

TRANSACTIONS

American Society for Metals

VOL. XXXIV

1945

TECHNICAL PROGRAM AND REPORTS OF OFFICERS AMERICAN SOCIETY FOR METALS—26TH ANNUAL CONVENTION, CLEVELAND, OCTOBER 16 to 20, 1944

FOR purposes of record and for the benefit of members who were not in attendance at the Twenty-sixth Annual Convention of the Society, held in Cleveland, October 16 to 20, 1944, the Technical Papers Program, the Production, Conservation and Post-War Planning Group Meetings, and Reports of Officers for 1944 are herewith published in full.

TECHNICAL PAPERS PROGRAM

MONDAY, OCTOBER 16

Lattice Room, Hotel Statler—9:30 A. M.

Session on Surface Hardening

Joint Chairmen—G. M. Cover and E. G. Mahin

Practical Aspects of the Selection of Frequency and Time Cycles for the Processing of Metallic Parts with Induction Heating, by W. E. Benninghoff and H. B. Osborn, Jr., Ohio Crankshaft Co.

Induction Hardening of Plain Carbon Steels, by D. L. Martin and F. E. Wiley, General Electric Co.

Shot for Metal Peening, by O. E. Harder and J. T. Gow, Battelle Memorial Institute.

Grand Ballroom, Hotel Statler—9:30 A. M.

Session on Hardenability Tests

Joint Chairmen—R. L. Dowdell and M. Gensamer

Rates of Tempering in Cobalt Steels, by E. A. Loria, Carnegie-Illinois Steel Corp.

Isothermal Transformation and End-Quench Hardenability of Some NE Steels, by R. L. Rickett, United States Steel Corp.; J. G. Cutton, C. B. Bernhart, Jr., Carnegie-Illinois Steel Corp.; and J. R. Millikin, U. S. Army Air Forces.

Further Developments of the End-Quenched Hardenability Test, by C. R. Wilks, Earnshaw Cook and Howard S. Avery, American Brake Shoe Co.

A Hardenability Test for Low Carbon and Shallow Hardening Steels, by O. W. McMullan, Bower Roller Bearing Co.

Euclid Ballroom, Hotel Statler, 9:30 A. M.

Session on Nonferrous Alloys

Joint Chairmen—W. J. Conley and J. O. Lord

A Survey of Wrought Magnesium Alloy Fabrication, by J. V. Winkler, Dow Chemical Co.

The Copper-Manganese Equilibrium System, by R. S. Dean, J. R. Long, T. R. Graham, E. V. Potter and E. T. Hayes, Bureau of Mines.

Properties of Transitional Structure in Copper-Manganese Alloys, by R. S. Dean, E. V. Potter and J. R. Long, Bureau of Mines.

Age Hardening Copper-Manganese-Nickel Alloys, by R. S. Dean, J. R. Long, T. R. Graham and C. W. Matthews, Bureau of Mines.

Grand Ballroom, Hotel Statler—11:30 A. M.

Victory Session

Captain T. A. Solberg, U.S.N., Head, Bureau of Research and Standards
Branch Bureau of Ships

Music Hall, Cleveland Public Auditorium—2:00 P. M.

Group Meeting on Metal Cutting and Tool Materials

Ballroom, Cleveland Public Auditorium—2:00 P. M.

Group Meeting on Light Weight Construction

Music Hall, Cleveland Public Auditorium—4:00 P. M.

Group Meeting on Surface Finishes and Protection

Ballroom, Cleveland Public Auditorium—4:00 P. M.

Group Meeting on Sub-Zero Treatments

Music Hall, Cleveland Public Auditorium—8:30 P. M.

Group Meeting on What's New in the Study of Corrosion (Round Table Discussion)

Ballroom, Cleveland Public Auditorium—8:30 P. M.

Group Meeting on Induction Heating (Electronics in Overalls)

TUESDAY, OCTOBER 17

Parlors 1, 2 and 3, Hotel Statler—9:30 A. M.

Session on Physical Properties

Joint Chairmen—R. L. Templin and B. B. Wescott

The Mechanism of Failure of 18 Cr-8 Ni Cracking Still Tubes, by C. L. Clark, Timken Roller Bearing Co., and J. W. Freeman, University of Michigan.

Capillarity of Metallic Surfaces, by E. R. Parker, University of California, and R. Smoluchowski, General Electric Co.

The Effect of Fiber on Notched Bar Tensile Strength Properties of a Heat Treated Low Alloy Steel, by G. Sachs, J. D. Lubahn, L. J. Ebert and E. L. Aul, Case School of Applied Science.

The Effects of Notches of Varying Depth on the Strength of Heat Treated Low Alloy Steels, by G. Sachs, J. D. Lubahn and L. J. Ebert, Case School of Applied Science.

Lattice Room, Hotel Statler—9:30 A. M.

Session on Hardenability

Joint Chairmen—M. F. Judkins and Clair Upthegrove

The Effect of Carbon Content on Hardenability, by E. S. Rowland, J. Welchner, R. G. Hill and J. J. Russ, Timken Roller Bearing Co.

Air-Hardenability of Steels, by C. B. Post, M. C. Fetzer and W. H. Fenstermacher, Carpenter Steel Co.

The Partition of Molybdenum in Steel and Its Relation to Hardenability, by Fred E. Bowman, Climax Molybdenum Co.

The Rate of Diffusion of Molybdenum in Austenite and in Ferrite, by John L. Ham, Climax Molybdenum Co.

Grand Ballroom, Hotel Statler—9:30 A. M.

Session on Aluminum and Magnesium Alloys

Joint Chairmen—H. E. Brown and H. W. Schmidt

New Developments in High Strength Aluminum Alloy Products, by E. H. Dix, Jr., Aluminum Company of America.

Aluminum Alloy Forging Materials and Design, by L. W. Davis, Aluminum Company of America.

The Properties of Aluminum Alloys Melted in an Induction Heated Crucible Furnace, by James W. Poynter, Army Air Forces, Wright Field.
Magnesium Sheet, by P. T. Stroup and G. F. Sager, Aluminum Company of America, and J. B. West, American Magnesium Corp.

Grand Ballroom, Hotel Statler—11:30 A. M.

Victory Session

Walter S. Tower, President American Iron & Steel Institute

Music Hall, Cleveland Public Auditorium—2:00 P. M.

Group Meeting on The Hardenability Band as a Basis for Purchase and Use of Steel

Ballroom, Cleveland Public Auditorium—2:00 P. M.

Group Meeting on Magnesium—Problems in Fabrication and Utilization

Music Hall, Cleveland Public Auditorium—4:00 P. M.

Group Meeting on Surface Peening to Increase Fatigue Resistance

Ballroom, Cleveland Public Auditorium—4:00 P. M.

Group Meeting on Instruments for Quality Control; A—Measurement of Linear Dimensions

Music Hall, Cleveland Public Auditorium—8:30 P. M.

Group Meeting on National Emergency Steels and Hardenability Specifications from the Consumer's Viewpoint

Ballroom, Cleveland Public Auditorium—8:30 P. M.

Group Meeting on Tin, Tin Alloys, Tin Coatings

WEDNESDAY, OCTOBER 18

Annual Meeting of the American Society for Metals

Grand Ballroom, Hotel Statler—9:30 A. M.

Edward de Mille Campbell Memorial Lecture, by Dr. George R. Fitterer, Head, Dept. of Metallurgical Engineering, University of Pittsburgh.

Some Fundamental Problems in the Manufacture of Steel by the Acid

Open-Hearth Process

Robert F. Mehl, Chairman

Music Hall, Cleveland Public Auditorium—2:00 P. M.

Group Meeting on Metals for Railroads

Ballroom, Cleveland Public Auditorium—2:00 P. M.

Group Meeting on New Trends in Metallurgical Heating

Music Hall, Cleveland Public Auditorium—4:00 P. M.

Group Meeting on Products From Metal Powders

Ballroom, Cleveland Public Auditorium—4:00 P. M.

Group Meeting on Instruments for Quality Control; B—Means to Establish Identity

Music Hall, Cleveland Public Auditorium—8:30 P. M.

Group Meeting on Manufacture of Quality Steels

Ballroom, Cleveland Public Auditorium—8:30 P. M.

Group Meeting on Instruments for Quality Control; C—Detection and Measurement of Internal Defects

THURSDAY, OCTOBER 19

Pine Room, Hotel Statler—9:30 A. M.

Session on Melting and Special Alloys

Joint Chairmen—O. E. Harder and Gilbert Soler

A Comparison of Aluminum and Titanium Deoxidation for Preventing Strain Aging Embrittlement in Low Carbon Steel, by G. F. Comstock and J. R. Lewis, Titanium Alloy Mfg. Co.

The Ar' Reaction in Some Iron-Cobalt-Tungsten Alloys and the Same Modified with Chromium, by W. P. Sykes, General Electric Co.

The Basic Electric Melting Procedure for High Quality Alloy Steels, by A. L. Ascik, Sorel Industries Limited.

Grand Ballroom, Hotel Statler—9:30 A. M.

Session on Tool Steels

Joint Chairmen—L. S. Bergen and J. P. Gill

The Dimensional Stability of Steel—Part I—Subatmospheric Transformation of Retained Austenite, by S. G. Fletcher and Morris Cohen, Massachusetts Institute of Technology.

A Study of Subzero Treatments Applied to Molybdenum-Tungsten High Speed Steel, by R. G. Kennedy, Jr., Cleveland Twist Drill Co.

Experiments of Sodium Cyaniding of High Speed Steel Prior to Hardening, by John McIntyre, International Business Machines Corp.

Lattice Room, Hotel Statler—9:30 A. M.

Session on X-Ray Studies

Chairman—A. O. Schaefer

A Comparison of Microhardness Indentation Tests, by Douglas R. Tate, National Bureau of Standards.

Improved Sensitivity in Double Exposure Radiography, by James Rigbey, Ford Motor Company of Canada.

The Interpretation of Radiographs: Particularly of Aircraft Parts, by Leslie W. Ball, Triplett & Barton, Inc.

Grand Ballroom, Hotel Statler—11:30 A. M.

Victory Session

Major General G. M. Barnes, Chief of Research and Development Service, Office of Chief of Ordnance

Music Hall, Cleveland Public Auditorium—2:00 P. M.

Group Meeting on New Aluminum Alloys for Peace-Time Uses

Ballroom, Cleveland Public Auditorium—2:00 P. M.

Group Meeting on Salt Baths

Music Hall, Cleveland Public Auditorium—4:00 P. M.

Group Meeting on Quality Control by Statistical Methods

Ballroom, Cleveland Public Auditorium—4:00 P. M.

Group Meeting on Instruments for Quality Control; D—Measuring Devices for Atmosphere and Combustion

Ballroom, Hotel Statler—7:00 P. M.

Annual Dinner of American Society for Metals

FRIDAY, OCTOBER 20

Euclid Ballroom, Hotel Statler—9:30 A. M.

Session on Chromium and Molybdenum Alloys

Joint Chairmen—R. S. Archer and G. A. Sellers

Chromium Steels of Low-Carbon Content, by Russell Franks, Union Carbide & Carbon Research Labs.

Characteristics and Properties of Some Cast Chromium-Molybdenum Steels, by N. A. Ziegler and W. L. Meinhardt, Crane Co.

The Segregation of Molybdenum in Phosphorus Bearing Alloyed Gray Cast Iron, by F. B. Rote, Wyman-Gordon Co., and W. P. Wood, University of Michigan.

Grand Ballroom, Hotel Statler—9:30 A. M.

Session on Fracture and Grain Study

Joint Chairmen—L. W. Kempf and J. T. Norton

Fractography—A New Tool for Metallurgical Research, by Carl A. Zapffe and Mason Clogg, Jr., Rustless Iron and Steel Corp.

Cleavage Structures of Iron-Silicon Alloys, by Carl A. Zapffe and Mason Clogg, Jr., Rustless Iron and Steel Corp.

Grain Shape and Grain Growth, by David Harker, General Electric Co. and Earl R. Parker, University of California.

Fracture Studies of Soldered Joints, by F. Berman and R. H. Harrington, General Electric Co.

Lattice Room, Hotel Statler—9:30 A. M.

Session on Rolling and Graphitization

Joint Chairmen—V. N. Krivobok and S. P. Watkins

Annealing Studies on Cold-Rolled Iron and Iron Binary Alloys, by C. R. Austin and R. W. Lindsay, Pennsylvania State College; L. A. Luini, Wright Aeronautical Corp.

The Effect of Cold Rolling on the Structure of Hadfield Manganese Steel, by Norman P. Goss, Cold Metal Process Co.

Factors Controlling Graphitization of Carbon Steels at Subcritical Temperatures, by C. R. Austin, Pennsylvania State College, and M. C. Fetzer, Carpenter Steel Co.

Grand Ballroom, Hotel Statler—11:30 A. M.

Victory Session

Lt. Col. Wm. Walter Phelps, Air Corps Area Representative, Army Air Forces, Materiel Command

Music Hall, Cleveland Public Auditorium—2:00 P. M.

Group Meeting on Heat Treatment

Ballroom, Cleveland Public Auditorium—2:00 P. M.

Group Meeting on Improved Gray Iron Castings

A.S.M. GROUP MEETINGS

MONDAY, OCTOBER 16

Music Hall, Public Auditorium—2:00 P. M.

Metal Cutting and Tool Materials

Chairman—Harry B. Knowlton, Materials Engineer, International Harvester Co., Chicago, Ill.

Summarizer—Orlan W. Boston, Chairman, Dept. of Metal Processing, College of Engineering, University of Michigan, Ann Arbor, Michigan

Improvements in Carbides and Tools, Especially Milling Cutters, by Harry W. Highriter, Chief Metallurgical Engr., Vascaloy-Ramet Corp., North Chicago, Ill.

Improved Grinding Tools and Techniques for Grinding Carbide Tools, by Charles K. Worthen, Engineer of Diamond Products, Norton Company, Worcester, Mass.

Film Showing High Speed Milling with Carbide Tools, by Michael Field, Engineer, Research Dept., Cincinnati Milling Machine Co., Cincinnati, Ohio.

Improved Heat and Cold Treatments for High Speed Steels, by Z. T. Crittenden, Supt. of Heat Treatment, Pontiac Division of General Motors Corp., Pontiac, Mich.

Improved Finishes in High Speed Tools (Chromium Plate and Superfinish), by Burns George, Met. Engr., Vanadium-Alloys Steel Co., Latrobe, Pa.

Recent Developments in the Use of Cast Alloy Tools, by Robert L. Lerch, Vice Pres., Haynes Stellite Co., Kokomo, Ind.

Metallurgical Factors Affecting Machinability, by S. B. Knutson, Senior Metallurgist, Standard Steel Spring Co., St. Louis, Mo.

Appraisal and Measurement of Finishes, by J. Manuele, Director of Quality Control, Westinghouse Elec. & Mfg. Co., E. Pittsburgh, Pa.

Summary by Orlan W. Boston.

Ballroom, Public Auditorium—2:00 P. M.

Light Weight Construction

Chairman—V. N. Krivobok, International Nickel Co., New York

Summarizer—Zay Jeffries, Nela Park, Cleveland, Ohio

A—General Considerations

Influence of the Metals Used (or Available) on the Design, by the Chairman.

Influence of Heat Treatments in the Saving of Dead Weight, by Horace C. Knerr, Philadelphia, Pa.

Influence of Fabrication Methods, Especially Welding, by Edward J. Charlton, Asst. to President, Lukenweld, Inc., Coatesville, Pa.

B—Specific Applications of the General Principles

Weight and Rigidity of Long Bridges, by E. C. Hartmann, Aluminum Research Labs., New Kensington, Pa.

Weight Saving in Railway Equipment, by Stephen H. Badgett, Mech. Engr., Passenger Car Div., Pressed Steel Car Co., Pittsburgh, Pa.

Weight Saving in Ordnance, by Col. S. B. Ritchie, Office, Chief of Ordnance, U. S. Army, Washington, D. C.

Weight Saving in Aircraft, by S. A. Gordon, Chief Test Engineer, Glenn L. Martin Co., Baltimore, Md.

Light Weight in Consumers' Goods, by J. Mathes, Dow Chemical Company, Midland, Michigan.

General Discussion by the Audience.

Summary by Zay Jeffries.

Music Hall, Public Auditorium—4:00 P. M.

Surface Finishes and Protection

Chairman—James Rowan Ewing, Asst. to Pres., Solventol Chemical Products, Inc., Detroit, Mich.

Summarizer—M. B. Roosa, Service Mgr., Parker Rust-Proof Company, Detroit, Mich.

Process Engineering of Surface Conditioning and Finish, by George Onksen, Manager of Industrial Engineering and Service, Solventol Chemical Products, Inc., Detroit, Mich.

Blast Cleaning, by P. J. Potter, Exec. Vice Pres., Pangborn Corp., Hagerstown, Md.

Surface Preparation of Cast Iron, by J. H. Shoemaker, Pres., Kolene Corp., Detroit, Mich.

Improvements in Zinc and Nickel Coatings, by Myron B. Diggin, Chief Chem., Hanson-Van Winkle-Munning Co., Matawan, N. J.

Improvements in Other Protective Metallic Plates, by R. B. Saltonstall, Technical Director, The Udyllite Corp., Detroit, Mich.

Chemical Finishes on Copper and Steel, by Walter Meyer, Tech. Dir., The Enthone Co., New Haven, Conn.

Chemical Finishes on Other Metals, by R. M. Thomas, Vice Pres., Rheem Research Products, Baltimore, Md.

General Discussion by the Audience.

Summary by M. B. Roosa.

Ballroom, Public Auditorium—4:00 P. M.

Refrigeration in Metallurgy (Sub-Zero Treatments)

Chairman—J. R. Tranter, Pres., Kold-Hold Mfg. Co., Lansing, Mich.

Summarizer—Ralph L. Dowdell, Prof. of Met., University of Minnesota, Minneapolis, Minn.

Dried Blast and Its Advantages, by L. L. Lewis, Vice Pres., Carrier Corp., Syracuse, N. Y.

Refrigerated Test Rooms, by L. D. Heath, Met., B. F. Sturtevant Co., Boston, Mass.

General Remarks on the Action of Metals at Very Low Temperature, by J. J. Kanter, Research Met., Crane Company, Chicago, Ill.

Sub-Zero Treatment of Tool Steel, by G. B. Berlien, Ch. Met., Lindberg Steel Treating Co., Chicago, Ill.

Size Stabilization of Precision Gages, by Stewart G. Fletcher, Dept. of Physical Metallurgy, Mass. Institute of Technology, Cambridge, Mass.

Sub-Zero Treatment of Aluminum Alloys, by H. F. Swenson, Sweden Freezer Mfg. Co., Seattle, Wash.

General Discussion by the Audience.

Summary by Ralph L. Dowdell.

Music Hall, Public Auditorium—8:30 P. M.

What's New in the Study of Corrosion (Round Table Discussion)

Interlocutor—Robert B. Mears, Chief, Chemical Metallurgy Division
Aluminum Research Laboratories, New Kensington, Pa.

Passivity and the Stainless Steels, by Russell Franks, Union Carbide & Carbon Research Lab., Niagara Falls, N. Y.

Nickel Alloys, Galvanic and Marine Corrosion, by F. L. La Que, Development & Research Div., International Nickel Co., New York City.

Mechanism of Corrosion; Protective Coatings, by R. M. Burns, Asst. Chem. Director, Bell Telephone Labs., New York City.

Light Alloys; Aircraft Corrosion Problems, by R. H. Brown, Asst. Chief, Metallurgical Div., Aluminum Research Labs., Aluminum Co. of America, New Kensington, Pa.

Organic Protective Coatings, by Robert J. Moore, Mgr. of Sales Development Labs., Bakelite Corporation, Bloomfield, N. J.

Questions Raised by the Audience.

Summary by The Interlocutor.

Ballroom, Public Auditorium—8:30 P. M.

Induction Heating (Electronics in Overalls)

Chairman—Wm. E. Benninghoff, Manager, Tocco Division, The Ohio Crankshaft Co., Cleveland, Ohio

Summarizer—H. E. Somes, Chief Engr., Budd Induction Heating, Inc., Detroit, Mich.

ABC of the Process and Special Generating Equipment for High and Low Frequencies, by J. P. Jordan, Industrial Heating & Welding Engrg. Dept. General Electric Co., Schenectady, N. Y.

Heating for Melting, by Howard F. Taylor, Metallurgist, Naval Research Laboratory, Anacostia, Washington, D. C.

Heating for Forging, by C. M. Campbell, Metallurgist, Chevrolet Transmission & Aluminum Forge, Saginaw, Mich.

Surface Hardening with High Frequencies, by Thomas E. Eagan, Ch. Metallurgist, Cooper-Bessemer Corp., Grove City, Pa.

Surface Hardening with Very High Frequencies, by J. W. Cable, Director of Research and Development, Induction Heating Corp., New York City.

Heating for Brazing, by Anthony M. Setapen, Industrial & Engineering Division, Handy & Harman, New York City.

Continuous Heat Treating of Metals with Varying Cross Section, by Eugene Mittelman, Director of Electronic Research, Illinois Tool Works, Chicago, Ill.

General Discussion by the Audience.

Summary by Howard E. Somes.

TUESDAY, OCTOBER 17**Music Hall, Public Auditorium—2:00 P. M.**

The Hardenability Band as a Basis for Purchase and Use of Steel

Chairman—Walter E. Jominy, Chief Met., Dodge Chicago Plant, Chrysler Corp., Chicago, Ill.

Summarizer—Marcus A. Grossmann, Director of Research, Carnegie-Illinois Steel Corp., Chicago, Ill.

The Development and Possibilities of Hardenability Bands, by John Mitchell, Met. Engr., Alloy, Carnegie-Illinois Steel Corp., Pittsburgh, Pa.

General Discussion by the Audience.

Application and Use of Hardenability Tests by the Consumer, by A. L. Boegehold, Head, Metallurgy Dept., General Motors Corp., Research Labs. Div., Detroit, Mich.

General Discussion by the Audience.

Summary by Marcus A. Grossmann.

Ballroom, Public Auditorium—2:00 P. M.*Magnesium—Problems in Fabrication and Utilization*

Chairman—E. S. Christiansen, Vice Pres., Apex Smelting Co., Chicago, Ill.
(and Pres. The Magnesium Assoc.)

Summarizer—J. D. Hanawalt, Director of Met. Res., Dow Chemical Co.,
Midland, Mich.

Economic and Commercial Considerations Favorable to Magnesium for Consumer and Durable Goods, by Leo B. Grant, Sales Manager, Magnesium Division, Dow Chemical Co., Midland, Mich.

Important Foundry Operations at Variance with Conventional Gray Iron Practice, by H. C. Nicholas, Quality Castings Co., Orrville, Ohio.

Important Points about Forging, Different from Other Non-Ferrous Practices, by Edward S. Bunn, Met. Mgr., Revere Copper & Brass, Inc., New York City.

Problems in Design and Manufacture of Magnesium Die Castings, by W. J. During, Executive V. P. and Ch. Engr., Precision Castings Co., Syracuse, N. Y.

Essential Heat Treatment Operations, by Oscar Blohm, Chief Metallurgist, Hills-McCanna Co., Chicago, Ill.

Machining of Magnesium and Its Alloys, by Ralph M. Heintz, Vice Pres., Jack & Heintz Co., Bedford, O.

Surface Finishes, by Robert T. Wood, Chief Met., American Magnesium Corp., Cleveland, Ohio.

General Discussion by the Audience.

Summary by J. D. Hanawalt.

Music Hall, Public Auditorium—4:00 P. M.*Surface Peening to Increase Fatigue Resistance*

Chairman—Maurice Olley, Detroit, Mich.

Summarizer—Oscar E. Harder, Asst. Director, Battelle Memorial Institute, Columbus, Ohio

Influence of Shot Peening on the Mechanical Properties of Metals, by The Chairman.

Shot Peening of Coil & Leaf Springs, by F. P. Zimmerli, Chief Engr., Barnes-Gibson-Raymond Div. of Associated Spring Corp., Detroit, Mich.

Improvement of Parts on Motive Power, by L. E. Simon, Ch. Met., Electro-Motive Div., G.M.C., La Grange, Ill.

Shot Peening as Applied to Ordnance Materiel, by Col. John H. Frye, Office of Chief of Ordnance, War Dept., Washington, D. C.

Relation of Shot Quality to the Results of Peening, by Arthur E. Proctor, Jr., Lab. Met., Ford Motor Co., Dearborn, Mich.

Industrial Equipment for Shot Peening, by L. L. Andrus, Vice Pres. in Charge of Sales, American Foundry Equipment Co., Mishawaka, Ind.

General Discussion by the Audience.

Summary by Oscar E. Harder.

Ballroom, Public Auditorium—4:00 P. M.*Instruments for Quality Control; A—Measurement of Linear Dimensions*

Chairman—Orlan W. Boston, Chairman, Dept. of Metal Processing, College of Engineering, University of Michigan, Ann Arbor, Mich.

Summarizer—A. H. d'Arcambal, Vice Pres., Pratt & Whitney, Hartford, Conn.
Accuracy Attainable or Desirable by Various Classes of Instruments and Methods, and as Affected by the Personal Equation, by The Chairman.

Rules, Micrometers and Calipers, by H. D. Hiatt, Supt., Gage Dept. 948, Plant 5, Allison Division, General Motors Corp., Indianapolis, Ind.

Comparators—Electric, Pneumatic, Optical and Mechanical, by W. H. Baker, Ch. Inspector, Packard Aircraft Division, Packard Motor Car. Co., Detroit, Mich.

Multiple & Automatic Gages, by S. C. Hurley, Jr., Electric Eye Equipment Company, Danville, Illinois.

Fixed Limit Gages; Such as Plugs, Rings & Snaps, by Col. H. B. Hambleton, Gage Section, Ordnance Dept., U.S.A., Washington, D. C.

Projectors, by G. F. Stocker, Manufacturing Methods Department, General Electric Co., West Lynn, Mass.

General Discussion by the Audience.

Summary by A. H. d'Arcambal.

Music Hall, Public Auditorium—8:30 P. M.

NE Steels and Hardenability Specifications from the Consumer's Viewpoint
Chairman—Charles H. Herty, Jr., Bethlehem Steel Co., Bethlehem, Pa.

Summarizer—Harry W. McQuaid, Manager, Process & Product Dev. Div., General Met. Dept., Republic Steel Corp., Cleveland, Ohio

Future Possibilities in the Automotive Industry, by Roy W. Roush, Met., Timken Detroit Axle Co., Detroit, Mich.

Future Possibilities for Aircraft Engines, by Arthur W. F. Green, Materials Engr., Pratt & Whitney Aircraft Corp. of Mo., Kansas City, Mo.

Future Possibilities for Aircraft Frames, by J. B. Johnson, Materiel Command, Army Air Forces, Wright Field, Dayton, Ohio.

Future Possibilities in the Tractor Industry, by Glen C. Riegel, Chief Met., Caterpillar Tractor Company, Peoria, Ill.

Future Possibilities in the Petroleum Industry, by Blaine B. Wescott, Met., Gulf Research & Development Co., Pittsburgh, Pa.

Future Possibilities in Mining and Heavy Power Equipment, by J. T. Jarman, Gen. Supt., Allis-Chalmers Mfg. Co., Milwaukee, Wis.

General Discussion by the Audience.

Summary by Harry W. McQuaid.

Ballroom, Public Auditorium—8:30 P. M.

Tin; Tin Alloys; Tin Coatings

Chairman—Erwin Vogelsang, Director, Tin, Lead & Zinc Div., War Production Board, Washington, D. C.

Summarizer—Bruce W. Gonser, Battelle Memorial Institute, Columbus, Ohio
Resources of Virgin Tin Now Available to the United States and the Continuing Necessity for the Utmost Conservation of Tin, by The Chairman.

Reclamation of Tin from Tin Cans, by Walton Smith, Vice Pres., Metal & Thermit Corp., New York City.

Bearings, Low in Tin, by Herman L. Smith, Ch. Met., Federated Metals Div., American Smelting & Refining Co., Pittsburgh, Pa.

Solders, Low in Tin, by Arthur Maupin, Consultant, Tin, Lead, Solder & Babbitt Metals Branch, Conservation Division, W. P. B., Washington, D. C.

Electrolytic Tin Plate, by J. C. Whetzel, Asst. Mgr. of Sales, Tin Plate Div., Carnegie-Illinois Steel Corp., Pittsburgh, Pa.

Tin Cans, Low in Tin, by Harley S. Van Vleet, Met. Engr., American Can Co., Maywood, Illinois.

General Discussion by the Audience.

Summary by Bruce W. Gonser.

WEDNESDAY, OCTOBER 18

Music Hall, Public Auditorium—2:00 P. M.

Metals for Railroads

Chairman—William M. Barr, Chief Chem. & Met. Engineer, Union Pacific Railroad Co., Omaha, Neb.

How Rail Failures Are Being Prevented, by R. E. Cramer, Spec. Research Asso. Prof. of Engineering Materials, Rails Investigation, University of Illinois, Urbana, Ill.

Improving the Fatigue Resistance of Axles, by Oscar J. Horger, In Charge of Railway Engineering & Research, Timken Roller Bearing Co., Canton, Ohio.

Detection & Prevention of Incipient Failure in Firebox & Boilers, by Ray McBrian, Engineer of Standards and Research, Denver & Rio Grande Western R.R. Co., Denver, Colo.

Metal Limitations in the Perfecting of Motive Power, by Paul L. Irwin, Engineer of Tests, Baldwin Locomotive Works, Paschall Station, Philadelphia, Pa.

Stress Analysis as a Means of Improving the Design of Railroad Rolling Stock, by W. M. Murray, Pres., Society for Experimental Stress Analysis, Mass. Inst. of Technology, Cambridge, Mass.

Improving the Railroad-Car Bearing, by J. R. Jackson, Engineer of Tests, Missouri Pacific Lines, St. Louis, Mo.

General Discussion by the Audience.

Ballroom, Public Auditorium—2:00 P. M.

New Trends in Metallurgical Heating

Chairman—G. George Segeler, Engr. of Utilization, American Gas Association, New York 17, N. Y.

Summarizer—Gordon T. Williams, Materials Engineer, Pratt & Whitney Aircraft, East Hartford, Conn.

Special Furnaces & Methods for Heavy Ordnance, by C. H. Carpenter, Sales Engr., Lee Wilson Engineering Co., Cleveland, Ohio.

High-Speed Heat Transfer by Pressure Combustion, by Harry W. Smith, Jr., Mgr., Technical Information Department, Selas Corp. of America, Philadelphia, Pa.

Developments in Heating by Convection Currents, by Slade B. Gamble, Lindberg Eng. Co., Chicago, Ill.

Heating Light Alloys Uniformly and Quickly to Moderate Temperatures Without the Possibility of Overheating, by Philip T. Stroup, Chief, Process Met. Div., Al. Res. Labs., Aluminum Co. of America, New Kensington, Pa.

Continuous Induction Heat Treatment of Rod and Bar Stock, by F. F. Vaughn, Asst. Chief Met., Caterpillar Tractor Co., Peoria, Ill.

"Flowing" of Electrolytic Tin Plate, by G. E. Stoltz, Mgr. Metal Working Sec., Industrial Engineering Department, Westinghouse Electric & Mfg. Co., East Pittsburgh, Pa.

Heat Treating at Radio Frequencies, by Emil R. Capita, Pres., Ecco High Frequency Corp., North Bergen, N. J.

General Discussion by the Audience.

Summary by Gordon T. Williams.

Music Hall, Public Auditorium—4:00 P. M.

Products from Metal Powders

Chairman—Charles Hardy, Pres., Hardy Metallurgical Co., New York City

Summarizer—John Wulff, Mass. Inst. of Technology, Cambridge, Mass.

Electrical & Magnetic Devices from Metal Powders, by A. B. Gibson, Gibson Electric Co., Pittsburgh, Pa.

Iron Powder & Products Therefrom

War-Time Applications of Powder Metallurgy That Will Influence Peace-Time Production, by Andrew J. Langhammer, Pres., Amplex Div., Chrysler Corp., Detroit, Mich.

Bonding Copper Powder Compacts to Steel, by F. De Marinis, S. K. Wellman Co., Cleveland, Ohio.

New Techniques & Tools from Cemented Carbides, by Edgar W. Engle, Consulting Met., The Carboloy Co., Inc., Detroit, Mich.

Problems Connected with Die Design & Pressing, by Richard P. Seelig, Ch. Engr., Powder Metallurgy Corp., Long Island City, N. Y.
Special Instruments for Controlling Powder & Product, by W. R. Toeplitz, Prod. Mgr., Bound Brook Oil-Less Bearing Co., Bound Brook, N. J.
General Discussion by the Audience.
Summary by John Wulff.

Ballroom, Public Auditorium—4:00 P. M.

Instruments for Quality Control; B—Means to Establish Identity
Chairman—John Quincy Adams, Sec., Committee on Application of Magnetic Materials, General Electric Co., Schenectady, N. Y.
Summarizer—John G. Thompson, Chief of Chemical Metallurgy Section, Met. Div., National Bureau of Standards, Washington, D. C.
Identometers (Thermo-Electric Devices), by Antony Doschek, Research Engr., American Tubular Elevator Co., Pittsburgh, Pa.
Magnetic Hysteresis and Permeability Devices, by J. J. Smith, Gen. Engineering Lab., General Electric Co., Schenectady, N. Y.
Magnetic High Frequency Devices, by P. E. Cavanagh, Chief Met., Allen B. Du Mont Laboratories, Inc., Passaic, N. J.
Spark Tests; Use and Limitations, by Walter G. Hildorf, Director of Metallurgy, Timken Roller Bearing Co., Canton, Ohio.
Chemical Spot Tests for Steels and Non-Ferrous Metals, by W. O. Philbrook, Foreman, Met. Div., Wisconsin Steel Works of International Harvester Co., Chicago, Ill.
X-Ray Diffractions, by David Harker, Metallurgist, Research Laboratory, General Electric Co., Schenectady, N. Y.
Spectroscope (Steeloscope), Microphotometer and Spectrophotometer, by R. A. Wolfe, Res. Physicist, University of Michigan, Ann Arbor, Mich.
General Discussion by the Audience.
Summary by John G. Thompson.

Music Hall, Public Auditorium—8:30 P. M.

Manufacture of Quality Steels
Chairman—C. D. King, Chairman of Operating Committees, U. S. Steel Corp. of Delaware, Pittsburgh, Pa.
Summarizer—Herbert W. Graham, Dir. of Met. & Res., Jones & Laughlin Steel Corp., Pittsburgh, Pa.
Relative Advantages of Electric, Openhearth and Duplex Processes, by E. C. Smith, Ch. Met., Republic Steel Corp., Cleveland, Ohio.
Modified Chemistry for Narrow Hardenability Ranges, by W. G. Bischoff, Met. Asst., Timken Steel & Tube Co., Canton, Ohio.
Rapid Control Methods (Checks) on Molten Bath, by F. M. Washburn, Supt. of Testing, Wisconsin Steel Works Chicago, Ill.
Reaction Alloys or Intensifiers, by Norman F. Tisdale, Metallurgist, Molybdenum Corp. of America, Pittsburgh, Pa.
General Discussion by the Audience.
Summary by Herbert W. Graham.

Ballroom, Public Auditorium—8:30 P. M.

Instruments for Quality Control; C—Detection and Measurement of Internal Defects
Chairman—Norman L. Mochel, Manager of Metallurgical Engineering, Westinghouse Electric & Mfg. Co., Philadelphia, Pa.
Summarizer—Ray McBrien, Engineer of Standards & Research, Denver & Rio Grande Western Railroad Co., Denver, Colo.
Electrical and Electronic Flaw Detectors, by W. E. Habig, Dev. Engr., Sperry Products, Inc., Hoboken, N. J.
Magnetic Devices, by Theodore Zuschlog, Chief Engineer, Magnetic Analysis Corp., Long Island City, N. Y.

Radiography and Micro-radiography, by L. W. Ball, Triplett & Barton, Burbank, Calif.

Supersonics, by Floyd A. Firestone, Asst. Prof. of Physics, University of Michigan, Ann Arbor, Mich.

Magnetic Particles and Fluorescent Penetrants, by Alfred V. deForest, Prof. of Mechanical Engineering, Mass. Institute of Technology, Cambridge, Mass.

Discussion by the Audience.

Summary by Ray McBrian.

THURSDAY, OCTOBER 19

Music Hall, Public Auditorium—2:00 P. M.

New Aluminum Alloys for Peace-Time Uses

Chairman—C. G. Stephens, Inspection Mgr., The Glenn L. Martin Co., Baltimore, Md.

Summarizer—Edgar H. Dix, Jr., Asst. Dir. of Research and Chief. Met., Aluminum Research Laboratories, Aluminum Co. of America, New Kensington, Pa.

Sheet and Extrusion Alloy 75-S and Its Post-War Uses, by Theodore W. Bossert, Asst. Ch. Met., Fabricating Div., Aluminum Company of America, Pittsburgh, Pa.

New Strong Aluminum Alloys R-301 and R-303 and their Post-War Uses, by T. L. Fritzlen, Ch. Research Met., Reynolds Research Institute, Reynolds Metals Co., New York City.

Al-Fin and other Brazing and Welding Methods, by F. P. Culbert, General Manager, The Al-Fin Corporation, Jamaica, Long Island, N. Y.

New Cast Alloys, Strong as Cast, by Hiram Brown, Chief Met., Frontier Bronze Corp., Niagara Falls, N. Y.

English Alloys for Castings, Used in America, by Muir L. Frey, Aircraft Met., Packard Motor Car Co., Detroit, Mich.

New Casting Alloys from Aircraft Scrap, by Walter Bonsack, Dir. of Labs., The National Smelting Co., Cleveland, Ohio.

General Discussion by the Audience.

Summary by Edgar H. Dix.

Ballroom, Public Auditorium—2:00 P. M.

Salt Baths

Chairman—Haig Solakian, Vice Pres., A. F. Holden Co., New Haven, Conn.

Summarizer—Leon D. Slade, Supt., Gleason Works, Rochester, N. Y.

Historical Development of Salt Baths into Definite Functions, by A. E. Bellis, President, Bellis Heat Treating Co., Branford, Conn.

High Temperature Baths for High Speed Steels, by Paul C. Farren, Pres., Springfield Heat Treating Corp., Springfield, Mass.

Neutral Hardening of Carbon and Alloy Steels.

Medium and Low Temperature Baths for Carburizing and Nitriding, by Warren A. Silliman, Ch. Met., Cleveland Tractor Company, Euclid, Ohio.

Baths for Heating Armor Plate, by M. L. Fox, Ch. Engr., Parish Pressed Steel Co., Reading, Pa.

Baths for Interrupted Quenching (Martempering and Austempering), by Arnold P. Seasholtz, Met. Engr., E. F. Houghton & Co., Philadelphia, Pa.

General Discussion by the Audience.

Summary by Leon D. Slade.

Music Hall, Public Auditorium—4:00 P. M.

Quality Control by Statistical Methods

Chairman—John W. Sullivan, Cleveland, Ohio

Summarizer—John V. Sturtevant, Chairman, Pittsburgh Quality Control Society; Metallurgist, Carnegie-Illinois Steel Corp., Pittsburgh, Pa.

I.—Attributes Quality Control Plans

Single Versus Double Sampling Plans for Acceptance Inspection, by The Chairman.

Sequential Sampling Plans for Acceptance Inspection, by Major Orville T. Church, Officer in Charge, Inspection Branch, Jeffersonville Quartermaster Depot, Jeffersonville, Indiana.

II.—Variable Quality Control Plans

Control Charts for Average and Standard Deviations for Mass Produced Articles, by Edwin G. Olds, Chief Statistical Consultant, Office of Production Research and Development, W.P.B., Washington, D. C.

Control Charts for Average and "Range" as used for Steel Manufacture, by H. J. Hand, Industrial Engineering Division, National Tube Co., Pittsburgh, Pa.

Control Charts for Dimensional Control, by J. O. Heide, Quality Engineer, U. S. Rubber Co., Passaic, N. J.

III.—Quality Control Plans in a Specific Industry

Use by the Airframes Industry, by P. A. Haythorne, Engineering Dept., Lockheed Aircraft Corp., Burbank, Cal.

General Discussion by the Audience.

Summary by John V. Sturtevant.

Ballroom, Public Auditorium—4:00 P. M.

Instruments for Quality Control; D—Measuring Devices for Atmosphere and Combustion

Chairman—C. E. Peck, Engineer, Heating Section, Westinghouse Electric & Manufacturing Co., East Pittsburgh, Pa.

Summarizer—Matthew H. Mawhinney, Consulting Engineer, Salem, Ohio.

Process and Combustion-Gas Analyzers, by J. F. Luhrs, Application Engineer, Bailey Meter Co., Cleveland, Ohio.

Dew Point Potentiometer and Recorder, by E. G. de Coriolis, Director of Research, Surface Combustion, Toledo, Ohio.

Flow Meters, by P. K. Kinyoun, Combustion Engr., Bethlehem Steel Corp., Lackawanna Plant, Buffalo, N. Y.

Furnace Pressure Meters and Controls, by E. W. Fitch, Combustion Engineer, Republic Steel Corp., Youngstown, Ohio.

Gas Mixing and Fuel Air Ratio Controls, by Ed. C. McDonald, Fuel Engineer, Republic Steel Corp., Cleveland District.

Discussion by the Audience.

Summary by Matthew H. Mawhinney.

FRIDAY, OCTOBER 20

Music Hall, Public Auditorium—2:00 P. M.

Heat Treatment

Chairman—E. C. Bain, Vice Pres., Carnegie-Illinois Steel Corp., Pittsburgh, Pa.

Summarizer—H. J. French, Asst. Mgr., Dev. and Res. Div., International Nickel Co, New York City

Short Cycle Annealing, by Peter Payson, Asst. Dir. of Res., Crucible Steel Co. of America, New York City.

Continuous Cooling-Transformation Diagrams (A Necessary Guide for Propeller Heat Treatment), by C. A. Liedholm, Ch. Engrg. Met., Propeller Div., Curtiss-Wright Corp., Caldwell, N. J.

Advanced Quenching Practice, by B. F. Shepherd, Ch. Met. Ingersoll-Rand Co., Phillipsburg, N. J.

Controlled Gas Carburizing, by Floyd E. Harris, Furnace Engr., Buick Motor Div., G.M.C., Flint, Mich.

Protective Atmospheres and Gas Quenching, by Orville E. Cullen, Met., Surface Combustion, Toledo, Ohio.

General Discussion by the Audience.

Summary by H. J. French.

Ballroom, Public Auditorium—2:00 P. M.*Improved Gray Iron Castings*

Chairman—Frank A. Steinebach, Editor, "The Foundry", Cleveland, Ohio
Summarizer—James T. MacKenzie, Ch. Met., American Cast Iron Pipe Co.,
Birmingham, Alabama

Problems Connected with the Poor Quality of Available Scrap.

Advantages of Hot Iron, Through Blast Control and Other Expedients, by V. A. Crosby, Met. Engr., Climax Molybdenum Co., Detroit, Mich.

Inoculants (Ladle Treatments) to Improve Uniformity of Castings, by R. G. McElwee, Mgr., Fdry. Div., Vanadium Corp. of America, Detroit, Mich.

Short Anneals to Improve Machinability.

Flame Hardening of Castings, by John Erler, Chief Met., Farrel-Birmingham Co., Inc., Ansonia, Conn.

Strong Alloy Castings, by W. A. Hambley, Works Met., Allis Chalmers Mfg. Co., Milwaukee, Wis.

General Discussion by the Audience.

Summary by James T. MacKenzie.

**ANNUAL MEETING OF
AMERICAN SOCIETY FOR METALS**

Cleveland, Wednesday, October 18, 1944

The meeting was called to order by President Grossmann, who announced that the first order of business was the President's report. He then asked Vice-President Van Horn to occupy the chair while he read his report. This is published in full beginning on page 24 of this volume of TRANSACTIONS.

VICE-PRESIDENT VAN HORN: You have heard the report of the President. There being no comments the report will stand as read. I now return the chair to the President.

PRESIDENT GROSSMANN: The next order of business will be the annual report of the Treasurer, Harry D. McKinney.

Treasurer McKinney presented his report which appears in full beginning on page 29.

PRESIDENT GROSSMANN: You have heard the report of the Treasurer. There being no objections it will stand as read. The next order of business is the report of the Secretary.

Secretary Eisenman presented his report which appears in full beginning on page 34.

PRESIDENT GROSSMANN: You have heard the report of the Secretary. There being no objections it will stand as read. The next order of business is the election of officers.

ELECTION OF OFFICERS

PRESIDENT GROSSMANN, *Presiding*: Complying with the constitution, I appointed on March 3, 1944, the following Nominating Committee, selected from the list of candidates suggested by eligible chapters prior to March 1, 1944:

A. O. Schaefer, Philadelphia Chapter, Chairman.
Joseph A. de Bondy, Manitoba Chapter.
J. B. Johnson, Dayton Chapter.
A. B. Kinzel, New York Chapter.
W. D. McMillan, Chicago Chapter.
W. J. Reagan, Warren Chapter.
G. C. Riegel, Peoria Chapter.

The Committee met in New York on May 26, 1944, and made the following nominations:

FOR PRESIDENT

Kent R. Van Horn, Aluminum Co. of America, Cleveland—1 year

FOR VICE-PRESIDENT

Charles H. Herty, Jr., Bethlehem Steel Co., Bethlehem, Pa.—1 year

FOR SECRETARY

W. H. Eisenman—2 years

FOR TRUSTEE

L. S. Bergen, Bergen Precision Castings, Inc., Pleasantville, N. Y.—2 years

FOR TRUSTEE

R. W. Schlumpf, Hughes Tool Co., Houston, Texas—2 years

A report of these nominations duly appeared in the REVIEW of May, 1944.

I have been informed by the Secretary that no additional nominations were received prior to July 15, 1944, for any of the vacancies occurring on the Board of Trustees. Consequently the nominations were closed. I shall now call upon the Secretary to carry out the provisions of the Constitution in respect to the election of national officers.

W. H. EISENMAN, *Secretary*: Conforming with the provisions and requirements of the constitution of the American Society for Metals, I hereby cast the unanimous vote of the members for the election of the aforementioned candidates who were regularly nominated May 26, 1944.

PRESIDENT GROSSMANN: The provisions of the constitution having been complied with, I hereby declare the candidates heretofore named to be duly and unanimously elected to the several specified offices, the terms of each beginning on the day following the close of this annual meeting.

When Mr. Herty was nominated for vice-president of the Society, he resigned as a trustee leaving one year of his unexpired term. The trustees filled the vacancy by electing Mr. Arthur E. Focke, whom I now introduce to the members.

President Grossmann then introduced the newly-elected trustees, Mr. L. S. Bergen, President, Bergen Precision Castings, Inc. (Mr. R. W. Schlumpf, Chief Metallurgist of Hughes Tool Co. was unable to be present), Secretary Eisenman, Vice-President-Elect Charles H. Herty, Jr., Asst. to the President of the Bethlehem Steel Co., and President-Elect Kent R. Van Horn, Research Metallurgist of the Aluminum Co. of America.

President-Elect Van Horn said a few words to the audience.

... President Grossmann then presented a certificate to Howard E. Handy, in recognition of his 20 years' service as secretary of the Boston chapter.

PRESIDENT GROSSMANN: The chair now recognizes Ray McBrian, Engineer of Standards and Research, Denver, Rio Grande & Western Railroad, of Denver, who is chairman of the National Committee on Constitution and By-Laws of the Society.

MR. MCBRIAN: I have here the resolutions for the proposed changes in the Constitution and By-Laws of the Society as recommended and approved by the Board of Trustees and the Constitution and By-Laws Committee of the Society, and assembled in proper legal phraseology by the Society counsel. These proposed amendments were published in full in the August issue of the METALS REVIEW.

Amendments to Constitution and By-Laws

WHEREAS, the Board of Trustees of American Society for Metals has proposed that Section 1 of Article IX of the Constitution and By-Laws of the Society be amended in the respects hereinafter in this resolution set forth; and

WHEREAS, said amendments have been proposed by an affirmative vote of two-thirds of the membership of the Board of Trustees, at a meeting of the Board duly called and held in Cleveland, Ohio, on April 28, 1944, notice of which stated that amendments to the Constitution and By-Laws were to be discussed at the meeting; and

WHEREAS, at least sixty days prior to this date, the Secretary gave to each member, and to the representative of each member firm and corporation, written notice of the action of the Board of Trustees in proposing said amendments and written notice that said amendments would be presented for adoption at this annual meeting of the members of the Society, setting forth in such notice the proposed amendments in their entirety;

NOW THEREFORE, BE IT RESOLVED, that Section 1 of Article IX of the Constitution and By-Laws of American Society for Metals be and the same are hereby amended to read as follows:

Section 1 (a). Selection of Committees for Nomination of Officers. A Nominating Committee shall be appointed each year. Each local chapter in good standing which is eligible to have a member on the Nominating Committee shall annually select one candidate for a Nominating Committee from the local chapter membership in such manner as the local chapter shall deem fit, and the name of the candidate shall be forwarded to the President prior to March 1st of each year. From the list of eligible candidates suggested by the various local chapters, the President shall appoint a Nominating Committee of nine (9) members. In appointing the Nominating Committee the President shall select members thereof in such a regional manner as to be equitable for all chapters of the Society. Any chapter having a member on the Nominating Committee in any given year shall not be eligible to have a member on the Nominating Committee during the two succeeding years and no member of the Nominating Committee may serve two or more successive years. The President shall designate one of the members of the Nominating Committee as Chairman of the Committee. Seven (7) members of the Nominating Committee shall constitute a quorum.

A Committee for Nomination of a Secretary for the Society shall be appointed each year in which the term of office of the Secretary expires. It shall consist of seven (7) members. The President shall be a member and shall serve as Chairman of the Committee for Nomination of a Secretary, and shall appoint the six (6) remaining members. The President shall appoint as members of the Committee the six (6) persons who have most recently held the office of President and who are living. In the event that there are fewer than six (6) of the past presidents of the Society who are living and qualified to serve on the Committee for Nomination of a Secretary, any other member or the representative of any member of the Society shall be eligible for membership thereon. Five (5) members of the Committee shall constitute a quorum.

Prior to April 15th of each year, the names of the Nominating Committee and of the Committee for Nomination of a Secretary for the Society, if any, shall be published by the President for the benefit of the members of the Society in one of the publications of the Society. If for any reason there should be a vacancy on either the Nominating Committee or the Committee for Nomination of a Secretary, after appointment and before the conclusion of its duties, the President shall fill such vacancy by appointment of any person who would originally have been eligible to serve in the place created by such vacancy.

(b) Duties of Nominating Committee and Committee for Nomination of a Secretary. On any day during the third full week in the month of May, the Nominating Committee shall meet at a place designated by the Chairman and shall name one candidate for each office which shall become vacant at the close of the next succeeding annual meeting of the members except for the office of Secretary. During the same period in each year in which the term of office of the Secretary expires, the Committee for Nomination of a Secretary for the Society shall meet at a place designated by its Chairman and shall name one

candidate for the office of Secretary. As an aid in making nominations each Committee, and particularly the Chairman of the Committee, may canvass the executive committees of local chapters for written endorsements for consideration by the Committee. Each Committee shall also give consideration to written endorsements forwarded to it for its consideration by individual members or representatives of members of the Society. Endorsements submitted by a local executive committee to the Nominating Committee shall be confined to members of its local chapter or representatives of firms or corporations which are members of its local chapter, but an individual member or representative of a member of the Society may suggest any qualified members or representatives of members of the Society for consideration by the Nominating Committee. Immediately after the candidates are thus nominated, each Committee shall report the names of its nominees to the Secretary of the Society and the report shall be published by the Secretary in one of the publications of the Society not later than June 15th of the same year.

(c) Additional Nominations. After publication of the names of the candidates nominated by the Nominating Committee and by the Committee for Nomination of a Secretary for the Society, if any, and at any time prior to July 15th of the same year, additional nominations for any or all of the vacancies may be made by written communications addressed to the Secretary of the Society and signed by any fifty (50) members and/or representatives of member firms or corporations.

(d) Voting at Annual Meetings. If no such additional nominations are received prior to July 15th, nominations shall be closed and the Secretary, at the next succeeding annual meeting of the members, shall cast the unanimous vote of all members for the election of the candidates so nominated.

(e) Voting at Special Meeting. If the Secretary receives additional nominations for officers of the Society prior to July 15th, the Secretary shall call a special meeting of the members to vote on all candidates nominated by such communications and all candidates nominated by the Nominating Committee and by the Committee for Nomination of a Secretary for the Society, if any. The special meeting shall be held prior to the annual meeting, and forms of proxies for voting at such special meeting shall be mailed by the Secretary to each member or to each representative of a member firm or corporation at least thirty (30) days prior to the date fixed for such special meeting.

(f) Procedure for Voting. All votes for officers shall be counted by the Committee of Tellers. The candidates for the respective offices who receive a plurality of the votes cast shall be the duly elected officers of the Society, and shall be so certified by the Committee of Tellers immediately upon completion of the count, and such certification shall forthwith be filed with the Secretary of the Society.

(g) No nominations for officers shall be permitted except as herein specifically provided.

AND BE IT FURTHER RESOLVED, that a copy of the aforementioned written notice, given by the Secretary to each member and to the representative of each member firm and corporation, be attached by the Secretary to the minutes of this meeting and made a part hereof.

AND BE IT FURTHER RESOLVED, that said amendments shall become effective immediately upon the adoption of this resolution.

Mr. President, as chairman of the Constitution and By-laws committee I move the adoption of these amendments to the Constitution and By-laws of the Society. Motion seconded and carried.

PRESIDENT GROSSMANN: Has anyone present anything to bring before the meeting for the benefit of the Society? If not, a motion to adjourn is in order. Meeting adjourned.

. . . Following the annual meeting, President Grossmann introduced the chairman of the Campbell Memorial Lecture, Dr. Robert Mehl, who introduced Dr. George R. Fitterer, Head, Department of Metallurgical Engineering, University of Pittsburgh, who presented the Nineteenth Campbell Memorial Lecture entitled "Some Fundamental Problems in the Manufacture of Steel by the Acid Open-Hearth Process."

The lecture is printed in full in this volume of *TRANSACTIONS* beginning on page 41.

A.S.M. ANNUAL DINNER

On Thursday evening, October 19, members and guests assembled in the Grand Ballroom of the Hotel Statler for the Annual Dinner of the Society. The attendance taxed the capacity of the facilities of the Statler, there being well over 1200 present.

Those persons seated at the speakers' table were: Waldemar Naujoks, chief engineer, Steel Improvement & Forge Company, and chairman, Cleveland Chapter of the A.S.M.; Dr. G. R. Fitterer, head of the Dept. of Metallurgical Engineering, University of Pittsburgh, and Campbell Lecturer for 1944; Dr. Arthur E. Focke, metallurgist, Diamond Chain & Mfg. Co., Indianapolis, and trustee of the A.S.M.; Dr. Richard A. Flinn, metallurgist, American Brake Shoe Co., Rahway, N. J., and recipient of Henry Marion Howe Medal for 1944; John A. Fellows, assistant chief metallurgist, American Brake Shoe Co., Rahway, N. J., and recipient of Henry Marion Howe Medal for 1944; Earnshaw Cook, chief metallurgist, American Brake Shoe Co., Rahway, N. J., and recipient of Henry Marion Howe Medal for 1944; W. P. Woodside, chairman of the board, Park Chemical Co., Detroit, and past-president and founder member of the A.S.M.; Walter E. Jominy, chief metallurgist, Dodge Chicago Plant, Chrysler Corp., Chicago, and recipient of the Albert Sauveur Achievement

Award for 1944; Herbert J. French, assistant manager, Development & Research Division, International Nickel Co., New York City, and past-president of the A.S.M., and recipient of President's Medal; Dr. W. T. Griffiths, president, British Institute of Metals; Dr. Kent R. Van Horn, research metallurgist, Aluminum Co. of America, Cleveland, Ohio, and vice-president and president-elect of the A.S.M.; Major General G. M. Barnes, chief, research and development service, office of Chief of Ordnance, presenting the Ordnance Distinguished Service Award to the A.S.M.; Dr. Marcus A. Grossmann, director of research, Chicago District, Carnegie-Illinois Steel Corp., and President, A.S.M.; Major George Fielding Eliot, principal speaker at this annual dinner on the subject "Fruits of Victory"; Robert C. Stanley, president, International Nickel Co., New York City, and recipient of A.S.M. Medal for the Advancement of Research; Dr. Zay Jeffries, chairman of the board, Carboloy Co., Detroit, and past-president and honorary member of A.S.M.; Dr. Charles H. Herty, Jr., assistant to the vice-president, Bethlehem Steel Co., Bethlehem, Pa., and trustee and vice-president-elect of A.S.M.; Colonel E. A. Lynn, district chief, Cleveland Ordnance District; Harry D. McKinney, vice-president, Driver-Harris Co., Harrison, N. J., and treasurer of A.S.M.; A. C. Weigel, vice-president, Combustion Engineering Co., Inc., New York City, and president, American Welding Society; Dr. V. N. Krivobok, International Nickel Co., New York City, and trustee of A.S.M.; A. L. Boegehold, head of the metallurgical dept., General Motors Corp., Research Labs. Div., Detroit, and trustee of A.S.M.; L. S. Bergen, president, Bergen Precision Castings, Inc., Pleasantville, New York, and trustee-elect of A.S.M.; Warren A. Silliman, Cleveland Tractor Company, and secretary, Cleveland Chapter of A.S.M.; W. H. Eisenman, secretary, American Society for Metals, and founder member.

Presentation of President's Medal

The annual presentation of the President's Medal to the previous year's president was made by President Grossmann to Herbert J. French, who most ably served the Society as president during the year 1943.

Presentation of Howe Medal

The Board of Trustees in 1922 established the first of its medals in honor of Dr. Henry Marion Howe, the distinguished scientist,

often called the dean of American metallurgists. The rules governing the award of this medal make the provision that it should be awarded to the author or authors of the paper judged of highest merit, presented before the A.S.M. and published during any one year in the TRANSACTIONS of the Society.

The medal for 1944 was awarded to the three authors of the paper entitled "A Quantitative Study of Austenite Transformation" which appeared in Vol. 31 of TRANSACTIONS, 1943, page 41. The authors who were honored are R. A. Flinn, Earnshaw Cook, J. A. Fellows. Each was presented a certificate, a gold medal and a bronze replica.

Albert Sauveur Achievement Award

In honor of Dr. Albert Sauveur, distinguished metallurgist and for many years an honorary member of the American Society for Metals, the Board of Trustees established in 1934 an award consisting of a metal plaque and certificate. The purpose of this award is to recognize a metallurgical achievement which has stood the test of time and stimulated others along similar lines to the extent that a marked basic advance has been made in the metal arts and sciences. The award for 1944 was made to Walter E. Jominy of the Chrysler Corp. as a tribute to his work in developing the well-known end-quench hardenability test which bears his name. A pioneer in the field of hardenability, he devised the test that is now a standard for this all-important criterion of steel performance.

Conferring of the A.S.M. Medal for the Advancement of Research

Dr. Zay Jeffries presented Robert Crooks Stanley as the candidate for the award of A.S.M. Medal for the Advancement of Research. In presenting him, he read the citation that appears on the certificate, as follows:

"Robert Crooks Stanley early recognized the importance of research to the mining and metallurgical industries. Upon becoming president of the International Nickel Company in 1922, one of his first official acts was the creation of a new Development and Research Department, thereby establishing research as a primary activity of the Company. Up until that time nickel still was regarded as a "war metal", useful almost solely for the

production of guns, armor plate and projectiles. Through Mr. Stanley's strong support and consistent maintenance of research, nickel has been developed into an industrial metal with widely diversified engineering applications.

"As an illustration, the early varieties of copper-nickel alloys which were characterized as corrosion resisting metals having the strength of rolled structural steel have been supplemented by new alloys with much higher strengths comparable to hardened alloy steels. Today these alloys form the basis of the products of the rolled nickel industry.

"The development of nickel alloyed cast irons not only created an entirely new group of alloyed metallurgical products, but served as well to enlarge the whole horizon for that basic metallurgical material known as cast iron.

"To these and other examples of broad significance resulting from research supported internationally by Robert Crooks Stanley must be added numerous developments which individually have been of smaller scope. But in total they have provided the information and experience from which nickel has become one of the foremost of the alloys for improving the engineering properties of other metals.

"This work not only has served well the Company which undertook it, but its well recognized results represent a pioneering and practical demonstration to the mining and metallurgical industries of the value and importance of organized corporate research."

Ordnance Distinguished Service Award

Major General G. M. Barnes, chief of the research and development service, Office of Chief of Ordnance, an honored guest at this dinner, presented the Ordnance Distinguished Service Award to the American Society for Metals. Dr. Grossmann, president, accepted the award on behalf of the Society. A photographic reproduction of the scroll is published herewith.

Address of the Evening

Major George Fielding Eliot, noted war commentator, presented the main address of the evening entitled the "Fruits of Victory."

Ordnance Distinguished Service Award



presented to

American Society for Metals

*In recognition of outstanding
and meritorious engineering advisory
services, in war and peace, for the
development, manufacture and
maintenance of Ordnance materiel.*

Award Authorized 20 July 1944

Ed Campbell Jr.

MAJOR GENERAL, U. S. ARMY
CHIEF OF ORDNANCE

T. Hays

MAJOR GENERAL, U. S. ARMY
CHIEF, INDUSTRIAL SERVICE

W. H. ...

MAJOR GENERAL, U. S. ARMY
CHIEF, RESEARCH AND DEVELOPMENT SERVICE

J. K. ...

MAJOR GENERAL, U. S. ARMY
CHIEF, FIELD SERVICE

W. H. ...

MAJOR GENERAL, U. S. ARMY
CHIEF, MILITARY TRAINING SERVICE

ANNUAL ADDRESS OF THE PRESIDENT

MARCUS A. GROSSMANN, *President**Twenty-sixth Annual Convention, Cleveland, October 18, 1944*

THE manifold and widespread activities of the American Society for Metals are of course so extensive that the annual reports can cover only certain of their aspects. Some of these will be discussed by the Secretary and some by the Treasurer. For my own theme, I have selected a question that was raised in a meeting with the Executive Committee of the Chicago Chapter—that question being “What makes the Society click?”

Note the inference in that remark—namely that there is no question that the Society does click. As to the question itself—why is this Society successful?—I think it is worthy of a few moments of our attention.

In the course of visits to the Chapters in the company of the Secretary, opportunities were afforded to meet with many of the Executive Committees of the Chapters, to discuss Society affairs. It was interesting to write down the topics discussed and the questions posed, and subsequently to review them in order to gain some perspective on the viewpoints of the Chapters.

First, it was interesting that, of the total number of questions raised, exactly half of them had to do with local activities of the Chapters, while the other half dealt with affairs of the National Society. This was a significant division, quite in accord with the thought that the local Chapters and the National Society are just about equally important in the success of the Society as a whole.

As to the individual questions, they fell into certain broad categories. The questions brought up most frequently for discussion involved the educational activities of the local Chapters. Indeed some concern was expressed because war conditions have interfered to some extent, due for example to pressure of war work in the case of those who might lead the educational activities, smaller attendance due to gasoline rationing, etc. It was inspiring to find that local educational activities, which present such an important opportunity for service, loom so large in the thinking of the responsible leaders in our Chapters.

Almost equally prominent in the discussions were the national publications of the Society. Many inquiries were made about the prospective date of the next edition of the *METALS HANDBOOK*, thus testifying to the great usefulness of this "Bible" of the metal industry. Great interest attached to the new *METALS REVIEW*, of which more anon. The *TRANSACTIONS* were also discussed in much detail, and *METAL PROGRESS* came in for its share of inquiry.

Another point of interest was the magnitude of the present membership. Many raised a question as to whether the Society wants any more members. Judging by the attendance at the present convention, the need for new members is something less than urgent (to put it mildly). Probably a fair statement is to say that the Society is no longer in need of more members, but would not exclude anyone genuinely interested in metals.

Turning now to another field, there was lively interest in the financial status both of the individual Chapters and of the National Society. There seemed to be full appreciation of the fact that the Society is in sound financial condition and there was healthy discussion of the amount of reserves needed by a Society of this size, engaged in such far-flung activities. There were some indeed who honestly felt that the Society should spend some of its reserves on certain worthy projects. Personally, I belong to the gloomy or worrying group, who anticipate the coming of certain years of sharply curtailed income. When such years come, the Society should be in a position to maintain the services to its members.

In addition to the preceding topics, there were many items of only current or local interest, which nevertheless attested the unflagging interest of the Chapter members. So much for the Chapter activities.

I have already indicated the impression that the success of the Society can be credited about 50 per cent to the Chapters and about 50 per cent to National Headquarters. And when I say National Headquarters I mean Bill Eisenman. It has been said that an institution is the lengthened shadow of a man, and, for the American Society for Metals, Bill Eisenman is that man. Though I have to say it in his blushing presence, I think Bill combines the two needed qualities, (1) of being an educator, and (2) of knowing how to finance the activities of the Society. Therefore, first, I want to pay tribute to the memories of Arthur Henry and Ted Barker, who had

the vision to induce the youthful schoolmaster from Elmhurst, Illinois, to take the helm of the young Society. This youthful schoolmaster has had a sixth sense throughout the years, knowing what activities and what publications would help the members to learn the art and the science of metals. Then, second, I want to pay tribute to his conscientious building-up of the Society's net worth. It is well known that a technical school or university must rely on endowments—the tuition alone, as paid by the students, is inadequate to finance their schooling. Just so, in the A.S.M., the \$10 per year paid by the members is insufficient to support the Society's activities and publications. Bill has known how to augment this income. As to Mr. Eisenman's activities during the year just past, I wish to mention just a few. The new *REVIEW*, with its digest of metallurgical literature strictly up to date each month, is his brain-child. Our distinguished honorary member, Dr. Zay Jeffries, said recently, "Considering the many reviews of metallurgical literature, it did not seem possible to produce a new, unique and valuable service in that field, and yet once again Bill has pulled another rabbit out of the hat." He has indeed. Another important item, having to do this time with the convention, was his realization that this was not an ordinary show but was both a war show and a prospective reconversion show. Instead of being satisfied with half the space, which was all that was available at first, he sensed the coming demand with the result that exhibitors this year are using 38 per cent more space than in the largest exhibit ever before sponsored by the A.S.M.

Then there is the Ordnance Award, a symbol of distinguished service, which is being awarded to the A.S.M. this week by the Army. It is to the credit of our Secretary that he originated practically all of the war services for which this diploma is being awarded to the A.S.M., and it is to the credit of the members that they carried out these suggestions so efficiently as to merit the award.

Finally, it should be mentioned that this year the Secretary had to show his mettle in travel, for only an iron constitution could have withstood the way he was jostled around the A.S.M. circuit, visiting about 28 chapters with me and about 17 with Vice-President Van Horn.

May I then summarize the view that the success of the Society may be credited in large part to the activities of the Chapters, and in equally large part to the ingenuity and resourcefulness of our

Secretary. And in mentioning the Secretary, high praise should go also to his loyal and efficient associates and staff, whose work you see each month in the publications, and each year in other publications and in this convention.

Certain special activities of the Society should also be recorded at this time.

New Chapters

New Chapters were established in Kansas City, North Texas, Fort Wayne, and the Ottawa Valley, bringing the number of Chapters to a total of 63.

1943 Award of Medals and Honors

The President's Medal was awarded to Dr. Bradley Stoughton.

The Henry Marion Howe Medal was awarded to Dr. Shadburn Marshall, for his paper entitled "The Carbon-Oxygen Equilibrium in Liquid Iron."

The Campbell Memorial Lecture was presented by Dr. C. H. Mathewson, on the subject "Structural Premises of Strain-Hardening and Recrystallization."

The Sauveur Achievement Award was presented to Dr. C. H. Herty, Jr., for his contributions to the physical chemistry of steel making.

The Gold Medal of the American Society for Metals was presented to Dr. Zay Jeffries, in recognition of his outstanding metallurgical ability in diversified fields.

The A.S.M. Medal for the Advancement of Research was awarded to Roy Arthur Hunt, President of the Aluminum Company of America, who over a period of years has consistently sponsored metallurgical research and development.

Founder Membership in our Society was conferred on William Hunt Eisenman in recognition of his untiring devotion to the affairs of the Society and in celebration of the completion of his 25th year as Secretary.

1943 National Metal Congress

Also at last year's National Metal Congress, 37 papers were preprinted, presented and discussed, and since then printed in

TRANSACTIONS. Further there were 17 large meetings of the Group or Panel type, a feature inaugurated by our Secretary five years ago and since then become popular in our own Society and emulated by others.

Pension Plan

Because the employes at headquarters are ineligible for social security under the present law, and because in the earlier struggling years of the Society it was impossible to make any provisions whatever, a committee under the chairmanship of Past President James P. Gill evolved a plan which has been approved by the Board of Trustees and which is in conformity with the plans of institutions similar to ours.

Standing Committees

The several standing committees, by their unselfish labors, contributed in very large measure to the successful functioning of the Society. For their continued efforts, we are all obligated to the individual members of the Publications Committee, the Finance Committee, the Metals Handbook Committee, the Educational Committee, the Metal Progress Advisory Committee, the Constitution and By-Laws Committee, and the Advisory Committee on Metallurgical Education.

Board of Trustees

The Board of Trustees held the customary four meetings in the course of the year. The Board has the responsibility of making certain major decisions for the Society, on behalf of the membership whose interests they promote, and I wish to pay tribute to the sober earnestness displayed by them in arriving at considered opinions for the welfare of the Society. Also, at the August meeting, the Board accepted the resignation of Dr. C. H. Herty, Jr., as trustee, in view of his nomination for the vice-presidency, and elected for the unexpired term of one year as trustee Dr. A. E. Focke, Diamond Chain Company, Indianapolis.

Convention Week, 1944

And so we arrive at the present time and this week's meeting. We are met here with four other societies, the American Welding Society,

the American Institute of Mining and Metallurgical Engineers, the American Industrial Radium and X-Ray Society, and the Society for Experimental Stress Analysis. To all of these great societies—Greetings! I hope each and every person who has come here, to attend this convention, will feel upon his departure that he (or she) has profited greatly.

And now, finally, a serious word in this war year. The American Society for Metals has sought to fulfill its deep obligations. Some of our members have suffered tragic and irretrievable losses. We can do no less than join, whole-souledly, in the task of inexorably crushing our enemies. Insofar as metals are concerned in this task, that is our mandate, and to it we dedicate ourselves.

TREASURER'S REPORT

HARRY D. MCKINNEY, *Treasurer*

The fiscal year ending on August 31, 1944, has been a very successful year for your Society, and it is a satisfaction to your Treasurer to submit this report.

The cash balance on August 31, 1944, was \$204,886.44 compared to \$99,873.40 for last year, exceptionally heavy advance receipts from the show accounting for a large portion of this increase.

Total assets increased from \$746,343.31 to \$1,002,394.65 or an increase of 34 per cent, but included in these assets are many receipts on behalf of the present convention, and considerable expense is to be deducted. It is anticipated that this adjustment will reduce the per cent increase of assets of this year over last year to about 29 per cent net.

Accounts Receivable decreased in total from \$24,335.37 to \$20,890.92 which reflects a very healthy condition of receivables with an average collection period of less than thirty days.

General Inventory has increased over \$5,000.00, due to a reprinting of a number of books during the year. Also, we have valuable stocks of paper, cover stock, and envelopes which are used from month to month in the handling of the publication of METAL PROGRESS, TRANSACTIONS, the METALS REVIEW, etc.

Office furniture and equipment has remained about the same, a few replacements being made but depreciation showing a slight decrease in net asset valuation.

The investment in A.S.M. headquarters has been increased by the recent purchase for \$18,500.00 of the property adjoining our original purchase and small improvements during the year. Depreciation of approximately \$1,800.00 was written off on buildings in accordance with the amortization program authorized by the Board of Trustees.

Security holdings of the Society increased the past year from \$489,440.68 to \$622,911.43 or 27.3 per cent. Surplus funds permitted the purchase of additional securities and strengthening of the security account.

The Finance Committee, Board of Trustees, and your officers are in constant touch with the A.S.M. fiscal agents, the Cleveland Trust Company, and a close contact with the investment market is maintained. Frequent meetings between Mr. W. W. Horner, Vice-President in charge of investments of the Cleveland Trust Co., Dr. Zay Jeffries, Dr. Kent R. Van Horn, and your Secretary, Mr. W. H. Eisenman, are held to consider investment problems.

Observations and studies have been made concerning the proportion of bonds and stocks in our portfolio, and we are pleased to advise that the proportion of bonds to stocks is on a ratio of approximately 55-45, and this proportion is very much in line with the percentages held by the largest trust-fund operations of this country.

Additional purchases of securities during the present year have added approximately \$60,000.00 to government holdings, \$35,000.00 to bond holdings, and \$48,000.00 to common stocks which will maintain a diversification program and hedge against inflation.

The investment portfolio now shows:

		Per Cent
Real Estate (Headquarters)	\$ 65,435.00	9.5
U. S. Govt. Bonds	243,500.00	35.5
Canadian Govt. and Canadian Utility Bonds.....	31,000.00	4.5
Public Utility Bonds	19,050.00	3.0
Railroad Bonds	27,000.00	4.0
Industrial and Miscellaneous Bonds	14,375.00	2.0
Common and Preferred Stocks	285,220.00	41.5
	<u>\$685,580.00</u>	<u>100.0</u>

As of August 31, 1944, the total cost of securities (not including Headquarters) was \$622,911.43, and the market value was approximately \$645,000.00.

Market value of securities	\$645,000.00
and Headquarters	65,435.00
Plus cash on hand	204,886.00
	<u>\$915,321.00</u>

The assets of the Society as shown above, plus cash on hand namely \$915,321.00, is a little more than double the total operating cost of the Society and the Chicago Exposition for 1943 which was \$448,275.26.

The interest at an average rate of 3 per cent that could be realized from this sum of \$915,321.00 (\$27,470.00) is, however, only 6 per cent of the total operating expense. To insure the continued high level of Society service to the membership, the metal industry, and the government, your officers, trustees and finance committee believe it is advisable to endeavor to maintain and improve these figures.

The statement of income and expense for the year ending August 31, 1944, by totals is as follows:

Income	\$618,996.23
Expense	448,720.35
	<hr/>
Net Income	\$170,275.88

This exceeds by \$27,815.02 last year's record of \$142,460.86. The increase is due to increases in volume of METAL PROGRESS advertising, membership dues, book sales, and Metals Handbook sales. Other activities maintained themselves satisfactorily.

TRANSACTIONS, as you know, has been discontinued as a quarterly publication, and will be published once a year in two bound volumes. The net cost to the Society for the past year was approximately \$24,000.00.

METAL PROGRESS continues to be a very successful activity, and its contribution to the income of the Society was of the order of \$100,000.00. Its qualities as a technical advertising medium of high standing and unquestioned acceptance are recognized generally.

The REVIEW has now been changed to the METALS REVIEW with a new editorial policy and with greatly increased quality and quantity of content. Advertising in this publication is being accepted. Last year's net cost to the Society for this publication was \$18,500.00, which includes considerable of the expense of setting up the new format and program.

Miscellaneous items such as reprints, books purchased for resale, pins and buttons, automobile emblems, etc., balance out on approximately equal cost and income.

Books published again maintained a high volume of sales and added an excess of \$20,367.00 to the total. This figure is approx-

imately \$3,000.00 less than 1943, and is due to the fact that several books were discontinued and the high demand of the past couple of years has slackened slightly.

Metals Handbook sales amounted to \$15,776.00 but as inventory cost and preparation costs for a new handbook amounted to only \$9,002.00, an excess of \$6,774.00 was added by this publication.

The 1943 Chicago National Metal Congress and Exposition was again an outstanding event in the metal industry, and its value in aiding the government in our war efforts and industry in its many metallurgical problems can hardly be measured. Financially the exposition was successful.

The membership, which is the foundation of the Society and the base for all our activities, again reached a new high point for this last fiscal year.

	Gross Total
1944	\$193,826.26
1943	179,497.83
1942	150,107.00
1941	131,471.00
1940	115,502.00
1939	108,000.00
1938	103,600.00
1937	105,600.00

Of the \$193,826.26 received from membership dues, \$78,160.00 was returned to the chapters, and approximately \$115,666.00 was retained by the National Headquarters for operations. This amount of approximately \$115,600.00 is less than 19 per cent of the total income of the Society, and is about 26 per cent of the expenses of operation of the National Organization.

The chapters now report that they have assets, in addition to those of the National Office, of approximately \$133,806.00, and this shows an addition of \$16,885.00 to the net worth reported a year ago. This reserve should substantially insure the continued activity and progress of the chapters.

Your Treasurer gratefully acknowledges the active and cooperative assistance of the Finance Committee, the Board of Trustees, our President, Dr. Grossmann, Secretary Eisenman, and Assistant Treasurer Mr. C. W. Ohlson.

CONDENSED AUDITED BALANCE SHEET

As of August 31, 1944

ASSETS	
Cash	\$ 204,886.44
Securities	622,911.43
Accounts Receivable	20,890.92
Inventories	45,573.22
Other Assets	4,423.19
Real Estate	65,435.26
Office Furniture, Fixtures and Equipment	13,470.75
Deferred Charges	24,803.44
	<hr/>
	\$1,002,394.65
LIABILITIES AND SURPLUS	
Accounts Payable	\$ 32,800.33
Reserves	135,000.00
Deferred Income	91,949.50
Surplus	742,644.82
	<hr/>
	\$1,002,394.65

INCOME AND EXPENSE STATEMENT

Year Ended August 31, 1944

INCOME	
METAL PROGRESS	\$307,520.59
Memberships	116,715.90
1943 Convention—Chicago	80,306.17
Metals Handbook	15,776.65
TRANSACTIONS	8,963.17
METALS REVIEW	5,813.67
	<hr/>
	\$535,096.15
Books published	54,195.61
Interest and dividends	20,117.10
General reprints	4,197.63
Discount earned	3,703.62
Books purchased for resale	237.34
Sundry	1,448.78
	<hr/>
TOTAL INCOME	\$618,996.23
EXPENSES	
METAL PROGRESS	\$206,461.28
1943 Convention—Chicago	62,499.39
Books published	33,828.25
TRANSACTIONS	32,330.33
Metals Handbook	9,002.24
Secretary's office	20,244.15
Membership	12,314.51
General expense	12,516.76
Accounting department	10,633.65
METALS REVIEW	24,314.73
Headquarters	6,849.50
Trustees' expense	3,515.27
President's office	3,430.39
National committees	2,014.85
	<hr/>
	\$439,955.30
General reprints	3,508.89
National defense research—War Products Advisory Committee	596.00
Loss on disposal of securities	301.25
Lectures	500.00
Books purchased for resale	201.51
Emblems purchased for resale	615.77
Medal fund expense	268.56
Books for library	237.49
Medals and awards	1,949.98
General Index	30.00
Research and educational contributions	555.60
	<hr/>
TOTAL EXPENSES	448,720.35
	<hr/>
NET INCOME	\$170,275.88

In our opinion, the accompanying balance sheet and related statements of income and expense and surplus present fairly the position of the American Society for Metals at August 31, 1944, and the results of its operations for the year, in conformity with generally accepted accounting principles applied on a basis consistent with that of the preceding year.

ERNST & ERNST
Certified Public Accountants

ANNUAL REPORT OF THE SECRETARY

WILLIAM H. EISENMAN, *Secretary*

The American Society for Metals on October 1, 1944, had a membership of 18,468. Of this number 16,881 or 91.4 per cent were the member classification; 1,175 or 6.4 per cent were sustaining members; while 388 or 2.1 per cent were juniors. There are 24 honorary and founder members.

On October 1, 1943, the Society had a total membership of 17,095. The membership this year showed a gain of 8 per cent.

TRANSACTIONS

Since the last annual meeting of the Society, the December 1943 (quarterly issue) and Vols. 32 and 33 of the TRANSACTIONS were published and distributed to the membership on request. These total 1358 pages and constitute 50 articles with their discussions.

The December 1943 issue contained the last of the papers presented at the 1942 Convention.

Vols. 32 and 33 contain all of the papers presented at the 1943 Convention held in Chicago with their discussions together with other interim papers received during the year. Vol. 32 also contained a report of the Convention. The president, secretary and treasurer's annual report for 1943 and other current items of record were also included in that volume.

METAL PROGRESS

History of METAL PROGRESS during the fiscal year of 1944 was marked chiefly by the rise in advertising volume and net income to unprecedented figures. This is shown by the Treasurer's report and the publishing statistics for six years:

Fiscal Year	Editorial Pages	Revenue Advertising	Circulation*
1939	612	816	10,303
1940	662	915	11,640
1941	645	1078	13,018
1942	699	1276	15,412
1943	688	1595	16,363
1944	648	1937	18,774

*Audit Bureau of Circulation figure for June.

Circulation has steadily mounted during this 1944 period, resulting in the largest number of the largest magazine ever circulated to our members. At the same time it has been necessary for the Society as a whole to reduce substantially the tonnage of paper it consumes, as a war measure, and this has imposed a change in publishing plans for *TRANSACTIONS*, as described elsewhere.

It will be observed that the number of editorial pages remains fairly steady, year after year. A recent analysis as to source indicated the following:

Staff production	16%
Purchased material	12%
Contributed manuscripts	63%
Society news	4%
Abstracts	5%

Most of the contributed manuscripts come from speakers before the various A.S.M. chapters or the Group Meetings at the annual convention, and therefore furnish an excellent record of contemporary advances in the field. The various departments (like "Bits and Pieces") continue to grow in popularity. The data sheets retain their unique position in technical publishing—in fact, a loose-leaf assembly of 79 of them has achieved wide sale by our book department. Among notable contributions to the reading pages during the year may be mentioned the series of articles on cartridge brass by L. E. Gibbs, the series on the theory and practice of gas carburizing by F. E. Harris, the continuous cooling transformation diagrams of important engineering alloy steels by C. A. Liedholm, and the widely quoted staff articles on weldability and on jet propulsion.

Finally I repeat what I said in my 1940 report, for it is equally applicable today:

"In conveying the thanks of the Society to the hundreds of members who have cooperated with us, both in securing editorial matter and advertising patronage, I wish to remind other members that *METAL PROGRESS* is their joint property, that it is unapproached in quality, that it has the cream of metallurgical circulation. It should therefore be their *first* thought when they learn of some desirable and practical article that is ready for publication."

METALS HANDBOOK

The personnel of METALS HANDBOOK Committee during the past year was as follows:

George V. Luerksen, Chairman
Gordon T. Williams
A. J. Herzig
A. L. Kaye
C. H. Lorig
J. T. MacKenzie
Lyall Zickrick

J. B. Johnson
Jerome J. Kanter
Harry W. McQuaid
Harold L. Maxwell
C. W. Obert
J. Edward Donnellan, Secretary.

The committee held one meeting during the year. This was the first meeting the committee has had since before the war.

The meeting was held on January 14 in the National offices of the Society in Cleveland. It is interesting to note that all of the members were present, which shows the interest these men have in the HANDBOOK work in times like these, when they are all so hard pressed with their own production problems.

METALS HANDBOOK Committee has given considerable thought to the size of METALS HANDBOOK. Several plans have been considered in order to keep the HANDBOOK data contained in one volume. A definite decision has not been made, but the committee will continue to work on the problem.

The former subcommittees, that prepared reports for the HANDBOOK, have been re-appointed and their programs are fairly well organized. Many new subcommittees have also been appointed, and much progress has been made in organizing their work for the preparation of reports.

It has been found, however, that it is difficult to make as much progress with HANDBOOK committee work as was hoped for when the work was organized and planned last January. However, as it is not planned to publish a new edition until after the war, it is the aim of the committee to accomplish as much work as possible so that all the detail work will not be accumulated for completion just before the next HANDBOOK publication date. As the HANDBOOK has grown to such a large size, it is necessary to get as much accomplished well in advance of the intended publication date as is possible.

The Nonferrous Data Sheet Committee of the A.I.M.E. is again very active and has had a number of meetings and conferences for the preparation of the nonferrous section of the Handbook. In this section it is planned to re-organize and consolidate several of the sections. For example, all the Constitutional Diagram articles are to be prepared according to a definite outline so that condensation can be maintained. These articles are also to be arranged alphabetically in the last section of the HANDBOOK.

Mr. Obert has very kindly agreed to continue as Chairman of the

committee on Welding, organized by the International Acetylene Association. This committee has been organized, and Mr. Obert has his plans under way for another good section in the HANDBOOK on Cutting and Welding.

Since the 1939 edition of the HANDBOOK was published, the Society was obliged to produce a second printing of the HANDBOOK. The second printing consisted of 15,000 copies. In stock, we now have only 1850 copies. This reveals how popular the HANDBOOK has become and shows the important place it has taken as a reference book in the metallurgical field.

METALS REVIEW

Early in 1944 the METALS REVIEW inaugurated an entirely new publication policy. Starting with the February issue the "A.S.M. Review of Current Metal Literature" was installed as a permanent monthly feature, and a new and valuable service to members of the American Society for Metals.

Designed to provide a complete, up-to-the-minute survey of the engineering, scientific and industrial journals of the world, the A.S.M. Review of Current Metal Literature consists of a classified list of articles that have appeared during the preceding month with brief annotations indicating their content or scope. It is prepared in the library of Battelle Memorial Institute, Columbus, Ohio. Filling the need for a complete, thorough and up-to-date classified review of each month's periodicals and books, it met with instant and enthusiastic approval on the part of A.S.M. members.

Two other new departments made their first appearance in the March 1944 issue. These are "New Products in Review" and "Manufacturers' Catalogs in Review". At the same time a new format and improved method of printing were adopted, *and advertising is now being accepted*. The name of the publication was changed in July from the REVIEW to the METALS REVIEW, thus giving a better indication of the scope of the publication. The METALS REVIEW, however, continues to carry reports of A.S.M. chapter meetings and activities. It thus constitutes a complete survey and digest of what's new in technical and business magazines, books, equipment, parts, materials, manufacturers' catalogs, and technical meetings.

The over-all size of the paper remains approximately the same, but with the inclusion of the new departments it has been increased from 8 pages to an average of 20 pages per issue. The September

1944 issue contained 40 pages devoted largely to the National Metal Congress and Exposition, and had a circulation of 47,000 copies among the members of the cooperating societies in the Congress and other technical organizations. It is now published twelve times a year with issues in July and September, months that were formerly omitted. Since the installation of the new departments in February the available space has been allotted approximately as follows:

	Per Cent
A.S.M. Review of Current Metal Literature	38
New Products and Manufacturers' Catalogs	19
Reports of Chapter and National A.S.M.	
Activities and Other Editorial Matter	22
Advertising	21

Books

During the past year there have been no new book titles published by this Society. There have been many of our previous titles reprinted in order to take care of the demand for these technical books during the war period.

During the year and since the last convention, more than 45,000 books of all titles published by the ASM were sold to the membership and others, including copies of the METALS HANDBOOK that were sold to non-members.

Publications Committee

The Publications Committee for the year 1943-44 was made up of the following personnel: E. G. Mahin, Chairman; J. B. Austin, R. M. Brick, Walter Crafts, R. E. Cramer, A. E. Focke, W. R. Frazer, W. E. Jominy, R. W. Roush, A. O. Schaefer, Gilbert Soler, Clair Upthegrove, T. S. Washburn, S. P. Watkins, B. B. Wescott, and Ray T. Bayless, Secretary.

During the year and up to the present time the Committee has reviewed and approved 42 papers and rejected 6.

The Publications Committee held one formal meeting in July 1944 at which time the final arrangements for the technical program at this Convention were made. Forty-two papers were approved and scheduled for presentation.

Preprints

The 42 papers that are presented on the technical program of the ASM during this 26th annual convention were all preprinted and distributed to those members of the Society who had requested them.

The total number of pages for the 1944 preprints is 1024. A total of 42,000 preprint copies have been distributed free to the membership to date.

Educational Committee

The Educational Committee for the year 1944 was made up of the following personnel: C. W. Mason, Chairman; J. L. Bray, O. W. Ellis, J. G. Jackson, J. O. Lord, W. D. McMillan, J. T. Norton, C. H. Shapiro, and Ray T. Bayless, Secretary.

The Committee held one meeting during the year, at the Hotel Pennsylvania in New York City on May 5th. The purpose of this meeting was to plan for the revision of certain educational courses that had been published by the Society and the planning of other educational courses for future distribution to the chapters. The Committee also discussed at length the subjects for educational courses to be presented at the annual convention in 1945, 1946 and 1947, and has made selections and laid plans for these several conventions to come.

Inasmuch as the educational film entitled "Metal Crystals" has been so favorably received by the chapters and other educational institutions, the Committee wishes to proceed with further work along these lines in the formulation and filming of other subjects in the metallurgical field. Up to the present date the "Metal Crystals" film has been booked for 106 showings throughout the Country and Canada.

During the year the Committee has made available to the membership a large sized iron-carbon equilibrium diagram of a size suitable for a wall-chart in class-room work. More than 50 charts have been distributed up to the present time. Other enlarged wall charts are under consideration and will be publicized when they are ready for distribution.

The Committee is also studying three dimensional visual educational methods and no doubt will have some very interesting items to offer in a short time.

Advisory Committee on Metallurgical Education

This committee is under the chairmanship of Dr. Robert Mehl, Director of Metals Research Laboratory, Carnegie Institute of Technology.

This committee is formulating plans for metallurgical education in the post-war period, and expects to be able to have a report and recommendations available for presentation before very long.

National Metal Exposition and Congress

It is not necessary that I should speak to this assembly about the size or the success of the present event. However, for the purpose of the permanent record it should be noted that this is the largest exposition ever to be held under the auspices of the Society during the twenty-six years in which it has conducted these events.

It is the largest industrial exposition devoted to the metal industry that has ever been held in America.

A total of 412 manufacturers have placed on display the new developments, processes and materials that have been developed by them during the period of defense preparation and war production.

These manufacturers realize that the National Metal Exposition offers them an exceptional opportunity to contact industry previous to its transfer from a war economy to a civilian economy.

166,000 square feet of space have been required to adequately present the products of these manufacturers. The attendance is outstanding, and from the information gathered from those present there will be made a definite contribution to a speedy completion of the reconversion-period problems.

Five national technical societies have again cooperated in this Metal Congress. Each has prepared and is presenting a program of exceptional merit and the space-taxing attendance bears clear witness to the efficacy of their planning.

The group meetings of the ASM have, since their establishment a few years ago, achieved outstanding recognition. Their organization, style of presentation and contribution of up-to-the-minute information and developments have made the attendance at these meetings the seventh-day wonder of a five-day meeting.

The Metal Congress is a unique institution. It is unparalleled in any country of the world. It has a niche in the Hall of Fame because it combines in one great event and at one time the universities and work laboratories of the metal industry.

Just so long as the event continues to meet with the approval of its 45,000 members, as evidenced by their attendance at the Congress, just so long will it continue to be a success.

SOME FUNDAMENTAL PROBLEMS IN THE MANUFACTURE OF STEEL BY THE ACID OPEN-HEARTH PROCESS

By G. R. FITTERER

EVERY year at this time the American Society for Metals dedicates this period of the National Metal Congress to the memory of Edward DeMille Campbell. For the past eighteen years the lecturers have aptly chosen a variety of interesting subjects dealing with basic problems of current interest. For the most part these lectures have dealt with the factors controlling the hardening of steels—a subject which was close to the heart of Professor Campbell. A few of the lecturers dealt with steel making principles so as to develop a better understanding of the problems involved in meeting the specifications while at the same time maintaining or improving the quality of the steel.

Some of the fundamental problems involved in the manufacture of steel by the acid open-hearth process will be presented in this, the nineteenth Campbell Memorial Lecture. In spite of the broad scope of the metallurgical experience represented by the audience, it is hoped that this statement of a fundamental steel manufacturing problem will be found interesting to all. The method of attack is presumably new and may find numerous applications in other steel refining processes. Perhaps, if nothing more, this paper may serve as a guide to future research in the realm of liquid steel.

The subject selected and its ramifications would have intrigued Professor Campbell because of his interest in both chemistry and metallurgy. Problems involving the chemistry of the acid, or Siemens', process have not been solved. Although it was the original open-hearth and has been studied by metallurgists and chemists, since the first heat which was made in 1858, many fundamental questions remain to be answered.

Today, the acid furnace is annually responsible for from two to three million tons of large forgings and castings which are required

This is the nineteenth Edward DeMille Campbell Memorial Lecture presented by Dr. G. R. Fitterer, head of the Metallurgical Engineering Department, University of Pittsburgh and Director of Research for the Acid Open-Hearth Research Association, Inc., of Pittsburgh, Pa. The lecture was presented October 18, 1944, during the Twenty-Sixth Annual Convention of the Society, held in Cleveland.

by Government and industry. Most of the steels so produced are medium-carbon and low-alloy types, whereas many semi-steels or high-carbon irons are also made. Large calibre guns, marine crankshafts and connecting rods, shafts for steam turbines, locomotive parts, roll housings and rolls are examples of its products.

Great strides have been made in this country in the past several years to reduce the refining time in the acid hearth to an exceptionally low figure. Many heats are produced with no more than a 2-hour period from the time the heat is completely melted until it is tapped. No losses of nickel or molybdenum are encountered. These alloying elements are retained from remelted scrap and may be charged or added at any time during the heat. Chromium losses are nominal and considerable amounts of chromium may be retained from the remelted scrap. These factors should be placed on the credit side of the ledger for the acid open-hearth and are some of the reasons for its continued use.

On the debit side are usually placed the facts that, first, a low phosphorus and sulphur charge must be used; and, second, it is generally considered undesirable to use light scrap because of the high formation of iron oxide and the subsequent erosion of the acid or silica lining.

The short refining period mentioned above is partially accomplished by using a low percentage of pig iron in the charge and the low sulphur and phosphorus requirements of the pig iron are minimized somewhat in this manner. The scrap, however, must still be low in these elements.

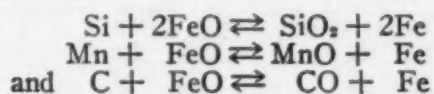
The use of light scrap in the acid open-hearth is quite common today, although heavy and medium scrap are to be preferred. No comparisons with other processes will be made herein. Instead, the process itself will be discussed in detail and some of the changes which have taken place in the practice will be reviewed. In addition, a new method for control of this process will be developed and recommended herein. The economics of the acid hearth have also changed in recent years, so that a reconsideration of its use may eventually be in order.

REVIEW OF ACID OPEN-HEARTH PRACTICE; HEAT LOGS

The refining of steel in the acid open-hearth furnace today consists chiefly of melting down a predetermined charge of pig iron and

scrap depending on various furnace characteristics. Sometimes spiegel and other deoxidizing materials are also charged in order to prevent an over-oxidized condition at "melt-down".

The principal reactions which occur during the refining period are the oxidation of silicon, manganese and carbon, respectively, according to the reactions:



The SiO_2 and MnO rise to the slag-metal interface where they become constituent parts of the slag. The slag already contains considerable amounts of these materials which were formed during the melt-down period. The carbon monoxide bubbles through the slag and into the gas.

Iron oxide (i.e., FeO) is soluble in both the slag and metal phases and is formed in large quantities during the "melt-down" period by the oxidizing action of the flame on the unmelted scrap.

Hence, whereas the metal bath contains variable quantities of carbon, manganese and silicon, as well as iron oxide, the slag contains chiefly SiO_2 , MnO and FeO .

Few refining additions are necessary in modern practice and when added, only small quantities are needed. Ore and limestone are the principal oxidizing agents for this purpose.

American Practice. Perhaps the best review of modern acid open-hearth practice can be obtained briefly from a study of typical heat logs such as is illustrated¹ in Fig. 1.

The manganese and silicon were reduced simultaneously to a low figure in the early stages of this heat. Essentially no carbon elimination took place until these two constituents were first reduced to a minimum. This is a desirable feature and common in American practice. Besides additions of ore and limestone, it is sometimes, although rarely, necessary to add sand, the main constituent of the slag. This is in contrast to the basic open-hearth where lime is the main constituent of the slag and it is necessary to add large quantities of this material in order to chemically balance the slag.

When limestone was added to this heat, the silicon and manganese were already eliminated and the carbon content began to drop immediately. The effect of limestone is evident in the figure because the iron oxide in the slag was "freed" by this addition so as

¹All discussion of American heats are presented by permission and courtesy of the Acid Open-Hearth Research Association, Inc., Pittsburgh, Pa.

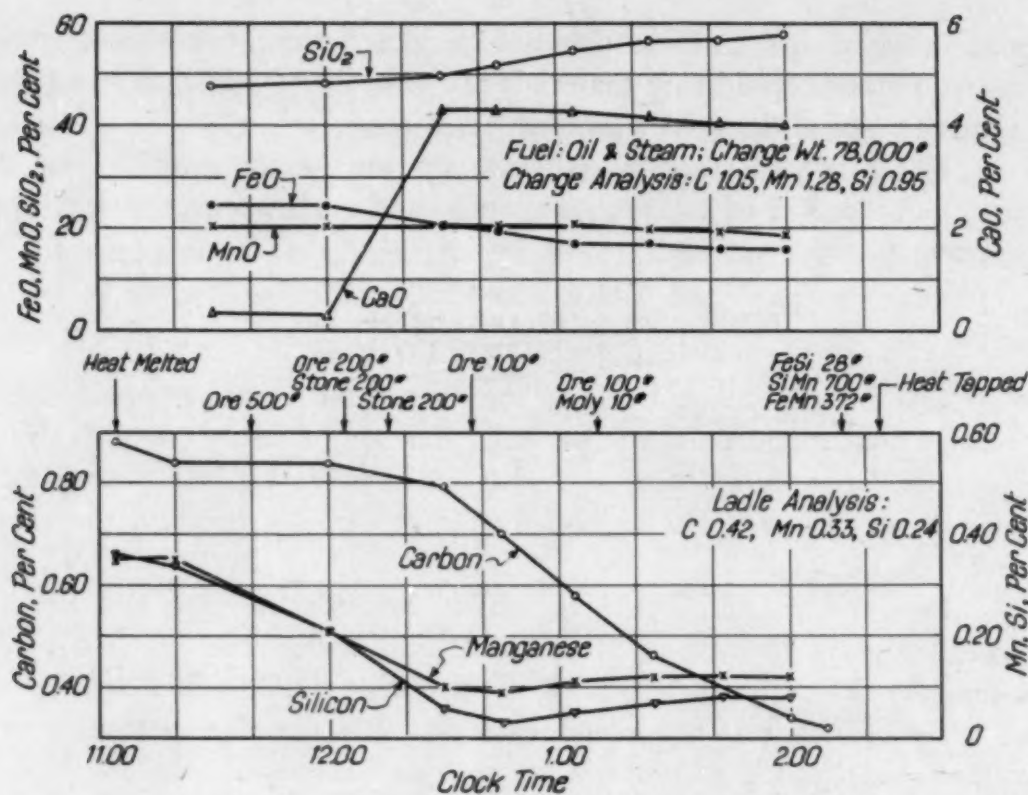


Fig. 1—Acid Open-Hearth Heat (American Practice).

to react with carbon in the bath. However, many heats are melted and refined without additions of either limestone or iron ore. This is a matter of judgment on the part of the melter after studying the action of the bath and its carbon content immediately after "melt-down".

It should be noted for the purpose of later technical discussion that the MnO content of the slag remained constant in this heat throughout the refining period. Also, as the heat progressed, the SiO₂ content increased appreciably with a corresponding decrease in FeO. The entire refining period (from "melt-down" to "tap") for this 40-ton heat involved only 3 hours.

If the charge contains somewhat less silicon and manganese than was the case in this heat, a shorter refining period results. Such a heat is illustrated in Fig. 2. Here the manganese and silicon at "melt-down" were low and, in addition, a simultaneous high rate of carbon elimination indicated a higher degree of oxidation than in the case of the first heat.

Here again, the MnO content of the slag was constant throughout the heat and the SiO₂ content increased regularly with a propor-

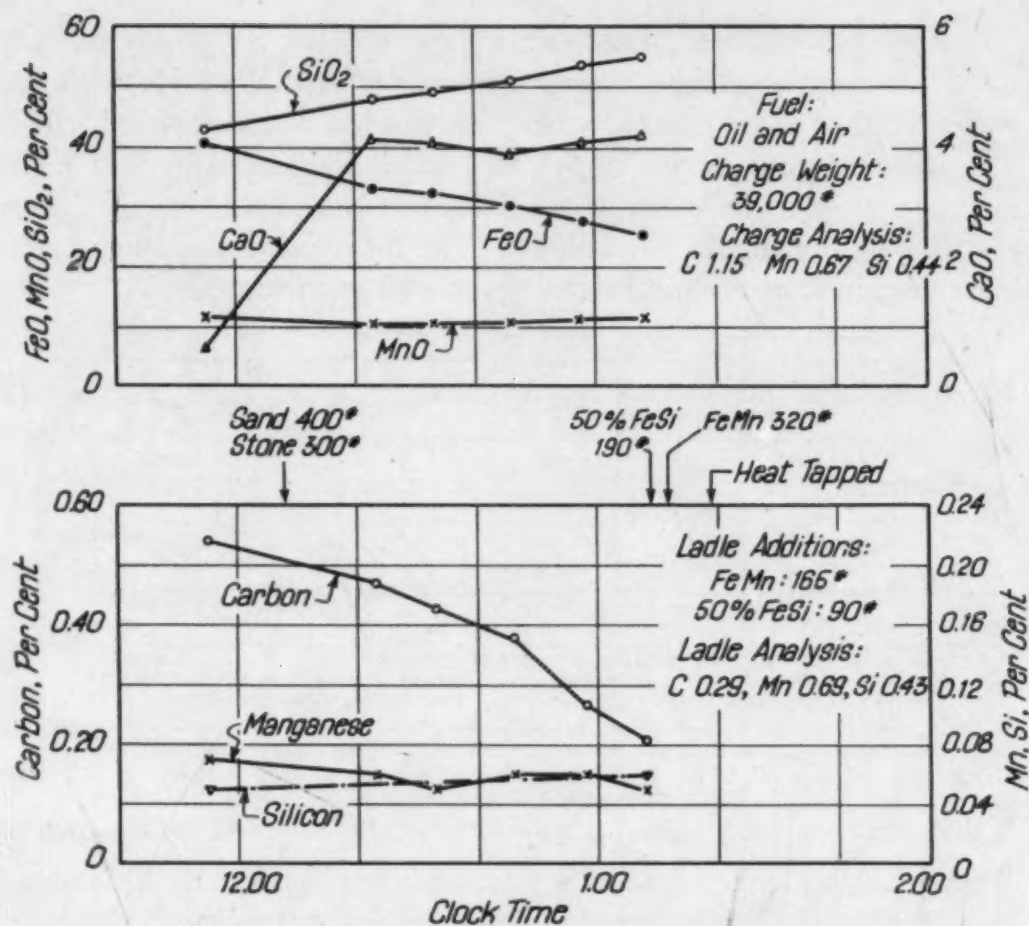


Fig. 2—Acid Open-Hearth Heat (American Practice).

tionate decrease in FeO. This heat was worked in the short period of 85 minutes and was consistent with modern American practice.

English Practice. In contrast to American practice a recent English heat may be cited.² This heat is shown in Fig. 3 and required a refining time of 6 hours and 43 minutes from melt-down to tap, in spite of the numerous ore and limestone additions. The percentage of MnO in the slag remained essentially constant throughout this heat, and in spite of the numerous additions of iron ore, the FeO content of the slag decreased steadily.

No more was accomplished in this heat than in the usual 1 to 3-hour refining period common to American practice. The carbon content at "melt-down" was higher than for a comparable American heat and this accounts in part for the longer refining period. However, the slow rate of operation may also be due to the furnace construction and/or the fuel.

²Iron and Steel Institute (London). Eighth Report on the Heterogeneity of Steel Ingots, Special Report No. 25, p. 11, 1939.

German Practice. Probably an extreme in European practice today but a typical acid open-hearth heat of from 10 to 15 years ago was published in Germany by Bardenheuer and Thanheiser.³ This heat had a refining period of 5 hours and is illustrated in Fig. 4. It may be seen that the trends throughout this heat were entirely different than in any of the other three. The manganese and silicon contents remained at an appreciable level, and even increased, through-

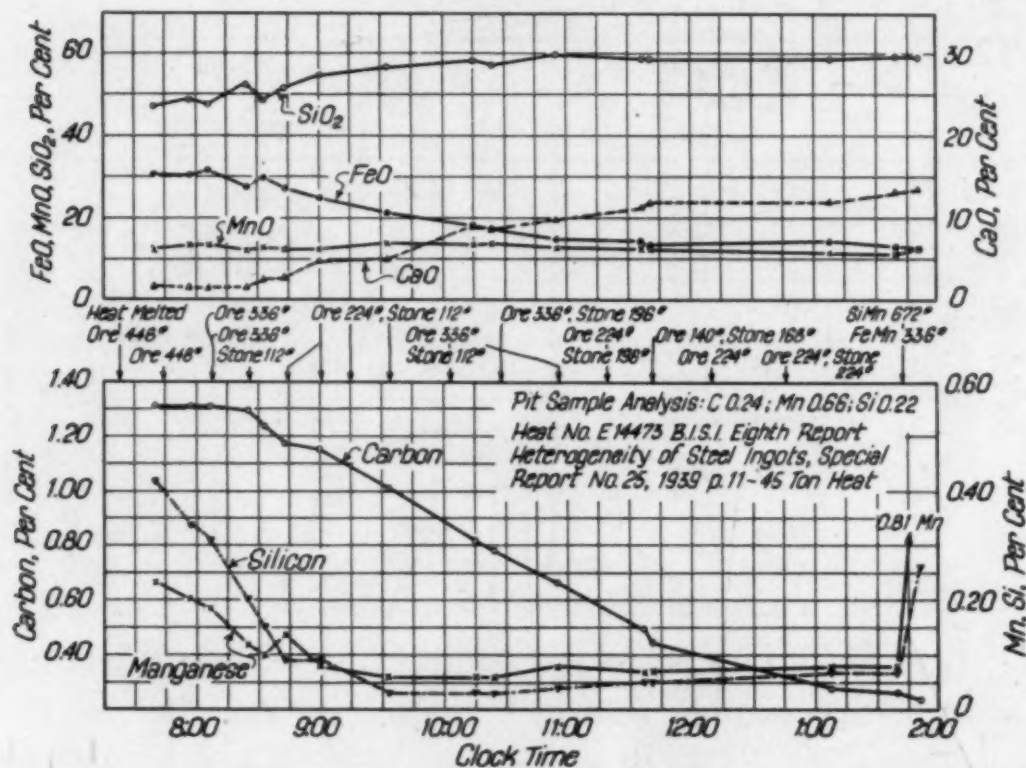


Fig. 3—English Acid Open-Hearth Heat.

out the heat, whereas the carbon dropped regularly. This is the reverse of American practice wherein manganese and silicon were essentially eliminated prior to any decrease in carbon and no appreciable pick-up in these elements was evident as the heat progressed. It is evident from the German heat that carbon may be eliminated in the presence of from 0.30 to 0.35 per cent each of manganese and silicon.

Bardenheuer and Thanheiser stated that this heat was of somewhat greater duration than the usual German practice because of the experimental samples taken during its operation. However, the true

³P. Bardenheuer and G. Thanheiser. Mitt. Kaiser-Wilhelm-Institut für Eisenf., Düsseldorf, Vol. 16, No. 17, 1934, p. 189-200.

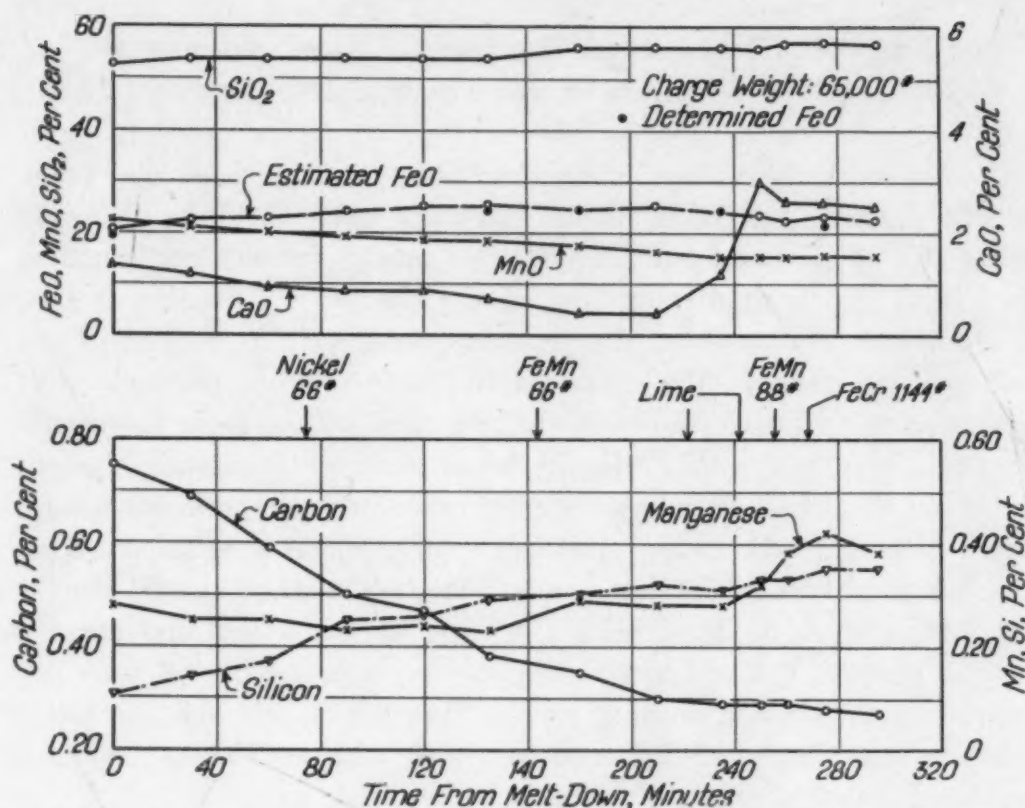


Fig. 4—German Acid Open-Hearth Heat According to Bardenheuer and Thanheiser.

explanation lies more in the method of charging and in the refining procedure than in the delays incurred by sampling. This heat was charged with greater percentages of manganese and silicon than is usual in American practice and, in addition, the heat "melted-in" at a much higher temperature. This is indicated by the high SiO₂ content of the slag at melt-down (52.6 per cent).

With a high "melt-down" temperature and a high metalloid content of the charge, the refining will be sluggish and considerable amounts of oxidizing materials such as ore and limestone are necessary in order to reduce the refining time. Late additions of limestone were made to reduce the carbon content in this heat but these had little effect. Such additions are much more effective at the early stages of the heat, when the temperature of the bath is low. It is possible that an ore addition followed by the limestone would have been more effective because this combination is extremely oxidizing.

It is also interesting to note that with the exception of the SiO₂ content, the trends in the slag composition were the converse of those observed in the heats described previously. The silica content increased gradually as the heat progressed, but the FeO also increased with a corresponding decrease in MnO content.

FURNACE CHARACTERISTICS, THE CHARGE, AND THEIR EFFECTS ON ACID OPEN-HEARTH PRACTICE

The marked decrease in refining time for American acid open-hearth practice has taken place gradually over the last 10 or 15 years and has been a result of developments in furnace construction, fuels and a better understanding of the charge.

Furnace Dimensions. In the acid open-hearth as well as in any steel-making process, the shape of the hearth has a marked effect upon the rate of operation. A shallow bath with a large slag-metal area results in more rapid refining unless more metalloids are charged to off-set this effect. One American furnace for example has a bath depth of only 14 inches and thus a large slag-metal area as compared with another furnace having approximately the same charge weight but a bath depth of 32 inches. Both use the same fuel and make a similar product. The former produces an average of 9.8 tons per hour with an average refining time of $1\frac{1}{2}$ hours, whereas the latter produces an average of 7.2 tons per hour with an average refining period of 2 to $2\frac{1}{2}$ hours duration.

Control Equipment. The acid open-hearth plants have trailed behind basic plants in the installation of fuel and temperature control equipment and many of the factors responsible for adverse opinions concerning the economics of the acid hearth may be attributed in part to this fact. The former lack of control equipment may have originated with production considerations. Acid open-hearth plants have not been so concerned with mass production as have the basic plants. In casting shops, for example, the decision as to when a furnace is to be tapped may be determined by the molding department as well as the furnace personnel.

Today, most acid shops in this country are equipped with modern control apparatus and now adjustments in fuel input may be made at will. This is recognized to be highly important because it is preferable to "melt-down" at a low temperature, or rate, in the acid furnace in order to eliminate the manganese and silicon during the melting period. Conversely, it is also desirable to be able to raise the temperature quickly after these metalloids are removed. Modern fuel control equipment together with a properly balanced charge permit this practice. As a result of these considerations, most American heats "melt-down" at a relatively low temperature with a subsequent rapid increase. The SiO_2 content of the slag increases with

the temperature and at a certain point in the heat when the temperature is sufficiently high, the carbon is eliminated rapidly as shown in Fig. 5.⁴

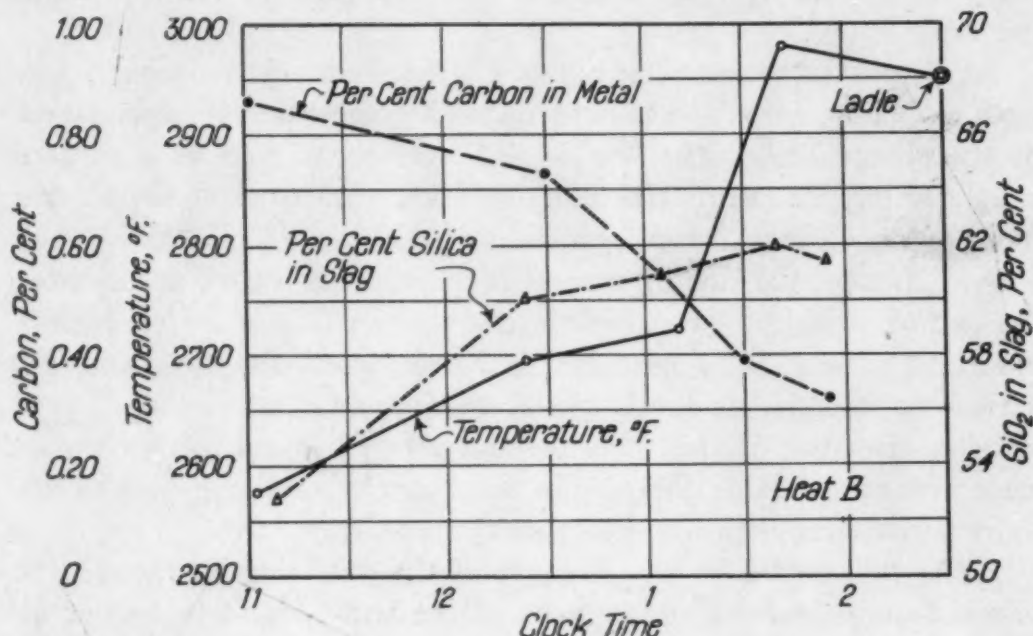


Fig. 5—Effect of Temperature on Slag Composition and Rate of Carbon Elimination in Acid Open-Hearth.

Types of Fuel. A survey of the acid open-hearth industry in this country reveals that three different types of fuel are in use: natural gas, oil and air, and oil and superheated steam.

Generally speaking, the heat input with oil and superheated steam (i.e., B.t.u. per hr.) is higher than that of either of the other two types of fuel as shown in the following table which gives a partial summary of American fuel consumption.

Table I
Fuels Used in American Acid Open-Hearth Plants

Type of Fuel	No. of Furnaces Considered	Million B.t.u./net ton, Average, Melt to Tap	Million B.t.u./net ton, Average, Charge to Tap	Net tons/Hour Charge to Tap	Million B.t.u. Per Hour
Natural Gas	14	0.95	4.42	5.0	21.0
Oil and Air	25	1.08	5.21	4.1	21.36
Oil and Superheated Steam	10	1.51	5.23	6.29	32.74

Shops producing ingots generally operate with a somewhat

⁴G. R. Fitterer, American Institute of Mining and Metallurgical Engineers, 21st Open-Hearth Proceedings, 1938, p. 38.

longer refining period than casting shops. This fact is reflected in the greater B.t.u. input in plants using oil and superheated steam, most of which are ingot producers. Similarly, most of the plants using oil and air are foundries and this accounts for the low B.t.u. per hour figure.

Oil and superheated steam gives the "sharpest-working", i.e., most oxidizing, flame and thus furnishes a greater degree of oxidation of the charge during the "melt-down" period as well as a greater supply of oxygen during the refining period. In turn, oil and air are more oxidizing than natural gas and air.

In Europe, the lack of natural fuels other than coal, necessitates the use of producer gas which is characterized by a softer or less oxidizing flame. This explains to some extent the long refining periods encountered in the English and German heats described previously. Because of this, it is possible that European plants would meet with considerable difficulty in reducing their refining time to the short periods commensurate to American practice.

The Balanced Charge. Because of the oxidizing characteristics of the flame, the metalloid content of the bath should be higher at melt-down in the oil—superheated steam practice than with other fuels in order to retain control of the heat during the refining period. If the carbon, manganese and silicon are too low at "melt-down", the heat may be highly oxidized with a subsequent excessive elimination of carbon, a high oxygen content of the bath, and possibly "dirtier" steel.

A summary of heats from 18 different plants is shown in Table II, wherein the general effect of metalloid content of the bath at "melt-down" on the refining period is shown. This table does not differentiate between the furnace capacities, the types of fuel used or the products, i.e., whether ingots or castings. However, it is obvious that in general the greater the metalloid content of the charge for a given type of heat, the longer will be the refining period. Most plants charge their heats with as small a quantity of total metalloids as possible, and this practice results in the high refining rates of from 0.3 to 0.8 tons per minute listed in the table. The heats in Table II in which high FeO was required to remove the metalloids, were under oxidized at melt-down and thus required large additions of limestone and ore to increase the refining rate. Those heats with spiegel additions were highly oxidized at "melt-down" and the operator retarded the refining rate by this deoxidizing addition.

Table II
The Effects of the Charge Analysis and Furnace Additions on the Rate of Refining
in Eighteen Acid Open-Hearth Furnaces. (All Different Plants)

Heat No.	Per Cent FeO Needed to Eliminate Metalloids (C, Mn and Si) Melt to Tap*	Refining Rate Net Tons/Min. Melt to Tap	Refining Additions Pounds
	Highly Oxidized	Heats: Spiegel	Added to Stop Action
1	1.00	0.391	1200 Spiegel
2	1.20	0.293	200 Spiegel
	Highly Oxidized	Heats: No Additions	
3	1.44	0.862	None
4	0.65	0.326	None
	Average Heats: Metalloids in Charge	Not Too High; Additions	Nominal
5	1.56	0.250	50 Ore
6	1.74	0.285	60 Stone
7	0.54	0.588	200 Ore
8	1.56	0.498	200 Ore
9	1.26	0.510	400 Ore
	Heats With Abnormally High Metalloid Charge or	Additions Too Small	
10	2.78	0.148	200 Ore, 25 Stone
11	1.95	0.239	300 Stone
12	2.67	0.125	400 Ore, 100 Stone
13	1.64	0.211	400 Ore, 120 Stone
14	3.56	0.212	800 Ore
	Heats With Abnormally High Metalloid Charge and High Additions		
15	2.74	0.361	800 Ore, 45 Stone
16	3.12	0.356	1000 Ore
17	3.13	0.451	2300 Ore
18	5.27	0.379	1900 Ore, 1200 Stone

Actually, the manganese and silicon contents are rarely over 0.03 to 0.10 per cent each at "melt-down" and the average is probably closer to 0.05 per cent. The carbon content at this time is often no more than 0.20 or 0.30 per cent above the "go-ahead" values just before the final additions are made. Several years ago, this practice would have resulted in many off-grade heats, since these principles were not thoroughly recognized at that time and the methods for their control were not known.

All of these factors concerning the furnace, the fuel and the charge are highly important and are inseparable from the discussion of the chemistry of the acid open-hearth which follows. In fact, all of these items introduce variables that complicate the treatment of acid open-hearth data even by statistical methods. Unless a sufficient number of these factors are held constant, statistical information becomes difficult to analyze.

PHYSICAL CHEMISTRY OF THE ACID OPEN-HEARTH: REVIEW OF PREVIOUS WORK

The statement has been made by many previous investigators that the acid open-hearth operates closer to equilibrium than any

other steel-making process. Unfortunately, this statement has never been clarified by a qualifying clause indicating specifically which phase of the process is at equilibrium. One objective of this paper is to seek a justification for this conclusion and to specify which equilibrium, if any, the acid open-hearth approaches.

Physical chemistry is a branch of science which deals with methods of determining: (1) which reactions can take place in a given system; (2) the extent to which they proceed. Investigations in this field usually involve attempts to determine equilibrium constants for the reactions and the manner of variation of such constants with temperature.

This type of information has accounted for the rapid strides made by the chemical industries only because the physical chemists have reduced equilibrium data to practice by the installation of control methods. Temperature and pressure control mechanisms, for example, establish the efficiency of many chemical processes as well as the quality and uniformity of their products.

The refining of steel by any process is similarly accomplished through chemical reactions, the physical chemical study of which is in order. However, such investigations should be directed towards subsequent control methods which may be used by the melt-shop personnel.

A critical survey of the available physical-chemical data has been made by the author to determine their usefulness to the acid open-hearth industry. This lecture deals specifically with a search for the equilibrium which the acid open-hearth reputedly approaches as so many previous investigators have stated.

Homogeneous Equilibria: Review of Previous Concepts. In the acid open-hearth there are both heterogeneous and homogeneous reactions to be considered since there are four phases involved: the solid (or the SiO_2) lining, the gas, the slag, and the metal bath. Strictly speaking, practically all of the reactions occurring in the process are heterogeneous in nature or are dependent upon other heterogeneous side reactions.

Most of the previous investigators have been concerned with the competing reactions of carbon, manganese and silicon with iron oxide in the metal bath. Practically all of these studies have involved attempts to explain the sources of iron oxide for purposes of these reactions. It is generally assumed that the oxygen is furnished to the metal by the slag and that the iron oxide is distributed between the

slag and metal in accordance with a distribution ratio. However, where the previous investigators attempted to explain the activity or the state in which the FeO is in the slag, they encountered a maze of contradictory data and found it necessary to resort to an arbitrary assumption in this regard.

For example, many excellent investigations such as those of Schenck,⁵ Styri,⁶ as well as Körber and Oelsen⁷ centered on the assumptions that iron oxide existed in the liquid slag as a definite chemical compound or ferrous silicate. This was dissolved in SiO₂ according to these authors and dissociated to some extent so that the slag was essentially composed of "free" FeO, "free" SiO₂ and some undecomposed silicate. The "free" FeO in turn diffused into the metal bath where it reacted with carbon and the other metalloids.

The reactions taking place according to this concept are as follows:

Reaction 1. $(\text{FeO})_2\text{SiO}_2 \rightleftharpoons 2 \text{FeO} + \text{SiO}_2$. All of these constituents are in the molten slag and the dissociation constant = $K_D = \frac{(\text{FeO})^2 (\text{SiO}_2)}{(\text{FeO})_2\text{SiO}_2}$.

Reaction 2. $(\text{FeO})_{\text{slag}} = [\text{FeO}]_{\text{metal}}$ and the distribution ratio $D. R. = \frac{[\text{FeO}]_{\text{metal}}}{(\text{FeO})_{\text{slag}}}$, then finally,

Reaction 3. $[\text{FeO}]_{\text{metal}} + \text{C} = \text{CO} + \text{Fe}$ and the equilibrium constant for this reaction becomes, $K_C = \frac{(\text{CO}) \text{ Fe}}{[\text{FeO}] \text{ C}}$.

In all of these constants, each constituent should be expressed according to the modern concept of chemical activity.

This procedure would be highly useful if it were not necessary to assume a value for the dissociation constant of the silicate as well as for the distribution ratio. The determination of K_D is the least difficult of the three constants.

There seems to be no ready and reliable experimental method for the verification of the assumed dissociation constants and none of this information promises to develop practical control methods in the near future. Inasmuch as this is the aim of the present investigation all of the previous data concerning the physical chemistry of the acid process will be reserved for future study. Instead, other methods

⁵H. Schenck and E. O. Brüggeman, *Arch. f. d. Eisenhüttenw.*, Vol. 9, 1936, p. 543.

⁶H. Styri, *Journal, Iron and Steel Institute (London)*, Vol. 108, II, 1923, p. 189.

⁷F. Körber and W. Oelsen, *Mitt. K.W.I. Eisenforsch.*, Vol. 14, No. 13, 1932, p. 181.

for control have been sought and this led the author to a study of heterogeneous equilibria or phase diagrams.

HETEROGENEOUS EQUILIBRIA; PHASE DIAGRAMS

The metallurgist uses phase diagrams for the explanation of heat treatment and the alloying of metals but rarely gives them a thought in connection with slag-metal reactions. This neglect is peculiar in that one would expect him to think primarily in these terms. Inasmuch as this type of study has received so little attention and because it appears to offer considerable promise, emphasis will be placed on phase diagram considerations in the following text.

The System FeO-SiO₂. In the study of acid open-hearth slags, the equivalent of the iron-carbon diagram in heat treatment is the system FeO-SiO₂ which will be the first to be considered herein. Very early work on this diagram may be eliminated from this discussion because of obvious inaccuracies. For example, the system by von Keil and Damman⁸ must be discounted because of the presence of as much as 8 per cent Fe₂O₃ in most of their samples.

The first important information to be published on this system was that of Greig⁹ who studied the high silica (and, therefore, the high temperature) end of the system. He found that mixtures of FeO and SiO₂ formed two immiscible liquids up to approximately 40 per cent of FeO. Beyond this percentage, the melting point was decreased and only one liquid was present in equilibrium with pure solid SiO₂ (cristobalite). These two liquids existed at a temperature above 1680 degrees Cent. (3056 degrees Fahr.). Shortly after the publication of Greig's work, Herty and Fitterer¹⁰ investigated the high/FeO end of the system and found two eutectics at 23 and 34 per cent silica, respectively, as well as the presence of the compound fayalite (2FeO-SiO₂) which melted at approximately 1350 degrees Cent. (2460 degrees Fahr.).

Later Bowen and Schairer¹¹ investigated practically the same range of composition and found much higher melting points between 40 and 60 per cent silica. After consideration of this work and the manner in which it was conducted, it is believed by the author that

⁸O. von Keil and A. Damman, *Stahl u. Eisen*, Vol. 45, 1925, p. 890.

⁹J. W. Greig, *American Journal of Science*, Vol. 14, 5th series, 1927, p. 479.

¹⁰C. H. Herty, Jr., and G. R. Fitterer, *Industrial and Engineering Chemistry*, Vol. 21, 1929, p. 51.

¹¹N. L. Bowen and J. F. Schairer, *American Journal of Science*, Vol. 24, 5th series, 1932, p. 177.

the FeO-SiO_2 system of Bowen and Schairer is more nearly correct than that of Herty and Fitterer. The former investigators used a method of quenching their samples which enabled them to determine the temperature at which the last portion of solid SiO_2 was dissolved by the liquid. This was not possible in the micropyrometer method

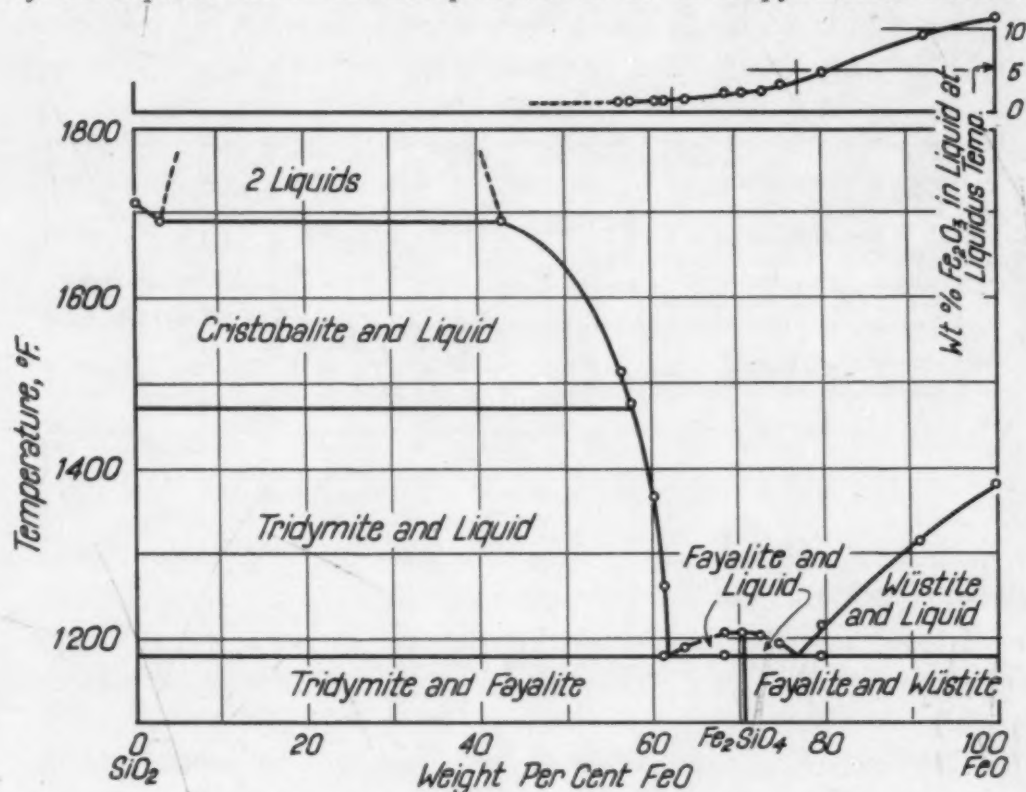


Fig. 6—The System FeO-SiO_2 . (Bowen and Schairer).

used by Herty and Fitterer and probably accounts for the discrepancies in their work. Because of this, the system according to Bowen and Schairer (Fig. 6), will be used exclusively in this study.

The System MnO-SiO_2 . White, Howat and Hay¹² investigated this system and used cooling curves as criteria for the determination of the liquidi. As will be shown later, it is more than likely that their temperatures in the intermediate silica range were too high. This is also true of the diagrams constructed by Benedicks and Löfquist¹³ from miscellaneous publications.

This system was also studied by Conley and Royer¹⁴ who used the micropyrometer method. After a survey of other work, it is be-

¹²J. White, D. D. Howat and R. Hay, *Journal of Royal Technical College of Glasgow*, Vol. 3, 1934, p. 231.

¹³C. Benedicks and H. Löfquist, "Non-Metallic Inclusions in Iron and Steel." Chapman and Hall (London), 1930.

¹⁴J. E. Conley and M. B. Royer, U. S. Bureau of Mines, R. I. 3081, p. 4, 1931.

lieved that their system (shown in Fig. 7) is more nearly correct than any other now available. This will be discussed in greater detail in connection with the ternary system FeO-MnO-SiO_2 .

The System CaO-SiO_2 . Limestone is a normal refining addition to acid open-hearth heats and is used to displace or free FeO from its combination with silica and thus increase the rate of oxidation, particularly of carbon. For this reason the system CaO-SiO_2 should

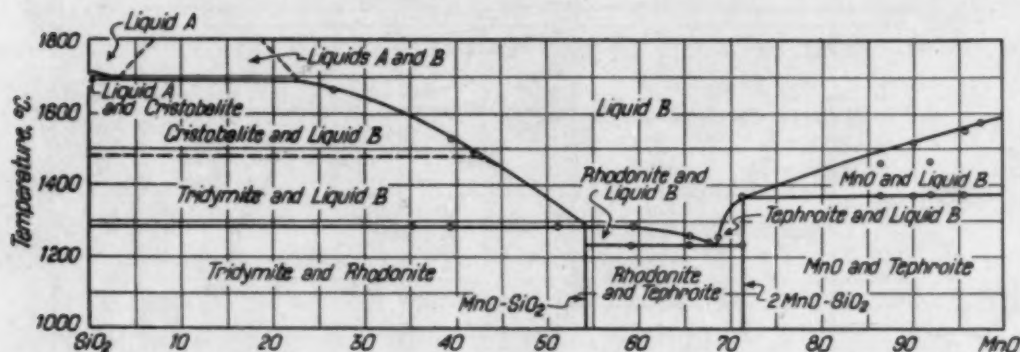


Fig. 7—The System MnO-SiO_2 (Conley and Royer).

be considered. The work of Day, Shepherd and Wright,¹⁵ Rankin and Wright,¹⁶ Greig,¹⁷ and Ferguson and Merwin¹⁸ is well established today and the portion of the diagram showing the saturation of SiO_2 with CaO in the steel making temperature range is shown in Fig. 8.

The interesting portions of these three binary systems from the standpoint of the acid open-hearth are plotted together in Fig. 9. All of these phase diagrams show a similar trend in the high silica range of composition. For example, liquid ferrous silicates are saturated with 40 per cent solid silica at 1400 degrees Cent. (2550 degrees Fahr.) and with 60 per cent at 1688 degrees Cent. (3070 degrees Fahr.). Manganous silicates are saturated with 52 per cent of solid silica at 1400 degrees Cent. (2550 degrees Fahr.) and 77 per cent at 1688 degrees Cent. (3070 degrees Fahr.). In addition the corresponding saturation values for liquid calcium silicates are 63 and 72 per cent at 1440 and 1688 degrees Cent. (2625 and 3070 degrees Fahr.), respectively.

The Ternary System FeO-MnO-SiO_2 . The ternary slags of

¹⁵A. L. Day, E. S. Shepherd and F. E. Wright, *American Journal of Science*, Vol. 22, 1906, p. 265.

¹⁶G. A. Rankin and F. E. Wright, *American Journal of Science*, Vol. 39, 4th series, 1915, p. 1.

¹⁷J. W. Greig, *American Journal of Science*, Vol. 13, 5th series, 1927, p. 1.

¹⁸J. B. Ferguson and H. E. Merwin, *American Journal of Science*, Vol. 48, 4th series, 1919, p. 81.

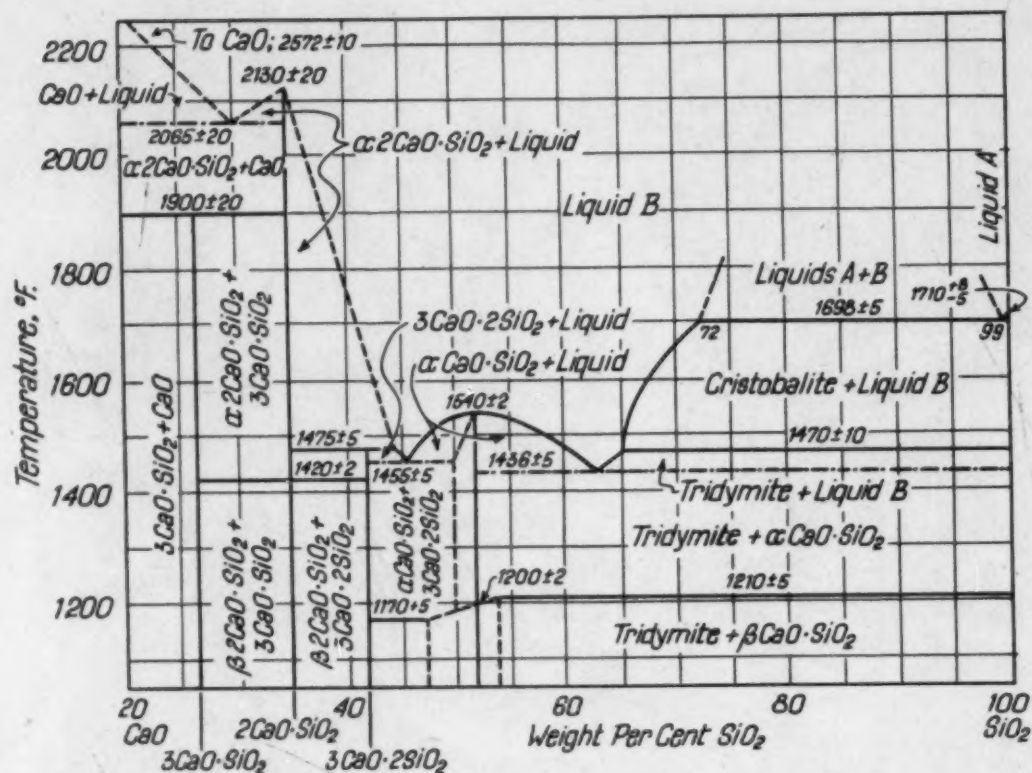


Fig. 8—System CaO-SiO_2 (Day, Shepherd, and Wright; Rankin and Wright; Greig; Ferguson and Merwin).

this system were investigated by Maddocks¹⁹ and, in general, the temperatures found appear to be extremely low, particularly in the range of composition of acid open-hearth slags. The ternary diagram of Conley and Royer¹⁴ also exhibits extremely low temperatures within the range of composition of acid open-hearth slags and in order to justify either of these systems it is necessary to assume that the acid open-heart slag is superheated to several hundred degrees above its melting point.

This assumption, in effect, implies that the acid open-hearth slag is far from equilibrium with the solid silica of the banks, a conclusion which cannot be justified on the basis of data given in this paper. The ternary diagram of Conley and Royer was partially extrapolated from the FeO-SiO_2 binary system of Herty and Fitterer¹⁰ which is admittedly incorrect as stated above.

For the purposes of this paper an entirely new ternary system has been constructed, in which the binary system FeO-SiO_2 according to Bowen and Schairer and the system MnO-SiO_2 by Conley and Royer have been combined. From the standpoint of acid open-hearth

¹⁹W. R. Maddocks, Iron and Steel Institute (London) Carnegie Scholarship Memoirs, Vol. 24, 1935, p. 51.

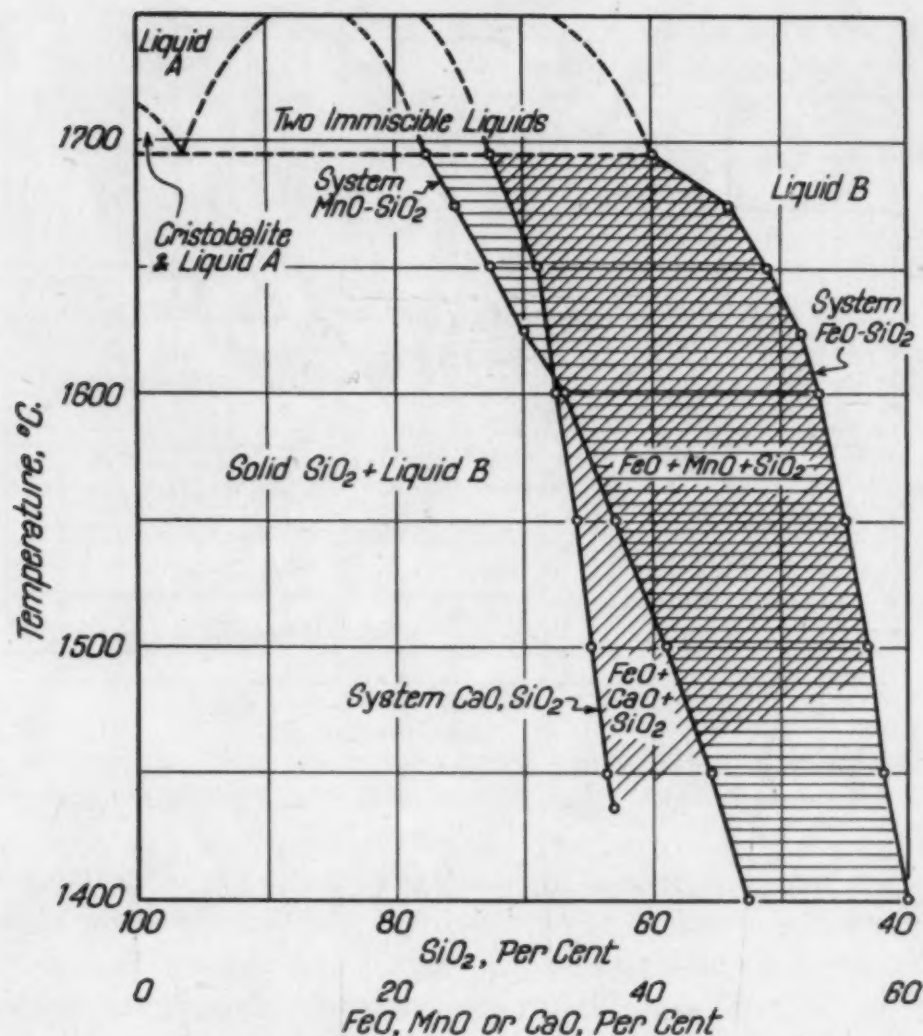


Fig. 9—Silica Saturation—Temperature Lines for the System FeO-SiO_2 (Bowen and Schairer). MnO-SiO_2 (Conley and Royer) and CaO-SiO_2 (Greig; Rankin and Wright).

slags only that portion of the system which represents slags between 40 per cent and 65 per cent SiO_2 and 5 to 25 per cent MnO need be considered.

In practically all of the previous studies of the ternary system, whether the determination has been by experiment or by extrapolation this portion of the diagram is shown as a plane made up of isotherms extending in straight lines across the ternary system from the saturation line on the FeO-SiO_2 to the comparable line on the MnO-SiO_2 binary. If the author may assume the same privileges taken by others, i.e., to draw such isotherms across the ternary system in accordance with the two above mentioned binaries, Fig. 10 is obtained.

The Relation Between Phase Diagrams and Acid Open-Hearth

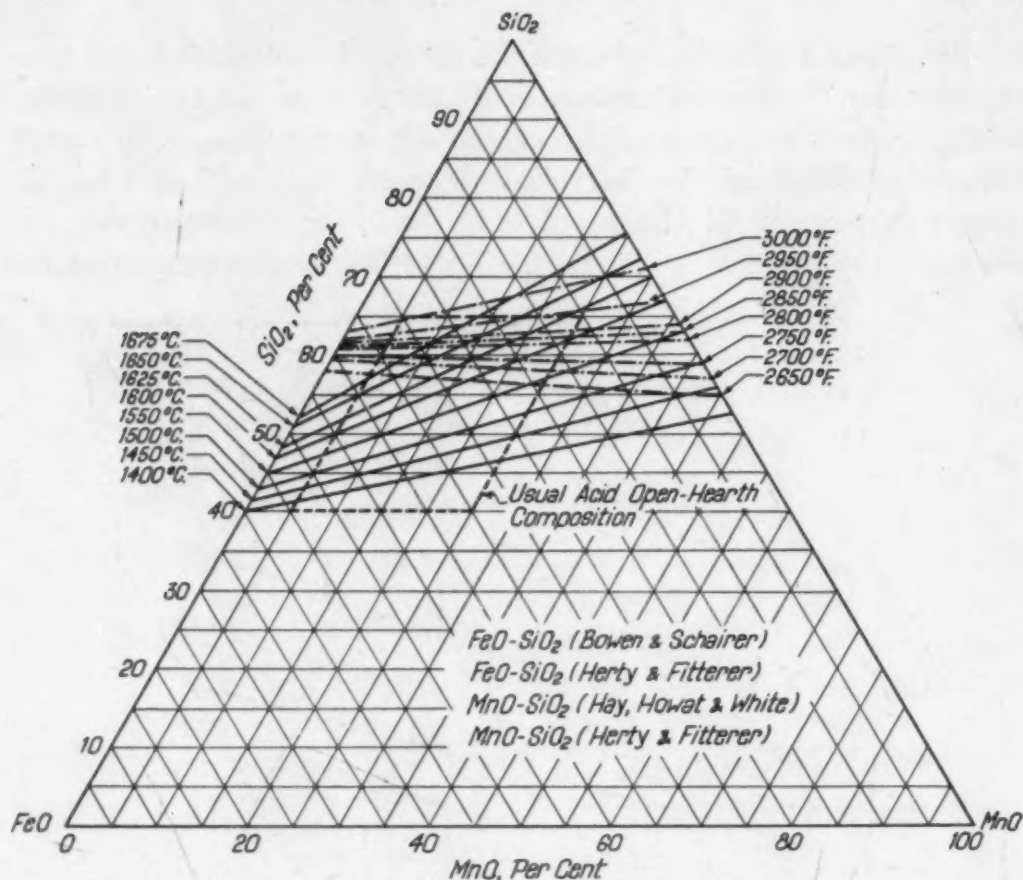


Fig. 10—The System FeO-MnO-SiO₂ Showing Usual Range of Acid Open-Hearth Slag Composition.

Operation. These isotherms may be compared with the usual compositions of acid open-hearth slags as indicated by the diamond shaped area outlined in the ternary diagram. It will be seen that the temperatures are quite reasonable and would represent feasible tapping temperatures particularly in the higher silica portion of the diamond which represents finishing slags in which the temperatures vary from 1540 to 1677 degrees Cent. (2800 to 3050 degrees Fahr.). If this ternary diagram is accepted, it then becomes possible to consider the possibility of the acid open-hearth slag being saturated with SiO₂ at all times unless upset temporarily by additions of limestone and ore. Sufficient data are available to prove that this unstable condition no longer exists within 10 or 15 minutes after the additions have been made and to show that the slag returns to its saturated condition within that period of time. The fact that temperatures of the White, Howat and Hay binary system are too high and the values for the FeO-SiO₂ system of Herty and Fitterer are too low to be practical is shown by the dotted lines in Fig. 10.

That the diamond represents the range of composition and temperature usually encountered in acid open-hearth slags is indicated in Fig. 11 in which the analyses of slags from fourteen plain carbon heats are plotted within the enlarged diamond shaped area of the ternary diagram. All of the points in the lower portion of this figure are early or melt-down slags. Those points represented at the

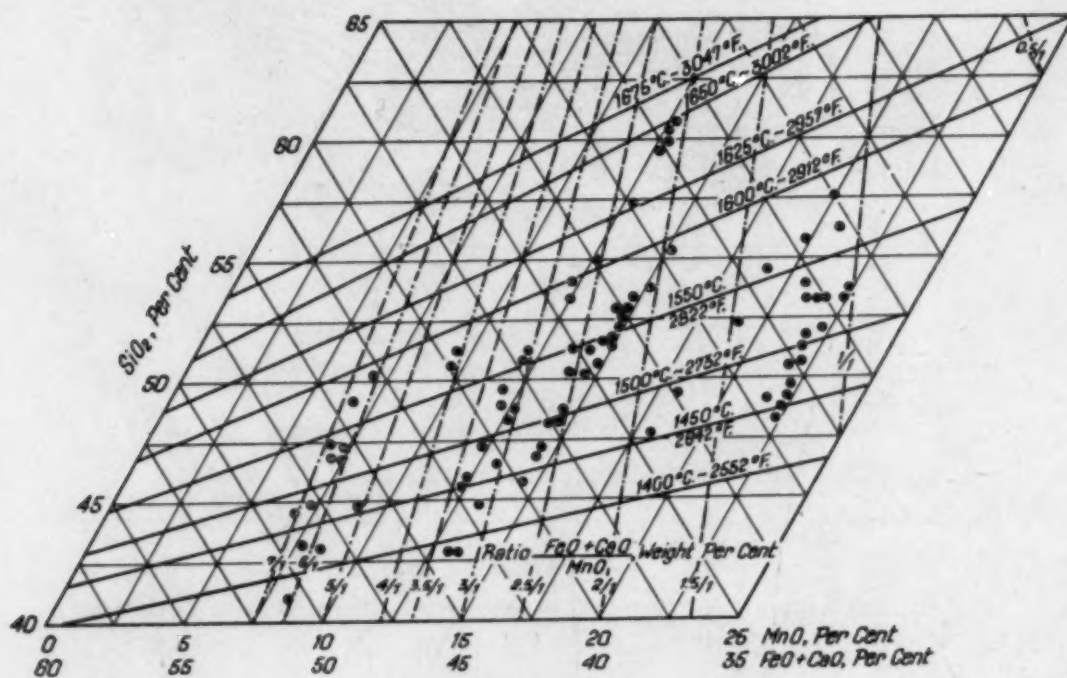


Fig. 11—Section of FeO-MnO-SiO₂ System Showing Composition of Slags from Fourteen Acid Open-Hearth Heats.

top of the figure are slags taken during the finishing stages of the heat and represent essentially the temperatures at which the heats were tapped. The points were plotted according to the method used by Whiteley and Hallimond²⁰ in which the SiO₂ content was plotted against the ratio of $\frac{\text{FeO} + \text{CaO}}{\text{MnO}}$ and, from the diagram, it can be seen that most of the heats were finished at temperatures varying from 1540 to 1650 degrees Cent. (2800 to 3000 degrees Fahr.).

The progression of a single heat may be followed from these points, since each individual heat is represented by a specific number. It is obvious that the MnO content of the slags in a given heat remained essentially constant, whereas the SiO₂ content increased with a proportionate decrease of the FeO and CaO contents.

²⁰J. H. Whiteley and A. F. Hallimond, *Journal, Iron and Steel Institute (London)*, Vol. 99, No. 1, 1919, p. 199.

There is no intention by the author to suggest that this diagram is exact. The manner in which it was constructed is open to criticism. However, its practical applications are sufficiently important to suggest experimental check work on the ternary system in this range of composition. Such work is already under way and in the meantime there is sufficient material on hand to check the theory in practice. Any corrections in this system, however, would be merely relative changes.

There already have been many experiments made which verify the conclusion that mixtures of FeO, MnO and CaO with SiO₂ form continuous solid and liquid solutions such as indicated in Figs. 10 and 11. This fact has been checked by X-ray and petrographic studies of slags in this range of composition. The index of refraction, the optical angle of rotation, the interplanar spacing distances as well as slag densities show a gradual change across this ternary system. The substitution of 2 or 3 per cent of CaO for FeO apparently does not appreciably disturb the general trends just described. (The fact that it is necessary to add lime to the slag in order to "free" the FeO is taken as an indication that these slags are near equilibrium at all times. This must be the equilibrium which the acid open-hearth reputedly approaches.

NON-EQUILIBRIUM CONDITIONS: OXIDATION PHENOMENA IN THE ACID OPEN-HEARTH

Oxidation from the Slag According to the Phase Diagram Concept. From the previous discussion it would appear that the acid open-hearth tends to approach a state of dynamic equilibrium, although it is unlikely that any heats reach that hypothetical state. However, it is apparent now that the acid slag continuously approaches a saturated state with respect to SiO₂ content. The reason that saturation is difficult to attain is that in usual American practice, the temperature is constantly increasing throughout the heat.

With increased temperature two phenomena may occur. First, since increased temperature demands a higher SiO₂ content of the slag for saturation, some SiO₂ may be absorbed from the furnace walls particularly by that portion of the slag which is in the proximity of the banks.

The slag in the center of the furnace, however, may approach saturation in a converse manner. A study of Figs. 6, 9 and 11 will

reveal that whereas an increased percentage of SiO_2 is required for the saturation of the slag at relatively higher temperatures, this may be accomplished not by an increase in SiO_2 but by a loss of FeO content. In other words, less FeO is required at relatively higher temperatures to saturate the silica and hence as the temperature increases it becomes free to react with the metalloids of the bath. Apparently both an increase in SiO_2 in the slag near the banks and a "precipitation" of FeO content in the center of the furnace occur simultaneously in most heats. The release of FeO for reaction with the metalloids undoubtedly accounts for part of the oxidation. However, a study of the oxygen balance of various heats indicates that this procedure may represent about 16 per cent of the total oxidation.

For this reason, an oxygen balance has been made on a recent heat (Tables IV and V). A total of 0.49 per cent carbon, 0.11 per cent manganese and 0.04 per cent silicon were removed during the refining period. On the basis of the 81,620 pounds charged, this represents a total of 2675 pounds of FeO required for the removal of the metalloids.

The next step was to calculate the slag weights at the "melt-down" and "go-ahead" periods on the basis of a manganese balance. The results of these calculations are shown in Table III, wherein it is indicated that some 449 pounds of FeO were released and lost from the slag during the refining period.

Table III
Changes in Slag Constituents During the Refining Period

Period of Heat	Slag Pounds	FeO Pounds	MnO Pounds	SiO_2 Pounds
At "Melt-Down"	5360	1515	1223	2552
At "Go-Ahead"	5910	1066	1334	3320
Change During Refining Period	+550	-449	+111	+768

This table shows that the pounds of SiO_2 increased whereas the pounds of FeO decreased during the heat as stated above. In addition it aids in the explanation of why the percentage of MnO does not change during most American heats. Although there is an increase of MnO content of 111 pounds, the slag weight also increased 550 pounds and hence, the percentage of MnO remained essentially constant by virtue of the dilution effect.

Oxidation by Means of Furnace Additions. Inasmuch as only 449 pounds of FeO are accounted for by loss from the slag and

since the total of 2675 pounds were needed to remove the metalloids some other source of oxidation must be sought.

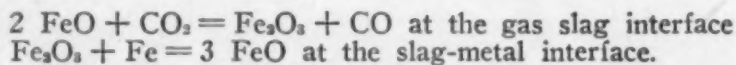
In spite of the FeO decrease in the slag, as above, a total of 300 pounds of ore and 400 pounds of limestone were added to this heat. The ore represented a total of 304 pounds of FeO. This was calculated on the basis of $\text{Fe}_2\text{O}_3 = 3 \text{ FeO}$ and that the ore contained 75 per cent Fe_2O_3 .

The limestone was assumed to furnish oxidation by two procedures: (1) the CaO content displaced a molecular equivalent of FeO; (2) the CO_2 in the limestone furnished a possible molecular equivalent of one FeO. The total amount of FeO available from the limestone additions was then 576 pounds, one half of which has already been included in the 449 pounds of FeO precipitated from the slag. Hence, the oxygen balance at this point would be

FeO needed for metalloids		2675 pounds
FeO "precipitated" from slag	449 pounds	
FeO from ore additions	304 pounds	
FeO from limestone (CO_2)	288 pounds	
Total		1041 pounds
FeO unaccounted for		1634 pounds

This would indicate that more than one half of the FeO needed to eliminate the metalloids must have originated from some other source than the slag or slag additions. This led to a more thorough study of the above heat and a consideration of the possibilities of oxidation from the gas.

Oxidation from the Gas. The common opinion concerning the mechanics of oxygen transfer through the acid open-hearth slag to the metal is that the Fe_2O_3 acts as a carrier agent according to the reactions



During the boil the convection currents cause the Fe_2O_3 which is formed at the top of the slag to be transferred to the metal surface where it is reduced to FeO. This is a feasible theory but requires an extremely rapid and continuous transfer of a very small quantity of Fe_2O_3 as a study of Tables IV and V will indicate.

If an average of 0.25 per cent Fe_2O_3 were present during the active part of the heat, since the average slag weight was 5635 pounds, then only 14.1 pounds of Fe_2O_3 must carry the oxygen from the gas to the metal according to the above reactions. Because 1634 pounds were needed, essentially 116 round trips for the Fe_2O_3 were

required during the refining period. In other words there would be a replacement of Fe_2O_3 about once every minute and a half on this basis. This is not inconceivable, but does not satisfactorily explain the entire mechanism by which oxygen is transferred from the gas to the metal phase.

The Metal Particle Theory. An extremely interesting suggestion was made by Whiteley and Hallimond,²⁰ who suggested the possibility of oxygen transfer by means of metal particles which are always present in the acid open-hearth slag particularly during the "boil". It was reported that as much as 50 per cent of the carbon may be eliminated by the gas oxidation of these particles which are forced into the slag by the boiling action. According to Whiteley and Hallimond, these globules were low in carbon content as compared with the metal bath. In addition, they absorbed iron oxide transferring it into the bath. As soon as the boil ceased, due to de-oxidizing additions, the amount of metal in the slag immediately decreased.

In order to determine the feasibility of this theory, the metal particles were separated from each slag sample in the heat on which the oxygen balance was made. The log for this heat is given in Tables IV and V. The amount of metal particles in the slag is shown in Fig. 12 together with their carbon content at various stages of the heat. It is obvious from these curves that Whiteley and Hallimond's work is verified and that there is a considerable amount of metal suspended in the slag throughout the active refining period of the heat. These particles were lower in carbon content than the metal bath throughout the boil. In early stages of the heat, there may have been sufficient manganese and silicon to prevent the oxidation of the carbon in the particles. Also, it is possible that at this time (i.e., prior to an active boil) the metal particles are not forced so violently into contact with the gas phase as they are later.

Throughout the boil period the metal particles constituted approximately 1 per cent of the slag. This would be equivalent to approximately 60 pounds of metal in the slag at any given moment in the heat under consideration. The question then arises as to how fast these particles must travel through the slag in order to account for the oxygen transfer required for the elimination of metalloids. If the assumption is made that 60 pounds of metal passes through the slag in the form of particles three times a second then the entire reduction of carbon content may be accounted for by means

of dilution alone. In other words, the low carbon particles continuously dilute the metal bath and thus lower the carbon content. According to the carbon dilution theory, the particles must necessarily be replaced from two to three times every second—an assumption which is not unreasonable. The metal particles have not yet been

Table IV
Log Sheet of Acid Open-Hearth. (See Fig. 12)

Clock Time	Additions and Remarks
7:15	Finished Charge Total 81,620 lbs. Average Analysis, 1.23% C, 1.35% Mn and 1.00% Si
10:05	Heat Melted
10:30	Slag and Metal Samples No. 1
10:40	200 lbs. Ore
10:45	Slag and Metal Samples No. 2
10:55	Slag and Metal Samples No. 3
11:10	Slag and Metal Samples No. 4
11:11	200 lbs. Limestone
11:19	Slag and Metal Samples No. 5
11:20	200 lbs. Limestone
11:30	Slag and Metal Samples No. 6
11:36	100 lbs. Ore
11:40	Slag and Metal Samples No. 7
11:50	Slag and Metal Samples No. 8
12:05	Slag and Metal Samples No. 9
12:15	Slag and Metal Samples No. 10
12:22	Slag and Metal Samples No. 11
12:25	224 lbs. FeMn, 750 lbs. SiMn
12:34	Heat Tapped

Table V
Metal and Slag Analysis

Sample No.	Per Cent in Metal			Per Cent in Slag						Metal Particles	% C in Metal Particles
	C	Mn	Si	SiO ₂	FeO	Fe ₂ O ₃	MnO	CaO			
1	1.01	0.20	0.12	47.66	28.29	0.71	22.82	0.16	0.45	1.02	
2	0.99	0.18	0.09	47.80	26.22	0.89	23.69	0.28	0.39	1.02	
3	0.99	0.11	0.07	47.96	26.22	0.91	22.95	0.34	0.27	1.02	
4	0.92	0.09	0.05	49.64	24.98	0.78	22.95	0.39	1.18	0.76	
5	0.87	0.07	0.04	51.10	23.18	0.52	22.88	1.85	0.86	0.75	
6	0.79	0.08	0.04	52.00	21.55	0.29	22.68	3.15	1.04	0.64	
7	0.72	0.10	0.05	53.20	20.56	0.20	22.60	3.19	0.89	0.60	
8	0.66	0.10	0.05	54.50	19.04	0.15	22.56	3.14	0.75	0.58	
9	0.57	0.08	0.06	53.26	18.22	0.13	22.35	3.25	1.09	0.51	
10	0.54	0.11	0.07	55.96	18.02	0.09	22.64	3.25	0.85	0.52	
11	0.52	0.09	0.08	56.08	18.02	0.13	22.56	3.20	0.72	0.49	

analyzed for FeO content and hence, no estimate of the amount of oxygen transferred by this means can be made at this time.

The metal particle theory should receive more attention and further investigation should be carried out in order to approve or disapprove its feasibility. From the figures given here it would seem reasonable that they play a large part in the transfer of oxygen from the gas and the slag to the metal phase. Also, the reduction of carbon content by dilution is a distinct possibility.

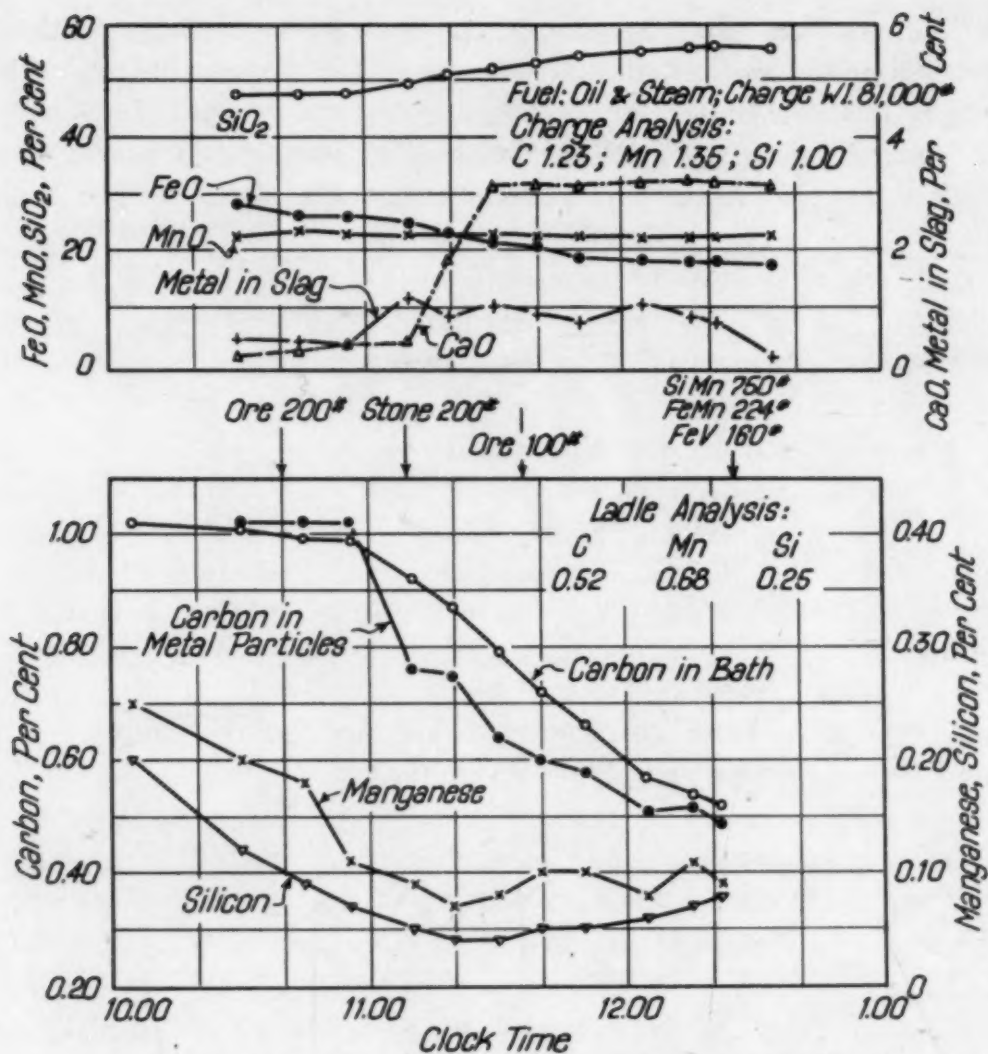


Fig. 12—No. 3 Acid Open-Hearth Heat (American Practice).

A METHOD OF SLAG CONTROL FOR THE ACID OPEN-HEARTH

At the beginning of this lecture, it was stated that the ultimate goal of any physical chemical study of steel-making processes should be the development of control methods which can be used by the melt-shop personnel. A possible control method for the acid open-hearth was the objective of this investigation.

It has been pointed out herein that as the temperature of an acid open-hearth heat increases, the SiO₂ content of the slag increases proportionally, whereas its FeO content decreases.

It was also shown that the MnO content of the slags remained essentially constant throughout American heats. Hence, it would appear that any quick test which would determine the SiO₂ content

of the slag would also permit the estimation of the temperature of the slag as well as its FeO content, provided of course, that the usual MnO value of the slag for the given practice is known.

This conclusion is logical because the location of any point on a ternary diagram may be found if the percentages of any two of the three constituents are known. In this case if the SiO_2 content of the slag may be determined quickly and the MnO content is set by charging practice, then the FeO content of the slag as well as its approximate temperature may be determined. This becomes apparent after a study of Fig. 11. Here it was shown that the composition of the slag with respect to SiO_2 and FeO contents were determined by the temperature and the MnO content.

The question now arises as to what quick and simple test may be taken by the melt-shop personnel and used to determine the course of the heat on this basis. The method of determination of slag fluidity similar to that described by Herty²¹ for basic open-hearth slags was selected for this purpose.

Juppenlatz²² and Kramerov²³ have shown that the fluidity of acid electric or acid open-hearth slags is a function of their SiO_2 content. This relation has been confirmed by the work of some of the authors' associates¹ and some recent data are shown in Fig. 13. The test mold used in this work has a $\frac{3}{8}$ -inch bore instead of $\frac{1}{4}$ -inch suggested by Herty. The former diameter has been found to be more universally useful for the acid open-hearth.

In this figure it may be seen that the flow or fluidity test is quite sensitive to changes in SiO_2 content of acid slags. One inch of flow is equivalent to plus or minus 1 per cent of SiO_2 . The slags having a long "run" (i.e., above 11 inches) are very early slags. As the heats progress the SiO_2 content increases and the fluidity decreases proportionally. Usually tapping slags run from 4 to 9 inches in this mold. Some plants aim towards a 4 to 5-inch tapping slag whereas others will tap on 8 to 9 inches depending principally on the product being made.

The points in Fig. 13 represent tests made on two heats from different plants—one a casting and the other an ingot shop.

The significance of this test is further clarified if the relation of fluidity to SiO_2 content is kept in mind while studying Fig. 14. These

²¹C. H. Herty, Jr., C. F. Christopher, H. Freeman and J. F. Sanderson. Carnegie Institute of Technology. Cooperative Bulletin 68, 1934, p. 26.

²²J. Juppenlatz, *Transactions, American Foundrymen's Association*, Vol. 50, 1942, 326.

²³A. Kramerov, *Metallurg (Russ.)*, Vol. 14, No. 8, 1939, p. 38.

curves were obtained directly from the ternary diagram of Figs. 10 and 11.

A heat charged to give 10 per cent MnO in the slag would tend to follow the 10 per cent curve of this figure as the temperature increases. The fluidity test may be taken at any time during the heat and the SiO_2 may be estimated from a curve such as Fig. 13. The

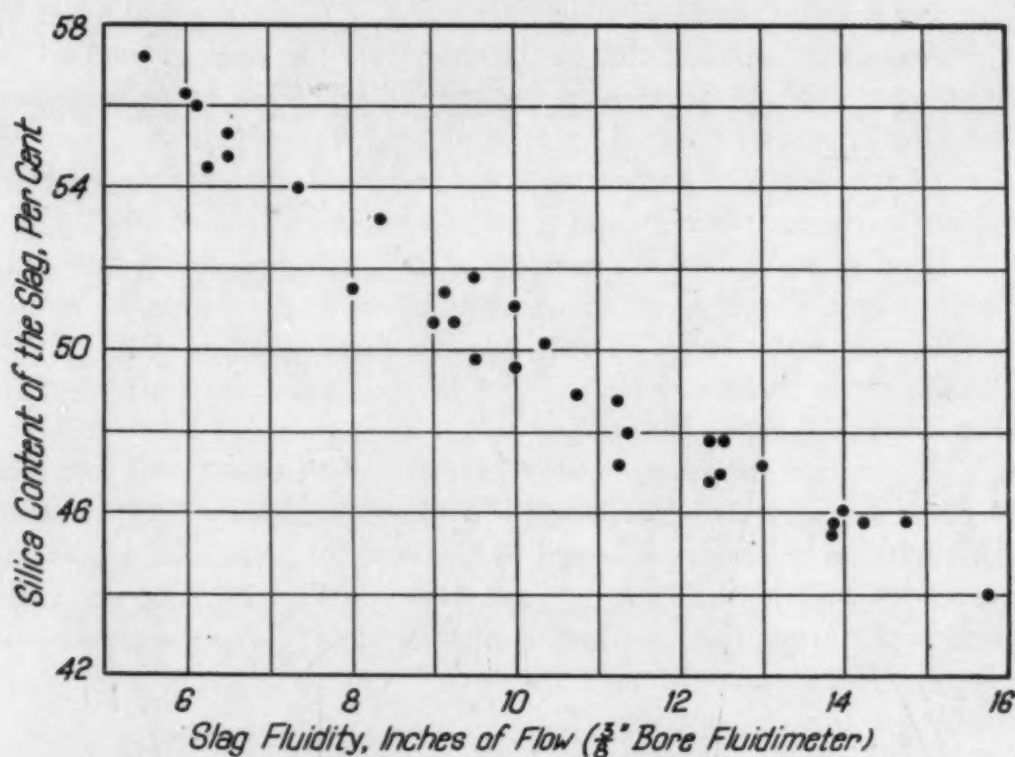


Fig. 13—Relation of Silica Content to Slag Fluidity in the Acid Open-Hearth.

$\text{FeO} + \text{CaO}$ content may then be determined from Fig. 11 since the SiO_2 and MnO contents are now known. The minimum temperature may also be determined by reference to either Figs. 11 or 14.

If for example the fluidity reading were 7 inches for a given slag then the SiO_2 content would be approximately 54 per cent (according to Fig. 13). With 54 per cent SiO_2 and 10 per cent MnO the ratio of $\frac{\text{FeO} + \text{CaO}}{\text{MnO}} = \frac{3.6}{1}$ according to Fig. 11. Hence, the $\text{FeO} + \text{CaO} = 36$ per cent. If no lime has been added to the heat, this represents essentially 36 per cent FeO. If, on the other hand, limestone is used and the usual slag contains 5 per cent of CaO then there is about 31 per cent of FeO present. In addition, it may be seen that the minimum temperature of this particular slag sample was about 2940 degrees Fahr. according to either Figs. 11 or 14.

A combination of Figs. 13 and 14 may then be used as a guide by the plant personnel. The fluidity values may be translated into SiO_2 and FeO contents of the slag as well as give an estimate of the temperature, providing the usual MnO content of the slag is known for the practice under consideration.

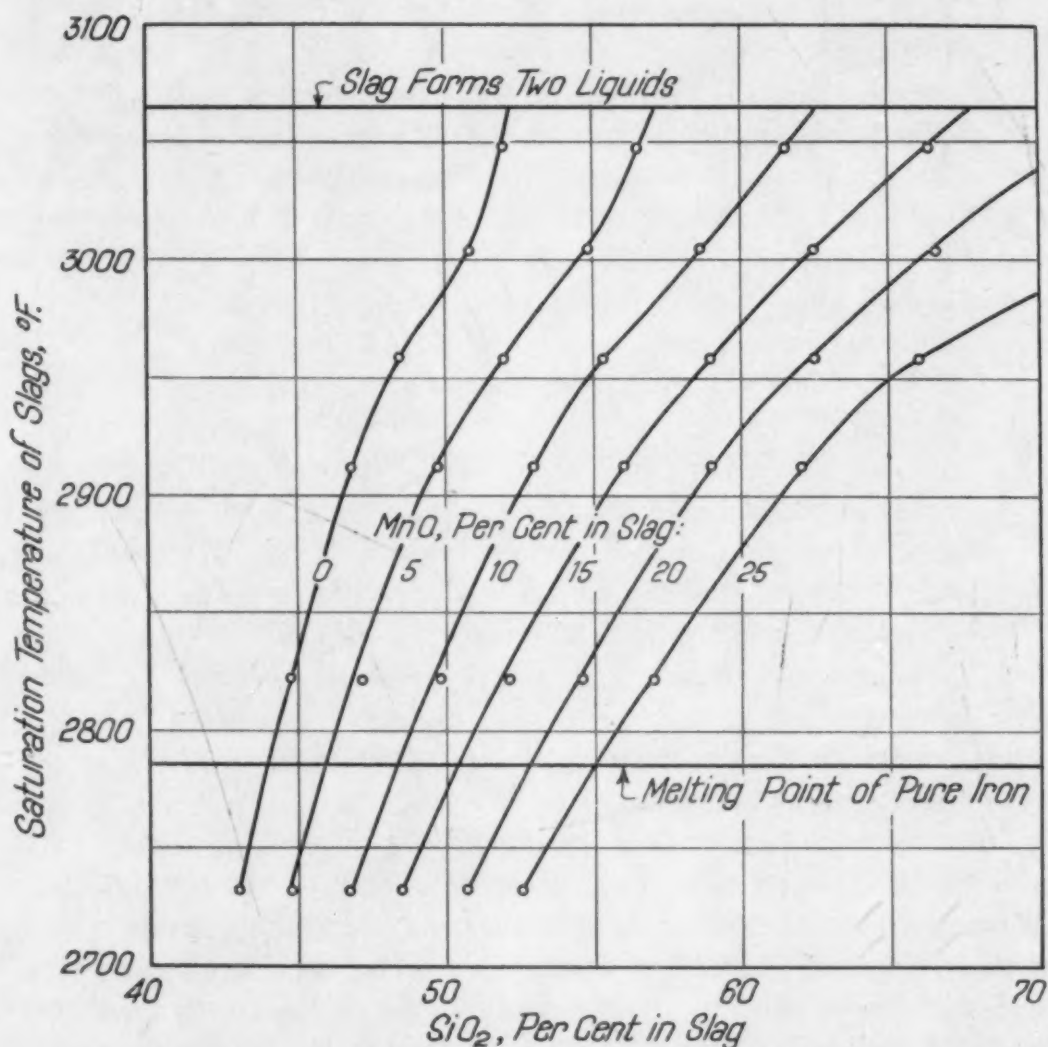


Fig. 14—Relation of Temperature of an Acid Open-Hearth Slag to Its Saturation with Silica.

Fluidity readings taken too soon after a limestone or an iron ore addition, should be avoided because the fluidity will be abnormally high. Some 10 to 15 minutes should be allowed after such additions in order to obtain a reliable fluidity value.

CONCLUSIONS

1. American acid open-hearth practice has improved considerably in recent years because of the use of fuel and draft

control equipment, a better understanding of the charge, and of the principles of refining.

2. The acid open-hearth slag is essentially saturated with SiO_2 at all temperatures as shown by phase diagram relationships.

3. Manganese oxide is essentially constant in the slag throughout a modern American heat.

4. The FeO content of the slag decreases with a proportionate increase in SiO_2 with a rise in temperature, because less FeO is required to saturate the slag at higher temperatures according to phase diagram relations. Some FeO is continually released from its combination with SiO_2 in this manner and is precipitated into the metal bath, where it subsequently reacts with the carbon, manganese, and silicon.

5. The slag fluidity is inversely proportional to the SiO_2 content of the slag.

6. The acid open-hearth may be controlled by charging a constant amount of manganese and by taking slag fluidity tests throughout the heat. The slag fluidity, the SiO_2 content and the temperature of the bath are all closely related as shown.

7. Metal particles are forced into the furnace atmosphere by the action of the boil. Here they are oxidized, and very shortly after, return to the bath. This is suggested as a strong possibility for the transfer of oxygen from the gas and/or the slag to the metal phase.

In conclusion, the author wishes to express his thanks and appreciation to the Officers and Research Staff of the Acid Open-Hearth Research Association for their assistance in preparing this work. Further, the author deeply appreciates the honor and privilege extended to him by the American Society for Metals in serving as the Nineteenth Campbell Memorial Lecturer.

FRACTOGRAPHY—A NEW TOOL FOR METALLURGICAL RESEARCH

BY CARL A. ZAPFFE AND MASON CLOGG, JR.

Abstract

Fractography is the name applied by the authors to the technique of studying untouched cleavage facets at high magnification.

As a supplementary metallurgical tool, fractography by definition offers many of the advantages of single-crystal methods, since the field is oriented about the cleavage plane; the field is nascent and untouched and therefore reveals much of the internal structure of the grain which cannot be seen after polishing and etching; the plane of weakness, which is often the plane of greatest interest, becomes ipso facto the field of observation; time may be saved by avoiding mounting, polishing, and etching; and tiny chips and otherwise unusable fragments are suitable for fractographic examination.

As a research tool, fractography has especially interesting aspects, for cleavage facets abound in detail, most of which remains to be explored. Examples are shown for numerous metallic and nonmetallic specimens.

INTRODUCTION

WHEN the French scientist de Réaumur, in 1722, first applied the microscope to metals, he studied the fractured facets of steel (1).¹ This elemental method of obtaining flat, microscopically useful facets by cleavage was a progeny of mineralogy (2), since the easy cleavage of many minerals lends itself to that simple procedure. Nearly two centuries then elapsed before Martens, who is generally accredited above de Réaumur as a founder of metallography, began his microscopical studies by examining fractures and became discouraged by the difficulties of focusing at high magnifications on such irregular surfaces (3).

In the meantime, Henry Clifton Sorby's interest was attracted to Williamson's work with thin slides of fossil wood. In 1849 Sorby

¹The figures appearing in parentheses pertain to the references appended to this paper.

A paper presented before the Twenty-sixth Annual Convention of the Society held in Cleveland, October 16 to 20, 1944. Of the authors, Carl A. Zapffe is assistant technical director, and Mason Clogg, Jr. is assistant metallurgist, Rustless Iron and Steel Corp., Baltimore, Md. Manuscript received June 20, 1944.

developed the first thin-section of rock and wrote a paper on "Calcareous Grit of Scarborough" in 1851 and another on "Slaty Cleavage" in 1853 (4). In 1857 he discussed his work on the "Microscopic Structure of Crystals" before an unappreciative audience comprising the Geological Society of London (5), and for many years received nothing but ridicule.

Martens' discouragement from the difficulties of examining such irregular surfaces led to an almost complete abandonment of the microscopical study of fractures. Sorby was also discouraged when he later tried to apply his petrographic thin-section technique to opaque metal; but this time the venture was no *cul-de-sac*, and the subsequent development of our modern cut-polish-and-etch technique is common knowledge.

With almost the single exception of Henry Marion Howe (6), whose omniscience will probably continue to antedate the "new" ideas of metallurgists yet to be born, metallographic observations using high magnification have been limited since the time of Martens to polished facets. Howe examined several suitable fracture facets in discussing his famous "X" bands (6); and mention might also be made of Goetz's more recent observations of a fractured bismuth crystal (7). Nevertheless, in no case has the technique been pursued as a study or developed as a research tool.

Often, however, the fracture of a metal holds much information for the metallurgist. Brittle fractures, fibrous fractures, and fractures caused by fatigue, corrosion, segregation and lamination—each has its characteristics and a story to tell; but, to date, only the macroscopic features of fractures are known. As an example of the information, or misinformation, contained in the appearance of fractures, we may recall the work of Ewing and Humfrey which exploded a metallurgical myth current years ago by showing that the "coarsely crystalline" appearance of certain fatigue fractures was not a matter of grain coarsening, but of fracture type (8).

At the turn of the present century, Ewing and Rosenhain provided a real basis for believing that valuable metallographic information might lie within a fracture (9 to 14). Stretching a polished specimen while examining it under a microscope, these eminent workers disproved another myth of that period by demonstrating that metal remains crystalline after plastic deformation. As shown years before with minerals (15), undisturbed blocks of the crystal become bounded by crystallographic deformation lines which develop

when the specimen is strained beyond its yield point. These we know today as "slip lines".

Furthermore, by copper-plating fractures to preserve their characteristics, these same authors examined polished cross sections and showed that even the most "fibrous" fracture of steel usually develops along flat, crystallographic cleavage planes, the only distinction between a "fibrous" and a "crystalline" fracture being in the extent of the individual cleavage (12 to 14).

In a recent research with embrittled metals (16) (17), one of the present authors became interested in the intrinsic differences that might exist between the facets which extend widely during brittle fracture, giving a mirror-like reflectivity, and those which comminute during deformation to provide a gray, fibrous appearance from the myriad of tiny, unresolved reflections. Once the discouragement afforded by irregularities and promontories on the fractured faces was surmounted, some surprising and satisfactory results were obtained, which led to the present paper. As possible advantages which one might gain by using a method and technique for studying with a microscope the individual facets on fractures, the following might be cited:

1. When cleaving crystallographically, the specimen attains many of the attributes of a single crystal which can be oriented with the microscope with all its structures crystallographically disposed.
2. Completely undisturbed by buffing or etching, these facets are nascent and therefore disclose the true interior of the grain without the superimposed effects of polishing and etching. As for the advantages of etching, a subsequent treatment is generally no more difficult than with a polished specimen.
3. The structures which are revealed are often new to the science and cannot be studied with orthodox polish-and-etch technique; furthermore, new information may be gained from known structures by observing them under these new conditions.
4. The plane of weakness, which is often the plane of greatest importance in studying the service and failure of metals, becomes *ipso facto* the plane of observation. The chances for studying the cause of the weakness may therefore be much greater than when using a random section.

5. Finally, there may be general advantages, which include:

- (a) Time-saving by avoiding mounting, polishing, and etching.
- (b) Applicability of odd sizes and shapes and tiny fragments, which are unsuited to orthodox examination.

Let it be clearly understood that these advantages represent optimum conditions and are rather heavily balanced against disadvantages which will probably never allow the method to be used as more than a supplementary metallographical tool. It especially implements the study of defective material, since the large facets of brittle failures favor this type of examination. Ductile material and fibrous fractures often make examination exceedingly difficult.

"Fractography" is the name we have applied to this technique. Reticence in introducing a new term is counteracted by the advantage in substituting one word for a phrase as long as "the micrographic study of cleavage facets on fractured metal specimens", which is the definition of fractography. In addition, the word fractography has some etymological correctness in stemming from roots similar to those affording metallography, for "fracto-" is the combining form of the Latin "fractus", meaning fracture.²

EXPERIMENTAL METHOD

Preparation of Specimens—The experimental technique is very simple, requiring only three accomplishments:

1. Obtaining a brittle fracture.
2. Orienting a facet with the axis of the microscope.
3. Obtaining the close approach of the lens to the specimen required for high magnification.

In regard to the first objective, because each cleavage facet constitutes a specimen, the metal should be made to break in such a manner that an individual facet covers most of the microscopic field at the magnification desired. Brittle metals generally conform to this without pretreatment, except for some which cleave irregularly

²More properly, the word for this study is regmatography, or regmagraphy, formed from derivations of the Greek words "graphos", meaning descriptive treatment, and "regma" or "regmatos", singular and plural, respectively, for fracture. However, mixed Latin and Greek derivatives are common in English, such as the word "automobile"; and fractography seems a more natural word, since derivatives of the Greek word for fracture are practically nonexistent in English.

or conchoidally. For normally ductile metals, sufficient brittleness can often be conferred in one of the following manners:

1. Rapid fracture, as by impact
2. Fracture at subnormal temperatures
3. Embrittlement with cathodic hydrogen
4. Other means, such as hydrostatic rupture

Any fractured face will usually serve, whether it is that of a standard tensile specimen, a failed article, or a mere chip from a sample.

Next, the problem is to orient one or several of the individual cleavage facets perpendicular to the axis of the microscope. A preliminary low-power examination with binoculars will aid in selecting the best facet. To accomplish the orienting, the simple orienting

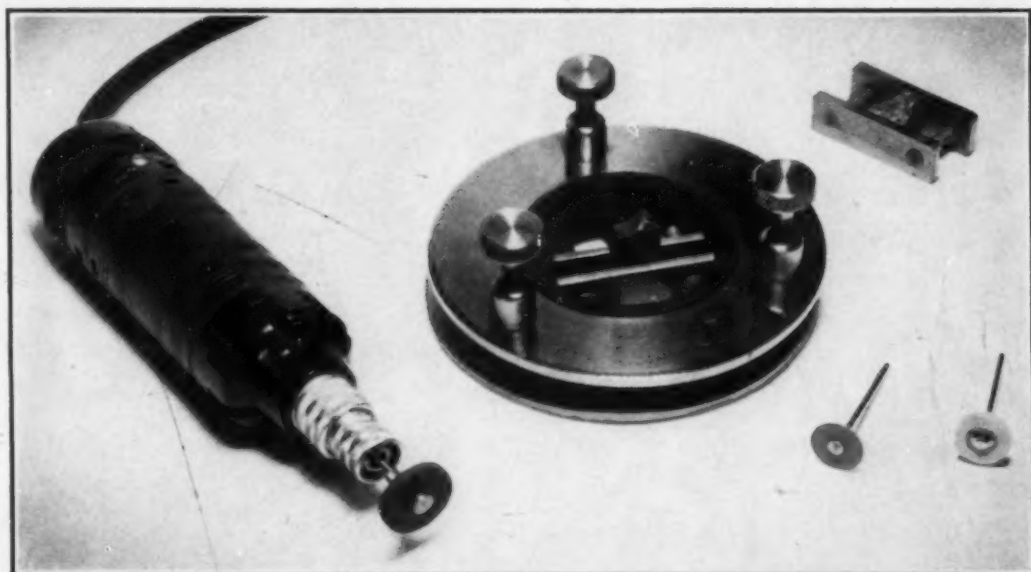


Fig. 1—Appliances Used in Fractography.

mechanism shown in Fig. 1 is used. This device consists of a base-plate, which fits into the annular opening in the stage of the microscope, and a superposed specimen holder supported by three screws whose bases are countersunk slightly into the base-plate. The base-plate may be threaded to fit the stage, or three bits of plasticene may be used at roughly 120-degree positions beneath the base-plate to give the structure steadiness. The specimen is held from above by any suitable means, such as clamps, bakelite, or plasticene in the central holder, with the facets of the specimen approximately horizontal. Starting with a low-power objective, one brings a given facet into approximate horizontality by means of the three leveling screws.

With practice, manipulation of the leveling screws becomes much easier by acquainting oneself with the relationship between focus and the motion of the three screws.

As for meeting the problem of surface irregularities, an electric hand-grinder of the type also shown in Fig. 1 is a simple answer. Working the tool while observing the specimen under binoculars, one can perform operations on interfering promontories sufficiently delicate to allow the use of a contact objective on almost any specimen. A variety of tips can be obtained for this instrument allowing grinding, drilling, or buffing, the latter operation being used for applying a polish-etch technique to individual cleavage structures. Needless to say, a long-nosed objective lens is especially suited for this work.

Materials Studied in This Research—In Table I the materials used in this research are listed and described.

OBSERVATIONS

Appearance of Grains and Grain Boundaries—In contrast to the appearance of a grain boundary in most polished and etched specimens as a narrow depression on a flat face, grain boundaries of fractographic specimens appear as shown in Fig. 2. The change in cleavage direction because of the different orientation of contiguous grains gives a ridge-like effect, the secondary grain being in shadow and generally proceeding out of focus away from the boundary of the focussed facet.

In this case, the specimen is a low silicon (1.59 per cent silicon) ferrite (See Table I). Note that the cleavage facet is intersected by visibly crystallographic planes, along with other natural markings of less regular characteristics whose nature remains to be explained. Since this alloy is known to cleave on $\{100\}$ planes (19), and since these intersecting markings are obviously cleavages because they actually bound fragmented and removed material, we can assume the markings also follow $\{100\}$ planes. The only visible planar angle is 90 degrees, which is in keeping with that assumption. If these markings represent planes other than $\{100\}$, such as $\{110\}$, $\{112\}$ or $\{123\}$ slip markings, or $\{112\}$ Neumann bands, which also can show 90 degree registrations on a $\{100\}$ cleavage, we would be confronted with interesting instances of cleavage occurring on slip or twinning planes. Furthermore, the same specimen subsequently deep etched (Fig. 2) proves that these crystallographic markings are either real

Table I
Materials Used in this Research

Specimen	Composition (In Per Cent)	Condition
Armco Ingot Iron	C = 0.013 Mn = 0.019 Si = 0.001 P = 0.003 S = 0.018 O = 0.03 N = 0.005 Cu = 0.041 Ni = 0.02 Sn = 0.008 As = 0.012 Others = 0.01	Commercial grade, hot-rolled. Specimen $\frac{1}{4}$ inch square cleaned by rough polishing, cathodized 60 minutes 10 per cent NaOH, 20 degrees Cent., 3 amps./in. ² Nicked with a saw and fractured by hammerblow.
Type 405 Stainless Steel (Modified)	Cr = 14.29 C = 0.047 Al = 0.23 Mn = 0.52 Si = 0.38 Ni = 0.23 S = 0.016 P = 0.020	Air-cooled after hot-rolling to $2\frac{1}{4}$ by $\frac{7}{8}$ inch.
Type 446 Stainless Steel	Cr = 26.10 C = 0.104 Mn = 0.45 Si = 0.63 Ni = 0.13 S = 0.010 P = 0.010	Annealed 40 hours at 1600 degrees Fahr. and water-quenched.
Silicon Ferrite	Si = 1.59 C = 0.034	Melted in induction furnace from Armco ingot iron and ferrosilicon (50 per cent). Cast in 5-lb. cast-iron molds. Fractured by hammerblow in as-cast condition.
Silicon Ferrite	Si = 4.24 C = 0.038	Ditto
Silicon Ferrite	Si = 4.96 C = 0.042	Kindly supplied by Dr. C. S. Barrett. (See Ref. No. 18, specimen from Allegheny Steel Co.). Commercial heat, 12 by 12 by 36-inch ingot cooled slowly under hot slag. As-cast crystals fractured by hammerblow.
Silicon Ferrite	Si = 11.84 C = 0.038	Same treatment as 2 per cent.
Silicon Ferrite	Si = 18.10 C = 0.052	Ditto
Silicon Ferrite	Si = 28.83 C = 0.040	Ditto
Silicon Ferrite	Si = 50.18 C = 0.122 P = 0.045	Commercial 50 per cent ferrosilicon as-cast. Fractured by hammerblow.
Silicon Ferrite	Si = 78.26 C = 0.045 P = 0.021	Commercial 75 per cent ferrosilicon as-cast. Fractured by hammerblow.
Antimony	Sb = 99.811 Pb = 0.035 As = 0.035 S = 0.04 Fe = 0.015 Cu = 0.01	Commercial antimony as-cast. Fractured by hammerblow.
Bismuth	Bi = 99.8 Ag = 0.01 Pb = 0.005 Fe = 0.01 Cu = 0.005 S = 0.01	Commercial bismuth as-cast. Fractured by hammerblow.
Rock Salt	NaCl = 98.51 Ca ₂ SO ₄ = 1.02 Moisture = 0.04 Other Imp. = 0.37	Commercial grade. Fractured by hammerblow.

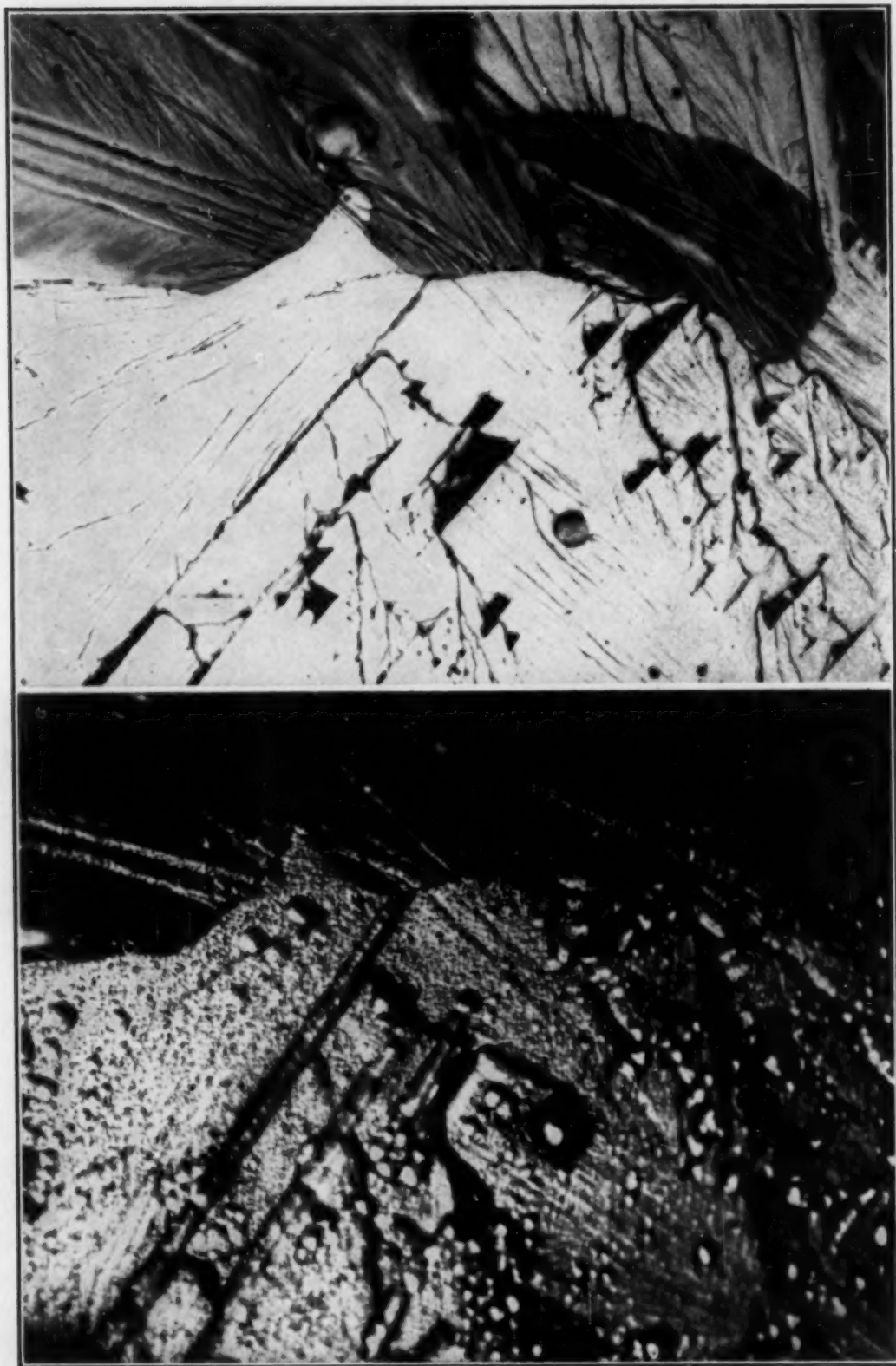


Fig. 2—Cleavage Facet of Cast 1.59 Per Cent Silicon Ferrite. (Above) Unetched. (Below) Heavily Etched. $\times 500$.

discontinuities or narrow zones of disorganized or reoriented material in the atomic structure.

Comparison of Metallic and Nonmetallic Cleavage Structures— Although metals are distinguished as a class by their unique deformability, when fractured in a brittle manner they often show informative similarities with nonmetallic crystals. Thus, ingot iron shows well-developed crystallographic markings on its fracture which are not unlike those shown by common salt (See Fig. 3). Note the passage of the markings through what appears to be a grain, or lineage, boundary of the ingot iron.

In rock salt, the similar crystallographic markings may be part of the rather well known imperfection structure of the NaCl lattice (20), a structure much argued for metals. Theoretically, NaCl should show a tensile strength of 285,000 pounds per square inch; actually, it shows a strength of only 5700 pounds per square inch, apparently because the lattice is not continuous. By suppressing the weakening effect of these discontinuities, the strength of rock salt has been increased from 5700 pounds per square inch to nearly 225,000 pounds per square inch (21), (22). Since metals similarly show an actual tensile strength of only one per cent or so of the theoretical, any possible analogy with the deformation of salt crystals obviously provides fascinating speculation. Perhaps precipitation hardening should be understood as the precipitation of a second phase within preexistent vacuities, the precipitate simultaneously lowering the ductility by keying adjoining blocks and raising the strength by welding across the vacuity. Tensile strengths have been raised several hundred per cent by precipitation hardening; but compared to the theoretical load the metal lattice should withstand, the present state of development by precipitation hardening is scarcely a beginning.

In Fig. 4, a much more complicated substructure shows itself. A 4.24 per cent silicon ferrite (See Table I) fractured in the as-cast condition revealed this intricate combination of fernlike, or lineage, network bounded and subdivided by a crystallographic cell-like structure, all within one grain. The detail of the lineage structure largely escapes resolution at this magnification, but close examination reveals an elaborate structure that is especially remarkable because of its small size.

Fragmentation in the lower right leads to designating the principal rectangular markings as $\{100\}$ cleavages. Note that the large

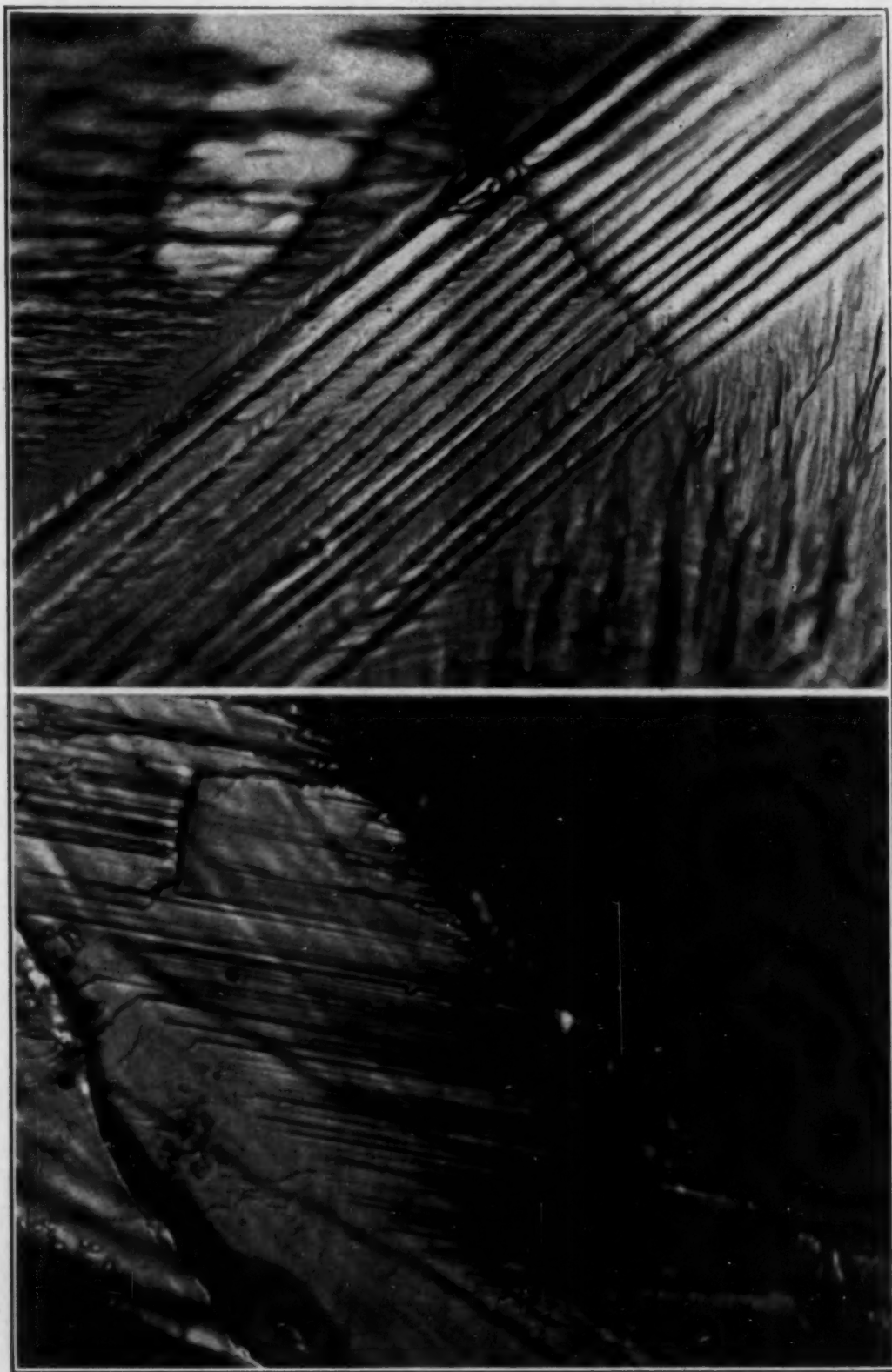


Fig. 3—Fracture Comparisons. (Above) Cathodized Armco Ingot Iron. $\times 750$.
(Below) Rock Salt. $\times 200$.

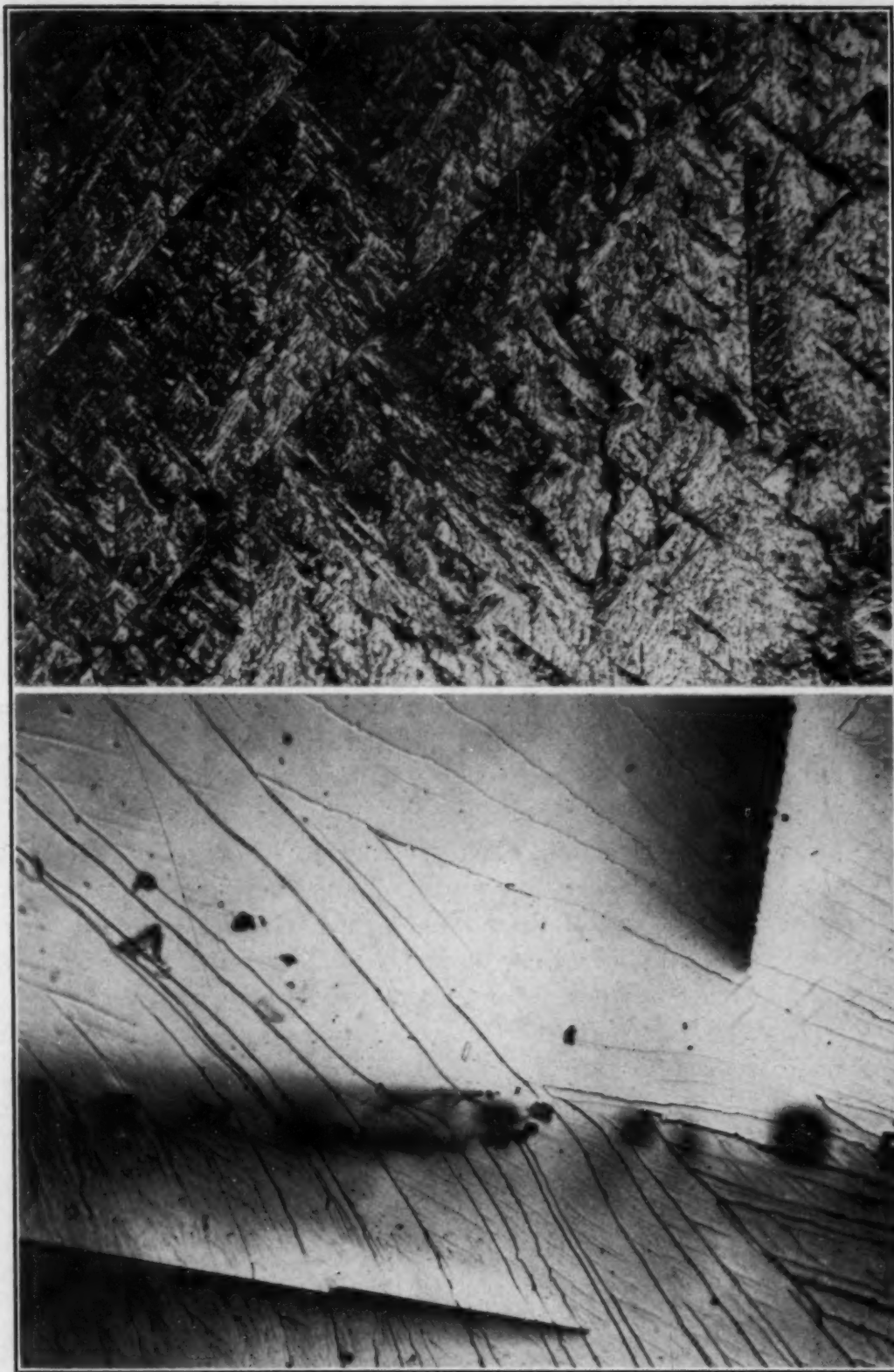


Fig. 4—Fracture Comparisons. (Above) As-Cast 4.24 Per Cent Silicon Ferrite. $\times 100$. (Below) Rock Salt. $\times 200$.

crystallographic markings appear slightly depressed. Also note the single contraposed crystallographic marking (vertical line to right center) at 45 degrees to the major markings. Obviously, this, too, cannot represent cleavage, which occurs on $\{100\}$ planes for this material (18) and therefore contains no 45-degree traces on a $\{100\}$ plane. Slip, which occurs here on $\{110\}$ planes, could have a 45-degree trace, as could twinning on $\{112\}$.

In comparison, the accompanying photomicrograph of fractured rock salt shows a possibly similar pattern, especially with respect to the effect of relief about the geometric markings. The nature of this relief seen in both these cases is not clear. As for the non-rectangular and semi-rectangular markings, close observation shows that their apparent direction is deceiving, and that they actually progress in a minute stepwise manner.

Fractured bismuth in Fig. 5 shows at least four separate structures, some known and some unknown. The darkest markings represent fissures whose crystallographic progression, as in the preceding case of rock salt, can be seen at high magnification to consist of minute steps. On a macroscopic scale, these fissures perhaps delineate the so-called lineage structure of the crystal (17).

The grey bands can be assumed to be twins, since bismuth belongs to that class of crystals which deform by twinning instead of by slipping (19), and their appearance here is typical of twin bands.

For that very reason, however, the fine background of *striae* at three well-marked 60-degree positions is especially puzzling. If slip were common to bismuth, these *striae* might be assigned to slip lines. If twins, they certainly show little resemblance in size, shape, and distribution to the other twins and consequently would offer some new information on the mechanism of twinning. In view of the basal cleavage of bismuth, and the 60-degree disposition of the *striae* on that basal plane, the *striae* can logically be identified as a function of prismatic or pyramidal planes. Perhaps under the conditions of fracture they represent some type of conjugate slip occurring during the separation of the cleavage faces; or they may be the $\{111\}$ "imperfect cleavages" discussed by Goetz (7).

Whatever these *striae* are, their complete and consistent failure to show a change of direction upon crossing the twin bands is notable. Certain planes, of course, are unaltered by the twinning mechanism, such as the twinning plane itself and those planes which are perpendicular to the twinning plane and contain the shear direc-

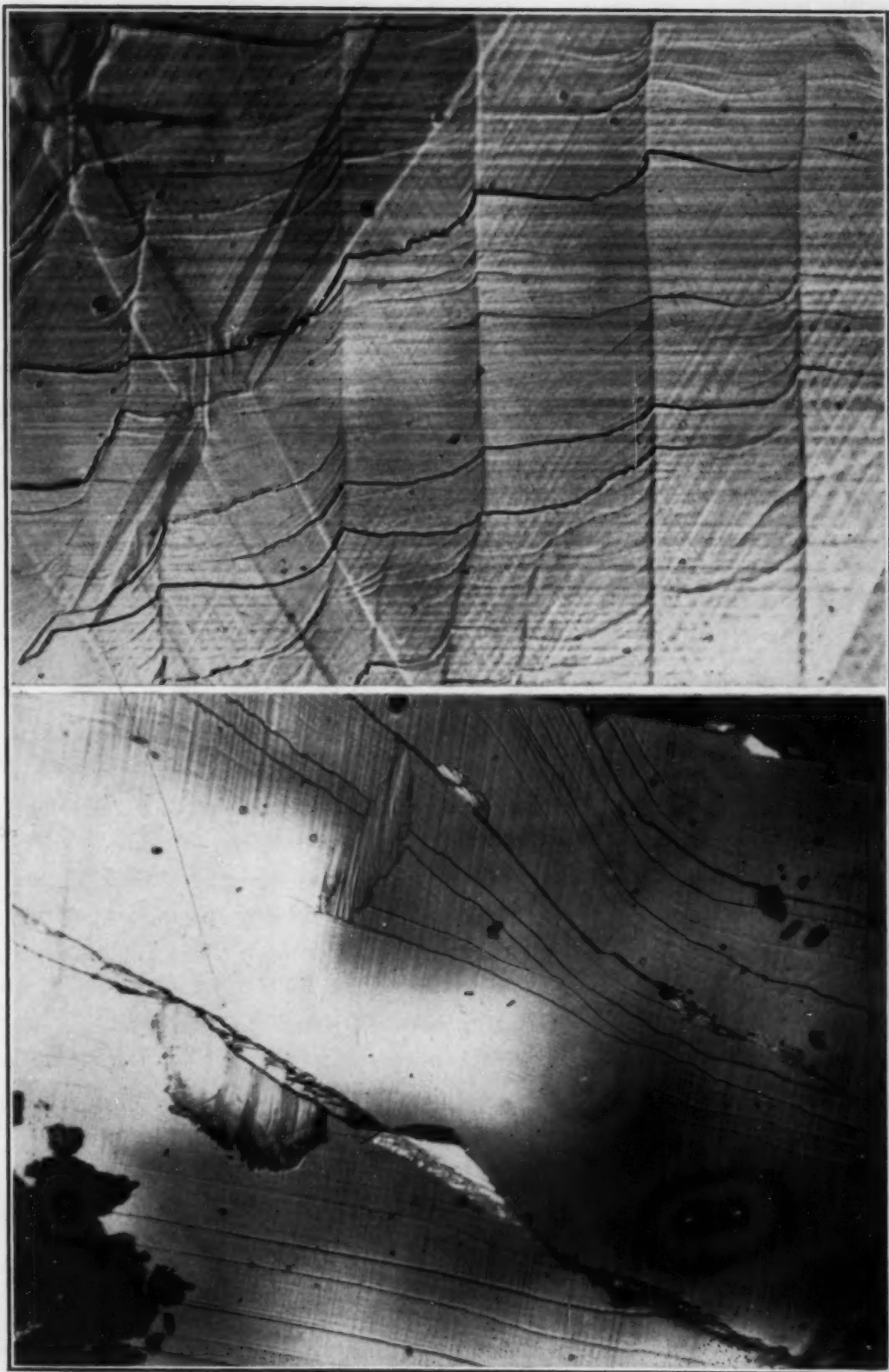


Fig. 5—Fracture Comparisons. (Above) Bismuth. $\times 500$. (Below) Rock Salt. $\times 200$.

tion. But the possibility that a network of markings lying along three directions and enclosing equilateral triangles, as this does, can traverse twinned zones without revealing the crystallographic shift in those zones, seems difficult to explain readily.

Similar background striae, incidentally, can also be seen on the rock salt fracture in this figure, and in the previous Fig. 3, though in this case they are at 90 degrees, conforming to the cubic symmetry of rock salt. In NaCl, deformation beyond 1 per cent splits the spots on a Laue pattern and apparently produces slip on one, or possibly two, systems of planes (23). These striae may be related to the {110} plane imperfections seen developing in rock salt crystals when stressed in a beam of polarized light (24).

An even more peculiar structure sometimes found in bismuth crystals is the ridge-like semi-crystallographic structure that one might refer to as rifflemarks (See vertical markings in upper photograph of Fig. 5). Lying at roughly 30 degrees to one family of twin bands and bisecting a 60-degree angle between striae, these markings strongly deflect the lineage fissures, show no interaction with the twin bands other than relief, and are crossed by the striae with no indication of any interaction whatsoever—the striae lying across all structures with an independence that suggests they are the last structure to be developed before actual cleavage.

This angular relationship of the rifflemarks seems necessarily to place them on a third family of planes. That is, the plane of the photograph being the basal cleavage plane, the one family of planes showing as striae concerns one set of intersecting planes, and the rifflemarks concern another. The very noticeable effect of the rifflemarks on the paths of the fissures suggests that the riffle mark is a cleavage marking, necessarily nonbasal, and that some separation or loosening has occurred along them, perhaps in a faulting action which was previous to the development of the fissure. If that is true, however, then the striae, which concern another set of planes, are not likely to be the imperfect cleavages claimed by Goetz (7), unless two such sets of imperfect cleavage exist.

At first an attempt was made to relate certain of these markings to superimposed stress patterns from a possible shock-wave or chattering effect during fracture; but the markings are always symmetrical with the crystal's orientation, and not with the direction of the fracturing force. They very likely represent some intrinsic and internal distribution of mass or stress, or both, which is part of the

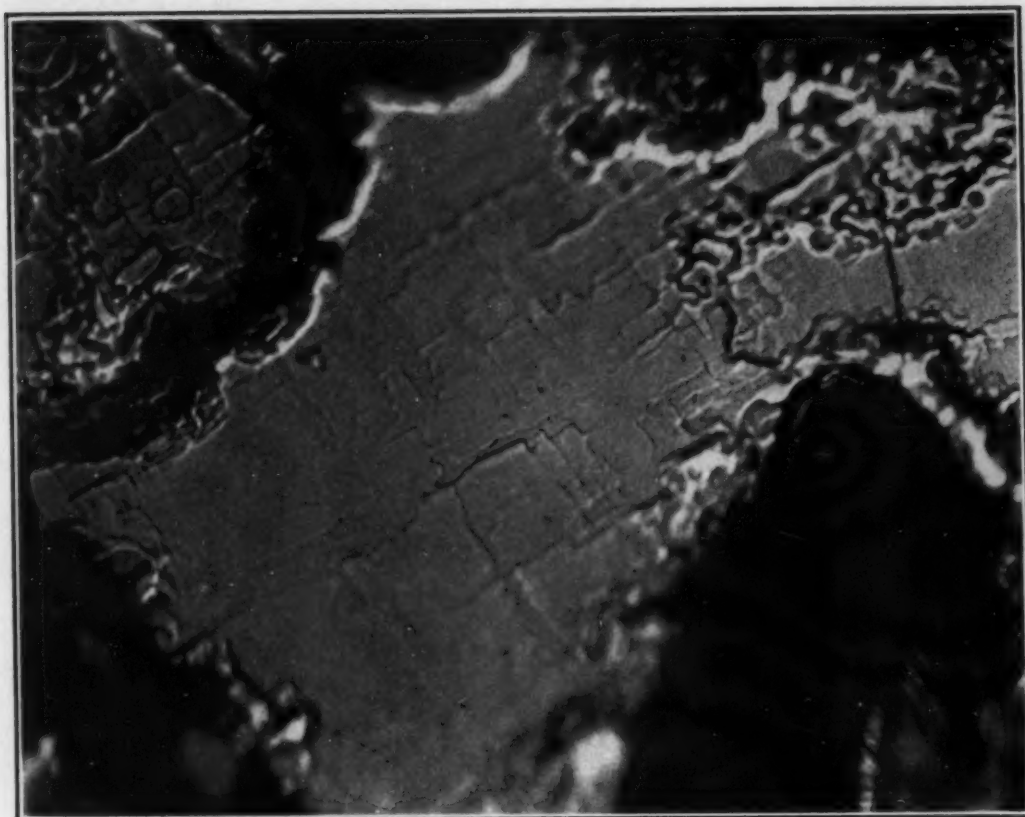


Fig. 6—Phase Determination with Fractography. Fractograph of 75 Per Cent Ferrosilicon Showing the Characteristic Fracture Pattern of Fe_2Si_5 . $\times 500$.

crystalline structure remaining to be explained. Perhaps these patterns are typical of real crystals, as opposed to ideal crystals, and depict crystalline adaptation to inhomogeneous constitution and internal stress. If that is the case, fractographic examination may become useful in searching for and studying these conditions.

Determination of Constitution by Fractography—Phases can usually be recognized on a fractograph as conveniently as on a polished and etched specimen, for the fracture type of a phase is as distinctive as its etch type. In Fig. 6, for example, a small chip of 75 per cent ferrosilicon observed fractographically immediately reveals its two phases without further treatment. The bright portion with the flat dendritic pattern is Fe_2Si_5 and may be recognized as such wherever it occurs (25). The iron-saturated silicon, or theta, phase, is friable and difficult to handle and comprises the dark, unresolvable background.

Etching techniques may be used, too, of course. Fig. 7 shows an ordinary polished-etched specimen of 18.10 per cent ferrosilicon, re-

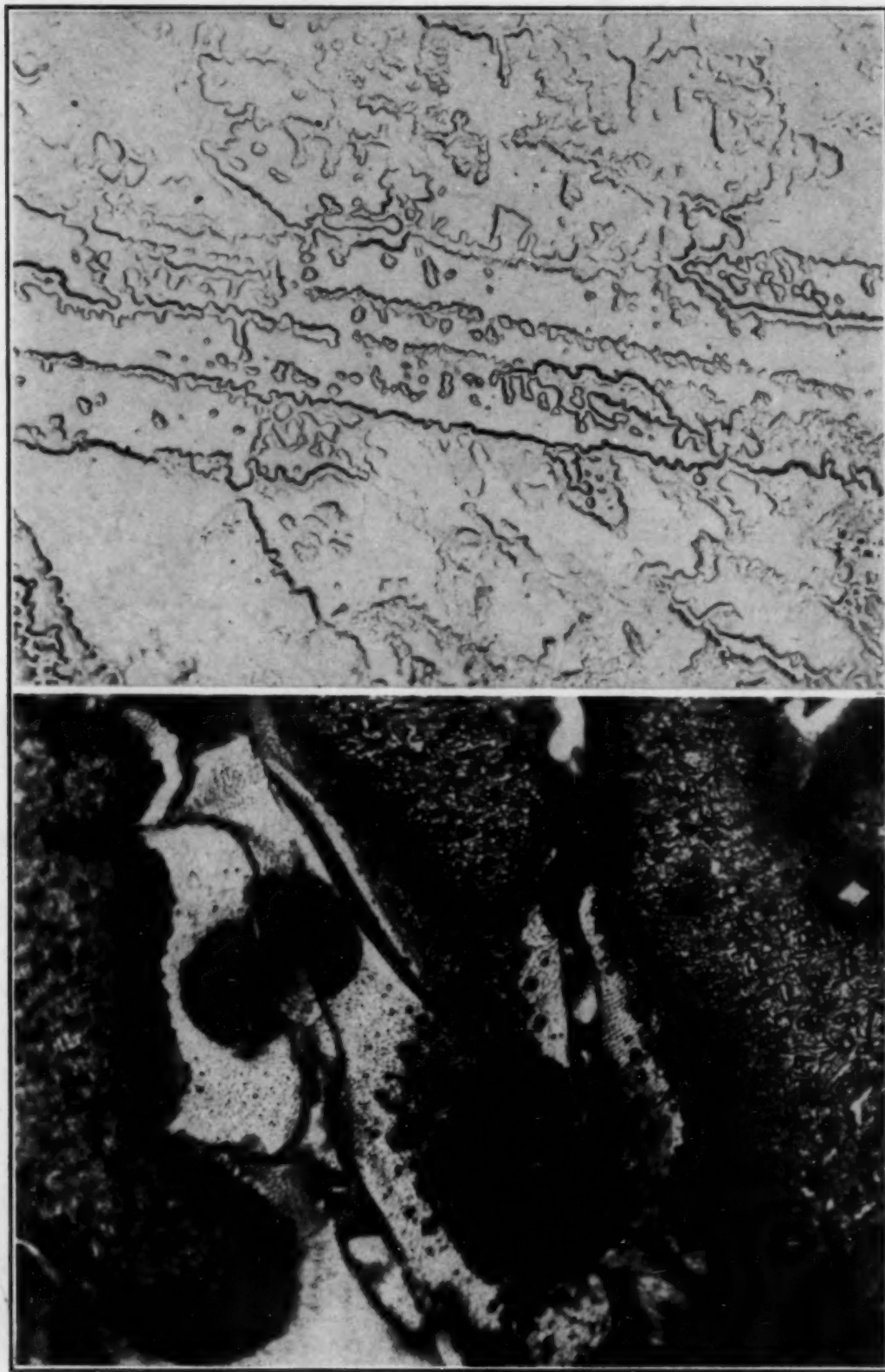


Fig. 7—Phase Determination with Fractography. (Above) Ordinary Polished Specimen of 18.10 Per Cent Ferrosilicon Etched with 25 Per Cent HNO_3 . $\times 100$. (Below) Heat-Etched Fracture. $\times 500$.

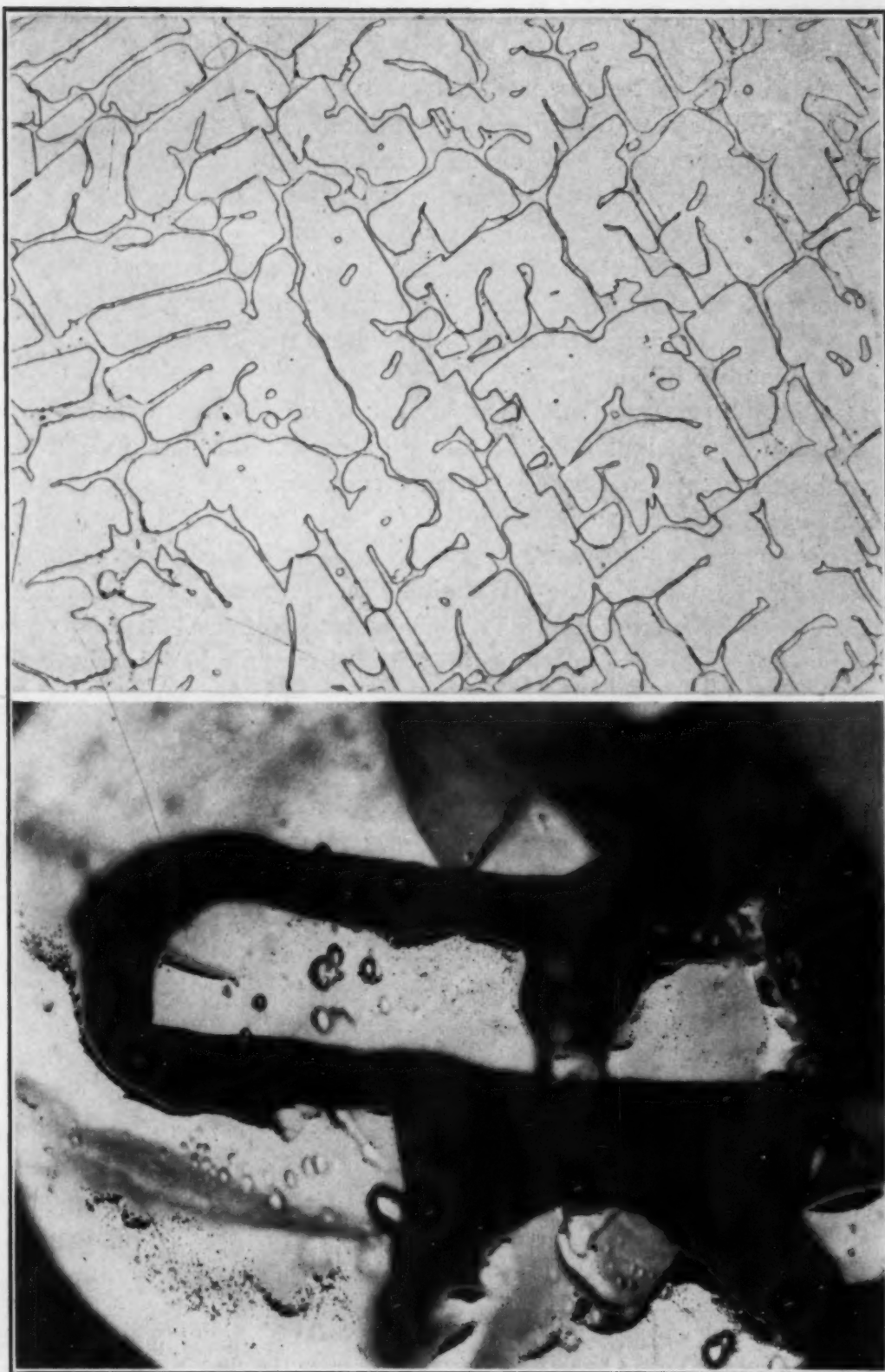


Fig. 8—Phase Determination with Fractography. (Above) Ordinary Polished Specimen of 28.83 Per Cent Ferrosilicon Etched with 25 Per Cent HNO_3 . $\times 100$. (Below) Fracture Etched with 20 Per Cent HNO_3 —20 Per Cent HF Solution. $\times 1000$.

vealing two phases which apparently are FeSi and either alpha iron containing silicon, or Fe_3Si (26). A chip of the material was heat-tinted in a brief treatment in an electric furnace at 1800 degrees Fahr. (980 degrees Cent.). Its heat-tinted fractograph, also shown in Fig. 7, revealed the two phases immediately. Furthermore, the two phases can be distinguished by tone from one another in the fractograph, the lighter being higher in silicon.

In Fig. 8, acid etching is compared for a polished specimen and a fractured specimen. In the fractured specimen, one phase has dissolved away, leaving the dendritic branch of the less soluble primary phase plainly visible.

*New Structures, and New Facts about Known Structures—*Probably a principal use of fractography will develop around expanding our information on known structures, since a simple, well-established microconstituent may show an astonishing assortment of new structures on a fracture. For example, in Fig. 9 a customary photomicrograph of Type 405 stainless steel (See Table I) is compared with its fractograph. This particular specimen had been overheated during hot rolling, and large brittle crystals had formed in a somewhat decarburized surface layer. Its condition made it ideal for fractographic examination, and the photographs were taken in this surface zone.

While the polished and etched field is typical and simple in appearance, the fractograph contains such a mass of large-scale and small-scale detail that much more work will be necessary to explain it all. Obvious lineage growths and block formation, all within a single grain, are but part of the story contained in this photograph.

In Fig. 10, a similar pair of photographs is shown for Type 446 27-Cr steel. The specimen was annealed for 40 hours at 1600 degrees Fahr. (870 degrees Cent.) and water-quenched to develop large grains and brittleness, making it especially suitable for fractographic examination. Once again, the polished and etched field is typically plain; whereas the fracture is a mass of detail. Much definition is lost in a reproduction; but under the microscope one sees tiny dendritic units, shown on the photograph as small white markings; and all changes in elevation appear to progress in discrete steps, or levels, which uniformly measure some fraction of a micron in thickness. Carbide particles, though probably not visible in the reproduction, can easily be seen in the microscope. The grain size is also estimable, since the grain boundary ends the flatness of a field.

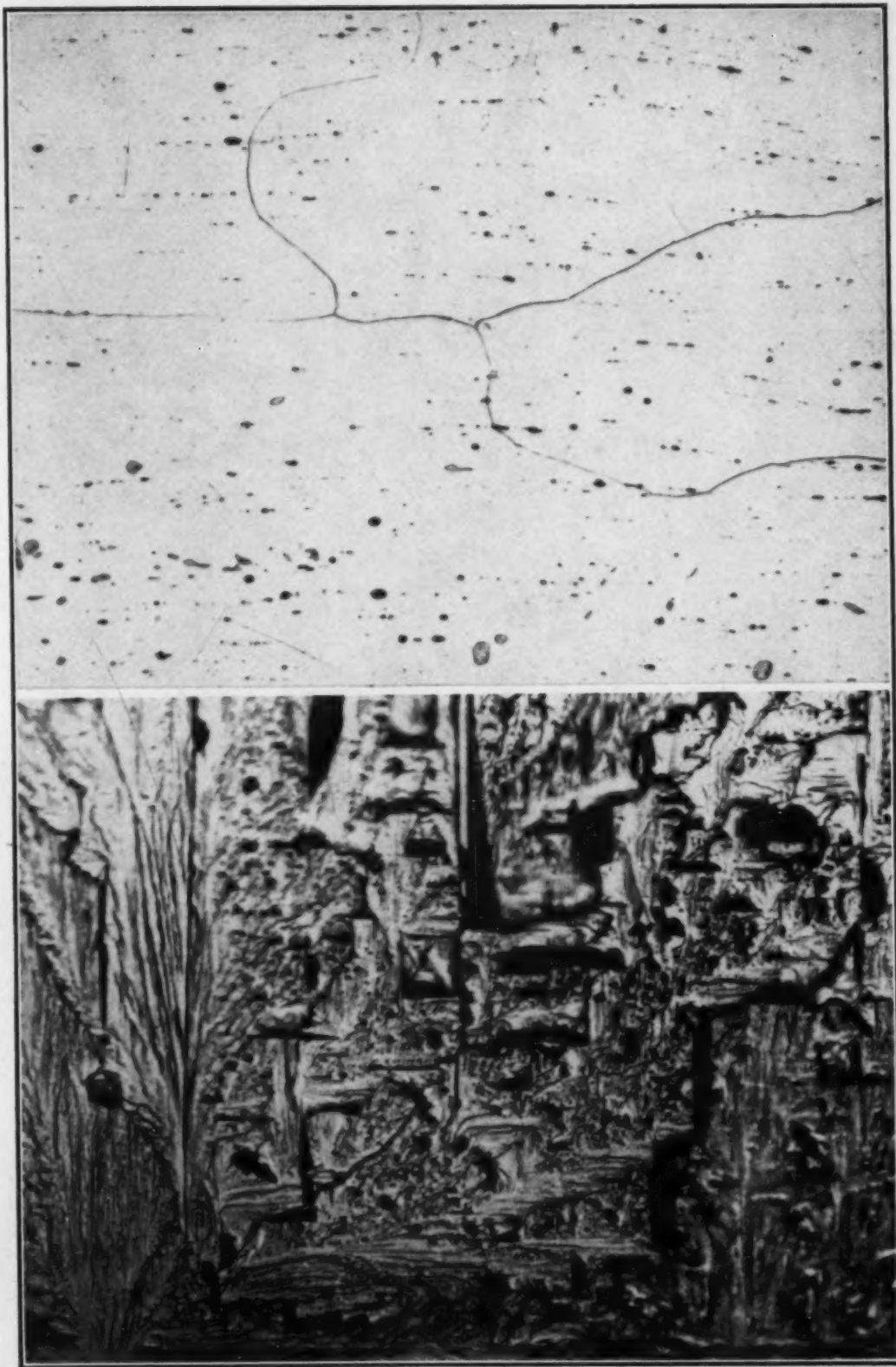


Fig. 9—Large-Grained and Decarburized Surface Layer of Type 405 Stainless Steel Air-Cooled from Hot-Rolling at 2000 Degrees Fahr. (1095 Degrees Cent.). (Above) Polished Specimen Etched in HCL—Picric Acid. $\times 100$. (Below) Fractograph. $\times 750$.

vealing two phases which apparently are FeSi and either alpha iron containing silicon, or Fe_3Si (26). A chip of the material was heat-tinted in a brief treatment in an electric furnace at 1800 degrees Fahr. (980 degrees Cent.). Its heat-tinted fractograph, also shown in Fig. 7, revealed the two phases immediately. Furthermore, the two phases can be distinguished by tone from one another in the fractograph, the lighter being higher in silicon.

In Fig. 8, acid etching is compared for a polished specimen and a fractured specimen. In the fractured specimen, one phase has dissolved away, leaving the dendritic branch of the less soluble primary phase plainly visible.

New Structures, and New Facts about Known Structures—Probably a principal use of fractography will develop around expanding our information on known structures, since a simple, well-established microconstituent may show an astonishing assortment of new structures on a fracture. For example, in Fig. 9 a customary photomicrograph of Type 405 stainless steel (See Table I) is compared with its fractograph. This particular specimen had been overheated during hot rolling, and large brittle crystals had formed in a somewhat decarburized surface layer. Its condition made it ideal for fractographic examination, and the photographs were taken in this surface zone.

While the polished and etched field is typical and simple in appearance, the fractograph contains such a mass of large-scale and small-scale detail that much more work will be necessary to explain it all. Obvious lineage growths and block formation, all within a single grain, are but part of the story contained in this photograph.

In Fig. 10, a similar pair of photographs is shown for Type 446 27-Cr steel. The specimen was annealed for 40 hours at 1600 degrees Fahr. (870 degrees Cent.) and water-quenched to develop large grains and brittleness, making it especially suitable for fractographic examination. Once again, the polished and etched field is typically plain; whereas the fracture is a mass of detail. Much definition is lost in a reproduction; but under the microscope one sees tiny dendritic units, shown on the photograph as small white markings; and all changes in elevation appear to progress in discrete steps, or levels, which uniformly measure some fraction of a micron in thickness. Carbide particles, though probably not visible in the reproduction, can easily be seen in the microscope. The grain size is also estimable, since the grain boundary ends the flatness of a field.

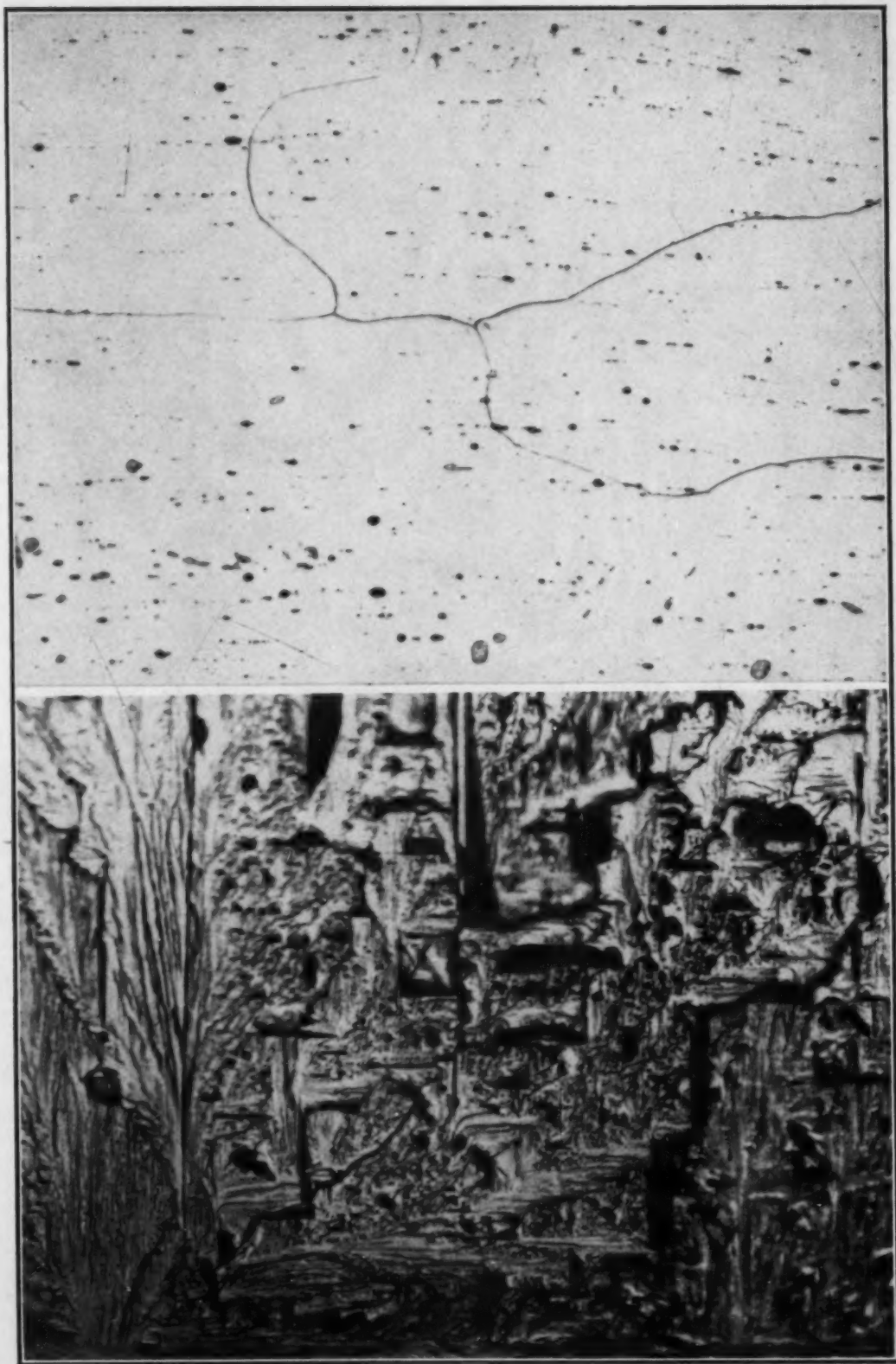


Fig. 9—Large-Grained and Decarburized Surface Layer of Type 405 Stainless Steel Air-Cooled from Hot-Rolling at 2000 Degrees Fahr. (1095 Degrees Cent.). (Above) Polished Specimen Etched in HCL—Picric Acid. $\times 100$. (Below) Fractograph. $\times 750$.

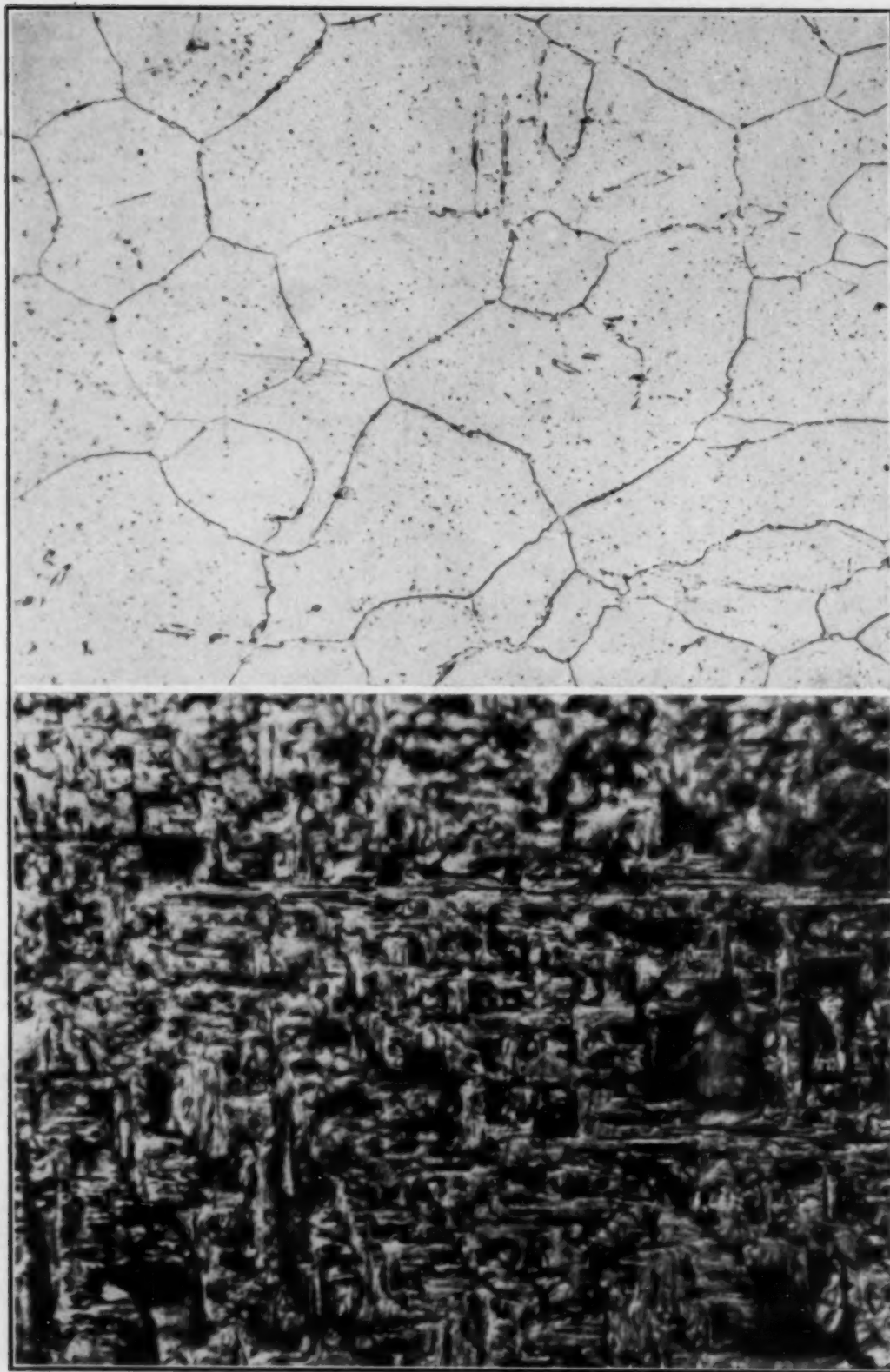


Fig. 10—Type 446 Stainless Steel Annealed 40 Hours at 1600 Degrees Fahr. (870 Degrees Cent.). Water-Quenched. (Above) Polished Specimen Etched with Mixed Acids in Glycerol. $\times 100$. (Below) Fractograph. $\times 750$.

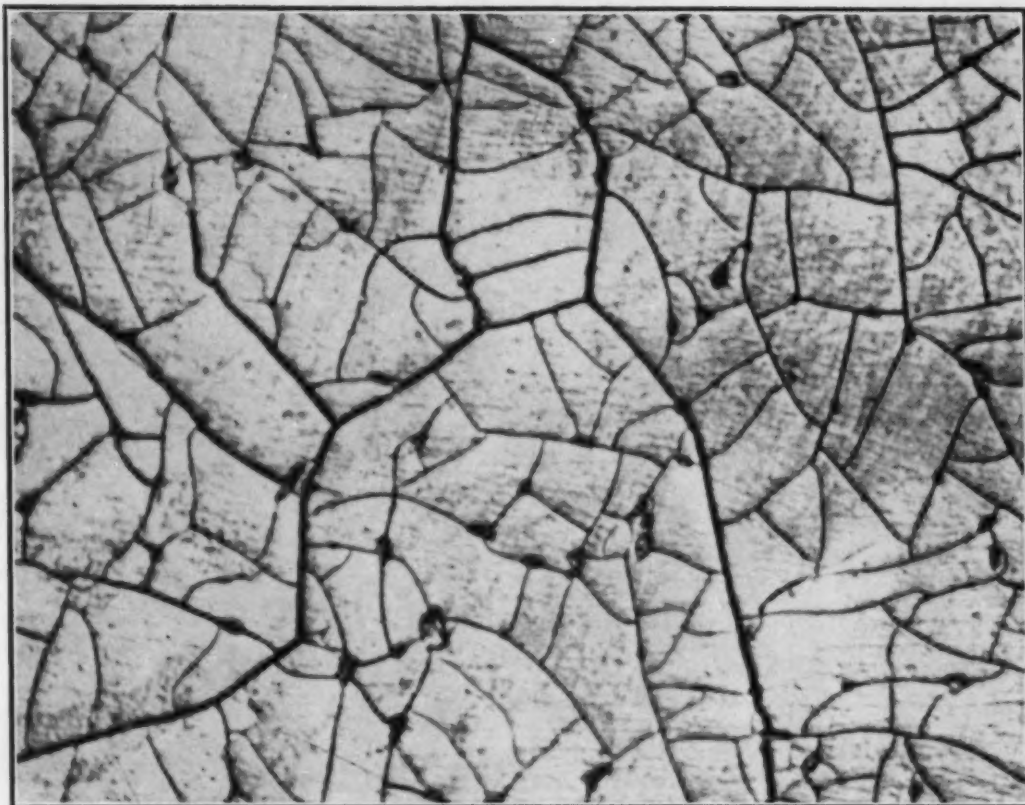


Fig. 11—Polished Specimen of 11.84 Per Cent Ferrosilicon Etched in 25 Per Cent HNO_3 . $\times 100$.

In other words, the fractograph conveys most of the information contained in a polished sample, and in addition displays an incredible amount of detail remaining to be cataloged. Discussion of this detail lies beyond the scope of the present paper.

As a further illustration of the prolific detail contained in some fractographs as compared to the polished and etched specimen, an 11.84 per cent ferrosilicon (See Table I) is depicted in Figs. 11, 12, and 13. Much argument has centered over alloys of approximately this composition, and most investigators agree that they lie within the alpha solid solution range of the binary diagram; yet, anomalies in their behavior are consistently reported which would indicate that they are not a simple solid solution.

Fig. 11 shows a customary polished specimen of cast 11.84 per cent ferrosilicon etched with 25 per cent HNO_3 . The microstructure is somewhat unusual because of the network of sub-boundary markings. Nevertheless, polishing and etching here reveals nothing but a single phase.

Fractographs, on the other hand, reveal a multiplicity of struc-

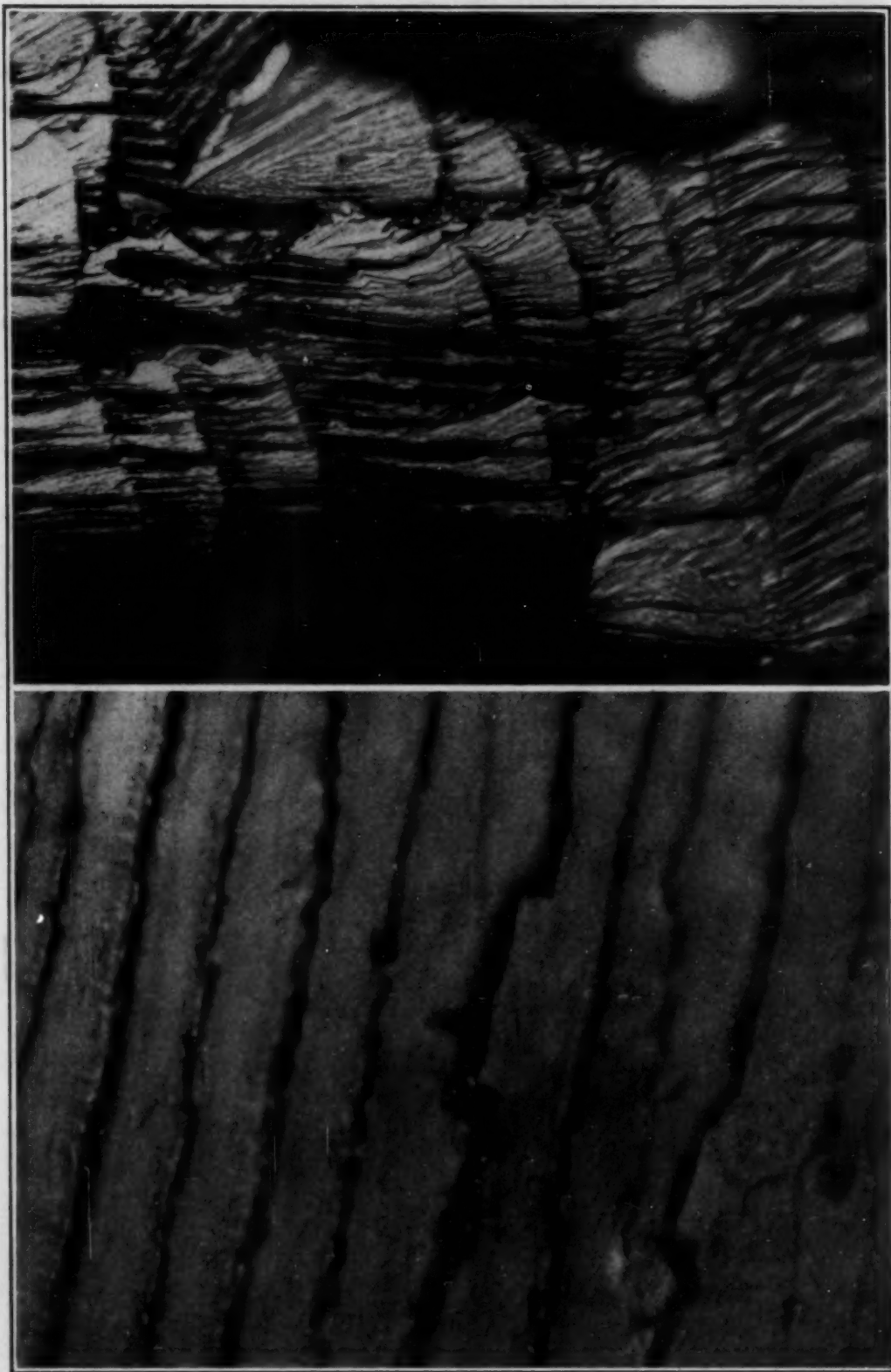


Fig. 12—Fractographs of 11.84 Per Cent Ferrosilicon. (Above) $\times 500$. (Below) $\times 2000$.

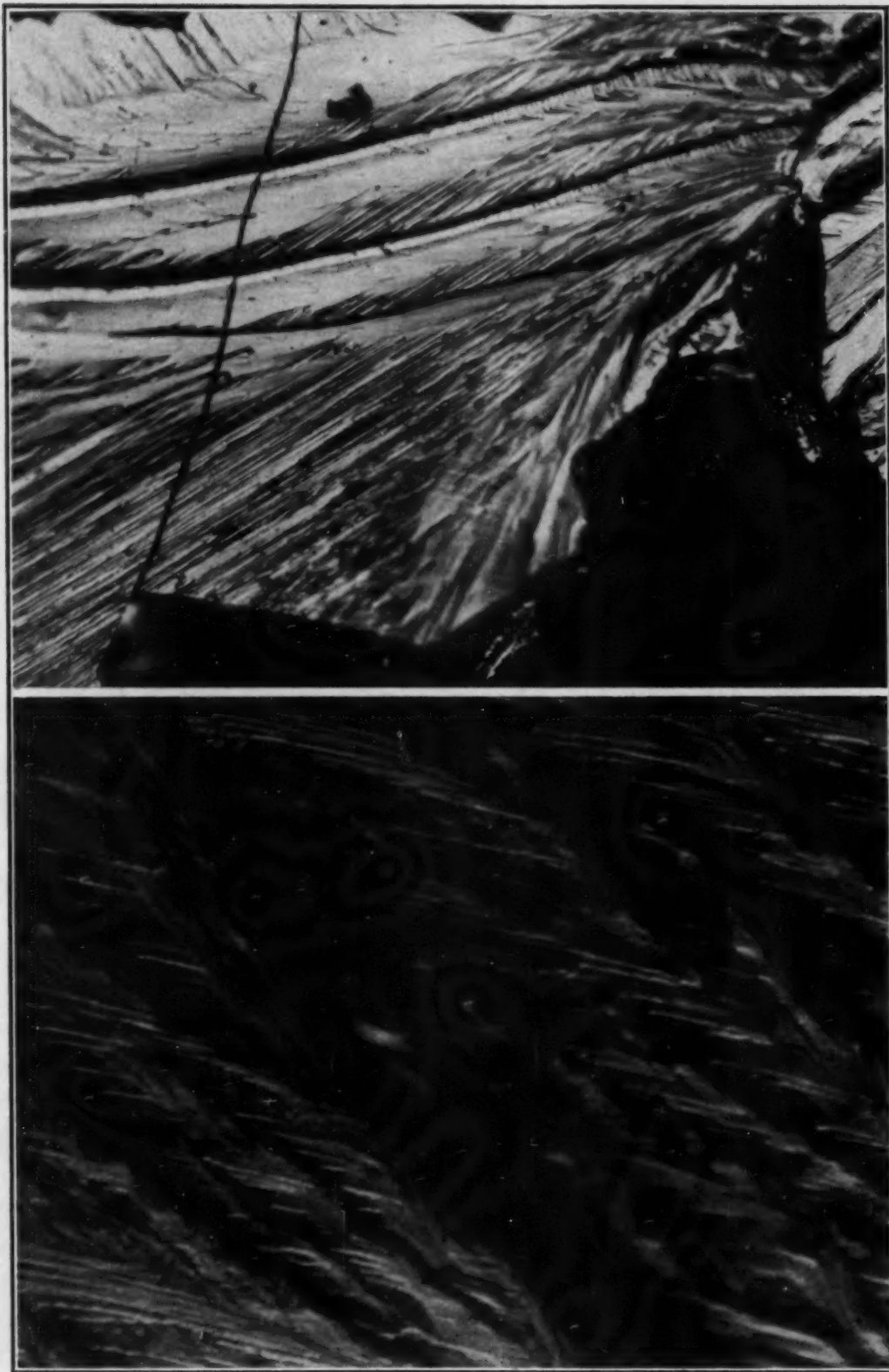


Fig. 13—Fractographs of 11.84 Per Cent Ferrosilicon. (Above) $\times 200$. (Below) $\times 2000$.

tures, which is not particularly consistent with what one might expect of a homogeneous solid solution, and which suggests some internal rearrangement characterizing this alloy. Four different fields selected throughout the casting are shown in Figs. 12 and 13.

The structure shown in the upper fractograph of Fig. 12 possibly resulted from a fracture parallel to the axis of a dendrite, which might account for the undulatory markings; or this pattern might be related to the markings on the specimens in the previous Fig. 4, and to the riffle marks in bismuth.

In the lower fractograph of Fig. 12, taken at 2000 diameters, one obtains a good view of the stepwise, or lamellar, nature of many fracture facets. Here we seem to have the basic structural pattern for pearlite in a metal which shows no pearlite. Etching only obliterates the structure. Since the dimensions of pearlite lamellae are nearly identical with the dimensions of this structure, one might speculate that the lamellar nature of pearlite, which has intrigued metallurgists for years, is the result of an action taking place within a structure whose characteristics of lamellar or block imperfection predetermine the disposition of the ferrite and carbide.

In the upper fracture of Fig. 13, a rib-like structure appears which is scarcely in keeping with the conception of a simple homogeneous phase. Of course, cast structures are not homogeneous. Nevertheless, a glance at the other alpha ferrosilicons in the previous Figs. 2 and 4 will show their almost complete dissimilarity with the fractures in Figs. 12 and 13. Although it is not so apparent here from the single fractographs of the 1.59 and 4.24 per cent ferrosilicon, these two alloys are rather similar in type (25). But the 11.84 per cent alloy shows radical departures which confirm opinions from other sources that some internal change, perhaps an ordering process, occurs in this portion of the alpha field (26).

The fourth and entirely different fractograph of the same alloy (See Fig. 13) shows a pattern not observed elsewhere. Based upon the same lamellar cleavage characteristics, discussed previously, the pattern here reminds one of a sheaf of wheat. Since this structure has no apparent relationship to another phase, it can be well explained on the basis of granular strains or imperfections whose existence is revealed only by fractography. None of these patterns was observed on polished and etched specimens.

DISCUSSION

As concluding examples of the new field for research afforded by such studies of cleavage facets at high magnification, Figs. 14 and 15 show structures which resist explanation on classical grounds. The pattern in Fig. 14, for example, is evidently a dendritic, or a growth pattern; yet, buffing this structure with a small buffing wheel

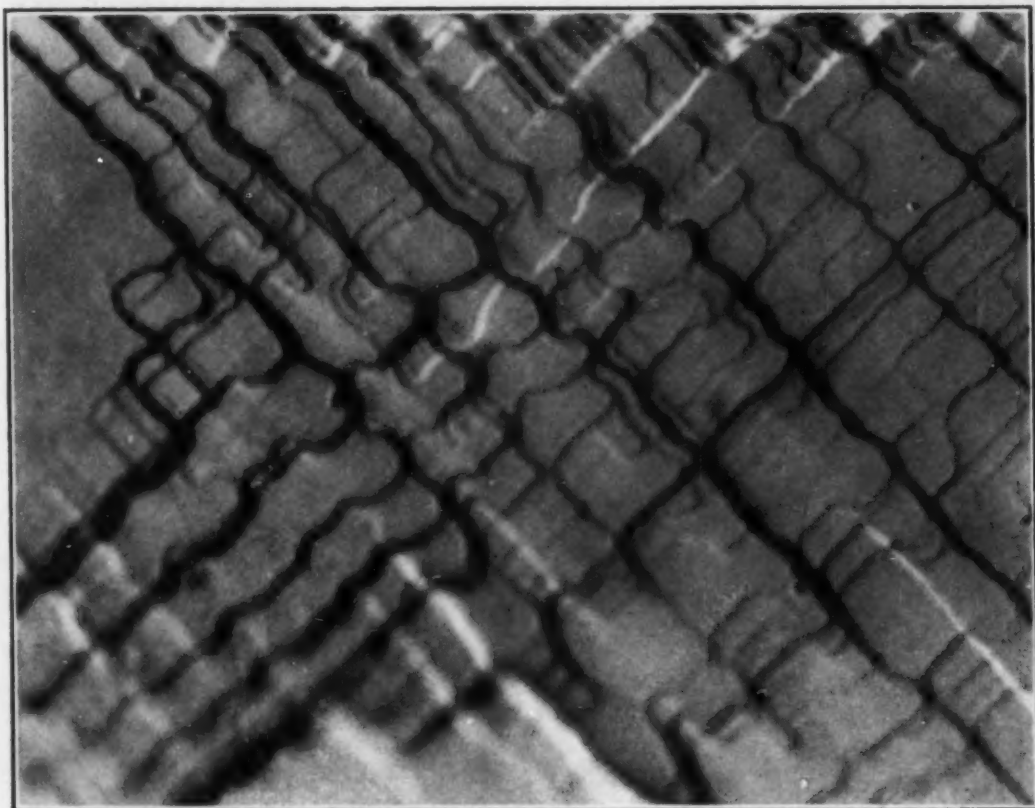


Fig. 14—Fractograph of Commercial 50 Per Cent Ferrosilicon Showing in Detail the Characteristic Cleavage Pattern of the Fe_2Si_5 Phase. $\times 2000$.

attached to the hand grinder and then etching the buffed surface with 20 per cent HNO_3 —20 per cent HF caused no reappearance of the pattern.

Certainly, such a cleavage pattern, existing as it does within a supposedly homogeneous phase, affords incontrovertible evidence that this is a pattern of lattice imperfection. The classic interpretation that deformation and cleavage are subject only to the spacing and density of certain atomic planes definitely fails here.

That is, the lamellar pattern in the lower part of the previous Fig. 12 could still be explained on classical grounds as a shift of cleavage from one set of planes to another parallel set because of some odd-angle direction of stress with respect to the cleavage direction; but the present pattern will allow no such argument. True, the cleavage in this ferrosilicon alloy undoubtedly follows classical cleavage planes; but these planes are in turn undoubtedly separated by

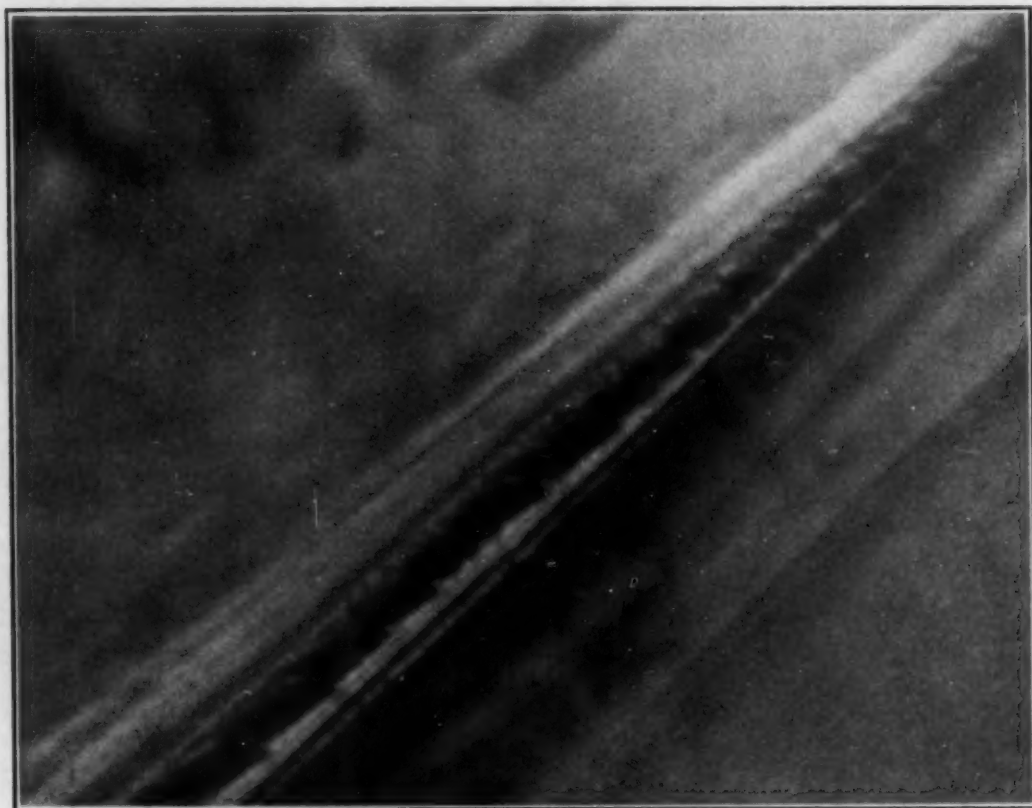


Fig. 15—Fractograph of 18.10 Per Cent Ferrosilicon Showing an Unusual Structure Within One of the Grains. $\times 4200$.

outright hiatuses which depict the pattern we observe and which represent sufficient weakness to influence and to deflect the path of cleavage as they do. One might presume that the growth of the grain in this case was dendritic or lineage, developing periodic discontinua, which, however, were too small to disrupt the gross crystallinity. This is in good agreement with the general understanding of imperfection structure in crystals, a conception that has been exceedingly slow in developing when one regards the vast simplification it offers to many fundamental metallurgical problems.

In Fig. 15, a structure with a remarkable appearance is shown.

Found in cast 18.10 per cent ferrosilicon, several of these needlelike formations lie within the grain. Its closest resemblance is perhaps a martensite needle, though this alloy should contain no martensite. Note the midrib declivity, the toothy markings, and the fainter parallel markings lying alongside. Also, note the magnification.

As this paper demonstrates, cleavage facets generally have a flatness which is as suitable for an oil immersion lens as the most carefully polished and etched specimen.

ACKNOWLEDGMENT

Acknowledgment is made to the Rustless Iron and Steel Corporation for the support of this work and permission to publish it as part of their program for fundamental research; and to Mr. A. L. Feild, Technical Director, under whose supervision the research was conducted.

References

1. R. A. F. de Réaumur, "The Art of Converting Iron Into Steel," Paris, 1722.
2. R. J. Haüy, "Traité de Minéralogie," Paris, 1801.
3. A. Martens, "The Microscopical Examination of Iron," *Z. Ver. deut. Ing.*, Vol. 21, 1878, p. 11-8.
4. "Dictionary of National Biography," Supplement, 1901-11, p. 355-6.
5. E. E. Jelley, "A Review of Crystallographic Microscopy," *Journal*, Royal Microscop. Society, Vol. 62, 1942, p. 93-102.
6. H. M. Howe, "Metallography of Steel and Cast Iron," N. Y., McGraw-Hill, 1916.
7. A. Goetz, "On the Experimental Evidence of the Mosaic Structure of Bi Single-Crystals," *Proceedings*, National Academy of Science, Vol. 16, 1930, p. 99-105.
8. J. A. Ewing and J. C. W. Humfrey, "The Fracture of Metals Under Repeated Alternations of Stress," *Transactions*, Royal Society, (London), Vol. 200A, 1902, p. 241-50.
9. J. A. Ewing and W. Rosenhain, "Experiments in Micro-Metallurgy: Effects of Strain. Preliminary Notice," *Proceedings*, Royal Society, (London), Vol. 65, 1899, p. 85-90.
10. J. A. Ewing and W. Rosenhain, "The Crystalline Structure of Metals," *Transactions*, Royal Society, (London), Vol. 193A, 1899, p. 353-75.
11. J. A. Ewing and W. Rosenhain, "The Crystalline Structure of Metals," *Transactions*, Royal Society, (London), Vol. 195A, 1900, p. 279-302.
12. W. Rosenhain, "Further Observations On Slip-Bands and Metallic Fractures," *Proceedings*, Royal Society, (London), Vol. 74, 1905, p. 557-62.
13. W. Rosenhain, "Deformation and Fracture in Iron and Steel," *Journal*, Iron and Steel Institute, (London), Vol. 70, 1906, p. 189-228.
14. W. Rosenhain, "Metallurgy: An Introduction to the Study of Physical Metallurgy," N. Y., Van Nostrand, 1st Edition, 1915.
15. O. Mügge, "On the Production of Artificial Twinning by Pressure on Antimony, Bismuth and Diopside," *Neues Jahrb. Mineral*, Vol. 1, 1886, p. 183-91.

16. C. A. Zapffe and C. E. Sims, "Hydrogen Embrittlement, Internal Stress, and Defects in Steel," *Metals Technology*, Vol. 8, Technical Publication 1307, 1941; also, *Transactions*, American Institute of Mining and Metallurgical Engineers, Vol. 145, 1941, p. 225-61; disc. p. 261-71.
17. C. A. Zapffe and G. A. Moore, "A Micrographic Study of the Cleavage of Hydrogenized Ferrite," *Metals Technology*, Vol. 10, Technical Publication 1553, 1943; also, *Transactions*, American Institute of Mining and Metallurgical Engineers, Vol. 154, 1943, p. 335-53; disc. p. 352-9.
18. C. S. Barrett, G. Ansel and R. F. Mehl, "Slip, Twinning and Cleavage in Iron and Silicon Ferrite," *TRANSACTIONS*, American Society for Metals, Vol. 25, 1937, p. 702-33; disc. p. 733-6.
19. C. S. Barrett, "Structure of Metals," N. Y., McGraw-Hill, 1943.
20. C. H. Desch, "The Chemistry of Solids," Ithaca, N. Y., Cornell University Press, 1934.
21. A. F. Joffé, "Mechanical and Electrical Strength and Cohesion," *Transactions*, Faraday Society, Vol. 24, 1928, p. 65-72.
22. A. F. Joffé, "The Physics of Crystals," N. Y., McGraw-Hill, 1928.
23. Yu S. Terminasov, "X-Ray Study of Plastic Deformation in Crystals. II," *J. Tech. Phys.*, (U.S.S.R.) Vol. 9, 1939, p. 769-81; cf. *J. Tech. Phys.* (U.S.S.R.) Vol. 7, No. 20-1, 1937; C. A. Vol. 33, p. 7638.
"X-Ray Investigation of the Plastic Deformation of Crystals. III," *J. Tech. Phys.* (U.S.S.R.) Vol. 9, 1939, p. 1740-4; cf. C. A. Vol. 33, p. 7638; C. A. Vol. 34, p. 2668.
24. I. V. Obreimov and L. V. Shubnikov, "An Optical Method of Studying Plastic Deformation of Rock Salt," *Z. Physik*, Vol. 41, 1927, p. 907-19; C. A. Vol. 21, p. 2205.
25. C. A. Zapffe and M. Clogg, "Cleavage Structures of Iron-Silicon Alloys," *TRANSACTIONS*, American Society for Metals, Vol. 34, 1945, p. 108.
26. E. S. Greiner, J. S. Marsh, and B. Stoughton, "The Alloys of Iron and Silicon." *Alloys of Iron Monograph*, Engineering Foundation, N. Y., McGraw-Hill, 1933, p. 457.

DISCUSSION

Written Discussion: By N. P. Goss, research metallurgist, Cold Metal Process Co., Youngstown, Ohio.

The authors are to be commended for having developed a new method for examining metal structures.

Heretofore, a fracture test was usually made to determine whether it was woody or silky, and the former associated with inferior quality.

The method worked out by the authors greatly extends the usefulness of the fracture test, for without question if we knew more about the structure of the metal at the place of failure, the cause of fracture would be more clearly understood.

The illustrations presented in this paper bring out the vast complexity of the fractographic structure, and in a most convincing manner disclose the sub-boundary structure, or block structure of the grains.

The block structure theory of metals is now being slowly developed, and fractography should play an important part in its development, especially when supplemented by X-ray diffraction methods.

It must be admitted that our concepts of the inner structure of the grains, and their behavior where subjected to forces of deformation are not completely understood, mainly because the block structure theory has never been widely

X-ray diffraction evidence, i.e., X-ray patterns are capable of showing the block displacements in mosaic crystals or grains. From the nature of the X-ray diffraction diagrams it was also evident that the strength and cohesive properties, varied throughout the grain but possessed a sort of periodicity, which was due to the block structure. In other words grains are not homogeneous entities. The evidence presented in this paper certainly proves that grains are not homogeneous even when they appear to be so under the microscope when examined conventionally. Fig. 14 discloses that the cleavage was entirely dependent upon the inherent block structure; that while the cleavage is parallel to the same plane (crystal face), it has many step-like discontinuities, as one can observe in the cleavage pattern. Evidently the forces of cohesion vary from block to block, and cleavage takes place on the surfaces having the least cohesive strength.

Also note that the block facets appear smooth (Fig. 14). This may indicate the blocks composing this mosaic to be homogeneous. However, if these block facets could be subjected to higher resolving power, they might disclose further irregularities in the lattice structure. This possible fine mosaic structure of the block facets is structure insensitive to cleavage, however, this may not be so for some other physical property. On the other hand, the "block" facets shown in Fig. 14 may be actually perfect lattice blocks, varying from 10^{-3} to 10^{-4} cm. Blocks smaller than this cannot be resolved under the microscope, and must be measured by X-ray diffraction methods.

The imperfections in grains are no doubt initiated when a metal undergoes the transition from the liquid to the solid state. Many factors can influence the type of imperfections developed during crystallization.

Obviously when all the blocks are perfectly aligned then we have a perfect crystal and this state is usually described by saying that the internal surface or the block disjuncture is zero. To produce large perfect crystals is highly improbable, but a crystal composed of perfect blocks, 10^{-3} cm or smaller, is a greater certainty.

Large grains are invariably mosaic, but in some block dislocations are quite small; however, even when the block alignment is nearly perfect, the periodic block structure is inherent. For it can easily be shown that a fine mosaic, when given but a slight plastic deformation, suffers block dislocations 10^{-6} cm apart. Slip does not start on every possible slip plane, but on planes spaced several thousand atom layers apart. The block dislocations are spaced in a periodic manner, and elastic as well as plastic deformations are strongly modulated by the inherent block structure. It should be pointed out that at each block disjuncture there is a slight increase in the lattice spacing,³ the magnitude depending upon the relative rotational block displacement. (This may vary from a few seconds up to 5 degrees of arc.)

As the authors point out, their results are in "agreement with the imperfection structure of crystals, a concept that has been exceedingly slow in developing when one regards the vast simplification it offers to fundamental metallurgical problems," and may I add they have ripped the field wide open.

Written Discussion: By Raymond G. Spencer, chairman, Metals and Minerals Research, Armour Research Foundation, Chicago.

Any new tool should be judged from the standpoint of its future possible uses rather than from any consideration of its initial success. It is from this viewpoint that I find myself much interested in this paper. I am not convinced that the paper has added anything to our knowledge of metals. However, fractography may find many significant applications in metals research.

Since the concept of a mosaic structure of crystals has previously been well established, the statement made by the authors that the fractographs indicate such a substructure should be interpreted as an indication of the usefulness of fractography as a tool to study crystals with, and not as proof of a mosaic structure.

Since the method is capable of giving some information about the mosaic structure of crystals, I would like to suggest two fields in metals research where it might possibly give us some much needed information.

One of these fields is precipitation hardening. In age hardening, there is often a marked effect even before precipitation has progressed far enough to be detectable by ordinary metallographic procedure or by X-ray diffraction techniques. Possibly fractographs would indicate whether or not this precipitation is occurring in the small faults between the mosaic or is entering directly into the crystal lattice.

It has been found that very small amounts of alloying elements often improve notch sensitivity of steels markedly. It is not possible by ordinary procedure to determine what these elements have done to the structure of the steel. Perhaps fractography might give some information that is obtainable in no other way.

The fractographs published in the paper show an amazing amount of detail and the authors should be commended for their skill and patience with a microscope.

Since the fractographs show such a wealth of detail and since the method is new in metallurgy, they will undoubtedly be incorrectly interpreted in some instances.

Written Discussion: By A. Nadai, consulting mechanical engineer, Westinghouse Electric & Manufacturing Co., E. Pittsburgh, Pa.

The authors have shown an interesting series of micrographs of metallic materials which have been obtained through the cleavage process. They are calling attention in their paper to a useful technique which may disclose fine details and has been described with particular reference to the cleavage fracture. It is believed that indeed many important details can be made observable in fractured surfaces if one does not polish these surfaces in the conventional manner used in ordinary micrography. In this connection it may interest perhaps the authors that a method has been described by the writer by means of which the fine distortions on the polished surfaces of specimens were observed which were obtained after deforming the specimens by small amounts. The method has been used by the writer since 1925 for observing, for example, the strain and flow figures (Lueders' lines) on mild steel specimens. Although the method was used primarily in macrographs there seems no reason why it could not be used also in micrography. The method was described in the writer's Edgar Marburg lecture presented at the 1931 meeting of the American

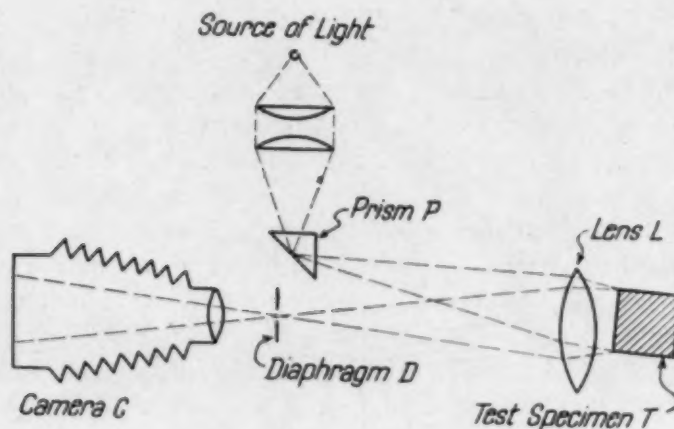


Fig. A—Schlieren Method for Observing Plastic Deformations.

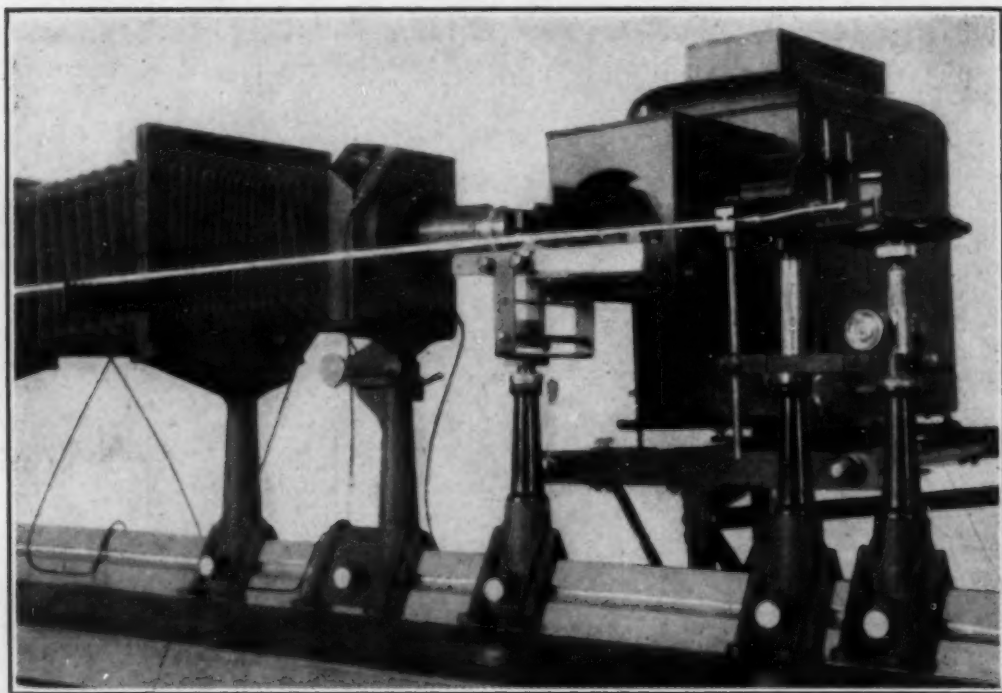


Fig. B—Optical Bench for Observing Distortions in Metals by Means of Schlieren Method. (The camera and lens arrangement are furnished by E. Leitz.)

Society for Testing Materials. It utilizes the Schlieren method for observing plastic deformations. As is well known, this method has been universally used for observing small changes in density or refractive power in transparent bodies, for example for inspecting lenses. It has extensively been used to study the supersonic flow of gases or the propagation of waves generated through fast moving objects (projectiles). Fig. A represents the Schlieren method for observing plastic deformations on the opaque but highly polished surface of metallic specimens after the specimens have been slightly deformed through plastic flow. It consists of an arrangement of lenses as indicated in Fig. A.

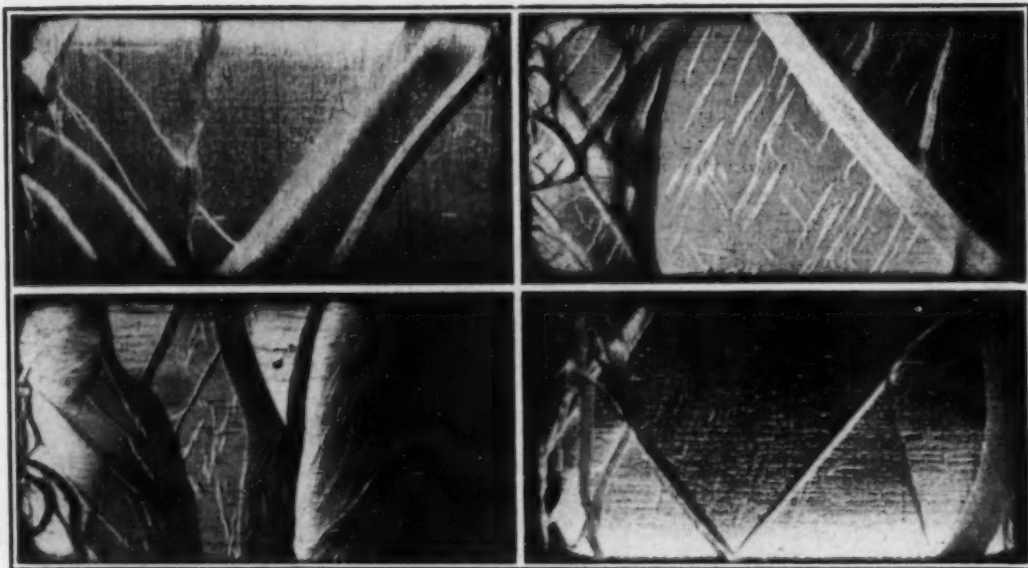


Fig. C—The Four Sides of a Mild Steel Prism of Square Cross Section After a Small Compression.



Fig. D—Meteoric Iron After Compression Test.

A small circular opening on the side of a prism *P* turned towards the test specimen *T* is assumed as a source of light serving to illuminate the test specimen *T*. This latter is, of course, turned with its polished surface towards the prism. By means of a very good lens *L* and the reflecting mirror surface of a test specimen *T* an image of the bright circular opening is thrown at a certain distance. This image appears as a light spot on the diaphragm *D* which might be inserted in the passage of the light beam. If slight disturbances are

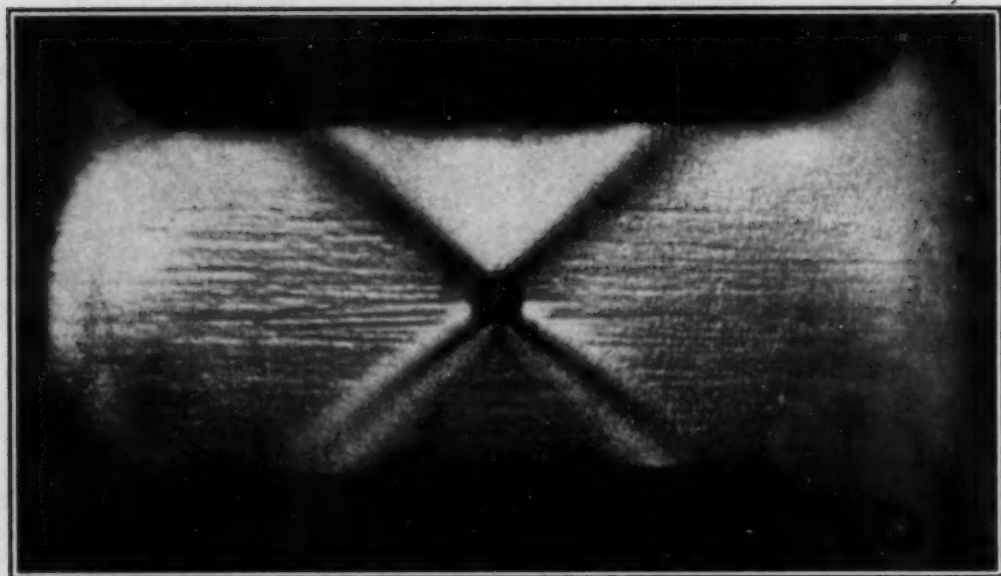


Fig. E—Hard Copper. Compression Test with Prism Having a Small Hole.

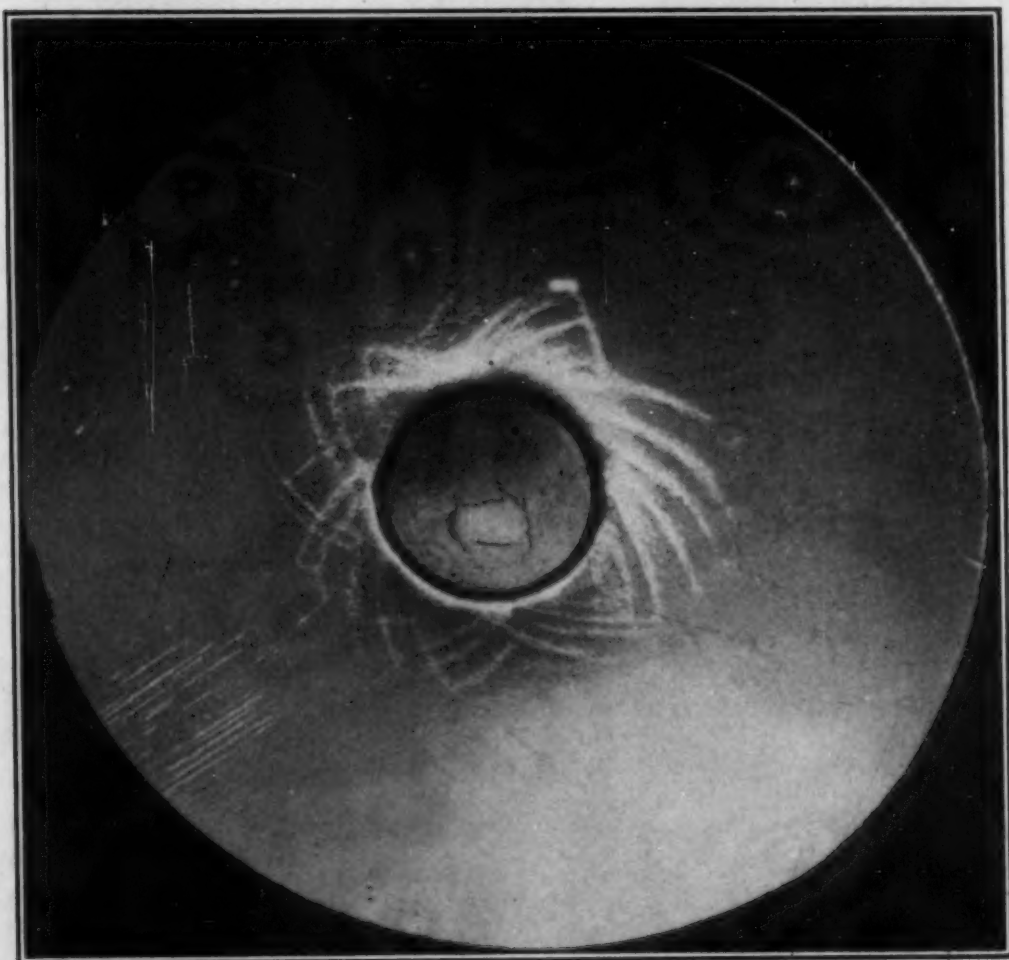


Fig. F—Impression of a Cylindrical Punch in Soft Steel.

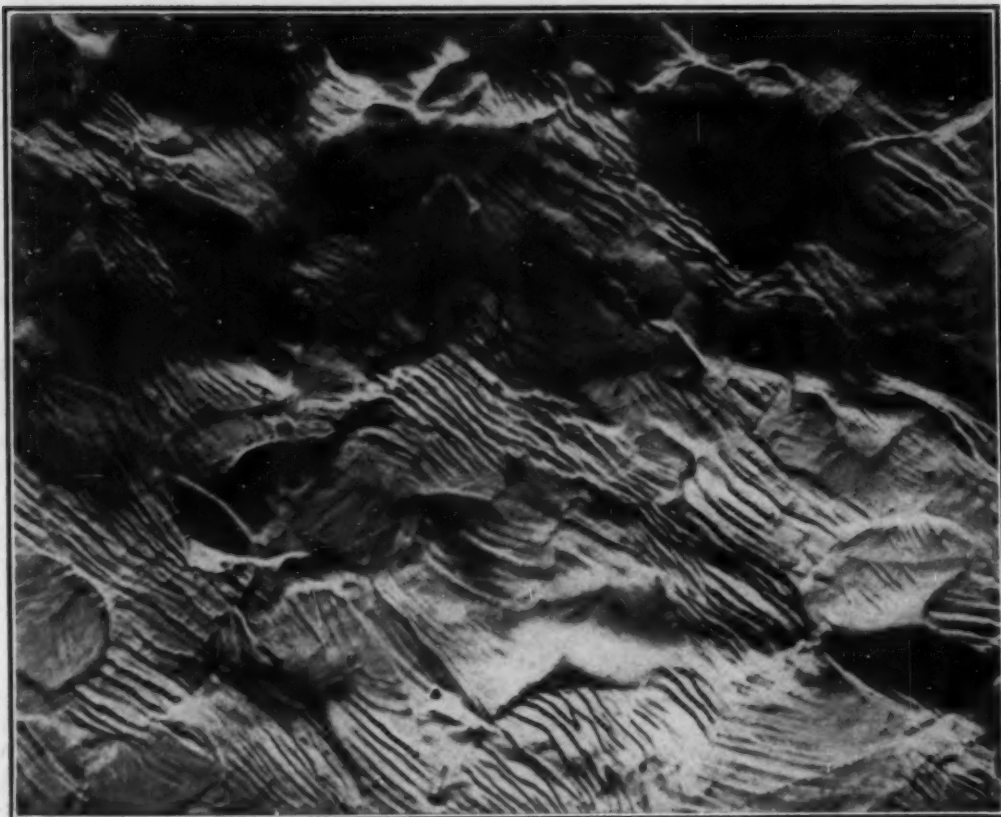


Fig. G—Micrograph. Plastically Deformed Grain Structure in a Flow Layer of a Compressed Mild Steel Prism.

present on the highly polished reflecting surface of the test specimen such as those produced by minute scratches or flow layers, the light coming from these places will not converge perfectly at D. Some light will pass around D, other light will be shut off. The result will be that the fine irregularities on the polished surface will become visible on the screen. Inserting the opaque screen at D will bring out at once minute details on the polished surface which otherwise under ordinary illumination would remain invisible. Fig. B shows an optical bench which was built for observing strain or flow figures using the Schlieren method. A few examples may illustrate this. Fig. C shows the four sides of a highly polished prism of square cross section of mild steel after a compression test. Fig. D shows the surface of a piece of meteoric iron having a small hole in the center also in a compression test. Fig. E shows a similar test with strain hardened copper after compression. Fig. F shows the polished surface of a steel block after a slight impression on the surface. Finally, Fig. G shows a micrograph of mild steel. This micrograph represents the structure of steel within one of the flow layers of the compression test shown in Fig. C. It will be noted how the surface has been distorted. Some crystal grains have been pushed out slightly from the surface while the remaining ones show a dense system of slip lines, most of which show a parallel orientation. This last example should illustrate that the above mentioned method can also be used with advantage in micrography.

Although the method described by the authors discloses very valuable fine details in the cleavage planes of broken metallic samples, which were not observed formerly, some concern must be expressed with regard to the real significance of some of the details which are visible for a correct interpretation of these details. The fact that the observations by the authors without exception refer to cases in which the object of observation was obtained through a cleavage process must limit somewhat the applicability of the method. It is believed by this writer that a number of details which appear in these micrographs may have been due to secondary reasons. As one of them, the fact must be remembered that a cleavage is produced by an impact process. It is suspected that some of the fine details may be due to the propagation modes of elastic or plastic or rupture waves. It is known that the conchoidal fracture in amorphous materials probably reflects some phenomena caused by the law of propagation of sound waves which were produced by sharp impacts. The writer hopes very much that the authors will have an occasion to investigate some of these important mechanical details in the future which might have been caused through elastic vibrations or also through other phenomena during the cleavage process and will assist readers by interpreting these details with great care before the method proves its usefulness in practical applications.

Oral Discussion

H. G. KESHIAN:^{*} This interesting paper is an effort to establish a relation between the fracture of a material and its constitutional and crystalline nature and if the authors continue their good work and succeed in their effort we will be in possession of another convenient method of studying metals.

The fracture of materials resulting from failure in service very often points to the possible cause of such failure. The appearance or the flow lines of the fracture oftentimes indicate the direction of the stress and the time element in the application of the stress which caused the failure. For instance, wrought iron if broken under a tension only slowly applied will show a fibrous fracture; but if it is broken under a stress suddenly applied its fracture would be crystalline.

The point which I wish to bring out is that the fractured surfaces which the authors showed us with the slides were no doubt caused under stresses, be they thermal or mechanical, suddenly or slowly applied. Therefore, it would be interesting to ask the authors whether they noticed any effect of fracturing their specimens by sudden blows or slow compression on the arrangement of striations or the flow lines of the fractures they studied.

Authors' Reply

We wish to thank Messrs. Goss, Nadai, Spencer, and Keshian for their contributions to this paper.

Dr. Nadai's 1931 Edgar Marburg lecture is known to us, and this present discussion of his Schlieren technique makes a valuable addition to our paper. As for his and Mr. Keshian's suggestion that the fine structure of fractographs

^{*}Metallurgist, Chase Brass and Copper Co., Waterbury, Conn.

may simply express propagation nodes of the impact force, we might repeat that the markings are always symmetrical with the crystal, regardless of the direction of the cleaving force, and that the markings have contours which could have no conceivable relationship to stress pattern and which must instead reflect heterogeneity of the crystal.

In addition, it might be mentioned that tensile fractures, which are not directly in the category of impact cleavages, likewise show these markings, even though the cleavage facets are greatly comminuted and are viewed in such cases with difficulty. The fracture patterns for amorphous material, as Dr. Nadai points out, can be related to a vibrational pattern; but they bear little resemblance to the structure shown here.

CLEAVAGE STRUCTURES OF IRON-SILICON ALLOYS

BY CARL A. ZAPFFE AND MASON CLOGG, JR.

Abstract

The metallographic technique referred to as fractography is applied to a series of alloys in the iron-silicon binary system. These alloys are especially suitable for this technique and provide a great number of interesting cleavage patterns, which are shown to reveal subtle intracrystalline processes not observable with the orthodox polish-and-etch technique.

Evidence is provided for a superlattice in alloys approaching the composition Fe_3Si ; the compounds epsilon (FeSi) and zeta (Fe_2Si_3) are identified by their characteristic and invariant fracture types; and the presence of eta (Fe_5Si_3) is indicated as a precipitation product within the alpha phase.

It is pointed out that the cleavage patterns, or fractographs, of these alloys, besides being useful as supplementary metallographic information, resist explanation on classical grounds of deformation and cleavage and clearly point to the pre-existence of an intracrystalline imperfection structure which must exert a tremendous influence upon the entire nature of the material.

INTRODUCTION

IN the course of developing the metallurgical technique referred to as fractography (1),¹ several iron-silicon alloys were examined along with a group of other specimens. These alloys were especially prolific in revealing new cleavage structures and invited further attention for two reasons in particular.

First, the structures observed in fractography are so novel that much exploratory work using many different kinds of specimens will evidently be necessary before the structures can be completely categorized and explained. The present study constitutes one such preliminary investigation designed to aid in the general understanding of cleavage patterns.

¹The figures appearing in parentheses pertain to the references appended to this paper.

A paper presented before the Twenty-sixth Annual Convention of the Society, held in Cleveland, October 16 to 20, 1944. Of the authors, Carl A. Zapffe is assistant technical director, and Mason Clogg, Jr. is assistant metallurgist, Rustless Iron and Steel Corp., Baltimore, Md. Manuscript received July 22, 1944.

Secondly, fractography is especially suited to the study of brittle metals; and the iron-silicon alloys advantageously present the rare combination of being commercially important and yet having easy cleavage from one end of their constitutional system to the other. Thus, with the numerous phases present in the iron-silicon system, an unusual opportunity is afforded for studying the effect of constitution on cleavage characteristics. Furthermore, iron-silicon alloys have received much study by other methods, and their nature is sufficiently well established to be quite helpful in interpreting fractographs.

EXPERIMENTAL PROCEDURE

A series of iron-silicon alloys was prepared in an induction furnace using a charge of Armco iron and 50 per cent ferrosilicon melted in a magnesia crucible. The specimens were cast in 5-pound cast iron molds. Their analyses appear in Table I; and in Fig. 1 the compositions are depicted on the Greiner, Marsh, and Stoughton constitutional diagram (2), (3). For the 50- and 78-per cent alloys, commercial ferrosilicon was used without remelting.

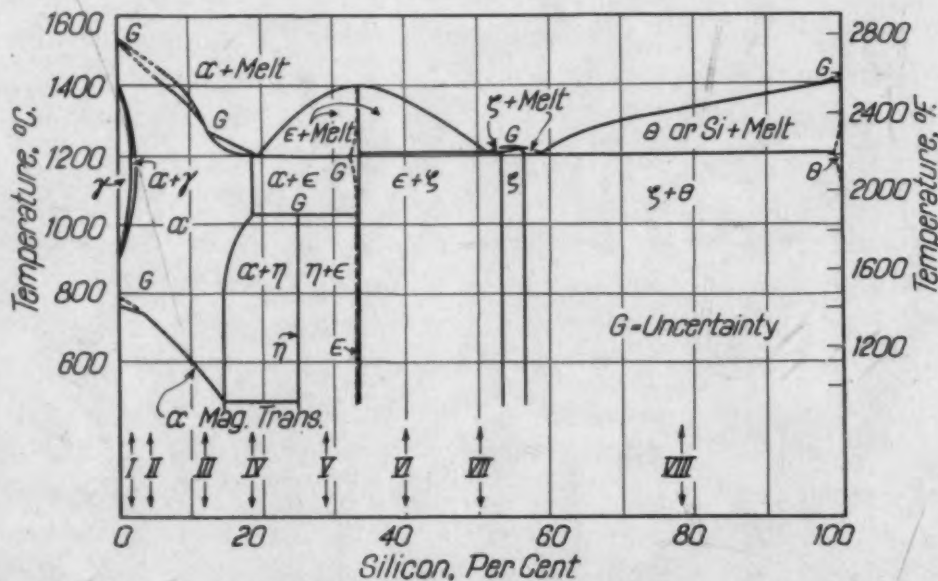


Fig. 1—Iron-Silicon Binary Diagram. According to Greiner, Marsh, and Stoughton, Showing the Alloys Studied in the Present Research.

Although the carbon contents are not high, the strong effect of carbon and other impurities on the constitution of the alloys must be kept in mind in interpreting the results, as must the fact that the observations are confined to specimens in the as-cast condition. Al-

Table I
Analyses of Iron-Silicon Alloys

	Silicon (Per Cent)	Carbon (Per Cent)
I	1.59	0.034
II	4.24	0.038
III	11.84	0.038
IV	18.10	0.052
V	28.83	0.040
VI	39.54	0.032
VII*	50.18	0.122
VIII*	78.26	0.045

*Commercial Ferrosilicon.

though several specimens were subsequently heat treated and re-examined, there were no changes in structure to be reported here.

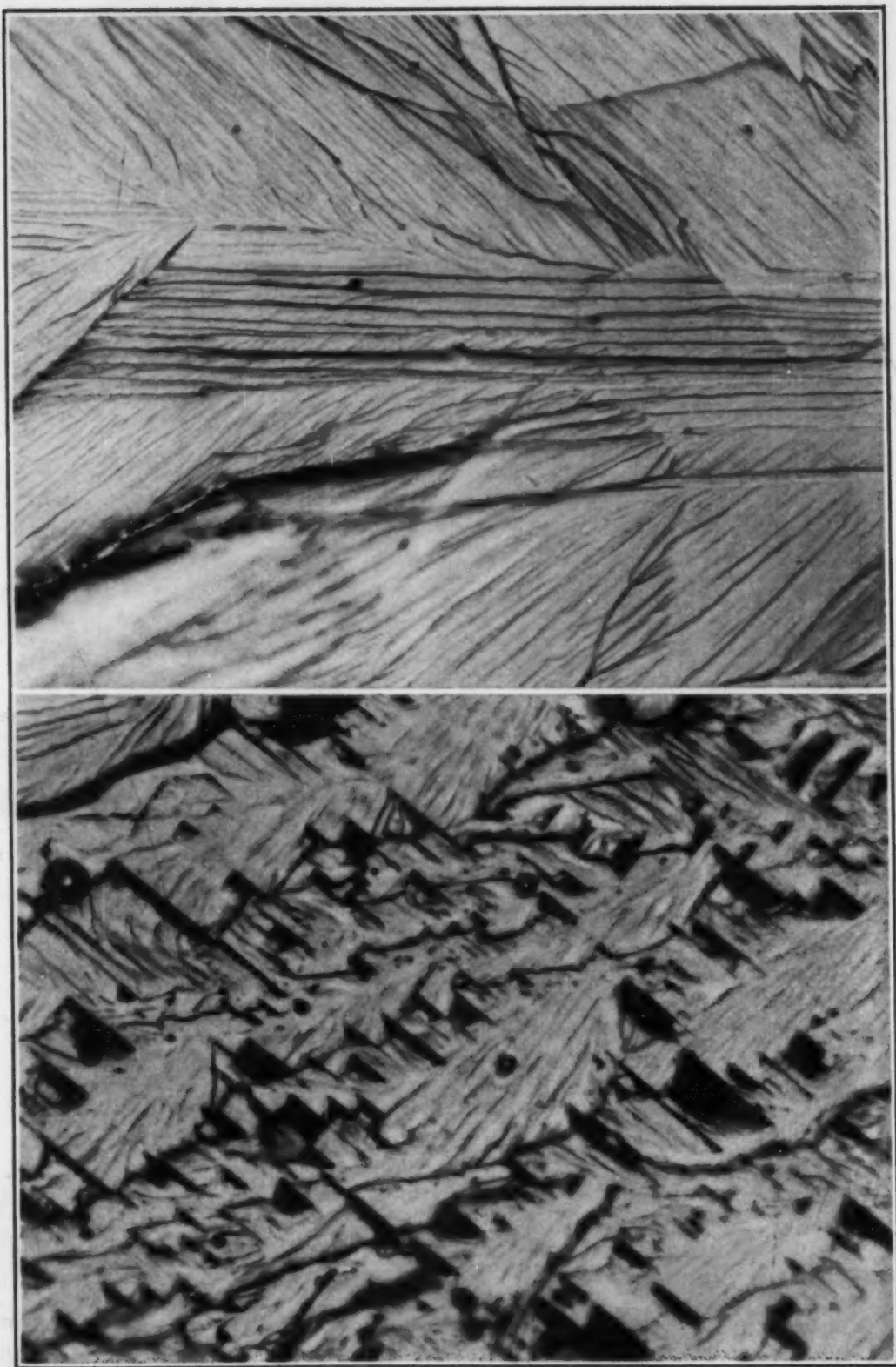
All specimens were broken by impact with a hammer. Their further preparation and the technique of examining the surfaces is described elsewhere (1).

OBSERVATIONS

Alloy I (1.59 Per Cent Silicon)—On the constitution of Alloy I, there is complete agreement among the various published researches that it is alpha iron containing the silicon in solution (3). A polished and etched section of Alloy I revealed nothing but this single phase.

Nevertheless, anomalies in the behavior of alloys of this composition have frequently been reported (3); and it is interesting to find that this alloy reveals some flexibility in cleavage pattern (see Figs. 2 and 3), a condition standing in sharp contrast to the characteristic patterns found later for other alloys. Perhaps the spread of results found at this composition can be explained by the multiplicity of planes that are available for deformation: {110}, {112}, and {123} for slip, and {112} for twinning (4), (5). With higher silicon contents, the number of available deformation planes becomes sharply limited (4), until certain brittle phases, as will be shown later, have only one characteristic cleavage pattern regardless of the conditions of fracture.

In Fig. 2, the faint subdivisional markings probably concern the so-called "lineage" structure, reported earlier for alpha iron containing no appreciable silicon (6). Generally speaking, the structural lines of a grain traverse a lineage boundary without the loss of their



Fractographs of Alloy I
Fig. 2—(Above) Assemblage of Lineages Traversed by Crystallographic Markings. $\times 500$. Fig. 3—(Below) "Block" Structure. $\times 750$.

gross crystallinity; but at the grain boundary, where a distinctly different orientation usually begins, the lines are interrupted or disrupted, depending upon the degree of offset between the axes of the two grains.

Also in Fig. 2 are some well developed crystal markings. The facet is believed to be one grain, as attested by these uniform horizontal markings, but incorporating subgranular lineage units which are at certain small angles of disarray, probably less than 2 degrees (7). The sharp 45-degree angle depicted by the crystallographic markings at the left of Fig. 2 eliminates the possibility that both sets belong to cleavage planes, since this material cleaves on {100}, and no 45-degree cleavage traces could appear on the cleavage facet. Slip, or twinning, could account for all the markings.

In Fig. 3, a marked block structure appears. The markings represent real openings, small blocks of material actually having been removed and lost. Etching with dilute nitric acid showed a vigorous attack over this area, the openings and fissures becoming enlarged from infiltration of the acid.

This block pattern is similar to that developed in iron if fractured when embrittled by hydrogen (6) and can be argued as striking proof that the grain is a composite, or mosaic, of smaller crystalline units whose boundaries are imperfect on an ultramicroscopic scale. During cleavage, certain of these weak boundaries fail so completely, even though they do not lie along the cleavage direction, that the segmented blocks of crystal between them are separated and lost from the structure.

Because of the strong evidence for a mosaic constitution of the grains in this material, a polished specimen was deep etched in 20 per cent HNO_3 in an attempt to reveal a similar structure by chemical attack. (See Fig. 4.) Platelets became clearly defined; and their thickness was of the order of the smallest observable contour on the blocks in the fracture. Although Stead observed the same etching structure in similar material half a century ago (8), and although investigators such as Pulsifer (9) have produced the same type of structure in most metallic crystals, the argument that these etched structures indicate intrinsic crystalline imperfection has never surmounted the classic argument of preferential attack on certain atomic planes. That classical picture, however, seems to require unnecessary faith in the homogeneous structure of crystals. So many observations, *viz.*, the so-called "structure sensitive" properties of

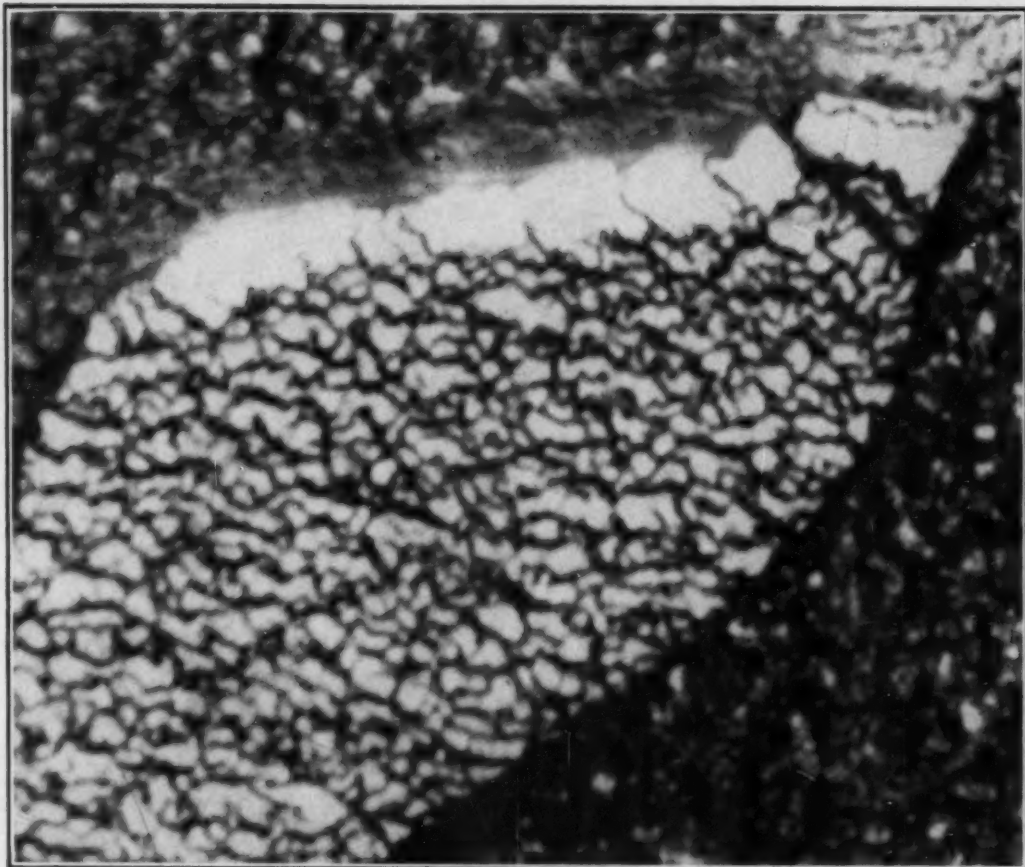
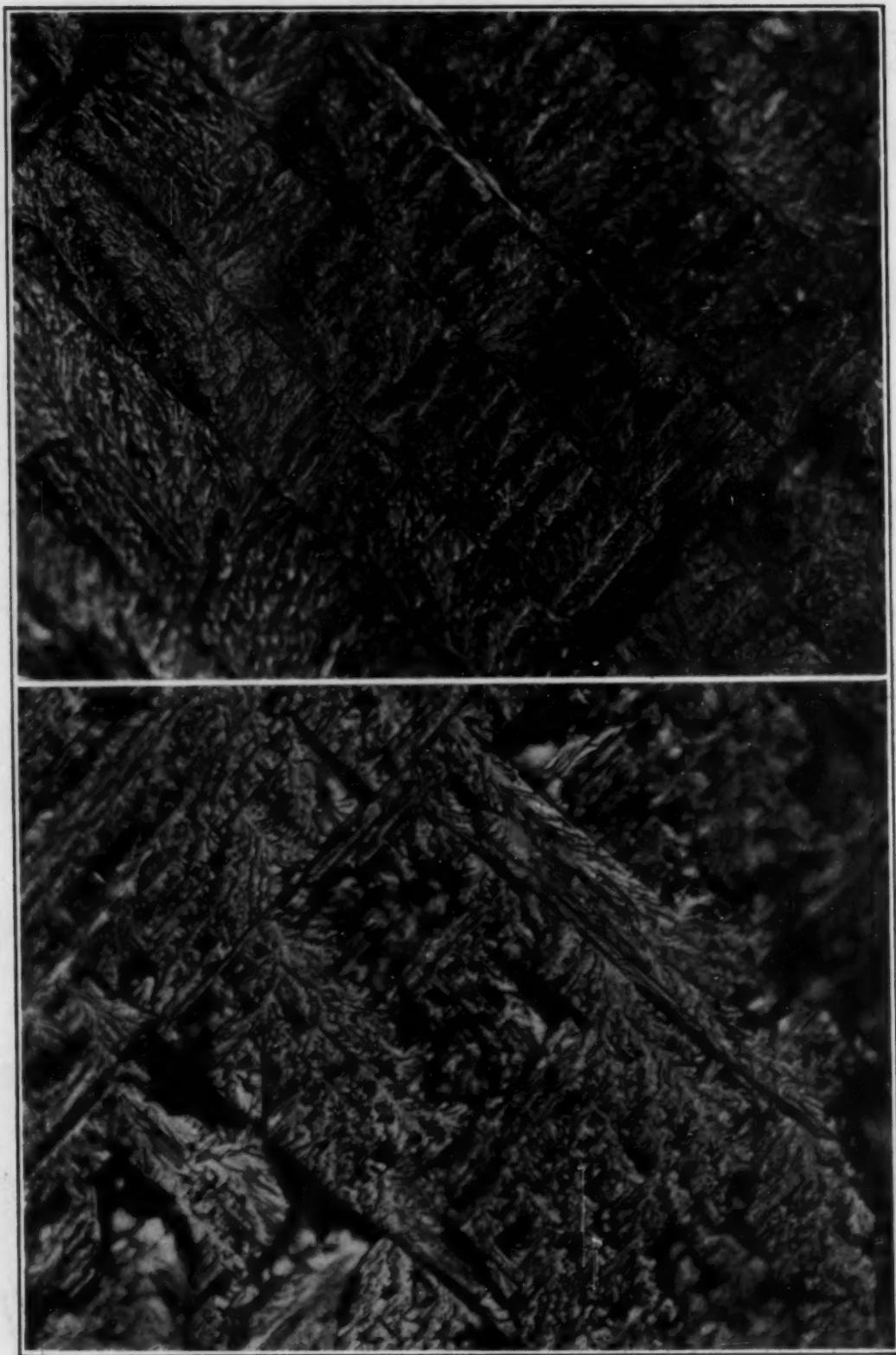


Fig. 4—Polished Specimen of Alloy I Deep-Etched with 20 Per Cent HNO_3 , Showing Mosaic Platelets. $\times 4000$.

crystals, cannot be explained on the classical ground; and they fit so conveniently into the picture of imperfection structure (7).

While the principal argument of the classical school is based upon the fact that different etching reagents often produce different etching structures on the same crystal, there is no reason for presuming that the imperfection structure is peculiar to but one family of planes. Depending upon the density and spacing of different planar families, their degree of imperfection should be expected to differ. The preference of a certain molecule of reagent for a certain interplanar disjunction can be accepted as readily as its supposed preference for a certain interplanar spacing in a perfect lattice.

Alloy II (4.24 Per Cent Silicon)—With this silicon content, the alloy is still agreed to be alpha iron (3). According to Barrett, Ansel, and Mehl (4), however, slip can no longer operate on $\{112\}$ and $\{123\}$. Consequently, all markings on the fractographs in Figs. 5 and 6 should relate to cleavage on $\{100\}$, or slip on $\{110\}$, or twinning on $\{112\}$.



Fractographs of Alloy II
Fig. 5—(Above) "Cell" and "Sub-Cell" Structure. $\times 500$. Fig. 6—(Below)
"Cell," "Sub-Cell," and "Block" Structure. $\times 500$.

In examining this alloy, it is clear that there are resemblances to those of the previous alloy, but that there are also marked differences; and, although a polished and etched specimen of Alloy II shows nothing but the same alpha phase, with fractography one alloy can be distinguished from the other.

For example, the marked cell-like pattern of Figs. 5 and 6 was not observed in Alloy I. In these patterns, at least one set of the rectangular markings can be identified as secondary cleavages on $\{100\}$, for rupture is evident. The thinner perpendicular set of lines may also be $\{100\}$ cleavage, or slip on $\{110\}$, or twinning on $\{112\}$.

Within the large segments, or cells, of Fig. 5, there are smaller sub-cells, each containing a tiny and elaborate lineage growth. Although much of their clarity is lost in reproduction, these sub-cells are still easily visible and can only be interpreted as being pre-existent and exhibiting the imperfection structure of the crystal. They were there first; and the location of the deformation markings between these small lineages was therefore predetermined by their presence.

Furthermore, these tiny lineages are also similarly bounded by the thin rectangular lines just discussed as possible slip or twinning markings. From that, one may conclude that the whole rectangular pattern expresses a pre-existent imperfection structure, whether the markings are cleavages, slip bands, or twins. In Fig. 6, the sub-cell structure reduces to a point where it cannot be distinguished from a block structure.

Classical homogeneous deformation is inconsistent with the spacing of the deformation markings in these figures, none of the small tree-like growths being crossed either by the heavy $\{100\}$ cleavage markings or by the lighter rectangular markings ascribed to cleavage, slip, or twinning. Since with polishing and etching these detailed markings do not appear, this inconsistency would not be noted on polished specimens.

Other evidence in these patterns can be similarly accepted as forthright proof that the crystals contain intrinsic internal imperfections which are on a minute and crystallographic scale and which must have tremendous influence on the whole mechanical and chemical behavior of the specimen. This conclusion is consistent with the information on the structure-sensitive properties of crystals and with the general argument for imperfection structure (7).

In Fig. 7 an unusual cleavage facet is shown which may represent a shock-wave pattern or a dendritic, or lineage, growth. The



Fig. 7—Fractograph of Alloy II, Showing an Unusual Pattern of Unknown Origin.
× 500.

origin of such a structure, found once again in an alloy of higher silicon content, is not clear.

Alloy III (11.84 Per Cent Silicon)—According to most investigators, the alpha lattice continues to be the only structure up to about 14.5 per cent silicon, since photomicrographs reveal only the one phase (3). Phragmén, however, found a rather irregular change of lattice parameter with silicon content over the presumed alpha range (10); and Jette and Greiner later showed that above 5 per cent silicon some subtle change in constitution occurs (11). While speculation (2) also involves the compound Fe_3Si , the more likely explanation is that atomic ordering occurs over a range of silicon content approaching the composition corresponding to Fe_3Si , as first proposed by Phragmén (10).

Although but one phase appears on a polished and etched specimen, the appearance of this phase is definitely abnormal. The remarkable sub-boundary structure shown in Fig. 8 under different

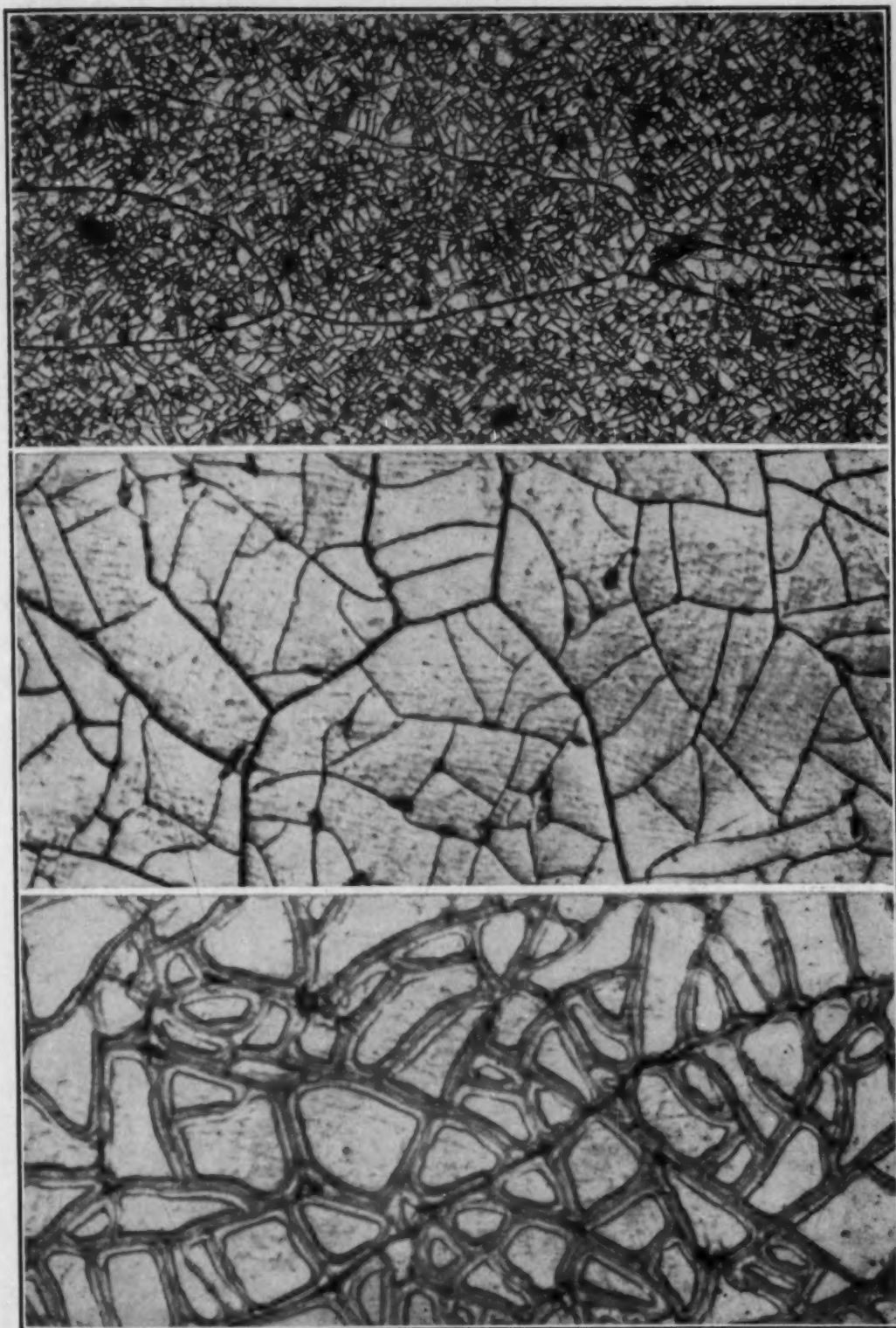


Fig. 8—Sub-Boundary Structure in Alloy III, Polished and Etched with 20 Per Cent HNO_3 . (Top) $\times 100$. (Center) $\times 1000$. (Bottom) Deep-Etched, Showing a Major Boundary in a Network of Sub-Boundary Markings. $\times 1000$.

conditions of magnification and etching is peculiar to this alloy. Annealing for 1 hour at 1000 degrees Cent. (1830 degrees Fahr.) and air cooling made the large grains equi-axed, but no noticeable change occurred in the sub-boundary structure.

A simple explanation for this sub-boundary structure is that it represents shrinkage from superlattice formation. Jette and Greiner's X-ray measurements show that the alpha lattice contracts at an increased rate when silicon exceeds about 5 per cent, which can be taken as an indication that an ordering process is decreasing the volume of the lattice beyond the decrease conforming to Vegard's Law. It is somewhat surprising, of course, to find such ordering in a cast structure where cooling is so rapid, and also after air cooling from an anneal at 1000 degrees Cent. (1830 degrees Fahr.), since the melting temperature of this alloy is only about 200 degrees higher, and superlattices are seldom found so near the melting point.²

A fractograph of the as-cast alloy etched with 20 per cent HNO_3 revealed the major boundary markings, but not the minor markings. (See Fig. 9.) The reason for this is not clear either; but it is possible that the ordering is anisotropic, causing the principal shrinkage to be normal to the cleavage and, therefore, unresolved on the cleavage facet. Neither is it understood why the cleavage markings show no interruption at these boundaries.

In Fig. 10, a photomicrograph of a deep-etched polished specimen shows a crosshatch structure that may have some significance in view of the similar "rippled regions" found by Harker in a 50 per cent Au-Cu alloy when annealed to develop a superlattice (12). The observation is presented as further indication that this portion of the binary diagram probably involves an ordered structure based upon the composition Fe_3Si . Alloy III, containing 11.84 weight per cent silicon, or 21.2 atomic per cent, closely approaches the stoichiometry of Fe_3Si .

Especially characteristic results occur in the fracture patterns, which are quite dissimilar to preceding fractographs and give further evidence that this composition is not simply alpha iron. In Fig. 11, for example, a lamellar structure is revealed which is reminiscent of pearlite, but lacks the two-phase constitution of pearlite. Perhaps these lamellae relate to the crosshatch structure in the previous Fig.

²Contemporary with this paper, Dean has shown a similar structure in Mn-Cu alloys containing 50 to 60 per cent Mn and quenched from an anneal at 700 to 850 degrees Cent. ("The Present Status of Electrolytic Manganese and Its Alloys," by R. S. Dean, *Metals Technology*, Vol. 11, No. 4, 1944.)

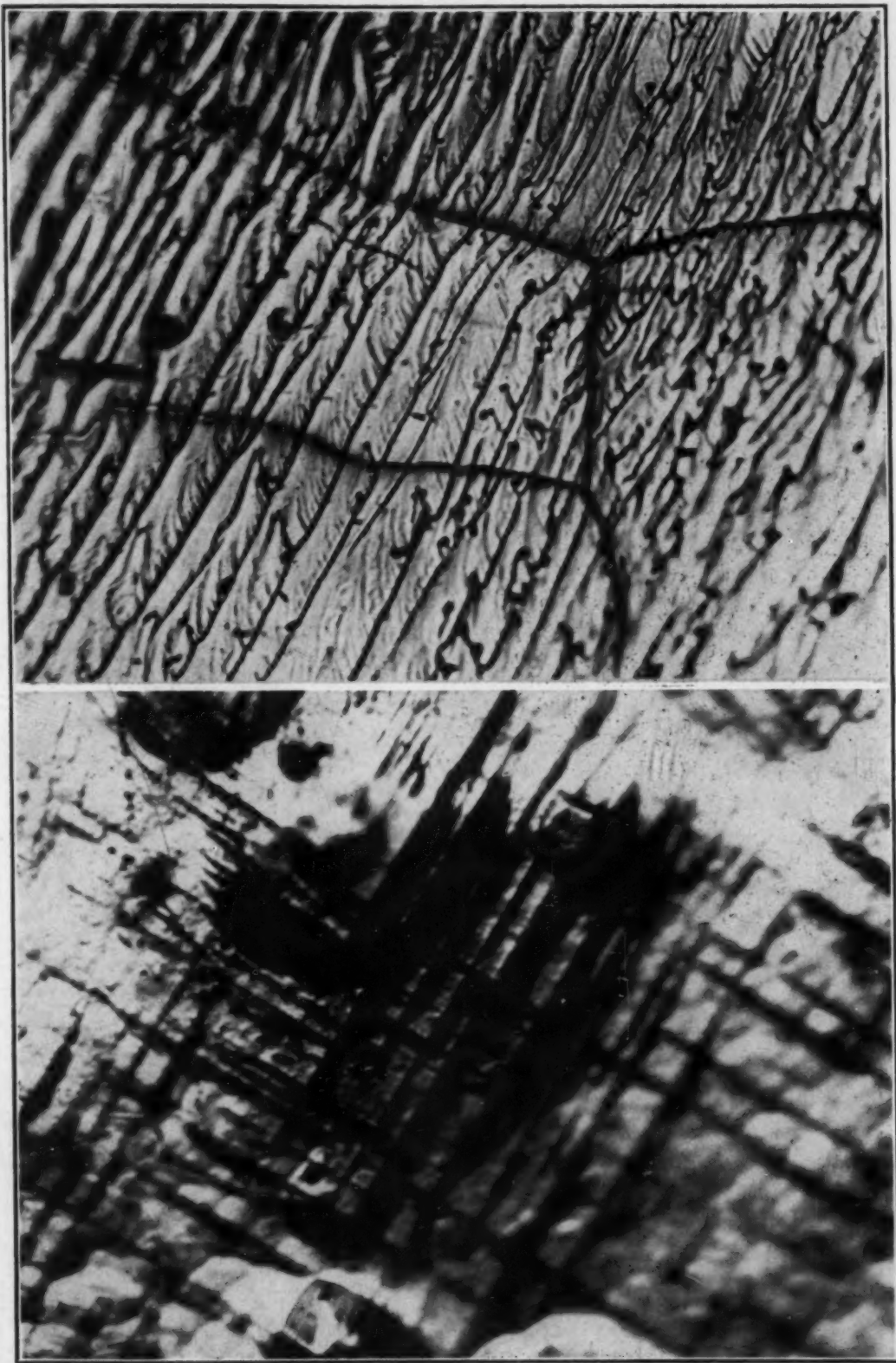
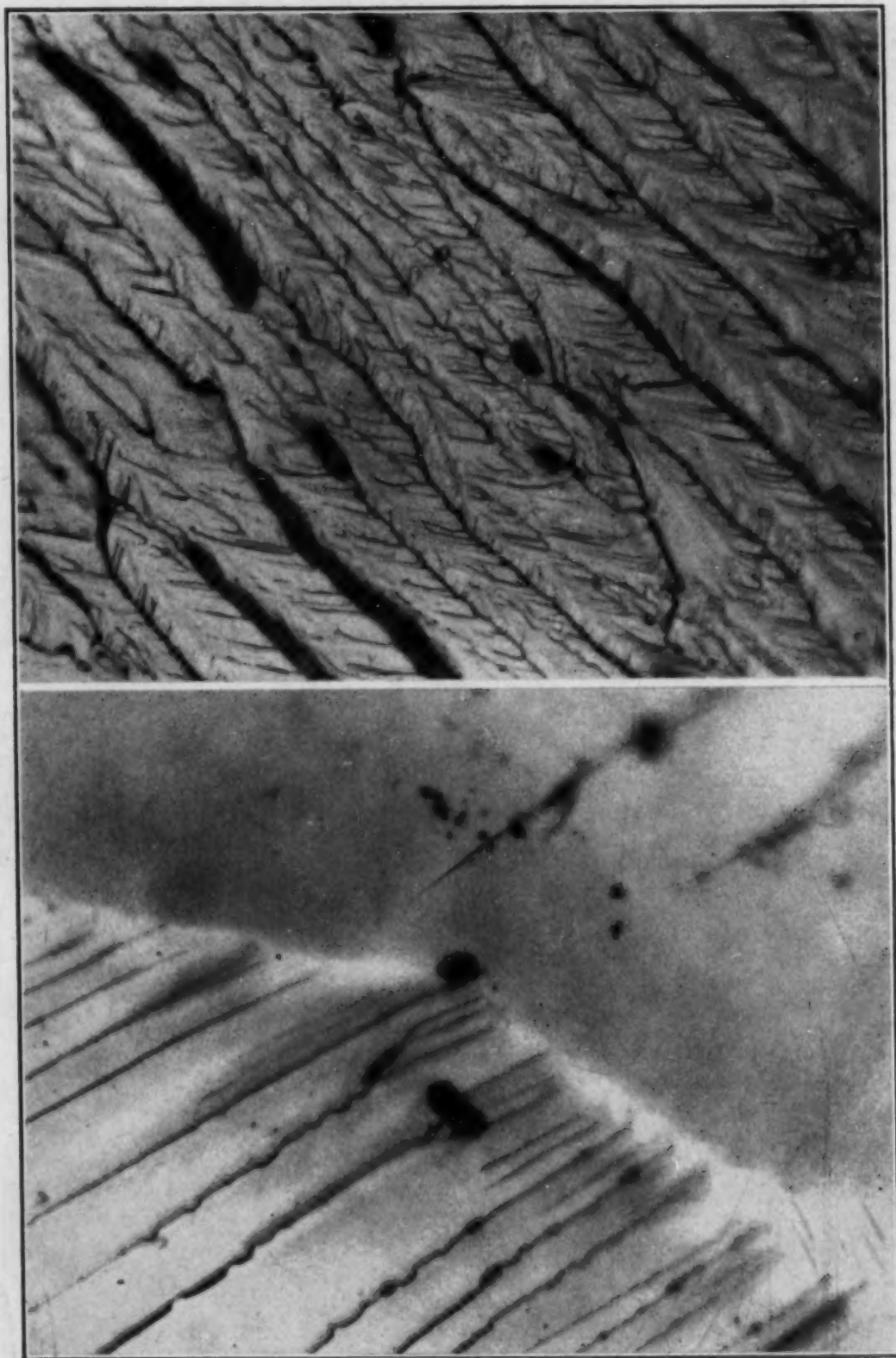


Fig. 9—(Above) Cleavage Facet of Alloy III, Etched in 20 Per Cent HNO_3 , Showing Only Major Boundary Markings. $\times 750$.

Fig. 10—(Below) Alloy III, Polished and Deep-Etched with 20 Per Cent HNO₃, Showing Markings Ascribable to Superlattice Formation. $\times 1000$.



Fractographs of Alloy III
Fig. 11—(Above) "Pearlite" Structure in a One-Phase, Non-Pearlitic Alloy. $\times 1000$. Fig. 12—(Below) "Stepdown Cleavage" and a Grain Boundary. $\times 2000$.

10. Whatever their nature, it is interesting to find the structural type of pearlite within a nonpearlitic, apparently homogeneous phase.

Another lamellar structure, but having different characteristics, appears in Fig. 12 and in the previous Fig. 9. This structure results from a "stepdown" type of cleavage which follows one plane a cer-



Fig. 13—Fractograph of Alloy III Showing Profile of "Stepdown" Cleavage. $\times 2000$.

tain distance and then shifts perpendicularly to a second parallel plane. The stepdown involves a lamellar unit of seemingly constant spacing in keeping with the block nature of deformation phenomena, and in general with the mosaic theory for crystals. Fig. 13 shows such a cleavage in profile. Although one might suppose that that pattern results simply from stress being applied at a low angle to the cleavage plane, the pattern is fairly distinctive and is not found in all alloys. The pattern of Fig. 11 was not found in any other alloy.

Two more fracture patterns for this alloy appear in Figs. 14 and 15. In Fig. 14, the odd stripes traversing the grain and showing

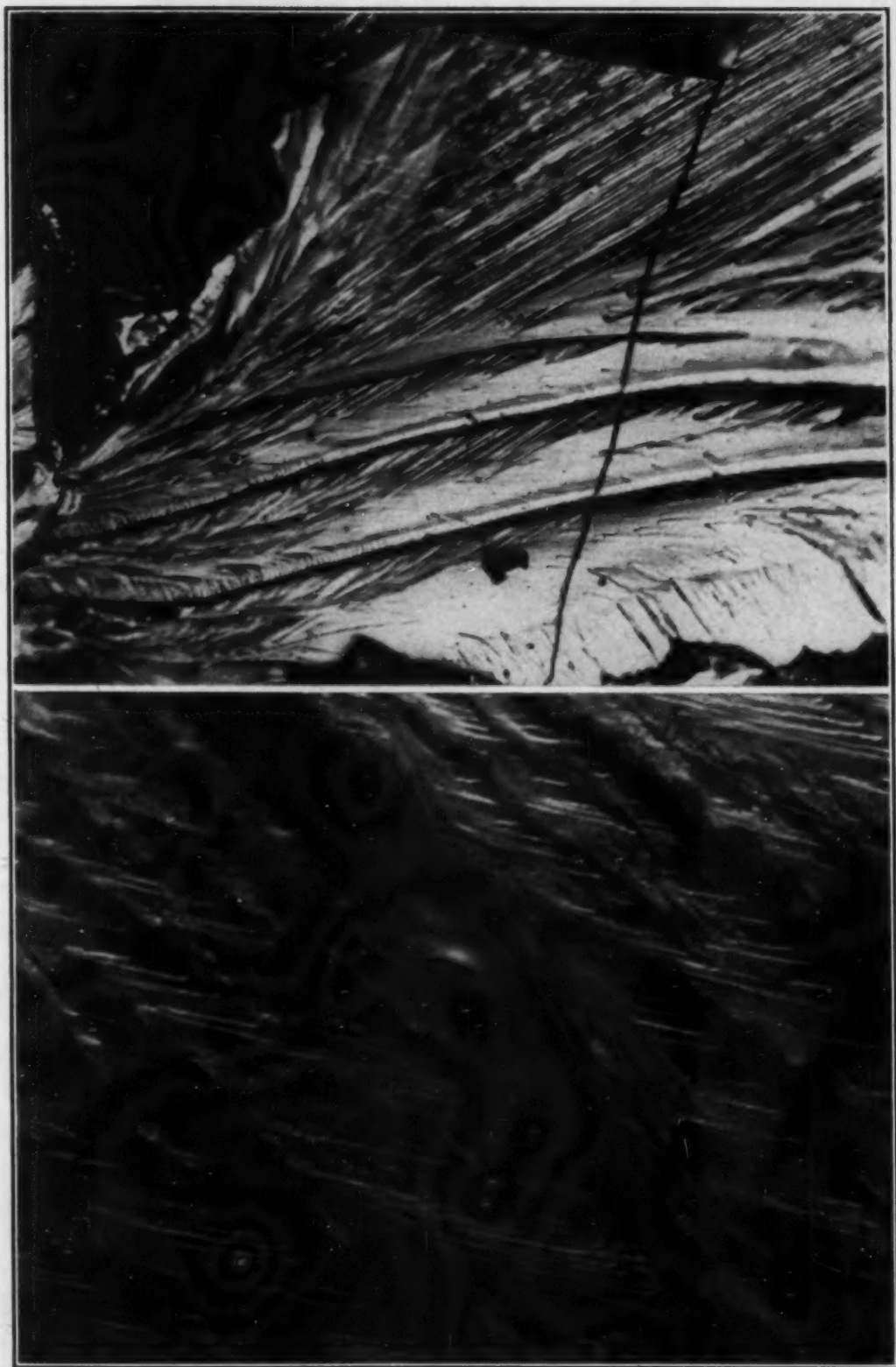
minute perpendicular striations across their breadths clearly indicate a departure from the simple constitution of alpha, although this structure may concern the carbide phase recently reported by Hurst and Riley for alloys of this composition (13). Incidentally, the previous Fig. 13 is an enlargement of part of the grain in Fig. 14 and shows one of these stripes in bold relief.

As for the remarkable pattern in Fig. 15, we will point out that once again the pattern can only be accepted as evidence of pre-existent imperfection, since cleavage could not conceivably follow such an elaborate course for any other reason. One might suggest that this is the structure responsible for the barley shell etch pattern discovered by Corson (14 to 16), if it were not for the recent clever research by Wrazej which apparently identifies that phenomenon simply as the scars left by iron fluoride crystals after etching with solutions containing HF (17).

Alloy IV (18.10 Per Cent Silicon)—According to Haughton and Becker (15) and Phragmén (10), Alloy IV, having 18.10 per cent silicon, should solidify as a eutectic of alpha and epsilon. Stoughton and Greiner (2) show Fe_3Si instead of alpha; and Osawa and Murata (18) complicate the picture further by proposing a peritectic reaction forming a superlattice, Fe_3Si , which subsequently reacts again peritectically to form a new superlattice, $\text{Fe}_{11}\text{Si}_5$, stable above 1030 degrees Cent. (1885 degrees Fahr.) and decomposing at lower temperatures to form an Fe_3Si superlattice plus Fe_3Si_2 .

Most diagrams agree in showing some type of decomposition reaction occurring below about 1030 degrees Cent. (1885 degrees Fahr.) producing alpha and an eta phase, which has been identified as Fe_3Si_2 until Weill's recent announcement that the compound is Fe_5Si_3 and is isomorphous with Mn_5Si_3 (19). Greiner and Jette then claim that this compound decomposes below 825 degrees Cent. (1520 degrees Fahr.) to form FeSi and more alpha, or some modification of alpha (20). On the other hand, Corson specifically denies the existence of such a compound (14).

Under the conditions of a rapidly cooled casting, it is anybody's guess how this complex constitution may resolve itself. The photomicrograph in Fig. 16 shows a two-phase structure which was not significantly changed by annealing for 1 hour at 1000 degrees Cent. (1830 degrees Fahr.) and air cooling. Phragmén's first investigation revealed only the compound FeSi , besides alpha, in this portion of the diagram (21); and the eta phase remained to be verified



Fractographs of Alloy III
Fig. 14—(Above) Unknown Structure Within Grain of Alpha. $\times 200$. Fig. 15—
(Below) Pattern of Crystal Imperfection (Oblique Light). $\times 2000$.

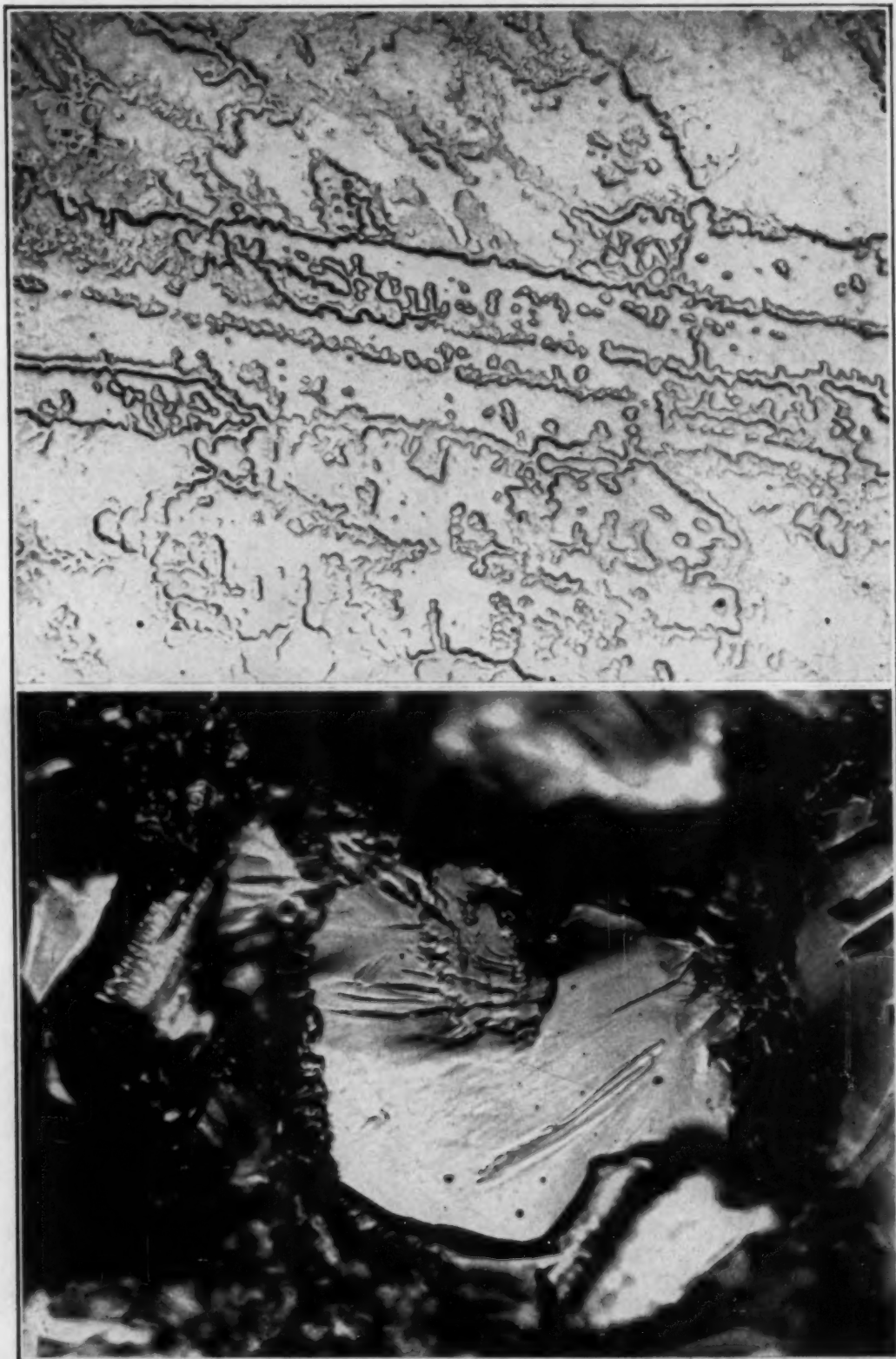


Fig. 16—Constitution of Alloy IV. (Above) Polished Specimen Etched with 20 Per Cent HNO_3 , Showing Alpha and Epsilon Phases. $\times 100$. (Below) Fractograph Showing Typical Cleavage Pattern of FeSi Phase (Central Facet). $\times 500$.

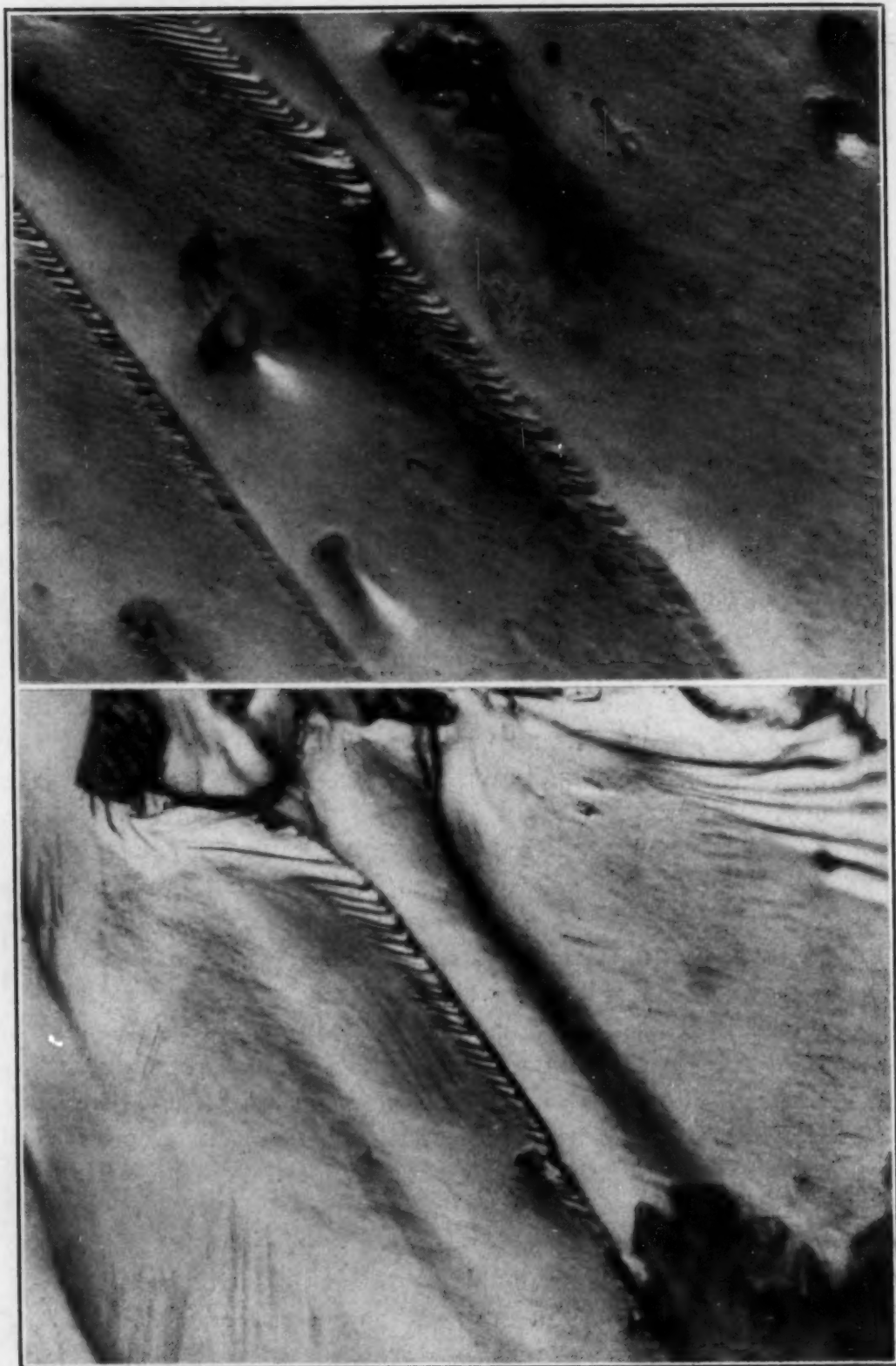
in his later investigation with carefully annealed alloys (10). We assume here that the photomicrograph in Fig. 16 shows alpha and epsilon, perhaps as the eutectic designated for this composition by Phragmén (10). A deep-etched specimen showed the markings in the alpha phase previously associated with an ordered structure in describing Alloy III.

Fractographs of this alloy plainly displayed the two phases; and the second phase, which we assume to be FeSi, is depicted in the fractograph also shown in Fig. 16. That fracture pattern is typical of this compound, and its discussion will be reserved for later attention in alloys having higher silicon content. A cleavage facet heat-tinted in a brief treatment at 1000 degrees Cent. (1830 degrees Fahr.) showed a discoloration from a brownish oxide developing on the iron-rich phase, thereby identifying it as alpha (1).

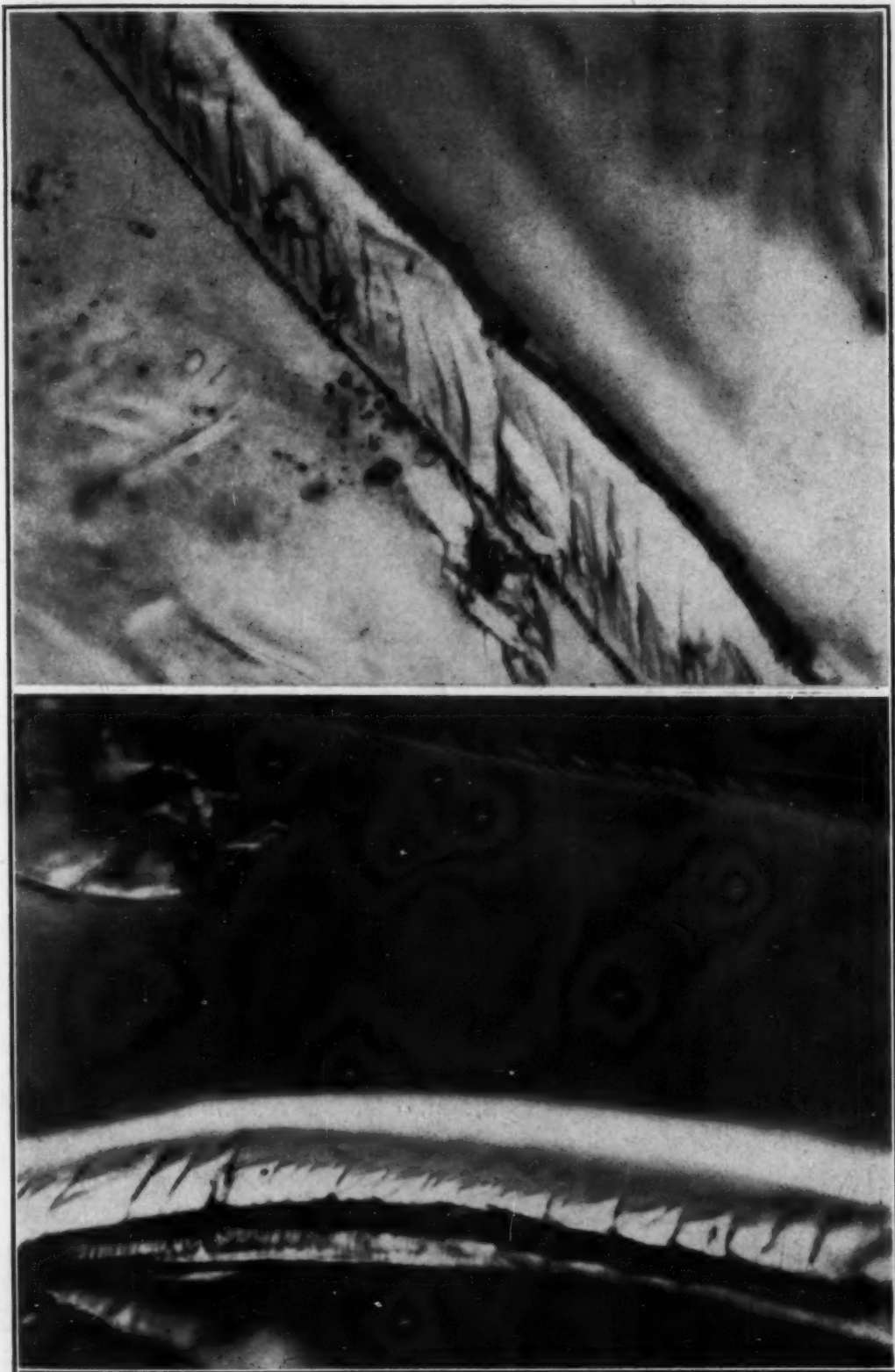
Although the fractured epsilon phase is structureless, from a fractographic standpoint, the alpha phase of this alloy shows an array of phenomena. For example, in Fig. 17 two odd outcrops of fine lamellae appear which were not observed in other alloys. Fig. 18 shows a similar outcrop, with faint markings in the lower and upper left of the photograph suggesting twinning. It is significant that the twin bands make an angle of 45 degrees with the lamellar bands. Note the fine detail in these outcrops and the constancy in the thickness of the lamellae. In Fig. 18, especially, there seem to be parallel lamellar bands which do not expose lamellae. The structureless patches surrounding the principal field in Fig. 18 belong to the epsilon phase.

None of the unusual structures in Figs. 19, 20, or 21 is clearly understood. The band in Fig. 19 is plainly a separate phase, but cannot be assigned to FeSi because of its cleavage pattern. We choose to regard the intrusive structures found in these fractographs as precipitations of the eta phase, Fe_5Si_3 . Note the rectangular, step-wise boundaries on the band in Fig. 19, suggesting that its origin is concerned with an inherent block structure of the crystal. That, of course, also points to its origin in the solid state, rather than the liquid, which is in keeping with the presumed origin of Fe_5Si_3 .

Although the peculiar double-ridged formation in Fig. 20 cannot be claimed to lie within the matrix of a single phase, and may represent some structural condition at a grain or dendrite boundary, the needlelike structures in Fig. 21 do lie within an otherwise homogeneous phase and are reminiscent of martensite, even showing a



Fractographs of Alloy IV
Fig. 17—(Above) Lamellar Outcrop in Alpha. $\times 2000$. Fig. 18—(Below) Lamellar Outcrop in Alpha, with Suggestion of Twinning in Upper and Lower Left. $\times 2000$.



Fractographs of Alloy IV

Fig. 19—(Above) Intrusive Structure Presumed to be the Solid-State Decomposition Product Fe_3Si_2 . $\times 2000$. Fig. 20—(Below) Further Evidence of Phase Change in Alpha. $\times 2000$.



Fig. 21—Fractograph of Alloy IV, Showing Needlelike Structures in the Alpha Phase. $\times 2000$.

pronounced midrib. Note the spiny markings along the midrib. These needlelike structures are especially suggestive of an eta phase precipitate.

In closing the discussion of this alloy, it might be remarked that Malashenko and Vasilevskaya recently applied magnetic measurement of Curie temperatures to the analysis of iron-silicon alloys and found marked obscuration of their results around this composition (21).

Alloy V (28.83 Per Cent Silicon)—With the silicon content increased to 28.83 per cent, the present alloy shows a fracture pattern which almost totally comprises the same type of facet described as FeSi in Alloy IV. (See Figs. 22 and 23.) The photomicrograph in Fig. 24 shows a predominance of primary FeSi crystals imbedded in a secondary structure which must be richer in iron and is very likely alpha-epsilon eutectic. In the same figure, a cleavage facet



Fractographs of Alloy V
Fig. 22—(Above) Typical Cleavage Pattern of FeSi. $\times 300$. Fig. 23—(Below)
Cleavage Pattern at Higher Magnification Showing Thin Shell of Alpha-Epsilon
Eutectic Surrounding Dendrite of FeSi. $\times 1000$.

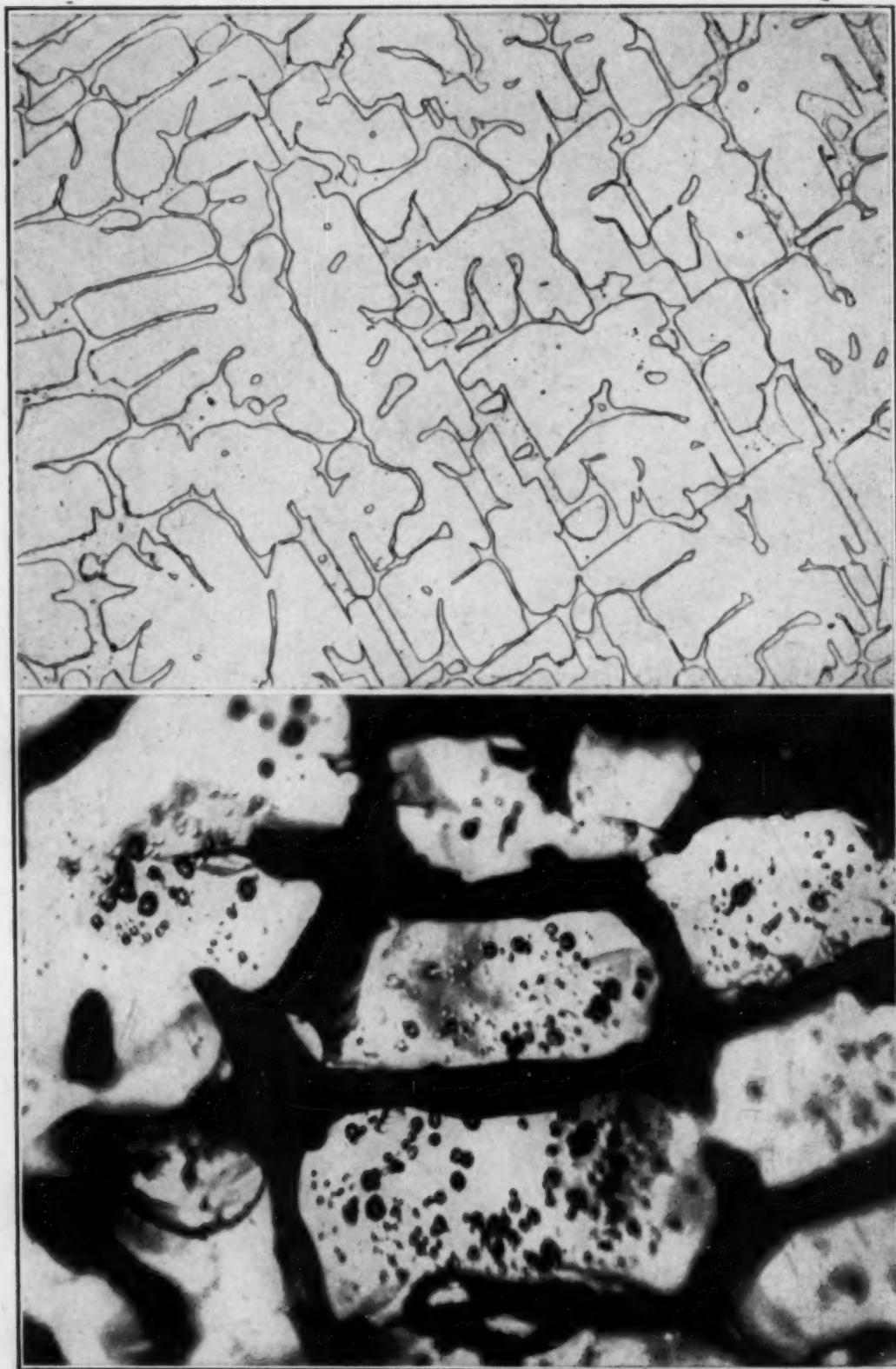


Fig. 24—Constitution of Alloy V. (Above) Polished Specimen Etched with 20 Per Cent HNO_3 , Showing Epsilon Dendrites Surrounded by Alpha-Epsilon Eutectic. $\times 100$. (Below) Cleavage Facet Etched with 20 Per Cent HNO_3 , Showing Epsilon Dendrites and Voids Where Eutectic Was Dissolved Away. $\times 750$.

etched with 20 per cent HNO_3 shows the primary dendrites of FeSi surrounded by deep voids where the iron-rich phase was dissolved away.

In passing, attention might be drawn to the fact that fractographs of this alloy show a complete absence of crystallographic detail, which is in marked contrast to the case with alloys richer in

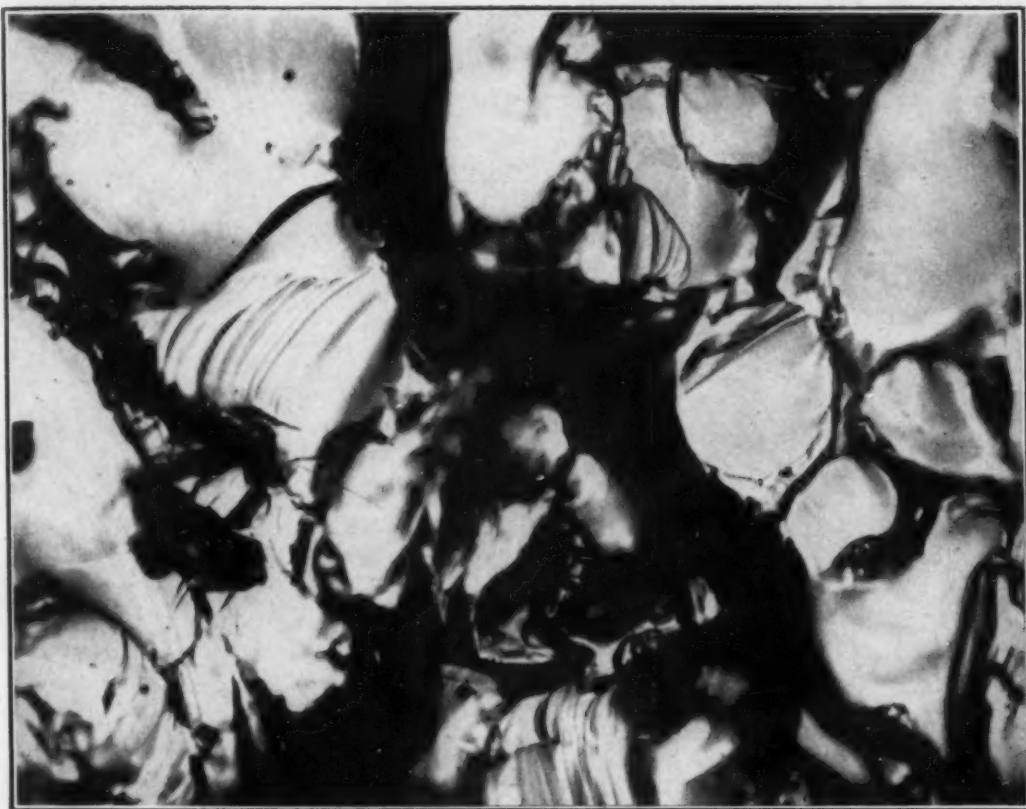


Fig. 25—Fractograph of Alloy VI, Again Revealing the Typical Fracture Pattern of FeSi. $\times 500$.

iron. Reviewing the earlier figures, which tended toward prolific variation in detail, one now finds that the single variable of silicon content has delimited the many fracture types through progressive additions of silicon until this one simple pattern remains near 33 per cent silicon. Furthermore, the progression of these many patterns, whose numbers tended to defeat interpretation when considering any one alloy, may now be seen in review to be somewhat orderly and probably highly meaningful. As the allotropy of the iron and its numerous systems of slip, twinning, and cleavage have been left behind, the cleavage patterns have taken on character, until the remaining two-thirds of the system, as will be shown, contains fracture pat-

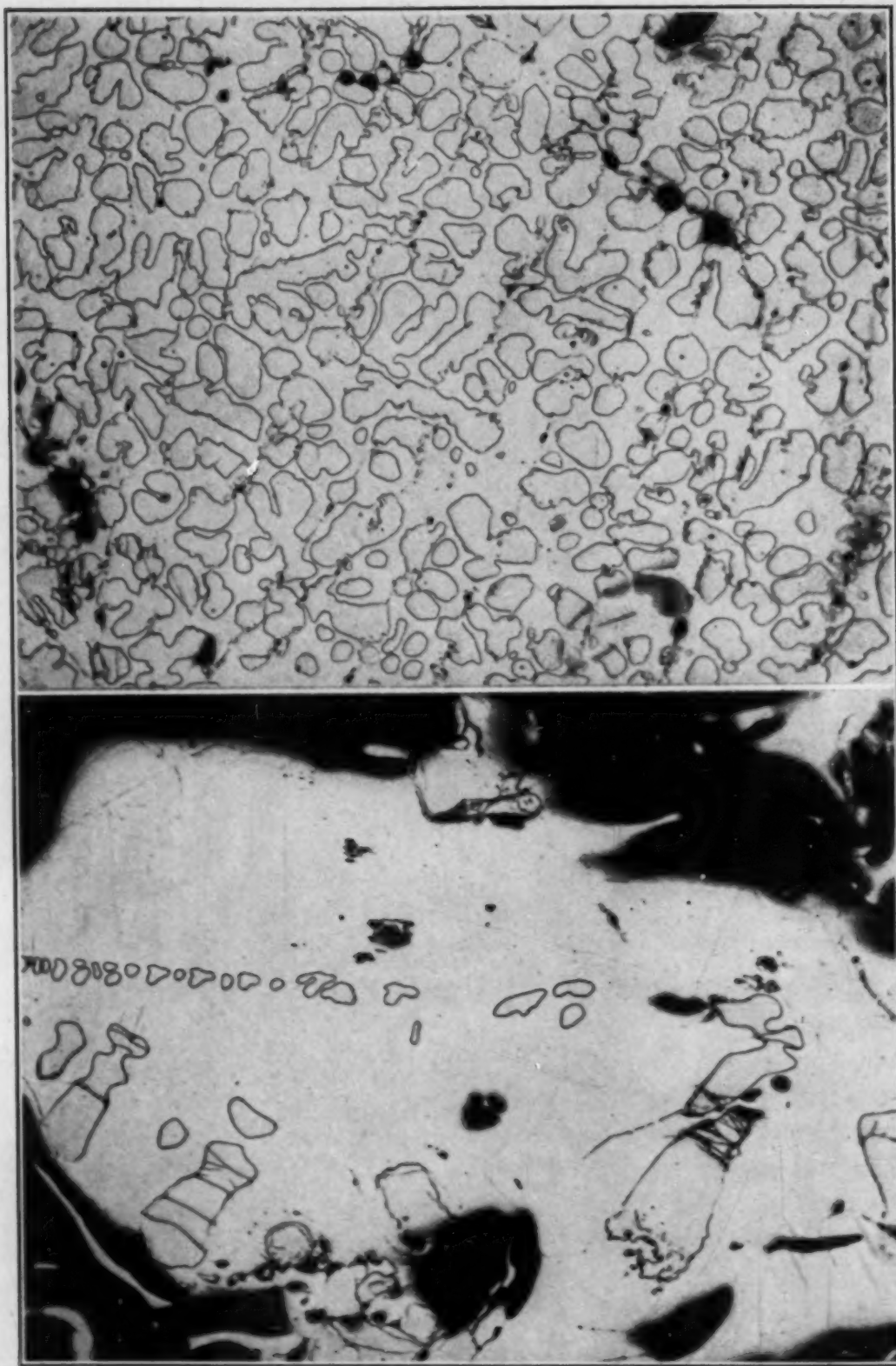


Fig. 26—Constitution of Alloy VI. Polished Specimen Etched with 20 Per Cent HNO_3 , Showing Epsilon Surrounded by Silicon-Rich Phase or Eutectic. $\times 100$.
Fig. 27—Constitution of Alloy VII. Polished Specimen Etched with $\text{HNO}_3\text{-HF}$ Solution, Showing a Primary Structure Imbedded in Zeta. $\times 100$.

terns which are in a large part highly characteristic and apparently invariant.

Alloy VI (39.54 Per Cent Silicon)—As may be seen in Fig. 23, the fracture pattern of this 39.54 per cent silicon alloy is seemingly identical with the fracture pattern of FeSi, already discussed. Referring back to the diagram in Fig. 1, one can conclude that the predominating phase is truly FeSi, but that the secondary phase is now a silicon-rich phase, or eutectic, in contrast to the preceding alloy. In the photomicrograph in Fig. 28, these two phases are readily evident.

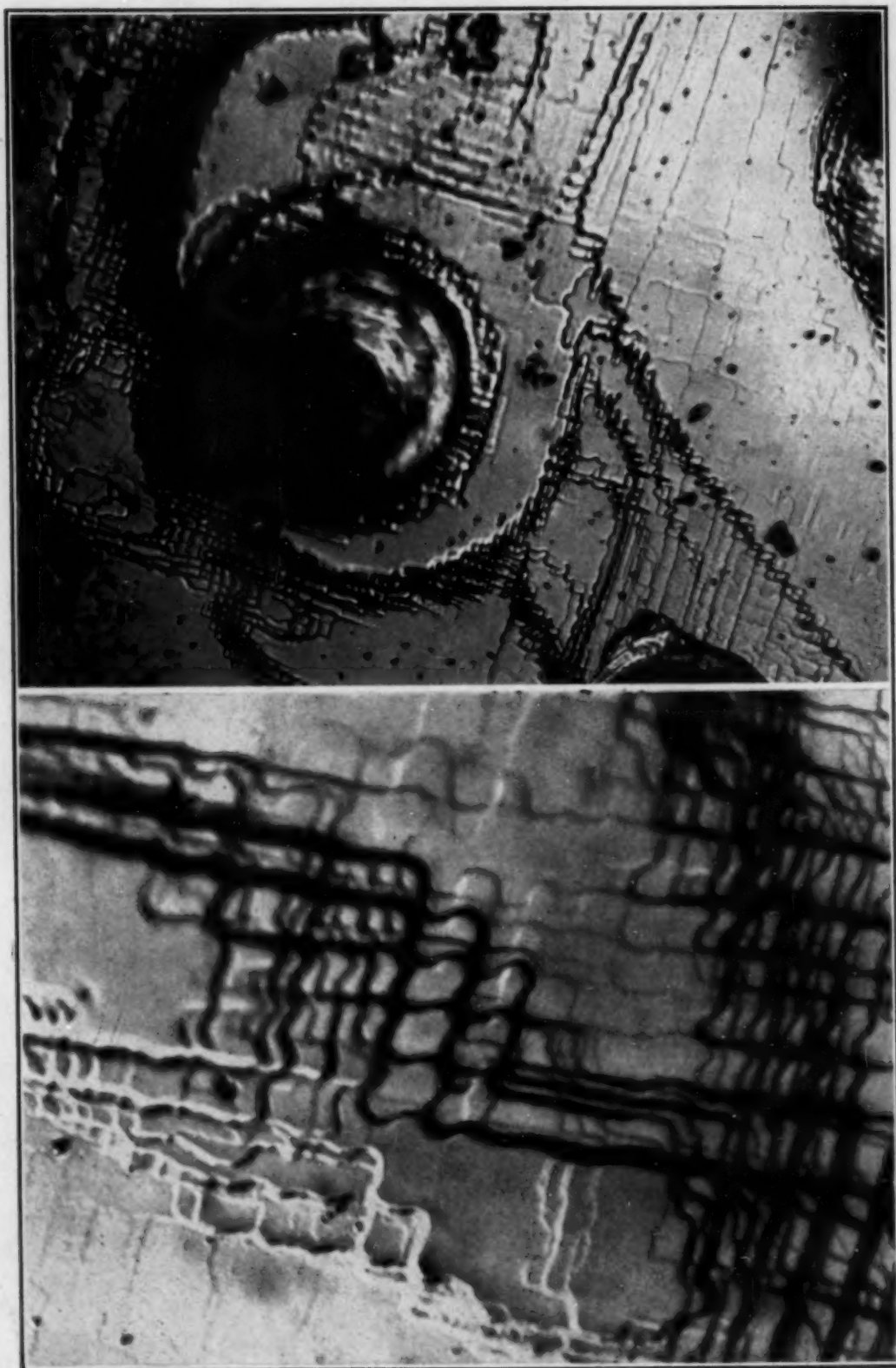
No pattern other than the one shown in Fig. 25 was ever observed in this alloy, or in Alloy V, making the identification of the epsilon phase exceedingly simple with fractography.

Alloy VII (50.18 Per Cent Silicon)—Alloys of this composition have involved a great deal of argument which has not yet resolved itself satisfactorily. A new silicide definitely forms in this range and was identified as FeSi₂ by Phragmén (10) who claimed a narrow range of miscibility for the compound. Haughton and Becker (15), however, believed the compound to be Fe₂Si₅ with a solubility range of about 8 per cent.

Recently, Ageev and several Russian colleagues (23) published an investigation which claimed to show that this zeta phase resulted from a peritectic reaction between FeSi and the residual liquid and lay in the range of 53 to 59 per cent silicon. This conforms with Haughton and Becker's work in indicating the compound Fe₂Si₅, originally proposed by Sanfourche (24).

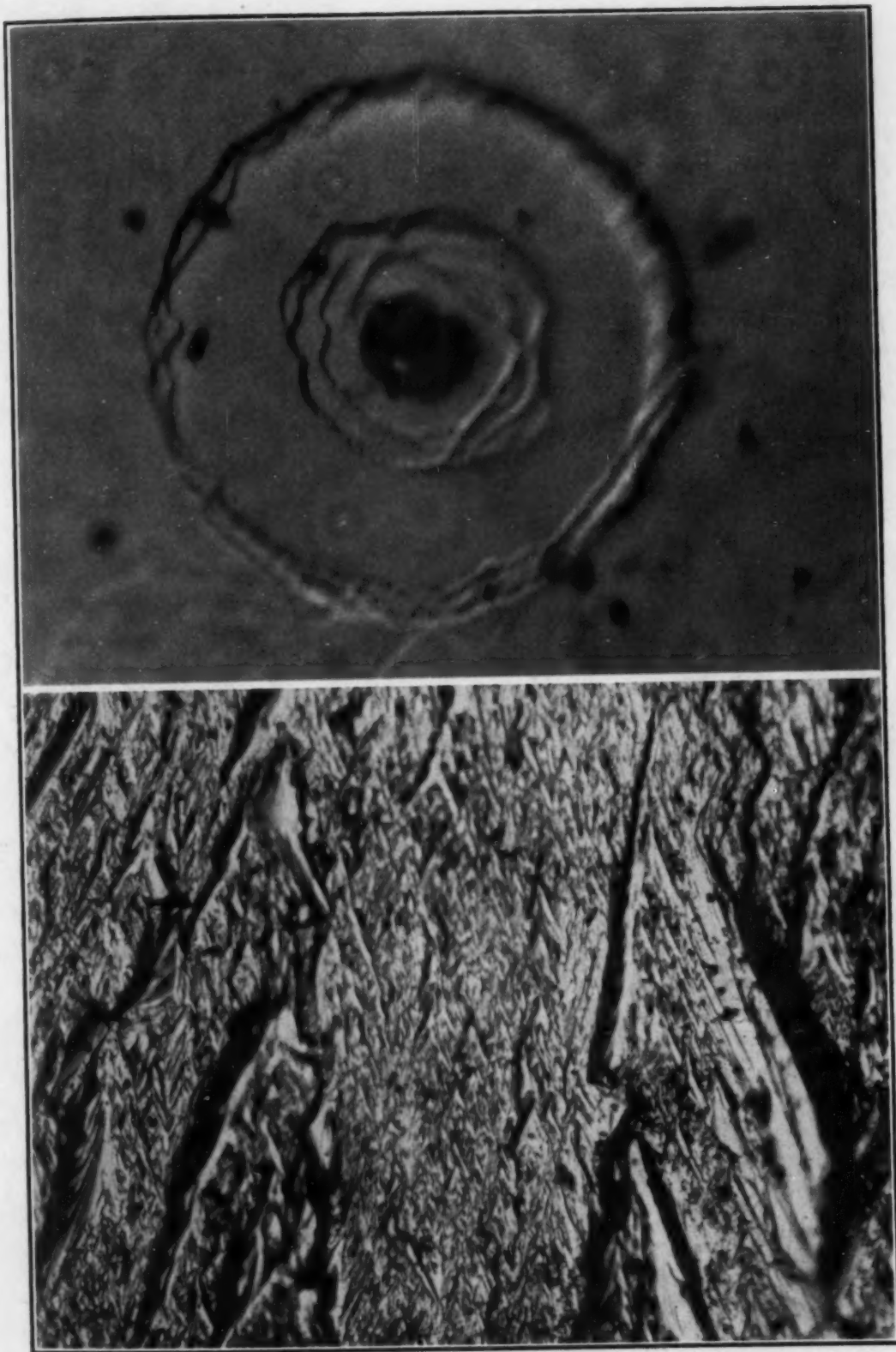
There is nothing in the present research to distinguish definitely between these compositions for the zeta phase; but photomicrographs taken of this alloy in the as-cast condition (see Fig. 27), and also after annealing for 1 hour at 1000 degrees Cent. (1830 degrees Fahr.) and air cooling, show two phases. The minority phase is plainly primary and dendritic and is highly suggestive of the epsilon phase shown in previous photomicrographs. If this observation is significant, then the composition of zeta must lie at silicon values greater than the 50.18 per cent content in this alloy, which suggests that Fe₂Si₅ is more likely than FeSi₂ for expressing the composition of zeta.

Fractography is especially applicable to these alloys because much of the confusion has resulted from the difficulty of polishing this friable material. As described elsewhere (1), a mere chip suffices for a specimen in fractography.



Fractographs of Alloy VII

Fig. 28—(Above) Characteristic and Apparently Invariant Fracture Pattern of the Zeta Phase. $\times 500$. Fig. 29—(Below) The Characteristic "Terrace Structure" at Higher Magnification. $\times 2000$.



Fractographs of Alloy VII
Fig. 30—(Above) Typical Example of a Concentric "Terrace Structure" Around
a Certain Type of Inclusion. $\times 2000$. Fig. 31—(Below) Unknown Structure. $\times 500$.

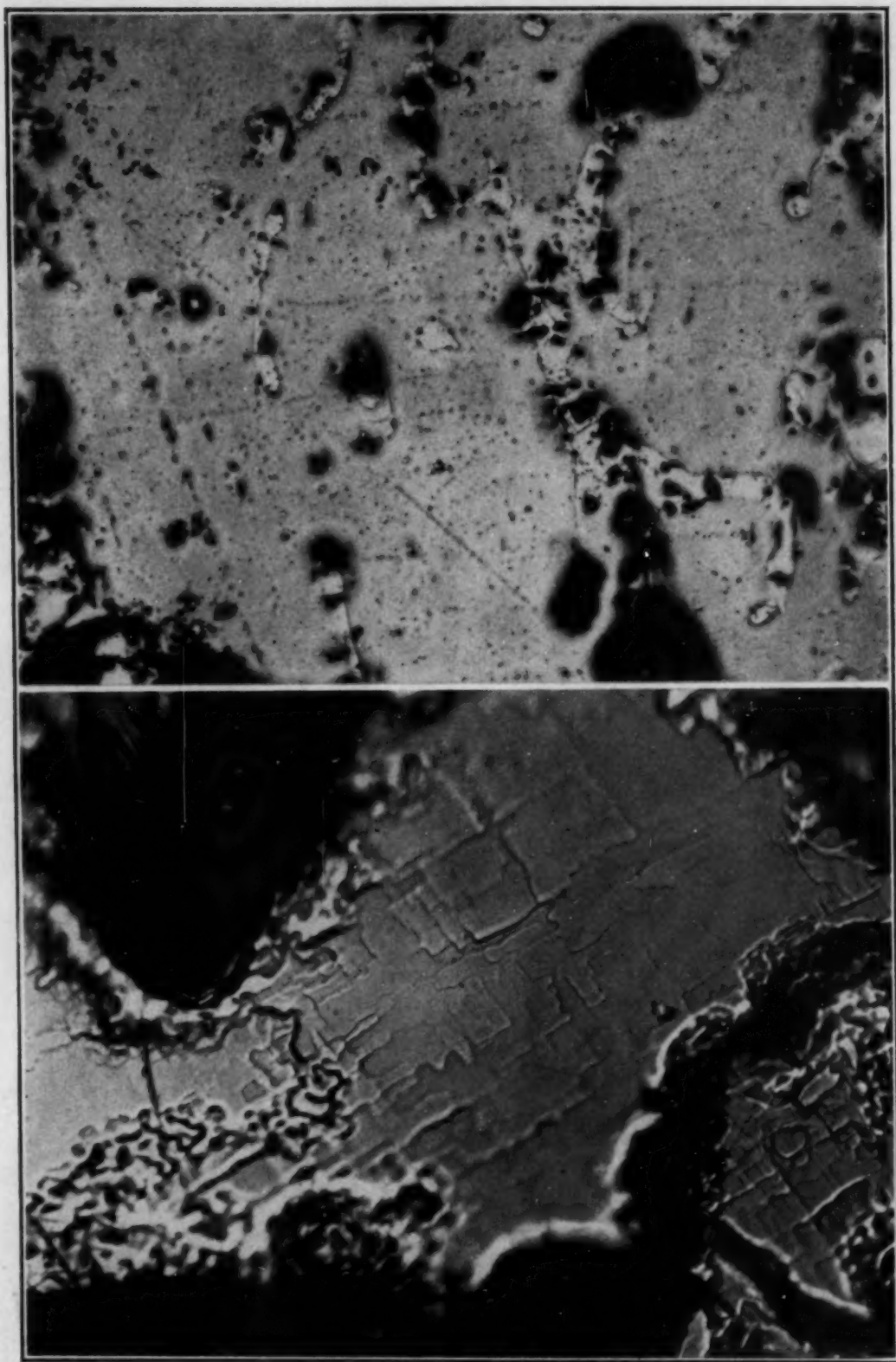


Fig. 32—Constitution of Alloy VIII. (Above) Polished Specimen Etched with HNO_3 -HF Solution, Showing Zeta and Theta Phases. $\times 100$. (Below) Fractograph Identifying the Zeta Phase by its Characteristic Cleavage. $\times 500$.

Under the microscope, a fracture presents a rather startling appearance, the zeta phase showing plainly as an elaborately terraced structure filled with a minute detail which is constant in appearance and completely characteristic of this phase. Figs. 28 and 29 present this typical pattern at different magnifications. A delicate buffing operation, performed with an electric hand-grinder (1), removed the terraced structure; and it could not be brought back by etching. The pattern is, therefore, characteristic of cleavage only.

A second remarkable observation is shown in Fig. 30. A circular terracing, symmetrical about an inclusion, is found throughout this material. Since this phenomenon is being investigated further, its discussion will be omitted here.

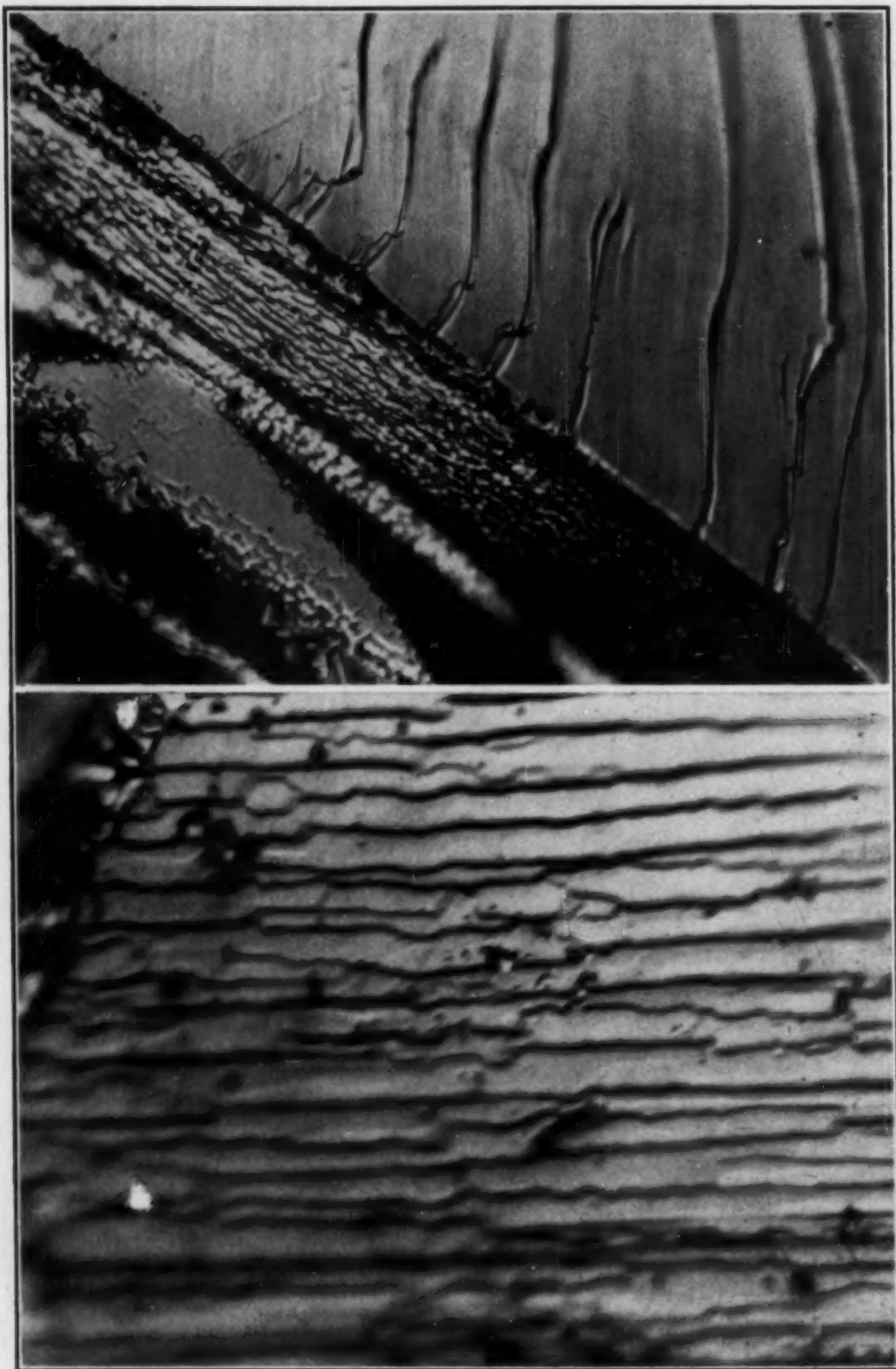
As for the primary phase just discussed, all the evidence on the fractographs points to its being epsilon. This is consistent with the observation made in discussing the photomicrograph in the previous Fig. 27 and confirms the formula Fe_2Si_5 for zeta. One fractograph, shown in Fig. 31, resembles nothing seen before. Perhaps it relates to the unknown "chi" phase recently mentioned by Ageev, et al., for alloys of this composition (23).

In closing the discussion of Alloy VII, it will be pointed out that the terraced structure must again denote intragranular imperfection, and on a scale which is sufficiently minute to escape detection by etching, and yet gross enough to predetermine the location of cleavage. The theoretical density of zeta, incidentally (3), is 5.02 gms./cc.; whereas the measured density is only 4.75 gms./cc., indicating an internal imperfection of considerable magnitude.

Alloy VIII (78.26 Per Cent Silicon)—While especially difficult to polish and examine in the customary manner, this alloy is studied conveniently by fractography. In Fig. 32, the photomicrograph shows two phases which can be interpreted as zeta and theta, the theta phase being nearly pure silicon with some small amount of iron in solution (3).

In contrast to this unsatisfactory photomicrograph, which required special and protracted metallographic treatment, the fractograph in the same figure immediately reveals the characteristic zeta pattern; and a small untreated chip, mounted and observed within a matter of minutes, served as the specimen.

As for the theta phase, its cleavage is often indistinct, although Fig. 33 shows this phase surrounding the characteristic terrace pattern of zeta in a small patch to the left center. A striking lamellar pattern of theta is also shown in Fig. 34.



Fractographs of Alloy VIII

Fig. 33—(Above) Cleavage Pattern Showing Theta Surrounding Small Pool of Zeta. $\times 500$. Fig. 34—(Below) Theta Cleavage at Higher Magnification. $\times 2000$.

CONCLUSIONS

An investigation of the structures on cleavage facets of iron-silicon alloys, using the metallographic technique referred to as fractography, shows that:

1. At 1.59 per cent silicon all patterns are of the lineage or mosaic type found in pure iron and are consistent with a single alpha phase. A certain secondary diversity found in these patterns can be accounted for on the basis of the allotropy and the numerous systems of deformation planes characteristic of alloys of this composition.

2. At 4.24 per cent silicon, although photomicrographs show only the same alpha phase, fractographs reveal some subtle structural change already occurring within that phase, such that this alloy can be distinguished from the preceding. The restriction of slip to {110} in this alloy may account for some of this change.

3. At 11.84 per cent silicon, photomicrographs still show only one phase, but fractographs reveal patterns which are entirely distinctive in comparison to the patterns of both previous alloys and which, along with other observations, are taken to express superlattice formation as the composition Fe_3Si is approached.

4. With 18.10 per cent silicon, a cleavage pattern occurs for one of the two phases present which is ascribed to FeSi and is highly distinctive because of its complete lack of crystallographic markings. The second phase is alpha, or a modification of alpha, within which unique structures appear. These intrusive structures are ascribed to precipitation of the compound Fe_5Si_3 .

5. With 28.83 per cent silicon, the entire fracture shows the characteristic and invariant cleavage of FeSi , with its dendrites imbedded in a secondary phase richer in iron.

6. Fractures of 39.54 per cent silicon alloys appear the same as the preceding, except that the primary FeSi is now surrounded with a secondary phase richer in silicon.

7. Commercial 50 per cent ferrosilicon shows a fracture pattern of the zeta phase which is completely distinctive and has a remarkably detailed structure. A primary phase also present can be identified as epsilon, thereby confirming Fe_2Si_5 as the composition of zeta. There is evidence of still another structure which is not clearly understood.

8. Commercial 75 per cent ferrosilicon clearly reveals the characteristic pattern of zeta imbedded in the high-silicon theta phase.

9. Many of the cleavage patterns, if not all, resist explanation on classical grounds of deformation and cleavage and clearly point to the pre-existence of an intracrystalline imperfection structure which must exert a tremendous influence upon the entire nature of the material.

10. The technique of fractography is especially applicable to the alloys in the iron-silicon system; and the new structures brought forth in this preliminary study hold some promise for further research.

ACKNOWLEDGMENT

Acknowledgment is made to the Rustless Iron and Steel Corporation, and to Mr. A. L. Feild, technical director, for the permission to publish this work.

References

1. C. A. Zapffe and M. Clogg, Jr., "Fractography—A New Tool for Metallurgical Research," *TRANSACTIONS, American Society for Metals*, Vol. 34, 1944, p. 71.
2. B. Stoughton and E. S. Greiner, "Progress Notes on the Iron-Silicon Equilibrium Diagram," *Transactions, American Institute of Mining and Metallurgical Engineers*, Vol. 90, 1930, p. 155-91.
3. E. S. Greiner, J. S. Marsh, and B. Stoughton, "The Alloys of Iron and Silicon," *Alloys of Iron Monograph*, Engineering Foundation, McGraw-Hill Co., New York, 1933, p. 457.
4. C. S. Barrett, G. Ansel, and R. F. Mehl, "Slip, Twinning and Cleavage in Iron and Silicon Ferrite," *TRANSACTIONS, American Society for Metals*, Vol. 25, 1937, p. 702-33; disc. p. 733-6.
5. Charles S. Barrett, "The Structure of Metals," New York: McGraw-Hill.
6. C. A. Zapffe and G. A. Moore, "A Micrographic Study of the Cleavage of Hydrogenized Ferrite," *Metals Technology*, Vol. 10, Technical Publication No. 1553, 1943, 19 pp.; also *Transactions, American Institute of Mining and Metallurgical Engineers*, Vol. 154, 1943, p. 335-52; disc., p. 352-9.
7. C. A. Zapffe and C. E. Sims, "Hydrogen Embrittlement, Internal Stress, and Defects in Steel," *Metals Technology*, Vol. 8, Technical Publication No. 1307, 1941, 37 pp.; also, *Transactions, American Institute of Mining and Metallurgical Engineers*, Vol. 145, 1941, p. 225-61; disc., p. 261-71.
8. J. E. Stead, "The Crystalline Structure of Iron and Steel," *Journal, Iron and Steel Institute*, Vol. 53, 1898, p. 145-89; disc., p. 190-205.
9. H. B. Pulsifer, "Microscopic Structure of Copper," *Transactions, American Institute of Mining and Metallurgical Engineers*, Vol. 73, 1926, p. 707-39; disc., p. 739-41.
10. G. Phragmén, "The Constitution of the Iron-Silicon Alloys," *Journal, Iron and Steel Institute*, Vol. 114, 1926, p. 397-404.
11. E. R. Jette and E. S. Greiner, "An X-Ray Study of Iron-Silicon Alloys Containing 0 to 15 Per Cent Silicon," *Transactions, American Institute of Mining and Metallurgical Engineers*, Vol. 105, 1923, p. 259-75.

12. D. Harker, "Order Hardening: Its Mechanism and Recognition," *TRANSACTIONS*, American Society for Metals, Vol. 32, 1944, p. 210-34; disc., 234-8.
13. J. E. Hurst and R. V. Riley, "The Occurrence of the Carbide Phase in High-Silicon Iron-Carbon Alloys," Iron and Steel Institute, Annual General Meeting, 1944, Preprint.
14. M. G. Corson, "The Constitution of the Iron-Silicon Alloys, Particularly in Connection with the Properties of Corrosion-Resisting Alloys of this Composition," *Transactions*, American Institute of Mining and Metallurgical Engineers, Vol. 80, 1928, p. 249-300.
15. J. L. Haughton and M. L. Becker, "The Constitution of the Alloys of Iron with Silicon," *Journal*, Iron and Steel Institute, Vol. 121, 1930, p. 315-32; disc., p. 333-5.
16. J. E. Hurst and R. V. Riley, "A Note on the Microstructure of High-Silicon Acid-Resisting Iron," Iron and Steel Institute, Annual General Meeting, October 1943, Preprint.
17. W. J. Wrazej, "The Apparent Microstructure Produced by Hydrofluoric Acid Etching Reagents on Pure Iron and Iron-Silicon Alloys Barley Shell Markings," Iron and Steel Institute, April 1944, Preprint.
18. A. Osawa and T. Murata, "The Equilibrium Diagram of the Iron-Silicon System," *Nippon Kinzoku Gakkai-Si*, Vol. 4, 1940, p. 228-42; C.A. Vol. 35, 1941, p. 423.
19. A. R. Weill, "Structure of the Eta Phase of the Iron-Silicon System," *Nature*, Vol. 152, 1943, p. 413.
20. E. S. Greiner and E. R. Jette, "X-Ray Study on the Constitution of Iron-Silicon Alloys Containing from 14 to 33.4 Per Cent Silicon," *Transactions*, American Institute of Mining and Metallurgical Engineers, Vol. 125, 1937, p. 473-81.
21. G. Phragmén, "On the Structure of Iron-Silicon Alloys," *Jernkontorets Annaler*, Vol. 107, 1923, p. 121-31.
22. S. V. Malashenko and Z. I. Vasilevskaya, "Rapid Determination of Si in Fe-Si," *Trudy Tsentral. Lab. Zavoda "Bol'shevik"* 1940, p. 200-3; *Khim. Referat. Zhur.*, Vol. 4, No. 4, 1941, p. 74; C.A. Vol. 37, 1943, p. 4987.
23. N. V. Ageev, N. N. Jurnakov, L. N. Guseva, and O. K. Konenko-Gracheva, "Physical-Chemical Investigation of Ferrosilicon," *Metalurg*, No. 1, 1940, p. 5-12; *Khim. Referat. Zhur.*, No. 8, 1940, p. 15.
24. A. Sanfourche, "Contribution to the Study of Iron-Silicon Alloys," *Rev. Mét.*, (Mem.), Vol. 16, 1919, p. 212-24.

DISCUSSION

Written Discussion: By David Harker, Research Laboratory, General Electric Co., Schenectady, N. Y.

I am sure that metallurgists will feel grateful to the authors for presenting this beautiful picture gallery of fractured surfaces. The explanations of their contours will doubtless furnish material for countless future discussions.

My own interest is mainly in the section of the paper concerning alloy III—the 11.84 per cent silicon in iron alloy. Figs. 8 and 10 show structures which the authors ascribe to superlattice formation.

Fig. 8 shows a network on a scale small compared to the grain structure of the specimen. This sub-boundary structure is explained by the authors as the result of shrinkage due to an ordering reaction. No doubt the authors

mean that the sub-boundary structure consists of cracks between regions which have shrunk away from one another during the ordering reaction. In my opinion, such a cracking could only occur if the external boundaries of the specimen were held fixed during the shrinkage; for if all parts of it shrank simultaneously, the result could only be a homogeneous decrease in size of the whole specimen. It makes no difference whether the shrinkage is due to ordering or to thermal contraction—the argument is the same. I suggest that the sub-boundaries are indeed due to cracks, but that they are caused by the inclusions present in the specimen. All the inclusions appearing in Fig. 8 (center) are on the sub-boundary lines, and most of them are at intersections of these lines. During cooling, the matrix doubtless shrinks more than the inclusions and so sets up inhomogeneous strains around them; when the metal is sectioned, polished, and etched, these strains are relieved by surface cracking. Fig. 8 (bottom) shows that the structure of the sub-boundary lines does not extend deep below the surface. The fractographs—Figs. 9, 11, 12, 13—show no structure similar to the sub-boundary structure, as they should, were this structure due to a network of shrinkage cracks.

Fig. 10 shows, I think, not a "ripple structure" (such as accompanies ordering reactions in which the shape of the unit cell changes), but rather the cube faces of one of the metallic crystals, exposed by preferential etching. The ordered structure proposed by Phragmén³ for Fe_3Si is cubic and so should not produce a ripple structure, since no anisotropic strains could be produced by its formation.

To sum up, I think the authors' evidence leaves the existence of an ordering reaction in Fe_3Si still in doubt.

Authors' Reply

Dr. Harker's comments are well received. However, we still believe shrinkage from ordering could cause this cellular structure, just as shrinkage of a mud flat causes a similar pattern. Homogeneous shrinkage occurs only over the zone developing from a single nucleus, and ordering very likely proceeds from many nuclei, each growing a zone which would shrink from the other. As for a fixed boundary, if such is important, the more rapid cooling at the surface of these rapidly cooled specimens would actually tend to fix a disordered boundary while the center had more time to become ordered.

We are glad to accept Dr. Harker's opinion on Fig. 10. Nevertheless, in none of the other specimens was such an etch pattern found.

³G. Phragmén, "Ueber dem Aufbau der Eisen-Silizium Legierungen," *Stahl und Eisen*, Vol. 45, 1925, p. 299.

FRACTURE STUDIES OF SOLDERED JOINTS

BY F. BERMAN AND R. H. HARRINGTON

Abstract

The method of fracture studies has been applied to the examination of the physical characteristics of "hard soldered" joints. Small pieces of copper were soldered end to end under various conditions, and were then bent at the joint to encourage fracture. In the case of vacuum applications, reheating of the joint in air, in the range of 500 to 700 degrees Cent. (930 to 1290 degrees Fahr.), will, upon subsequent fracturing, disclose oxidized surfaces, indicative of joints that would leak. In any case, much can be learned from the exposed fracture surfaces in conjunction with metallographic examination and occasional leak tests. The investigation showed, relative to vacuum-tight assemblies, that some copper to copper joints are best made with eutectic Ag-Cu alloy by soldering at 800 degrees Cent. (1470 degrees Fahr.) rather than at the conventionally higher temperatures.

THE purpose of this report is to cite the usefulness of fracture studies of soldered joints in conjunction with metallographic examination and, depending upon the use of the assembly, with leak tests at reduced pressures. Simplicity of procedure, ease of machining specimens, and clarity of results are outstanding features of this test. Effects on the joint are rather readily revealed for the following factors:

1. Cleanliness of brazed surfaces.
2. Brittleness or ductility.
3. Surface tension effects of molten solder.
4. Shrinkage properties of solders.
5. Porosity, often due to hydrogen liberation.
6. Effects of reheating in oxidizing atmospheres.
7. Variations in clearance.

DEFINITIONS

There has, in the past, been considerable confusion of definition of *soft soldering*, *hard soldering* and *brazing*. In the earlier

A paper presented before the Twenty-sixth Annual Convention of the Society, held in Cleveland, October 16 to 20, 1944. Of the authors, F. Berman is research assistant, and R. H. Harrington is research metallurgist, General Electric Research Laboratories, Schenectady, N. Y. Manuscript received June 24, 1944.

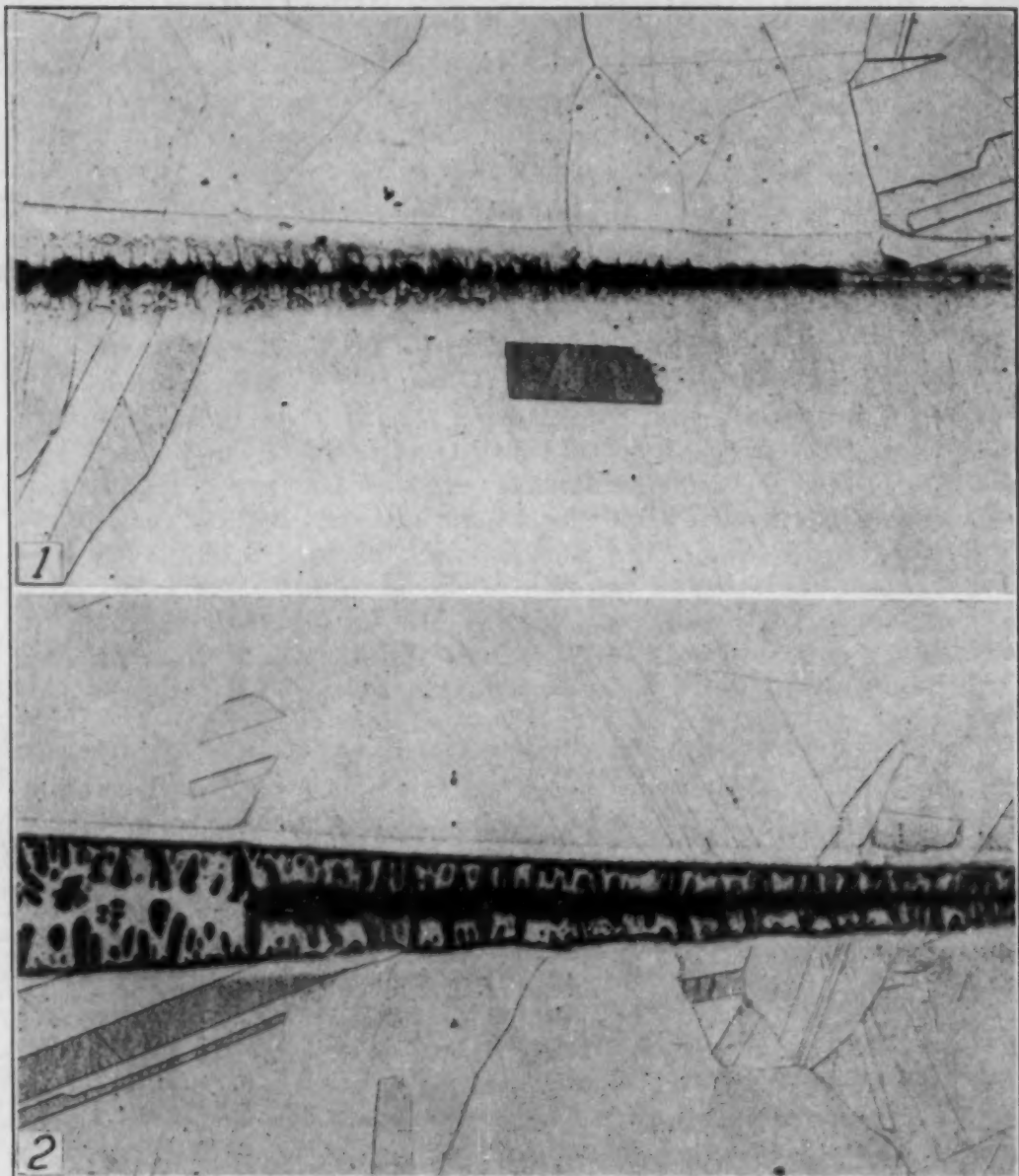


Fig. 1—Eutectic Silver Soldered Joint (No. 7), Copper to Copper. Soldered at 875 to 900 Degrees Cent. (1605 to 1650 Degrees Fahr.). Standard Ammonia Plus Hydrogen Peroxide Etch. $\times 100$.

Fig. 2—Eutectic Silver Soldered Joint (No. 8), Copper to Copper, After Subsequent Heating for 3 Hours at 550 Degrees Cent. (1020 Degrees Fahr.). Soldered at 875 to 900 Degrees Cent. (1605 to 1650 Degrees Fahr.). Standard Ammonia Plus Hydrogen Peroxide Etch. $\times 100$.

years, pure tin was called a hard solder while lead constituted a soft solder, and brazing referred to the use of brass as a solder. Through use in the art, the meaning of the first two was altered in recent years to yield the definition of *solder* given in the 1937 issue of Webster's Collegiate Dictionary: "Solder: a metal or metallic alloy used, when melted, to join metallic surfaces. Solders which melt

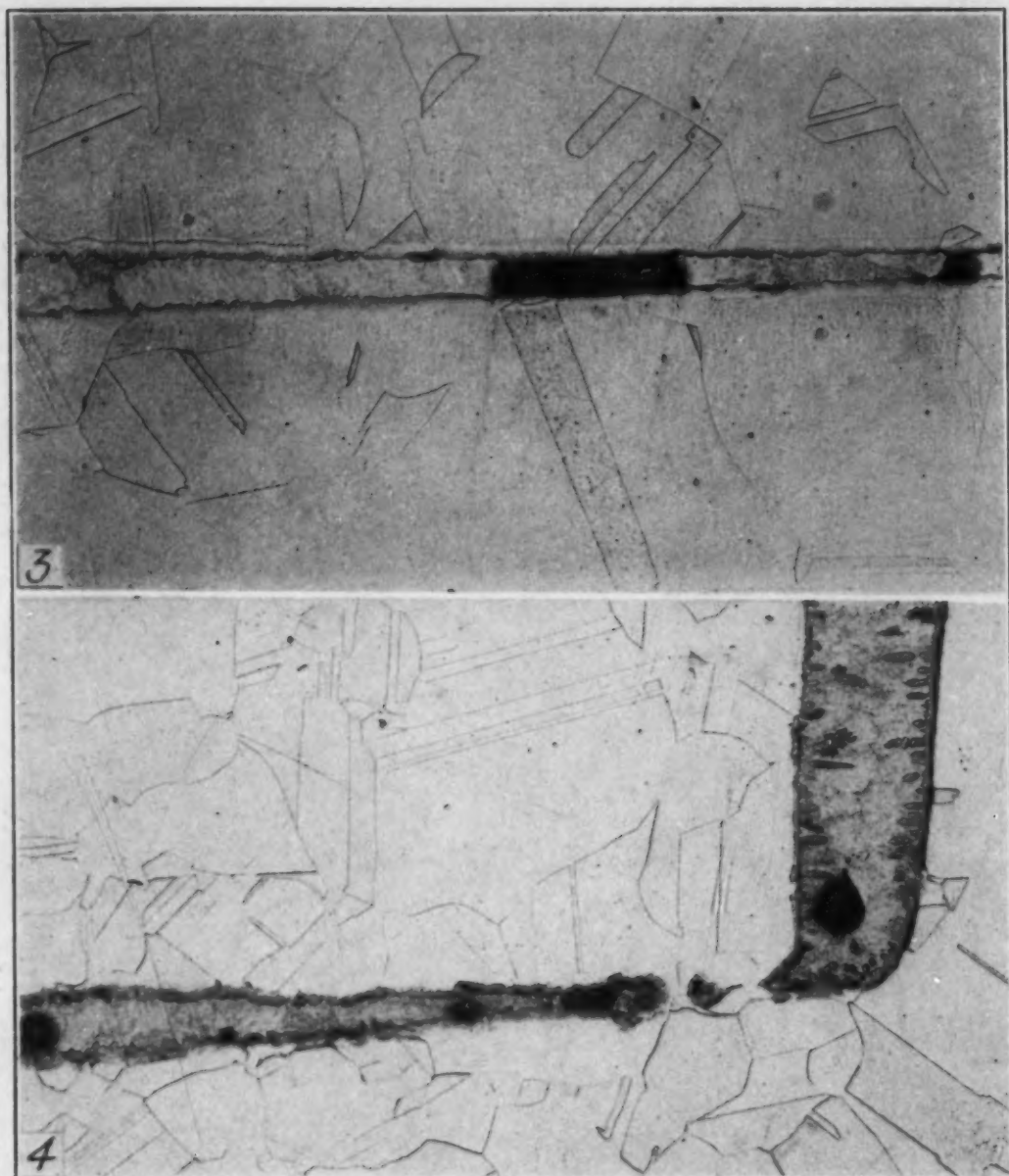


Fig. 3—Eutectic Silver Soldered Joint (No. 16), Copper to Copper. Soldered at 800 Degrees Cent. (1470 Degrees Fahr.). Only the Two Small Defects in the Whole Joint. Standard Ammonia Plus Hydrogen Peroxide Etch. $\times 100$.

Fig. 4—Eutectic Silver Soldered Joint, Copper to Copper. Soldered at 900 Degrees Cent. (1650 Degrees Fahr.). Standard Ammonia Plus Hydrogen Peroxide Etch. $\times 100$.

readily are *soft solders*; others fusing at a red heat are *hard solders*." This definition is adhered to by the Handbook of the American Welding Society. Still more recently preference has been shown to designate the use of *hard solders* as *brazing*. While all the joints described in this report are thus of the brazed type, the word *solder* has been retained since the method of fracture study is useful relative to all soldered joints.

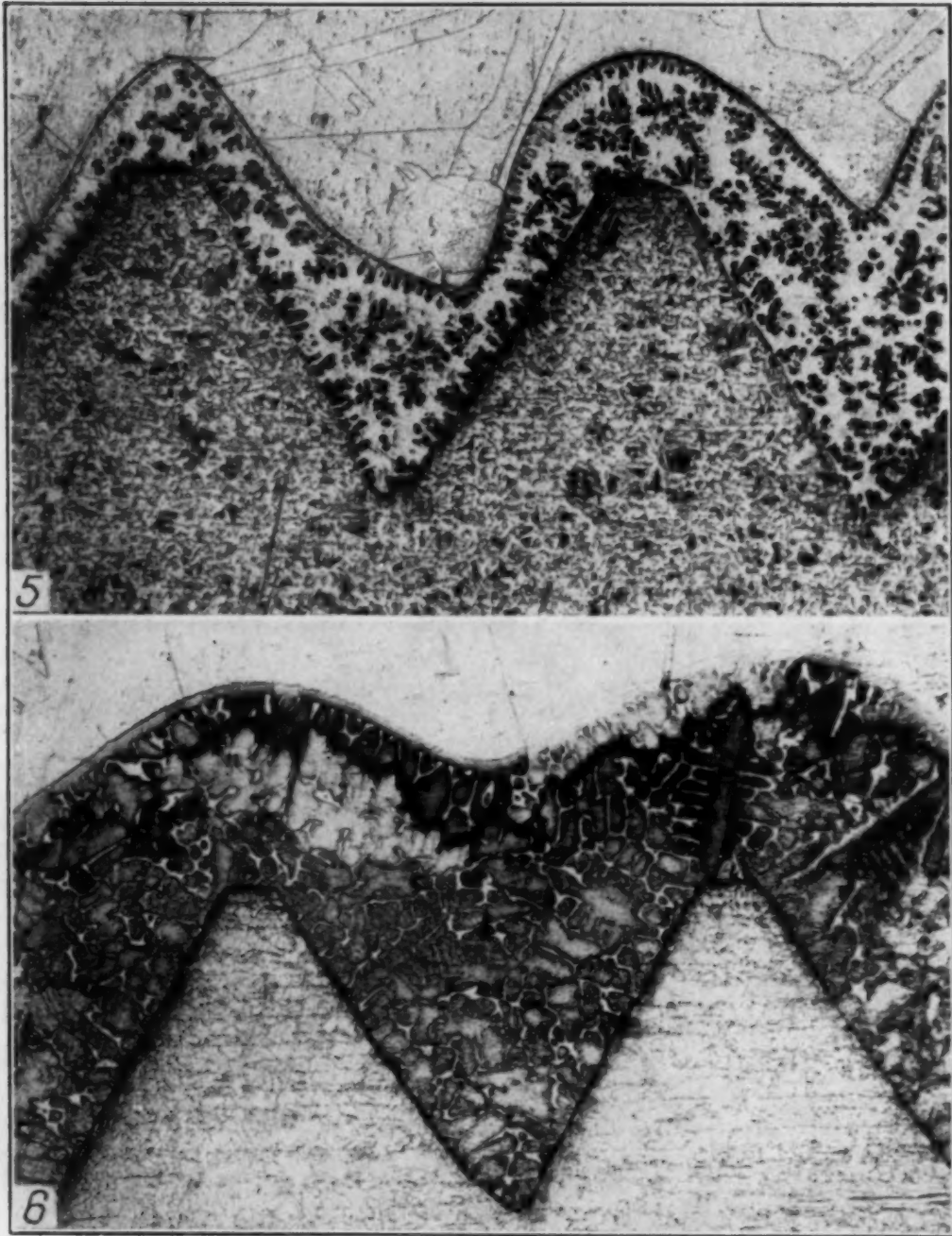


Fig. 5—Eutectic Silver Soldered Joint, Copper to Steel. Soldered at 900 Degrees Cent. (1650 Degrees Fahr.), Reheated 3 Hours at 500 Degrees Cent. (930 Degrees Fahr.). Ammonia Plus Hydrogen Peroxide Followed with 1 Per Cent Nital Etch. $\times 50$.

Fig. 6—60 Copper-40 Silver Soldered Joint, Copper to Steel. Soldered at 1000 Degrees Cent. (1830 Degrees Fahr.), Reheated 3 Hours at 500 Degrees Cent. (930 Degrees Fahr.). Ammonia Plus Hydrogen Peroxide Followed with 1 Per Cent Nital Etch. $\times 50$.

SOME TYPICAL DEFECTS THAT MAY BE ENCOUNTERED

During development of a complicated soldered assembly, metallographic studies revealed a variety of defects as shown in Figs. 1

through 7. This assembly had to withstand subsequent vacuum and service temperatures up to about 500 degrees Cent. (930 degrees Fahr.). Figs. 1, 2, and 3 are from three of the fracture samples herein described while Figs. 4 through 7 show defects from several other types of joints. Metallographic examination, alone, cannot disclose that these defects are harmful nor which are leakers. Defects shown in Figs. 1, 2, 4, 6, and 7 may cause leaks.

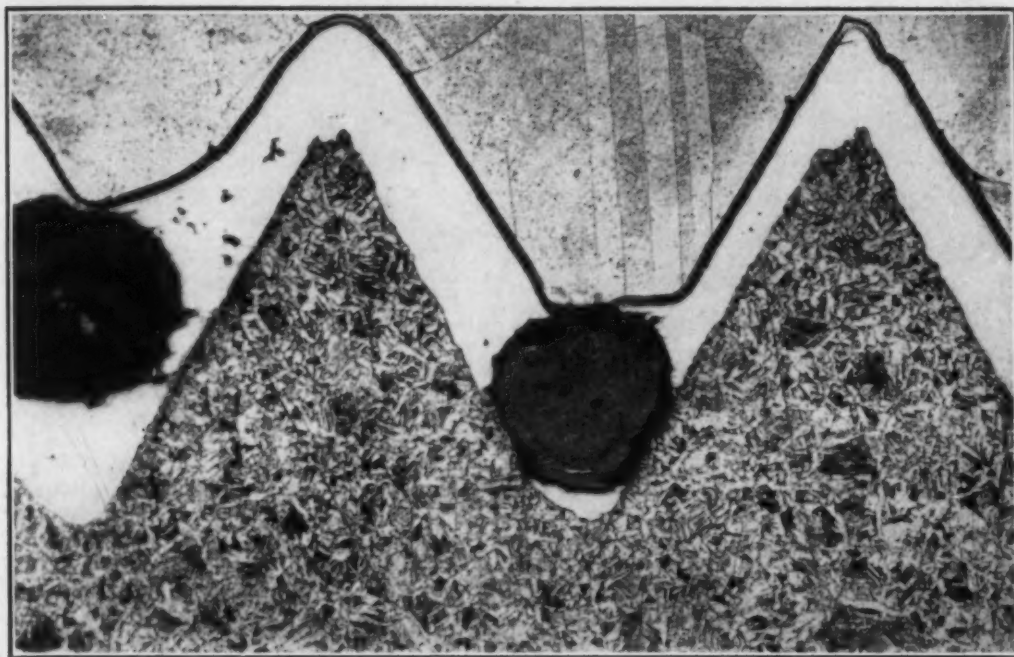


Fig. 7—Gold Soldered Joint, Copper to Steel, Soldered at 1000 Degrees Cent. (1830 Degrees Fahr.), Reheated 3 Hours at 500 Degrees Cent. (930 Degrees Fahr.). Ammonia Plus Hydrogen Peroxide Followed with 1 Per Cent Nital Etch. $\times 50$.

Comparison of Fig. 2 with Fig. 1 shows effect of diffusion of copper into the eutectic silver soldered joint caused by reheating the brazed joint for 3 hours at 550 degrees Cent. (1020 degrees Fahr.). Fig. 3 shows two minor defects, the only ones in an entire joint, due to slightly dirty areas on soldered surfaces. Fracture showed this joint to be leak proof. Fig. 4 appears to show porosity due to rejection of hydrogen from molten solder as it solidified. Fig. 5 shows the rounding off of threads in the copper side due to diffusion of copper into the solder while the steel threads are relatively unaffected. Fig. 5 is from a satisfactory joint but comparison with Fig. 6 shows, in Fig. 6, a continuous interdendritic shrinkage (a dark band) near the copper side probably due to the high shrinkage of 60 copper-40 silver (as compared with eutectic alloy of Fig. 5) and

more rapid cooling from the copper side of the joint. Fig. 7 shows a cross section of a practically continuous *cork screw* porosity, apparently due to rejection of hydrogen from the gold solder as it solidified.

PROCEDURE FOR FRACTURE STUDY

The joints made for this study consist of two pieces of OFHC copper $\frac{3}{16} \times 1\frac{1}{4} \times 1\frac{1}{4}$ inch, butt soldered on the $1\frac{1}{4}$ -inch side. The spacing between them was accomplished by means of steel sheet of 2 mils thickness placed in both ends of the joints. Each piece was chamfered at the top edge of the surface facing its mate, so as to keep the solder in place. Prior to assembling, all parts were etched lightly with 50 per cent nitric acid. The two pieces were held during soldering by a simple jig, with which they were clamped tightly. A thin sheet of steel, coated with chromium oxide paste, was placed beneath the joints to prevent excessive solder flow. The ends of the joints touching the jig were also painted with chromium oxide paste to keep them from being soldered in place.

Solder was applied in the form of wire either $\frac{1}{32}$ inch square or $\frac{1}{32}$ inch round. Two pieces of the solder, $1\frac{1}{4}$ inch long, were laid in the groove formed by the chamfered sections of copper. The actual soldering operation took place in 3-inch hydrogen muffle furnaces. All joints were held at soldering temperature for 3 minutes, after being brought up to that temperature as rapidly as possible.

Duplicate sets of most joints were made with each solder and at each temperature. Of each pair of joints, one was fractured as soldered, while the other was heated for 3 hours in air at either 550 or 700 degrees Cent. (1020 or 1290 degrees Fahr.) before being fractured. Before fracturing any joint, a $\frac{1}{4}$ -inch section was cut from one end, to be used for metallographic examination if desired. Heating in air causes oxidation of any open interface, or cavity, or exposed surface, which shows up clearly in the subsequent fracture.

In order to fracture these joints, one side was held firmly in a vise, and the free end was struck with a hammer until it was either fractured completely or bent at a right angle. The chamfered side of the joint was kept on the outside of the bend. If this was not sufficient to bring about fracture, the joint was bent double by pressing its ends together in the vise. The steel spacers, transverse at the ends of the joint, have no effect on the character of the fracture

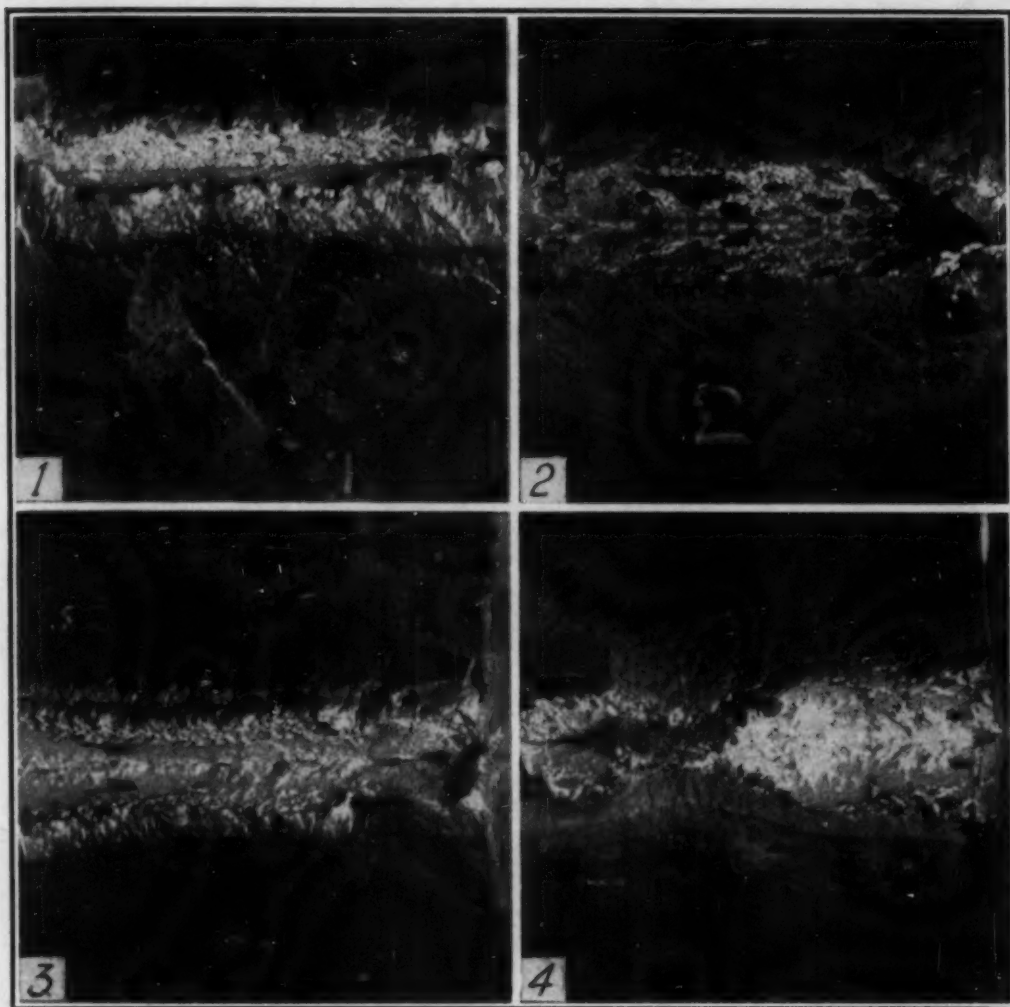


Fig. 8—Photograph of Joints 1 Through 4. $\times 2$.

as they are parallel to the direction of bending. The fracture takes place essentially as though the steel spacers had not been present.

DATA AND RESULTS

Table I summarizes all of the conditions pertaining to each sample joint, the joints being numbered consecutively from 1 to 18. Fractures of the corresponding joint numbers are shown in Figs. 8 through 12.

Soldering of samples 1-14 inclusive was done in an atmosphere of hydrogen purified by passing through sulphuric acid, sodium hydroxide pellets, and phosphorous anhydride. Samples 15-18 were soldered in an atmosphere of unpurified *line* hydrogen.

Both the joints made with 60/40 solder, (Nos. 1 and 2 in Fig. 8), had hemispherical voids on their fracture surfaces, these being about $\frac{1}{16}$ inch in average diameter. The samples fractured readily when bent at right angles. Reheating of No. 2 in air resulted in strongly oxidized fracture surfaces, indicating the existence of a continuous passage for air in the soldered joint. Samples 3 and 4



Fig. 9—Photograph of Joints 5 and 6. $\times 2$.

Table I
Conditions for Soldered Joints

No.	Solder	Spacing of Joint	Soldering Temperature Degrees Cent.	Reheat- ing Time	Reheating Temperature Degrees Cent.
1	60/40*	4 mils	975-1000	0	...
2	60/40	4 mils	975-1000	3 hrs.	700
3	eutectic†	4 mils	875- 900	0	...
4	eutectic	4 mils	875- 900	3 hrs.	700
5	gold	4 mils	975-1000	0	...
6	gold	4 mils	975-1000	3 hrs.	700
7	eutectic	2 mils	875- 900	0	...
8	eutectic	2 mils	875- 900	3 hrs.	550
9	eutectic + 2% Sn	2 mils	875- 900	0	...
10	eutectic + 2% Sn	2 mils	875- 900	3 hrs.	550
11	gold	2 mils	975-1000	0	...
12	gold	2 mils	975-1000	3 hrs.	550
13	silver	2 mils	875- 900	0	...
14	silver	2 mils	825- 850	3 hrs.	550
15	eutectic	2 mils	825	0	...
16	eutectic	2 mils	800	0	...
17	eutectic	2 mils	800	3 hrs.	550
18	eutectic	2 mils	900	0	...

*60% Cu, 40% Ag. †71.5% Ag, 28.5% Cu.

(eutectic solder), (Fig. 8), fractured equally readily, but contained fewer and smaller voids. The fracture surface of No. 4 was oxidized only slightly.

Joints 5 and 6 (soldered with pure gold, Fig. 9) had to be bent double before any appreciable fracturing occurred. There were

only very few small holes in the fracture surfaces. The only difference effected by reheating in air (No. 6) was a continued diffusion alloying between gold and copper resulting in greater resistance to fracture.

Joints 7, 8, 9 and 10 (Fig. 10) differed in fracture very little from one to another. (Joints 1 through 6 were made with a 4-mil

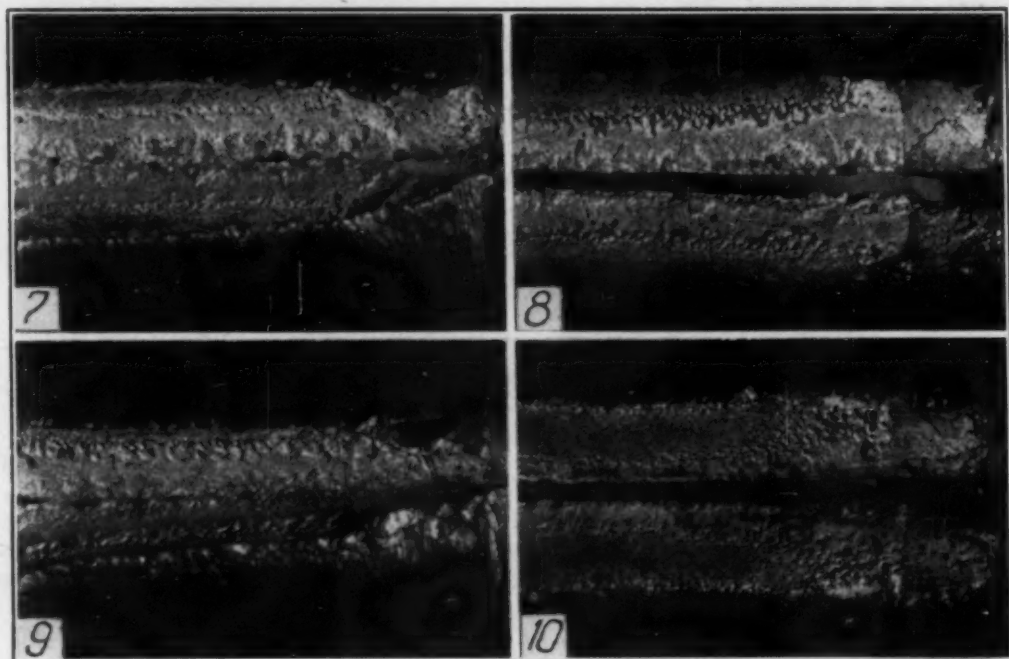


Fig. 10—Photograph of Joints 7 Through 10. $\times 2$.

solder space while joints 7 through 18 were constructed with only a 2-mil solder space.) Joints 7 and 8 were made with eutectic silver-copper solder while 9 and 10 were soldered with an alloy of eutectic + 2 per cent tin. All fractured readily through the solder, disclosing only a few round gas pockets. Reheating in air had no visible effect on the joints of samples 8 and 10. However, the appearance of the fractures indicated that the joint was broken by shrinkage cavities that might have been initiated by surface tension effects of the molten solder. Polished sections through joints 7 and 8 are shown, respectively, in Figs. 1 and 2. These photomicrographs appear to support the theory that combined surface tension and shrinkage caused the solder to separate along its central plane, resulting in the dendrite-lined split-cavity. The reheated sample (No. 8, Fig. 2) showed a higher degree of diffusion of copper into the original eutectic solder zone.

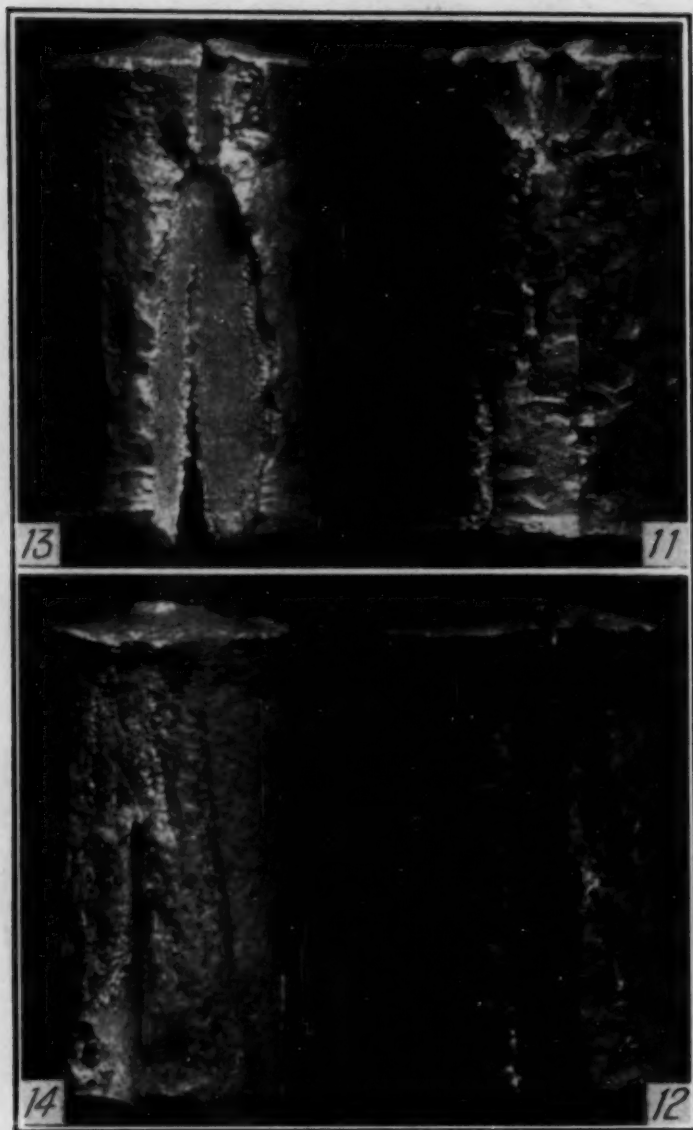


Fig. 11—Photograph of Joints 11 Through 14. $\times 2$.

Samples 11 and 12 (Fig. 11), soldered with gold, cracked only very slightly, even when bent double. Again, reheating (Sample 12), causing increased diffusion of gold and copper, had a beneficial effect on the strength of the bond. Although the melting point of gold is 1063 degrees Cent. (1945 degrees Fahr.), samples 5 and 6 and 11 and 12 were *actually soldered* in the range of 975 to 1000 degrees Cent. (1785 to 1830 degrees Fahr.). This is due to the rapid solid state diffusion of each of these metals in the other. With inter-diffusion of copper and gold at the contact surfaces of the gold solder with the copper plates, the melting point is progressively

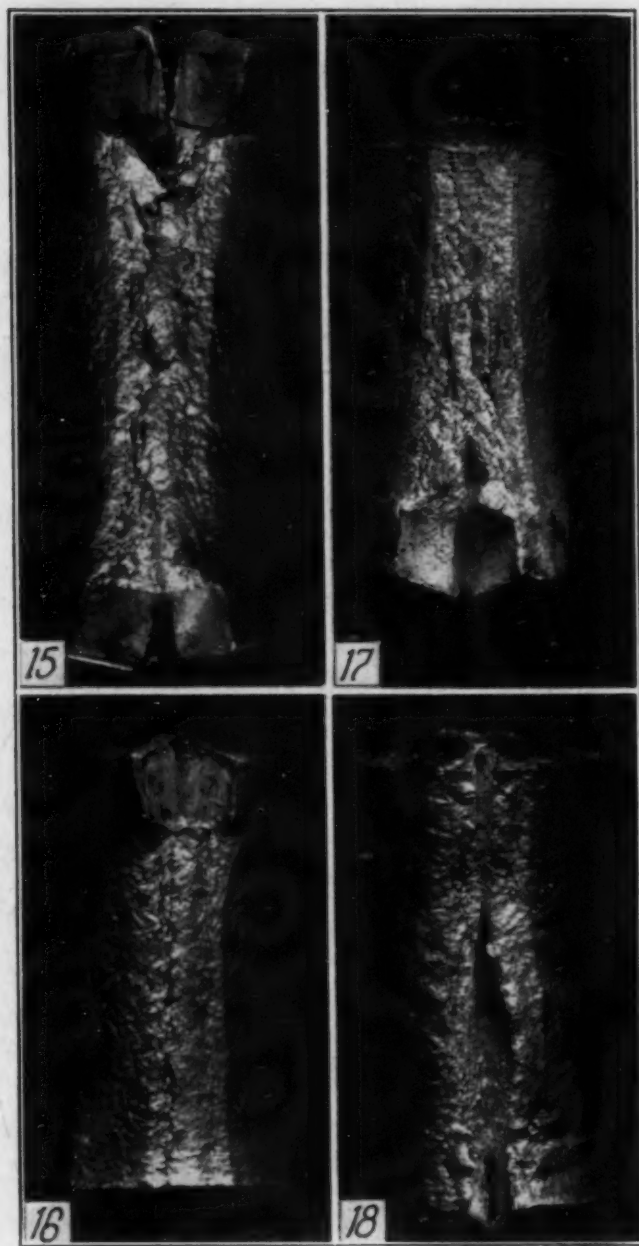


Fig. 12—Photograph of Joints 15 Through 18. $\times 2$.

lowered to 1000 to 975 degrees Cent. (1830 to 1785 degrees Fahr.) for copper contents (in the original gold) of 5 to 10 per cent.

The results observed for these gold-soldered joints suggested that the rapid alloying which occurs during their making was responsible for the satisfactory bonding properties. It was thought that similar characteristics might be obtained with pure silver. Samples 13 and 14 were prepared to check this possibility for silver. Both

joints were soldered at a temperature below the melting point of pure silver [961 degrees Cent. (1760 degrees Fahr.)] but above the silver-copper eutectic temperature [778 degrees Cent. (1435 degrees Fahr.)]. Both fractures (Fig. 11) were somewhat superior to those obtained previously for eutectic-soldered joints, but not as good as those for the joints soldered with gold.

Since it seemed that much of the previously observed inconsistency of eutectic-soldered joints might have been due to surface tension of the molten solder, an attempt was made to minimize this effect by keeping the solder more viscous. Lower soldering temperatures might accomplish this. Consequently test joints were made with eutectic solder in furnaces only slightly above the melting point of the eutectic alloy. The results achieved were surprisingly good. All three joints, Nos. 15, 16 and 17 (Fig. 12), appeared to be as good, if not actually better than the samples soldered with gold. Sample 15 was soldered at 825 degrees Cent. (1515 degrees Fahr.) while Nos. 16 and 17 were soldered at 800 degrees Cent. (1470 degrees Fahr.) with Sample 17 subsequently reheated 3 hours at 550 degrees Cent. (1020 degrees Fahr.) in air. They cracked open only slightly and even then the small tears were in the base metal, unalloyed copper. Fig. 3 shows a polished section through joint No. 16. The area chosen for the photomicrograph contains the only evidence of porosity in the whole joint. There are almost no darkened grains in the solder film, indicating only a small degree of alloying, if any, by diffusion of copper from the plate into the solder film whereas narrow edge zones of the plate do show slight alloying by diffusion of silver from the solder into the copper plate.

Sample 18 (Fig. 12) was eutectic soldered at 900 degrees Cent. (1650 degrees Fahr.) in the same furnace as the preceding three joints to establish the fact that temperature, and not furnace characteristics, was responsible for the improved quality of the joint of Samples 15, 16 and 17. The fracture of joint 18 matched that of joint 7, proving this point.

CONCLUSIONS

As a result of relatively few fracture samples, much was ascertained about soldered joints that could otherwise be deduced only by interpretation from other types of tests.

It is certain that a solder of 60 copper-40 silver cannot be suc-

cessfully used if joints are soldered at 975 to 1000 degrees Cent. (1785 to 1830 degrees Fahr.). The 60 copper-40 silver alloy has considerably greater shrinkage characteristics than the eutectic alloy (71.5 silver-28.5 copper).

The addition of 2 per cent tin does not appear to improve the eutectic alloy for soldering copper parts (as had previously been thought).

Gold makes an excellent soldered joint between copper parts when clearances are kept small. Excellent results are obtained with gold when the soldering temperature is kept below its melting point. However, gold holds no advantage over eutectic solder when this silver-copper alloy is used at the low soldering temperatures of 800 to 825 degrees Cent. (1470 to 1515 degrees Fahr.).

Much is gained, of course, by minimizing the clearance in the joints to be soldered.

Most important of all (for leak-proof joints between copper parts), the quality of joints soldered with eutectic silver-copper alloy can be greatly improved by keeping soldering temperatures as low as possible. The lower soldering temperatures reduce shrinkage, surface tension effects, diffusion of base metal into the solder film, and the amount of hydrogen dissolved in the initially molten solder.

Reheating soldered joints in air, previous to fracture test, often discloses oxidized fracture surfaces indicative of serious leak conditions relative to intended use of the joint for either pressure or vacuum applications.

For the photomicrographs, Figs. 1 through 7, the following etching reagents were used:

- a). For joints between two parts of copper: the standard ammonia plus hydrogen peroxide etchant.
- b). For joints of one part of copper to one of steel: ammonia plus hydrogen peroxide followed by an etch with 1% Nital.

ACKNOWLEDGMENT

The authors wish to express their appreciation for the preparation of the photomicrographs and photomacrographs by Miss I. G. MacLeod of the Metallographic Section of the General Electric Research Laboratories.

GRAIN SHAPE AND GRAIN GROWTH

BY DAVID HARKER AND EARL R. PARKER

Abstract

Arguments are presented to show that the ability of a metal to show grain growth depends not at all on grain size, but only on grain shape. When all grains in a metal have flat faces making 120-degree angles with adjacent faces, there can be no grain growth, no matter what the grain size. The distribution of the angles at which grain boundaries meet on the surface of a metallographic specimen provides a criterion for the growth stability of its grain structure. This distribution is calculated for the ideal stable structure in which only 120-degree angles exist between adjacent faces. It is shown experimentally that the distribution of grain boundary junction angles approaches the calculated one as a metal is annealed, no matter what the final grain size. Some specimens show grain growth on annealing, others do not; but the grain shape always approaches that of the ideal stable structure.

over simplification
2.
1.
A SPECIMEN of metal always consists of a number of regions in each of which the atomic arrangement is periodic, at least for short distances. To say it more vividly, but in not quite such well defined words, a piece of metal consists of more or less perfect crystals. The reason for this is that metal atoms are held together mainly by their attraction for the electron cloud in which they float. They tend to surround themselves compactly with other atoms, so that all the atoms may be as close as possible to the entire electron cloud. There is only a small number of ways in which an atom can be surrounded by a large number of other atoms. It is, therefore, not surprising that the surroundings of atoms at different places in a metal are similar. The structure of a metal is thus composed of a large number of atoms whose surroundings are all alike. This state of things automatically brings about a structure that repeats itself—a periodic structure, or crystal. Such a periodic arrangement of atoms does not arise full formed at all points of a large volume

A paper presented before the Twenty-sixth Annual Convention of the Society, held in Cleveland, October 16 to 20, 1944. Of the authors, David Harker is a member of the Research Laboratory, General Electric Co., Schenectady, N. Y., and Earl R. Parker is on the staff of the College of Engineering, University of California, Berkeley, Cal. Manuscript received July 14, 1944.

simultaneously. One atom, say, finds itself surrounded by others in one of the ways leading to closest packing. As a consequence, its neighbors are partially so surrounded and need not wait as long as the original atom to find themselves also surrounded by a close-packed arrangement. And so the periodic structure grows out from the original cluster until all the disorganized structure is used up.

The motion required to rearrange atoms into the best positions is furnished by the heat energy of the system. The higher the temperature, the more rapidly and violently the atoms move, and the more rapidly any change in the structure of a group of atoms can occur. Were this thermal motion absent, no changes in atomic positions could occur and no crystallization (or any other chemical reaction) could take place.

When a piece of metal is deformed (by hammering, rolling, bending, etc.), the perfection of the periodic structure in the metal's crystals is destroyed and a new rearrangement of the atoms becomes possible. This rearrangement will occur at a greater rate the higher the temperature. The smaller the deformation, the more nearly each atom is at equilibrium with its surroundings and the less likely is the new arrangement to have an orientation appreciably different from the old. If the deformation is large, the new structure may have an entirely different orientation from the old one. In either case, equilibrium nuclei form first and the new crystals grow from these nuclei.

The rate at which disturbed material produces a certain total volume of nuclei must be much less than the rate at which that same material can deposit itself on an advancing crystal boundary. To form a nucleus requires the simultaneous positioning of several atoms in a favorable arrangement, while subsequently the atoms in contact with the equilibrium structure have only to locate themselves individually in order to achieve a stable neighborhood. More formally, one could say that the free energy of activation is higher for nucleation than for growth. At low temperatures, then, only a few nuclei will form in a given volume of distorted material before it is totally filled by the new crystals growing from the first nuclei. At higher temperatures, a greater density of nuclei is expected before the volume is filled with equilibrium material.

After this recrystallization process is complete, the metal is composed of crystals, each extending in all directions from the point at which a nucleus was formed. Where two crystals growing from

different nuclei meet, there is a transition zone in which atoms do not belong to either crystal.

This zone can hardly be more than two or three atoms thick, since interatomic forces decrease very rapidly with distance. In this zone are atoms that belong permanently to neither one crystal nor the other, but, moving about due to their thermal energy, attach themselves first to one, then to the other of the two structures. Since the structures are equally stable, there is no more reason for an atom to stick to one more than the other. If, then, the average surroundings of an atom belonging to the crystal on one side of the transition zone are the same as those of one on the other side, as many atoms will leave one side per unit time as leave the other, and the transition zone will remain fixed in the specimen of metal. In other words, the atoms in the transition zone may be thought of as merely oscillating between the two crystals so that the position of this transition zone will remain fixed.

The material composing one homogeneous crystal surrounded by transition zones to other crystals is called a "*grain*" of the metal—the transition zone is called the "*grain boundary*." A grain is a solid block whose shape is determined by the shapes of the neighboring grains. The grain boundary is the surface surrounding each grain and separating it from neighboring grains.

A grain boundary is composed of *faces*, *edges*, and *vertices*. A face exists between every two grains in contact across a boundary. Each grain that is not completely surrounded by another grain—and very few are—is enclosed by a boundary that meets other boundaries. The meeting places between the boundary of one grain and the boundaries of neighboring grains are edges: each edge is the line along which three boundaries meet. Thus, a grain with only two neighbors will be enclosed by a boundary composed of two faces and one edge. If a grain has more than two neighbors, it will have more than one edge. The point at which three (or more) edges meet is a vertex. Fig. 1 depicts these features.

When a metal is examined under the microscope, the presence of grains and grain boundaries is revealed by means of a plane section through the specimen. The specimen is cut along such a plane, which is then polished and etched. The etching removes material at different rates from different grains, because the plane of section cuts across them in different crystallographic directions. The grain

boundaries are visible on the etched section as the transitions between the different levels produced by etching, or, sometimes, because they themselves etch more rapidly than any grain. Where the plane of section crosses a grain face, a line is visible. It crosses an edge or (very rarely) a vertex at a point. Three lines on the plane of section meeting at a point show that the plane of section is crossing three grain faces meeting at an edge. Four lines meeting at a point is observed very rarely and could mean either that the plane

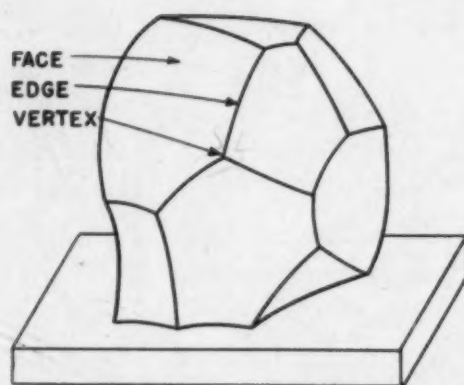


Fig. 1—A Grain, Showing that Faces and Edges May Be Curved.

of section passes through a vertex at that point, which is an improbable occurrence, or that four faces meet there at a common edge, another very improbable occurrence. In general, each grain exposed on the plane of section is bounded (in the section) by "lines," which are the traces of grain faces, and points where three lines meet (called "junctions" hereafter), which are the traces of grain edges. Almost all the observations of grains in metals are made on such sections.

Grain growth is the process by which a specimen of metal becomes composed of larger grains than when originally observed. If a section cut through a specimen is found to contain 1000 grains per square centimeter before the specimen is heated, and if another section is found to contain only 100 grains per square centimeter after the heating, grain growth is said to have occurred in the specimen. Since the grains cannot reasonably be expected to have turned over in the specimen in order that neighboring grains could match their crystallographic orientations and thus become indistinguishable,

the grain growth process must have occurred through motion of the grain boundaries.

It is, therefore, necessary to set up a mechanism by means of which grain boundaries will move. First of all, it is easy to see that a plane face should not move. Consider two crystal grains, A and B, of different orientation and in contact across a plane. The atoms in the boundary plane belong neither to one structure nor the other. Due to thermal motion, these atoms will wander from one side of the transition zone to the other, adapting themselves alternately to the structures of crystal A and crystal B. Since the boundary is plane, the average vacant position next the boundary in A is as much surrounded by the A structure as is the similar position in the B structure. Therefore, the energy required for an atom next the boundary zone in A to escape into the boundary is the same, on the average, as that required for escape from B. Since energy fluctuations occur with the same frequency at each point in the whole region at a given temperature, the rate at which atoms escape from A will be the same as the rate at which they escape from B. Furthermore, the rate of escape from the boundary into one of the neighboring crystals will be the same in either direction. *Therefore, both crystals A and B are forming and disappearing at the same rate at all points of the plane boundary, and the boundary will not move (except for local fluctuations of atomic dimensions).*

Now suppose that the grain boundary between crystals A and B is curved so that it is concave toward A and convex into B. Then, on the average, an atom next the boundary zone in crystal A will be less surrounded by the structure of crystal A than will an atom, next the boundary zone in crystal B, be surrounded by the structure of crystal B. Consequently, the rate of escape of an atom from crystal A into the boundary zone should be greater than that of an atom from crystal B, and, therefore, crystal A should "dissolve" in the boundary faster than B, while the boundary continues to "crystallize out" on both crystals at the same rate. This situation results in a net loss of atoms from crystal A to crystal B, while the boundary moves toward A, leaving behind it on the B crystal the atoms which it acquires from A. This process will continue as long as the boundary is curved. *This argument shows that a grain face should always move in such a way as to reduce its curvature; more rapidly the greater the curvature and the higher the temperature.*

(The argument just presented holds only for a pure metal—one

radius do

composed entirely of only one kind of atoms. It should doubtless be modified to take into account the presence of several kinds of atoms. It can be said, however, that the effect of foreign atoms which can "dissolve" in the crystal structure of the metal should be merely to retard the motion of grain boundary faces toward their concave sides.)

An example of this motion would be the behavior of a single grain A completely surrounded by grain B. The boundary of A consists of a single face completely surrounding A and on the aver-

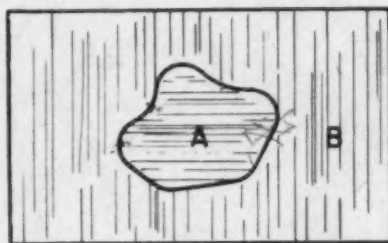


Fig. 2a—Section Through a Grain Completely Surrounded by Another Grain.

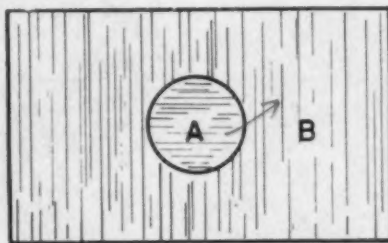


Fig. 2b—The Same as Fig. 2a, After Some Heating.

age concave toward A. A section through A would appear as in Fig. 2a.

The system being heated, the first motions of the boundary would be toward its concavity at each point, so that the grain would tend toward a spherical shape, as shown in Fig. 2b. The spherical grain, A, would then continue to shrink, at an accelerating linear rate, until it finally vanished. This behavior would be expected not only on the basis of the argument presented here, but also from the idea that a grain boundary is a high energy region and should decrease its extent with time, according to the laws of thermodynamics. The equilibrium state of this system is, on either argument, a region consisting entirely of crystal B.

The conditions at a grain edge will be discussed next. A grain edge is the line along which three grains meet. (If more than three grains meet at a line, the condition is at best metastable and cannot maintain itself.) A grain edge is always common to three (or more) grains.

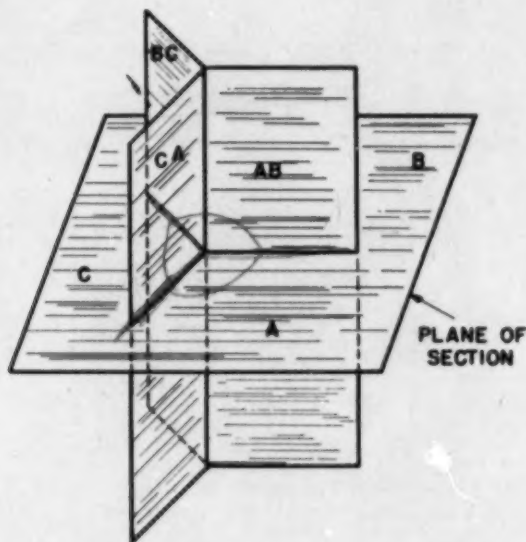


Fig. 3—Three Plane Grain Faces Meeting at An Edge Perpendicular to the Plane of Section.

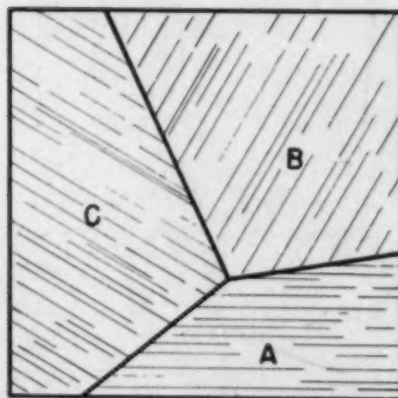


Fig. 4—Section Perpendicular to Grain Edge. Angle A Greater than 120 Degrees.

Suppose three grains, A, B, C, meet along a line. This line is the meeting place of the grain faces AB, BC, and CA. At any point the edge will be nearly straight over a short distance and the faces which meet there will be nearly plane. Consider, therefore, the ideal situation in which three plane grain faces meet in a straight grain edge, as shown in Fig. 3. A section perpendicular to the edge will

be perpendicular to the faces, which will cut it in three straight lines, as shown in Fig. 4. The angles between these lines measure the angles between the faces: the angle lying in grain A will be called angle A, and so on. Angle A is the angle between faces CA and AB, etc.

An atom in the edge ABC can move under the action of thermal motion either into one of the boundaries AB, BC, or CA; or onto

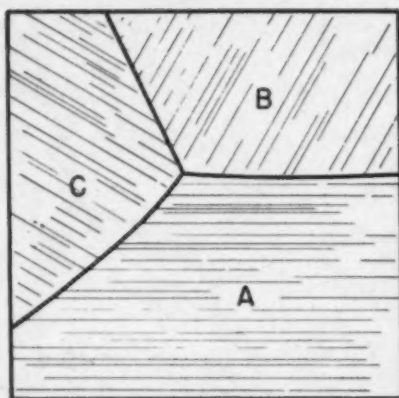


Fig. 5—The Section of Fig. 5 After Some Heating. Note curvature of faces AB and CA, and motion of edge away from grain A.

one of the crystals A, B, or C, in which case it becomes a part of the structure of that crystal. Suppose angle A is the largest of the three; then an atom at the edge of crystal A makes more contact with the structure of crystal A than the similarly located atoms of crystals B and C make with their respective structures. The rate of escape of atoms at angle A from the structure of crystal A into the edge should, therefore, be less than the rates of escape of atoms at angles B or C. Thus, grains B and C should lose atoms to grain A "through" the edge and the edge should move away from crystal A. As the edge moves it draws the faces CA and AB after it, thus bending them so that they become convex to grain A. This condition is shown in Fig. 5. The faces CA and AB will then move, respectively, toward grain C and grain B. As this motion goes on angle A continues to decrease until it is no longer the largest of A, B, and C. The edge will, perhaps, then keep on moving in some other direction until all three angles are equal—which occurs when

they are all 120 degrees. The grain edge is then at equilibrium and will not move further.

We are thus faced with the conclusion that the grain boundaries in a metal should move in such a way as to (a) make all grain faces flat and (b) make the angles between grain faces all equal to 120

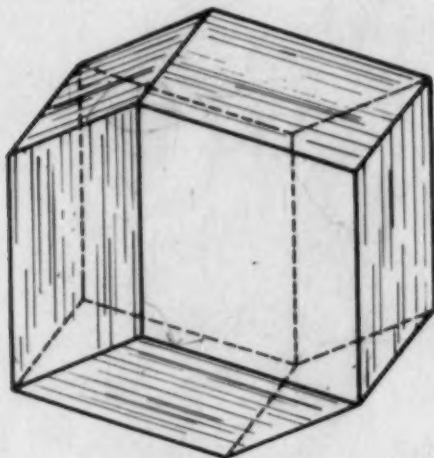


Fig. 6—A Stable Grain Shape: the Rhombic Dodecahedron.

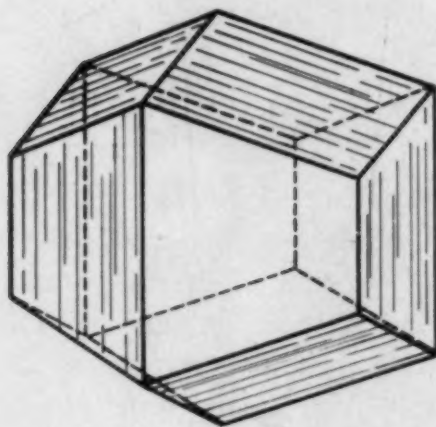


Fig. 7—Another Stable Grain Shape.

degrees. If the grain structure of a metal is such that these conditions are fulfilled, no grain growth should occur no matter what the grain size.

A question that arises at once is this: Can the conditions that all grain faces be flat and all interfacial angles 120 degrees be fulfilled? That is: Can a set of geometrical solids fulfilling these conditions fit together so as to fill space? The answer is yes. An example of such a figure is the rhombic dodecahedron, familiar to crys-

Example

tallographers. It is depicted in Fig. 6. It is a twelve-faced solid, each face of which is congruent to all the others. These faces are in the shape of a rhombus—a parallelogram with four equal sides—whose obtuse internal angle is 109.5 degrees. Another example of a suitable solid is obtained by cutting the rhombic dodecahedron in

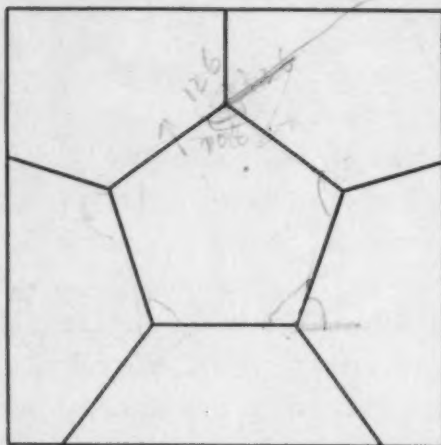


Fig. 8a—Section Through a Grain with Five Parallel Edges Perpendicular to the Plane of Section.

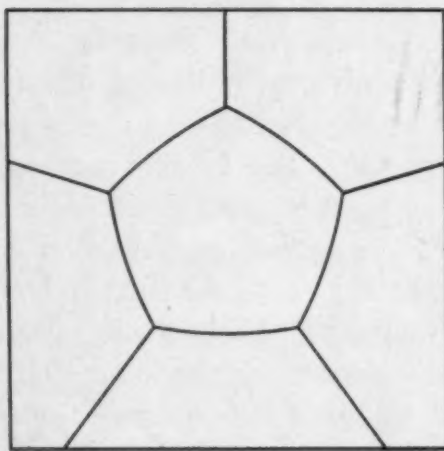


Fig. 8b—Same Section as Fig. 8a, After Some Heating.

two in the plane of its hexagonal section and rotating one-half 60 degrees before sticking it to the other half again. This is another twelve-faced solid, but its faces are not all the same shape. It is shown in Fig. 7. Either of these solids can be packed together to fill all space and so provide a possible equilibrium grain structure for a metal. These two solids—and certain distortions of them—are the only possible equilibrium grain shapes.

If the metal is composed of grains all in the shape of rhombic dodecahedra of the same size, the grain centers will be arranged on a face-centered cubic lattice; that is, they will be in the relationship to each other of the centers of spheres arranged in cubic closest packing. The other dodecahedron as a grain shape places the grain centers in the relative positions of the sphere centers in hexagonal closest packing.

"Grain growth" can only occur if the number of grains in the specimen of metal decreases. Hence, the situations leading to the disappearance of grains must be examined. Such situations must be characterized by the fact that they provide structures in which grain faces are not flat, interfacial angles are not 120 degrees, or both.

One such situation is the following: A grain is such that a certain plane section through it is in the form of a pentagon; each of the five faces, whose traces on the section are the sides of the pentagon, stands perpendicular to the plane of section and, therefore, the five edges cut by the section are also normal to its plane. Not more than three of the interfacial angles can be as great as 120 degrees at once. If all angles are equal, they are all 108 degrees. Suppose all the angles to be 108 degrees between these faces, as shown in Fig. 8a. If the metal is heated, all the edges will move inwards toward the grain's center, leaving the faces concave toward the grain, as shown in Fig. 8b. The faces will then move inward, thus decreasing the angles. These two processes will continue until this grain has vanished. A similar grain with less than five faces, all normal to the plane of section, would suffer the same fate.

If a grain like the one just described is bounded by more than six faces normal to the plane of section, it will grow outward at the expense of its neighbors by much the same mechanism as described in the last paragraph. This is true because the average value of the interfacial angles is greater than 120 degrees. Only if such a grain is bounded by six faces normal to the plane of section is it possible for its boundaries to be stable, for only then can the faces be flat and at the same time make 120-degree angles with one another.

It must not be concluded that a grain showing a different number of faces than six on an arbitrary section is unstable, since these faces are usually not perpendicular to the plane of section. For instance, a regular rhombic dodecahedron—a stable grain shape—can be cut by an arbitrary plane so that 3, 4, 5, 6, 7, 8, or 9 faces are traversed. Counting the faces cut by the plane of section on a metal-

lographic specimen will provide no criterion for the stability of its grain structure. Such a criterion is provided by another line of attack, as will be seen later. The foregoing paragraphs were merely intended to describe situations leading to grain growth.

It should be pointed out that the size of grains gives no clue to the stability of a grain structure; if the grains in a specimen of metal achieve flat faces and 120-degree interfacial angles at a small grain size, the structure is just as stable as one satisfying the same conditions at a much larger grain size. It is a well known fact that some specimens of metal show no grain growth, although the grains are very small, while others with very large grains show grain growth.

THE CRITERION OF GRAIN STABILITY

A study of the angles at which the traces of grain faces meet in the plane of section seems to provide a criterion for grain stability. If these traces meet at 120 degrees, are straight lines, and if it is known that the grain edges stand perpendicular to the plane of section, it can be said with some assurance that these grain edges will not move when the specimen of metal is heated. This statement is not true if the grain faces are curved, for these will tend to flatten and, in doing so, may change the interfacial angles from 120 degrees. The grain edges will then move. However, if it could be shown that all the interfacial angles in a specimen of metal were 120 degrees, it would be very likely to have a stable grain structure. Unfortunately, it is usually impractical to measure these angles, since grain edges usually are not perpendicular to the actual plane of section.

What can be measured are the angles between the traces of grain faces in the plane of section—the “junction angles” as they will be called hereafter. It will now be shown how these lead to a criterion of stability.

In general, there is no reason to expect a grain edge to be intersected by the plane of section at one angle rather than another, so that it can be assumed, at least in most cases, that if enough edges are intersected, all angles will be represented in the proportions of their inherent probabilities.

To calculate the distribution function of the angle, θ , at which grain edges are intersected by an arbitrary plane, it is convenient to think of a metal specimen's grain structure as consisting of a network of grain edges. Each edge is joined at each end to three (or,

rarely, more) other grain edges at the points where four grains meet. In a perfectly stable structure, the four edges meeting at a point make angles of 109.5 degrees with one another; this is a corollary of the condition that all interfacial angles be 120 degrees.

In a structure which forms under the same general conditions at all points, the probable number per unit of volume of grain edges of a given length does not vary from place to place. Consider the grain edges parallel to a given direction, whose lengths lie between l and $l + \delta l$. The chance that one of them will be intersected by an arbitrary plane is proportional to $l \cos \theta$, where θ is the acute angle

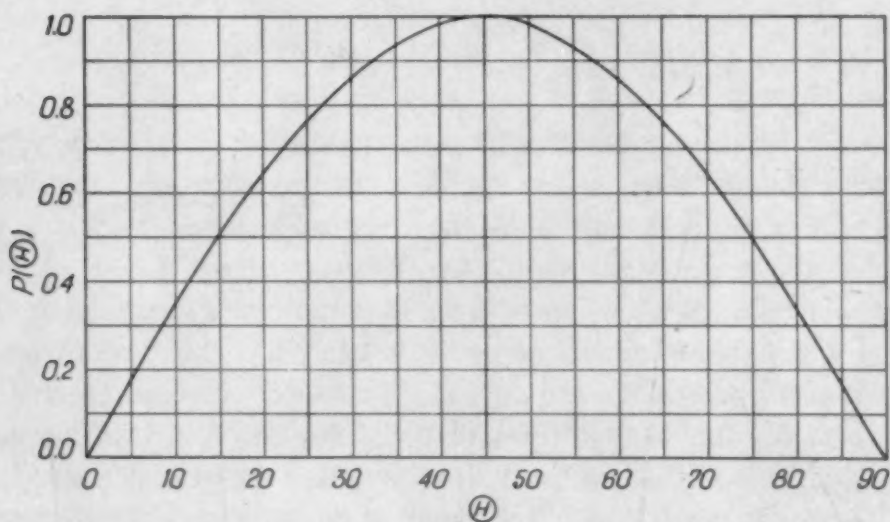


Fig. 9— $P(\theta)\delta\theta$ is the Chance that a Straight Grain Edge Makes an Angle Between θ and $\theta + \delta\theta$ with the Normal to the Plane of Section. (θ should be measured in radians.)

between these grain edges and the normal to the intersecting plane. If the whole set of grain edges pointing in all directions and with lengths between l and $l + \delta l$ is considered, the number intersected by an arbitrary plane at an angle lying between θ and $\theta + \delta\theta$ is proportional to $l \cos \theta \sin \theta \delta\theta$. This is so since $\sin \theta \delta\theta$ is the solid angle (area on the unit sphere) within which lie directions inclined to the plane normal at angles between θ and $\theta + \delta\theta$. This can be written $\frac{1}{2}l \sin 2\theta \delta\theta$. The function giving the probability that a grain edge whose length is between l' and $l' + \delta l'$ is intersected by an arbitrary plane at an angle lying between θ and $\theta + \delta\theta$ is, similarly, proportional to $\frac{1}{2}l' \sin 2\theta \delta\theta$. If the length of the grain edge is unimportant, it can be said in general that the chance that a given grain edge intersected by an arbitrary plane makes an (acute) angle between θ

and $\theta + \delta\theta$ with the plane normal is proportional to $\frac{1}{2} \sin 2\theta$
 $\delta\theta = \frac{1}{2}\delta(\sin^2\theta)$.

Each grain edge is the meeting place of three (or rarely more) grain faces. These faces cut the arbitrary plane of section in three lines which meet at the point where the grain edge passes through the plane. Supposing that the grain faces actually make 120-degree angles with one another measured in a plane normal to the grain

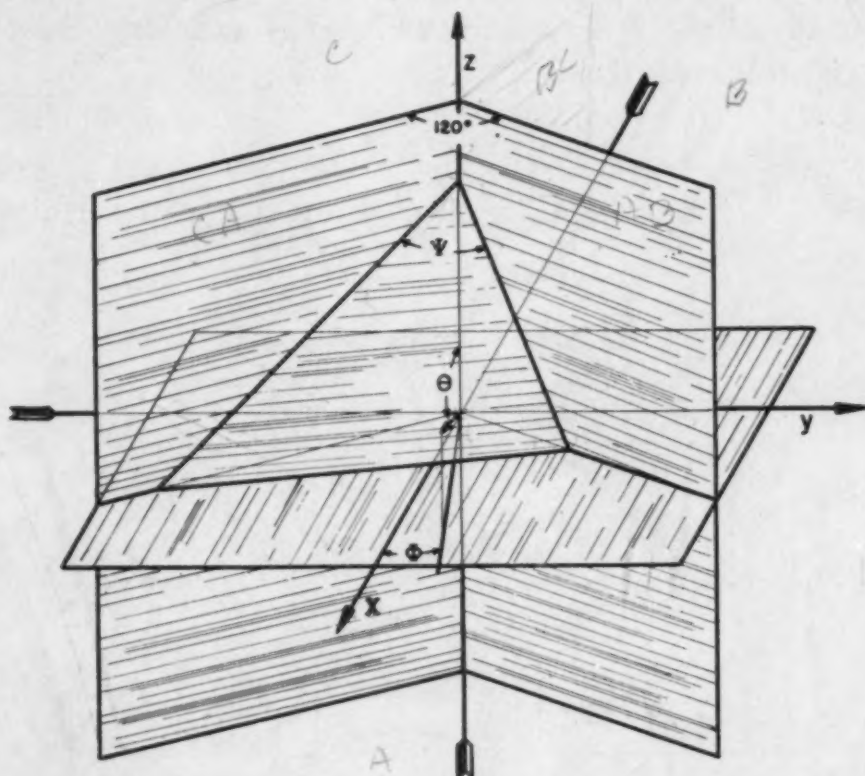


Fig. 10—Two Planes Meet Along the z -Axis at 120 Degrees (Measured in the xy -Plane). Their intersections with the plane of section make an angle ψ with one another. The normal to the plane of section makes an angle θ with the z -axis; its projection on the xy -plane makes an angle ϕ with the x -axis.

edge, what angles do they make with one another in the arbitrary plane? These angles clearly depend upon the direction of the arbitrary plane. To describe the direction of the plane of section, a cartesian coordinate system is set up related to the grain edge, as follows: The z -axis is along the grain edge, the x -axis is normal to the z -axis and in the direction bisecting the 120-degree angle between the two grain faces CA and AB. The y -axis is normal to the x - and z -axes in a direction to make the sequence $x y z$ right-handed. In this set of axes the grain edge lies along the line $x = y$

$= 0$, the line whose direction cosines $[a, \beta, \gamma]$ are $[0, 0, 1]$. The grain face AB lies in the plane $\sqrt{3}x - y = 0$, and the grain face CA lies in the plane $\sqrt{3}x + y = 0$. (The grain face BC lies in the plane $y = 0$, but will not be considered until much later in the problem.) The arbitrary plane of section has a direction defined by the direction cosines $[a, \beta, \gamma]$ of its normal. Of these, $\gamma = \cos \theta$ defines the angle between the grain edge and the normal to the plane of section; the other two, γ and β , define the relationship between the grain faces and the plane of section. A set of spherical polar co-ordinates is set up such that

$$\begin{aligned} x &= r \sin \theta \cos \phi, \\ y &= r \sin \theta \sin \phi, \\ \text{and } z &= r \cos \theta. \end{aligned}$$

The direction cosines of a line through the origin in the direction

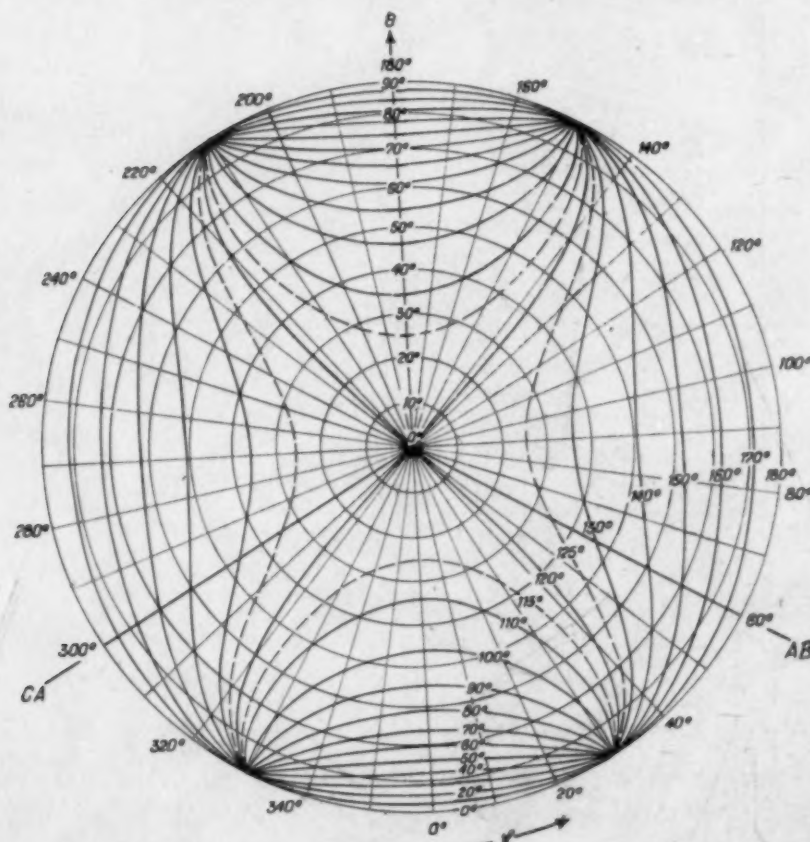


Fig. 11—Contours of Equal ψ Drawn on a Polar Map of ϕ and θ .

$[a, \beta, \gamma]$ are given by the co-ordinates of a point on it at unit distance from the origin, thus:

$$\begin{aligned} x &= a = \sin \theta \cos \phi, \\ y &= \beta = \sin \theta \sin \phi, \\ z &= \gamma = \cos \theta. \end{aligned}$$

The direction cosines of the normal to the plane of section through the origin can be related in this way to the angle, θ , it makes with the grain edge and the angle ϕ , its projection on the grain edge's normal plane makes with the bisector of the angle between the grain faces CA and AB. Fig. 10 shows these relationships.

The angle between the traces on the plane of section of the grain faces CA and AB is called Ψ . It is given, in terms of ϕ and θ , by the formula*

$$\tan \Psi = \frac{\sqrt{3} \cos \theta}{\sin^2 \theta (\cos 2\phi + \frac{1}{2}) - 1}$$

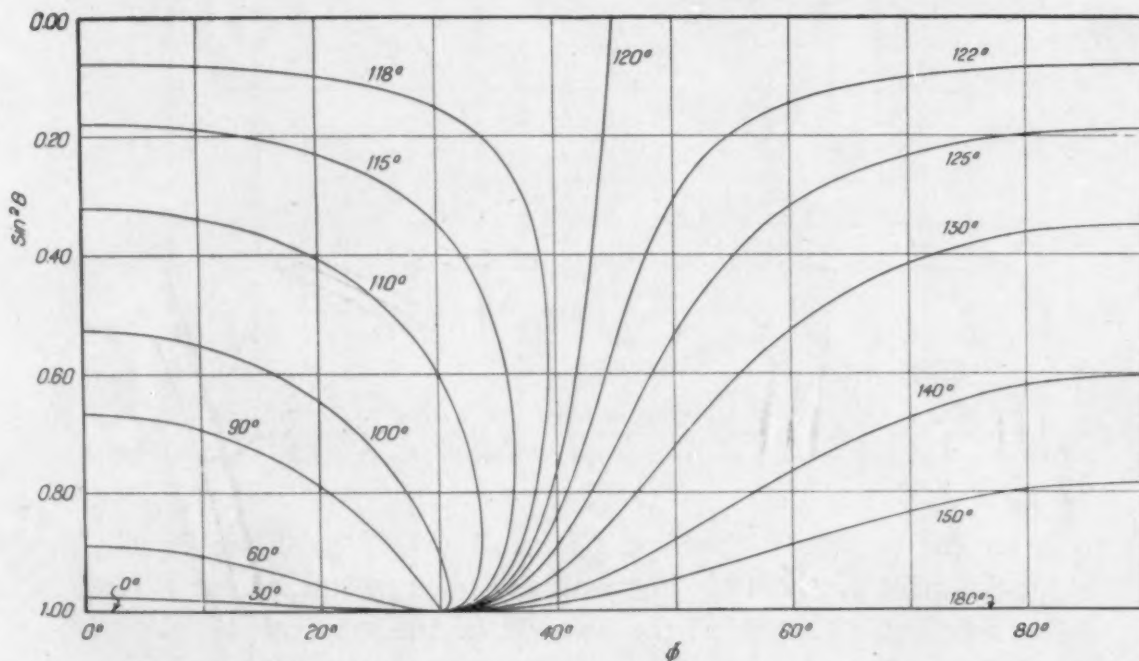


Fig. 12—Contours of Equal Ψ Drawn on a Map of ϕ and $\sin^2\theta$. Areas on this map are proportional to the probabilities of the corresponding ranges of Ψ .

Fig. 11 is a contour map of the values of Ψ plotted against ϕ and θ on an equiarea polar projection. It is seen that if $\theta = 0$, $\Psi = 120$ degrees, as would be expected. For other values of θ , Ψ can vary from 0 degrees to 180 degrees, however. The problem is to determine the relative probabilities of occurrence of the different values of Ψ . These can then be compared with the frequencies of occurrence of these angles as measured on a plane section. If the calculated relative probabilities and the observed relative frequencies cor-

*If the angle between the grain faces is x , instead of 120 degrees, the formula for Ψ is

$$\tan \Psi = \frac{2 \sin x \cos \theta}{\sin^2 \theta (\cos 2\phi - \cos x) + 2 \cos x}$$

respond for a given specimen, it is quite likely that its interfacial angles are all equal to 120 degrees. The assurance with which the frequencies can be used as probabilities increases with the number of angles measured.

If the values of Ψ are plotted on a cartesian map whose elements of area are proportional to the relating probabilities of finding those particular values of ϕ and θ , the problem can be solved by measuring

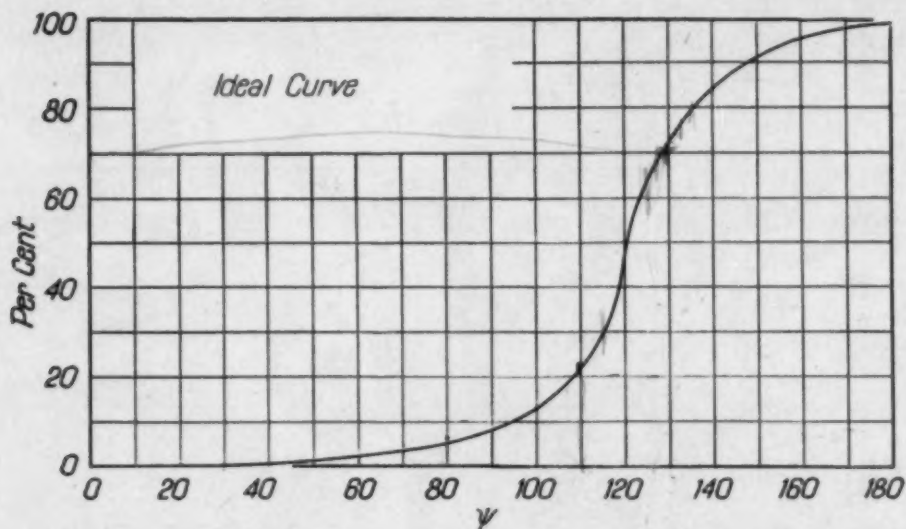


Fig. 13—Cumulative Distribution Curve for Ψ , the Angle Between the Intersections of the Plane of Section with Two Planes at 120 Degrees. The ordinate at any Ψ is the per cent of the observed angles expected to be less than Ψ .

areas on the map. In the first place, all values of ϕ are equally likely; the arbitrary plane is just as likely to slope toward one direction as another. Therefore, the abscissa of the map can be plotted on a linear scale in ϕ . We have seen before that the chance of finding a grain edge cutting an arbitrary plane at an angle θ to the plane's normal is proportional to $\frac{1}{2} \delta (\sin^2 \theta)$. Consequently, the ordinates on this map can be plotted on a linear scale in $\sin^2 \theta$. Such a map appears in Fig. 12. Relative areas on this map are proportional to the relative probabilities of the corresponding ranges of Ψ . Thus, for instance, it can be seen that the chance of finding a junction angle Ψ smaller than 90 degrees is small compared with the chance of finding a junction angle between 90 and 180 degrees, and that the chance of finding a junction angle within 5 degrees of 120 degrees is larger than the chance of finding the angle in any other 10-degree range.

The cumulative probability curve appears in Fig. 13 and in Table I. The values of the junction angle Ψ are plotted as abscissae;

the ordinate at any Ψ is the percentage probability that a junction angle smaller than Ψ will be observed. The data for this curve were obtained by numerical integration of areas on the map of Ψ , Fig. 12.

From the curve, the probability of any range of Ψ can be found by subtracting the ordinate for the bottom of the range from that for the top. For instance, the chance of finding an angle between 115 and 125 degrees is $64.0 - 29.5 = 34.5$ per cent, or about one-third. Thus one junction angle in three should be within five degrees of 120 degrees.

Table I

Junction Angle Ψ	Chance of Angle $< \Psi$ Per Cent	Junction Angle Ψ	Chance of Angle $< \Psi$ Per Cent
0	0.0	90	7.9
5	0.0	95	9.9
10	0.0	100	12.5
15	0.1	105	16.1
20	0.2	110	21.4
25	0.3	115	29.5
30	0.4	120	46.3
35	0.5	125	64.0
40	0.7	130	73.8
45	1.0	135	80.6
50	1.3	140	85.7
55	1.7	145	89.6
60	2.1	150	92.7
65	2.7	155	95.1
70	3.4	160	97.0
75	4.2	165	98.4
80	5.1	170	99.3
85	6.3	175	99.8
90	7.9	180	100.0

Or again, the chance of finding an angle between 95 and 145 degrees is $89.6 - 9.9 = 79.7$ per cent, or about four-fifths. Consequently, four junction angles out of five should lie within 25 degrees of 120 degrees. It is interesting to note that the junction angles of the traces of grain faces in a random plane are calculated to cluster so closely around the actual interfacial angle.

It is not difficult to measure junction angles to an accuracy of five degrees, that is, to state that a certain angle is within five degrees of (say) 110 degrees. Consequently, in collecting data to compare with the calculated probabilities the measured angles are grouped in classes defined as 90 ± 5 , 100 ± 5 degrees, and so on. The numbers of angles observed in these classes can be compared with the calculated probabilities of finding angles in these classes. These calculated probabilities are listed in Table II, and are shown as a block diagram in Fig. 14.

In order to discover whether the interfacial angles in a specimen

of metal are really 120 degrees or not, one hundred (say) of the junction angles in the plane of a metallographic section are measured. The number of angles within five degrees of each of the multiples of ten is recorded and these numbers compared with the percentage

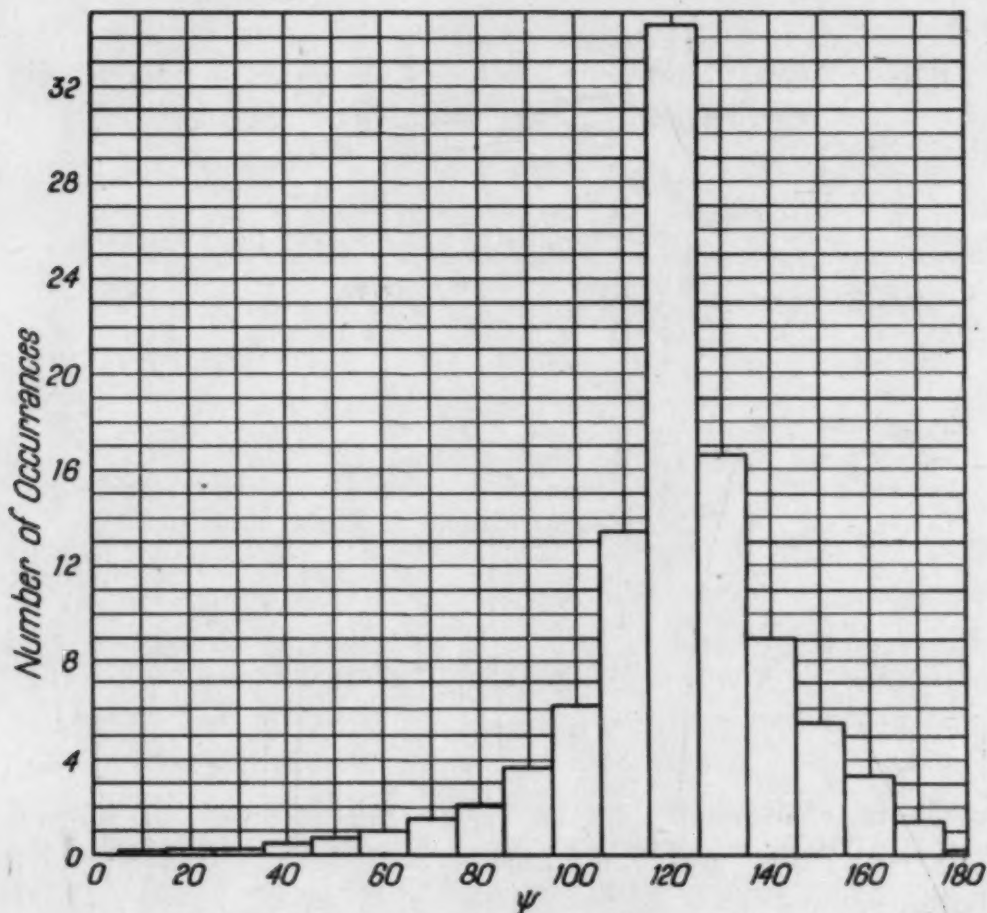


Fig. 14—Block Diagram of the Distribution of Ψ . The height of a block is the per cent chance of finding an angle within ± 5 degrees of the corresponding Ψ .

probabilities in Table II. *If there is agreement to the nearest couple of integers, there is a high probability that the interfacial angles of the grains in the specimen are really 120 degrees, and the grain structure is probably stable. Such a specimen would not be expected to show grain growth on heating, no matter what its grain size.*

Poor agreement between the calculated and observed frequencies can be due to three main causes:

- (1) The interfacial angles in the specimen are not all 120 degrees.
- (2) The directions of grain edges in the specimen are not distributed at random.

(3) A non-representative set of angles was selected for measurement.

Table II

Junction Angle at Range Center Ψ	Probability of Finding $\Psi \pm 5$ Degrees Per Cent
0	0.0
10	0.1
20	0.2
30	0.2
40	0.5
50	0.7
60	1.0
70	1.5
80	2.1
90	3.6
100	6.2
110	13.4
120	34.5
130	16.6
140	9.0
150	5.5
160	3.3
170	1.4
180	0.2

The first of these kinds of disagreement shows up as a spreading in the distribution function—more small and more large angles will be found than predicted on the basis of 120-degree interfacial angles. Such a spreading of the observed distribution function can be interpreted to mean that the grain structure of the specimen is unstable and that grain growth can occur. It is interesting to watch the distribution function of junction angles “peak-up” at 120 degrees as the grain structure of a specimen approaches stability.

The second kind of disagreement shows itself as too high a peak in the distribution function at 120 degrees, or as peaks at other angles. Too high a peak at 120 degrees means that the specimen contains a high proportion of 120-degree interfacial angles and that too many of the grain edges intersect the plane of section nearly at right angles. A columnar cast structure sectioned perpendicular to the length of the grains shows this effect.

The third kind of disagreement can produce any imaginable effect on the observed distribution function and is due to bad luck in collecting data. It is not a serious matter to measure another set of angles if this effect is suspected. It is extremely unlikely that the distribution function will be in error twice in succession in the same way because of honestly unlucky selection of data. If two similar distribution functions are obtained from the same specimen, each

from a different set of junction angles, the cause of their disagreement (if any) with the ideal distribution function must be due to conditions (1) or (2).

This, then, is the angle criterion of grain stability: that the junction angles of the traces of grain faces on a plane section be distributed according to the curve of Figs. 13 and 14 or Tables I and II.

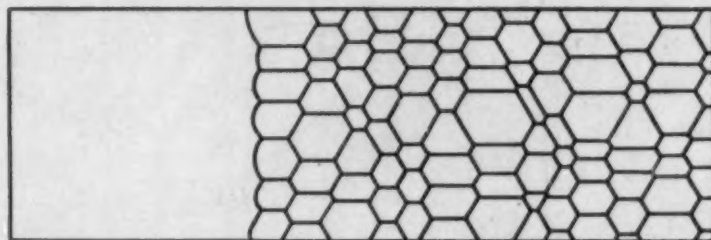


Fig. 15—A Structure Expected to Show Grain Growth. On heating, the small grains will be absorbed by the large one.

THE EFFECT OF GRAIN SIZE GRADIENTS

Grain size gradients are said to exist in a specimen of metal if the average volume of the grains in the neighborhood of a point in the specimen changes as the point moves through the specimen. Less exactly, a grain size gradient is present in a specimen if large grains exist in one region of the specimen and small grains in another.

An extreme case is furnished by a bar specimen consisting of a single grain at one end abutting on a fine-grained region at the other. A longitudinal section through such a bar might appear as in Fig. 15.

The conditions at the boundary between the large grain and the small grains are similar to those at the boundary of a grain with more than six parallel edges passing normally through the plane of section. The bounding faces of the large grain are convex into the large grain and concave toward the small grains as a result of the effort of the interfacial angles to become 120 degrees. These bounding faces will, therefore, move toward the small grains, consuming them as they go, while the large grain continues to grow larger. This explains the "grain size contrast" effect. It will produce grain growth whenever a few grains in a specimen are sufficiently larger than their immediate neighbors.

A grain size gradient need not lead to an unstable grain structure, as is shown by Fig. 16. This is a section through a hypothetical

columnar structure in which all grain edges stand perpendicular to the plane of section. All faces are flat and all interfacial angles are 120 degrees; therefore, such a structure will show no grain growth.

The presence of a grain size gradient is consequently not necessarily indicative of an unstable grain structure and predictions of the grain growth behavior of such systems should be made cautiously and only after a detailed consideration of the grain structure.

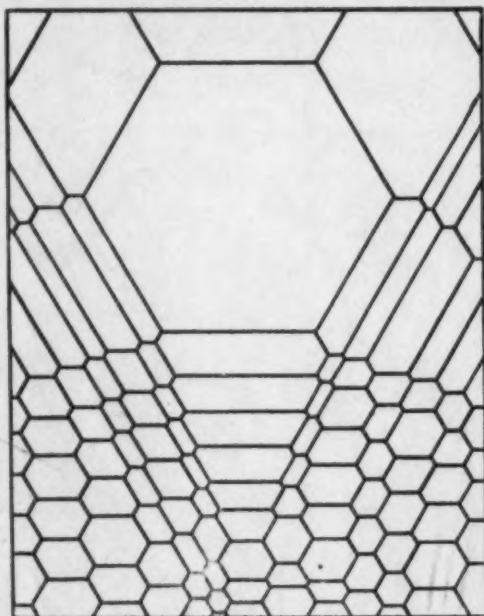


Fig. 16—A Stable Grain Structure. All angles between grain faces are 120 degrees.

THE ESTABLISHMENT OF A GRAIN STRUCTURE IN A SPECIMEN

As noted earlier, grains are produced by the nucleation and growth of undistorted crystals from plastically deformed material. The geometry of the final equilibrium grain structure is determined by the positions and times at which nuclei occur as well as by the rate at which the crystals grow out from them.

It seems to be a fact that the *linear* rate of crystal growth is constant, once a nucleus has been "activated." That is: a crystal growing under constant conditions extends itself in each direction at a rate characteristic of that direction. Most of the common metals belong to the cubic system and their most frequent growth forms are the cube, octahedron, and dodecahedron, all of which are not too far from the spherical shape. It is, therefore, not too bad an assump-

tion to say that crystals grow out from nuclei as spheres whose radii increase at a constant rate. A crystallization process proceeding in this way will be called *ideal*.

In the ideal case, then, spheres start growing from nuclei at various positions and at various times, and each sphere increases in radius at the same rate until its growth is stopped by meeting other spheres or the boundaries of the specimen.

Imagine two nuclei which start growing at the same instant separated by a distance, l . The two (spherical) crystals will meet when their radii are both equal to $\frac{1}{2}l$ at the halfway point between

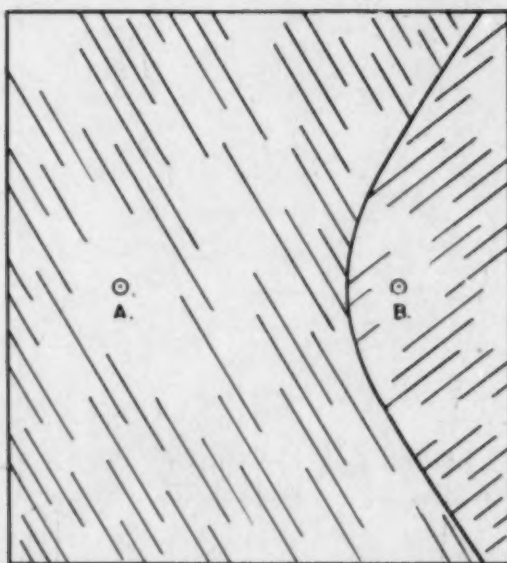


Fig. 17—Section Through a Grain Face Formed Between the Crystals Growing from Nuclei A and B. Nucleus A started growing before nucleus B.

the positions of the two nuclei. From this time on, the two crystals will be in contact across a plane which bisects perpendicularly the line between the two nuclei; their free surfaces continue spherical.

Next consider two nuclei which start growing at different times: one of them starts the growth of a sphere at t_1 , the other at t_2 . If R is the linear rate of growth, then the first sphere has a radius of $R(t_2 - t_1)$ at the time the second sphere starts growing. The two spheres will make contact at t_3 when

$$\frac{r_1}{r_2} = \frac{l + R(t_3 - t_1)}{l - R(t_3 - t_1)},$$

i. e., when r_1 is greater than r_2 . As they continue to grow, they will

be separated by a surface in the shape of one sheet of a hyperboloid of revolution concave toward the crystal that started growing at the later time. Fig. 17 shows a section through such a boundary. The concavity will be greater, the later the second crystal started growing. On further heating, the first crystals that nucleate will grow at the expense of those that were born later, due to the motion of boundaries toward their concavities.

In a large specimen of distorted metal, nuclei appear here and there from time to time and start growing. In general, the nuclei that form first will grow into crystals whose boundaries are concave toward the crystals whose nuclei were formed later. On further heating, the first formed crystals grow at the expense of those formed later and usually consume them entirely; only rarely will the geometry be such that the structure contains many crystals whose



Fig. 18—Grain Structure of Sheet in Which the Nuclei Were Farther Apart than the Thickness of the Sheet. Grain faces are nearly normal to the plane of the sheet (θ is small).

nuclei formed much later than the first ones. In consequence, the equilibrium grain structure of an annealed specimen of metal consists mainly of crystals whose nuclei formed during a short period at the start of the recrystallization. The relative positions in space of these initial nuclei determine the shapes and sizes of the final structure.

The statements made in the last few paragraphs should still be approximately true if the growth shape of the crystals is not spherical, provided only that the shape is not too elongated or flattened—any more or less equiaxed growth shape would lead to the same general conclusions.

Suppose, now, that the specimen of distorted metal is in the form of a thin sheet, and that the initial nuclei are spaced at distances from each other considerably larger than the thickness of the sheet. Then the grains in the annealed specimen will be large compared to the thickness of the sheet and their boundaries will extend through it. These boundaries will be almost plane surfaces nearly normal to lines connecting the original nuclei, and, therefore, also to the plane of the sheet, as shown in Fig. 18. Grain edges will,

therefore, also be mostly nearly normal to the plane of the sheet. A section of such a specimen parallel to the plane of the sheet should show many more angles near 120 degrees than would a random section of a specimen large compared to its grain size. This effect operates in the case of the bismuth specimen, annealed after compressing to a sheet, as will be seen later.

When a liquid metal is cooled, the nuclei first form at its surfaces. Unless it is cooled very slowly, not enough other nuclei form throughout the body of the metal to prevent the crystals growing from the surface nuclei from consuming all, or most of, the liquid. This situation gives rise to what are known as "columnar grains." A section parallel to the surface from which the metal was cooled meets the grain faces nearly at right angles, and, therefore, the grain edges also stand about perpendicular to the surface. If such grains are brought to equilibrium by heating, the junction angles in the section just mentioned should all be near 120 degrees.

If a section is made at right angles to the cooled surface of the cast metal, the axes of the columnar grains are more or less parallel to the plane of section and many grain edges meet the surface at very small angles. Reference to Fig. 11 shows that in this case, even if all interfacial angles are 120 degrees, many very small and very large junction angles will be found in the section.

In order to verify these conclusions, a study was made of the junction angles in various plane sections through a block of OFHC copper which consisted of large columnar grains. The results of this study are among those described in the next section.

EXPERIMENTAL

One hundred junction angles were measured on each of a number of specimens. The measurements were recorded thus: 110 ± 5 , 120 ± 5 , 130 ± 5 degrees, etc. An angle lying between (say) 105 degrees and 115 degrees would be recorded as 110 degrees, and so on. A table was then constructed showing the number of angles recorded in each ten-degree range. From this table the total number of angles less than any odd multiple of five degrees was obtained by adding. For example, a specimen of pure zinc, slowly cooled from above the melting point to a low temperature, provided the data shown in the tabulation on the next page.

Range Degrees	No. of Junction Angles	No. of Angles Less Than Top of Range	Predicted
0 to 75	0	0	4
80 \pm 5	1	1	6
90 \pm 5	7	8	10
100 \pm 5	13	21	16
110 \pm 5	17	38	29
120 \pm 5	28	66	64
130 \pm 5	15	81	81
140 \pm 5	10	91	89
150 \pm 5	4	95	95
160 \pm 5	4	99	98
170 \pm 5	1	100	100
175 to 180	0	100	100



Fig. 19—Zinc, Slowly Cooled Through Solidification. $\times 8$.

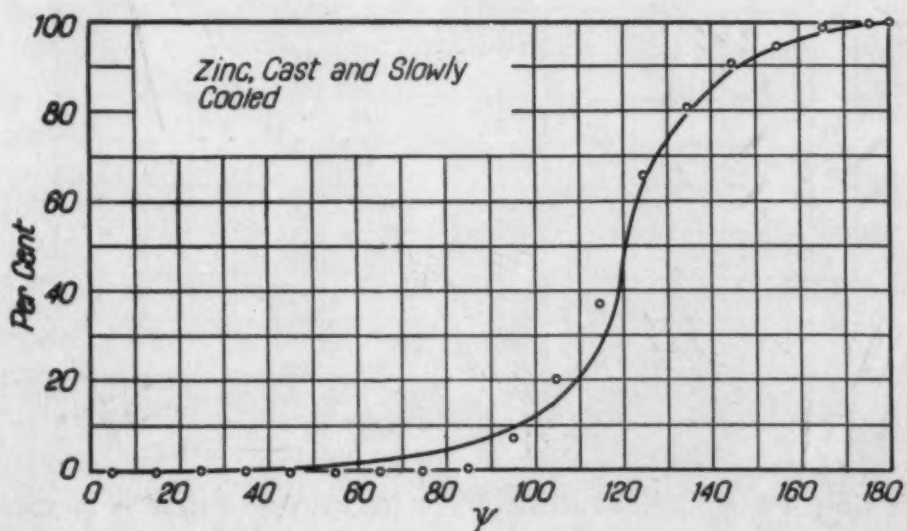


Fig. 20—Cumulative Distribution of Junction Angles for the Zinc Specimen of Fig. 19, Compared with the Ideal Curve of Fig. 13.

These data are plotted in Fig. 20 on the same graph with a curve drawn according to theory. Many other specimens were analyzed in a similar way. Each is discussed separately in the following:

Zinc—The specimen was made by accident during an attempt to prepare a single crystal. It is an example of very slow cooling

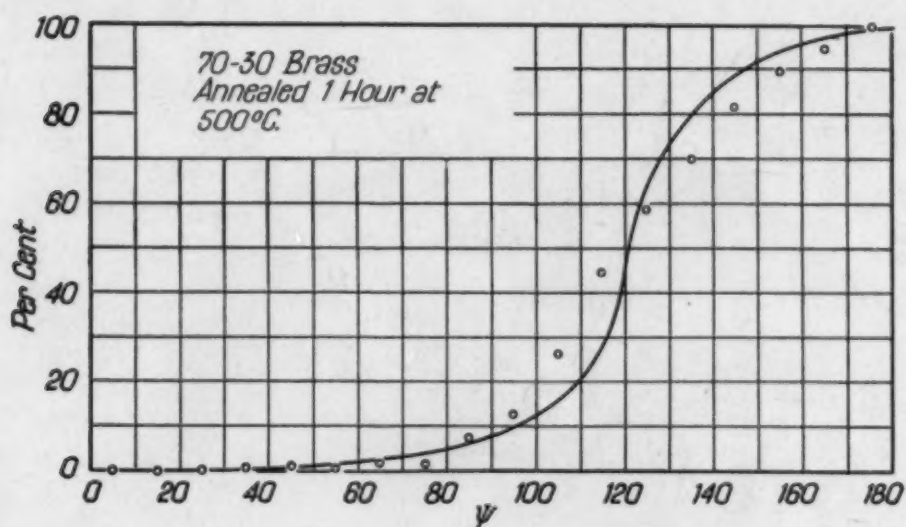


Fig. 21—Cumulative Distribution of Junction Angles for 70-30 Brass, Annealed at 500 Degrees Cent. for 1 Hour, Compared with the Ideal Curve of Fig. 13.

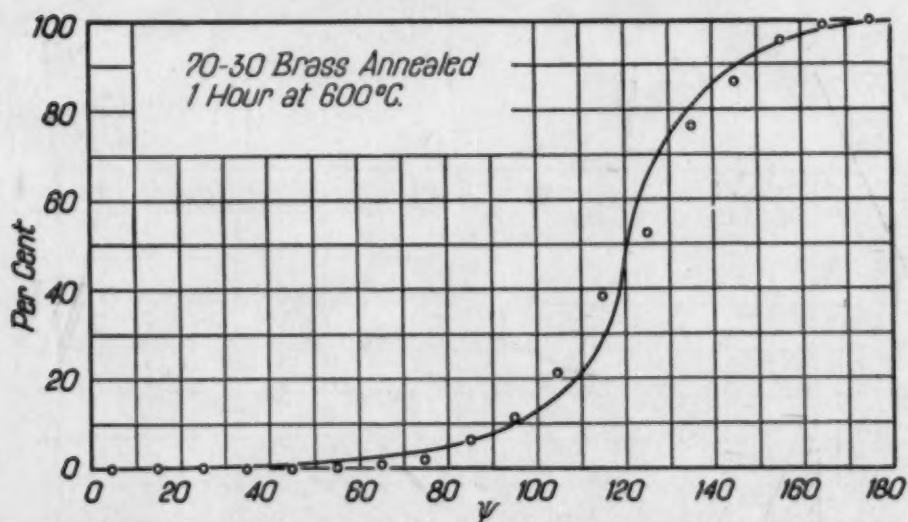


Fig. 22—Cumulative Distribution of Junction Angles for 70-30 Brass, Annealed at 600 Degrees Cent. for 1 Hour, Compared with the Ideal Curve of Fig. 13.

through the melting temperature. The plane of section is perpendicular to the long dimension of the specimen. The structure is shown by Fig. 19 and the distribution of angles by Fig. 20. Somewhat too few junction angles are less than 90 degrees and a few too

many lie between 100 and 120 degrees; however, the agreement with the ideal curve shows that the assumption of 120-degree interfacial angles must be very near the truth. This specimen should show little, if any, grain growth on further annealing.

Brass—Four specimens of 70-30 brass were annealed, respec-

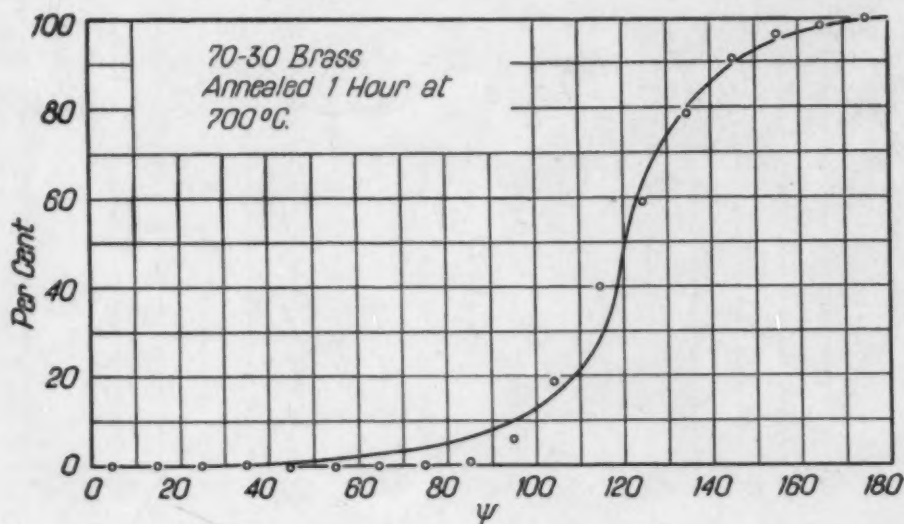


Fig. 23—Cumulative Distribution of Junction Angles for 70-30 Brass, Annealed at 700 Degrees Cent. for 1 Hour, Compared with the Ideal Curve of Fig. 13.

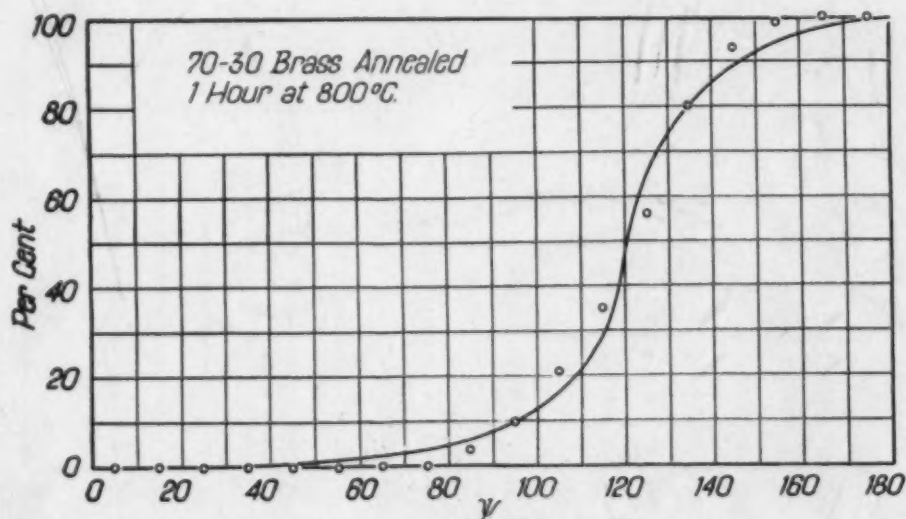


Fig. 24—Cumulative Distribution of Junction Angles for 70-30 Brass, Annealed at 800 Degrees Cent. for 1 Hour Compared with the Ideal Curve of Fig. 13.

tively, at 500, 600, 700, and 800 degrees Cent. (930, 1110, 1290, and 1470 degrees Fahr.). The grain sizes of these specimens increased in the same order. The distribution curves of their junction angles appear in Figs. 21, 22, 23, and 24. It is seen that the specimen an-

nealed at 500 degrees Cent. (930 degrees Fahr.) shows many more small and large junction angles than would a specimen containing only 120-degree interfacial angles. It contains, therefore, interfacial angles different from 120 degrees. The specimen annealed at 600 degrees Cent. (1110 degrees Fahr.) has junction angles more nearly

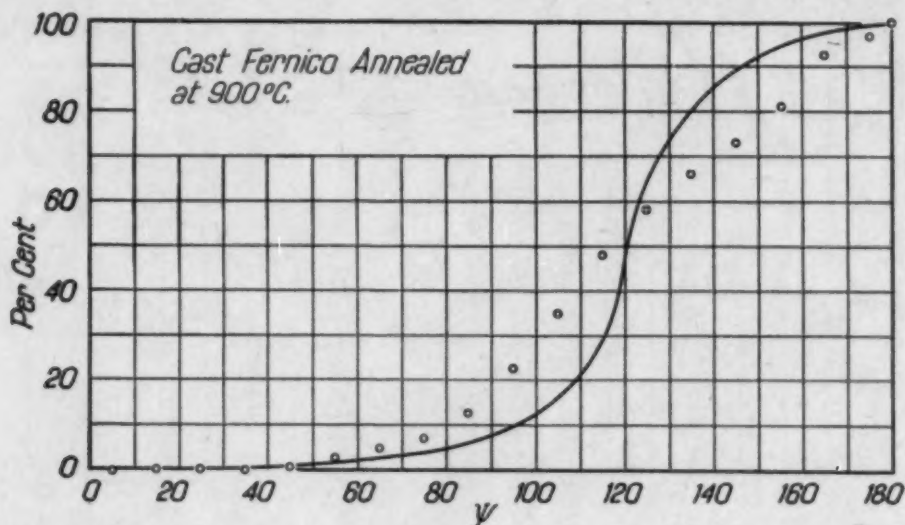


Fig. 25—Cumulative Distribution of Junction Angles, for Cast Fernico, Annealed at 900 Degrees Cent. for 1 Hour, Compared with the Ideal Curve of Fig. 13.

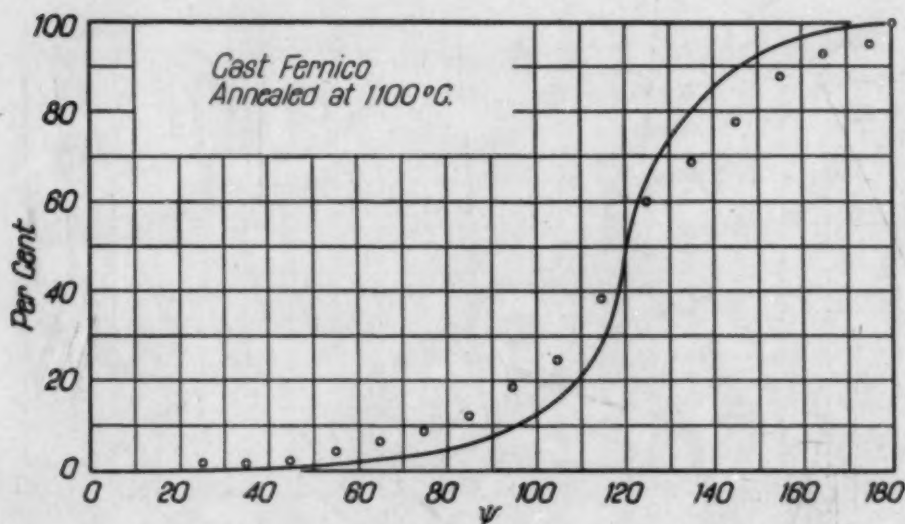


Fig. 26—Cumulative Distribution of Junction Angles for Cast Fernico, Annealed at 1100 Degrees Cent. for 1 Hour, Compared with the Ideal Curve of Fig. 13.

distributed according to the curve expected for a specimen having 120-degree interfacial angles. Thus, the grains, in growing, have adjusted their interfacial angles toward 120 degrees. This tendency continues in the next two specimens—annealed at 700 and 800 de-

grees Cent. (1290 and 1470 degrees Fahr.) respectively, which have distributions of junction angles agreeing fairly well with the assumption of 120-degree interfacial angles. This set of specimens proves that grain growth is accompanied by an adjustment of the interfacial angles toward 120 degrees.

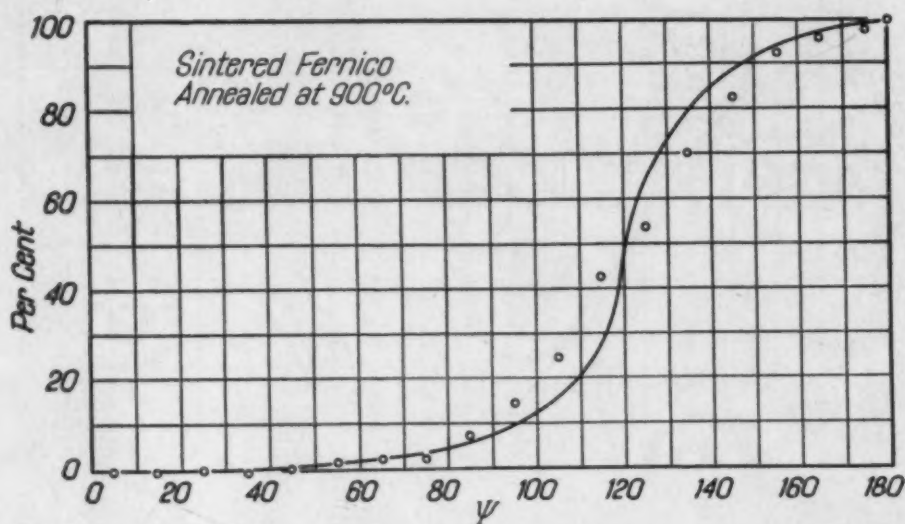


Fig. 27—Cumulative Distribution of Junction Angles for Sintered Fernico, Annealed at 900 Degrees Cent. for 1 Hour, Compared with the Ideal Curve of Fig. 13.

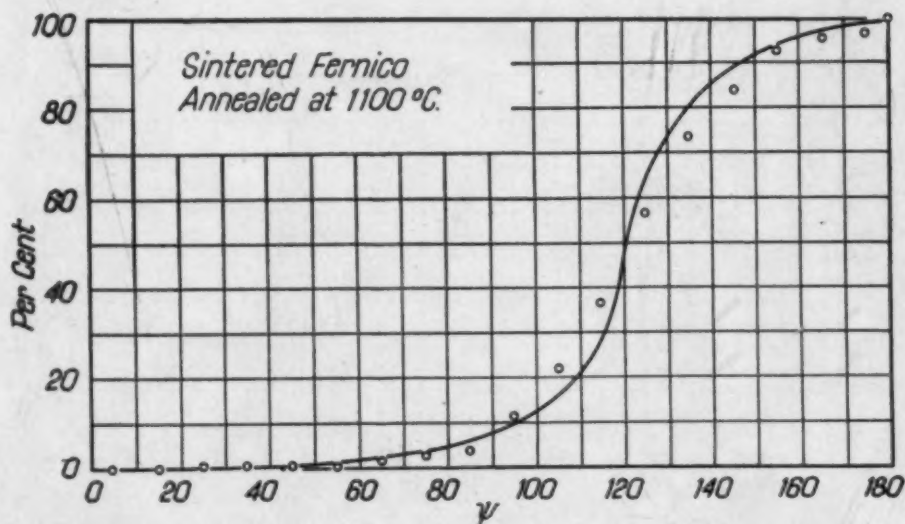


Fig. 28—Cumulative Distribution of Junction Angles for Sintered Fernico, Annealed at 1100 Degrees Cent. for 1 Hour, Compared with the Ideal Curve of Fig. 13.

Fernico—Cast and cold-worked Fernico shows considerable grain growth after the start of recrystallization. Figs. 25 and 26 show the distribution of junction angles in cast and worked Fernico annealed at 900 and 1100 degrees Cent. (1650 and 2010 degrees Fahr.). The

approach to 120-degree interfacial angles shows up clearly. Sintered Fernico shows little or no grain growth, although the angular distribution approaches that required by 120-degree interfacial angles, as shown in Figs. 27 and 28. This example proves that it is pos-

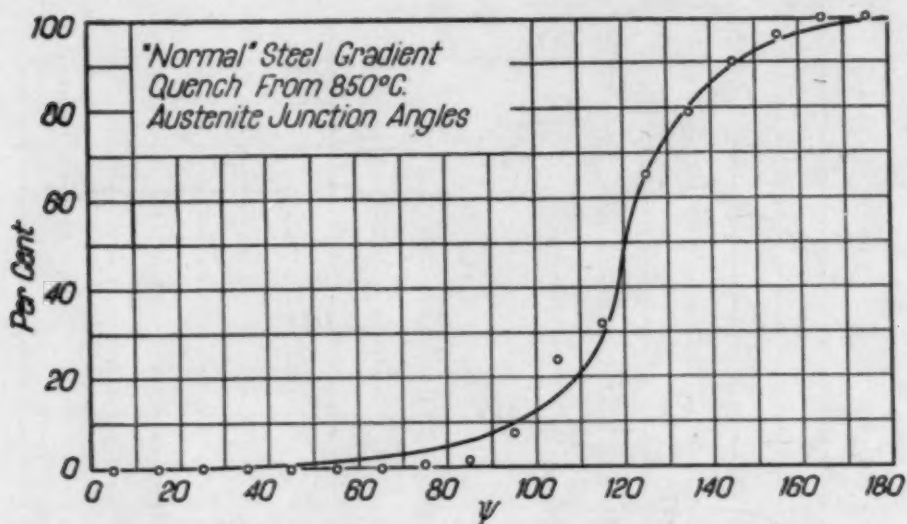


Fig. 29—Cumulative Distribution of Austenite Junction Angles for "Normal" Steel, Gradient Quenched from 850 Degrees Cent., Compared with the Ideal Curve of Fig. 13.

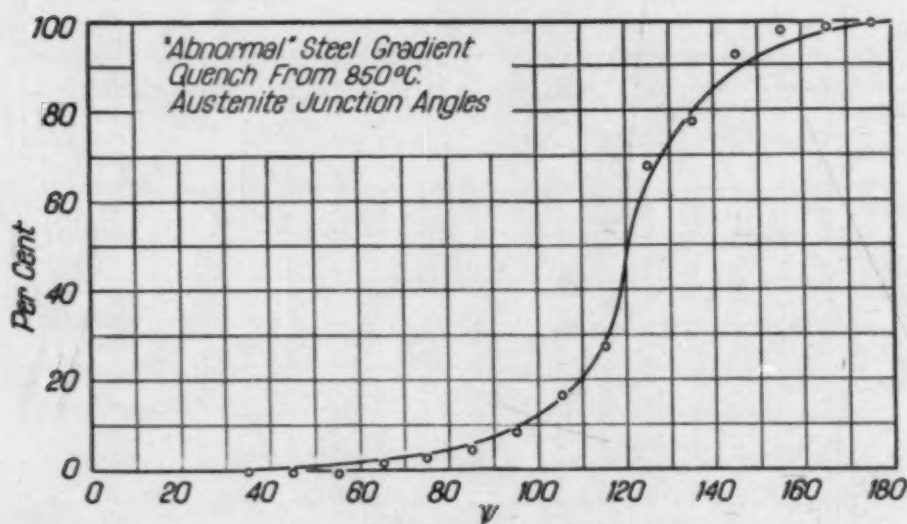


Fig. 30—Cumulative Distribution of Austenite Junction Angles for "Abnormal" Steel, Gradient Quenched from 850 Degrees Cent., Compared with the Ideal Curve of Fig. 13.

sible for grain boundaries to achieve equilibrium without an increase in the average grain size.

Steel—Eutectoid steel quenched at the proper rate from temperatures above the gamma-alpha transformation shows the outlines of the austenite grains traced in pearlite against a martensite back-

ground. In this way the junction angles of the austenite can be measured. Two bars of 0.8 per cent carbon steel—one “normal”, the other “killed” with aluminum and “abnormal”—were held for an hour at 850 degrees Cent. (1560 degrees Fahr.) and quenched

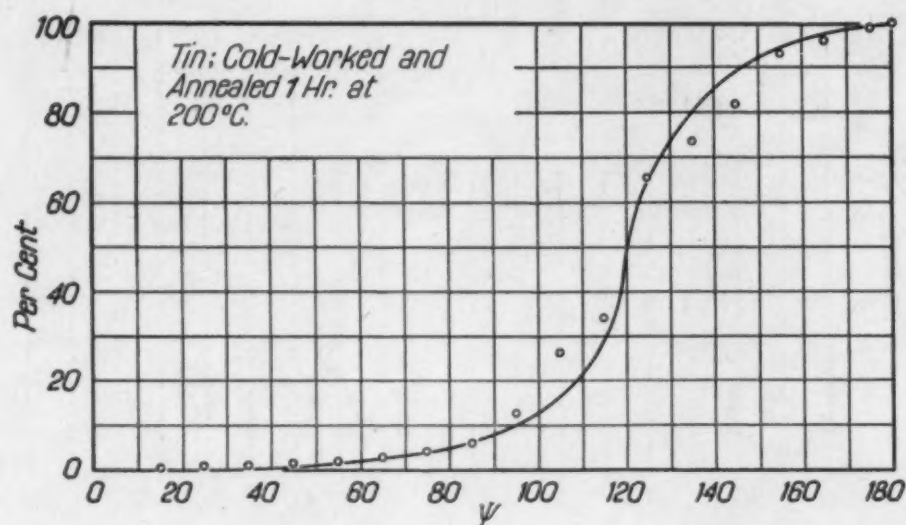


Fig. 31—Cumulative Distribution of Junction Angles for Pure Tin, Cold-Worked and Annealed at 200 Degrees Cent. for 1 Hour, Compared with the Ideal Curve of Fig. 13.

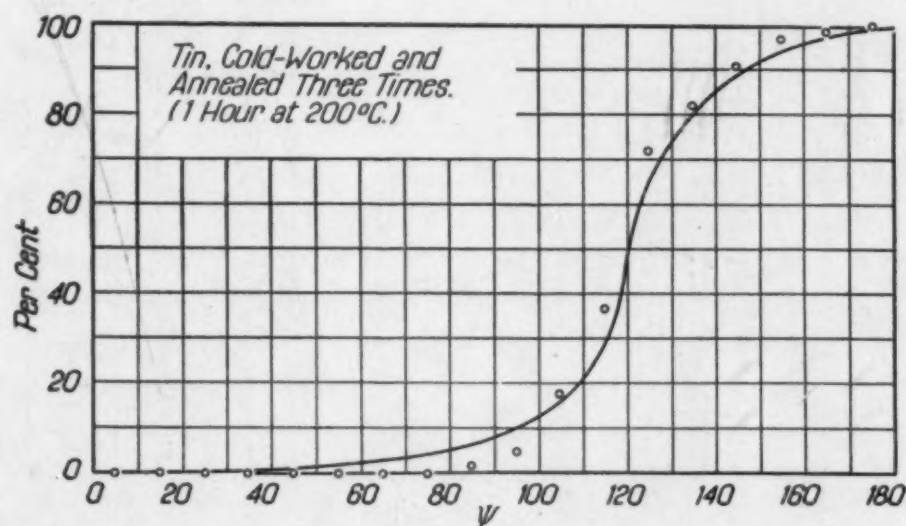


Fig. 32—Cumulative Distribution of Junction Angles for Pure Tin, Cold-Worked and Annealed at 200 Degrees Cent. for 1 Hour Three Times, Compared with the Ideal Curve of Fig. 13.

from one end, so that a range of cooling rates was present in the bars. In each bar a region was found where the austenite grain boundaries could be observed; this was coarse in the normal and fine in the abnormal steel. Measurements of the junction angles showed both steels to have possessed 120-degree interfacial angles when they

consisted of austenite. The distributions of these angles are shown in Figs. 29 and 30. Neither of these steels should have shown much change in austenite grain size on longer heating before quenching. (Reheating of the quenched steels to above the gamma-alpha transi-

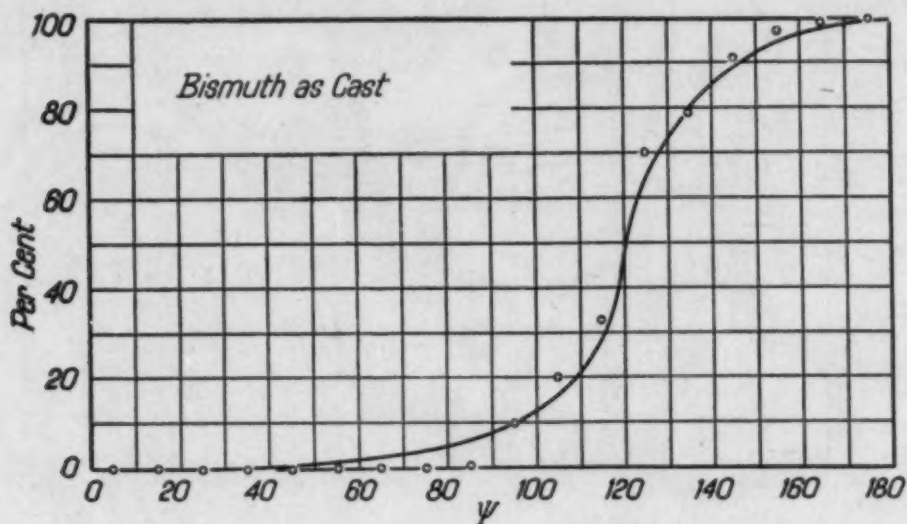


Fig. 33—Cumulative Distribution of Junction Angles for Pure Bismuth, As-Cast, Compared with the Ideal Curve of Fig. 13.

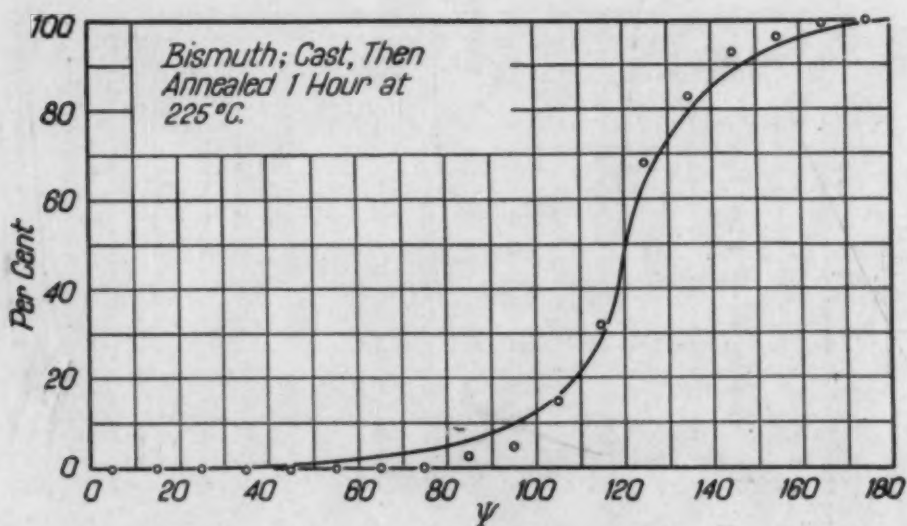


Fig. 34—Cumulative Distribution of Junction Angles for Pure Bismuth, Cast and Annealed at 225 Degrees Cent. for 1 Hour, Compared with the Ideal Curve of Fig. 13.

tion would, of course, establish a new set of austenite grains, which might have sizes different from those originally present.)

Tin—A block of pure tin was compressed first in one direction, then in another, until the whole mass had been subjected to considerable plastic deformation, although the external dimensions had been

restored approximately to their original values. The block was then annealed at 200 degrees Cent. for an hour and the junction angles measured. The angular distribution is shown in Fig. 31. It is seen that there are too many large and small junction angles, so that it is concluded that not all the interfacial angles are 120 degrees. The

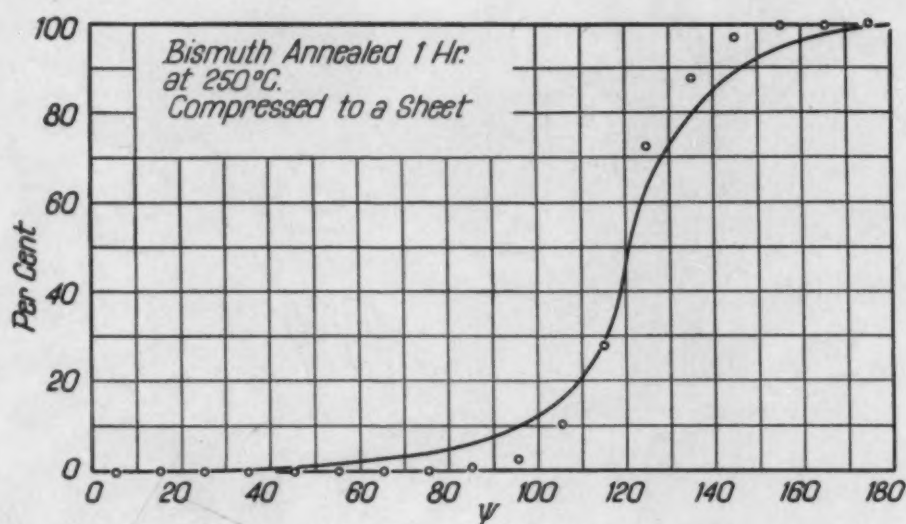


Fig. 35—Cumulative Distribution of Junction Angles for Pure Bismuth, Compressed to a Sheet and Annealed at 250 Degrees Cent. for 1 Hour, Compared with the Ideal Curve of Fig. 13. Plane of section parallel to sheet.

tin block was then subjected to the working and annealing process twice more, and the junction angles measured again. As is seen from Fig. 32, the block now consists of grains whose faces meet at 120 degrees.

Bismuth—A block of pure bismuth was examined as cast and again after annealing for an hour at 225 degrees Cent. (435 degrees Fahr.). The distribution of junction angles—Figs. 33 and 34—shows these specimens to contain 120-degree junction angles. There was no appreciable grain growth during the annealing.

A piece of this block was worked by slowly compressing it at 200 degrees Cent. (390 degrees Fahr.). It was possible to reduce the thickness by 80 per cent in this way, without fracturing the specimen. This worked sheet was then annealed for an hour at 250 degrees Cent. (480 degrees Fahr.) and examined on a section normal to the direction of compression. The resulting junction angles had the distribution plotted in Fig. 35. It is seen that there are many more angles near 120 degrees than predicted by the calculated curve. Such a result indicates that more of the grain edges meet the plane of

section nearly perpendicularly than is predicted from a random distribution of edge directions.

This result can be explained by the fact that the grains are large compared to the thickness of the sheet in which they nucleate and grow, as explained in the section on the establishment of grain structures.



Fig. 36—Silver Bearing OFHC Copper, As Cast. Section parallel to axes of columnar grains. $\times 3.5$.

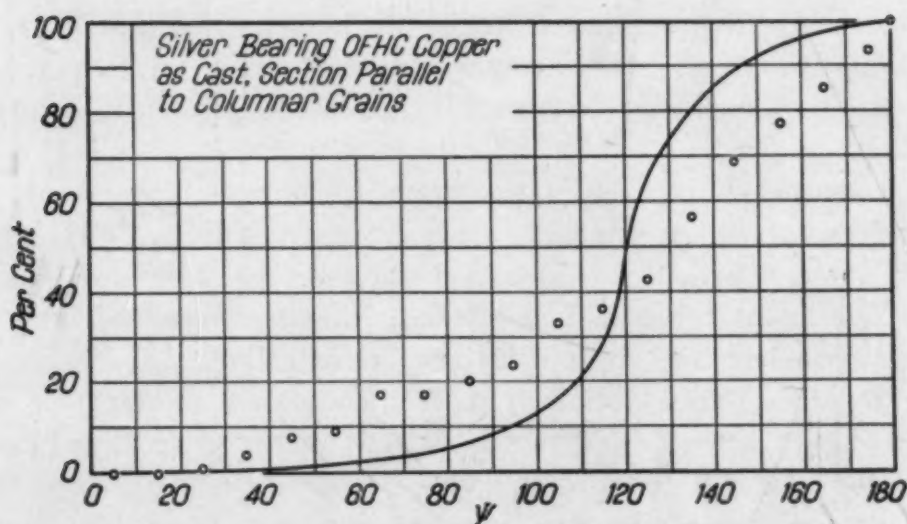


Fig. 37—Cumulative Distribution of Junction Angles for the Copper Specimen of Fig. 36, Compared with the Ideal Curve of Fig. 13.

Copper—A block of silver bearing (0.05 per cent) OFHC copper consisting of columnar grains was cut from a large cast bar. A section was cut approximately parallel to the long axes of the grains

and the junction angles measured. Figs. 36 and 37 show the section and a graph of the distribution of junction angles. It is seen that the grains appear very elongated and that there are many too many small and large angles. Another section, cut at right angles to the long axes of the columnar grains, gave the results shown in Figs. 38

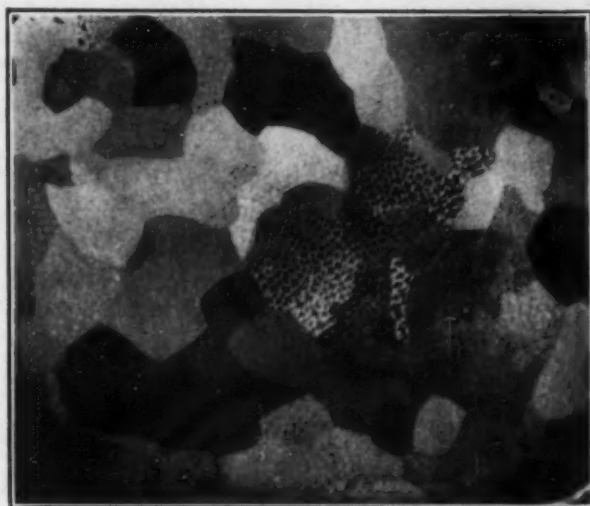


Fig. 38—Silver Bearing OFHC Copper, As Cast, Section Normal to Axes of Columnar Grains. $\times 3.5$.

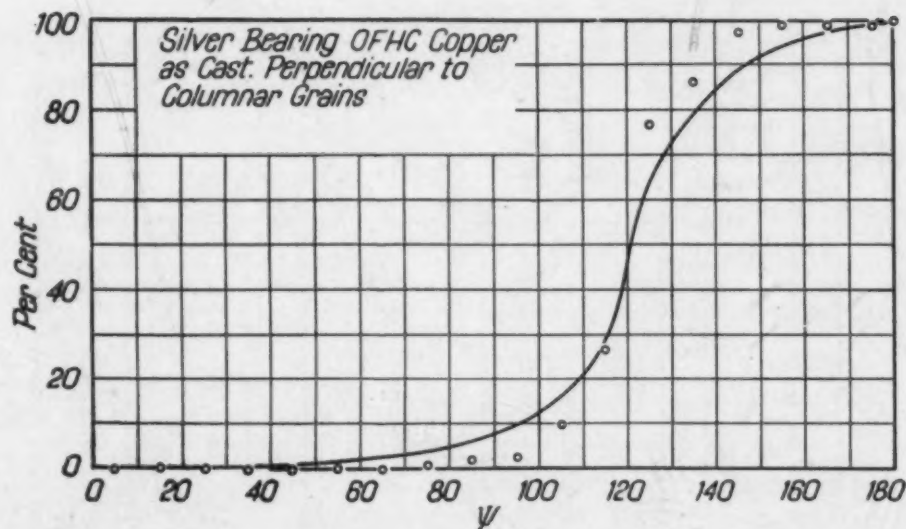


Fig. 39—Cumulative Distribution of Junction Angles for the Copper Specimen of Fig. 38, Compared with the Ideal Curve of Fig. 13.

and 39. In this section the grains appear as equiaxed polygons, but there are many more junction angles near 120 degrees than expected in a section through a random grain structure.

The copper block was then annealed for half an hour at 1000

degrees Cent. (1830 degrees Fahr.) and the two sections repolished, etched, and their junction angles measured. In both cases the numbers of small and large junction angles decreased somewhat, as shown in Figs. 40 and 41. This result reflects the adjustment of the interfacial angles toward 120 degrees on annealing.

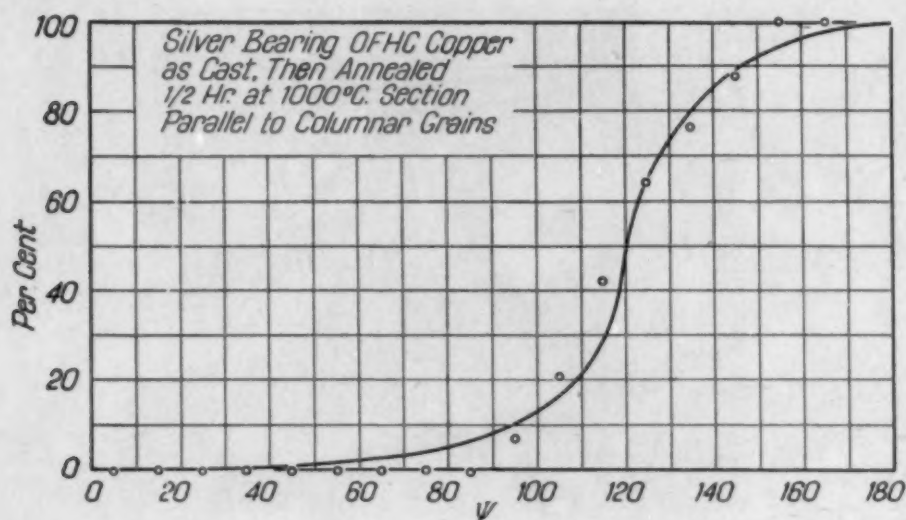


Fig. 40—Cumulative Distribution of Junction Angles for Silver Bearing OFHC Copper, Cast and Annealed at 1000 Degrees Cent. for $\frac{1}{2}$ Hour, Compared with the Ideal Curve of Fig. 13. Plane of Section Parallel to Axes of Columnar Grains.

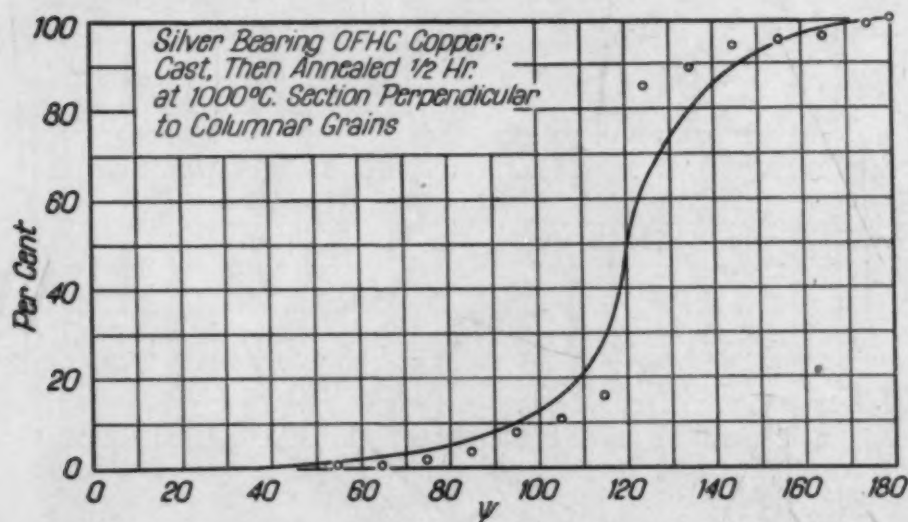


Fig. 41—Cumulative Distribution of Junction Angles for Silver Bearing OFHC Copper, Cast and Annealed at 1000 Degrees Cent. for $\frac{1}{2}$ Hour, Compared with the Ideal Curve of Fig. 13. Plane of section normal to axes of columnar grains.

It was expected that the section at right angles to the long axes of the columnar grains would show junction angles almost all within 5 degrees of 120 degrees, since the grain edges should all be about

normal to the plane of section and the 120-degree interfacial angles should, therefore, appear almost unchanged as junction angles. Fig. 11 shows that a grain edge where three faces meet at 120 degrees may be tilted 25 degrees to the section normal before any junction angle deviates from 120 degrees by as much as 5 degrees.

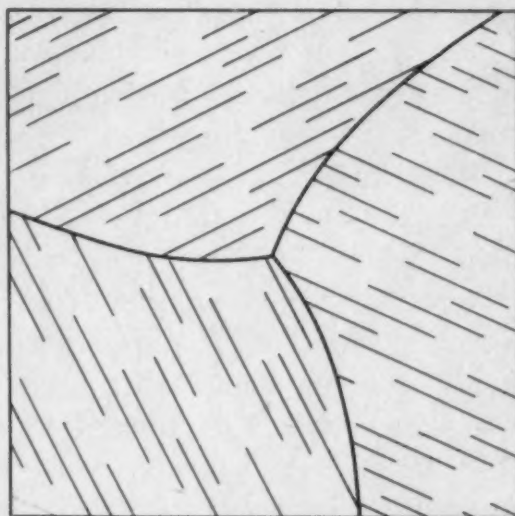


Fig. 42—A "Turbine" Type Junction, Sectioned Normal to the Grain Edge.

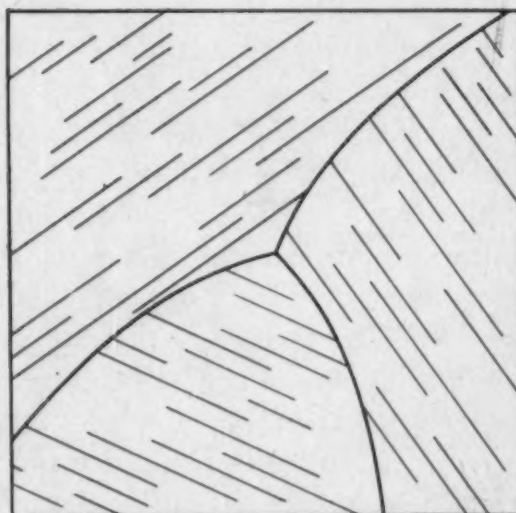


Fig. 43—A "Two Against One" Type Junction, Sectioned Normal to the Grain Edge.

The conclusion is that the interfacial angles are not all 120 degrees in even the well annealed specimen. Indeed, the distribution of junction angles must be a fair representation of the distribution of interfacial angles in a specimen, if the plane of section is normal to

the long axes of the grains. The reasons for believing that the equilibrium grain structure contains only plane grain faces and 120-degree interfacial angles are so cogent, however, that a detailed examination of the section was made.

It became apparent that most of the grain boundaries were curved. Three curved boundaries can meet at an edge in two principal ways: I, the "turbine," in which all three curvatures bend the faces in the same rotational sense about the edge as shown in Fig. 42; and II, the "two against one," in which one of the faces bends in the opposite rotation sense to the other two, as shown in Fig. 43. On annealing, the faces tend to flatten at a rate increasing with their curvatures. At the "turbine" type of edge, all faces can flatten simultaneously without changing the angles from 120 degrees; the result is merely a rotation of the three grain faces about the edge. The "two against one" type of edge cannot behave so simply. As the faces attempt to flatten, the angle toward which two faces are concave is forced to become more acute, while the angle toward which two faces are convex is forced to become more obtuse. The tendency toward flat faces thus opposes the tendency toward equal angles and the result is that neither state is achieved. The best that can be done is to distribute the deviations from the ideal state as well as possible by bending faces and moving the edge toward the acute angle. Examination of the photomicrograph of the section across the columnar grains, Fig. 38, shows that grain faces will bend considerably in order to adjust the interfacial angles toward 120 degrees. Only if the curvature is quite sharp are the angles very different from the equilibrium value. These effects retard the attainment of 120 degrees for every interfacial angle, so that there usually will be a few more large and small junction angles in every section than predicted from the assumption of 120 degrees.

The examples just discussed show that: (a) the grain structure of an annealed specimen of metal is really determined by the geometry of the grains and not by their sizes; (b) the interfacial angles of grains tend toward 120 degrees on annealing and the faces of grains tend toward flatness, although the achievement of these two goals becomes very slow as equilibrium is approached.

ACKNOWLEDGMENT

It is a pleasure to record here our debt of gratitude to those who have helped us in developing this paper. Our discussions with

Drs. R. Smoluchowski, H. A. Liebhafsky, and R. H. Harrington have been particularly helpful in clarifying and sharpening our statements. To Mrs. C. Riisness, who made many of the angle measurements; to Mrs. C. Brodie, who carried out the metallography; and to Mr. J. Kilfoyle, who drew the figures, we tender our appreciation for their painstaking work.

REFERENCES

An attempt to list the authors whose published work has contributed to the background of this paper would be almost hopeless. Nearly every paper we have read dealing with metallography, metallurgy, physics, chemistry, or crystallography has contributed in some way to our thought on this subject.

We have, therefore, decided to leave out all references.

DISCUSSION

Written Discussion: By E. J. Eckel, department of mining and metallurgical engineering, University of Illinois, Urbana, Ill.

The authors have capably presented both in theory and experimental results a new and interesting aspect of the ever important phenomenon of grain growth, namely, that as grains grow the junction angles approach 120 degrees. However, the conclusion of the authors that grain growth cannot take place once the angles reach 120 degrees is open to question. From the theoretical standpoint, the fact that the junction angles should approach 120 degrees does not prove that after this value is reached the grains should not continue to grow while maintaining the same shape, and thus reach a lower energy level.

If the authors stated that 120-degree angles are approached but never reached, their conclusion would be difficult to check since the result would be practically the same whether the grains grew to form perfect junction angles of 120 degrees or to reduce the boundary area. If growth is merely incidental to the forming of 120-degree angles, the process must be very inefficient in view of the tremendous increase in grain size that can be brought about by grain growth. With 70-30 brass an increase of 60,000 times by volume is possible by means of coalescence after recrystallization.

The authors in their experimental results mention that measurements of the junction angles of austenite grains in a fine-grained aluminum-killed steel indicated that the angles were practically all 120 degrees, and therefore they conclude that an increased temperature of heating before quenching would not have shown much change in grain size. It is well known that all aluminum-killed steels will coarsen if the temperature is high enough, and if the authors will repeat the work on steels, using a temperature of 2200 degrees Fahr. (1205 degrees Cent.), they will find that the grain size of the aluminum-killed

steel will be as coarse if not coarser than that of the coarse-grained steel. The coarsening of aluminum-killed steels results in an increase in grain size of 200 or more times by volume. If this much growth can take place after the attainment of junction angles of 120 degrees, certainly the angle is not the stabilizing factor.

The authors also mention that they detected negligible growth in cast zinc and bismuth. The impossibility of bringing about growth in unstrained cast single-phase metals, whether the grains be small, large, equiaxed, or columnar, has been long an accepted fact. The inhibitor in this case is believed to be impurities that are concentrated in the last liquid to solidify at the grain boundaries.

In conclusion, this paper reveals that during grain growth the junction angles approach 120 degrees but does not prove that grain shape is the controlling factor in grain growth. In fact some of the experimental results might well be used to show that the end point in grain growth is not 120-degree junction angles.

Written Discussion: By H. L. Walker, department of mining and metallurgical engineering, University of Illinois, Urbana, Ill.

This paper contains a number of interesting observations on the shape of grains which grow in solid metals where the growth is hindered by contact with other grains. I have no objections to make to the observed data which indicate that solid grains of metal tend to form dodecahedrons; however, it does not seem to me that good proof has been established to substantiate the statement that metal grains will not continue to grow in size when a statistical arrangement based upon 120-degree interfacial angles has been reached.

I also wish to question the statement in paragraph four, page 157, "At low temperatures, then, only a few nuclei will form in a given volume of distorted material before it is totally filled by new crystals growing from the first nuclei. At higher temperatures, a greater density of nuclei is expected before the volume is filled with equilibrium material." While the statement is perhaps theoretically correct, it is at variance with observations upon the grain size produced at just complete recrystallization, without appreciable coalescence having taken place for cold-rolled cartridge brass. For cartridge brass, it has been found that the recrystallized grain size is independent of time and temperature of annealing and for the given metal is dependent only upon the amount of cold deformation.

As an example of the independence of recrystallized grain size upon time and temperature, the following data are offered for cartridge brass:

Per Cent Cold Deformation	Annealing Conditions		Recrystallized Grain Diameter in mm.
	Time	Temperature, Degrees Cent.	
70	2 hr.	350	0.016
70	16 min.	400	0.016
70	2 min.	450	0.015
70	30 sec.	500	0.015
70	15 sec.	600	0.016
43	4 hr.	400	0.033
43	16 min.	450	0.028
43	4 min.	500	0.031
43	2 min.	550	0.029
43	15 sec.	600	0.030

When a whole series of deformations is annealed and the recrystallized grain sizes are plotted against the per cent of cold deformation, prior to annealing, a smooth curve of the exponential type $y = MX^n$ is produced. If these data are plotted as \log_{10} grain size versus $\sqrt{\text{per cent deformation}}$ a straight line is produced. Therefore, if the number of nuclei formed, for a given deformation, is a function of temperature, then the rate of disappearance of nuclei must equal the rate as which new nuclei are formed, otherwise, a difference would be found in the grain size produced.

Any discussion of the grain growth phenomena should distinguish between growth due to recrystallization, i.e., when an unstrained area is feeding upon a strained area, and growth due to coalescence, i.e., when one unstrained area grows at the expense of another unstrained area. This latter is probably due to a difference in surface energies. The shape of the grain may very well have something to do with grain growth, as proposed on page 160. However, many instances have been observed in polished sections of cartridge brass where one grain whose boundary was convex was feeding on a neighboring grain whose boundary was concave to the feeding grain. This phenomenon has been observed in growth due to either recrystallization or to coalescence.

Since grain growth may take place by the process of an unstrained area feeding upon another area containing strain (process of true recrystallization) then we may actually have an increase in the number of grains present as a result of nucleation and grain growth. As an example: if a specimen of brass with an average grain diameter of 0.50 mm. is cold-rolled to 70 per cent reduction in thickness and then recrystallized, the recrystallized grain size is found to be 0.015 mm. diameter. This is in direct contradiction to the statement on page 166, i.e., grain growth can only occur if the number of grains decreases. Once recrystallization is complete, however, there must be a decrease in number of grains during grain growth by coalescence.

A direct comparison of the grain growth characteristics of cast and cold-worked Fernico with sintered Fernico cannot be made because of the probability of contamination of the surfaces of the sintered grains, such as by an oxide, which would act as an obstruction to the free exchange and diffusion of intergranular atoms. At some higher temperature than 1100 degrees Cent. (2010 degrees Fahr.) the sintered material may very well show a great amount of growth. Likewise the same objection is raised to the experiment with aluminum-treated steel. It is well known that steels treated with aluminum produce small grains after heating to normal heat treating temperatures; however, they are prone to coarsen very rapidly at temperatures in excess of approximately 925 degrees Cent. (1700 degrees Fahr.). The temperature of approximately 850 degrees Cent. (1560 degrees Fahr.) used in the experiment gives no criterion, regardless of grain shape, for the growth characteristics at higher temperatures.

Normally, a cast metal which has been slowly cooled will nucleate solid crystals, which feed upon the liquid metal and grow in a comparatively free manner, and without appreciable strain. Such a cast metal does not show coalescence of grains upon annealing, unless the metal or alloy exhibits an allotropic modification, in which case nucleation and grain growth take place by a change in atomic configuration.

In the case of silver-bearing O.F.H.C. copper, as cast, and exhibiting columnar grains, I would not expect a change in grain shape or size to take place. However, I have not had an opportunity of examining a section of columnar copper after annealing at a temperature close to its melting point. The data as presented do indicate that some change in the grain structure has taken place, or else a more favorable section was measured after the annealing cycle. I regret that a photomicrograph of the structure after annealing is not included in the paper.

The value of this paper lies in its presentation of data which indicate that a stable grain tends to assume the configuration of a rhombic dodecahedron, or more probably a pyritohedron. The force responsible for coalescence is generally considered to be a reduction in total surface energy. The lowest possible surface energy is connected with a sphere of largest possible diameter; however, solid grains are not free to form spheres. Therefore they tend to assume the closest possible configuration approaching a sphere.

The process of coalescence in solid grains is different from coalescence of liquids, but the end product is the same, i.e., greater stability through an increase in size. To remove the concept of surface energy as the driving force for coalescence and substitute therefor a stable geometric configuration without regard to size does not seem justified.

We should also be aware of the influence exerted by similar and dissimilar orientation of atomic planes in neighboring grains. Two grains in contact and having similar orientations can coalesce more easily than two grains having radically different orientations, all other conditions being the same. Van Arkel* has presented experimental evidence that coalescence is a function of the orientation of individual grains. According to Van Arkel's experiments the amount of coalescence is limited to grains having an orientation very close to that of the growing grain and a grain in one domain cannot grow at the expense of another grain in a domain of widely different orientation.

Authors' Reply

First we should like to thank Doctors Eckel and Walker for the thorough consideration they have given our paper. Next, we should like to reply to some of their criticisms.

Both the discussers seem to feel that we would interpret agreement between the junction angle distribution of a specimen and the calculated ideal curve as proof that its grain structure was stable and could show no further change. This impression is one we did not wish to make. In the first place (as stated in the first paragraph of the section on "The Criterion of Grain Stability"), we feel that the grain faces must not only meet at 120 degrees, but must also be planes, if the grain structure is to be really stable; knowing that the angles are 120 degrees is only half the story. In the second place, agreement—even perfect—with the ideal curve is at best a statistical result and means only that the interfacial angles are very likely to be within 5 degrees of 120 degrees.

*Van Arkel, "Some Phenomena of Recrystallization," *Revue de Metallurgie*, Vol. 33, 1936, p. 197-202.

What we believe we *have* proved is that the interfacial angles of grains in a specimen of metal approach 120 degrees as the time of annealing increases, whether or not there is an increase in average grain size.

We have presented what we believe to be a sound theory which predicts the cessation of grain growth after the achievement of flat faces and 120-degree interfacial angles by all the grains. The experimental fact that the angles do approach 120 degrees is in agreement with a prediction of the theory and gives weight to its other predictions. We, therefore, do not expect grain growth to continue in a specimen whose junction angles are distributed according to the ideal curve.

It can, and does, happen that the junction angle distribution of a specimen is in good agreement with the ideal one while the grain boundaries are still somewhat curved. Fig. 19 shows this condition in cast zinc. As noted on the last couple of pages of the paper, we think the velocity of grain face flattening decreases greatly as the radius of curvature of the face increases, i.e., as the face approaches flatness. Thus, grain growth can still proceed in structures such as that of the cast zinc, but only very slowly. This effect may account for the behavior of brass, as follows: Up to about 700 degrees Cent. (1290 degrees Fahr.) 1-hour anneals produce grain growth by adjustment of interfacial angles toward 120 degrees, as well as by flattening faces. After the 700-degree Cent. (1290-degree Fahr.) anneal, the angles are all within 5 degrees of 120 degrees, but the faces are not all flat. Grain growth, therefore, continues by further adjustment of the structure toward a condition involving flat faces as well as 120-degree interfacial angles.

As a face flattens, the angles it makes with adjoining faces must change, and, if they were originally 120 degrees, they are no longer so. The flattening of a face thus produces a tendency for its edges to move; consideration of Figs. 4 and 5 will show the edges will move in the same direction as the center of the face as it flattens. The whole face, edges and all, will therefore move toward its concavity, if its adjoining interfacial angles were originally 120 degrees. In moving it will sweep across the grain in its path; if it sweeps across it completely, that grain vanishes from the specimen, the average grain size increases and "grain growth" occurs.

The only polyhedra, all of whose interfacial angles are 120 degrees, are those illustrated in Figs. 6 and 7. The interfacial angles of a pyritohedron are not 120 degrees, but either 113.6 or 126.9 degrees. The only distortions of the pyritohedron that have all their interfacial angles equal to 120 degrees are the two dodecahedra mentioned and distortions of them produced by moving planes parallel to themselves. Some of these distortions are far from spherical—one produced by lengthening a hundred fold all the vertical edges in Fig. 6, for instance—yet they are still stable grain shapes.

We should like to point out that the tendency of grains to assume flat faces and 120-degree interfacial angles can be predicted just as easily on the basis of surface energy arguments as on the mechanistic basis used in this paper. For this purpose the grain boundaries are to be thought of as high energy regions separating crystals of different orientations. The minimum area of grain surface that can be achieved under a given set of initial conditions will be the final grain structure. It is easy to see that this leads to flat faces and 120-degree

interfacial angles. For intuitive purposes, the boundaries can be compared to the cell walls in a foam of soap bubbles, but differing from soap foam in that the air can pass fairly easily from one cell to another through the cell walls. When a grain face is flat and makes 120-degree angles with adjoining faces, it cannot move without increasing the total area of grain boundary material in the specimen (except by moving so as to leave it flat and at 120 degrees to adjoining faces). Thus, there is nothing in the surface energy argument that would lead to any other conclusions than those stated in the paper.

Whenever a grain boundary moves it does so because of conditions in its immediate neighborhood. Its motion cannot be conditioned by the average grain size in the specimen. Whenever a grain boundary is flat and makes 120-degree angles with neighboring grain boundaries, it has no reason to move and, therefore, will not do so. When all grain boundaries in a specimen satisfy this condition, the surface energy is at a minimum compared to the surface energies which would be produced by motion of the grain boundaries, so the grain structure is stable. Any deviations from this behavior must arise from such factors as strained grains, concentration differences between grains, inclusions, etc., whose effects were not considered in setting up the theory presented in this paper, but may form the subjects of future ones.

The word "coalescence" we take to mean the formation of a grain by the disappearance of the boundaries between several smaller grains. We agree with Van Arkel in saying that this happens only when the grains have almost the same orientation. Such a situation is quite rare in the specimens of metal ordinarily observed and has been ignored in this paper. The only process of grain growth considered here is that of the "absorption" of grains by neighboring grains, which takes place by the sweeping of grain boundaries completely across the grains being absorbed. This is the way grain growth usually occurs.

Dr. Walker's data on the grain size of just barely recrystallized brass are very interesting and seem to show that the nuclei on which the recrystallization of his specimens initiated were produced during cold working. The relative motion of atoms in a specimen during cold working must be quite extensive and it is not surprising—indeed, it is gratifying—to find that stable atomic constellations are produced during these motions. Our statements referred to the production of nuclei due to thermal motion of atoms in distorted material and we still feel it to be correct for nuclei so produced. There are probably three ways in which nuclei can be produced: by cold work, by thermal motion, and by the survival of fragments of the original annealed material. Nuclei produced by cold work seem to predominate in Dr. Walker's brass; other specimens of metal may show other types.

As mentioned before, the theory of this paper applies to the changes in grain structure occurring in a specimen consisting entirely of crystals with the equilibrium atomic arrangement. The remarks in the first two pages of the paper are mainly intended to present to the reader the picture of atomic behavior on the basis of which the subsequent theory was set up. We have referred to *recrystallization* as the process during which strained or disorganized crystals disappear from the specimen by absorption into growing grains of

stable crystal structure, and to "*grain growth*" as the process during which grains of stable crystal structure change shape and size at each other's expense after all strained or other nonequilibrium material has disappeared from the specimen. Under this definition—the usual one, we believe—"grain growth" involves a decrease in the number of grains in a specimen. Grains growing at the expense of nonequilibrium material are not exhibiting "grain growth."

The effect of impurities—either dissolved or as inclusions—on the motion of grain boundaries has not been considered in the theory outlined in this paper. It would be expected that inclusions larger than the thickness of a grain boundary would tend to prevent grain boundary motion, while inclusions smaller than the thickness of a grain boundary would have little effect. If the thickness of grain boundaries increases with temperature—a not unreasonable assumption—the hindrance to grain boundary motion would suddenly decrease at the temperature where the grain boundary's thickness became greater than the size of the inclusions. The behavior of the austenite grain size in aluminum-killed steel might be explained in this way. The sintered Fernico, too, contains included nonmetallic particles which prevent grain boundary motion, but do not prevent the adjustment of the interfacial angles toward 120 degrees. The boundaries are, of course, quite curved and irregular.

Cast metal shows some grain growth, although not much. We do not believe all cast metal can be dirty or impure enough to envelop all grains and prevent their mutual contact. Their lack of grain growth, it seems to us, is probably connected with their interfacial angles being close to 120 degrees and their grain faces having only slight curvatures. Some castings, of course, do contain large amounts of impurities and, in these cases, the grains may be isolated from one another by foreign material; grain growth could not take place in such a specimen.

EXPERIMENTS ON SODIUM CYANIDING OF HIGH SPEED STEEL PRIOR TO HARDENING

By JOHN McINTYRE

Abstract

This paper describes experimental work on the cyaniding of three types of high speed steel prior to hardening. Hardness values of Rockwell C 68-70 have been obtained throughout sections of 1-inch diameter. Following a cyanide treatment at 1450 degrees Fahr. (790 degrees Cent.) for one and one-half hours, the experimental pieces were hardened and tempered in accordance with normal high speed steel practice. It was found that pieces retained hardness values of C 70 with drawing temperatures as high as 1150 degrees Fahr. (620 degrees Cent.). Tools treated in the manner described in this paper have shown unusually long life in production service during the last eight months. Photomicrographs illustrating the structures obtained in the experimental pieces are included and show a marked difference from structures obtained by hard casing procedures as applied to high speed steel. The work described in the paper is a beginning and is being followed by further studies.

FOR some time there have been attempts by various metallurgists to improve on the hardness of high speed steel. The most notable of these attempts have been with some nitrogenous medium applied to the steel after it has been hardened, tempered and ground. However, these treatments produce on the steel only a superficial case which, though extremely hard, is readily removed by light grinding. This paper presents a method whereby high speed steel can be made extremely hard not only at the surface but throughout sections of 1-inch diameter. The process is simple and is applicable to both the tungsten and molybdenum high speed steels.

MATERIAL TESTED

In these experiments three types of high speed steel were used. These are listed as Type A, Type B, and Type C and the chemical analyses are given in Table I.

A paper presented before the Twenty-sixth Annual Convention of the Society, held in Cleveland, October 16 to 20, 1944. The author, John McIntyre, is manager, heat treating department, International Business Machines Corp., Rochester, N. Y. Manuscript received June 15, 1944.

Table I
Composition of Steels Tested

Type	W	Mo	Cr Per Cent	V	C
A	18.00	4.00	1.00	0.70
B	5.50	4.25	4.00	1.65	0.80
C	1.50	8.00	4.00	1.00	0.80

TYPE OF CYANIDE BATH USED

When the cyanide bath was first started, it was filled with commercial sodium cyanide of the 96 per cent NaCN, 4 per cent inert type, and as the bath was depleted from oxidation and drag-out, this same composition was used to replenish it. This bath has been in use for two years and the normal running temperature over the period has been 1450 degrees Fahr. (790 degrees Cent.). At the time the experiments were run, the NaCN content of the bath was between 20-30 per cent. The cyanide pot was of the 35 per cent nickel-15 per cent chromium type and was 12 inches in diameter and 18 inches deep. The chromel-alumel thermocouple in a protection tube was immersed in the pot to within 3 inches of the bottom and was connected to an automatic temperature control instrument. To avoid fouling of the atmosphere in subsequent hardening treatments, each specimen, after removal from the cyanide bath, was washed in a boiling solution of oakite to remove adhering cyanide and was then degreased.

OTHER EQUIPMENT USED IN HARDENING, TEMPERING AND TESTING

The high temperature furnace was of the carbon muffle type and was controlled by an automatic temperature controlling and recording instrument.

The tempering furnace was the forced circulation type and was also controlled automatically.

All hardness tests were made with a Rockwell Superficial Hardness Tester using a 45-kilogram load.

SURFACE PREPARATION AND IDENTIFICATION OF SPECIMENS

The specimens used were of different sizes so that depth of hardness could be checked from one size to the next. The stock used was of the hot-rolled type with mill scale still on it while

some was high speed drill rod and some was hardened tool bits which first had to be annealed before cyaniding. On cylinders of hot-rolled stock, the cut-off ends were surface ground parallel to provide testing surfaces. This was also performed on the drill rod specimens. Hardened tool bits first were packed in cast iron chips and annealed at 1600 degrees Fahr. (870 degrees Cent.), then ground on four sides to eliminate any scale or decarburization from the annealing, approximately 0.010 inch being removed from each side. These were then cut into half-inch lengths and the cut ends ground parallel for hardness testing.

All specimens were lettered with A, B, or C to identify the type of steel.

HEAT TREATMENT OF SPECIMENS

A $\frac{3}{8}$ -inch diameter by 3-inch long piece of Type A steel was cut into four pieces so that there would be two pieces $\frac{1}{2}$ inch long and two pieces 1 inch long. These were numbered as A1, A2, A3, and A4. Two of these, A1 and A4, were suspended in the cyanide for $1\frac{1}{2}$ hours. They were then air-cooled and cleaned to remove cyanide after which they were heated to 2300 degrees Fahr. (1260 degrees Cent.) and oil-quenched. They were then given a double draw at 1050 degrees Fahr. (565 degrees Cent.).

Numbers A2 and A3 were then heated to 2300 degrees Fahr. (1260 degrees Cent.), quenched into cyanide bath at 1450 degrees Fahr. (790 degrees Cent.) and held at that temperature for 1 hour after which they were oil-quenched and given a double draw at 1050 degrees Fahr. (565 degrees Cent.).

A1 and A2 were then surface ground to a depth of 0.005 inch to remove any scale from hardening or tempering. A3 and A4 were broken and the broken faces surface ground for hardness readings. Transverse tests were then taken beginning at the center and moving towards the edge, the final one being taken as close to the edge as possible. The tests were made with a Rockwell Superficial Hardness Tester using the 45N scale. Table II lists hardness readings obtained and also the equivalent Rockwell C conversions.

It was evident, due to the great increase in hardness readings of specimens A1 and A4, that a change had occurred somewhere in the heat treatment. To check for the same hardness values, another series of the same steel was prepared. Four pieces of $\frac{3}{8}$ inch diam-

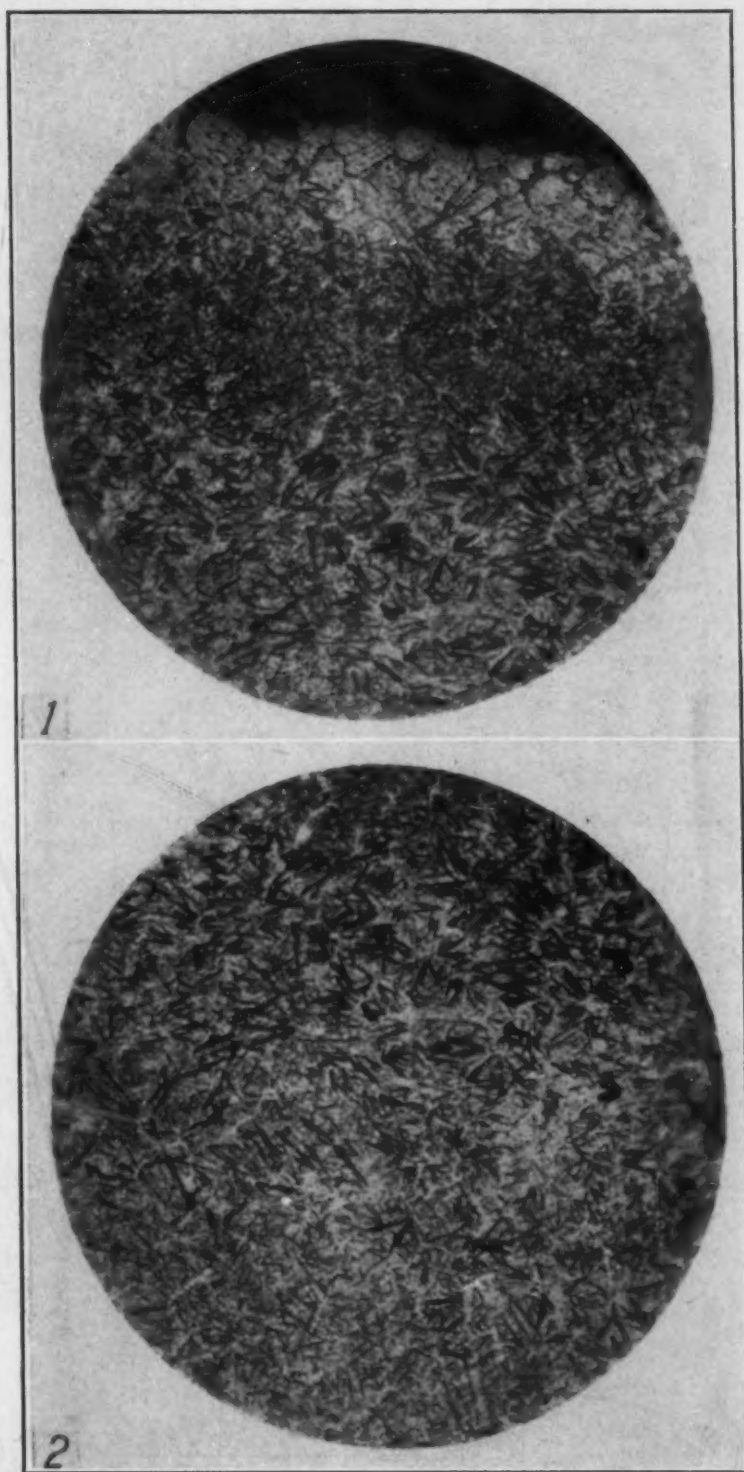


Fig. 1—Type A Steel $\times 200$ Etched in 4 Per Cent Picral Showing 3 Zones.

Fig. 2—Type A Steel $\times 200$ Etched in 4 Per Cent Picral Showing Third Zone and Core.

Table II
Hardness Readings

		1st Reading (Center)	2nd	3rd	4th (Edge)	Equivalent Rockwell C
45N)	A1	77.5	76.5	77.5	77.5	70
45N)	A4	77.5	77.5	77.5	77.5	70
45N)	A2	73	72	73	73	65-66
45N)	A3	73	72	73	72	65-66

eter by $\frac{1}{2}$ inch long were stamped A5 to A8 inclusive. These were given the same heat treatment as A1 and A4 of the previous test; cyanide at 1450 degrees Fahr. (790 degrees Cent.) for $1\frac{1}{2}$ hours, air-cooled, followed by washing, heated to 2300 degrees Fahr. (1260 degrees Cent.) oil-quenched and drawn. After tempering, 0.005 inch was removed by grinding to eliminate scale or decarburization, then hardness readings were taken on a transverse section as before.

Table III lists the Rockwell 45N readings and also the Rockwell C conversions.

Table III
Hardness Readings

Type A	1st Reading (Center)	2nd	3rd	4th (Edge)	Equivalent Rockwell C
45N) A5	76	77	77.5	77	68-70
45N) A6	77	77.5	77	77	69-70
45N) A7	77.5	76	76	76	69-70
45N) A8	77.5	77.5	77	76	69-70

A third test was then prepared and included three types of high speed steel: Types A, B, and C. Type A was included as a check and consisted of five pieces of $\frac{3}{4}$ -inch diameter by 1-inch long hot-rolled stock, numbered A9 to A13 inclusive. Type B was $\frac{1}{2}$ -inch diameter by 1-inch long hot-rolled stock and was numbered B1 to B5 while Type C was $\frac{1}{2}$ inch square by $\frac{3}{4}$ inch long, numbered C1 to C4.

To avoid repetition of hardening and tempering procedures, an outline of these is given at this time.

All types were cyanided, previous to hardening, at 1450 degrees Fahr. (790 degrees Cent.) for $1\frac{1}{2}$ hours.

Type A was then austenitized at 2300 degrees Fahr. (1260 degrees Cent.) while Types B and C were austenitized at 2250 degrees Fahr. (1230 degrees Cent.). All specimens were then oil-quenched and given two 1-hour draws at 1050 degrees Fahr. (565 degrees Cent.). After hardening and tempering all pieces, had 0.005 inch

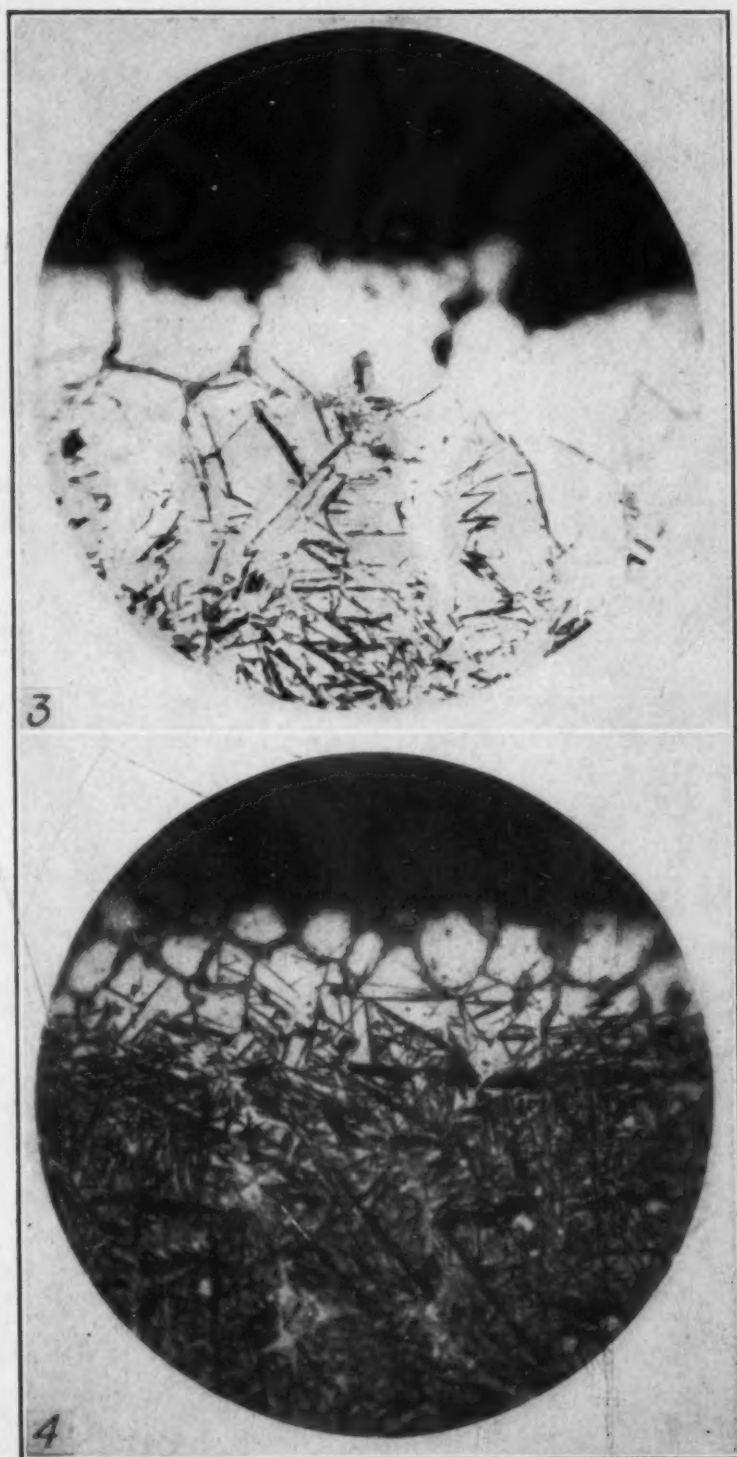


Fig. 3—Showing First Zone of Fig. 1 at $\times 500$ Etched in 4 Per Cent Picral.

Fig. 4—Type A Steel $\times 500$ Etched in 4 Per Cent Picral Showing Light Area Typical of Nitrided Surface.

removed from faces to be tested, by surface grinding and transverse readings taken on each piece. Table IV lists hardness readings taken on Rockwell 45N scale and equivalent Rockwell C readings.

Table IV
Hardness Readings

Type A	1st Reading (Center)	2nd	3rd	4th (Edge)	Equivalent R.C.
9	75.5	76.5	76.5	77.5	68-70
10	76.5	77	76	77	68-70
11	76	77	76	77	68-70
12	77.5	77	77.5	77.5	69-70
13	77.5	76	76	77.5	69-70
Type B					
1	74	74	74.5	74	67-68
2	74.5	74.5	74.5	74.5	67-68
3	74.5	74	74	74.5	67-68
4	75	74	74	74	67-68
5	74.5	74.5	74.5	74.5	67-68
Type C					
1	75.5	76.5	77	77	68-70
2	75.5	76.5	75.5	75.5	68-69
3	76.5	76.5	77	77.5	69-70
4	76.5	78.5	77	77.5	69-71

Table V
Hardness Readings

Type A	1100 Degrees Fahr. Draw	Equivalent R.C.	1150 Degrees Fahr. Draw	Equivalent R.C.
9	75.5-77.5	68-70	75.5-77.5	68-70
10	76.5-77.5	69-70	76 -77.5	69-70
11	77.5-78.5	70-71	77.5-78.5	70-71
12	76.5-78.5	69-71	76.5-78.5	69-71
13	76.5-77.5	69-70	76.5-77.5	69-70
Type B				
1	75.5-76.5	68-69	76.5-77.5	69-70
2	75.5-76.5	68-69	75 -77.5	67-70
3	74 -76.5	67-68	76.5-77.5	69-70
4	75 -75.5	67-68	76.5-77.5	69-70
5	75 -76.5	68-69	75.5-78.5	68-71
Type C				
1	75.5-76.5	68-71	76.5-78.5	69-71
2	75.5-76.5	68-69	76.5-78.5	69-71
3	75.5-77.5	68-70	76.5-78.5	69-71
4	76.5-78.5	69-71	76.5-78.5	69-71

After taking hardness readings on all specimens it was decided to increase the drawing temperatures until the hardness started to drop off. Each successive draw was increased by 25 degrees Fahr. until at 1175 degrees Fahr. (635 degrees Cent.) the hardness readings became slightly lower. Table V lists two different drawing temperatures, 1100 degrees Fahr. (595 degrees Cent.) and 1150 degrees Fahr. (620 degrees Cent.) with the high and low readings obtained on the 45N scale and equivalent Rockwell C conversions.

A 1-inch diameter by 4-inch long bar of Type C steel was hardened by this process to determine how deep the hardness would penetrate. After hardening and tempering, the bar was nicked and broken. The broken faces were surface ground and hardness readings taken on transverse faces. The readings obtained from the center to the edge were Rockwell 45N-75.5-76.5, the equivalent of Rockwell C 68-69.

CHEMICAL ANALYSES

To determine the cause of this extreme hardness, it was decided to make chemical analyses of some of this steel. To do this, specimens $\frac{1}{2}$ inch diameter by 2 inches long of Type A drill rod were cyanided, hardened, and annealed in cast iron chips. The specimens were cut in half, and the mating ends faced off for nitrogen determination. After analyses, it was found that the average nitrogen content was 0.018 per cent.

To determine the carbon, pick up turnings were taken in six progressive cuts of 0.002 inch on the radius starting at the surface. There were drillings also taken from the core. Table VI lists the carbon content of the analyzed chips.

Table VI
Composition of Chips

Original C Content	1st Cut	2nd Cut	3rd Cut	4th Cut	5th Cut	6th Cut	Core
0.70	0.98	1.20	1.25	1.16	1.07	1.11	0.70

DISCUSSION OF HARDNESS RESULTS

Although it appears from the hardness values of Table V that Type B steel does not attain full hardness until tempered at 1100 degrees Fahr. (595 degrees Cent.) yet this is not so. Other experiments have shown that this type of steel will reach its maximum hardness value on drawing at 1050 degrees Fahr. (565 degrees Cent.). Why it should have shown up low in this instance is unknown.

Readings were taken on the Rockwell Superficial Tester because it was the only tester available at all times when these experiments were being run. Although there were no hardness tests taken on the hot-rolled surface after hardening, it was found that the surface was file hard.

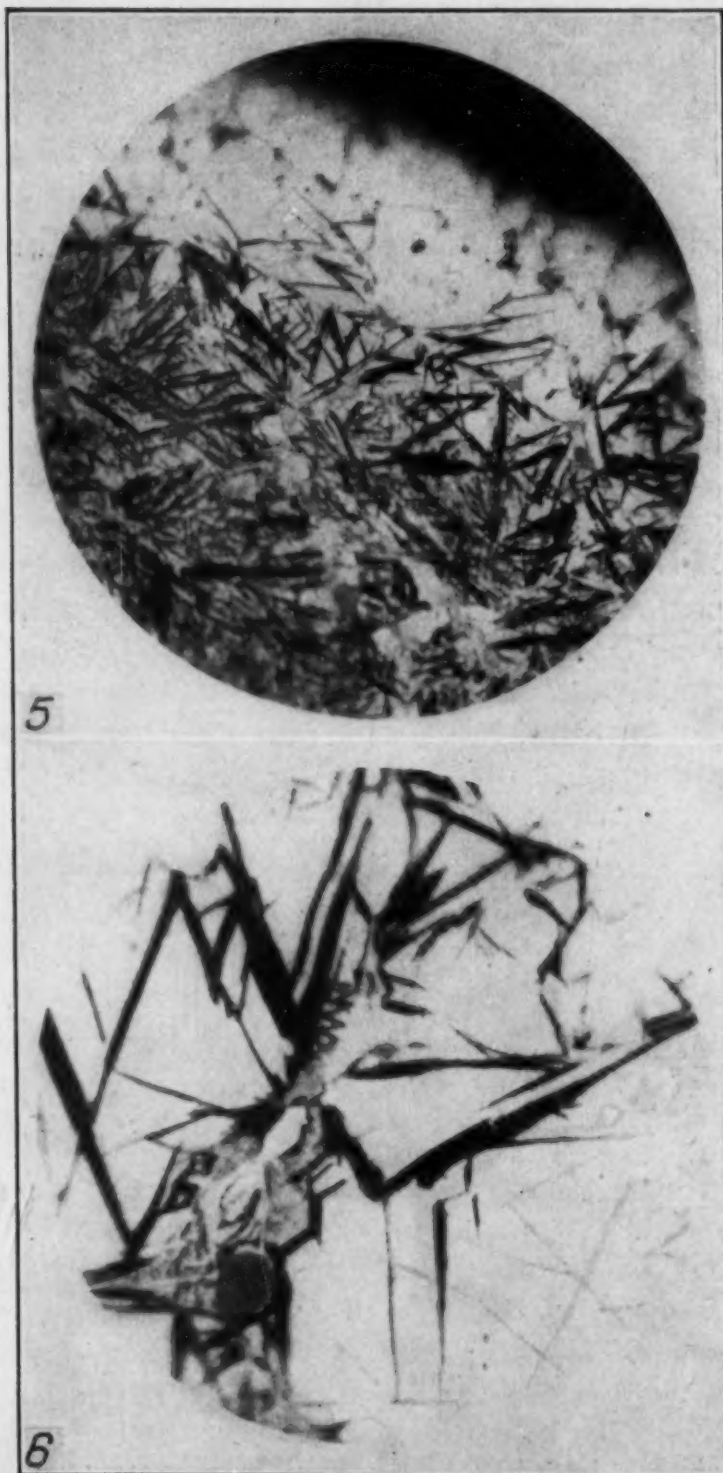


Fig. 5—Type A Steel $\times 500$ Etched in 4 Per Cent Picral Showing Internal Face of Specimen A4.

Fig. 6—Type A Steel $\times 1500$ Etched in 4 Per Cent Picral Showing Some Coarse Martensite and an Eutectic-Like Structure.

As is to be expected on steel with such high hardness, the specimens were brittle. Where this brittleness is not a governing factor in tool life, however, tools will have greatly prolonged life as has been demonstrated in lathe tool bits. These tools hardened by the described method gave 400 per cent better production between grinds.

The fact that maximum hardness is retained at a draw of 1150 degrees Fahr. would tend to point to the fact that high speed steels hardened in this manner would have greater red hardness than steels hardened in the usual manner. It will be noted that in all cases maximum hardnesses obtained were from 2 to 4 points Rockwell "C" higher than high speed steel hardened in the ordinary manner.

DISCUSSION OF MICROSTRUCTURES

All photomicrographs are of Type A steel but are typical of B and C types also. Specimens were mounted in bakelite and surface ground before preparation. Preparation was carried out on emery papers down to 3/0, followed by polishing with levigated alumina. Etching was done with 4 per cent picral.

Each steel when polished and etched shows a definite case of approximately 0.0125 inch. However, this case is not appreciably harder than the core as the tabulated hardness readings indicate. This core consists of 3 distinct zones. The first zone is light in color and similar to a nitrided case and has very coarse martensite scattered through it. The second zone is a dark layer with finer martensite than in the first zone. The third zone is much lighter than zone two but not as light as zone one and the martensite is coarser than in zone two but not as coarse as that in zone one. This third zone blends into a core which is much like that of a normally hardened structure of high speed steel.

Fig. 1, specimen A5, shows this 3-zone case at $\times 200$ while Fig. 2 shows the same specimen in position to show zone number 3 and the core. From the light area of first zone it would seem as if the specimen is decarburized. However, this is unlikely because a file could not cut this specimen; also, from the carbon analysis it was found that the first 0.002 inch was much higher in carbon than the original carbon of the specimen before heat treating. Fig. 3 shows the light edge or first zone of Fig. 1 at $\times 500$.

Fig. 4, specimen A1, at $\times 500$ again shows up the white layer typical of nitrided high speed steel while the martensite appears

coarser and more plentiful. The gray area at the grain boundaries indicates overheating, but it does not show up in steels treated by this method until it has been at room temperature for some time.

Fig. 5, specimen A4, is the broken and polished face of that specimen. This shows the same general structure of coarse martensite and the white area at the edge. Fig. 6, specimen A5, at $\times 1500$ shows some coarse martensite and an eutectic-like structure at the grain boundary.

CONCLUSIONS

The results of the tests conducted show that high hardness values can be obtained on both tungsten and molybdenum high speed steels by a treatment in molten sodium cyanide before the actual hardening operation. This treatment consists of the following steps:

1. Heat part in molten sodium cyanide at 1450 degrees Fahr. for $1\frac{1}{2}$ hours.
2. Air cool.
3. Remove excess cyanide.
4. Heat to hardening temperature—2300 degrees Fahr. for tungsten type and 2250 degrees Fahr. for molybdenum type high speed steel.
5. Quench in oil.
6. Double draw in air at 1050 degrees Fahr. for 1-hour intervals.

It was found that by treating bars up to 1-inch diameter by this method, hardness values of Rockwell "C" 68-70 could be obtained in the center of the bar, and this hardness could be maintained at temperatures up to 1150 degrees Fahr.

That this treatment has practical value has been shown by the fact that it has produced substantial increases in tool life over that obtained by the usual hardening methods.

ACKNOWLEDGMENTS

The author wishes to extend thanks to International Business Machines, Rochester, New York, for the time spent on the preparation of this paper and for the use of their facilities. Also to the Engineering Department of the University of Rochester, Rochester, New York, for the use of the metallurgical equipment.

DISCUSSION

Written Discussion: By Stewart G. Fletcher, research associate, Massachusetts Institute of Technology, Cambridge, Mass.

It appears at first glance that this paper presents a method of hardening high speed steel throughout to much higher hardnesses than heretofore possible. As is pointed out, this additional hardness is not confined to the case, as it is in normal cyaniding treatments, but extends throughout sections up to 1 inch in diameter. The treatment proposed to produce this extraordinary effect is a cyaniding treatment of 1½ hours at 1450 degrees Fahr. (790 degrees Cent.), prior to hardening.

Previous investigations on the cyaniding of high speed steels generally have been limited to temperatures up to about 1250 degrees Fahr. (675 degrees Cent.), while cyaniding at higher temperatures (1450 degrees Fahr. and up) has been applied only to the low carbon steels. Typical results from these investigations indicate a maximum nitrogen penetration of 0.002 to 0.003 inch in 30 minutes at 1250 degrees Fahr. (675 degrees Cent.),¹ and a maximum case depth of 0.010 inch for 90 minutes at 1500 degrees Fahr. (815 degrees Cent.).² It is hardly likely that the high heat treatment following the cyaniding allows the high carbon and nitrogen contents of the case to diffuse to the very center of a 1-inch diameter piece. Furthermore, even if this extreme condition were to prevail (and if we assume the prior presence of a 0.010-inch case with average carbon content of 1.00 per cent and nitrogen content of 0.25 per cent) the average overall carbon increase would be but 0.04 per cent, and nitrogen about 0.1 per cent, compared with the original of 0.70 per cent carbon and 0.02 per cent nitrogen. These increases are not likely to be significant with respect to hardness.

In addition, Mr. McIntyre has reported 0.018 per cent nitrogen in his steel after cyaniding. Nitrogen is commonly present in varying amounts in all steels. To determine whether or not this 0.018 per cent was an above-average nitrogen content, two pieces of high speed steel drill rod, spheroidize-annealed, not cyanided, were analyzed for nitrogen by the vacuum-fusion method. I am indebted to Dr. N. J. Grant for these analyses. One steel was an 18-4-1 type, the other a 6-6-2 variety. The former was found to contain 0.010 per cent N₂ and the latter 0.033 per cent N₂. This would indicate that the 0.018 per cent N₂ reported in this paper was well within the realm of normal nitrogen contents for high speed steel. It would also tend to show that the cyaniding treatment, followed by hardening, is not effective in adding sufficient total nitrogen throughout to act as a contributory hardening agent in the steel.

A study of Mr. McIntyre's photomicrographs further suggests the possibility that the steels had been overheated. The presence of very coarse martensite (Figs. 1 and 2), and of the eutectic structure (Figs. 4 and 6) tend to support this assertion. The very high carbon content of the case (Table VI), extending more or less uniformly to a depth of at least 0.012 inch,

¹J. G. Morrison and J. P. Gill, "Introductory Study of the Nitriding of Hardened High Speed Steel by the Use of Molten Cyanides," *TRANSACTIONS, American Society for Metals*, Vol. 27, 1939, p. 935-1014.

²B. B. Beckwith, "Liquid Bath Carburizing," *Symposium on Carburizing*, American Society for Metals, 1937.

coupled with the large amounts of retained austenite and relative absence of carbides, also indicates overheating. The high carbon of the case could easily have come from the carbonaceous heating atmosphere if the overheating conditions prevail.

Such an overheated, high carbon structure would be expected to resist tempering, and therefore to maintain full hardness at higher temperatures. It would be accompanied, of course, by extreme brittleness.

Two factors may contribute to the exceptionally high hardness reported by Mr. McIntyre. The first of these is the probable overheating mentioned above, giving a higher carbon martensite, and thus higher hardness. The second is the definite possibility that the Rockwell 45N values are open to question. The author has failed to show any hardness readings for a high speed steel heat treated in a normal manner, so actually it is impossible to base this statement on any data given in the paper. However, we have found that a specimen of 18-4-1, hot-quenched 1 hour at 1450 degrees Fahr. (790 degrees Cent.) in lead, then oil-quenched and double tempered at 1050 degrees Fahr. (565 degrees Cent.) (duplicating the thermal treatment of specimens A2 and A3) gave a hardness of Rockwell "45N" 60.5, and of Rockwell "C" only 55. This is considerably lower than the Rockwell "45N" 73 equivalent to Rockwell "C" 65 reported in the paper.

Hot quenching at 1450 degrees Fahr. (790 degrees Cent.) in molten cyanide could not produce a case deeper than 0.010 inch, as mentioned above. Aside from that, the thermal treatment alone, involving hot quenching considerably higher than the 1000 to 1100 degrees Fahr. (540 to 595 degrees Cent.) normally used, would result in a considerable amount of proeutectoid carbide precipitation,³ lowering the carbon content of the martensite and resulting in decreased hardness. Again, overheating could have retarded this action somewhat, and produced slightly higher values of hardness, but not very likely enough to take care of the 10-point Rockwell "C" discrepancy noted above.

There is some doubt in my mind as to whether or not the hardness readings given in Tables IV and V were made on transverse sections cut through the centers of the heat treated pieces, or whether they were merely made on the end of the pieces after a 0.005-inch grind, as I would interpret the accompanying text to imply. If the latter is the case, all the hardness readings were made the same distance from the outside surface, and the "center" and "edge" readings lose significance.

In view of the above discussion it is doubtful that cyaniding at 1450 degrees Fahr. (790 degrees Cent.) prior to hardening should produce the results reported by Mr. McIntyre, particularly with respect to carrying increased hardness throughout a 1-inch section. However, his proposed treatment might conceivably have a beneficial effect on the case itself, making it deeper and lowering somewhat the steep carbon and nitrogen gradients. This would lead to a tougher case, and one less liable to chipping, but also one which would undoubtedly be softer than the more conventional cyanide cases produced at 1050 degrees Fahr. (565 degrees Cent.) or thereabouts.

³P. Gordon, M. Cohen, and R. S. Rose, "The Kinetics of Austenite Decomposition in High Speed Steel," *TRANSACTIONS, American Society for Metals*, Vol. 31, 1943, p. 161-217.

Author's Reply

According to information received from the Vanadium Alloys Corp. the nitrogen content of high speed steel is 0.006 per cent or less. This is also the normal nitrogen content claimed by J. P. Gill and associates in the 1944 edition of "Tool Steels".

The analyses for these two sources were made by Battelle Memorial Institute. In view of this, 0.018 per cent would represent quite a large increase. Had these specimens been overheated they would not have withstood the production demands to which they were subjected, and overheating would not have increased the hardness value to such an extreme value.

It is possible that the higher carbon content resisted tempering but in view of the fact that some of the specimens received seven 1-hour draws this is hardly likely. Also when the final draw temperature reached 1150 degrees Fahr. (620 degrees Cent.) the hardness started to drop but did not drop to the point one would expect for such a high draw.

After duplicating the thermal treatment as given in this paper, for specimens A2 and A3, Dr. Fletcher reports a hardness value of (45N) 60.5 and of Rockwell C 55. This would appear as a good check on the conversion of the 45N scale to the C scale as these values coincide on chart published by Wilson Mechanical Instrument Co.

It is poor practice to quench high speed steel at 1450 degrees Fahr. (790 degrees Cent.) as is suggested by Dr. Fletcher but the fact that a Rockwell C hardness of 65 to 66 was obtained by this type of hot quench is indicative that the cyanide had some effect on the steel.

The transverse tests were made on specimens A3, A4 and on the 1-inch section after breaking and grinding them, but on the other specimens only 0.005 inch was ground off for hardness tests.

THE DIMENSIONAL STABILITY OF STEEL PART I—SUBATMOSPHERIC TRANSFORMATION OF RETAINED AUSTENITE

BY STEWART G. FLETCHER AND MORRIS COHEN

Abstract

In view of the general usage of low temperatures for dimensional stabilization of heat treated gage steels, it becomes essential to obtain a more precise picture of the subatmospheric decomposition of retained austenite than is available at the present time. In this paper, a combined X-ray and dilatometric procedure is described for making a quantitative study of subcooling transformations. Detailed charts are given to show the extent of austenite decomposition as a function of subatmospheric temperature and time of prior aging at room temperature. Room temperature aging lowers the temperature at which the retained austenite starts to transform and reduces the amount of decomposition attained by cooling to any selected temperature. However, the cooling transformation continues down to -250 to 260 degrees Fahr. (-155 to 160 degrees Cent.), irrespective of the aging treatment.

PREFACE

A LONG range investigation of the dimensional stability of steel was started in 1942 at the Massachusetts Institute of Technology at the request of The Sheffield Foundation of Dayton, Ohio. For the time being emphasis is being focused on the high carbon steels because of their wide usage for gage, tool and die applications in which dimensional stability is a major requirement.

The problem of dimensional stability of high carbon steels received considerable attention in this country during World War I when the manufacture of gage blocks was undertaken. "Seasoning" was then carried out by cycling the hardened and tempered gages several times between -5 and 220 degrees Fahr. (-20 and 105

This paper is from a study sponsored by The Sheffield Foundation of Dayton, Ohio.

A paper presented before the Twenty-sixth Annual Convention of the Society held in Cleveland, October 16 to 20, 1944. Of the authors, Stewart G. Fletcher is research associate, and Morris Cohen is associate professor of physical metallurgy, Massachusetts Institute of Technology, Cambridge, Mass. Manuscript received July 7, 1944.

degrees Cent.), and then storing them for several months (1).¹ Later, as a result of further study by the Bureau of Standards (2), it appeared that 10 to 80 alternate dips in oil at 390 degrees Fahr. (200 degrees Cent.) and in ice water were more efficacious. It was observed, however, that after the steels had been "seasoned" by this method, their hardness was substantially lower than that usually specified for gages. Scott (3) also felt that the spontaneous expansion so often encountered on prolonged aging at room temperature could likely be eliminated by repeated heating and cooling through an appropriate temperature cycle. However, no specific data were obtained as to the magnitude of the effect or the optimum stabilizing treatment to use.

On the other hand the National Physical Laboratory (4) recommended a prolonged tempering at 300 degrees Fahr. (150 degrees Cent.) for stabilizing. It was demonstrated that this treatment was successful from a dimensional standpoint, but also softened the gage steels to an undesirable degree.

In recent years, there has been a marked tendency toward the use of lower subzero temperatures as a part of the stabilizing treatment, the objectives being to avoid long drawn-out seasoning procedures and to attain maximum hardness. Boyle (5) reports the most common treatment as tempering at 300 degrees Fahr. (150 degrees Cent.) and cooling in dry ice (-105 degrees Fahr.) several times. A number of similar operations have been reviewed by Phair (6), most of which involve cyclic treatments, with the cold end ranging from -25 to -120 degrees Fahr. (-32 to -85 degrees Cent.). Knight (7) has recorded the actual stabilizing cycles practiced by several companies.

From a comparative study of the published stabilizing methods, it is evident that no common agreement exists on the subject. In fact, the lack of positive knowledge concerning the specific benefits of the different treatments has often been deplored. Master gages which were supposed to have been stabilized have been found to expand as much as 0.0001 inch in 4 inches over a period of $6\frac{1}{2}$ years (8).

In the present program, the ultimate goal is to establish the fundamental reason for the dimensional instability of heat treated high carbon steels, and to develop the most effective means of minimizing the spontaneous dimensional changes that occur in service

¹The figures appearing in parentheses pertain to the references appended to this paper.

or in storage after heat treatment. This paper constitutes only an initial step in the approach to the general problem. Other contributions will be published from time to time.

INTRODUCTION

Inasmuch as the principal type of dimensional instability observed in heat treated steels is *growth*, it is natural to regard retained austenite and its gradual decomposition on aging as a potential cause of progressive dimensional change. It is now well-known that retained austenite is amenable to decomposition on cooling to low temperatures, and this is undoubtedly an important reason for the adoption of subzero "seasoning" treatments.² Unfortunately, however, there is a dearth of trustworthy information on the austenite contents retained by the common gage steels; and the quantitative relationships between subatmospheric cooling and austenite transformation are unknown. For example, such questions as "what fraction of the retained austenite is convertible by cooling?" or "how much austenite can be decomposed by cooling to a given temperature?" and "does it make any difference whether the cooling is conducted right after hardening or some time later?" are but a few of the many issues that must be resolved before subzero cooling can be employed on a rational basis.

This paper describes a combined X-ray and dilatometric analysis which permits the precise measurement of retained austenite and its transformation during cooling to temperatures as low as -321 degrees Fahr. (-196 degrees Cent.). For the first time, quantitative data are presented in the form of subatmospheric transformation charts. Even though no correlation with dimensional stability is available as yet, the recent widespread interest in subzero cooling phenomena makes it desirable to report on the transformation studies now.

PREVIOUS WORK ON AUSTENITE DECOMPOSITION BELOW ROOM TEMPERATURE

Relatively little attention seems to have been devoted to subatmospheric transformations in straight carbon and low alloy steels, such as form the basis of this paper. Mathews (10) found that

²Retained austenite can also be converted by tempering (9), but the temperatures required are sufficiently high to cause excessive softening for most gage, tool and die applications.

retained austenite in hardened 0.70 per cent carbon, 3.60 per cent tungsten steel could be decomposed by cooling in liquid air. Similar results were observed by Schroeter (11) on a steel containing 1.89 per cent carbon and 2.22 per cent manganese. Sykes and Jeffries (11a) reported the effect of austenitizing temperature on the hardening produced by cooling 1.00 to 1.58 per cent carbon steels in liquid oxygen.

Tammann and Scheil (12) showed that subcooling quenched straight carbon steel (1.25 and 1.72 per cent carbon) caused an increase in volume (as measured at room temperature) starting at -4 degrees Fahr. (-20 degrees Cent.) and continuing to -240 degrees Fahr. (-150 degrees Cent.). They attributed this expansion to the transformation of retained austenite into martensite, and established that the conversion took place on cooling, not on holding at the low temperatures. Andrew, Fisher and Robertson (13) arrived at similar conclusions independently.

There has been a considerable number of subcooling investigations on high alloy steels, such as nickel (14), chromium (15), chromium-nickel (16), high carbon, high chromium (14, 17), and high speed steels (14, 18, 19). However, even for most of these materials precise data are completely lacking.

EXPERIMENTAL DETAILS

Steels Investigated—The steels used throughout this work are listed in Table I. All of these materials were purchased in the form of $\frac{3}{8}$ -inch diameter drill rod.

		Table I Analyses of Steels									5	3	6	4
Steel	Type	C	Si	Mn	S	P	W	Cr	V	Mo				
M	Carbon aluminum deoxidized	0.70	0.22	0.28	0.023	0.021				
L	Carbon	1.06	0.33	0.33	0.014	0.014				
K	Carbon aluminum deoxidized	1.07	0.23	0.25	0.014	0.011				
J	Ball Bearing	1.04	0.34	0.35	0.012	0.014	1.54	0.20				
H	Manganese Die	0.94	0.21	1.17	0.016	0.020	0.82	0.59	0.24				
G	Tungsten Die	1.24	0.39	0.33	0.007	0.022	1.59	0.76	0.20	0.22				

Except for the 0.70 per cent carbon steel, these grades are typical of straight carbon and low alloy gage steels. High alloy gage steels, such as the high carbon, high chromium and high speed vari-

eties, will be covered separately. The 0.70 per cent carbon analysis was included to indicate the effect of carbon content. Steels L and K have substantially the same chemistry, but the latter was deoxidized with aluminum. Steel J is a water-hardening grade of low alloy gage steel, while Steels H and G contain sufficiently more alloy to make them oil hardening.

Heat Treatment—All the specimens were heat treated as $\frac{3}{8}$ -inch diameter rounds according to the commercial practice outlined in Table II. In each case, complete hardening was achieved; that is, even the center of the specimens contained only martensite and retained austenite with or without undissolved carbides. The quench-

Table II
Heat Treatment Data

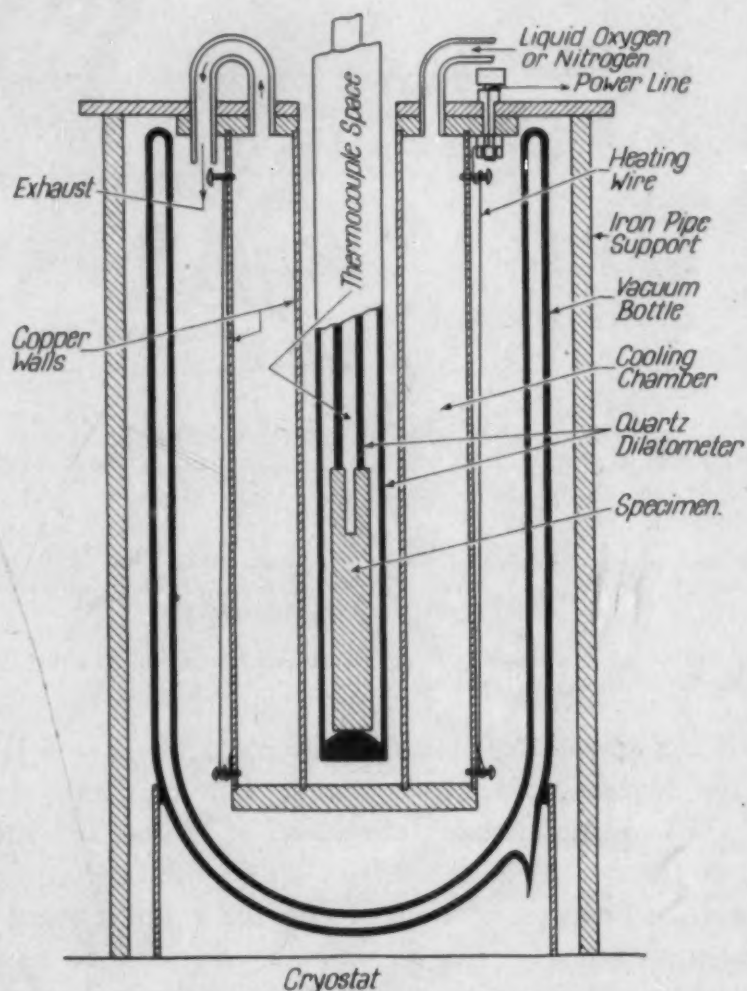
Steel	Type	Austenitizing		Quenching Medium	Fracture Grain Size	Hardness As Quenched Rockwell C
		Temperature Degrees Fahr.	Time Minutes			
M	Carbon	1500	30	Water	7-8	65.4
L	Carbon	1450	30	Water	8-9	66.1
K	Carbon	1450	30	Water	8-9	66.3
J	Ball Bearing	1450	30	Water	9-10	66.4
H	Manganese Die	1450	30	Oil	9-10	65.2
G	Tungsten Die	1600	30	Oil	9-10	66.7

ing medium, whether water or oil, was held at 75 to 85 degrees Fahr. (24 to 30 degrees Cent.). Room temperature aging was carried out at 68 degrees Fahr. (20 degrees Cent.).

X-Ray Technique—The retained austenite contents of the hardened steels were determined by Gardner's method (20) of X-ray line densities. Briefly, it consisted of comparing photometrically the densities of two diffraction lines in an X-ray pattern, one of the lines coming from an aluminum reference foil and the other from the austenite in the test specimen. The foil was calibrated with the aid of specimens of known austenite content, the latter specimens being produced by quenching the steels under consideration from fairly high temperatures so as to coarsen the structure and thus permit the measurement of the austenite by metallographic means (20). Once calibrated, the X-ray method was utilized to determine the austenite contents of regularly hardened specimens in which the structure was too fine to apply metallographic measurements.

The sensitivity of these X-ray determinations was improved by using the (111) lines instead of the weaker (200) lines selected by Gardner (20). Ordinarily, the (111) line of the austenite is partially overlapped by the (101)—(110) doublet of the tetragonal

martensite, but this difficulty was circumvented by tempering the hardened steel for 30 minutes at 350 degrees Fahr. (180 degrees Cent.). Such tempering did not affect the austenite content (9), but did collapse the martensite doublet into a single ferrite line, leaving the austenite line in the clear. This practice led to reliable austenite determinations (± 0.25 per cent) down to contents of $1\frac{1}{2}$ per cent austenite.



Note: Horizontal Scale Exaggerated 2:1

Fig. 1—Schematic Diagram of Cryostat Used for Cooling and Heating the Dilatometer at Controlled Rates Below Room Temperature.

Dilatometric Technique—While the above X-ray method was employed for establishing the retained austenite contents of the hardened steel, it turned out more convenient to measure the subcooling transformations by means of a dilatometer, taking advantage of the large expansion which accompanies the decomposition of austenite

into martensite. The dilatometer used was similar to one previously described (21), but was modified to accommodate a 4-inch long by $\frac{3}{8}$ -inch diameter specimen. The dial gage provided a sensitivity of 5 millionths of an inch per inch.

The subzero cooling was carried out in the cryostat shown schematically in Fig. 1 with either liquid oxygen at -297 degrees

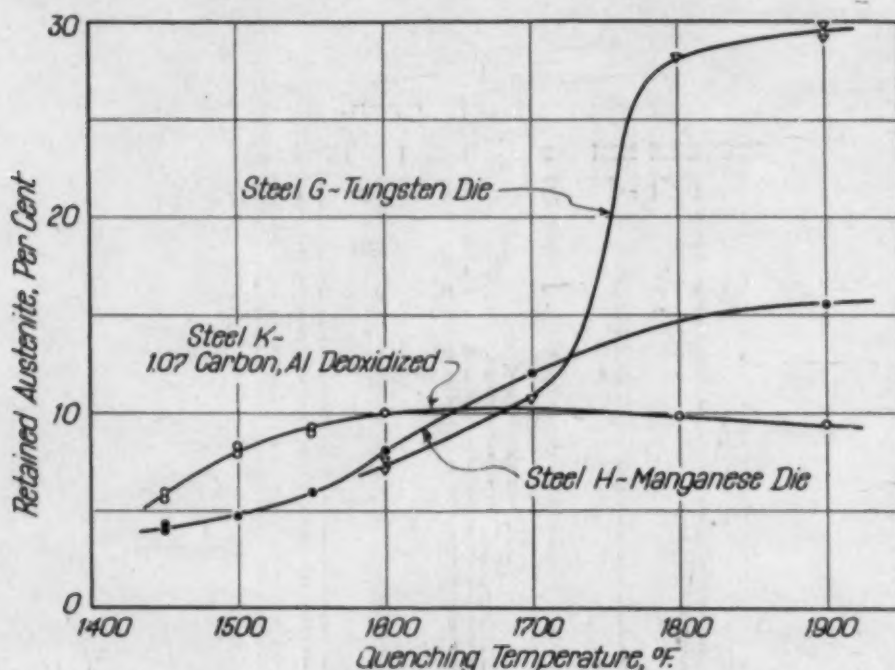


Fig. 2—Effect of Austenitizing Temperature on Amount of Retained Austenite in Steels K, H and G.

Fahr. (-182 degrees Cent.) or liquid nitrogen at -321 degrees Fahr. (-196 degrees Cent.) as coolants. The cryostat consisted of a double-walled copper cylinder, closed off at the bottom and resting in a vacuum bottle. The dilatometer fitted into the inner copper tube, and the coolant was introduced into the annular space between the inner and outer walls. In order to help minimize temperature gradients, the exit cold gases were led into the surrounding space within the vacuum bottle. Insulated resistance wire was wound around the outer copper tube, so that the rate of heating back to room temperature could be controlled. The rate of cooling was regulated by adjusting the addition of the coolant. Generally, the temperature gradient from one end of the specimen to the other was about 1 degree Fahr.

In making a subcooling run, the hardened specimen was placed in the dilatometer, the cryostat was raised to surround the dila-

tometer, and after a predetermined hold at room temperature (68 degrees Fahr.), the cooling was started. Readings were taken for every 5-degree Fahr. change in temperature, and the rates of cooling and heating were maintained at 4 to 6 degrees Fahr. per minute.

DISCUSSION OF RESULTS

Austenite Content of Hardened Steels—The amounts of austenite retained in the six steels are given in Table III. Some of the specimens were suitable for metallographic as well as X-ray determinations of the austenite content, and in such cases, both values are listed. The results for Steels K, H and G are plotted in Fig. 2.

Table III
Effect of Hardening Temperature on Amount of Retained Austenite

Steel	Type	Hardening Temperature Degrees Fahr.	Quenching Medium	Per Cent Retained Austenite		Fracture Grain Size
				X-ray	Metallographic	
M	Carbon (0.70 per cent) aluminum deoxidized	1500	Water	2.7, 3.0	7-8
		1700	Water	2.9, 3.1	7-8
L	Carbon (1.06 per cent)	1450	Water	6.7, 6.6	8-9
		1700	Water	11.8	6-7
K	Carbon (1.07 per cent) aluminum deoxidized	1450	Water	5.7, 5.9	8-9
		1500	Water	7.9, 8.2	8-9
		1550	Water	9.2, 8.9	8-9
		1600	Water	10.0	8-9
		1800	Water	9.8	4-5
		1900	Water	9.4	9.4	3-4
J	Ball Bearing	1450	Water	4.6	9-10
		1700	Water	12.7	8-9
H	Manganese Die	1450	Oil	4.2, 4.0	9-10
		1500	Oil	4.7	9-10
		1550	Oil	5.9	9-10
		1600	Oil	8.0	9-10
		1700	Oil	12.0	9-10
		1900	Oil	16.0	15.5	4-5
G	Tungsten Die	1600	Oil	7.0, 7.5	9-10
		1700	Oil	10.7	9-10
		1800	Oil	28.2	8-9
		1900	Oil	28.8, 30.2	29.1, 29.8	5-6

As might be expected, the amount of retained austenite increases with the austenitizing temperature until the carbides are completely dissolved. In Steel K (1.07 per cent carbon), the maximum amount of austenite is retained when quenched from 1600 degrees Fahr. (870 degrees Cent.) which is just above the A_{cm} temperature. Higher austenitizing temperatures actually bring about a slight decrease in the austenite content. In Steel H (manganese die steel), the retained austenite steadily increases as the austenitizing temperature is raised to 1900 degrees Fahr. (1040 degrees Cent.). At 1700 degrees Fahr. (930 degrees Cent.), microscopic examination showed

some carbide still out of solution, whereas all the carbides were dissolved at 1900 degrees Fahr. (1040 degrees Cent.). High quenching temperatures produce relatively large amounts of retained austenite in Steel G (tungsten die steel) primarily because of the high carbon content of this material (1.24 per cent). However, minor amounts

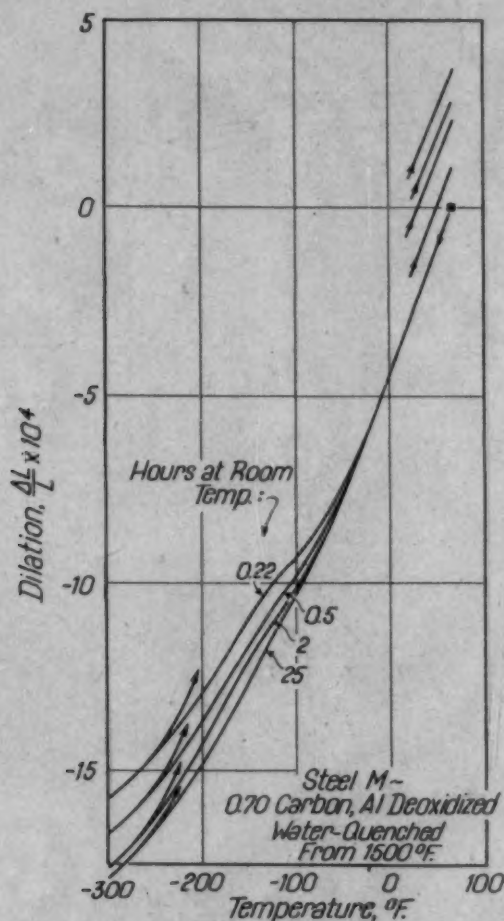


Fig. 3—Dilatometric Changes During the Subatmospheric Cooling and Heating of Steel M After Hardening and Aging at Room Temperature for the Times Shown.

of carbides were still undissolved after both the 1800 and 1900-degree Fahr. (980 and 1040-degree Cent.) treatments.

It is interesting to note that at the lower hardening temperatures, the alloyed steels retain less austenite than the straight carbon steels, L and K (1.06 and 1.07 per cent). Undoubtedly, this is due to the more difficultly soluble carbides keeping carbon out of solution, thus causing a higher M-point (22) for the alloy steels and

more austenite conversion during the hardening quench. However, when the alloy carbides are dissolved by exposure to suitably high austenitizing temperatures, the solution of both the carbon and alloying elements lower the M-point sufficiently (23, 24) to result in the retention of large amounts of austenite.

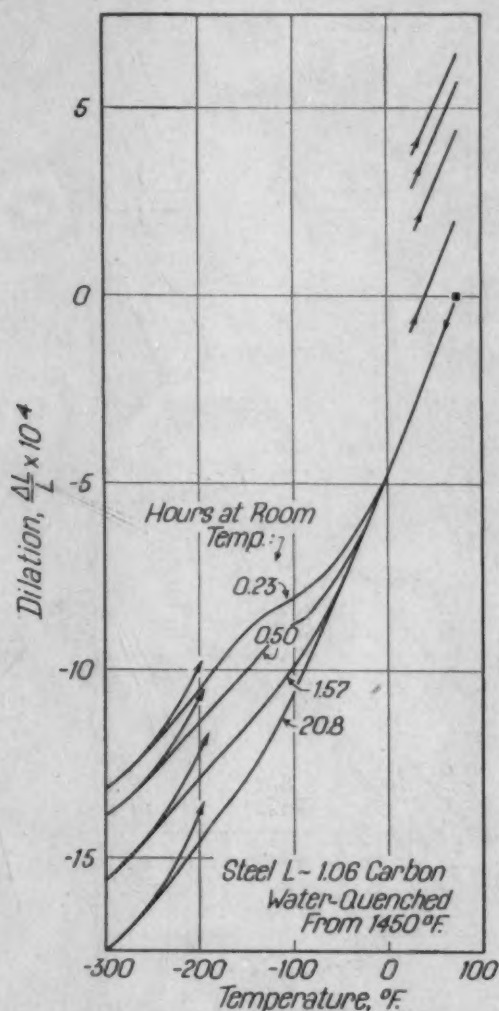


Fig. 4—Dilatometric Changes During the Subatmospheric Cooling and Heating of Steel L After Hardening and Aging at Room Temperature for the Times Shown.

The 0.70 per cent carbon steel, M, retains no more than 3 per cent austenite even when all the carbon is put into solution.

Dilatometer Curves on Subcooling—Figs. 3 to 6 depict the dilatometric changes observed on cooling hardened samples of Steels M, L, K, and H after various holding times at room temperature.

The expansions superimposed on the normal contraction curves indicate the subatmospheric transformation of the retained austenite. In all instances, the extent of this transformation is markedly lessened by aging at room temperature, even though no appreciable amount of austenite decomposes during such aging.

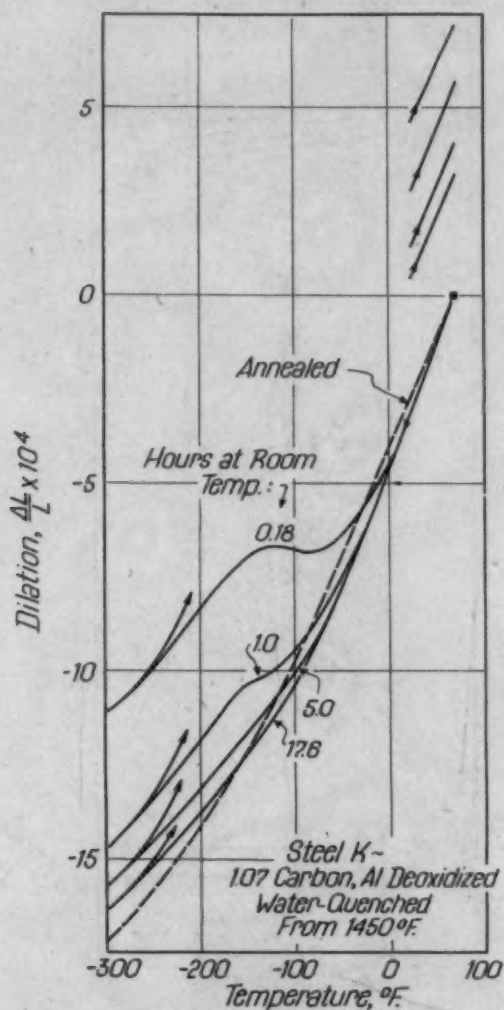


Fig. 5—Dilatometric Changes During the Subatmospheric Cooling and Heating of Steel K After Hardening and Aging at Room Temperature for the Times Shown.

No transformation occurs during the heating, and for the sake of clarity, only the beginning and end of the heating curves are shown. The broken line in Fig. 5 represents the heating and cooling curve of Steel K in the annealed condition. No hysteresis was found, the heating and cooling points being coincident. This fact

testifies to the absence of temperature gradients in the dilatometer specimen.

The quantitative dependence of the subzero transformation on the cooling temperature and on the prior room temperature aging is derivable from the dilatometric curves of Figs. 3 to 6. The analyti-

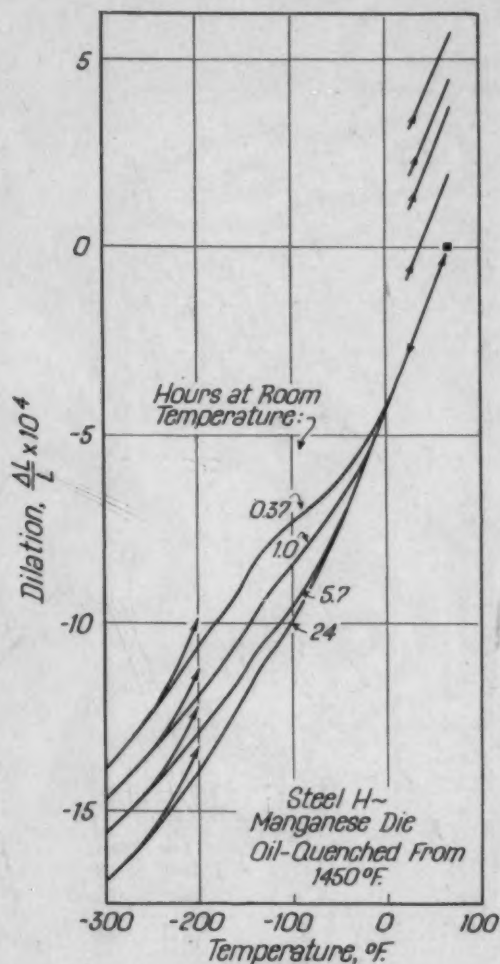


Fig. 6—Dilatometric Changes During the Subatmospheric Cooling and Heating of Steel H After Hardening and Aging at Room Temperature for the Times Shown.

cal steps are as follows: In the typical dilatometric run shown in Fig. 7, the dashed line AB represents the hypothetical contraction curve if no austenite were to transform on subcooling. The values used to plot this curve were taken from the cooling curve of a similar specimen tempered at 300 degrees Fahr. (150 degrees Cent.) for 1 hour, this tempering being sufficient to stabilize the austenite

against transformation on subsequent subcooling.³ The segments *m* and *n* are then recorded at 5-degree Fahr. temperature intervals from room temperature down to -300 degrees Fahr. (-185 degrees Cent.). Segment *w* as measured at any given temperature is

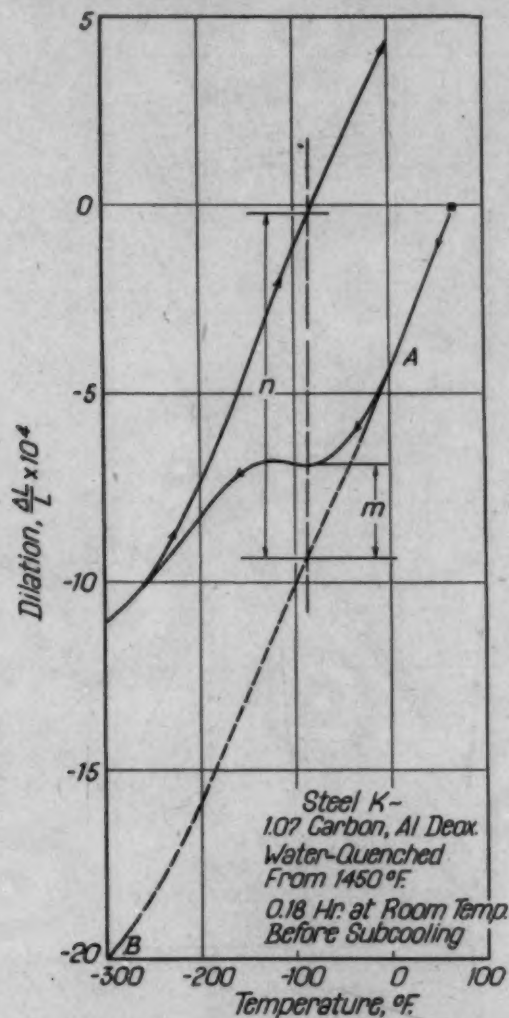


Fig. 7—Sample Dilatometric Run Showing How the Segments *m* and *n* are Measured to Obtain the Trend of the Subatmospheric Transformation of the Retained Austenite.

the length change due to the retained austenite decomposition down to that temperature, and *n* is the length change (referred to the same temperature) due to the total subcooling transformation down to -300 degrees Fahr. (-185 degrees Cent.). This total subcooling transformation does not constitute the complete decomposition of the

³The details of the effect of tempering on subatmospheric transformations will be published later.

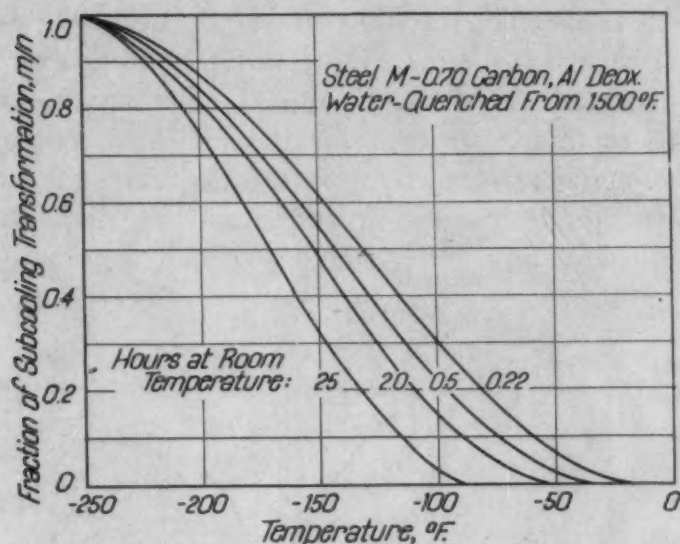


Fig. 8—Fraction of Total Subatmospheric Transformation Achieved by Subzero Cooling Steel M After Hardening and Aging at Room Temperature for the Times Shown.

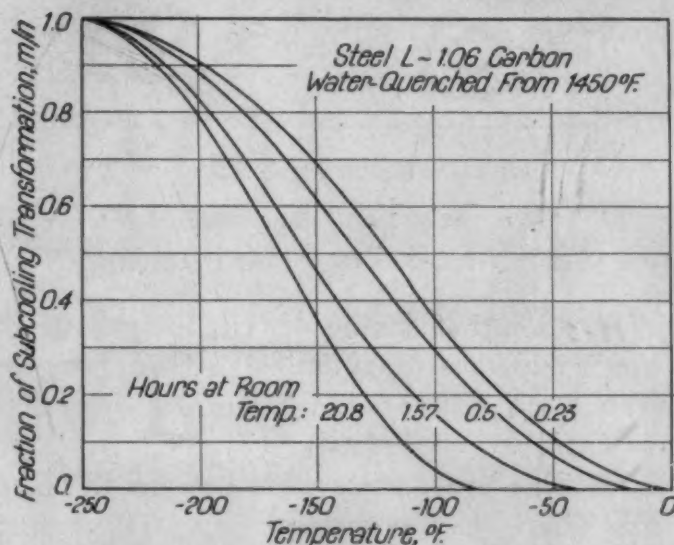


Fig. 9—Fraction of Total Subatmospheric Transformation Achieved by Subzero Cooling Steel L After Hardening and Aging at Room Temperature for the Times Shown.

retained austenite, but only the maximum degree of decomposition attainable by subzero cooling under the conditions at hand, inasmuch as the transformation invariably stops before -300 degrees Fahr. (-185 degrees Cent.) is reached. Consequently, the ratio m/n at each temperature yields the fraction-of-the-total-subatmospheric-transformation which takes place on cooling to that temperature.

Retained Austenite Transformation on Subcooling—The course

of the retained austenite transformation on subcooling is shown in Figs. 8 to 11 in which the m/n values are plotted against subcooling temperature for Steels M, L, K and H after aging the hardened specimens at room temperature for the indicated lengths of time. In each case, aging at room temperature depresses the onset of the retained austenite decomposition and also lowers the temperature required to achieve any given fraction of the maximum attainable

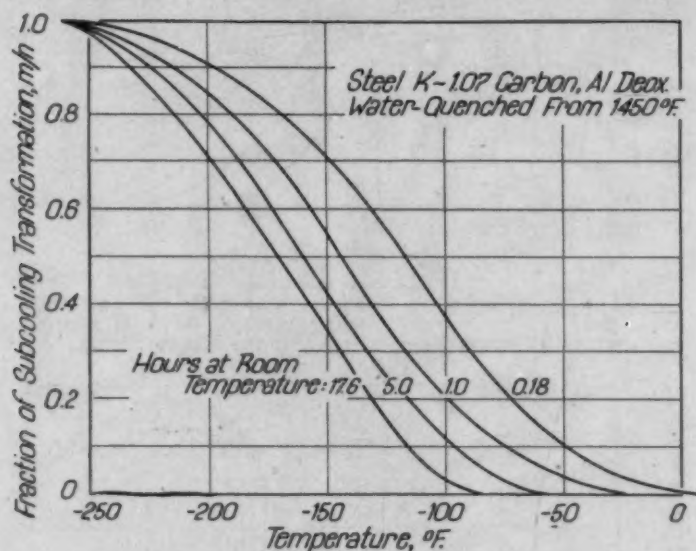


Fig. 10—Fraction of Total Subatmospheric Transformation Achieved by Subzero Cooling Steel K After Hardening and Aging at Room Temperature for the Times Shown.

subzero transformation, but has no detectable influence on the temperature at which the transformation ceases. In fact, the transformation in all the steels stops at -250 to 260 degrees Fahr. (-120 to 125 degrees Cent.).

These phenomena are similar in nature to those observed in high speed steel (18). However, the cooling transformation in the latter material only continues down to -150 degrees Fahr. (-100 degrees Cent.). 95 per cent of the maximum attainable subcooling transformation in high speed steel is achieved by cooling to -100 degrees Fahr. (-73 degrees Cent.), but the steels under investigation here require cooling to at least -210 degrees Fahr. (-135 degrees Cent.) for an equivalent fraction of transformation.

The austenite decomposition in Steel H (Fig. 11) is of particular interest because of the two-stage nature of the transformation. Down to about -140 degrees Fahr. (-95 degrees Cent.), the transformation proceeds more readily than in the other steels. Then be-

tween -140 and -160 degrees Fahr. (-95 and -107 degrees Cent.), there is a range of inactivity. Below -160 degrees Fahr. (-107 degrees Cent.) the decomposition sets in again, and continues very much the same as in the straight carbon steels. It is almost as though this manganese die steel exhibits a transition behavior intermediate between that of the straight carbon steels on the one hand and the high speed steel on the other.

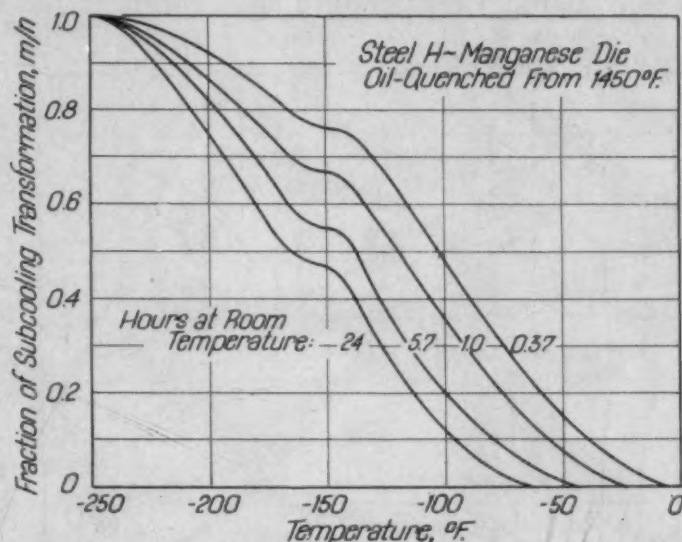


Fig. 11—Fraction of Total Subatmospheric Transformation Achieved by Subzero Cooling Steel H After Hardening and Aging at Room Temperature for the Times Shown.

Magnitude of Austenite Transformation Attainable by Subcooling—The absolute amount of austenite transformable by subatmospheric cooling can be evaluated if the relative specific volumes of austenite and its decomposition product, martensite, are known. The increase in volume when austenite transforms to martensite is comparatively insensitive to the carbon and alloy content, and turns out to be about 4.6 per cent when referred to room temperature.⁴ Therefore, for each 1 per cent of austenite decomposition into martensite, there is a fractional change in volume of $\frac{\Delta v}{v} = 0.00046$ cubic inch per cubic inch as measured at room temperature. This corresponds to a fractional change in length of $\frac{\Delta l}{l} = 1/3 (0.00046) = 0.00015$ inch per inch. Hence, by measuring the overall change

⁴The expansion was computed from an average of X-ray data reported by Honda and Nishiyama (25), Ohman (26), and Hagg (27).

in length as a result of subcooling to below -250 degrees Fahr. (-155 degrees Cent.) (where the transformation stops) and returning to room temperature, the corresponding amount of sub-atmospheric austenite decomposition can be calculated.

Fig. 12 shows the fractional change in length caused by cooling Steels M, K, L and H to -300 degrees Fahr. (-185 degrees Cent.) and the per cent of austenite decomposed by such cooling, as a function of the time at room temperature aging prior to the subcooling.

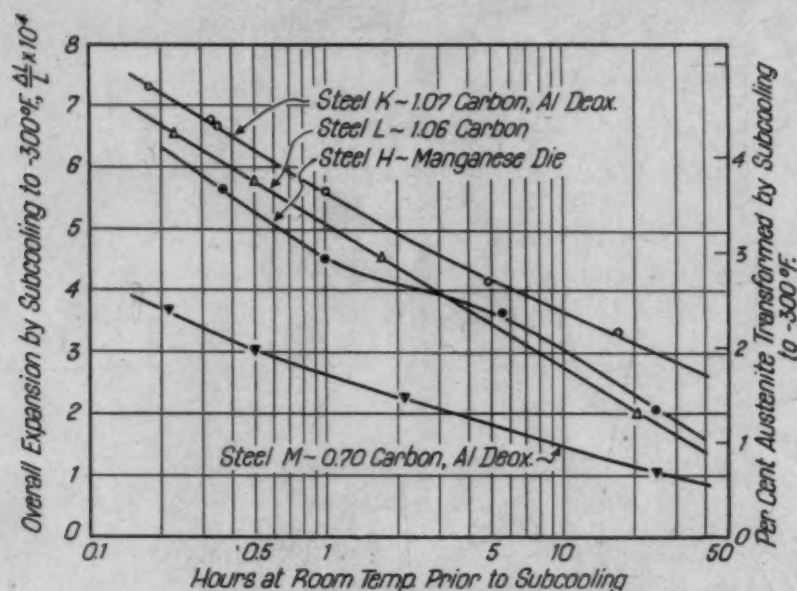


Fig. 12—Effect of Room Temperature Aging on the Overall Expansion (Referred to Room Temperature) and on the Amount of Austenite Transformed on Subzero Cooling to -300 Degrees Fahr.

The aging exerts a potent stabilizing effect on the retained austenite, and makes it more reluctant to decompose on subsequent cooling. The amount of austenite in the 0.70 per cent carbon steel convertible by subcooling is small because of the low austenite content in the hardened steel. Somewhat more austenite is transformable in the aluminum-deoxidized steel, K, than in the mating steel, L. Again the manganese die steel displays a two-stage behavior.

Subatmospheric Transformation Charts—It is now possible to put the entire course of the subcooling transformation on an absolute basis by combining Fig. 12 with each of Figs. 8 to 11. The latter curves indicate the fraction-of-the-total-subcooling-transformation that is attained by cooling to any given temperature, while Fig. 12 gives the total subcooling transformation itself. Accordingly, multiplication of the corresponding values yields the amount of

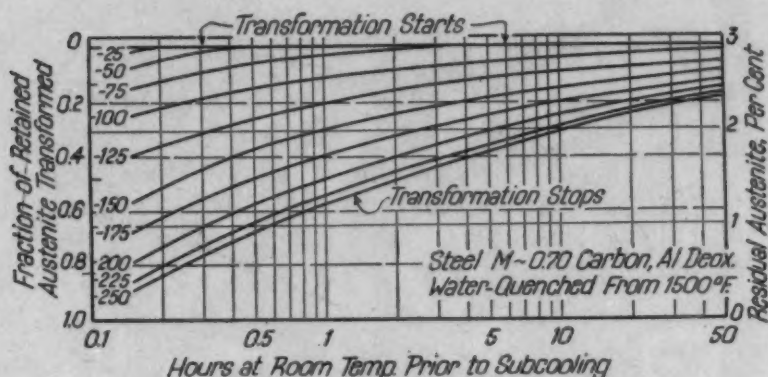


Fig. 13—Subatmospheric Transformation Chart for Steel M, Showing the Fraction of the Retained Austenite that Transforms and the Amount of Residual Austenite Left After Room Temperature Aging and Subzero Cooling to the Indicated Temperatures.

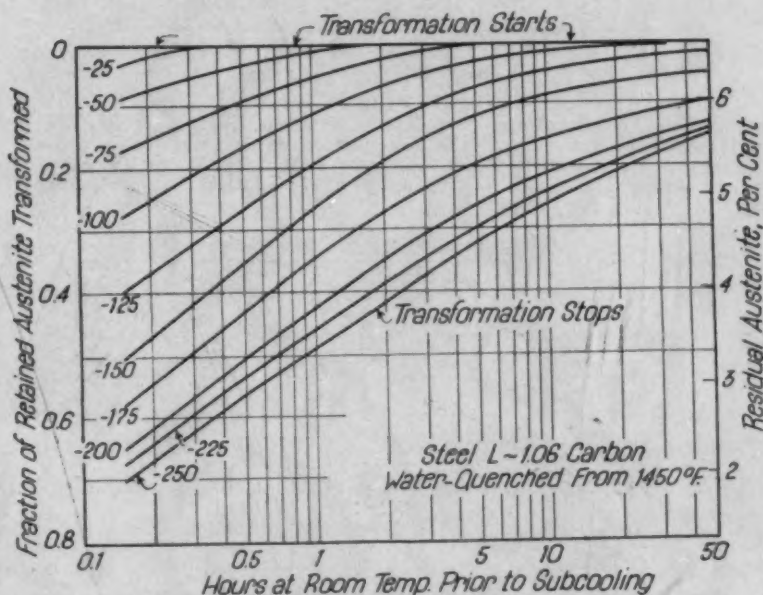


Fig. 14—Subatmospheric Transformation Chart for Steel L, Showing the Fraction of the Retained Austenite that Transforms and the Amount of Residual Austenite Left After Room Temperature Aging and Subzero Cooling to the Indicated Temperatures.

austenite transformed by cooling to any selected subatmospheric temperature. From this, the fraction of the retained austenite which transforms and the amount of austenite left can be easily determined.

The resulting data are plotted in the form of subatmospheric transformation charts, as shown in Figs. 13 to 16 for Steels M, L, K and H. These charts demonstrate quantitatively how the subcooling temperature and the prior time at room temperature affect both the fraction of the retained austenite transformed and the per cent of austenite remaining after the transformation.

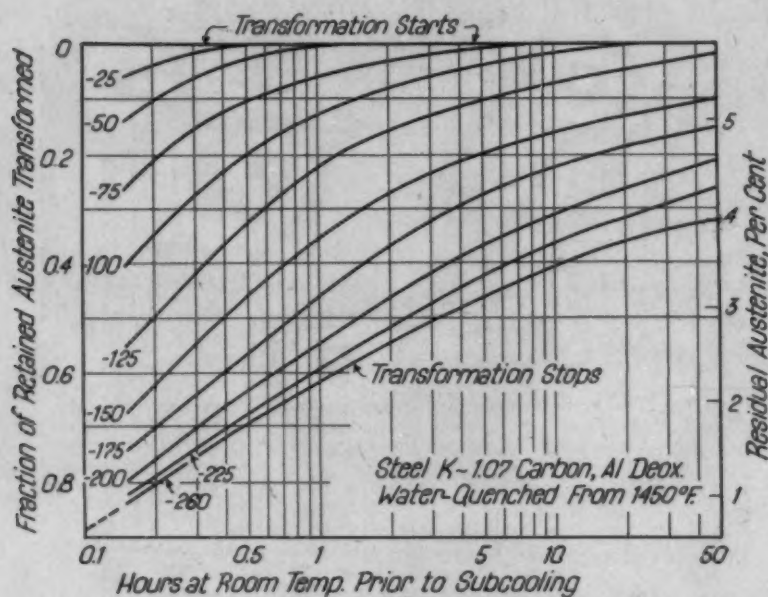


Fig. 15—Subatmospheric Transformation Chart for Steel K, Showing the Fraction of the Retained Austenite that Transforms and the Amount of Residual Austenite Left After Room Temperature Aging and Subzero Cooling to the Indicated Temperatures.

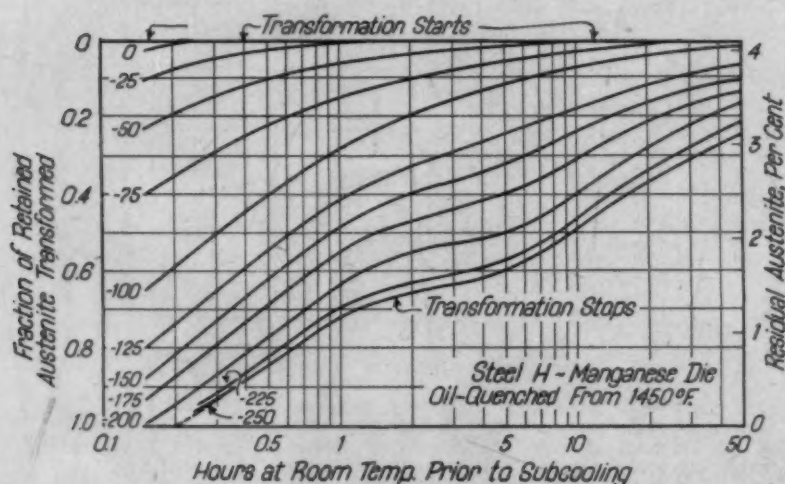


Fig. 16—Subatmospheric Transformation Chart for Steel H, Showing the Fraction of the Retained Austenite that Transforms and the Amount of Residual Austenite Left After Room Temperature Aging and Subzero Cooling to the Indicated Temperatures.

It is evident from Figs. 13 to 16 that subcooling to a particular temperature becomes less effective (from an austenite conversion standpoint) the longer the time of prior holding at room temperature. Practically all of the retained austenite can be decomposed by subcooling if the time of room temperature aging is kept sufficiently short. For example, extrapolations of the -250 to -260 -degree

Fahr. (-155 to -160 -degree Cent.) curves indicate that the retained austenite can be completely decomposed by cooling to this temperature if the holding at room temperature is less than 5, 2.4 and 12 minutes for Steels M, K and H respectively. (The extrapolation for Steel L is too uncertain to be justified.) By way of comparison, only 60 per cent of the retained austenite in high speed steel can be converted by subcooling. The principal reason for this difference is that the transformation in high speed steel stops below -150 degrees Fahr. (-100 degrees Cent.), whereas in the lower alloy steels, it continues down to -250 to -260 degrees Fahr. (-155 to -160 degrees Cent.). Thus, there may be good reason for cooling the latter materials to considerably lower temperatures than those used for high speed steel.

It is important to note that the room temperature aging factor cannot be divorced from subatmospheric transformation studies, and must be taken into account because of its suppressing effect on the austenite transformation. This behavior has appeared in all the steels that have been investigated so far, and may be quite general. From a fundamental viewpoint, it means that interruption of the austenite-martensite reaction (i. e., stopping the hardening quench at room temperature) may inhibit both the resumption and extent of the remaining transformation on further cooling. The authors believe that a detailed study of this phenomenon will provide new information concerning the basic nature of the austenite-martensite transformation, and will tie in with the reasons for the large amounts of austenite retained in high speed steel on arrested quenching (28). Conceivably, the stresses set up by the volume change accompanying the transformation facilitate the progress of the reaction on continuous cooling, and if the cooling is stopped within a suitable temperature range, enough stress relief may occur to alter the natural course of the decomposition when the cooling is resumed.

CONCLUSIONS

(A) The subatmospheric transformation of retained austenite in straight carbon and low alloy gage steels has been investigated by X-ray and dilatometric methods.

(B) Quantitative relationships between the extent of austenite decomposition, the subcooling temperature and the prior holding time at room temperature are presented in the form of subatmospheric transformation charts.

(C) Aging at room temperature between the hardening and subcooling treatments lowers the temperature at which the retained austenite starts to transform on subcooling and reduces the amount of transformation achieved by any given cooling treatment.

(D) However, the subatmospheric transformation in these steels continues down to -250 to -260 degrees Fahr. (-155 to -160 degrees Cent.), irrespective of the holding time at room temperature.

(E) Virtually complete decomposition of the retained austenite can be accomplished by subcooling to -250 to -260 degrees Fahr. (-155 to -160 degrees Cent.) if the prior time at room temperature is kept within several minutes.

ACKNOWLEDGMENTS

The authors wish to thank the Sheffield Foundation of Dayton, Ohio, for permission to publish this paper. They are also indebted to Mr. Fay Aller, Director of Research of the Foundation, for his interest in this work.

References

1. F. D. Jones, "How Precision Gage Blocks Are Made," *Machinery*, Vol. 26, 1920, p. 697-708.
2. H. J. French, "Artificial Seasoning of Steel," *American Machinist*, Vol. 55, 1921, p. 768-771.
3. H. Scott, "Dimensional Changes Accompanying the Phenomena of Tempering and Aging Tool Steels," *TRANSACTIONS, American Society for Steel Treating*, Vol. 9, 1926, p. 277-304.
4. F. H. Rolt, "Gauges and Fine Measurements," Macmillan & Co., London, 1929, 2 vol.
5. W. P. Boyle, "Aging Tools and Gages," *Steel*, Vol. 109, Sept. 22, 1941, p. 71.
- ✓ 6. W. A. Phair, "Cold Treatment of Metals," *Iron Age*, Vol. 151, Feb. '25, 1943, p. 37-43.
- ✓ 7. H. A. Knight, "Sub-Zero Stabilizing of Steel Gages and Parts," *Metals and Alloys*, Vol. 19, Mar. 1944, p. 610-614.
8. National Physical Laboratory Reports, 1928, p. 182.
9. D. P. Antia, S. G. Fletcher and M. Cohen, "Structural Changes during the Tempering of High Carbon Steel," *TRANSACTIONS, American Society for Metals*, Vol. 32, 1944, 290-332.
10. J. A. Mathews, "Retained Austenite—A Contribution to the Metallurgy of Magnetism," *TRANSACTIONS, American Society for Steel Treating*, Vol. 8, 1925, p. 565-588.
11. K. Schroeter, "On the Transformation of Austenite to Martensite in Liquid Air," *Zeitschrift für anorg. u. allgemeine Chemie*, Vol. 169, 1928, p. 157-160.
- 11a. W. P. Sykes and Z. Jeffries, "On the Constitution and Properties of Hardened Steel," *TRANSACTIONS, American Society for Steel Treating*, Vol. 12, 1927, p. 871-904.
12. G. Tammann and E. Scheil, "Transformation of Austenite to Martensite in Hardened Steel," *Zeit. für anorg. u. allgemeine Chemie*, Vol. 157, 1926, p. 1-21.

13. J. H. Andrew, M. S. Fisher and J. M. Robertson, "Some Physical Properties of Steel and Their Determination," *Proceedings*, Royal Society, London, Vol. 110A, 1926, 391-422.
14. O. E. Harder and R. L. Dowdell, "Decomposition of Austenite in Liquid Oxygen," *TRANSACTIONS*, American Society for Steel Treating, Vol. 11, 1927, p. 391-398.
15. K. Honda and K. Iwase, "Decomposition of Austenite in Liquid Air," *TRANSACTIONS*, American Society for Steel Treating, Vol. 11, 1927, p. 399-412.
16. G. V. Luerssen and O. V. Greene, "The Cold Treatment of Certain Alloy Steels," *TRANSACTIONS*, American Society for Steel Treating, Vol. 19, 1932, p. 501-552.
17. N. Minkevich, O. Ivanov, and Y. A. Dovgalevsky, "Influence of Low Temperatures on Two Quenched Steels," *Stal*, 1938, No. 4, 63-65; Abstracted in *Journal*, Iron and Steel Institute, Vol. 139, 1939, p. 63A.
- ✓ 18. P. Gordon and M. Cohen, "The Transformation of Retained Austenite in High Speed Steel at Subatmospheric Temperatures," *TRANSACTIONS*, American Society for Metals, Vol. 30, 1942, p. 569-591.
19. A. Gulyaev, "Transformation of Retained Austenite at Subzero Temperatures in High Speed Steel," *Metallurg*, Vol. 14, 1939, p. 64-77.
20. F. S. Gardner, M. Cohen, and D. P. Antia, "Quantitative Determination of Retained Austenite by X-rays," *Transactions*, American Institute of Mining and Metallurgical Engineers, Iron and Steel Division, Vol. 154, 1943, p. 306-317.
- ✓ 21. P. Gordon, M. Cohen and R. S. Rose, "The Kinetics of Austenite Decomposition in High Speed Steel," *TRANSACTIONS*, American Society for Metals, Vol. 31, 1943, p. 161-217.
22. A. B. Greninger, "The Martensite Thermal Arrest in Iron-Carbon Alloys and Plain Carbon Steels," *TRANSACTIONS*, American Society for Metals, Vol. 30, 1942, p. 1-26.
23. V. Zyuzin, V. Sadovskii, and S. Baranchuk, "Influence of Alloy Elements on Position of Martensite Point, Quantity of Retained Austenite, and Stability of Retained Austenite During Tempering," *Metallurg*, Vol. 14, Nos. 10-11, 1939, p. 75-80.
24. P. Payson and C. H. Savage, "Martensite Reactions in Alloy Steels," *TRANSACTIONS*, American Society for Metals, Vol. 33, 1944, p. 261-280.
25. K. Honda and Z. Nishiyama, "On the Nature of the Tetragonal and Cubic Martensites," *Science Reports*, Tohoku Imperial University, Series 1, Vol. 21, 1932, p. 299-331.
26. E. Ohman, "X-Ray Investigations on the Crystal Structure of Hardened Steel," *Journal*, Iron and Steel Institute, Vol. 123, 1931, p. 445-463.
27. G. Hagg, "X-Ray Investigation on the Structure and Decomposition of Martensite," *Journal*, Iron and Steel Institute, Vol. 130, 1934, p. 439-451.
28. P. Gordon, M. Cohen, and R. S. Rose, "Effect of Quenching-Bath Temperature on the Tempering of High Speed Steel," *TRANSACTIONS*, American Society for Metals, Vol. 33, 1944, p. 411-454.

DISCUSSION

Written Discussion: By R. F. Harvey, metallurgist, Brown & Sharpe Mfg. Co., Providence, R. I.

The authors have effectively emphasized the need for more reliable and complete quantitative information on the subatmospheric transformation of retained austenite in plain carbon and low alloy steels. Many different commercial stabilizing treatments have been adopted with little or no data to support the use of any particular procedure.

The authors show that as plain carbon and low alloy steels cool from the hardening temperature, the retained austenite starts to transform to martensite on cooling to about 0 to -25 degrees Fahr. providing the holding time at room temperature is within a few minutes, and continues to transform on continuous cooling until a temperature of about -260 degrees Fahr. (-160 degrees Cent.) is reached where substantially complete transformation of the austenite is accomplished. The authors further show that the longer the cooling is interrupted at room temperature, the lower will be the temperature at which transformation starts. Also, the amount of transformation will be less for a given cooling treatment if the hardened plain carbon or low alloy steel is aged at room temperature.

With reference to Steels L and K (aluminum deoxidized) which were both high carbon tool steels similar in analysis and fracture grain size after hardening, the question arises as to why with about 1 per cent more austenite at room temperature more transformation during subcooling was obtained with the latter steel for any given cooling treatment.

It is common commercial practice to stabilize gages by drawing at temperatures of about 300 degrees Fahr. (150 degrees Cent.) followed by cold treatment. As the authors have pointed out in Fig. 7, the cooling curve for a plain carbon tool steel drawn at 300 degrees Fahr. (150 degrees Cent.) for 1 hour stabilized the austenite so that no transformation at all was obtained on cooling down to about -300 degrees Fahr. (-185 degrees Cent.). It is evident, therefore, that when the tempering treatment precedes the subatmospheric cooling the greater dimensional stability obtained must be independent of any residual austenite transformation.

Other commercial stabilizing procedures employ cyclic treatments involving numerous repetitions of subjecting the steel to alternate cold and hot temperatures. By employing extreme cold followed by moderate heat after hardening, the low temperature treatment results in further conversion of austenite to martensite and the draw should be beneficial in relieving stress developed as a result of the martensite formation. However, there is no evidence advanced in the literature to show that many repetitions of this cycle will produce results not accomplished in the first cold and hot treatment except, of course, for the additional softening and stress relief as a result of prolonged drawing. Would the authors care to comment on the possible benefits, if any, that may be expected from numerous repetitions of the same cold treatment?

Although liquid nitrogen at -321 degrees Fahr. (-195 degrees Cent.) and liquid oxygen at -297 degrees Fahr. (-183 degrees Cent.) are used experimentally, commercial refrigerating systems commonly employed for stabilizing steel operate at temperatures down to about -120 degrees Fahr. (-85 degrees Cent.). The present paper points out the possibilities of obtaining greater austenite conversion and dimensional stabilization by employing much lower temperatures than are now used.

As the authors have pointed out, the principal type of dimensional instability observed in heat treated parts is growth. However, stress relief may occur over a period of time to cause distortion and warping particularly in intricate-shaped parts. In the case of straight edges and squares, distortion

or warping is more detrimental than growth. Do the authors plan to study the effect of stress in causing dimensional instability?

Written Discussion: By Stewart M. DePoy, metallurgist, Delco Products Div., General Motors Corp., Dayton, Ohio.

Subatmospheric treatment of steels is becoming more important in industry daily. Engineers have been discussing the effects and reasons for this treatment on a theoretical basis for the past 2 years. Messrs. Fletcher and Cohen have finally given us some factive evidence with which we may use this treatment on a better known basis.

The thoroughness with which the authors prove the stabilizing effect of aging at room temperature explains beyond a doubt the nonuniformity which exists between the results obtained at various industrial plants from this process. It is now very evident that subzero cooling should follow immediately after the quench. However, it is still this discussor's belief that this is a dangerous practice. Thermal shock and dimensional change in the untempered part is almost sure to cause a large amount of cracking. The authors do not show the effect of tempering before subzero cooling. What would be the effect of the following treatment on Steels L and J?

Austenitize at 1440 degrees Fahr. (780 degrees Cent.) for L and 1525 degrees Fahr. (830 degrees Cent.) for J. Water-quench L and oil-quench J to approximately 100 to 150 degrees Fahr. Temper both at 350 degrees Fahr. Subzero treat at -120 degrees Fahr. for 2 hours and retemper at 350 degrees Fahr.

This treatment has worked splendidly at Delco Products Division, G.M.C. With it we are able to hold tolerances within ± 0.000025 to -0.00000 inch. This has been checked by room temperature aging from 24 hours to 6 months. The latter is probably the life of an industrial gage. Hardness obtained on these gages by the above treatment will range from 62 to 66 Rc. However, a chrome flash of 0.000025 inch on the diameter of the finished gage has lengthened the life of our gages quite materially.

For master gages it is quite apparent that subzero cooling to 250 degrees Fahr. will speed up their manufacture and probably is the only way to make a perfect gage. The paper infers that absolutely complete transformation of all austenite in a steel would be impossible. At least, this is the theory at this writing. However, it does not seem plausible that what is left after proper hardening and subzero treatment could transform by room temperature aging. The authors are to be congratulated for their splendid work. This paper is truly an important contribution to the literature on this subject, and it will surely stimulate much more work on this process in the industrial field.

Written Discussion: By Robert S. Rose, sales metallurgist, Vanadium-Alloys Steel Co., Boston.

The identification of the metallurgical phenomena responsible for the dimensional instability of hardened steel at or near room temperature is of both academic and industrial importance. Yet, despite this importance and the researches of many able investigators, the isothermal reactions appear vague, complex and inconsistent. Hence, the present authors are deserving of praise in undertaking an extended investigation fraught with so many difficulties.

It is probably unfair and premature to attempt to draw from them an expression of the relationship between the transformation of residual austenite and dimensional instability at room temperature, yet the data presented here and in two previous reports^{5,6} seem to argue that no relationship or dependence does, in fact, exist.

The stability of residual austenite in as-quenched steel has been shown to increase with time at room temperature, at least with respect to its susceptibility to transformation by supercooling. It is presumed that this stability is affected by the structural changes occurring in the co-existing martensite. Hence, while not serving as proof that room temperature transformation of austenite cannot and does not take place, the increased stability with time would be expected to deter, not hasten, the reaction. Doubtlessly the authors have aged some as-quenched specimens much longer than the 24 hours employed here prior to supercooling. It would be of considerable interest to learn whether any change in quantity of austenite was observed as a direct result of aging only. Strangely enough, the dimensional instability indicated by the known room temperature structural changes (in the martensite) is a contraction, not a growth.

To an even greater extent, tempering as low as 300 degrees Fahr. (150 degrees Cent.) stabilizes the residual austenite against transformation during supercooling and certainly most gages receive the benefit of this heat treatment. If the tempering precedes the subcooling operation, as it frequently does, then the residual austenite is immunized and any reduction in dimensional instability is accomplished without previous change in its quantity.⁷

Progressively higher tempering treatments (above 300 degrees Fahr.) at first further stabilize and then decompose the residual austenite—it disappearing in straight carbon steel altogether at about 475 degrees Fahr. (245 degrees Cent.) in 1 hour. The room temperature aging of specimens given various prior temperings, it seems to me, despite an alteration of stress, would give some further insight into the relationship, if any, between dimensional instability and residual austenite.

Even though this subject is beyond the scope of the present paper, perhaps the authors would be willing to offer their comments.

Written Discussion: By L. D. Jaffe, Laboratory of Physical Metallurgy, Harvard University, Cambridge, Mass.

Were any X-ray measurements made of the amount of austenite remaining after the material was cooled to -190 degrees Cent. and reheated to room temperature? It would seem that these would serve as a check of the calculations based upon the specific volumes of austenite and martensite.

Written Discussion: By W. E. Bancroft, chief metallurgist, Pratt & Whitney Division, Niles-Bement-Pond Co., W. Hartford, Conn.

It is indeed gratifying to note that at last some scientific light is going to be shed on the mysterious matter of stabilization of hardened tool steels.

⁵Dara P. Antia, Stewart G. Fletcher and Morris Cohen, "Structural Changes During the Tempering of High Carbon Steel," *TRANSACTIONS, American Society for Metals*, Vol. 32, 1944, p. 290.

⁶Stewart G. Fletcher and Morris Cohen, "The Effect of Carbon on the Tempering of Steel," *TRANSACTIONS, American Society for Metals*, Vol. 32, 1944, p. 333.

⁷It is probable that with very large quantities of residual austenite (30 per cent or over) that higher drawing temperatures may be necessary for complete stabilization.

As a first chapter in an extensive investigation of this subject, this paper is certainly a valuable contribution. Its usefulness will be increased as further data are developed showing the true relationship between conversion of austenite and actual stabilization. As a unit by itself, this present paper seems rather difficult to discuss. The painstaking methods of procedure and the orderly presentation of results leave very little to be desired. It certainly provides adequate information for more intelligent usage of subzero treatments in so far as austenite transformation only is concerned.

Perhaps this paper's only fault might be said to lie in its brevity. It whets the appetite and stimulates all sorts of questions which are as yet unanswered. It is recognized that this is but a preliminary report, but nevertheless there are some points which might logically have been included in this study of transformation. For example, a comparison of the effect of multiple cooling treatments with that of single treatments would be of interest. As stated by the authors most of the literature on stabilization and presumably most of the practical experience to date have indicated that alternate heating and cooling cycles are desirable in developing stabilization, so eventually the effect of such treatments on austenite conversion should be developed. Then there is the matter of hardness. Possibly it may be assumed that none of the treatments reported upon in this paper had a significant effect on hardness but a direct statement by the authors concerning this might be in order.

Some of the points which are brought out in the paper are of particular interest. Fig. 2 and Table III showing the absolute amounts of austenite retained on quenching and the effect of overheating are quite valuable. However, they do give rise to the question of how thoroughly the larger amounts of austenite resulting from overheating can be transformed by subzero cooling.

The fact that the steels covered in this paper transform through a much lower range than high speed steel is of great importance. The curves in Figs. 13 to 16 show that a temperature of -100 degrees Fahr. produces less than 50 per cent of the transformation that can be achieved in any of the steels under the most favorable conditions, with the possible exception of Steel H. From a practical standpoint this precludes the usefulness of dry ice or any mechanical refrigeration equipment now available. It means that liquid gases must be used if anywhere near complete transformation is to be obtained—unless multiple treatments will work differently.

The effect of room temperature aging on the completeness of transformation which can be obtained is quite similar to that which has been observed in high speed steel. This is a point which will bear close watching in connection with stabilization because it appears to have been pretty well established that good stabilization can actually be developed by multiple treatments or others, wherein the cooling has been applied after extensive room temperature aging or even tempering, which, according to the data in this paper, would not permit transformation of any of the retained austenite! Can it be that austenite conversion is not the all-important factor that it has been believed to be in promoting stabilization?

It is hoped and expected that subsequent reports on this valuable investigation will answer the foregoing and many other important questions.

Written Discussion: By Otto Zmeskal, research metallurgist, Universal-Cyclops Steel Corporation, Bridgeville, Pa.

The authors have given us another one of their illuminating and precise studies of transformation phenomena in plain carbon and low alloy steels. The writer has obtained some data on the subatmospheric transformation of a high-carbon, high-chromium cobalt-bearing die steel which he would like to present to permit a comparison of the reaction of the authors' steels and a more complex steel to cold treatment.

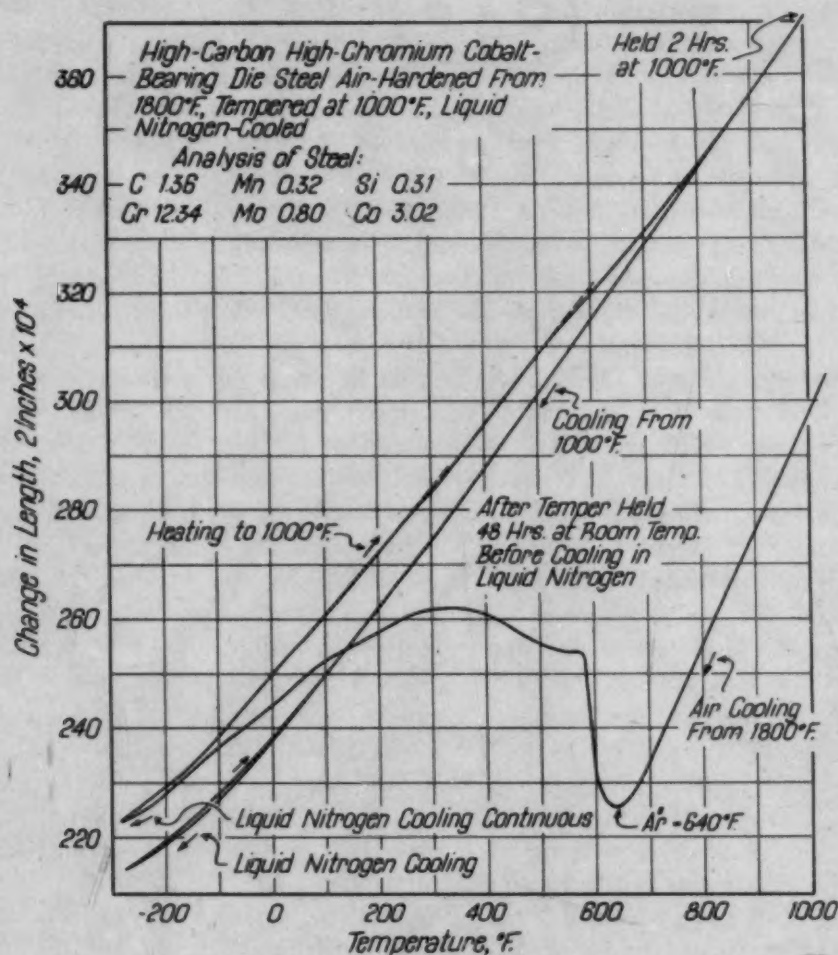


Fig. A

The steel used for this work had the following analysis:

C	Mn	Si	S	P	Cr	Ni	Mo	Co	Cu
1.36	0.32	0.31	0.012	0.014	12.34	0.28	0.80	3.02	0.04

It was used in the shape of $\frac{1}{4}$ -inch diameter rods, 2 inches long, and centerless ground from $\frac{3}{8}$ -inch diameter hot-rolled-and-annealed rods. The dilatometer was similar to that described by Gordon, Cohen, and Rose.⁵ All specimens

⁵Paul Gordon, Morris Cohen, and Robert S. Rose, "The Kinetics of Austenite Decomposition in High Speed Steel," TRANSACTIONS, American Society for Metals, Vol. 31, 1943, p. 166.

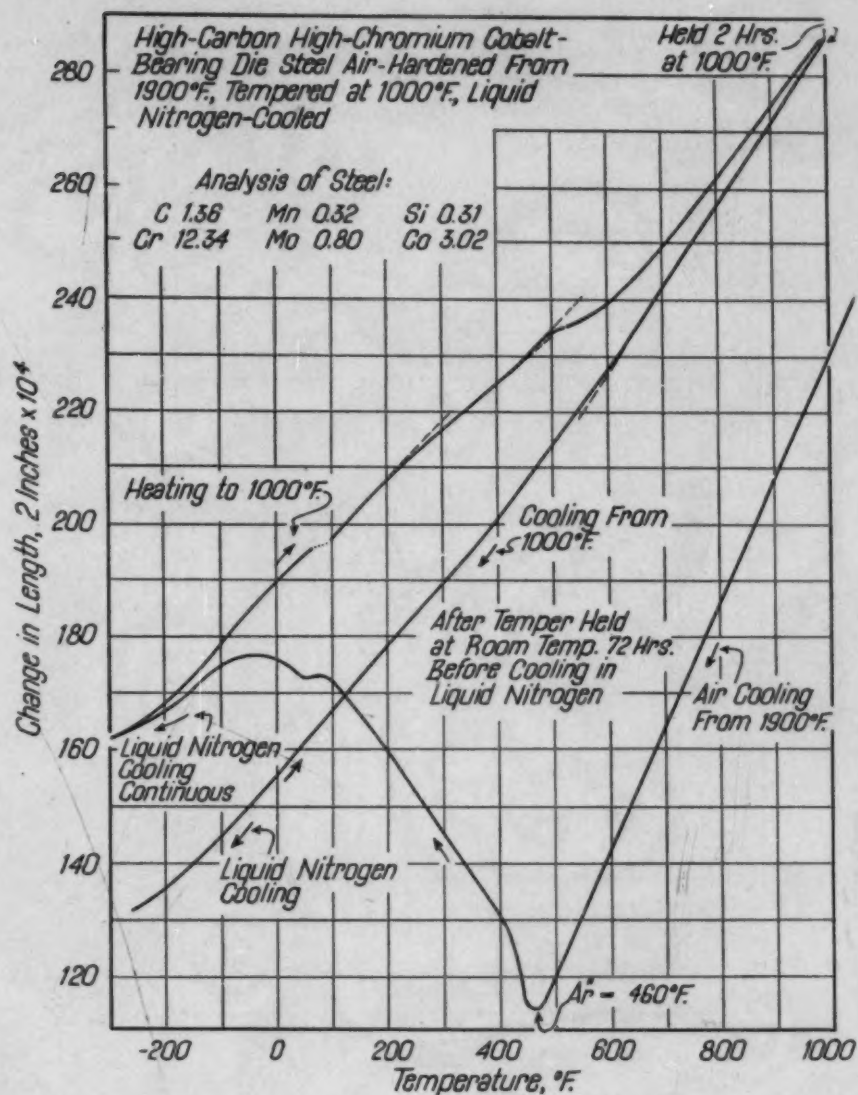


Fig. B

were hardened in a Sentry combustion furnace in an atmosphere of nitrogen. Each was held 2 minutes at temperature. The specimen temperature was determined by a platinum thermocouple. The specimen was removed from the furnace and quickly placed into the dilatometer, enabling readings of the contraction to be made from 1300 degrees Fahr. (705 degrees Cent.) down. Liquid nitrogen cooling was effected by placing the dilatometer tube in a test tube and then placing this unit in a Dewar flask containing the coolant. The cooling rate was low enough to permit readings every 10 degrees. The results are presented in Figs. A to E. In these figures the ordinate values were taken arbitrarily.

Increasing the austenitizing temperature lowers the temperature of the primary austenite transformation. This is shown in the table on the following page.

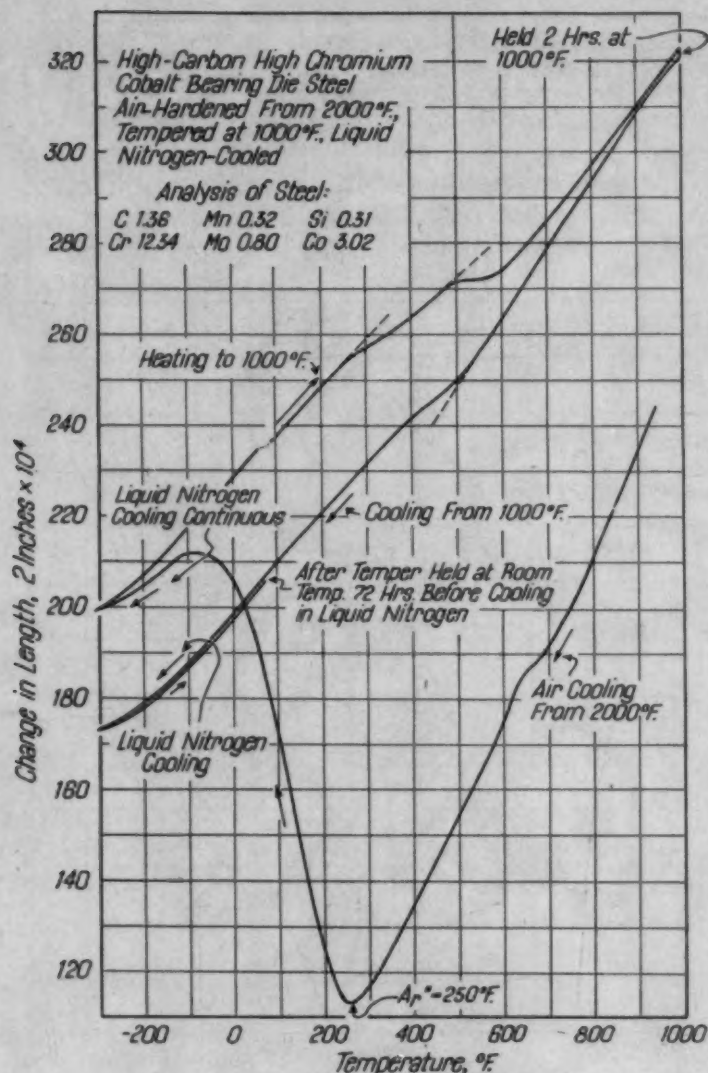


Fig. C

Effect of the Austenitizing Temperature of a 1.3 C-12.3 Cr-0.8 Mo-3 Co Steel on the Transformation Temperature of the Primary Austenite

Austenitizing Temperature Degrees Fahr.	Transformation Temperature Degrees Fahr.
1800	640
1900	460
2000	250
2100	100
2200	-30

In each case the cooling from the hardening temperature was carried out continuously down to the temperature of liquid nitrogen (-320 degrees Fahr.). However, if the austenite was so stabilized that it remained untransformed down to room temperature, the period of holding at room temperature before subatmospheric cooling was without effect on the subsequent transformation.

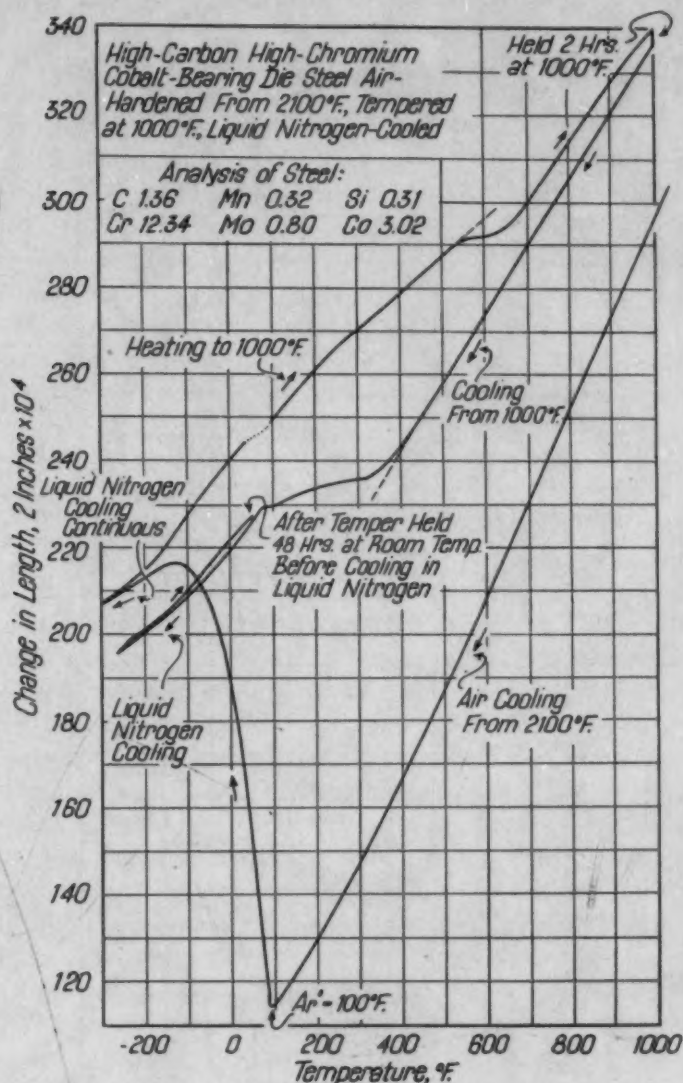


Fig. D

An interesting fact that may be interpolated here is that a similar high-carbon high-chromium die steel but without the cobalt would not exhibit any transformation on cooling to -320 degrees Fahr. when hardened from 2200 degrees Fahr. Thus, cobalt raises the Ar'' of these steels as it does in simpler steels, as reported by Chiswik and Greninger⁶. In order to stabilize the austenite of the cobalt-bearing die steel so as to resist transformation on cooling to -320 degrees Fahr. it is necessary to harden it from 2300 degrees Fahr. (1260 degrees Cent.) (a temperature which results in slight eutectic formation at the grain boundaries).

When the austenite stability is diminished to the point where transformation occurs above room temperature (whether it is the primary or the secondary

⁶H. H. Chiswik and A. B. Greninger, "Influence of Nickel, Molybdenum, Cobalt and Silicon on the Kinetics and Ar'' Temperatures of the Austenite to Martensite Transformation in Steels," *TRANSACTIONS, American Society for Metals*, Vol. 32, 1944, p. 514.

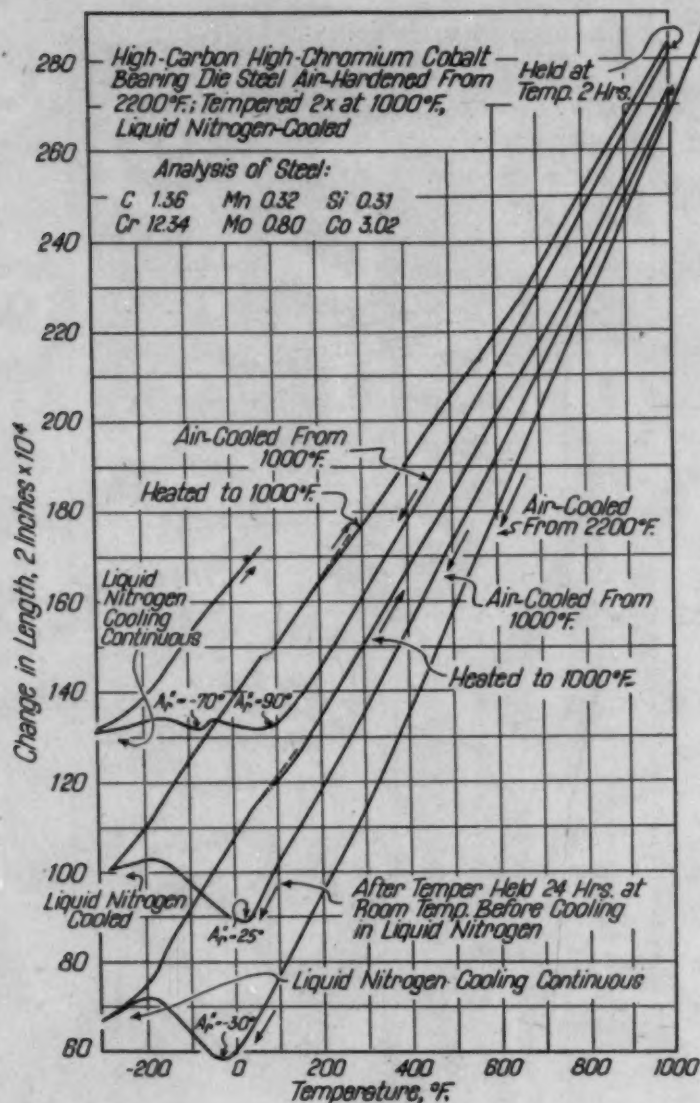


Fig. E

transformation) the stabilization effect of room temperature holding becomes apparent. Attention is called to the stabilization effect of a 48-hour hold at room temperature on the retained austenite of the specimen hardened from 2100 degrees Fahr. (1150 degrees Cent.) for 2 hours (Fig. D). The transformation that was in process during cooling to room temperature was completely stopped by the hold at room temperature.

The primary austenite transformation has several peculiarities that relate to the stability of the austenite. On cooling from an austenitizing temperature of 1800 degrees Fahr. (980 degrees Cent.) (Fig. A) the austenite transformed in three stages, two stages strongly apparent between 640 and 70 degrees Fahr. and one slightly apparent on subatmospheric cooling. At a 1900-degree Fahr. (1040-degree Cent.) austenitizing temperature (Fig. B) the three stages were

still apparent, but the subatmospheric stage was more pronounced. The two peaks that occurred at 580 and at 350 degrees Fahr. in the 1800 curve were depressed in the 1900 curve to 80 and -40 degrees Fahr. On austenitizing at 2000 degrees Fahr. (1095 degrees Cent.) (Fig. C) and above, the transformation was one continuous stage. In the very stable austenite of the 2200-degree Fahr. (1205-degree Cent.) hardened specimen (Fig. E), two peaks appeared in the subatmospheric cooling after the second temper at 1000 degrees Fahr. (540 degrees Cent.).

On heating during the tempering operation each curve showed two inflection points, both being contractions superimposed upon the normal expansion. The first, occurring between 200 and 300 degrees Fahr. (95 and 150 degrees Cent.), was due to the transformation of tetragonal martensite to cubic martensite; the second, occurring between 450 and 550 degrees Fahr. (230 and 290 degrees Cent.), was due to the formation of carbides from the transitional phase precipitated. The magnitude of the contraction effects is dependent upon the amount of martensite that is formed during the primary austenite transformation, being greatest for the specimen hardened from 2000 degrees Fahr.

In one instance, the 1900 curve, an additional inflection, this time an expansion, occurring just before the second contraction, was noticed. This was due to retained austenite transformation on heating. Supercooling completely transformed the austenite in the 1800 specimen, and the retained austenite in the 2000 specimen was too stable to transform on heating, but in the 1900 specimen, heating through 450 to 500 degrees Fahr. (230 to 260 degrees Cent.) transformed part of the austenite left untransformed by the supercooling. The remainder transformed on cooling through 600 degrees Fahr.

No austenite transformation occurred at temperature during the 2-hour temper at 1000 degrees Fahr. (540 degrees Cent.) for any of the hardening temperatures. The only phenomenon that took place was the precipitation of carbides from the retained austenite. On subsequent cooling, transformation of the retained austenite took place. The amount of austenite that transformed on cooling from the tempering temperature increased as the amount retained increased and as the amount transformed by the supercool decreased.

There is no advantage in using high temperatures in the hardening of high-chromium high-carbon steel for gages. Too much austenite is retained and that retained is too stable. Examination of the 1800 curve shows that austenite transformation is complete after a supercooling to -150 degrees Fahr. from the hardening temperature. For complete stability, however, it is believed that any transformation which leads to dimensional stability should be consummated. That is, the tetragonal martensite should be converted to cubic martensite and the transitional precipitate occurring therefrom should be converted to the carbide by tempering through 650 degrees Fahr.

The future contributions of the authors to the science of dimensional stabilization are awaited with great interest.

Authors' Reply

The problem of dimensional instability in hardened gage and die steels has been recognized for many years. Yet, even at this late date, the authors do not

pretend to know the "final answers" to the pertinent questions that have been raised by the several discussers. It is quite evident, however, that most of the low temperature treatments which have been reported to yield dimensional stability actually do not convert the potentially unstable retained austenite. One must face the thought-provoking conclusion that either the room temperature decomposition of retained austenite is not the principal cause of growth during aging, or the subcooling process makes the retained austenite more resistant to decomposition during subsequent aging, even though the austenite is not converted during the subcooling. The evidence does not justify further speculation at this time.

Mr. Harvey has noted the small, but definite, difference in behavior that was observed between Steels L and K (similar analyses, Steel K being aluminum-killed). As yet, it is not known whether the difference is truly a function of the state of deoxidation, or whether such differences are to be expected from heat to heat of supposedly the same steel. One should not assume, however, that steels with more retained austenite will necessarily undergo more transformation during subcooling than steels with less austenite. The authors wish to thank Mr. Harvey for pointing out the case of distortion and warpage in straight edges and squares. Eventually, we hope to give due consideration to stress and stress relief as factors in dimensional stability.

It is true, as Mr. DePoy states, that refrigeration immediately after hardening is apt to be a hazardous practice from the standpoint of cracking. Tempering before subcooling certainly minimizes the danger of cracking during subcooling, but the low temperature transformation of the retained austenite is likewise inhibited. Perhaps it would be well to emphasize here that the subcooling conversion of austenite after hardening is not a matter of thermal shock, that slow cooling is effective in transforming austenite, and definitely lessens the probability of cracking. In the last paragraph of his discussion, Mr. DePoy mentions that this paper infers complete transformation of the austenite to be impossible. Actually, complete transformation is attainable in these straight carbon or low alloy steels if the time at room temperature, prior to subcooling, is sufficiently short (cf. p. 235).

The authors have performed no experiments with the treatments described by Mr. DePoy, but are interested to know that they result in dimensional stabilization. An attempt will be made to incorporate such treatments in our future research.

In line with Mr. Rose's suggestion, the relationship between time and temperature of tempering and the extent of dimensional stability on subsequent aging is scheduled for study in due course. As yet, no measurements of the changes in austenite content during room temperature aging have been made. Such determinations will prove most difficult. Observations of changes in length, volume, magnetization, or electrical resistance can be made very precisely, but are also affected by martensite decomposition and stress relief. The X-ray method for austenite measurement is more absolute and holds promise, but its sensitivity is much lower than that of the other techniques.

Mr. Rose's discussion brings up the fact that the stabilizing of retained austenite must be considered in two ways, first with respect to its possible iso-

thermal decomposition during aging, and secondly, with respect to its possible conversion during subcooling. A treatment which inhibits the austenite transformation in one of these ways may not have a similar effect on the other type of transformation.

Table A is submitted in answer to Mr. Jaffe's question. The X-ray work was held to a minimum when dealing with small amounts of austenite because the dilatometer results offered a simpler and more accurate method of securing the same answer. However, wherever cross checks were made, reasonable agreement was obtained.

Table A
Comparison of Calculated and X-Ray Determinations of
Retained Austenite After Subzero Cooling

Steel K (1.07 Carbon, Al. Deox.), Water Quenched from 1450 Degrees Fahr.	Time at Room Temperature Hours	Minimum Cooling Temperature Degrees Fahr.	Per Cent Retained Austenite Calculated from Dilation	X-ray Results
	0.08	-300	about 0.5	**
		-125	about 1.9	1.5*
	0.5	-300	1.8	**
		-125	4.0	3.7
	5.0	-300	3.1	2.9
		-125	5.2	4.9
	25.0	-300	3.8	**
		-125	5.5	5.5

*The X-ray method is reliable only when more than 1.5 per cent austenite is present, and then only to about ± 0.3 per cent austenite.

**No determination has been made.

As Mr. Bancroft rightly points out, many questions are stimulated by the present paper. The effects of overhardening and of multiple subcooling cycles are to be investigated as a part of our immediate program. Hardness studies are under way, and the available trends show a qualitative correlation between austenite conversion and increase in hardness, the maximum increase in these normally hardened steels being about one Rockwell C point.

We are indebted to Dr. Zmeskal for the interesting subatmospheric data that he has presented for a high-carbon high-chromium steel containing cobalt. It is important to note that the stabilizing influence of room temperature aging with respect to austenite decomposition on subcooling does not exist if the primary M-point lies below room temperature. In other words, the austenite-martensite transformation must be interrupted by the room temperature aging in order for the latter to have a suppressive action on the rest of the transformation during further cooling.

The three-stage behavior of the austenite decomposition in this steel after austenitizing at 1800 and 1900 degrees Fahr. (980 and 1040 degrees Cent.) appears quite complex. This may be partly due to the very short austenitizing time used. Insufficient solution of the carbides might well lead to some bainite formation during air cooling, with an unpredictable effect on the course of the austenite-martensite transformation. Faster cooling, longer austenitizing times or higher austenitizing temperatures would tend to suppress possible interference by bainite formation.

A STUDY OF SUBZERO TREATMENTS APPLIED TO MOLYBDENUM-TUNGSTEN HIGH SPEED STEEL

BY RALPH G. KENNEDY, JR.

Abstract

The effects of cooling to subzero temperatures on hardened molybdenum-tungsten high speed steel have been studied by means of dilation, specific volume, hardness, static torsion, mutual indentation hardness tests at elevated temperatures, and by metallographic examination and tool performance tests.

The effects on physical properties of such factors as the subzero temperature reached, the time of holding at this temperature and the time of aging at room temperature before subzero cooling, have been studied. The effect of subzero cooling before and after tempering has been examined in conjunction with the usual heat treatment variables of hardening temperature, tempering temperature, and quenching temperature attained before tempering.

Tensile, torsion and transverse bend tests have been made with specimens from the same heat of high speed steel in order to furnish correlation factors with which the static torsion test results of the present experiments may be compared with the results of tensile and transverse bend tests previously published for various types of high speed steels.

Tool performance tests in which all variables were controlled as closely as possible have been run with ordinary hardening compared to various types of subzero hardening.

PREVIOUS WORK

RECENT studies of subzero decomposition of retained austenite in 18-4-1 high speed steel by Gordon and Cohen (1)* have rekindled interest in the use of low temperature treatments. Decomposition of austenite at low temperatures in high speed steels has been demonstrated some years ago by Harder and Dowdell (2), Scott (3), and Gulyaev (4).

*The figures appearing in parentheses refer to the bibliography appended to this paper.

A paper presented before the Twenty-sixth Annual Convention of the Society held in Cleveland, October 16 to 20, 1944. The author, Ralph G. Kennedy, Jr., is research metallurgist, The Cleveland Twist Drill Co., Cleveland, Ohio. Manuscript received June 23, 1944.

Harder and Dowdell (2) found a large increase in hardness and specific volume after liquid air immersion of high chromium and high nickel steels and a slight increase for high speed steel. They could detect no change in the microstructure of high speed steel due to the low temperature treatment.

Many previous investigators (5-12) have detected low temperature transformation of austenite to martensite as evidenced by increases in hardness, specific volume, magnetization, and strength properties. Sykes and Jeffries (8) showed that in carbon and alloy steels this low temperature transformation of austenite does not depend on the time of holding at the low temperature but only on the temperature reached, and that all of the low temperature transformation is complete when a minimum temperature of -148 degrees Fahr. (-100 degrees Cent.) has been reached.

The part which stresses due to thermal shock play in the decomposition of austenite at low temperatures has been investigated by Honda and Iwase (7), Bain and Waring (9), and Nielsen and Dowdell (10). Apparently thermal stresses are not essential to the formation of martensite from austenite although Tammann (13) and Honda and Iwase (7) advance evidence to show that such stresses may help.

Some twelve years ago experiments in the author's laboratory revealed that liquid air treatment of hardened special high speed steels with very stable austenite, containing in one case 7 per cent nickel, and in another case 4.5 per cent manganese, gave increases of hardness as high as 15 points on the Rockwell C scale. Subsequent tempering at temperatures which normally gave maximum secondary hardness (1050-1150 degrees Fahr.) (565-620 degrees Cent.) eliminated the hardness increases caused by the liquid air immersion so that approximately equal hardness was obtained with specimens which had been immersed in liquid air after hardening and those which had not received such treatment.

More recently the kinetics of the subatmospheric austenite transformation in high speed steel has been rather thoroughly investigated by Gulyaev (5) and Gordon and Cohen (1). Gulyaev investigated the austenite transformation by means of magnetic measurements and showed that the transformation is dependent on the hardening (quenching) temperature and that it extends well below room temperature as shown in Fig. 1 reproduced from Gulyaev's (5) work.

Both Gulyaev (5) and Gordon and Cohen (1) showed that if the cooling to subzero temperature is interrupted at room temperature for even short periods of time, the amount of transformation is decreased and the temperature of the beginning of transformation is lowered. In addition, Gordon and Cohen (1) demonstrated that room temperature aging after quenching results in no change in specific volume, although an increase in magnetic induction occurs. Cohen and Koh (14) have also shown that aging hardened 18-4-1 high speed steel at room temperature results in no change in specific volume after tempering at 1000 degrees Fahr. (540 degrees Cent.) for various periods of time.

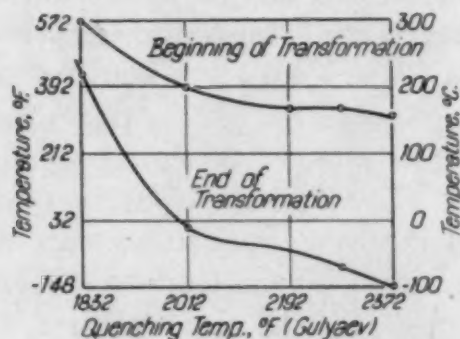


Fig. 1—Effect of Quenching Temperature on the Temperature of the Beginning and the End of the Austenite-Martensite Transformation in High Speed Steel. [Gulyaev (5)]

An important part of the investigation of Gordon and Cohen (1) on subzero hardening of high speed steels appears to be that they have measured by means of transverse bend tests, a considerable increase in ductility over that obtained by regular hardening and tempering treatments.

Gill and Roberts (15) have conducted an interesting investigation of 18-4-1 high speed steels, subzero hardened, and regularly hardened. They found that the increment of hardness gained by subzero cooling after quenching to room temperature is maintained with tempering temperatures below 1000 degrees Fahr. (540 degrees Cent.) while above 1000 degrees Fahr. the specimens not supercooled were the hardest. They also conducted an experiment in which the specimens were (a) cooled to -110 degrees Fahr. prior to tempering, (b) cooled to 70 degrees Fahr. prior to tempering, and (c) cooled to 250-300 degrees Fahr. (120-570 degrees Cent.) prior to tempering. They found that the subzero treated specimens were

the hardest after tempering at temperatures up to 1000 degrees Fahr. (540 degrees Cent.) and those quenched to 250-300 degrees Fahr. were the softest. However, with tempering times of 1 hour or more at temperatures above 1050 degrees Fahr. (540 degrees Cent.) the hot-quenched specimens were considerably harder than the other types.

With regard to cutting quality of high speed tools as influenced by subzero treatments many reports have been published. One of the most detailed of these concerns the work of DePoy (16). This series of tests involved determination of the proper place in the heat treating operation to interpose subzero treatment. Subzero cooling between the first tempering and the second tempering operation gave better tool performance than a subzero treatment after quenching and prior to tempering. Microstructures of subzero hardened tools were claimed to show slightly finer martensitic structures than were shown by regularly hardened tools.

Table I
Composition of High Speed Steel Studied

Diameter of Stock Inches	Type of Test	Steel No.	Per Cent				
			C	Cr	W	V	Mo
$\frac{1}{8}$	Torsion	LG	0.80	3.68	1.64	1.00	8.24
$\frac{1}{8}$	Specific Volume	LG	0.80	3.68	1.64	1.00	8.24
$\frac{1}{8}$	Rockwell Hardness	LG	0.80	3.68	1.64	1.00	8.24
$\frac{1}{8}$	Dilatometric	LG	0.80	3.68	1.64	1.00	8.24
$\frac{1}{8}$	Torsion	FT	0.78	3.81	1.58	1.18	8.36
$\frac{1}{8}$	Drill	FT	0.78	3.81	1.58	1.18	8.36
$\frac{1}{8}$	Drill	FT	0.78	3.81	1.58	1.18	8.36
$\frac{1}{8}$	Transverse Bend	FT	0.78	3.81	1.58	1.18	8.36
$1\frac{1}{8}$	Tensile	FT	0.78	3.81	1.58	1.18	8.36
$\frac{1}{2}$	Mutual Indentation Hot Hardness	Z 6952	0.81	3.97	1.42	1.13	8.32
$\frac{1}{8}$	Drill	W 7483	0.81	3.73	1.63	1.13	8.28
$\frac{1}{8}$	Drill	A 7150	0.79	3.80	1.37	1.04	9.20
$\frac{3}{8}$	Drill	W 6055	0.74	3.90	1.54	1.10	8.85
$\frac{1}{2}$	Drill	W 6520	0.74	3.83	1.40	1.08	8.06
$\frac{1}{2}$	Drill	6255	0.79	3.91	1.73	1.14	8.92
$1\frac{1}{8}$	Drill	Z 6963	0.74	3.83	1.40	1.08	8.06
$1\frac{1}{8}$	Milling Cutter	W 6266	0.75	3.82	1.53	1.08	8.37
$1\frac{1}{8}$	Milling Cutter	6411	0.79	3.78	1.68	1.07	8.66

The milling cutters were the type used for milling the flutes in twist drills.

EXPERIMENTAL DETAILS

Materials Studied and Preparation of Specimens—In Table I are listed the various molybdenum-tungsten high speed steels studied.

The static torsion test specimens were made from $\frac{5}{16}$ -inch diameter ground rod according to the dimensions found to be most suit-

able by Emmons (17). Hardness and specific volume measurements were also made on the torsion test specimens.

The transverse bend test specimens were rough ground from $\frac{5}{16}$ -inch round stock to a square cross section of 0.220 inch and were then cut to 5-inch lengths. After heat treatment they were ground and lapped to a square cross section of 0.2000 to 0.2002 inch with care being taken to eliminate all transverse surface grinding marks or scratches.

Tensile test specimens were machined oversize and ground after heat treatment to the dimensions shown in the sketch, Fig. 2.

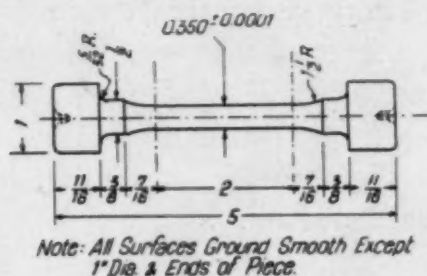


Fig. 2—Tensile Test Specimen.

Fig. 3 is a photograph of the torsion, transverse bend, and tensile test specimens.

The dilatometer specimens were ground from $\frac{5}{16}$ -inch round stock to 0.250-inch diameter and were cut and ground to a length of $4.00 \pm .01$ inch. A $\frac{5}{64}$ -inch thermocouple hole was drilled to a depth of $1\frac{3}{8}$ inches along the axis of each specimen.

Specimens for measuring hot hardness by the mutual indentation method consisted of small cylinders which were accurately ground after heat treatment to a diameter of 0.3937 inch (1 centimeter) and, also, to a length of 0.3937 inch in accordance with the method suggested by Cowdrey (18) and developed by Harder and Grove (19).

The various drills used in the drilling tests were made from round stock of the sizes indicated in Table I. After heat treatment they were finish ground to size. Care was taken to produce drills with as uniform shape as possible so that all the drills in one test would be exactly alike with respect to shape and dimensions.

Heat Treatments—The high heat treatments of all types of tools and test specimens, except the dilatometer specimens, were carried out in salt bath furnaces. Hardening temperatures ranged from 2000 ± 5 to 2240 degrees Fahr. (1095 to 1225 degrees Cent.).

The dilatometer specimens were hardened at 2200 degrees Fahr. (1205 degrees Cent.) in a globar furnace provided with a carbonaceous muffle to minimize scaling and decarburization. Quenching was done in oil, salt, air or a lead-tin bath with automatic temperature control in most instances. Where subzero cooling was interposed in the heat treating cycle, continuous cooling from the quench bath temperature or the tempering temperature, through room temperature to the subzero temperature was employed unless otherwise

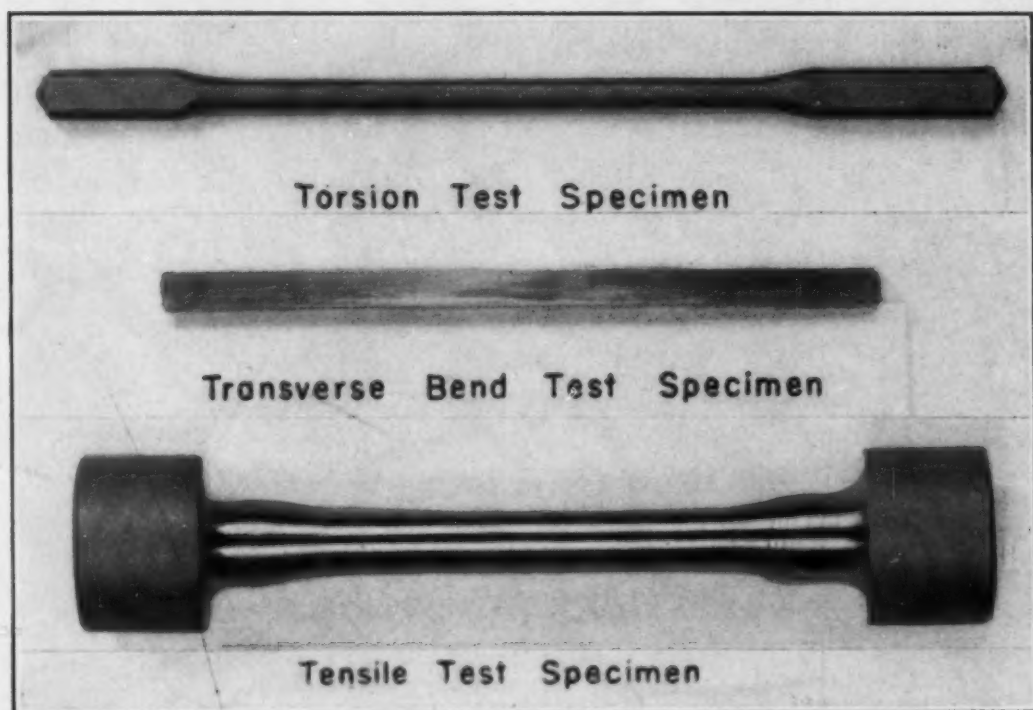


Fig. 3—Photograph of the Torsion, Transverse Bend, and Tensile Test Specimens.

noted. Temperatures down to -120 degrees Fahr. (-84 degrees Cent.) were obtained in a commercial chilling unit of the cascade type while liquid nitrogen was used for temperatures of -310 degrees Fahr. (-190 degrees Cent.). The dilatometer specimens were tempered in an electrically heated tubular air furnace which contained a copper sleeve and was specially wound to give uniform temperature distribution over a 5-inch zone. All other tools and specimens were tempered in an electrically heated lead bath furnace in which tempering temperatures were automatically controlled to ± 5 degrees Fahr.

Torsion Tests—The technique applied to the torsion testing procedure has been fully described elsewhere (17), (20). Usually

five specimens were tested for each heat treatment variation to obtain a reliable average. In some cases, particularly with heat treatments not including tempering, as many as fifteen specimens were tested for each type of heat treatment. Results for modulus of rupture values showed a maximum spread of 7.5 per cent for individual values in a group of five. The accuracy of modulus of rupture values listed in the various tables is, therefore, ± 3.8 per cent. The ultimate torque at rupture was measured directly on the Emmons torsion testing machine in pounds at 1-inch radius. These ultimate torque values were converted to modulus of rupture values using the formula:

$$S = \frac{Tr}{J} \quad \text{Where } S = \text{Modulus of Rupture} = \text{Tensile Unit Stress in the Outer Fibers}$$

$$T = \text{Ultimate Torque in pound-inches}$$

$$r = \text{Radius of cross section of specimen in inches}$$

$$J = \text{Polar moment of inertia}$$

$$= \frac{\pi d^4}{32}$$

For the torsion test specimen used in these experiments

$$d = 0.1875 \text{ inch}$$

Substituting for r and d above:

$$S = \text{Modulus of Rupture} = 773T$$

The values for plastic strain were calculated from values for plastic deformation which were directly measured on the torsion machine as angles of twist in degrees (circular). Plastic strain values, representing unit plastic strain in the outer fibers, were computed from the formula:

$$E = r\phi \quad \text{Where } E = \text{Elongation in outer fibers}$$

$$r = \text{Radius of specimen in inches} = 0.09375 \text{ inch}$$

$$\phi = \text{Angle of twist in radians}$$

$$\text{Then elongation in outer fibers} = E = 0.000545 \theta \text{ inches per inch where}$$

$$\theta = \text{Angle of twist in degrees}$$

The method of calculating plastic unit strain values may be better understood after considering a typical calculation.

$$\begin{aligned} \text{Example: Ultimate angle of twist at rupture} &= 133 \text{ degrees} \\ \text{Ultimate torque at rupture} &= 442 \text{ lb.-inches} \end{aligned}$$

After plotting a stress-strain curve the angle of twist representing the elastic portion of the total deformation is found to be 65 degrees. Then the plastic deformation may be represented as the difference between total deformation and elastic deformation or $133 - 65 = 68$ degrees. The plastic unit strain in the outer fibers is then computed as $E = 0.000545 \times 68$
 $= 0.0371$ inches per inch.

The plastic strain values are reproducible within ± 15 per cent considering the widest discrepancies. An accuracy of at least ± 10 per cent was obtained for most of the tempered specimens.

Proportional limit values have been listed with two significant figures only, since the stress-strain curves break away from the straightline (elastic) portions very gradually.

The values for modulus of elasticity in torsion have been calculated from the formula:

$$\text{Torsional Modulus of Elasticity, } G = \frac{583 \text{ TL}}{d^4 \theta}$$

Where T = Torque in pound-inches

L = Gage length of specimen

= 3 inches plus a correction for tapered ends.

d = Diameter of gage length in inches

θ = Angle of twist in degrees

For the torsion test specimens used in these investigations

$$G = 1,508,000 \frac{T}{\theta}$$

The values for modulus of elasticity depend somewhat on how accurately the straight line portion of the stress-strain curves can be plotted. No claim is made concerning the accuracy of the absolute values of modulus of elasticity, due to the method used to determine torsional strain, and to the correction applied to the gage length for the tapered portions of the torsion test specimen. A comparison between elastic properties associated with different heating and cooling treatments is all that was desired in these experiments.

Metallographic Technique—The specimens used for microstructure examination were cut from the flattened portion of the torsion test pieces transverse to the longitudinal axis. The etching reagent used was 6 per cent nital. Since it has been observed that the time required for etching a freshly polished specimen varies with the amount and condition of the tempered martensite in the structure, the etching times have been recorded. The photographic conditions of exposure, developing and printing time, and temperature, were maintained as constant as possible for the photomicrographs. Etching time was

adjusted to give a moderate density to the photomicrographs so that over-etching would not obscure fine details of the martensite.

Hardness Tests at Room Temperature—Rockwell "C" hardness measurements were made on the flat portions of the torsion specimens. Five readings were usually made on each piece and, since there were at least five test specimens for each heat treatment, the Rockwell hardness values listed in the various tables represent average values of at least 25 individual hardness measurements. No cracking was observed around impressions on any specimens.

Hardness Tests at Elevated Temperatures—The hot hardness tests were made in accordance with the method of Harder and Grove (19). Duplicate specimens, representing each type of heat treatment, were tested at 1150 degrees Fahr. (620 degrees Cent.) and another set of duplicate specimens was tested at 1300 degrees Fahr. (705 degrees Cent.). In making a test, the special dies made of heat resistant steel were first heated to the testing temperature. Then the assembly was lowered from the furnace, the specimens carefully inserted, and the assembly raised into the furnace again. About 5 to 10 minutes were required for the specimens to reach the testing temperature. They were then held at the testing temperature 20 minutes, after which the load was applied for 30 seconds. A 3000-kilogram load was used for the tests at 1150 degrees Fahr. (620 degrees Cent.) and a 1000-kilogram load was used for tests at 1300 degrees Fahr. (705 degrees Cent.). Several difficulties were encountered in making the tests. One of them was the tendency for the die parts to stick together so that they had to be pried apart with some force after many of the tests at 1150 degrees Fahr. (620 degrees Cent.). Another difficulty was to insert both specimens in the dies so that they were in exact contact along their full length. It was found that a slight overhanging would cause a considerable error in the hardness readings. Some trouble was also experienced with reading the width of the flats. It was found advisable to lightly run a fine stone over the flats to remove part of the scale. With this method the width readings could be checked within 2 parts in 100. The "Cylinder Hardness" was calculated as:

$$\text{Cylinder Hardness} = \frac{\text{Applied load in kilograms}}{\text{Area of indentation in square millimeters}}$$

"Cylinder Hardness" values were converted to conventional Brinell hardness numbers using a multiplying factor of 1.52 (18), (19).

The actual calculations of Brinell hardness were made as follows:

$$\text{For tests at 1150 degrees Fahr. (620 degrees Cent.) BHN} = \frac{1.52 \times 3000}{10 \times \frac{\text{Width of Indentation in mm.}}{10}}$$

$$\text{For tests at 1300 degrees Fahr. (705 degrees Cent.) BHN} = \frac{1.52 \times 1000}{10 \times \frac{\text{Width of Indentation in mm.}}{10}}$$

Specific Volume Measurements—The specific volume determinations were made by the usual method of weighing in air and in distilled water. Specimens were very carefully cleaned of all scale and rust and were degreased in a clean solvent. A trace of wetting agent was used to reduce the tendency for air bubbles to cling to the specimen or its supporting wire. Some slight rusting of the specimens during the weighing in water was eliminated by adding a drop of dichromate to the distilled water. The specific volume measurements were all referred to a room temperature of 72 degrees Fahr. after making the usual corrections for the suspension wire and density of the water. An accuracy of ± 3 parts in 10,000 was obtained from sample to sample.

Dilatometric Technique—The dilatometer consisted of an outer quartz tube 20 inches long by $\frac{7}{8}$ inch outside diameter and a special inner quartz tube $15\frac{1}{2}$ inches long by $\frac{1}{4}$ inch outside diameter. The inner tube was constructed with a web along its entire length, separating its cross section into two equal parts. This construction made it unnecessary to use separate insulators for the portion of the 28-gage chromel-alumel thermocouple which was contained within the inner tube. The hot junction of the thermocouple projected $1\frac{3}{8}$ inches below the $\frac{1}{4}$ -inch tube. Light metallic spacers were used to prevent the $\frac{1}{4}$ -inch tube from moving in any direction except along the longitudinal axis of the outer tube. The apparatus was similar to that used by Gordon, Cohen, and Rose (21) with the exception that specimens were inserted in the dilatometer from the top. Length changes were measured by means of a dial gage, readable to ± 0.00001 inch.

In making a run it usually took about a minute to transfer the specimen by means of special tongs from the high heat furnace to the dilatometer, lower the $\frac{1}{4}$ -inch tube so that the end rested firmly on the specimen with the hot junction of the thermocouple inside

the specimen hole, tap the tube so that the specimen rested firmly on the dome-shaped bottom and made good contact with the $\frac{1}{4}$ -inch tube, and clamp the dial gage in position. To insure continuous cooling through room temperature down to -310 degrees Fahr. (-190 degrees Cent.) a Dewar flask containing ice water was raised around the outer quartz tube when the temperature of the specimen had dropped to about 150 - 200 degrees Fahr. Later when the specimen temperature had dropped below room temperature the ice water was replaced by chilled trichlorethylene at temperatures in the neighborhood of -60 to -90 degrees Fahr. (-51 to -68 degrees Cent.). Still later, a flask containing liquid nitrogen replaced that containing the cold solvent. In this manner continuous cooling was obtained through room temperature down to the temperature of liquid nitrogen (-310 degrees Fahr.). At -310 degrees Fahr. (-190 degrees Cent.) heavy frost tends to form inside the dilatometer. This was prevented by installing a small diameter tube inside the outer quartz tube, the end of the small tube being located at the bottom of the dilatometer and in a position which did not interfere with the specimen or the $\frac{1}{4}$ -inch inner quartz tube. Nitrogen gas, which was dried by passing through a two-unit chemical drying train, was slowly circulated through the dilatometer to eliminate frosting.

Tensile Tests—The tensile tests were made on a Baldwin-Southwark 60,000-pound capacity tensile testing machine. Twelve specimens of the form shown in Figs. 2 and 3 were tested. It was found necessary to insert lead washers between the surfaces of the adapters and the specimens in order to improve the contact between them. In this way the load was applied as uniformly as possible to the specimens. With this testing method the maximum spread of tensile strength values was 2700 psi., representing an accuracy of ± 3.7 per cent.

Transverse Bend Tests—The transverse bend tests were made with a Riehle 10,000-pound capacity machine. A 3-inch span was used with a two-point loading system to provide pure bending over the middle third of the specimen. The load was applied in small increments and the resulting tensile stresses in the outer fibers were calculated from simple beam theory.

Twenty-six specimens of the form shown in Fig. 3 were tested. The accuracy of the calculated average modulus of rupture was ± 18 per cent.

Drill Testing—The test drill sizes were $\frac{1}{4}$, $\frac{1}{2}$, $\frac{57}{64}$ and 1-inch

diameter. From two to four drills were used to represent each heat treatment studied. In most cases all drills were tested from two to four grinds in each of four different types of material so that the average performance ratings represent the cutting ability of a general purpose drill. A typical example of conditions under which the drilling tests were run is shown in Table XIX.

Drills with regular heat treatment were used as standards of comparison, the results of each test being calculated as a percentage with the performance of the regularly heat treated tools taken as 100 per cent. The percentages earned by drills (having a certain heat treatment) in each material were then averaged together to obtain a final performance percentage. Thus the final average performance percentages in each test report represent from twelve to twenty-four individual tests of different sizes of drills in a wide variety of materials and under different operating conditions. In order to obtain some general comparisons between heat treatments in which subzero cooling was interposed, a summary of all of the tool tests was made. In this summary (see Table XX) five general types of heating-cooling treatments were compared to regular heat treatment. Since the various test reports, averaged together to obtain the final performance percentages, represent different numbers of individual tests, the test report percentages were multiplied by the number of individual tests which they represent and these weighted percentages were entered in Column 1 of the summary performance Table XX. The corresponding total numbers of individual tests represented by the percentages in Column 1 were entered in Column 2 as "Total Number of Grinds." Average performance ratings for the five types of heating-cooling treatments were calculated by dividing Column 1 values by Column 2 values. It is believed that this method of computing the average performance ratings eliminates some of the errors inherent in calculating relative performance ratings with unweighted averages.

The following example illustrates the method of computing average performance ratings described above. Suppose that we are required to average the results of two test reports in order to compute average performance ratings. Let us further assume that Test Report No. 1 represents six individual tests in each of four different materials, while Test Report No. 2 represents three individual tests in only two materials. Example:

Heating-Cooling Treatment	Test Report No. 1								Total No. Tests	Weighted Percentages
	Material A No. Tests	Material A Per-cent-age	Material B No. Tests	Material B Per-cent-age	Material C No. Tests	Material C Per-cent-age	Material D No. Tests	Material D Per-cent-age		
Type 1	6	80	6	120	6	110	6	130	24	$480 + 720 + 660 + 780 = 2640$
Type 2	6	100	6	100	6	100	6	100	24	$600 + 600 + 600 + 600 = 2400$

Treatment	Test Report No. 2				Total No. Tests	Weighted Percentages
	Material A No. Tests	Material A Per-cent-age	Material B No. Tests	Material B Per-cent-age		
Type 1	3	100	3	70	6	$300 + 210 = 510$
Type 2	3	100	3	100	6	$300 + 300 = 600$

The average performance ratings for Type 1 and Type 2 heating-cooling treatments would then be computed as follows:

Treatment	Total No. Grinds	Weighted Percentages	Average Performance Ratings Per Cent
Type 1	30	$2640 + 510 = 3150$	$\frac{3150}{30} = 105$
Type 2	30	$2400 + 600 = 3000$	$\frac{3000}{30} = 100$

Thus the 5 per cent performance superiority of Type 1 over Type 2 could be accepted with some confidence.

If the above method of weighting the performance percentages had not been used, but instead the usual method of averaging together unweighted percentages, the relative performance of the two types of heating-cooling treatments might have been computed as follows:

Heating-Cooling Treatment	Test Report No. 1				Average Performance
	Material A	Material B	Material C	Material D	
Type 1	80	120	110	130	110
Type 2	100	100	100	100	100

Treatment	Test Report No. 2		Average Percentage
	Material A	Material B	
Type 1	100	70	85
Type 2	100	100	100

Average Performance Rating—Per Cent		
Type 1	$\frac{110 + 85}{2} = 97$	
Type 2	$\frac{100 + 100}{2} = 100$	

In such a case it might be thought that Type 2 treatment is slightly superior to Type 1. The above examples explain the reason for adopting the method used for computing the average performance ratings in Table XX, and described on pages 261 and 262.

DISCUSSION

A preliminary dilatometer run (see Fig. 4A) was made using ordinary hardening and double tempering at 1040 degrees Fahr. (560 degrees Cent.) to give some idea of the amounts of retained austenite transformed during cooling from each tempering operation. In order to check the amount of austenite transformed, a series of specific volume measurements was made as shown in Table II.

Table II

High Heat °F.	Quenched to	Tempered	Average Specific Volume	Rockwell Hardness
2200	Room temp.	None	0.12619	65.3
2200	Room temp.	800° F., 1 hr.	0.12593	61.6
2200	Room temp.	1040° F., 1 hr.	0.12656	65.8
2200	Room temp.	1100° F., 1 hr.	0.12654	63.9
2200	Room temp.	1100° F., ½ hr. +		
		1100° F., ½ hr.	0.12652
2200	Room temp.	1150° F., 1 hr.	0.12649	61.7
2200	Room temp.	1150° F., ½ hr. +		
		1150° F., ½ hr.	0.12648

It is believed from the specific volume data of Table II that a tempering cycle of 1040 degrees Fahr. (560 degrees Cent.) for 1 hour gives practically complete decomposition of austenite retained on quenching from a hardening temperature of 2200 degrees Fahr. (1205 degrees Cent.) to room temperature. For this series of tests 100 per cent decomposition of austenite is calculated from the volume increase due to decomposition of retained austenite only, and is represented by the difference between the specific volume obtained by tempering at 800 degrees Fahr. (425 degrees Cent.) and by tempering at 1040 degrees Fahr. (560 degrees Cent.) or higher. This specific volume increase is 0.00063, or 0.50 per cent. Fig. 4A indicates that total decomposition of austenite corresponds to a linear increase of 19×10^{-4} inches per inch or 0.19 per cent which equals a volume increase of 3×0.19 or 0.57 per cent. The slightly greater austenite decomposition shown in the dilatometer chart, Fig. 4A, as compared to that computed from specific volume changes may be due to the fact that somewhat more austenite was carried into the tempering operation by quenching to 140 degrees Fahr. before tempering (dilatometer test) than by quenching to room temperature (specific volume data, Table II) as has been demonstrated by Gordon, Cohen and Rose (22).

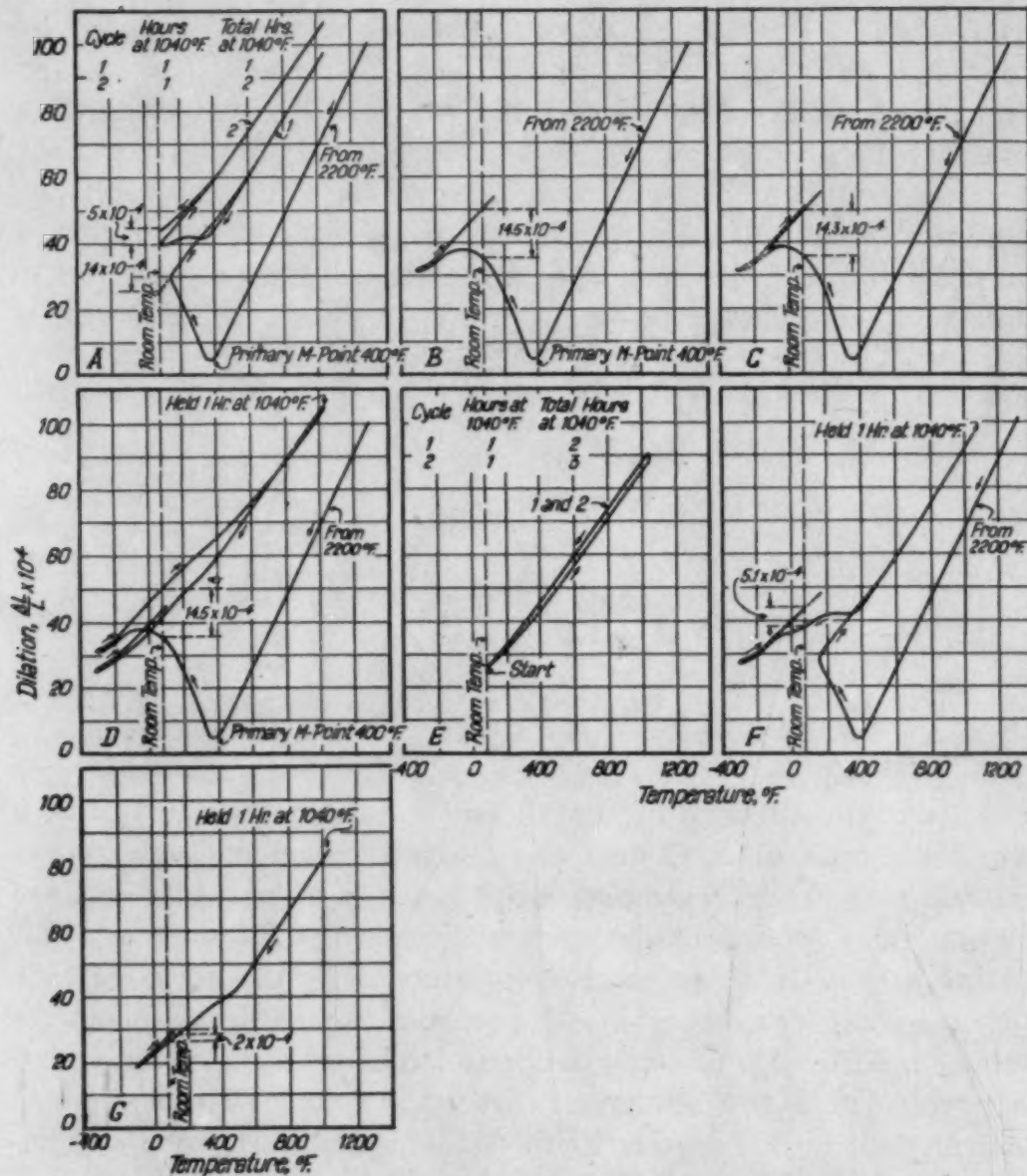


Fig. 4—Dilation Curves. A. Regular Hardening Plus Double Tempering at 1040 Degrees Fahr. (560 Degrees Cent.). B. Effect of Continuous Cooling from 2200 to -310 Degrees Fahr. (1205 to -190 Degrees Cent.). C. Effect of Continuous Cooling from 2200 to -120 Degrees Fahr. (1205 to -84 Degrees Cent.). D. Effect of Continuous Cooling from 2200 to -310 Degrees Fahr. (1205 to -190 Degrees Cent.) plus Tempering at 1040 Degrees Fahr. (560 Degrees Cent.) followed by Continuous Cooling a Second Time to -310 Degrees Fahr. (-190 Degrees Cent.). E. Effect of Multiple Tempering at 1040 Degrees Fahr. (560 Degrees Cent.) after the Heating-Cooling Cycles Shown in Curve D. F. Effect of Continuous Cooling from a Tempering Temperature of 1040 to -310 Degrees Fahr. (560 to -190 Degrees Cent.). G. Effect of Continuous Cooling from a Tempering Temperature of 1040 to -120 Degrees Fahr. (560 to -84 Degrees Cent.). (Quenched to Room Temperature Before Tempering.) (Average Cooling Rates Were 80 Degrees Fahr. per Minute from 2200 to 200 Degrees Fahr., and Were 12 Degrees Fahr. per Minute from 200 to Subzero Temperatures.)

Fig. 4B shows the effect of continuous cooling from the high heat to a subzero temperature of -310 degrees Fahr. (-190 degrees Cent.). The transformation of austenite to martensite produced by the subzero cooling in this case amounts to a linear expan-

sion of 14.5×10^{-4} inches per inch or 0.145 per cent, corresponding to a cubical expansion of 3×0.145 or 0.43 per cent. This increase checks well with the measured specific volume increase of 0.0005 (see Table III) or 0.40 per cent for specimens continuously cooled from 2200 to -120 degrees Fahr. (1205 to -84 degrees Cent.). However, Fig. 4C shows that the linear expansion due to continuous cooling to -120 degrees Fahr. (-84 degrees Cent.) is 14.3×10^{-4} inches per inch or 0.143 per cent corresponding to a cubical expansion of 3×0.143 or 0.43 per cent, which also checks well with the specific volume increase noted in Table III. Since the dilatometer curves of Fig. 4C and Fig. 4 B indicate that 95 per cent or more of the low temperature transformation occurring on continuous cooling to -310 degrees Fahr. (-190 degrees Cent.) also occurs on continuous cooling to -120 degrees Fahr. (-84 degrees Cent.), the latter temperature was used for most of the subzero treatments of torsion specimens and test tools.

Fig. 4D shows the effect of tempering at 1040 degrees Fahr. (560 degrees Cent.) for 1 hour after subzero hardening. The subzero transformation of a considerable part of the retained austenite has left only a portion to transform during tempering and the attendant expansion of this remainder on tempering is considerably overshadowed by the contraction which occurs on heating up in the range 200 to 800 degrees Fahr. (95 to 425 degrees Cent.). This contraction has been shown to be due to transformation of tetragonal martensite to tempered martensite and to slight carbide precipitation (14). Specific volume and hardness measurements on a series of specimens tempered at various temperatures after regular hardening and after subzero hardening are listed in Table III. They definitely show that after subzero hardening only a limited amount of austenite remains to transform to martensite on subsequent tempering.

Table III

Tempering	Subzero Hardened (2200° F. to -120° F.)		Regularly Hardened (2200° F. to Room Temperature)	
	Rockwell C	Specific Volume	Rockwell C	Specific Volume
None	67.8	0.12669	65.3	0.12619
400° F., 1 hr.	64.9	0.12646	62.3
800° F., 1 hr.	64.2	0.12619	61.6	0.12593
1040° F., 1 hr.	64.7	0.12651	65.8	0.12656
1100° F., 1 hr.	63.7	0.12654	63.9	0.12654
1150° F., 1 hr.	60.5	0.12649	61.7	0.12649

The volume increase due to tempering after subzero hardening is 0.00032 or 0.25 per cent. Since the transformation of all the retained austenite by tempering (after hardening at 2200 degrees Fahr.) is attended by a volume increase of 0.00063 or 0.50 per cent, it is evident that $\frac{0.25}{0.50}$ or 50 per cent of the retained austenite remains untransformed after the subzero cooling to -120 degrees Fahr. (-84 degrees Cent.). Consequently 50 per cent of the retained austenite transforms on continuous cooling after hardening to -120 degrees Fahr. (-84 degrees Cent.) and the accompanying volume change is 0.40 per cent as already mentioned.

As a further explanation of the overall contraction of the dilatometer specimen (Fig. 4D) after subzero hardening and tempering at 1040 degrees Fahr. (560 degrees Cent.) for 1 hour, it can be seen from Table III that the specific volume after tempering the subzero hardened specimen at 1040 degrees Fahr. (560 degrees Cent.) is 0.12651 which is considerably less than the volume (0.12669) before tempering.

The second subzero cooling cycle shown in Fig. 4D produced only a very slight expansion indicating that practically all of the retained austenite had transformed as a result of the previous subzero cooling and tempering. The same specimen which was subjected to two subzero cooling cycles and one tempering treatment in Fig. 4D was next retempered twice at 1040 degrees Fahr. (560 degrees Cent.) as shown in Fig. 4E. No overall expansion occurred as a result of this multiple tempering and this fact further substantiated the conclusion that all retained austenite had been transformed.

Dilatometric investigation of the effects of subzero cooling after tempering are shown in Figs. 4F and 4G. Fig. 4F shows the dilation of a specimen quenched from 2200 to 140 degrees Fahr. (1205 to 60 degrees Cent.), immediately tempered at 1040 degrees Fahr. (560 degrees Cent.) for 1 hour and continuously cooled to -310 degrees Fahr. (-190 degrees Cent.) from the tempering temperature. Fig. 4G shows the tempering and subzero cooling of a specimen which had been quenched from 2200 degrees Fahr. to room temperature and aged at room temperature 24 hours before tempering. Subzero cooling has resulted in a linear expansion of 0.02 per cent representing a cubical expansion of 0.06 per cent. This is somewhat larger than the corresponding 0.024 per cent increases observed in specific volume on cooling to a subzero temperature of -120 degrees Fahr. after tempering.

Torsion and Hardness Tests—Having made a preliminary investigation of the behavior of molybdenum-tungsten high speed steel during subzero cooling before and after tempering, a series of hardness and torsion tests was carried out to determine the effect on physical properties of the variables connected with subzero cooling. For these tests subzero cooling to a temperature of -120 degrees Fahr. (-84 degrees Cent.) was used, although, temperatures be-

Table IV

Rate of Cooling °F. Per Min.	Rockwell "C" Hardness	Modulus of Rupture (Lb. Per In. ²)	Torsional Modulus of Elasticity	Proportional Limit (Lb. Per In. ²)	Plastic Strain (Inches Per Inch)
80	65.1	332,000	10,200,000	193,000	0.040
0.6	64.7	328,000	10,200,000	180,000	0.036

tween -25 and -120 degrees Fahr. (-33 and -84 degrees Cent.) were also investigated.

Effect of Rate of Cooling to -120 degrees Fahr. (-84 degrees Cent.)—Torsion and hardness tests were made on a series of specimens in which the rate of cooling to -120 degrees Fahr. (-84 degrees Cent.) after quenching and before tempering was varied from approximately 80 degrees Fahr. (26 degrees Cent.) per minute to 0.6 degrees Fahr. per minute. The results of these tests (Table IV) show that the rate of cooling to -120 degrees Fahr. after harden-

Table V
Effect of Time of Holding at -120 Degrees Fahr. After Hardening
(No Subsequent Tempering)

Time at -120° F. Minutes	Rockwell C Hardness	Modulus of Rupture (Lb. Per In. ²)	Torsional Modulus of Elasticity	Proportional Limit (Lb. Per In. ²)	Plastic Strain
1	67.3 ^a	294,000	9,500,000	170,000	0.016
10	67.4	266,000	9,700,000	140,000	0.009
60	67.6	277,000	9,900,000	130,000	0.010
120	67.9	266,000	9,400,000	170,000	0.007
1440	67.2	279,000	9,700,000	120,000	0.010

Table VI
Effect of Time of Holding at -120 Degrees Fahr. After Hardening
(Subsequently Tempered at 1040 Degrees Fahr. 1 Hour)

Time at -120° F. Minutes	Rockwell C Hardness	Modulus of Rupture (Lb. Per In. ²)	Torsional Modulus of Elasticity	Proportional Limit (Lb. Per In. ²)	Plastic Strain
1	65.0	333,000	10,500,000	200,000	0.028
10	64.9	332,000	10,100,000	170,000	0.030
60	64.6	328,000	10,200,000	200,000	0.027
120	64.7	328,000	10,400,000	180,000	0.029
1440	64.5	331,000	10,200,000	180,000	0.029

ing has no appreciable effect on such physical properties as hardness, strength and plasticity after tempering at 1040 degrees Fahr. for 1 hour.

Effect of Time of Holding at -120 degrees Fahr. (-84 degrees Cent.)—The effect of the time of holding at -120 degrees Fahr. (-84 degrees Cent.) after continuous cooling from a hardening temperature of 2200 degrees Fahr. (1205 degrees Cent.) was studied with a series of specimens which were subzero hardened, but not tempered, and with a series which were subzero hardened and subsequently tempered at 1040 degrees Fahr. (560 degrees Cent.) for 1 hour. The results of these tests are shown in Tables V and VI.

The results of Tables V and VI indicate that no significant changes in hardness, strength or plasticity are produced by increasing

Table VII
Effect of Time of Holding at -120 Degrees Fahr. After Tempering

Time at -120° F. Minutes	Rockwell C Hardness	Modulus of Rupture (Lb. Per In. ²)	Torsional Modulus of Elasticity	Proportional Limit (Lb. Per In. ²)	Plastic Strain
10	66.1	338,000	10,100,000	150,000	0.031
120	65.9	342,000	10,100,000	180,000	0.039
1440	65.4	339,000	10,200,000	170,000	0.035

the time of holding at -120 degrees Fahr. (-84 degrees Cent.) beyond 10 minutes. These conclusions are in agreement with tests made with 18-4-1 high speed steel by Gordon and Cohen (1).

Effect of Time of Holding at -120 degrees Fahr. After Tempering—A series of specimens were hardened at 2200 degrees Fahr. (1205 degrees Cent.), quenched in oil to about 1000 degrees Fahr. (540 degrees Cent.), air-cooled to room temperature and tempered at 1040 degrees Fahr. (560 degrees Cent.) for 1 hour. They were then continuously cooled from the tempering temperature to -120 degrees Fahr. (-84 degrees Cent.) and held for various periods of time. The results of these tests are listed in Table VII.

The results of Table VII indicate that variations in the time of holding at -120 degrees Fahr. (-84 degrees Cent.) after tempering have no effect on hardness, strength, or plasticity. Apparently the full effect of subzero treatment at -120 degrees Fahr. (-84 degrees Cent.), either before or after tempering, can be attained by short holding times at the low temperature. In practice this means holding at -120 degrees Fahr. (-84 degrees Cent.) long enough to ensure that the entire piece has attained the low temperature.

Effect of Various Subzero Temperatures—The effects of various subzero temperatures were studied with two series of specimens. The first was hardened at 2200 degrees Fahr. (1205 degrees Cent.) and continuously cooled to subzero temperatures ranging from -25 to -120 degrees Fahr. (-33 to -84 degrees Cent.) without subsequent tempering. The second series was hardened at 2200 degrees Fahr. (1205 degrees Cent.), cooled to temperatures ranging from -25 to -120 degrees Fahr., and subsequently tempered at 1040 degrees Fahr. (560 degrees Cent.) for 1 hour. Specific volume

Table VIII
Effect of Various Subzero Temperatures After Hardening
(No Subsequent Tempering)

Continuously Cooled After Hardening to a Subzero Temperature of	Rockwell C Hard- ness	Modulus of Rupture (Lb. Per In. ²)	Torsional Modulus of Elasticity	Proportional Limit (Lb. Per In. ²)	Plastic Strain (Inches Per Inch)	Specific Volume
80° F. (Reg.)	65.3	236,000	9,400,000	91,000	0.017	0.12619
— 25° F.	67.2	252,000	9,400,000	130,000	0.009	0.12650
— 50° F.	67.4	249,000	9,400,000	130,000	0.007	0.12654
—100° F.	67.3	257,000	9,400,000	160,000	0.007	0.12658
—120° F.	67.9	266,000	9,400,000	170,000	0.007	0.12669

Table IX
Effect of Various Subzero Temperatures After Hardening
(Subsequently Tempered at 1040 Degrees Fahr.—1 Hour)

Continuously Cooled After Hardening to a Subzero Temperature of	Rockwell C Hard- ness	Modulus of Rupture (Lb. Per In. ²)	Torsional Modulus of Elasticity	Proportional Limit (Lb. Per In. ²)	Plastic Strain (Inches Per Inch)	Specific Volume
80° F. (Reg.)	65.8	342,000	10,200,000	160,000	0.037	0.12656
— 25° F.	65.2	325,000	9,900,000	210,000	0.020	0.12656
— 50° F.	65.2	330,000	9,900,000	200,000	0.026	0.12648
—100° F.	65.1	328,000	10,200,000	209,000	0.028	0.12649
—120° F.	64.7	328,000	10,400,000	180,000	0.029	0.12651

measurements were made on these specimens in addition to the hardness and torsion tests. Results are shown in Tables VIII and IX.

The results of Table VIII are interesting because they reveal that enough retained austenite is transformed to martensite by continuous cooling to only -25 degrees Fahr. (-33 degrees Cent.) to cause a distinct increase in hardness, volume, modulus of rupture, and proportional limit and a decrease in plasticity as compared to cooling to room temperature. Another very interesting point is that subzero transformation of 50 per cent of all the retained austenite gives no increase in modulus of elasticity. However, when the subzero hardened specimens are tempered (Table IX) transforming

Table X
Effect of Various Subzero Temperatures After Tempering

Continuously Cooled After Tempering to a Subzero Temperature of	Rockwell C Hardness	Modulus of Rupture (Lb. Per In. ²)	Torsional Modulus of Elasticity	Proportional Limit (Lb. Per In. ²)	Plastic Strain (Inches Per Inch)
80° F. (Reg.)	65.8	342,000	10,200,000	160,000	0.037
- 25° F.	65.9	345,000	9,900,000	190,000	0.046
-120° F.	65.9	342,000	10,100,000	180,000	0.039

the remaining 50 per cent of the retained austenite and tempering the primary martensite formed by the subzero cooling, a significant increase in modulus of elasticity is obtained.

Table IX reveals that tempering at 1040 degrees Fahr. (560 degrees Cent.) for 1 hour after cooling to various subzero temperatures causes the untransformed austenite to transform to martensite, and results in an increase of strength and plasticity (compare with Table VIII). As compared with the data for regularly hardened and tempered specimens, the subzero hardening treatments have resulted in lower strength, hardness and plasticity. Apparently subzero transformation of up to 50 per cent of the retained austenite allows the martensite thus formed to be so thoroughly softened on subsequent tempering at 1040 degrees Fahr. (560 degrees Cent.) that it does not contribute its full share to the hardness and strength of the structure. The transformation of the 50 per cent of untransformed austenite to martensite on cooling from the tempering temperature is not sufficient to offset the overall softening effect due to overtempering the martensite formed during subzero cooling, and due to the relief of quenching stresses.

Inserting a cooling treatment of -25 or -120 degrees Fahr. (-32 or -84 degrees Cent.) after tempering (Table X), produced little change in the physical properties associated with regular hardening and tempering. This is not surprising since the data of Table III show that tempering at 1040 degrees Fahr. (560 degrees Cent.) for 1 hour transforms practically all of the retained austenite, leaving none to transform during subsequent cooling to subzero temperatures.

Effect of Aging at Room Temperature Prior to Subzero Cooling—A series of tests was made to determine the effect of aging at room temperature after hardening and before cooling to subzero temperature. As already mentioned, Gulyaev (5) and Gordon and Cohen (1) have noted the marked stabilizing effect of room tempera-

Table XI
Effect of Aging at Room Temperature Prior to Cooling to -120 Degrees Fahr.
(No Subsequent Tempering)

Time of Aging at Room Temperature	Rockwell C Hardness	Modulus of Rupture (Lb. Per In. ²)	Torsional Modulus of Elasticity	Proportional Limit (Lb. Per In. ²)	Plastic Strain (Inches Per Inch)
None (Continuous cooling)	67.9	266,000	9,400,000	170,000	0.007
20 min.	67.7	221,000	9,400,000	150,000	0.003
24 hrs.	67.1	223,000	9,400,000	150,000	0.004

ture aging in the case of 18-4-1 high speed steel. In the present investigation three series of specimens were hardened at 2200 degrees Fahr. (1205 degrees Cent.). The first series was quenched in oil to about 1000 degrees Fahr. (540 degrees Cent.), and air-cooled to

Table XII
Effect of Aging at Room Temperature Prior to Cooling to -120 Degrees Fahr.
(Subsequently Tempered at 1040 Degrees Fahr.—1 Hour)

Time of Aging at Room Temperature	Rockwell C Hardness	Modulus of Rupture (Lb. Per In. ²)	Torsional Modulus of Elasticity	Proportional Limit (Lb. Per In. ²)	Plastic Strain (Inches Per Inch)
None (Continuous cooling)	64.7	328,000	10,400,000	180,000	0.029
20 min.	64.9	329,000	10,500,000	180,000	0.027
1 hr.	64.4	326,000	10,500,000	180,000	0.027
24 hr.	64.5	325,000	10,500,000	180,000	0.022

140 degrees Fahr. A group of specimens was then continuously cooled to -120 degrees Fahr. (-84 degrees Cent.). Other groups were aged at room temperature for periods of time up to 24 hours

Table XIII
Effect of Aging at Room Temperature After Tempering and Prior to Cooling to -120 Degrees Fahr.

Time of Aging at Room Temperature	Rockwell C Hardness	Modulus of Rupture (Lb. Per In. ²)	Torsional Modulus of Elasticity	Proportional Limit (Lb. Per In. ²)	Plastic Strain (Inches Per Inch)
None (Continuous cooling)	65.9	342,000	10,100,000	180,000	0.039
20 min.	66.1	350,000	9,900,000	160,000	0.044
1 hr.	66.3	345,000	10,200,000	150,000	0.041
24 hrs.	66.2	348,000	9,900,000	160,000	0.045

after which they were cooled to -120 degrees Fahr. (-84 degrees Cent.). In the second series, specimens were treated in a similar manner to those of the first series except that the subzero cooling was followed by tempering at 1040 degrees Fahr. (560 degrees

Cent.) for 1 hour. The third series of tests was made by first hardening at 2200 degrees Fahr. (1205 degrees Cent.), oil quenching to 1000 degrees Fahr. (540 degrees Cent.), air cooling to room temperature and tempering at 1040 degrees Fahr. (560 degrees Cent.) for 1 hour. One group of this series was continuously cooled from the tempering temperature to -120 degrees Fahr. (-84 degrees Cent.). Other groups were aged at room tempera-

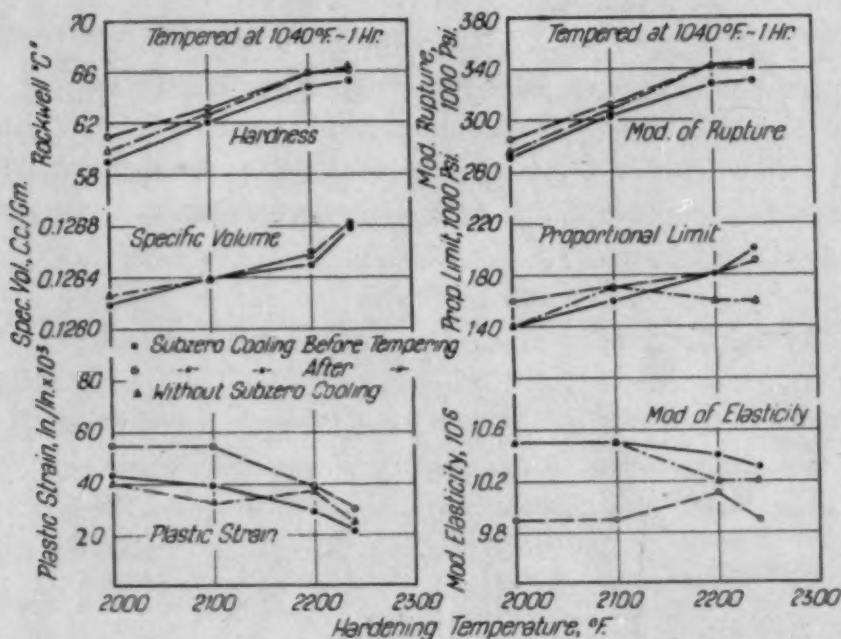


Fig. 5—Effect of Subzero Cooling to -120 Degrees Fahr. (-84 Degrees Cent.) in Conjunction with Hardening at Various Temperatures.

ture for various periods of time before cooling to -120 degrees Fahr. (-84 degrees Cent.). Tables XI, XII, and XIII show the results of the three series of tests.

Table XI reveals that room temperature aging prior to subzero cooling decreases the amount of martensite formed during subsequent cooling to -120 degrees Fahr. (-84 degrees Cent.) as evidenced by lower hardness and strength.

Table XII reveals that the stabilizing effect of room temperature aging noted in Table XI is not so evident after subsequent tempering.

Table XIII shows no significant effect on hardness, strength or plasticity as a result of aging at room temperature after tempering.

Effect of Austenitizing at Various Temperatures in Conjunction With Subzero Cooling to -120 degrees Fahr.—Since Gulyaev (5)

showed that higher hardening temperatures lower the austenite-martensite transformation range of 18-4-1 high speed steel to temperatures below room temperature, it was decided to investigate this point with respect to molybdenum-tungsten high speed steel. Three series of tests were carried out. The first series consisted of austenitizing several sets of specimens at temperatures from 2000 to 2240 degrees Fahr. (1095 to 1225 degrees Cent.), followed by regular oil quenching to approximately 1000 degrees Fahr. (540 degrees Cent.), air cooling to room temperature and tempering at 1040 degrees Fahr. (560 degrees Cent.) for 1 hour. The second series was similar to the first except that subzero cooling to -120 degrees Fahr. (-84 degrees Cent.) was interposed in the heat treating cycle after quenching and prior to tempering. In the third series subzero cooling was interposed after tempering. The results of these three series of tests are shown in Fig. 5.

Effect of Various Hardening Temperatures Without Subzero Cooling—A study of Fig. 5 shows that there is a general increase in hardness, specific volume, strength and proportional limit and a decrease in plasticity as the hardening temperature is raised. The increases indicate that at the higher hardening temperatures the structure is composed of more martensite or that the martensite is intrinsically more stable, possibly due to a higher carbon content. Such a concept is in line with the theory developed by Emmons (23) that the stability of both austenite and martensite is dependent on the amount of carbon in solid solution.

Effect of Various Hardening Temperatures in Conjunction with Subzero Cooling Prior to Tempering—A comparison between the curves illustrating the effect of various hardening temperatures on specimens cooled to subzero temperature *before tempering* (solid dots—Fig. 5) and the curves for *normal heat treatment* (triangles—Fig. 5) shows that the subzero treatment causes a general lowering of hardness, specific volume and strength. The following explanation is offered for this behavior. Subzero cooling after quenching from the hardening heat causes transformation of part of the retained austenite as evidenced by significant increases in specific volume and hardness (see data in Tables III and VIII). As a result of this low temperature transformation, more primary martensite and less retained austenite are carried into the subsequent tempering operation. Consequently, less secondary martensite forms on cooling from the tempering temperature and the structure, after tempering,

consists of more fully tempered primary martensite and less untempered secondary martensite. This condition results in the observed general decrease in hardness and strength mentioned above.

Reference to Fig. 5 reveals that hardening temperatures as low as 2000 and 2100 degrees Fahr., in conjunction with subzero cooling before tempering, result in the lower hardness and strength already mentioned, but also result in an increase in plasticity as compared to normal heat treatment. At higher hardening temperatures such as 2200 and 2240 degrees Fahr., however, subzero cooling before tempering results in decreased hardness, strength and plasticity as compared to normal heat treatment.

Effect of Various Hardening Temperatures in Conjunction with Subzero Cooling After Tempering—Subzero cooling after tempering produces a slight increase in hardness, specific volume, and strength and a marked increase in plasticity at hardening temperatures as low as 2000 to 2100 degrees Fahr. (1095 to 1150 degrees Cent.). This increment of plasticity is rather interesting in view of the accompanying increment of hardness and strength. It is possible that subzero cooling after tempering might be employed with lower hardening temperatures to give extra toughness where maximum strength and hardness are not necessary. The marked increase in plasticity with slight improvement in strength and hardness which subzero cooling after tempering gives when the hardening temperature is below normal (i. e., below that at which the combination of hardness, strength, and toughness is a maximum), may account for the improvement in tool performance noted frequently in trade journal reports. It is possible that many tools purchased on the market may be accidentally or purposely underhardened, and would show a slight improvement in hardness and toughness when subjected to subzero treatment. At hardening temperatures which develop maximum hardness and strength, 2200 to 2240 degrees Fahr. (1205 to 1225 degrees Cent.), subzero cooling after tempering gives about the same hardness, specific volume, strength and ductility as does regular hardening. This is to be expected in view of the fact that the slight increase in specific volume and dilation (Fig. 4G) accompanying subzero cooling to -120 degrees Fahr. (-84 degrees Cent.) after tempering at 1040 degrees Fahr. (560 degrees Cent.) for 1 hour indicates that practically all of the retained austenite transforms on cooling from the tempering temperature to room temperature, leaving only a very small amount to transform on further cooling to sub-

zero temperatures. In this respect it is interesting to note that Fig. 4F shows more subzero transformation of austenite after tempering when the steel is quenched to 140 degrees Fahr. prior to tempering than when it is quenched to room temperature. This is to be expected since more austenite is carried into the tempering operation as the temperature reached during quenching is raised (22). In order to study the effects of subzero cooling in conjunction with heat treat-

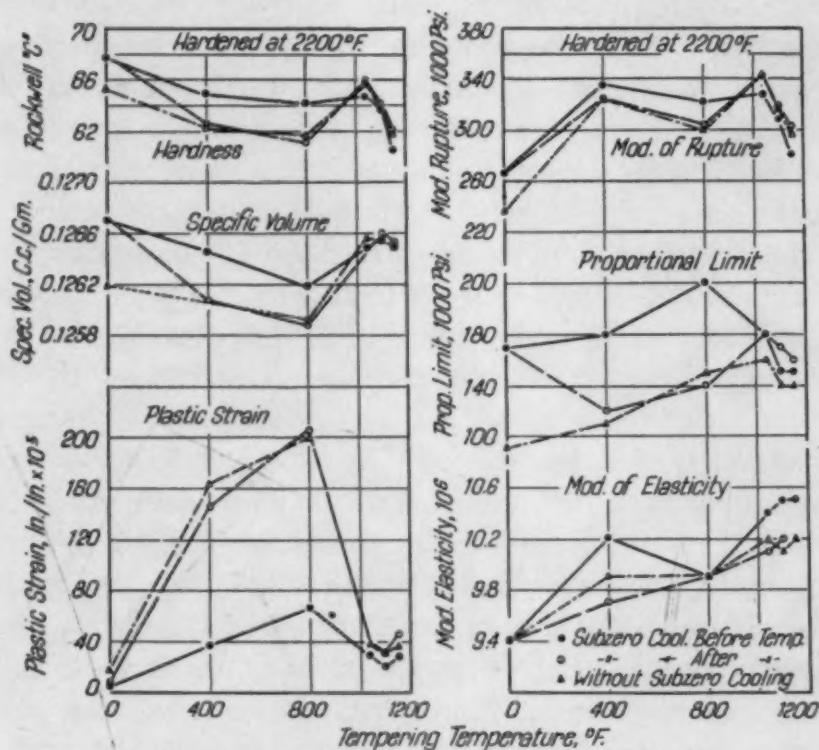


Fig. 6—Effect of Subzero Cooling to -120 Degrees Fahr. (-84 Degrees Cent.) Before and After Tempering at Various Temperatures.

ments which induce the retention of increasing amounts of austenite, several treatments involving quenching at temperatures above room temperature were later applied to test drills (Table XIX) and torsion test specimens (Tables XIV and XV).

Effect of Subzero Cooling Before and After Tempering at Various Temperatures—Three series of tests were undertaken to investigate the effect of tempering in conjunction with subzero cooling. The first series consisted of hardening a set of specimens at 2200 degrees Fahr. (1205 degrees Cent.), quenching in oil to approximately 1000 degrees Fahr. (540 degrees Cent.), air cooling to room temperature and tempering at various temperatures up to 1150 degrees Fahr. (620 degrees Cent.) for 1 hour. The second series

was similar to the first except that subzero cooling to -120 degrees Fahr. (-84 degrees Cent.) was interposed in the heat treatment cycle after quenching and prior to tempering. In the third series subzero cooling was placed after the tempering. The results of these three series of tests are shown in Fig. 6.

Effect of Subzero Cooling Prior to Tempering at Various Temperatures—Fig. 6 reveals that there is a pronounced difference in the effect of subzero cooling prior to tempering (solid dots—Fig. 6) depending on whether the tempering is carried out below or above 1000 degrees Fahr. (540 degrees Cent.). With tempering temperatures less than 1000 degrees Fahr. (540 degrees Cent.), subzero cooling increases hardness, specific volume, strength and proportional limit and decreases plasticity as compared to normal heat treatment. These effects appear to be due to the presence of the extra martensite formed as a result of the subzero treatment. When the tempering temperature is 1040 degrees Fahr. (560 degrees Cent.) or above, subzero cooling results in slight decreases in hardness, specific volume, plasticity, and strength, while the proportional limits and modulus of elasticity are increased. The advantage in hardness and strength associated with regular hardening and tempering at 1040 degrees Fahr. (560 degrees Cent.) (triangles—Fig. 6) over subzero hardening and tempering is probably due to the presence of more untempered martensite in the normally heat treated specimens. The additional untempered martensite produced by normal heat treatment gives a slight increase in ductility rather than a decrease as one might expect. Fig. 6 shows that normal hardening gives superior plasticity as compared to subzero hardening at all tempering temperatures up to 1150 degrees Fahr. (620 degrees Cent.). The greatest increase in plasticity is shown at a tempering temperature of 800 degrees Fahr. (425 degrees Cent.). At this temperature normal hardening gives three times the plasticity that subzero hardening gives. It is possible that the martensite formed at -120 degrees Fahr. (-84 degrees Cent.) is more resistant to softening up to tempering temperatures around 800 degrees Fahr. (425 degrees Cent.) than is the primary martensite formed on quenching. The results shown in Fig. 6 with respect to comparisons between regular and subzero hardening are somewhat similar to those observed for 18-4-1 high speed steel by Gordon and Cohen (1) and by Roberts and Gill (15).

Effect of Subzero Cooling After Tempering at Various Temperatures—With regard to subzero cooling after tempering (curves

—Fig. 6)—the effects are much less than with subzero cooling prior to tempering. At 400 degrees Fahr. (205 degrees Cent.) subzero cooling produces little change in hardness and strength although the plasticity is somewhat less as compared to normal heat treatment. At 800 degrees Fahr. (425 degrees Cent.) there is also little change effected by subzero cooling. At 1040 and 1100 degrees Fahr. (560 and 595 degrees Cent.) subzero cooling after tempering shows an increase in hardness which is too small to be considered significant. The amount of subzero transformation after tempering for 1 hour at 1040 degrees Fahr. (560 degrees Cent.) or higher is considerably less than was observed for 18-4-1 high speed steel (1), while with no tempering it is somewhat greater. At 1150 degrees Fahr. (620 degrees Cent.) subzero cooling shows some small increases in hardness, strength, and plasticity, but again the increases cannot be considered significant.

The "as-quenched" hardness data of Fig. 6 suggests an additional explanation for some of the tool performance improvements due to subzero cooling mentioned in the literature. Finish grinding of very hard tools often causes a very thin layer of the tool surface to be heated above the critical temperature. Consequently this layer has been hardened but has not been tempered. (Its presence may sometimes be detected as an unetched white zone in microspecimens which have been cut and polished in a plane perpendicular to a ground tool surface.) If the improperly ground tool is used in this condition it will likely perform poorly due to the softness of the untempered surface layer. When the same tool is cooled to subzero temperatures the hardness of the untempered layer may increase 3 or more points on the Rockwell C scale and this additional surface hardness may give improved wear resisting qualities to the tool.

Effect of Subzero Cooling in Conjunction with Hot Quenching at 1100 degrees Fahr.—The effect of subzero cooling in conjunction with hot quenching at 1100 degrees Fahr. (595 degrees Cent.) was studied with the subzero cooling interposed in the heat treatment cycle (a) before single tempering at 1040 degrees Fahr. (560 degrees Cent.), (b) before and between multiple tempering treatments at 1000 degrees Fahr. (540 degrees Cent.), and (c) before and between multiple tempering treatments at 1040 degrees Fahr. (560 degrees Cent.). The results of these tests are listed in Table XIV. It is apparent that hot quenching for even 10 minutes at 1100 degrees Fahr. (595 degrees Cent.) has stabilized the austenite to such an

Table XIV
Effect of Hot Quenching at 1100 Degrees Fahr. with Subzero Cooling Interposed (a) Before Single Tempering at 1040 Degrees Fahr., (b) Before and Also During a Multiple Tempering Cycle at 1000 Degrees Fahr., and (c) Before and During Multiple Tempering Cycles at 1040 Degrees Fahr.

Treatment	Rockwell Hardness ("C" Scale)	Modulus of Rupture (Lbs. Per In. ²)	Torsional Modulus of Elasticity	Proportional Limit (Lbs. Per In. ²)	Plastic Strain (Inches Per Inch)	Specific Volume C.C. Per Gm.
Normal Practice: Austenitized at 2200° F. Quenched to approximately 1000° F. Air-cooled to room temperature. Tempered at 1040° F., 1 hour	65.8	342,000	10,200,000	160,000	0.037	0.12656
Austenitized at 2200° F. Salt bath quenched at 1100° F., held 10 minutes. Air-cooled to approximately 150° F. Continuously cooled to -120° F. and held 2 hours.						
Subsequently:						
Not tempered	67.1	234,000	9,900,000	120,000	0.005	0.12652
Tempered at 1040° F., 1 hour	64.2	325,000	10,300,000	180,000	0.033	0.12662
Tempered at 1000° F., 3 hours. Continuously cooled to -120° F. and held for 2 hours. Retempered at 1000° F., 3 hours.	64.4	325,000	10,500,000	210,000	0.025	0.12650
Tempered at 1040° F., 30 minutes. Continuously cooled to -120° F. and held for 2 hours. Retempered at 1040° F., 30 minutes.	64.0	322,000	10,500,000	140,000	0.035
Tempered at 1040° F., 1 hour. Continuously cooled to -120° F. and held for 2 hours. Retempered at 1040° F., 1 hour.	64.0	322,000	10,500,000	170,000	0.028

extent that continuous cooling to -120 degrees Fahr. (-84 degrees Cent.) produces only part of the subzero transformation produced after ordinary quenching. This is shown by the fact that the specific volume of the hot-quenched specimens is 0.12652 and hardness is 67.1, as compared to 0.12669 and 67.8 respectively for specimens subzero hardened without hot quenching (Table III). Tempering at 1040 degrees Fahr. (560 degrees Cent.) specimens which have been hot-quenched at 1100 degrees Fahr. (595 degrees Cent.) and continuously cooled to -120 degrees Fahr. (-84 degrees Cent.) causes a marked increase in specific volume from 0.12652 to 0.12662, whereas such tempering causes a considerable decrease in specific volume with specimens subzero hardened without hot quenching at 1100 degrees Fahr. (595 degrees Cent.). This is a further demonstration that hot quenching stabilizes the austenite so that it does not transform as freely on cooling to -120 degrees Fahr. (-84 degrees Cent.), leaving a larger percentage to be carried into the tempering operation.

Interposing single or multiple subzero cooling treatments in the heat treating cycle before and between multiple tempering operations produces no improvements in the hardness, strength or plasticity of the hot-quenched specimens.

Effect of Subzero Cooling in Conjunction with Hot Quenching at 320 degrees Fahr.—The effect of subzero cooling in conjunction with hot quenching in the martensite region at 320 degrees Fahr. (160 degrees Cent.) was studied with subzero cooling interposed in the heat treating cycle (a) before single tempering at 1040 degrees Fahr. (560 degrees Cent.), and (b) before and between multiple tempering operations at 1040 degrees Fahr. The results of these tests are shown in Table XV. The data of Table XV reveal no substantial changes in hardness, strength, or plasticity as compared with ordinary hardening or subzero hardening without hot quenching.

Some of the heat treatment variations listed in Tables XIV and XV were applied to test drills in order to study their effect on tool performance. Results of these drilling tests are included in the performance summary, Table XX.

Mutual Indentation Hot Hardness Tests—Mutual indentation hardness tests were made at 1150 and 1300 degrees Fahr. (620 and 705 degrees Cent.) in order to determine whether any effects of subzero cooling might persist at high tempering temperatures. In these

Table XV

Effect of Hot Quenching in the Martensite Region at 320 Degrees Fahr. with Subzero Cooling Interposed (a) Before Single Tempering at 1040 Degrees Fahr., and (b) Before and Also During Multiple Tempering at 1040 Degrees Fahr.

Treatment	Rockwell "C" Hardness	Modulus of Rupture (Lbs. Per In. ²)	Torsional Modulus of Elasticity	Proportional Limit (Lbs. Per In. ²)	Plastic Strain (Inches Per Inch)
Normal Practice: Austenitized at 2200° F. Quenched to approx. 1000° F. Air-cooled to room temperature. Tempered at 1040° F., 1 hour.....	65.8	342,000	10,200,000	160,000	0.037
Austenitized at 2200° F. Quenched to approx. 1000° F. Air-cooled to 320° F. Subsequently: Held at 320° F., 30 mins. Continuously cooled to -120° F. and held 2 hours. Tempered at 1040° F., 1 hour.....	64.9	326,000	10,500,000	180,000	0.031
Held at 320° F., 24 hours. Continuously cooled to -120° F. and held 2 hours. Tempered at 1040° F., 1 hour.....	65.0	333,000	10,300,000	200,000	0.028
Held at 320° F., 24 hours. Continuously cooled to -120° F. and held 2 hours. Tempered at 1040° F., 30 mins. Continuously cooled to -120° F. and held 2 hours. Retempered at 1040° F., 30 mins.	64.5	324,000	10,300,000	210,000	0.026

Table XVI

Mutual Indentation Hardness Tests at Elevated Temperatures

Treatment	Testing Temp.	
	1150° F. (Load 3000 Kg.)	1300° F. (Load 1000 Kg.)
Hardened at 2200° F. Normal practice.	No. 1 Austenitized at 2200° F. Quenched to approx. 1000° F. Air-cooled to 140° F. Tempered at 1040° F., 1 hour....	411 143
Hardened at 2200° F. Subzero cooling before tempering.	No. 2 Austenitized at 2200° F. Quenched to approx. 1000° F. Air-cooled to 140° F. Continuously cooled to -120° F. and held 2 hours. Tempered at 1040° F., 1 hour.....	407 136
Hardened at 2200° F. Subzero cooling after tempering.	No. 3 Austenitized at 2200° F. Quenched to approx. 1000° F. Air-cooled to 140° F. Tempered at 1040° F., 1 hour. Continuously cooled to -120° F., held 2 hours.....	422 137
Hardened at 2240° F. Normal practice.	No. 4 Austenitized at 2240° F. Remainder of cycle similar to No. 1 above.....	430 138
Hardened at 2240° F. Subzero cooling before tempering.	No. 5 Austenitized at 2240° F. Remainder of cycle similar to No. 2 above.....	432 147
Hardened at 2240° F. Subzero cooling after tempering.	No. 6 Austenitized at 2240° F. Remainder of cycle similar to No. 3 above.....	430 145

tests subzero cooling was interposed in the heat treating cycle before and also after single tempering at 1040 degrees Fahr. (560 degrees Cent.), and these variations were compared with normal heat treating practice. The method of making the tests and the difficulties encountered have already been described. The results are listed in Table XVI.

No significant effect on hot hardness is produced by subzero cooling either before or after tempering.

Correlation of Tensile, Transverse Bend, and Torsion Tests—

Many methods of testing have been used to evaluate the strength and toughness of high speed steels. Transverse bend, torsion impact, static torsion, Charpy and unnotched Izod impact, and tensile tests have been chiefly used. D'Arcambal (24) measured moduli of rupture as high as 550,000 pounds per square inch with transverse bend tests of 18-4-1 and 14-4-2 types of high speed steel, while with tensile tests the moduli for the same steels were in the range 200,000 to 300,000 pounds per square inch. Page (25) recorded a modulus of rupture of 304,000 pounds per square inch with tensile tests of a 14 per cent tungsten high speed steel. Gordon and Cohen (1) measured modulus of rupture from 386,000 to 444,000 pounds per square inch with transverse bend tests of 18-4-1 high speed steel, while Cohen and Koh (14) with the same type of tests registered moduli of rupture from 94,000 to 526,000 pounds per square inch. Gordon, Cohen, and Rose (22) recorded moduli of rupture from 287,000 to 434,000 pounds per square inch with transverse bend tests of 6-5-1.5 type of high speed steel. All of these tests involved high speed steel specimens which had been given various heat treatments. It is appar-

Table XVII
Torsion, Tensile and Transverse Bend Tests of High Speed Steel "FT"

Type of Test	Number of Pieces Tested	Average Modulus of Rupture	Ratio of Torsion Modulus of Rupture to Others, Per Cent
Torsion	20	337,600	88
Tensile	12	382,800	88
Transverse Bend	26	539,100	63

ent that modulus of rupture values obtained by tensile testing are considerably lower than those obtained from transverse bend tests. Since the modulus of rupture values recorded in the present work were obtained by static torsion tests, it was believed desirable to perform additional transverse bend and tensile tests in order to have

a basis of comparison with published data referred to on page 281.

The tensile, transverse bend, and torsion test specimens used to obtain correlated modulus of rupture values were made from a single heat of molybdenum-tungsten high speed steel (Steel "FT," Table I). The preparation of the three types of specimens has already been described. Figs. 2 and 3 illustrate the various specimen forms. All three series of specimens were heat treated under carefully controlled conditions. Hardening was done in a salt bath at 2200 degrees Fahr. (1205 degrees Cent.). Quenching was done in oil. Tempering at 1040 degrees Fahr. (560 degrees Cent.) for 1 hour was performed in a forced convection air furnace.

The torsion test specimens required 48 seconds to reach 2200 degrees Fahr. (1205 degrees Cent.), were soaked at this temperature for 30 seconds, quenched in oil to room temperature, and were subsequently tempered.

The tensile test specimens required $2\frac{1}{2}$ minutes to attain the hardening temperature of 2200 degrees Fahr. (1205 degrees Cent.). They were held at this temperature for 45 seconds and were then quenched in oil to room temperature and subsequently tempered.

The transverse bend test specimens required 50 seconds to reach 2200 degrees Fahr. (1205 degrees Cent.) and were held at this temperature for 30 seconds. They were quenched in oil to room temperature and subsequently tempered.

All specimens had a Snyder (26) grain size of 10 and Rockwell hardness in the range C 65.5 to 66.0 (Table XVII).

The results presented in Table XVII indicate that the static torsion test gives modulus of rupture values which are 88 per cent as large as those obtained by tensile tests. The ratio of modulus of rupture values obtained by torsion tests and by transverse bend tests is 63 per cent. With these correlation factors available it is possible to compare the various modulus of rupture values obtained from the torsion tests in the present work with previously published values for high speed steels.

Effect of Subzero Cooling on Microstructure of Mo-W High Speed Steel—Photomicrographs of steel "LG" are shown in Figs. 7 to 13. Fig. 7 shows the "as-hardened" structure, while Fig. 8 shows the subzero hardened structure. Grain size and carbide distribution are identical. The primary martensite has no visible structure since it does not etch dark until tempered. Fig. 9 shows the structure of the same specimen as Fig. 7 after it has been tempered just enough

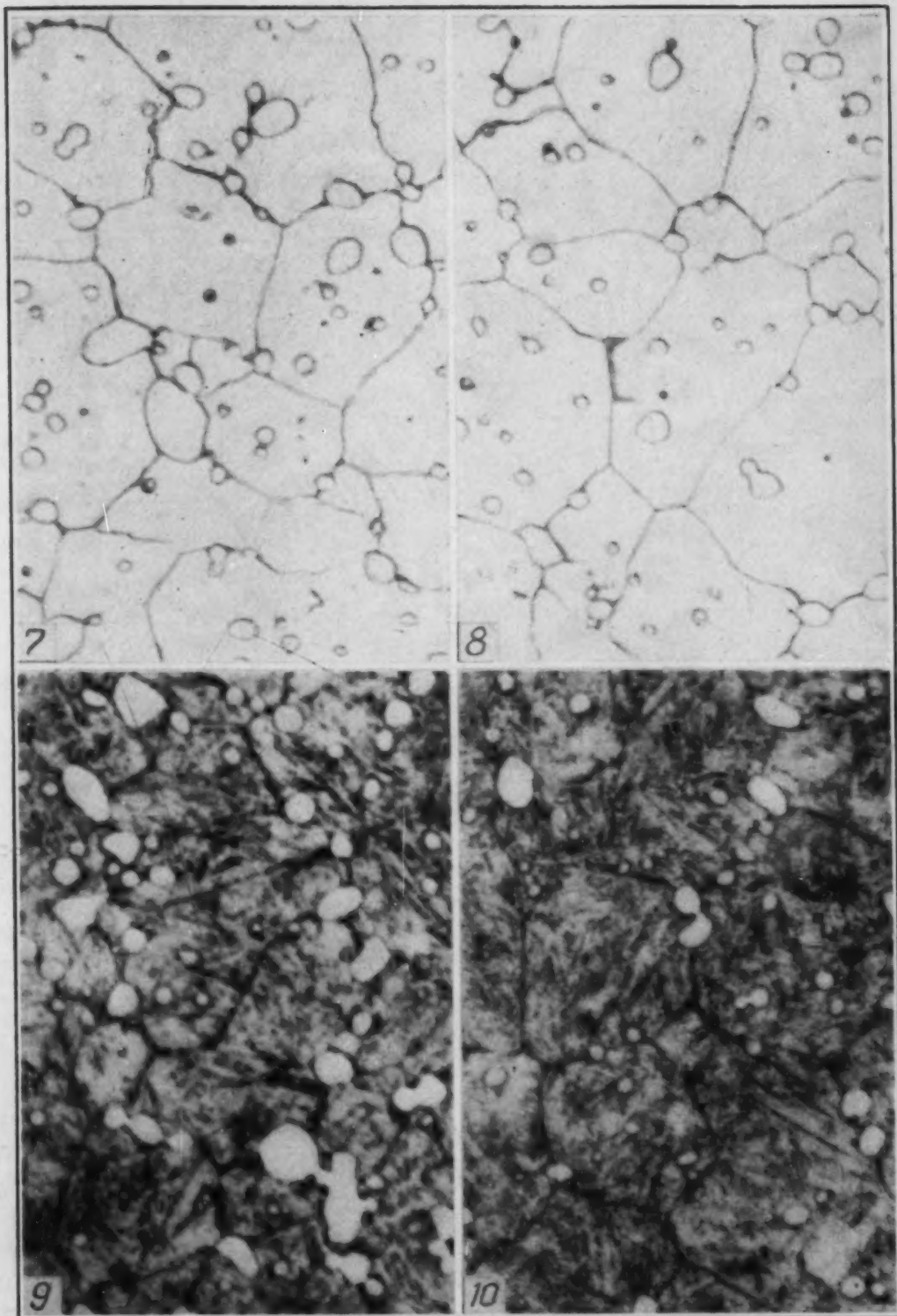


Fig. 7—Steel LG, Hardened at 2200 Degrees Fahr. (1205 Degrees Cent.). Not Tempered. Etched 5 Minutes in 6 Per Cent Nital. $\times 2000$.

Fig. 8—Steel LG, Hardened at 2200 Degrees Fahr. (1205 Degrees Cent.). Continuously Cooled to -120 Degrees Fahr. (-84 Degrees Cent.) and Held 2 Hours. Not Tempered. Etched 5 Minutes in 6 Per Cent Nital. $\times 2000$.

Fig. 9—Steel LG, Hardened at 2200 Degrees Fahr. (1205 Degrees Cent.). Tempered at 1040 Degrees Fahr. for 2 Minutes. Etched $1\frac{1}{2}$ Minutes in 6 Per Cent Nital. $\times 2000$.

Fig. 10—Steel LG, Hardened at 2200 Degrees Fahr. (1205 Degrees Cent.). Continuously Cooled to -120 Degrees Fahr. (-84 Degrees Cent.) and Held 2 Hours. Tempered at 1040 Degrees Fahr. (560 Degrees Cent.) for 2 Minutes. Etched $1\frac{1}{2}$ Minutes in 6 Per Cent Nital. $\times 2000$.

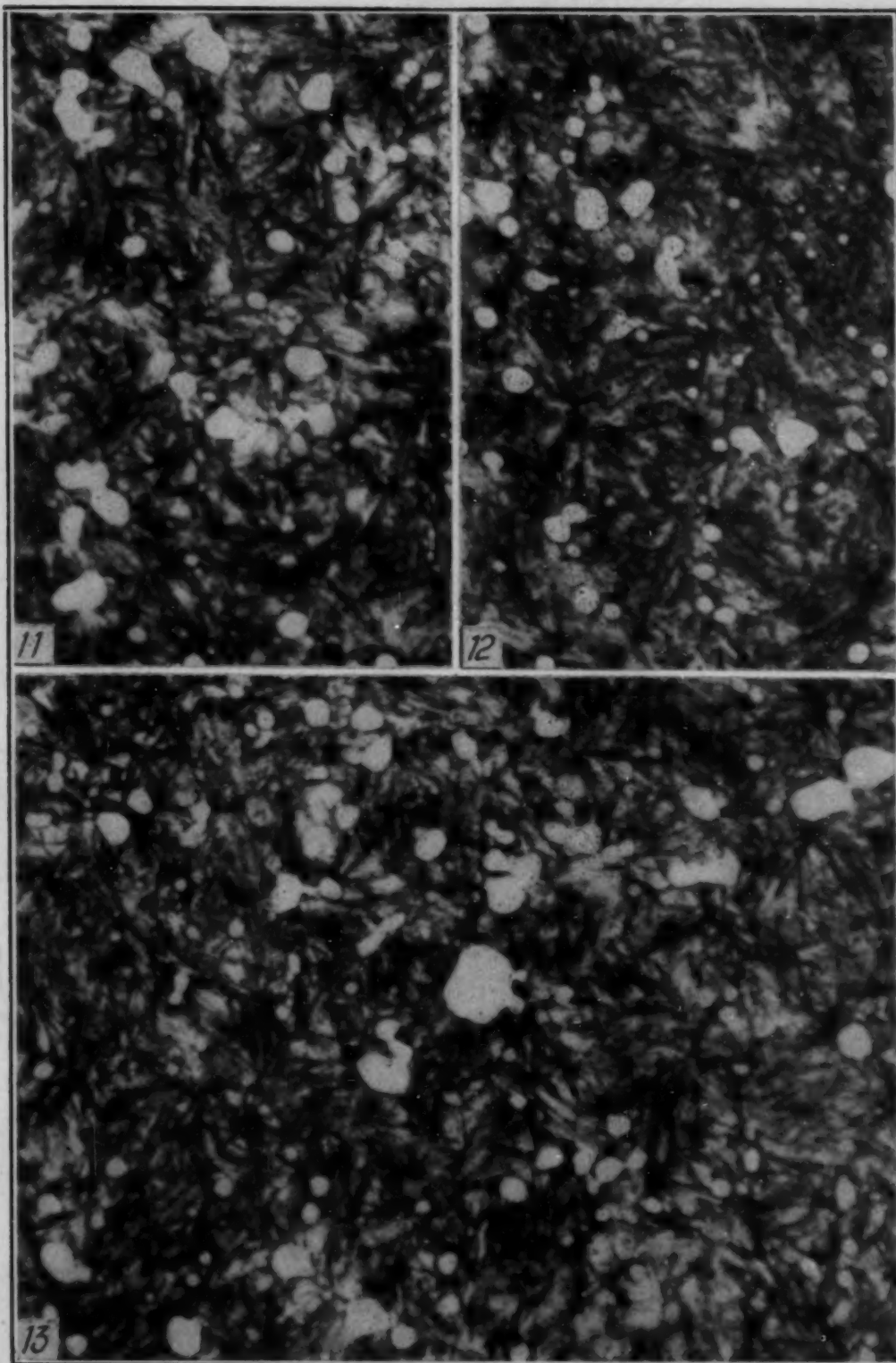


Fig. 11—Steel LG, Hardened at 2200 Degrees Fahr. (1205 Degrees Cent.). Tempered at 1040 Degrees Fahr. (560 Degrees Cent.) for 1 Hour. Etched 18 Seconds in 6 Per Cent Nital. $\times 2000$.

Fig. 12—Steel LG, Hardened at 2200 Degrees Fahr. (1205 Degrees Cent.) Continuously Cooled to -120 Degrees Fahr. (-84 Degrees Cent.) and Held 2 Hours. Tempered at 1040 Degrees Fahr. (560 Degrees Cent.) for 1 Hour. Etched 18 Seconds in 6 Per Cent Nital. $\times 2000$.

Fig. 13—Steel LG, Hardened at 2200 Degrees Fahr. (1205 Degrees Cent.). Tempered at 1040 Degrees Fahr. (560 Degrees Cent.) for 1 Hour. Continuously Cooled from Tempering to -120 Degrees Fahr. (-84 Degrees Cent.) and Held 2 Hours. Etched 18 Seconds in 6 Per Cent Nital. $\times 2000$.

Table XVIII
Heating-Cooling Treatments Used for Test Tools

Treatments	Hardening Temp. °F.	Quenched to Approx. °F.	Air-Cooled to °F.	Continuously Cooled to -120° F. and Held For	First Tempering	Continuously Cooled to -120° F. and Held For	Second Tempering
	2180 to 2240 (According to tool size)		Room Temp.		1040° F. 1 hr.		
A Normal Practice		800		1040° F. 1 hr.
A ₁ Normal Practice	"	800	140	1 hr.
B Subzero before single tempering	"	800	140	2 hrs.	1040° F. 1 hr.
C Subzero after single tempering	"	800	140	1040° F. 1 hr.	2 hrs.
D Subzero between multiple tempering	"	800	140	1040° F. 1 hr.	2 hrs.	800° F. 1 hr.
E Subzero between multiple tempering	"	800	140	1040° F. 1 hr.	2 hrs.	1040° F. 30 min.
F Subzero before and after single tempering	"	800	140	2 hrs.	1040° F. 1 hr.	2 hrs.
G Multiple subzero and multiple tempering	"	800	140	2 hrs.	1040° F. 1 hr.	2 hrs.	800° F. 1 hr.
H Multiple subzero and multiple tempering	"	800	140	2 hrs.	1040° F. 1 hr.	2 hrs.	1040° F. 30 min.
I Hot quenching plus subzero hardening	"	1100 10 min.	140	2 hrs.	1040° F. 1 hr.
J Hot quenching plus multiple subzero and multiple tempering	"	1100 10 min.	140	2 hrs.	1000° F. 3 hrs.	2 hrs.	1000° F. 3 hrs.
K Hot quenching plus multiple subzero and multiple tempering	"	1100 10 min.	140	2 hrs.	1040° F. 30 min.	2 hrs.	1040° F. 30 min.
L Hot quenching plus subzero hardening	"	1000 3 min.	525 30 min.	2 hrs.	1040° F. 1 hr.
M Hot quenching plus subzero hardening	"	1000 3 min.	525 24 hrs.	2 hrs.	1040° F. 1 hr.
N Hot quenching plus multiple subzero and multiple tempering	"	1000 3 min.	525 24 hrs.	2 hrs.	1040° F. 30 min.	2 hrs.	1040° F. 30 min.
O Hot quenching plus subzero hardening	"	1000 3 min.	320 30 min.	2 hrs.	1040° F. 1 hr.
P Hot quenching plus subzero hardening	"	1000 3 min.	320 24 hrs.	2 hrs.	1040° F. 1 hr.
Q Hot quenching plus multiple subzero and multiple tempering	"	1000 3 min.	320 24 hrs.	2 hrs.	1040° F. 30 min.	2 hrs.	1040° F. 30 min.

to reveal the primary martensite but not enough to cause decomposition of retained austenite. Likewise Fig. 10 shows the structure of the same specimen as Fig. 8 after a short tempering to reveal the primary martensite. The photographic conditions under which all of the photomicrographs were taken have been held as constant as possible so that slight differences in the background pattern or con-

trast might be attributed to subzero cooling effects. There appear to be no significant differences between the fine martensitic patterns of Figs. 9 and 10.

Fig. 11 shows a normally hardened and tempered structure etched lightly enough to reveal some details of the martensitic matrix. Fig. 12 shows a subzero hardened and tempered structure. The tempered martensite of Fig. 12 is very slightly finer or less acicular than that of Fig. 11, but the difference is not marked enough to definitely ascribe the finer martensite to subzero cooling. Fig. 13 shows a hardened and tempered structure which has been cooled to subzero temperatures after the tempering operation. It is very similar to the normally hardened and tempered structure shown in Fig. 11. A general observation which can be made about Figs. 7 to 13 is that subzero cooling has not affected the microstructure to any significant extent.

Heating-Cooling Treatments Applied to Test Tools—The heating-cooling treatments which were applied to test drills and milling cutters are listed in Table XVIII. In general the hardening temperature used was 2200 degrees Fahr. (1205 degrees Cent.), although temperatures of 2180 to 2240 degrees Fahr. (1195 to 1225 degrees Cent.) were also used depending on the tool size and carbon content of the high speed steel. Treatments A to H in Table XVIII represent normal hardening and quenching practice in conjunction with subzero cooling interposed in the heat treating cycle before and after single or multiple tempering. Treatments I to Q represent normal hardening with hot quenching in the range 320 to 1100 degrees Fahr. (160 to 595 degrees Cent.) in conjunction with subzero cooling before and after single or multiple tempering.

Normal Quenching Treatments—Treatments A to H in Table XVIII represent normal hardening and quenching cycles. Types A and A₁ represent normal practice with no subzero cooling and are used as a basis of comparison for all of the other treatments. Type B represents subzero hardening or subzero cooling prior to single tempering. Type C represents subzero cooling after single tempering. Types D and E are similar to Type C with retempering added after subzero cooling to temper any martensite formed during the previous tempering and subzero cooling treatments. Type F represents subzero cooling before and after single tempering. Types G and H are similar to Type F with retempering added to temper any martensite formed in the previous tempering and subzero cooling.

Table XIX
Drill Size 1/4 Inch H. S. Steel "FT"

	1"	1 1/2"	1"	1" Hard	
Material	S.A.E. 52100	Armor Plate	S.A.E. 1040	Cast Iron	
Brinell Hardness ..	321	255	170	212	
Cutting Speed					
Ft./Min.	30	60	100	110	
Penetration Rate					
In./Min.	0.458	3.2	9.9	11.76	Performance
	Av. In	Av. In	Av. In	Av. In	Average
Treatment	Per Per	Per Per	Per Per	Per Per	in Four
Type A ₁ (Normal)	Grind Cent	Grind Cent	Grind Cent	Grind Cent	Materials
B	7.92 100	50.3 100	58.8 100	102.7 100	Per Cent
C	4.58 58	68.4 136	46.7 79	104.6 102	100
D	7.75 98	54.9 109	71.6 122	114.1 111	94
E	6.33 80	54.7 109	66.6 113	116.2 113	110
F	6.54 83	59.8 119	81.0 138	92.0 90	104
G	5.17 65	56.6 112	81.7 139	99.3 97	108
H	4.67 59	65.4 129	71.0 121	85.7 83	103
	6.83 86	51.0 101	51.7 88	88.3 86	98
					90

Each value of "Av. In Per Grind" represents 6 individual grinds for a grand total of 24 grinds in four materials.

Table XX

Group	Types	Treatment and Description	Performance		
			Column		Average Performance Col. 1 ÷ 2 Per Cent
			1	2	
			Total Percentage Weighted According to Number of Grinds	Total Number Grinds	
I	B, I, L, M, O and P	Subzero cooling interposed in heat treating cycle <i>before</i> single tem- pering	18,866	189	100
II	C	Subzero cooling interposed in heat treating cycle <i>after</i> single temper- ing	17,869	163	110
III	D, E	Subzero cooling interposed in heat treating cycle between multiple tempering	21,263	223	95
IV	F	Multiple subzero cooling interposed in heat treating cycle before and after single tempering	7,786	76	102
V	G, H, J, K, N and Q	Multiple subzero cooling interposed in heat treating cycle before, after or between multiple tempering	24,952	243	103
VI	A and A ₁	Standard—no subzero cooling	18,400	184	100

Hot Quenching Treatments—Treatments I to Q represent hot quenching in the range 1100 to 320 degrees Fahr. (595 to 160 degrees Cent.) in conjunction with various subzero cooling and tempering treatments. Types I, J, and K represent hot quenching for a short time at 1100 degrees Fahr. (595 degrees Cent.) in conjunction with various subzero cooling and tempering cycles. Types L, M, and N represent hot quenching in the bainite region of 525 degrees Fahr. (275 degrees Cent.) in conjunction with subzero cooling and tempering cycles. Types O, P, and Q represent hot quenching at 320

degrees Fahr. (160 degrees Cent.) (below the primary M-point) in conjunction with subzero cooling and tempering cycles.

Many of the heating-cooling cycles listed in Table XVIII are those which have been advocated in various articles recently published in some of the technical journals. In general the treatments tend to produce fully tempered or slightly overtempered structures. As such they cover only a very narrow portion of the possible treatments.

Twist drills and milling cutters, subjected to the treatments listed in Table XVIII, were tested in from two to four different kinds of materials at several different cutting speeds and penetration rates. Many such tests were carried out and the performance averages were calculated according to the procedure described on pages 261 and 262. As already stated, all conditions in the tests were controlled as closely as possible in order to get a true comparison between normally heat treated tools and those subjected to subzero treatments. An example of a typical drilling test is given in Table XIX and a summary of all the tests is reported in Table XX.

Typical Drill Test in Four Different Materials—Table XIX shows the performance results for a typical drilling test run with $\frac{1}{4}$ -inch diameter drills. The test conditions in each material are listed at the top of the table. Performance results are listed in "Average Inches Drilled per Grind" and in percentages. Each value of "Average Inches Drilled per Grind" represents two separate tests on each of three different drills, making a total of six different grinds. The average performance percentages listed in the last column of Table XIX represent an average of twenty-four different grinds. Table XIX is typical of many test results which were added together as described on page 261 in order to obtain the summarized results listed in Table XX.

Summary of Tool Performance Tests—In order to obtain an overall comparison between heat treatments involving subzero cooling and regular heat treatment, the performance data for six different groups of tests involving a total of 1078 grinds have been summarized in Table XX. It is not claimed that the method of grouping the various treatments is the only correct one from a metallurgical standpoint. However, the groupings shown in Table XX do give an overall picture of the effect of subzero cooling interposed in the heat treating cycle before and after single tempering and in conjunction with multiple tempering.

The best results obtained in Table XX were with treatments involving subzero cooling to -120 degrees Fahr. (-84 degrees Cent.) after single tempering at 1040 degrees Fahr. (560 degrees Cent.) for 1 hour. In a general way this observation checks with the torsion and hardness test results which showed that (Figs. 5 and 6) subzero cooling after tempering at 1040 degrees Fahr. (560 degrees Cent.) gave physical properties equal to or very slightly better than those obtained with normal heat treatments. It is possible that shorter tempering times and temperatures lower than 1040 degrees Fahr. (560 degrees Cent.) would show better performance results in conjunction with subzero cooling since the cooling acts to transform retained austenite as does tempering.

SUMMARY AND CONCLUSIONS

This entire series of experiments is to be regarded as a reconnaissance of a limited portion of the field and not as a complete coverage. Some of the physical tests and practically all of the tool performance tests are concerned with subzero cooling in conjunction with a fully tempered condition. There still exists a wide range of possibilities to be investigated in the region of subzero cooling plus an undertempered condition. This field should prove interesting in view of the observed tendency for subzero cooling to act as an auxiliary to the tempering operation by causing the transformation of some of the retained austenite.

It is possible that certain combinations of subzero cooling and tempering will be found which will provide advantages over a normally hardened, fully tempered tool. As yet no outstanding case of this has been observed.

Bearing in mind that the effect of the size or mass of the tool or specimen has not been investigated and that these results have been obtained with small sized specimens and drills, the following conclusions have been reached with respect to subzero cooling of the molybdenum-tungsten steels studied:

1. Continuous cooling to -120 degrees Fahr. (-84 degrees Cent.) from a hardening temperature of 2200 degrees Fahr. (1205 degrees Cent.) results in the subzero transformation of at least 95 per cent of the amount of austenite which would transform if cooled to temperatures as low as -310 degrees Fahr. (-190 degrees Cent.).

2. The formation of additional martensite during subzero cooling after hardening (no subsequent tempering) gives an increase in specific volume, hardness, and strength as compared to normal hardening.

3. The increment of hardness and strength gained by subzero hardening is maintained up to tempering temperatures of at least 800 degrees Fahr. (425 degrees Cent.), but at 1040 degrees Fahr. (560 degrees Cent.) it has disappeared.

4. Subzero hardening followed by tempering 1 hour at 1040 degrees Fahr. (560 degrees Cent.) produces a decrease in plasticity as compared to normal hardening.

5. Subzero cooling after tempering 1 hour at 1040 degrees Fahr. (560 degrees Cent.) produces little change in hardness, strength or plasticity when hardening temperatures of 2200 degrees Fahr. (1205 degrees Cent.) or higher are employed. At lower hardening temperatures subzero cooling after tempering yields some increases in hardness and strength, and a marked increase in plasticity.

6. Subzero cooling before or after tempering in conjunction with hot quenching at 1100 or 320 degrees Fahr. (595 or 160 degrees Cent.) produces no significant change in hardness, strength or plasticity.

7. No significant change in the mutual indentation hardness at elevated temperatures is produced by subzero cooling before or after tempering at 1040 degrees Fahr. (560 degrees Cent.).

8. No significant effect on the appearance of the microstructures is produced by subzero cooling to -120 degrees Fahr. (-84 degrees Cent.) before or after tempering at 1040 degrees Fahr. (560 degrees Cent.).

9. Subzero cooling before tempering at 1040 degrees Fahr. (560 degrees Cent.) gives tool performance results equal to those obtained with normal heat treatment and slightly inferior to those obtained by subzero cooling after tempering at 1040 degrees Fahr. (560 degrees Cent.).

10. Many more controlled tests will be necessary to determine whether the observed 10 per cent improvement in tool performance due to subzero cooling after tempering at 1040 degrees Fahr. (560 degrees Cent.) is a significant increase.

ACKNOWLEDGMENTS

The generous aid furnished by Mr. J. V. Emmons and Mr. A. S. Townsend in reviewing the manuscript is gratefully acknowledged. The author also wishes to express his thanks to Professor H. D. Churchill of Case School of Applied Science for his supervision of the tensile and transverse bend tests, to Mr. G. H. Seaver for the preparation of the photomicrographs, to Mr. H. R. Stack for the specific volume measurements, to Mr. W. L. Emerson for the chemical analyses, to the members of the Research Division of the Laboratory for their assistance throughout the entire series of experiments, and to the Misses Kundtz and Eichele in arranging the tabulated data.

Bibliography

1. P. Gordon and M. Cohen, "The Transformation of Retained Austenite in High Speed Steels at Subatmospheric Temperatures," *TRANSACTIONS, American Society for Metals*, Vol. 30, 1942, p. 569-591.
2. O. E. Harder and R. L. Dowdell, "The Decomposition of the Austenite Structure in Steels with Use of Liquid Oxygen," *TRANSACTIONS, American Society for Steel Treating*, Vol. 11, January 1927, p. 391-399.
3. H. Scott, "Relation of High Temperature Treatment of High Speed Steel to Secondary Hardening and Red Hardness," *Scientific Papers, Bureau of Standards*, Vol. 16, 1920, p. 521-536.
4. A. Gulyaev, "Improved Heat Treatment of High Speed Steel," *Metallurg*, Vol. 12, No. 12, 1937, p. 65-70.
5. A. Gulyaev, "Transformation of Retained Austenite at Subzero Temperatures in High Alloy Steels," *Metallurg*, Vol. 14, No. 3, 1939, p. 64-71.
6. J. A. Mathews, "Retained Austenite—A Contribution to the Metallurgy of Magnetism," *TRANSACTIONS, American Society for Steel Treating*, Vol. 8, 1925, p. 565-583.
7. K. Honda and K. Iwase, "The Transformation of Retained Austenite into Martensite by Stress," *TRANSACTIONS, American Society for Steel Treating*, Vol. 11, 1927, p. 399-405.
8. W. P. Sykes and Z. Jeffries, "On the Constitution and Properties of Hardened Steel," *TRANSACTIONS, American Society for Steel Treating*, Vol. 12, 1927, p. 871-898.
9. E. C. Bain and W. S. N. Waring, "Austenite Decomposition and Length Changes in Steel," *TRANSACTIONS, American Society for Steel Treating*, Vol. 15, 1929, p. 69-95.
10. H. P. Nielsen and R. L. Dowdell, "Effect of Thermal Stresses on Austenite," *TRANSACTIONS, American Society for Metals*, Vol. 22, Sept. 1934, p. 810-832.
11. G. V. Luerssen and O. V. Greene, "The Cold Treatment of Certain Alloy Steels," *TRANSACTIONS, American Society for Steel Treating*, Vol. 19, 1931, p. 501-552.
12. H. S. VanVleet and C. Upthegrove, "Austenite Decomposition and the Changes in Magnetic Properties," *TRANSACTIONS, American Society for Steel Treating*, Vol. 18, 1930, p. 729-759.
13. G. Tammann, "Textbook of Metallography," The Chemical Catalog Co., translated by Dean and Swenson, 1925, p. 251-253.

14. M. Cohen and P. K. Koh, "The Tempering of High Speed Steel," *TRANSACTIONS, American Society for Metals*, Vol. 27, 1939, p. 1015-1051.
15. G. A. Roberts and J. P. Gill, "Some Effects of Subzero Cooling," *Iron Age*, March 23, 1944, p. 53-56.
16. S. M. DePoy, "Subzero Treatment of High Speed Steels," *Iron Age*, April 13, 1944, p. 52-55.
17. J. V. Emmons, "Some Physical Properties of Hardened Tool Steel," *Proceedings, American Society for Testing Materials*, Vol. 31, 1931, p. 47-76.
18. I. H. Cowdrey, "Hardness by Mutual Indentation," *Proceedings, American Society for Testing Materials*, Vol. 30, 1930, p. 559-571.
19. O. E. Harder and H. A. Grove, "Hot Hardness of High Speed Steels and Related Alloys," *Transactions, American Institute of Mining and Metallurgical Engineers, Iron and Steel Div.*, Vol. 105, 1933, p. 88-132.
20. "ASM Metals Handbook," 1939 Edition, p. 667-668.
21. P. Gordon, M. Cohen, R. S. Rose, "Kinetics of Austenite Decomposition in High Speed Steel," *TRANSACTIONS, American Society for Metals*, Vol. 31, 1943, p. 161-217.
22. P. Gordon, M. Cohen, R. S. Rose, "Effect of Quenching Bath Temperature on the Tempering of High Speed Steel," *TRANSACTIONS, American Society for Metals*, Vol. 33, 1944, p. 411-454.
23. J. V. Emmons, "Some Physical Properties of High Speed Steel," *TRANSACTIONS, American Society for Steel Treating*, Vol. 19, 1932, p. 289-332.
24. D'Arcambal, "Physical Tests on High Speed Steels," *TRANSACTIONS, American Society for Steel Treating*, Vol. 2, 1922, p. 586-601.
25. A. Page, "Mechanical Properties of High Speed Steel at Elevated Temperatures," *Metallurgia*, April 1930, p. 239-241.
26. R. W. Snyder and H. F. Graff, "Study of Grain Size in Hardened High Speed Steel," *METAL PROGRESS*, April 1938, p. 377-380.

DISCUSSION

Written Discussion: By Stewart M. DePoy, metallurgist, Delco Products Div., General Motors Corp., Dayton, Ohio.

The author is to be congratulated on the thoroughness of his research. His approach and results, although being highly technical, nevertheless make it possible to make a practical interpretation.

Mr. Kennedy's results and conclusions show subzero cooling after a preliminary temper to give the highest tool productivity. These results check with those obtained by the writer. However, the increase in production obtained by the latter were in the range of 30 to 50 per cent, whereas that of the author's only averaged 10 per cent. Nevertheless the tendency for increased productivity is pointed out by subzero treatment after a preliminary draw.

All the discussor's work was done with a temper following the subzero treatment, regardless of where the latter was inserted in the treatment cycle. It is reasonable to believe that untempered martensite would be dangerous on a tool cutting edge. However, a high temperature is not required for tempering the primary martensite. Consequently a tempering at 400 degrees Fahr. (205 degrees Cent.) following the subzero treatment is practiced at Delco Products Division. The preliminary tempering is at 1050 degrees Fahr. (565 degrees

Cent.) following a short quench at 1100 degrees Fahr. (595 degrees Cent.) in salt and a cool in air to room temperature.

The writer has reported and published photomicrographs intending to show a definite difference in microstructure between the normal and subzero treated materials. Since publication of these photos, it is believed that the difference shown was due to differential etching. This is substantiated by Mr. Kennedy's photos. However, it is still the writer's belief that either a new structure or a different form of martensite is formed by supercooling. At this writing there is no evidence to prove this theory.

It is interesting to note from Table XIX that the C treatment was more effective when operating at 100 F.P.M. than it was at 30 F.P.M. Actual production applications at Delco Products have shown the subzero treated tools to be more effective at slow surface speeds.

The author offers the opinion that there are possibilities existing in the range of subzero treated and undertempered conditions. This does not seem possible to the writer due to the fact that most tools reach a high tempering temperature on the cutting edge while working. This would probably obliterate any accurate results on such tools, especially if they are allowed to cool between cuts as is the general practice.

It must be remembered that all the writer's experience has been on the 6-5-4-2 type (M-2) and the 18-4-1 type (T-1) high speed steels. However, the tendencies of these and the 9-1-4-1 1/2 type (M-1) reported by Mr. Kennedy are the same. To the writer's knowledge no work on this latter type has been reported in the past, and consequently Mr. Kennedy's contribution to the literature on this subject is very important and useful.

Written Discussion: By Stewart G. Fletcher, research associate, Massachusetts Institute of Technology, Cambridge, Mass.

Mr. Kennedy has certainly done an excellent job of studying the effects of subcooling in one widely used high speed steel. His paper has been well organized in its presentation of data.

There has been nothing in this paper which would indicate that the behavior of the particular high speed steel in question is any different from the behavior of other high speed steels, such as the 18-4-1 and 6-6-2 varieties. Mr. Kennedy has definitely strengthened the conviction which has gradually been growing that if the steel is properly hardened and thoroughly tempered, little or no advantage may be gained by subcooling treatments. His data do show, however, that if a high speed steel is underhardened, a slightly better performance may be attained by subcooling after tempering, though the reason for this improvement is still obscure.

It is entirely possible that if the steel had been overheated, refrigeration after quenching or just after the first temper would be advantageous. This would arise from the fact that the higher hardening temperature would result in considerable quantities of retained austenite, and normal tempering procedures may not be adequate to bring about its decomposition to a point consistent with maximum tool life.

The statement is made on page 263 of the paper that "... a tempering cycle of 1040 degrees Fahr. (560 degrees Cent.) for 1 hour gives practically

complete decomposition of austenite retained on quenching from a hardening temperature of 2200 degrees Fahr. (1205 degrees Cent.) to room temperature." This is not supported by the accompanying dilation curves. In Fig. 4A, for example, a definite expansion is observed during the cooling from a *second* temper at 1040 degrees Fahr. (560 degrees Cent.), and much of this is undoubtedly due to decomposition of austenite left after the first cooling. Also, in Fig. 4G, after 1 hour's tempering at 1040 degrees Fahr. (560 degrees Cent.) (quenched to room temperature before tempering) enough retained austenite remains at room temperature to give a definite expansion on further subcooling to -120 degrees Fahr. For a steel of almost identical analysis, and also hardened at 2200 degrees Fahr. (1205 degrees Cent.), it was found in the Massachusetts Institute of Technology laboratories that at least 3 hours at 1040 degrees Fahr. (560 degrees Cent.) was required to bring about complete austenite transformation on subsequent cooling to room temperature.¹

With regard to interpretation of the various dilatometric curves in Fig. 4, particularly Fig. 4A, it is dangerous to use increases in length (measured at room temperature) as a criterion of the amount of austenite decomposed, when the specimen has been subjected to heating between the measurements. Such heating is likely to bring about a contraction by decomposing the prior untempered martensite (note the contraction in Fig. 4D on first heating). This would be superimposed upon any net expansion due to austenite decomposition, and thus apparently lower the amount of austenite decomposed. On the other hand, when cold treatment alone is involved, any expansion at room temperature is directly related to the amount of austenite. No other reactions are possible to mask the resultant expansion in this case.

Mr. Kennedy's results of drill tests, tabulated in Table XX, indicate that if the subzero treatment is used after a single temper, the improvement in tool performance is at a maximum. It is, however, difficult to assign a positive reason for this fact, particularly in terms of the metallographic structure. Could it be possible that the final subzero cooling can upset the normal condition of surface stresses, reducing the surface tensile stresses and thus contributing to improved tool performance? If so, many of the phenomenal results reported for such a treatment, despite little or no evidence of structural change, may be entirely a function of the nature of the residual stresses.

Written Discussion: By Otto Zmeskal, research metallurgist, Universal-Cyclops Steel Corporation, Bridgeville, Pa.

Mr. Kennedy's paper presents the results of a carefully conducted, excellent, and thorough investigation. After the first years of enthusiasm in which cold treatment has been advocated as an adjunct to heat treatment of all kinds, we are gradually building up facts, scientifically attained, from which the proper applications of cold treatment may be derived. The work of Mr. Kennedy is a pillar in this structure.

The writer has sporadically studied the effects of cold treatment on high speed steels during the past two years and has, as a result, certain information which he would like to present in discussion of some of the details of this fine research of Mr. Kennedy.

¹J. I. Bluhm, B. S. Thesis, Massachusetts Institute of Technology, 1941.

In an investigation of the effect of time at -320 degrees Fahr. after tempering for a tungsten-molybdenum (6-6-2) high speed steel no difference was found in hardness for a period at the low temperature of over 100 hours. The data are presented in the table. Completely tempered specimens were unaffected by the cold treatment. The insufficiently tempered specimens had some retained austenite which was transformed by the cooling to the low temperature.

The table shows the effect of time at -320 degrees Fahr. on the Rockwell C hardness of specimens ($\frac{5}{8}$ inch square by $\frac{1}{2}$ inch long, hot-rolled and annealed) of 6-6-2 high speed steel. The specimens were oil-quenched to black from $1\frac{1}{2}$ minutes at 2250 degrees Fahr. (1230 degrees Cent.), cooled in air to room temperature and tempered as shown.

Rc Hardness After the Following Times at -320 Degrees Fahr. After Tempering							
Temper	0	5 min.	1 hr.	3 hr.	10 hr.	30 hr.	100 hr.
1000-1x-1 hr.	65.5	66.8	66.9	66.7	66.3	66.3	66.1
1000-2x-1 hr.	66.7	66.9	66.8	67.1	66.6	66.5	66.7
1000-3x-1 hr.	66.5	67.3	66.6	66.4	66.7	66.4	66.2
Steel Used:							
0.86 C	5.77 W	3.96 Cr	1.54 V	5.41 Mo			

In regard to the rate of cooling, although the physical properties are not affected, quenched pieces are very prone to crack if the cooling rate is too high. This is especially true if deep punch marks in a decarburized surface are present. No cracking was found in specimens that had been drawn prior to cold treatment regardless of the time at -320 degrees Fahr., nor in those that had been hot-quenched to 1000 degrees Fahr. (540 degrees Cent.) for 1 hour before cold treatment. All of the specimens continuously quenched down to -320 degrees Fahr. were cracked.

In the treatments of tool bits to be described later it was found that 18-4-1 high speed steel was much more susceptible to cracking on cold treatment than was molybdenum-tungsten high speed steel.

In his summary the author states that a wide range of possibilities is to be expected in the region of subzero cooling plus an undertempered condition. This writer does not believe that many possibilities exist if undertempering is taken to indicate tempering below 950 degrees Fahr. (510 degrees Cent.). Fig. 6 of the author's paper shows that subzero cooling does not transform the retained austenite in specimens of molybdenum-tungsten high speed steel tempered at 400 to 800 degrees Fahr. (205 to 425 degrees Cent.). Gordon and Cohen have shown that the retained austenite in 18-4-1 high speed steel is stabilized to subzero transformation by tempering temperatures as high as 900 degrees Fahr. (480 degrees Cent.).² Recently, the writer attempted to transform the retained austenite in an undertempered molybdenum-tungsten high speed steel by subzero cooling. The specimens had previously been tempered at 850 degrees Fahr. (455 degrees Cent.) after a quench from 2150 degrees Fahr. (1175 degrees Cent.) (59 Rc). No increase in hardness resulted from either cold treatment at -110 degrees Fahr. or at -320 degrees Fahr., for refrigerating

²Paul Gordon and Morris Cohen, "The Transformation of Retained Austenite in High Speed Steel at Subatmospheric Temperatures," *TRANSACTIONS, American Society for Metals*, Vol. 30, 1942, p. 580.

periods ranging from 1 to 120 hours. It was only after tempering above 950 degrees Fahr. (510 degrees Cent.) that precipitation occurred in the austenite and conditioned it for transformation on subzero cooling (63 Rc).

Attention has been called to the marked increase in plasticity that resulted by subzero cooling after a 1040 temper of specimens of molybdenum-tungsten

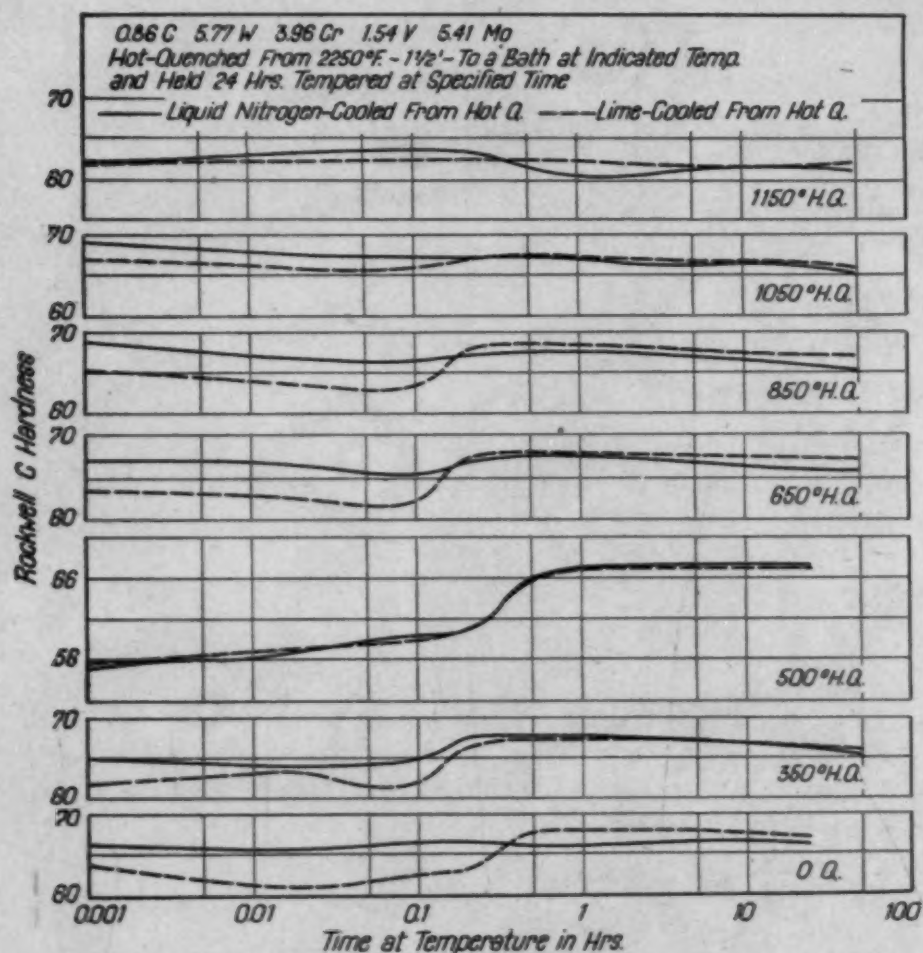


Fig. A—Effect of Time at a Tempering Temperature of 1000 Degrees Fahr. on the Hardness of Hot-Quenched 6-6-2 High Speed Steel.

high speed steel hardened at temperatures lower than 2200 degrees Fahr. (1205 degrees Cent.) (The author's Fig. 5). The writer believes that a superior combination for toughness is a low draw after a 2200-degree Fahr. hardening. Subzero cooling has no effect here. For high strength the regular 1040-degree Fahr. draw after a 2200-degree Fahr. hardening seems entirely satisfactory. The comparison data were taken from the author's Figs. 5 and 6, and Table X.

Hardening Temperature Deg. F.	Draw	Subzero Treatment	Hardness Rc	Modulus of Rupture Psi.	Plastic Strain In. per In.
2100	1040-1 hr.	After draw	63	310,000	0.055
2200	800-1 hr.	None	61	305,000	0.210
2200	1040-1 hr.	None	65.8	342,000	0.037
2200	1040-1 hr.	After draw	65.9	342,000	0.034

The high plasticity of the molybdenum-tungsten steel specimens tempered at 800 degrees Fahr. (425 degrees Cent.) must be due to the retained austenite present in the structure. The fully hard, stress-free martensite is embedded in a binder of relatively soft austenite, which lowers the apparent hardness but greatly increases the plasticity. A temper of 400 degrees Fahr. (205 degrees

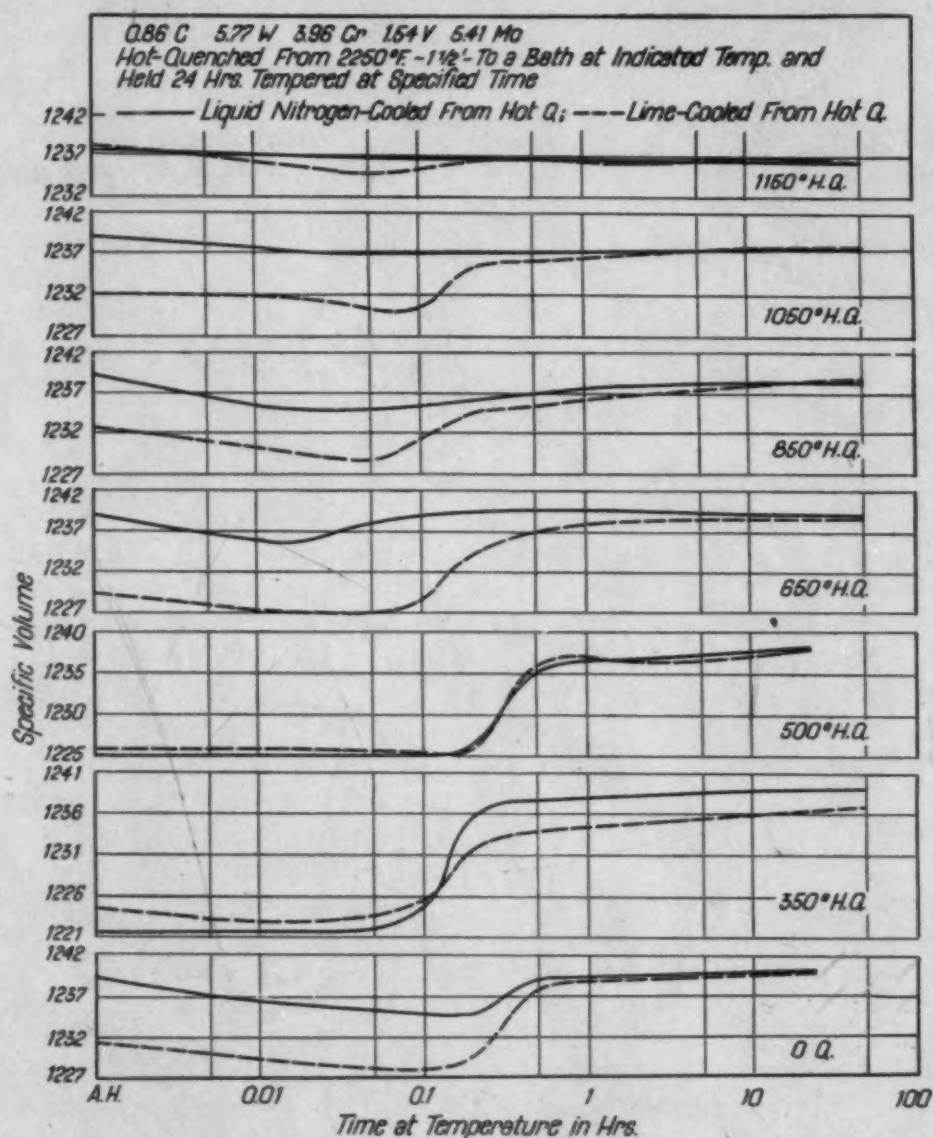


Fig. B—Effect of Time at a Tempering Temperature of 1000 Degrees Fahr. on the Specific Volume of Hot-Quenched 6-6-2 High Speed Steel.

Cent.) will transform the tetragonal martensite of the quenched structure to cubic martensite and will result in a marked gain in plasticity over that of the quenched structure. The 800-degree Fahr. (425-degree Cent.) temper, however, completes the precipitation processes in the martensite and relieves the stresses.

It would be of interest to determine the plasticity of a stress-free structure containing 50 per cent rather than 20 per cent retained austenite. Such a struc-

ture could be obtained by hot quenching to 500 degrees Fahr. (260 degrees Cent.) for 24 hours, slowly cooling to room temperature, and tempering at 800 degrees Fahr. (425 degrees Cent.). In applications where high toughness is desired and hardness at elevated temperatures is not required such a heat treatment might be very beneficial.

Cold treatment is useful in specimens that have been insufficiently tempered, that is, for specimens tempered in the range wherein precipitation occurs from the austenite and conditions it to transform during cooling (above 950 degrees Fahr.) but not for the time sufficient to allow all of the retained austenite to transform during cooling. Where the austenite is stabilized by very high hardening temperatures (to produce grain sizes of 4 to 6 Snyder), what is considered normal tempering is not enough to completely decompose the austenite. Cold treatment after this incomplete tempering is beneficial.

The author has found that a 10-minute hot quench at 1100 degrees Fahr. (595 degrees Cent.) stabilized the austenite for subzero transformation. The effect of hot quenching 6-6-2 high speed steel for 24 hours at various temperatures will be of interest in this connection. Figs. A and B give the change in hardness and in specific volume for tempering times of 1 second to 60 hours at 1000 degrees Fahr. (540 degrees Cent.). It has been shown before by Gordon, Cohen, and Rose that 24-hour hot quenches in the range 400 to 600 degrees Fahr. (205 to 315 degrees Cent.) for both 6-6-2 and 19-4-1 high speed steels result in large amounts of retained austenite³. Fig. A shows that this austenite is also very stable as it does not transform on cold treatment.

Part of the retained austenite left by the other hot quenches (except at 1150 degrees Fahr.) as well as by the cold oil quench was transformed by the cold treatment. The specific volume curves of Fig. B show that the remainder of the retained austenite left untransformed by the cold treatment transformed during tempering at the same time as the specimens not cold treated.

No advantages in hardness result from cold treatment in connection with multiple tempering. An experiment was conducted on 6-6-2 steel in which specimens quenched from 2260 degrees Fahr. (1240 degrees Cent.), half of them cold-quenched to -320 degrees Fahr. and half quenched to room temperature, were drawn seven times at 1000 degrees Fahr. (540 degrees Cent.). The cold-quenched specimens were also cold-treated after each temper, while the other set was air-cooled. Except in the as-quenched condition, the specimens not cold-treated were harder at all draws than were those that had been cold-treated.

It is true that cold treatment permits the earlier attainment of the maximum secondary hardness in a specimen but this maximum secondary hardness is always less than the maximum secondary hardness attained by regular treatment.

As Roberts and Gill have found for cold treatments at -110 degrees Fahr. our experiments have also shown that specimens regularly treated resist softening at the higher tempering temperatures to a greater extent than do those treated at -320 degrees Fahr. before tempering⁴.

³Paul Gordon, Morris Cohen and Robert S. Rose, "The Kinetics of Austenite Decomposition in High Speed Steel," *TRANSACTIONS, American Society for Metals*, Vol. 31, 1943, p. 193.

⁴*Iron Age*, March 23, 1944, p. 52.

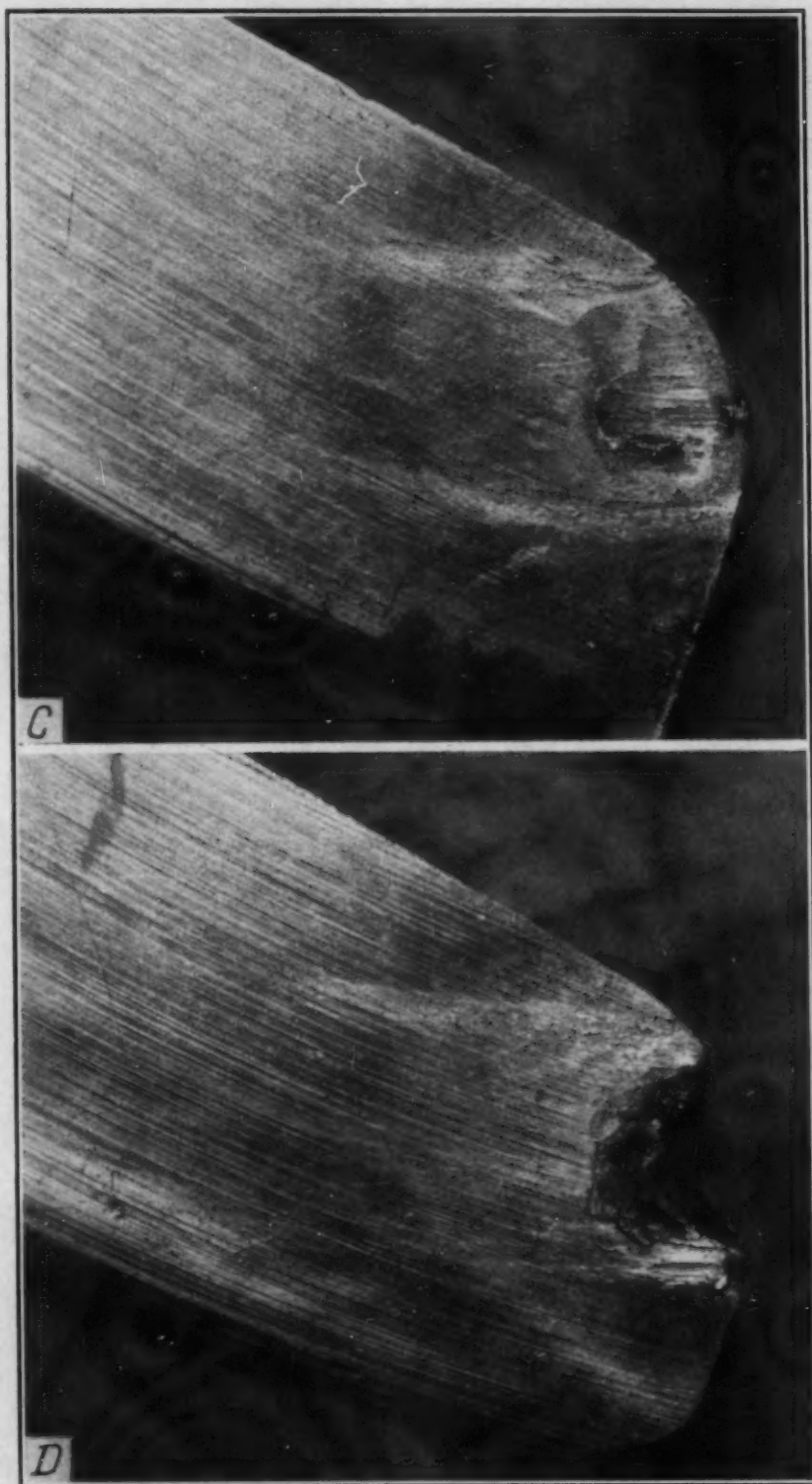


Fig. C—Crater Formation in High Speed Steel Lathe Bit.
Fig. D—Failure of High Speed Steel Lathe Bit.

Table B
Effect of Cold Treatment After Tempering on the Cutting Performance of 18-4-1 High Speed Steel
 (Oil Quenched from 2350 Degrees Fahr.—1½ Ft.)
 0.71 C 18.28 W 3.86 Cr 0.99 V 0.23 Mo

Identification	Hi-Heat °F.	Time Min.	Draw	Cold Treatment	Grain Size Snyder	Hardness After Treatment RC	Cutting Speed at Failure, F.P.M.			Performance Based on 94 F.P.M. as 100%
							End 1	End 2	Avg.	
Reg. Lo-Hi Draw Deep Freeze	2350	1½	850-2 Hrs. +	None	12	65.0	94.98	94.71	94.85	101
	2350	1½	1050-2 Hrs. 1050-2 Hrs.	-120, 2 Hrs. After draw	12	65.0	96.41	93.46	94.94	101
Reg. Double Draw Deep Freeze	2350	1½	1050-2x-2 Hrs.	None	12	64.0	95.61	91.97	93.79	100
	2350	1½	1050-2x-2 Hrs.	-120, 2 Hrs. After draw	11	64.1	96.62	97.31	96.97	103
Reg. Single Draw Deep Freeze	2350	1½	1050-1x-1 Hr.	None	11	65.1	92.83	95.11	93.97	100
	2350	1½	1050-1x-1 Hr.	-120, 2 Hrs. After draw	11	65.5	94.25	94.36	94.31	101
Reg. Multiple Draw Deep Freeze	2350	1½	1050-4x-2 Hrs.	None	12	63.6	101.43	98.73	100.08	107
	2350	1½	1050-4x-2 Hrs.	-120, 2 Hrs. After draw	12	63.8	96.37	96.45	96.41	103
Average of Regular Treatments							Average of Regular Treatments			102
Average of Deep Freeze Treatments							Average of Deep Freeze Treatments			102

Table C
Effect of Cold Treatment on the Cutting Performance of Molybdenum High Speed Steel

Identification	Treatment (All Previously Preheated at 1500°—15' in 10% CO and Hi-Heated at 2175°—1½' in 10% CO)	Grain Size Snyder	Hardness After Treatment RC	Cutting Speed at Failure F.P.M.		Performance Based on 94 f.p.m. as 100 per cent
				End 1	End 2 Avg.	
Continuous Cool to —320	Quench to black, then to —320, then draw at 1025, 2X, 2 hrs.	13	63.9	96.46	93.16	94.81
Interrupted Cool to —320	Quench cold, then to —320, then draw at 1025, 2X, 2 hrs.	14	63.9	94.94	96.68	95.81
—320 after 10-hi draw	Quench cold, draw 850, 2 hrs., + 1025, 2 hrs., then to —320	14	65.2	93.69	94.36	94.03
—320 between lo-hi draw	Quench cold, draw 850, 2 hrs., to —320 draw 1025 2 hrs.	14	65.2	93.83	97.02	95.43
—320 after double draw	Quench cold, draw 1025, 2X, 2 hrs., then to —320	15	64.4	100.76	93.66	97.21
—320 between double draw	Quench to cold, draw 1025, 2 hrs., to —320, draw 1025 2 hrs.	14	64.7	99.09	95.32	97.20
—320 after double draw	Quench cold, draw 1050, 2X, 2 hrs., then to —320	14	63.7	96.72	90.87	93.80
—320 between double draw	Quench cold, draw 1050, 2 hrs., to —320, draw 1050, 2 hrs.	14	64.5	94.98	93.22	94.10
—320 after single draw	Quench cold, draw 1025, 1 hr., to —320	14	66.0	96.76	94.31	95.54
—320 after multiple draw	Quench cold, draw 1050, 1 hr., to —320	14	65.7	91.13	93.46	92.30
—320 between multiple draw	Quench cold, drawn 1025, 4X, 2 hrs., then to —320	14	64.0	98.71	94.50	96.61
	Quench cold, draw 1025, 2 hrs., to —320, draw 1025, 2 hrs., to —320, draw 1025, 2 hrs.	15	64.7	94.25	98.23	96.24

Table C (Continued)
Effect of Cold Treatment on the Cutting Performance of Molybdenum High Speed Steel

Identification	Treatment (All Previously Preheated at 1500°—15' in 10% CO and Hi-Heated at 2175°—1½' in 10% CO)	Grain Size Snyder	Hardness After Treatment RC	Cutting Speed at Failure F.P.M.		Performance Based on 94 f.p.m. as 100 per cent
				End 1	End 2	
Continuous Cool to -110	Quench to black, then to -110, then draw at 1025, 2X, 2 hrs.	14	63.5	97.35	98.84	104
Interrupted Cool to -110	Quench cold, then to -110, then draw at 1025, 2X, 2 hrs.	15	63.0	91.01	91.70	97
-110 after lo-hi draw	Quench cold, draw 850, 2 hrs. + 1025, 2 hrs., then to -110	14	65.3	90.86	91.38	97
-110 between lo-hi draw	Quench cold, draw 850, 2 hrs. to -110, draw 1025, 2 hrs.	15	65.2	96.49	91.65	100
-110 after double draw	Quench cold, draw 1025, 2X, 2 hrs. then to -110	14	64.0	94.73	91.15	99
-110 between double draw	Quench cold, draw 1025, 2 hrs. to -110, draw 1025, 2 hrs.	14	65.2	95.09	93.06	100
-110 after double draw	Quench cold, draw 1050, 2X, 2 hrs. then to -110	14	64.2	98.23	95.00	103
-110 between double draw	Quench cold, draw 1050, 2 hrs. to -110, draw 1050, 2 hrs.	14	64.0	87.68	93.62	97
-110 after single draw	Quench cold, draw 1025, 1 hr. to -110	14	64.1	90.44	89.90	96
-110 after multiple draw	Quench cold, draw 1050, 1 hr. to -110	15	65.0	92.87	95.00	100
-110 between multiple draw	Quench cold, draw 1025, 4X, 2 hrs. then to -110	14	65.0	89.64	88.28	95
	Quench cold, draw 1025, 2 hr. to -110 Draw 1025, 2 hrs. to -110, draw 1025, 2 hrs. to -110, draw 1025, 2 hrs.					
				Two bits cracked		
				Average		100

Table D
Effect of Cold Treatment on the Cutting Performance of 18-4-1 High Speed Steel

Identification	Treatment (All Previously Preheated at 1500°—15' in 5% CO and Hi-Heated at 2350°—1½' in 5% CO)	Grain Size Snyder	Hardness After Treatment RC	Cutting Speed at Failure F.P.M.		Performance Based on 94 f.p.m. as 100 per cent
				End 1	End 2	
Continuous Cool to -320	Quench to black, then to -320, then draw at 1050, 2X, 2 hr.	12	63.3	97.33	95.67	103
Interrupted Cool to -320	Quench cold, then to -320, then draw at 1050, 2X, 2 hr.	12	64.0	97.18	97.81	104
-320 after lo-hi draw	Quench cold, draw 850, 2 hrs. + 1025, 2 hrs., then to -320	13	65.2	94.25	94.50	100
-320 between lo-hi draw	Quench cold, draw 850, 2 hrs., to -320, draw 1050, 2 hrs., to -320			two tools cracked		
-320 after double draw	Quench cold, draw 1050, 2 hrs., 2X, then to -320	12	64.1	99.51	97.04	105
-320 between double draw	Quench cold, draw 1050, 2 hrs., to -320, draw 1050, 2 hrs., to -320			two tools cracked		
-320 after single draw	Quench cold, draw 1050, 1 hr., 1X, then to -320	13	66.0	94.31	93.04	100
-320 after multiple draw	Quench cold, draw 1050, 2 hrs., 4X, then to -320			two tools cracked		
-320 between multiple draw	Quench cold, draw 1050, 2 hrs., to -320, draw 1050, 2 hrs., to -320, draw 1050, 2 hrs., to -320, draw 1050, 2 hrs.	13	63.7	92.70	94.42	100

Table D (Continued)
Effect of Cold Treatment on the Cutting Performance of 18-4-1 High Speed Steel

Identification	Treatment (All Previously Preheated at 1500°—15' in 5% CO and Hi-Heated at 2350°—1½' in 5% CO)	Grain Size Snyder	Hardness After Treatment RC	Cutting Speed at Failure F.P.M.		Performance Based on 94 f.p.m. as 100 per cent
				End 1	End 2	
Continuous Cool to -110	Quench cold, then to -110, then draw 1050, 2X, 2 hrs.	12	65.0	95.67	96.26	95.97
Interrupted Cool to -110	Quench cold, then to -110, then draw 1050, 2X, 2 hrs.	11	65.7	94.69	92.16	93.43
-110 after lo-hi draw	Quench cold, draw 850, 2 hrs., + 1050 2 hrs., then to -110	12	64.1	96.76	98.46	97.61
-110 between lo-hi draw	Quench cold, draw 850, 2 hrs., to -110, draw 1050, 2 hrs.			two tools cracked		104
-110 after double draw	Quench cold, draw 1050, 2 hrs., 2X, then to -110	12	63.7	99.84	95.36	97.60
-110 between double draw	Quench cold, draw 1050, 2 hrs., -110, draw 1050, 2 hrs.	12	64.9	96.11	98.65	97.38
-110 after single draw	Quench cold, draw 1050, 1 hr., 1X, then to -110			two tools cracked		101
-110 after multiple draw	Quench cold, draw 1050, 2 hrs., 4X, then to -110	12	64.1	92.53	98.12	95.33
-110 between multiple draw	Quench cold, draw 1050, 2 hrs., to -110, draw 1050, 2 hrs., to -110, draw 1050, 2 hrs., to -110, draw 1050, 2 hrs.			two tools cracked		102
				Average		102

A series of lathe tests was conducted to determine the effect of subzero cooling on cutting quality. This test consisted of running a facing out across a disk from the center to the point where the tool failed. The speed at failure is calculated from the radius at which failure occurs. A sturdy lathe, with a 24-inch chuck, 21-inch wide bed, 11-inch wide cross slide, variable speed, and a gear drive was used for the test. The bed was clamped securely during a run to reduce chatter to a minimum. The face of the work after the tests showed perfectly uniform cuts.

The tool blanks were cut $5\frac{1}{2}$ inches long from $\frac{5}{8}$ -inch square hot-rolled and annealed bar stock. After treatment they were ground to $\frac{1}{2}$ inch square and accurately nosed by a grinding jig to the specifications given in the following table:

Tool Bit Angles in Degrees						
Back Rake	Side Rake	End Relief	Side Relief	End Cutting Edge	Side Cutting Edge	Nose Radius (inches)
7	14	12	12	15	25	.090

A 14.75-inch diameter turned forging of SAE 3275 steel heat treated to a Brinell hardness of 250 was used as the disk. The cut was started from a 2.22-inch diameter center hole. The depth of the cut was 0.055 inch and the feed was 0.023 inch. The disk rotated at 40 RPM.

On this test, with high speed steels assigned a 100 per cent rating, cast nonferrous alloy tools have been tested to a rating of 250 per cent and sintered carbide tools to a rating of over 700 per cent. The nature of the failure in a tool bit is shown in Figs. C and D. The reader is looking down on the top surface of the tool nose. Fig. C shows the cratering that resulted from the chip wear. It can be seen that the crater occurred behind the point. The progressive deepening of the crater leaves finally a cutting lip too thin to dissipate the frictional heat and the lip becomes red hot and is rubbed down, yielding the appearance shown in Fig. D. This is the point of failure of the tool.

The hardening temperatures used for these tool bits resulted in a finer grain size than that attained in the specimens of Mr. Kennedy's tests (12 to 15 Snyder compared to 10 Snyder grain size), which factor would tend to diminish any advantages of cold treatment.

The first set of tests was aimed at evaluating cold treatment after the tempering treatment. Blanks of molybdenum-tungsten high speed steel and of 18-4-1 high speed steel were hardened and tempered in duplicate. One set was then sent to the Motor Products Corporation where they were placed in -120 degrees Fahr. deep freeze, containing a convection fluid, for 2 hours. The tools were then ground and tested; the results are given in Tables A and B. No significant difference was found to result from the cold treatment.

The second set of tests was aimed at evaluating cold treatment at various points in the treatment cycle. Continuous cooling down to the subzero temperature, interrupted subzero cooling, subzero cooling between draws, subzero cooling after draws, and subzero temperatures of -320 degrees Fahr. (liquid

nitrogen) and of -110 degrees Fahr. (dry ice and methanol) were applied to blanks of the same heats of steel used in the first set of tests. After treatment the blanks were ground and tested. The results are given in Tables C and D. No outstanding improvement resulted from any of the treatments.

In conclusion, no significant advantage of cold treatment at any stage of the treatment process over the regular treatment properly conducted has been found.

Oral Discussion

R. S. ROSE:⁵ I would also like to comment on Mr. Kennedy's very excellent paper. It is a comparatively minor point but on page 263 of the paper Mr. Kennedy concludes that a 1-hour temper at 1040 degrees Fahr. (560 degrees Cent.) is sufficient to virtually complete the conditioning of residual austenite and bases it on specific volume measurements and dilation curves. In his Fig. 4A, as I interpret it, he extrapolated the dilation obtained by quenching to 140 degrees Fahr., down to room temperature and obtained the difference between that figure and in cooling from a single draw, but it is observed that when he draws the second time there is a very definite expansion which would seem to indicate that it would require more than 1 hour to condition all the residual austenite. Furthermore, as Dr. Fletcher previously pointed out, due to the primary martensite contraction on heating, the difference between the as-quenched condition and the total dilation after the single and double draw would doubtlessly be much greater if this contraction were taken into consideration. Finally, in Fig. 4G, after holding 1 hour at 1040 degrees Fahr. (560 degrees Cent.) and then subsequently supercooling, there is a further expansion indicated after returning to room temperature which would seem to substantiate the fact that 1 hour at 1040 degrees Fahr. (560 degrees Cent.) had not been sufficient to condition all the residual austenite.

A. H. D'ARCAMBAL:⁶ This subject, covering the subzero treatment of high speed steel cutting tools, is a most controversial one. Mr. Kennedy has performed a real service in publishing this paper, his scientific investigation clearly showing that the subzero treatment on high speed steel does not improve the physical properties nor tool life. Booklets have been published stating that high speed steel cutting tools given the subzero treatment show anywhere from 100 to 500 per cent increase in tool life as compared with the same tools given the usual hardening treatment. We have also read with interest leading articles and trade journals quoting similar figures.

Instead of attacking this problem in a scientific manner we took the easy way out by merely giving various types of cutting tools the subzero treatment, comparing the cutting life of these tools with tools made on the same order but given the regular hardening treatment. These 12 to 15 tests, covering such high speed steel tools as taps, reamers and cutters, were carefully conducted in some of the large manufacturing plants throughout the country, no increase in cutting efficiency being noted in a single case on tools given the subzero treat-

⁵Sales metallurgist, Vanadium-Alloys Steel Co., Boston, Mass.

⁶Vice-president and consulting metallurgist, Pratt and Whitney Division, West Hartford, Conn.

ment at -120 degrees Fahr. as compared with tools given the standard hardening treatment. In some cases the tools were given the cold treatment after the quench, others between the two high draws, and still others after finish grinding.

It has always been our belief, although we had to pay \$2500 for a unit to prove same, that when you properly harden and draw high speed steel cutting tools, resulting in all of the austenite being converted to martensite, the subzero treatment will not in any way affect the physical properties or the cutting efficiency of the tool, and we believe that the carefully conducted tests above outlined definitely prove that this statement is correct. Undoubtedly tools that are not properly hardened and drawn will show some benefit from the subzero treatment but even in these cases the increase in cutting life should not be nearly as great as claimed by many investigators.

In closing we wish to have it thoroughly understood that we are not condemning this type of equipment. In our opinion there are certain types of steels that possibly will be benefited by the subzero treatment and moreover there are so many other important industrial uses for these cold units that companies manufacturing same should enjoy a great demand for their product during the postwar period. Our discussion applies only to the results obtained on high speed steel cutting tools given the subzero treatment.

Author's Closure

The discussions presented are very welcome. It was my hope that metallurgists who have actually carried out comparative test programs would add their data and criticisms to the paper. I wish to thank all of them for their contributions.

Dr. Zmeskal's careful and exhaustive work adds greatly to my own findings on subzero treatments. His tests on 6-6-2 and 18-4-1 high speed steels indicate that these steels react to cold treatment in a manner similar to that of the molybdenum-tungsten high speed steels studied in the present paper. His data pertaining to the effect of hot quenching on the stabilization of austenite add to the work of Gordon, Cohen, and Rose. The type of tool failure produced in the disk test indicates that this test measures not only resistance to wear, but also resistance to tempering. Dr. Zmeskal's tool performance data shown in his tables agree with the results of the tool tests shown in Table XX, and also check the hot hardness data of Table XVI showing that subzero treatments have no significant effect on hot hardness or resistance to tempering.

Mr. DePoy's comments are quite interesting and appreciated. With regard to the possible effect of subzero treatment on appearance of the martensite, we are in agreement that no significant effect has been shown to date with optical microscopes. It is hoped that electron microscope pictures may throw more light on this question in the near future.

I am in agreement with Dr. Fletcher's views that very little advantage can be gained by subzero cooling treatments applied to high speed tools which have been properly hardened and tempered. As regards refrigeration showing more improvement with overheated tools, it is possible that more austenite would be retained by hardening at higher temperatures. However, such tem-

peratures will damage the tool by causing extreme brittleness. The highest hardening temperature used was 2240 degrees Fahr. (1225 degrees Cent.) and at this temperature, reference to Fig. 5 will show that plasticity has already dropped. Any further drop in plasticity would certainly prove dangerous to many tools.

Dr. Fletcher and Mr. Rose are correct in warning against using increases in length or volume as a criterion of the amount of austenite transformed when the specimen has been heated between measurements. As they have pointed out, heating tempers the martensite already formed with the marked shrinkage noted in the dilatometer curves 4A and 4D. Admittedly, my conclusion that 1-hour tempering at 1040 degrees Fahr. (560 degrees Cent.) conditions the retained austenite so that all of it transforms on cooling from the tempering temperature should not have been based on the specific volume and dilatometric data presented in the paper. However, although such a tempering cycle may not result in transformation of 100 per cent of the retained austenite as revealed by volume changes, it does result in obtaining optimum physical properties as shown by the following table:

Effect of Tempering Time at 1040 Degrees Fahr. on Two Molybdenum-Tungsten High Speed Steels

Tempering Time at 1040 Degrees Fahr.*	Rock. C Hardness		Mod. of Rupture 1000 Psi.		Plastic Strain Inches per Inch	
	Steel No. 1	Steel No. 2	Steel No. 1	Steel No. 2	Steel No. 1	Steel No. 2
1 hour	65.6	65.7	346	352	0.045	0.052
2 hour	65.1	65.3	338	346	0.042	0.055
3 hour	65.2	64.9	337	340	0.042	0.046

*All test pieces were hardened at 2200 degrees Fahr. (1205 degrees Cent.) and quenched in oil to room temperature.

I appreciate Mr. d'Arcambal's comments as they serve to substantiate my own conclusions in a very practical way. With regard to the effect of subzero treatments applied before or after finish grinding the tools, some additional data have been obtained. We have applied subzero treatments to a series of milling cutters before sharpening them and also to a series of cutters after they have been sharpened. These cutters have been used mostly in milling the flutes in high speed drills. To date, no significant difference in performance has been noted between cutters which are regularly treated, those which have been subzero treated before being sharpened, and those which have been subzero treated after sharpening.

PRACTICAL ASPECTS OF THE SELECTION OF FREQUENCY AND TIME CYCLES FOR THE PROCESSING OF METALLIC PARTS WITH INDUCTION HEATING

BY W. E. BENNINGHOFF AND H. B. OSBORN, JR.

Abstract

The wider acceptance and more general usage of induction heating has placed this equipment in a large number of manufacturing and metal processing plants. The ready adaptation of this relatively new tool requires a knowledge of the various inherent characteristics and behavior of high frequency energy. Frequency, time cycles and inductor design and their relationship to the shape and dimensions of the part being treated are extremely important. This paper deals with a practical approach to the understanding and application of such knowledge, and dispenses with the consideration of the more detailed and involved theoretical aspects.

INTRODUCTION

MUCH has been written describing the underlying principles which control the heating of metals by high frequency currents. Theoretical considerations involving the role played by hysteresis and eddy currents cannot be dismissed too casually. Magnetic materials lose their magnetism at a temperature below that used for heat treating, heating for forging, etc. Nonmagnetic substances such as carbon, aluminum, copper, and brass respond readily to induction, as do the nonmagnetic steels. The heat generated due to hysteresis is therefore probably of negligible importance, and that resulting from the eddy currents is the controlling factor. Therefore, any material which is capable of conducting a current, when placed within the confines of a conductor carrying alternating current, will become heated. Specifically chosen frequencies of 960, 1920, 3000, 9600, and upwards of 100,000 cycles are being used extensively at this time.

The high frequency currents mentioned above, carried through an inductor designed to produce a specific heating result, generate

A paper presented before the Twenty-sixth Annual Convention of the Society held in Cleveland, October 16 to 20, 1944. Of the authors, W. E. Benninghoff is manager, and H. B. Osborn, Jr., is research director, TOCCO Division, Ohio Crankshaft Co., Cleveland. Manuscript received July 17, 1944.

a magnetic field within the space it encircles and induce a flow of current in any conductive material close enough to have the magnetic flux lines cut through it. The intensity of the field is greatest at the midpoint of the width of the inductor and near its inside face. The inductively heated part has thus become the secondary of a simple transformer wherein the inductor is the primary. Much of the mystery which apparently enshrouds the understanding of the principles of induction heating processes may be cleared away by thinking of it as I^2R heating. Since the substance which carries the induced current has the ability to act as a conductor, it also has an electrical resistance to this flow of energy. We may then compare induction heating to straight resistance heating and establish it as I^2R heating. That is, there is a flow of current (I) and a resistance to the flow (R) which combined are responsible for the generation of heat. However, the unusual characteristic of high frequency heating upon which all surface hardening applications depend, is its tendency to concentrate on the surface of the conductor through which it flows. This phenomenon, called skin effect, is a function of frequency. Other factors being equal, the higher the frequency, the shallower the depth of penetration. The limitations of this relationship are discussed in detail in subsequent portions of this paper.

When the temperature of an inductively heated magnetic steel bar arrives at the critical point, all heating due to hysteresis ceases and that due to eddy currents continues at a reduced rate. The rate of heating decreases with time as the electrical resistance to the flow of current increases with temperature. Since the entire action goes on in the surface layers, only that portion is affected. The original core properties can be maintained, and surface hardness secured by quenching when complete carbide solution has been attained. Continued application of power causes an increase in depth of heating, for, as each layer of steel is brought to temperature, the current density shifts to the layer beneath, which offers a lower resistance. Additional depth results from heat by conduction with longer time of heating.

It is obvious that the selection of the proper frequency and the control of power and heating time make possible the fulfillment of any desired specifications of surface hardening or through-heating for heat treating, annealing, normalizing, brazing, or forging or forming.

There are certain relationships between frequency and diameter

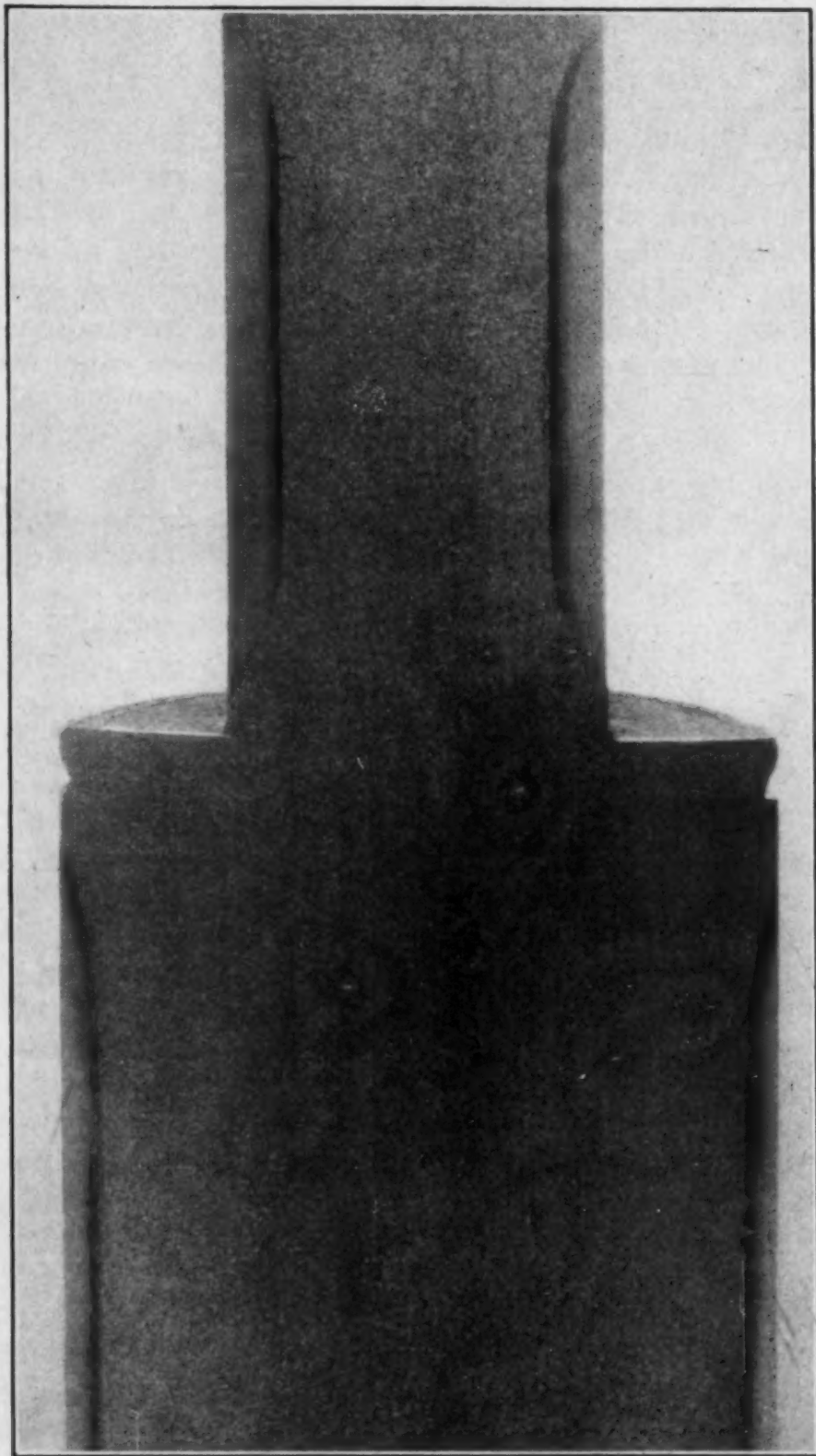


Fig. 1—End of 48-Inch Long Roller Induction Hardened with 9600 Cycles. S.A.E. 1045 Steel. 2-inch diameter hardened progressively at 0.33 inch per second with 65 KW, pilots with a "single shot" at 80 KW for 2.5 seconds.

or thickness of stock treated upon which may depend the selection of the specific frequency to be used for a particular application. Currently, however, it has been found that more than 95 per cent of all induction heating problems can be solved successfully by the use of energy of 9600 cycles or less.

All induction heating equipment consists of an inductor, quenching auxiliaries if needed for hardening, suitable transformers and capacitors, automatic timing controls, and a high frequency generator. In addition, provisions are made for handling the parts intermittently or continuously, depending upon production requirements and hardening specifications. Fig. 1 shows bearing surfaces on a mill roller, the large diameter having been hardened progressively, and the small diameter with a "single shot."

The inductor may be a single turn of copper to fit the piece to be heated, or several turns of copper tubing shaped for the same purpose. Careful design is essential at this point to insure maximum efficiency. However, symmetrical inductors may be used to heat unsymmetrical objects because of the natural tendency of the high frequency current to follow the contour of the piece. The quenching medium is supplied through the inductor by means of orifices which are an integral part of it, Fig. 2. The same timing device which controls the heating cycle operates an electric quench valve and controls the quenching cycle to the same degree of accuracy and also indexes parts in and out of the inductor when necessary.

Fixtures for holding parts and necessary inductors are specially designed, but are adjustable and adaptable to a wide variety of parts. Furthermore, the change from one fixture and inductor assembly to another takes but a few minutes, since the mounting positions of the equipment are generally standard. The change involves no more effort than change of a fixture on a machine tool. A single induction heating unit may be used for economical processing of hundreds of different parts.

Automatic control and accuracy are keynotes in induction hardening from two standpoints. First, because of precise design of equipment, there is automatic positioning, assuring exact locations of hardened areas (more than one area can be treated simultaneously), and automatic control of heating, quenching, and indexing cycles to within 0.1 second accuracy. Second, this control makes each heating operation and treated object an exact duplicate of all others processed with the same set-up. Further, total elimination of human error

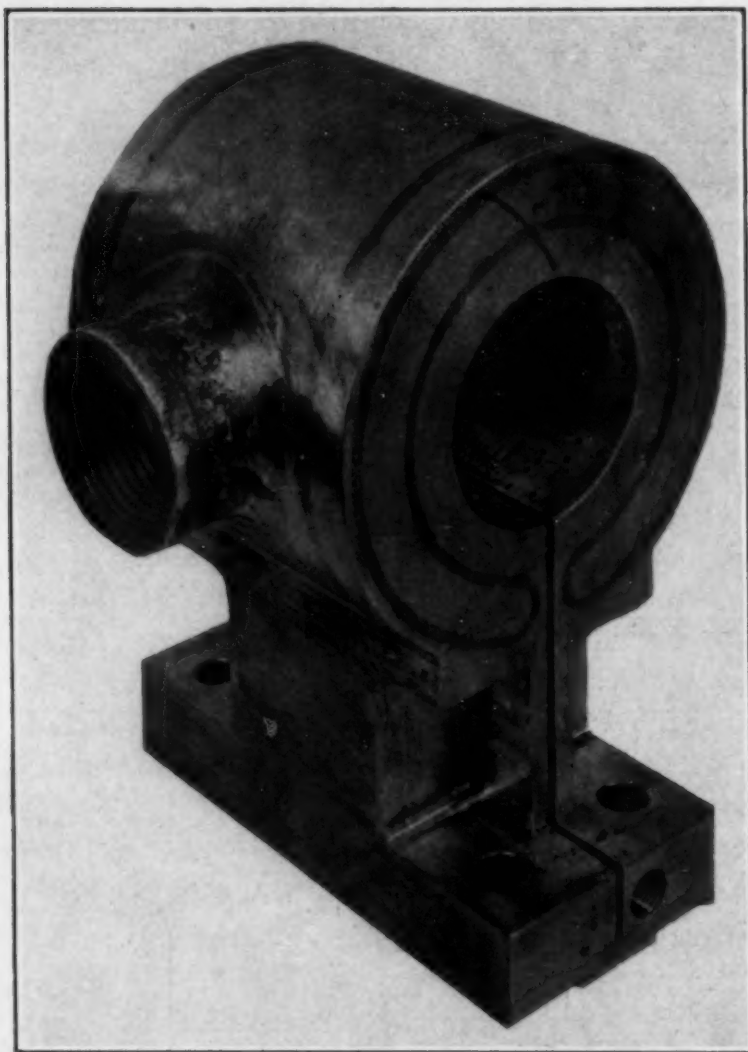


Fig. 2—Typical Inductor Block for "Single Shot" Hardening. Note cooling water inlets in base and quench holes on inside diameter for instantaneous quenching.

avoids the usual variations and mistakes so characteristic of manual control.

A complete description of the different types of induction heating units, and various metallurgical aspects as well as applications for the process, have been described in detail in earlier publications by the writer (1), (2).¹

FREQUENCY AND ITS RELATIONSHIP TO DIAMETER OF STOCK

Numerous equations have been presented involving the use of Bessels functions and hyperbolics which attempt to establish a for-

¹The figures appearing in parentheses pertain to the references appended to this paper.

mula permitting calculation of the minimum optimum frequency suited for specific work. In its simplest form, it includes such factors as diameter, permeability of material, and constants. Strangely enough, however, it can be demonstrated that such relationships, while acceptable from a theoretical standpoint, do not prove correct in actual practice.

Since the main purpose of the paper is to present simple usable data, we propose the following equation to be used as a guide in the selection of the minimum optimum frequency suited for inductively heating cylindrical stock to temperatures above the magnetic transformation point (i.e., normal temperature used for heat treating and heating for forming, forging, normalizing, etc.) where the magnetic permeability of the material is unity.

$$F = \frac{180}{R^2} \quad (1)$$

F = Min. Opt. Frequency — cycles per second.
R = Radius — inches.

As a limitation to the above, note that frequencies of less than approximately 1000 cycles are not generally used because of electrical problems of equipment design and power factor correction. No factor of efficiency is to be considered since it can be shown that with correctly designed inductors and properly applied time cycles, the conversion of kilowatts to B.t.u. energy in the metal is substantially independent of frequency. This is true especially if the index ratio is above 2.5, being equal to the radius in cm. divided by the specific resistance of the material in ohms/cc. See N. R. Stansel on this and other related factors (3). Further, this equation makes no attempt to define concentration of energy or distribution of heat through a cross section, but only the heat developed in the surface layers. The effect of time of heating, energy per unit of surface area, and transfer of heat by thermal conductivity to the core is described in a following portion of this paper.

For illustrative purposes, the following data show *approximately* the correct order of magnitude of the factors given in the above equation, as affecting the treatment of cylindrical stock, of a hardenable analysis, quenched immediately following a heating time of short duration and one which permits a minimum of heat transfer by thermal conduction.

A 1/2-inch diameter bar heated with 1920 cycles would heat sub-

stantially throughout its entire cross section and very little, if any, decremental of hardness would result. Treated with 9600 cycles, surface hardening to a depth of approximately 0.080 inch is generally obtained, and shallower depths with excessive power input per unit of surface area or with higher frequencies.

A $\frac{1}{4}$ -inch diameter bar heated with 1920 cycles could not be effectively heated to temperatures which would permit hardening, although this frequency is satisfactory for annealing or low temperature drawing. Heated with 9600 cycles, this bar would show adequate temperature for hardening, but as with the $\frac{1}{2}$ -inch diameter stock on 1920 cycles, hardness would be throughout the entire cross section. Surface hardening would dictate the need for frequencies well above 9600 cycles.

A $\frac{1}{8}$ -inch diameter bar could not be effectively heated to hardening temperatures with 1920 cycles, although 9600 cycles is being used for subcritical annealing or drawing. Obviously, such work is generally confined to the progressive treating of wire. Frequencies above 100,000 cycles are needed for through hardening such stock. Surface hardening of material of these dimensions is not considered practical.

Although special low frequency inductors have been designed for the processing of strip stock which shows considerable merit, the above data, as well as the equation, will be approximately correct for such items with thickness of plate being substituted for diameter.

DEPTH OF PENETRATION OF ELECTRICAL ENERGY

The depth of penetration of the induced electrical energy for a bar subjected to high frequency energy for hardening [temperature approximately 1500 degrees Fahr. (816 degrees Cent.)] is approximately defined by the following equation:

$$D = \sqrt{\frac{4}{F}} \quad (2)$$

D = Depth of penetration of electrical energy-inches
 F = Frequency in cycles per second.

Unfortunately, however, this factor of depth has no physical significance, since it assumes that time is zero. Since no metallurgical transformation can take place in zero time, the depth of penetration of hardness will always be considerably in excess of the above calculated depth when time assumes a significant value and heat flows by conduction from the surface, to layers beneath, as described in a previous section of this paper.

The depth of metal carrying the induced current does not have a uniform current density; the surface has a value of maximum intensity and this value decreases vectorially through the zone to zero at the depth calculated by the above equation. The heat resulting from this energy is proportional to the square of the current density and thus the temperature differential between the surface and bottom of heated zone falls off faster than the current density. This phenomenon would seem to offset the tendency for greater depths of hardness resulting than the calculated depth of electrical energy, but the heat flow by conduction is so rapid and begins the instant any temperature gradient is developed, that only if time were but infinitesimally greater than zero would such an effect be noticeable.

At the present time, it is not considered practical to use heating times for single shots of much less than 1 second due to the limitations imposed by control equipment.

Since a heating time of 1 second has a significant value and is appreciably more than an amount infinitesimally greater than zero, the resulting depth of hardness is, in general, several times that of the theoretical depth calculation of equation No. 2. Obviously, the microstructure must be such that it will respond to a short heating cycle if we are to approach these minimum values. For the production of a fine homogeneous martensite, a sorbitic structure is ideal, a normalized structure usually satisfactory, depending upon the coarseness of the pearlite, and a spheroidized structure not desirable unless containing very fine, well distributed carbides. The sluggishness of certain metallic carbides found in alloy steels must also be taken into consideration. Due to short heating cycles, induction heating is not bound by the usual limitations of coarsening temperatures, and we can overcome the reticence of certain structures to go into solution by heating to temperatures several hundred degrees above the upper critical with no deleterious effects.

Assuming reasonable response of structure, the following table shows the absolute minimum depths of hardness which should be considered for production work:

Frequency Cycles Per Second	Approximate Minimum Practical Depth of Hardness Inches	Approximate Theoretical Depth of Penetration of Electrical Energy Inches
3,000	0.060	0.035
9,600	0.040	0.020
120,000	0.030	0.006
500,000	0.020	0.003
1,000,000	0.010	0.002

The foregoing depths of hardness data represent actual results obtained with structures which respond very readily to heat and are values noted with both single and progressive methods of treatment with power input of at least 15 KW per square inch of surface area. Note that the depths are considerably greater than the theoretical depths calculated from equation No. 2. Obviously, the diameter of the stock must be sufficient to offer a reasonable core, since, for example, the flow of heat is so rapid in a piece of steel that regardless of frequency or power, material of less than $\frac{1}{8}$ -inch diameter cannot be surface hardened. A similar condition exists with tubing. If we are hardening such a part, the wall thickness should be at least twice the depth of hardness anticipated. Although other factors such as the relationship of wall thickness to diameter assume importance in such instances, it is not considered appropriate to discuss them here (4).

FREQUENCY VERSUS POWER INPUT PER UNIT OF SURFACE AREA

Fullest advantage of the skin effect of high frequency heating is obtained only if the surface area can be brought up to hardening temperature in a very few seconds. To do this, we must introduce a sufficient amount of energy into the inductor block to induce adequate current in the surface of the zone to be heated. The width of the inductor is slightly greater than the area heated but may be considered the same for the sake of discussing surface energy relationships. The power introduced into the inductor is measured in kilowatts, and we, therefore, speak of the power input as kilowatts per square inch of surface area heated. Unless we maintain certain minimum values for this factor, flow of heat by thermal conduction will result in increase of the depth of hardness.

As the area increases due to a greater width being required, the number of kilowatts required for a specific part increases proportionally. For example, if a 1-inch wide bearing on a 2-inch diameter shaft required 60 KW, then to harden a 2-inch wide area on the same shaft to the same depth of hardness would necessitate power of the order of 120 KW.

If the area increases due to an increase in diameter, the kilowatt requirement increases also, but not in direct proportion. Purely as a guide, and to illustrate this condition, note Fig. 3 which shows kilowatt requirement per square inch to produce a depth of approxi-

mately 0.100 to 0.150 inch using a frequency of 9600 cycles. This curve has been plotted from an accumulation of data collected over the past several years.

To maintain minimum depths of hardness, we must provide certain minimum power input per unit of area. Due to limitations of power from the high frequency sets operating above 100,000 cycles,

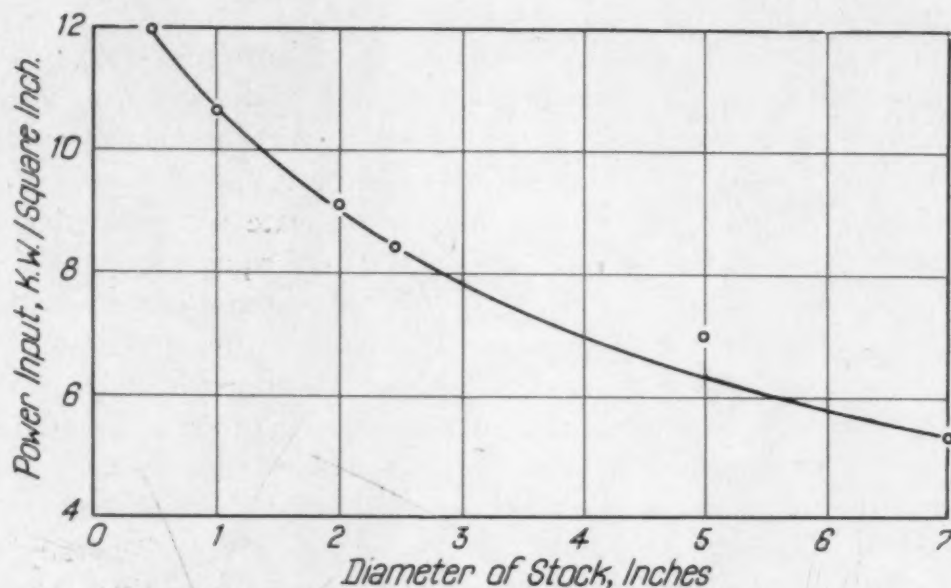


Fig. 3—Suggested Minimum Values of Power Input Per Unit of Surface Area Plotted Against Diameter. Frequency 9600 cycles, average depth of hardness 0.100 to 0.150 inch. Data suitable for higher frequencies but not to minimum depths.

we cannot harden large parts to depths which dictate such frequencies. The higher the frequency, the more important becomes this power per unit area requirement. Where 5 KW per square inch of surface area may maintain minimum depth requirements at 9600 cycles, a minimum of 10 KW on a large diameter or 30/40 KW per square inch on small diameters might be needed at 500,000 cycles to obtain the shallower depths associated with this higher frequency. The intensity of the magnetic field is greatest at the inside face of the inductor and the space between the part being heated and the inductor is held as small as possible, but not to a point which will introduce mechanical problems of locating and handling. Increase of the gap results in slower rates of heating for fixed power input and thus greater depths of hardness. To offset this, power must necessarily be increased.

EFFECT OF HEATING TIME ON DEPTH OF HARDNESS AND MICROSTRUCTURE

Discussion thus far has stressed the factors affecting minimum depth control. Some reference has been made to the mechanism by which depth of hardness increases with heating time. We shall now consider more specifically the various factors associated with the production of controlled depth of heating.

When a particular part is to be induction hardened, we obviously must rely upon some data to guide us in the selection of power and heating time. The effect of frequency and power input has been described in previous pages, but once we have established these factors (assume 9600 cycles) we can roughly estimate a heating time requirement of approximately 35 KW seconds per square inch. For example, for an area 1 inch wide on a 2-inch diameter bar, we would try 58 KW (Fig. 3) for 3.8 seconds, followed by a quench at sufficient pressure and duration to cool the part to approximately 200 degrees Fahr. (93 degrees Cent.). Observation of this initial trial might note a temperature in excess of that required for hardening. (Different prior structures show marked differences at final temperatures under identical conditions of power and time. Generally, coarsely spheroidized structures attain less temperature than one which is finely pearlitic, due to a difference in specific resistance.) A decrease in power input would then be tried and a check on the surface hardness made to see if the material has hardened to values anticipated because of its analysis. Assuming results are acceptable, the specimen is then cut, polished, and etched, and subsequent action governed by its examination, both under the microscope and hardness tester. The following tabulation may then be used for reference:

Microstructure	Depth	Remedy
Incomplete solution	Satisfactory but may be increased	Increase heating time
Incomplete solution	Satisfactory but may be increased	Increase power input
Complete solution	Too deep	Increase power input and decrease heating time
Complete solution	Too shallow	Increase heating time and decrease power input
Coarsened	Satisfactory but may be decreased	Decrease power
Coarsened	Satisfactory but may not be decreased	Decrease power and increase time
Coarsened	Too deep	Decrease power and decrease time
Coarsened	Too shallow	Decrease power and increase time

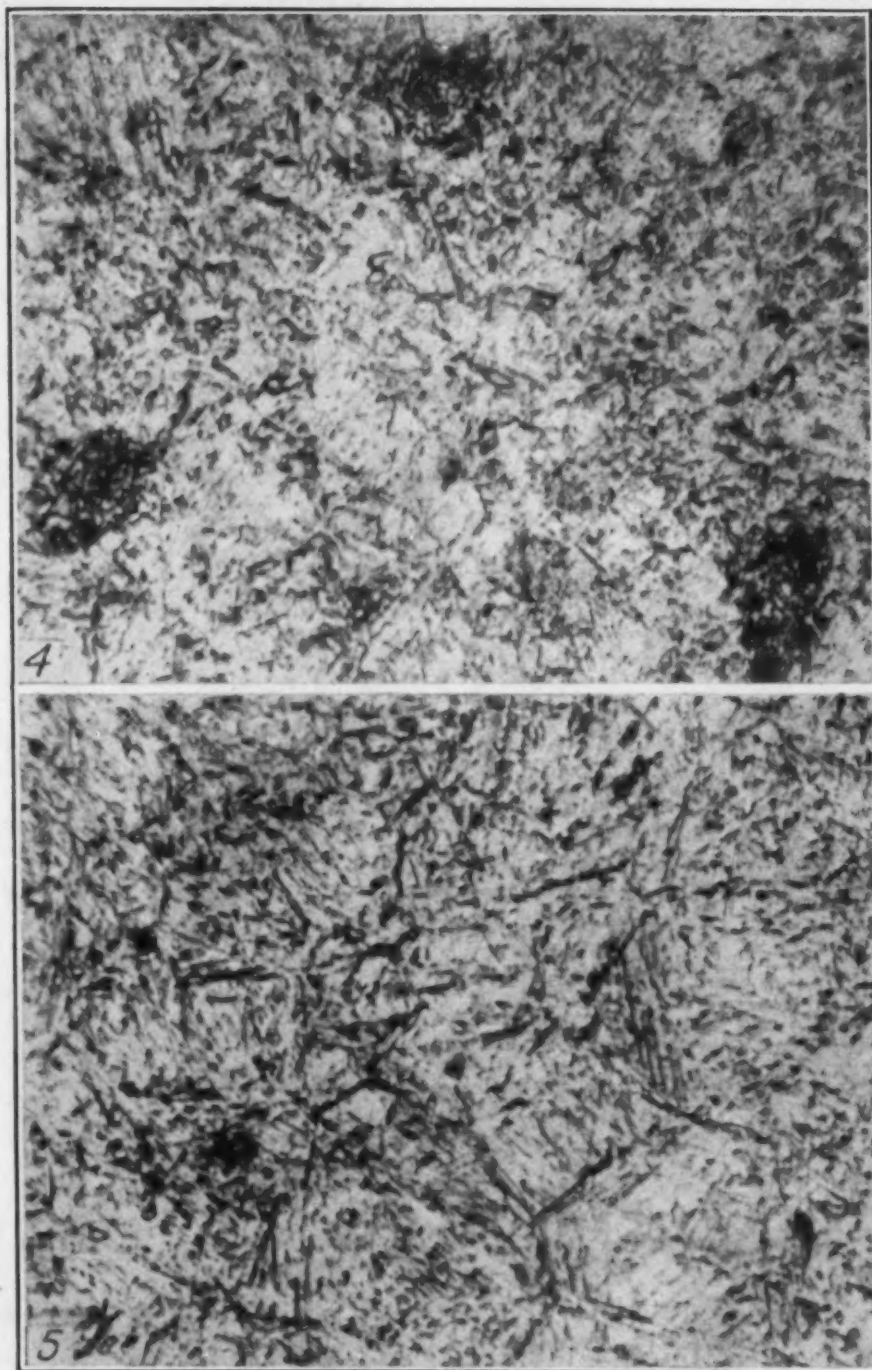


Fig. 4—Photomicrograph at $\times 500$ Showing Hardened Structure of a 40-Millimeter A.P. Projectile. WD4150 Steel. Original pearlite and residual carbides show incomplete transformation.

Fig. 5—Photomicrograph at $\times 500$ Showing Hardened Structure of a 40-Millimeter A.P. Projectile. WD4150 Steel. Overheating has resulted in coarsening.

Obviously, no values of percentage can be assigned to the recommended modifications of power and time. Fortunately, the short

heating times of induction heating permit considerable latitude in heat treating temperatures, and one modification of a preliminary cycle will generally suffice.

A most important item of control in all induction heating applications is that of the delay time between end of the heating period and the beginning of the quench. Quite often, a modification of delay time or introduction of the same is used in preference to, or in conjunction with, changes in power and heating time. Since a delay period permits additional time for heat penetration and carbide solution, an increase may be used in preference to increasing power or time to prevent the necessity of heating to higher temperatures.

Quenching technique varies as do time cycles, but general practices prevail in that the cooling must be in excess of the critical

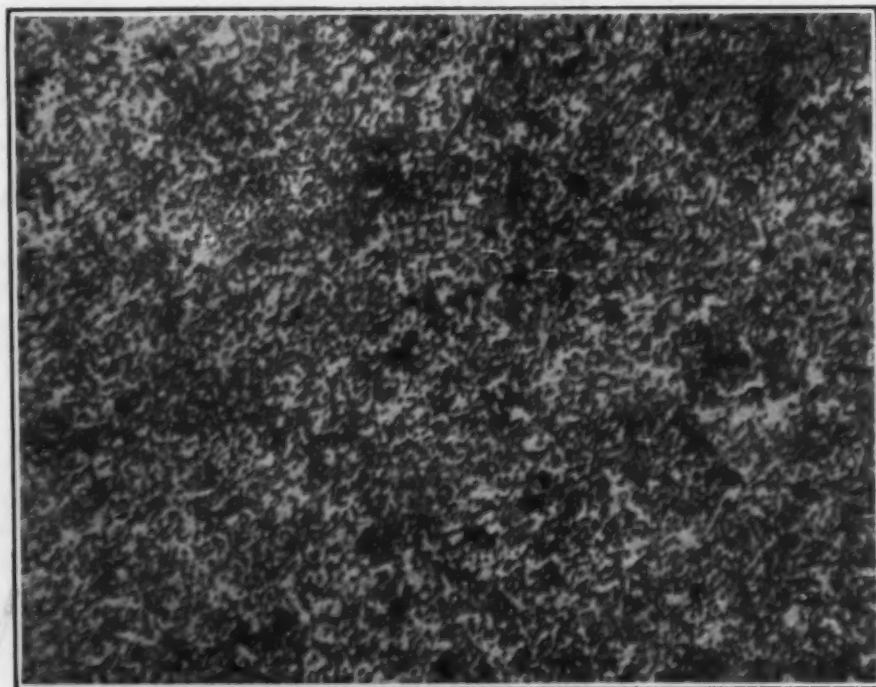


Fig. 6—Photomicrograph at $\times 500$ Showing Hardened Structure of a 40-Millimeter A.P. Projectile. Shot from same lot as used in Figs. 4 and 5 treated with modified cycle to produce desired microstructure.

cooling rate with usual precautions given to undercooling or too rapid cooling and the production of stresses which lead to cracking.

High power inputs for short periods of time produce shallow depths of hardness. Application of lower power per unit of area for long periods permits heat flow by conduction. There are certain limiting features of frequency which we will not present here involv-

ing maximum frequencies for through heating as related to diameters. Obviously, frequencies of several hundred thousand cycles would not serve for through heating of bars approximately 1 inch in diameter and larger, due to the concentration of energy on the surface. To overcome the more marked skin effect on these higher frequencies, the power input would have to be reduced to such a low value that the heating time would be unusually long, and radiation losses appreciable.

9600-cycle equipment has been used very successfully in the heat treatment of large cross sections. The most outstanding example of this has been the heat treatment of armor-piercing shot, including 20, 37, 40, 57, 75, and 90 millimeter, as well as a 5-inch A.A. shell. Control of cycles is just as important for such parts as for surface hardening. However, our only concern is microstructure and hardness. On a standard armor-piercing shot machine cycles are checked and may be modified for each heat of steel. Fig. 4 shows the microstructure of a 40-mm. shot (Material WD4150) hardened with a power input of 10 KW and 70 seconds heat, 20 seconds delay, and 30 seconds quench. Note the incomplete solution of the pearlite and the presence of carbides. Fig. 5 shows a structure resulting from overheating. These shot were below specifications in hardness, and would no doubt have failed on ballistic test. Requisite modification of treating cycle can be made in three ways. Shot from the same lot were hardened and the resulting satisfactory microstructure is shown in Fig. 6. The hardness deficiency was also corrected. An increase of power input, increase of heating time, or an increase in delay time, or combinations of same, correct deficiencies of the structure shown in Fig. 5. Decrease of power, decrease of heating time, or both, overcome coarsening difficulties.

PROGRESSIVE OR CONTINUOUS HEATING

Increase of surface area resulting from increasing width of area requires additional power in direct proportion to the area in order to maintain the same energy input per square inch for surface hardening. Obviously, processing of a long bar would be somewhat impractical with the "single shot" method to which we have confined previous discussion. To minimize the amount of power required, it is a very simple matter to heat a narrow band on the surface and by moving the stock progressively through the inductor to continue

heating the surface with a maintained high power input. The forward (or downward) motion of the bar carries it into the quench which is continuously flowing in a sheet from the inductor. The angle of incidence of this quench may be modified to suit specific conditions. Increasing or decreasing of the angle has the same effect as increasing or decreasing the delay period in the "single shot" method. Further, change in the rate of travel of the stock through the inductor accomplishes the same effect as modifying the heating time.

The selection of the rate of travel for various diameters and

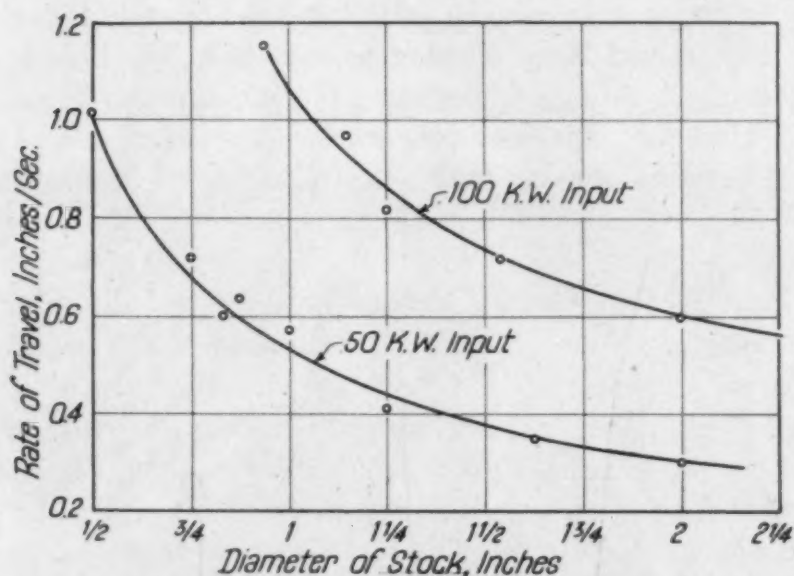


Fig. 7—Progressive Surface Hardening of Cylindrical Stock. 9600 cycles to average depth of 0.100 inch. Data includes S.A.E. 3140, 4130, 1045, 52100 steels. Complete solution may not be obtained for full depth at 100 K.W.

power inputs depends somewhat on the width of inductor used and depth of penetration selected. Fig. 7 may serve as a guide, since it shows the relationship of these factors at 50 KW and 100 KW introduced through an inductor approximately 1 inch wide to harden approximately 0.100 inch deep. Steel is assumed to be in a condition which will respond readily to a short cycle. Further, the inductor must be relatively closely coupled, i.e., the space between the surface of the bar and the I.D. of the inductor should be approximately 0.100 inch. Increase of this gap places the surface of the bar in a weaker portion of the magnetic field, and as with "single shot" methods, the power at the inductor must be increased if we are to maintain the same depth of hardness. A slower rate of travel in the continuous method or increase of heating time for a "single

shot" will offset this coupling deficiency, but only at the sacrifice of shallowness of depth.

Fig. 8 illustrates the effect of rate of travel on depth of hardness for a 1 $\frac{3}{4}$ -inch diameter track pin of S.A.E. 1050 steel, hardened to 60 Rockwell "C" minimum, with 150 KW at 3000 cycles.

Further development of the technique so successfully used for the surface hardening of cylindrical stock now finds use in the through heat treatment of bar stock free of scale and absolutely uniform throughout cross section and length. Equipment handles sizes from $\frac{1}{2}$ inch up to 3 inches in diameter and by adjustment of

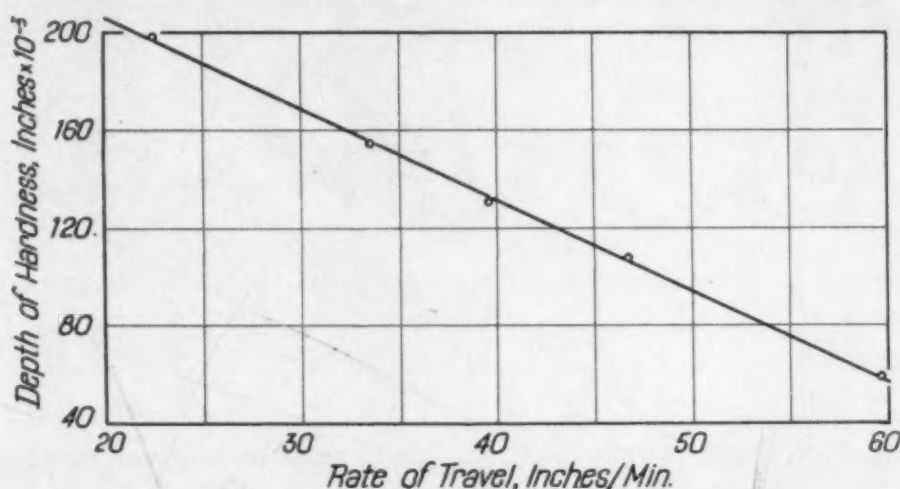


Fig. 8—Effect of Rate of Travel on Depth of Hardness for 1.5-Inch Track Pins. S.A.E. 1050 steel, 60 Rockwell "C" minimum, 3000 cycles at 150 KW.

rate of travel and power input, bars are heated uniformly to necessary hardening and drawing temperatures. The inductors consist of several turns of copper tubing providing a large amount of area and thus a low power input per square inch so that heat is generated slowly on the surface and flows by conduction to the center of the bar. Power of less than 0.5 KW per square inch is used, depending upon the stock size. Fortunately, the inductor can be spread out to cover large areas and special designs are used to insure complete and uniform heating of the entire cross section of stock. Two coils operate in the same line, the first controlled for heating to hardening temperatures [approximately 1500 degrees Fahr. (815 degrees Cent.)] following which the bar is quenched to full hardness and the second for heating to adequate drawing temperature depending upon analysis for the production of requisite hardness for specified physicals. Processing of tubing is carried on in the same manner,

although most applications require but one heating such as the annealing of stock coming directly from a welding machine or subsequent cold drawing to relieve cold work of a previous operation. Stainless steel tubing is a particularly good example of the latter.

The temperature obtained for through heating may be raised to forming and forging values with stock fed as long bars, or billets, or short slugs going directly to the press.

Energy conversions are rather interesting and show values of from 5 to 15 pounds of stock heated per kilowatt-hour of energy

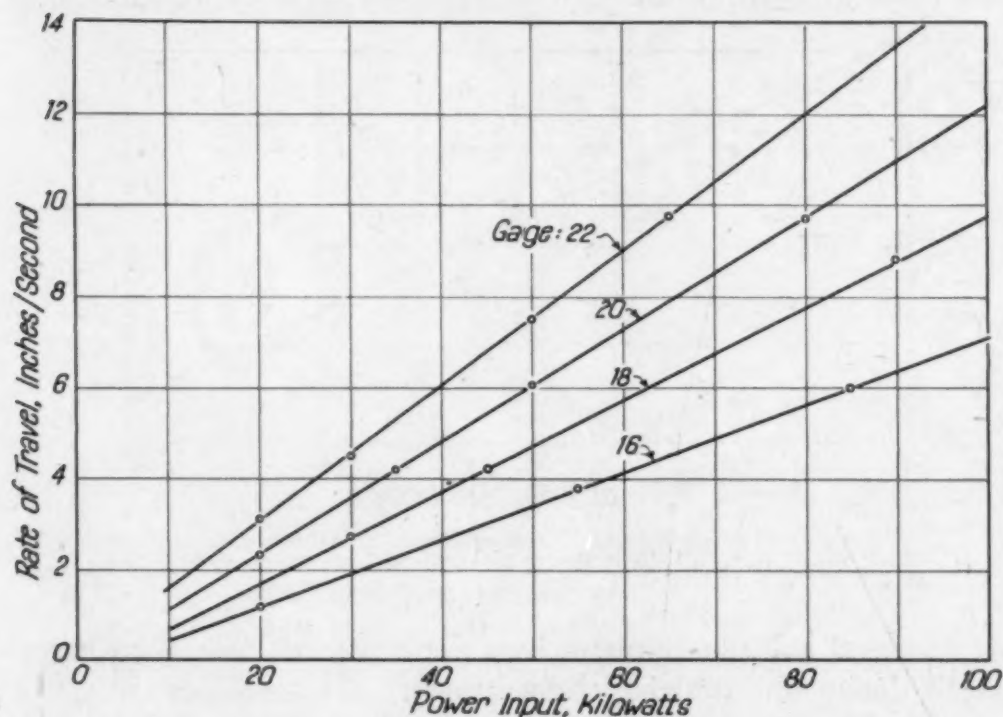


Fig. 9—Effect of Power Input on Rate of Travel for Continuous Through Heating of X4130 Tubing to 1600 Degrees Fahr. (870 Degrees Cent.). 9600 Cycles. Data for $\frac{1}{4}$ to 1-inch O.D. tubing but suitable for larger diameters and for higher frequencies on smaller diameters.

input, depending upon temperature. Progressive heating of tubing (for annealing, heat treating, normalizing, brazing) is perhaps the most efficient application for induction heating. When the wall thickness approaches the same order of magnitude as the depth of penetration of the electrical energy, our energy conversions are increased over the values given above. For equation showing this effect, and discussion, see article by R. M. Baker (4). Fig. 9 shows data for processing of X4130 tubing at 1600 degrees Fahr.

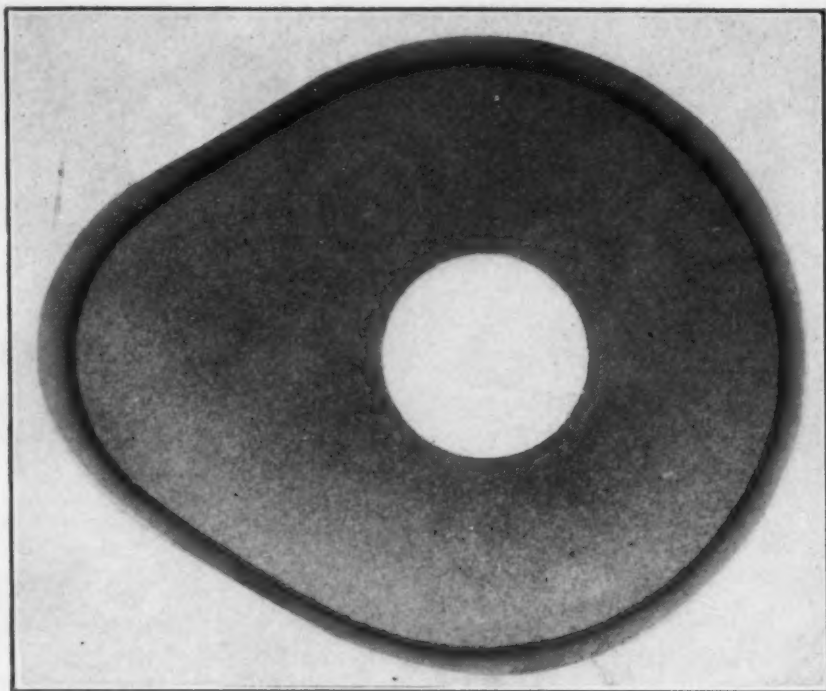


Fig. 10—Pearlitic Malleable Brake Cam Hardened with 1920 Cycles. Round inductor.

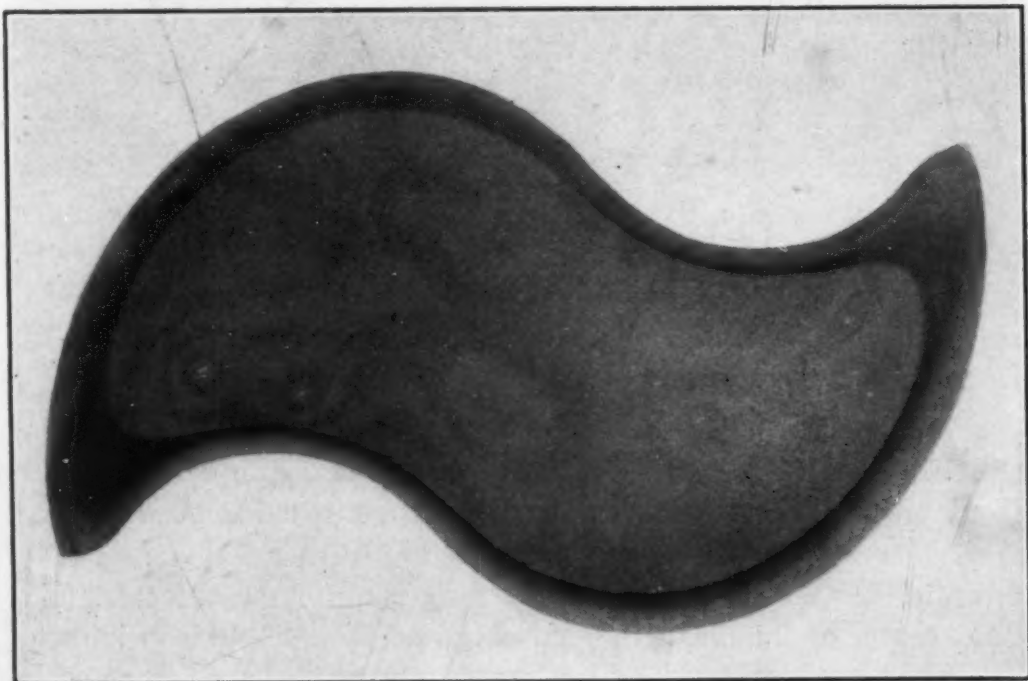


Fig. 11—Demonstrating Low Frequency Contour Hardening. 4-inch (tip to tip) S.A.E. 1045 brake cam hardened in a round inductor with 1920 cycles. Round inductor.

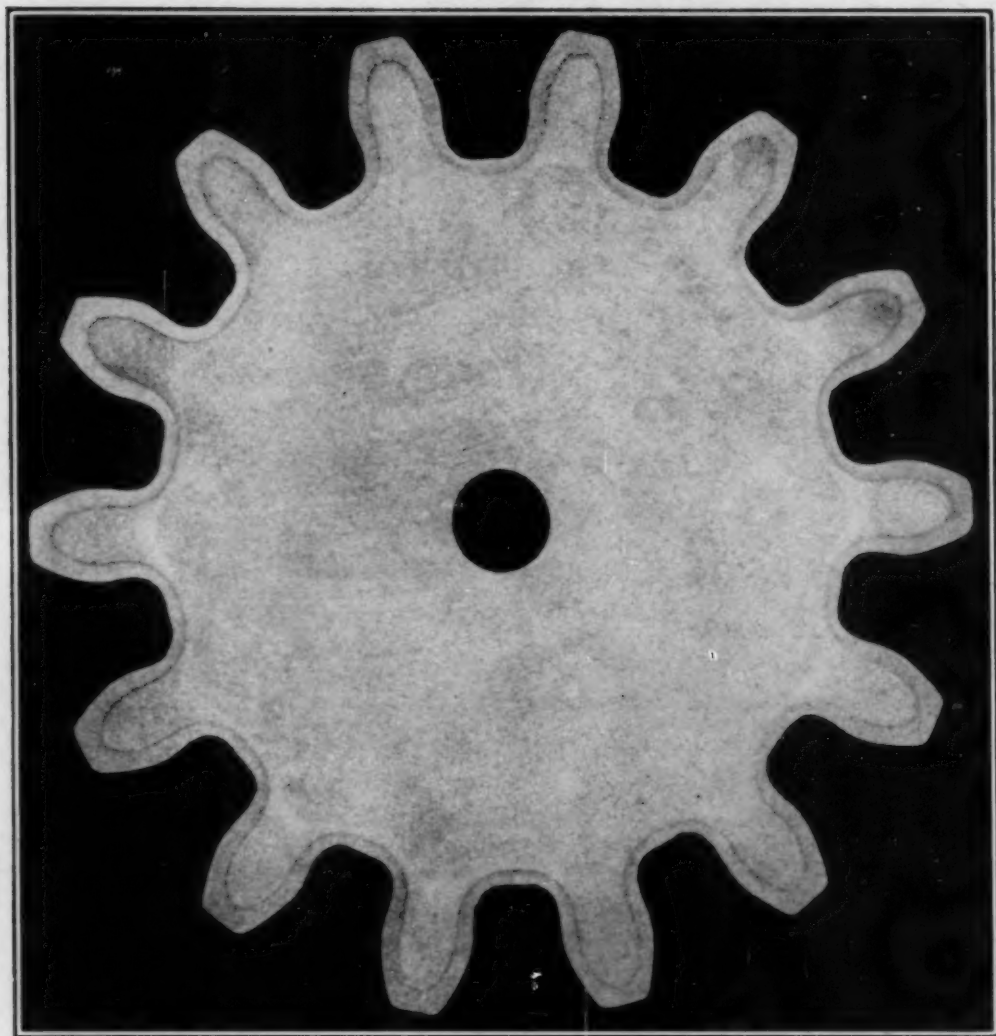


Fig. 12—Contour Hardening of a 4-Inch Diameter Spur Gear with 450,000 Cycles.

RELATIONSHIP OF FREQUENCY AND POWER PER UNIT OF AREA
TO CONTOUR OF HARDENING

The skin effect of the high frequency energy from a round inductor holds the induced current to the surface of the object being heated. Fig. 10. Regardless of frequency, the depth of heat is perfectly uniform on a cylindrical surface provided it has been centered in the magnetic field. A part heated well off center will show greater depth in the area subject to the closer coupling of the inductor. The exact center of the magnetic field produced by a single loop inductor is not the geometric center, due to the effect of the point at which the current leaves and enters the loop. At higher frequencies, this effect is more noticeable, but may be overcome by moving the part just slightly toward this area or by rotation during the heating cycle.

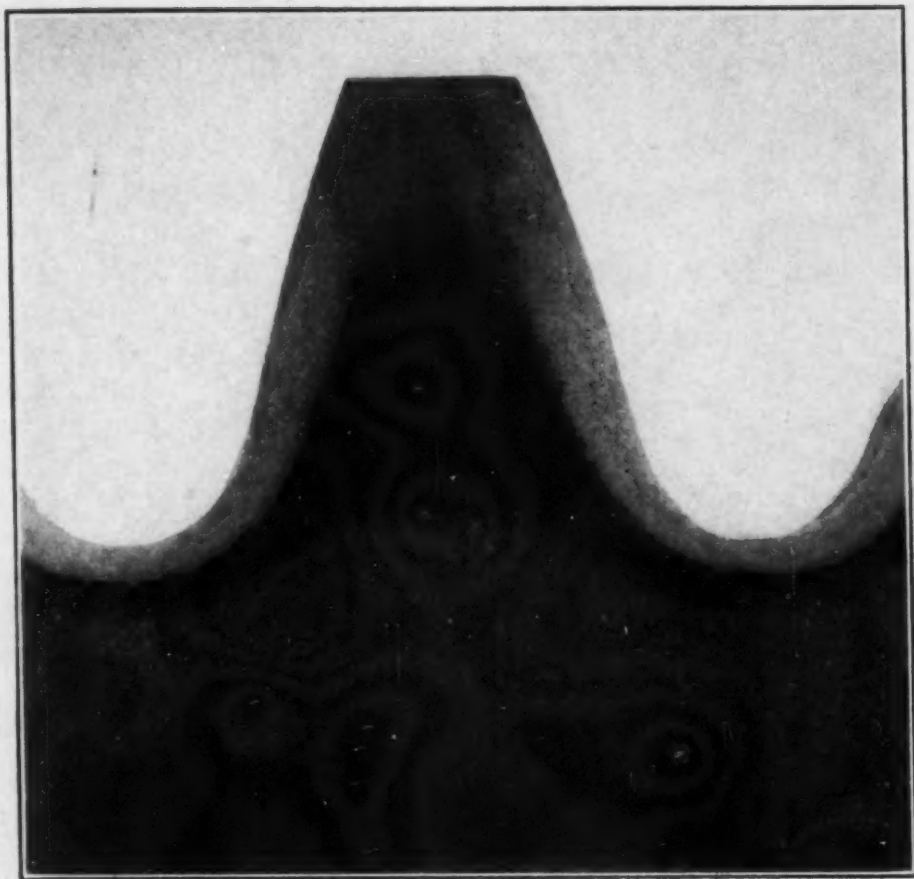


Fig. 13—Contour Hardening of a Large 26-Inch Diameter by 5-Inch Face, 275-Pound Final Drive Gear. Photo shows section including 1 tooth. S.A.E. 1045, 9600 cycles, 500 KW.

As we depart from a perfect cylindrical surface, the skin effect tends to produce uniform depth of heating, even when treated with round inductors. High frequencies exhibit this tendency more strongly than lower frequencies, but we must not fall below the recommended minimum values of kilowatts per square inch lest we lose the benefit of the skin effect and have heat flow by conduction produce contours not wanted. To illustrate, see Fig. 11 which shows a brake cam which has been contour hardened with a round inductor but with a low frequency of 1920 cycles.

A gear is nothing more than a cylinder with a distorted surface and contours which follow the tooth form perfectly are obtainable, but with definite limitations. Fig. 12 shows a spur gear which has been hardened with 450,000 cycles. The tooth spacing and pitch is of such a nature that the depth of hardness is quite uniform. Were we to process a finer pitch gear and introduce almost uniform energy

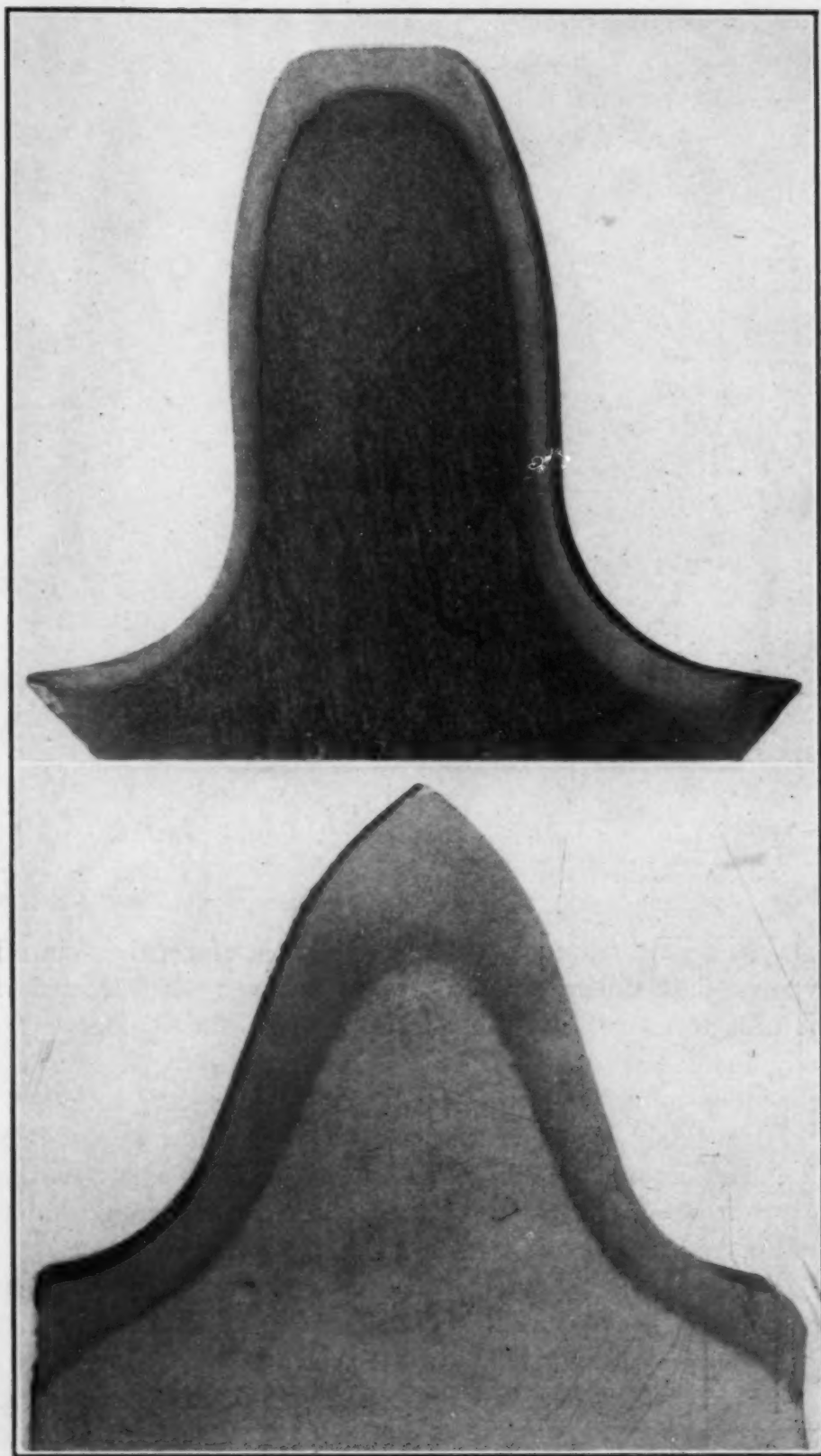


Fig. 14—Teeth from Two Typical Tank Sprockets. 9600 cycles with formed inductor, one tooth at a time.

over the surface, the depth of hardness would be greater on the sides of the tooth than at the root, due to the lesser volume of metal beneath in proportion to the surface area. This condition makes it practically impossible to contour harden a very fine pitch gear, regardless of frequency or power. We believe that contour hardening is limited to gears of less than approximately 5 to 7 pitch. Fig. 13 illustrates the contour hardening of a large final drive gear, 26-inch diameter by 5-inch face, with 9600-cycle energy.

Many unusual phenomena are noted when we attempt to harden



Fig. 15—Fixture for Automatic Indexing of Sprockets. Former inductors are used and several sprockets hardened simultaneously, depending upon production requirements.

gears and the relationship of frequency to tooth form and pitch and gear diameter will bear careful investigation. One notes that under certain conditions and with specific frequencies, the heating will start in the root, other times at the pitch diameter, and others at the tip. Further, areas which heat first are not necessarily the first to arrive at hardening temperatures.

To conserve on power requirements and to meet special contour needs, formed inductors are used very extensively to develop uniform rates of heating in the surfaces to be hardened. Fig. 14 shows two large tank sprocket teeth which have been hardened in

this manner. Fig. 15 shows the automatic equipment which indexes the sprocket into the inductor for hardening two teeth simultaneously, one on each of two sprockets.

Space does not permit the discussion of the various factors to be considered in the design of special inductors. We wish to stress, however, the strict adherence to sufficient power per unit of surface area so as to make possible the use of a heating cycle sufficiently short to prevent excessive flow of heat by conduction. In some instances, flow of heat by conduction enables us to heat areas which cannot be inductively raised to hardening temperature regardless of inductor design.

HEATING OF INTERNAL SURFACES

This paper has been confined to the use of induction heating wherein the heating has been done by placing the part within or adjacent to the inductor. The heating of hollow objects with the inductor inside of the part has been the means developed for surface hardening of cylinder liners and similar parts. By using lower power inputs than those required for such applications, internal heating has been applied likewise to the heating of small shell noses for forming or forging and for the brazing of assemblies which, because of design, cannot be readily heated from the outside.

Generally, the power input per unit of surface area of inductor is considerably above the values noted heretofore, since the force of the electrical energy is considerably weaker outside of the inductor loop. The use of iron cores within the inductor has been found quite advantageous for such work, particularly at the lower frequencies. It tends to concentrate more of the flux towards the surface of the surrounding steel object.

The hardening of the surface of holes less than 1 inch in diameter is not considered practical due to limitations imposed by the inductor design. Such parts as 30 and 50-caliber bullet dies and the like are precisely surface hardened on the bore by heating inductively throughout the entire cross section, followed by jet quenching of the I.D. after a carefully determined and automatically controlled delay period during which all metal but the surface of the bore has cooled below the critical temperature.

For description of internal hardening equipment and the limited number of applications for which it is required, see article by H. E. Somes (5).

HIGH FREQUENCY OSCILLATORS

Since we have discussed the effect of frequency, it seems to be in order to briefly cover some information relative to the type of equipment used to generate the alternating currents.

There are three sources of high frequency current which find commercial acceptance for induction heating.

The original alternator used for induction heating as applied to surface hardening on a production basis was a motor generator set operating at 1920 cycles. Such was the type of energy used for the hardening of crankshafts, camshafts, axle shafts, track pins, etc. Recent installations on similar parts now use 3000-cycle generators with some benefit derived from the slightly higher frequency.

Spark gap oscillators later entered the picture because of their higher frequencies (100,000 to 400,000 cycles) and are used for heating of small parts. Power output of standard equipment is limited to less than 25 KW.

Following a period of dissatisfaction with the spark gap circuit for critical hardening applications, a 9600-cycle generator was developed which has proved to be the most widely used type of induction heater. These generators are available in complete self-contained machines with a wide selection of power ratings.

Simultaneously with the above development, the use of vacuum tube oscillators was exploited for induction heating, and where the higher frequencies are needed as described in the earlier pages of this paper, they provide the necessary energy. As with the spark gap sets, however, present standard equipment is limited in power to approximately 50 KW maximum output. Special units at higher power ratings are in use, but the prevailing cost of such installations precludes their consideration for general use. Frequency of this equipment runs generally upwards of 450,000 cycles well into the megacycle range.

CONCLUSION

It has been the intention of this paper to present data and information which will serve as a guide in the selection of the correct frequency as well as an approximate time cycle to accomplish a certain result. Stress has been put on the 9600-cycle motor generator equipment because it occupies the leading place in industry and is

adaptable to a wider range of applications than other frequencies and is not hampered by power limitations.

Conversion of the available induction heating equipment to post-war work is of extreme importance today, and it is hoped that this article will serve in some measure to establish correct methods of processing of parts which will benefit from the use of induction heating.

The equations given have been simplified to permit use by the layman and all control data must be applied knowing that the variations of metallurgical structure and their behavior will often necessitate modifications. However, used with full knowledge of the limitations set forth, one can quickly arrive at cycles for standard production and hold to close tolerance limits.

For a thorough and concise discussion of factors involving frequency, permeability, and other controlling features, reference to a recent presentation by N. R. Stansel (3) is suggested. Mr. Stansel establishes relationships of technical accuracy and introduces a term called "Index Ratio" which should prove very useful in the more theoretical considerations of the conditions discussed in this paper.

ACKNOWLEDGMENT

The authors wish to express their appreciation to the engineering and research personnel of the TOCCO Division of the Ohio Crankshaft Company for their many helpful suggestions and co-operation in the preparation of this manuscript.

References

1. M. A. Tran and H. B. Osborn, Jr., "Inherent Characteristics of Induction Hardening," *TRANSACTIONS, American Society for Metals*, Vol. 1, 1941, p. 49.
2. H. B. Osborn, Jr., "Surface Hardening by Induction," *Transactions, Electrochemical Society*, Vol. 79, 1941, p. 215.
3. N. R. Stansel, "Induction Heating—Selection of Frequency," a paper presented at the A.I.E.E. summer technical meeting, St. Louis, Mo., June 26-30, 1944.
4. R. M. Baker, "Heating of Non-Magnetic Electrical Conductors by Magnetic Induction," *Electrical Engineering*, Vol. 63, No. 6, p. 273.
5. H. E. Somes, "The Development of High Speed Induction Heating for the Hardening of Internal Diameter," *Transactions, Electrochemical Society*, Vol. 79, 1941, p. 45.

DISCUSSION

Written Discussion: By T. E. Eagan, chief metallurgist, The Cooper-Bessemer Corp., Grove City, Pa.

The success or failure of an adventure in the use of induction heating depends a great deal on the proper choice of equipment. In general the people who have use for such equipment are not too well versed in the subject of high frequency currents which when considered from a theoretical aspect become rather complicated. The question of how these currents are generated can be left up to the manufacturer of such equipment. The question of how they can be used is of prime importance. This paper is an able attempt to boil down the highly theoretic calculations necessary to a simplified form which can easily be applied.

Most induction hardening units are applied to cases where large production allows the machine to be set up for a long run. Time and effort can be then profitably spent on the design of the inductor blocks and the setting of the timing cycle and power input requirements. However, there are units which are used to harden small lots of pieces in which such effort cannot be profitably expended. In such cases the information given in this paper becomes very valuable as it can be used to determine, first, the practicability of applying induction hardening to the part; second, what size of inductor block would be necessary; third, the operator of the unit can be given some idea as to the power required and the time cycle. Without such information as is given in this paper, the above factors must be determined by a rather long experimental procedure using the cut and try method.

Written Discussion: By J. R. Konold, metallurgist, Armstrong Cork Co., Lancaster, Pa.

The authors are to be commended on their paper for the presentation of practical data which should be of value to all users of induction heating of metallic parts. Their comments on the rate of heating and resulting microstructure were of interest to us, especially the data on the 40-millimeter A.P. Shot made from WD4150.

We have done considerable work on 20-millimeter A.P. shot made from WD4150 and some of our results are not in accordance with our interpretation of the authors' paper. We are, therefore, presenting the results of some of our work for general information and further discussion.

All of our work was done on two 20-KW Tocco machines of 9600 cycles, each machine having two stations and each station consisting of 10 inductor coils made of copper tubing.

In trying to work out a heating cycle for a heat of steel in which the annealed structure varied from 90 per cent spheroidized to 90 per cent lamellar pearlite, we made a number of temperature determinations on each of the four heads in order to calibrate the power input with temperature. We used an optical pyrometer, but the results were not very satisfactory so we tried inserting a thermocouple into the center of the shot through a $\frac{1}{8}$ -inch hole as illustrated in Fig. A. The temperatures determined by this method were very consistent and when checked by the optical pyrometer, they were within 10 degrees

Fahr. The optical was set for a predetermined temperature and in a definite position as established by a previous test, the table was lowered after the shot had been heated for a definite time. The thermocouple reading of the center of the shot did check with the optical pyrometer setting. A typical time-temperature curve was similar to that of curve "B-center" of Fig. A. This curve will vary with power input, but in every case we would get a break in the curve between 1300 and 1400 degrees Fahr. (705 and 760 degrees Cent.).

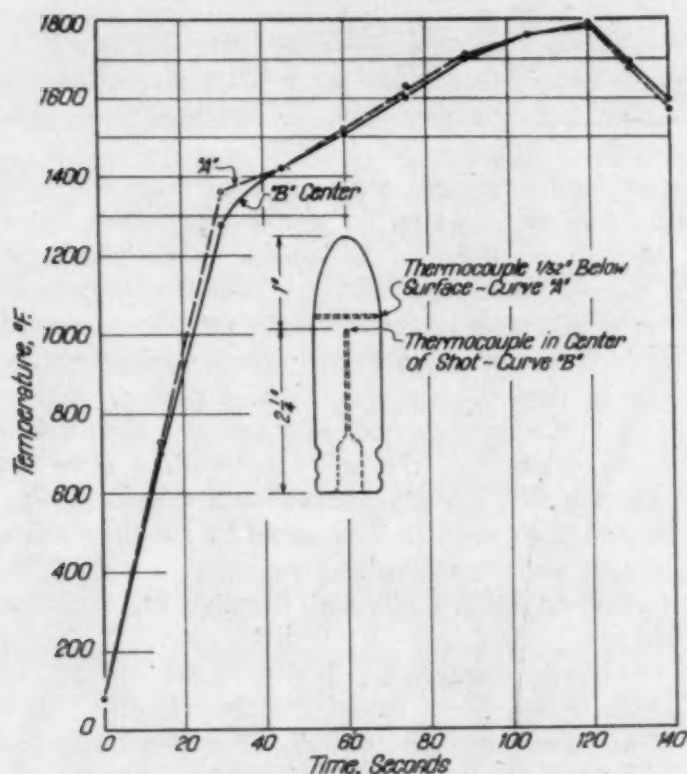


Fig. A—Time-Temperature Curves. Center and Surface of 20-Millimeter A.P. Shot. WD4150 Steel. 120 Seconds Heating Cycle.

We made a number of tests to determine the heating curves of the surface and center of the shot. In these tests the thermocouples were inserted in the center of the body of the shot through the body to within $\frac{1}{2}$ inch of the surface as shown in Fig. A. The temperatures were read simultaneously using two potentiometers. A typical curve is shown in Fig. A which indicates that the outside surface heats faster than the center until it reaches the critical point and then it heats as a unit.

A similar test was made by comparing the temperature of the center of the body of the shot with the surface of the nose. The location of thermocouples and resulting curves are shown in Fig. B. This curve again indicates that the surface heats faster than the center until the critical point is reached, but in this case the surface of the nose heats at a slower rate than the center of the body. We believe that this is a normal condition because the nose is far-

ther away from the inductor coil than the sides of the shot and also being a smaller diameter, it is subjected to greater radiation losses. The microstructure of the nose was different from that of the bourrelet and the hardness of the nose was less than that of the body. These factors helped to substantiate the curves.

The authors recommend a delay period between the heating cycle and the quench in order to secure additional time for heat penetration and carbide solution. If our curves are correct, the reason for a delay period would be to secure additional carbide solution and to decrease the temperature prior to quench-

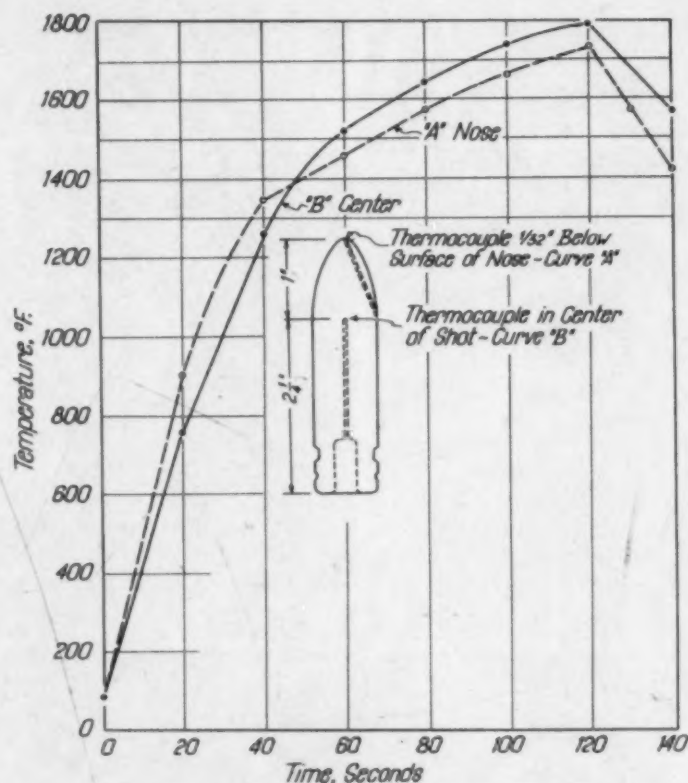


Fig. B—Time-Temperature Curves. Center and Nose of 20-Millimeter A.P. Shot. WD4150 Steel. 120 Seconds Heating Cycle.

ing as 1800 degrees Fahr. (980 degrees Cent.) would be too high a quenching temperature for 4150 steel.

The authors recommend a TOCCO structure as shown in Fig. 6 of their paper as the desired structure for best ballistics and control the cycles by hardness pattern and microstructure. We have found by a number of ballistic tests that we secure the best results by holding our shot to a 5 to 6 Shepherd grain size fracture test and a definite hardness pattern. The microstructure of our shot is shown in Figs. C and D. They were made from the prestructures as shown in Figs. E and F. Both structures were given the same treatment, i. e., heated for 110 seconds, delayed for 10 seconds and quenched for 15 seconds. The power input was the same for both structures and the resulting

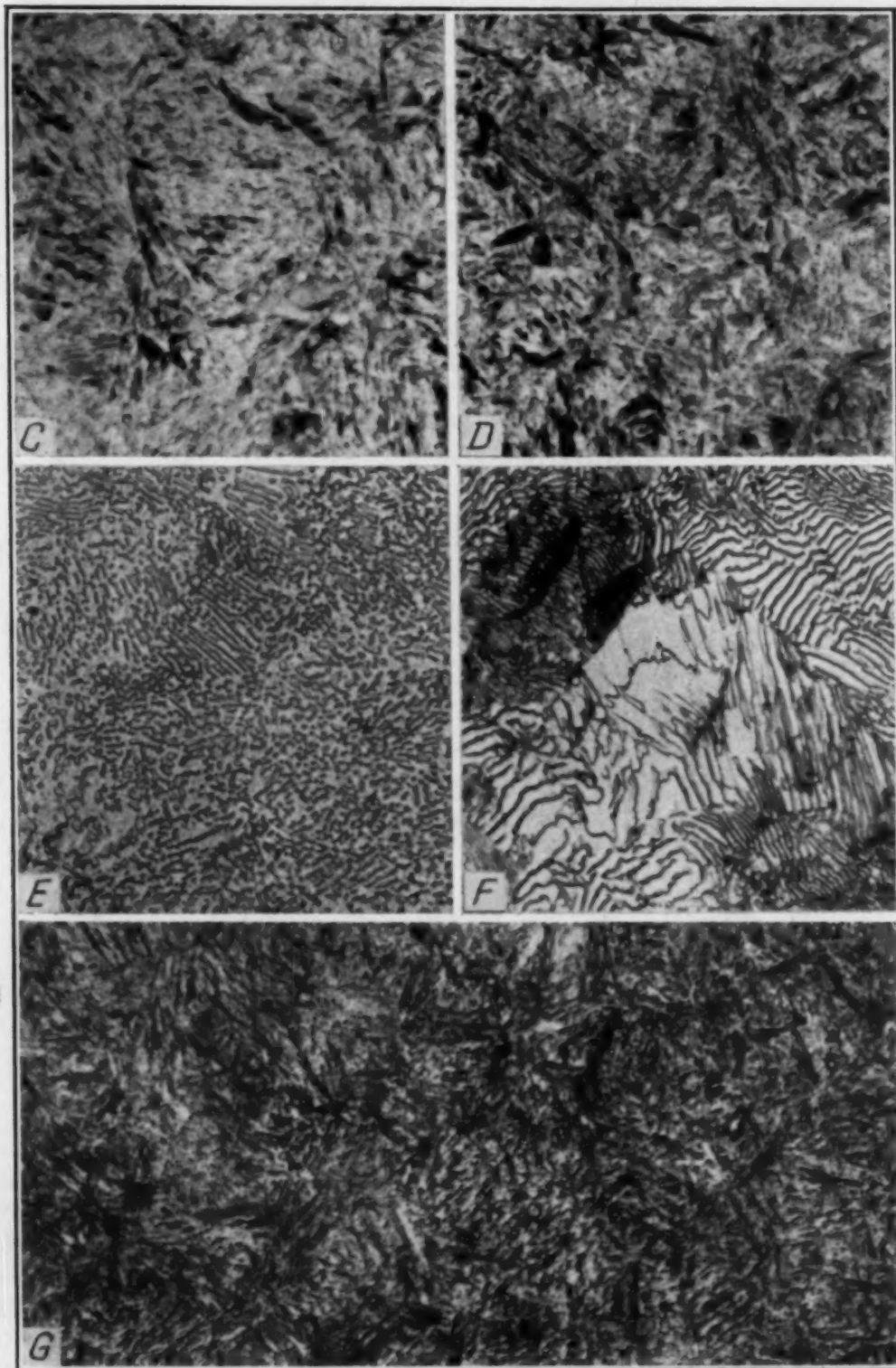


Fig. C—Spheroidized Structure of Fig. 4A in the As-Quenched Condition Heated to 1840 Degrees Fahr., Quenched at 1720 Degrees Fahr. $\times 750$.

Fig. D—Pearlitic Structure of Fig. 4A in the As-Quenched Condition. Heated to 1840 Degrees Fahr., Quenched at 1720 Degrees Fahr. $\times 750$.

Fig. E—Spheroidized Anneal, $\times 750$.

Fig. F—Lamellar Pearlitic Anneal. $\times 750$.

Fig. G—Structure of Regular Production Shot Heated to 1800 Degrees Fahr. (Approx.)—Quenched at 1700 degrees Fahr. (Approx.)—Tempered at 300 Degrees Fahr. for 4 Hours.

grain size fracture was the same (5 to 6). The ballistic results were the same in both cases (6 completes out of 6 shot) except that the spheroidized prestructure gave larger fragments than the lamellar structure. This coarse microstructure is typical of our standard production as shown in Fig. G.

We are of the opinion that the coarse grain size fracture gives better ballistics than the fine grain because the coarse grain has a dampening effect on the vibration of the metal as the projectile strikes the plate. We have fired shot having an 8 grain size with a structure similar to the authors' Fig. 6 and the shot hardly made a mark on the plate; it practically exploded on impact. A shatter test was recently conducted on 3 to 4, 5 to 6 and 7 grain size at increasing velocities; the 5 to 6 grain size gave the best results.

By using the fracture test as a method of control, we have been able to adjust the temperatures in the four heads to within a maximum variation of 35 degrees Fahr. This method will also readily detect variations in each coil and each heat of steel. The temperature must be adjusted for each heat of steel depending on structure, grain size and chemistry.

Based on the above data, we would appreciate having the authors' comments on the following:

1. In securing the data for the curves in Figs. A and B, would the effect of the inductive field on thermocouples be sufficient to materially affect the results? If so, why did we get such a close check with the optical pyrometer?
2. Is it possible that the $\frac{3}{4}$ -inch round section would be a critical section which would be a factor in securing the heating curves as shown in Fig. A?
3. In comparing your recommended microstructure for A.P. shot and ours (your Fig. 6 and our Figs. C, D, and G), do you believe that the size of the projectile might have any influence on the desired structure?
4. Do you have any comments on the use of the grain size fracture test as a control for the operation of the induction heating equipment?

Written Discussion: By N. R. Stansel, General Electric Co., Schenectady, N. Y.

The factors that determine the electrical performance of an assembly for induction heating are:

- (a) the resistivity of the material of the charge
- (b) the permeability of the material of the charge
- (c) the shape of the charge
- (d) the radius, or one-half the thickness, of the charge
- (e) the frequency

Of these the frequency is the only factor that can be chosen.

No one of these factors of performance can be considered separately. Their joint effect is taken into account in the circuit equations by the relations noted below.

Solid Cylindrical Charges.

$$\text{Index Ratio, } \Delta = \frac{a}{\rho} \quad (1)$$

$a = \text{radius of charge, cm.}$

Solid Plates

$$\text{Index Ratio, } \nabla = \frac{\sqrt{2}c}{\rho} \quad (2)$$

c = one-half the thickness of the charge, cm.

$$\rho = \frac{3560\sqrt{\rho}}{\sqrt{\mu f}}, \text{ cm.} \quad (3)$$

ρ = resistivity of the material of the charge at its maximum temperature, ohm-cm².

μ = permeability of the material of the charge at its maximum temperature.

f = frequency, cycles per second.

An assembly for induction heating is a form of transformer. The index ratio is the measure of the technical and economic merits of this device.

Consider a given assembly and assume that a range of frequency is available. The efficiency of the transformation from electric energy to heat increases with increase of frequency until the index ratio reaches a certain value. Beyond that value the efficiency is not affected by further increase of frequency.

In general the index ratio value 2.50 is as low as is advisable to use as a basis of design. The corresponding frequency is termed the base frequency of the assembly.

It can be shown that as the frequency is increased beyond the base frequency value that the KVA required for a given rate of heat development (watts) first decreases and then increases. The range of frequency between the base frequency and the frequency with which the KVA is the same as the KVA required with the base frequency is termed the optimum frequency range for the assembly. The closer the coupling between the charge and the primary coil (the air-gap ratio) the wider is the optimum frequency range.

With the air-gap ratios of general practice the width of the optimum frequency range permits the selection of a standard frequency for a given service and in addition makes practicable the use of one frequency for a considerable range of diameters of charges of a given material.

Written Discussion: By J. J. Fox, Lepel High Frequency Laboratories, Inc., Chicago.

Since there is a great deal of interest at present in induction heating, and since the advantages and merits of the various types of equipment are not clearly understood by the great majority of those who are interested in acquiring further knowledge of the process, any printed statement relative to induction heating, or equipment, appearing in a reputable publication, is seized upon avidly and regarded as the statement of a competent authority. Hence, it is only fair and proper that all facts be correctly stated, and I am quite certain that both Mr. Benninghoff and Dr. Osborn will welcome this opportunity to bring their information up to date.

On page 333 the statement is made that spark-gap equipment has a frequency range of from 100,000 to 200,000 cycles. Actually, the frequency range on Lepel spark-gap units (to which all reference is made hereafter) is from 100,000 to above 450,000 cycles, the actual frequency used being determined by the part being heated and the particular work coil utilized. (This is the operation referred to as tuning, wherein the unit is tuned to a resonant frequency with the inherent frequency of the inductor, or work coil, and the part to be heated. This variable range of frequency is one of the basic advantages of the spark-gap type of unit, and accounts to a great extent for its remarkable degree of flexibility and its high efficiency.)

The statement is also made (page 333) that spark-gap equipment is not satisfactory for critical hardening applications, with the further inference that only 9000-cycle generator equipment is satisfactory. Modern spark-gap and tube equipment, as proven by thousands of satisfactory installations, is doing a most excellent job in this respect.

Several other inaccuracies have been pointed out to me in previous reprints of papers by the same authors, published in *TRANSACTIONS* of the American Society for Metals, and I am taking the liberty of discussing these also at this time.

The statement is made that these units have a maximum power input of 25KVA, and are suitable only for use on small parts. The KVA rating is antiquated, since for the past several years modern spark-gap equipment has been built with power factor corrected to unity at full rated load, and such equipment has consequently been rated in KW. The largest unit manufactured at present is rated at 30KW, equivalent to a 35-KVA, or even 40-KVA, unit with uncorrected power factor. This 30-KW limitation is largely a matter of physical size, as the manufacturers have been reluctant to produce a unit of such size that it would lose the advantage of easy mobility in the user's plant. This size unit is today successfully handling fairly sizable applications—for example, heat treating of a 10-inch gear with 1-inch face. Larger parts are being handled in many cases by the applications of ingenious progressive feed arrangements.

The additional statement has been made that this type of unit has an operating efficiency of 50 per cent. This is not quite correct, since the overall efficiency of the unit under favorable conditions will be about 70 per cent. However, it is only fair to state, without any intention or desire to enter into lengthy discussions, that the efficiency of any unit will depend upon a number of factors—i.e., type of material being treated (ferrous or nonferrous), type of coil (I.D. or O.D.), coupling of the work to the coil, etc. Many induction units are rated on an output basis, which is a theoretical figure based on output at the terminals under ideal laboratory conditions, and in no wise represents the actual power delivered to the work in a varying range of applications. Thus, an application for the heat treating of the I.D. of a certain part would represent a rather poor application (though it might still be highly preferable to other methods), since in this case only that portion of the lines of force surrounding the *outside* of the work coil can be utilized, rather than the heavy concentration *inside* the work coil, and consequently the amount of power available at the work would represent only a fraction of that for which the machine might be rated. It has always been our opinion at Lepel that a power rating based on input, with its fairly constant factors, is more conservative engineering practice than any other basis of rating.

Written Discussion: By J. W. Cable, director of research and development, Induction Heating Corp., New York, N. Y.

Since the adoption of induction heating as an accepted production tool, industry has looked forward to such a paper as Messrs. Benninghoff and Osborn have made available in their presentation, "Practical Aspects of the Selection of Frequency and Time Cycles for the Processing of Metallic Parts with Induction Heating". These gentlemen are to be complimented on the completeness

and thoroughness of the data covered in this paper. The facts discussed represent the results of research work of considerable magnitude and the analysis of data compiled from years of experience with motor generator type induction heating equipment, which until recently was the predominant type in commercial use.

A considerable amount of equipment of the vacuum tube type having an output frequency of 375,000 cycles per second is now in use, and the writer believes that an expansion of these same fundamental principles to apply to higher frequencies is desirable to make this paper have equal value for all concerned with the application of induction heating. Disregarding the virtues of the equipment supplying the high frequency energy, the resultant effect to be considered in the utilization of different frequencies is ably brought forth in the table at the bottom of page 317. Analyzing these data, it can be seen that energy at 9600 cycles per second concentrates itself in a theoretical layer of approximately 0.020-inch thickness at the surface of the metal, while, by interpolation, this layer becomes only 0.004 inch thick at 375,000 cycles. As pointed out by the authors, these values represent zero time functions, and are therefore purely theoretical.

Any finite value of time will effect a typical heat penetration into the metal in accordance with its thermal conductivity. This penetration ranges from the minimum practical value shown in the above mentioned table achieved at a heating time of approximately one second, to through heating of the mass at time values of long duration. As this heating period increases, it is obvious that the effect of the depth of electrical penetration decreases, until it becomes negligible when the theoretical penetration is a negligible percentage of the total required heat depth. Hence, it can be concluded that very little difference is noted in the through heating of objects regardless of frequency, provided the kilowatt per square inch into the metal is maintained at such a value as to preclude overheating of the surface which might cause objectionable metallurgical changes. On the other hand, the fact that an advantage can be obtained by the use of the higher frequency in the production of thin cases is quite evident from the respective theoretical and practical depths of penetration set down by the authors.

An operating frequency of 375,000 cycles per second has shown itself in practice, with a general acceptance by industry, to give results comparable to 9600 cycles in through heating operations and deep penetrating applications involving heating periods of fifteen seconds duration or greater with corresponding rates of power input per unit surface area into the work. Such results are evident in the hardening of 37 and 57-millimeter armor piercing caps by induction heating, where large installations of both 9600-cycle and 375,000-cycle equipment were used. Slight variations in the inductor design were necessary to compensate for the higher energy loss in the metal at the higher frequency, since the eddy current losses increase as approximately the square root of the frequency at this order of magnitude. Since these results were obtained on such large diameters, there is no doubt that 375,000 cycles could effectively through heat 1-inch stock without any difficulty.

However, when the effect opposite from through or deep heating is desired,

the 375,000-cycle energy offers, as mentioned before, a distinct advantage. While the production of thin cases is not often required in large masses, it is extremely desirable in the hardening of small diameter parts. A hardened case of 0.020 inch is readily obtained in production with stock diameters of $\frac{1}{8}$ inch using 375,000-cycle energy at input levels of approximately 35 KW per square inch, and the effective heating of wire stock to hardening and annealing temperatures has been accomplished on diameters as small as 0.009-inch. Conclusions should not be drawn, however, that unlimited frequencies can be used in practice to obtain extremely thin cases. Since the depth of penetration given in equation (2) of the authors' paper is shown to be an inverse function of the square root of the frequency, this would appear feasible, but in actual application very little if any advantage is obtained by going higher than 375,000 cycles, because of the added difficulties in obtaining high power input levels.

Since induction heating is a function of the magnetic flux density, which, in single turn inductors, depends on the current flow, terminal voltages for equivalent flux densities go up directly with the frequency. The minimum clearance between the coil and work is dictated by the terminal voltage, and must be held at a sufficient value to prevent electrical flash-over which would damage the surface of the work and also the coil. Since a small change in gap or coupling greatly affects the flux density, a stalemate condition is reached whereby increased frequency means increased voltage, which in turn means increased air gaps and no gain is accomplished. It has been proven the 375,000-cycle energy will permit the use of clearances small enough to give high flux densities, and still gain the advantages of the lesser penetration thus obtained.

In summation it should be noted that the equation (1) for frequency has very little value to the average engineer in the choice of the frequency of equipment involved, since only extremely small diameters would indicate a frequency now commercially used on a large scale for induction heating; also that frequencies ranging from 9600 cycles to 375,000 cycles show very little difference in resultant heat patterns with corresponding energy input levels, thus allowing practically any heating operation to be done with this range of frequency; and finally, that added benefits in the production of thin cases, and the heating of small diameters can be obtained with the use of frequencies of the order of 375,000 cycles over those of the order of 9600 cycles.

Written Discussion: By O. W. Ellis, director, department of engineering and metallurgy, Ontario Research Foundation, Toronto, Canada.

This paper by Benninghoff and Obsorn is a most useful contribution to the literature on induction heat treatment. I have been particularly interested in the remarks on page 323 where the heat treatment of A.P. shot is referred to. I am in complete agreement with the authors' findings with regard to overheating. It is not surprising that overheated shot were below specification in hardness and it is most probable that they would have failed on ballistic test. What I would like to stress, however, is that, while it is undoubtedly most desirable to standardize the structures of steel before induction heat treatment, these structures, insofar as they relate to A.P. shot, seem capable of variation over quite a wide range without adversely affecting ballistic properties. Such varied prehardening treatments as the following have, in one well-established case at least, resulted in the production of quite acceptable material—

1. As-rolled
2. Heated for 72 hours at 1350 degrees Fahr. (730 degrees Cent.)—fully spheroidized
3. Heated to 1950 degrees Fahr. (1065 degrees Cent.) for 2 hours, cooled in air to room temperature, re-heated to 1325 degrees Fahr. (720 degrees Cent.) for 7 hours, cooled in air
4. Heated to 1950 degrees Fahr. for 2 hours, cooled rapidly to 1225 degrees Fahr. (665 degrees Cent.), held at 1225 degrees Fahr. (665 degrees Cent.) for 7 hours, cooled to 925 degrees Fahr. (495 degrees Cent.) at a uniform rate of 100 degrees per hour.

The cycles of induction treatment which followed the above treatments were the same in every case. It was such as to leave the steel with definite traces of the prehardening structures, e.g., pseudomorphs of iron carbide in martensite in case No. 1, pseudomorphs of pearlite (heterogeneous martensite) in case No. 3, etc. In short, induction heat treatment did not result in every case in the formation of martensite approaching the orthodox in character. Nevertheless, shot made from steel having all the prehardening structures referred to above passed muster and, to all intents and purposes, behaved in exactly the same manner during proof. The further point might well be made that they showed up just as well as A.P. shot hardened by more usual methods of heat treatment. This, I believe, speaks well for the versatility of the induction method of heat treatment and suggests strongly that studies of the properties of such rather unusual structures as are obtained as a result of such prehardening treatments should be carefully investigated.

Oral Discussion

JOHN V. RUSSELL:² I have just one short question. I would like to have returned that slide on the large pinion gear.

It will be noted that below the light outer case, there is a considerable dark area which includes the whole tooth and a small part of the tooth root. I would like to inquire if the authors have any measurement of the hardness of that area, and of the hardness in relation to the main body of the gear.

Authors' Reply

In reply to Mr. Cable's comments, let us state that we agree heartily with what he has said. The importance of kilowatts per square inch cannot be overlooked. However, because of the limitation in the power output of currently available vacuum tube oscillator equipment, we are unable to apply it to as wide a variety of work as is possible with the motor generator equipment. This is especially true when we have large parts and the generator units are the only ones which are available with sufficient power to maintain adequate power input per square inch.

There is a further limitation, of course, with the high frequency equipment, and that is through heating of large diameters. By large, I mean a few inches. On a 1-inch diameter, it would not make any difference from the standpoint

²Metallurgist, Republic Steel Corp., Chicago.

of efficiency whether you used 500,000-cycle equipment or 2000-cycle equipment to heat all the way through the entire cross section, but with two inches and three inches in diameter, your concentration of energy on the surface, regardless of how low the kilowatt input per square inch, would make it perhaps not impossible, but quite impractical to use the high frequencies for through heating of such stock, especially to hardening temperatures and higher.

The hardening of the 57-millimeter cap, to which Mr. Cable refers, required the use of an inductor which covered portions of the nose and the heat was thereby generated such that the linear flow necessary to produce through heating was considerably less than the radius of a bar 57 millimeters in diameter. It would be somewhat impractical to through heat a bar of this size with the 375,000-cycle energy. As a matter of fact, we designed our 57-millimeter, 75-millimeter, and 3-inch A.P. cap, 9600-cycle hardening inductors along the same general lines, to permit more rapid heating.

We agree that there are limitations to the equation " F equals $\frac{180}{R^2}$." However, it was used to show that although the theoretical aspects of the whole induction heating field are quite involved, we can get down to some bare fundamentals which will give us a general idea as to how we can express ourselves in interpreting relationships between diameter and frequency. Similar equations published in many texts yield calculations of frequency approximately ten times greater, which we know are definitely in error.

For Mr. Russell's information, the large gear that was shown is a final drive gear for a tractor. The material is SAE 1045. In some cases it was just normalized and in others it was actually heat treated and drawn back to about 220 Brinell and, then, induction hardening imposed upon it as a final operation. There is no finishing treatment at all.

The martensitic case around that gear runs approximately 58 Rockwell C. From there on there is a gradual transition in hardness and structure down through the demarcation zone to the original core. Most of the dark area is a subcritical area. Although since the gear is of extremely coarse pitch (1.5) the contour of hardness is somewhat affected by hardenability. For details of hardness, see Fig. H.

To Mr. Konold, we should like to say that although many facilities making the armor piercing shot of the 20-millimeter size have used the Shepherd grain size method of fracture for control and determination of hardening cycles, investigation made by the Integrating Committee of the armor piercing shot manufacturers was not entirely conclusive. Further, since the identity of the fracture or the grain size of the fracture is completely lost after a 300-degree draw, and since all the shot are fired under these conditions, we are not too enthusiastic about that being used as a definite method of control for all types of shot, particularly the larger sizes. It is admitted, however, that it is an excellent method for establishing standards, and thereby modify cycles to produce the fracture grain indicated by such standards.

The nose of the 20-millimeter shot is not heated by induction, due to limitations explained in the paper when discussing the relationship between the diameter and frequency. The nose of the shot is very small, and the 9600 cycles used on the 20-millimeter shot machines will not heat it by induction. The heat

flow is by thermal conduction of the energy introduced into the bourrelet. The radiation losses, of course, go up once we reach 1300 degrees Fahr. (705 degrees Cent.), but we do not believe the effect is too pronounced.

Mr. Konold, incidentally, did not have an opportunity to present, verbally, several questions that he has in his written discussion and we should like to answer these at this time.

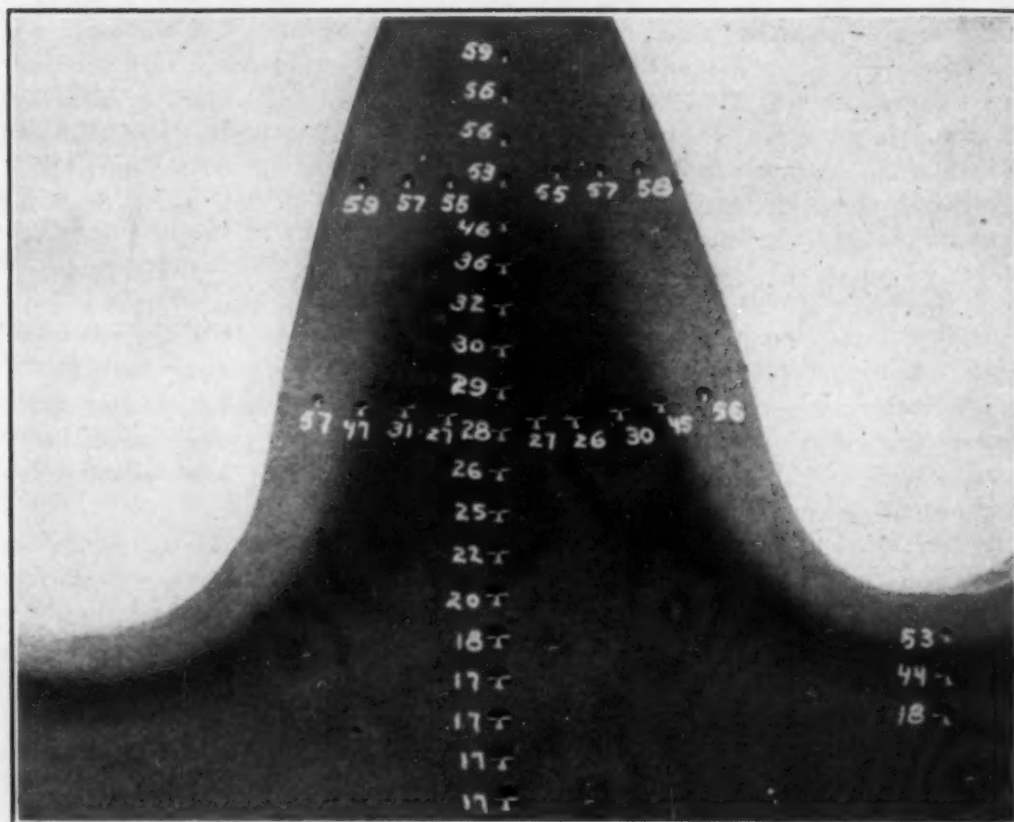


Fig. H—Rockwell C Survey—TOCCO Hardened Tooth of 275-Pound Main Drive Gear for 17.5-Ton Tractor. Entire Gear Hardened at Once.

There is no appreciable effect of the high frequency on the thermocouples, at 9600 cycles, because of the small diameter and one should not expect any induced current to flow in the wires. Therefore, a determination made with an optical pyrometer or a regular thermocouple in the shot should be substantially the same.

For hardening the 20-millimeter diameter shot, the power input used is approximately one-third of a kilowatt per square inch and, therefore, the heat flow by conduction is sufficient to prevent very little temperature differential being created from the center of the shot to the outside. On larger diameters of two inches or three inches, you would not find this lack of temperature differential from the surface to the center.

The photomicrograph of the 40-millimeter shot that we had in our paper was not intended to express our thoughts as to the type of structure needed for best ballistics on the 40-millimeter shot. Merely, it was a handy set of photo-

micrographs to show what happened when you underheated or overheated. As a matter of fact, we are inclined to believe that in some cases, on certain calibers of shot (nothing you can say about one caliber shot is necessarily true for all sizes), a tendency toward a slight coarsening has been found quite desirable in the production of satisfactory ballistics.

The grain size fracture, as stated before, is to be recommended, provided standards can be used. However, it would only be suitable for the through heating of small parts and would hardly be satisfactory for establishing cycles for large diameters.

Mr. Eagan, we think, agreed with most of the things we said. We do not believe any comments are necessary, other than an expression of appreciation for his pointing out something which the manufacturers of induction heating equipment have been stressing, namely: an induction heating unit is not a single purpose machine, but can be readily and economically adapted to an extremely wide variety of parts.

Mr. Ellis has raised a point which is of extreme interest to all users of induction hardening equipment. Although we have been somewhat reticent about recommending complete disregard of pretreatment, we do know that hardening cycles can be set which will produce a satisfactory microstructure almost regardless of prior structure. Since coarse structures generally require longer heating times, which of course will cause solution of finer structure as well, we need have little concern for initial structure when processing parts which are through hardened or hardened to reasonable depths.

A typical example is that of a large diesel engine crankshaft made of SAE 1050. The cams have a base circle diameter of 2 inches and are hardened to a depth of approximately 0.180 to 0.200 inches.

An identical induction heating cycle was used for several test shafts and the resultant microstructure of the hardened areas did not show sufficient difference to warrant selection of any one as being better than the other. All were satisfactory despite variation of prior treatment which was as follows:

1. As-rolled
2. Annealed—(Standard mill practice)
3. Slow cooled from 1600 degrees Fahr. (870 degrees Cent.) after standard mill
4. Normalized from 1600 degrees Fahr. (870 degrees Cent.)
5. Heat treated—quenched and drawn back to approximately 250 BHN.

We accept Mr. Fox's correction of our statement with reference to the frequency of the spark gap equipment and have modified it to read 100,000 to 400,000 cycles. However, the correction of our statement depends on how it is read. We are citing some historical facts and actually at the time the spark gap equipment was first used for heating of metals, the frequency range was approximately 100,000 to 200,000 cycles.

However, we are not so disposed on several other points mentioned by Mr. Fox and present rebuttal herewith.

Due to the fact that efficient operation of a spark gap set requires careful tuning of the circuit to resonance, depending upon the design of the work coil, type of material being heated, etc., the frequency of operation varies for different jobs and is not something obtained at a pre-selected value. In other words,

we cannot put the cart in front of the horse—the frequency is a product of the operation and although variable is not controllable to limits of any consequence. Further, the frequency of a particular spark gap circuit varies within limits which would have very little effect on final results.

When a piece of steel is heated, its electrical resistance increases and therefore the electrical characteristics of the inductor assembly complete with part being heated will change during the heating cycle. Thus, the power absorbed by the piece falls off and although of no real consequence, when processing small parts or even large parts when adequate power is available to permit short heating cycles, such a condition makes it impossible to take advantage of the skin effect of the high frequency when surface hardening the majority of parts so treated. Automatic regulation of output voltage or automatic addition of capacitance holds the power input to the piece constant with motor generator equipment. With a spark gap circuit this change in external electrical characteristics throws the unit completely out of resonance and although of little importance on short heating cycle results, with long heating cycles the benefit of the high frequency heating is completely lost since a longer heating time is needed to offset the drop in power. Unless we are able to take advantage of the high frequency of the spark gap circuit, there is no basic reason for having a unit capable of producing it—the maintenance of such equipment and the initial cost per unit of power input is far greater than the generator type which requires nothing more than oiling of the bearings of the motor generator.

We repeat that the spark gap type of equipment is not suitable for critical hardening operation whereas the motor generator sets or the tube sets are satisfactory. This is especially true of high production work. If a spark gap set were running on a part which called for a specific energy input for 1.5 seconds, any variation in either power or heating time might conceivably produce a part not up to specifications of structure, hardness and depth. With high production of say 1500 parts per hour a single adjustment of tuning for resonance or of the spark gaps would not hold stable for continuation of a long run of many hours. Spacing of the spark gaps must be set regularly and the period of such adjustment is dependent upon the use of the equipment. Many units which are used for high production now require adjustment every 8 hours and this cannot be done in a matter of a few minutes.

We are aware of the changes which have taken place in the design of spark gap equipment and should like to point out that our statement referring to its maximum power input as 25 KVA was made in articles published several years ago. In the paper now under discussion and submitted at the 1944 ASM Convention, we state, on page 333, that power output of standard spark gap equipment is limited to less than 25 KW. Thus, even if a 35-KW input unit could operate at 70 per cent efficiency, the output would be as stated—less than 25 KW. Special units could be manufactured at higher ratings, but only at a marked increase in cost and in sizes which would not be accepted by users of this equipment. Such a 35-KW unit sells for approximately \$250 per KW output, which is considerably more than a complete generator set of the same rating. Further, as generator ratings increase, the cost per KW output falls off quickly—to less than \$100 per KW for units of several hundred KW output capacity at 9600 cycles and still less at lower frequencies. A complete 200-KW

output motor generator is no larger in size than the currently manufactured 35-KW input spark gap unit.

We have stressed the fact that to take advantage of the shallow depths of heating of any high frequency equipment, heating time must be minimized to prevent heat flow by conduction. This requires the use of adequate power input per unit of surface area. Thus, the use of a 35-KW input spark gap unit cannot possibly average over the total heating time more than $\frac{1}{3}$ to $\frac{1}{2}$ KW per square inch, on a 10-inch diameter by 1-inch face gear (based on pitch diameter); the heating time with such low power input would be so long that no difference in final result could be noted whether processed at 9600 cycles, 300,000 cycles, or 500,000 cycles.

We do not believe that even under the most ideal conditions could a spark gap set be made to operate at 70 per cent efficiency but assuming such to be the case, this would only be true at the beginning of the heating cycle under which condition the set has been tuned for resonance. As heating progresses, the set passes quickly out of resonance and only by re-tuning and doing so continuously could any semblance of good efficiency be maintained. Obviously such a practice would be most impractical in production work and precludes the advisability of using such equipment on large parts.

The efficiency of any induction heating set-up is, of course, dependent upon the coil design and proximity of the work to the coil, i.e., coupling. Correct coil design and reasonably close coupling are first necessary before a spark gap set can be tuned for efficient operation. With the motor generator set single adjusted of power factor and field excitation of the generator can correctly match the set to the characteristics of the inductor and work to provide efficient operation. Moreover additional adjustment of this type can be made automatically during the heating cycle to maintain this efficiency.

The ratings of the motor generator sets and vacuum tube oscillators are output ratings and represent actual energy delivered to the inductor or step-down transformer if using low inductance work coils. These transformers operate at 95 per cent efficiency or better. The KW meter on the motor generator set and the R.F. meter on the tube oscillator are accurate measures of such energy and make it possible to re-establish exact operating power requirements when a part is to be processed in accordance with control data established as necessary for the production of critical hardening operations.

Motor generator equipment is being used for the heating of shell tube ends for nosing and a correctly designed inductor for I. D. heating using a laminated core, to force the flow into the inside surface of the shell, heats just as efficiently as one which heats from the O. D.

Due to the nature of the paper which we have presented, we naturally did not elaborate on many items which have appeared to be of a controversial nature. As a summary we should like to state that TOCCO equipment is manufactured with both motor generators and vacuum tube oscillators as a source of high frequency energy. Power ratings of the M.G. units range from 7.5 to 200 KW output at 9600 and 3000 cycles in complete machines or as high as required (some installations used 1250-KW generators) for special installations. The vacuum tube unit called the TOCCOTRON operates at 450,000 cycles and at 20-KW output. Recommendations for equipment are made based on appli-

cation requirements and, due to the lower cost, the motor generator units are always selected unless the high frequency is indicated for shallow depths of heating or the processing of small diameters.

For most brazing work either type may suffice as does its spark gap equipment since power input is generally set at less than 1 KW per square inch of surface area. However, for heating of large cross sections, the skin effect of the high frequency of the spark gap and vacuum tube units is a disadvantage.

Therefore, while each type of equipment can be used for a wide variety of work, the economies inherent with the purchase and use of the motor generator equipment make this equipment more desirable, provided we are not processing extremely small diameters.

INDUCTION HARDENING OF PLAIN CARBON STEELS: A STUDY OF THE EFFECT OF TEMPERATURE, COM- POSITION, AND PRIOR STRUCTURE ON THE HARDNESS AND STRUCTURE AFTER HARDENING

BY D. L. MARTIN AND FLORENCE E. WILEY

Abstract

The results of an investigation of the effect of temperature, composition and prior structure upon the induction hardening characteristics of plain carbon steel are presented in this paper.

The basic metallurgical principles of induction hardening were observed to be no different from those for conventional hardening methods. The properties of induction hardened steel are frequently different but that is due to the surface layer of martensite and the lack of homogenization in the austenite.

The maximum heating temperature is the important variable in induction hardening. To obtain satisfactory properties, it is necessary to heat the steel to a high temperature where diffusion of carbon is rapid.

Increasing the carbon content of a steel facilitates the formation of austenite during induction heating, and increases the maximum hardness in the quenched samples.

The distribution of cementite in the ferrite matrix greatly influences the hardening characteristics of steel. A sorbitic structure was found to transform to austenite at a lower heating temperature than either a furnace-cooled or air-cooled structure.

HIGH frequency induction heating has been widely applied in the past few years for surface hardening of steel. The advantages of induction hardening over the conventional methods are related to the rapid heating of the surface of the metal sample without an appreciable rise in temperature of the core. This condition makes possible case hardening of a plain carbon steel part in a few seconds with very little, if any, distortion and without the formation of an oxide scale or a decarburized zone. As a result of these and

A paper presented before the Twenty-sixth Annual Convention of the Society held in Cleveland, October 16 to 20, 1944. The authors, D. L. Martin and Florence E. Wiley, are associated with the Research Laboratory, General Electric Co., Schenectady, N. Y. Manuscript received June 16, 1944.

other advantages, applications of induction heating methods for the hardening of steel articles have been numerous (1-8).¹

The theory of induction heating has been described in detail by Sherman (3), Jordan (8), and Babat and Losinsky (10). The basic principles may be summed up by two equations:

$$(1) \Delta P = \frac{k I^2 N^2 \sqrt{\rho \mu f}}{8}$$

where ΔP = power dissipated as eddy currents

k = constant

I = coil current

N = effective number of turns in the coil

ρ = resistivity of charge

μ = permeability of charge

f = frequency

$$(2) p = \frac{1}{2\pi} \sqrt{\frac{\rho}{\mu f}} = \text{depth of penetration of current.}$$

Examination of these equations reveals that the rate of heat input is directly proportional to the square root of the frequency, resistivity, and permeability; and that the depth of penetration varies directly with the square root of resistivity and inversely with the square root of permeability and frequency. The metallurgical importance of these principles is that it is possible by induced high frequency currents to heat a thin surface layer to temperatures above the A_{e_3} temperature in a matter of seconds, and thus provide a method for the rapid surface hardening of steel.

The question arises whether or not the transformation reactions and properties of the hardened steel are different due to the extremely fast heating rate. Evidence offered by previous investigators indicates that unusual properties and structural changes do result from induction hardening of steel. In fact, a few of the effects, such as rapid solution of carbide, hardening below the critical temperature, "superhardness", pearlite "ghosts", appear to be anomalous.

Rapid Solution of Carbides—Steels have been induction hardened in extremely short times. For example, Sherman (3) has surface hardened steel samples with 5 megacycle current in as short a heating time as 0.6 second, while Tran and Osborn (1) have estimated that 0.2 to 0.3 of a second above the lower critical temperature was time enough to obtain "complete carbide solution and homogeneity" in an S.A.E. 1050 steel, with a suitable prior structure.

¹The figures appearing in parentheses pertain to the references appended to this paper.

Iron carbide has a higher specific resistance than ferrite and therefore, according to Osborn (12), should be heated to a higher temperature than the ferrite for a given current induced by high frequency. This temperature gradient, he assumed, accelerated the solution of carbide. Vaughn (6) attributes the rapid austenitizing to the high surface temperatures produced by induction heating compared to conventional heat treating temperatures, and as a result, diffusion of carbon within the heated zone is very rapid, yet time at temperature is so short that excessive grain growth does not occur.

Hardening Below Critical Temperature—Osborn (11) has claimed that it is possible to obtain thoroughly diffused martensite in S.A.E. 1045 steel by heating between Ae_1 and Ae_3 with complete elimination of free ferrite. In addition, he reports that steels heated to temperatures below the lower critical and quenched have "definite evidence of hardness and microscopic transformations which theoretically should not take place until critical temperatures have been reached." If these observations are true, then the critical temperature for the formation of austenite is a function of the heating rate.

Superhardness—Induction hardened steel has frequently been observed to possess a higher hardness than samples of the same steel furnace hardened (1), (2). This higher hardness has been referred to as "superhardness"; although the term is misleading in that the 2 to 5 points Rockwell C increase which has been observed hardly makes the steel "super." Vaughn, Farlow and Meyer (2) attribute the higher hardness to quenching stresses present to a greater degree in induction hardened samples than in furnace treated samples. They demonstrated that high compressive stresses were present in the hardened case.

The finer martensitic structure generally found in induction hardened samples has been suggested by Tran and Osborn (1) as a factor which might account for the higher hardness. McQuaid (13) goes one step further and explains the extra hardening by assuming that the austenite formed by induction heating is nonhomogeneous; as a result, the martensitic structure formed from nonhomogeneous austenite consists of less retained austenite, compared to martensite formed from a homogeneous austenite. Furnace treated samples will in general be heated long enough to insure a homogeneous austenite, and will therefore have a higher per cent of retained austenite which in turn will result in a lower hardness.

Pearlite "Ghosts"—The term *pearlite "ghosts"* has been used to

describe a structural constituent found in hardened steels, possessing the approximate hardness of martensite but resembling pearlite in microstructure. The structure is the product of nonhomogeneous austenite and has been observed in furnace as well as induction treated samples (10), (14), (15). Ellis (10) has described this constituent as pseudomorphs of pearlite and suggests that it may possess unusual properties.

The extremely short heating time, higher hardness and stresses, hardening below the critical, finer martensite—all tend to verify Osborn's remark (11) that "induction heating is somewhat unusual in so far as the metallurgical results are concerned." The results are certainly different from those generally obtained for furnace hardened steels; but, is the metallurgy different? The answer to this question will depend for the most part upon verification of Osborn's observations (11) that austenite is formed below the A_{e1} temperature in induction heated samples.

The object of the investigations described later in this paper was to study the effect of temperature, composition, and prior microstructure on the hardness and microstructure of induction heated steels to ascertain if the results are in agreement with existing information on the formation of austenite and martensite by conventional heating methods.

EXPERIMENTAL METHODS

Materials and Treatments—Five plain carbon steels covering the range 0.2 to 1.1 per cent carbon were studied in this investigation. The analyses of these steels are listed in Table I. Steels A and B were obtained as 1-inch diameter hot-rolled bars from commercial stocks and were machined to $\frac{7}{8}$ -inch diameter to eliminate surface decarburization. Steels C and D were prepared in 50-pound heats in a laboratory induction furnace and cast into molds 2 inches in diameter. The ingots were hot-forged to 1-inch diameter bars which in turn were machined to $\frac{7}{8}$ -inch diameter. The 1.1 per cent carbon steel (Steel E) was ground, $\frac{7}{8}$ -inch diameter commercial drill rod.

The $\frac{7}{8}$ -inch diameter bars were cut into 1-inch cylinders which were then heat treated to yield the prior structures noted in Table I. After austenitizing for 1 hour at the designated temperature, in a nitrogen atmosphere to prevent decarburization, the specimens were cooled to produce the desired structure.

Our precautions to prevent decarburization were not quite thorough enough, for irregularities later observed in a few of the induction heated samples were definitely traced to decarburization. For example, examination of one induction hardened sample (Fig. 1) showed considerable free ferrite at the surface. Apparently, this sample was heated in improperly deoxidized nitrogen since a similar

Table I
Analysis and Prior Treatments of the Steels

Steel	Per Cent			Austenitizing ² Degrees Cent.	Treatments ¹				
	C	Mn	Si		F.C. ³	A.C. ⁴	Q. ⁵	T. ⁶	S. ⁷
A	0.17	0.87	nil	900	*
B	0.30	0.66	0.18	900	*
C	0.47	0.19	0.13	850	*
D	0.80	0.34	0.27	800	*	*	.	*	*
E	1.10	0.44	0.19	900	*	.	.	.	*

¹The asterisk (*) marks the treatments given to the steels.

²The steels were austenitized for 1 hour at temperature in purified nitrogen.

³Furnace-cooled at the rate of 100 degrees Cent. (210 degrees Fahr.) per hour.

⁴Cooled in air.

⁵Brine-quenched from 800 degrees Cent. (1470 degrees Fahr.).

⁶Tempered at 500 degrees Cent. (930 degrees Fahr.) for 1 hour after quenching.

⁷Steel D was spheroidized by holding the normalized samples at 650 degrees Cent. (1200 degrees Fahr.) for 50 hours. Steel E was spheroidized in the as-received condition.

steel was not decarburized when heated in purified nitrogen. Oxygen was removed from the nitrogen by passing over hot copper chips and water vapor by passing over P_2O_5 ; however, with time the copper chips become ineffective due to oxidation and have to be renovated by deoxidation with hydrogen. It is apparent that a closer check should have been made to insure a neutral atmosphere. The results obtained on decarburized samples (about six out of over 50 samples) will accordingly have to be interpreted with this factor in mind.

All the steels were induction hardened in the furnace-cooled condition. In addition, Steels C, D and E were also treated to produce other structures since the distribution and size of the phases has previously been shown to have a definite effect on austenite formation and thus on the hardening characteristics. The treatments used to produce the desired prior structures are listed for all the steels in Table I.

Induction Heating Equipment—A General Electric electronic heater was used for induction heating the steels. For this investiga-

tion the oscillator was adjusted to produce alternating currents with a frequency of 530,000 cycles. The maximum power input to the sample was approximately 10 kilowatts up to the Curie temperature where it dropped to a value of approximately 4 kilowatts. The heating rate for these conditions was from 275 to 300 degrees Cent.

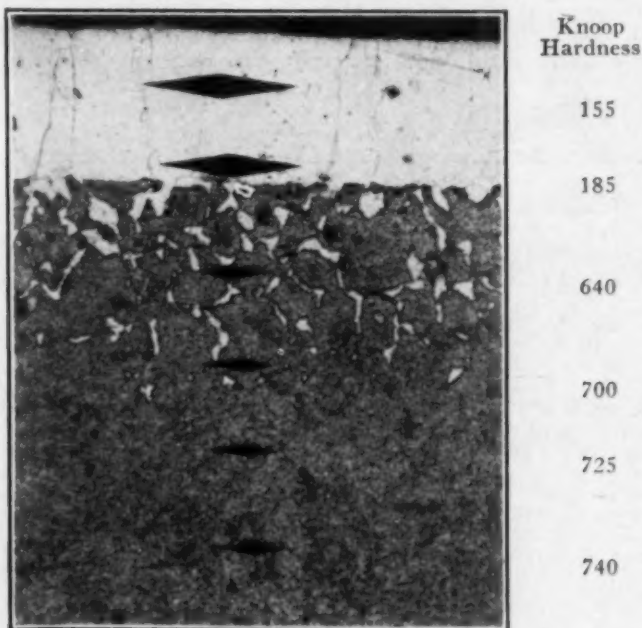


Fig. 1—Knoop Hardness Indentations in an Induction Hardened Sample of Steel E; $\times 75$. Note the decarburized layer resulting from austenitizing in improperly deoxidized nitrogen. The indentations are 0.005 inch apart.

(500 to 540 degrees Fahr.) per second up to the Curie temperature and about 50 degrees Cent. (90 degrees Fahr.) per second above that critical temperature due to the change in permeability.

The induction heating fixture shown in Fig. 2 was made in order to obtain uniform heating for all the samples. The component parts of this fixture are the copper inductor coil which carries the high frequency currents, the electrical terminals, and the water quench ring for quenching the sample after heating. Water cooling of the inductor coil is required to prevent overheating; this is accomplished by attaching the terminals to a water supply as well as to the electronic heater.

The size of the sample, as mentioned before, was standardized at a height of 1 inch and a diameter of $\frac{7}{8}$ inch. A brass table with

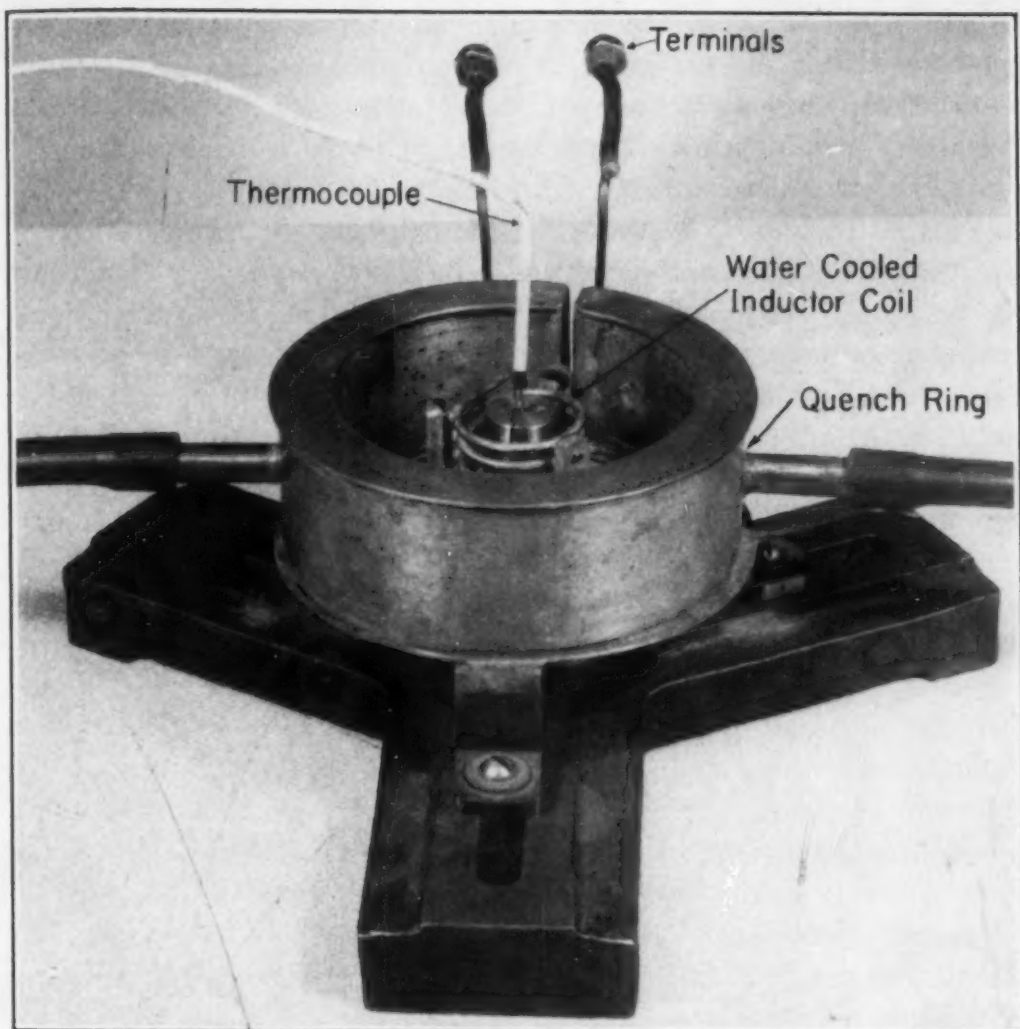


Fig. 2—The Induction Heating Fixture with the Sample and Thermocouple in Position.

a centering pin supported the sample and helped to center it in the inductor coil. When in position the surface of the sample was approximately $\frac{1}{4}$ inch from the coil, although this distance varied $\pm \frac{1}{16}$ inch around the sample. As a result of this difference in coupling, the heating was not quite uniform. In practice, this effect is minimized by rotation of the sample; however, because the thermocouple was attached to the sample this practice was not feasible. Instead, the location of the thermocouple was marked and hardness and metallographic data were obtained in proximity of that point.

Temperature Measurement—The influence of temperature on the austenitizing reaction is so great that it would be impossible to make an intelligent study of the effect of composition and prior

structure without knowing the approximate maximum surface temperature. Tran and Osborn (1) in their work determined the time-temperature curves for one of their test pieces using an optical pyrometer to measure the temperature. This they did by setting the pyrometer at a certain temperature above 760 degrees Cent. (1400 degrees Fahr.) and measuring the time to heat to that temperature. Their method is sound; however, it is doubtful whether their data are accurate because of the difficulty in deciding when the sample temperature corresponds to the pyrometer calibration. For example, a hesitation of 1 second in determining when the filament disappeared would result in a sample temperature 70 to 210 degrees Cent. (130 to 380 degrees Fahr.) higher than the pyrometer temperature, assuming heating rates to be essentially as shown in their curves. This temperature error could easily account for the hardening below the critical which Osborn has claimed (11), particularly, since the heating rate below the critical is higher than that above.

For the present study it was decided to use a chromel-alumel thermocouple and a high speed photoelectric recorder, which has recently been developed (33), to measure the temperature of the induction heated samples. One end of each wire of the thermocouple was spot welded to the side of the sample about $\frac{1}{8}$ inch apart and about $\frac{1}{2}$ inch down from the top. Preliminary tests with this arrangement showed that the recorder could trace heating curves of 200 to 300 degrees Cent. per second. High frequency currents are induced in the thermocouple wires, but they are very small since the wires are parallel to the flux lines. Whatever their magnitude the induced currents did not appear to influence the temperature readings for there was no sudden change when the power was shut off as would be expected if the high frequency currents had an effect.

During the course of one run the thermocouple leads parted from the sample, due to overheating, and short circuited the inductor coil. This had tragic effects, for the high amperage currents from the inductor coil burned out the coils in the photoelectric recorder making it necessary to measure the temperature with another photoelectric-type instrument—a controller instead of a recorder.² This instrument is generally employed to control the temperature of a furnace; however, it may also be used to measure temperatures. A method similar to that of Tran and Osborn's was found to give satis-

²If the thermocouple is held rigidly there is little chance for short circuiting of the inductor coil, thus damaging the instrument. The photoelectric recorder is best for this type of work since a heating curve is obtained for each sample.

factory results. The instrument was set at a certain temperature and the sample heated inductively to the predetermined temperature at which point the power was shut off. An electronic timer in the power circuit recorded the heating time so that a heating curve could be obtained by covering a number of temperatures. The advantage of this photoelectric instrument over the optical pyrometer is that it is much easier to determine the instant when the sample is at the desired

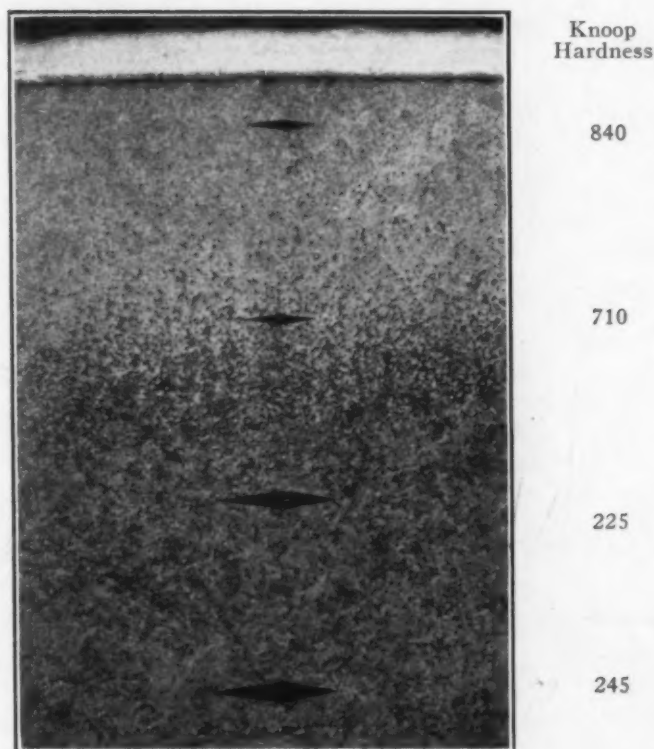


Fig. 3—Hardened Case in an Induction Hardened Sample of Steel D; $\times 75$. The indentations are 0.010 inch apart. The white surface layer is chromium. This sample was heated twice to 750 degrees Cent. (1290 degrees Fahr.) and quenched.

temperature. During heating the galvanometer light on the controller is green, when at temperature it is white, and when beyond the designated temperature, it is red. It is very easy to follow the light and stop the heating at the designated temperature (the white light). The temperature error is estimated to be less than 20 degrees Cent. (35 degrees Fahr.) at temperatures above 700 degrees Cent. (1290 degrees Fahr.).

The general test procedure followed was to heat separate sam-

ples to temperatures in the range 700 to 1000 degrees Cent. (1290 to 1830 degrees Fahr.) and then water-quench until cold. About 1 second delay occurred between the shut-off of the power and the water quenching. The temperature changes due to cooling in air are estimated to be less than 10 degrees Cent. (20 degrees Fahr.) during this interval.

Hardness Measurements—Hardness was measured with a Tu-

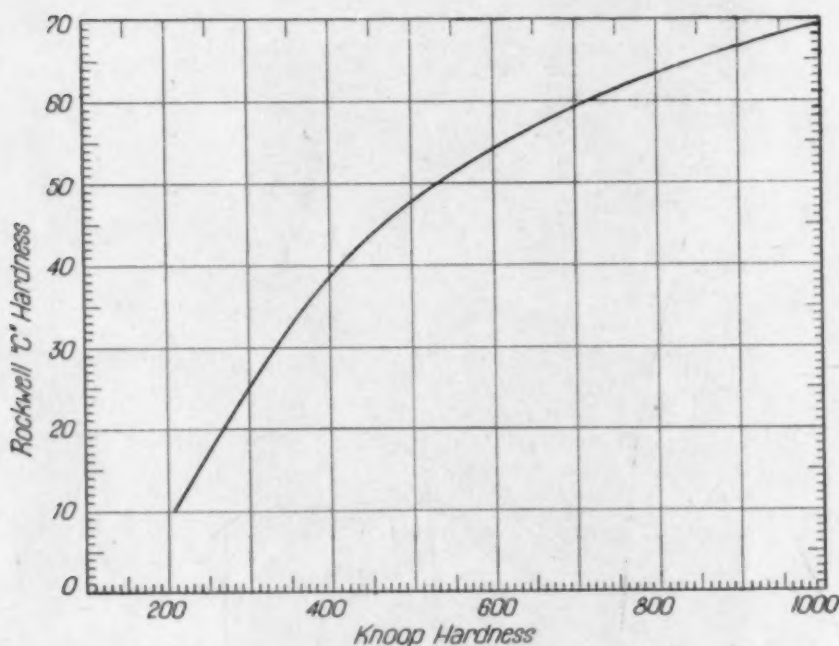


Fig. 4—Knoop-Rockwell "C" Hardness Conversion Chart.

kon tester. The advantages of this tester for measuring the hardness of thin surface layers (hard or soft) are obvious when Fig. 1 is examined. Rockwell "C" hardness determination of the ferrite layer or of the hardened case in Fig. 5 would be impractical. At least five microhardness readings (called Knoop hardness) could be made in a row in the same hardened zone. The Tukon tester is ideal for such applications. One disadvantage is that considerable time is required to prepare the sample for the test since a metallographic polish is required.

The induction hardened samples were cut transversely through the center (under a water spray) and Knoop hardness readings at 0.010-inch intervals were made across the hardened case into the

core (as in Fig. 3).³ The procedure and equipment for measuring Knoop hardness are those described recently by Mrs. C. B. Brodie (34). The Knoop hardness is very sensitive to the structural condition of the area tested, and therefore it was necessary to run two or more series of readings across the hardened case to insure consistent results. Rockwell "C" readings were made on the outside round surface and across the diameter of all samples, although the



Fig. 5—Steel D After Being Induction Heated to 700 Degrees Cent. (1290 Degrees Fahr.) and Water-Quenched; $\times 1000$. Note the absence of martensite. The layer at the surface (less than 0.001 inch) is ferrite.

values did not have much significance when the martensitic zone was less than 0.050 inch.

A hardness conversion chart for Knoop and Rockwell "C" is given in Fig. 4. This was prepared from hardness data made on small samples of Steels D and E which were first furnace hardened and then tempered at different temperatures to cover the entire hardness range.

Metallographic Examination—The samples were repolished and etched for microscopic examination after the hardness measurements

³Most of the samples were chromium plated to prevent rounding of the edges during polishing and mounted in bakelite.

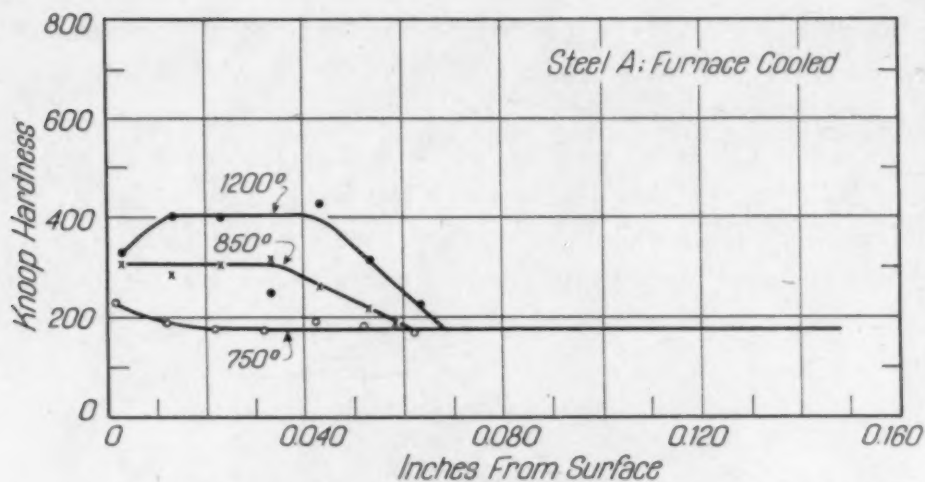


Fig. 6—Hardness Penetration Curves for Steel A (0.17 Per Cent Carbon) with a Furnace-Cooled Prior Structure. The temperature values are degrees Cent. The low hardness value for the 1200-degree Cent. sample at about 0.035 inch is probably due to undissolved ferrite.

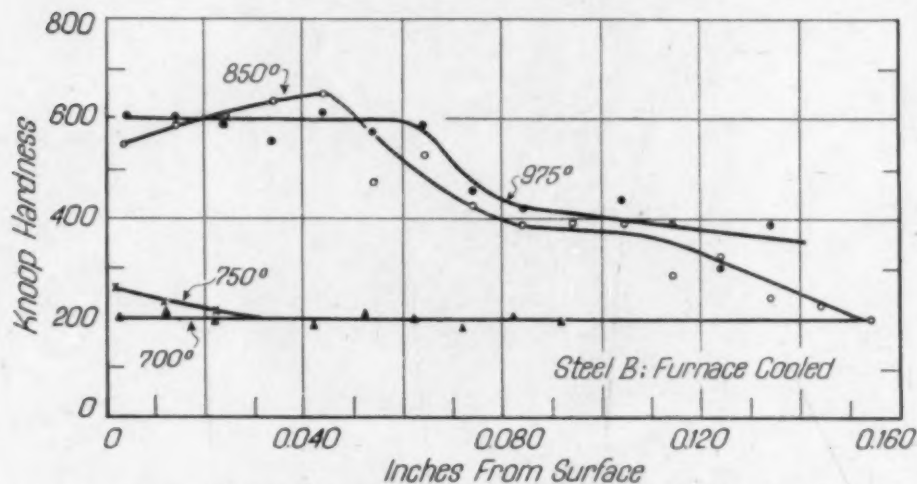


Fig. 7—Hardness Penetration Curves for Steel B (0.30 Per Cent Carbon) with a Furnace-Cooled Prior Structure. The temperature values are degrees Cent.

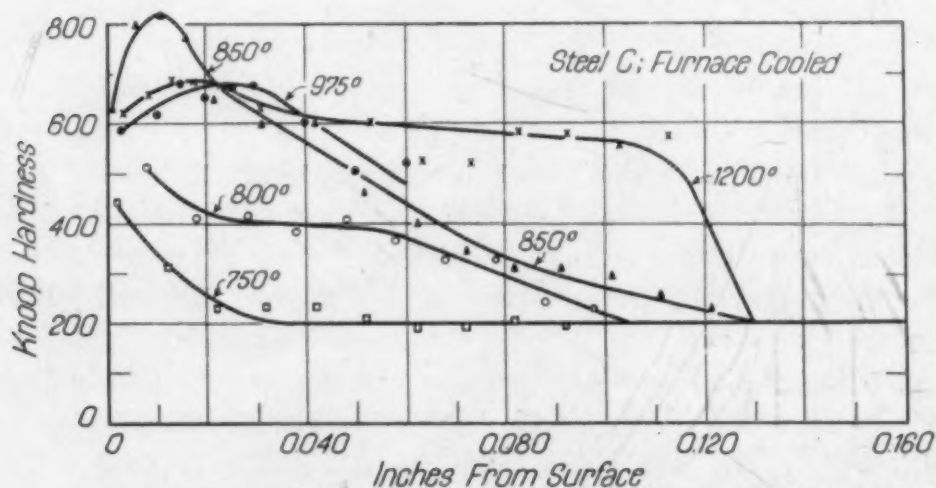


Fig. 8—Hardness Penetration Curves for Steel C (0.47 Per Cent Carbon) with a Furnace-Cooled Prior Structure. The temperature values are degrees Cent.

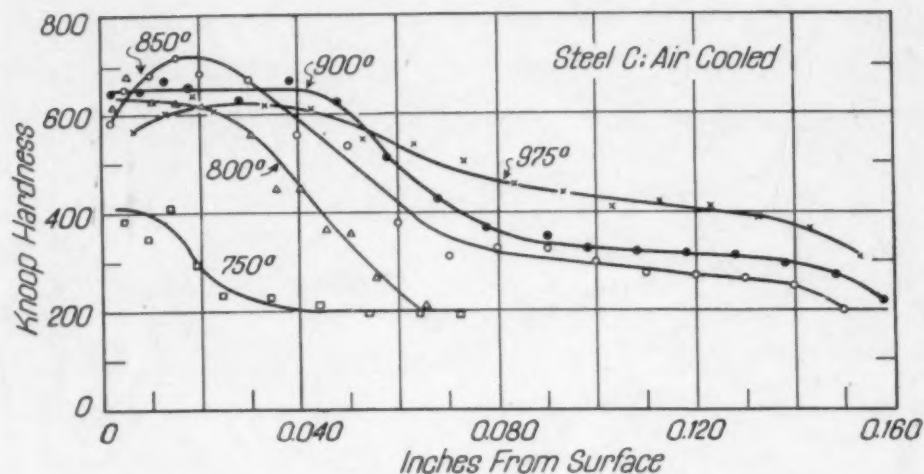


Fig. 9—Hardness Penetration Curves for Steel C (0.47 Per Cent Carbon) with an Air-Cooled Prior Structure. The temperature values are degrees Cent.

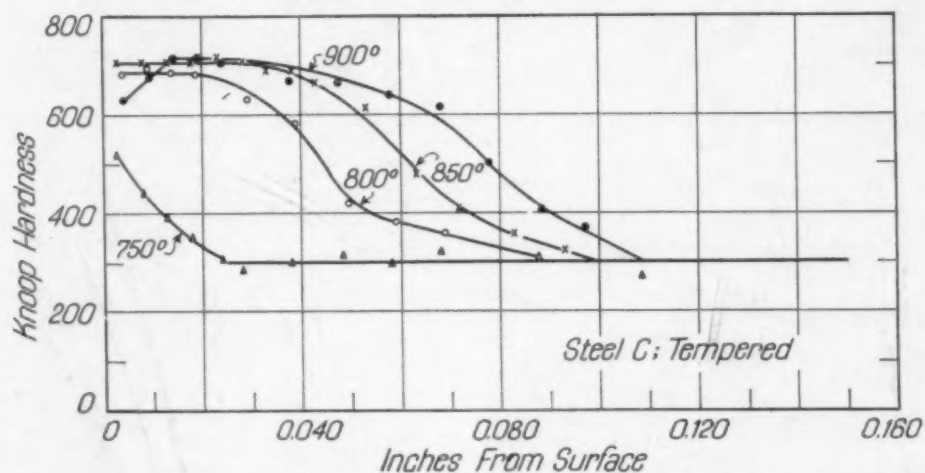


Fig. 10—Hardness Penetration Curves for Steel C (0.47 Per Cent Carbon) with a Sorbitic Prior Structure. The temperature values are degrees Cent.

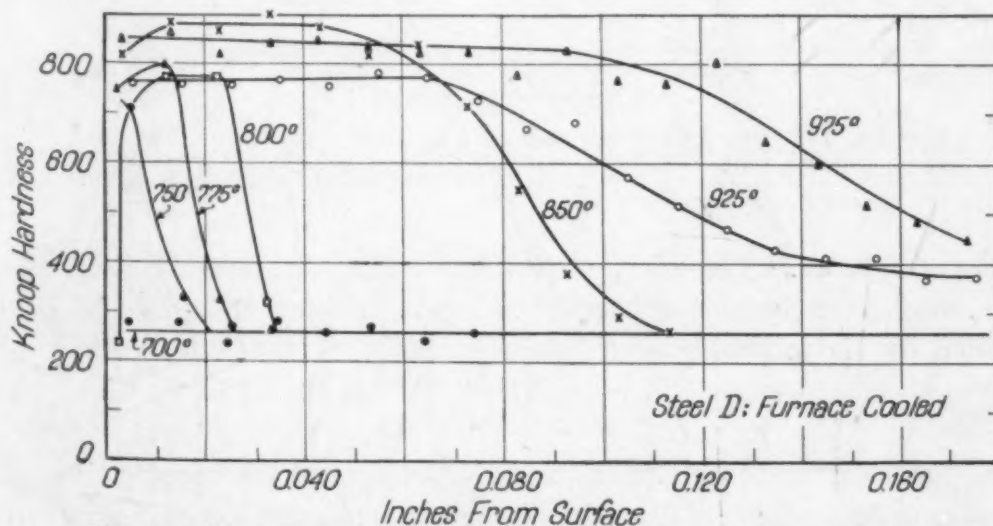


Fig. 11—Hardness Penetration Curves for Steel D (0.80 Per Cent Carbon) with a Furnace-Cooled Prior Structure. The temperature values are degrees Cent. The 800-degree Cent. sample was decarburized at the surface.

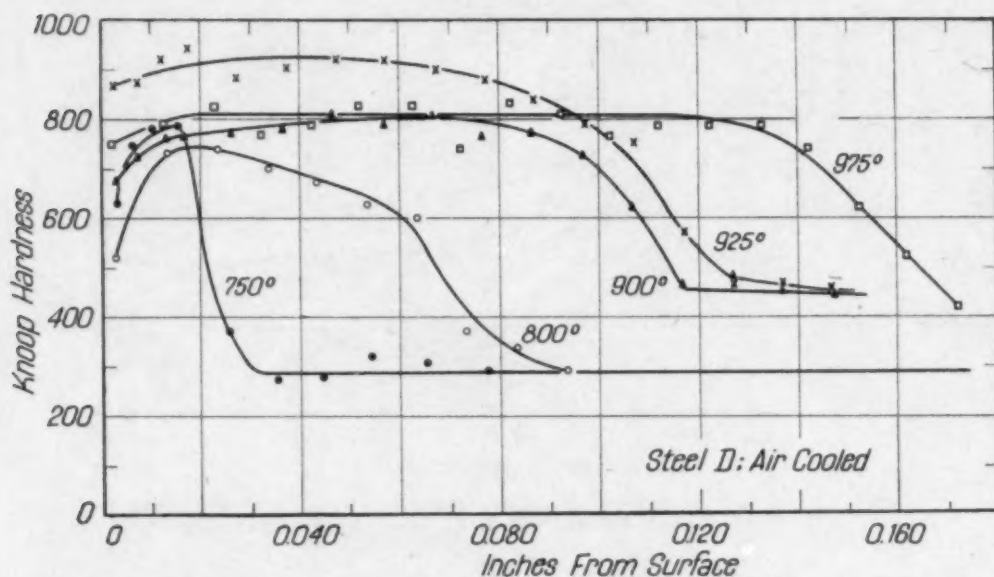


Fig. 12—Hardness Penetration Curves for Steel D (0.80 Per Cent Carbon) with an Air-Cooled Prior Structure. The temperature values are degrees Cent. The 750 and 800-degree Cent. samples were decarburized at the surface.

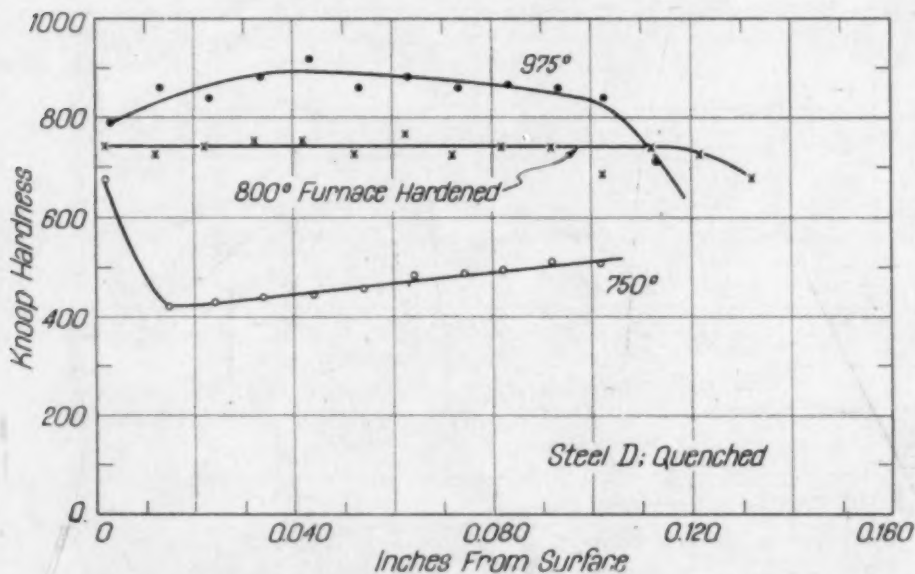


Fig. 13—Hardness Penetration Curves for Steel D (0.80 Per Cent Carbon) with a Martensitic Prior Structure. The temperature values are degrees Cent. Note the slight softening of the base material near the transition of the 750-degree Cent. sample.

were completed. Photomicrographs illustrating the structural changes resulting from induction heating along with other data will be presented in the following sections.

RESULTS

Metallographic and microhardness studies of the samples heated to 700 degrees Cent. (1290 degrees Fahr.) showed no indication of

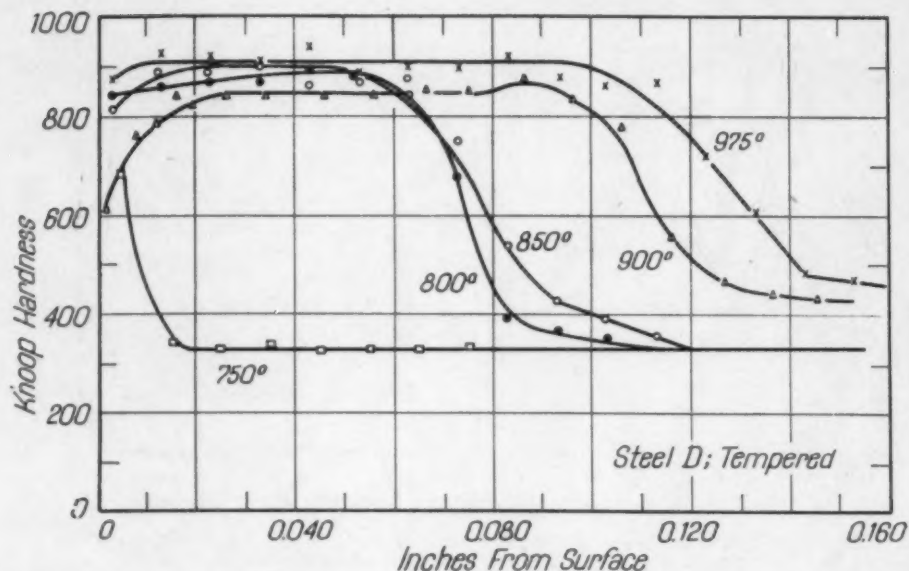


Fig. 14—Hardness Penetration Curves for Steel D (0.80 Per Cent Carbon) with a Sorbitic Prior Structure. The temperature values are degrees Cent. The low hardness of the 900-degree Cent. sample near the surface is probably due to decarburization.

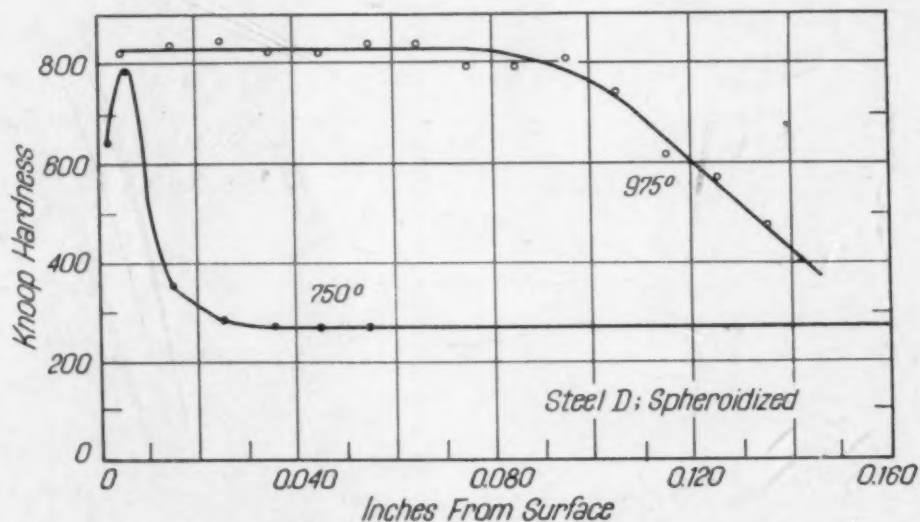


Fig. 15—Hardness Penetration Curves for Steel D (0.80 Per Cent Carbon) with a Spheroidized Prior Structure. The temperature values are degrees Cent.

hardening, although hardening did result when the samples were heated to 750 degrees Cent. (1380 degrees Fahr.) or higher. The furnace-cooled sample of Steel D shown in Fig. 5 is representative of all steels heated to 700 degrees Cent. (1290 degrees Fahr.). Fig. 3 is for the same steel after a 750-degree Cent. (1380-degree Fahr.) treatment and reveals that austenite has formed when heated to that temperature (intermediate temperatures were not checked).

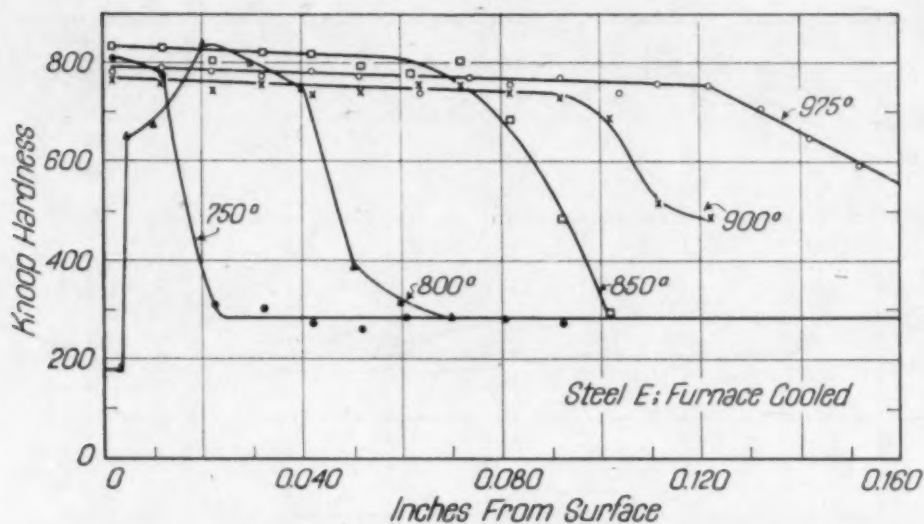


Fig. 16—Hardness Penetration Curves for Steel E (1.10 Per Cent Carbon) with a Furnace-Cooled Prior Structure. The temperature values are degrees Cent. The 800-degree Cent. sample was decarburized at the surface.

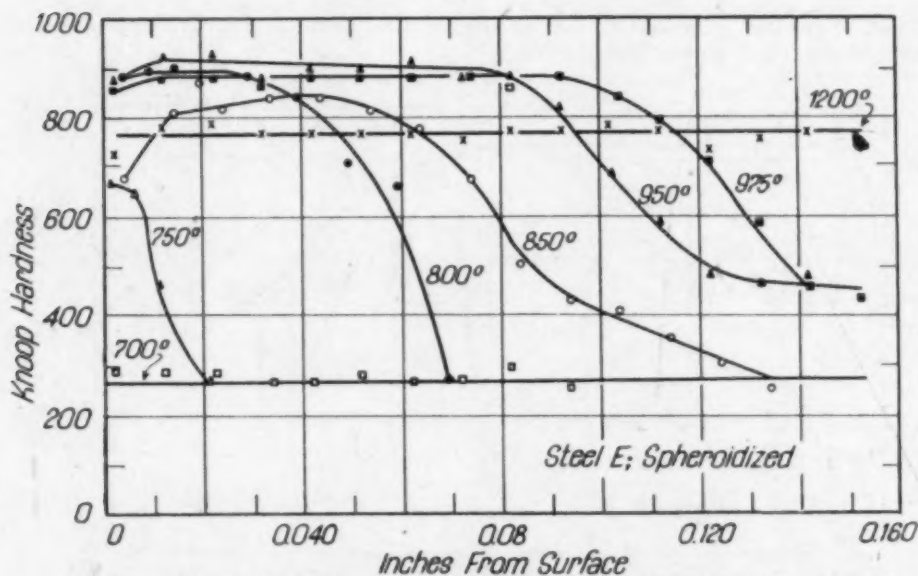


Fig. 17—Hardness Penetration Curves for Steel E (1.10 Per Cent Carbon) with a Spheroidized Prior Structure. The temperature values are degrees Cent. These samples should be free of any decarburizing effects since they were hardened as received.

The temperature at which the five plain carbon steels will start to transform to austenite on slow heating will be between 725 and 735 degrees Cent. (1335 and 1355 degrees Fahr.).⁴ The results presented above indicate that the temperature at which austenite starts to form is between 700 and 750 degrees Cent. (1290 and 1380 degrees Fahr.) for induction heating. A more detailed study is needed than was made in this investigation, to determine if there is an effect of

⁴As given in the 1939 A.S.M. METALS HANDBOOK, p. 475 for comparable S.A.E. steels.

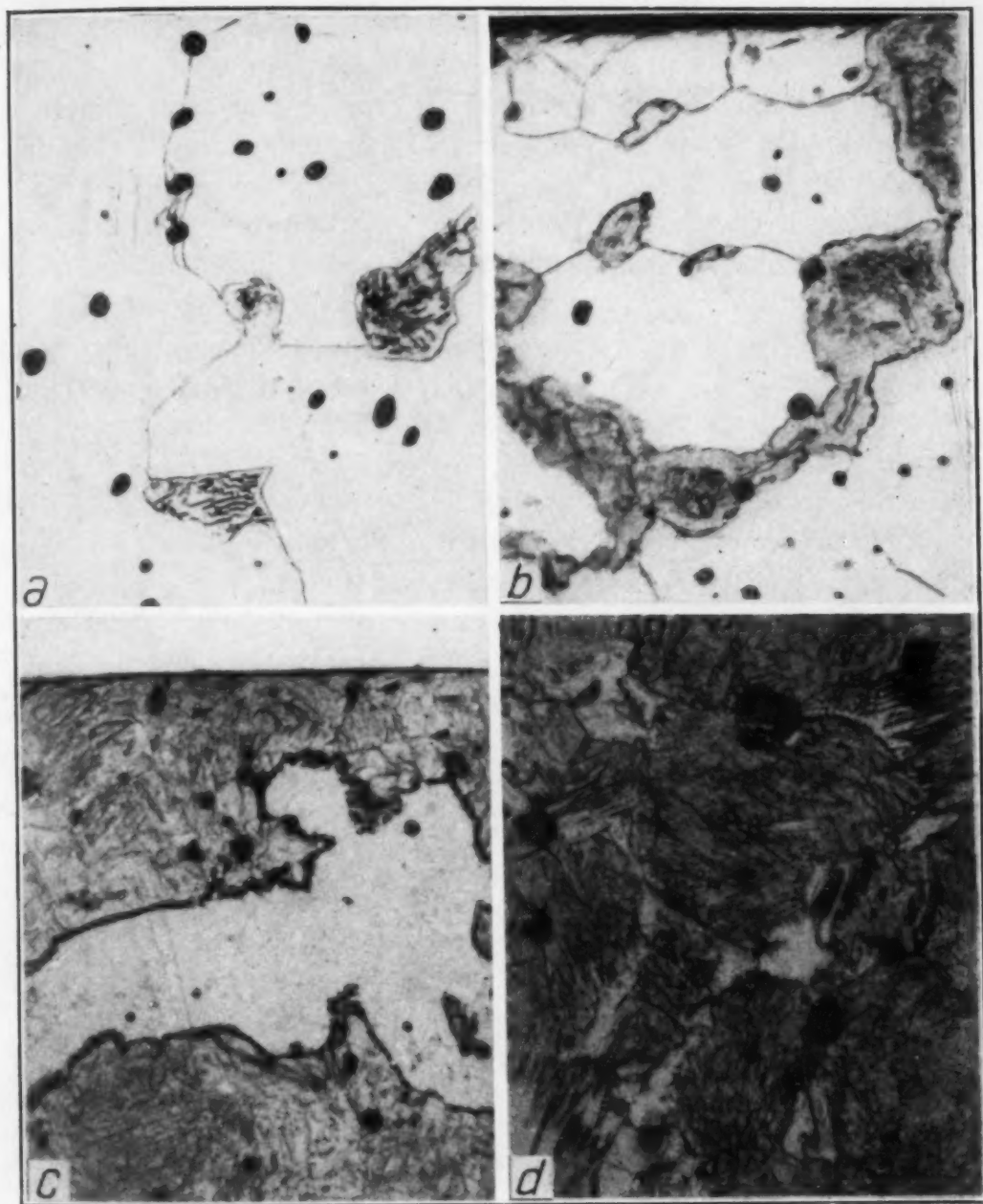


Fig. 18—Effect of Increasing Induction Heating Temperature on the Microstructure of Steel A; $\times 1000$. Fig. 18a—Original furnace-cooled structure. Fig. 18b—Heated to 750 degrees Cent. (1380 degrees Fahr.): martensite (10%) and ferrite. Taken at the surface. Fig. 18c—Heated to 850 degrees Cent. (1560 degrees Fahr.): martensite (50%) and ferrite. Taken at the surface. Fig. 18d—Heated to 1200 degrees Cent. (2190 degrees Fahr.): martensite (90%) and ferrite. Taken near the surface.

induction heating on the Ac_1 temperature as at the present there appears to be no effect of any practical consequence.

The rate of formation of austenite from ferrite:carbide aggregates is greatly accelerated as the temperature is increased above the Ae_1 . This statement applies regardless of the method of heating but

is of particular importance in the induction hardening of steel, where the heating rate is extremely high. The temperature of the sample increases continuously with the heating time so that an interrelation between time and temperature exists, i. e., the temperature or heating time may be varied but not the time at a certain temperature. To obtain full hardening by induction heating, the sample has to be heated to a temperature at which austenite forms almost instantaneously. It follows that the important variable in induction hardening is temperature and not time (at least for heating rates comparable to those used in this study). Time and temperature are of equal importance in furnace hardening which usually involves an isothermal transformation.

The hardness penetration curves for the five steels clearly illustrate the importance of temperature in induction hardening of steel. These curves for various temperature and structural conditions are presented in Figs. 6 to 17. They can be discussed conveniently on the basis of carbon composition:

Steel A. A maximum surface temperature of 1200 degrees Cent. (2190 degrees Fahr.) was not high enough to harden completely this 0.17 per cent carbon steel (Fig. 6). This is understandable when the prior structure of the furnace-cooled samples shown in Fig. 18a is considered. In fact, it is remarkable that over 90 per cent of the sample could be converted to austenite during the 15 seconds required to heat to 1200 degrees Cent. (2190 degrees Fahr.). The progressive increase in the formation of austenite with increasing temperature is illustrated in the photomicrographs in Fig. 18. The pearlitic areas are first converted to austenite; as the temperature is increased the austenite areas grow by diffusion of carbon into gamma iron, that is, into what formerly were free ferrite areas. At temperatures above 1200 degrees Cent. (2190 degrees Fahr.) for the steel a homogeneous austenite is obtained.

The undissolved ferrite areas in the quenched steels result in erratic Knoop hardness values. Thus, in Fig. 6 there is a low hardness value of about 250 Knoop at a distance of 0.035 inch from the surface for the 1200-degree Cent. (2190-degree Fahr.) sample which is low probably due to free ferrite (Fig. 18d).

Steel B. Increase in the carbon content to 0.30 per cent facilitates the formation of austenite during induction heating. Full hardness was obtained in this steel when heated to 850 degrees Cent. (1560 degrees Fahr.) although some undissolved ferrite still re-

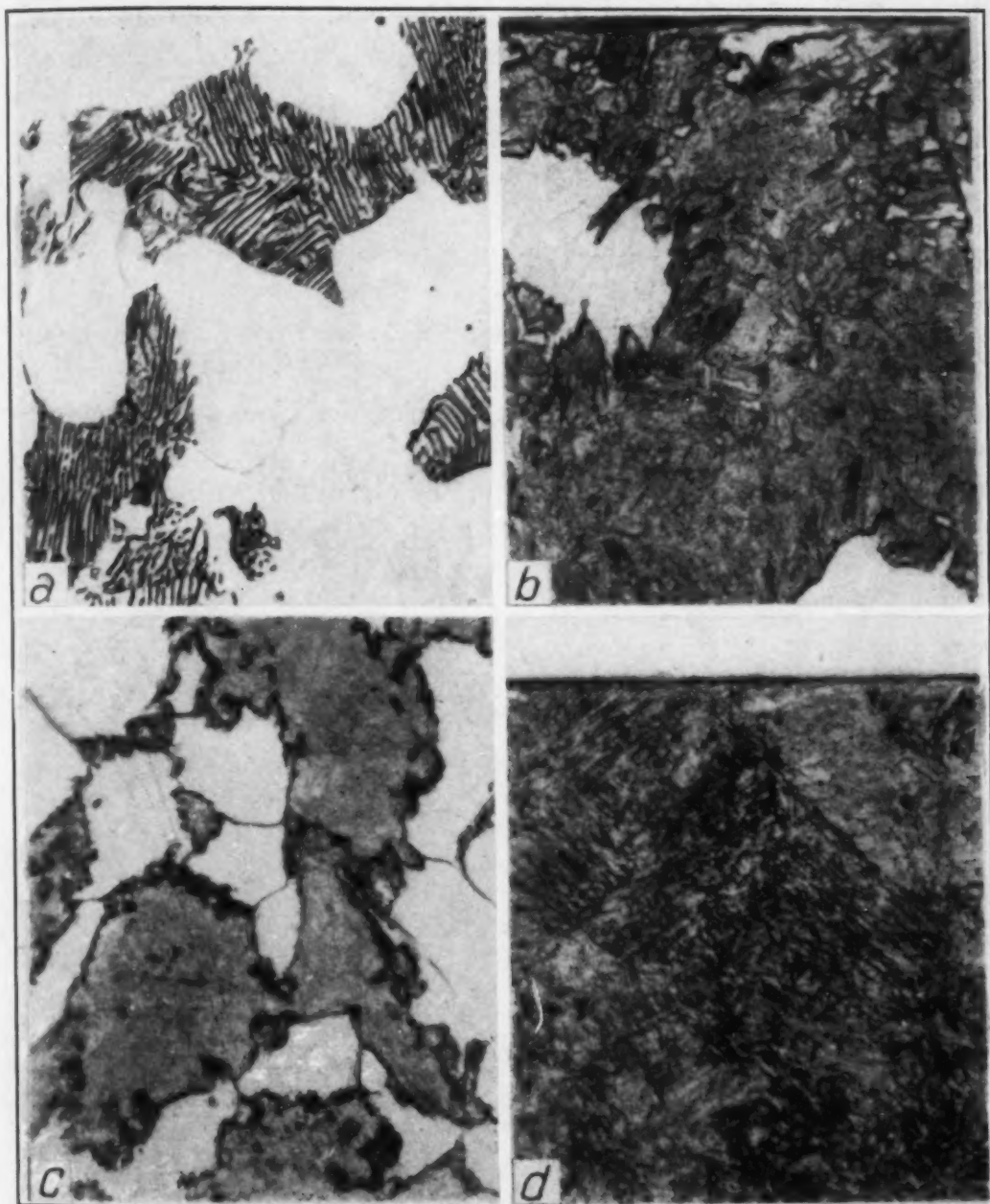


Fig. 19—Effect of Increasing Induction Heating Temperature on the Microstructure of Steel B; $\times 1000$. Fig. 19a—Original furnace-cooled structure. Fig. 19b—Heated to 850 degrees Cent. (1560 degrees Fahr.): martensite and ferrite. Taken at the surface. Fig. 19c—Same sample as (B): martensite, ferrite, and low carbon pearlite. Taken in the transition zone. Fig. 19d—Heated to 975 degrees Cent. (1785 degrees Fahr.): martensite. Taken at the surface.

maintained (Figs. 7 and 19b). The scatter in the points [850-degree Cent. (1560-degree Fahr.) curve] near the transition zone probably results from the mixed microstructure of martensite, ferrite, and pearlite found there. Fig. 19c illustrates the nature of the transition zone. This steel is completely austenitized at some temperature be-

tween 850 and 975 degrees Cent. (1560 and 1785 degrees Fahr.). The structure in Fig. 19d is typical of the martensite found in any hardened low carbon steel.

The increase in Knoop hardness of the 850-degree Cent. (1560-degree Fahr.) sample (Fig. 7) with depth of penetration has been observed for other samples (Figs. 8, 9, 11, 12, etc.). There are several possible explanations for the occurrence of the maximum hardness at some distance from the surface:

1. The surface may have been decarburized. However, examination of the surface of this sample (Fig. 19b) indicates no decarburized zone so that some other factor or factors must be responsible for the phenomenon.

2. There is less free ferrite at the surface of this sample than near the transition zone (Figs. 19b and 19c) due to a higher temperature at the surface. As a result, the martensite at the surface will be lower in carbon than the martensite in the transition. The low carbon martensite will have a lower hardness in accord with our knowledge on the effect of carbon content on martensitic hardness. Thus, the presence of undissolved ferrite is indirectly responsible for increasing the hardness. Of course, that will depend upon where the hardness indentation is made; if on the high carbon martensitic matrix, the hardness will be higher than that for a low carbon homogeneous martensite at the surface; whereas, if the indentation is made on or near a ferrite island, the hardness will be unusually low. The Tukon tester makes a very small indentation so that in a structure consisting of 80 to 90 per cent martensite the chances are very favorable for measuring the hardness of high carbon martensite instead of ferrite. A Rockwell or Brinell measurement on such a sample would give an average hardness of the two constituents.

This explanation would apply only to hypoeutectoid steels containing appreciable amounts of free ferrite (less than about 0.60 per cent carbon) and not to an eutectoid or hypereutectoid steel. Since these higher carbon steels also exhibit the described phenomenon of higher "transition" hardness there must be other possible interpretations.

3. Internal stresses may account for the higher hardness occurring at a distance from the surface. There are high compressive stresses in the hardened case of an induction hardened sample. This condition exists because the core will not allow the martensitic case to expand to its full volume. It will be shown later that internal com-

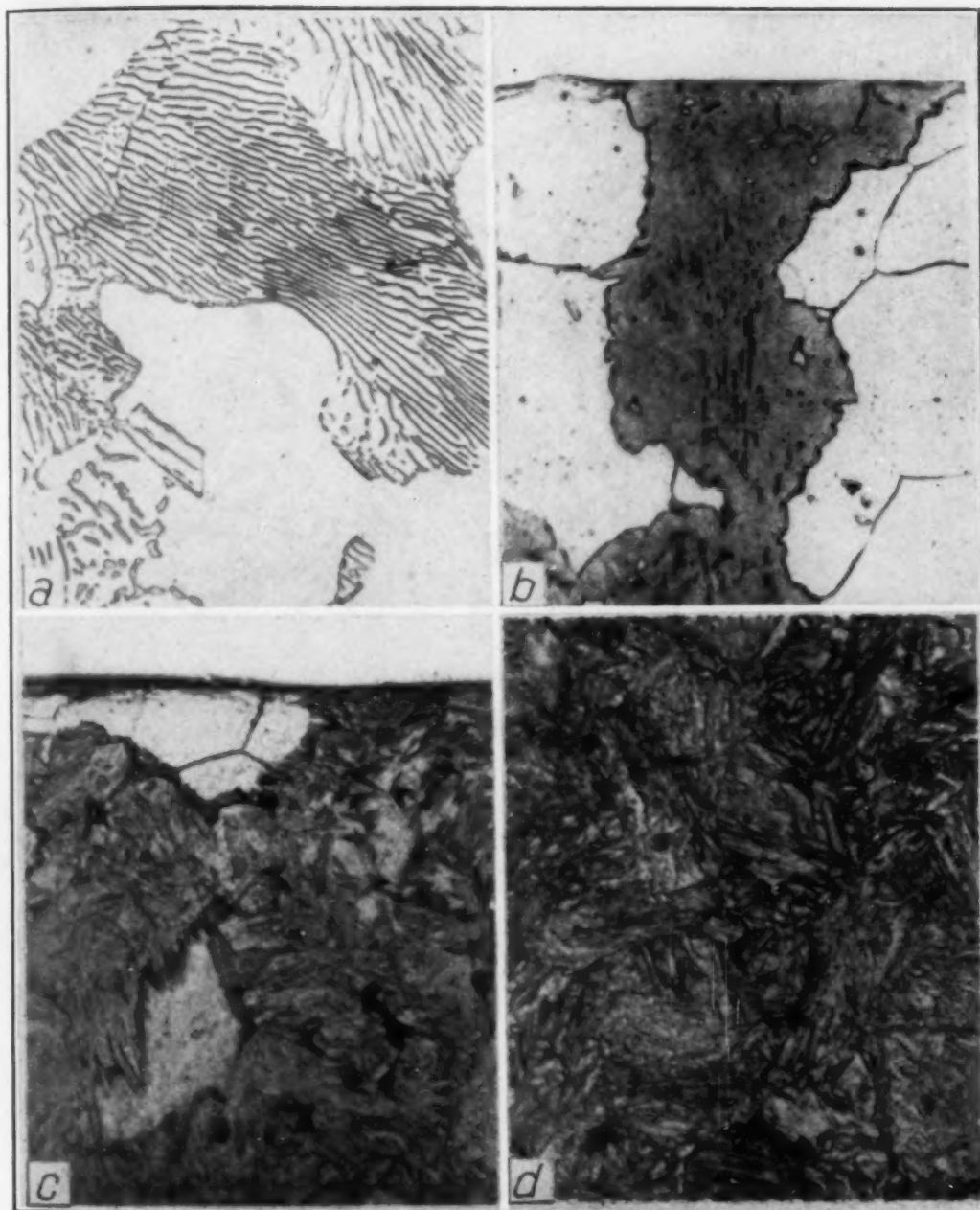


Fig. 20—Effect of Increasing Induction Heating Temperature on the Microstructure of Steel C; $\times 1000$. Fig. 20a—Original furnace-cooled structure. Fig. 20b—Heated to 750 degrees Cent. (1380 degrees Fahr.): martensite and ferrite. Taken at the surface. Fig. 20c—Heated to 850 degrees Cent. (1560 degrees Fahr.): martensite and ferrite. Taken at the surface. Fig. 20d—Heated to 975 degrees Cent. (1785 degrees Fahr.): martensite. Taken near the surface.

pressive stresses increase the hardness and residual tensile stresses decrease the hardness of a metal sample (also reference 39). The restraining action of the core should be greatest near the transition zone and thus the hardness also higher near there. As the depth of the hardened case increases this effect should diminish since the pre-

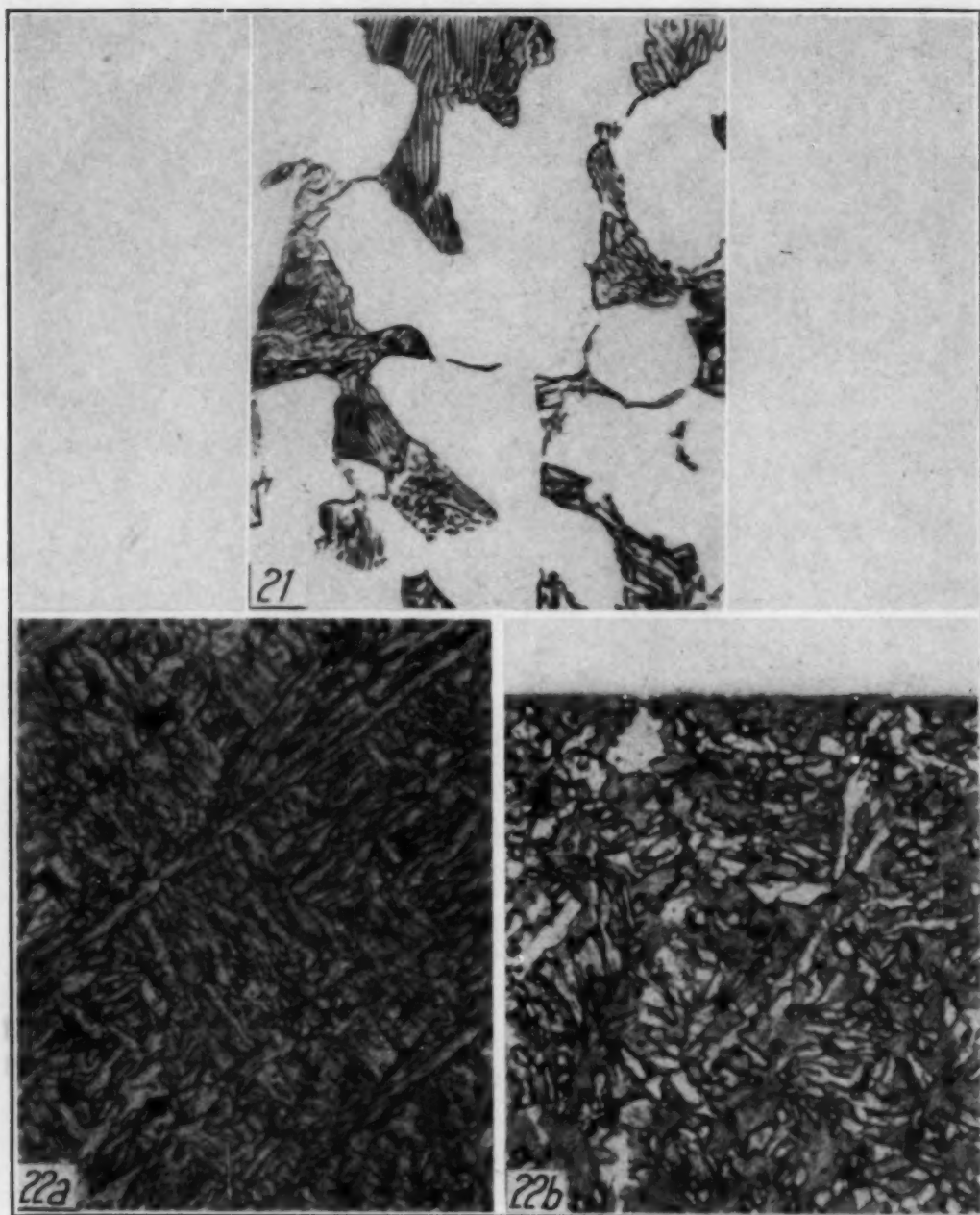


Fig. 21—Air-Cooled Structure of Steel C; $\times 1000$.
Fig. 22—Effect of Induction Heating on the Microstructure of Steel C; $\times 1000$.
Fig. 22a—Original tempered structure: sorbite. Fig. 22b—Heated to 750 degrees Cent. (1380 degrees Fahr.): martensite and ferrite. Taken at the surface.

requisite conditions for compressive stresses are a martensitic case and an unhardened core. This appears to be true, for the samples heated to high temperatures [above 900 degrees Cent. (1650 degrees Fahr.)] have in general a more uniform hardness distribution. However, the high temperatures would also produce a more homogeneous austenite and thus eliminate the high carbon martensitic areas if any existed.

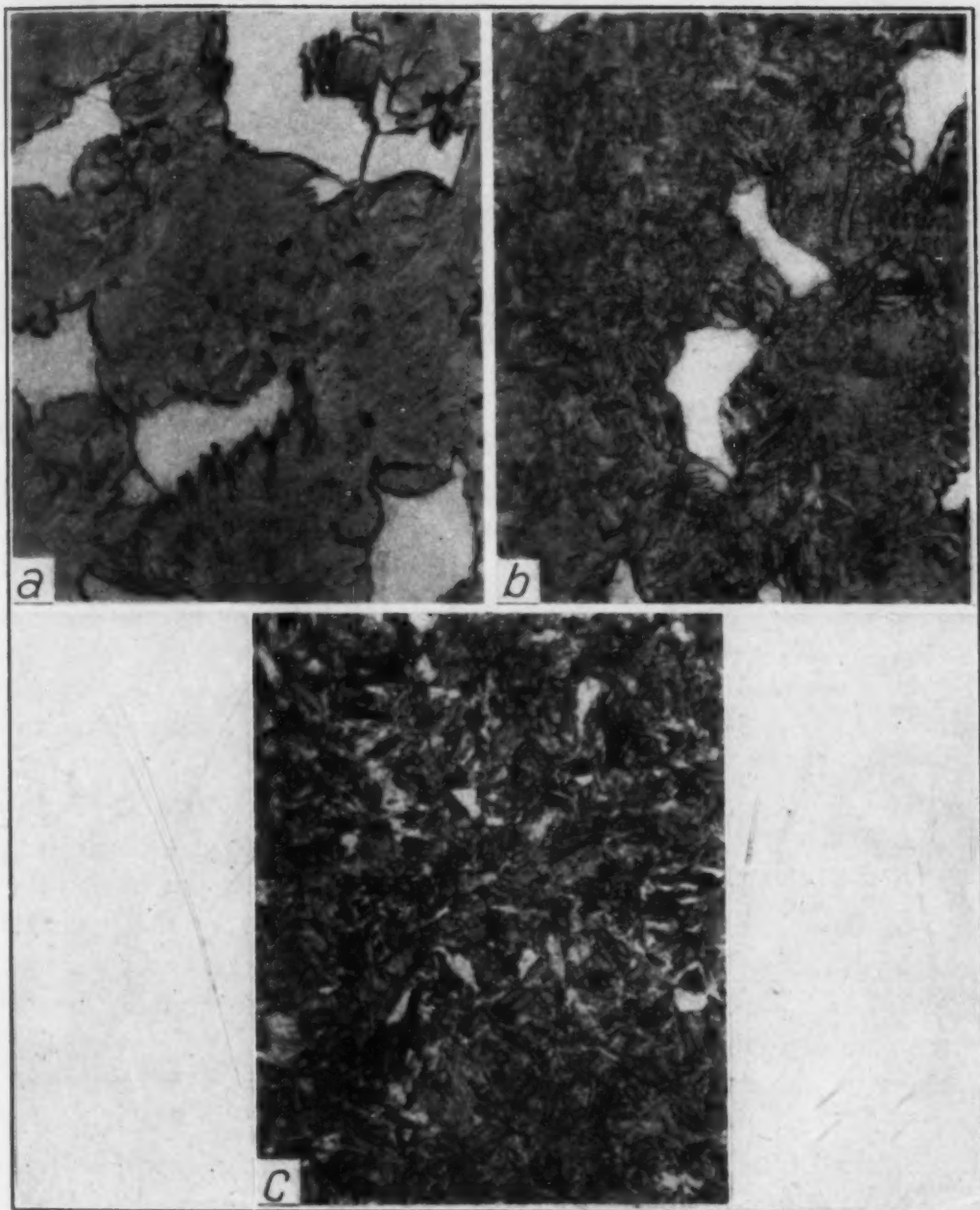


Fig. 23—Effect of Various Prior Structures on the Induction Hardening of Steel C; $\times 1000$. Fig. 23a—Furnace-cooled: martensite and ferrite. Fig. 23b—Air-cooled: martensite and ferrite. Fig. 23c—Tempered: martensite. All pictures were taken near the edge. The samples were heated to 800 degrees Cent. (1470 degrees Fahr.).

4. Retained austenite is another possible condition which could account for the lower surface hardness. In view of the photomicrographs in Fig. 29 which show less retained austenite at the surface than near the center of the sample this factor seems to be eliminated.

Probably internal stresses and nonhomogeneous martensite are

each effective in producing the frequently observed increase in hardness with depth into the hardened case.

Steel C. This steel with a carbon content of 0.47 per cent has higher hardness when quenched than Steels A or B.

Note in Fig. 8 that the 850-degree Cent. (1560-degree Fahr.) sample has a much higher hardness than any sample heated to a lower or higher temperature. The photomicrograph of this specimen, reproduced in Fig. 20c, shows undissolved ferrite; therefore the martensite will be of a higher carbon content, and thus have a higher hardness than the martensite shown in Fig. 20d which formed from a more uniform austenite.

The lower surface hardness of the 975 or 1200-degree Cent. samples can also be explained, as previously discussed for Steel B, by assuming that the stresses near the transition are compressive to a greater degree than those at the surface.

The air-cooled series plotted in Fig. 9 do not differ appreciably from the furnace-cooled samples in Fig. 8. The depth of hardening for the air-cooled samples is slightly greater than the furnace-cooled samples as is to be expected from a comparison of the prior microstructures (Figs. 20a and 21).

The samples of Steel C with a prior sorbitic structure responded most favorably to induction heating (Fig. 22). The sample heated to 800 degrees Cent. (1470 degrees Fahr.) was martensitic at the edge compared to mixtures of martensite and ferrite for the furnace-cooled and air-cooled samples (Fig. 23). The maximum hardness obtained in this series is essentially the same for all samples heated to temperatures above 800 degrees Cent. (1470 degrees Fahr.). The hardness of the hardened case is also quite uniform from surface to transition for two of the hardened samples plotted in Fig. 10 (the third, heated to 900 degrees Cent. (1650 degrees Fahr.), will be discussed in the next paragraph). Since the sorbitic structure of these samples was most favorable of those studied for the formation of austenite, the resulting martensite should be quite uniform in composition from surface to transition zone. For this reason, it appears that carbon segregation effects are responsible for any difference in hardness measured in the hardened case of hypoeutectoid steel.

The sharp drop in hardness of the 900-degree Cent. (1650-degree Fahr.) sample near the surface appears irregular. Examination of the sample showed an etching effect in the approximate area of the hardness indentations. This etching mark resembled the tem-

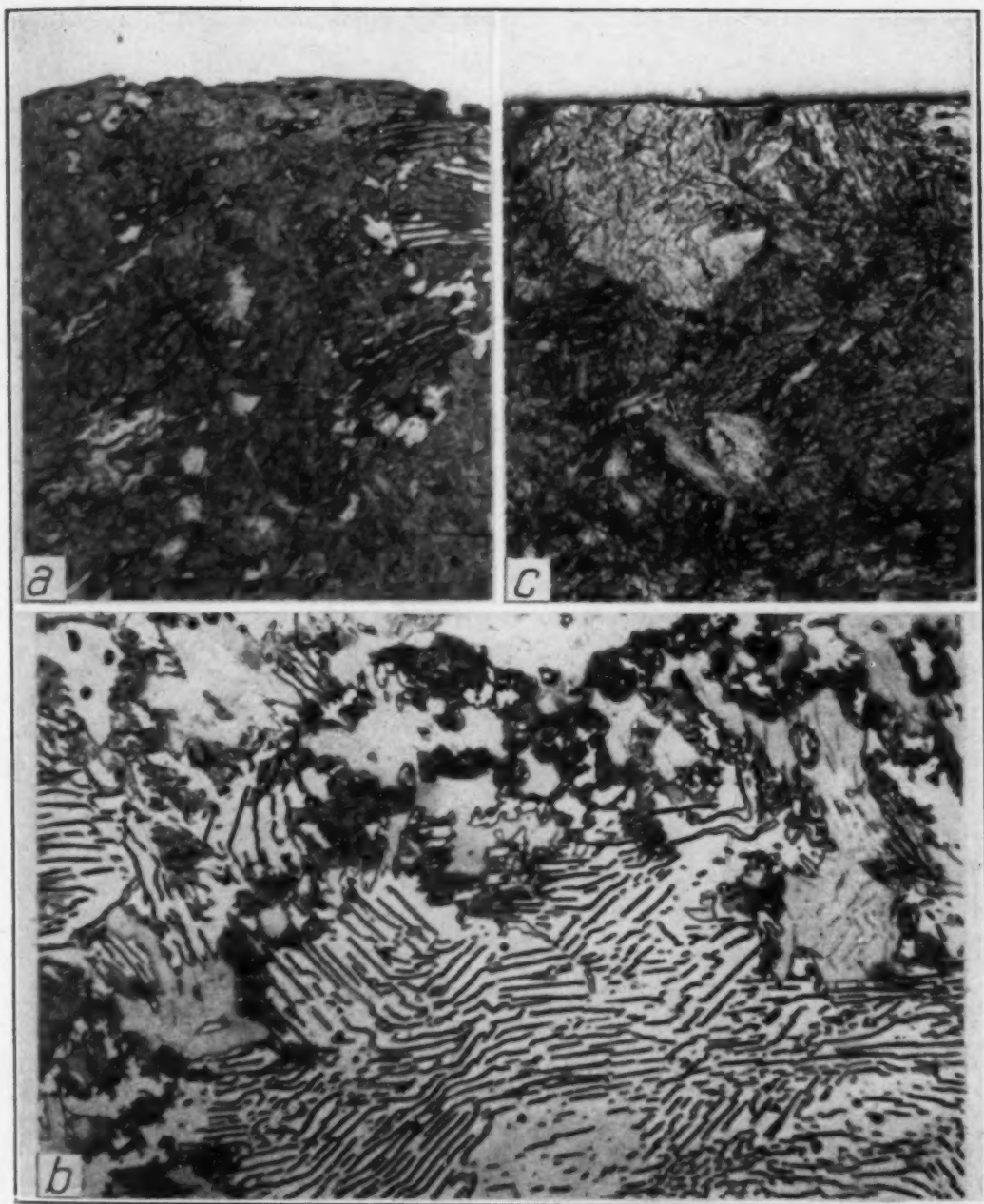


Fig. 24—Effect of Increasing Induction Heating Temperature on the Microstructure of Steel D; $\times 1000$. Fig. 24a—Heated to 775 degrees Cent. (1425 degrees Fahr.): martensite and ferrite. Taken at the surface. Fig. 24b—Same treatment as (a): martensite and pearlite. Taken near the transition zone. Fig. 24c—Heated to 975 degrees Cent. (1785 degrees Fahr.): martensite. Taken at the edge.

pered streaks obtained on hardened samples which are overheated during the cutting-off operation. The present specimens were cut under a water spray but overheating is nevertheless a possibility. Tempering during the cutting operation is, therefore, another factor to be considered in regard to any drop in hardness. Grinding and

polishing of the samples for hardness measurements should remove any superficial tempered areas and in general that appears to have been the case for the other samples did not show etching streaks.

Steel D. The maximum Knoop hardness was obtained in this eutectoid steel when heated to 850 degrees Cent. (1560 degrees Fahr.). A slight drop in hardness resulted with higher temperatures (Fig. 11). This may be explained by assuming that the compressive stresses are highest in the 850-degree Cent. (1560-degree Fahr.)

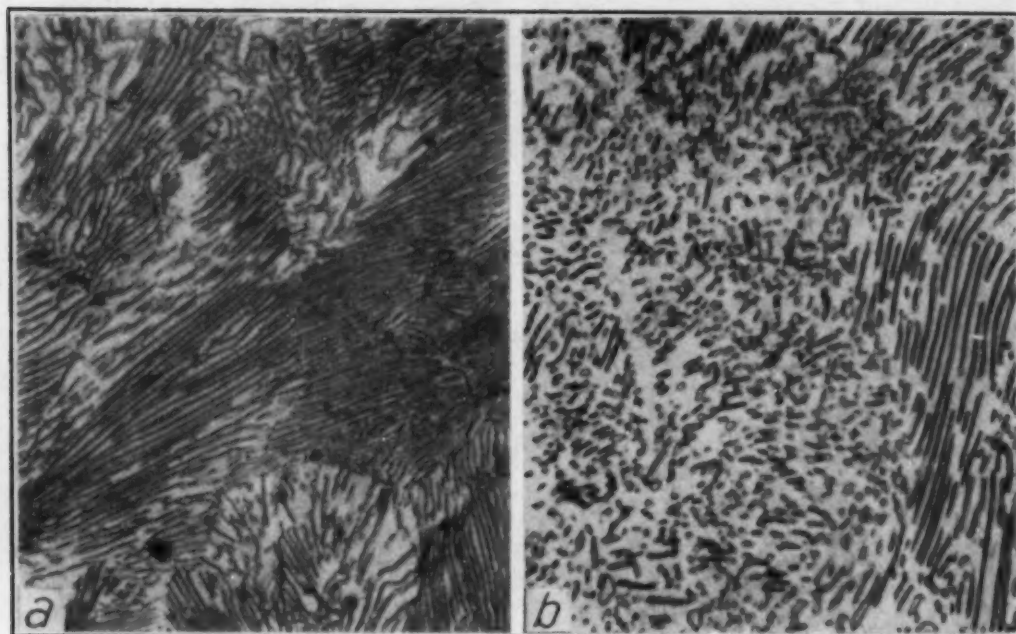


Fig. 25—Prior Structure of Steel D; $\times 1000$. Fig. 25a—Air-cooled. Fig. 25b—Spheroidized.

sample and thus the hardness is also highest. Another factor to consider is the increase in the amount of untransformed austenite as the heat treating temperature is increased; this would likewise result in a lower hardness. Detailed information is needed to evaluate the effect of each factor on the hardness.

The furnace-cooled sample of Steel D heated to 775 degrees Cent. (1425 degrees Fahr.) had a surface layer consisting of martensite and undissolved ferrite as shown in Fig. 24a. Higher temperatures produced a martensitic structure similar to that in Fig. 24c.

The transition zone is fairly sharp at low magnifications (as in Fig. 3), but at high magnifications we find an irregular zone consisting of a heterogeneous martensitic structure and pearlite. The nature of the heterogeneous martensite is illustrated in Fig. 24b; it

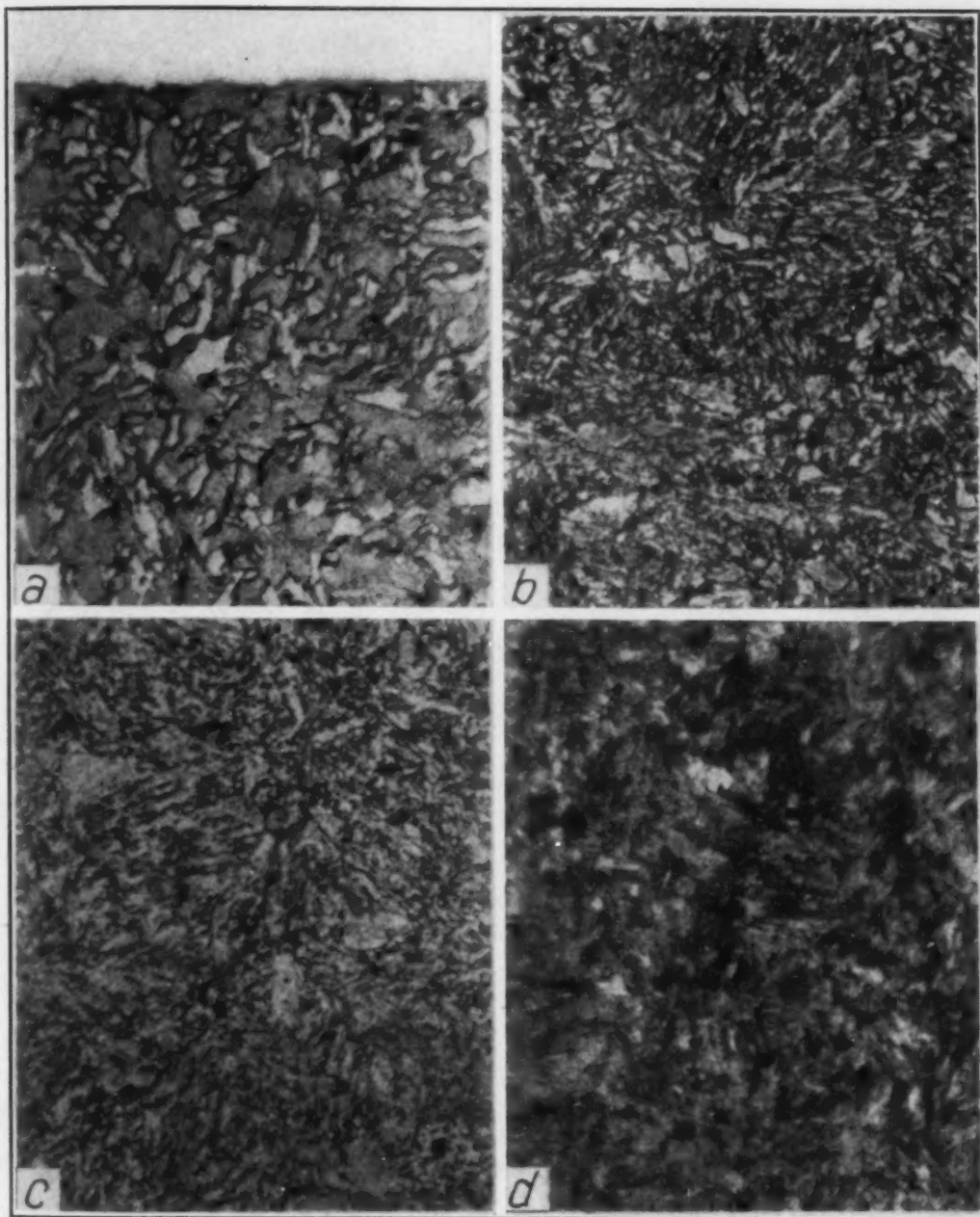


Fig. 26—Effect of Induction Heating Temperature on the Microstructure of Steel D; $\times 1000$. Fig. 26a—Quenched sample heated to 750 degrees Cent. (1380 degrees Fahr.). Taken near the edge. Fig. 26b—Same sample as in (a); sorbite. Taken in the transition zone. Fig. 26c—Basic tempered structure: sorbite. Fig. 26d—Heated to 800 degrees Cent. (1470 degrees Fahr.): martensite. Taken near the surface.

will be noted that traces of the carbide lamellae are still observed. This structure is called pearlite "ghosts" or pseudomorphs of pearlite. Additional facts on this interesting constituent will be presented later.

As expected, the fine pearlitic structure shown in Fig. 25a transforms to austenite slightly faster than does the coarse pearlite in the

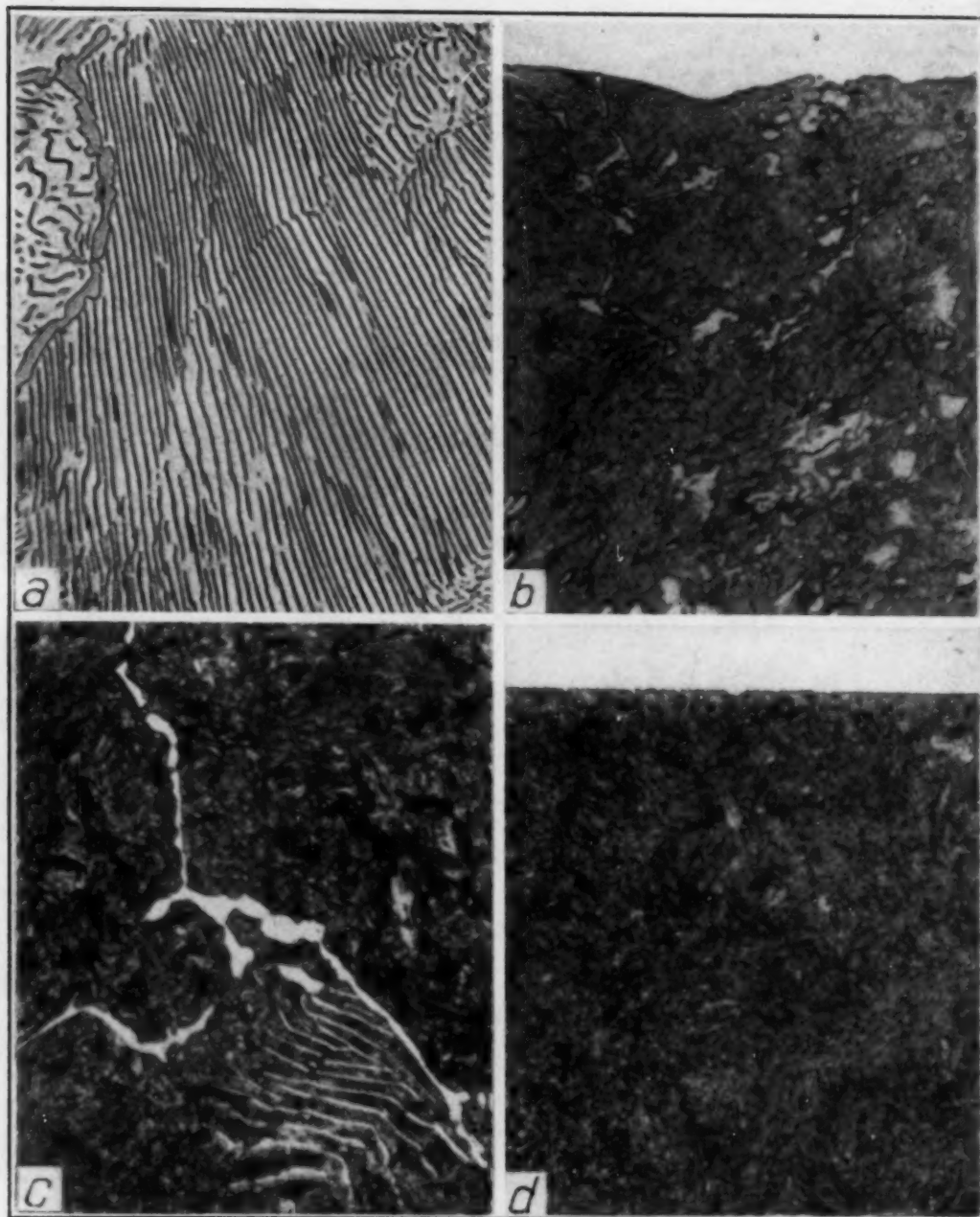


Fig. 27—Effect of Induction Heating Temperature on the Microstructure of Steel E; $\times 1000$. Fig. 27a—Original furnace-cooled structure. Fig. 27b—Heated to 750 degrees Cent. (1380 degrees Fahr.): martensite and undissolved carbide. Taken at the surface. Fig. 27c—Same treatment as for (a): martensite and undissolved carbide. Taken in the transition zone. Fig. 27d—Heated to 900 degrees Cent. (1650 degrees Fahr.): martensite. Taken at the edge.

furnace-cooled samples. The depth of hardening is likewise greater as the lamellae spacing is decreased (Fig. 12). The 925-degree Cent. (1695-degree Fahr.) sample had maximum hardness in the air-cooled series. With higher temperatures a decrease in hardness was

observed. The microstructural changes are similar to those presented for the coarser pearlite samples (Fig. 24).

The results plotted in Fig. 13 are of interest. The prior structure of the samples was martensite, the hardness curve of which is also included in the diagram. It will be noted that the induction hardened sample [975-degree Cent. (1785-degree Fahr.) curve] is considerably harder than the furnace-hardened specimen, although the depth of hardening is not as great.

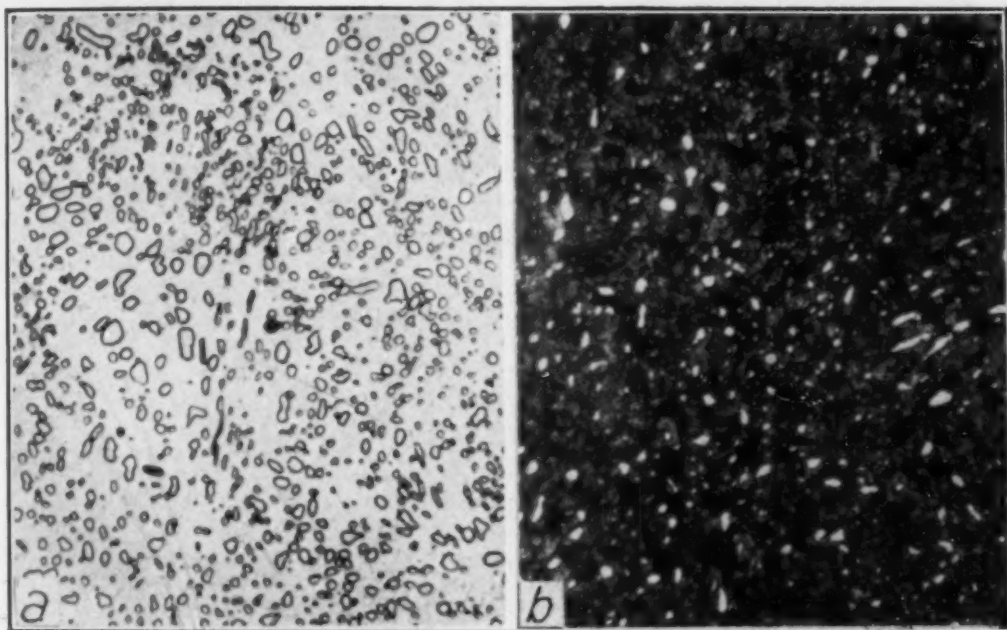


Fig. 28—Effect of Induction Heating on the Microstructure of Steel E; $\times 1000$. Fig. 28a—Spheroidized structure. Fig. 28b—Heated to 800 degrees Cent. (1470 degrees Fahr.): martensite and undissolved carbide. Taken near the surface.

During induction heating the original martensite decomposes into ferrite and carbides, which in turn transform into austenite above the A_{c1} temperature. The surface of the sample heated to 750 degrees Cent. (1380 degrees Fahr.) is shown in Fig. 26a. The considerable amount of free ferrite in this sample indicates that the decomposition of martensite and growth of carbide occurs very rapidly on heating, since the total heating time for this sample was 3.1 seconds. The tempering effect of the prior martensite extended into the unhardened core and the low hardness values near the transition zone (Fig. 13) are due to the tempered structure.

The tempered series (Fig. 14) act similarly to the quenched samples in their response to induction heating. The fine distribution of carbide is very favorable for rapid austenitizing (Fig. 26d), al-

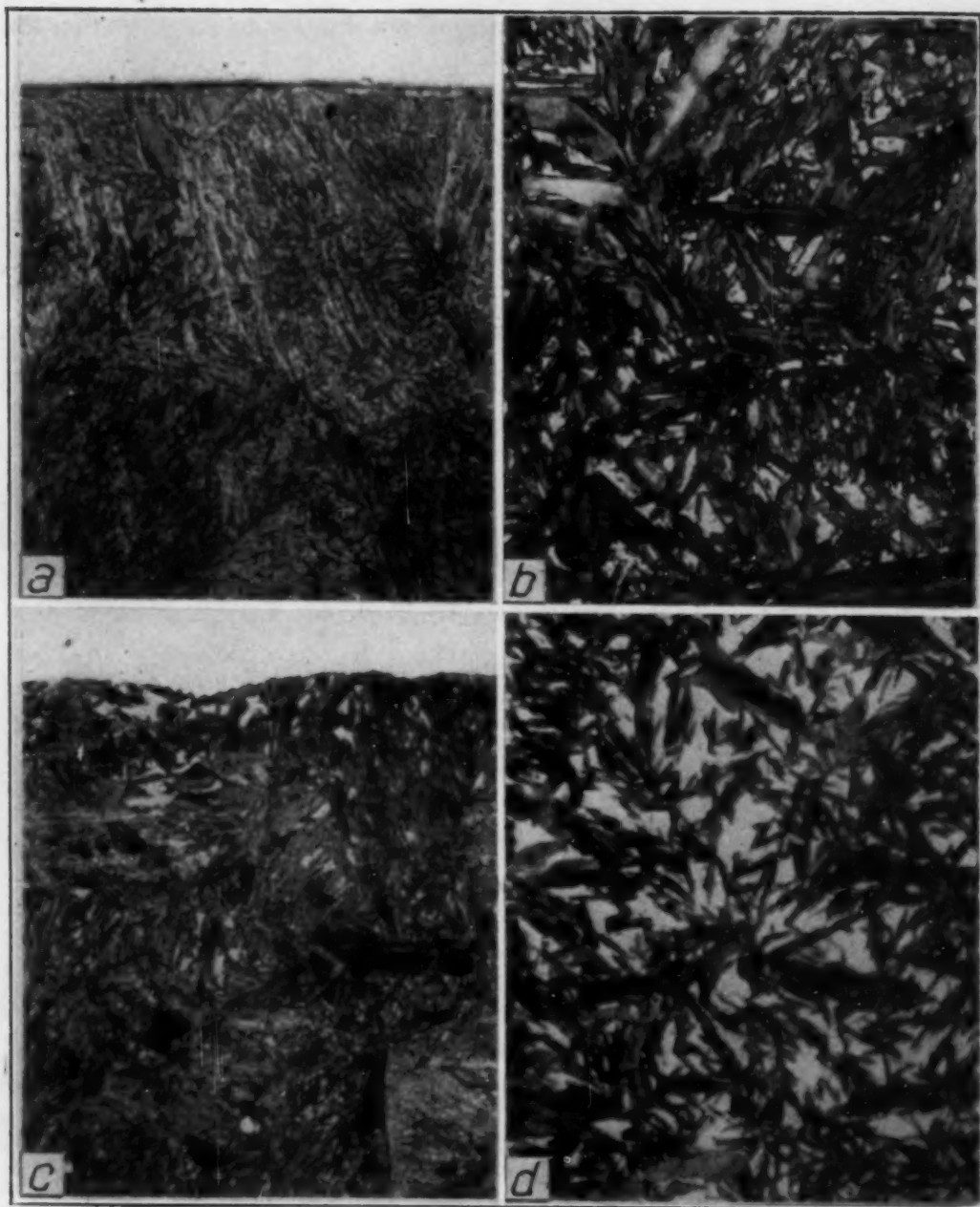


Fig. 29—Retained Austenite in Steel E; $\times 1000$. Fig. 29a—Spheroidized sample heated to 1200 degrees Cent. (2190 degrees Fahr.): martensite. Taken at the surface. Fig. 29b—Same as (a): martensite and austenite. Taken a distance from the surface. Fig. 29c—Furnace-cooled sample heated to 975 degrees Cent. (1785 degrees Fahr.): martensite and austenite. Taken at the surface. Fig. 29d—Same sample as in (c): martensite and austenite. Taken a distance from the surface.

though this factor is not as important in a high carbon steel as in a medium steel where the ferrite and carbide distribution is of major importance.

The Knoop hardness results are not appreciably different from those obtained for air-cooled samples. The microstructure for the

800-degree Cent. (1470-degree Fahr.) sample is given in Fig. 26d. Spheroidizing of the eutectoid steel produces no great changes in hardness compared to the other structures in this group (Fig. 15). This is to be expected since the general distribution of carbide is not much different (Fig. 25b).

Steel E. The structure of the furnace-cooled 1.10 carbon steel is reproduced in Fig. 27a. When this structure is heated to 750 degrees Cent. (1380 degrees Fahr.) austenite is formed in the pearlitic areas leaving a network of undissolved carbides (Figs. 27b and 27c). Since the carbide does not impair the hardness, essentially full martensitic hardness is obtained in this sample. Heating to higher temperatures to dissolve the carbide (Fig. 27d) results in minor changes in hardness, although the depth of hardening does increase (Fig. 16).

The Knoop hardness of the spheroidized steel (Figs. 17 and 28a) is in general about 100 units higher than the furnace-cooled samples (Fig. 16). There is no apparent explanation for this difference.

However, there are logical reasons for the lower hardness of the samples (Figs. 16 and 17) heated to temperatures above 900 degrees Cent. (1650 degrees Fahr.)—retained austenite and probably lower stresses. The photomicrograph in Fig. 27d is in sharp contrast to those in 29b and 29d. A very interesting point is that there appears to be less retained austenite at the surface of the samples in Fig. 29. This is in agreement with the results of Mathews (26) and others (19), (28) that oil quenching produces more untransformed austenite than water quenching, i.e., the faster the cooling rate, the higher is the percentage of martensite formed.

DISCUSSION

The information presented in the preceding section may best be discussed in terms of temperature, structural, and composition effects.

Effect of Temperature—The metallurgical reactions which occur during induction hardening are no different from those occurring during furnace hardening. There is, however, a wide difference in the importance of time and temperature in the two methods of heat treatment. Furnace hardening is essentially a long time isothermal treatment at a low temperature, whereas induction hardening in-

volves a continuous heating operation to a high temperature where the formation of austenite is extremely rapid. The temperature to which a plain carbon steel sample has to be heated by induced high frequency currents to obtain full hardness is greatly dependent upon the carbon composition and the prior structure. A surface temperature of over 1200 degrees Cent. (2190 degrees Fahr.) is required to surface harden a 0.17 per cent carbon steel (Fig. 6), whereas a minimum temperature of 750 degrees Cent. (1380 degrees Fahr.) is re-

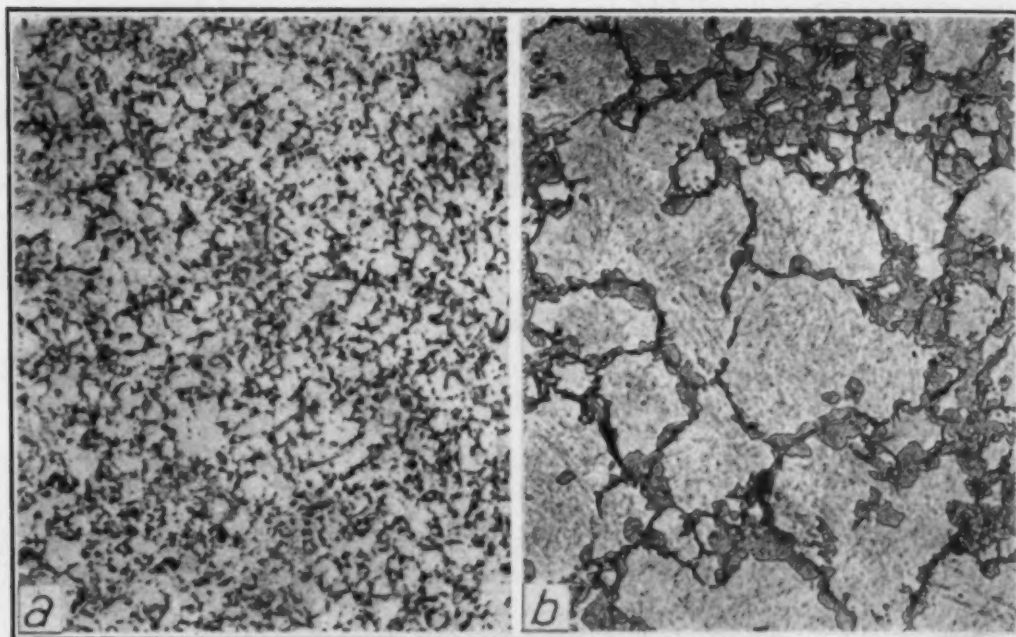


Fig. 30—Comparison of Austenite Grain Size Obtained During Furnace and Induction Heating of Steel B; $\times 100$. Fig. 30a—Induction heated to 975 degrees Cent. (1785 degrees Fahr.); air-cooled to 675 degrees Cent. (1245 degrees Fahr.) and water-quenched. Fig. 30b—Held at 975 degrees Cent. (1785 degrees Fahr.) in furnace for 15 minutes.

quired to induction harden a 1.10 per cent carbon steel (Fig. 16).

Temperatures below this "minimum" result in incomplete austenitizing. The lowest temperature for the formation of austenite has been found to be between 700 and 750 degrees Cent. (1290 and 1380 degrees Fahr.) indicating that A_{c1} temperature is probably not lowered by rapid induction heating.

Increase in the induction heating temperature above the minimum temperature for full hardening results in several changes in hardness and structure:

1. The hardness is increased slightly at first, followed generally by a decrease (as in Fig. 17). Several factors appear to be operating to effect these changes: (a) changes in the internal stresses;

(b) homogenization of austenite; (c) retained austenite. These factors may exert separate effects or be interrelated to each other. That is, retained austenite is probably related to grain size, homogenization, and internal stresses.

2. The depth of the hardened case increases with increasing temperature. The stresses at the surface can be tensile or compressive depending upon the depth of hardening; and if tensile the hardness will be lower than if compressive (39). Therefore, the hard-

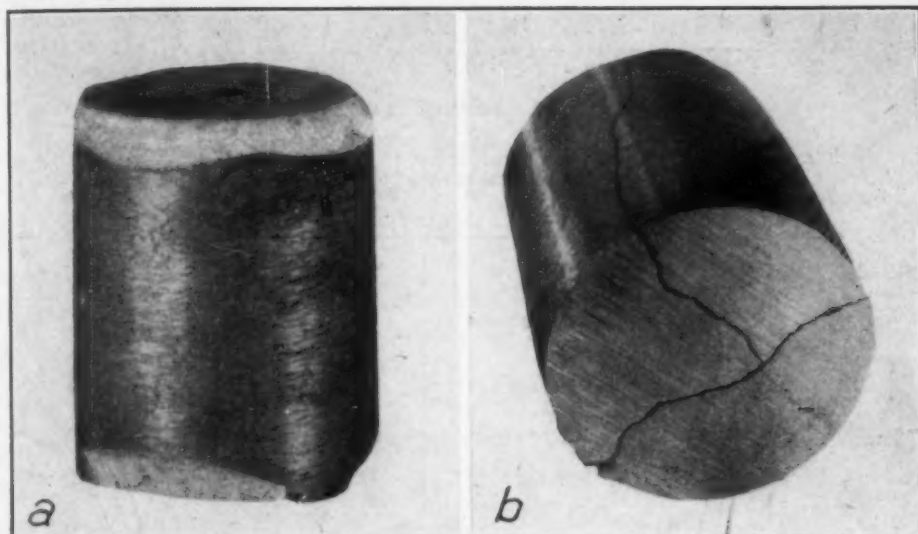


Fig. 31—Fractures Which Occurred During Induction Hardening; $\times 1.5$.
Fig. 31a—Spalling in a sample of Steel D heated to 925 degrees Cent. (1695 degrees Fahr.). Fig. 31b—Cracking in a sample of Steel E heated to about 1300 degrees Cent. (2370 degrees Fahr.).

ness should eventually decrease as the depth of hardening increases since the prerequisite conditions for compressive stresses are a martensitic case enveloping an unhardened core.

3. The austenite becomes increasingly homogeneous as the induction hardening temperature is increased. In a hypoeutectoid steel, higher heating temperatures result in the elimination of "free ferrite" areas, which lowers the average carbon composition of the martensitic areas and thus causes a reduction in the hardness. Higher temperatures also effect elimination of carbon segregation in hyper-eutectoid steels but not necessarily with increase in hardness since the per cent untransformed austenite increases with carbon content.

4. The austenite grain size of induction heated steels has never been thoroughly studied; however, it seems logical to expect a general increase in grain size with temperature for a constant rate of heating. The results in Fig. 30 should be of interest. The induction

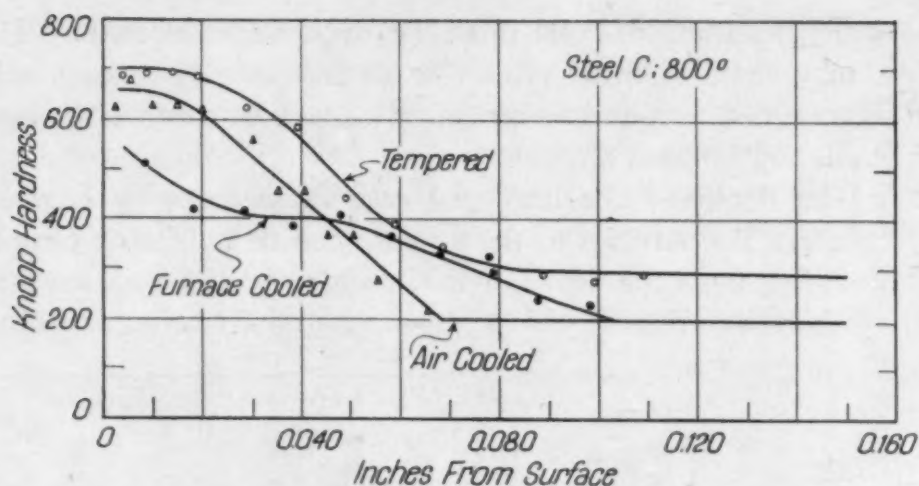


Fig. 32—Effect of Prior Structure on the Hardness Penetration for Steel C. All samples were induction heated to 800 degrees Cent. (1470 degrees Fahr.).

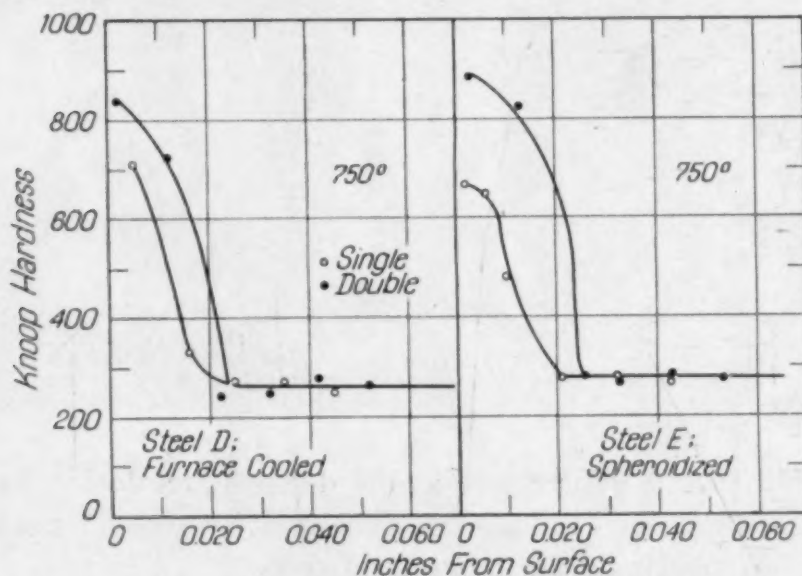


Fig. 33—Effect of Double Hardening Treatment on the Hardness Penetration of Steels D and E. The samples were induction heated to 750 degrees Cent. (1380 degrees Fahr.).

heated sample has a decidedly smaller austenite grain size when heated to the same temperature as the furnace-heated sample (i. e., not considering any time effect).

5. Cracking and spalling tendencies increase as the induction heating temperature is raised. In particular, this was observed to be true for the high carbon steels. The examples in Fig. 31 illustrate spalling (a) and cracking (b). The hypoeutectoid steels which are generally used in commercial practice for induction hardening applications were found to be free from cracking and spalling at the temperatures studied.

Effect of Prior Structure—A sorbitic structure is the ideal prior structure for the induction hardening of medium carbon steels (1), (13). The results in Fig. 32 show a sorbitic structure to be best of the three structures tested. Higher hardness and greater depth of hardening result from the even distribution of carbide and ferrite in a tempered steel. The improvement resulting from even distribution of carbide and ferrite is quite evident in Fig. 23 where the microstructures of the samples heated to 800 degrees Cent. (1470 de-



Fig. 34—Effect of Carbon Content Upon Knoop Hardness of Hardened Samples. Curve A—Samples were heated to about 50 degrees Cent. (90 degrees Fahr.) above upper critical temperature, and water-quenched. Curve B—The furnace-hardened samples (a) were first given a low temperature transformation treatment (LTT treatment) in liquid nitrogen, and then tempered at 100 degrees Cent. (210 degrees Fahr.) for 2 hours. Curve C—Maximum hardness value obtained for the induction hardened steels.

grees Fahr.) are compared. The effect of prior structure is less at high heating temperatures. It follows, that the prior structure would be of utmost importance in the production of an extremely thin hardened layer.

It is not always feasible to furnace treat samples to produce the desired prior structure. In that case a double induction hardening treatment will yield satisfactory results. This is illustrated in Fig. 33 for two steels given a double treatment at 750 degrees Cent. (1380 degrees Fahr.). The double treatment could be varied in many ways, for example, the first treatment involving a high temperature hardening, and followed by a second low temperature hardening.

There is an additional practical significance of double treatments. Frequently, in determining the heating time to harden a given part, several treatments are repeated on the same sample; since each treatment will alter the structure they likewise will alter the hardening characteristics of the steel. The heating data obtained on samples given multiple treatments will not be representative of the basic material. The correct procedure would be to heat a number of parts for various time periods, instead of multiple treatments on the same sample.

Effect of Carbon Content—From an induction hardening viewpoint, increasing the carbon content of a steel is definitely advantageous because a higher hardness is obtained, the hardening temperature is lower, and the influence of prior structure is less important.

The curves in Fig. 34 give us a comparison of the hardened steels by various treatments. In Curve C the *maximum* hardness values obtained on the induction hardened samples are plotted against the carbon content of the steels. In addition, curves for (A) the furnace-hardened samples, and for (B) the furnace-hardened samples given a low temperature transformation (L.T.T.) treatment followed by a tempering anneal at 100 degrees Cent. (210 degrees Fahr.). The maximum hardness obtained for the induction hardened samples was found to be higher than the values obtained on the furnace-hardened samples; but not always higher than the furnace-hardened samples given the L.T.T. treatment followed by tempering.

The higher hardness of induction hardened samples has been attributed to several factors: internal stresses, less retained austenite, finer martensite and incomplete carbon diffusion. These factors require additional discussion and for convenience will be regrouped into two subjects (A) internal stresses and (B) nonhomogeneous austenite.

A. Vaughn, Farlow and Meyer (2) demonstrated the presence of high stresses in induction surface-hardened steels and related the higher hardness to this condition. However, they did not differentiate between the effect of tensile and compressive stresses. Earlier work by Fink and Van Horn (38) showed that internal tensile stresses decrease the hardness of metals.

Crampton (39) reasoned from this evidence of Fink and Van Horn that if internal tensile stresses decreased the hardness then internal compressive stresses should increase the hardness. Likewise,

he assumed that relief of the internal tensile stresses should effect an increase in hardness compared to a decrease when compressive stresses were relieved. Furthermore, he proved this to be true for a drawn brass tube with internal tensile stresses at the outside surface and internal compressive stresses at the inside surface.⁵

Crampton's results have a direct application to our present problem of higher hardness in induction hardened samples. Surface-hardened samples have high compressive stresses in the hardened case due to the difference in specific volume of the martensite in the case and the unhardened metal in the core. Furnace-hardened samples which are generally hardened to a much greater depth (at least for hardness determinations) will have either tensile stresses or low compressive stresses at the surface.⁶ Accordingly, the induction hardened steel should have a higher hardness due to the high compressive stresses. However, if the induction hardened steel was hardened all the way through a hardness difference should not exist. Likewise, a furnace-treated sample hardened only at the surface should have higher hardness than a sample completely hardened.

The results reported by Bain verify our assumption (Fig. 90, page 156 of reference 16). By changing the austenite grain size he was able to vary the depth of hardening in a 1-inch diameter bar. The shallow hardened samples have a higher maximum hardness than the completely hardened bars. The presence of more retained austenite in the coarse-grained samples could account for these results, except that the lowest hardness was obtained in the sample with an intermediate grain size—probably the sample with the highest internal tensile stresses.

Reduction of the internal compressive stresses by tempering (also by cutting the sample longitudinally) results in a decrease in hardness. This was observed by Vaughn, Farlow and Meyer (2) and further checked by tempering of many of the induction samples in this present study. A drop of several points on the Rockwell "C" scale results from tempering at 100 degrees Cent. (210 degrees Fahr.). Since the high compressive stresses in the surface layer

⁵The different effect of tensile and compressive stresses on hardness can be easily demonstrated by measuring the hardness on the concave and convex surface of a metal strip which has been bent elastically. The side of the strip under tension (the convex surface) will have a lower hardness than the side under compression.

⁶High tensile stresses have been determined at the surface of furnace hardened samples (35). Relief of these stresses by a low temperature anneal should result in an increase in hardness. The increase in hardness frequently observed when quenched steels are tempered may thus be due to relief of internal tensile stresses and not to precipitation hardening as suggested by Fletcher and Cohen (27).

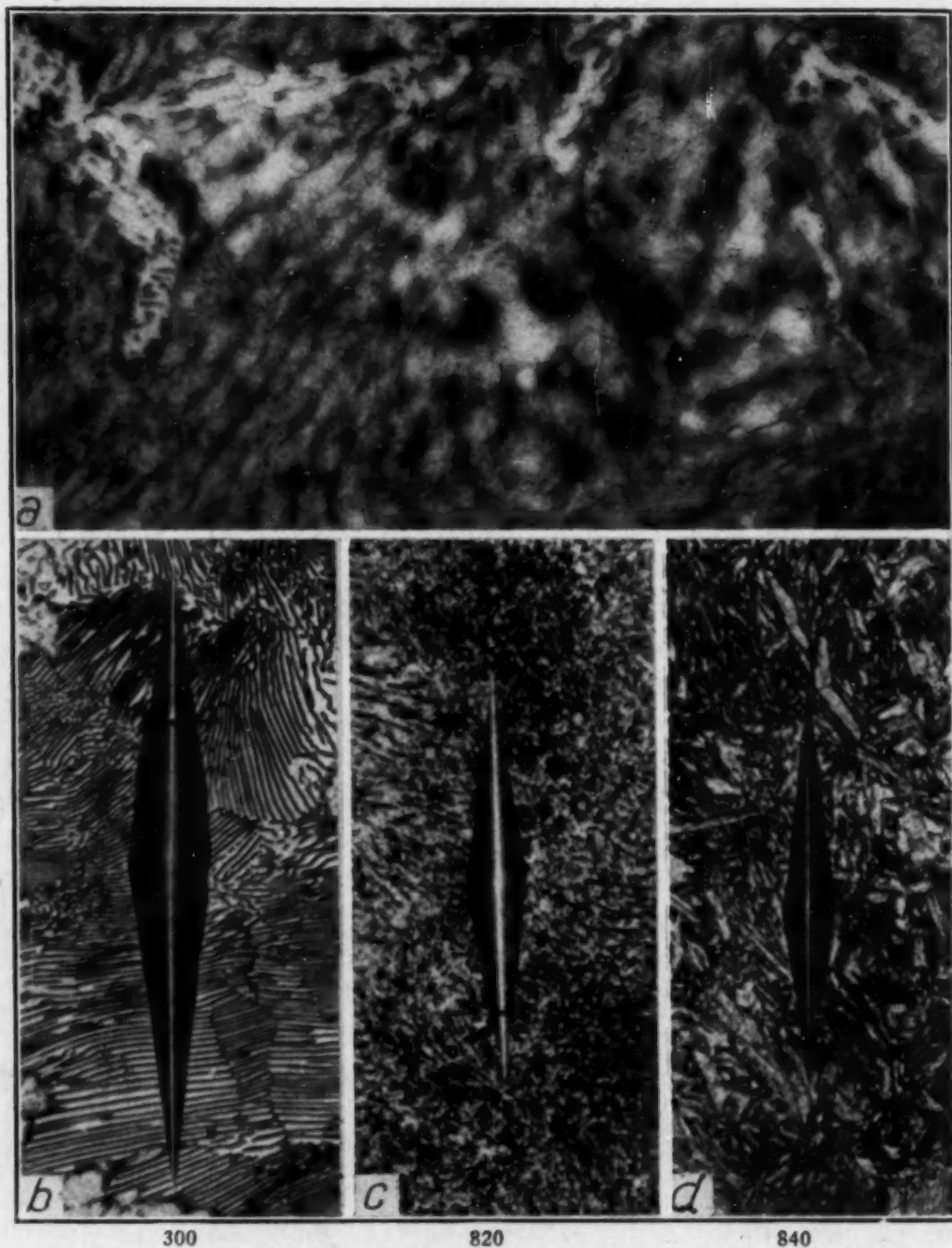


Fig. 35—Hardness Comparison of Pearlite, Pearlite Ghosts, and Martensite in an Eutectoid Steel; $\times 1000$. Fig. 35a—Microstructural appearance of pearlite ghosts (cored martensite). Fig. 35b—Pearlite. Fig. 35c—Pearlite ghosts. Fig. 35d—Martensite.

also improve the fatigue properties,⁷ it is not always desirable to temper induction hardened parts. Cracking of the untempered in-

⁷As fatigue failures are tensile failures, it is possible to partially neutralize external tensile stresses by placing the surface in compression and thus improve the fatigue properties. This can be accomplished by any of a number of surface hardening methods (shot blasting, nitriding, induction hardening). Horger and his associates have effected improvements of over 200 per cent by flame-hardening methods (36), (37).



Fig. 36—Electron Micrograph of Induction Hardened Sample of Steel D; $\times 9000$.

duction hardened parts is not likely to occur due to the uniform hardened layer and the high compressive stresses.

B. Incomplete carbon diffusion during induction heating is also a contributing factor toward the higher hardness of induction hardened steels (13). Examination of photomicrographs of induction hardened steels (for example, Figs. 20 and 27) reveals undissolved ferrite or carbide (for the samples heated to a low tempera-

ture) and a fine martensite (1). The per cent of retained austenite is likely to be less in a fine martensite than in a coarse martensite (as in Fig. 29). In general, furnace-hardened samples have a coarser martensite, due probably to its formation from a homogeneous austenite, and thus the hardness will be lower than for a fine martensite induction sample. The difference is due to retained austenite and not fine martensite, per se. The basic factor, however, is the incomplete carbon diffusion during heating. This results in nonhomogeneous austenite which in turn is responsible for a fine martensite with less retained austenite.

Retained austenite has a greater effect in high carbon steels since they have inherently more untransformed austenite. This is evident from the increase in hardness which results when a furnace-hardened steel is given a low temperature transformation treatment (Fig. 36).

Incomplete carbon diffusion is responsible for the interesting case in which a sample containing free ferrite is harder (at least, the Knoop hardness is higher) than one containing all martensite. This unusual condition results from the higher carbon content of the martensitic areas in the incompletely transformed sample and has been discussed previously in regard to the results obtained for Steels B and C.

To summarize, compressive stresses, less retained austenite, and carbon segregation (incomplete carbon diffusion) tend to increase the hardness of a quenched steel. Induction hardening favors each of these factors, although the influence of each factor is not the same for all steels. Internal stresses are likely to be equally effective for all carbon contents. The high carbon steels will be most affected by retained austenite and the hypoeutectoid steels will be influenced most by the carbon segregation effect. Furnace-hardened samples may be treated to have high compressive stresses, less retained austenite, etc., in which case they too will be harder.

Pearlite "Ghosts"—Austenite when it first forms is not homogeneous but contains undissolved carbide and carbon concentration gradients. Martensite formed from such a nonhomogeneous austenite will frequently resemble pearlite in appearance (i. e., if there were pearlite in the original structure), but have the hardness of martensite. This structural constituent has been called pearlite "ghosts", or pseudomorphs of pearlite (10), (14), (15), and might also be called *cored martensite* since the lamellae appearance is an etching effect due to carbon concentration gradients in the martensite. The

microscopic appearance of this structure is shown in Fig. 35a. A comparison of the Knoop hardness of pearlite, pearlite "ghosts", and martensite is made in Fig. 35. The cored martensite possesses a hardness very close to that of the homogeneous martensite in this steel. However, it is likely that the cored martensite structure in a hypoeutectoid steel will have a higher hardness than the homogeneous martensite which is of lower carbon content.

An electron micrograph of a pearlite ghost area is given in Fig. 36 at a magnification of 9000. The most interesting feature of this picture is not the cored martensite but the large undissolved carbide and the pearlite surrounding it. Note that the pearlite carbide is nucleated by the large cementite particle. Apparently the carbide lamellae traces in the pearlite ghost area were previously nucleated by the same undissolved carbide since they are definitely related to the new pearlite lamellae. The heterogeneity of the cored martensite is quite clear in this micrograph.

SUMMARY AND CONCLUSIONS

The results obtained on over 50 samples indicate that the basic metallurgical principles of induction hardening are no different than those for conventional hardening methods. The results obtained are, to be sure, much different but nevertheless, the reactions are still the same. Austenite forms upon heating above the A_{c1} temperature and martensite is the transformation product when quenched.

The pearlite starts to transform during induction heating to austenite at a temperature between 700 and 750 degrees Cent. (1290 and 1380 degrees Fahr.). As the heating temperature is increased, the austenite areas grow by solution of the undissolved carbide or free ferrite. A minimum temperature is reached at which full hardness is obtained when quenched. This "minimum" temperature is greatly dependent upon the distribution of cementite in the ferrite matrix, varying with carbon content and prior structure. For furnace-cooled structures, the "minimum" temperature for full hardening ranged from 750 degrees Cent. (1380 degrees Fahr.) for the 1.1 per cent carbon steel to over 1200 degrees Cent. (2190 degrees Fahr.) for the 0.17 per cent carbon steel.

Only about 90 per cent martensite is required to obtain essentially full hardness in an induction heated sample. Thus, the structure of samples heated to the "minimum" will be 90-95 per cent mar-

tensite (after quenching) and the balance undissolved ferrite or carbide. The complete elimination of ferrite is probably desirable for applications involving fatigue since cracks will form in this weak constituent at a much lower stress than the surrounding martensite.

Induction heating to high temperatures above the "minimum" will result in complete transformation to austenite and elimination of carbon concentration gradients. For extreme temperatures, the hardness of all steels decreases due to homogenization and deeper penetration of the hardened layer. At intermediate temperatures (above the minimum), the hardness may be at a maximum due to optimum internal stress and microstructural conditions.

The high compressive stresses in the hardened layer, less retained austenite, and carbon segregation effects all contribute toward a slightly higher hardness in an induction hardened steel compared to a completely furnace-hardened sample of the same steel. In general, as the induction hardening temperature is increased, these effects are eliminated due to greater depth of hardening and homogenization, and the hardness decreases. The drop in hardness is not serious so that a wide temperature range exists above the "minimum" hardening temperature where satisfactory properties are obtained (for fast heating rates the time may be critical). For applications where fatigue properties are important, it may be necessary to limit the upper heating temperature in order to obtain optimum internal compressive stresses in the hardened case.

Prior structure is of major importance in hypoeutectoid steels in which a shallow depth is desired. A sorbitic structure has been found to transform to austenite at lower temperatures and at a faster rate. For applications where furnace equipment is not available for correct prior heat treatment, it is possible to obtain equally satisfactory results by a double induction hardening treatment. The purpose of the first treatment is to obtain a satisfactory carbon distribution, generally by heating to a high temperature and quenching. The second treatment is to produce the desired hardened layer at the surface.

Increasing the carbon content of an induction hardened steel is desired since it facilitates formation of austenite, increases the maximum hardness, and decreases the influence of the prior structure. Normalized steels above approximately 0.45 per cent carbon respond satisfactorily to induction hardening methods.

Tempering of induction hardened samples at low temperatures

relieves, at least in part, the high compressive stresses in the hardened case. Due to the beneficial improvements resulting from internal compressive stresses (improved hardness and higher endurance limit), tempering is not advised where wear resistance and fatigue are of major importance. Cracking or spalling of induction hardened samples is not likely to occur due to the uniform hardened layer and the high compressive stresses.

To conclude, it has been found that:

(a) The metallurgical principles, which have been determined by conventional heating methods, apply likewise to induction hardening methods. The properties and structures are different due to (a) a surface layer of martensite, and (b) the lack of homogenization in the prior austenite.

(b) The heating temperature is the most important variable in induction hardening. To obtain satisfactory properties, it is necessary to heat to a high temperature where carbon diffusion is sufficiently rapid. For a 0.45 per cent carbon steel, a temperature of approximately 850 degrees Cent. (1560 degrees Fahr.) is usually satisfactory.

(c) Extreme heating temperatures [greater than 1000 degrees Cent. (1830 degrees Fahr.)] should be avoided. The increased depth of hardening and homogenization, which result generally, effect a decrease in hardness and fatigue properties. High temperature will also alter the grain size, but no information was obtained on this property other than that one induction heated sample had a much finer grain size than a sample of the same steel heated in a furnace to the same temperature.

(d) Prior microstructure is important if rapid austenitizing is desired at a low temperature. A sorbitic structure was found to transform to austenite at a lower temperature than any of the other structures studied.

(e) The higher carbon steels are desired for induction hardening applications since they have lower austenitizing temperatures, higher hardness, and do not require any special prior structure.

(f) Tempering of induction hardened parts is not recommended for parts in which maximum wear resistance or fatigue properties are desired. A low temperature anneal reduces internal compressive stresses which contribute towards higher hardness and endurance limits.

ACKNOWLEDGMENT

The authors are indebted to many persons for assisting in the experimental work and in the preparation of this paper.

We wish to express our appreciation to Mrs. Catharine Riisness, Dr. R. Smoluchowski, Mr. E. R. Parker, Mr. W. E. Ruder, Mr. Lyall Zickrick, and Mrs. C. B. Brodie for assistance and helpful discussions during the progress of the investigation and in the writing of the paper.

The members of the Industrial Heating and Welding Engineering Department, General Electric Company, in particular Messrs. J. P. Jordan, R. D. Frazier, and R. A. Gehr were most helpful in the induction hardening of the samples.

Our thanks also to Messrs. Roy Adams, Harold Vail and E. A. Smith for help in the preparation and heat treatment of the samples.

We are indebted to Miss Margaret Murphy for preparing the electron micrograph in Fig. 36.

References

1. M. A. Tran and H. B. Osborn, Jr., "Inherent Characteristics of Induction Hardening," *Surface Treatment of Metals*, published by American Society for Metals, 1941, p. 209.
2. F. F. Vaughn, V. R. Farlow and E. R. Meyer, "Metallurgical Control of Induction Hardening," *TRANSACTIONS, American Society for Metals*, Vol. 30, 1942, p. 516.
3. V. W. Sherman, "Thin Case Hardening with Radio-Frequency Energy," *Aero. Eng. Rev.*, Vol. 2, 1943.
4. R. LeGrand, "New Uses of Induction Heating," *American Machinist*, Oct. 1, 1942, p. 1079; Oct. 15, 1942, p. 1158.
5. H. E. Somes, "The Development of High Speed Induction Heating for the Hardening of Internal Diameters," *Transactions, Electrochemical Society*, Vol. 79, 1941, p. 45.
6. F. F. Vaughn, "Differential Hardening with High Frequency Current," *METAL PROGRESS, American Society for Metals*, Vol. 45, March 1944, p. 493.
7. F. W. Curtis, "Heating Gears for Hardening by High-Frequency Induction," *Machinery*, July, 1943.
8. J. P. Jordan, "The Theory and Practice of Industrial Electronic Heating," *General Electric Review*, December 1943.
9. G. Babat and M. Losinsky, "Heat Treatment of Steel by High-Frequency Currents," *Journal, Institute of Electrical Engineers*, Vol. 86, 1940, p. 161.
10. O. W. Ellis, "Pseudomorphs of Pearlite in Quenched Steel," *TRANSACTIONS, American Society for Metals*, Vol. 32, 1944, p. 270.
11. H. B. Osborn Jr., Discussion to Reference 10, p. 284.
12. H. B. Osborn, Jr., "Surface Hardening by Induction," *Transactions, Electrochemical Society*, Vol. 79, 1941, p. 215.
13. H. W. McQuaid, Discussion to Reference 1, p. 233.
14. G. A. Roberts and R. F. Mehl, "The Mechanism and the Rate of Formation of Austenite from Ferrite-Cementite Aggregates," *TRANSACTIONS, American Society for Metals*, Vol. 31, 1943, p. 613.

15. M. Baeyertz, "Effect of Initial Structure on Austenite Grain Formation and Coarsening," *TRANSACTIONS, American Society for Metals*, Vol. 30, 1942, p. 458.
16. Edgar C. Bain, "The Alloying Elements in Steel," published by American Society for Metals, 1939, p. 100-113.
17. R. H. Lauderale and O. E. Harder, "Study of Carbide Solution in Hypoeutectoid Plain Carbon and Low Alloy Commercial Steels," *TRANSACTIONS, American Society for Metals*, Vol. 27, 1939, p. 581.
18. R. F. Mehl, "The Physics of Hardenability," *Hardenability of Alloy Steels*, American Society for Metals, 1939, p. 1.
19. H. Carpenter and J. M. Robertson, *Metals*, Oxford University Press, 1939, Vol. II, 879-891.
20. A. B. Greninger and A. R. Troiano, "Kinetics of the Austenite to Martensite Transformation in Steel," *TRANSACTIONS, American Society for Metals*, Vol. 28, 1940, p. 537.
21. A. B. Greninger, "The Martensite Thermal Arrest in Iron-Carbon Alloys and Plain Carbon Steels," *TRANSACTIONS, American Society for Metals*, Vol. 30, 1942, p. 1.
22. E. R. Saunders and J. F. Kahles, "A Study of Martensitic Formation by a Photometric Method," *TRANSACTIONS, American Society for Metals*, Vol. 30, 1942, p. 1139.
23. M. Cohen, Discussion to Reference 22, p. 1157.
24. P. Payson and C. H. Savage, "Martensite Reactions in Alloy Steels," *TRANSACTIONS, American Society for Metals*, Vol. 33, 1944, p. 261.
25. H. A. Chiswick and A. B. Greninger, "Influence of Nickel, Molybdenum, Cobalt and Silicon on the Kinetics and Ar¹ Temperatures of the Austenite to Martensite Transformation in Steels," *TRANSACTIONS, American Society for Metals*, Vol. 32, 1944, p. 483.
26. J. H. Mathews, "Austenite and Austenitic Steels," *Transactions, American Institute of Mining and Metallurgical Engineers*, Vol. 71, 1925, p. 568.
27. S. G. Fletcher and M. Cohen, "The Effect of Carbon on the Tempering of Steel," *TRANSACTIONS, American Society for Metals*, Vol. 32, 1944, p. 333.
28. F. S. Gardner, M. Cohen and D. P. Antia, "Quantitative Determination of Retained Austenite by X-Rays," *Transactions, American Institute of Mining and Metallurgical Engineers*, Vol. 154, 1943, p. 306.
29. G. A. Roberts and R. F. Mehl, "Effect of Inhomogeneity in Austenite on the Rate of the Austenite-Pearlite Reaction in Plain Carbon Steels," *Transactions, American Institute of Mining and Metallurgical Engineers*, Vol. 154, 1943, p. 318.
30. G. Freedman, Discussion to Reference 28, p. 316.
31. J. L. Burns, T. L. Moore and R. S. Archer, "Quantitative Hardenability," *TRANSACTIONS, American Society for Metals*, Vol. 26, 1938, p. 1.
32. D. P. Antia, S. G. Fletcher and M. Cohen, "Structural Changes During the Tempering of High Carbon Steel," *TRANSACTIONS, American Society for Metals*, Vol. 32, 1944, p. 290.
33. D. F. Lang, "Photoelectric Recorder," *General Electric Review*, Vol. 46, November 1943, p. 623.
34. Constance B. Brodie, "The Microhardness Tester as a Metallurgical Tool," *TRANSACTIONS, American Society for Metals*, Vol. 33, 1944, p. 126.
35. O. V. Greene, "Estimation of Internal Stress in Quenched Hollow Cylinders of Carbon Tool Steel," *TRANSACTIONS, American Society for Steel Treathers*, Vol. 18, 1930, p. 369.
36. O. J. Horger and T. V. Buckwalter, "Fatigue Strength Improved by Flame Treatment," *Iron Age*, Vol. 148, Dec. 18, 1941, p. 47.
37. O. J. Horger and H. R. Neifert, "Effect of Surface Condition on Fatigue Properties," *Surface Treatment of Metals*, published by American Society for Metals, 1941, p. 279.

38. W. Fink and K. Van Horn, "Lattice Distortion as a Factor in the Hardening of Metals," *Journal, Institute of Metals*, Vol. 44, 1930, p. 241.
39. D. K. Crampton, "Some Effects of Internal Stress on Properties of Drawn Brass Tubes," *Transactions, American Institute of Mining and Metallurgical Engineers*, Vol. 104, 1933, p. 209.

DISCUSSION

Written Discussion: By Arthur E. Focke, research metallurgist, Diamond Chain and Manufacturing Co., Indianapolis.

This very instructive paper contains much information which is valuable to those of us who are attempting to apply induction hardening commercially.

However, the writer feels that some of the authors' conclusions must be accepted with caution. For example, while in many cases the authors' conclusion, that tempering is not only unnecessary but is actually undesirable if the induction hardened zone is to resist wear or fatigue, cannot be denied, it has been our experience that if the parts have thin sections or are irregular in outline so that the heated zone is nonuniform, tempering is essential particularly if the steel has high hardenability.

Similarly the authors' suggestion of a double induction treatment to provide the most uniformly martensitic surface without the necessity of prior furnace treatment to produce an initial sorbitic structure is valuable, but it has been our experience that thin or irregularly shaped parts cannot always be reheated by induction without cracking, and it is our practice to temper our parts at about 1000 degrees Fahr. (540 degrees Cent.) before rehardening whenever such rehardening may be required.

Also the writer encountered difficulty in attempting to compare the authors' results with the data which we have obtained on other types of units. It seemed necessary to make the comparison on the basis of time to reach various temperatures, but the individual times are not recorded in the data of the paper except in two cases: (1) for a sample heated to 1380 degrees Fahr. (750 degrees Cent.) for which the time was reported as 3.1 seconds (page 379), and (2) for a sample heated to 2190 degrees Fahr. (1200 degrees Cent.) in 15 seconds (page 368), but if the heating rate of 500 to 540 degrees Fahr. up to the Curie point and 90 degrees Fahr. above that temperature, which the authors report on page 356 is used, and if 1410 degrees Fahr. is assumed as the Curie point, these times should have been:

$$\frac{1380-70}{500} = 2.6 \text{ seconds and } \frac{1410-70}{500} + \frac{2190-1410}{90} = \frac{1340}{500} + \frac{780}{90} = 2.7 + 8.6 = 11.3 \text{ seconds respectively.}$$

In addition, in our work we would consider a clearance of $\frac{1}{4}$ inch between the surface of the sample and the coil to be quite loose coupling and we wonder why the authors set up the delay period of 1 second between the end of the heating and the start of the quench. In many of the tests this second must have represented a large part of the time the surface was over the Ac_1 and naturally one wonders how much the data reported would have been altered if the coupling had been closer and if the delay had been omitted.

It is our sincere hope that the authors will continue their work in this field and that they will set up a program to study the physical properties such as resistance to fatigue and impact of test parts treated under the same series of variables studied in this report.

Written Discussion: By Samuel J. Rosenberg, metallurgist, National Bureau of Standards, Washington, D. C.

The pleasure and value of reading this paper are considerably diminished by doubt as to the extent to which decarburization affected the hardness of the surface layers of the steels tested. In view of the manner in which the various specimens were treated prior to induction hardening, the possibility of decarburization to a greater or lesser degree existed in all samples and the authors mention several cases in which such decarburization was found to exist. This condition imposes an uncontrolled variable which, it appears, could readily have been eliminated by the simple expedient of pretreating the samples in slightly oversize sections and then either machining or grinding to size so as to definitely eliminate any decarburized surface layers. This seems so obvious that it is impossible to conceive that the authors did not consider it. Is it possible that they felt that mechanical distortion of the surface layers might have introduced an even greater variable? If so, it surely could have been minimized by careful machining and the resultant distortion would have been relieved still further by the induction heating itself.

As it is, the suspicion that decarburization may be present casts doubt upon the validity of the hardness values secured either at or adjacent to the induction hardened surfaces of all of the samples. Many of the curves presented in the paper show an increase in hardness below the surface. Is it not possible that in many cases this phenomenon is merely the result of partial decarburization?

It has been mentioned that the authors noted decarburization in some of their samples. Such a phenomenon can be readily detected under the microscope if it has progressed to the point where the surface layer is practically pure iron, as is illustrated in the authors' Fig. 1. If decarburization, however, has progressed only slightly, so that the surface layers are somewhat lower in carbon than the base material, and the material has been quenched from above the A_{c3} of the lower carbon surface layers, the resulting martensite will be quite similar in appearance to the martensite of the base material and differentiation under the microscope would be extremely unlikely. Since it has been fairly well established that the hardness of martensite is dependent upon the carbon content, at least up to 0.60 per cent carbon, the lower hardness of the martensitic surface layers of many of the test specimens could easily be due to a deficiency in carbon as related to the base material.

As a case in point, reference may be made to the authors' Figs. 6 and 7. In Fig. 7, which gives the hardness penetration curves for Steel C (0.47 per cent carbon) with an originally annealed structure, it may be observed that the specimens quenched from 850, 975 and 1200 degrees Cent. (1560, 1790 and 2190 degrees Fahr.) all have a somewhat lower hardness at the surface than at some distance below the surface—the surface hardness of all three of these samples is approximately 600 with the Knoop indenter. If the surface of these samples had been only partially decarburized (so that the average carbon

content were, say, 0.30 per cent) the surface layers could reasonably be expected to show a somewhat lower hardness than the underlying layers, provided, of course, that the induction heating penetrated sufficiently to bring the higher carbon subsurface layers to above their A_{c3} . As a matter of interest, reference to Fig. 7 indicates that the maximum hardness obtained in the 0.30 per cent carbon steel slightly below the surface is actually slightly greater than the surface hardness obtained on the 0.47 per cent carbon steel, an indication that the surface layers of the latter steel may actually have contained only about 0.25 or 0.30 per cent carbon.

Incidentally, it is interesting to compare the hardness of these induction hardened steels with that which may be obtained by normal quenching procedure. According to the curve published by Burns, Moore, and Archer⁸ the maximum hardness obtainable in 0.30 and 0.47 per cent carbon steels (presumably by quenching furnace-heated steels) is R_c 56 and 64, respectively. Using the curve shown in the authors' Fig. 4 as a basis of conversion, these Rockwell numbers correspond to Knoop numbers of 640 and 810. It will be noted that these values agree quite closely with the values for maximum hardness of the 0.30 and 0.47 per cent carbon steel as shown in the authors' Figs. 7 and 8, and are considerably higher than the maximum values for the 0.47 per cent carbon steel shown in Figs. 9 and 10. The curves shown in the authors' Fig. 34 appear to indicate an appreciably higher hardness in induction hardened steels as compared with steels hardened in the orthodox fashion. According to their Curve A for "furnace-hardened" steel, a carbon content of 0.47 per cent results in a Knoop hardness of 600. Using their conversion curve given in Fig. 4, this corresponds to R_c 54, which, it will be recognized, is extremely low for fully hardened 0.47 per cent carbon steel. The curve of Burns, Moore, and Archer shows that a steel containing 0.47 per cent carbon should harden to about R_c 63-64. As a matter of interest the writer quenched a $\frac{1}{4}$ -inch section of steel containing 0.49 per cent carbon and secured a hardness of R_c 63. Again using the authors' Fig. 4 for conversion, this corresponds to a Knoop hardness number of 810, which is just about what the authors show in Fig. 34 for induction hardened steel.

The curve giving the conversion of Knoop to Rockwell numbers (shown by the authors in Fig. 4) would be very useful if the indenting load had been given. Unfortunately the Knoop numbers are influenced to a considerable extent by the loads used, particularly with the lower loads, as is shown by Tate⁹ in a paper presented at another session of this convention. He states that "It is evident that an indentation number can have little meaning unless the indenting load in addition to the indenter is specified." The authors overlooked giving the load used in establishing this conversion curve, as well as the loads used in the hardness surveys of the several test specimens, and it is hoped that they will supply these data in their closure. Fictitiously high Knoop numbers may be obtained under very low loads and it is possible that some of the exceptionally high hardness values reported for induction hardened steels may be due to this.

⁸J. L. Burns, T. L. Moore, and R. S. Archer, "Quantitative Hardenability," *TRANSACTIONS, American Society for Metals*, Vol. 26, 1938, p. 1.

⁹Douglas R. Tate, "A Comparison of Microhardness Indentation Tests," *TRANSACTIONS, American Society for Metals*, Vol. 35, 1945, p. 373.

The writer is intrigued by the authors' reasoning that superhardness in the hypoeutectoid steels may be explained by the incomplete solution of ferrite in austenite which then results in martensite of higher hardness than if complete solution had been obtained. This is undoubtedly true on a microscopic scale but is surely wrong on a macroscopic scale since the increased hardness of the higher-carbon martensitic areas would be more than offset by the decreased hardness of the soft ferritic areas. The writer doubts the validity of this hypothesis as an explanation of the lower surface hardness observed in many of the steels and is inclined to believe, as mentioned before, that partial surface decarburization is the cause.

In connection with their theory that incomplete solution of ferrite may be the cause of higher hardness in induction hardened steels, the authors note that the complete elimination of ferrite is probably desirable for applications involving fatigue since cracks will form in the weak ferrite at a much lower stress than in the surrounding martensite. This is undoubtedly true and would indicate that in induction hardening the heating cycle should be timed so as to assure complete solution of ferrite prior to quenching. Induction hardening is also used for parts subjected to wear and the presence of free ferrite at the surface of such parts would be decidedly injurious to the wear resistance. It is definitely better metallurgical practice to treat for a uniform martensitic surface.

The authors also postulate that higher internal stresses may be another cause of the slight increase in hardness of subsurface layers. Micrographs are presented in the authors' Fig. 29 which show retained austenite at a distance from the surface. The writer would appreciate the authors' advice as to how far below the surface such retained austenite was observed. If higher stresses do exist in the subsurface layers should that not be conducive to a more complete transformation of austenite to martensite? Harder and Dowdell¹⁰ showed many years ago that stress favors this transformation. They stated that tension stresses should favor the gamma to alpha transformation while compression stresses should oppose it. Neilsen and Dowdell¹¹ also indicate that tensile stress tends to facilitate the formation of martensite. It may be noted in passing that the authors' statement that compressive stresses tend to increase the hardness of quenched steels whereas tension stresses act in the reverse direction should be considered as tentative until definite evidence is produced as proof. The references cited by the authors in this connection contain no proof of this statement. Vaughn, Farlow and Meyer (reference 2 of the paper) make such a statement but it is only a conjecture; the work of Crampton (reference 39 of the paper) refers to the effect of internal stress on the hardness of cold-drawn brass. His conclusion that in drawn brass internal compressive stresses result in higher hardness than do internal tensile stresses is not necessarily applicable to quenched steel.

This discussion has attempted to emphasize the fact that the various hypotheses offered as an explanation of the higher subsurface hardness as compared with the surface hardness observed in many of the specimens are, per-

¹⁰Oscar E. Harder and Ralph L. Dowdell, "The Decomposition of the Austenitic Structure in Steel—Part VI," *TRANSACTIONS, American Society for Steel Treating*, Vol. 12, 1927, p. 51.

¹¹H. P. Neilsen and R. L. Dowdell, "Effect of Thermal Stresses on Austenite," *TRANSACTIONS, American Society for Metals*, Vol. 22, 1934, p. 810.

haps, unnecessary. The writer believes that positive elimination of any surface decarburization might eliminate this hardness differential. It would be interesting if the authors would, in their closure, include tests to either prove or disprove this belief. The writer also wishes to emphasize the fact that the maximum hardness reported in the various induction hardened steels is no greater, using the authors' conversion curve, than would be expected by orthodox quenching.

Written Discussion: By H. B. Osborn, Jr., research and development engineer, TOCCO Division, The Ohio Crankshaft Co., Cleveland.

At the time we presented our paper before the American Society for Metals in 1941, we expressed the hope that it would stimulate immediate interest and investigation of the factors controlling and results obtainable with induction heating. With the exception of the paper by Vaughn, presented in 1942, and that of Ellis presented in 1944, our challenge had gone unanswered until today. Mr. Martin and Miss Wiley have presented in their paper much data which will enable us to understand many of these factors and results.

The authors have been painstaking and very thorough in attempting to show that the metallurgical reactions which occur during induction heating are not unusual. While they are to be commended for the preparation and presentation of an excellent paper, they have overlooked several important points.

The frequency employed for their tests, namely 530,000 cycles, heats only the surface of the metal to a depth of 0.003 to 0.005 inch by electrical induction. The balance of the cross section is heated by conduction. The power input to the piece was a maximum of 4 KW per square inch at the beginning of the heating cycle, and dropped to less than half this amount at the end. Only by using power inputs per unit of surface area which will permit the surface of a part to reach austenitizing temperature in but a very few seconds, and also perhaps using frequencies which permit heating of greater depths can we establish conditions which permit the study of the behavior of metals inductively heated. That is to say, all metallurgical and physical examinations made by the authors were not limited to that portion of the sample which was heated exclusively, or even primarily, by induction.

We have changed many of our ideas during the past few years, and are now reasonably convinced that the higher hardness of an inductively hardened part is closely associated with internal stresses. Such condition, however, is not limited to surface hardening, and therefore cannot be conclusively explained on the same basis as a furnace-treated specimen hardened only on the surface and which exhibits higher hardness than a sample through hardened. There have been many thousands of armor-piercing shot inductively hardened to hardnesses above that obtainable from the most drastic conventional methods of treatment. In some cases, these parts have shown a tendency to drop slightly in hardness when drawn at moderate temperatures which would not ordinarily affect the structure at such hardness levels. In all such cases we are referring to a through hardened sample on projectiles up to 90 millimeters in diameter.

A further study of parts inductively hardened, both on the surface and through the cross section, will no doubt reveal many interesting facts. However, by control of heating and quenching cycles, the stresses introduced can be either tensile or compressive, or a combination of both.

Authors' Reply

We agree with Mr. Focke's suggestion that tempering may be necessary in samples of irregular shapes. Tempering may not be required for parts in which the hardened zone is uniform in contour; however, until more information is available the best rule is to test the sample in each condition to determine which treatment gives the best results.

The heating rates given in the text are only crude approximations as Mr. Focke found in trying to check some of our test results. There is still a wide spread in the heating rates depending upon the alloy and its microstructure (also the frequency, power input, and coupling); therefore, comparison of results on the basis of heating is unlikely to be significant. For example, the heating periods for two different steels are listed in Table A. (The equipment and procedure used are those described in the paper.) Note that the alloy steel is sluggish in the range 750 to 900 degrees Cent. (1380 to 1650 degrees Fahr.)

Table A
Comparison of Time to Induction Heat the Surface of Two Steels to Various
Temperatures with 530,000-Cycle Current

Material	Heating Time in Seconds					
	Temperature Degrees Cent.					
	700	750	800	850	900	950
Steel D (0.80C)	2.3	3.3	5.8	9.4	11.0	12.1
Normalized						
NE 9255	2.4	5.0	8.1	10.0	11.5	12.7
Normalized						

but that there is only a slight difference in heating time for temperatures above or below this range. Since austenitizing also occurs in the same temperature range during induction heating it is possible that the sluggishness on the part of the NE 9255 steel is due to a lower rate of diffusion of carbon in this steel.

The maximum surface temperature and the total time in the austenitic range offer a better basis for comparison of induction hardening results, except that those particular values are very difficult to measure.

The clearance of $\frac{1}{4}$ inch between the surface of the sample and the coil was much greater than the recommended coupling for commercial operation (about $\frac{1}{8}$ inch); however, the reason for the loose coupling was to enable a thermocouple to be placed on the surface without interfering with the test procedure.

The delay between the end of heating and the start of the quench was estimated to be about 1 second and was not a prearranged time delay. The water quench was automatically turned on when the oscillator was turned off; however, a short interval of time passed before the water actually reached the surface of the sample—estimated to be about 1 second.

The values of the effective penetration of the induced currents given by Dr. Osborn are apparently for room temperature conditions. For temperatures in the austenitic range a much greater depth of penetration is obtained since the resistivity increases and the permeability decreases with temperature (the relation between frequency, resistivity, permeability, and depth is given in Equa-

tion 2). Vologdin¹² gives values for the effective penetration of the induced currents in 1045 steel at 15 degrees Cent. (60 degrees Fahr.) and 850 degrees Cent. (1560 degrees Fahr.) which illustrate the increase in depth of penetration when the steel becomes austenitic. For example, note in Table B that the penetration is about 25 times as deep at 850 degrees Cent. (1560 degrees Fahr.) as at 15 degrees Cent., and for a frequency of 500,000 cycles per second a depth of 0.035 inch is given for a 1045 steel at 850 degrees Cent. (1560 degrees Fahr.). It would seem, therefore, that the portion of the samples heated primarily by induction was much greater than indicated by Dr. Osborn. However, we do not consider it necessary to distinguish between the areas heated primarily by electrical induction and those heated by conduction since induction heating will always involve both types, although to varying degrees. From a metallurgical viewpoint the important variables are temperature and austenitizing time and not method of heating in itself. That is, the atoms in the steel

Table B
Effect of Temperature on the Depth of Penetration of Current for a 1045 Steel
(After Vologdin)

Frequency Cps	Depth in Inches	
	15 Degrees Cent.	850 Degrees Cent.
50	0.12	3.5
1,000	0.03	0.81
10,000	0.008	0.260
100,000	0.003	0.081
500,000	0.0012	0.035
1,000,000	0.0008	0.026

will not differentiate between the method of heating if the time and temperature conditions are the same.

The high hardness in steel samples induction hardened through to the center may not be due to internal stresses but instead to less retained austenite than found in furnace-hardened samples. The austenite formed during induction heating is usually less homogeneous than that formed in a furnace-treated steel. The presence of undissolved carbides in the austenite lowers the Ms temperature and raises the Mf temperature (21, 24); the net effect of this is a steel with less retained austenite and probably also of somewhat higher hardness. This would be particularly true for alloy steels. Dr. Osborn could check this by determining the retained austenite in samples given varying induction and furnace treatments.

Mr. Rosenberg concluded his discussion with the statement that positive elimination of any surface decarburization might eliminate the hardness differential which we observed in numerous samples between the surface and subsurface layer; and suggested that we offer tests to prove or disprove his belief. Additional tests have been made on a commercial 1050 steel and the results indicate that no significant difference in hardness exists between the surface and the subsurface layer of the steel sample after induction hardening. However, the results also show that 5 or more series of readings are probably required

¹²V. Vologdin, "Surface Hardening Through High-Frequency Currents," *Metallurg.*, Vol. 12, No. 12, 1937, p. 9. Translation No. 529 by Henry Bratcher, Altadena, Calif.

in order to obtain representative hardness penetration curves as a single series of readings may show an increase in hardness below the surface.

In this experiment the $\frac{7}{8}$ -inch diameter induction samples were machined from a 1-inch diameter bar after the austenitizing and furnace cooling treatment to eliminate any decarburized layer which may have formed during the heat treatment. This is unquestionably the safest method of preparation of the induction samples and the main reason we did not follow the same procedure in our earlier work is because preliminary treatments in a purified nitrogen atmosphere showed no evidence of decarburization in the test pieces.

The induction hardening equipment and procedures described in the text were followed in hardening the 1050 steel. The microhardness results (500-gram load) for the sample induction heated to 825 degrees Cent. (1515 degrees Fahr.) before quenching are given in Fig. A. The microhardness indentations

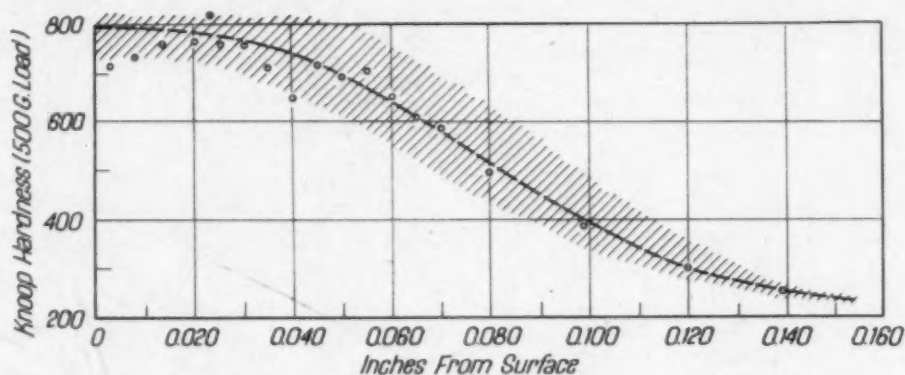


Fig. A—Hardness Penetration Data for a 1050 Steel with an Initial Furnace-Cooled Structure. The sample was induction heated to 825 degrees Cent. before quenching. The full circles indicate the results for a complete series of Knoop measurements; the hatched area gives the spread in hardness values; and the dashed line represents the best curve for all data.

were spaced about 0.005 inch apart up to the transition zone and at about 0.020 inch into the core. The average curve for six series of readings, given by the dashed line in the drawing, shows no increase in hardness below the surface. However, a single series of measurements did show an increase, as indicated by the plotted points in Fig. A. In view of the wide spread of microhardness values in the martensitic zone a variation of values in a single series of less than 100 Knoop units cannot be considered significant. The nonhomogeneous martensitic structure found in induction hardened steels is probably responsible for this wide spread of microhardness values.

Reviewing the curves in Figs. 6 to 17 with this spread in mind we find only a few samples in which the hardness below the surface can be considered to be higher than at the surface and most of those are samples which were definitely decarburized during the pretreatment. Decarburization may be the cause of low surface hardness in one or two other instances where free ferrite did not show at the edge to indicate decarburization.

In Fig. 13 the sample induction heated to 975 degrees Cent. (1790 degrees Fahr.) shows an increase in hardness below the surface. Additional measurements on this sample (Fig. B) show a slightly lower hardness was obtained at the surface; indicating perhaps that the sample was slightly decarburized.

The higher microhardness values in the subsurface layers of the 850-degree Cent. sample in Fig. 8 is the result of chance. This sample has a mixed structure consisting of undissolved ferrite and martensite of about eutectoid composition near the surface (Fig. 20-C). Whenever the indentations fall on a martensitic area a high value will be obtained and, conversely, a low value will be measured when the impression is made on ferrite. For example, note in Fig. B that a Knoop hardness of 840 was obtained at a depth of 0.035 inch in contrast to much lower values nearer the surface. It is obvious that the high hardness value is misleading in view of the considerable amount of ferrite in the sample. A Rockwell measurement on such a sample would give a more representative value of hardness but even the Rockwell hardness does not indicate the presence of small amounts of ferrite (14).

This discussion has emphasized the limitations of the Tukon hardness

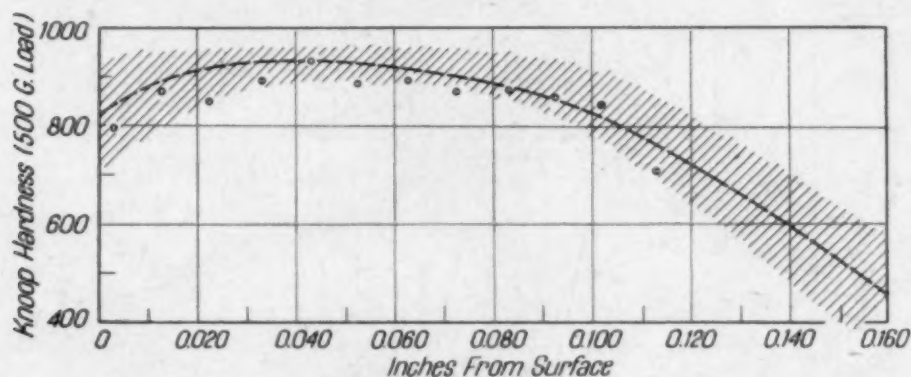


Fig. B—Additional Hardness Data for the Sample of Steel D Induction Hardened from 975 Degrees Cent. The full circles are the values given in Fig. 13 for this sample. The spread in the Knoop hardness is indicated by the hatched area, and the average curve for all data by the dashed line.

tester for measuring the hardness of mixed structures. However, it should also be pointed out that in general it is a very useful tool to measure the hardness of case hardened samples provided a sufficient number of readings are taken to obtain a representative curve and the microstructure is examined to insure proper interpretation of the data.

Mr. Rosenberg has observed that the hardness of Steel C (0.47 carbon, 0.19 manganese, 0.13 silicon) in the furnace hardened condition is much lower than would be expected from the work of Burns, Moore, and Archer, and further that the maximum hardness obtained in the induction hardened samples was no greater than would be expected by orthodox quenching. In other words, is the hardness of induction hardened samples higher than that obtained by furnace hardening of the same steel? Previous investigators have shown that the maximum hardness obtained by induction methods is several points Rockwell "C" higher than obtained by conventional hardening methods (1, 2). Our results also show a difference, although the actual values are lower than expected, at least, for the 0.47 carbon steel.

Additional experimentation on Steel C has shown it to be quite different in hardening characteristics from a commercial 1050 steel. In Table C the two steels are compared. There is a surprising difference in the maximum hardness obtained in these two steels of identical carbon analysis (the analyses were

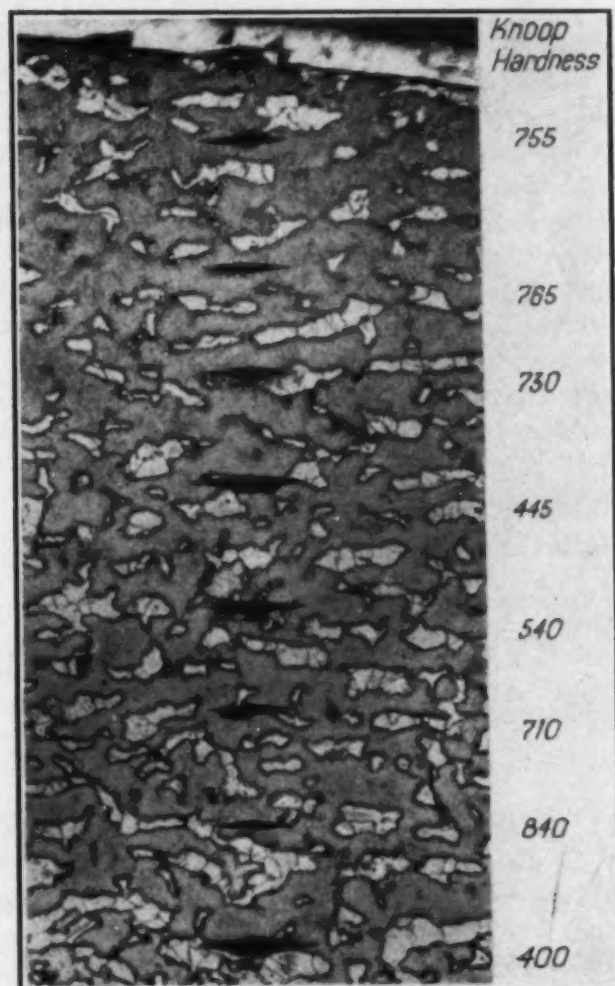


Fig. C—Variation of Knoop Hardness in an Induction Heated Sample of Steel C Containing Undissolved Ferrite and Martensite. The sample was heated to 850 degrees Cent. before quenching. The hardness measurements were made at 0.005 spacings and with a 500-gram load; $\times 90$.

checked). In particular note that the maximum hardness by induction hardening is higher than the hardness obtained by furnace treatment of small samples.

A possible explanation of the difference in the hardening characteristics of the two steels is that the lower manganese content of the laboratory prepared steel lowers the hardenability to a degree where the critical cooling rate is higher than the quenching rate obtained in the various hardening operations, in which case the full hardness (as represented by the commercial steel) is not obtained. The Jominy test is not a sensitive indication of hardenability for shallow hardening steels so that we were not able to determine the relative hardenabilities by that method; however, the induction hardening results (Fig. A vs. Fig. 8) indicate that the commercial 1050 steel with higher manganese is deeper hardening.

We would like to point out that while the curve of Burns, Moore, and Archer relating martensitic hardness to carbon content is very useful it should also be recognized that wide deviations occur in practice from the values given

on the curve. Recent work has shown that hardness values 5 or more Rockwell "C" units lower than the ideal values may be expected in the standard Jominy bar.¹³ (That is, the maximum is lower.)

Regarding the higher hardness of the induction hardened steel we would like only to add that the present information points strongly toward high compressive stresses and nonhomogeneous austenite as being the factors responsible for the increase in hardness. Additional investigations will be required to prove the role of each factor.

In view of the work by Tate which Mr. Rosenberg discusses, it is important that the indenting load be given when citing Knoop hardness values. In our work a 500-gram load was used for all measurements.

Mr. Rosenberg has suggested that "if higher stresses do exist in the sub-surface layer should that not be conducive to a more complete transformation

Table C
Comparison of the Hardening Characteristics of a Commercial
and a Laboratory 1050 Steel

Steel		Analysis			Rockwell "C" Hardness		
		C	Mn	Si	Jominy Bar	Furnace Hardened	Induction Hardened
Commercial	1050	0.47	0.73	0.11	59	62	65
Laboratory	1050	0.47	0.19	0.13	54	55	59
(Steel C)							

of austenite?" The answer is yes if the stresses are tensile, no if they are compressive. In Fig. 29 the amount of retained austenite was shown to be higher below the surface than at the edge (the micrographs were taken about 0.050 inch from the edge) and internal stresses may very well have been the influencing factor; however, it is difficult to predict what the stress conditions were at the time of transformation since they are profoundly changed as a result of the transformation. It should be pointed out that the core of the samples shown in Fig. 29 was above the critical temperature due to the high surface temperatures and as a result the conditions are different from those obtained during surface hardening as it is generally understood (in the samples heated to 850 degrees Cent. for example).

In closing we would like to thank Messrs. Focke, Osborn, and Rosenberg for discussions which have added to the usefulness of our paper and which will be of great help to us in continuing this work on alloy steels.

¹³J. Welchner, E. S. Rowland and J. E. Ubben, "Effect of Time, Temperature and Prior Structure on the Hardenability of Several Alloy Steels", *TRANSACTIONS, American Society for Metals*, Vol. 32, 1944, 521.

RATES OF TEMPERING IN COBALT STEELS

BY EDWARD A. LORIA

Abstract

The effect of cobalt on the tempering characteristics of carbon-cobalt steels is studied by means of hardness measurements. Changes during the tempering of such steels are shown to be similar in nature to those of a plain carbon steel. The cobalt promotes a small increase in hardness following tempering due to its solid solution hardening of ferrite. One steel shows a very slight secondary hardening, but this behavior is not general.

INTRODUCTION

THE effect of cobalt in steel is of considerable interest. From a practical standpoint, cobalt resists tempering in complicated high speed steels especially at red heat, and thus contributes to the remarkable resistance to softening which these steels exhibit at high temperatures. It would be of interest to learn the effect of cobalt during tempering in the absence of complications from large amounts of tungsten, chromium and other alloying elements which may be used. The present paper presents the results of a study of the effect of cobalt in the tempering of plain carbon-cobalt steels by the interpretation of hardness measurements. The literature does not contain any information on this subject, but the recent papers by Cohen and his associates (1-4)¹ furnish excellent information on the theory of tempering and the methods of investigation. The maximum solubility of cobalt in pure gamma iron is infinite and maximum solubility of cobalt in pure alpha iron is nearly 80 per cent (5). Bain (6) states that the carbide-forming tendency is about that of iron or slightly stronger, and its principal function is to resist softening with elevation in temperature when dissolved in ferrite. Just how much of an increase in hardness is obtained at a particular tempering temperature over that of a plain carbon steel is the primary concern of this paper.

¹The figures appearing in parentheses pertain to the references appended to this paper.

A paper presented before the Twenty-sixth Annual Convention of the Society held in Cleveland, October 16 to 20, 1944. The author, Edward A. Loria, is associated with the Carnegie-Illinois Steel Corp., Pittsburgh. Manuscript received June 14, 1944.

EXPERIMENTAL METHOD

Materials used—The measurements reported here were made on five steels, the analyses of which are given in Table I. For the experimental work, the specimens were disks of $\frac{1}{2}$ -inch diameter and from $\frac{1}{8}$ to $\frac{3}{8}$ -inch thickness. No specimens greater than $\frac{1}{8}$ inch thick were used for steels D and E because of the necessity of obtaining martensite on quenching.

In connection with previous work on carbon-cobalt steels in this laboratory, steels A, B, C, D and E had been prepared from the same heat of steel. After ingot A was poured an addition of cobalt was made to the furnace. Ingot B was then poured. Another addition of cobalt to the furnace was made and ingot C was then poured. This procedure was repeated until ingot E was made. The ingots were forged into bar stock and all surface defects and decarburization were removed by machining.

Table I
Chemical Analyses

Steel	C	Co	Per Cent by Weight				Austenitizing	
			Mn	Si	S	P	Temp. °C.	Temp. °F.
A	0.76	nil	0.42	0.26	0.026	0.026	860	1580
B	0.71	1.95	0.42	0.26	0.026	0.026	860	1580
C	0.71	4.20	0.42	0.29	0.026	0.026	880	1615
D	0.68	7.40	0.43	0.26	0.026	0.026	960	1760
E	0.68	11.20	0.42	0.26	0.026	0.026	960	1760

Heat treatment—Since the principal object of this work was to investigate the effect of tempering, it was essential to austenitize the steels completely prior to quenching. The austenitizing was conducted in a lead bath except for steels D and E. In order to attain the necessary austenitizing temperature, steels D and E were heated in an electric resistance (globar) furnace equipped with an automatic temperature control and a protective atmosphere to prevent decarburization. The quenching medium in all cases was brine. A lead bath was used because of the protection which it affords against decarburization and scaling during austenitizing and tempering.

Tempering temperatures were invariably held to better than ± 3 degrees Cent. by means of a potentiometric control system. The experiments were carried out by tempering specimens for different lengths of time at suitable temperatures and then cooling to room temperature for hardness readings.

Hardness—Rockwell C hardness measurements were made according to standard technique. Throughout the course of this work, at least six hardness readings were taken on each specimen. Thus every plotted point on the hardness-tempering curves represents the average of six or more hardness determinations.

DISCUSSION OF RESULTS

In order to correlate hardness changes with the different stages of tempering, a detailed hardness investigation was made at various tempering temperatures and times.

Fig. 1 shows the effect of tempering temperature on the hardness of the plain carbon steel A. It is evident that softening occurs more rapidly as the tempering temperature is raised, in line with the greater solubility and diffusivity of carbon in ferrite at the higher temperatures. The curves are typical of medium carbon steels.

Figs. 2, 3, 4, 5 and 6 show the hardness-tempering curves for steels B, C, D and E. It is readily seen from these curves that the hardness and strength of these steels fall off smoothly with rise in tempering temperature.

The first set of values obtained for steel D indicated that there may have been retained austenite in the as-quenched specimens because of what appeared to be a stability in hardness in the 275 to 385-degree Cent. (525 to 725-degree Fahr.) temperature range. Since the rate of softening during tempering is dependent upon the initial structure of the steel, the procedure was repeated, using two specimens with the same as-quenched hardness initially, and then immersing one of them in an acetone-dry ice solution to attempt the transformation of any retained austenite which might be present. For check purposes, this experiment was run twice using a temperature of -78 degrees Cent. and a holding time of one-half hour to assure that the specimens reached the bath temperature. The dry ice treatment increased the average as-quenched hardness only $\frac{1}{2}$ point Rockwell C and this is believed to be within the experimental error. The values obtained upon tempering both as-quenched and dry ice treated specimens are shown by different symbols in Fig. 4. The apparent stability in hardness in the 275 to 385-degree Cent. (525 to 725-degree Fahr.) temperature persists and may be due therefore to one of the two possibilities:

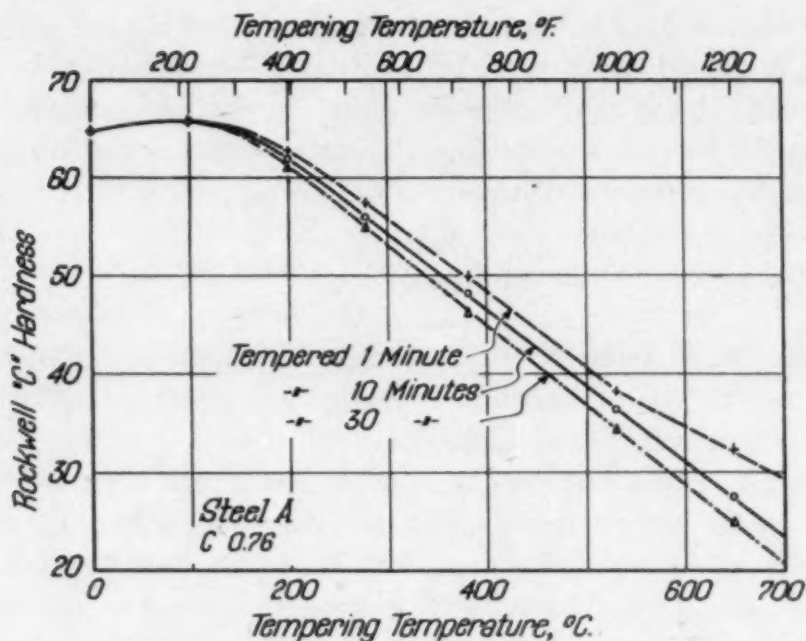


Fig. 1—Hardness-Tempering Curves for Steel A (0.76 Per Cent Carbon).

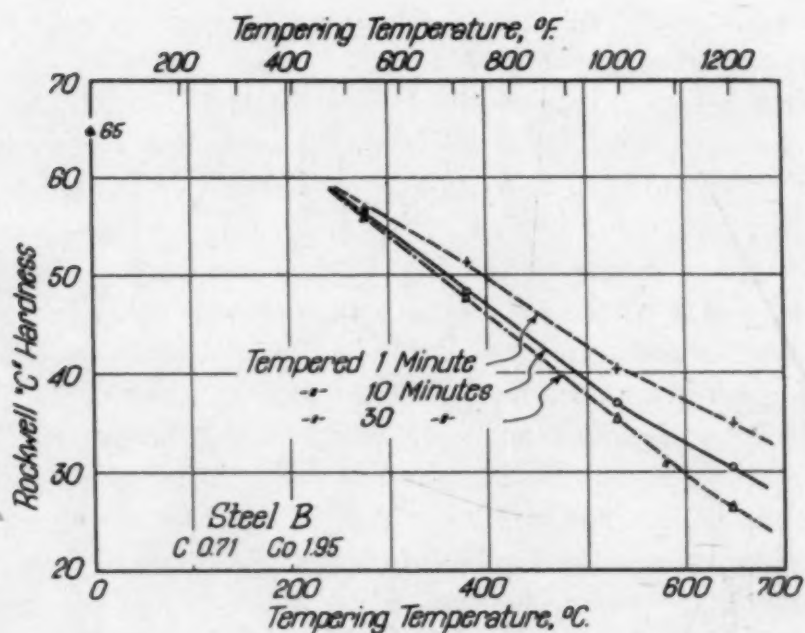


Fig. 2—Hardness-Tempering Curves for Steel B (0.71 Per Cent Carbon, 1.95 Per Cent Cobalt).

- (a) Retained austenite (for cold treatment does not absolutely guarantee its removal).
- (b) A true secondary hardness.

However, speculation would lead to the belief that (b) is more likely

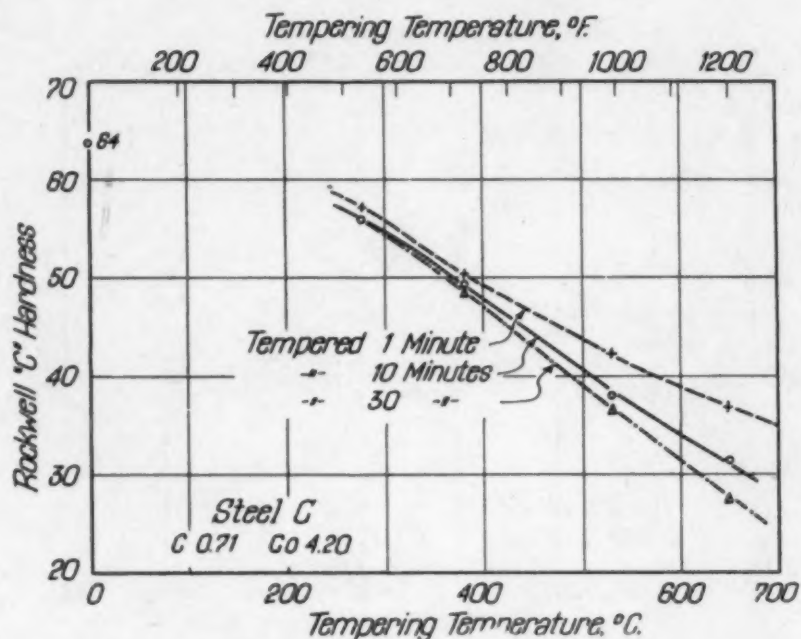


Fig. 3—Hardness-Tempering Curves for Steel C (0.71 Per Cent Carbon, 4.20 Per Cent Cobalt).

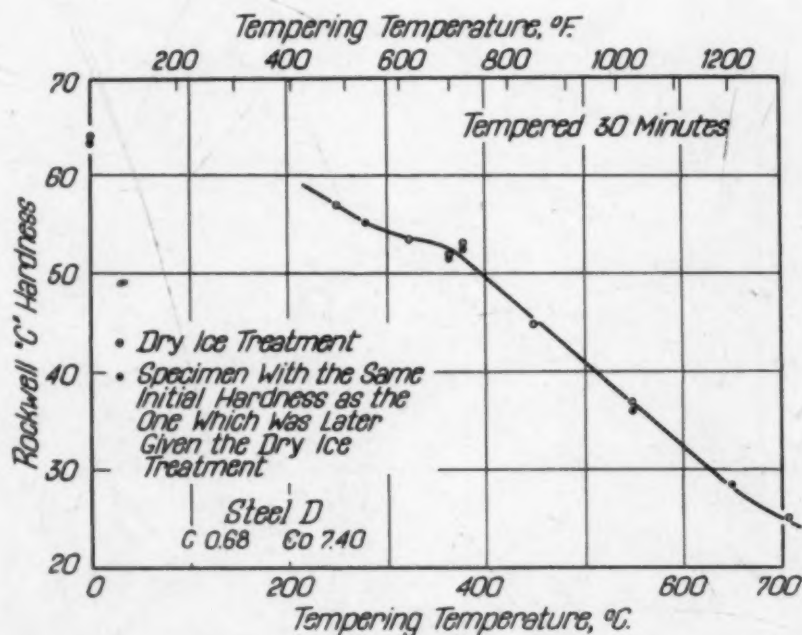


Fig. 4—Hardness-Tempering Curves for Steel D (0.68 Per Cent Carbon, 7.40 Per Cent Cobalt).

than (a) because cobalt raises the $A_{r''}$ point. Hence, steel D should be less likely to show an effect of retained austenite than steels A, B, and C (which showed no effect). To the objection that steel E should show an even greater effect than steel D, if it is a matter of

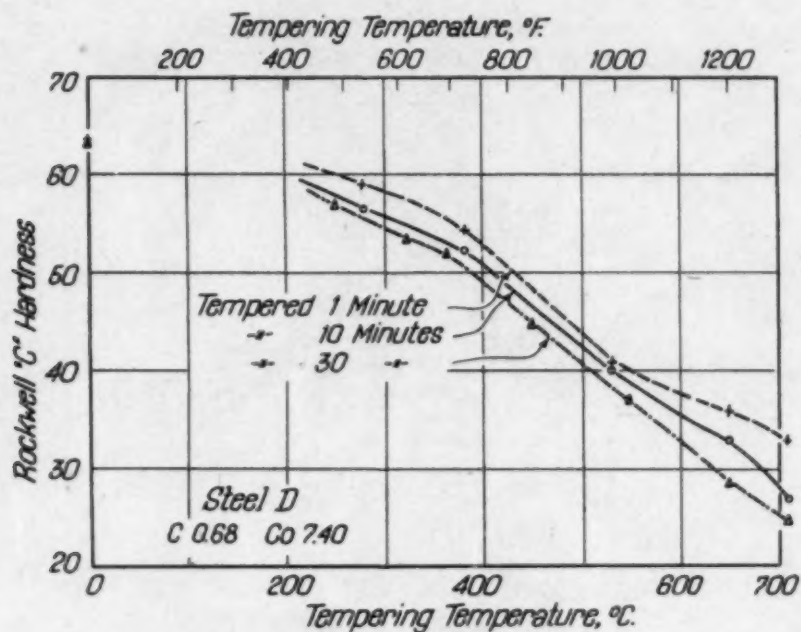


Fig. 5—Hardness-Tempering Curves for Steel D (0.68 Per Cent Carbon, 7.40 Per Cent Cobalt).

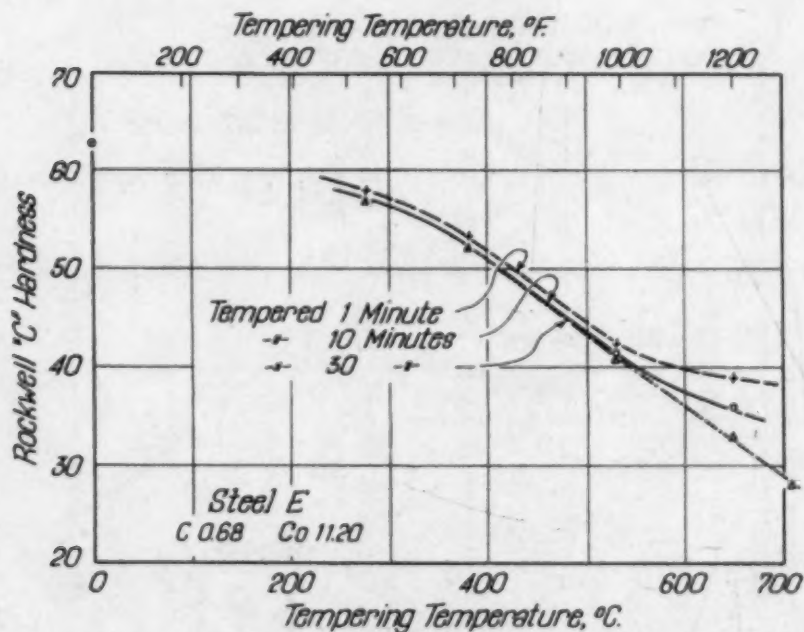


Fig. 6—Hardness-Tempering Curves for Steel E (0.68 Per Cent Carbon, 11.20 Per Cent Cobalt).

secondary hardness, it is possible that a higher austenitizing temperature is required for secondary hardness in steel E than in steel D because cobalt raises the A_1 temperature.

Figs. 7 and 8 compare the five steels when tempered for 10 and

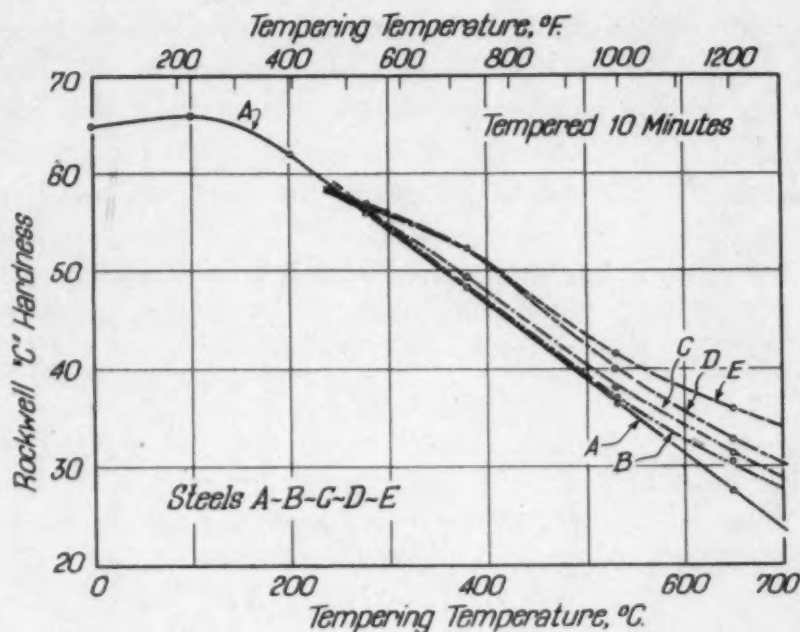


Fig. 7—Hardness-Tempering Curves, Showing Hardness After 10-Minute Tempering at Various Temperatures.

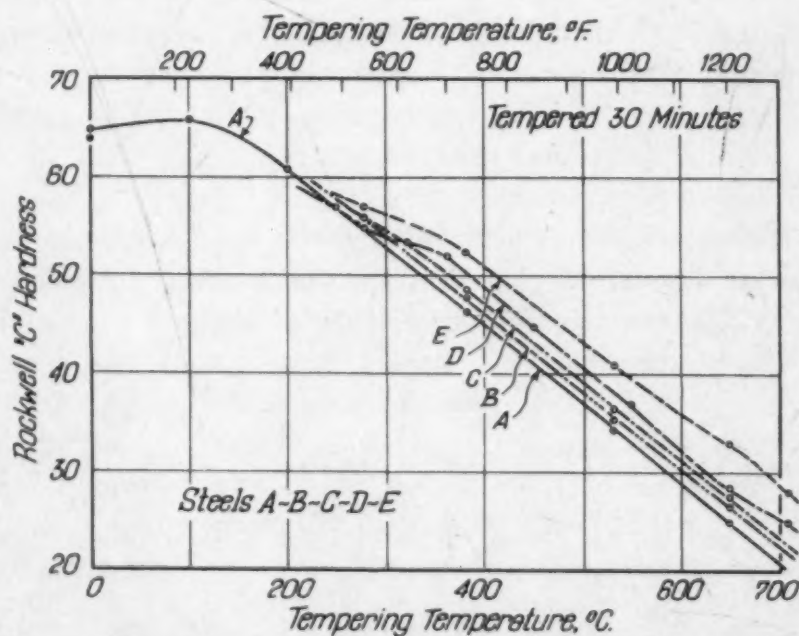


Fig. 8—Hardness-Tempering Curves, Showing Hardness After Half-Hour Tempering at Various Temperatures.

30 minutes respectively. Both sets of curves show that all five steels follow the same general softening pattern (with the exception of a very slight secondary hardening effect in the 7.40 per cent cobalt steel) and that the cobalt, when present in an increasing proportion,

acts to elevate the hardness of tempered steels which have been suitably quenched. One may assume, since cobalt in all probability is not present in any large proportion in the carbide, that its effect is to strengthen the ferrite in which the gradually coarsening carbides are dispersed. As the cobalt content is increased to 2, 4, 7 and 11 per cent respectively, the average Rockwell C hardness of specimens tempered for 30 minutes in the range of 250 to 710 degrees Cent. (480 to 1310 degrees Fahr.) increases 1, 2.5, 4, 6.5 points respectively.

SUMMARY

The hardness of plain Fe-C-Co steels tempered over the range 250 to 710 degrees Cent. (480 to 1310 degrees Fahr.) is similar to that of plain carbon steels tempered over the same range. The cobalt present promotes a small increase in hardness after tempering by solid solution hardening of ferrite. A 7.40 per cent cobalt steel shows a very slight secondary hardening in the range 275 to 385 degrees Cent. (525 to 725 degrees Fahr.). This effect is very small compared to that found in high speed steels and it was not observed in an 11.20 per cent cobalt steel.

ACKNOWLEDGMENT

The author wishes to acknowledge the kind assistance of Mr. M. F. Hawkes in various phases of this work. The facilities of the Metallurgical Laboratories of the Carnegie Institute of Technology were used.

References

1. D. P. Antia, S. G. Fletcher and M. Cohen, "Structural Changes During the Tempering of High Carbon Steels," *TRANSACTIONS, American Society for Metals*, Vol. 32, 1944, p. 290-332.
2. S. G. Fletcher and M. Cohen, "The Effect of Carbon on the Tempering of Steel," *TRANSACTIONS, American Society for Metals*, Vol. 32, 1944, p. 333-362.
3. D. P. Antia and M. Cohen, "The Tempering of Nickel and Nickel-Molybdenum Steels," *TRANSACTIONS, American Society for Metals*, Vol. 32, 1944, p. 363-380.
4. M. Cohen and P. K. Koh, "The Tempering of High Speed Steel," *TRANSACTIONS, American Society for Metals*, Vol. 27, 1939, p. 1015-1051.
5. M. Hansen, "Der Aufbau der Zweistofflegierungen," J. Springer, 1936.
6. E. C. Bain, "Functions of the Alloying Elements in Steel," American Society for Metals Publication, 1943.

THE Ar' REACTION IN SOME IRON-COBALT-TUNGSTEN ALLOYS AND THE SAME MODIFIED WITH CHROMIUM

BY W. P. SYKES

Abstract

Within a range of limited compositions, the ternary alloys of iron, cobalt, and tungsten exhibit a behavior similar to that of the steels as regards the eutectoidal decomposition, $\gamma = \alpha + \epsilon$.

The times required for the beginning and completion of this reaction have been approximated for one composition.

Chromium, when present in this type of alloy, delays the onset of the reaction and appears to depress the position of the three-phase field in which γ is stable.

IT has been previously shown (1)¹ that alloys of iron, cobalt and tungsten similar to composition No. 165 in Table I undergo an eutectoidal decomposition when slowly cooled through a temperature of about 900 degrees Cent. (1650 degrees Fahr.). The upper and lower limits of the Ar' range have also been approximated for certain alloys of this type.

In the following pages are reported some data bearing upon the characteristics of the Ar' isothermal reaction, the resulting microstructures, and hardness changes and the influence of small additions of chromium to the base alloy which lies in the ternary section shown in Fig. 1. The compositions listed in Table I all yield substantially single-phase structures when quenched to room temperature from a solution treatment at 1350 degrees Cent. (2460 degrees Fahr.). Details of melting and working these alloys have been described elsewhere (2).

METHODS OF THERMAL TREATMENT

Specimens for thermal treatment, about $\frac{3}{8}$ inch in length, were cut from swaged rods $\frac{1}{2}$ inch in diameter. Solution treatments were carried out in a hydrogen atmosphere at 1350 degrees Cent. (2460

¹The figures appearing in parentheses refer to the bibliography appended to this paper.

A paper presented before the Twenty-sixth Annual Convention of the Society held in Cleveland, October 16 to 20, 1944. The author, W. P. Sykes, is metallurgical engineer, Wire Works, Incandescent Lamp Dept., General Electric Co., Cleveland. Manuscript received May 23, 1944.

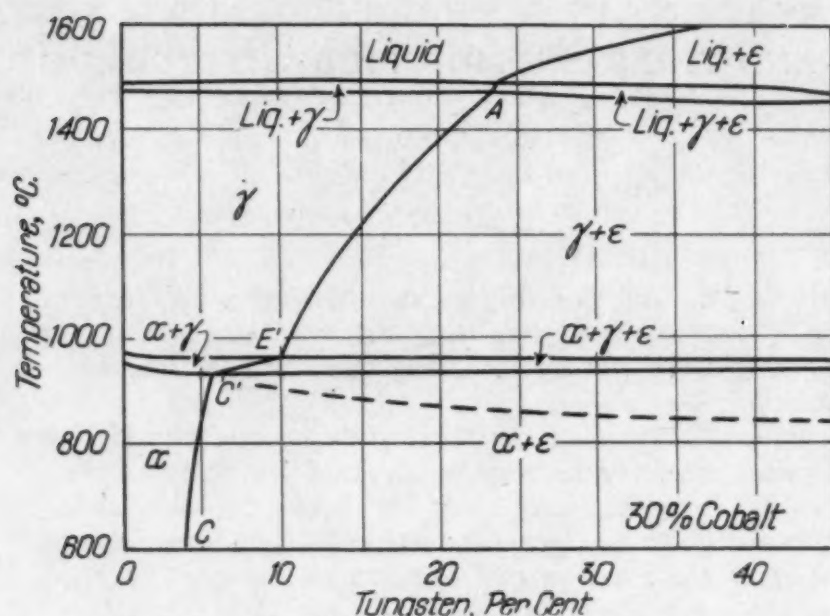


Fig. 1—Section Through Ternary System at 30 Per Cent Cobalt.

degrees Fahr.) for 1-hour periods and the specimens quenched in molten salt or lead at some selected temperature between 550 and 900 degrees Cent. (1020 and 1650 degrees Fahr.). After holding at temperature for the desired period the alloys were water-quenched. For the extended periods at 900 degrees Cent. (1650 degrees Fahr.) the specimens were rapidly transferred from the molten bath to the hydrogen atmosphere of a tube furnace held at 900 degrees Cent. (1650 degrees Fahr.).

THE AR' RANGE IN ALLOY No. 165

At 900 degrees Cent. (1650 degrees Fahr.) the isothermal decomposition of the γ phase in this alloy begins after a period of about 30 minutes as evidenced by the appearance of the dark etching nodules, a duplex formation, located at the boundaries of the γ grains

Table I
Composition of Alloys

Alloy No.	Per Cent			Iron
	Cobalt	Tungsten	Chromium	
165	29.50	17.76	Balance
196	29.30	17.21	1.85	Balance
166	29.10	17.33	2.76	Balance
	Silicon0.10 to 0.13 per cent		
	Manganese0.13 to 0.17 per cent		
	Carbon0.03 to 0.05 per cent		

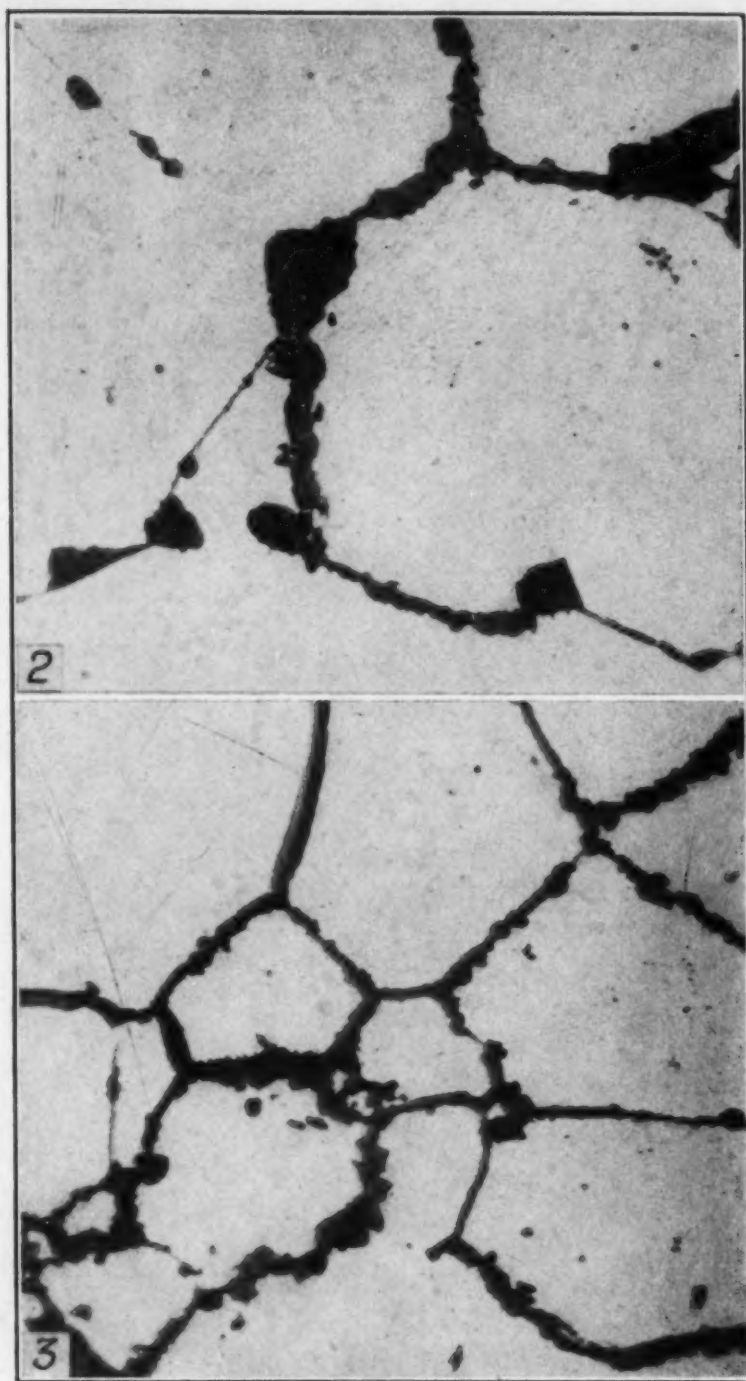


Fig. 2—Alloy No. 165. Quenched from 1350 Degrees Cent. (2460 Degrees Fahr.) Into Salt Bath at 900 Degrees Cent. (1650 Degrees Fahr.), Held for 1 Hour and Water-Quenched. Etched 5 Seconds in 4 Parts H_2O_2 , 1 Part H_3PO_4 . $\times 200$.

Fig. 3—Alloy No. 165. 800 Degrees Cent. (1470 Degrees Fahr.) for 5 Minutes. Etching Same as Fig. 2. $\times 200$.

and shown in Fig. 2. The reaction $\gamma = \alpha + \epsilon$ is completed at 900 degrees Cent. (1650 degrees Fahr.) in the course of some 25 hours.

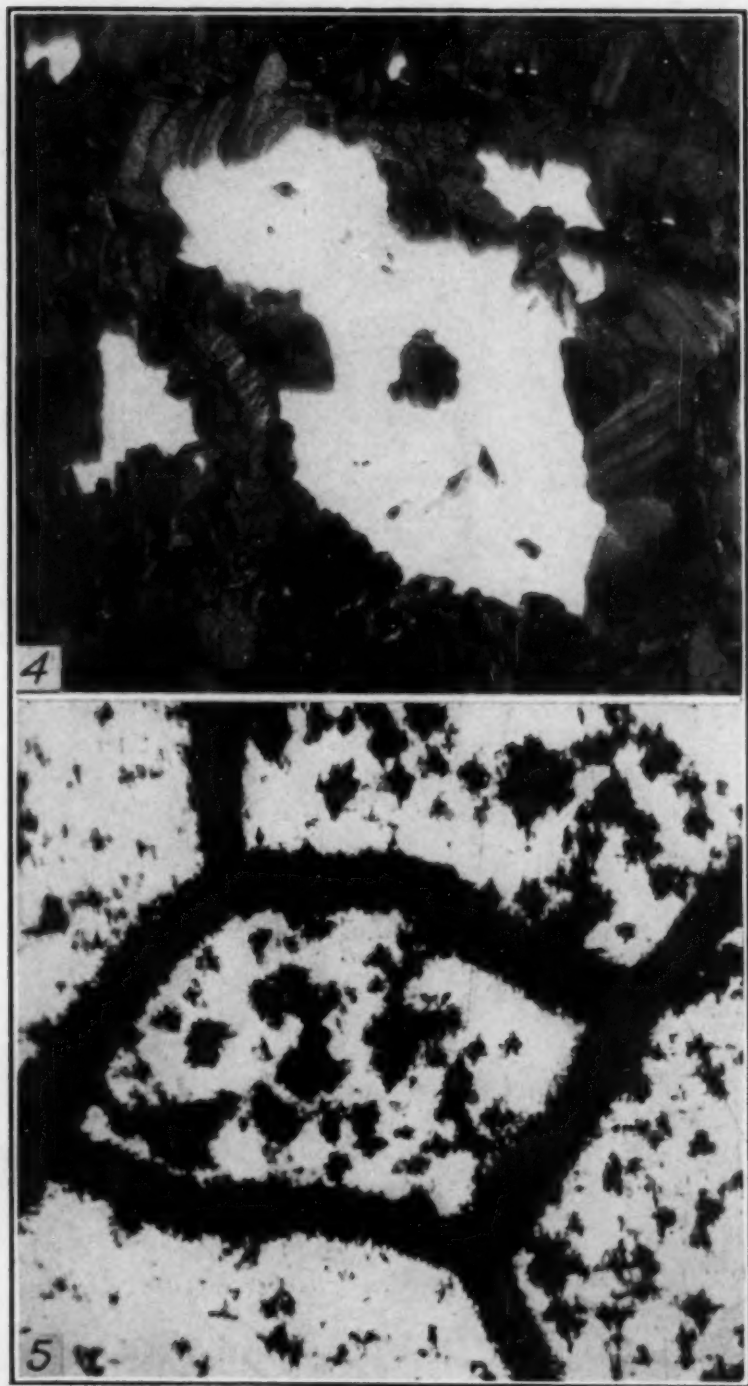


Fig. 4—Alloy No. 165. 800 Degrees Cent. (1470 Degrees Fahr.) for 30 Minutes. Etching Same as Fig. 2. $\times 200$.

Fig. 5—Alloy No. 165. 600 Degrees Cent. (1110 Degrees Fahr.) for 10 Hours. Etching Same as Fig. 2. $\times 200$.

Three minutes at 800 degrees Cent. (1470 degrees Fahr.) suffices to initiate the reaction, yielding the structures illustrated in Figs. 3 and 4. As the temperature of decomposition is further low-

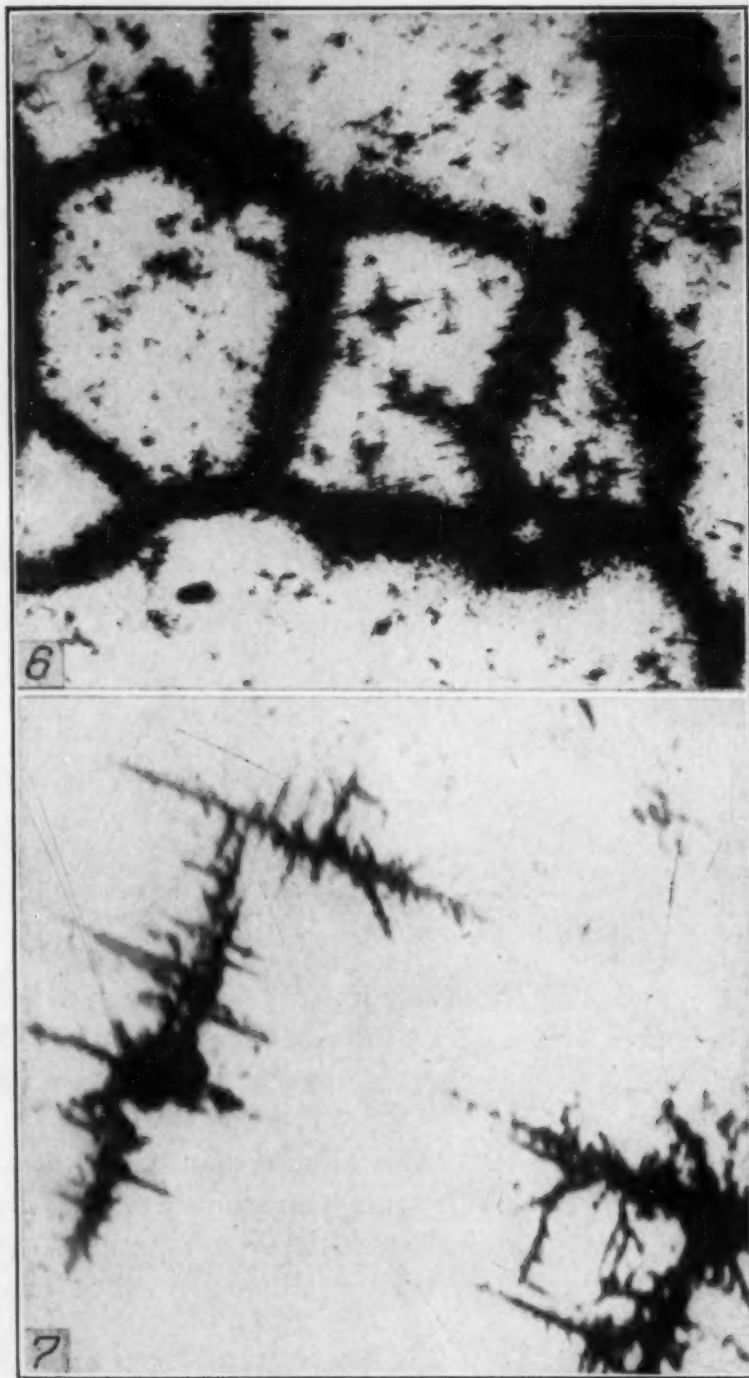


Fig. 6—Alloy No. 165. 550 Degrees Cent. (1020 Degrees Fahr.) for 100 Hours. Etching Same as Fig. 2. $\times 200$.
Fig. 7—Alloy No. 165. 550 Degrees Cent. (1020 Degrees Fahr.) for 50 Hours. Etching Same as Fig. 2. $\times 2000$.

ered the areas representing the products of the reaction tend to assume a directional habit suggestive of a Widmanstätten pattern to be observed in Figs. 5, 6 and 7.

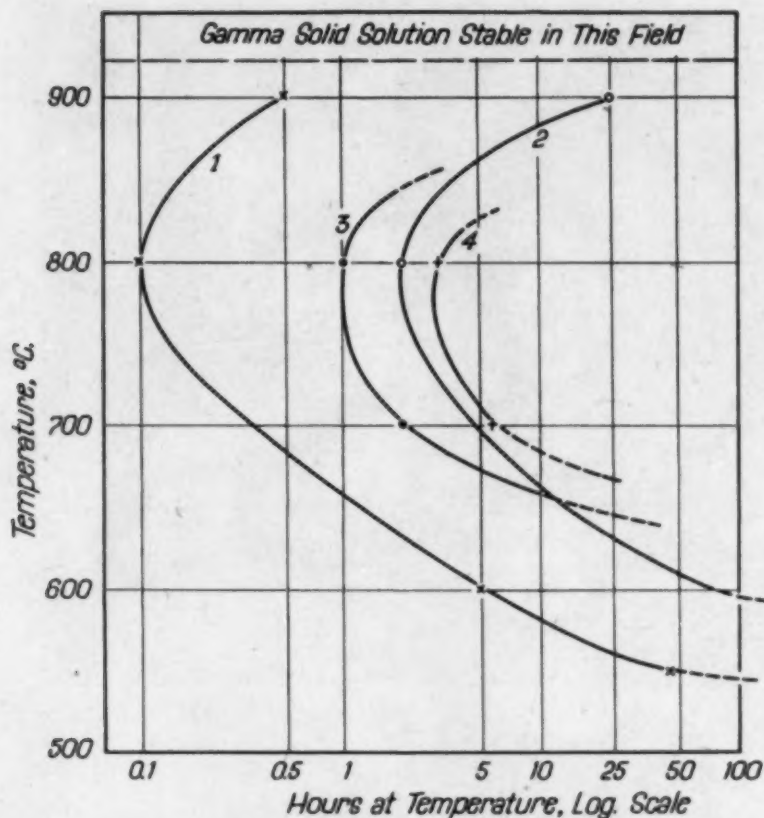


Fig. 8—Curves Showing Temperature-Time Relationships of Ar' Reaction. Curve 1—Reaction Starts in Alloy No. 165.
Curve 2—Reaction Completed in Alloy No. 165.
Curve 3—Reaction Starts in No. 196.
Curve 4—Reaction Starts in No. 166.

Curves 1 and 2 in Fig. 8 indicate the relationship between decomposition temperature and the time intervals required for the beginning and completion of the reaction as observed in the case of Alloy No. 165.

As previously shown (3) this alloy if quenched to 525 degrees Cent. (975 degrees Fahr.) from a temperature within the γ field develops a structure of the martensitic type reproduced in Fig. 9. The amount of this acicular structure thus formed at temperatures between 525 and 350 degrees Cent. (975 and 660 degrees Fahr.) is substantially independent of time and increases only as the temperature is lowered. It therefore presumably results from the γ to α transformation and hence the upper limit of the Ar'' range must lie between 525 and 550 degrees Cent. (975 and 1020 degrees Fahr.) for this composition.

EFFECTS OF CHROMIUM ADDITIONS

Alloy No. 196 differs from No. 165 mainly in that it contains

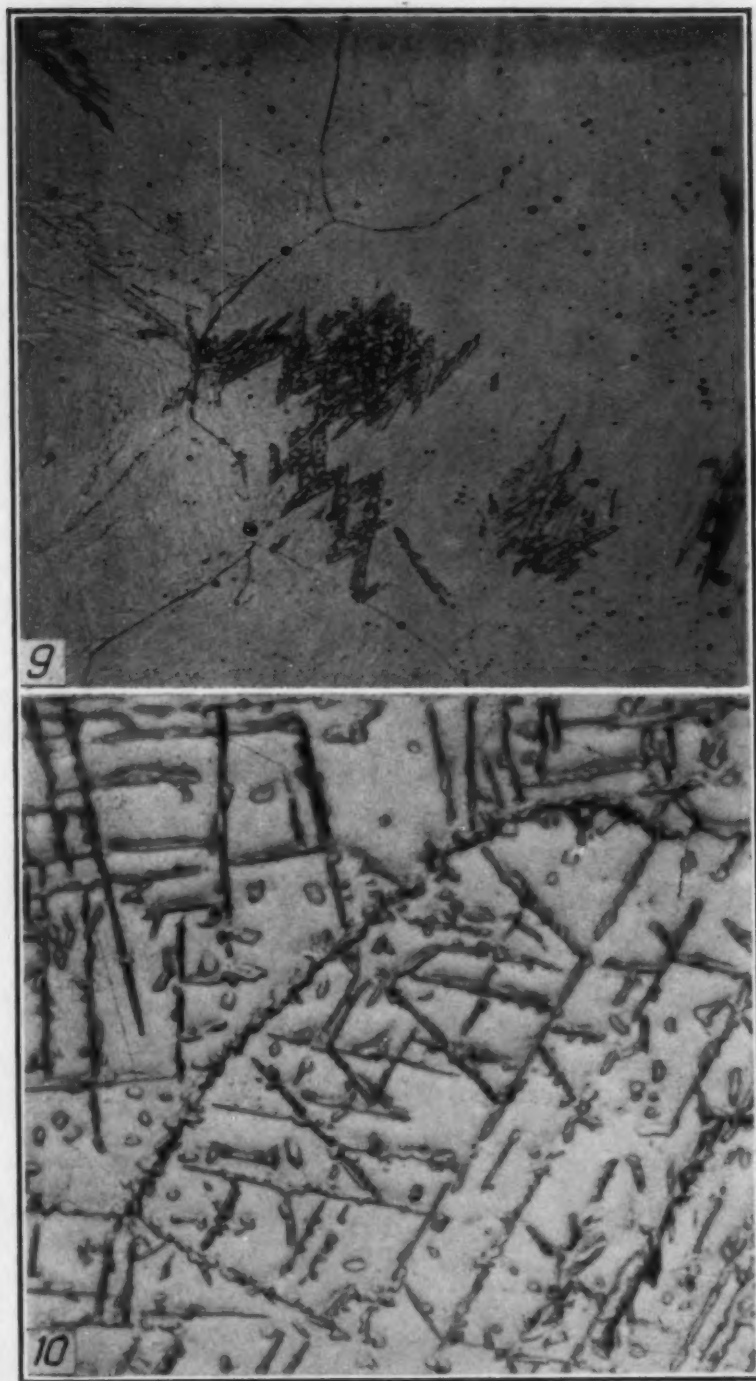


Fig. 9—Alloy No. 165. Quenched from 1350 to 525 Degrees Cent. (2460 to 975 Degrees Fahr.). Held for 15 Minutes and Water-Quenched. Etching Same as Fig. 2. $\times 200$.

Fig. 10—Alloy No. 196. Quenched from 1350 to 900 Degrees Cent. (2460 to 1650 Degrees Fahr.). Held for 100 Hours. Etching Same as Fig. 2. $\times 500$.

1.85 per cent of chromium which replaces a like amount of iron. When quenched to 900 degrees Cent. (1650 degrees Fahr.) and held

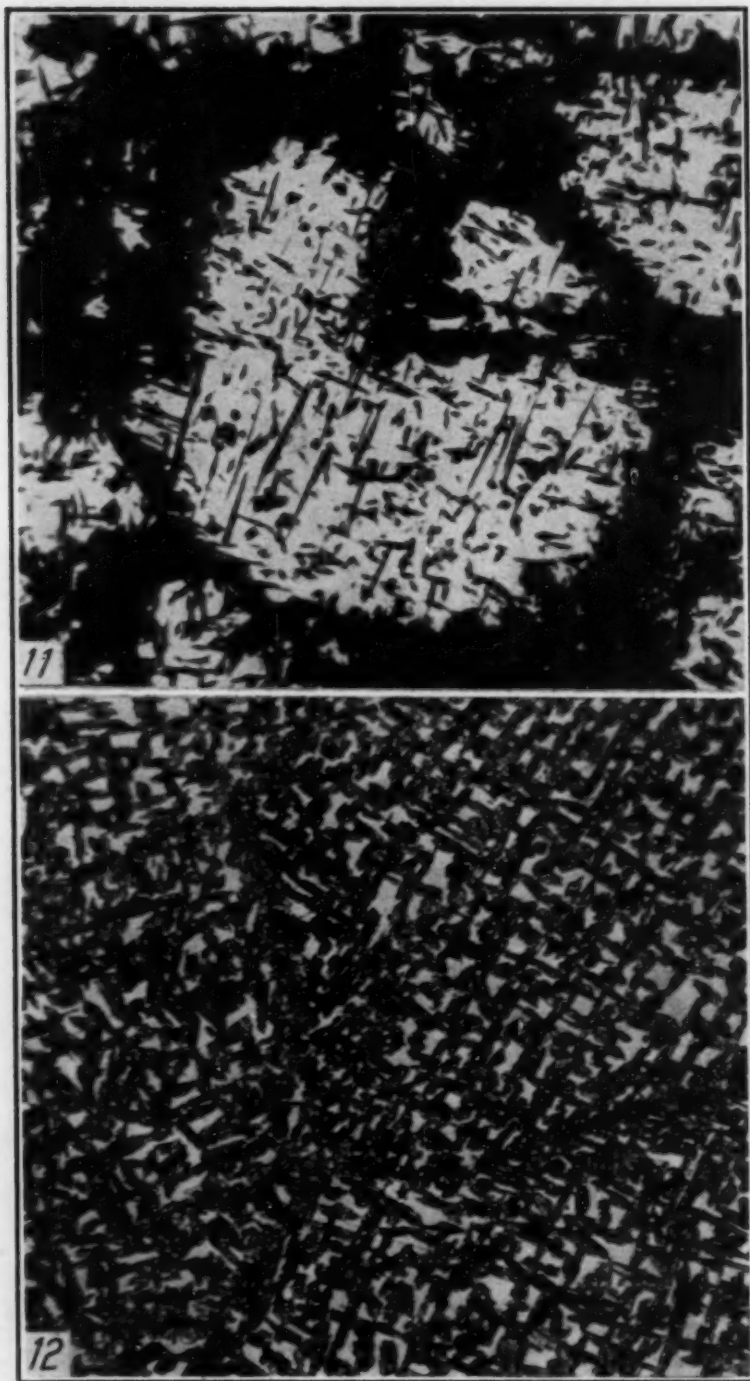


Fig. 11—Alloy No. 196. 800 Degrees Cent. (1470 Degrees Fahr.) for 25 Hours. Etching Same as Fig. 2. $\times 200$.
Fig. 12—Alloy No. 166. 800 Degrees Cent. (1470 Degrees Fahr.) for 300 Hours. Etching Same as Fig. 2. $\times 200$.

at this temperature for a period in excess of 100 hours it exhibits no evidence of the Ar' decomposition. The resulting structure seen in Fig. 10 represents the normal precipitation of ϵ from γ which occurs

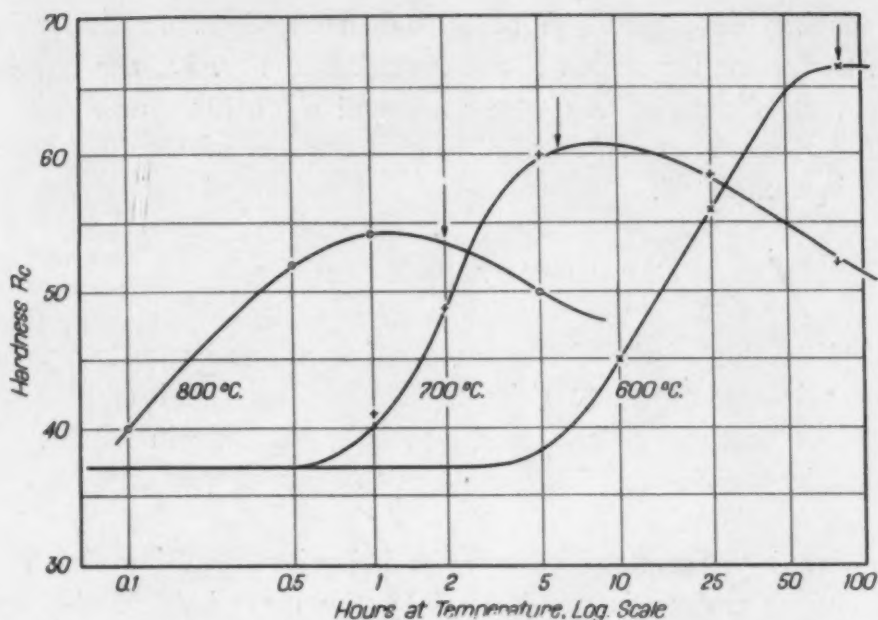


Fig. 13—Hardness Changes Accompanying Ar' Decomposition in Alloy No. 165.

upon cooling from the γ field into the $\gamma + \epsilon$ field. This alloy, however, quenched to 800 degrees Cent. (1470 degrees Fahr.) shows evidence of the Ar' decomposition after a period of 1 hour and the structure indicates that the reaction is completed at the end of 50 hours. In Fig. 11 appears the microstructure corresponding to a period of 25 hours at 800 degrees Cent. (1470 degrees Fahr.).

From Curve 3 in Fig. 8, it may be seen that the time required for the beginning of decomposition at 700 degrees Cent. (1290 degrees Fahr.) has increased to about 3 hours while at 600 degrees Cent. (1110 degrees Fahr.) no indication of the reaction was observed after 100 hours. As might be expected, alloy No. 166, containing 2.76 chromium, shows no evidence of the reaction at 900 degrees Cent. (1650 degrees Fahr.). At 800 degrees Cent. (1470 Fahr.) it has started after about 3 hours but is still uncompleted at the end of 300 hours, as may be seen from Fig. 12.

HARDNESS CHANGES ACCOMPANYING THE Ar' DECOMPOSITION

Soon after the reaction sets in an increase in hardness is observed which passes through a maximum at about the time of completion. The time-hardness curves of Alloy No. 165 for three temperatures of decomposition are reproduced in Fig. 13. Here the arrows mark approximately the end of the reaction at each tempera-

ture. During decomposition at 900 degrees Cent. (1650 degrees Fahr.), the curve for which is not included in Fig. 13, the hardness reaches a maximum of Rc 44 at the end of 1 hour and decrease thereafter of a period of 25 hours to a final value of Rc 40 when the reaction is completed.

DISCUSSION AND SUMMARY

The behavior of the chromium-bearing alloys suggests that one effect of this element is to shift the three-phase field ($\alpha + \gamma + \epsilon$) to lower temperatures as indicated by the broken line in Fig. 1. This could explain the failure of these alloys to react at 900 degrees Cent. (1650 degrees Fahr.).

A second pronounced change in behavior resulting from the presence of chromium is manifested by the remarkable stability of the solid solution at 600 degrees Cent. (1110 degrees Fahr.). At this temperature no indication of decomposition was observed within an interval of 100 hours.

Bibliography

1. W. P. Sykes, "Structural and Hardening Characteristics of Some Iron-Cobalt-Tungsten Alloys," *TRANSACTIONS, American Society for Metals*, 1937, Vol. 25, p. 953.
2. W. P. Sykes, "Hardening Characteristics of an Iron-Cobalt-Tungsten Alloy," *TRANSACTIONS, American Society for Metals*, 1942, Vol. 30, p. 147.
3. W. P. Sykes, "The Ar" Range in Some Iron-Cobalt-Tungsten Alloys," *TRANSACTIONS, American Society for Metals*, 1943, Vol. 31, p. 284.

A COMPARISON OF ALUMINUM AND TITANIUM DEOXIDATION FOR PREVENTING STRAIN AGING EMBRITTLEMENT IN LOW CARBON STEEL

BY GEORGE F. COMSTOCK AND JOHN R. LEWIS

Abstract

The strain aging of low-carbon steel, melted in an induction furnace, deoxidized with silicon, aluminum, or titanium, and forged from small ingots, was studied by three different methods, and this paper reports the results as affected by differences in forging practice and heat treatment, as well as by different deoxidation. The three methods of testing were (1) the work brittleness method, involving impact tests after cold drawing with and without subsequent aging, (2) impact tests after tensile straining, with and without aging, and (3) Brinell hardness tests at increasing temperatures up to 500 degrees Fahr. These methods gave results in close agreement, the work-brittleness test being preferred as the most informative. Strain aging embrittlement can be eliminated as effectively with titanium deoxidation as with aluminum if sufficient titanium is used. The minimum amount required to equal 2 or 3 pounds aluminum per ton depends on the forging practice and heat treatment, 15 pounds ferro-carbon-titanium per ton being generally effective, although 10 or 12 pounds per ton appear to be sufficient with the best conditions of forging and heat treatment.

STRONG deoxidation of steel with aluminum is generally recognized to be effective for preventing susceptibility to loss of notch-toughness when the steel is aged after straining. This effect of aluminum on steel has been thoroughly described¹ and it has become standard practice to use aluminum-killed steel for applications where strain aging embrittlement might develop and would be objectionable, as in high-pressure tubing. Steel fully killed with aluminum is not,

¹B. N. Daniloff, R. F. Mehl and C. H. Herty, Jr., "The Influence of Deoxidation on the Aging of Mild Steels," TRANSACTIONS, American Society for Metals, Vol. 24, 1936, p. 595.

Graham and Case (U. S. Patent 2,174,740, October 1939).

A paper presented before the Twenty-sixth Annual Convention of the Society, held in Cleveland, October 16 to 20, 1944. Of the authors, G. F. Comstock is metallurgist, and J. R. Lewis is associate metallurgist, The Titanium Alloy Manufacturing Co., Niagara Falls, N. Y. Manuscript received June 13, 1944.

however, entirely free from disadvantages; it tends to be more or less dirty from alumina inclusions which have a decided tendency to segregate in streaks, and recently it has been found to be more apt than ordinary steel to lose strength by graphitizing under certain conditions of high temperature service. Thus there is a definite incentive to find other methods, than by the use of aluminum, for preventing strain aging embrittlement. Silicon deoxidation has been found to be ineffective, but the effect of titanium deoxidation seems not to have been separately investigated, although it is well known to give cleaner steel than aluminum. How it compares with aluminum in controlling strain aging embrittlement is reported in this paper.

MATERIAL AND METHODS USED

This investigation was carried out entirely with S.A.E. 1015 steel forged from 17-pound ingots melted in a magnesia-lined induction furnace. The same melting stock, containing 0.16 per cent carbon, 0.39 per cent manganese, 0.13 per cent silicon, 0.014 per cent phosphorus, and 0.039 per cent sulphur, was used for all the ingots. The melting loss in carbon was made up with 1 per cent silicon low-phosphorus pig iron, and a little extra manganese and silicon were also added in the form of the customary ferro alloys. Aluminum and titanium alloy additions were made at the top of the slag-free bath about 2 minutes before the power was shut off and the ingot poured. The ferrotitanium chiefly used for deoxidation was medium-carbon FCT containing about 20 per cent titanium, 4.5 per cent carbon, 2.5 per cent silicon, and 1.5 per cent aluminum; in a few ingots, however, the regular grade of low-carbon ferrotitanium was used, with about 40 per cent titanium, 0.08 per cent carbon, 3.5 per cent silicon, and 8 per cent aluminum, in order to obtain higher titanium contents.

The ingots were forged to $\frac{7}{8}$ -inch round bars by two different methods, designated as A and B. Forging practice A involved heating slowly to 2000 degrees Fahr. (1095 degrees Cent.), holding at that temperature for about 1.5 hours, and forging rather slowly with a 200-pound Bradley hammer, with several reheatings of the stock before finishing at a dull red heat, or about 1400 degrees Fahr. (760 degrees Cent.). With forging practice B the ingots were first heated 4 hours at 2200 degrees Fahr. (1205 degrees Cent.) as would be done with large commercial ingots in a soaking pit, and then air-

cooled. Later they were reheated to 2100 degrees Fahr. (1150 degrees Cent.) and forged at that temperature with a heavy steam hammer and without any subsequent reheating, being finished below a red heat. The effects of these different forging practices, as well as of the different methods of deoxidation, are compared.

The deoxidation, forging practice, and composition of the ingots used for this work are given in Table I.

Table I
Deoxidation, Composition, and Forging of the Ingots

Steel No.	Final Additions Lbs. per Net Ton			Chemical Analysis, Per Cent				Heating and Forging Practice
	Al	FCT	40% FeTi	C	Mn	Si	Ti	
0A	0	0	0	0.17	0.45	0.25	A
0B	0	0	0	0.17	0.39	0.31	0.005	B
1B	0.5	0	0	0.145	0.26	0.11	0.006	B
1A	1	0	0	0.15	0.45	0.21	A
2A	2	0	0	0.16	0.44	0.23	A
2B	2	0	0	0.14	0.42	0.25	0.005	B
3A	3	0	0	0.165	0.45	0.26	A
4B	0	4	0	0.165	0.42	0.22	0.014	B
8A	0	8	0	0.155	0.47	0.25	0.020	A
8B	0	8	0	0.165	0.43	0.23	0.030	B
10A	0	10	0	0.16	0.49	0.24	0.028	A
10B	0	10	0	0.15	0.46	0.24	0.031	B
12A	0	12	0	0.155	0.44	0.25	0.042	A
12B	0	12	0	0.15	0.45	0.24	0.038	B
15A	0	15	0	0.14	0.40	0.22	0.047	A
15B	0	15	0	0.16	0.48	0.29	0.056	B
16A	1	10	0	0.155	0.44	0.23	0.048	A
17A	0	0	6	0.16	0.46	0.24	0.099	A
18A	0	0	15	0.16	0.47	0.25	0.225	A

The forged bars were tested in two conditions of heat treatment, either stress-relieved 3 hours at 1100 degrees Fahr. (595 degrees Cent.), or normalized 1.5 hours at 1680 degrees Fahr. (915 degrees Cent.). Three different methods of testing for susceptibility to strain aging were used, namely:

1. The work-brittleness test as described by Graham and Work² involving Izod impact tests of tapered specimens strained by cold drawing through a die. Duplicate specimens were tested as soon as possible, or within 3 or 4 hours, after the cold work, and also after a period of aging, respectively. The aging treatment included in all instances $\frac{1}{2}$ hour at 450 degrees Fahr. (235 degrees Cent.), and 14 to 20 days at room temperature.

2. Straining about 5 per cent in tension, followed by Izod im-

²Graham and Work, *Proceedings, American Society for Testing Materials* Vol. 39, 1939, p. 571.

pact tests within 4 hours of straining, and after a period of aging. The aging treatment was the same as described above.

3. Brinell hardness tests at room temperature and at increasing temperatures up to 500 degrees Fahr. (260 degrees Cent.). This method was suggested by S. L. Case, formerly of the Jones and Laughlin Research Laboratory, as being simpler, though equally effective, than hot tensile tests that have previously been used to determine susceptibility to strain aging. Care was taken, by means of a thermocouple embedded within a dummy specimen, to ensure that the specimens were actually at the desired temperatures when the Brinell impressions were made. A Kennametal Brinell ball was used to resist deformation at the higher temperatures. The load used was only 2000 kilograms, as the available specimens were thought to be rather small and soft to resist spreading under the heavier standard load.

WORK-BRITTLENESS TEST RESULTS

The results of the work-brittleness tests are reported graphically in Figs. 1 to 5 inclusive, which are believed to be self-explanatory. The extent of the downward slope of the full lines indicates the strain-sensitivity of the steels, and the spread between the full and broken lines indicates the susceptibility to strain aging embrittlement.

Figs. 1 and 2 confirm the elimination of strain aging embrittlement by deoxidation with 2 or 3 pounds aluminum per ton, while only 1 pound per ton as in steel 1A is slightly less effective, and $\frac{1}{2}$ pound per ton as in steel 1B gives no less strain sensitivity or aging embrittlement than in the silicon-deoxidized steels 0A and 0B. These results were found with both stress-relieved and normalized specimens, and with both forging practices. According to the results from steel 4B, 4 pounds FCT per ton gives somewhat better control of strain sensitivity than $\frac{1}{2}$ pound of aluminum, but not much less aging embrittlement.

In Figs. 3 and 4 the results with 8 to 15 pounds FCT per ton are plotted, and they are seen to depend partly on the heat treatment of the specimens and the forging practice, as well as on the amount of FCT used for deoxidation. With forging practice A the results with stress-relieved and normalized specimens are practically the same, indicating that 8 or 10 pounds FCT per ton give about the

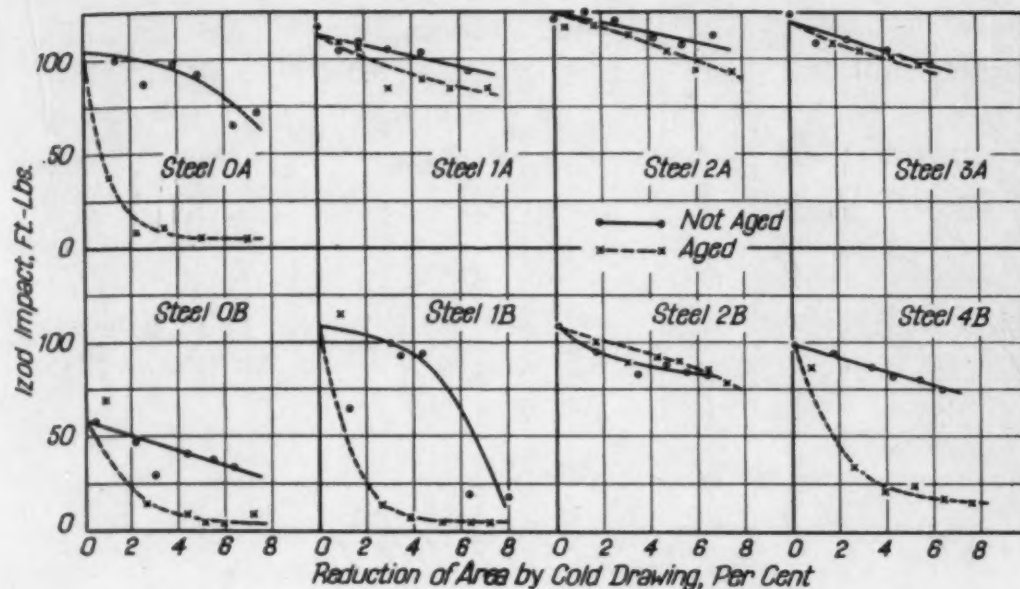


Fig. 1—Work-Brittleness Tests of Stress-Relieved Specimens.

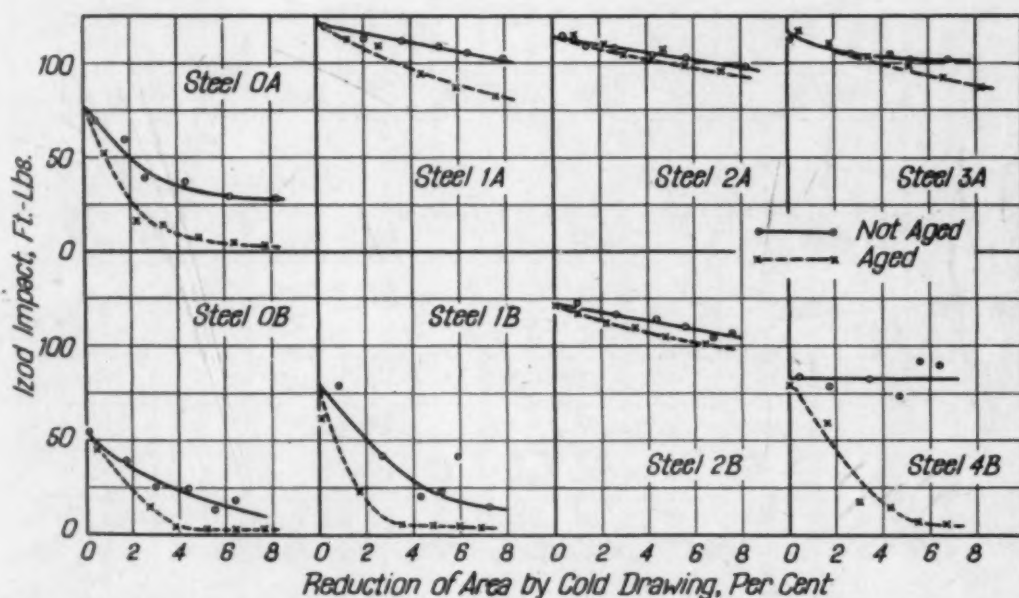


Fig. 2—Work-Brittleness Tests of Normalized Specimens.

same control of strain aging embrittlement as 1 pound of aluminum while 12 or 15 pounds FCT are about equivalent to 2 or 3 pounds of aluminum. With forging practice B much better results were obtained with stress-relieved than with normalized specimens, and 15 pounds FCT per ton were required for the same effect as with 2 or 3 pounds of aluminum per ton.

To determine the reason for the difference in results between

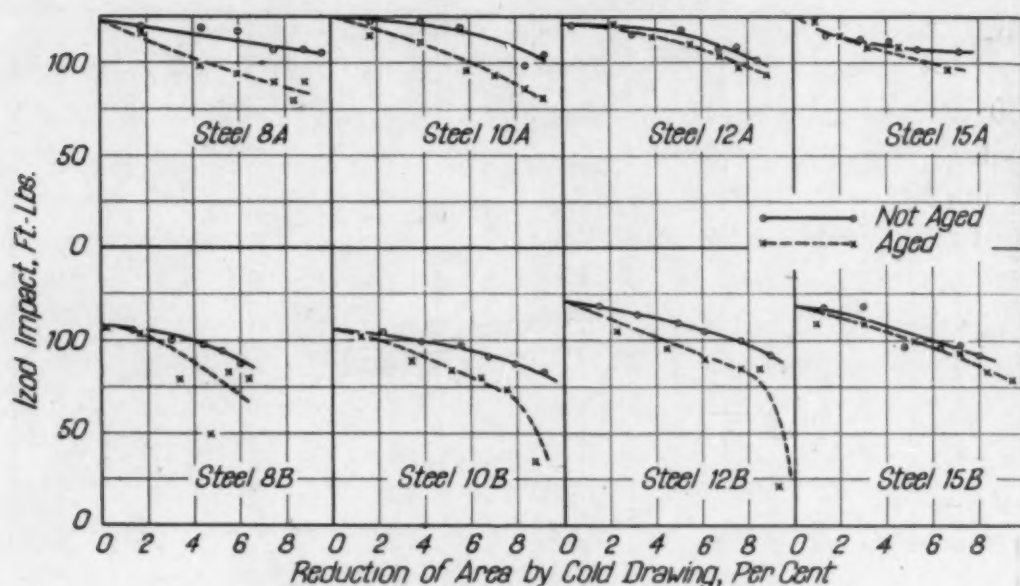


Fig. 3—Work-Brittleness Tests of Stress-Relieved Specimens.

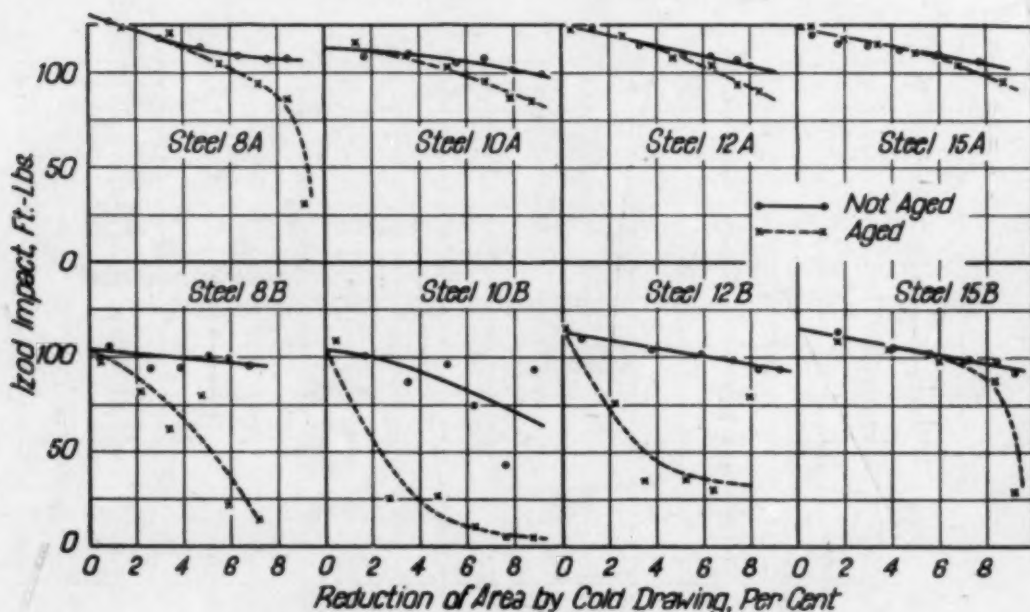


Fig. 4—Work-Brittleness Tests of Normalized Specimens.

the two forging practices, the microstructures of the unstrained ends of the normalized specimens of steels 10A, 10B, 12A, and 12B were examined, and these are illustrated in Fig. 6. The grain size is seen to be partly coarse in the bars forged by practice B, while the others are entirely fine-grained. Since all the specimens were normalized in exactly the same way, some feature of the forging practice B must have lowered the grain-coarsening temperature of the steel as compared with the other forging practice. This difference

in structure undoubtedly accounts for the different work-brittleness results shown for the 10B and 12B steels in Fig. 4 as compared with 10A and 12A, but it is interesting to note that the unstrained impact value is reduced very little by the coarser grain size, which thus is found to affect the impact resistance seriously only after straining and aging.

Fig. 5 gives the results of some work-brittleness tests on steels deoxidized by both aluminum and titanium. In steel 16A, 1 pound of aluminum was added with 10 pounds FCT per ton, as reported

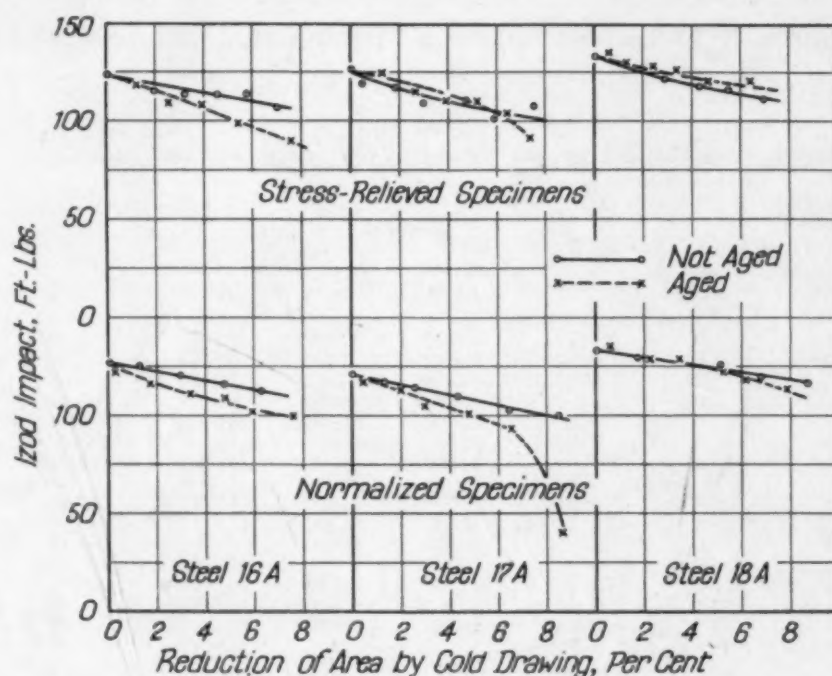


Fig. 5—Work-Brittleness Tests of Steels 16A, 17A and 18A.

in Table I, and in the other two steels appreciable amounts of aluminum were added as part of the low-carbon ferrotitanium used. This amounted to about $\frac{1}{2}$ pound per ton in the case of steel 17A, and about 1.2 pound per ton in 18A. In the latter steel, with over 0.2 per cent residual titanium in addition to thorough deoxidation, the impact values are higher than in any of the other steels tested, and strain aging embrittlement is more completely eliminated than with even 3 pounds aluminum per ton as in steel 3A. This improvement with higher titanium contents was checked with a number of other ingots which are not included in this paper because some of the test specimens were unfavorably affected by unsoundness or "pipe".

IMPACT TESTS AFTER TENSILE STRAINING

In the second method of testing, tensile test specimens of about 0.46-inch diameter and with 6-inch gage length were strained to 5 per cent elongation or about 4 or 5 per cent reduction of area, and then cut in half and notched for Izod impact tests. Each half was long enough for two notches. The impact tests were made on one half as soon as the strained specimens could be notched, and on the other half after aging as has been described. When the bars were strained the yield point was determined by the drop of the beam, and also the stress required to produce 5 per cent elongation

Table II
Yield Strengths and Impact Values of Specimens Strained in Tension

Steel No.	Lbs. Added		Ti Content	-Lbs. per Sq. In.-		Izod Impact Value, Ft. Lbs.		Avg. Loss by Aging
	Per Ton			Yield Point	Stress for 5% Strain	Not Aged	Aged	
	Al	FCT						
Stress-Relieved Specimens:								
0A	0	0	55100	61200	63-68	12-14	52.5
0B	0	0	0.005	60200	71500	62-42	22-15	33.5
1B	0.5	0	0.006	59200	69800	90-29	4-6	54.5
1A	1	0	47000	55600	92-95	90-90	4.0
2A	2	0	52300	58900	105-107	99-110	1.5
2B	2	0	0.005	57100	69000	92-93	89-85	5.5
3A	3	0	47000	54700	112-111	109-110	2.0
4B	0	4	0.014	53000	65500	91-92	31-17	67.5
8A	0	8	0.020	58400	63200	116-112	102-93	16.5
8B	0	8	0.030	59200	66400	89-91	85-73	11.0
10A	0	10	0.028	56000	59800	105-117	97-100	12.5
10B	0	10	0.031	57700	66000	102-95	80-72	22.5
12A	0	12	0.042	57500	62300	112-116	95-98	17.5
12B	0	12	0.038	48200	53000	107-113	92-90	19.0
15A	0	15	0.047	54600	113-115	115-115	0.0
15B	0	15	0.056	50400	57200	100-104	98-94	6.0
16A	1	10	0.048	50200	55000	117-120	103-112	11.0
17A	0	(6 FeTi)	0.099	46100	53500	123-112	112-73	25.0
18A	0	(15FeTi)	0.225	54200	58600	118-124	120-119	1.5
Normalized Specimens:								
0A	0	0	51200	60500	53-37	20-18	26.0
0B	0	0	0.005	48900	63000	35-22	12-8	18.5
1B	0.5	0	0.006	40900	53100	70-76	10-6	65.0
1A	1	0	51600	53100	113-105	104-107	3.5
2A	2	0	50500	54200	108-112	105-106	3.0
2B	2	0	0.005	57400	112-114	101-97	14.0
3A	3	0	48000	53600	86-105	103-102	0.0
4B	0	4	0.014	44000	55700	71-58	35-15	39.5
8A	0	8	0.020	49300	56600	118-117	97-99	19.5
8B	0	8	0.030	43700	55100	98-99	43-32	61.0
10A	0	10	0.028	51900	56700	110-110	102-96	11.0
10B	0	10	0.031	43000	54400	98-66	28-64	36.0
12A	0	12	0.042	47900	54800	113-111	109-106	4.5
12B	0	12	0.038	43300	51500	103-104	40-95	36.0
15A	0	15	0.047	48600	50600	115-117	115-118	0.0
15B	0	15	0.056	45500	52300	99-101	96-99	3.5
16A	1	10	0.048	50500	114-118	115-115	1.0
17A	0	(6 FeTi)	0.099	45900	51500	113-113	110-108	4.0
18A	0	(15 FeTi)	0.225	51700	53600	126-125	127-129	0.0

was recorded. These results, together with the impact values in duplicate, are reported in Table II.

The yield strength values in Table II do not seem to bring out any comparisons of special interest between the steels, but the stress-relieved specimens were in general stronger than the normalized. In estimating the amount of strain aging from Table II, it is necessary to consider not only the right-hand column giving the loss in impact value on aging, but also the next to the last column giving the actual impact values obtained. The normalized specimen of steel 0B, for instance, should be graded as definitely inferior to 4B, 10B, or 12B, even though 0B shows a smaller loss in impact value.

In general these impact results on specimens strained in tension support the evidence obtained from the work-brittleness tests. Deoxidation with 1 to 3 pounds aluminum per ton, or with 15 pounds FCT per ton, or with low-carbon ferrotitanium giving about 0.2 per cent residual titanium content, is seen to eliminate strain aging embrittlement according to this method of testing. Deoxidation with only 8 to 12 pounds FCT per ton gave somewhat variable results, and the evidence from Table II, which was obtained with only about 5 per cent strain, is undoubtedly less reliable for these intermediate comparisons than that provided by the work-brittleness tests where a wider range of strain was used. The results in Table II should best be used therefore merely as a rough check on the work-brittleness diagrams. The effect of the coarser grain of the normalized specimens of steels 10B and 12B, as illustrated in Fig. 6, is well reflected in Table II, the forging practice A in most instances giving the better results.

HOT HARDNESS TESTS

Typical Brinell hardnesses of these steels at various temperatures are reported graphically in Fig. 7. Similar tests were made also on most of the other steels, but the results merely checked those reported, and are omitted from Fig. 7 to avoid confusion. Steels 15A and 15B, deoxidized with 15 pounds FCT per ton, are seen to be entirely free from hardening at temperatures up to 500 degrees Fahr. (260 degrees Cent.), like steel 2B with 2 pounds aluminum per ton. Steel 12A, deoxidized with 12 pounds FCT per ton, shows less hardening with increasing temperature than 1A with 1 pound aluminum per ton, especially after normalizing, but steel 12B, forged in a different way, shows more. The steels treated with less titanium

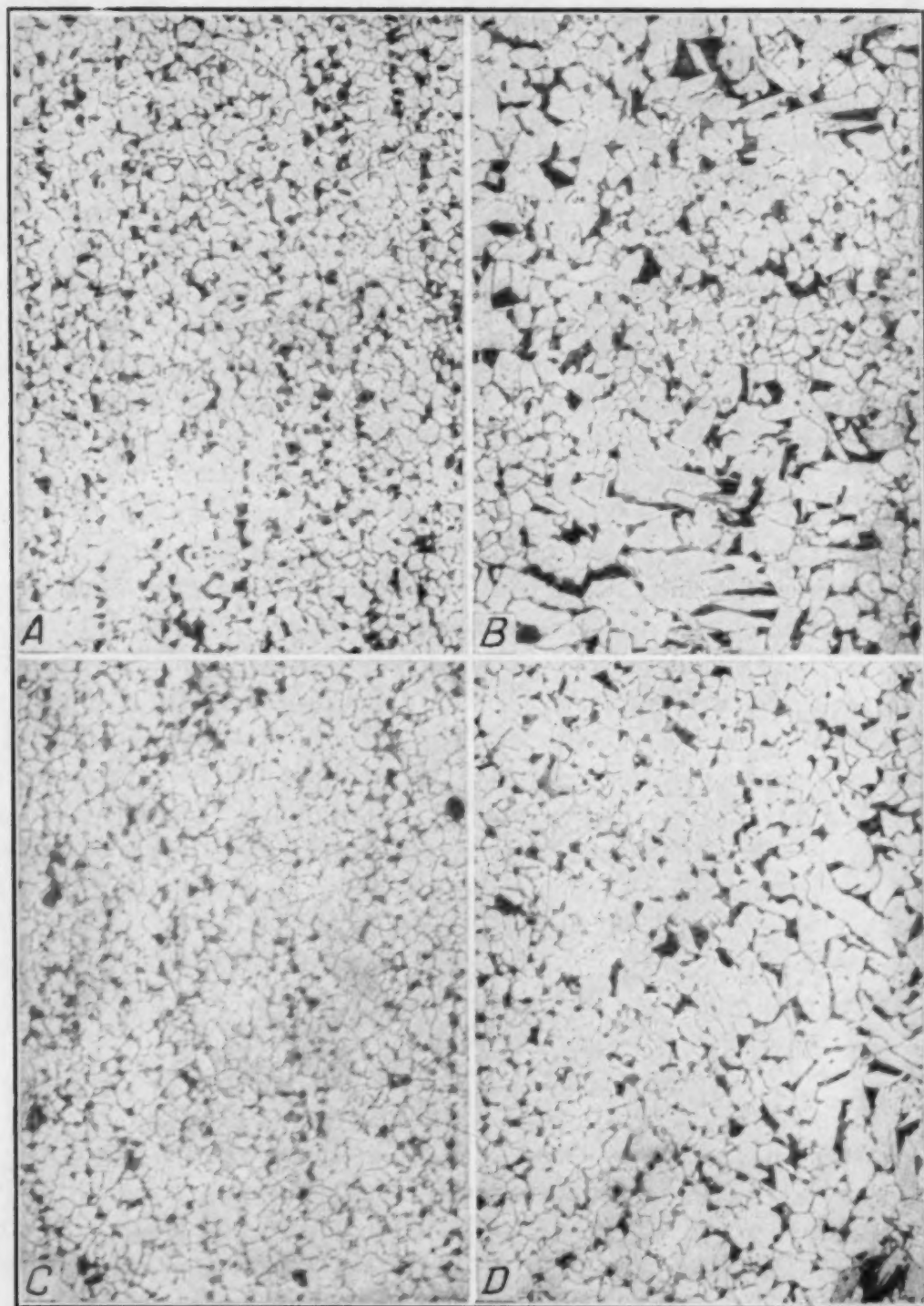


Fig. 6—Typical Microstructures of Lengthwise Sections of the Unstrained Ends of the Work-Brittleness Test Specimens Normalized at 1680 Degrees Fahr. and Aged, Nital Etched. $\times 100$.

Fig. 6A—Steel 10A, 10 pounds FCT per ton. Forging Practice A.
Fig. 6B—Steel 10B, 10 pounds FCT per ton. Forging Practice B.
Fig. 6C—Steel 12A, 12 pounds FCT per ton. Forging Practice A.
Fig. 6D—Steel 12B, 12 pounds FCT per ton. Forging Practice B.

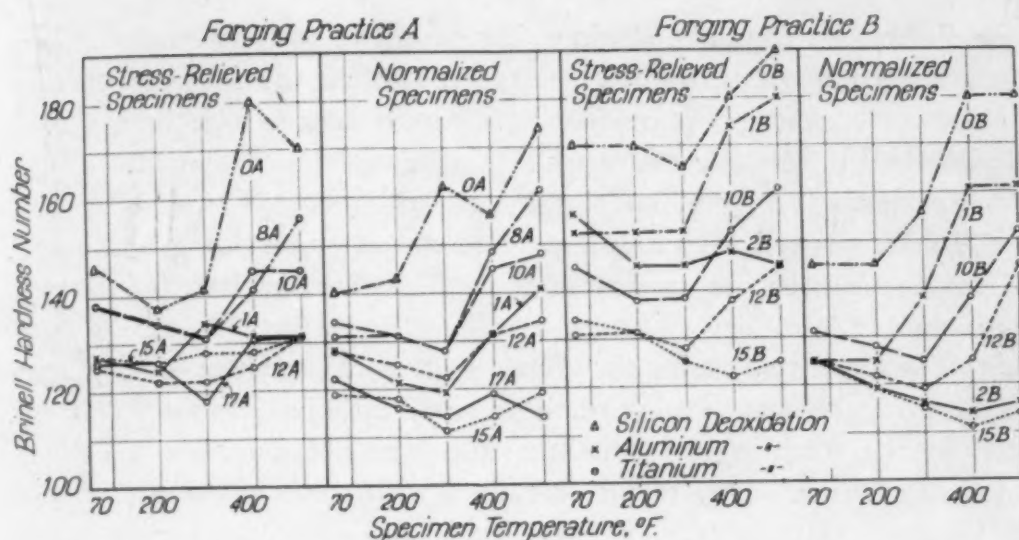


Fig. 7—Brinell Hardness at Different Temperatures.

are definitely inferior by this method of testing, though generally better than steels 0A, 0B and 1B deoxidized with only silicon or $\frac{1}{2}$ pound aluminum per ton. These results are in close agreement with those obtained by the other methods involving impact tests. It is interesting to note that steel 17A, deoxidized with low-carbon ferrotitanium, and containing nearly 0.1 per cent titanium, appears about as free as any of the steels in Fig. 7 from high-temperature hardening, indicating that the single low impact value for this steel in Fig. 5 might reasonably be disregarded.

GENERAL DISCUSSION OF RESULTS

The elimination of susceptibility to strain aging embrittlement in low-carbon steel is shown by this work to depend not only on the degree of deoxidation of the steel, but also in part on the heating and forging practice and the resulting microstructure. The influence of the ingot heating and forging practice by itself is relatively slight, as indicated by the minor differences between the A-series and B-series curves in Figs. 3 and 7 where grain size differences due to heat treatment are absent or ineffective. With the best forging practice, less FCT seems to suffice for restricting the strain aging embrittlement, or hardening at increased temperature. With the normalized specimens, on account of the use of a normalizing temperature as high as 1680 degrees Fahr. (915 degrees Cent.) the effect of grain size differences became important on the impact results, and

the differences found in strain aging embrittlement between the bars forged by the two methods were greater because the forging practices also affected the grain coarsening. Grain coarsening, however, is definitely not the sole cause of strain aging embrittlement, for the microstructures of the stress-relieved specimens of steels 0B and 1B, which showed very low impact values after straining and aging, were found to be just as fine as those illustrated in Fig. 6 for steels 10A and 12A.

The exact reason for the effects of the difference in forging practice on the grain coarsening of these steels on subsequent normalizing, and on the strain aging embrittlement, was not determined because of lack of time. Any results obtained with these small ingots need to be checked by commercial practice, where the reduction in rolling would be very much greater and finished structures similar to those illustrated for steels 10A and 12A in Fig. 7 should be obtainable regularly without any trouble. These tests do indicate, however, that at least in the laboratory-melted steel, strain aging embrittlement can be completely eliminated by the use of titanium for deoxidation, without any aluminum additions. Whether the expense of the titanium for this purpose would be justified commercially depends on how serious the dirtiness of the aluminum-killed steel might be for any particular application, and whether the graphitizing tendency on long service at moderately high temperatures would be eliminated by the substitution of titanium for aluminum. This latter feature of titanium-deoxidized low-carbon molybdenum steels is at present under investigation.

CONCLUSIONS

The conclusions arrived at from this work should be understood to apply to steels melted in an induction furnace and forged from small ingots, and to be subject to confirmation with steel rolled under commercial conditions with the normal amount of reduction from ingot to bar in rolling. With this limitation accepted, the following conclusions can be drawn:

(1) Strain aging embrittlement is practically absent in low-carbon steel deoxidized with 2 or 3 pounds aluminum per ton, and is slight with 1 pound per ton, but may be as serious with only $\frac{1}{2}$ pound per ton as it is in silicon-deoxidized steel without any aluminum or titanium.

(2) Strain aging embrittlement of low-carbon steel is eliminated

equally well by deoxidation with 15 pounds ferro-carbon-titanium per ton, as with 2 or 3 pounds aluminum per ton, and with the most suitable forging practice only 10 or 12 pounds FCT may be sufficient for equally satisfactory results.

(3) Low-carbon steel containing as much as 0.2 per cent titanium derived from low-carbon ferrotitanium, from which some aluminum is also absorbed by the steel, is even more resistant to strain aging embrittlement than aluminum-killed steel.

(4) Susceptibility to strain aging embrittlement is accompanied in low-carbon steel by increasing hardness at temperatures up to 500 degrees Fahr., while steels not subject to embrittlement by strain aging do not harden when so heated. Thus hot Brinell hardness tests may be used as an indication of the comparative resistance of steels to strain aging embrittlement.

ACKNOWLEDGMENTS

The authors gratefully acknowledge the help of many of their associates with this work, especially that of Mr. A. S. Yocco who melted all the steel used and forged many of the ingots. Thanks are due also to the Titanium Alloy Manufacturing Company for supplying the facilities required for the investigation and for permission to publish the results.

DISCUSSION

Written Discussion: By S. L. Case, research engineer, Battelle Memorial Institute, Columbus, Ohio.

Messrs. Comstock and Lewis' paper makes an interesting contribution to a vital subject. The equivalence of 15 pounds per ton of ferro-carbon-titanium and 2 pounds per ton of aluminum in their effect on strain aging embrittlement might prove a strong economic deterrent to the use of titanium for this purpose, unless, as pointed out by the authors, some concurring improvements attributable to titanium should justify the extra cost. In this connection, it may be pertinent to point out that the work-brittleness tests, as carried out in the present work, measure more than mere strain aging embrittlement. Taken alone, the "not aged" curves reflect work sensitivity, i.e., the embrittlement due to cold work, while the spread between the "aged" and "not aged" curves on each steel indicates its strain aging characteristics. From this point of view, the addition of only 4 pounds per ton of FCT apparently had a marked beneficial effect on work-sensitivity, although 15 pounds per ton of FCT were required for complete elimination of strain aging embrittlement.

In comparing aluminum and titanium deoxidation, one is tempted to speculate on the results the authors might have obtained on their strain aging embrittlement tests if instead of employing a standard work-brittleness test specimen, with a 0.025-inch taper, they increased the taper to 0.050 inch. On the standard test specimen, tapered from 0.450-inch diameter to 0.475-inch diameter, the maximum amount of cold work at the last notch is approximately 8.5 per cent reduction of area. If the specimen were tapered from 0.450-inch diameter to 0.500-inch diameter, the reduction of area at the last notch would be about 16.5 per cent, which would bring the test within the range of commercial cold drawing practice. There is a possibility that with an increase in cold work the equivalence of 15 pounds per ton of FCT and 2 pounds per ton of aluminum may no longer hold. Under normal steel-making practice, deoxidation with aluminum does not appear to be sufficient to hold the work-brittleness curve at a high level when the cold work exceeds 10 to 12 per cent reduction of area. If titanium, or some combination of titanium and aluminum, should succeed in doing so, this could prove to be of practical importance.

The so-called hot-hardness tests given in the paper are very interesting. In the true sense, these tests measure aging behavior rather than hardness. If the test is performed on nonferrous metals or on nonaging steels, the hardness curves always slope downward from the original room temperature point. When it is made on aging steels, strain aging is accelerated with an increase in testing temperature, and this reverses the downward trend of the curve. The temperature at which strain aging reaches its maximum appears also to be a function of some inherent difference in steel quality as well as of the rate of load application. In dynamic hardness tests, the maximum may occur at a considerably higher temperature than in static hardness tests. As shown by the authors in Fig. 7, the hardness-temperature curves on all steels slope downward until a temperature of 300 degrees Fahr. is reached; at this point the rate of aging is sufficiently accelerated to reverse the direction of the curves. In this connection, one wonders whether the top temperature employed in these tests was sufficiently high to bring out the maximum strain aging effects on all steels. At 500 degrees Fahr. the direction on most of the curves is still upwards. The tests might have proved more illuminating if they were continued until the curves started to slope downward, indicating completion of aging.

Written Discussion: By G. H. Enzian, Research and Development Division, Jones & Laughlin Steel Corporation, Pittsburgh.

The authors have presented interesting information concerning the use of titanium for preventing strain aging embrittlement in low carbon steels. Whether or not the use of titanium in the large amounts suggested here might be open to the same objections as those cited for aluminum (i.e., dirtiness and tendency to promote graphitization) remains to be seen and preferably, as the authors suggest, with production heats rolled under commercial conditions. There are a few points I should like to mention in connection with the interpretation of the test results and with our experience in the use of titanium.

In the present paper the work-brittleness test has been used as a measure of both strain-sensitivity (by testing as soon as possible after cold working) and of strain aging embrittlement by noting the difference between the test results

in the supposedly not-aged condition and after an accelerated aging treatment. The time lapse encountered between cold working and testing was, however, 3 to 4 hours; with a rapidly aging steel, we believe that aging may progress substantially in this length of time and the results, therefore, may not provide a reliable basis for measure of the extent of strain aging.

For example, the test results shown in Fig. 2 of the paper for steels 0B and 1B, normalized, indicate that these steels are "strain-sensitive" but not as subject to aging as, let us say, steels 10B and 12B in Fig. 4, as measured by the spread between the full and the broken lines. However, the hot hardness test results given in Fig. 7 for these same steels show that the former are the more susceptible to strain aging in that they exhibit the greater increases in hardness from room temperature to 500 degrees Fahr. (260 degrees Cent.). In the case of steels 0B and 1B, then the time lapse of 3 to 4 hours was evidently sufficient for strain aging to be substantially complete and therefore the difference between the two work-brittleness curves for each steel probably is not a true indication of the extent of strain aging.

It has been our practice to use the work-brittleness test as a measure of sensitivity to cold work. However, since it is impractical to make the test without aging taking place to some degree in the interval between cold drawing and testing, we prefer to eliminate that variable by making all tests in the fully aged condition and to determine the extent of strain aging by means of blue heat tests such as hot hardness or hot tensile. Thus the combination of the two tests, work-brittleness and blue heat, can often provide information concerning strain-sensitivity and strain aging which could not be determined by either test alone.

The results given in the paper indicate that the strain aging embrittlement of steel in the hot-rolled or forged condition is somewhat dependent on the rolling or forging practice used; studies we have made substantiate this. Therefore, in order to determine the effect of an alloying element or deoxidation practice, it has been found desirable to make the comparisons after some standard heat treatment such as normalizing.

While it is recognized that normalizing may not completely eliminate the effect of fabricating variables in all cases, the extent to which such variables are eliminated might possibly be considered a function of the steel itself. For example, considering only the aged work-brittleness test results on the normalized steels, it will be seen that heats 2A and 2B, made with 2 pounds per ton of aluminum, have similar curves. However, for all other steels where a comparison of the two forging practices can be made, and even for the two steels treated with 15 pounds per ton of FCT, there are slight differences. The authors state that "some feature of the forging practice B must have lowered the grain coarsening temperature of the steel as compared with the other forging practice." This was true in the titanium-treated steels but not, apparently, in the steels treated with 2 pounds per ton of aluminum.

With further reference to the effects of aluminum and titanium, the authors show, in Fig. 5, that the normalized steel 16A, with 1 pound of aluminum and 10 pounds of FCT per ton, has a slightly better work-brittleness curve than steel 10A made with 10 pounds per ton of FCT alone. It would be interesting to know the effect of forging practice B on a steel deoxidized in the same manner as

heat 16A. It has been our experience that the properties of titanium-treated steels can be markedly improved through the use of small amounts of aluminum in addition to the titanium. Evidently titanium alone is not quite as effective as aluminum in grain size or strain aging control, but when the two are used in combination the desired results may be obtained with relatively small additions of each. It might have been helpful also if the authors had included in their data aluminum and nitrogen contents of the various steels, as it is known that these two elements have a pronounced effect on strain aging.

The effect of titanium on the properties and behavior of low-carbon steels and the mechanisms whereby strain aging in steel is controllable are indeed interesting and useful subjects for study; it is to be hoped that the authors will continue their excellent work along these lines.

Oral Discussion

H. B. WISHART:³ The authors are to be congratulated on their very interesting paper on strain aging embrittlement of low-carbon steels. There are several points of interest on this subject which while not exactly covered in this paper can possibly be answered by the authors.

It is noted that some work was done in connection with a study of hardness variation with increasing temperature in order to predict strain aging. According to the authors the work-brittleness method was preferred over the hardness method as being the most informative. The work-sensitivity test requires a certain amount of sample preparation which is of course time consuming on a large number of tests. If hardness readings could be obtained rather than impact values after the steel was drawn it would simplify the testing. The first question therefore is—have the authors attempted to obtain a correlation between hardness and impact strength on the steel after drawing and, if so, is it indicated that hardness can be used in lieu of impact values?

It is of course noted that all the work in this paper was done on induction heats. Because of this the next question may be a little out of order but I would like to ask whether the authors would care to comment as to whether titanium with reasonable additions would have the same effect on eliminating strain aging in liquid metal steels as on the induction steels.

R. W. HOLT:⁴ I would like to ask what difference in hot shortness, if any, was noticed between the steels deoxidized with aluminum and the steels deoxidized with FCT.

MR. COMSTOCK: Hot shortness is generally due to high sulphur and is corrected by the addition of manganese so that manganese sulphide rather than iron sulphide is formed. According to the evidence that we have, titanium is about as effective as manganese for preventing hot shortness if there is sufficient titanium present.

MR. HOLT: Did you notice any difference between these specific steels killed with aluminum and titanium?

MR. COMSTOCK: We noticed no difference whatever. The manganese was fairly high in all of them.

³Supervisor of Research, Gary Works, Carnegie-Illinois Steel Corp., Gary, Indiana.

⁴Research laboratory, Chicago Steel and Wire Co., Chicago.

Authors' Reply

We appreciate very much the discussions that were offered on this paper.

In reply to Mr. Enzian's comment as to whether titanium-deoxidized steel is any cleaner or any less free from graphitizing tendency than aluminum-deoxidized steel, we can only say that these points were not investigated in these small induction furnace heats. Experience over a great many years in testing steels for cleanliness has shown, however, that while titanium may not make steel entirely clean, it is very much less apt to cause segregated streaks of inclusions, which are a typical result of aluminum deoxidation, especially with large amounts of aluminum. The aluminum oxide shows a great tendency to segregate into streaks or seams, while titanium, as far as the evidence has shown, does not have that tendency.

In regard to graphitizing tendency, we have no evidence as to what the effect of titanium deoxidation would be as compared with aluminum, but that question is being investigated at Battelle Memorial Institute in connection with the research project that is being conducted there on graphitizing of low-carbon steels. We hope to have some information on that later.

Mr. Enzian also pointed out a difference that he thought occurred in the curves that were shown for steels 2A and 2B as compared with 15A and 15B. Except for a single low impact value for steel 15B, however, we would consider the differences in these curves within the experimental error and not to be significant. The test is probably not accurate enough to place any reliance on such small differences.

Mr. Enzian is quite correct in pointing out the possibility that considerable aging may have occurred in steels 0B and 1B in the few hours required for notching the cold-drawn specimens, so that probably there were no "not aged" work-brittleness tests actually made on those steels. His suggestion that hot hardness tests should be used along with the work-brittleness tests on such steels seems reasonable, if it is ever possible for a steel to be strain-sensitive without being subject to strain aging also.

In reply to Mr. Wishart, we did not determine the cold hardness of our steels after straining and we do not think that strain aging embrittlement can be determined even approximately by cold hardness tests, since hardness probably has no relation to the impact values.

In regard to the effect of titanium in decreasing strain aging embrittlement in steel melted in other ways than by electric induction, we have no direct evidence on that, but I believe it was brought out by Mr. Wright a year or so ago that Bessemer steel, if sufficiently deoxidized, showed no greater tendency toward strain aging embrittlement than open-hearth steel. It is a question of deoxidation rather than steel-making practice, and we know of no reason why the effect of titanium should be any different in Bessemer or open-hearth steel than it is in induction fur-

nace steel if the addition can be made effectively. That remains to be proven by actual tests, however, and perhaps different amounts of titanium would be effective.

Mr. Case's discussion was very helpful and his suggestions as to additional work that might be done on this subject are especially appreciated. We are now engaged in investigating the effect of a greater amount of strain, using specimens tapered so that they are larger at the larger end and, therefore, would have greater reduction of area in drawing at the larger end, but we have no comparable results that can be reported now.

We are grateful to Mr. Case for pointing out the improvement in work-sensitivity brought about by the addition of only 4 pounds of ferro-carbon-titanium per ton.

THE COPPER-MANGANESE EQUILIBRIUM SYSTEM

BY R. S. DEAN, J. R. LONG, T. R. GRAHAM, E. V. POTTER
AND E. T. HAYES

Abstract

A study of the transition temperatures in pure electrolytic manganese confirms the existence of three points and places the alpha-beta change at 705 ± 5 degrees Cent. (1300 degrees Fahr.), the beta-gamma at 1092 ± 3 degrees Cent. (2000 degrees Fahr.), and the gamma-delta at 1135 degrees Cent. (2075 degrees Fahr.).

Examination of copper-manganese alloys by thermal analysis, X-ray diffraction and metallographic methods established a copper-manganese equilibrium diagram differing from previously published diagrams by (A) the transition point in pure manganese, (B) position of the solidus, (C) extent of the gamma-beta field, and (D) placement of the alpha-gamma phase boundary.

THE alloys of the copper-manganese system include a series of compositions with unusual damping, electrical and thermal characteristics which have by no means been fully exploited. Recent development and expansion of the electrolytic manganese production have made available commercial quantities of the metal and have opened this and other fields of alloy research. In the course of investigating alloys made with electrolytic manganese in the laboratories of the Federal Bureau of Mines, results were obtained that were not consistent with published diagrams, and it was apparent that discrepancies between these diagrams would have to be cleared up to facilitate a correlation of the properties of alloys in this system. The allotropy of manganese itself has been a problem of academic interest, with a variance of opinion as to the num-

Published by permission of the Director, Bureau of Mines, U. S. Department of the Interior.

A paper presented before the Twenty-sixth Annual Convention of the Society held in Cleveland, October 16 to 20, 1944. Of the authors, R. S. Dean is assistant director, Bureau of Mines, U. S. Department of the Interior, Washington, D. C.; J. R. Long and T. R. Graham are senior metallurgists, E. V. Potter is senior physicist and E. T. Hayes is associate metallurgist, Bureau of Mines, Intermountain Experiment Station, Salt Lake City, Utah. Manuscript received June 3, 1944.

ber of allotropes as well as the temperature of transition. Many of these inconsistencies were due, in part at least, to the impurities normally associated with furnace grades of the metal. Several workers, however, have performed limited experiments with carefully distilled manganese without complete agreement.

TRANSFORMATION POINTS OF MANGANESE

The transformation points found in pure manganese by various investigators are listed in Table I.

Table I
Transformation Points Found in Manganese by Various Investigators

Investigator	Alpha-Beta		Beta-Gamma		Gamma-Delta		Melting Point
	Heating	Cooling	Heating	Cooling	Heating	Cooling	
Gayler	742	682	1043	1005	1188	1195	1244
Yoshisaki	712	701	1093	1087	1148	1152	1254
Grube	736	677	1072	1062	1152	1162	1245
Sieverts & Moritz	770	670	1070	1050	1165	1145	1244
Bureau of Mines		705	1092	1090	1133	1134	1246

Gayler (1)¹ was the first to determine the points of thermal arrest on vacuum-distilled manganese. While three arrests were observed, only three modifications of the metal were recognized; the first, designated as the alpha phase, stable up to 742 degrees Cent. (1370 degrees Fahr.), the second, or beta phase, stable from 742 to 1191 degrees Cent. (1370 to 2175 degrees Fahr.), and the third, gamma, stable from 1191 degrees Cent. (2175 degrees Fahr.) to the melting point, 1244 degrees Cent. (2270 degrees Fahr.). No modification of manganese was attributed to the observed 1005 to 1043-degree Cent. (1840 to 1910-degree Fahr.) point. X-ray investigations of Westgren and Phragmen (2), Bradley and Thewlis (3), Preston (4), and others established alpha and beta manganese as belonging to the cubic system having complex structures with 58 atoms in the unit alpha cube and 20 atoms in the beta unit. Gamma manganese was shown to have a simple face-centered tetragonal structure with an axial ratio of 0.934. Persson (5) and Sekito (6) agreed with Gayler's conclusions. Yoshisaki's (7) results, obtained by ingenious density measurements in molten sodium chloride for the higher temperatures and by dilatometric methods for the 712-degree Cent. (1310-degree Fahr.) point, show a better agreement between the points on heating and cooling than those of Gayler.

¹The figures appearing in parentheses pertain to the references appended to this paper.

Grube's (8) work in 1936, like Gayler's, was conducted by thermal analysis on vacuum-distilled manganese. Neither Yoshisaki nor Grube identified the fourth modification of manganese, but Grube attributed the 1162-degree Cent. (2120-degree Fahr.) point to a delta form and incorporated it in his copper-manganese (9) and palladium-manganese diagrams. The data of Sieverts and Moritz

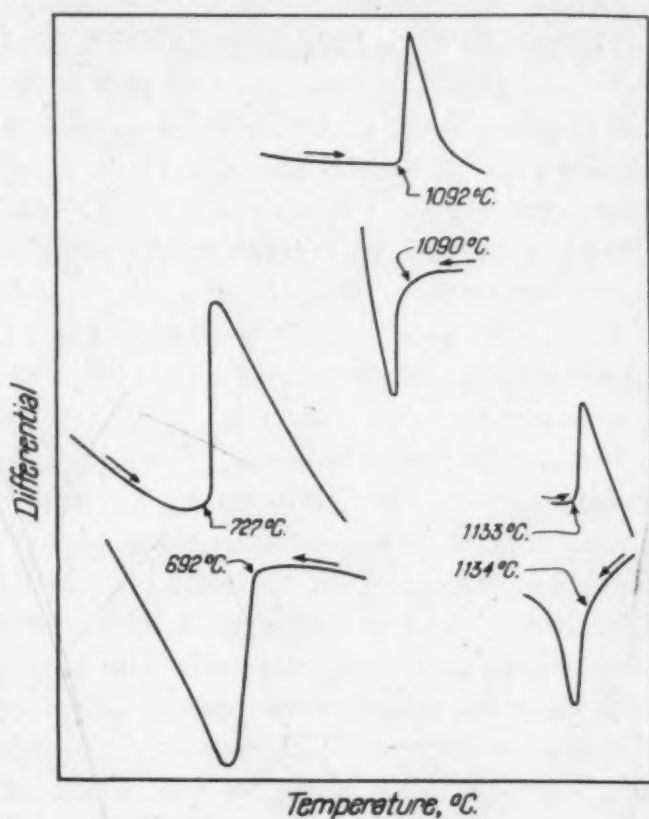


Fig. 1—Differential Curve for Electrolytic Manganese.

(10) on solubility of hydrogen in manganese showed distinct changes corresponding fairly well to the accepted transition points.

Thermal analysis on high-purity electrolytic manganese, conducted in these laboratories, definitely confirms the existence of three arrests. Differential methods with heating and cooling rates of approximately 2 degrees Cent. per minute were used, and the metal was carefully protected from active gases by an atmosphere of purified helium.

As can be seen from the representative curves of Fig. 1, the alpha-beta change occurred at 727 degrees Cent. (1340 degrees Fahr.)

and the reverse at 692 degrees Cent. (1280 degrees Fahr.). This lag, though large, is characteristic of thermal studies on manganese and suggests that the true equilibrium temperature is somewhat below that usually accepted. The reproducibility of the higher temperature and the inconsistencies in the lower temperature found by the various workers has led them to accept the former as the more accurate. This however, is not necessarily the case, for Yoshisaki's dilatometric results give a smaller range and suggest a lower temperature (712 to 701 degrees Cent.) (1310 to 1295 degrees Fahr.). Also thermal studies of copper-manganese alloys show that the change occurs from 705 to 735 degrees Cent. (1300 to 1355 degrees Fahr.) varying with the heating rate, and on cooling it can be depressed well below the lowest temperature noted in the table. Since the results obtained by thermal studies are not reliable because of the sluggishness of the transformation, the temperature has been placed at 705 degrees Cent. (1300 degrees Fahr.) by results of X-ray studies on copper-manganese alloy. This data is considered more accurate and is discussed in the section on X-ray work.

The beta-gamma transformation occurred at 1091 degrees Cent. (1995 degrees Fahr.), with practically no lag between heating and cooling. This temperature is higher than those given by the data of Gayler, Grube, and Sieverts and Moritz, but checks Yoshisaki quite well and is also checked by hydrogen-solubility data (11) obtained in these laboratories. It is reproducible within 3 degrees Cent. and probably is a close approach to the true temperature.

The gamma-delta change at 1133 degrees Cent. (2070 degrees Fahr.) is quite a bit lower than given by any of the other investigators but like the previous point is reproducible within 3 degrees Cent. and has a negligible hysteresis. In addition, it is closely checked by hydrogen-solubility data. Work on copper-manganese alloys has shown similar arrests at high manganese contents, but X-ray and metallographic examination has failed to reveal any differences between material quenched from above and below this temperature range. These data, then, indicate the presence of a fourth form of manganese, but its nature is unknown.

On the basis of this work the transformation points of manganese are placed at 705 ± 5 degrees Cent. (1300 degrees Fahr.), for the alpha to beta change, 1091 ± 3 degrees Cent. (1995 degrees Fahr.) for the beta-gamma, and 1133 ± 3 degrees Cent. (2070 degrees Fahr.) for the gamma-delta.

THE COPPER-MANGANESE SYSTEM

Solidus-Liquidus Lines—A survey of the published diagrams, particularly the later ones, shows reasonable agreement on the liquidus line but considerable disagreement on the course of the solidus line beyond 35 per cent manganese. In the phase diagram published by Lewis (12) in 1902, the minimum in the liquidus occurred at about 50 per cent manganese, and the solidus line was roughly horizontal from this point up to 80 per cent. Wologdine (13) followed in 1907 with another diagram which differed from Lewis' in that a maximum occurred in the liquidus at 80 per cent manganese and a second minimum at 90 per cent. Zhemchuzny (14) and co-workers published results in 1908 with a minimum at 30 per cent manganese; the solidus followed the liquidus quite closely on both sides of the minimum, showing only a small liquid-solid temperature range as compared with previous work. Zhemchuzny's work is worthy of note because of the care taken to minimize the effect of dendritic segregation. In the same year Sahmen (15) published a diagram which approximated Lewis' with the solidus horizontal, or nearly so, from 35 to 70 per cent manganese. Except for Wologdine these investigators believed copper-manganese to form a complete series of solid solutions.

In 1929 Ishiwara (16) presented a diagram (Fig. 4) in which the liquidus and the solidus followed the same general course as those of Lewis and Sahmen and proposed a eutectic horizontal extending from 35 to approximately 75 per cent manganese. Broniewski and Jaslan (17), in a report of investigation published in 1937, proposed a diagram closely paralleling Ishiwara's. Koronev (18) investigated this system and, although he did not present an original diagram, agreed with the general outline given by Ishiwara.

None of these diagrams could be considered final, since all of these investigators used impure manganese made by the Goldschmidt process in preparing their alloys, and this material contained 2 to 10 per cent impurities, including iron, silicon, carbon, and aluminum. Vacuum-distilled metal was first used by Persson in 1932 and later by Grube in 1939. Grube's results were the most complete of all the investigators'. The liquidus line was in general agreement with previous work, and the solidus line on the manganese-rich side of the diagram took an intermediate position between that of Zhemchuzny and that of Lewis. Grube's diagram (Fig. 5) differs from Persson's

(Fig. 6) in that he included his fourth modification of manganese stable between 1067 and 1157 degrees Cent. (1950 and 2115 degrees Fahr.). In 1941 Dean and Anderson redetermined the solidus and liquidus, using electrolytic manganese and pure copper. Their results agreed very well with those of Sahmen as far as the liquidus and solidus were concerned but did not confirm the existence of Grube's delta phase.

The excellent agreement between the results of Grube and Persson with distilled manganese and Dean and Anderson with electrolytic manganese on the general course of the liquidus suggests that it is essentially correct. However, the discrepancies in the solidus curves, particularly beyond 35 per cent manganese, indicate that dendritic segregation, known to be persistent in these alloys, may have brought about considerable error with the methods of thermal analysis used. With this in mind, it was believed that the usual methods of thermal analysis were not applicable and that microscopic examination of specimens quenched from successively higher temperatures would give better results.

For such a study, copper-manganese alloys ranging from 30 to 95 per cent manganese in 5 per cent increments, carefully prepared from electrolytic manganese and pure copper, were forged and then rolled to $\frac{3}{4}$ -, $\frac{1}{2}$ -, $\frac{3}{8}$ -, and $\frac{1}{4}$ -inch square bars. The $\frac{1}{4}$ -inch bar was used in the cold-rolled condition; the others after quenching from two hours at 850 degrees Cent. (1560 degrees Fahr.) following the hot rolling. Specimens of each alloy taken from the different size bars were heated in a tube furnace for 40 minutes, quenched, sectioned parallel to the direction of rolling, and examined microscopically for evidence of melting. Furnace temperatures were adjusted in accordance with results obtained by microscopic examination and the temperatures at which melting occurred were determined for each alloy. The temperature for alloys above 40 per cent manganese was accurate to ± 6 and to 2 degrees Cent. in the neighborhood of the minimum.

As a general rule, specimens taken from larger bars showed melting at lower temperatures than those taken from the smaller bars. This is illustrated by the microstructures of the 69.4 per cent manganese alloy heated at 1010 degrees Cent. (1850 degrees Fahr.) in Fig. 2. Banding is quite noticeable here, and melting has taken place preferentially in the areas of greatest segregation. It can also be seen that the $\frac{3}{4}$ - and $\frac{1}{2}$ -inch bars show melting, while the $\frac{3}{8}$ -inch

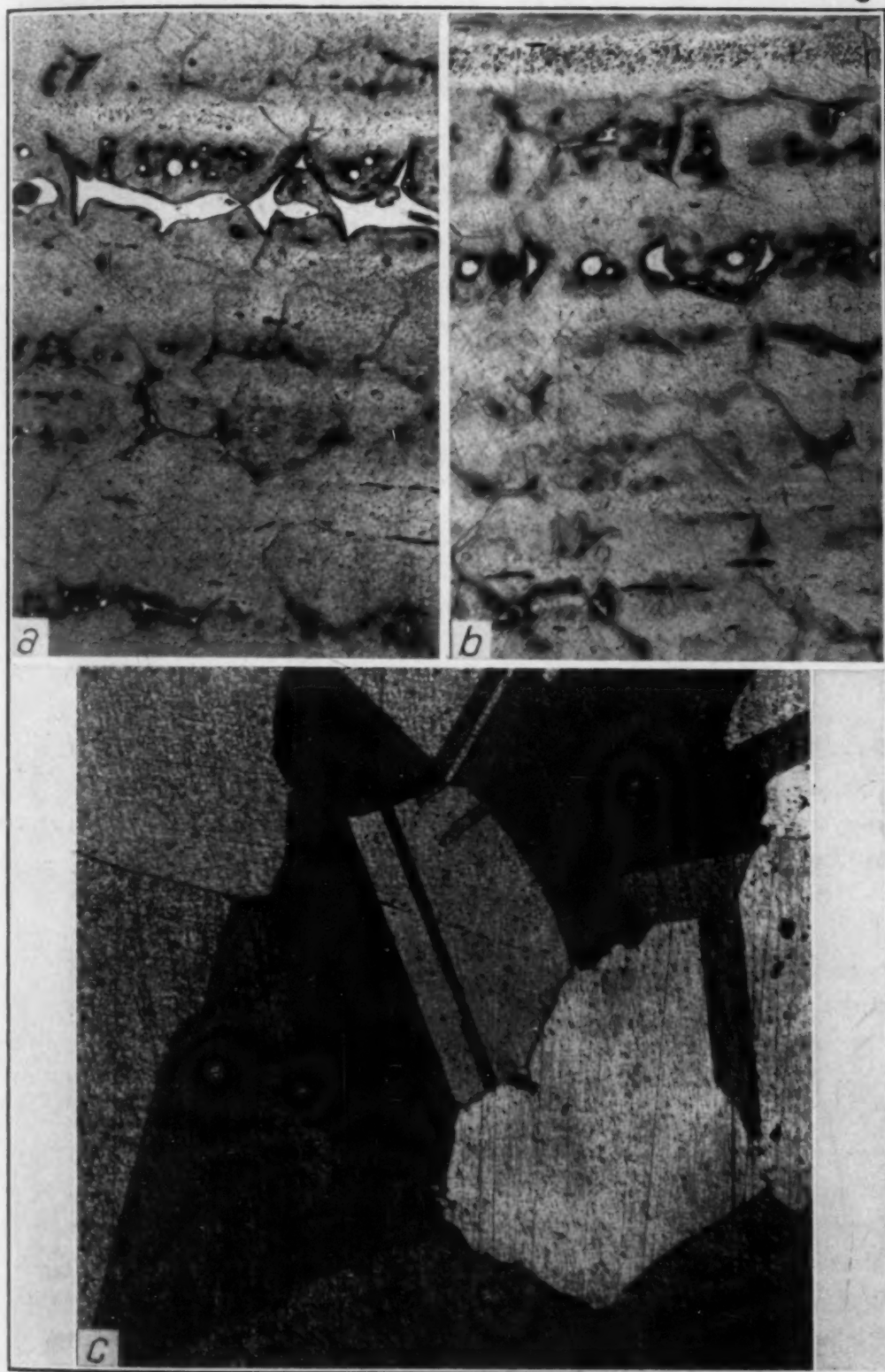


Fig. 2—69.4 Per Cent Manganese at 1010 Degrees Cent. $\times 100$. (a) Three-Quarter Inch Bar. (b) One-Half Inch Bar. (c) Three-Eighths Inch Bar.

bar does not. The $\frac{1}{4}$ -inch bar of this composition had to be heated to 1014 degrees Cent. (1855 degrees Fahr.) before any evidence of melting could be detected. In each alloy the most probable position of the solidus was considered to be the highest temperature to which it could be heated without showing microscopic signs of melting. Results of this work are plotted in Fig. 3 along with data from other workers. The solidus line is considerably higher, as determined in

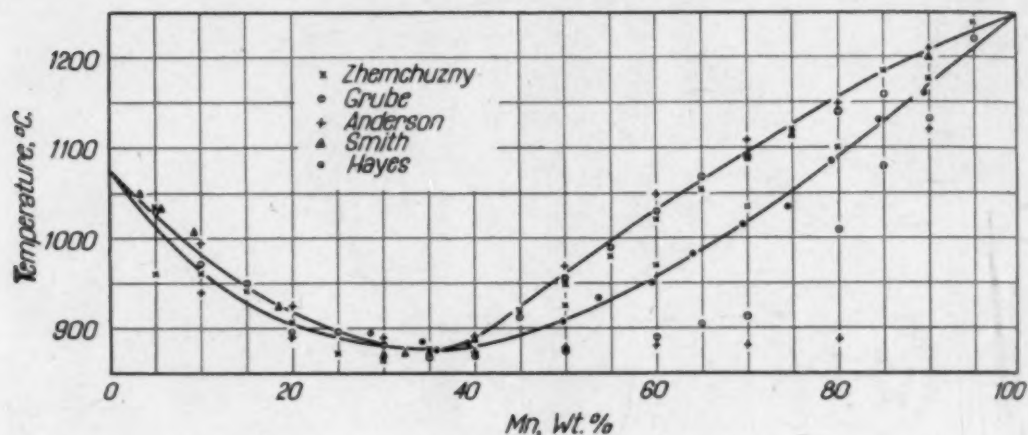


Fig. 3—Solidus and Liquidus Lines of Copper-Manganese System.

these tests, than was indicated by Grube and Persson. The difference is in all probability due to the segregation which takes place in these alloys upon solidification and reduces the accuracy usually expected of thermal studies.

Solubility of Manganese in Copper—Early workers believed that copper and manganese formed a continuous series of solid solutions at both high and low temperatures. Bain (20), Patterson (21), and Corson (22) have, however, noted ranges of compositions that produced heterogeneous alloys. Ishiwara (Fig. 4) placed a solubility limit of manganese in copper at about 32 per cent at the solidus, and showed this decreasing to 22 per cent at room temperature. He also indicated a solubility of copper in gamma manganese with a eutectoidal decomposition into the low manganese solution and beta manganese. Beta manganese is also shown as a stable phase up to 70 per cent copper. This diagram, like those preceding it, is open to question because of the impure grades of manganese used. Persson (Fig. 4) and later Grube (Fig. 5), working with vacuum-distilled manganese, found complete solubility at high temperatures and limited solubility at low temperatures. The results and interpretations of these workers, however, differed in a number of respects.

Persson, noting that the change in axial ratio transformed the face-centered cube of the high copper solutions to the tetragonal face-centered structure of the high manganese solution, suggested phase boundaries to separate these forms. Grube, on the other hand, noting the change was gradual rather than abrupt, considered this to be the normal result of the solution of a cubic metal in a tetragonal one and omitted these boundaries. He also introduced a delta phase and a peritectic reaction at high manganese content.

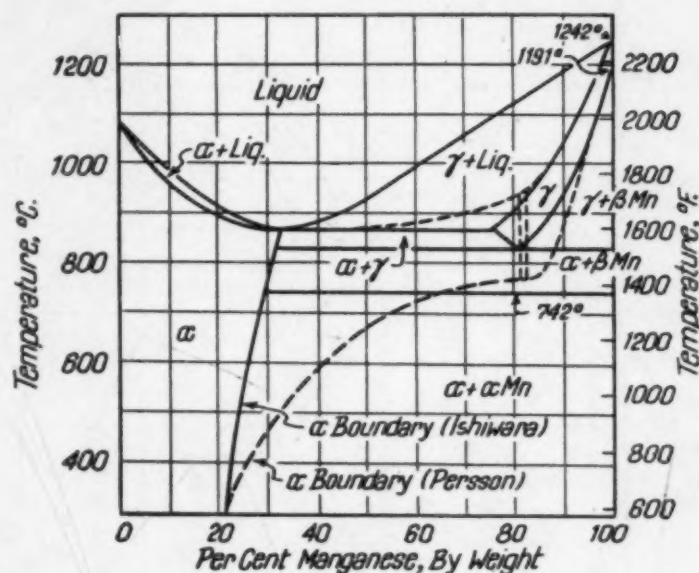


Fig. 4—Equilibrium Diagrams of Ishiwara and Persson (A.S.M. METALS HANDBOOK).

For the work performed in these laboratories, copper-manganese alloys with compositions ranging from 18 to 97 per cent manganese were prepared from electrolytic manganese and high grade copper and treated by schedules calculated to minimize segregation. The manganese used was typical of the electrolytic product and contained only traces of silicon and iron, with no carbon and very low sulphur. The copper showed no significant impurities and was carefully checked from lot to lot to avoid impurities that might interfere with hot working or with other properties of interest. In general, the alloys were chill-cast into 4 by 4-inch ingots, soaked several hours at temperatures known to be in the solid solution range, hot-forged into 1-inch square bars, soaked again, and quenched. These bars were then hot-rolled to $\frac{3}{4}$ -inch square, again soaked in the solid solution range, quenched, and cold-rolled to $\frac{1}{4}$ -inch bars with inter-

mediate heat treatment as required, usually finishing up with material 60 per cent cold-reduced after the last heat treatment.

For the first approximation of the solubility line cold-worked specimens were heated for 24 hours to temperatures ranging from 350 to 850 degrees Cent. (660 to 1560 degrees Fahr.) at temperature intervals of 50 degrees Cent. These were then sectioned longi-

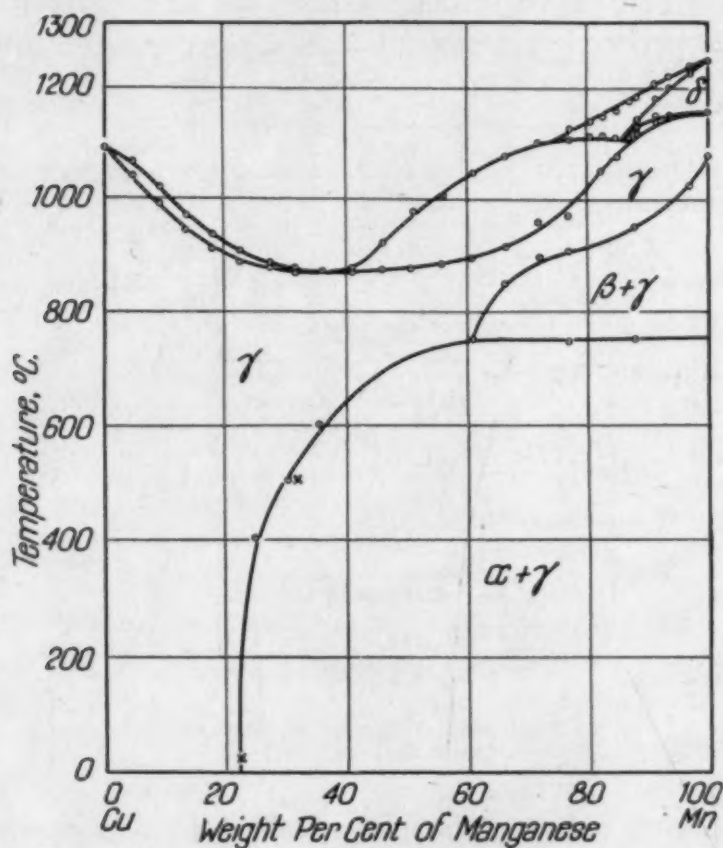


Fig. 5—Copper-Manganese Equilibrium Diagram by Grube.

tudinally and examined under the microscope for evidence of two-phase structures. Wherever two phases were found in specimens heated to approximately 700 degrees Cent. (1290 degrees Fahr.), X-ray examination showed these two phases to consist of alpha manganese with a parameter corresponding to that of the pure metal and a solid solution of manganese and copper. Two-phase structures at 750 degrees Cent. (1380 degrees Fahr.) and above were found to consist of beta manganese with a parameter corresponding to the pure metal and the solid solution. Single-phase structures varied from the face-centered cube of copper to the face-centered tetragonal of gamma manganese, according to the manganese content. After

the initial identification of the phases encountered, alpha manganese and the solid solution phase could be readily recognized under the microscope, but alpha and beta manganese could not be easily distinguished from each other. X-ray examination was, therefore, necessary to place the boundary of the change from alpha to beta manganese.

Rough approximations of the phase boundaries were made from

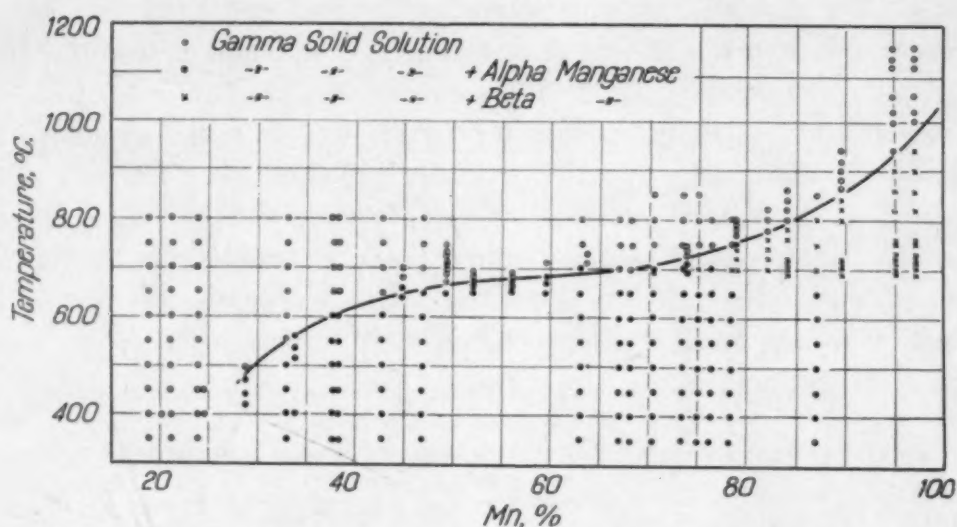


Fig. 6—Solubility Line from Metallographic Data.

these data, and temperatures chosen for the second set of specimens to place the boundaries more accurately. Additional checks were made where necessary and the phase boundaries finally drawn as shown in the plot of the data in Fig. 6. According to this plot, the solubility curve of manganese in copper rises rather gradually from 24 per cent at 400 degrees Cent. (750 degrees Fahr.) to 40.4 per cent at 620 degrees Cent. (1150 degrees Fahr.), cuts across the diagram to 67 per cent at 700 degrees Cent. (1290 degrees Fahr.) with a small slope, and then rises steeply to 1092 degrees Cent. (2000 degrees Fahr.) at 100 per cent manganese. The limiting temperatures found for the alloys examined are given in Table II along with the temperature intersection of the final phase boundaries taken from the graph.

X-RAY STUDIES

The X-ray studies of this investigation were guided by those of Persson and Grube, since only they report any considerable amount

of such data. This part of the work had three objectives, first, to determine the parameters of the gamma solid solution, second, to check the manganese solubility curve, and third to place the alpha-beta boundary.

Iron radiation without filters was used in practically all cases and required an exposure of $1\frac{1}{2}$ hours, with 7-centimeter radius, full circular cameras, when the tube was operated at 40KV and 9 milliamperes. The cameras were designed to accommodate powder, wedge, or wire specimens. It was found that the last two types gave the most satisfactory results, and these were used wherever possible. Systematic errors in the parameter values were eliminated as far as possible by graphical projection or by calculation using Cohen's (23) method. The values obtained by the graphical method were found to check the calculated values within 0.1 per cent and since the former method was much simpler, the latter was used only in a few cases (usually where tetragonal structures were involved).

Table II
Temperature Limits of Single-Phase and Two-Phase Structures from
Metallographic Data

Per Cent Manganese	Upper Limit of Two Phases	Lower Limit of Single Phase	Curve	Per Cent Manganese	Upper Limit of Two Phases	Lower Limit of Single Phase	Curve
18.7	59.5	670	685	690
21.1	63.5	650	700	690
23.9	400	67	650	700	700
24.5	400	450	405	68.2	700	750	700
28.8	470	495	480	69.5	690	705	702
33	450	550	545	73.5	700	750	720
33.9	535	550	550	76.3	700	750	730
37.6	550	600	590	78.3	700	750	750
38.25	550	600	545	78.8	760	775	760
38.8	595	615	605	82.1	780	800	785
42.8	600	650	630	84.1	800	820	800
44.8	640	600	645	87.3	800	850	830
49.3	650	670	665	89.6	840	860	850
52	670	680	670	94.9	900	940	932
56	670	680	670	97	940	1000	970

The parameter curves were obtained on two types of materials, alloys made by regular fusion methods previously described, and alloys prepared by powder methods. The powder alloys were sintered at 850 degrees Cent. (1560 degrees Fahr.) and given 60 per cent reduction by cold rolling prior to final heat treating. Alloys of each group were homogenized by soaking for time periods from 16 to 24 hours at temperatures found to produce single-phase gamma solid-solution structures.

The parameter values were obtained on alloys ranging in compo-

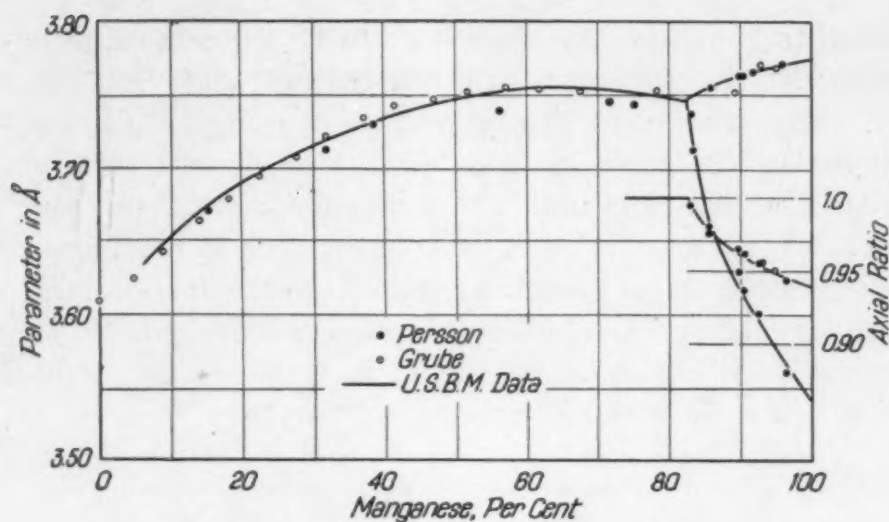


Fig. 7—Parameter Curve for Solid Solution Alloys.

Table III
Gamma Solid-Solution Parameters

Powder Alloys				Fusion Alloys					
Per Cent Mn	Parameter	Per Cent Mn	Parameter	Per Cent Mn	Parameter	Per Cent Mn	Parameter (a)	Axial Ratio	Parameter (c)
6.1	3.634	45	3.741	20.3	3.692	64.6	3.753
10.8	3.658	50	3.745	24.6	3.706	69.0	3.752
15.4	3.674	55	3.749	28.8	3.720	74.0	3.751
20.1	3.688	60	3.754	33.7	3.731	79.0	3.749
24.0	3.702	65	3.755	38.9	3.739	82.0	3.747	1000
27.5	3.709	70	3.752	44.3	3.745	84.1	3.751	.985	3.695
30	3.714	75	3.752	49.1	3.748	89.2	3.761	.963	3.622
35	3.725	80	3.747	53.9	3.750	94.0	3.767	.950	3.579
40	3.735	60.0	3.752	97.1	3.771	.944	3.560
..	100.0	3.774	.938	3.540

sition from 6 to 97 per cent manganese, and the averages of several independent determinations are given in Table III. The error in the average values does not exceed 0.001 Å. The powder alloys show somewhat lower parameters from 20 to 50 per cent manganese and are considered to be the more reliable. From 50 to 80 per cent manganese, both sets of values agree closely. The parameter curve (Fig. 7) was drawn through the powder-alloy values up to 65 per cent manganese and through the fusion-alloy values from there on. The curve is in substantial agreement with the data of the earlier workers, although Persson's values are slightly lower from 40 to 80 per cent.

The solution of manganese in copper increases the parameter value of copper to a peak value of 3.753 Å for 65 per cent manganese

and further addition of manganese up to 82 per cent causes a slight decrease; the structure remains a face-centered cube throughout this range. The solution of copper in gamma manganese likewise expands the lattice, increasing the "c" axes of the tetragonal and increasing the axial ratio until it becomes unity at 82 per cent manganese. This change in axial ratio, transforming the face-centered tetragonal structure of gamma manganese to the face-centered cubic structure at 82 per cent manganese, is gradual, and, as noted by Sekito and Grube, can be considered as a reasonable result of the solution of a cubic metal in a tetragonal one.

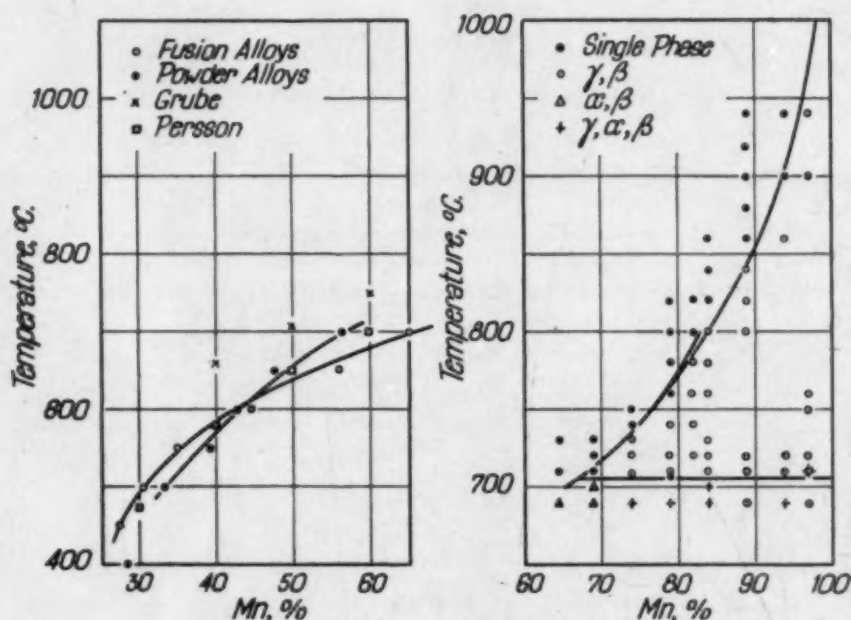


Fig. 8—Solubility of Manganese from X-Ray Data.

The solubility of manganese in copper was determined on alloys heated to temperatures from 400 to 700 degrees Cent. (750 to 1290 degrees Fahr.) until they had reached equilibrium. In some cases this required four weeks. These heat treatments generally produced two-phase alloys containing a gamma solid solution and alpha manganese. When equilibrium was reached, the parameter of the gamma solid solution in the two-phase alloys was constant within experimental error. The average gamma solid-solution parameters obtained for the various temperatures with the corresponding solubilities are shown in Table IV. The solubility curves are given in Fig. 8, along with the data obtained by Persson and Grube. These solubility curves are not consistent with each other or with that in Fig.

6, obtained by microscopic methods. Since the latter method gives lower values and is much more sensitive, the X-ray data were not considered in the final equilibrium diagram.

To place the alpha-beta boundary, cold-worked solid solution alloys were heated to various temperatures ranging from 680 to 800

Table IV
Solubility Limits

Temperature Degrees		Powder Alloys		Fusion Alloys	
Cent.	Fahr.	Parameters A	Solubility	Parameters A	Solubility
700	1290	3.752 ± 0.001	56.5 ± 1.0	3.753 ± 0.003	65 ± 10
650	1200	3.743 ± 0.002	47.5 ± 2.0	3.751 ± 0.002	56 ± 5
600	1110	3.737 ± 0.001	42.8 ± 0.7	3.745 ± 0.002	44.5 ± 3
550	1020	3.732 ± 0.002	39.2 ± 1.5	3.733 ± 0.002	35 ± 1.2
500	930	3.722 ± 0.002	33.3 ± 1.5	3.724 ± 0.003	30.5 ± 1.0
450	840	3.716	27.5
400	750	3.711 ± 0.003	28.4 ± 1.2

degrees Cent. (1255 to 1470 degrees Fahr.). The initial precipitation in these alloys was beta manganese in all cases. However, at 700 degrees Cent. (1290 degrees Fahr.) the beta phase gradually transformed into alpha manganese but did not transform at 710 degrees Cent. (1310 degrees Fahr.). The alloy containing 70 per cent manganese transformed in 72 hours, while longer times were required to complete the transformation at higher manganese contents. These results indicate that the alpha-beta boundary is a horizontal line at approximately 705 degrees Cent. (1300 degrees Fahr.), as shown in Fig. 8, copper having no effect on this transformation. Lattice parameters determined on alpha and beta manganese in the alloys are slightly higher than published results for the metal but are within 0.1 per cent of the values formed for high-purity electrolytic manganese. These data are given in Table V, where they are compared with data on pure manganese. This indicates that there is no appreciable solubility of copper in manganese, and projection to 100 per cent manganese places the alpha-beta transformation in the pure metal at 705 degrees Cent. (1300 degrees Fahr.).

Table V
Parameters of Alpha, Beta, and Gamma Manganese

Phase	Published Values For Manganese	Electrolytic Manganese USBM	Values For Cu-Mn Alloy
Alpha	8.894	8.913	8.904
Beta	6.300	6.317
Gamma	3.774, 0.940	3.774, 0.938

The solubility line in Fig. 6 was further checked by X-ray methods in the temperature range from 700 to 1050 degrees Cent. (1290 to 1920 degrees Fahr.). The temperature and compositions at which beta manganese occurred agreed well with this curve as can be seen in Fig. 8. The gamma solid solution found in this two-phase field was cubic at temperatures up to 780 degrees Cent. (1435 degrees Fahr.) and tetragonal above this. The cubic to tetragonal shift in the gamma solid solution at 82 per cent manganese is in complete agreement with the parameter curve, Fig. 7.

No data have been obtained on the delta phase, and all the alloys which have been quenched from the region in which this phase might appear show only the normal gamma solid solution. This suggests that if the delta phase does exist, it cannot be retained by quenching.

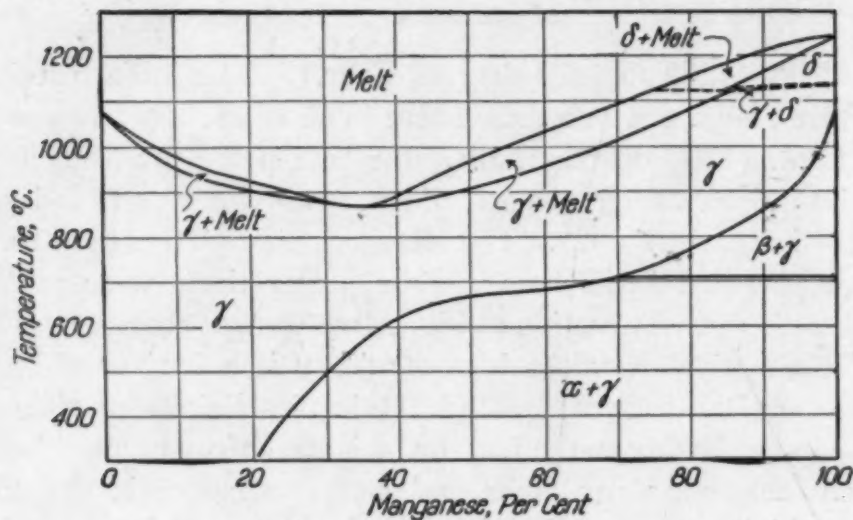


Fig. 9—Copper-Manganese Equilibrium Diagram.

THE EQUILIBRIUM DIAGRAM

The equilibrium diagram for the copper-manganese system assembled from the foregoing data is given in Fig. 9. While this diagram is in general accord with those of Persson and Grube, it differs in several important respects: First, in the location of the transformation points in pure manganese; second, the shape and position of the solidus; third, the extent of the beta-gamma field; and finally, differences in the placement of the alpha-gamma phase boundary.

In this diagram four modifications of manganese are shown: Alpha stable to 705 degrees Cent. (1300 degrees Fahr.), beta stable

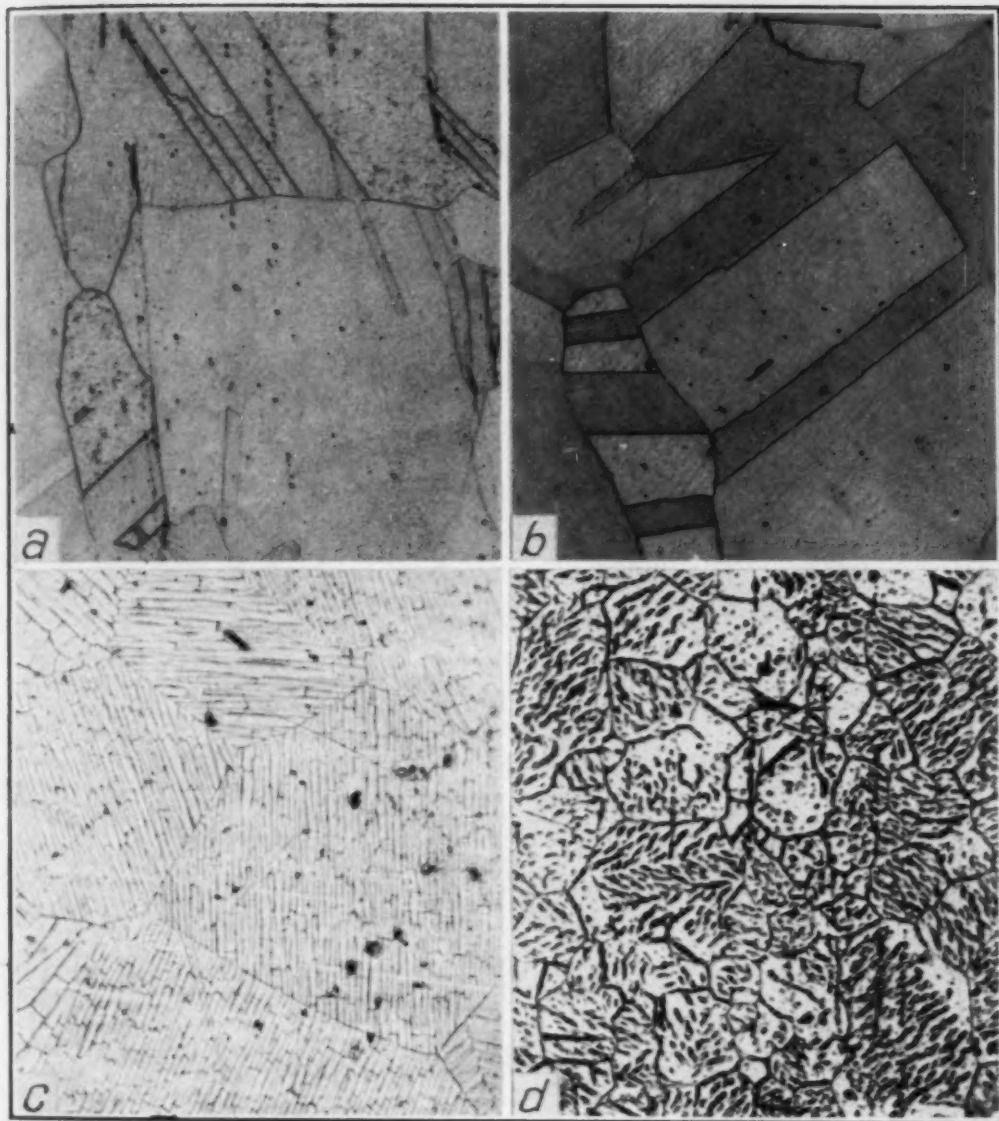


Fig. 10—Typical Structures of Solid Solution Alloys. $\times 150$. (a) 20 per cent manganese, 80 per cent copper, 500 degrees Cent. (b) 40 per cent manganese, 60 per cent copper, 500 degrees Cent. (c) 50 per cent manganese, 50 per cent copper, 850 degrees Cent. (d) 75 per cent manganese, 25 per cent copper, 850 degrees Cent.

from 705 to 1092 degrees Cent. (1300 to 2000 degrees Fahr.) and delta stable from 1133 degrees Cent. (2070 degrees Fahr.) to the melting point, 1244 degrees Cent. (2270 degrees Fahr.). The liquidus and solidus are drawn as shown in Fig. 3, except for the region of the delta phase. Here a peritectic reaction has been dotted in to correlate the 1135-degree Cent. (2075-degree Fahr.) point found in pure manganese with the heat effect observed in the alloys. Thermal studies definitely show heat effects here, but they are beclouded by segregation and are not sufficiently complete to be satisfactorily in-

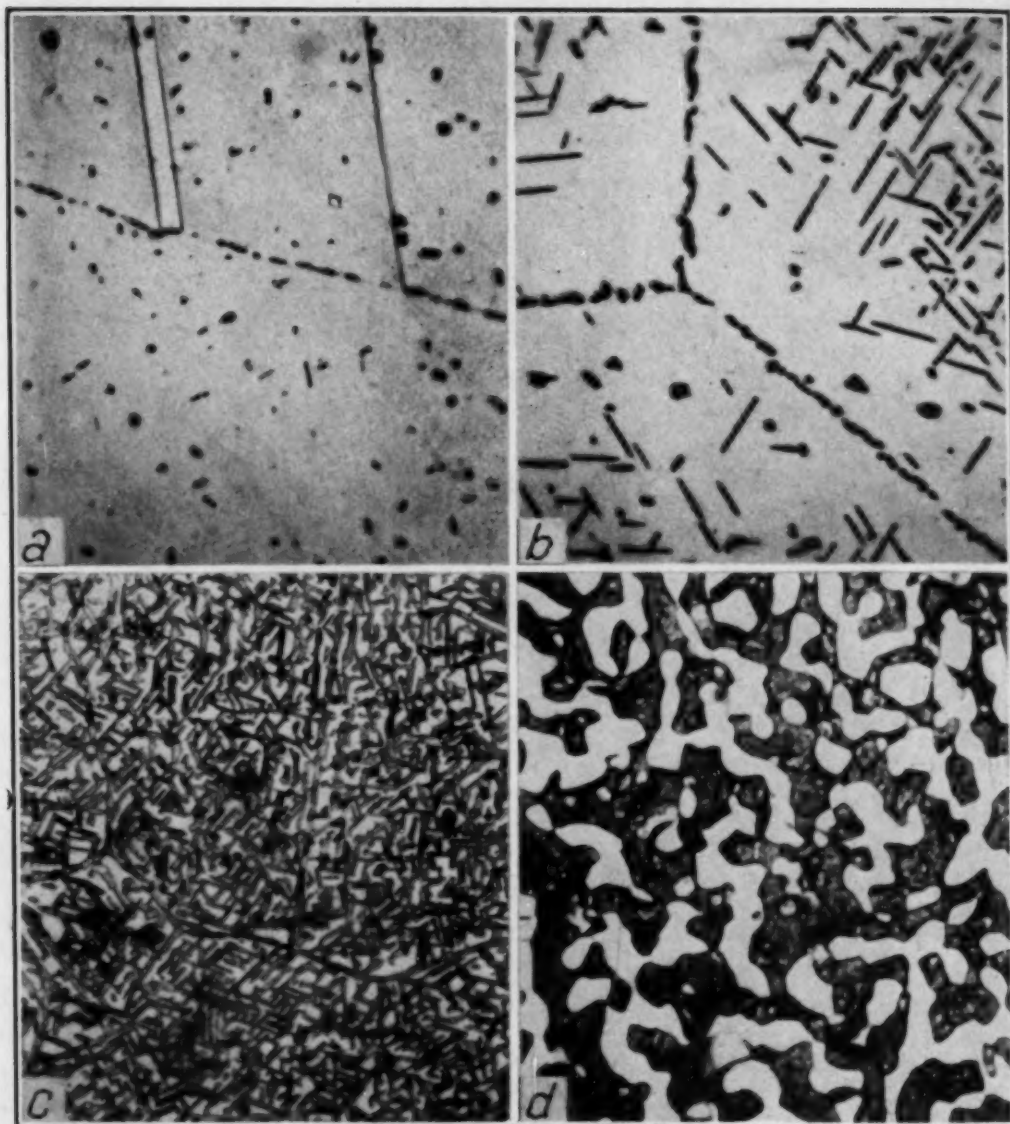


Fig. 11—Typical Microstructures of the Two-Phase Field. $\times 500$. (a) 33.5 per cent manganese, 66.5 per cent copper, 500 degrees Cent. (b) 40 per cent manganese, 60 per cent copper, 500 degrees Cent. (c) 75 per cent manganese, 25 per cent copper, 600 degrees Cent. (d) 85 per cent manganese, 15 per cent copper, 700 degrees Cent.

terpreted. The delta phase in the alloy apparently cannot be retained by quenching and hence cannot be followed by microscopic or X-ray methods.

The other phase boundaries are drawn in accordance with Figs. 6 and 8. Copper is shown to be soluble in gamma manganese, with a continuous solid solution field across the diagram at the higher temperatures. This solution breaks down at lower temperatures when the manganese content exceeds 25 per cent and precipitates alpha or beta manganese. Copper appears to be insoluble in both of these

forms. The gamma-beta transformation is lowered from 1093 to 705 degrees Cent. (2000 to 1300 degrees Fahr.) with 30 per cent copper and entirely suppressed beyond this. The alpha-beta transformation is placed at 705 degrees Cent. (1300 degrees Fahr.) from 0 to 70 per cent copper. Beyond this alpha manganese precipitates directly from the gamma solid solution.

Typical microstructures of the alloys in the various fields of the diagram are shown in Figs. 10 and 11. Fig. 10 shows structures occurring in the gamma solid solution field. Up to approximately 45 per cent manganese, simple polyhedral twinned structures are found and are typical of copper solid solutions. In the range of 50 to 80 per cent manganese a veined or block structure occurs. The significance of this structure is not clear as yet, but it may be related to the tendency for these alloys to coat with copper during etching and also, in part, to grinding and polishing operations. Another view previously expressed by one of the authors (25) suggests that it represents heterogeneity in this field and indicates the co-existence of two or more solid solutions closely related to each other. If this be the case, the diagram is much more complex in this area. Alloys above 80 per cent manganese again have a simple twinned structure.

Fig. 11 shows the microstructure that occurs in the gamma-alpha and gamma-beta fields. Alpha manganese precipitates in the grain boundaries and with prolonged treatment below the solubility line occurs as an oriented precipitate throughout the grain. This is particularly well developed in the 75 per cent manganese alloy. Beta manganese usually occurs in a massive form, as shown in the 85 per cent manganese alloy. When present in large amounts the alpha and beta may often be distinguished by their mode of occurrence, but in small amounts X-ray examination must be resorted to.

It is believed that this diagram is substantially correct and that the difference between it and those previously published are due to dendritic segregation in the alloys, the persistence of this segregation throughout treatment, and the general sluggishness which they exhibit to changes in state. In some cases impurities present in the manganese used have also contributed to these differences.

SUMMARY

The transition points in pure electrolytic manganese have been studied and placed at 705 ± 5 degrees Cent. (1300 degrees Fahr.)

for the alpha to beta, 1092 ± 3 degrees Cent. (2000 degrees Fahr.) for the beta to gamma and 1133 ± 2 degrees Cent. (2070 degrees Fahr.) for the gamma to delta. This has been followed by a review of the copper-manganese alloys resulting in an equilibrium diagram differing in several respects from that previously accepted. Thermal structures in the delta field have confirmed the existence of such a field but have not been sufficient to permit a determination of its limits.

References

1. M. L. V. Gayler, "Alloys of Iron Research, Part 6—Preparation of Pure Manganese," *Journal, Iron and Steel Institute*, Vol. 115, 1927, p. 393.
2. A. Westgren and G. Phragmen, "The Crystal Structure of Manganese," *Zeit. Phys.*, Vol. 33, 1925, p. 777.
3. A. J. Bradley and J. Thewlis, "Crystal Structure of Alpha Manganese," *Proceedings, Royal Society (London)*, A 115, 1927, p. 456.
4. G. D. Preston, "Crystal Structure of Beta Manganese," *Phil. Mag.*, Vol. 5, 1928, p. 1207.
5. E. Persson, "Röntgenanalyse der Kupfer-Manganlegierungen," *Z. physik. Chemie, Abt. B.*, Vol. 9, 1932, p. 25.
6. S. Sekito, "Crystal Structure of Manganese," *Z. Kristallographie*, Vol. 72, 1929, p. 406.
7. H. Yoshisaki, "On the Transformation of Manganese," *Zeit. für Kristallographie*, Vol. 72, 1929, p. 406.
8. G. Grube, K. Bayer and H. Bumm, "Das System Palladium-Mangan," *Zeit. Elektrochem.*, Vol. 42, No. 11, 1936, p. 104.
9. G. Grube, E. Ostreiche, and O. Winkler, "Das System Mangan-Kupfer," *Zeit. Elektrochem.*, Vol. 10, 1939, p. 770.
10. A. Sieverts and H. Moritz, "Mangan und Wasserstoff," *Z. physikal. Chem.*, A180, 1937, p. 249.
11. To be published at an early date.
12. E. A. Lewis, "Alloys of Copper-Manganese," *Journal, Society of Chemical Ind.*, Vol. 21, 1907, p. 842.
13. S. Wologdine, "Alliages de Manganese et de Cuivre," *Rev. Met.*, Vol. 4, 1907, p. 25.
14. S. Zhemchuzny, G. Urasow and A. Rykowski, "Legierungen des Mangans mit Kupfer und Nickel," *Zeit. anorg. Chemie*, Vol. 57, 1908, p. 253.
15. R. Sahmen, "Über die Legierungen des Kupfers mit Kobalt, Eisen, Mangan und Magnesium," *Zeit. anorg. Chemie*, Vol. 57, 1908, p. 1.
16. T. Ishiwara, "On the Equilibrium Diagrams of the Aluminum-Manganese, Copper-Manganese and Iron-Manganese Systems," *Tohoku Imperial University Science Reports*, Vol. 19, 1930, p. 499.
17. W. Broniewski and S. Jaslan, "Sur les Alliages de Cuivre avec le Manganese," *Am. Acad. Sci. Tech. Varsovie*, Vol. 3, 1936, p. 141.
18. N. I. Koronev, "Concerning Alloys of Manganese with Copper," *Acad. Sci., U.S.S.R. (Institute of General and Inorganic Chem.)*, *Annals of Section on Physics-Chemical Analysis*, Vol. 11, 1938, p. 47.
19. R. S. Dean, C. T. Anderson, Moss, Cresop and P. M. Ambrose, "Manganese and Its Alloys," *U. S. Bureau of Mines, R. I. 3477*, 1939. (Revised in 1941 and reprinted as R. I. 3580.)
20. E. C. Bain, "Crystal Structure of Solid Solutions," *Transactions, American Institute of Mining and Metallurgical Engineers*, Vol. 68, 1923, p. 625.
21. R. A. Patterson, "Crystal Structure of Copper-Manganese Alloys," *Phys. Rev.*, Ser. 2, Vol. 23, 1924, p. 552.

22. M. G. Corson, "Manganese in Non-Ferrous Alloys," *Transactions, American Institute of Mining and Metallurgical Engineers, Institute of Metals Division*, Vol. 78, 1928, p. 483.
23. M. U. Cohen, "Precision Lattice Constants from X-ray Powder Photographs," *R.S.I.*, Vol. 6, 1935, p. 68.
24. R. W. G. Wyckoff, "The Structure of Crystals," Second Edition, American Chemical Society Monograph, The Chemical Catalog Company, New York, 1931.
25. R. S. Dean, C. T. Anderson and J. H. Jacobs, "The Alloys of Manganese and Copper: Microstructure of the Alloys," *TRANSACTIONS, American Society for Metals*, Vol. 29, 1941, p. 881.

DISCUSSION

F. M. WALTERS, JR.:¹ This paper is a noteworthy contribution to our knowledge of the copper-manganese equilibrium diagram. The experimental technique used in the determination of the solidus is particularly commendable.

The inclusion of "delta" manganese in the diagram does not seem warranted. The heat evolution observed at 1130 degrees Cent. (2065 degrees Fahr.) is unusual for a phase change; it occurs at a higher temperature on cooling than it does on heating. This fact, as well as the lack of any substantiating X-ray or microscopic evidence, makes the existence of "delta" doubtful.

JOSEPH G. JACKSON:² The paper is interesting and of distinct value.

It is somewhat unrelated to the subject of the paper, but I am wondering whether the authors would care to comment on the resistance of the various phases of manganese to atmospheric corrosion. I am particularly interested in whether all the phases corrode readily at ordinary temperature, or whether certain phases are most resistant to corrosion.

Authors' Reply

Answering Mr. Jackson's question, we have found no difference in the resistance to corrosion among the forms of manganese.

We agree with Dr. Walters that the existence of the "delta" phase is not fully established. Some other data, particularly that on hydrogen solubility, however, confirms its existence. We are, therefore, inclined to accept Grube's inclusion of this phase in the equilibrium diagram pending a more complete study.

Additional data obtained after the paper had been submitted have shown the alpha-beta transformation to take place between 680 and 690 degrees Cent. (1255 and 1275 degrees Fahr.), rather than the 705 degrees Cent. (1300 degrees Fahr.) given. These data are the result of long-time heat treatments of specimens previously quenched from temperatures at which alpha manganese (600 degrees Cent.) and beta manganese (750 degrees Cent.) were precipitated. The specimens were reheated for 50, 100 and 224 hours at 680, 690, 700, 710, 720 and 730 degrees Cent. (1255, 1275, 1290, 1310, 1330 and 1345 degrees Fahr.). Those originally containing alpha manganese were not changed by heating to 680 de-

¹Division of Physical Metallurgy, Naval Research Laboratory, Washington, D. C.

²Metallurgist, War Department, Office of the Chief of Ordnance, Engineering and Inspection Control, Washington, D. C.

grees Cent. (1255 degrees Fahr.), but at 690 degrees Cent. (1275 degrees Fahr.) some beta was formed after 50 hours in alloys ranging from 85 to 96 per cent manganese. After 224 hours, the alpha manganese was transformed into beta with only very small amounts of alpha manganese remaining. These traces of the low temperature form persisted even after 224 hours at 710 degrees Cent. (1310 degrees Fahr.) but had disappeared in specimens heated to 720 degrees Cent. (1330 degrees Fahr.) for that time. Specimens originally containing the beta constituent transform more rapidly, and 50 hours at 680 degrees Cent. (1255 degrees Fahr.) was sufficient for complete transformation. Those heated to 690 degrees Cent. (1275 degrees Fahr.) and higher retained the beta without any change.

It is apparent from these data that the transformation occurs between 680 and 690 degrees Cent. (1255 and 1275 degrees Fahr.) and that the alpha-beta change is much more sluggish than the reverse.

PROPERTIES OF TRANSITIONAL STRUCTURES IN COPPER-MANGANESE ALLOYS

BY R. S. DEAN, E. V. POTTER, J. R. LONG, AND R. W. HUBER

Abstract

Certain anomalies observed in the properties of copper-manganese alloys have been explained on the basis of a suggested mechanism for decomposition of the gamma solid solution. This mechanism consists of distortion of the gamma lattice, eventually producing a definite intermediate tetragonal lattice designated as epsilon. This later breaks down to give a succession of face-centered cubic solutions and alpha manganese, ending with the equilibrium phases. The mechanism is based on X-ray data which give a fairly complete picture, particularly at the higher manganese content, and give the parameter of epsilon at 3.760 Å, with 0.96 axial ratio.

Single-phase tetragonal structures and high damping capacities found in furnace-cooled alloys are considered to result from strained lattice conditions in the initial stages of the decomposition. Anomalies in the resistivity and temperature coefficient of resistance are traced to the presence of epsilon.

DURING the investigation of the copper-manganese alloy system carried on in the laboratories of the Federal Bureau of Mines, the physical properties of a large number of alloys heat treated in a number of ways were determined. These data, in conjunction with microstructure and X-ray data, led to the establishment of an equilibrium diagram which has been presented in another paper (1).¹ A considerable amount of these data, however, cannot be explained by the diagram and have caused much confusion in the interpretation of the data as a whole.

The phenomena that have received particular attention are:

¹The figures appearing in parentheses pertain to the references appended to this paper.

Published by permission of the Director, Bureau of Mines, U. S. Department of the Interior.

A paper presented before the Twenty-sixth Annual Convention of the Society held in Cleveland, October 16 to 20, 1944. Of the authors, R. S. Dean is assistant director, Bureau of Mines, U. S. Department of the Interior, Washington, D. C.; E. V. Potter is senior physicist, J. R. Long is senior metallurgist, and R. W. Huber is associate metallurgical engineer, Bureau of Mines, Intermountain Experiment Station, Salt Lake City, Utah. Manuscript received June 3, 1944.

(a) The occurrence of a single-phase, face-centered tetragonal structure in alloys containing less than 80 per cent manganese, which should always be cubic under equilibrium conditions.

(b) The occurrence of a single-phase microstructure where equilibrium conditions require two-phase structures.

(c) The abnormally low value of electrical resistivity found in slowly cooled alloys.

(d) The high value of the temperature coefficient of resistance found in slowly cooled alloys.

(e) The high damping capacity of alloys given certain heat treatments, compared to those in the equilibrium condition.

As these effects appeared to be associated with nonequilibrium conditions arising from the general sluggishness of the transitions and the mechanism of decomposition of the alloys, attempts were made to approach equilibrium by various means, checking these anomalies at various stages in the process. The specimens were in the form of cold-worked wire and rod in the following heat treated conditions:

(a) Heated to temperatures ranging from 400 to 900 degrees Cent. (750 to 1650 degrees Fahr.) for 24 hours and quenched.

(b) Heated to 850 degrees Cent. (1560 degrees Fahr.) for 24 hours, quenched, reheated to temperatures between 400 and 850 degrees Cent. (750 and 1560 degrees Fahr.) for 24 hours and quenched.

(c) Heated to 850 degrees Cent. (1560 degrees Fahr.) for 24 hours and cooled to room temperature at rates from 40 to 2.5 degrees Cent. per hour.

(d) Heated to 850 degrees Cent. (1560 degrees Fahr.) for 24 hours, rapidly cooled to temperatures between 500 and 550 degrees Cent. (930 and 1020 degrees Fahr.) and held for 24 to 330 hours.

The lattice parameter, electrical resistivity, temperature coefficient of resistance, microstructure, and damping capacity were determined on the alloys.

DISCUSSION OF X-RAY DATA

The equilibrium diagram for these alloys as published in another paper is given here in Fig. 1. The gamma phase in the diagram has a face-centered cubic structure up to 82 per cent manganese and a face-centered tetragonal structure from 82 to 100 per cent manganese, as shown by the parameter curve in Fig. 2. The axial ratio changes gradually from 0.938 to 100 per cent manganese to unity at

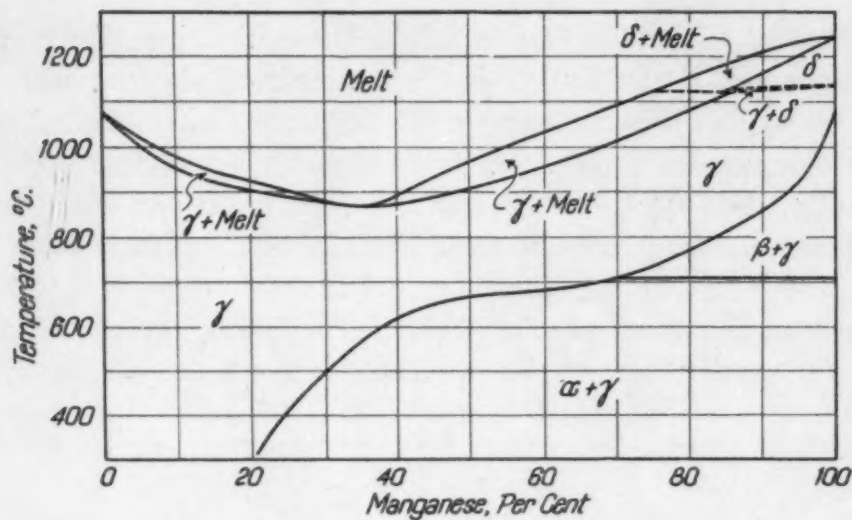


Fig. 1—Equilibrium Diagram.

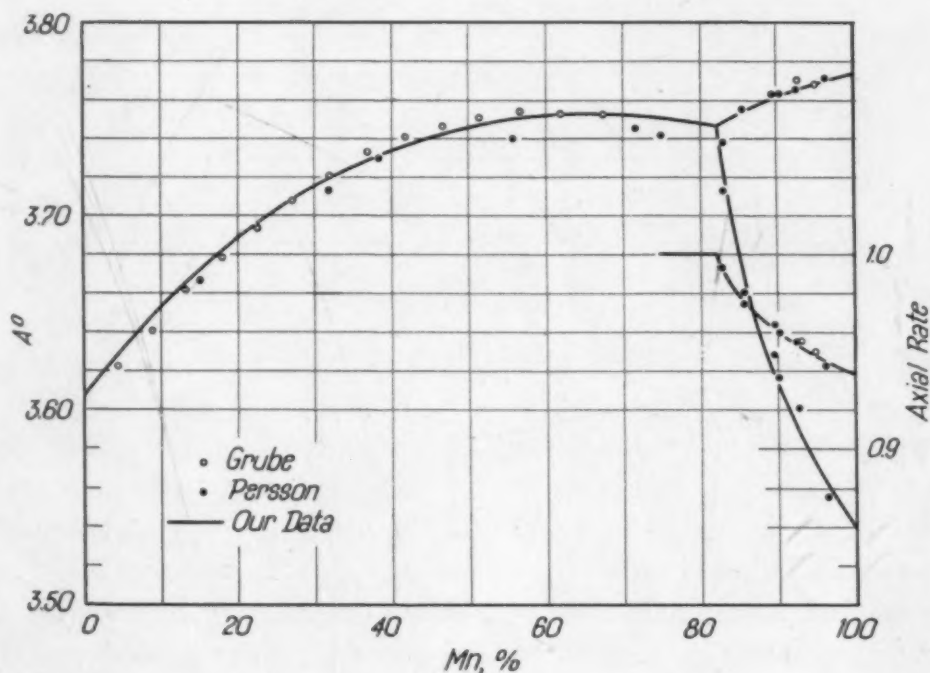


Fig. 2—Parameter Curve, Solid Solution.

82 per cent manganese and the structure remains cubic from here on. The alpha and beta phases show a small solubility for copper, their parameters being essentially the same as those obtained on pure manganese. In the two-phase fields gamma is cubic up to 780 degrees Cent. (1435 degrees Fahr.) and tetragonal above.

The diffraction patterns on alloys cooled at various rates were

not in accord with those expected from the equilibrium diagram. The furnace-cooled alloys had single-phase instead of two-phase structures up to 89 per cent manganese and two-phase structures with higher manganese content. Up to 36 per cent manganese, the single-phase alloys had a face-centered cubic lattice, but above this they were face-centered tetragonal with axial ratios varying from 0.96 to unity. These data are shown graphically in Fig. 3 along with similar data obtained by Ellsworth (2). Ellsworth found single-phase structures up to 90 per cent and two phases at higher manganese contents. The

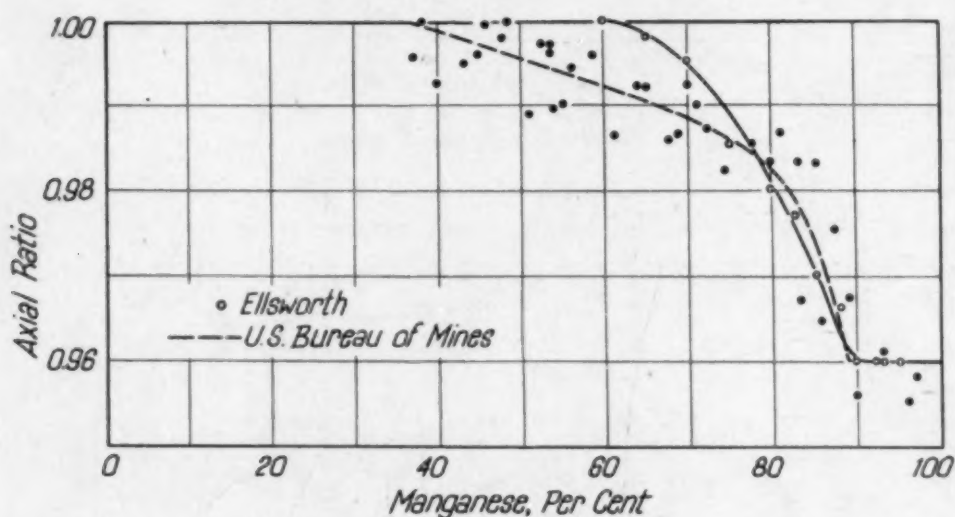


Fig. 3—Axial Ratio, Furnace-Cooled Alloys.

single-phase alloys were cubic up to 65 per cent and tetragonal from 65 to 90 per cent manganese. In each case, the two-phase alloys contained alpha manganese and a tetragonal phase with a parameter of about 3.77 Å and an axial ratio of 0.96. The fact that Ellsworth did not find tetragonal structures below 65 per cent is probably due to a difference in cooling rates between the two sets of data. The axial ratio curve for the alloys heat treated in these laboratories is an average curve, and the axial ratios of the individual alloys showed considerable scatter from this average.

The diffraction patterns of alloys cooled at 20 to 40 degrees Cent. per hour showed broad lines and indicated single-phase structures up to 79 per cent manganese. The 220 line was especially broad but could not be resolved into more than one line. Beyond 79 per cent the lines were sharper, and alpha manganese was present. The 79 per cent alloy cooled at 20 degrees Cent. per hour showed

well-defined lines, corresponding to a single-phase, face-centered tetragonal structure having a parameter of 3.766 Å and an axial ratio of 0.958. These are obviously not equilibrium structures, since the diagram requires a face-centered cubic solid solution and alpha manganese for this field.

These structures were much better resolved in alloys cooled at 2.5 and 4.2 degrees Cent. per hour. In the 4.2-degree-Cent.-per-hour series, the alloys were single-phase up to 40 per cent manganese and definitely three-phase at 50 per cent and above. The 45 per cent alloy showed broadened lines which could not be readily resolved. The three-phase alloys contained alpha manganese and two solid solutions. One was a face-centered cubic structure with a parameter ranging from 3.708 to 3.716 Å, the other a face-centered tetragonal having an average parameter of 3.764 and an axial ratio of 0.959. In the 50 per cent alloy this third phase could not be positively identified as either a cube or tetragonal structure, but it was quite definitely tetragonal at 60 per cent and beyond.

In the series cooled at 2.5 degrees Cent. per hour the results were similar, with the 45 per cent alloy showing three phases. One of these phases was alpha manganese, the second was a cubic solid solution, and the third also appeared to be a cubic solid solution. From 60 per cent up, the three phases were: Alpha manganese, a cubic phase varying from 3.705 to 3.720 Å, a tetragonal phase with an average parameter of 3.762 Å, and an axial ratio of 0.961. The patterns obtained from the alloys in the 2.5 and 4.2-degree-Cent.-per-hour series were characterized by the appearance of two or three distinct lines in place of the fuzzy 220 line previously seen.

Evidently the gamma solid solution is decomposed by several intermediate stages, forming rather definite lattices that are highly developed in the more slowly cooled alloys.

The face-centered, tetragonal, solid solution phases found in the 79 per cent alloy cooled at 20 degrees Cent. per hour, in the alloys above 60 per cent cooled at 2.5 and 4.2 degrees Cent. per hour and in the two-phase furnace-cooled alloys are identical, indicating that they represent a definite stage common to all the alloys containing 60 per cent or more manganese. For the sake of simplicity and clarity in the discussion, it will be referred to as epsilon from here on.

Epsilon was also found in alloys permitted to transform at constant temperatures but never as the only constituent. The accompanying phases were alpha manganese and a cubic solid solution.

Alpha manganese predominated above and the cubic solid solution predominated below 80 per cent manganese. A few of the alloys held at 500 degrees Cent. (930 degrees Fahr.) showed epsilon present at the end of 72 hours, but after 161 hours only a cubic solid solution and alpha manganese were present. Upon holding at 550 degrees Cent. (1020 degrees Fahr.), epsilon occurred in most of the alloys containing 60 per cent or more manganese. It persisted in the 80 per cent alloy as long as 120 hours but was not present in any of them after 168 hours. Quenched alloys reheated to 600 and 650 degrees Cent. (1110 and 1200 degrees Fahr.) for 24 hours showed traces of epsilon, but the pattern did not have a sufficient number of lines to positively identify the phase and permit determination of the parameter.

The X-ray evidence from these series of heat treatments indicates rather definitely that epsilon is a transitional constituent formed by decomposition of the gamma solid solution. It suggests further that alloys above 80 per cent manganese first precipitate manganese and form epsilon, while those below form a cubic phase and epsilon, and that epsilon later decomposes with the precipitation of manganese and the formation of the various cubic solutions noted above.

It is believed that the structures found in the furnace-cooled alloys represent still another stage in the decomposition of the gamma solid solution and occur before the formation of epsilon. They do not appear to be a homogeneous tetragonal structure but probably represent distorted conditions resulting from partial rearrangement of the high temperature solid solutions. The wide variation in axial ratio of the individual alloys plotted in Fig. 3 and the broad lines obtained in the diffraction patterns support this conclusion. In addition, these variable tetragonal structures have been found only in furnace-cooled alloys that have been cooled at rates exceeding 40 degrees Cent. per hour for the first 200 to 300 degrees Cent. It appears then that the single-phase tetragonal structures occur before the formation of epsilon and are preserved by the fast cooling rate, while 20 degrees Cent. per hour permits epsilon to form and the still slower rates, 4.2 and 2.5 degrees Cent. per hour, allow it to partially decompose. The rate of dissolution of epsilon is dependent upon temperatures. At 600 to 650 degrees Cent. (1110 to 1200 degrees Fahr.) the decomposition appears to be almost complete in 24 hours, while 72 to 168 hours at temperature are required for 500 and 550 degrees Cent. (930 and 1020 degrees Fahr.). Epsilon can be pre-

served by slow cooling, probably because the treatment allows sufficient time for its formation but insufficient time for complete decomposition.

The initial cubic solutions accompanying epsilon and those formed by its decomposition are not generally those required by equilibrium conditions. That is, the alloys are not necessarily in equilibrium when epsilon has been completely decomposed. The time required to attain true equilibrium at 550 degrees Cent. (1020 de-

Table I
Time Required to Reach Equilibrium at 550 Degrees Cent.

Mn, Per Cent	Time, Hours	Mn, Per Cent	Time, Hours
40	126-330	70	24-48
45	168-216	75	48-72
50	0-24	80	168-216
60	216-330	85	24-48
65	48-72	90	72-96

grees Fahr.) is given in Table I and ranges from 24 to 216 hours. The 50 per cent manganese alloy reaches equilibrium in the shortest time, while the 40 and 60 per cent alloys require the longest time.

At 80 per cent the long time required can be attributed to the lack of other phases which could act as nuclei and accelerate decomposition of the epsilon. At 60 and 65 per cent manganese, the large difference between average composition and that of the epsilon phase probably retards its initial formation. Once epsilon forms it appears to decompose readily. The sharp decrease in decomposition time for the 50 per cent alloy suggests that a different mechanism may be followed by alloys below 60 per cent manganese. When true equilibrium conditions were attained, the lattice parameters of the solution phases became constant at values corresponding to those given in the paper on the copper-manganese equilibrium system.

The single-phase microstructures reported earlier (3) in these alloys are, therefore, due to these transitional tetragonal structures and their relatively slow decomposition to alpha manganese and the equilibrium solutions. The amounts of precipitated manganese observed in alloys cooled at 4.2 and 2.5 degrees Cent. per hour and in those maintained at 500 and 550 degrees Cent. (930 and 1020 degrees Fahr.) are consistent with the X-ray data. That is, the maximum precipitation of manganese occurs in about the time indicated in Table I. It may, therefore, be concluded that the tetragonal lattices and the single-phase microstructures can be satisfactorily explained by

the data presented and the suggested mechanism of decomposition of the gamma phase.

RESISTIVITY AND TEMPERATURE COEFFICIENTS OF RESISTANCE

The resistivities of cold-worked alloys heated to 500, 600, 650, 700, 800, and 900 degrees Cent. (930, 1110, 1200, 1290, 1470, and 1650 degrees Fahr.) and quenched are plotted against composition in Fig. 4. The 800 and 900-degree Cent. (1470 and 1650-degree Fahr.) curves are typical of gamma solid solution values, and

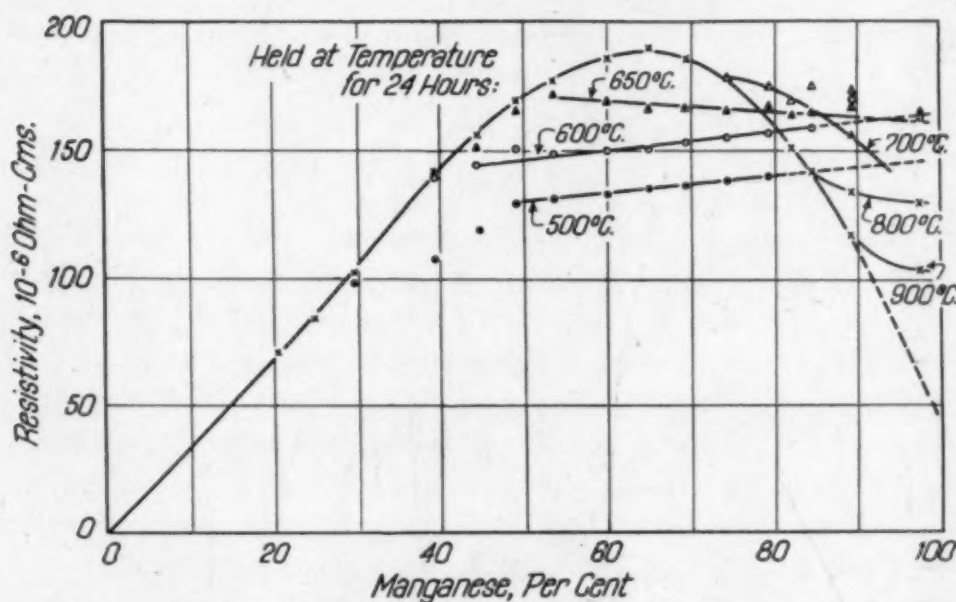


Fig. 4—Resistivity Curves, Cold Worked, Heated and Quenched Alloys.

agree with previously published data (4). However, recent measurements in the Bureau laboratories have indicated a value for gamma manganese of about 45 times 10^{-6} per ohm-centimeter, which is considerably lower than that extrapolated from the earlier data. We have, therefore, projected the curve to this lower value for gamma manganese. The results for the 500, 600, and 650-degree Cent. (930, 1110, and 1200-degree Fahr.) treatment depart from the curve at progressively higher percentages of manganese and then fall on straight lines showing little variation with composition. These may be extrapolated to a value of 145 to 164 times 10^{-6} ohm-centimeters at 100 per cent manganese. The curves for alloys heated to 700, 800, and 900 degrees Cent. (1290, 1470, and 1650 degrees Fahr.) deviate from the gamma solid solution curve on the high manganese

side of the maximum and tend toward low values of resistivity because of the presence of beta manganese preserved by quenching from these temperatures.

The curves of Fig. 5 were obtained by measuring the resistivity of alloys at temperatures ranging from 450 to 850 degrees Cent. (840 to 1560 degrees Fahr.). The alloys were held at temperature for prolonged periods of time until the resistivity values stabilized. These curves for 400 to 600 degrees Cent. (750 to 1110 degrees Fahr.) are exactly what would be expected from consideration of the equilibrium diagram. Theoretically, the resistivity should follow straight lines which start at 100 per cent manganese and intersect the solid solution resistivity curve at a composition corresponding to

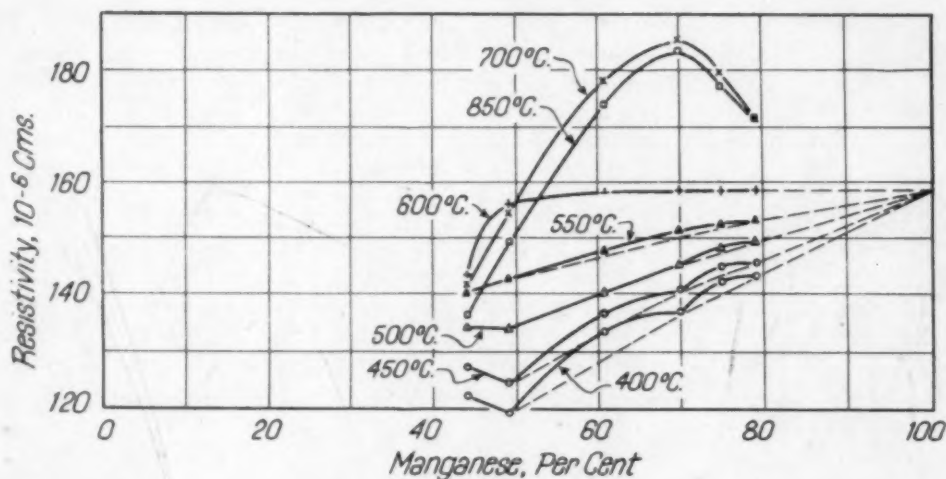


Fig. 5—Resistivity Curves, Alloys at Temperature.

the solubility of manganese in copper at that particular temperature. These data place the resistivity of alpha manganese at 159×10^{-6} ohm-centimeters, in reasonable agreement with values obtained from Fig. 4 and with determinations made on electrolytic manganese shown in Table II. These data also indicate that alpha manganese has a very low temperature coefficient of resistance at least up to 600 degrees Cent. (1110 degrees Fahr.) and that the gamma solid solution has a negative coefficient in the range 600 to 850 degrees Cent. (1110 to 1560 degrees Fahr.).

The temperature coefficients of resistance for the alloys cold-worked, heated to temperatures ranging from 600 to 900 degrees Cent. (1110 to 1650 degrees Fahr.) and quenched are shown in Fig. 6. All the alloys from 20 to 65 per cent manganese have small

negative values for all treatments. For alloys heated to 900 degrees Cent. (1650 degrees Fahr.) the curve rises sharply above 75 per cent manganese. This is characteristic of the gamma solid solution phase. By projection, a value of 40 times 10^{-4} is obtained at 100 per cent manganese, and this checks well with published values for gamma manganese (5, 6,), Table II. The deviation above 85 per cent is due, as previously noted, to the presence of beta manganese. The 700, 750,

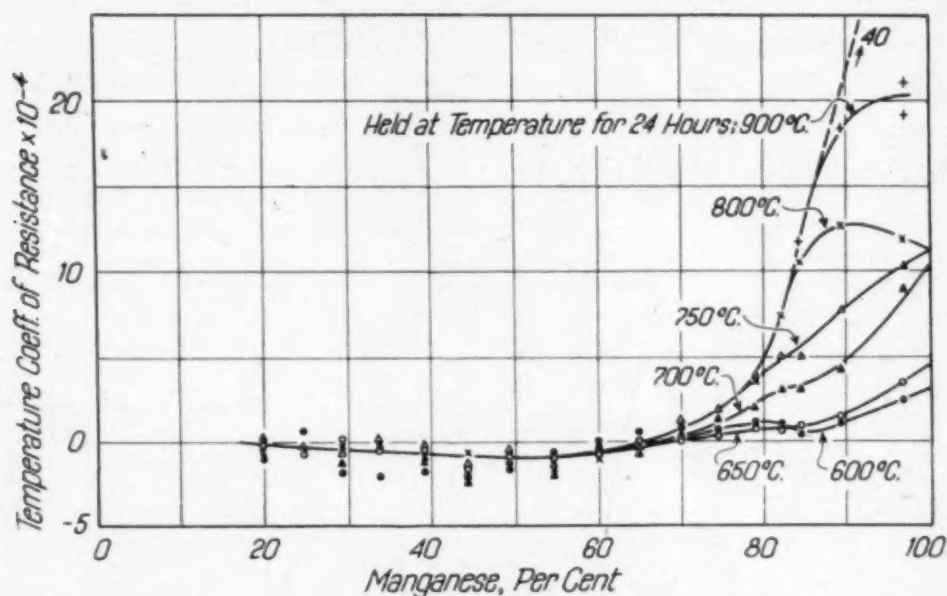


Fig. 6—Temperature Coefficient of Resistance, Cold-Worked, Heated and Quenched Alloys.

and 800-degree Cent. (1290, 1380, and 1470-degree Fahr.) curves also show the effect of beta and may be projected to about 11 times 10^{-4} for beta manganese, in good agreement with published values (5, 7), (Table II). The curves for 600 and 650 degrees Cent. (1110 and 1200 degrees Fahr.) project to values of 3 and 4.2 times 10^{-4} at 100 per cent manganese, corresponding well to those obtained on electrolytic alpha manganese.

Figs. 7 and 8 show the resistivities and temperature coefficients of resistance for alloys cooled at controlled rates of 40 to 2.5 degrees Cent. per hour from 850 degrees Cent. (1560 degrees Fahr.) to room temperature. The decrease in resistivity and the increase in temperature coefficient beyond 40 per cent manganese do not agree with the equilibrium results in Figs. 4 to 6. The resistivities are abnormally low and appear to have a minimum in the neighborhood of 80 per cent manganese. The coefficients rise rapidly from 40 per cent manganese to a peak at 80 to 85 per cent and then decrease.

The 20 to 40-degree-Cent.-per-hour cooling rates gave the highest values and the 2.5-degree-Cent.-per-hour the lowest. These differences are attributed to nonequilibrium conditions resulting from the heat treatment.

The slower cooling rates of 2.5 to 4.2 degrees Cent. per hour would normally be expected to produce a reasonably close approach to equilibrium conditions. However, X-ray diffraction patterns on the alloys so treated definitely show them to be in a nonequilibrium state. On the other hand, the alloys cold-worked and heated to various temperatures were in equilibrium and composed of alpha manganese and the gamma solid solution stable at the temperature of treatment.

Table II
Properties of Alpha, Beta and Gamma Manganese and 80 Per Cent Tetragonal Phase

	Resistivity	Temperature Coefficient	Damping Capacity
Alpha manganese	189×10^{-6} U.S.B.M. Elec. Mn $145 = 160$ U.S.B.M. Alloys	$+ 4.2 \times 10^{-4}$ U.S.B.M. 1.7×10^{-4} Brunke	Appears low
Beta manganese	91×10^{-6} Brunke	Bridgman $8-14 \times 10^{-4}$ 13.6 Brunke	Appears low
Gamma manganese	44.5×10^{-6} Elec. Mn	Brunke $39-53 \times 10^{-4}$ (Brunke, Valentiner, Becker)	Appears high
80 per cent tetragonal	94.2 U.S.B.M. (20°/hr.)	19.4×10^{-4} U.S.B.M. (20°/hr.)	Seems low

In general, alloys in the metastable condition can consist of at least three phases, a cubic solid solution phase with varying compositions, epsilon and alpha manganese. The relative amounts are dependent upon the heat treatment, composition and time. A series of alloys heat treated in the same manner will not reach the same degree of equilibrium, and the properties determined on them cannot be expected to follow a smooth curve. The curves shown in Figs. 7 and 8 illustrate typical values obtained on metastable alloys. Since minimum amounts of other phases were present at 79 and 82 per cent manganese in the slow-cooled alloys, it is believed that the composition of epsilon lies in this range. The 79 per cent alloy cooled at 20 degrees Cent. per hour appeared to be single-phase epsi-

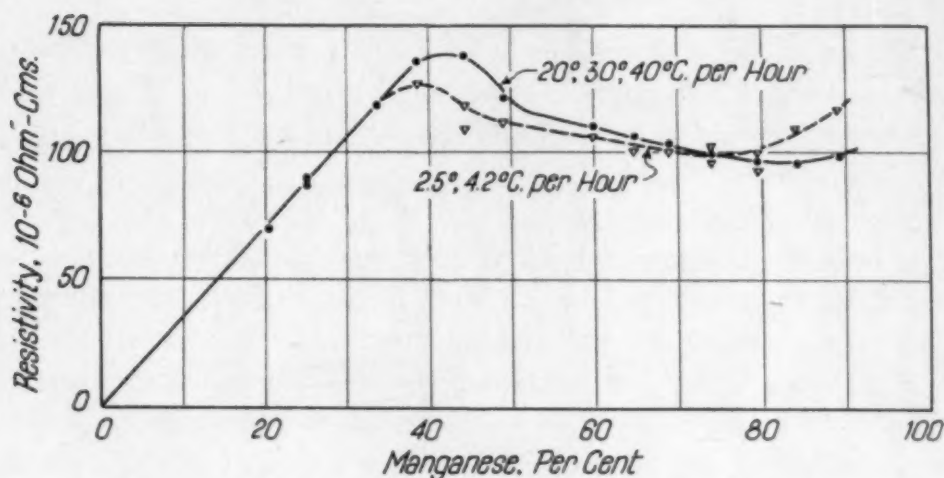


Fig. 7—Resistivity Curves, Slowly Cooled Alloys.

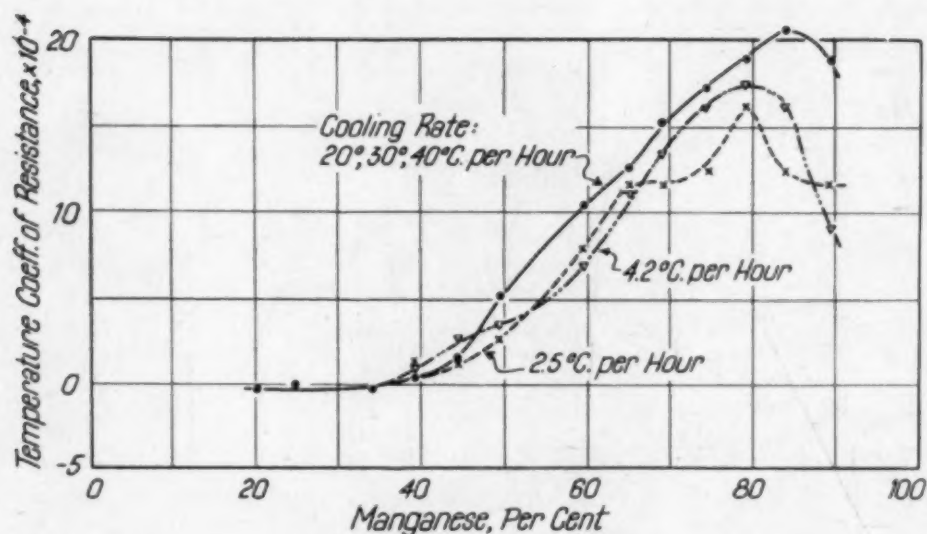


Fig. 8—Temperature Coefficient of Resistance, Slowly Cooled Alloys.

ion, and its properties have been assumed to be representative of the epsilon phase. (Table II.)

The low values of resistivity in Fig. 7 can then be explained by the presence of epsilon predominating at 79 per cent manganese. The increase noted above and below 79 per cent is due to the increasing amounts of other constituents (alpha manganese and nonequilibrium cubic solid solutions). The temperature coefficients of resistance of Fig. 8 can be explained in a similar manner; that is, epsilon, the controlling constituent at 79 per cent manganese, has a

value of 19 times 10^{-4} , and variations on either side of this are due to the presence of smaller amounts of epsilon and increasing amounts of other constituents.

DAMPING CAPACITY

The damping capacity observed in the 850-degree Cent. (1560-degree Fahr.) quenched alloys is shown in Fig. 9. The values, low up to 80 per cent manganese, rise sharply at this point to about 10 per cent, and drop off beyond 88 per cent manganese, where beta manganese is present. Furnace-cooled alloys, however, show appreciable

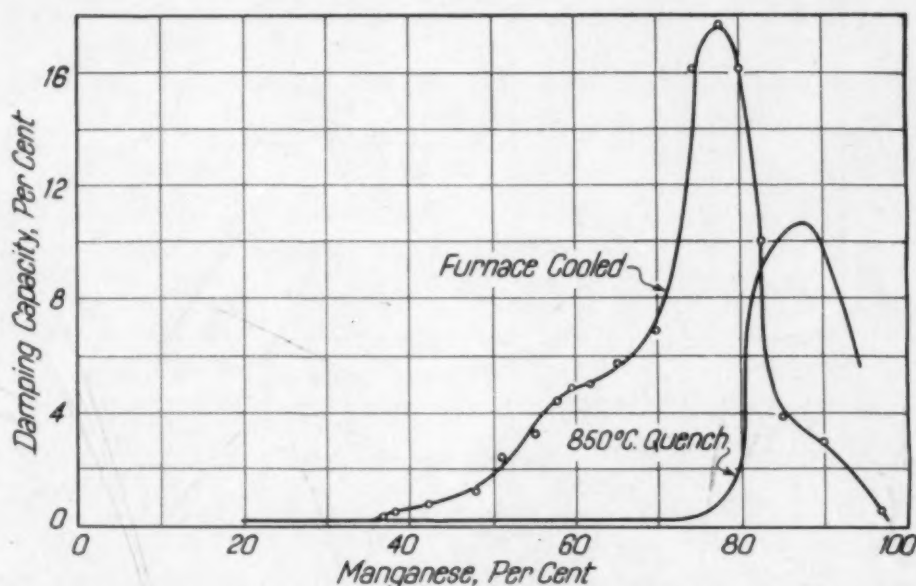


Fig. 9—Damping Capacity, 850 Degrees Cent. (1560 Degrees Fahr.), Quenched and Furnace-Cooled Alloys.

damping capacity as low as 36 per cent manganese, reaching a peak of 17.5 per cent at 77.5 per cent manganese and dropping rapidly with higher manganese contents. Cooling rates (from 2.5 to 40 degrees Cent. per hour) show a similar type of curve (Fig. 10) but the peak damping is considerably lower and occurs between 60 and 70 per cent manganese. The faster cooling rates, in general, give the higher damping, and the slower cooling rates give considerably lower values. They are, however, higher than those obtained by quenching from 850 degrees Cent. (1560 degrees Fahr.) in the range 35 to 80 per cent manganese. While the mechanism of decomposition of the high-temperature solid solution is probably responsible for these high damping capacities, they cannot be wholly explained by the occurrence of epsilon. This is indicated by the alloys showing low damp-

ing capacities in Fig. 10, especially the 79 per cent alloy cooled at 20 degrees Cent. per hour, which is essentially single-phase epsilon. Other treatments producing low damping capacities show structures consisting of epsilon, alpha manganese, and well-defined cubic solid solutions, leading to the conclusion that these phases possess low damping capacities. Alloys showing the high damping capacities in Fig. 10 have structures which are cubic and produce broad lines in the diffraction patterns, while the furnace-cooled alloys with high

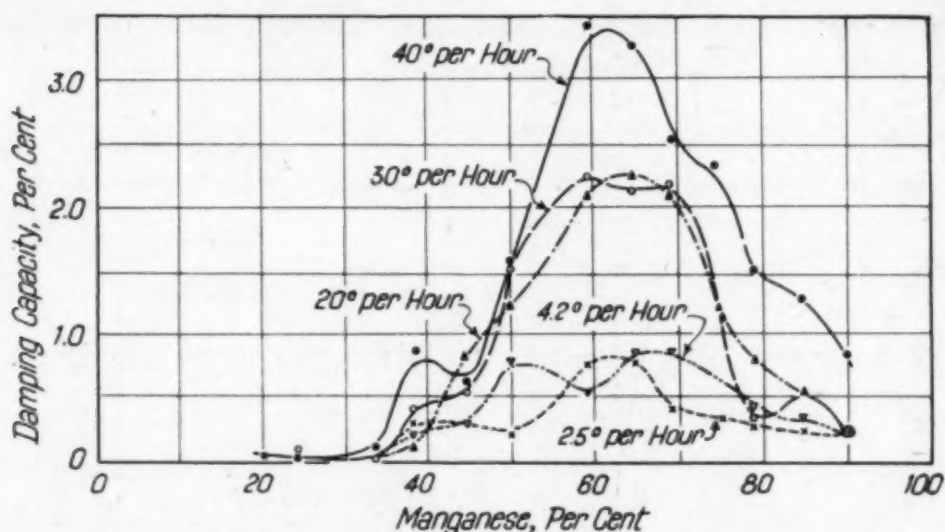


Fig. 10—Damping Capacity, Slowly Cooled Alloys.

damping in Fig. 9 have tetragonal patterns with axial ratios varying as shown in Fig. 3.

These high damping capacities, therefore, appear to be associated with transitional single-phase structures which exist before epsilon is formed. The lattices and the high damping capacities result from strained conditions occurring in the initial stages of decomposition of the gamma solid solution. The high damping capacity of the quenched alloys may be due also, in part, to strained conditions brought about by the quenching but appears to be largely a property of the high temperature equilibrium tetragonal solid solution containing more than 82 per cent manganese. The decrease in the damping capacity, noted in the curve beyond 89 per cent manganese, is the result of quenching from 850 degrees Cent. (1560 degrees Fahr.). At this temperature the higher manganese alloys contain beta manganese.

SUMMARY

The anomalies listed in the first part of this paper have been explained on the basis of a suggested mechanism of decomposition of the high temperature phase to form alpha manganese and a low manganese solid solution.

The first step appears to be a distortion of the solid solution lattices to produce single-phase tetragonal structures having axial ratios that vary and approach 0.960 as a limit. This step ends with the formation of a tetragonal lattice of this axial ratio (designated as epsilon) accompanied by the precipitation of alpha manganese above 80 per cent manganese and by the formation of a series of cubic solid solution below. The second step consists of a breaking down of epsilon by precipitation of more manganese and nonequilibrium cubic solid solutions. The third step consists of a breaking up of these cubic solid solutions to form the equilibrium solid solutions and more alpha manganese.

The single-phase, face-centered tetragonal structures below 80 per cent manganese occur as initial stages in the decomposition of the gamma solid solution to form epsilon.

The single-phase microstructures are the result of these tetragonal lattices and the slow rate of precipitation of alpha manganese.

Abnormally low resistivities and high temperature coefficients of resistance appear to be due to the influence of epsilon which appears to have a relatively low resistivity and a high temperature coefficient of resistance.

The high damping capacity of certain slowly cooled alloys may be correlated with the occurrence of tetragonal structures before the formation of epsilon and attributed to strained conditions in the lattices.

References

1. R. S. Dean, J. R. Long, T. R. Graham, E. V. Potter, and E. T. Hayes, "The Copper-Manganese Equilibrium System," *TRANSACTIONS, American Society for Metals*, Vol. 34, 1945, p. 443-464.
2. Louis D. Ellsworth and F. C. Blake, "An X-Ray Study of the Copper-Manganese Binary Alloys," *Journal of Applied Physics*, Vol. 15, No. 6, June 1944, p. 507-512.
3. R. S. Dean, C. Travis Anderson, and J. H. Jacobs, "The Alloys of Manganese and Copper. Microstructure of the Alloys," *TRANSACTIONS, American Society for Metals*, Vol. 29, 1941, p. 881-898.
4. R. S. Dean and C. Travis Anderson, "The Alloys of Manganese and Copper. The Electrical Resistance and Temperature Coefficient of Electrical Resistance," *TRANSACTIONS, American Society for Metals*, Vol. 29, 1941, p. 788-801.

5. Fritz Brunke, "Investigations on Pure Alpha, Beta and Gamma Manganese," *Ann. d. Physik*, Vol. 5, 1934, p. 139.
6. S. Valentiner and G. Becker, "Susceptibility and Electrical Conductivity of Copper-Manganese Alloys," *Zeit. f. Phys.*, Vol. 80, 1933, p. 735.
7. P. W. Bridgman, *Proceedings*, American Academy Arts and Sciences, Vol. 64S, 1929, p. 55.
8. R. S. Dean, C. Travis Anderson, and E. V. Potter, "The Alloys of Manganese and Copper. Vibration Damping Capacity," *TRANSACTIONS*, American Society for Metals, Vol. 29, 1941, p. 402-414.

AGE HARDENING COPPER-MANGANESE-NICKEL ALLOYS

By R. S. DEAN, J. R. LONG, T. R. GRAHAM, AND C. W. MATTHEWS

Abstract

Hardenable copper-manganese-nickel alloys containing 22 to 24 per cent manganese and equal amounts of nickel are shown to have the ability to harden to Rockwell C 45 and higher. The optimum treatment consists of a solution treatment at 650 degrees Cent. (1200 degrees Fahr.) followed by aging at 350 to 450 degrees Cent. (660 to 840 degrees Fahr.). Hardness may be controlled by regulation of aging times. Material hardened from the cold-worked condition responds more rapidly than the simple solution treated material. The physical properties of the alloy compare quite favorably with those of copper-beryllium alloys. The alloy made with electrolytic manganese has greater elongation at all hardness levels than when made with ordinary commercial manganese and is also somewhat easier to fabricate.

THE scarcity of copper and beryllium and the great war-time demands for the hardenable alloys of these metals prompted a consideration of the copper-manganese-nickel alloys as substitutes. An investigation was made to determine the optimum heat treatment for, and the physical properties that may be obtained in, alloys containing 20, 22, and 24 per cent manganese and equal quantities of nickel.

The preliminary work on copper-manganese-nickel alloys conducted in the Bureau of Mines laboratories was published in a series of three papers by R. S. Dean, C. T. Anderson, and E. V. Potter (1), (2), (3).¹ These papers reported the results of an investigation of electrical properties, coefficient of expansion, and response to heat treatment. It was shown that some of these alloys were

¹The figures appearing in parentheses pertain to the references appended to this paper.

Published by permission of the Director, Bureau of Mines, U. S. Department of the Interior.

A paper presented before the Twenty-sixth Annual Convention of the Society held in Cleveland, October 16 to 20, 1944. Of the authors, R. S. Dean is assistant director, Bureau of Mines, U. S. Department of the Interior, Washington, D. C.; J. R. Long and T. R. Graham are senior metallurgists and C. W. Matthews is assistant metallurgist, Bureau of Mines, Intermountain Experiment Station, Salt Lake City, Utah. Manuscript received June 3, 1944.

susceptible to age hardening, particularly those containing approximately equal quantities of manganese and nickel. Hardness values as high as Rockwell C 45 to C 50 were reported.

In selecting compositions for detailed study a number of alloys were carefully examined, and only those which hardened to Rockwell C 35 or better were considered. This hardness level is readily attained by the copper-beryllium alloys and was assumed as a minimum for all alternate materials. It was found that the composition range capable of maximum hardening corresponded roughly to the pseudo binary line from copper to the compound MnNi as suggested by Dean and Anderson.

PREPARATION OF ALLOYS

The alloys were prepared in heats of about 50 pounds each from electrolytic nickel, wire bar grade copper and high purity electrolytic manganese chips. High-frequency induction furnaces with magnesia crucibles were used for melting and alloying. The most advantageous alloying method consisted of melting the copper and the nickel down together and adding the manganese gradually after the bath was completely molten. When the manganese was completely dissolved, the metal was deoxidized with about 0.5 per cent pure aluminum and cast into pigs. These pigs were remelted and chill cast at a pouring temperature of 1350 to 1375 degrees Cent. (2460 to 2500 degrees Fahr.) into 4 by 4-inch Gathmann molds with sand rammed hot tops. The ingots were hot stripped and soaked at 785 degrees Cent. (1445 degrees Fahr.) prior to forging. Chemical analyses of the heats are given in Table I.

Table I
Chemical Analyses of Copper-Manganese-Nickel Alloys

Alloy Designation	Per Cent Copper	Per Cent Manganese	Per Cent Nickel
MN 20	60.0	19.9	22.0
MN 22	56.2	21.6	22.0
	56.4	21.4	21.8
	56.1	21.8	22.0
	56.0	21.6	21.6
MN 24	52.0	23.6	23.7

Initial forging of the ingots had to be carefully done with frequent reheating. However, after they had been completely broken down, they were readily forged and rolled at temperatures of 700 to 850 degrees Cent. (1290 to 1560 degrees Fahr.). All heats were

hot-worked into 0.4-inch plate, annealed by heating to 650 degrees Cent. (1200 degrees Fahr.), quenched, cold-rolled to 0.2-inch thickness, annealed again, and cold-rolled further to 0.080 inch (60 per cent cold reduction in thickness). Half of the material from each ingot was again annealed by the 650-degree Cent. (1200-degree Fahr.) treatment and the remainder was used in the cold-rolled condition.

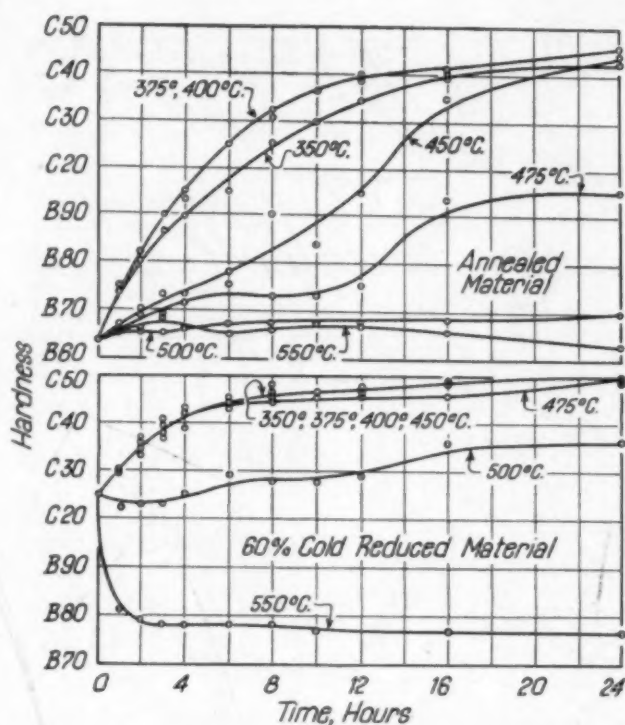


Fig. 1—Time-Hardness Curves for Alloy MN 20.

HEAT TREATMENT

The heat treatment originally recommended for these alloys as being most satisfactory consisted of heating to 850 to 900 degrees Cent. (1560 to 1650 degrees Fahr.) for solution, quenching, and aging at 450 degrees Cent. (840 degrees Fahr.) for 12 hours. However, since this solution temperature produced a rather large grain size which might decrease the ductility at high hardness levels, a series of cold-worked samples of each alloy were solution treated for 1 hour at temperatures ranging from 650 to 900 degrees Cent. (1200 to 1650 degrees Fahr.) and then aged at 450 degrees Cent. (840 degrees Fahr.) for time periods ranging from 4 to 24 hours. Hardness values determined on these samples (Table II) indicated that a

solution temperature of 650 degrees Cent. (1200 degrees Fahr.) would give the most rapid hardening rate and the highest final hardness. Lower solution temperatures were not explored because of the relatively high hardness obtained on material annealed below 650 degrees Cent. (1200 degrees Fahr.) and because the recrystallization range of these alloys was relatively high extending to 550 degrees Cent. (1020 degrees Fahr.) for MN 24. Since this alloy hardens

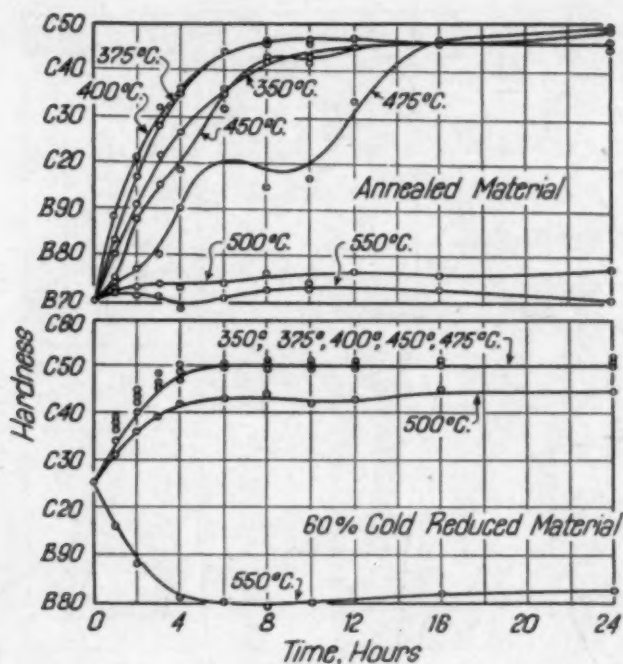


Fig. 2—Time-Hardness Curves for Alloy MN 22.

slightly at the latter temperature, a temperature of 650 degrees Cent. (1200 degrees Fahr.) was consequently used for all subsequent solution treatment. The grain size of the alloys solution treated at this temperature ranged from 0.010 to 0.015 millimeter compared to 0.120 to 0.150 millimeter for the 900-degree Cent. (1650-degree Fahr.) treatment.

To establish the effect of aging time and temperature on material solution treated at 650 degrees Cent. (1200 degrees Fahr.), specimens were hardened at temperatures ranging from 350 to 550 degrees Cent. (660-1020 degrees Fahr.) and for time periods up to 24 hours. These specimens were aged from both the solution treated and cold-worked states. Hardness data obtained and plotted in Figs. 1 to 3 show that temperatures from 350 to 450 degrees Cent. (660 to 840 degrees Fahr.) produced satisfactory hardening in all three

alloys in 24 hours or less. As previously noted, the cold-worked material hardened more rapidly than the solution treated material; alloy MN 24 hardened at the fastest rate and MN 20, at the slowest rate. At 475 degrees Cent. (885 degrees Fahr.) satisfactory hardening was obtained on all alloys as cold-worked but MN 20 did not harden beyond B 90 from the solution treated state. At 500 degrees Cent. (930 degrees Fahr.) none of the alloys hardened from the soft

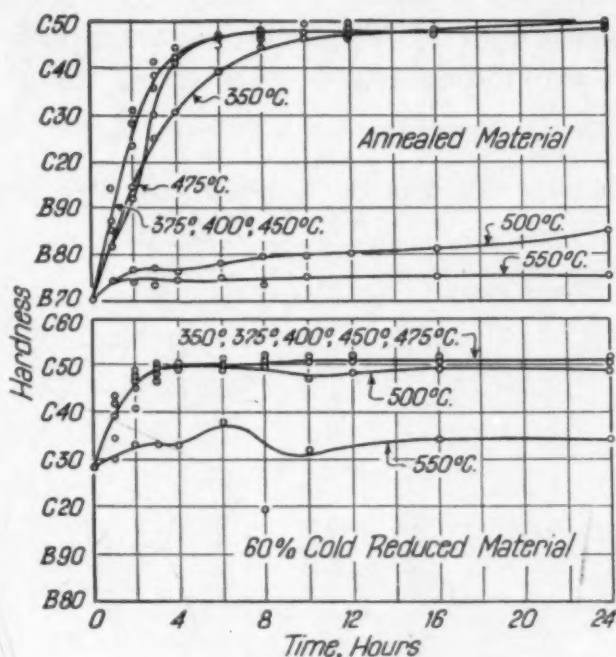


Fig. 3—Time-Hardness Curves for Alloy MN 24.

state, and although they all responded from the cold-worked state, the hardness was slightly lower for MN 22 and MN 24, and considerably lower for MN 20. At 550 degrees Cent. (1020 degrees Fahr.) only the cold-worked MN 24 hardened and that barely reached C 34. The maximum hardness obtained in this series of tests was Rockwell C 52 for the MN 24 alloy.

From these results it was concluded that after solution treatment at 650 degrees Cent. (1200 degrees Fahr.), aging at 350 to 450 degrees Cent. (660 to 840 degrees Fahr.) would produce satisfactory hardening, and that the rate of hardening was such as to permit control of the aging time to obtain any desired hardness in the alloys from Rockwell C 30 to C 45. These data were used in subsequent work to predict the time required to produce a given hardness. Different lots of cold-worked alloys were hardened to within 2 points of

the predicted value. The solution treated material did not respond quite as well.

To note the effects of prolonged treatment at aging temperatures, specimens of each alloy were aged for periods up to 4 weeks at 375 degrees Cent. (705 degrees Fahr.) and at 450 degrees Cent. (840 degrees Fahr.). The results (Table III) show no tendency for overaging at 375 degrees Cent. (705 degrees Fahr.), but at higher temperatures a perceptible decrease in hardness occurs at the end of the second week. This decrease is quite definite at the end of the fourth week; the MN 20 alloy shows the greatest change.

Table II
Change in Hardness With Time at 450 Degrees Cent. After Various Solution Temperature Treatments

Solution Temperature Degrees Cent.	0	4	8	12	16	20	24
MN 20 Alloy							
650	B70	C22	C33	C42	C40	C43	C40
705	B59	B86	C28	C31	C36	C40	C41
760	B58	B83	C21	C34	C37	C42	C40
815	B57	B82	C19	C24	C31	C38	C40
870	B55	B73	B94	C23	C28	C35	C35
900	B52	B74	B38	C18	C25	C36	C34
MN 22 Alloy							
650	B74	C36	C41	C46	C46	C45	C43
705	B61	B93	C32	C34	C37	C41	C41
760	B60	B97	C32	C41	C39	C39	C39
815	B58	B91	C30	C42	C32	C40	C38
870	B55	B86	C24	C42	C29	C35	C36
900	B55	B79	C23	C26	C28	C34	C34
MN 24 Alloy							
650	B76	C43	C45	C47	C48	C45	C46
705	B67	C23	C37	C45	C41	C43	C42
760	B64	C21	C34	C45	C41	C44	C41
815	B63	C97	C37	C43	C35	C42	C38
870	B62	B93	C29	C40	C34	C34	C38
900	B60	B94	C30	C37	C34	C37	C37

Apparently overaging does not readily occur in these alloys, and can only take place at temperatures above 375 degrees Cent. (705 degrees Fahr.) after very long periods of time. This suggests that the alloys can be used successfully at moderate temperatures.

MICROSCOPIC EXAMINATION

Microscopic examination of the hardened alloys shows two different types of structures are developed depending on the aging temperature. When aged at temperatures up to and including 400 degrees Cent. (750 degrees Fahr.), a finely divided precipitate appears in the grain boundary areas and this spreads gradually throughout the grains as illustrated in Figs. 4 and 5. Fig. 5 also suggests that the grains have been considerably altered in the process of precipita-

tion. Aging at 450 degrees Cent. (840 degrees Fahr.) and above produces a grain boundary phase that has but little tendency to spread through the grains themselves. Normally the amount also increases with time and hardness as shown in Figs. 6 and 7. Prolonged aging does not seem to affect the finely divided precipitate, as illustrated by Figs. 8 and 10 for material aged at 375 degrees Cent. (705 degrees Fahr.) for 1 week and 4 weeks, respectively. The amount of grain boundary precipitate formed at 450 degrees Cent. (840 degrees Fahr.) tends to decrease after aging for 4 weeks as shown by a comparison of Figs. 9 and 11 with each other and with Fig. 7. The

Table III
Effect of Extended Aging Time

Alloy	Aging Temperature Degrees Cent.	Initial Condition	Rockwell Hardness				
			24 Hours	1 Week	2 Weeks	3 Weeks	4 Weeks
MN 20	375	Annealed	C46	C49	C49	C50	C50
MN 22	375	Annealed	C49	C50	C51	C52	C52
MN 24	375	Annealed	C50	C52	C52	C52	C52
MN 20	375	60% Cold Red.	C50	C51	C51	C52	C52
MN 22	375	60% Cold Red.	C52	C53	C53	C54	C54
MN 24	375	60% Cold Red.	C52	C55	C54	C55	C54
MN 20	450	Annealed	C44	C44	C43	C42	C40.5
MN 22	450	Annealed	C45	C48	C46	C45	C43
MN 24	450	Annealed	C48	C49	C48	C48	C46
MN 20	450	60% Cold Red.	C48	C47	C45	C43.5	C42
MN 22	450	60% Cold Red.	C50	C48	C47	C46	C44
MN 24	450	60% Cold Red.	C51	C50	C48	C47.5	C46

cold-worked structure in Fig. 11 tends to mask the precipitate, but even taking that into account the amount appears to be less than shown in Fig. 7.

The precipitate responsible for the hardening has not been identified as yet. Dean and Anderson have suggested that an ordered phase corresponding to manganese-nickel may be formed, and its formation at the aging temperature brings about the hardening. X-ray data show two phases to be present after the prolonged aging period. The groundmass has a face-centered cubic structure and is probably a simple solid solution of manganese and nickel in copper; the second phase is undoubtedly the precipitate. There are definite changes in electrical resistance with aging, the resistivity dropping from 87 to 67 microhms per centimeter cube when aged from the solution treated state and from 88 to 63 microhms per centimeter cube when aged for the cold-worked condition. This agrees with the metallographic evidence since precipitation should decrease the re-

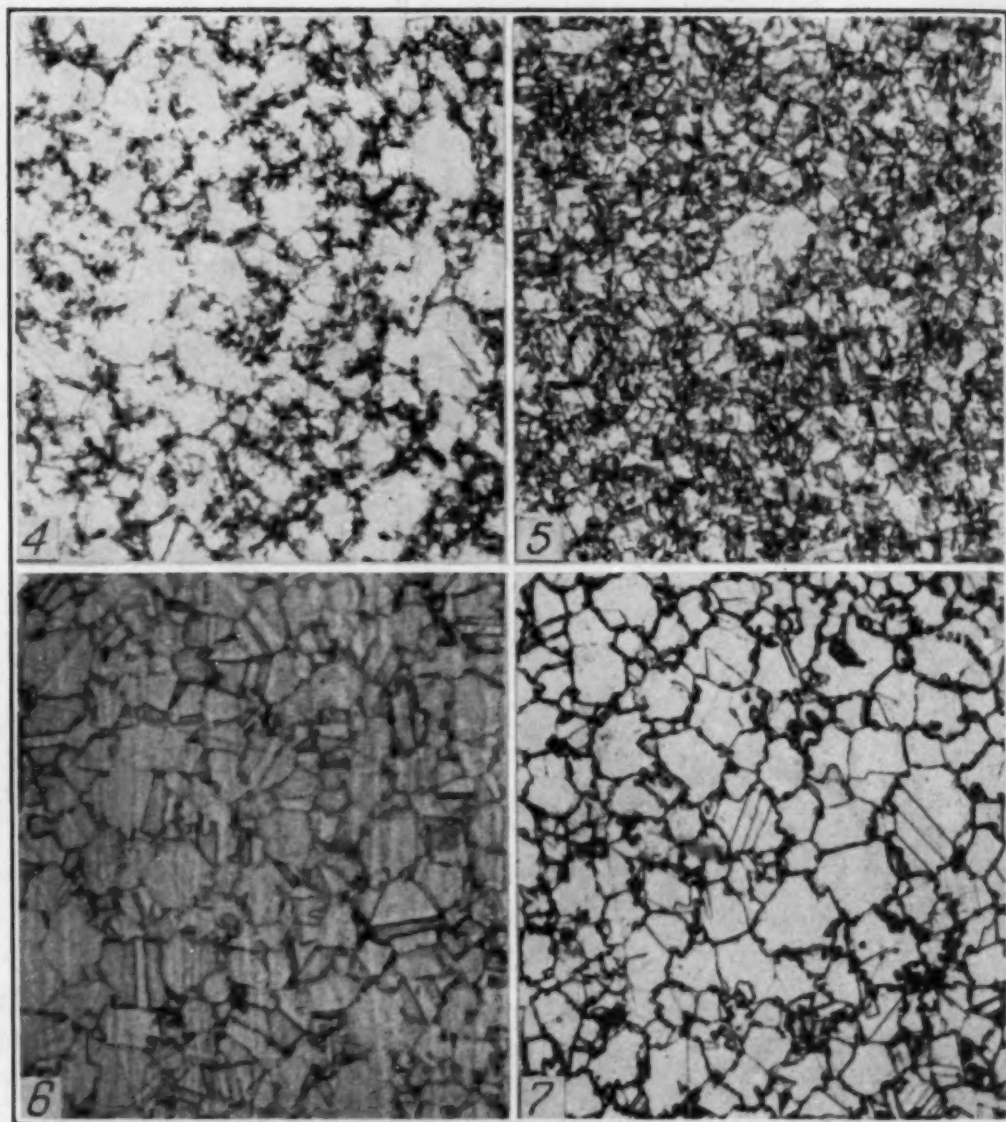


Fig. 4—MN 22. Solution Treated Aged 3 Hours 400 Degrees Cent. (750 Degrees Fahr.). Hardness C38. $\times 250$.

Fig. 5—MN 22. Solution Treated Aged 16 Hours 400 Degrees Cent. (750 Degrees Fahr.). Hardness C48. $\times 250$.

Fig. 6—MN 22. Solution Treated Aged 3 Hours 450 Degrees Cent. (840 Degrees Fahr.). $\times 250$.

Fig. 7—MN 22. Solution Treated Aged 16 Hours 450 Degrees Cent. (840 Degrees Fahr.). Hardness C36. $\times 250$.

sistivity. Formation of an ordered phase would have a similar effect. Fragmentary data indicate that these alloys undergo a volume change at the aging temperature.

TENSILE PROPERTIES

The average tensile properties of the alloys in the annealed state and as cold-worked are given in Table IV. Tensile and yield strengths increase with added manganese and nickel, but the elongation remains

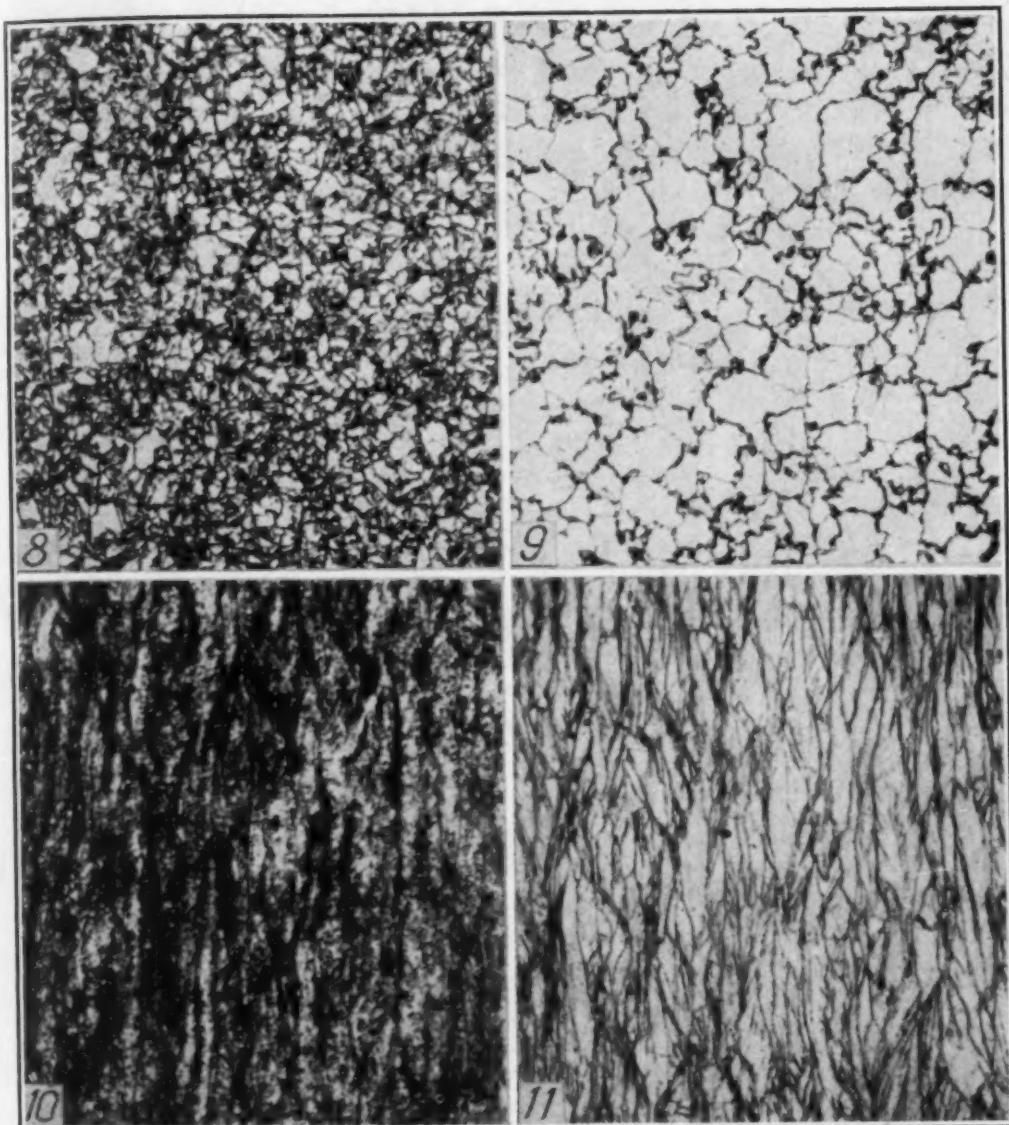


Fig. 8—MN 22. Solution Treated Aged 4 Weeks at 375 Degrees Cent. (705 Degrees Fahr.). Hardness C52. $\times 250$.

Fig. 9—MN 22. Solution Treated Aged 4 Weeks at 450 Degrees Cent. (840 Degrees Fahr.). Hardness RC44. $\times 250$.

Fig. 10—MN 22. Cold Reduced Aged 1 Week at 375 Degrees Cent. (705 Degrees Fahr.). Hardness RC53. $\times 250$.

Fig. 11—MN 22. Cold Reduced Aged 1 Week at 450 Degrees Cent. (840 Degrees Fahr.). Hardness RC48. $\times 250$.

constant at 40 per cent for annealed material. Cold work raises the tensile strength about 50 per cent or more and quadruples the yield strength with a corresponding increase in the proportional limit, and a decrease in elongation.

Tensile data for specimens of MN 22 after hardening at 350, 400, and 450 degrees Cent. (660, 750 and 840 degrees Fahr.) to hardness levels of C 30, C 35, C 40, and C 45 are given in Tables V

and VI. These values are rounded averages taken from the plots of tensile properties versus hardness in Figs. 12 to 17. The plots show the spread of the data for 9 or 10 tensile specimens at each hardness level. The variation in tensile properties for any given hardness is within the limits of experimental error. Considering that several

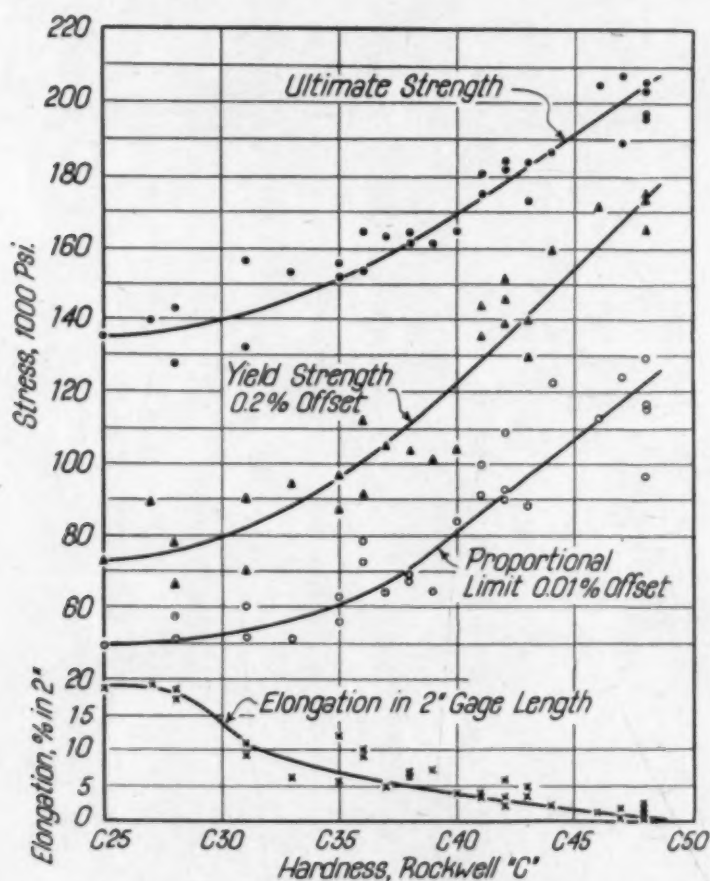


Fig. 12—Tensile Properties of MN 22 Solution Treated and Aged at 350 Degrees Cent. (660 Degrees Fahr.).

different heats of the alloy were involved in this work the spread of the data is not excessive.

In general, more variation occurs in material hardened from the solution treated state (Figs. 12 to 14) than material hardened from the cold-worked state (Figs. 14 to 17). This is probably due to differences in grain size and hardness that occur in the solution treatment and are accentuated by the aging, but which are not significant if the material is cold-worked to 60 per cent reduction in thickness prior to aging. The tensile properties increase regularly with hardness for both conditions, and at all three aging temperatures. The maximum properties of 215,000 psi. tensile, 202,000 psi. yield, and

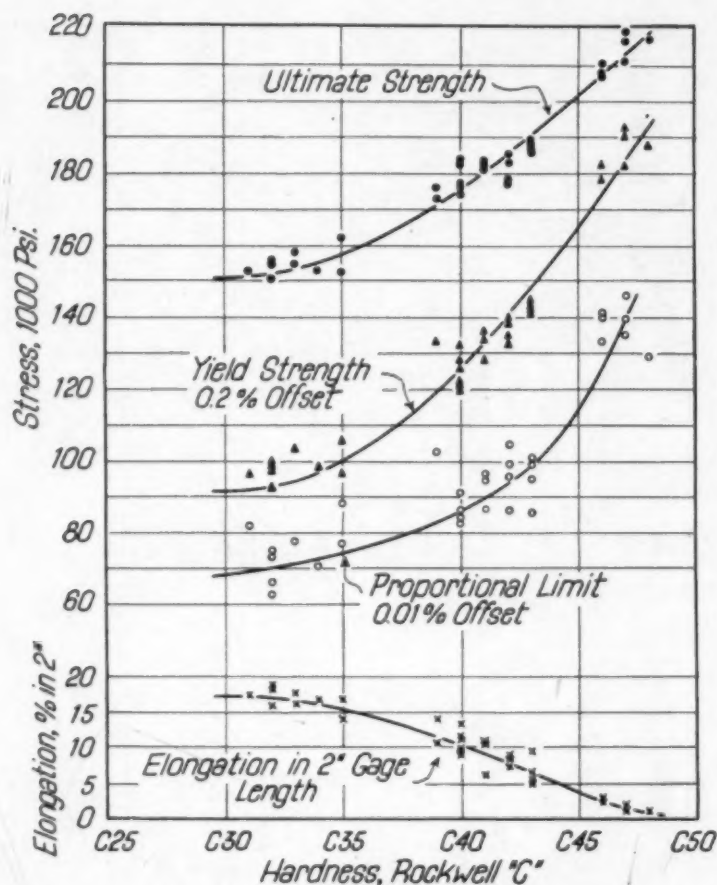


Fig. 13—Tensile Properties of MN 22 Solution Treated and Aged at 400 Degrees Cent. (750 Degrees Fahr.).

Table IV
Physical Properties of Copper-Manganese-Nickel Alloys. Material in Sheet Form as Cold-Worked and as Annealed

Alloy	Condition	Ultimate Strength Psi.	Yield Strength Psi.	Proportional Limit Psi.	Elongation Per Cent	Rockwell Hardness
MN 20	Annealed	84,000	37,000	32,000	39	B74
MN 20	60 Per Cent CR	127,000	124,000	90,000	3.2	C23
MN 22	Annealed	87,000	38,500	27,000	40	B77
MN 22	60 Per Cent CR	134,000	127,500	90,000	3.0	C24
MN 24	Annealed	90,000	42,500	32,000	40.2	B79
MN 24	60 Per Cent CR	136,000	133,000	83,000	3.0	C26

170,000 psi. proportional limit are obtained with a hardness of C 45 at an aging temperature of 450 degrees Cent. (840 degrees Fahr.). The elongation decreases with increasing hardness to a minimum of 1 per cent for the highest tensile values. This decrease is quite regular for the solution treated and hardened material, but the cold-worked and hardened material shows a maximum in the elongation-

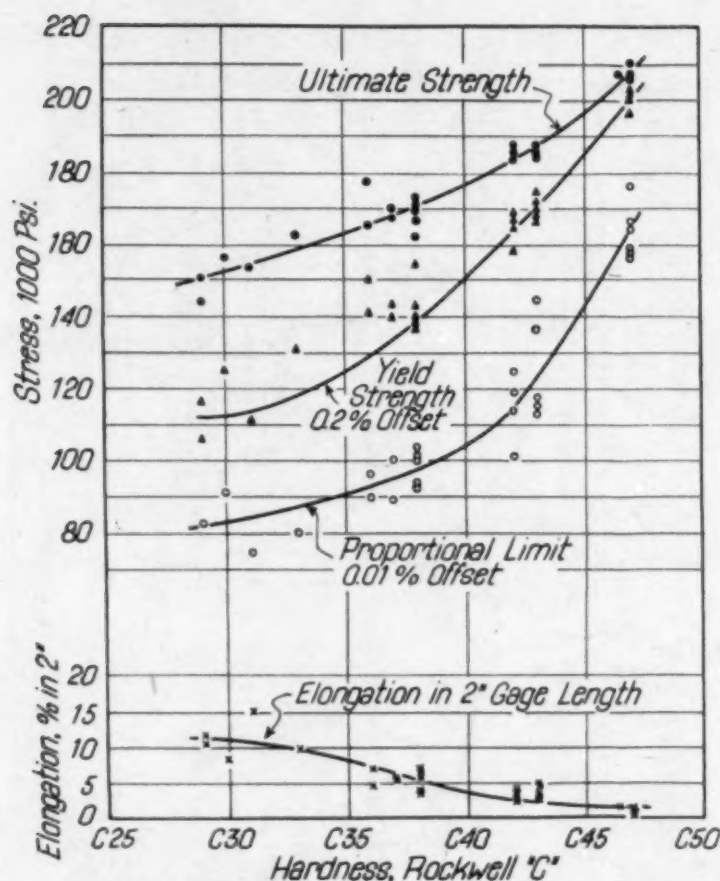


Fig. 14—Tensile Properties of MN 22 Solution Treated and Aged at 450 Degrees Cent. (840 Degrees Fahr.).

Table V
Physical Properties of Alloy MN 22 Solution Treated and Aged to Given Hardness Levels at Various Aging Temperatures. Specimens in Sheet Form.

Aging Temperature Degrees Cent.	Ultimate Strength Psi.	Yield Strength 0.2 Per Cent Offset	Proportional Limit Psi. 0.01 Per Cent Offset	Elongation Per Cent in 2 Inches	Rockwell Hardness
350	139,000	79,000	52,000	13	C30
400	150,000	92,000	68,000	17.5	C30
450	152,000	112,000	82,000	12	C30
350	152,000	96,000	60,000	7	C35
400	158,000	100,000	74,000	15.5	C35
450	163,000	125,000	91,000	8	C35
350	169,000	122,000	81,000	4	C40
400	175,000	125,000	86,000	10.0	C40
450	177,000	150,000	104,000	4	C40
350	192,000	155,000	107,000	2	C45
400	202,000	163,000	115,000	4	C45
450	196,000	185,000	143,000	2	C45

hardness curve at C 30 to C 35.

Material hardened from the solution treated state develops the highest tensile properties when aged at 450 degrees Cent. (840 de-

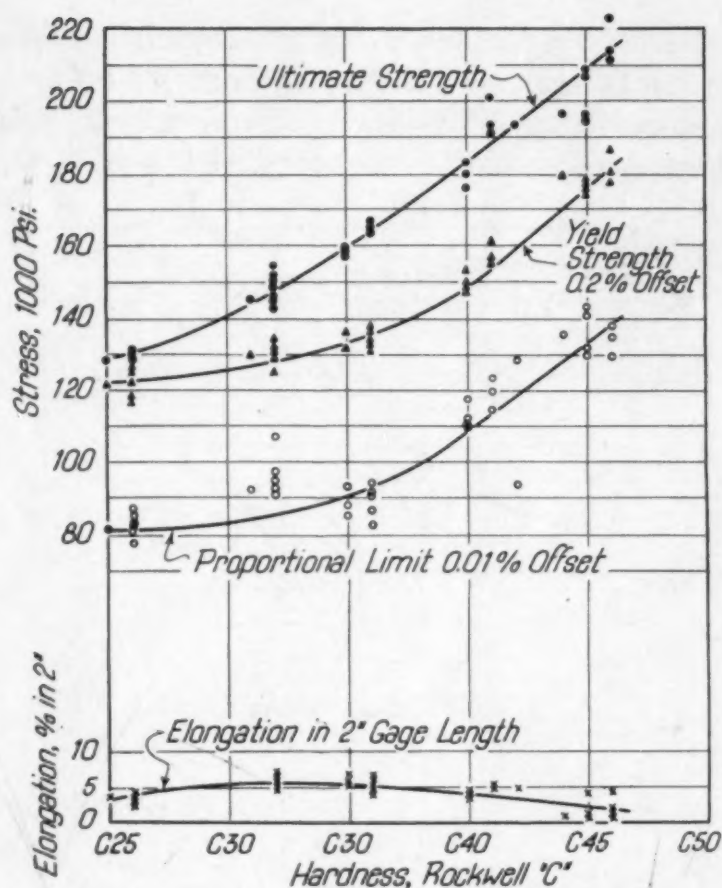


Fig. 15—Tensile Properties of MN 22 Solution Treated, Cold-Worked (60 Per Cent) and Aged at 350 Degrees Cent. (660 Degrees Fahr.).

Table VI
Physical Properties of Alloy MN 22 Solution Treated, Cold Reduced 60 Per Cent and Aged to Given Hardness at Various Aging Temperatures. Specimens in Sheet Form

Aging Temperature Degrees Cent.	Ultimate Strength Psi.	Yield Strength 0.2 Per Cent Offset	Proportional Limit Psi. 0.01 Per Cent Offset	Elongation Per Cent in 2 Inches	Rockwell Hardness
350	140,000	126,000	84,000	5.0	C30
400	141,000	132,000	96,000	7.5	C30
450	140,000	128,000	96,000	7.5	C30
350	159,000	132,000	91,000	6.0	C35
400	161,000	143,000	108,000	6.5	C35
450	162,000	147,000	118,000	6.5	C35
350	183,000	148,000	108,000	4	C40
400	188,000	169,000	132,000	3.5	C40
450	187,000	174,000	143,000	4	C40
350	208,000	155,000	132,000	2	C45
400	214,000	200,000	160,000	1.5	C45
450	213,000	202,000	168,000	2	C45

grees Fahr.) but has the greatest elongation when aged at 400 degrees Cent. (750 degrees Fahr.). At any hardness level moderately high strength and high elongation can be obtained by aging at 400 degrees

Cent. (750 degrees Fahr.), and a maximum strength with somewhat lower elongation by aging at 450 degrees Cent. (840 degrees Fahr.). Material hardened from the cold-worked state shows higher tensile properties when hardened at 450 degrees Cent. (840 degrees Fahr.),

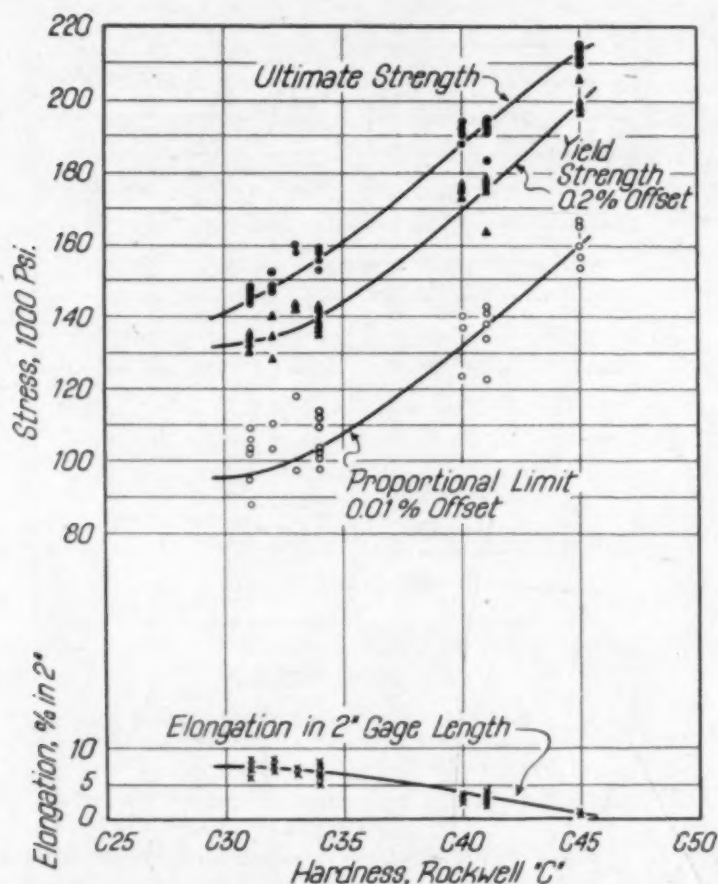


Fig. 16—Tensile Properties of MN 22 Solution Treated, Cold-Worked (60 Per Cent) and Aged at 400 Degrees Cent. (750 Degrees Fahr.).

particularly for the range Rockwell C 40 to 45, but the elongation is not affected by aging temperature, and appears to depend only on the hardness. Physical properties at hardness levels beyond C 45 were not explored because a few tests indicated that elongation approaches the vanishing point at C 50.

A comparison was also made between the physical properties of all three alloys hardened from both conditions. Average results from ten individual samples for each hardness are plotted in Figs. 18 to 20. Alloys MN 20 and MN 24 respond in the same manner as MN 22. As hardened from the cold-worked state, the spread of the tensile properties is well within that obtained on MN 22 alone. How-

ever, alloy MN 20, hardened from the solution treated state, had higher yield strengths and proportional limits and somewhat lower elongations than either MN 22 or MN 24 in similar conditions.

Since MN 20 cannot be hardened to quite the same level as the

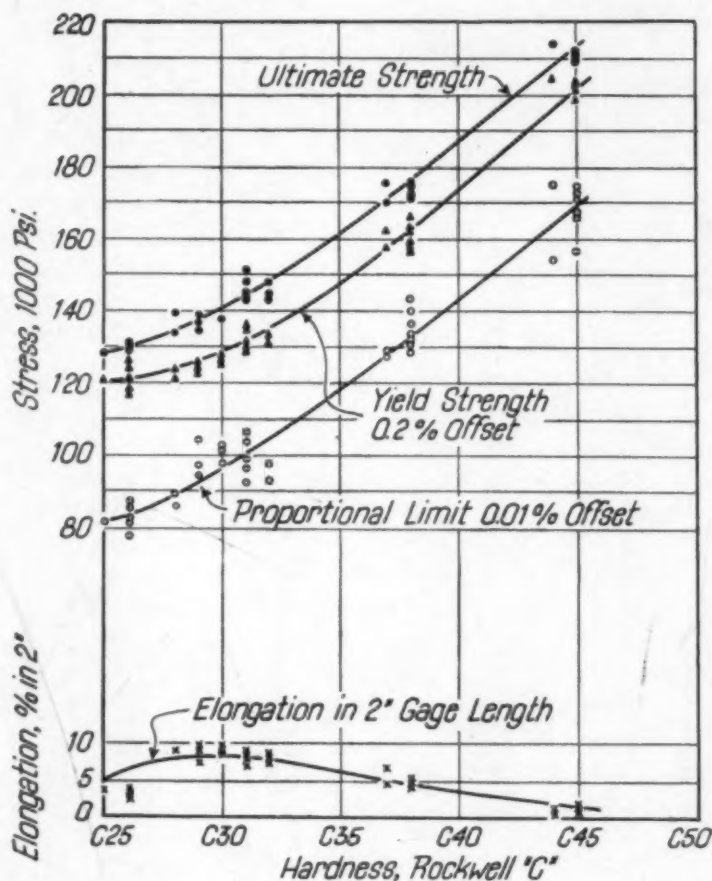


Fig. 17—Tensile Properties of MN 22 Solution Treated, Cold-Worked (60 Per Cent) and Aged at 450 Degrees Cent. (840 Degrees Fahr.).

other two alloys, the optimum composition appears to lie between 22 and 24 per cent each of manganese and nickel. The tensile strength of 87,000 psi., with 40 per cent elongation at a hardness of Rockwell B 77 in the annealed condition, may be varied by cold working to a tensile strength of 137,000 psi., to 3 per cent elongation when cold-rolled to 60 per cent reduction in thickness. By proper heat treatment the hardness can be varied from C 30 to C 45, the tensile strength from 137,000 to 213,000 psi., and the elongation from 13 to 2 per cent respectively. This range of properties offers many possibilities for application of the alloy. The modulus of elasticity as

determined on the tensile specimens ranged from 21 to 23 x 10⁶ psi. and as determined by dynamic methods, from 21 to 22 x 10⁶ psi. Incomplete fatigue data indicate that material hardened to C 40 will have an endurance limit of about 40,000 psi. for 10⁸ cycles.

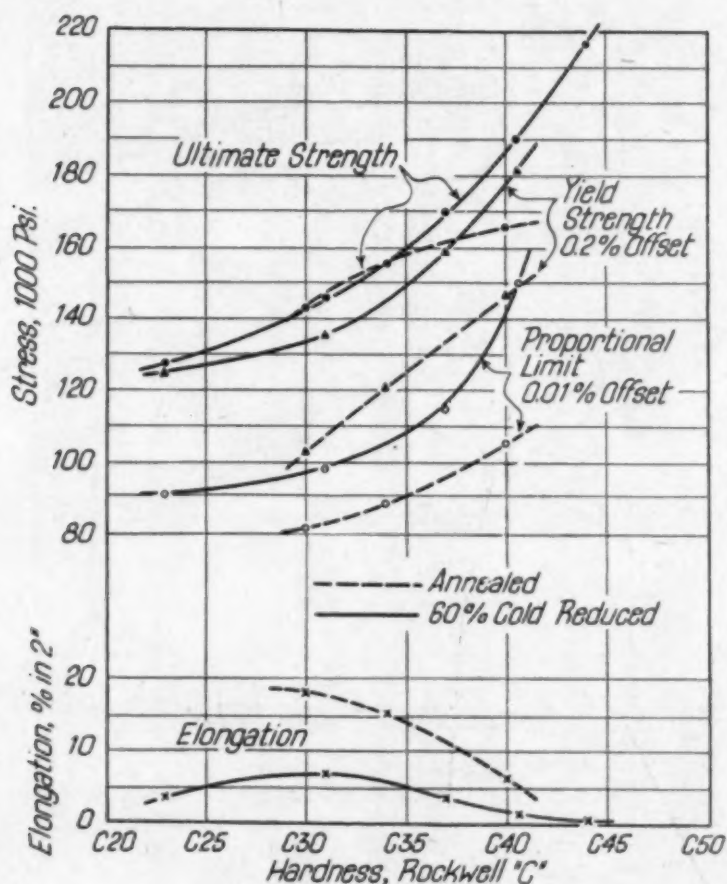


Fig. 18—Tensile Properties of MN 20 Hardened at 400 Degrees Cent. (750 Degrees Fahr.).

COMPARISON WITH COPPER-BERYLLIUM ALLOYS

A comparison of the physical properties of the MN 22 alloy with copper-beryllium alloys is given in Table VII. Data on the 2-2.25 per cent beryllium alloy were taken from tentative A.S.T.M. specifications B 120-41 T for limiting values, and from the Metals Handbook for average values. Data for the MN 22 alloy were taken from Table IV and Fig. 8 and were chosen to correspond to the average hardness of the beryllium alloy. The MN 22 alloy compares very favorably in all conditions listed, meets the A.S.T.M. minimum specifications and is equal or superior to the average values

given for the beryllium alloy. The high yield strength is remarkable considering that it was determined on 0.2 per cent offset from the modulus line, while the other data were determined on 0.75 per cent offset. It should also be noted that the percentage elongation is

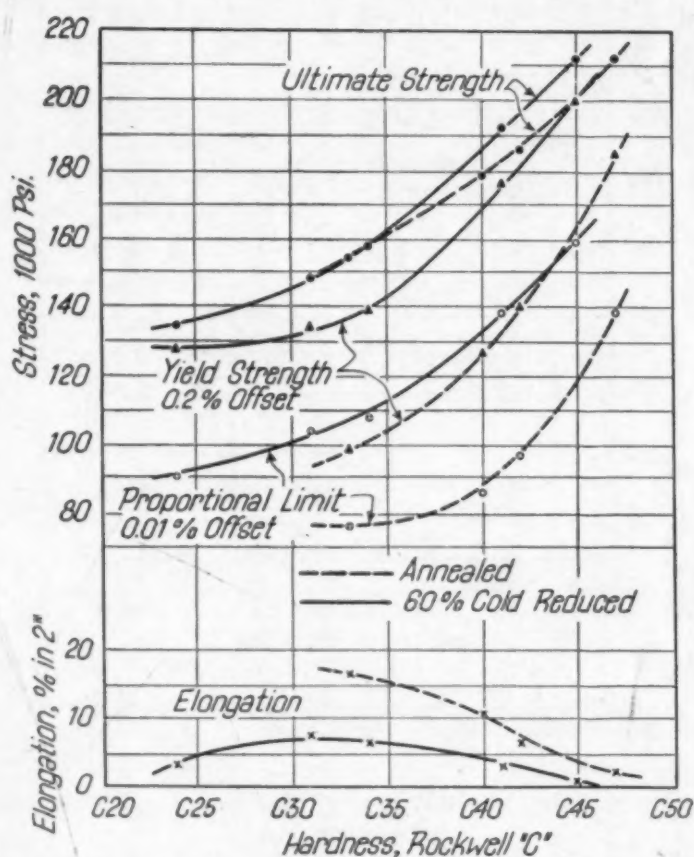


Fig. 19—Tensile Properties of MN 22 Hardened at 400 Degrees Cent. (750 Degrees Fahr.).

higher than that of the beryllium alloy of the same hardness. For material aged from the solution treated condition, the MN alloy has twice the elongation of the other. The properties of MN alloy compare very favorably with those of copper-beryllium alloy. While it requires 23 per cent of nickel and 23 per cent of manganese, the supplies of these metals are much more elastic than that of beryllium.

THE ALLOY MADE WITH COMMERCIAL MANGANESE

A series of the alloys have also been made with the commercial grade of manganese metal to compare with those made with the electrolytic grade. These alloys were much more difficult to fabricate but once the ingot structure had been broken down, they could

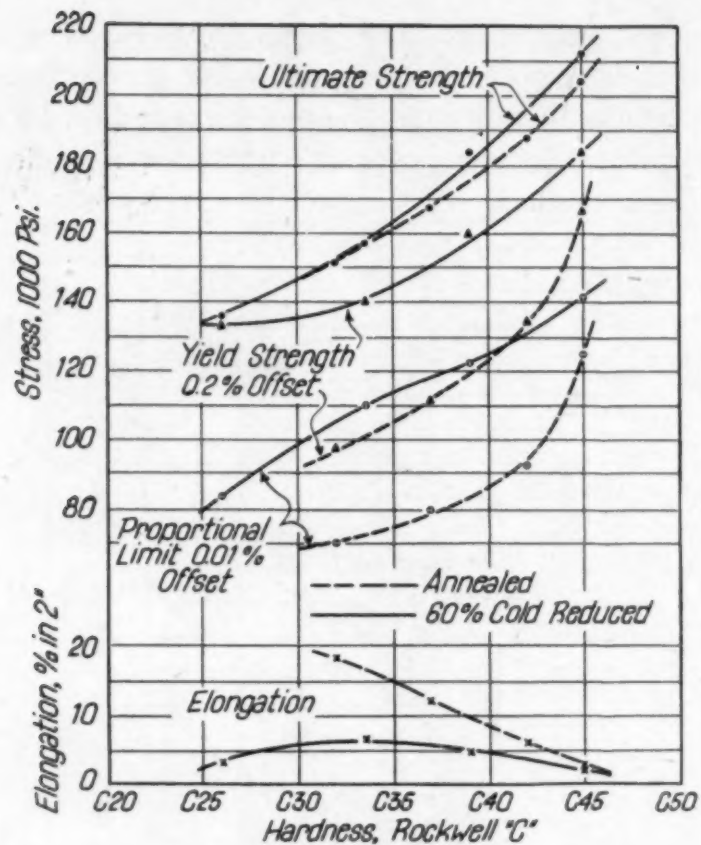


Fig. 20—Tensile Properties of MN 24 Hardened at 400 Degrees Cent. (750 Degrees Fahr.).

Table VII
Comparison of Copper-Beryllium Alloys with Alloy MN 22 in Various Conditions

Alloy	Conditioner (a)	Tensile Strength Psi.	Yield Point Psi. (b)	Proportional Limit (c) Psi.	Elongation (Per Cent)	Rockwell Hardness	Source
Be	A	80,000 (d)	35 (e)	B80 (d)	ASTM
Be	A	70,000	31,000	8,000	45	B70	ASM
MN 22	A	87,000	38,500	27,000	40	B77	Table 4
Be	H	95,000 (e)	2 (e)	B93 (e)	ASTM
Be	H	118,000	105,000	39,000	4.3	C24	ASM
MN 22	H	134,000	127,000	90,000	3.0	C24	Table 4
Be	AT	150,000 (e)	90,000	5 (e)	C35 (e)	ASTM
Be	AT	175,000	134,000	46,000	6.3	C38	ASM
MN 22	AT	170,000	118,000	86,000	12	C38	Fig. 8
Be	HT	180,000 (e)	95,000	1 (e)	C39 (e)	ASTM
Be	HT	193,000	138,000	55,000	2	C41	ASM
MN 22	HT	192,000	176,000	138,000	3	C41	Fig. 8

(a) A—solution treated; H—hard temper; AT—aged from A condition; HT—aged from H condition.

(b) Yield strength at 0.75 per cent offset for Be alloys, and 0.2 per cent offset for MN.

(c) Proportional limit at 0.01 per cent offset for MN alloy.

(d) Maximum.

(e) Minimum, all other are average values.

be hot- and cold-rolled if carefully handled. In general they were harder, stronger, and less ductile than the manganese alloys of comparable composition. In the cold-worked state their response to heat treatment was similar to that of the MN alloy, while as solution treated they started from a higher hardness level, and hardened more

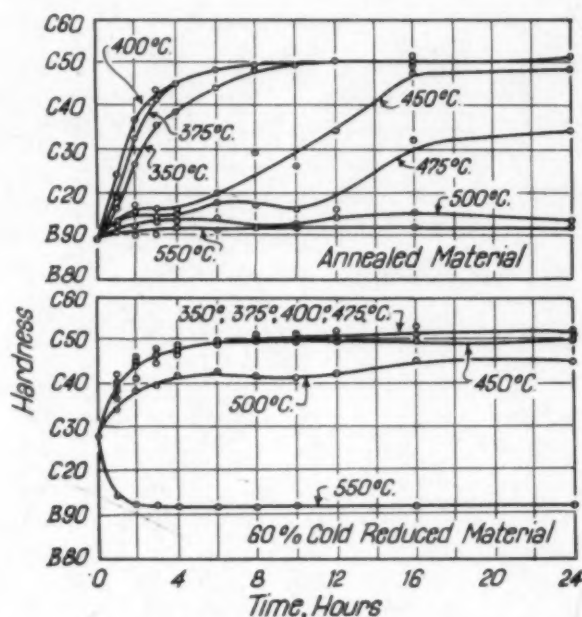


Fig. 21—Time Hardness Curves of an Ordinary Manganese MN 22 Alloy, 60 Per Cent Cold-Worked.

rapidly. As heat treated the tensile strength, yield strength and proportional limits are not very different from those of the MN alloy although the material hardened from the solution treated condition does tend to have slightly higher values. The elongation, however, is definitely lower than that of the MN alloy for any given hardness. These points are well illustrated by the data obtained on the 22 per cent manganese, 22 per cent nickel alloy given in Figs. 21 to 23 and in Table VIII. The first figure shows the hardenability curves for the various hardening temperatures, and the last two show the relationship between the physical properties and hardness for the material hardened at 400 degrees Cent. (750 degrees Fahr.). Table VIII gives the values of the properties taken from Figs. 22 and 23 and also the properties as cold-worked and as annealed. The chemical analysis of the alloy shows considerably higher iron and silicon content than the MN alloy, as shown in Table IX.

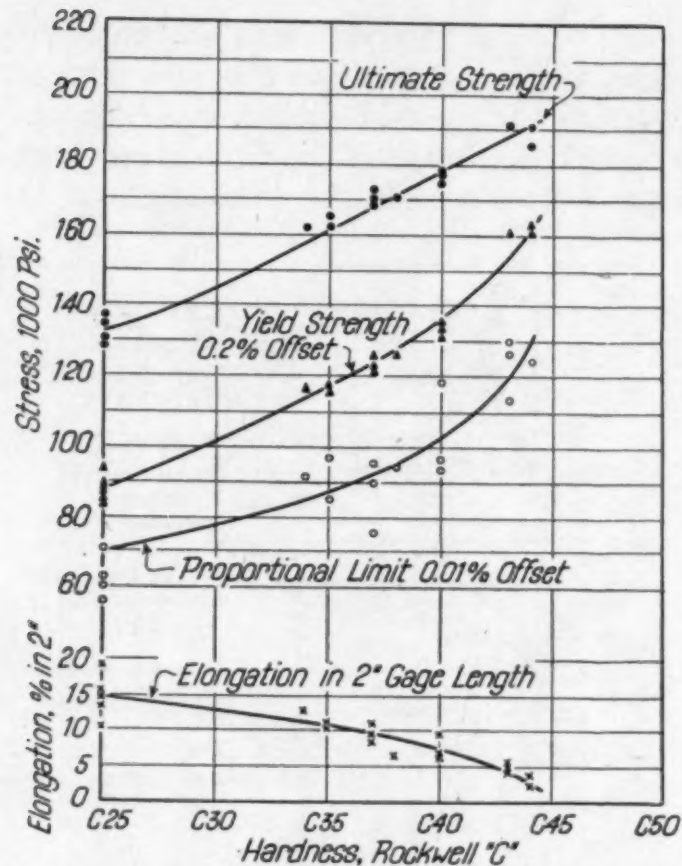


Fig. 22—Physical Properties of Material, Made with Ordinary Manganese, Annealed 650 Degrees Cent. (1200 Degrees Fahr.) Aged 400 Degrees Cent. (750 Degrees Fahr.).

Table VIII
Physical Properties of Material Made With Ordinary Manganese and Age-Hardened at 400 Degrees Cent.

Ultimate Strength	Yield Strength	Annealed then age-hardened			Elongation
		Proportional Limit	Hardness		
100,000	59,000	54,500	B91	31 as anneal	
132,000	87,500	70,000	C25	15	
145,000	102,000	78,000	C30	13	
162,000	117,000	86,000	C35	11	
178,000	135,000	103,000	C40	7.5	
192,000	162,000	130,000	C44	2.5	
60 per cent cold reduced then age-hardened					
140,000	130,000	84,000	C27	2.0 as CW	
144,000	132,000	90,000	C30	3.0	
161,000	149,000	109,000	C35	3.5	
189,000	173,000	136,000	C40	3	
210,000	198,000	164,000	C45	1.5	

SUMMARY

Copper-manganese-nickel alloys, containing about 22 to 24 per cent manganese and an equal amount of nickel, respond very well

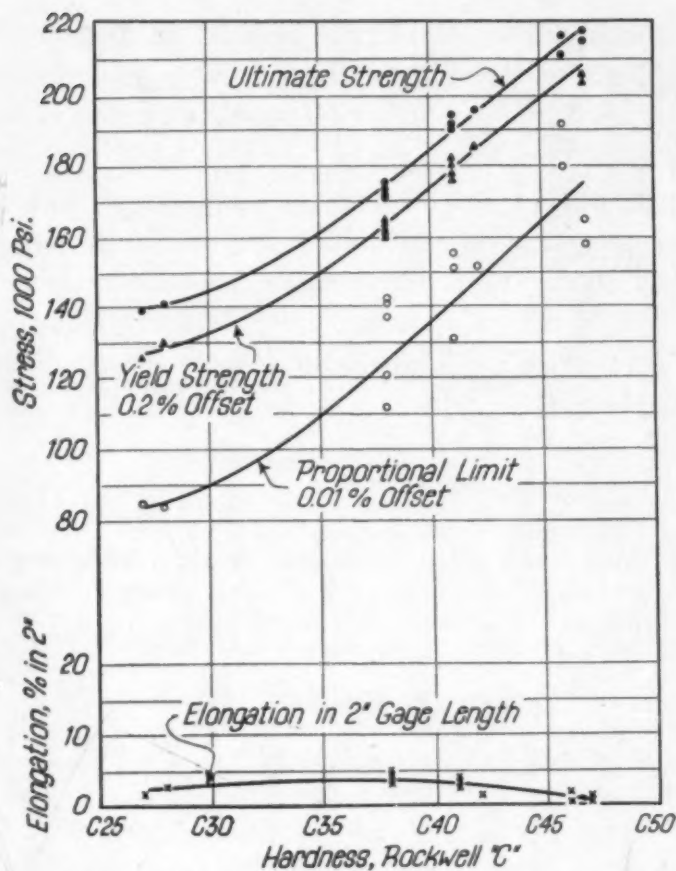


Fig. 23—Physical Properties of Material, Made with Ordinary Manganese, 60 Per Cent Cold Reduced. Aged 400 Degrees Cent. (750 Degrees Fahr.).

Table IX
Composition of MN 22 Made With Ordinary and With Electrolytic Manganese

	Electrolytic Manganese Alloy	Ordinary Manganese Alloy
Cu	55.4	56.5
Mn	21.6	21.75
Ni	21.8	20.25
Fe	0.017	0.67
Si	Nil	0.10

to age hardening treatments and possess physical properties similar to those of the copper-beryllium alloys. Quenching from 650 degrees Cent. (1200 degrees Fahr.) followed by aging at 350 to 450 degrees Cent. (660 to 840 degrees Fahr.) for periods up to 24 hours, depending on the hardness and other properties desired, has been found quite satisfactory. The hardness and physical properties obtained are reproducible within reasonable limits. Like copper-beryllium, these alloys age more rapidly from the cold-worked condition than from the solution treated condition. Material hardened from the

solution treated condition shows the highest elongation upon aging at 400 degrees Cent. (750 degrees Fahr.). In general, the maximum tensile properties for a given hardness are obtained by aging at 450 degrees Cent. (840 degrees Fahr.). The physical properties obtained on aging can be varied over extremely wide ranges under appropriate conditions of heat treatment. While the major portion of the data presented was obtained on alloys made with electrolytic manganese, several heats of the alloys were made with commercial grades of manganese for comparison. These alloys were more difficult to fabricate and had lower elongation for any given hardness and strength.

References

1. R. S. Dean and C. T. Anderson, "The Alloys of Manganese-Copper and Nickel: Hardening in the pseudo-binary system, Cu-MnNi," *TRANSACTIONS, American Society for Metals*, Vol. 29, 1941, p. 808.
2. R. S. Dean and C. T. Anderson, "Alloys of Manganese-Nickel and Copper: The Electrical Resistance and Temperature Coefficient of Electrical Resistance," *TRANSACTIONS, American Society for Metals*, Vol. 29, 1941, p. 899.
3. R. S. Dean, C. T. Anderson, and E. V. Potter, "Alloys of Manganese-Nickel and Copper: The Coefficient of Thermal Expansion," *TRANSACTIONS, American Society for Metals*, Vol. 29, 1941, p. 907.
4. U. S. Patent No. U. S. 2,234,552, March 11, 1941.

DISCUSSION

Written Discussion: By Stanley R. Hood, chief engineer, W. M. Chace Co., Detroit.

The authors have made a welcome addition to the data available on these alloys and at a time when widespread interest is developing in the commercial application of the materials. Our work in determining the physical properties of these alloys is in good agreement with their results with the exception that higher tensile values have been obtained through the use of a slightly different thermal treatment. We have consistently obtained tensile values of 220,000 psi. for alloy MN 20, and 230,000 psi. for MN 22 on samples which have been cold-rolled to a 60 per cent reduction and then aged.

The analysis shown for sample MN 20 in this paper is 2 per cent high in nickel content. This is more than twice the commercial tolerance. This deviation from the required 1:1 ratio of nickel to manganese producing maximum hardenability contributes to the difference they have shown between the properties of MN 20 and the other alloys tested. While the solution temperature of 1200 degrees Fahr. (650 degrees Cent.) which they used is only slightly higher than we would use for the alloys high in Ni and Mn content, it is about 150 degrees Fahr. higher than the optimum solution temperature for MN 20. This lower solution treatment results in higher hardness and a more rapid hardening rate. Also MN 20 is hardened more rapidly at 750 degrees Fahr. (400 degrees Cent.) than at the temperature of 840 degrees Fahr. (450 degrees Cent.) used in their tests. The use of these lower temperatures for MN 20 also considerably

reduces the difference in age hardness of soft and cold-rolled material. While these are minor differences, I wish to say that the alloys are even less critical in respect to heat treatment and composition than is indicated by the paper.

It is assumed that all solution treatments refer to water quenching from the solution temperature. An unusual and highly desirable characteristic of these alloys is their insensitiveness to rate of cooling from the solution temperature. Air-cooled and water-quenched samples will have identical time-hardness curves on being aged. Furnace-cooled samples will partially harden on passing through the hardening range of 900 to 500 degrees Fahr. (480 to 260 degrees Cent.). Hardening can then be continued at the normal rate by reheating to the aging temperature. Isothermal hardening can be accomplished either by quenching from the solution temperature to the aging temperature or by slow cooling from the solution temperature to the aging temperature and holding for the required time. Instead of requiring closely controlled conditions characteristic of many age hardening alloys, these alloys cannot be subjected to a thermal or mechanical handling which will prevent hardening on their being subsequently heated to the aging temperature.

When a hardened sample is heated from the aging temperature to the solution temperature there is a gradual decrease in hardness as "resolution" takes place. At any intermediate temperature a comparatively fixed amount of "resolution" will take place, the amount being primarily a function of temperature rather than time. It is therefore possible to "draw" the hardness back to any predetermined value with considerable accuracy. The time at the "drawing" temperature may be varied from a few minutes to as much as 4 hours without affecting the resultant hardness. Full hardness can be restored after drawing by reheating to the aging temperature. Rehardening takes place at approximately the normal rate. This process is perfectly reversible and may be repeated any number of times.

Recrystallization, solution and aging temperatures are in slightly overlapping ranges. It is possible to select a temperature which will first soften a cold-rolled strip after which age hardening will begin. This is due to the sluggishness of the hardening mechanism as compared to the short time required for annealing and resolution. Springs made of these alloys can be heat treated for minimum "drift" by a preliminary stress relieving treatment of heating to just below the annealing temperature followed by the regular aging treatment. While the stress relieving treatment softens the material slightly, it does not affect the hardening rate or maximum obtainable hardness.

The overaging referred to in the paper and for which photomicrographs are shown may be the resolution of precipitate taking place along the grain boundaries where it originally formed. This resolution would gradually spread through the grains until resolution is completed. I would like to ask the authors if the new phase developed by overaging is not the same phase present in solution treated metal.

Authors' Reply

The solution temperature of 1200 degrees Fahr. (650 degrees Cent.) was chosen for this work to suit all three of the alloys and at the same time provide

reasonable softening for subsequent cold working. Lower solution temperatures down to 950 degrees Fahr. (510 degrees Cent.) can be used for the lower manganese and nickel alloys. For MN 24, however, the solution temperature must be in excess at 1022 degrees Fahr. (550 degrees Cent.). We, however, have made no particular study of solution temperatures below 1200 degrees Fahr. (650 degrees Cent.) and are interested in learning that the MN 20 Alloy has been successfully handled from 1050 degrees Fahr. (565 degrees Cent.). We are also interested in the suggestions that the hardness-of the alloys can be further regulated by tempering operations which Mr. Hood described. This feature should contribute to the precise control of hardness.

To answer Mr. Hood's question on the precipitate developed by over-aging, as far as we know, it is the same one which is present in normally aged material. It has not, however, been identified.

THE EFFECT OF FIBER ON NOTCHED BAR TENSILE STRENGTH PROPERTIES OF A HEAT TREATED LOW ALLOY STEEL

BY GEORGE SACHS, J. D. LUBAHN, L. J. EBERT AND E. L. AUL

Abstract

Regular and notched bar tensile tests were made on specimens taken in both the longitudinal and transverse directions from 1½ and 2¾-inch diameter, hot-rolled rod of a low alloy steel, S.A.E. 3140. Most of the specimens were heat treated to a strength level of 190,000 psi., but some transverse tests were made on specimens heat treated to 140,000 and 220,000 psi., respectively. The rod size and location of the specimens had little effect on the results of either the regular or the notched bar tensile tests in the longitudinal direction. In the transverse direction, the ductility was considerably less than in the longitudinal direction. According to regular tensile tests it was lower in the 2¾-inch diameter rod, but according to the notched bar tensile tests it was lower in the 1½-inch diameter rod. Neither rod size nor fiber direction had any effect on the ultimate strength. Both the regular and the notched bar tensile tests yielded a continuous decrease in ductility with increasing strength level, the percentage difference in ductility between longitudinal and transverse specimens becoming larger with increasing strength level. The concentric notch ductility and the eccentric notch strength measured the ductility of the metal, as influenced by rod size and fiber direction, in nearly the same manner as shown in previous investigations.

IN this investigation, the tensile strength properties of hot-rolled bars of a low alloy steel were investigated in both the longitudinal and transverse directions. In addition to this major variable (a), the direction of testing, the following additional factors were varied: (b) the thickness of the hot-rolled section, (c) the strength level, and (d) the type of test.

This paper is the sixth report on the research program conducted at Case School of Applied Science under the sponsorship of The International Nickel Co.

A paper presented before the Twenty-sixth Annual Convention of the Society held in Cleveland, October 16 to 20, 1944. Of the authors, George Sachs is professor of physical metallurgy, J. D. Lubahn, L. J. Ebert and E. L. Aul are research assistants, department of metallurgical engineering, Case School of Applied Science, Cleveland. Manuscript received May 25, 1944.

The properties determined were (a) the regular tensile strength and contraction in area of cylindrical tensile test bars, and (b) the ultimate strength or "notch strength" of test bars provided with a sharp and deep notch, subjected to both concentric and eccentric tension, and the notch ductility of concentrically tested bars.

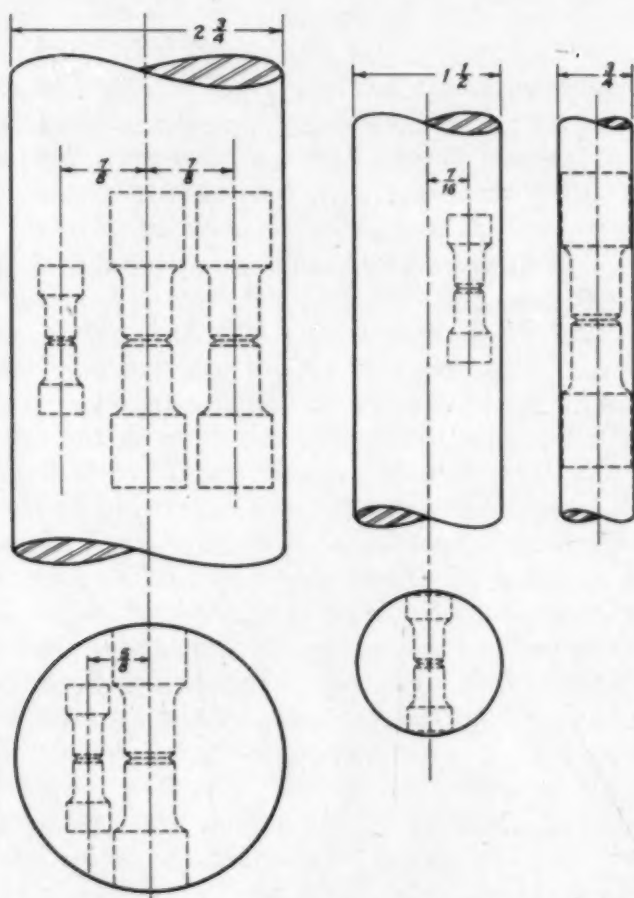


Fig. 1—Position of Specimens in the Various Size Rods.

It appears that no data are available on the notch strength of steels in the transverse direction, at present, except for some results of notched bar impact tests. Such tests, and also regular tensile tests in the transverse direction, have been carried out by a number of investigators (1)¹, in order to reveal the effects of "fiber" or "directionality." Such a directionality develops with progressing reduction from the ingot to a forged or rolled billet or rod. The strength properties in the transverse direction of a steel section are generally inferior to those in the longitudinal direction (1). This inferiority appears primarily in the ductility and impact energy but

¹The figures appearing in parentheses pertain to the references appended to this paper.

usually not in either the yield or tensile strength of a steel. The first mentioned transverse properties improve on working the ingot until a reduction in area of 50 to 75 per cent has been reached in a similar manner to the longitudinal properties. However, they are adversely

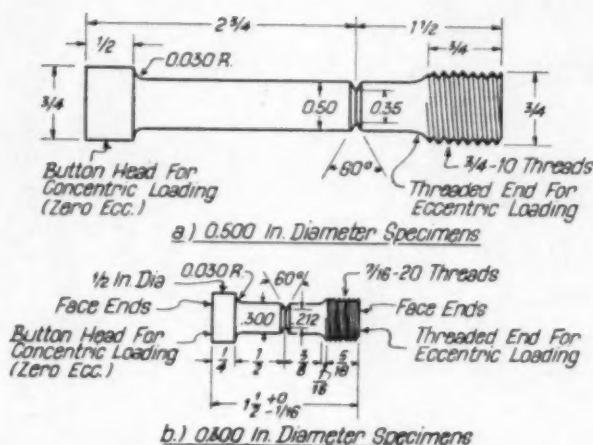


Fig. 2—50 Per Cent Sharp Notched Specimens.

affected by greater reductions, and approach a rather low level for the high reductions to which commercial billets and rods have been subjected. No definite conclusions can be drawn from previous work regarding the effect on the transverse properties of heat treating a steel to a high strength level.

MATERIAL AND PROCEDURE

S.A.E. 3140 steel of the previous analysis (2) was used in the investigation. Three different sizes of hot-rolled rod were available, having diameters of $\frac{3}{4}$ inch, $1\frac{1}{2}$ inches, and $2\frac{3}{4}$ inches, respectively. Regular tensile test specimens and notched bar tensile test specimens were cut from various positions in the rods, Fig. 1, to show the effects of rod size, fiber, specimen size, and location of the specimen in the rod. Two specimen sizes were employed as follows: The first was the previously used specimen, Fig. 2a, 3 inches long (or $2\frac{3}{4}$ inches where necessary) and having a 0.50-inch diameter gage length; and the second was $1\frac{1}{2}$ inches long with a 0.30 or 0.20-inch diameter (depending upon the strength level), Fig. 2b.

Threaded-end, unnotched specimens were used to determine the ultimate and yield strengths, contraction in area, and elongation where the specimen was long enough to permit a gage length of four times the diameter. Specimens provided with a 50 per cent sharp notch were used for both the concentric and eccentric tests.

The specimens for concentric loading were provided with button-heads, and those for eccentric loading with threaded ends.

The specimens were heat treated in the same manner as in the previous investigations (2).

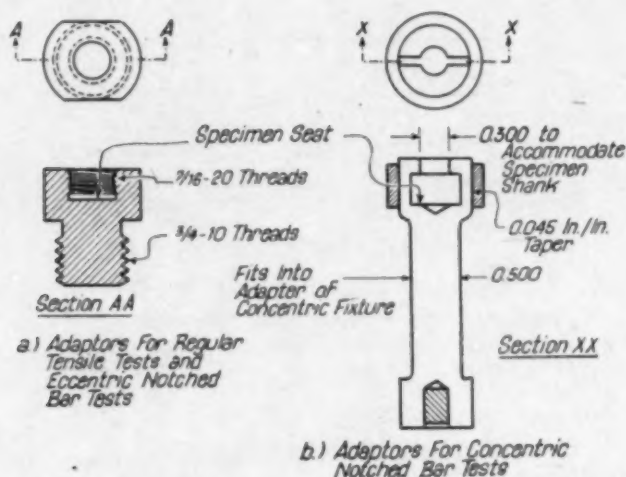


Fig. 3—Adapters for Testing Small Specimens in the Fixtures for Standard Size Specimens.

To permit the testing of the small specimens in the various test fixtures, special adapters were made, Fig. 3. The adapters for the regular tensile tests and the eccentric notched bar tensile tests, Fig. 3a, consisted of plugs to accommodate the diameter and threads of the small specimens. The ends of the specimens were faced in a lathe and the ends of the tapped holes in the adapters were recessed and faced to permit the specimen to be screwed completely into the adapter. The adapters were tightened with a wrench so that the ends of the specimen were seated rigidly on the bottom of the hole in the adapter. The adapters and specimens were made to such a length that a rigid assembly of specimen and adapters, 3 inches long, was obtained. Thus, the small specimens could be tested in the eccentric fixtures under reproducible conditions of bending, Fig. 4. The effective length between the points of application of the tensile load (the ball seats) was held relatively constant ($10 \pm \frac{1}{4}$ inches) to assure a constant bending moment.²

The adapters for the small, buttonhead type specimens, Fig. 3b, were split, and the outside surface of the end that held the specimen was tapered. A ring with a matching taper was forced on this

²Some of the small eccentricity specimens were made two inches long by mistake. In testing these specimens, a new left-hand thread adapter, Fig. 4, $\frac{1}{2}$ inch shorter than the regular one, was made so that the total length of the assembly, and consequently the bending moment, was still constant.

end to hold the two halves together with the specimen inside. A small hardened pin was inserted in the other end, which fitted into the adapters, to maintain the necessary 0.50-inch shank diameter

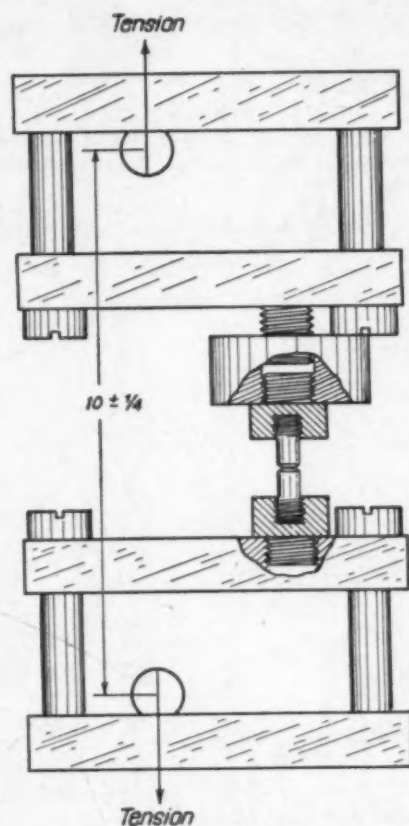


Fig. 4—Schematic Diagram of a Small Specimen in Position for Testing in the Eccentric Fixtures.

(diameter of the standard size specimen). The entire assembly was 6 inches long, and was then treated as a standard specimen. The results of the tests are shown in Table I and Figs. 5 to 11.

RESULTS OF REGULAR TENSILE TESTS

It is known that the tensile strength of a steel of a given composition is not affected by the size of the section from which the test bar has been machined, and that it is practically the same in the with-grain and cross-grain directions. This has been confirmed for the S.A.E. 3140 steel, heat treated to strength levels between 125,000 and 240,000 psi., according to Fig. 5. The tensile strength of a large number of various test specimens, tempered at a temperature of 830 degrees Fahr. (445 degrees Cent.), agreed within ± 9000 psi., or ± 5 per cent; and this indicated a rather uniform carbon content of all the rods from which test bars were taken.

The contraction in area of the longitudinal test bars, which is a measure of the ductility of a steel, was also found to be practically independent of the section thickness of the hot-rolled rod for the one strength level of approximately 190,000 psi. investigated, Fig. 5.

Table I
Summary of Regular and Notched Bar Tensile Tests on S.A.E. 3140 Specimens Cut from Different Positions in Various Size Rods

Position in Bar	Tempering Temp. Degrees Fahr.	Outside Diameter In.	Notch† Depth Per Cent	Initial Ecc. In.	Ultimate Strength 1000 Psi.	Yield Strength 1000 Psi.	Contr. in Area Per Cent	Elong. Per Cent	Specimen Length In.
2¾-Inch Diameter Rod									
Long. from center	830	0.375	0	0	185	175	59	..	3
	830	0.501	50	0	276	5½
	830	0.500	51	0.03	264	...	2.6	..	3
	830	0.500	51	0.12	213	...	1.8	..	3
	830	0.500	50	0.22	144	...	1.0	..	3
Long. from edge	830	0.499	51	0.42	65	...	0.3	..	3
	830	0.375	0	0	192	179	58	..	3
	830	0.374	0	0	195	185	56	..	3
	830	0.501	51	0	271	...	1.8	..	5½
	830	0.501	50	0	274	...	2.4	..	5½
	830	0.500	50	0.04	268	...	1.6	..	3
	830	0.500	49	0.12	206	...	1.5	..	3
	830	0.500	50	0.25	129	...	0.7	..	3
	830	0.500	51	0.47	53	...	0.1	..	3
	830	0.300	0	0	181	170	59	16	2
	830	0.301	0	0	189	175	60	17	2
	830	0.299	50	0	268	...	4.9	..	2
	830	0.299	51	0	267	...	4.2	..	2
	830	0.300	51	0.05	258	2
	830	0.301	51	0.10	237	2
	830	0.300	51	0.10	237	2
	830	0.302	53	0.23	150	2
	830	0.300	53	0.24	138	2
	830	0.300	51	0.46	50	2
2¾-Inch Diameter Rod									
Transverse	830	0.375	0	0	185	177	12	..	2¾
	830	0.375	0	0	187	178	11	..	2¾
	830	0.500	50	< 0.05	200	2¾
	830	0.496	48	< 0.05	208	2¾
	830	0.500	50	0.05	213*	...	0.9	..	2¾
	830	0.500	50	0.05	206†	...	0.5	..	2¾
	830	0.500	50	0.08	158†	...	0.6	..	2¾
	830	0.500	51	0.09	160*	...	0.4	..	2¾
	830	0.500	50	0.21	83*	...	0.1	..	2¾
	830	0.500	50	0.21	88†	2¾
	830	0.500	51	0.44	38*	...	0.0	..	2¾
	830	0.500	50	0.46	35†	...	0.0	..	2¾
	830	0.300	0	0	181	171	12	5	2
	830	0.300	0	0	181	...	10	3	2
	830	0.300	50	0	235	...	2.9	..	2
	830	0.299	49	0	250	...	2.0	..	2
	830	0.300	51	0.04	212	2
	830	0.301	52	0.11	180	2
	830	0.298	49	0.12	188	2
	830	0.301	54	0.23	93	2
	830	0.301	50	0.24	93	2
	830	0.299	50	0.46	30	2
1½-Inch Diameter Rod									
Long. from edge	830	0.300	0	0	181	...	61	16	2
	830	0.296	49	0	274	...	3.8	..	2
	830	0.299	50	0	274	...	5.8	..	2
	830	0.299	51	0.04	260*	2
	830	0.300	50	0.10	236*	2
	830	0.301	51	0.12	228*	2
	830	0.300	50	0.24	152*	2
830	0.297	50	0.44	45*	2

Table I—(Continued)
Summary of Regular and Notched Bar Tensile Tests on S.A.E. 3140 Specimens Cut from Different Positions in Various Size Rods

Position in Bar	Tempering Temp. Degrees Fahr.	Outside Diameter In.	Notch† Depth Per Cent	Initial Ecc. In.	Ultimate Strength 1000 Psi.	Yield Strength 1000 Psi.	Contr. in Area Per Cent	Elong. Per Cent	Specimen Length In.
1½-Inch Diameter Rod									
Transverse	650	0.200	0	0	242	217	9	..	1½
	650	0.201	0	0	239	216	11	..	1½
	650	0.290	48	0	159	...	0.0	..	1½
	650	0.291	48	0	181	...	0.0	..	1½
	650	0.300	48	0.03	132	1½
	650	0.301	47	0.09	97	1½
	650	0.301	48	0.10	79	1½
	650	0.301	48	0.22	40	1½
	650	0.301	47	0.23	38	1½
	650	0.301	47	0.42	18	1½
	830	0.301	0	0	193	181	21	..	1½
	830	0.300	0	0	191	183	18	..	1½
	830	0.291	47	0	243	...	0.0	..	1½
	830	0.291	46	0	238	...	1.1	..	1½
	830	0.301	49	0.06	172	1½
	830	0.301	48	0.10	140	1½
	830	0.301	44	0.12	112	1½
	830	0.301	47	0.21	65	1½
	830	0.300	48	0.22	58	1½
	830	0.300	49	0.45	18	1½
	1200	0.300	0	0	127	121	35	..	1½
	1200	0.300	0	0	122	112	36	..	1½
	1200	0.291	48	0	183	...	3.8	..	1½
	1200	0.291	49	0	179	...	3.8	..	1½
	1200	0.301	49	0.05	184	1½
	1200	0.300	49	0.10	158	1½
	1200	0.301	48	0.11	159	1½
	1200	0.301	48	0.23	88	1½
	1200	0.301	48	0.23	81	1½
	1200	0.301	48	0.44	26	1½

*Tested with fiber direction parallel to the plane of bending.

†Tested with fiber direction perpendicular to the plane of bending.

‡All notches have 0.000-inch radii.

The contraction in area of transverse test bars, however, was lower for the 2¾-inch diameter rod than for the 1½-inch diameter rod. This difference was rather consistent; however, no conclusions can be drawn regarding the effect of rod size from a few tests of this type, as the transverse ductility may vary considerably for the different parts of a heat.

The difference between the longitudinal and transverse ductilities increased considerably with increasing strength level, from a difference of approximately 40 per cent of the longitudinal values at a strength level of 125,000 psi., to a difference of 80 per cent at a strength level of 240,000 psi., for the test bars machined from 1½-inch diameter rod. Thus, a transverse brittleness develops rather rapidly on increasing the strength level of a heat treated steel.

The same fact has been observed previously regarding the circumferential ductility of S.A.E. 2340 tubing which was subjected to

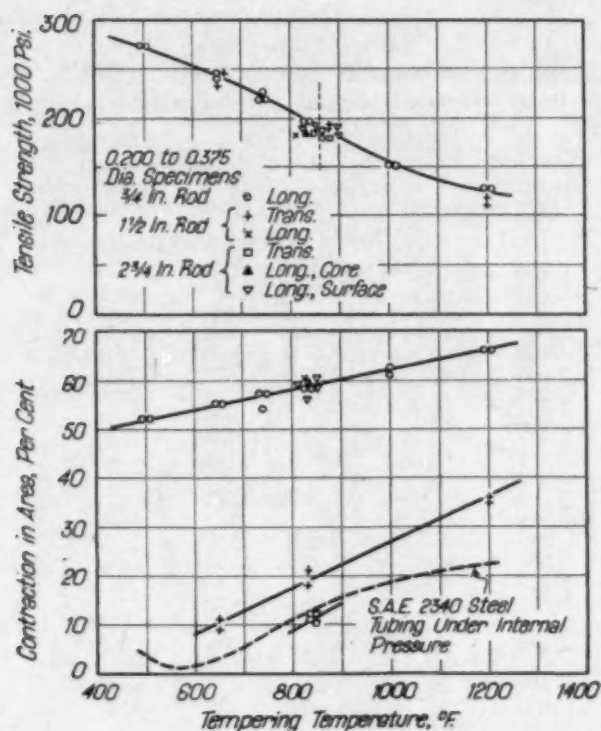


Fig. 5—Effect of Tempering Temperature, Rod Size and Direction of Testing on the Tensile Strength and Ductility of S.A.E. 3140 Steel.

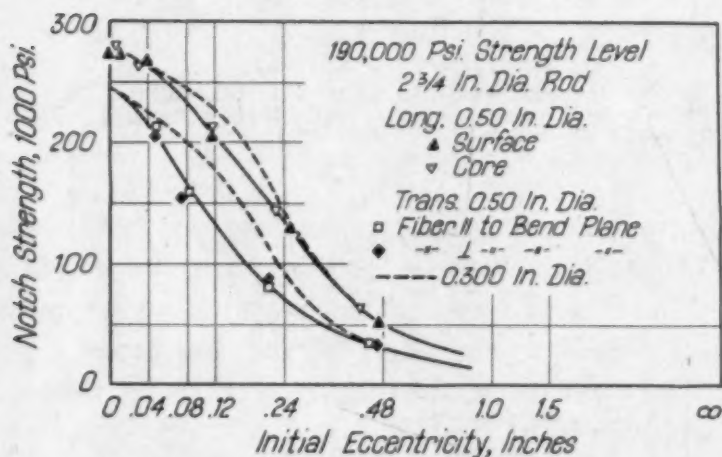


Fig. 6—Effect of Eccentricity, Fiber Direction, Specimen Size and Specimen Position on the Notch Strength of Bars from 2.75-Inch Diameter Hot-Rolled Rod.

internal pressure, Fig. 5 (4). In these tests, a longitudinal tension was also present which apparently had only a slight effect on the relation between strength level (tempering temperature) and ductility. It appears interesting that the circumferential ductility of thin-walled tubing is as low or less than the transverse ductility of rod.

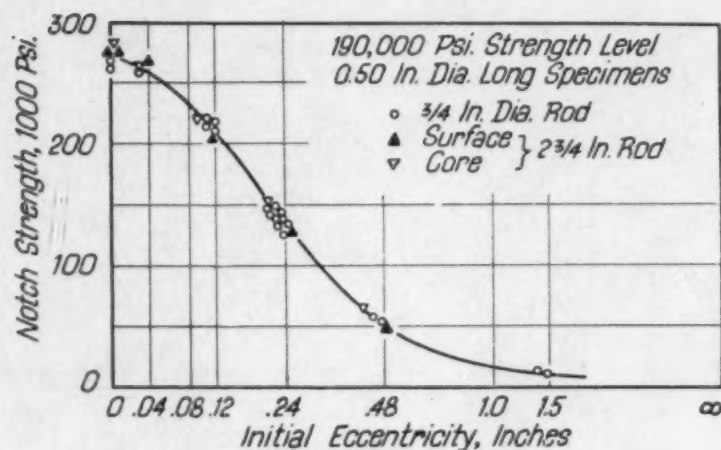


Fig. 7—Effect of Eccentricity, Rod Size and Specimen Position on the Longitudinal Notch Strength of 0.50-inch Diameter Specimens.

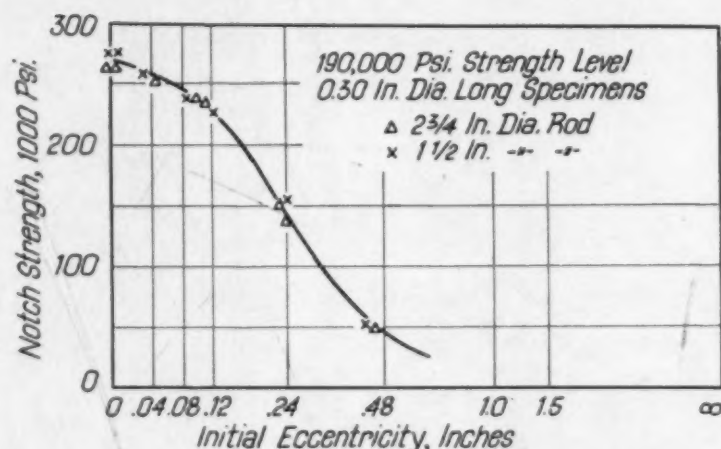


Fig. 8—Effect of Eccentricity and Rod Size on the Longitudinal Notch Strength of 0.30-inch Diameter Specimens.

RESULTS OF NOTCHED BAR TENSILE TESTS

The two different sizes of notched tensile test specimens yielded, according to Fig. 6, slightly different results, the effect of eccentricity being smaller for the smaller diameter. This difference was pronounced for intermediate eccentricities. It became insignificant for zero eccentricity and for larger eccentricities, e.g., $\frac{1}{4}$ inch.

The longitudinal notch strength was found to be practically identical for all rod sizes over the entire range of eccentricities tested; and it was found also to be the same for test bars taken from the core and from the surface of the $2\frac{3}{4}$ -inch diameter rod, Figs. 7 and 8. Such a comparison was carried through only for the strength-level of 190,000 psi.; but if the notch strength and notch

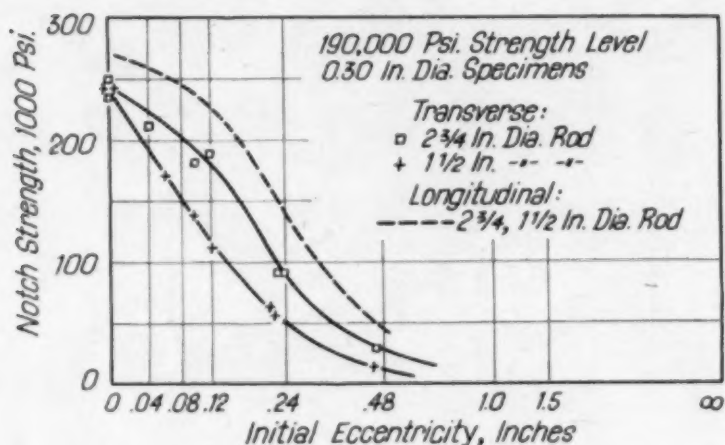


Fig. 9—Effect of Eccentricity, Rod Size and Fiber Direction on the Notch Strength of 0.30-Inch Diameter Specimens.

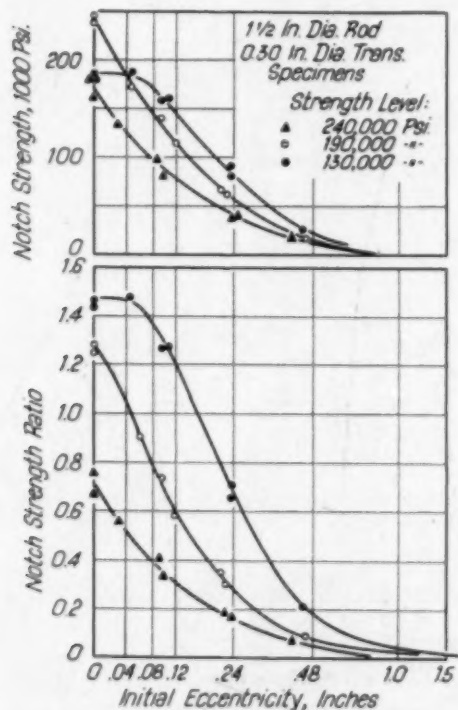


Fig. 10—Effect of Eccentricity and Strength Level on the Transverse Notch Strength and Notch Strength Ratio of 1.5-Inch Diameter Hot-Rolled Rod (0.30-Inch Diameter Specimen).

ductility were dependent upon the rod size at all this should appear in the eccentric tests at any strength level.

The rod size,³ however, had a considerable effect on the transverse notch strength, Fig. 9. Such a difference in notch strength was

³This effect should not be confused with the effect of the "section size" of the test specimen.

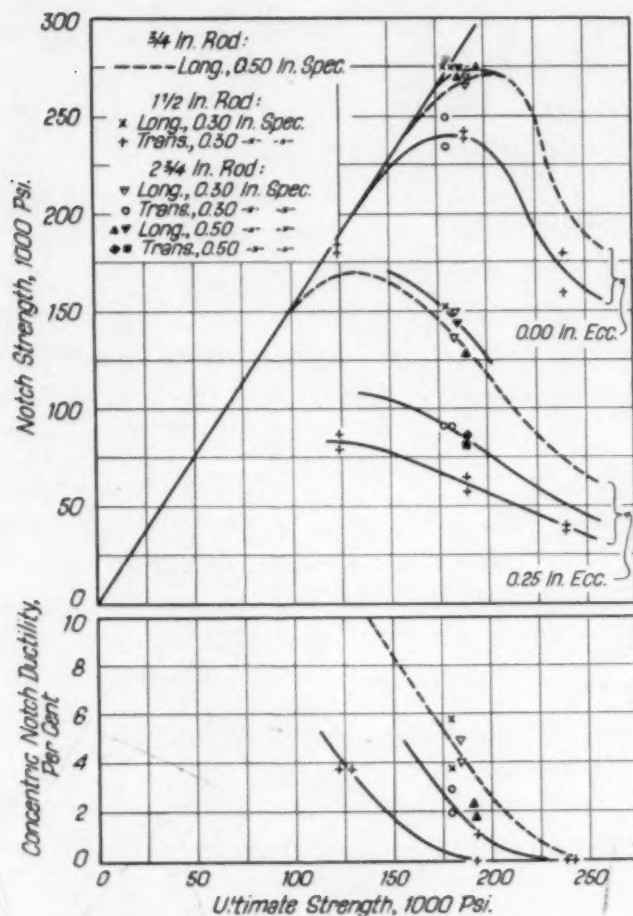


Fig. 11—Effect of Strength Level, Rod Size, Fiber Direction and Specimen Position on the Notch Strength and Notch Ductility of 50 Per Cent Notched Tensile Bars Eccentrically and Concentrically Loaded.

not observed in the concentric tests, on specimens having a strength level of 190,000 psi., but at higher eccentricities, $\frac{1}{8}$ inch or more, the test bars machined from the $1\frac{1}{2}$ -inch rod exhibited a transverse notch strength of only approximately 60 per cent of those machined from the $2\frac{3}{4}$ -inch rod. This result disagrees with the ductility values obtained on unnotched test bars, Fig. 5. However, it appears from practical experience that the harmful effect of a fiber on ductility generally increases with decreasing section size (3). If this should be confirmed, the notched bar tensile test would again yield strength characteristics of a heat treated steel which conform more closely to practical performance than those derived from regular tensile tests.

The relation between strength level and transverse notch strength was investigated for the $1\frac{1}{2}$ -inch diameter rod (0.30-inch diameter specimens). The effect of eccentricity on the notch strength in-

creased with increasing strength level, yielding a family of notch-strength ratio versus eccentricity curves, Fig. 10, similar to those of longitudinal test bars. Such a transverse curve for a certain strength level approximately corresponds to that of a longitudinal curve for a higher strength level. However, identical values of notch-strength ratios in the transverse and longitudinal direction, respectively, occurred at values of strength level that were more nearly equal for concentric than for eccentric specimens, see Fig. 11.

The notch strength of the concentrically tested transverse specimens remained the same as that of longitudinal specimens up to a strength level of approximately 160,000 psi., Fig. 11. The notch-strength ratio in this range is generally approximately 1.5 for 50 per cent notched specimens (2), being characteristic for "notch-ductile" heat treated steels. With increasing strength level, however, the transverse notch strength became increasingly smaller than the longitudinal. At a strength level of 220,000 psi., the transverse notch strength of concentric specimens was only approximately 80 per cent of the longitudinal notch strength, indicating a corresponding difference in notch ductility.

The concentric tests showed no difference between the transverse notch strengths of $1\frac{1}{2}$ -inch and $2\frac{3}{4}$ -inch diameter rod heat treated to a strength level of 190,000 psi. However, a considerable difference in notch ductility was observed, Fig. 11. As has been shown in a previous investigation (2), the notch ductility of concentric specimens is nearly a linear function of the eccentric notch strength for a suitably selected eccentricity, say $\frac{1}{4}$ inch. This generalization is further supported by the results in Fig. 11 which show a similar effect of rod size and direction of testing on the notch ductility, as measured either by the eccentric notch strength or the concentric notch ductility. With $\frac{1}{4}$ -inch eccentricity, the transverse notch strength was 65 per cent of the longitudinal notch strength for the $2\frac{3}{4}$ -inch rod and only 50 per cent for the $1\frac{1}{2}$ -inch rod.

References

1. G. Sachs, "Properties of Heavy Forgings," *Steel*, Vol. 110, 1942, No. 14, p. 76-77, 101-109.
2. G. Sachs, J. D. Lubahn, and L. J. Ebert, "Notched Bar Tensile Test Characteristics of Heat Treated Low Alloy Steels," *TRANSACTIONS, American Society for Metals*, Vol. 33, 1944, p. 340-395.
3. G. Sachs, "Some Observations on the Forging of Strong Aluminum Alloys," *Journal, Institute of Metals (London)*, Vol. 64, 1939, p. 261-281; *Metal Industry (London)*, Vol. 54, 1939, p. 366-373.
4. G. Sachs and J. D. Lubahn, "Bursting Tests on Notched Alloy Steel Tubing," *TRANSACTIONS, American Society for Metals*, Vol. 31, 1943, p. 71.

THE EFFECTS OF NOTCHES OF VARYING DEPTH ON THE STRENGTH OF HEAT TREATED LOW ALLOY STEELS

BY GEORGE SACHS, J. D. LUBAHN AND L. J. EBERT

Abstract

The effects of notches of various depths on the strength properties of metals have attracted considerable attention because of the fundamental significance which has been attributed to them regarding the "cohesive strength." The combined effects of notch depth and notch radius on the tensile strength of a low alloy steel, heat treated to various strength levels between 145,000 and 240,000 psi., were found to be considerably different from previously observed effects. The notch strength increases with increasing notch depth, approximately linearly, only if the strength of the steel is rather low or the notch radius is large. On the contrary, sharply notched high strength steels exhibit a minimum in the notch strength at intermediate notch depth; and this is explained by a corresponding minimum in the notch ductility.

This paper concludes a series of investigations on the factors which determine the notch strength properties of heat treated low alloy steels at room temperature. The effect of notch depth on the notch strength ratio can be represented by a single family of curves, the same curve applying to a sharply notched steel of rather low strength and to a high strength steel, provided with a well-rounded-off notch.

The investigation also makes possible the separation of the two fundamental effects occurring in notched bar tensile (and bending) tests: That of triaxiality and that of stress concentration. The cohesive strength of a heat treated steel increases with increasing triaxiality, only slightly less rapidly than the flow stress (shear stress), confirming McAdam's conceptions. The closeness of these two relations accounts for the rapid changes from a ductile to a brittle condition, which may be caused by small changes in metal structure or type of load application.

A paper presented before the Twenty-sixth Annual Convention of the Society held in Cleveland, October 16 to 20, 1944. Of the authors, George Sachs is professor of physical metallurgy, J. D. Lubahn and L. J. Ebert are research assistants, department of metallurgical engineering, Case School of Applied Science, Cleveland. Manuscript received May 25, 1944.

INTRODUCTION

THE changes in the properties of notched tensile test bars with increasing notch depth, other conditions being constant, have attracted numerous investigators.¹ According to Kuntze's conceptions, any metal should gradually approach the condition of total brittleness, with increasing notch depth, provided that the notch is sufficiently sharp. Thus, tensile tests on bars with deep, sharp notches should yield metal characteristics which measure the elusive property called "cohesive strength."

These conceptions, however, have been proved to be based on incorrect conclusions (1).² While a deep notch reduces considerably the ductility of any metal, the resulting condition may or may not be "brittle," depending primarily upon the inherent properties of the metal. Certainly, the "strength" of the notched test bar is not a characteristic stress value, but only an average of the stresses, the variations of which over the cross section are unknown. Regarding the effects of notch depth, it rather appears that a maximum embrittling effect is not attained with an extremely deep notch, but with a notch removing 30 to 70 per cent of the cross sectional area (1), (2).

It is thus recognized that the stress and strain relations in deeply notched, plastically stretched bars are very complex. On the other hand, the results of such tests have opened a new approach to the century-old problem of brittle or brittle-appearing failures in metals which are considered as ductile according to conventional measures. The full significance of the metal characteristics revealed by such tests is not yet known; and it will be necessary to fully analyze the notched bar tensile test for this purpose. It is rather clear, at present, that this problem can be solved, if at all, only by a tedious gradual experimental approach.

A certain amount of fundamental information has been obtained from the investigation of two factors, the notch radius and the eccentricity of loading (5). In continuation of this work, it was expected that a detailed study of the effects of notch depth for notches having various radii would yield another piece of fundamental information. As previously mentioned, a considerable quantity of experimental

This paper is the fifth report on the research program conducted at Case School of Applied Science under the sponsorship of The International Nickel Co.

¹For a complete bibliography until 1942, see (1), (2). Several more recent papers also deal with this subject (3), (4).

²The figures appearing in parentheses refer to the bibliography appended to this paper.

material has been accumulated on this phase of notched bar tensile testing and, consequently, some of the experimental relations can be considered as definitely established.

The stress state present in the narrowest section of a notched tensile test bar, Fig. 1, can be approximately described by two characteristic values: the ratio of maximum to average longitudinal stress, or "stress concentration factor," and the average value of transverse stress. Regarding these two characteristics, the following information can be derived from previous investigations:

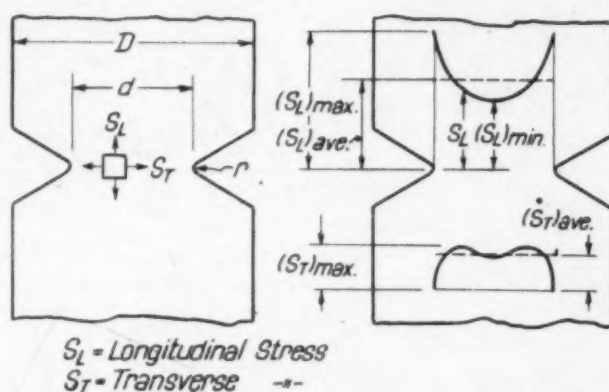


Fig. 1—Schematic Diagram of the Stress Distributions Across the Minimum Section of a Notched, Round Tensile Test Specimen.

The stress concentration is known for the range of elastic loading from photoelastic tests (6) and theoretical investigations (7). For test bars of a given diameter (D) and possessing a notch of a given radius (r) but varying in depth, the stress concentration should first increase with increasing notch depth, then go through a maximum for a notch depth of approximately 40 per cent, and eventually the stress distribution should become uniform for a 100 per cent notch, Fig. 2a. This latter decrease of stress concentration is explained by the fact that a notch of given finite radius becomes relatively less sharp the deeper the notch is, terminating in a theoretically cylindrical bar if the notched section becomes very small. If the notch radius were not constant, or proportional to the unnotched diameter, but proportional to the diameter of the notched section (d), the stress concentration would first increase with increasing notch depth and then approach a constant value for notch depths over about 50 per cent, Fig. 2b.

The stress concentration factor rapidly decreases with progressing plastic stretching (5). It appears that after a certain minimum

amount of stretching, say 2 to 5 per cent, the residual stress concentration is practically independent of the original notch radius, within wide limits, zero to approximately 0.1 of the diameter. Consequently, the properties of notch ductile test bars having notches with such radii are almost identical, see Fig. 6.

The effect of stress concentration factor is most clearly observed in the notch ductility, i. e., the average contraction in area (at failure) of the notched section (1), (2), (4). For a constant notch

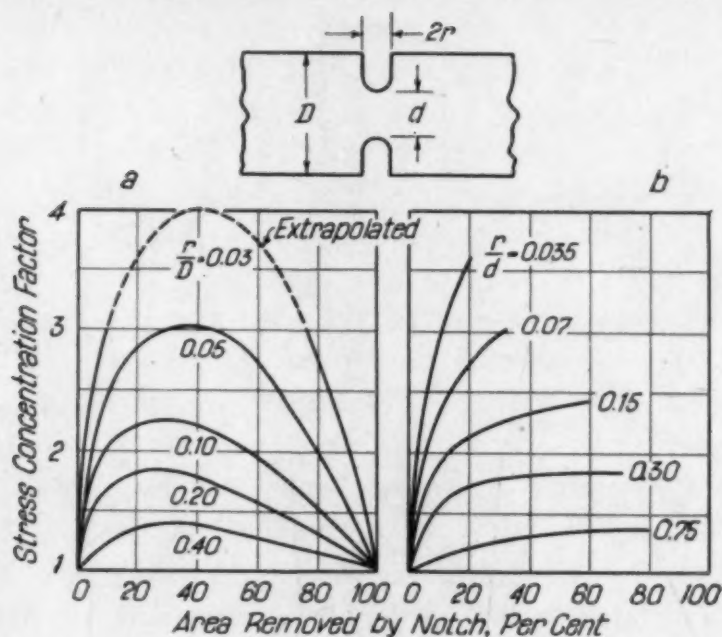


Fig. 2—Effect of Notch Depth and Notch Radius on Stress Concentration in a Flat-Notched Bar. (Derived from Frocht.)

radius, the notch ductility first decreases rapidly with increasing notch depth, and then apparently passes through a flat minimum; the following increase for very deep notches is, however, not definitely established as yet. The higher the inherent ductility, (e. g., the lower the strength level of a heat treated steel) and the larger the notch radius, the larger is the minimum notch ductility, the curves for various metals being almost parallel, Fig. 3.

The lateral stress increases almost linearly with the notch depth, i. e., the cross section removed by notching. This has been derived both from the elastic strains of the notched sections and particularly from the change of the average tensile strength, or notch strength, with increasing notch depth (1). From previous experimentation, it might be assumed that a linear increase of the notch strength with increasing notch depth is the general relation for any ductile and

homogeneous metal (1). Thus, if the notch strength ratio, or ratio of notch strength to ultimate strength, is plotted versus the notch depth, straight lines are obtained for many ductile metals. Such a straight line frequently terminates, for a sharp notch, having a 100 per cent notch depth, in a value of approximately twice the ultimate strength of the metal, Fig. 3a. This relation is explained by a corresponding increase in lateral stress. The notch radius, within the limits previously discussed, should not affect this relation (5); and

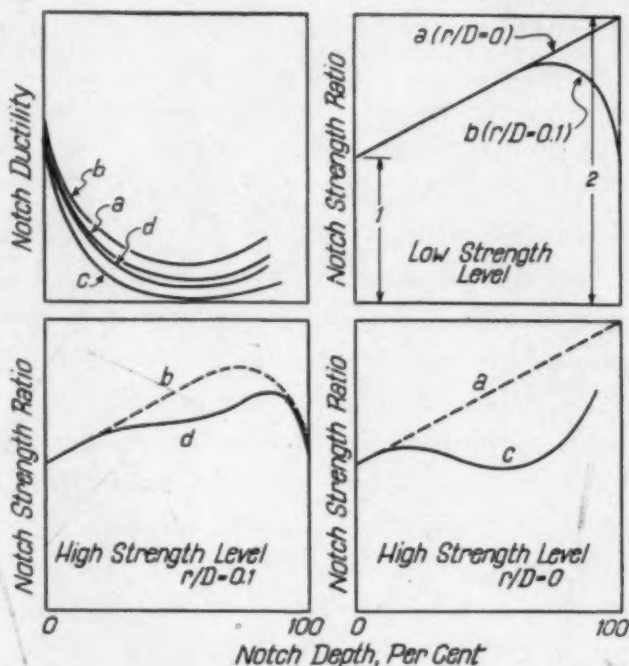


Fig. 3—Schematic Representation Showing the Effect of Notch Depth on the Properties of Notched Tensile Test Bars.

the lateral stress correspondingly should be little dependent upon the notch radius.

If, however, the notch radius exceeds a certain limit, both the lateral stress and the notch strength decrease, approaching again the tensile strength for an infinitely large radius (5).

Consequently, for notches having a constant radius, the linear trend of the notch strength versus notch depth curve should terminate at a certain notch depth and a reversal of the trend or decrease of notch strength, with increasing notch depth, should become noticeable, Fig. 3b. The notch strength should again approach the ultimate strength. As the radius becomes larger, the reversal of the trend occurs at smaller notch depths. Thus, for various notch radii,

notch strength versus notch depth curves are expected, which are almost identical straight line relations for a considerable range of notch depth, but then fan out to lower values for large notch depths.

Furthermore, this linear increase of notch strength with increasing notch depth only applies to notch ductile metals. The ductility of such metals must be sufficiently high to cause the tensile load to reach a maximum. It was observed that notch tensile test bars of heat treated low alloy steels exhibit a decrease in load before failure if their notch ductility exceeds approximately 5 per cent, or approximately the same value as the uniform reduction in area of an un-notched bar (2), (5).

If, on the contrary, the metal is notch brittle, the notch strength should deviate from the basic curves (for notch ductile metals) to lower values. This deviation should become larger as the notch ductility becomes smaller, and the ductility in turn is dependent upon the retained stress concentration. As previously discussed, the retained stress concentration is determined primarily by two factors, the inherent ductility of the metal and the initial stress concentration. For a notch of given small radius, therefore, if the stress concentration possesses a maximum at intermediate notch depth, a wavy notch strength versus notch depth curve should result, Fig. 3c, as discussed in detail in a previous publication (2). In addition, if the radius is large, such a curve should show a reversal at very deep notches, so that the notch strength approaches the tensile strength; and this reversal should occur earlier as the radius becomes larger, Fig. 3d.

The following investigation refers primarily to these relations between the notch strength, notch depth, and notch radius. The laws governing the fracture stress of unnotched and notched test bars are also the subject of this investigation. Further work will be done also on other characteristics of notched tensile test bars, such as the yield strength values corresponding to various strains. The peculiar changes of the notch ductility with increasing notch depth present an additional problem. If these complex relations were fully recognized and reduced to superimposed simpler effects, considerable progress would have been made towards the analysis of the stress-strain relations in notched structures of ductile metals.

PROCEDURE

Tests on notched test bars possessing notches varying in both

the radius and the depth offer a rather unique opportunity to confirm or discount previously developed fundamental conceptions. Therefore, a detailed study was made of various strength levels of S.A.E. 3140 steel, Table I, subjected to concentric notched bar tensile tests (5).

The test bars were provided with notches having depths of 15, 30, 50, 65, 80, and 90 per cent notch, and radii of 0.000, 0.008, and

Table I
Properties of S.A.E. 3140 Steel Oil-Quenched from 1525 Degrees Fahr.

Temperature (1 Hr.) Degrees Fahr.	Specimen Diameter In.	Yield Strength 1000 Psi.	Tensile Strength 1000 Psi.	Contraction in Area Per Cent	Strength Level 1000 Psi.
500	0.351	233	273	52	
	0.351	233	273	52	270
650	0.350	216	241	55	
	0.350	218	242	55	240
740	0.501	200	211	..	
	0.501	198	215	..	
	0.355	...	220	57	
	0.355	...	220	57	
	0.301	...	222	54	220
830	0.500	181	188	57	
	0.500	178	186	57	
	0.300	185	196	58	
	0.299	184	195	58	190
1000	0.500	133	147	60	
	0.500	130	144	60	
	0.300	140	152	62	
	0.300	141	153	61	145
1200	0.500	110	128	62	
	0.500	112	129	62	
	0.300	113	130	66	
	0.300	113	130	66	130

All specimens were cut longitudinally from 3/4-inch diameter hot-rolled rod.

0.031 inch. The preparation of the specimens and equipment has been described previously (5).

The results of the tests are assembled in Table II and Figs. 4 to 6. The agreement between notch strength values determined under identical conditions is better than ± 5 per cent in all cases. It was possible to determine the notch ductility with sufficient accuracy only for the highest strength levels. The accuracy of the measurements of notch ductility is particularly poor for comparatively large notch ductilities, at present. The moment of rupturing of notched specimens which fail at decreasing loads cannot be determined by the transverse strain gage definitely; and the accuracy of microscopic measurements is not better than ± 2 per cent. Consequently only measurements by the gage are shown in Table II, and even these must be considered unreliable when the ductility is large.

RESULTS

The results of the various tests again showed clearly the universal significance of the *notch ductility*. All the curves of notch ductility versus notch depth, Fig. 4, were of the same general type. The notch reduced the average contraction in area of the notched section

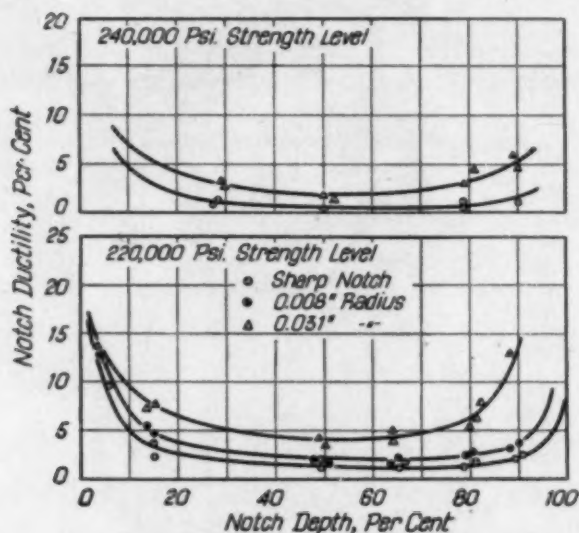


Fig. 4—Effect of Notch Depth, Strength Level, and Notch Radius on the Notch Ductility of S.A.E. 3140 Steel.

to a value which decreased with decreasing notch radius and increasing strength level, and which, within the limits of accuracy, assumed a flat minimum at notch depths between 40 and 60 per cent. These relations can be considered as a rather convincing proof that the stress concentration, which is responsible for the embrittlement, possesses a maximum in an intermediate range of notch depths.

The *notch strength* of the lowest investigated strength level, 145,000 psi., increased with the notch depth almost linearly, in agreement with previous observations on comparatively ductile, wrought metals, Fig. 5. The test bars provided with the sharp notch, 0.000-inch radius, yielded such a relation very closely approaching a value of twice the tensile strength for a 100 per cent notch. The larger notch radius, 0.031 inch, affected the notch strength only very slightly, up to a notch depth of approximately 75 per cent. For deeper notches, however, the notch strength increasingly deviated from that for sharply notched bars, exhibiting a flat maximum at a notch depth of approximately 85 per cent.

The steels having higher strength levels yielded complex notch

Table II
Results of Notched Bar Tensile Tests on S.A.E. 3140 Steel

Notch Depth Per Cent	Notch Radius Inch	Notch Strength 1000 Psi.	Notch Strength Ratio	Notch Ductility Per Cent	Fracture Stress 1000 Psi.	Outside Diameter of Test Bar Inch	Notch Sharpness (Notch Radius Notch Diameter)
145,000 Psi. Strength Level							
0	∞	152	1.00	62	261	0.300	∞
0	∞	153	1.00	61	257	0.300	∞
49	0.000	223	1.53	5.9	229	0.492	0.000
50	0.000	211	1.45	13.7	235	0.500	0.000
50	0.031	228	1.56	12.8	251	0.500	0.088
80	0.000	266	1.84	0.500	0.000
80	0.000	262	1.81	5.4	277	0.500	0.000
80	0.031	248	1.71	18.1	283	0.500	0.137
80	0.031	262	1.81	18.2	295	0.500	0.137
89	0.000	267	1.84	0.500	0.000
89	0.000	274	1.89	0.500	0.000
90	0.031	262	1.81	18.2	308	0.500	0.191
90	0.031	262	1.81	18.8	310	0.500	0.191
190,000 Psi. Strength Level							
0	∞	196	1.00	58	310	0.300	∞
0	∞	195	1.00	58	302	0.299	∞
49	0.000	266	1.39	3.9	277	0.492	0.000
49	0.000	267	1.40	4.0	278	0.498	0.000
51	0.031	281	1.47	9.3	306	0.481	0.092
50	0.031	297	1.56	7.7	322	0.500	0.088
50	0.031	287	1.50	7.9	310	0.500	0.088
80	0.000	310	1.62	3.8	322	0.499	0.000
80	0.000	307	1.61	4.0	320	0.499	0.000
80	0.031	332	1.74	13.7	364	0.499	0.139
80	0.031	320	1.68	13.7	371	0.499	0.139
90	0.000	331	1.73	4.7	348	0.499	0.000
90	0.000	319	1.67	5.0	336	0.500	0.000
90	0.031	341	1.79	10.4	381	0.499	0.200
89	0.031	337	1.77	10.5	377	0.499	0.202
220,000 Psi. Strength Level							
0	∞	222	1.00	54	...	0.301	∞
0	∞	220	1.00	57	334	0.355	∞
0	∞	220	1.00	57	327	0.355	∞
5	0.000	234	1.05	15.1	260	0.292	0.000
6	0.000	233	1.05	11.5	254	0.296	0.000
4	0.008	229	1.03	11.6	237	0.300	0.027
4	0.031	234	1.05	18.2	253	0.300	0.105
4	0.031	232	1.04	15.7	248	0.300	0.105
15	0.000	245	1.10	7.1	264	0.301	0.000
15	0.000	247	1.11	6.4	264	0.301	0.000
14	0.008	251	1.13	5.6	266	0.301	0.029
15	0.008	248	1.12	5.7	263	0.301	0.029
14	0.031	253	1.14	8.4	270	0.301	0.111
14	0.031	252	1.14	8.4	262	0.301	0.111
32	0.000	268	1.21	0.500	0.000
31	0.000	269	1.21	0.500	0.000
30	0.008	267	1.20	0.500	0.019
30	0.008	267	1.20	0.500	0.019
28	0.031	278	1.25	0.501	0.073
29	0.031	276	1.24	0.501	0.073
49	0.000	266	1.20	2.8	274	0.500	0.000
49	0.000	272	1.23	1.8	277	0.501	0.000
49	0.008	298	1.34	0.5	300	0.500	0.022
50	0.008	294	1.32	0.6	296	0.501	0.023
49	0.031	322	1.45	4.4	337	0.501	0.086
50	0.031	324	1.46	2.8	333	0.501	0.087
66	0.000	293	1.32	2.7	301	0.501	0.000
66	0.000	272	1.23	0.4	273	0.500	0.000
64	0.008	305	1.37	2.0	311	0.501	0.027
65	0.008	316	1.42	0.0	316	0.500	0.027
64	0.031	350	1.58	2.6	359	0.500	0.104
64	0.031	344	1.55	0.0	344	0.500	0.104
79	0.000	279	1.26	12.7	319	0.500	0.000
81	0.000	303	1.36	2.6	311	0.501	0.000

Table II—(Continued)
Results of Notched Bar Tensile Tests on S.A.E. 3140 Steel

Notch Depth Per Cent	Notch Radius Inch	Notch Strength 1000 Psi.	Notch Strength Ratio	Notch Ductility Per Cent	Fracture Stress 1000 Psi.	Outside Diameter of Test Bar Inch	Notch Sharpness ($\frac{\text{Notch Radius}}{\text{Notch Diameter}}$)
80	0.008	352	1.58	0.0	352	0.500	0.036
80	0.008	354	1.59	0.0	354	0.497	0.036
81	0.031	357	1.61	1.0	361	0.501	0.140
80	0.031	350	1.58	8.0	381	0.500	0.138
82	0.031	364	1.64	7.4	393	0.501	0.145
80	0.062	317	1.43	9.7	343	0.500	0.279
80	0.062	312	1.41	8.0	383	0.500	0.277
81	0.250	264	1.19	22.3	301	0.500	1.132
81	0.250	254	1.14	25.4	296	0.500	1.136
90	0.000	320	1.44	7.2	345	0.500	0.000
90	0.000	348	1.57	0.0	348	0.500	0.000
89	0.008	374	1.68	0.0	374	0.501	0.048
89	0.008	380	1.71	0.0	380	0.500	0.048
88	0.031	354	1.60	10.4	395	0.499	0.181
240,000 Psi. Strength Level							
0	∞	241	1.00	55	350	0.350	∞
0	∞	242	1.00	55	348	0.350	∞
28	0.000	254	1.05	1.0	257	0.300	0.000
28	0.000	267	1.10	1.1	270	0.300	0.000
29	0.016	298	1.23	3.0	307	0.300	0.063
29	0.016	299	1.24	2.8	308	0.300	0.064
51	0.000	210	0.88	0.500	0.000
50	0.000	183	0.76	0.3	184	0.500	0.000
52	0.031	326	1.35	1.3	330	0.500	0.089
50	0.031	326	1.35	1.6	330	0.500	0.088
79	0.000	222	0.92	0.5	223	0.499	0.000
80	0.000	259	1.07	1.1	262	0.499	0.000
80	0.031	376	1.55	2.9	388	0.500	0.137
81	0.031	390	1.61	4.5	408	0.499	0.143
90	0.000	300	1.24	1.2	304	0.499	0.000
90	0.031	386	1.59	4.4	403	0.499	0.195
89	0.031	373	1.54	6.1	397	0.499	0.191

strength versus notch depth curves throughout. These are of two types, the one type for the sharper notches, and the other type for the notch of larger radius. The tests on the sharply notched bars, having 0.000 and 0.008-inch radius, resulted in wavy notch strength versus notch depth curves, of the general trend predicted previously (2). These curves can be described best by comparison with straight lines extending from the tensile strength, for the unnotched bar, to twice the tensile strength, for the limiting condition of a 100 per cent notched bar, Fig. 3a. The experimental curves invariably deviated from such a straight line relation, exhibiting a maximum deviation at a notch depth between 60 and 70 per cent. The magnitude of this deviation increased with both increasing strength level and decreasing notch radius, i. e., with decreasing notch ductility, Fig. 5.

The notch strength versus notch depth curves for bars provided with a 0.031-inch radius notch possessed a peculiar shape, which can be readily explained as resulting from a superposition of

the two effects that have been discussed. The increasing strength level causes a slightly increasing waviness of the curves, and the large notch radius causes a universal reduction of the values for the deepest notches.

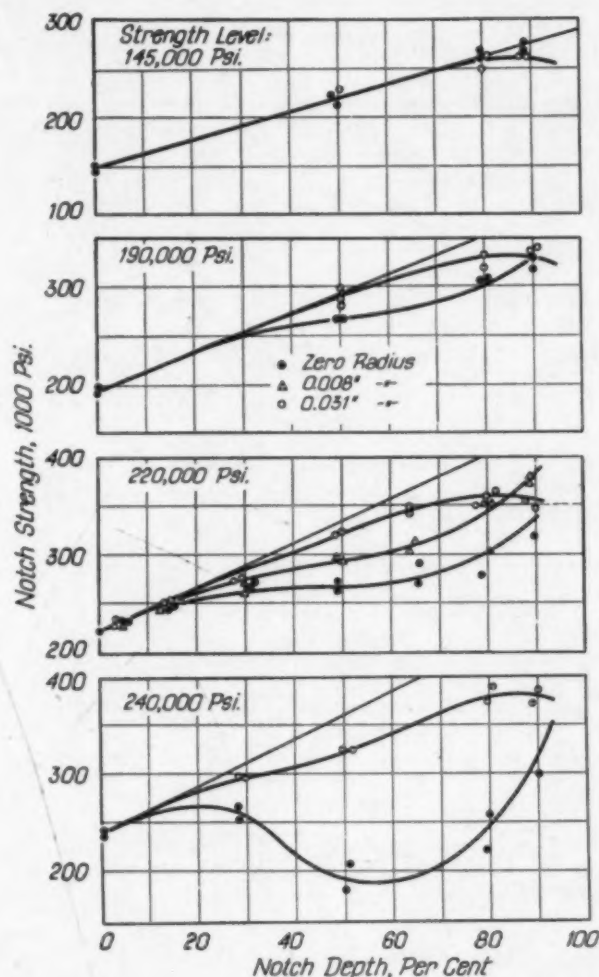


Fig. 5—Effect of Strength Level and Notch Radius on the Notch Strength Versus Notch Depth Curves.

The effect of notch radius is further illustrated in Fig. 6. For 50 per cent notched bars, it was observed previously that the radius affected the notch strength for notch ductile conditions only slightly in the range of 0.000 to 0.031 inch. For 80 per cent notched bars, it has been found now that the notch strength for the notch ductile condition remains constant for notch radii only up to approximately 0.025 inch. For both notch depths the notch strength then decreases with increasing notch radius, approaching the tensile strength for an infinitely large radius. The reduction of the notch strength with

increasing strength level is large for sharp notches but becomes insignificant if the notch radius exceeds approximately 0.062 inch.

The various strength levels of a heat treated steel can be compared more extensively with each other by reducing the notch strength values to a common basis. This is achieved by dividing them by the strength level. The resulting *notch strength ratios*

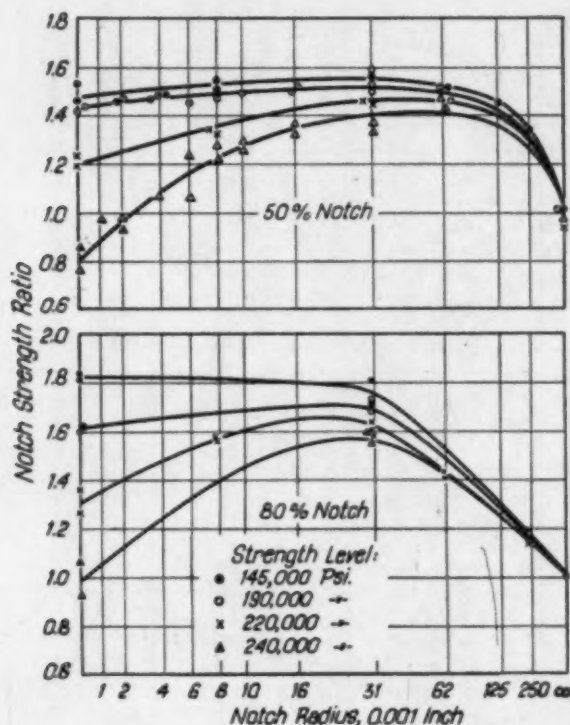


Fig. 6—Effect of Strength Level and Notch Depth on the Notch Strength Ratio Versus Notch Radius Curves.

plotted versus the notch depth now follow trend curves, Fig. 7, which appear to belong to a single family of curves, for the sharper notches. For the lowest strength level, having a relatively high notch ductility, such a curve is again practically a straight line extending from the value 1.0 for zero notch depth to a value close to 2.0 for a 100 per cent notch depth. The curves of Fig. 7 actually agree better with straight lines which are slightly different for the different strength levels. The limiting notch strength ratio for the highest strength level may be as low as 1.85 rather than 2.0. These variations, however, do not exceed sufficiently the limits of accuracy to justify definite conclusions. The curves for conditions having lower ductilities follow this basic curve for shallow notches, but gradually fall below it as the notch depth increases. Then, for very

deep notches the curves appear again to approach the basic straight line, but the extent of this last effect is rather indefinite, according to the test results available at present.

The notch strength ratio versus notch depth curves for test bars provided with a 0.031-inch radius notch follow up to a notch depth of approximately 70 per cent, the same curves as those that

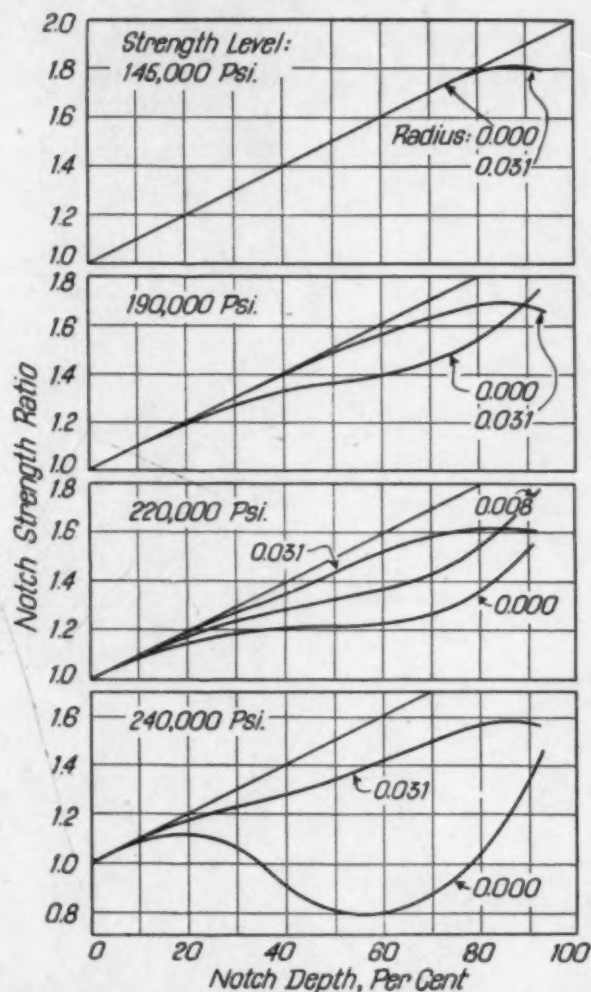


Fig. 7—Effect of Notch Depth, Strength Level and Notch Radius on the Notch Strength Ratio of S.A.E. 3140 Steel.

apply generally to tests with sharply notched bars. For deeper notches, however, they gradually deviate to lower values; and for notch depth values over 80 per cent, these notch strength values decrease rather than increase. The trend of these curves is explained by the fact that for a constant diameter of the cylindrical portion (cylindrical diameter) the diameter of the notched section (notch diameter) approaches zero as the notch depth becomes large. Con-

sequently, the constant radius of 0.031 inch becomes large in comparison to the notch diameter, for deep notches.

Thus, the results of the experimentation agree well with the qualitative conceptions developed in the introduction.

FUNDAMENTAL RELATIONS

Fundamentally, it appears that the "sharpness" of a notch should be measured by the ratio (r/d) of notch radius to notch

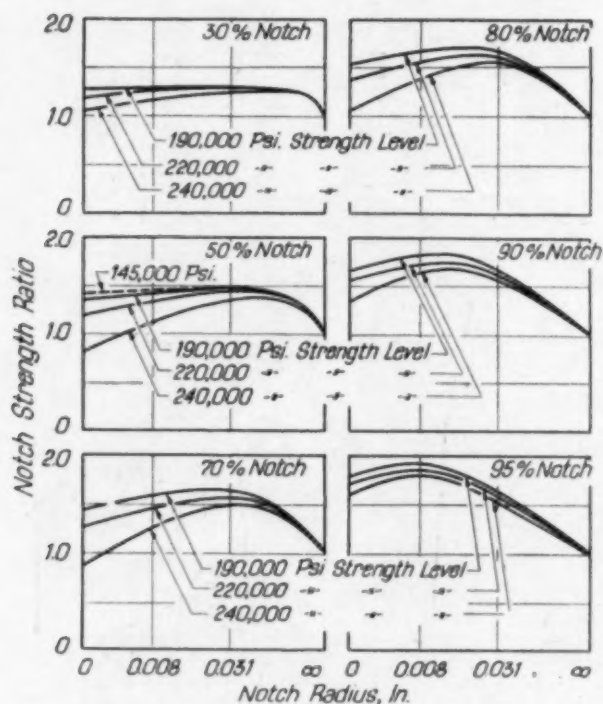


Fig. 8—Effect of Notch Depth and Strength Level on the Notch Strength Ratio Versus Notch Radius Curves.

diameter rather than by the ratio (r/D) of notch radius to cylindrical diameter. However, it would be inconvenient to determine experimentally the notch strength for specimens possessing varying notch depth and such a constant "notch sharpness".

On the contrary, a notch strength versus notch depth curve for a constant "notch sharpness" can be readily obtained by graphical construction. Experimental data on the effect of sharpness are available for two notch depths, 50 and 80 per cent, Fig. 6, as previously discussed. The corresponding relations for other notch depths can be developed by interpolation and extrapolation; and such curves

were constructed for notch depth values of 30, 70, 90, and 95 per cent, Fig. 8.

For convenience, the same data can also be assembled in families of curves (one set for each strength level) illustrating the effect of the notch radius on the notch strength ratio for various notch depths, Fig. 9.

From these fundamental curves, Figs. 8 and 9, notch strength

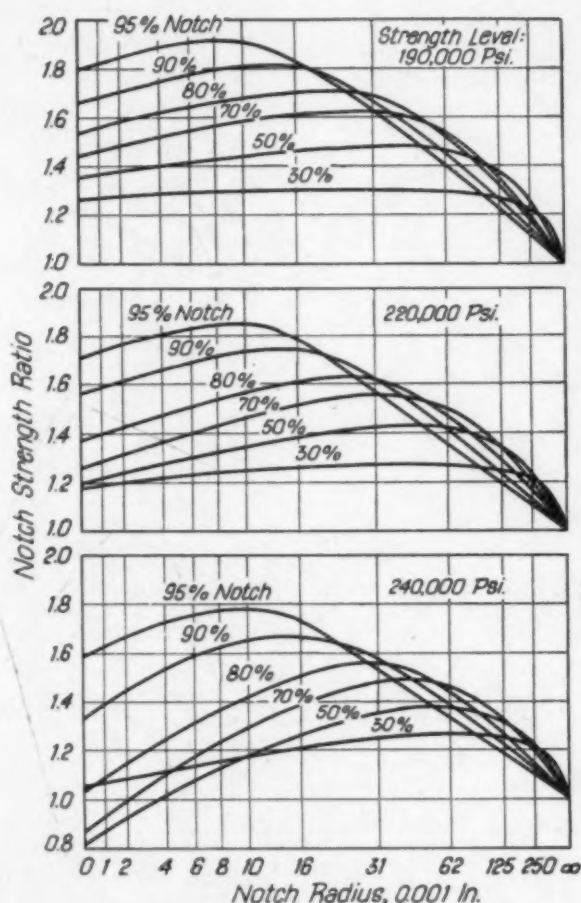


Fig. 9—Effect of Notch Depth and Strength Level on the Notch Strength Ratio Versus Notch Radius Curves.

ratios for a constant notch sharpness (r/d) can be taken for various notch depths. These values have been plotted for all strength levels and for three values of notch sharpness, $r/d = 0.000$, 0.029 , and 0.089 which correspond to actual specimens with 50 per cent notches and radii of 0.000 , 0.008 , and 0.031 inch respectively.

These derived curves, Fig. 10, in contrast to the experimental notch strength ratio versus notch depth curves, Fig. 7, can be made readily to approach a limiting notch strength ratio of 2.0 , for a 100

per cent notch. This proves that the reversal of the curves for test bars having a 0.031-inch radius notch, at a large notch depth, is purely a geometrical effect, associated with the variation of the notch diameter with the notch depth. This effect is eliminated from the derived curves, Fig. 10, which now emphasize the embrittling effect of both notch sharpness and strength level. The embrittlement caused by a sharp notch and/or a high strength level can be meas-

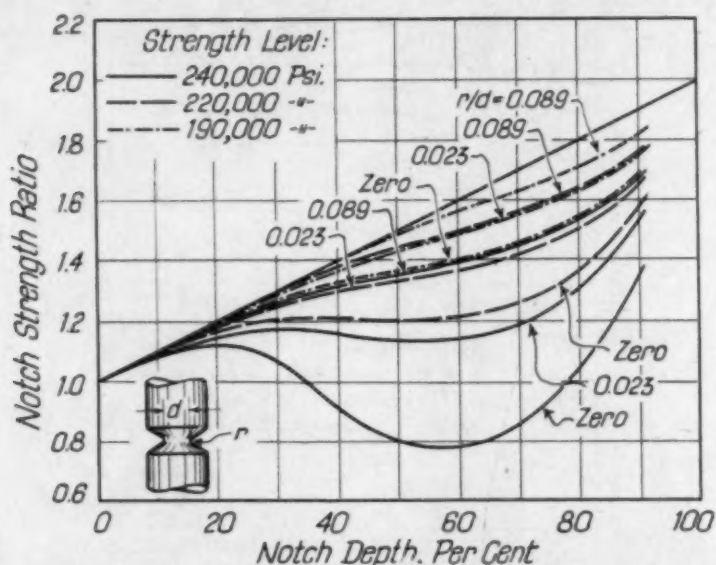


Fig. 10—Derived Curves Showing Effect of Notch Depth, Strength Level and Notch Sharpness on Notch Strength Ratio. Numbers at Curves Denote Notch Sharpness r/d .

ured by the belly depth of a particular curve; the greater the deviation of the curve from the limiting straight line, the larger is the embrittling effect.

The derived notch strength ratio versus notch depth curves for the various strength levels have been assembled in Fig. 10, in order to illustrate the universal nature of this representation. Apparently, for the range of strength levels investigated, the effects of notch sharpness and strength level are interchangeable; for example, the same notch strength ratio versus notch depth curve is obtained for a strength level of 240,000 psi. and a notch sharpness (r/d) of 0.089 as for a strength level of 190,000 psi. and a notch sharpness of zero. Thus, within the limits of experimental accuracy, these notch strength ratio versus notch depth curves represent a single family of curves.³ There were some irregularities in the shape of the origi-

³Similarly, a single family of curves was obtained in eccentric notched bar tensile tests on test specimens possessing various strength levels and radii and a notch depth of 50 per cent. Therefore, the effects of the factors strength level, notch radius, notch depth, and eccentricity can be represented by a single family of surfaces.

nal curves of Fig. 10, which may be ascribed to the fact that a comparatively small number of tests have been considered as sufficient to reveal the complex, fundamental relations that have been discussed. In order to obtain the final curves, the various steps of the procedure were repeated several times, some corrections of the trend curves being made in order to avoid intersection of the derived curves. This was found to be possible, without exceeding the limits of experimental accuracy.

THE SIGNIFICANCE OF THE FRACTURE STRESS AND THE TECHNICAL COHESIVE STRENGTH

The average value of stress observed at or immediately preceding the failure of a tensile test specimen is generally considered an important characteristic of the metal. This fracture stress is therefore frequently taken as the (technical) cohesive strength of the metal. This is true, however, only if the stress is uniformly distributed at fracture and if the condition of the metal has not been altered during the test by a large plastic strain, according to the previous definition of the term (3).

The fracture stress of a brittle metal, failing by tensile stresses, may be an important physical constant. Such a metal does not undergo changes during the application of the load; and with proper testing technique the load can be applied uniformly over the cross section (pure tension). For example, it has been found that the normal stress on the cleavage plane of brittle metal crystals does not depend upon the orientation of the crystal (8).

However, a ductile metal subjected to a regular tensile test undergoes two important changes which affect the metal characteristics. First, the properties of the metal change with progressing plastic flow; and second, the necking which develops prior to the failure introduces a triaxial stress state and a nonuniform distribution of stress, which may also affect the metal properties.

Regarding the influence of plastic strains on the fracture stress, the conception has been introduced by Ludwik (9) that the cohesive strength increases with progressing plastic flow, in a manner slightly different from the simultaneous increase in yield strength (or strain hardening). Tests by Davidenkov and Wittmann (10) and Hollomon (11) on specimens drawn or stretched at room temperature and tested at the temperature of liquid air confirmed this effect of plastic flow on the fracture stress.

The necking of a tensile test specimen creates a stress state which is identical with that of a rather deep but large-radius notch. The action of a notch on the fracture stress consists of two effects which are practically independent, according to the previous tests on heat treated low alloy steels (1), (2), (5). McAdam and Mebs (3) concluded that the fracture stress increases with increasing tri-

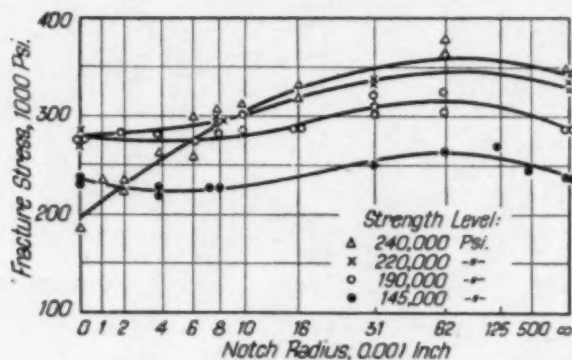


Fig. 11—Effect of Notch Radius on the Fracture Stress of Heat Treated S.A.E. 3140 Steel Tensile Specimens. (50 Per Cent, 60 Degree, V-Notch.)

axiality; while the stress concentration or nonuniform stress distribution present at the moment of failure should generally reduce the (average) fracture stress.

The degree of triaxiality has been found (1) to increase, practically linearly, with the notch depth (reduction in cross sectional area by notching). It decreases with increasing opening angle of the notch. The radius at the notch bottom has practically no influence as long as it is smaller than approximately 1/10 of the notch diameter; beyond this limit the triaxiality decreases rapidly with increasing notch radius (5).

The degree of stress concentration is determined primarily by the notch radius and the extent of plastic flow preceding the failure. The smaller the notch radius, the larger the initial stress concentration present in the elastic state. However, during plastic flow the stress distribution becomes progressively more uniform. Thus, within the range of constant triaxiality, the fracture stress of a (notch-) brittle metal, such as a heat treated steel having a strength level of 240,000 psi., has been found to decrease with decreasing notch radius, Fig. 11 (5). However, if the notch ductility exceeded 2 to 3 per cent, such as in a heat treated steel having a strength level of 190,000 psi., the notch radius had little effect on the fracture stress.

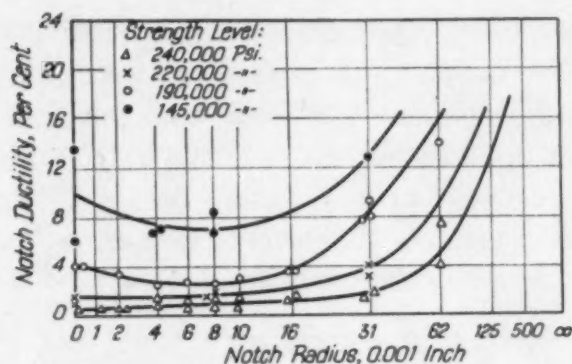


Fig. 12—Effect of Notch Radius on the Ductility of Heat Treated S.A.E. 3140 Steel Tensile Specimens. (50 Per Cent, 60 Degree, V-Notches.)

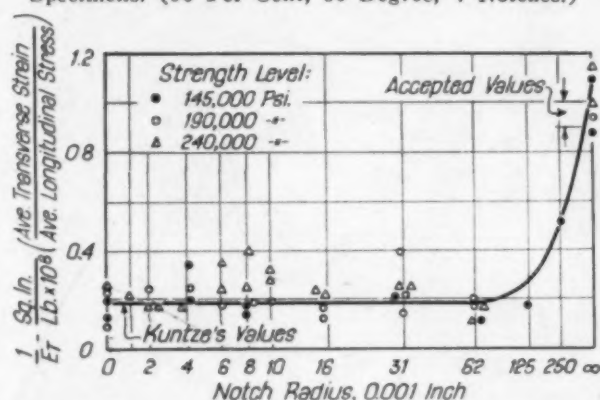


Fig. 13—Effect of Notch Radius on the Inverse Transverse Modulus of Heat Treated S.A.E. 3140 Steel Tensile Specimens with 50 Per Cent Notches.

Consequently, the initial stress concentration is almost eliminated by plastic strains of this order.

If no stress concentration is present, the shape of the fracture stress versus notch radius curve is governed by two factors, the ductility and the stress state. The dependence of these characteristics upon the notch radius is shown in Figs. 12 and 13 (5). Within the range of constant triaxiality (zero to 0.062-inch radius for a 50 per cent notch) the fracture stress reflects the ductility, Fig. 12, showing a slight minimum where the ductility is at a minimum, and increasing with increasing radius in the same manner as the ductility.

Above 0.062-inch radius, the triaxiality, as indicated by the (inverse) transverse elastic modulus, Fig. 13, decreases rapidly with increasing radius to zero at infinite radius. In this range of notch radii, the fracture stress, Fig. 11, should decrease correspondingly, as explained later. Apparently this effect is greater than that of increasing ductility, since the combined effects cause a decrease of fracture stress from 0.062 inch to infinite radius.

The above relations explain the trend of the fracture stress versus notch depth curves for heat treated steel specimens provided with notches of different radii, Table II and Fig. 14. The shape of the curve depends upon whether the (notch) ductility does or does not exceed a critical value of 2 to 3 per cent. If the ductility is below this limit, the fracture stress versus notch depth curve becomes very complex, such as for the S.A.E. 3140 steel, having a strength

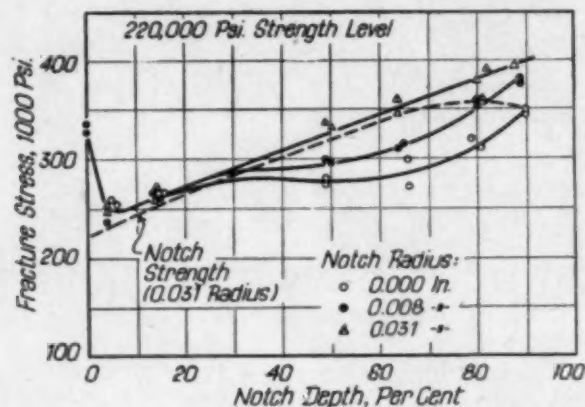


Fig. 14—Effect of Notch Depth and Notch Radius on the Fracture Stress of S.A.E. 3140 Steel Tensile Specimens. (60-Degree, V-Notches.)

level of 220,000 psi. and notch radii of 0.000 or 0.008 inch, Fig. 14. Because of the unknown magnitude of the stress concentration retained at failure, such curves cannot be analyzed in detail, at present. If, however, the notch ductility is above the limit of 2 to 3 per cent, such as for the S.A.E. 3140 steel specimens having a strength level of 220,000 psi. and a notch radius of 0.031 inch, the (initial) stress concentration has no influence, and the fracture stress versus notch depth curve assumes a universal and fairly simple appearance. With increasing notch depth, the fracture stress decreased first rapidly to a minimum, at 5 to 10 per cent notch depth, and then increased again, following a course slightly above the notch strength versus notch depth curve (because of the effect of plastic strain).

From the curve for the 0.031-inch notch radius, the dependence of the fracture stress upon the degree of triaxiality can now be evaluated. Within a range of notch depth between 15 and 80 per cent, the notch ductility of the test bars varied but little, between 4 and 7 per cent, Fig. 4; consequently the effect of the plastic strain preceding the failure should not affect materially any relation between fracture stress and notch depth that can be derived from the above curve.

For shallow notches (less than 15 per cent) the relations are very complex because of the large strains that occur previous to fracture and because of changes in the shape of the notch. While it should be possible to evaluate quantitatively the effect of the shape in the necked portion of an unnotched bar, the influence of plastic strain on the fracture stress cannot be determined, at present. The occurrence of large plastic strains in shallow-notched and unnotched

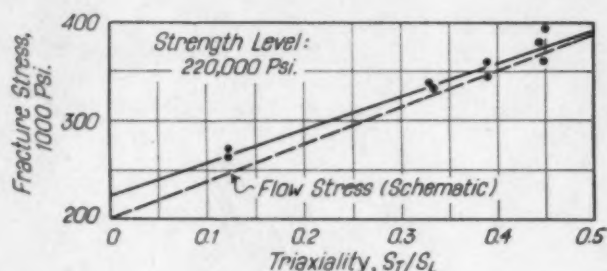


Fig. 15—Effect of Stress State on the Fracture Stress of Heat Treated S.A.E. 3140 Steel.

bars probably explains the high values of fracture stress generally observed on such specimens.

For the very deep notches (greater than 80 per cent) the somewhat larger ductility probably has an insignificant effect on the fracture stress. However, the relative increase in radius with increasing notch depth must be considered. As explained previously, the triaxiality no longer bears the same relation to notch depth as for intermediate notch depths, if the diameter at the root of the notch decreases to a value less than 10 times the notch radius.

However, for the range of notch depth between 15 and 80 per cent, the degree of triaxiality as determined by the notch depth becomes the only significantly differing factor. In this range, the fracture stress (S_F) usually is only slightly higher than the notch strength (S_L); and both increase in practically the same manner with increasing notch depth (R), following approximately the simple relation:

$$S_F \approx S_L = S_n(1 + R),$$

where S_n is the regular tensile strength, and the notch depth (R) is expressed as the fraction of the cross sectional area removed by notching.

According to general conceptions regarding plastic flow, the transverse stress (S_T) should be:

$$S_T = S_L - S_n = S_n \times R$$

Table III
Calculation of Triaxiality from Notch Depth

Notch Depth Per Cent	Fracture Stress 1000 Psi.	R	$R/(1 + R) = S_T/S_L$
14	270	0.14	0.123
12	262	0.14	0.123
49	337	0.49	0.329
50	333	0.50	0.333
64	359	0.64	0.390
64	344	0.64	0.390
80	381	0.80	0.444
81	361	0.81	0.448
82	393	0.82	0.450

The triaxiality can then be defined as the ratio of transverse to longitudinal stress:

$$\frac{S_T}{S_L} = \frac{R}{1 + R}$$

By means of this relation, the fracture stress can be plotted as a function of the triaxiality, Table III and Fig. 15. Confirming McAdam and Meb's (3) conceptions, the fracture stress of a ductile steel increases almost linearly with increasing triaxiality, within the range of triaxiality subject to investigation. No conclusions can be drawn from these results regarding the fracture stress under higher values of triaxiality. In particular, any extrapolation to total triaxiality, $S_T/S_L = 1$, is not justified.

As previously mentioned, the effect of triaxiality on the fracture stress or cohesive stress can be derived from notched bar tensile tests only in the case of a metal condition for which the (notch) ductility exceeds a certain rather small value. It is rather surprising that the rate of increase of fracture stress with increasing triaxiality in the range subject to investigation is almost the same as the rate of increase of the flow stress. If the two fundamental failure characteristics of a steel were really affected in the same manner, the phenomenon that a steel becomes increasingly brittle with increasing triaxiality could not be explained. Apparently, the fracture stress increases with increasing triaxiality slightly less rapidly than the flow stress, Fig. 15. However, it has not been possible to establish this basic relation for heat treated steels with sufficient accuracy, as yet.

Bibliography

1. G. Sachs and J. Lubahn, "Effects of Notching on Strained Metals," *Iron Age*, Vol. 150, 1942, Oct. 8, p. 31-38; Oct. 15, p. 48-52.

2. G. Sachs and J. D. Lubahn, "Notched Bar Tensile Tests on Heat Treated Low Alloy Steels," *TRANSACTIONS, American Society for Metals*, Vol. 31, 1943, p. 125-160.
3. D. J. McAdam and R. W. Mebs, "An Investigation of the Technical Cohesive Strength of Metals," *Metals Technology*, August, 1943.
4. C. W. McGregor and J. C. Fischer, "Relations Between the Notched Beam Impact Test and the Static Tension Test," *Journal of Applied Mechanics*, Vol. 11, 1944, p. A-28-34.
5. G. Sachs, J. D. Lubahn and L. J. Ebert, "Notched Bar Tensile Test Characteristics of Heat Treated Low Alloy Steels," *TRANSACTIONS, American Society for Metals*, Vol. 33, 1944, p. 340-395.
6. M. M. Frocht, "Factors of Stress Concentration Photoelastically Determined," *Journal of Applied Mechanics*, Vol. 2, 1935, p. A67-68.
7. H. Neuber, "Exact Elastic Solutions Concerning the Notch Effect on Plates and Bodies of Rotational Symmetry," *Z. angew. Mathematik*, Vol. 13, 1933, p. 439-442.
8. E. Schmid and W. Boas, "Plasticity of Crystals," Berlin, 1935, p. 176, 258.
9. P. Ludwik, "The Significance of Flow and Rupture Resistance in Material Testing," *Z. Ver. Deut. Ing.*, Vol. 71, 1927, p. 1532-1538.
10. N. Davidenkov and F. Wittmann, "Mechanical Analysis of Impact Brittleness," *Tech. Phys., U.S.S.R.*, Vol. 4, 1937, No. 4, p. 3-17.
11. J. H. Hollomon, "The Notched-Bar Impact Test," *Metals Technology*, April, 1944.

DISCUSSION

Written Discussion: By D. J. McAdam, Jr., G. W. Geil and R. W. Mebs, National Bureau of Standards, Washington, D. C.

This paper contains much valuable information. Some of the conclusions, however, have been expressed with insufficient regard for the limited scope of the experiments, and thus are not generally true. Although all the experiments were made with steels and with one notch angle (60 degrees), the authors have discussed the results as if they apply to any metal and any notch angle. As shown by the writers,^{4,5,6} curves representing the influence of notch characteristics on mechanical properties are not qualitatively the same for all metals. Moreover, a complete picture of the influence of notch depth can be obtained only by considering also the influence of the notch angle.⁴

The authors begin the discussion of their results (page 524) by saying: "The results of the various tests again showed clearly the universal significance of the notch ductility. All the curves of notch ductility were of the same general type." Curves of the type shown, however, are not obtained with all metals; the curves for some metals have at least one reversal. Moreover, even if the curves for all metals were qualitatively similar, the paper does not reveal any "universal significance of the notch ductility". Suitable experiments with notched specimens make it possible to study the qualitative influence of the radial stress ratio (S_2/S_1) on the relation between flow stress, cohesion limit, and ductility, but reveal no reason for assigning any significance to ductility.

⁴D. J. McAdam, Jr. and R. W. Mebs, "An Investigation of the Technical Cohesive Strength of Metals," American Institute of Mining and Metallurgical Engineers, Technical Publication No. 1615, p. 63, *Metals Technology*, Vol. 10, August 1943.

⁵D. J. McAdam, Jr. and R. W. Mebs, "The Technical Cohesive Strength and Other Mechanical Properties of Metals at Low Temperatures," *Proceedings, American Society for Testing Materials*, Vol. 43, 1943, p. 661.

⁶D. J. McAdam, Jr., R. W. Mebs, and G. W. Geil, "The Technical Cohesive Strength of Some Steels and Light Alloys at Low Temperatures," American Society for Testing Materials, Preprint No. 27, 1944.

Two of the writers have shown the variation of the ultimate stress with notch depth for several ferrous and nonferrous metals.⁴ That paper shows also the variation of the breaking stress with the notch angle, but not with notch depth. Figs. 16 and 17, derived from data in the paper referred to,⁴ show the influence of notch depth on ultimate stress and breaking stress, for various notch angles. Fig. 16B also shows the influence of notch depth on theoretical

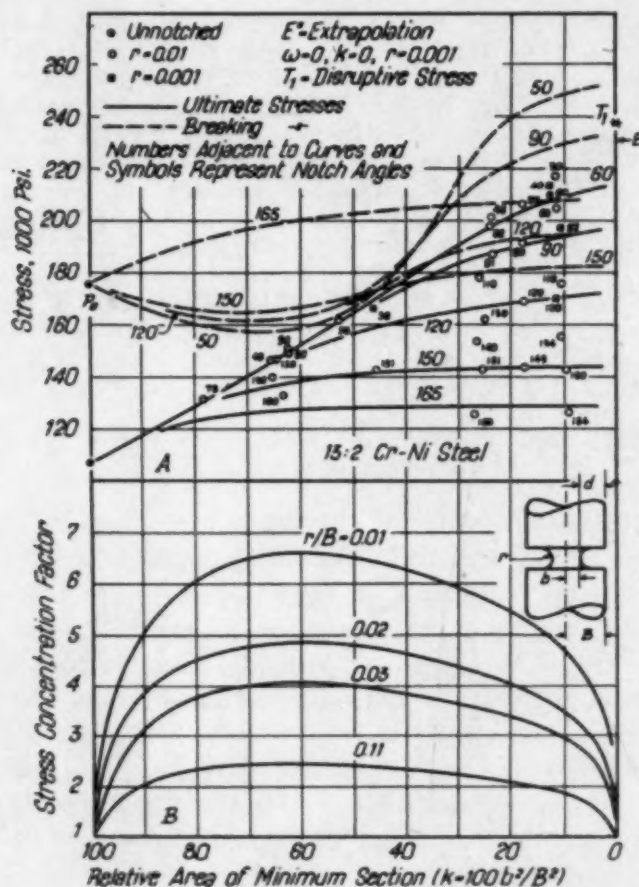


Fig. 16—Effect of Notch Depth on Initial Stress Concentration, on Ultimate Stress, and on Breaking Stress of 13:2 Chromium-Nickel Steel.

(initial) stress concentration. The curves of ultimate stress are of two kinds. Curves of simple form were obtained with annealed copper (Fig. 17B); curves of the same form were obtained with 13:2 chromium-nickel steel (Fig. 16A) and with cold-rolled copper (Fig. 17A) when the notch angle was large (150 degrees or more). All the curves of this form rise at a continuously decreasing rate. Curves of complex form were obtained with the 13:2 chromium-nickel steel and the cold-rolled copper when the notch angle was not more than 120 degrees; these curves rise first at increasing then at decreasing rate.

The initial course of the complex curves is influenced directly or indirectly by stress concentration. As shown in Fig. 16B, theoretical stress concentration is at a maximum at an abscissa ($k = b^2/B^2$) of 60 per cent, but the rate of increase of stress concentration is greatest as the notch begins to

form ($k=100$ per cent). The complex form of some of the curves of ultimate stress in Figs. 16A and 17A is due to the depressing influence of stress concentration; stress concentration also causes the crowding together of the curves throughout an abscissa range representing shallow notches.⁴

For wide angled notches, the stress concentration is small even when the notches are shallow. This is illustrated by the curves of theoretical stress concentration in Fig. 18B. Curves of ultimate stress obtained with wide angled

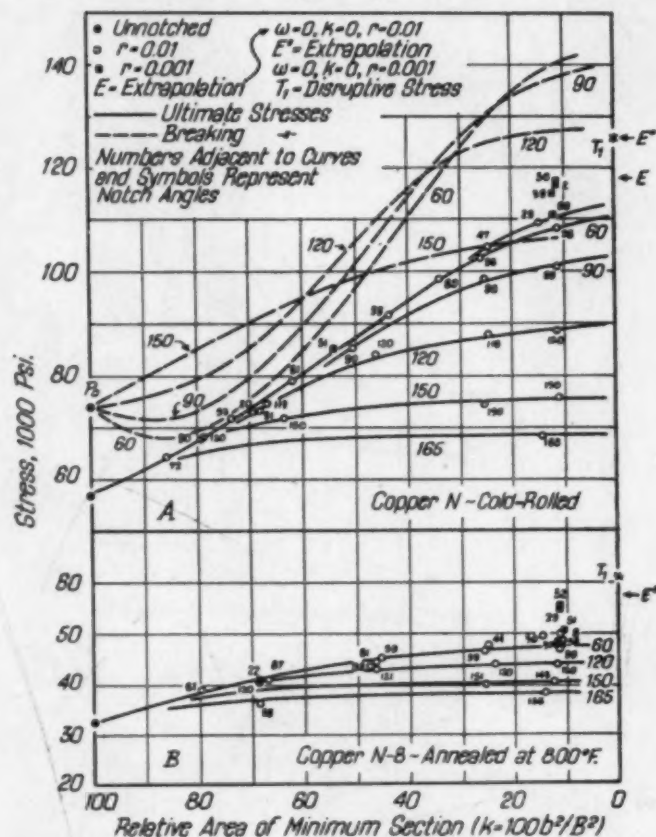


Fig. 17—Effect of Notch Depth, for Various Notch Angles on Ultimate Stress and Breaking Stress; Oxygen-Free Copper.

notches, therefore, are not influenced qualitatively by stress concentration, and consequently are of simple form.

The variation of ultimate stress with notch depth evidently is not generally linear. The approximately linear variation reported by Kuntze and by the authors probably is a fortuitous relationship obtained with notch angle 60-degrees, and is due to the combined variation of stress concentration and radial stress ratio.

In discussing the influence of notches on the breaking stress, the authors say (page 536): "If, however, the notch ductility is above the limit of 2 to 3 per cent,, the (initial) stress concentration has no influence, and the fracture stress versus notch depth curve assumes a universal and fairly simple appearance." However, the nearly linear variation shown in the paper for a range of notch depths from 15 to 80 per cent (85 to 20 per cent for k)

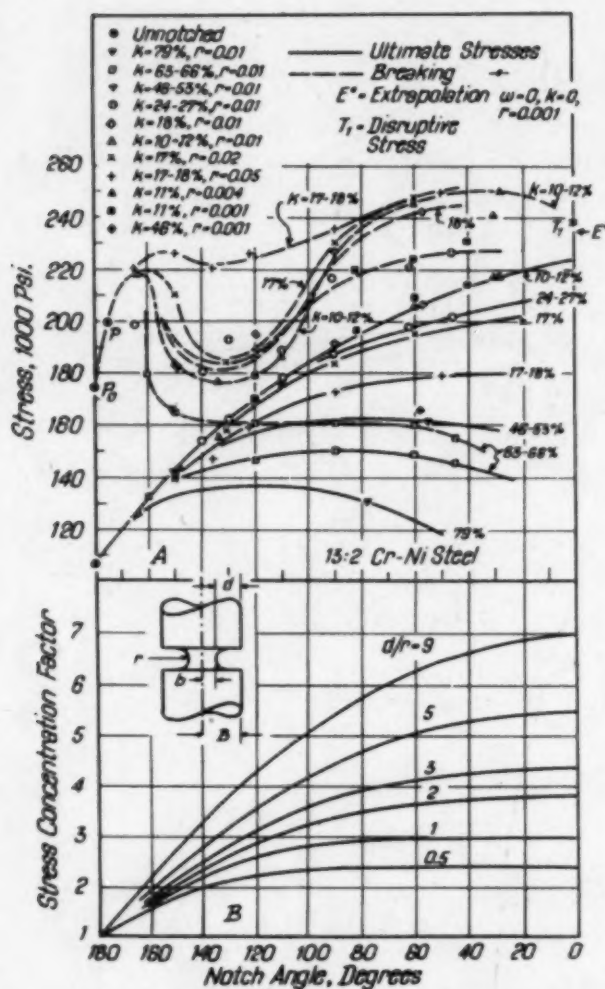


Fig. 18—Effect of Notch Angle on Initial Stress Concentration, on Ultimate Stress, and on Breaking Stress of 13:2 Chromium-Nickel Steel.

is not "universal". As shown in Figs. 16A and 17A the variation of the breaking stress for the metals indicated depends on the notch angle. For notch angles greater than a limiting value the curve is of simple form; for smaller notch angles the curve is complex.

The complexity of a curve of breaking stress, unlike the complexity of a curve of ultimate stress, is not due primarily to stress concentration. This is illustrated by Fig. 18 in which abscissas represent notch angles. The stress concentration rises at a decreasing rate with decrease of the notch angle, although the curves of ultimate stress are of the same simple form, the curves of breaking stress for this metal are of complex form. (For copper and monel metal, the curves of breaking stress are of simple form).

As shown in previous papers by the writers,^{4, 7, 8} the course of a locus of

⁷D. J. McAdam, Jr., "The Technical Cohesive Strength of Metals," *Transactions, American Society of Mechanical Engineers*, Vol. 63; *Journal of Applied Mechanics*, Vol. 8, December 1941, p. A 155-165.

⁸D. J. McAdam, Jr., "The Technical Cohesive Strength and Yield Strength of Metals," *American Institute of Mining and Metallurgical Engineers, Technical Publication No. 1414*, p. 47, January 1942; also *Transactions, Iron and Steel Division*, Vol. 150, 1942, p. 311-357.

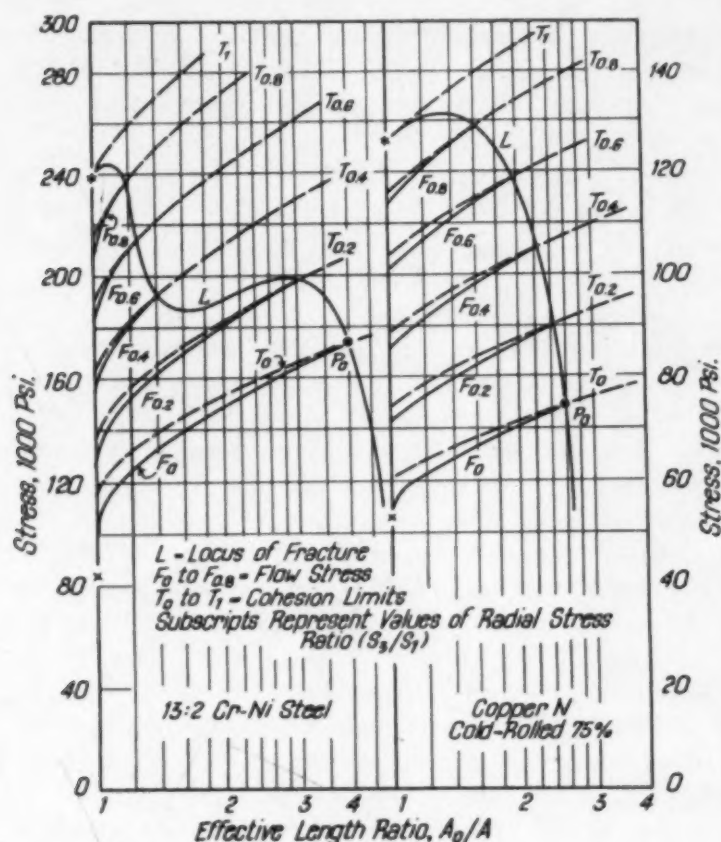


Fig. 19—Influence of Radial Stress Ratio on Flow Stress, Technical Cohesion Limit and Ductility; 13:2 Chromium-Nickel Steel and Oxygen-Free Copper.

breaking stresses depends largely on the differential effect of the radial stress ratio (S_2/S_1) on flow stress and cohesion limit. This differential effect governs the variation of the ductility with the radial stress ratio and thus governs the variation of any specific cohesion limit, because a specific cohesion limit (a cohesion limit corresponding to a specific value of the radial stress ratio) increases with prior plastic deformation. A cohesion limit, as illustrated in Fig. 19, increases less rapidly than the corresponding flow stress.^{4,7,8} The curves shown are qualitative representations. They are assumed to be free from the distorting influence of stress concentration and deformation gradient.

It is gratifying to know that the authors confirm the conclusions of the writers,⁴⁻⁸ about the influence of the radial stress ratio on the breaking stress. In the abstract of the paper, however, the term "cohesive strength" is used in a confusing way. A distinction should be made between "technical cohesive strength" and "technical cohesion limit". The technical cohesive strength of a metal at any instant could be represented by a three-dimensional diagram with the three principal stresses as co-ordinates.^{4,7,8} Any point on such a diagram represents a technical cohesion limit. Technical cohesive strength varies with temperature, rate of deformation, etc., but not with the stress combination.

Although no method of extrapolation can give an exact value of the disruptive stress (the cohesion limit under polarsymmetric tension), an approximate

estimate can be made by curvilinear extrapolation according to the method described by two of the writers.⁴ For example, curvilinear extrapolation by means of Figs. 16A and 18A to zero values of w and k gives the point E'' representing a value of the ultimate stress. The point T_1 (representing the disruptive stress) probably should be above E'' , but below the highest points representing fracture after plastic deformation.

Authors' Reply

We appreciate the contribution of Dr. McAdam, who has carried out some valuable work on notched bar tensile tests including various materials and various notch angles not investigated by us. We have studied the results of his work and cannot find any serious discrepancies between corresponding results such as regarding the shapes of the curves of notch strength and notch ductility vs. notch depth. Our conclusions do not depend upon a straight line relation between notch strength and notch depth; but such a linear function is very convenient, and its existence simplifies the analysis of the more complex relations. Also, we do not claim that the transverse fracture strain, which has been designated as notch ductility, is a fundamental quantity, but only that this value is dependent upon the fundamental factors, stress concentration and triaxiality, in a considerably simpler manner than the notch strength; and, therefore, a clearer conception of the complex relation can be obtained by considering the ductility as the basis of any analysis.

At the present, we do not feel that the problem is sufficiently clarified to standardize terms; however, any strength or limit designates, according to our conception, only an individual value and never an entire function. Consequently we have used cohesive strength in the same sense as McAdam's cohesion limit, and we would prefer some term such as "cohesive strength surface" to designate the whole range of values, for various combinations of the three principal stresses.

The opinion of Dr. McAdam that the complex appearance of the fracture stress vs. notch depth curve can be explained simply by corresponding variations of the stress concentration does not conform with our conceptions, and it appears that he neglected both the direct effect of varying triaxiality and its indirect effect through the ductility. The complex and varying shapes of the fracture stress curves presented by McAdam can be explained by the wide variations in the relative notch radii, and the ductilities exhibited by the material used. An approximately linear relationship over a considerable range of notch depth may be observed only for conditions where the notch ductility varies within a narrow range and the notch sharpness (r/d) does not exceed a certain limit. Regarding the combined effects of stress-concentration, triaxiality, and plastic strain (preceding failure) we intend to explain our conceptions in a more exacting manner in a paper which is now in preparation.

THE INTERPRETATION OF RADIOGRAPHS; PARTICULARLY OF AIRCRAFT PARTS

BY LESLIE W. BALL

Abstract

The purpose of this paper is to outline a basic policy and procedure for the interpretation of radiographs. The objectives of radiography in the aircraft industry are stated. A system of identifying radiographic images with metallurgical defects is presented and methods are suggested for assessing the acceptability of defective parts.

BASIC POLICY

RADIOGRAPHY is used by industry to achieve certain specific objectives, among which the reduction of service failures and of wasted machining costs are predominant. To insure its own future, radiography must achieve these objectives in a more reasonable and a more economical way than any alternative procedure. Both reasonableness and economy depend on the application of a sound basic procedure and on a clear policy of radiographic interpretation.

The X-ray interpreter is often an intermediary between the producer of a raw part and the manufacturer of a finished product. In the case of aircraft, the interpreter is invested by the manufacturer with responsibility for applying quality standards to the acceptance and rejection of raw parts such as castings. The interpreter's standards have to insure that no unserviceable part goes into an airplane, but also, he must realize that his decisions can mean the difference between profit and loss to a producer, such as for example, an aluminum foundry. Some disagreement over X-ray rejections is inevitable, but if these rejections are not supported by a clear and consistent policy, disagreement can lead to extravagant condemnation of the whole X-ray function.

The existing published data and standards for radiographic interpretation are very meager. In the case of steel castings, the U. S. Navy Standards (1)* are excellent, but their application is limited to

*The figures appearing in parentheses pertain to the references appended to this paper.

A paper presented before the Twenty-sixth Annual Convention of the Society, held in Cleveland, October 16 to 20, 1944. The author, Leslie W. Ball, is assistant technical director, Triplett and Barton, Inc., Burbank, Cal. Manuscript received June 7, 1944.

very large parts. In the case of steel welds, the radiographic sections of the Boiler Code (2) are useful for a limited class of construction, and the Ordnance Standards (3) are very helpful for some other applications. In the aircraft field, only a very few correlations between strength and specific defects have been made. Most rejections are still based on unpublished and often confidential experiences. The Air Corps Technical Report No. 4796 was a very necessary first step; but its substance covers only a few aspects of the interpretation problem. Its static test requirements are very welcome and valuable when used as a general guide, but if applied as an absolute criterion of aircraft serviceability, these static load tests would probably lead to service failures under nonstatic loading. Moreover, when defective metal is accepted because an overdesigned part withstands a static test, producers are liable to demand acceptance of defective metal in all aircraft parts. Thus at the present time, the X-ray interpreter cannot rely solely on reference to established standards. His procedure must be based on the application of his own laboratory's knowledge, judgment and testing facilities, to fulfilling the objectives for which his radiography is intended.

In the aircraft industry, the general requirement for safe and serviceable parts can be broken down into seven specific objectives, as follows:

1. The first objective is for adequate service strength. After it has been machined and assembled in the airplane, each part must have sufficient strength to withstand continuously the types and degree of stress for which it was designed.
2. The second objective is for adequate assembly strength. Each part must have sufficient strength to withstand the forces introduced during its assembly into the plane, e. g., riveted sections must be able to withstand the shock of the riveting gun and attachment brackets must have sufficient ductility to overcome imperfection in seating.
3. The third objective is that all parts accepted by X-ray shall pass the shop inspections. Each part must be free from cavities that will be revealed by machining and which then would be rejected. Shop rejections may be based on:
 - a. Unsatisfactory machinability as, e. g., a blowhole causing a twist drill to go out of alignment.
 - b. Stress concentration due to the position of a cavity in the surface.

c. Probable corrosion because a surface cavity will not be sealed by the ordinary anti-corrosion treatment.

d. Lack of confidence in the aircraft, caused by reports from the assembly line of the use of defective even though serviceable material.

4. The fourth objective of aircraft radiography is that parts subject to hydraulic pressure must be free from any condition which may allow seepage of the hydraulic fluid, e. g., those parts in which the hydraulic seal is formed by a honed surface must be free from even minute cavities in the honed area.

5. The fifth objective is that parts that are to be assembled by welding must be free from conditions which make welding difficult. They must be free from dross pockets.

6. A sixth objective concerns composite parts which are X-rayed to determine the position of concealed sections. In these parts even sound material is only acceptable when the required tolerances are attained.

7. A seventh objective occurs in several alloys. Some conditions seen on radiographs may lead to corrosion followed by stress failure, even though at the time the radiograph is made, the part has ample strength.

The degree of defectiveness that justifies rejection because of one or more of these seven considerations varies from part to part. Also it varies with the location of the defect in the part and it depends on the design factors and the shop inspection standards of the consuming aircraft company.

Amid this complexity, the radiographic interpreter can draw on two fairly simple conceptions. One of these is "commercially perfect metal." A commercially perfect casting is one which can be produced consistently by a good foundry, working with adequate controls and with a well designed pattern. A commercially perfect casting is of course free from major defects such as shrink cavities, but it may contain a few minor imperfections. Even for aircraft use, the interpreter can accept without hesitation any casting of this standard. When radiography reveals a lower quality, acceptance must be based on definite knowledge of limitations in the service requirements.

When the interpreter has no knowledge of limitations in the service requirements, he must presume that the casting is a "normal

structural aircraft part." This hypothetical part is subject to all types of stress including bending, impact and fatigue, and also corrosion. However, when the interpreter does have a blueprint or other written data which shows limitations, for example, that fatigue stress is not applied to the part, then he can adjust his rejection standard accordingly.

Few parts are loaded uniformly, so the interpreter must determine from the blueprint where stress concentrations occur. If he is unable to do so, he must presume the most unfavorable stress distribution.

Obviously, the more information that the aircraft manufacturer provides for the radiographic interpreter, the less will be the rejections.

Perhaps the most vital "ignorance factor" which leads to unnecessary rejections is the ratio of the actual strength of a defective part to the service load. If this ratio is high, the interpreter may accept relatively poor quality material, but if this ratio is low, even slightly defective material must be rejected. Unfortunately this ratio, of actual strength to service load, can seldom be determined satisfactorily. Theoretical design calculations involve wide approximations and the jigs used for static tests seldom reproduce the service stresses.

It is because of these limitations in determining this ratio that the aircraft designers with whom we are associated are often unwilling to accept defective material, even when it cannot be proved that the defective part will fail in service. On the other hand, the foundries are unwilling to scrap large quantities of defective, but apparently serviceable parts.

The radiographer can experience a further difficulty, in that the engineering and the purchasing departments of the same company sometimes demand two vitally different policies. The engineers are proud that their combat planes come back even when seriously damaged and they may wish at all times to use only commercially perfect material. On the other hand, the purchasing department may be so pressed by delivery dates and procurement difficulties that they demand acceptance of any part which can get by the minimum specifications.

The job of compromising between these attitudes has to be faced by the radiographic interpreter. His decisions are guided by the function of the part as well as by the loading factors. Any part

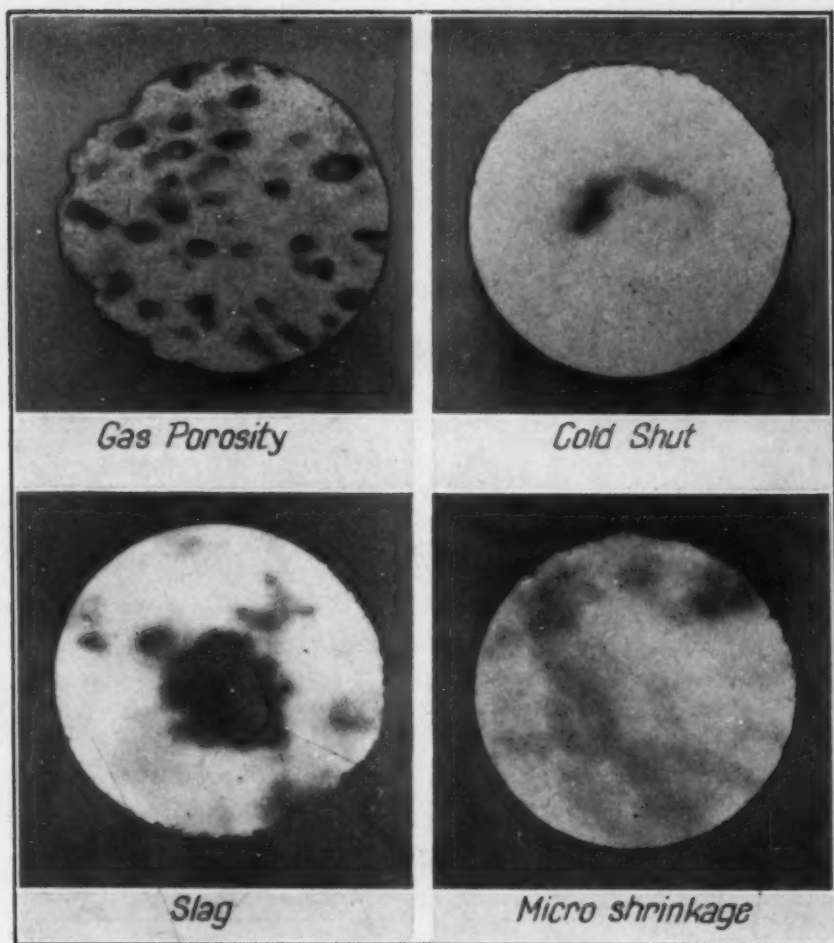


Fig. 1—Images Produced by Secondary Radiation.

whose failure would cause disaster to the plane should be subject to 100 per cent X-ray inspection and the interpreter should accept only commercially perfect material. Of course the interpreter must realize that a part which is difficult to make will carry a slightly lower standard than one of more simple design. In the case of castings, about one quarter of the total number of parts in a plane are of this 100 per cent X-ray class.

Rejection of parts whose failure will not cause disaster should be based on a rough calculation of the reduction in the physical strength of the part. To make this calculation the interpreter must be able to do three things. First, he must have enough knowledge of engineering to visualize possible modes of failure. Second, he must have enough knowledge of radiographic metallurgy to identify the defective condition. Third, he must have data such that the decrease in strength can be deduced from the radiographic appearance.

Table I
Defect Code Terminology

1. Sharp Discontinuity	2. Shrinkage	3. Holes
1.1 Crack*	2.1 Cavity	3.1 Gas*
1.2 Cold Shut: Lap, Fold	2.2 Sponge	3.2 Cluster Porosity*
1.3 Hot Tear	2.3 Pipe	3.3 Dross*
1.4 Surface*	2.4 Centerline	3.4 Surface*
4. Dispersed Defects	5. Heterogeneities	6. Welding (Also*)
4.1 Gas Porosity*	5.1 Light Inclusions*	6.1 Incomplete Fusion
4.2 Shrink Porosity	5.2 Heavy Inclusions*	6.2 Undercut
4.3 Microshrinkage	5.3 Segregation	6.3 Draw
4.4 Microtears	5.4 Stress Segregation	6.4 Linear Porosity
9. Misc.	9.1.....	
	9.2.....	

Before dealing with the identification and assessment of genuine defects, it should be noted that there are many radiographic appearances which are not due to defects in the material. For example, Fig. 1 shows four types of image produced by secondary radiation. Training in the recognition of the several types of false images is a prerequisite for all radiographic interpretation (4).

IDENTIFICATION

To deal with identification and strength assessment in an orderly manner we have found it convenient to use six groups of defects. Table I shows this grouping. The titles of the groups correspond to types of radiographic appearances, but the terms within the groups conform to common metallurgical usage.

For example the first title is "sharp discontinuities." The radiographic appearance of each of the defects in this group consists of one or more dark narrow lines. One advantage of this grouping is that although different interpreters may disagree on the exact identification of a defect, they will agree on its general radiographic appearance and so they will both assign it to the same group.

Another advantage is that the same sort of strength tests and acceptance standards apply to the defects within each group. For example, in Group 1 sharp discontinuities are all assessed as stress raisers. They are almost always rejectable, because they will propagate through the section. This distinction between sharp and dull defects was recognized in the Canadian Radiographic Code in 1940 (5) and in the Army Air Corps Technical Report No. 4976 in 1942. The defects in Group 1 are illustrated by Figs. 2 to 5. Fig. 2 shows a crack. Fig. 3 shows a cold-shut. Fig. 4 shows a hot tear. Fig. 5

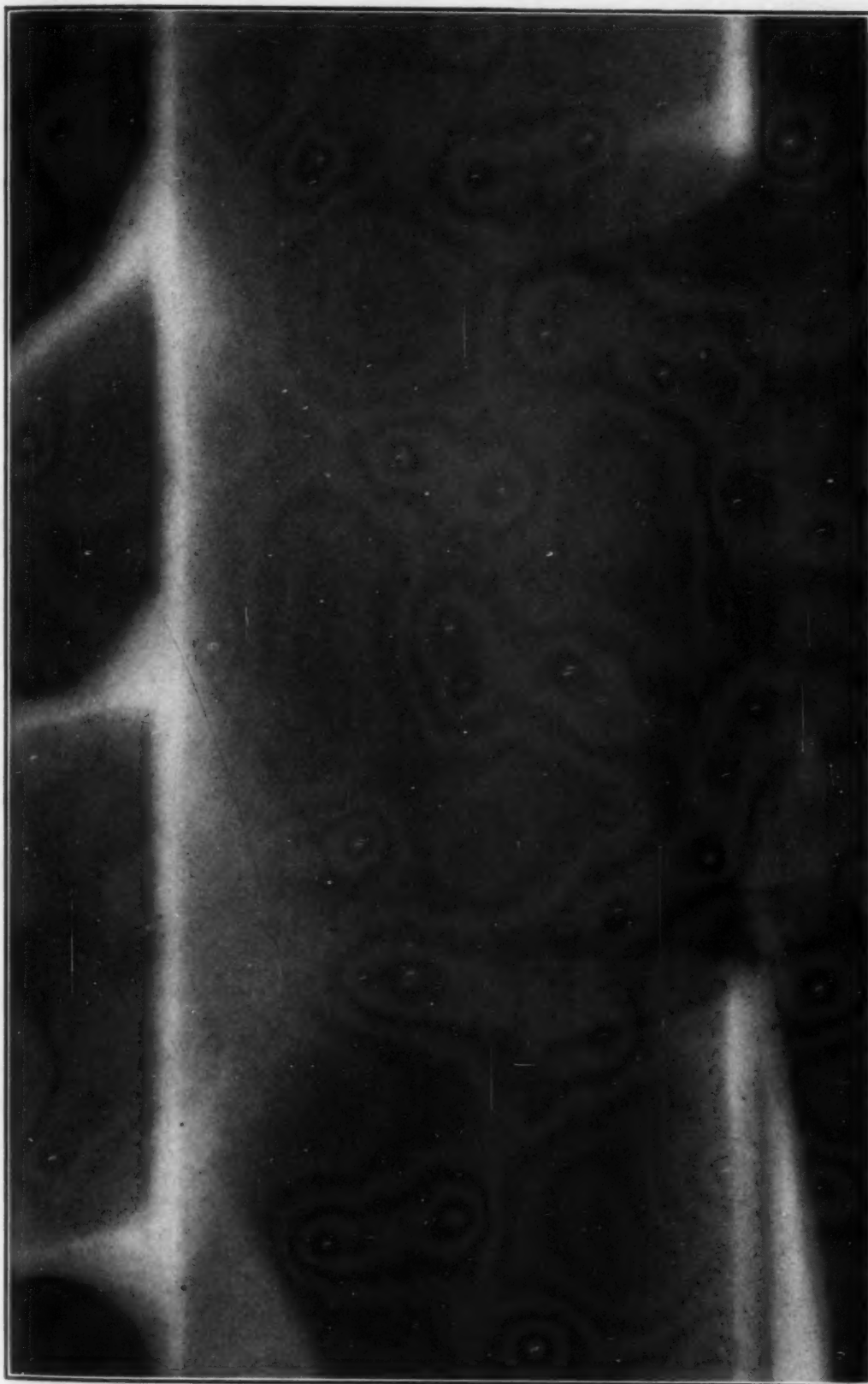


Fig. 2—Radiograph of Welding Crack.

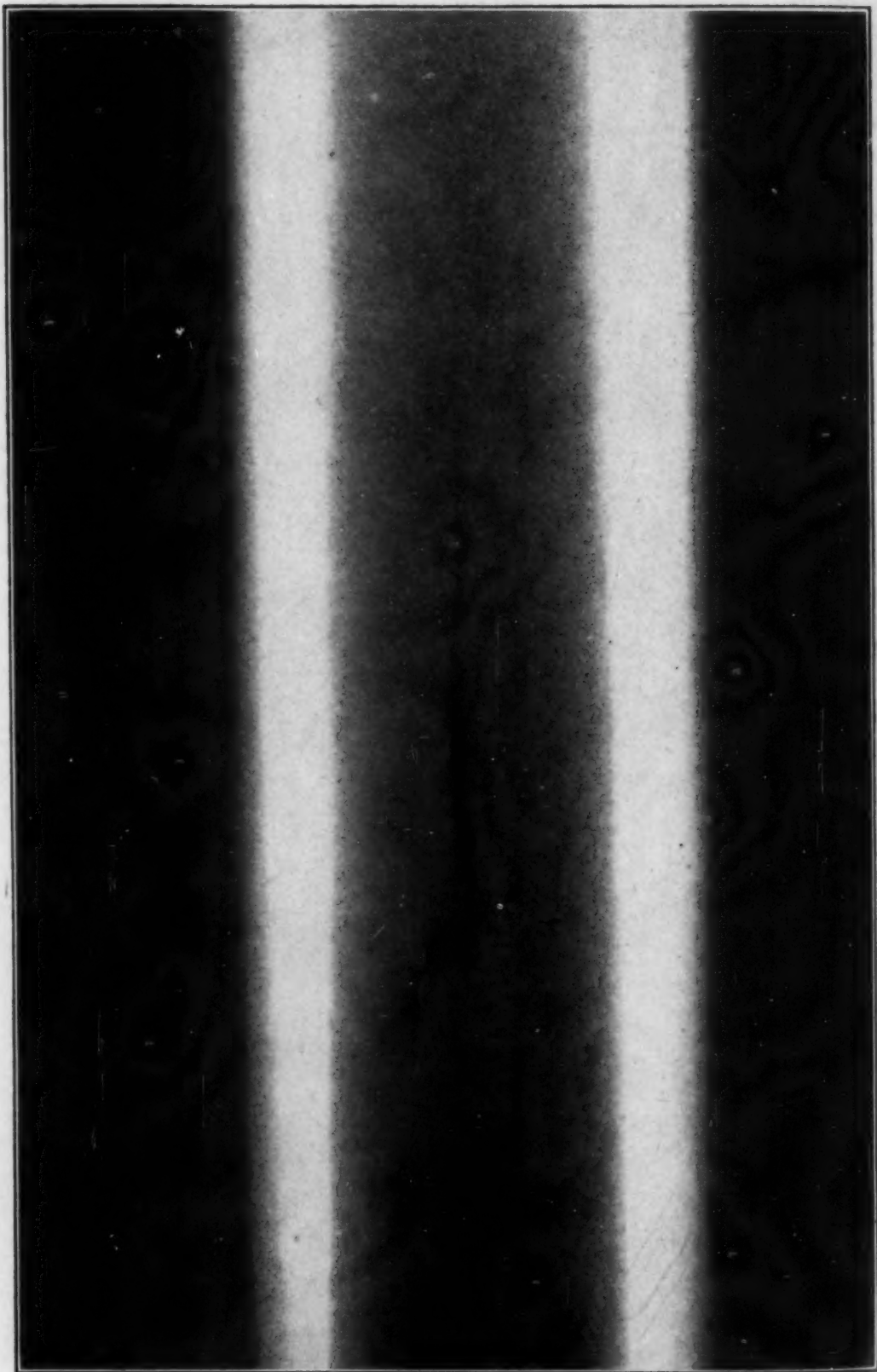


Fig. 3—Radiograph of Cold-Shut.

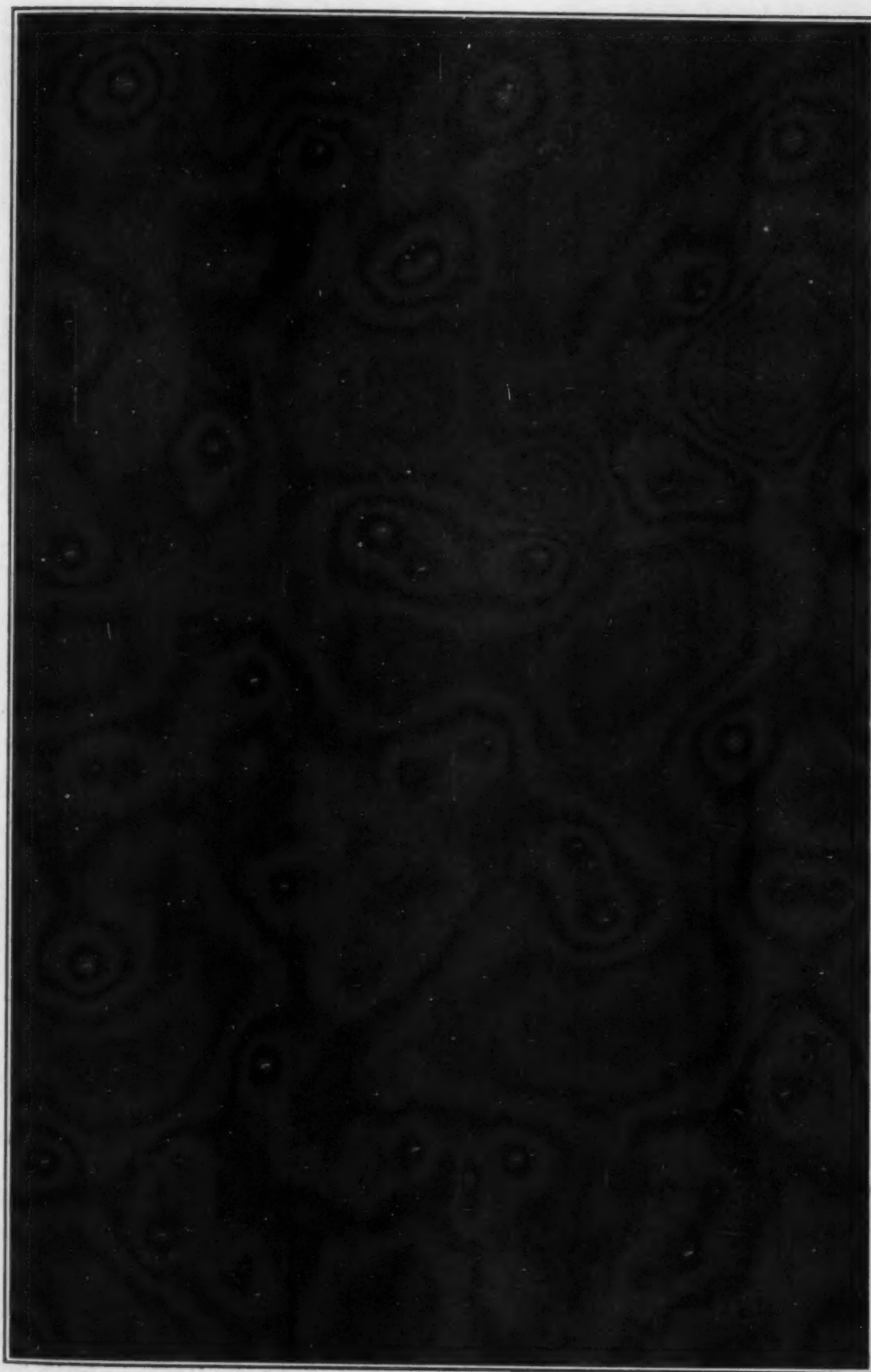


Fig. 4—Radiograph of Hot Tear.

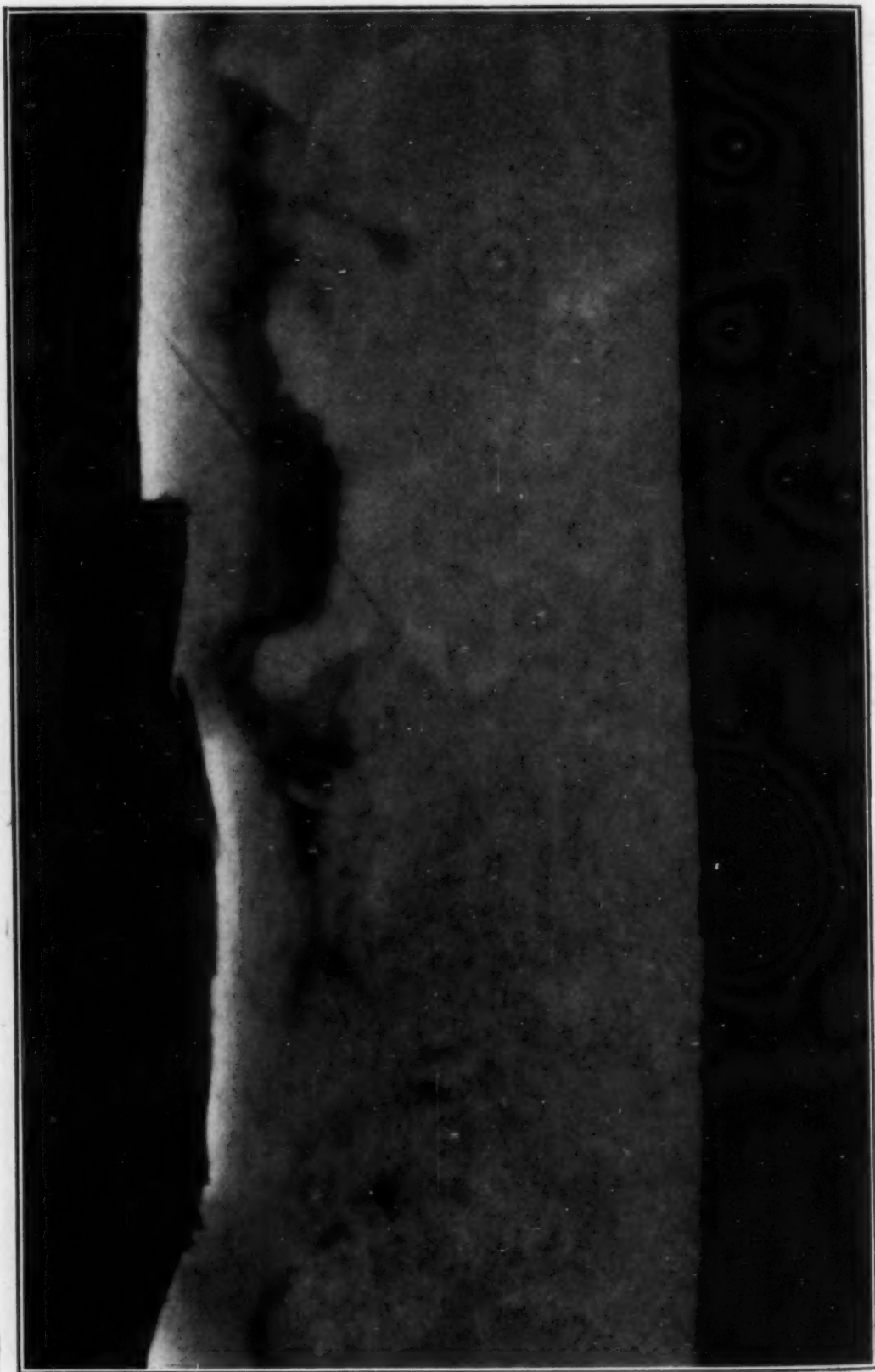


Fig. 5—Radiograph of Surface Sharp Discontinuity, Identified as a Sand Fall.

shows a surface gap. These four sharp discontinuities are cause for rejection in all classes of castings, forgings, and extrusions. Only occasionally is one of these defects so orientated that it is acceptable.

The second group of defects is entitled, "shrinkage." The radiographic appearances of shrinkage are related to each other by their position in the casting. Variations in shape and pattern of shrinkage images depend on the alloy, method of fabrication and geometry of the individual part. However, after suitable training, the interpreter is able to identify shrinkage with fair certainty. Figs. 6 to 9 illustrate the subdivision of "shrinkage" into four individual types. Fig. 6 shows "cavity." Fig. 7 shows "sponge." Fig. 8 shows "pipe." Fig. 9 shows "centerline." Three of these, the cavity, pipe, and centerline, appear in the form of discrete images that can be easily identified. Since they represent bad foundry practice they are just cause for rejection in the 100 per cent X-ray class of casting. However, these defects do occur in forms so slight that they are acceptable in other classes of casting.

By contrast, "sponge shrinkage" does not appear as a discrete defect, but as an area on the radiograph corresponding to a volume of imperfect metal. Although honeycombed with tiny voids, the metal may have considerable strength. Without a background of investigation, the radiographer cannot tell either the extent of the sponge in the direction of the X-rays or the strength of the affected region.

In our laboratories, we have sought to provide this background in two steps. The first step was the making and radiographing of slices through selected sponge sections. This procedure showed both the extent of the sponge and the degree of honeycombing. The interpreter is now guided by comparing the contrast and general appearance of radiographs with these test cases. The second step is to estimate the strength and corrosion resistance of the different types of sponge. In general the coarser the honeycomb the weaker the metal, but no adequate series of test-bar measurements are available.

The third group of defects is entitled "holes." Their radiographic appearances correspond to discrete voids of easily visible size and whose width, breadth and depth are roughly equal. Fig. 10 shows "gas holes." These are smooth walled, spheroidal holes and occur individually. Fig. 11 shows "pin holes" (or cluster porosity). This condition is distinguished by the occurrence of small spheroidal

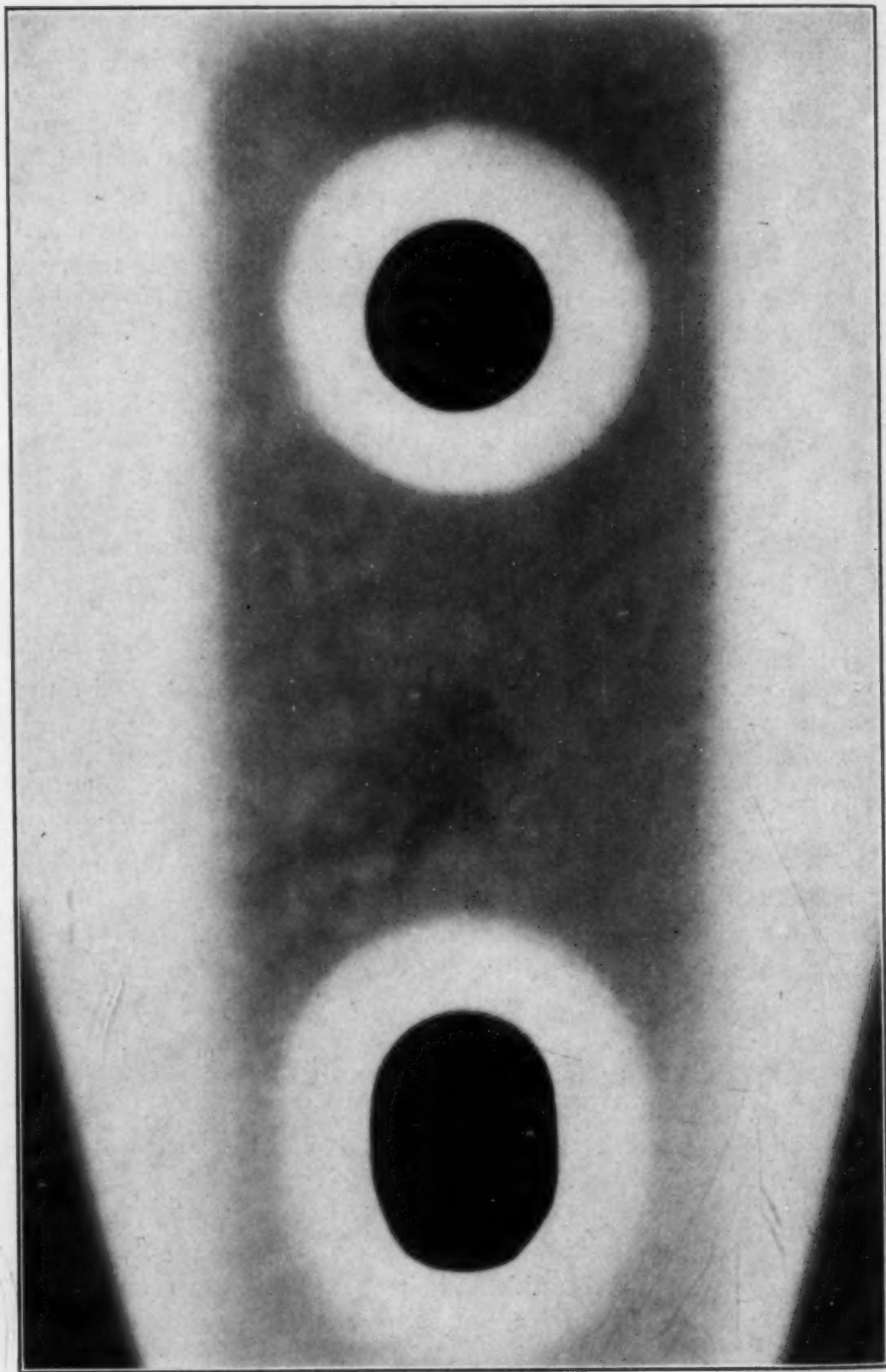


Fig. 6—Radiograph of Shrink Cavity.

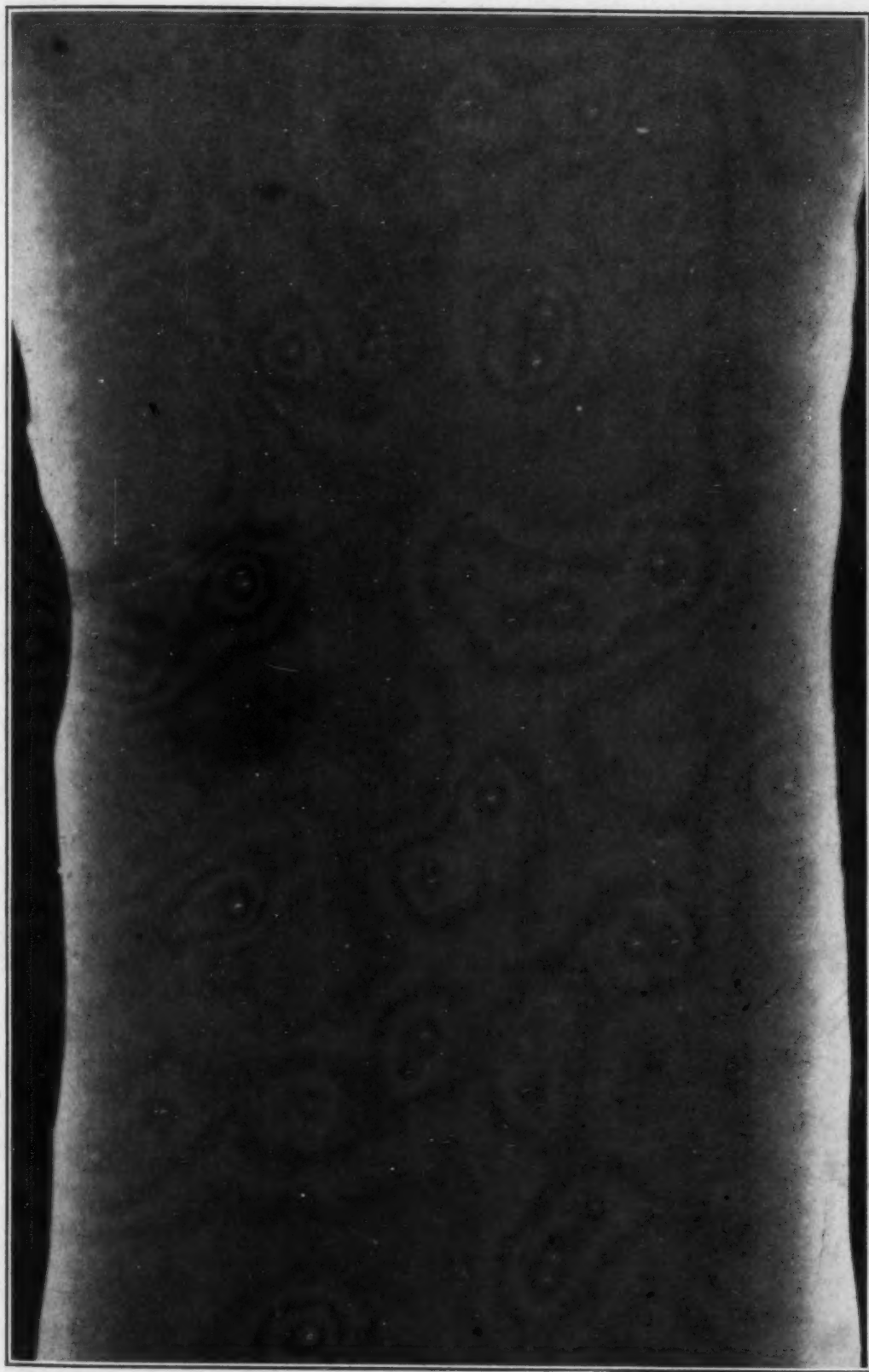


Fig. 7—Radiograph of Shrink Sponge.

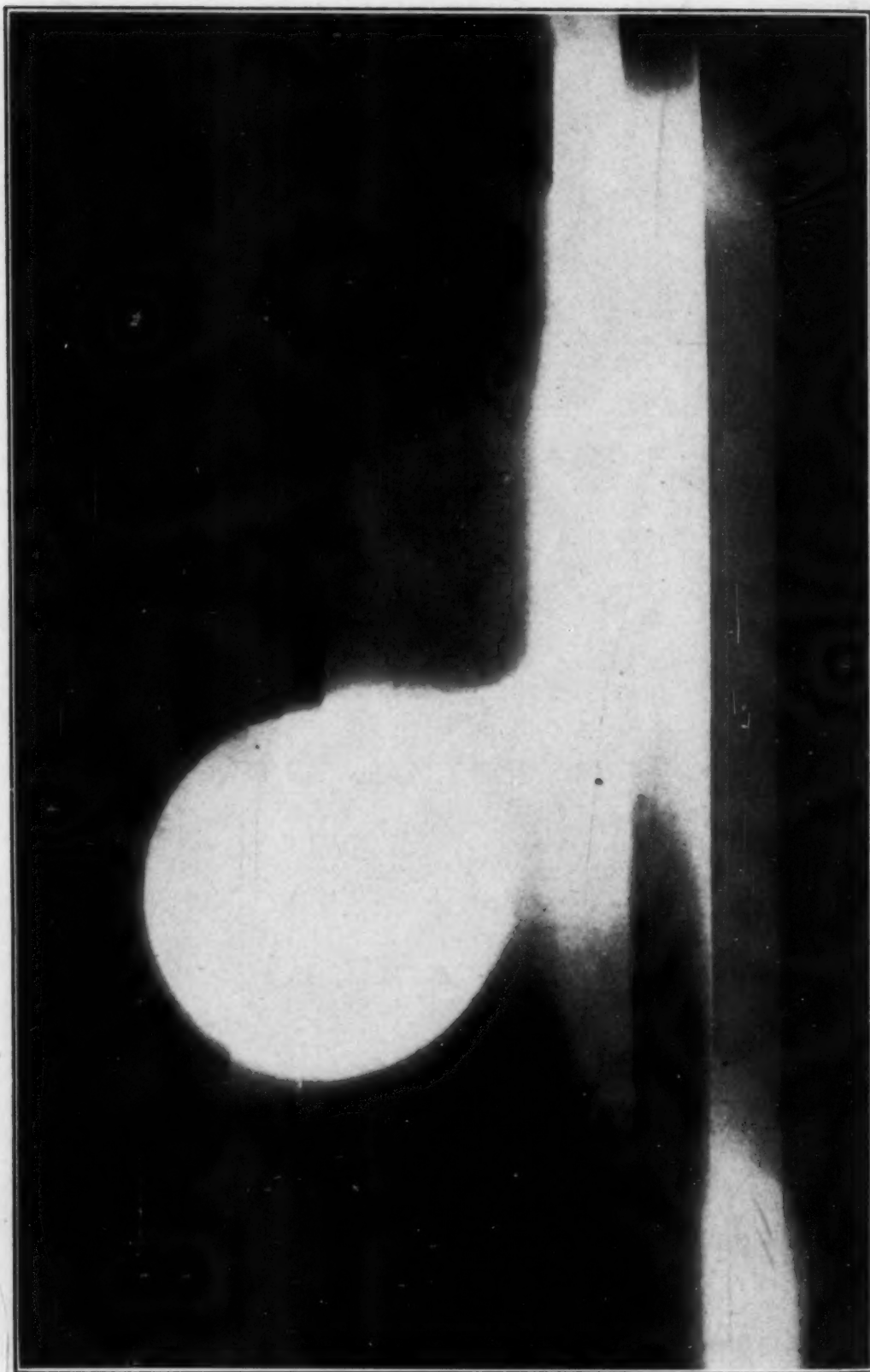


Fig. 8—Radiograph of Shrink Pipe.



Fig. 9—Radiograph of Shrink Centerline.

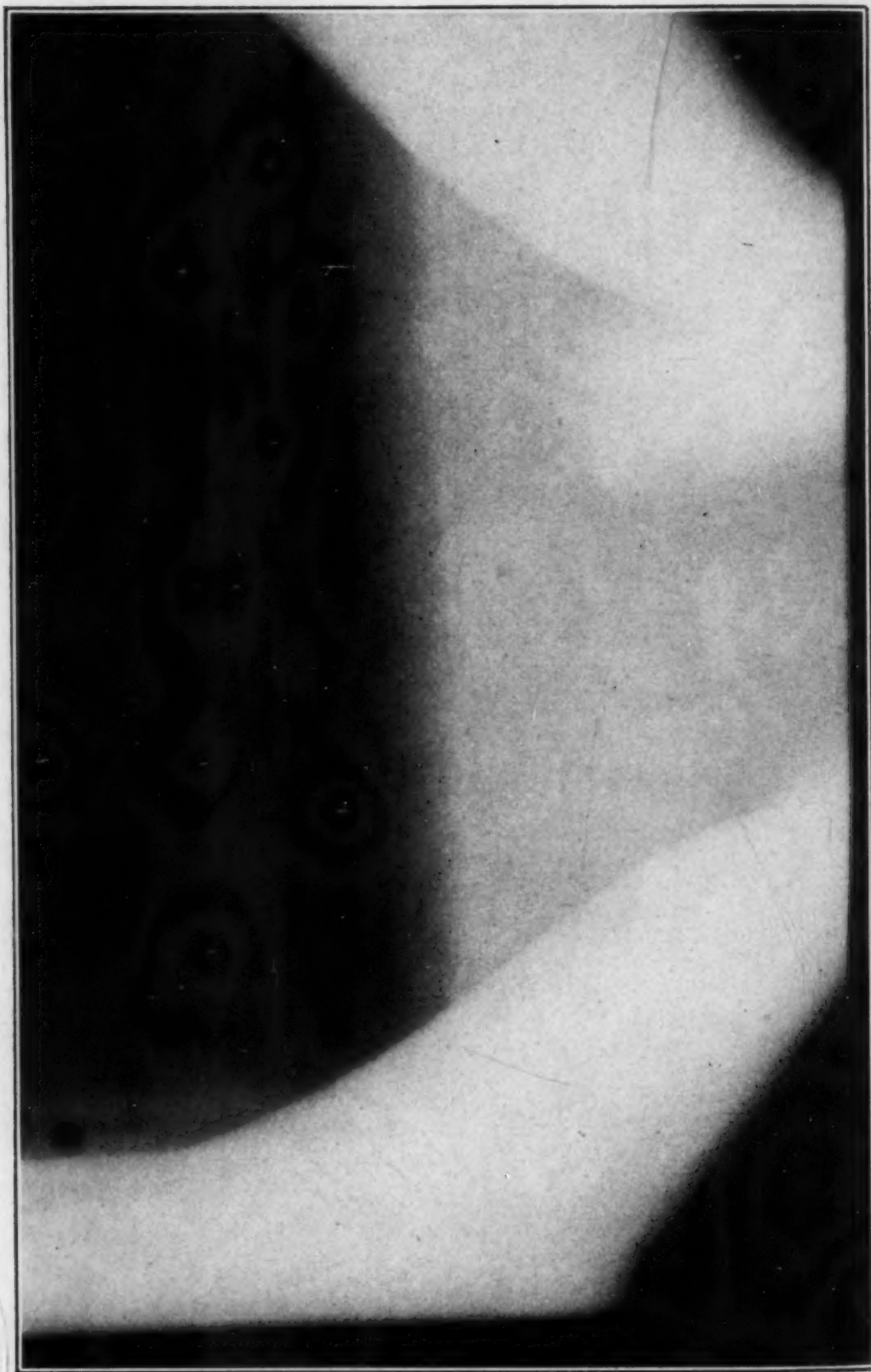


Fig. 10—Radiograph of Gas Holes in Aluminum Casting.

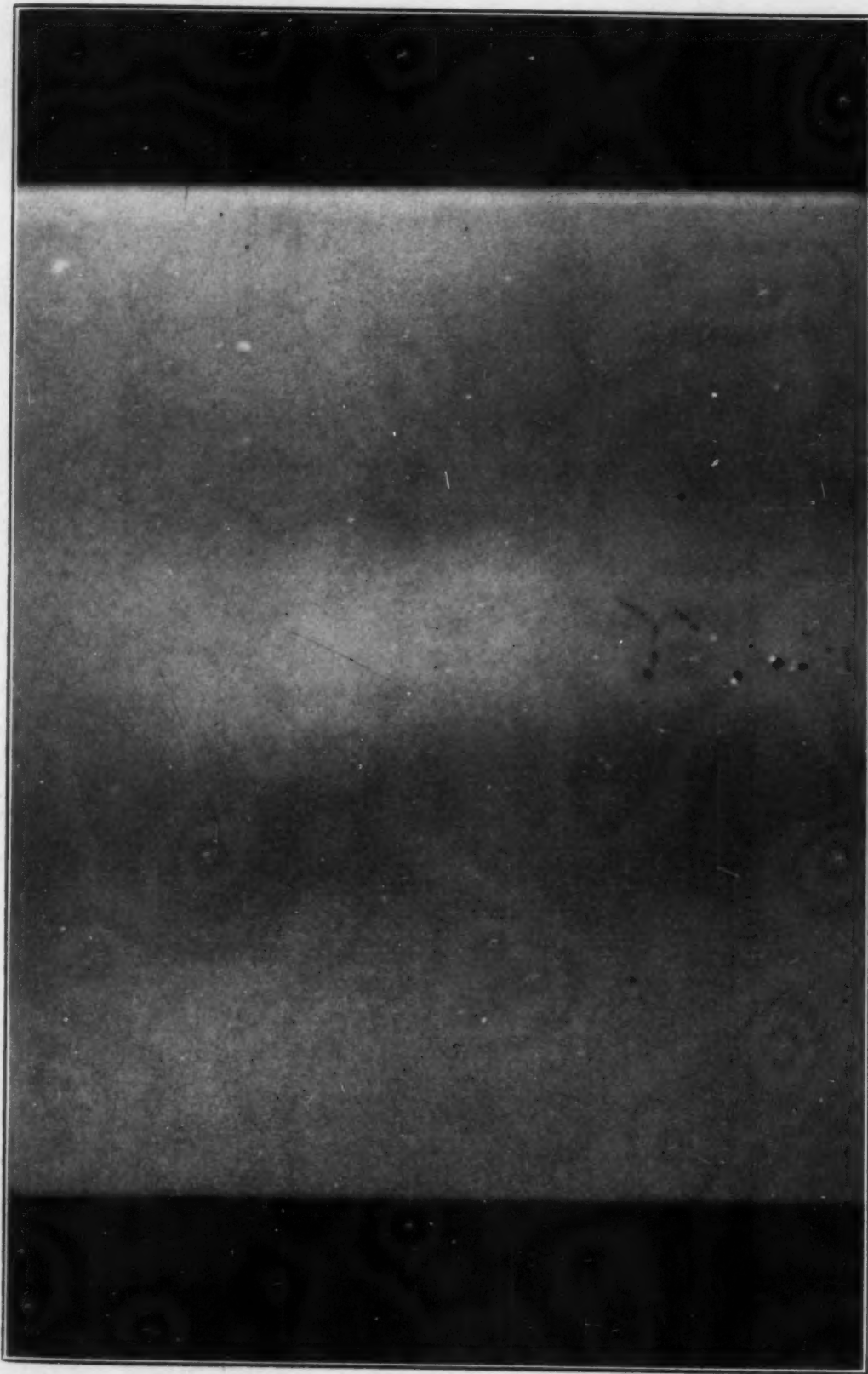


Fig. 11—Radiograph of Cluster Porosity.

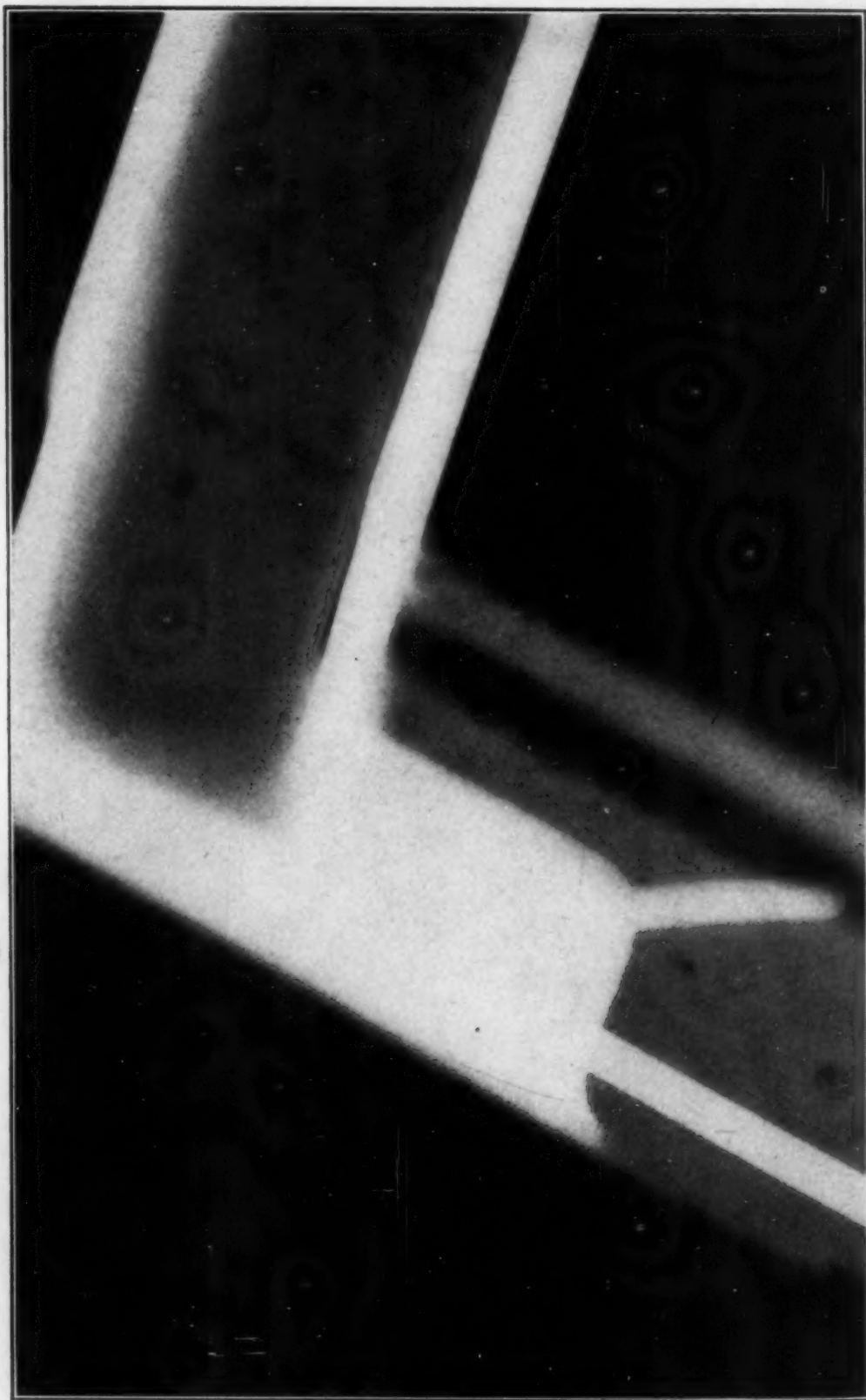


Fig. 12—Radiograph of Dross Holes.

voids in a group. Fig. 12 shows "dross holes." They are characterized by their irregular shape and distribution. Surface holes occur as an innumerable variety of sand failures, etc., and their appearances are correspondingly varied.

It is not possible to establish universal standards for holes of any type, particularly in an aircraft casting. Rejections must be based first on the feasibility that a fracture of the part could pass through the holes and secondly on the size, shape, orientation, and distribution of the holes relative to the fracture surface. G. C. Laurence included a useful study of this relation in the Canadian Code in 1940.

The majority of rejections, because of holes, are based on machine shop standards. This means that the interpreter has to predict if the hole will be revealed by machining. One other consideration is that holes, particularly dross holes, are evidence of turbulent pouring or bad mold design. When the interpreter considers these deduced metallurgical factors are unsatisfactory his report should indicate the need for improved foundry practice.

To guide our interpreters' rejection standards, we have among our reference films several dozen cases where holes have been carefully assessed. Satisfactory judgment can be acquired by an interpreter through studying these reference films.

The fourth group of defects we have called "dispersed defects." They consist of metallurgical conditions in which tiny voids are scattered throughout part or all of a casting. They are very prevalent in light alloy castings.

On radiographs, dispersed defects give rise to a wide range of appearances such as mottling, dark streaks, speckles or very small tears. With sections of metal more than $\frac{1}{2}$ inch thick, it is rarely possible to distinguish many discrete images corresponding to the individual voids. However, radiographs of slices of metal about twenty thousandths of an inch thick do show the presence of those individual voids.

To enable our radiographic interpreters to identify each of the four subdivisions of dispersed defects, we have prepared enlargements of from 2 to 200 diameters of radiographs of scores of slices of aluminum and magnesium alloys. Our library of reference films correlates the appearance of the nondestructive radiograph with the sliced X-ray micrograph.

Figs. 13, 14 and 15 show X-ray micrographs of gas porosity,

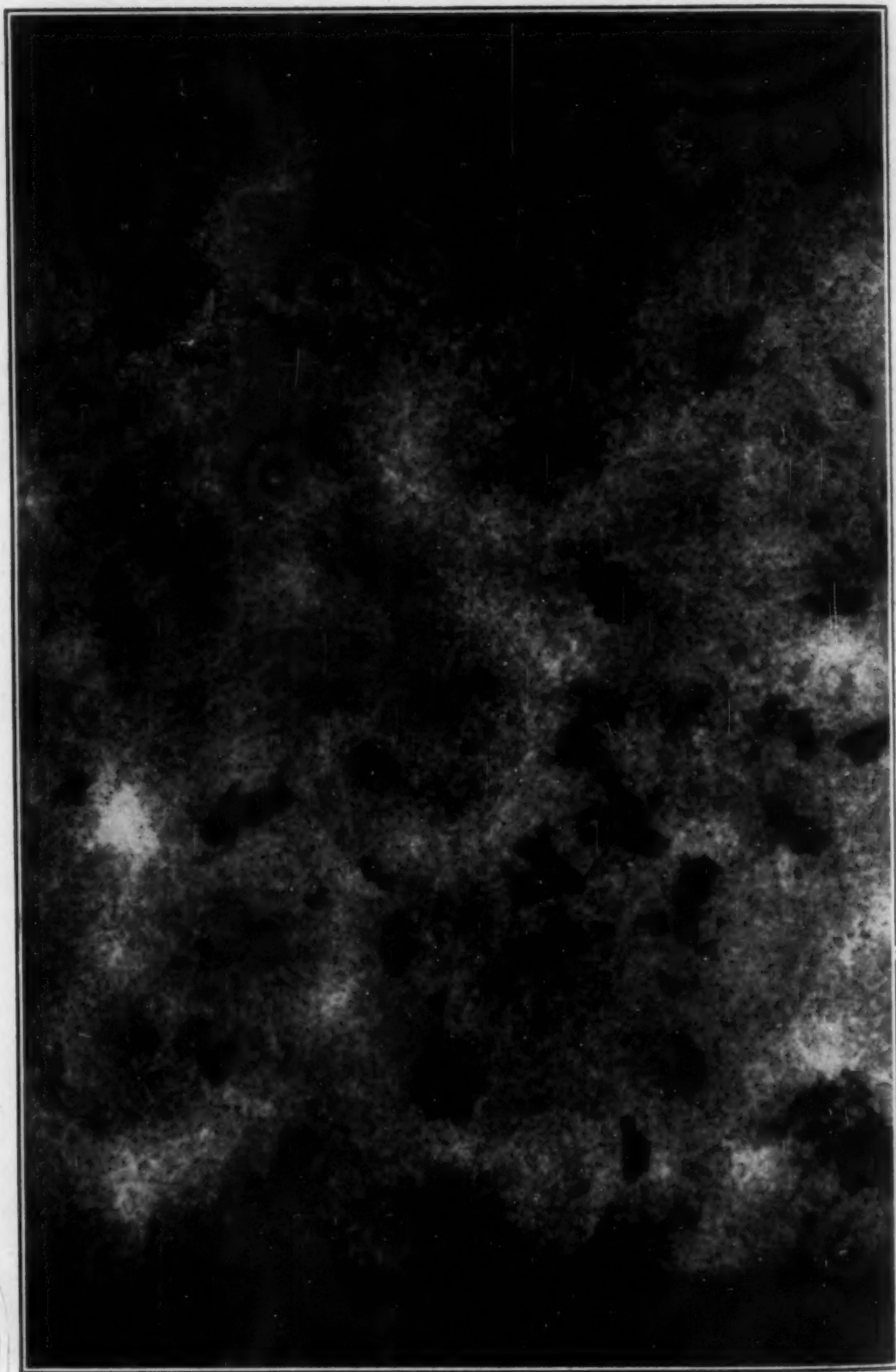


Fig. 13—X-ray Micrograph of Gas Porosity. $\times 10$.



Fig. 14—X-ray Micrograph of Shrink Porosity. $\times 30$. 220 alloy.

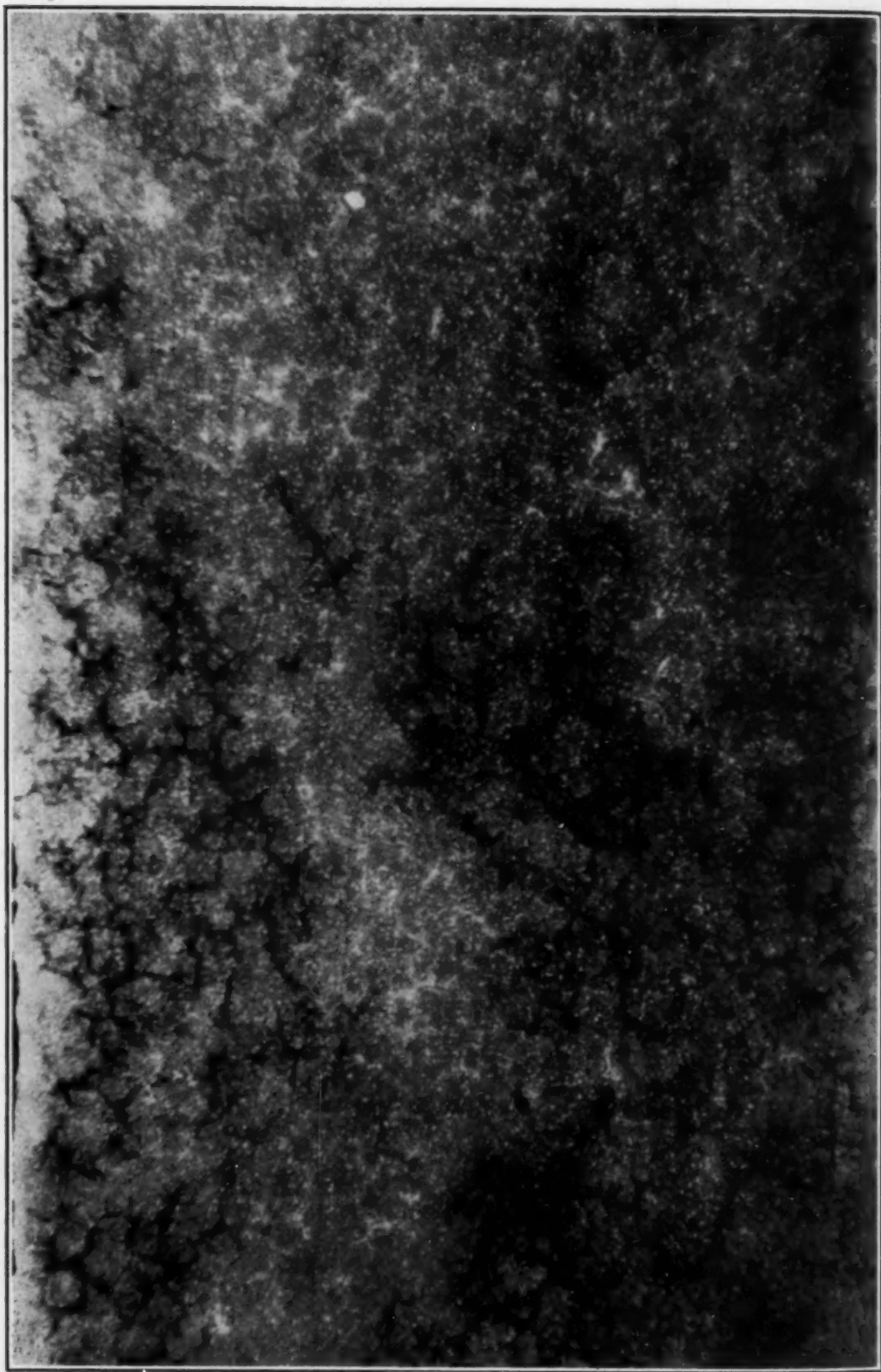


Fig. 15—X-ray Micrograph of Magnesium Microshrinkage. $\times 25$.

shrink porosity and magnesium microshrinkage respectively.

The assessment of acceptability of material containing dispersed defects should be based on extensive series of correlations between the radiographic appearance and the physical characteristics of test coupons. Tests on complete castings are a useful supplement, but they rarely provide fatigue, impact or elongation data. Moreover, by this method it is impossible to investigate the scores of variations that occur in the shape, size and orientation of microcavities.

The deleterious effect of shrink porosity depends greatly on the dimensions of the section in which it occurs. Perhaps the greatest pitfall in the radiographic interpretation of aircraft parts is the failure to reject castings containing shrink porosity in sections which are cast thick, but are machined thin. For example, in a certain engine cowl bracket the cast section is 1 inch thick, but the flanges left by machining are only $\frac{1}{8}$ inch thick. The same shrink porosity that reduces the strength of the original section by 10 per cent can reduce the service strength by 75 per cent. The majority of casting assembly failures which occur in aircraft production are due to reduced ductility caused by shrink porosity.

There are a few published researches correlating dispersed defects in test coupons with physical properties but many more are needed. Even these few are not too readily applicable to general use. This is because the appearance of the radiograph, corresponding to a certain degree of dispersed defect, depends on the thickness of the section, the contrast and graininess of the film, the tube potential and several other factors.

We believe that we have partially solved this particular problem of dispersed acceptability standards. The method will be described in detail in a separate paper (6), but very briefly it is as follows:

For a particular alloy at least 50 test coupons covering a range of defectiveness are obtained from one heat of similar castings. In addition to these test bars, thin slices of metal are cut from regions giving the same radiographic appearances as the test coupons. X-ray micrographs at 2 to 50 diameters are made of each slice. The coupons are broken and their physical properties are correlated with both their own radiographic appearance and the X-ray micrograph appearance of the slices.

To apply the test results to production radiography requires the destruction of a borderline rejectable casting. Slices are cut from the defective region of this casting and X-ray micrographs are made

from them. Inspection of these X-ray micrographs determines the proper rating of the metal. A re-examination of the routine radiograph of the destroyed part shows to what extent section thickness, etc., modifies the radiographic appearance of the defective condition.

The fifth group of defects is entitled, "heterogeneities." These appear on the film as variations in film blackening not corresponding to variations in thickness or to the presence of cavities or scatter. They are due to nonuniformity in composition or in the density of the material.

Both light and heavy inclusions are well understood. Their identification by the radiographic interpreter is based on a knowledge of the metallurgy of the product being examined. A light inclusion in steel may be identified as a sand pocket, but in aluminum it would more probably be a dross pocket. Again in our laboratory, interpreters acquire satisfactory judgment of this type of defect through studying a library of carefully analyzed films.

The rejectability of inclusions is based on considerations similar to those described under "holes." The standards are rather more severe where corrosion or damage to a machine tool is possible.

General segregation seldom is cause for rejection in castings, but in forgings and extrusions, excessive striations on the radiograph in the direction of the flow lines are associated with cracks and may cause rejection. Figs. 16 to 19 show the four types of heterogeneity.

In Group 6 those defects which are peculiar to steel welding are listed. There are several extensive papers in which these defects are discussed. In the case of magnesium welding, there are a few causes for rejection which do not occur in steel. We have in our library sets of films for identifying these magnesium defects and physical test data are being added.

This completes the list of defects. The assignment of code

Table II
Serviceability Rating Code Terminology

The Interpretation Code Consists of the View Number and a Rating Followed by the Group and Then the Type of Defect. e.g., 1-4-4.1 Means View 1 Has a Rating of 4 on a Dispersed Type of Defect Identified as Gas Porosity.

Normally Acceptable		Normally Not Acceptable	
—1—	Trace	—5—	Excessive
—2—	Some	—6—	Heavy
—3—	Appreciable	—7—	Extra Heavy
—4—	Considerable	—8—	Extreme
—Q—	Questionable	—9—	
Insufficient Eng. Data to Grade			



Fig. 16—Radiograph of Light Inclusion.

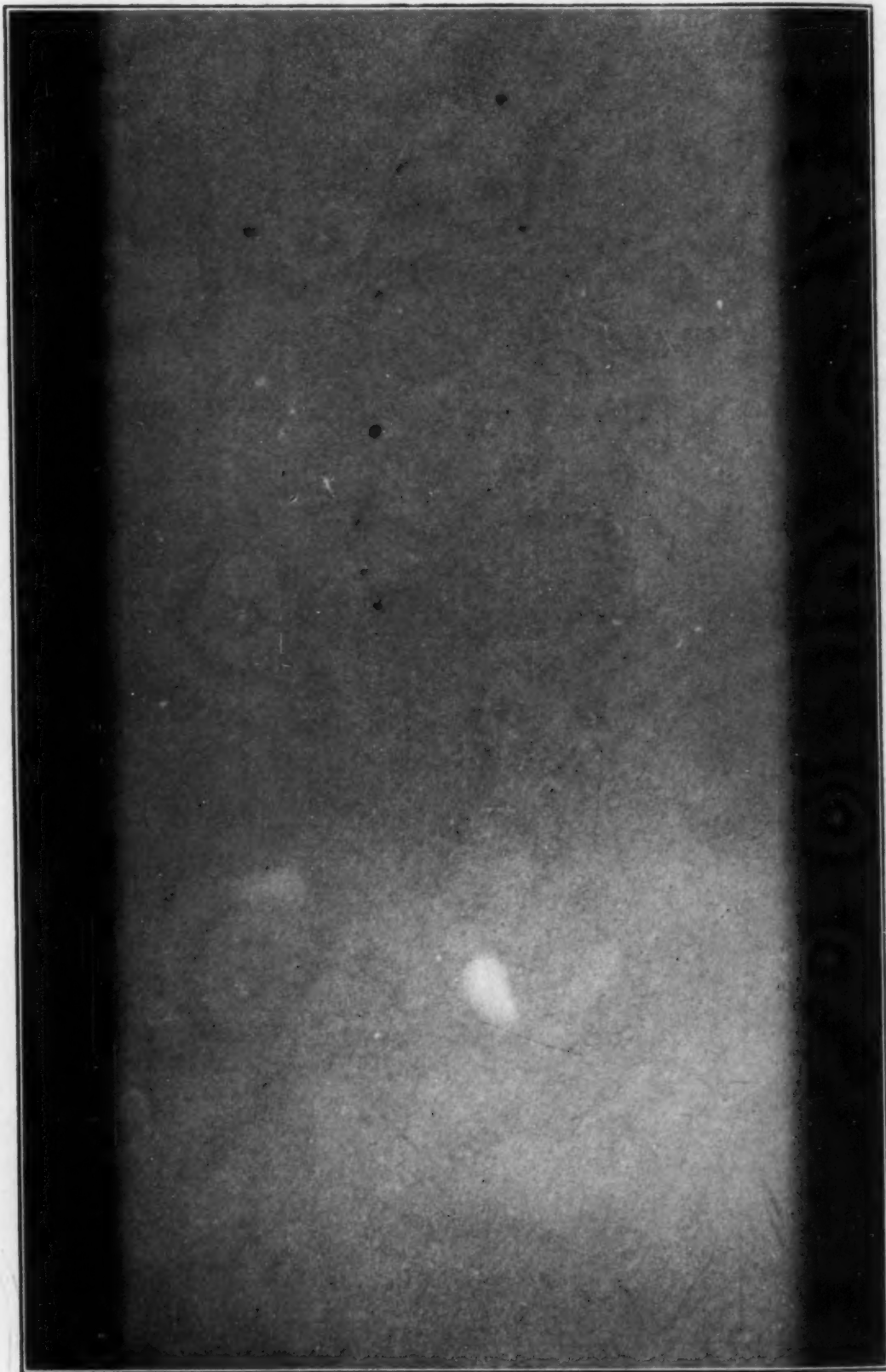


Fig. 17—Radiograph of Heavy Inclusion.

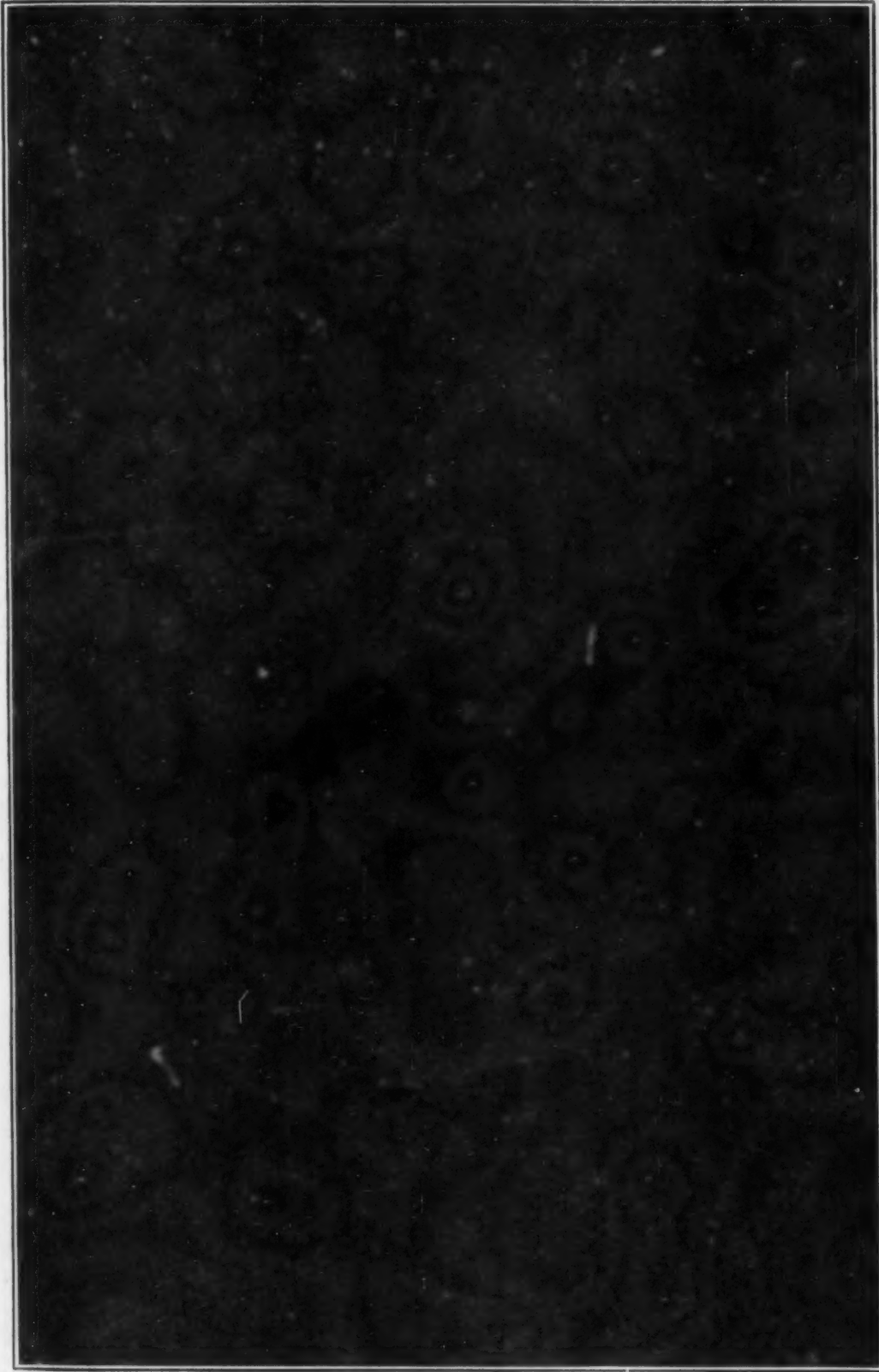


Fig. 18—Radiograph of Segregation.



Fig. 19—Radiograph of Stress Segregation.

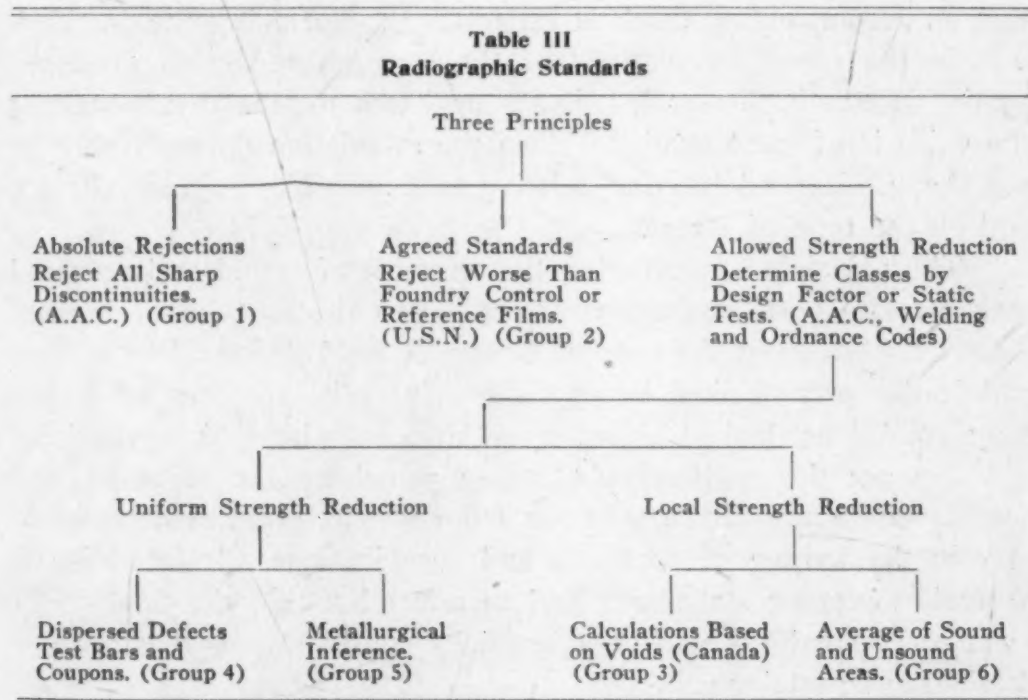
numbers of 1 through 6 to the groups, and numbers of 0.1 through 0.4 to the items in the groups, is invaluable, both in writing reports and in making statistical analyses. This need for coding on X-ray reports is quite important in the aircraft industry. The addition of a degree of rating code, of 1 through 8, allows the summarizing of all the conditions in more than a hundred defective castings on a single page. Table II shows a rating code that has proved to be satisfactory.

PRINCIPLES FOR REJECTION AND ACCEPTANCE

Earlier in this paper it was stated that one advantage of the grouping of defects was that the same sort of acceptance standards apply in each group. The corresponding fact is that different sorts of standards apply to the different groups.

At the present time, radiographic inspection standards are based on three distinct principles.

Table III shows the relation of these principles to the standards used for each of the six groups of defects.



Absolute rejection of cracks, cold-shuts and hot tears in light alloys is satisfactory to all concerned. However, the placing of

shrinkage in this category is not satisfactory because this condition occurs in some very minor forms.

The use of agreed standards is satisfactory for conditions which occur persistently in the same place. Shrinkage is one of these conditions. Most foundries are willing to include in their contract an agreement that the degree of shrinkage shown on the foundry control radiographs shall be the maximum permitted in production parts.

Under the third principle of allowable strength reduction it is necessary to know whether a 10, 20 or even 40 per cent reduction can be tolerated. This is accomplished partially by assigning classes based on the ratio of the allowable to the service load. Static tests are of great value in the determination of these classes (7).

Dispersed defects reduce the strength of the metal throughout a section of the whole of a part. The test bar researches of Bean (8) and of Busk (9) are good examples of the basis for rejection in this group.

The principle of metallurgical inference can be illustrated by rejections for stress segregation. Although the radiographic interpreter may see only the relatively innocent segregation, the inference that an accompanying crack is very likely to form is quite justified.

In the rough calculations of the strength reduction produced by the defects in Group 3, it is assumed that the metal surrounding the voids is of good quality. Then the calculation depends only on the shape, size and location relative to a possible fracture surface and on the type of stress.

The principle of averaging the strength of sound and unsound area across a possible fracture is applied to all cases, but it is most clearly applicable in the case of Group 6, weld defects. In a weld a defective area flanked by good areas may be accepted while the same conditions flanked by imperfect area may have to be repaired.

Because the application of these principles for rejection and acceptance of aircraft parts is far from simple, great care is necessary in the writing of contracts and specifications. It is advisable to avoid sweeping statements and to remember that the final judgment of acceptability will be affected by considerations that are too detailed to be catalogued.

In conclusion, I will repeat my opening thesis, namely, that the future use of radiography is dependent on its providing a more reasonable and economical method of performing certain tasks than

any alternative. The reasonableness of radiography is very much in the hands of the production interpreters, even when they are guided by an engineer. So, development of professional status and recognition for them is of vital importance. Is this development taking place? The answer is yes, but all too slowly.

References

1. Radiographic Standards for Steel Castings, *Bureau of Ships*, July 1, 1942.
2. ASME Code for Power Boilers.
3. Army Ordnance Welding Standards.
4. Leslie W. Ball, "Diffraction and Secondary Radiation as Factors in Industrial Radiography", presented to the Los Angeles Chapter of the A.I.R. & X.S. To be published in *Industrial Radiography*.
5. "Radiographic Inspection Procedure for Light Alloy Castings", Used in the National Research Laboratories Limited Circulation by the National Research Council Radiographic Section, Ottawa, Canada.
6. "A New Basis for Radiographic Standards on Dispersed Defects", to be presented to ASTM Committee E-7, June 1945.
7. Frank S. Wyle, "The Use of Static Tests as a Method of Determining the Radiographic Classification of Castings."
8. Zarifa Bean, "The Fatigue and Tensile Properties of Cast 355 Aluminum Alloy in Relation to Treatment of the Melt to Eliminate Porosity and in Relation to Corresponding X-Ray Characteristics." Antioch Foundry, Yellow Springs, Ohio.
9. R. S. Busk, "A Correlation of the Mechanical Properties and Radiographic Appearance of Magnesium Alloy Castings." ASTM Symposium on Radiography, 1944.

DISCUSSION

Written Discussion: By G. F. Jenks, North American Aviation, Inc., Inglewood, Calif.

Mr. Ball's paper is an excellent presentation of a very timely subject. There is need of a national standard by which a common language is used to describe the irregularities seen in radiographs. It is remarkable that the radiographic industry has expanded so widely without the development of such standards. Whatever the factors are which have delayed this standardization work, they should not be permitted to postpone it longer.

The primary classifications of defects used by Mr. Ball appear excellent. Question may be raised as to whether all the subdivisions are necessary and whether they can be distinguished in the radiograph. Any not required should be omitted.

The ideal system of interpretation is one by which a radiograph may be so described that a stress engineer can judge the acceptability of the part without seeing the radiograph. Any system of interpretation devised should keep this ideal in mind. It is believed that such a system would answer the needs of the foundry, because the stress engineer must know the origin and nature of defects before he can judge their effect. Merely to tell the stress engineer that

there is a region of irregular shaped low density metal does not give him a concept that he can associate with behavior of the part during fabrication or in service. The radiograph interpreter acquires through training the ability to correlate the appearance of the radiograph and the physical nature and origin of the defect in the metal. A complete statement of why certain appearances in the radiograph are interpreted as a given defect should accompany any standard of interpretation.

The system proposed by Mr. Ball includes symbols for degree or intensity of defects. Those are not the only factors that the stress engineer must consider. Important factors are size, orientation, location and distribution as pointed out by Mr. Ball. The system of interpretation should include those factors. Defective structure must be located in respect to areas of given intensities of stress, or of special fabrication requirements.

If the stress engineer is to receive such service he must co-operate in making complete information available to the radiographic laboratory and to the foundry as to the magnitude, direction and type of stress in various sections of the casting and the special requirements for hydraulic tests, integrity of machined surfaces and other factors which influence foundry practice and radiographic interpretation.

The rating code proposed by Mr. Ball appears to be overdeveloped. It must meet the demands of the stress engineer and of the foundry, but it must provide steps of sufficient magnitude that the interpreter may make a proper classification. These ratings mean little unless there is an illustration to show exactly what is intended. It should be noted also that the appearance of radiographs will vary with wall thickness. It is suggested that each degree of defect must be illustrated for at least three thicknesses of castings.

The use of such terms as "excessive" and "questionable" in rating defects is objectionable in that it prejudges whether a material is acceptable. Whether a given defect of given intensity and location can be tolerated depends upon the service to which that section of the casting is put. In other words, acceptability will be placed at varying degrees of defect ratings according to the requirements of fabrication and service.

The preparation of standards indicating limiting types and intensity or rating of defects which can be tolerated in a given product, that is, under specified service conditions, cannot be satisfactorily prepared until a standard of classifying and rating radiographic defects is available. It is hoped that such a standard can be prepared and accepted in the near future. It would be of great assistance to the airframe industry.

Written Discussion: By H. W. Hiemke, formerly with the Bureau of Ships, Navy Dept., now with the War Metallurgy Committee of the National Research Council, Washington, D. C.

Mr. Ball has made a very useful contribution to the codification and standardization of radiographic images—a subject which merits a great deal more attention than has been given it in the technical literature.

Any new inspection procedure has to undergo a development period when the knowledge of the principles underlying its application gradually come to be appreciated. In the case of radiography, the development period has been

prolonged by virtue of the almost universal usefulness of the method in non-destructive testing, necessitating the training and indoctrination of a very large number of engineers and inspection personnel in the use of the process.

The writer has been greatly interested in the standardization and interpretation of radiographs for a number of years. In the field of welded pressure vessels, a condition of confusion regarding the interpretation of radiographs existed until the Bureau of Engineering of the Navy Department introduced a set of 18 X-ray films as standards for welded Naval boiler drums, in June 1936. These standard films may be described, in the language of the author, as requiring "A commercially perfect" product. Sharp discontinuities (cracks and lack of fusion) are considered to be cause for rejection regardless of the degree of such defects. In the case of slag inclusions, the length of inclusion permitted is based on its ratio to the thickness of the boiler drum. Blowholes are classified as acceptable or nonacceptable, based almost entirely on the ability of producers to meet such a standard without resorting to unusual control measures.

During 1937 and 1938, similar standards were accepted by the Joint AFI-ASME Unfired Pressure Vessel Code and the ASME Power Boiler Code.

In 1942, the Bureau of Ships, Navy Dept., established a set of radiographic standards for steel castings. In these standards, defect types are illustrated in various degrees of severity. There is also a classification of ship castings into five classes, depending on section thickness and severity of service. In applying these standards, the acceptability of a given radiographic image is determined by first determining the type and degree of defect, and next by determining the acceptability for the class of casting involved. A given radiographic image may be considered unacceptable for one class of casting, borderline for the next lower class of casting, and acceptable for other classes, lower in order of required soundness.

There has been frequent criticism of both the above-mentioned standards on the basis that they are quite arbitrary and are therefore not suitable "minimum safety" standards. It must be admitted that they are arbitrary—that they constitute arbitration standards between the desire for perfection on the part of the consumer, and the desire for a more liberal standard, or no radiographic inspection at all, on the part of at least some of the producers. As arbitration standards, radiographic standards are no more or less arbitrary than physical standards. In the opinion of the writer, it is just as reasonable to base the acceptance or rejection of a casting on its radiographic soundness as it is to accept or reject a casting or a group of castings on the basis of the strength and ductility of a separately cast coupon.

Mr. Ball and the company with which he is associated have developed an excellent background of "approved reference films" for aluminum aircraft castings, and have reached agreements with both the aircraft manufacturers and the foundries on what he describes as the "agreed quality standard for commercially perfect material." It is hoped that these agreements may assume the form of a nationally accepted standard in the not-too-distant future.

Written Discussion: By Herbert R. Isenburger, president, St. John X-Ray Service, Inc., Long Island City, New York.

May I compliment Mr. Ball on the excellent presentation of his paper with

the same words Harvey R. Anderson wrote to me exactly thirteen years ago on a similar occasion:¹

"The classifying and illustrating of all possible objectionable internal conditions which radiography may reveal in castings or welds is no small task and the extent to which you have succeeded in so doing calls for congratulations. This is a field in which more standardization is needed, both in the technique employed and in the interpretation of results. It is to be hoped that other papers dealing with this problem will appear in the near future."

Other papers on this subject did appear from time to time but none so well suited as Mr. Ball's paper to form a basis for real standardization work. The latter is just as badly needed today as it was thirteen years ago. Today we have the co-operation of consumers and producers whose material is to be X-rayed. They are really the ones who should get together and decide what is acceptable and what is not under the different circumstances. With thirteen years more experience and more than twenty times the number of qualified workers in this field, we ought to be able to finish this job if it ever can be finished.

If I understand Mr. Ball correctly, his examples apply to all types of castings, that is, aluminum as well as steel. If this is so, I would suggest another type of serious defect to be included in Group 1 of Table I, which is the *shrinkage crack*. There seems to be a distinct difference, particularly in steel castings, between hot tears (Fig. 47-7) and shrinkage cracks (Fig. 48a).² The first being more sharply defined and the latter has too much a crack-like appearance than that it could be called merely pipe shrinkage (Figs. 47-4 and 47-5) or shrinkage cavity (Fig. 47-3).

There is one other consideration which to my mind requires some differential treatment: That is to distinguish between Pilot-Casting Inspection³ and routine examination. The former may require more rigid standards.

One point that should be mentioned in this connection is the fact that only too often two sections may be superimposed. And what appears to be an acceptable defect may in machining turn out to be quite objectionable, just because some of its ramifications have been covered by additional thickness of sound metal during the exposure. This is just as true for weldments as it is for castings. Similarly, defects or portions thereof may be missed because they penetrate the material at an angle which is not advantageous for detection by the X-ray beam.

I do not expect Mr. Ball to supply the answer to all these problems. They are only thoughts to stimulate further discussion of a vital problem which can only be solved if we have the co-operation of all concerned.

Written Discussion: By Robert H. Lace, in charge, and J. Oyster, radiologist, Quality Control Division, Lear Avia Inc., Piqua, Ohio.

Although the percentage of Class A-1 castings is not high among the various castings we use, those castings which are structurally vital must be checked very carefully.

In our effort to establish radiographic standards for our A-1 castings it

¹*Mechanical Engineering*, 1931, Vol. 53, p. 729-35.

²Figures refer to *Industrial Radiology*, John Wiley & Sons, New York, 1943.

³*Heating, Piping, Air Conditioning*, 1935, Vol. 7, p. 530.

was necessary first to radiograph the castings at various angles at different potentials, in order to produce a radiograph that would be acceptable to Government Standards. With the technique established, we then issued a film position chart of the casting. This chart is used as a guide in positioning film in relation to source of radiation for further radiographic inspection. We felt this was necessary, inasmuch as the particular part might be made by two or more foundries, and might be X-rayed by as many different laboratories.

The first set of radiographs of any design were interpreted and the condition classified radiographically, as to acceptable or unacceptable, no defects being permitted. All unacceptable castings were then subjected to a static, proof load, or destructive tests. The correlation between the various tests, and the radiographic findings, was the basis of establishing radiographic standards of acceptance and rejection for each individual design.

As is standard, any crack, cold-shut, or misruns are automatic cause for rejection.

All further radiographs were compared or interpreted against the established standard. On the basis of relation to critical section, casting defects were classified as follows:

- 1—Acceptable radiographically
- 2—Unacceptable radiographically
- 3—Borderline

Castings that had evidence of unacceptable conditions were scrapped.

Castings with borderline conditions were accepted or rejected upon higher authority.

Apparently, each casting has an inherent tendency to a particular type of defect, dependent upon design and mold layout. This is particularly true where a permanent mold pattern is used and where casting conditions are approximately uniform. In the case of sand castings, the foundryman may change his locations of gates and risers from batch to batch and thus change the casting conditions.

We have thus been able to limit the casting methods as well as to reduce the number of views necessary on complex castings without endangering the safety of the complete unit, by specifying the location and type of allowable defects on our radiographic standards.

The above procedure in regard to Class A-1 castings is now being followed through, almost from the moment the blueprint is issued. The print gives us information as to critical sections, proof loading methods and stresses. We then check against a standardized chart for exposure times, voltage, etc., and are able to issue specific instructions to the foundry's X-ray laboratories in time for the initial run of castings to be properly X-rayed.

With each new aircraft design, new radiographic techniques are developed, to assure safety and promote quality.

Written Discussion: By Wm. W. Austin, Jr., inspection foreman, Consolidated Vultee Aircraft Corp., Nashville, Tenn.

Since his coming to this country, Mr. Ball's contributions toward the solutions of our radiographic problems have been indeed outstanding. The presentation of this paper will definitely mark an important milestone in our progress toward ideally uniform standards of radiographic interpretation, and it is hoped

that the keen interest and the spirit of co-operation which have been so admirably demonstrated in Mr. Ball's work will inspire and promote further development in this field.

It is feared that any discussion of this paper may tend to add to the complexity which the author has striven to eliminate. However, one or two points of discussion may be mentioned, it is hoped, without too much disorganizing effect. To the well chosen list of seven specific objectives of radiographic inspection the addition of an eighth objective is suggested, namely, the use of radiographic inspection for the maintenance of a given standard of quality in a product regardless of its actual service requirements.

This idea may be frowned upon by producers of castings since it could conceivably lead to the rejection of serviceable material in an effort to force the foundry to maintain a certain high quality level. However, it is not necessary that the application of this principle result in the actual rejection of castings. On the contrary, far better results could be obtained by closer co-operation and co-ordination between the X-ray laboratory and the foundry before the rejections are made. For example, when production radiographs indicate that the quality of a certain casting is tending to fall below the desired level, the forwarding of X-ray reports to the foundry will give advance notice of the undesirable tendency so that corrective action may be taken before any actual rejections are necessary. It is believed that the application of this objective will lead to a better understanding between producers and consumers, as well as to a general improvement in the quality of castings.

Another point worthy of further discussion is the reiteration of Mr. Ball's comments concerning the need of the radiographic interpreter for adequate engineering information regarding the material he is inspecting. It is obviously necessary for the designer of castings to possess a thorough knowledge of strength of materials, and to have a detailed breakdown of the stress analysis and functional requirements of the system at hand before a suitable design can be arrived at. It seems only logical, therefore, that at least part of this information should be placed in the hands of the radiographer if he is to be expected to make an intelligent interpretation of the films under consideration. This point is of course well recognized by radiographic laboratories, yet all too often engineers and designers are prone to neglect requests for engineering information as being irrelevant, or not necessary for inspection purposes. As Mr. Ball has pointed out, the lack of such information forces the radiographer to assume the existence of the most unfavorable service conditions which naturally results in excessive rejection rates. During the present war emergency this should not be permitted, and as we emerge into the post-war era when keen competition will enforce maximum operating efficiency, rejections based on such assumptions cannot be reconciled with sound economy. Consequently, it is imperative that our engineering departments be impressed with the urgency of the radiographer's need for appropriate data regarding load direction and magnitude, functional requirements, and service conditions of all castings requiring radiographic inspection.

Written Discussion: By A. E. Cartwright, chief metallurgist, The Robert Mitchell Co., Ltd., Montreal, Canada.

The present contribution by Mr. Ball to the systematic interpretation of

radiographs is another step along the path that he has pioneered; first, in molding Canadian standards and, subsequently, in his present connection in the United States.

It is always a difficult problem to adequately convey through the medium of articles and technical papers the measure of a critical improvement in radiographic interpretation owing to the shortcomings of reproduction of radiographs in print. It is apparent, however, that Mr. Ball's application of radiographic and microradiographic techniques supplemented by mechanical tests can be used as a basis for standard gradation for purposes of comparisons.

I would like to ask Mr. Ball if he visualizes the methods described as routine practice to be adopted by individual laboratories or as the basis for preparation of standards by an institution such as A.S.T.M., Bureau of Standards, etc. The latter would seem to the writer a more effective application of the principles, with some national or international body preparing and distributing standard comparison films.

From another angle, it has always seemed to the writer that the onus of correlating radiographic appearances with their effects on aircraft parts in service has been placed on the radiologist with much too comfortable resignation on the part of designing, production and operating engineers.

The result of this attitude is that "ignorance factors" are responsible for more uncertainties and rejections than would be the case if a greater degree of contributive information was furnished by the engineer. There is a studious avoidance of including, on the blueprint of most aircraft components, any information regarding type, direction, magnitude or localities of stress. There is ample space on most blueprints to allow for some description relating to the function, operating limitations and specific localized demands on portions of a part. A small diagram indicating the relative location and function of the part in the structure would often be invaluable.

The writer has never seen a blueprint containing any such information but has had plenty of experience in having to guess and deduce from indirect evidence most of these data. Uncertainties of this nature most generally result in penalizing the foundry in order to be on the safe side.

To this extent radiographic interpretation of serviceability of aircraft parts is lop-sided. There is constantly becoming less excuse for the magnitude of ignorance factors when aircraft engineers can chart stresses on parts in actual service by means of brittle lacquers, resistance strain-gages, etc.

If this information is acquired, there is no valid excuse for excessively comfortable overdesigning or for failing to interpret it right through to the blueprint for the metallurgist's and radiologist's guidance.

Written Discussion: By Milton A. Miner, Douglas Aircraft Co., Inc., Santa Monica, Cal.

Mr. Ball's paper is very timely in view of the tremendous growth of X-ray inspection of castings in the aircraft industry over the past two or three years. His basic thesis that radiography to insure its own future must achieve certain definite objectives bears repetition. Only concrete and positive results which correlate with actual experience will be justification for the use of radiographic inspection on finished castings. However, this writer believes that the emphasis should be placed on foundry control by means of radiographs rather than on

inspection of finished parts but that is a somewhat divergent subject.

Going into specific detail, I cannot agree with the general statement that the interpreter be responsible for preventing any unserviceable part from being used. The interpreter should be qualified and expected to read the radiograph in terms of known standards and report exactly what he finds. His responsibility should not include responsibility for acceptance or rejection of those castings which fall in the doubtful range; i.e., castings whose disposition depends on their end use. The means for handling such problems is of fundamental importance to the prime contractor, the aircraft manufacturer, and should be handled by extending salvage systems already in operation. Of course, there will be a large majority of castings that can be accepted or rejected without difficulty based on standards agreed upon by the radiographic reader and the prime contractor's stress analyst. In all controversial cases, however, the radiographic reader should be required to interpret the X-ray only to the extent of assaying defects in terms of their expected effect on physical properties. It is strongly felt that the decision to accept or reject parts should remain with a salvage engineer who has access to all pertinent information regarding the part.

A second point of discussion is raised on the use of test bars to evaluate the various defects shown on radiographs. The size and shape effect both in foundry technique and test results is very difficult to correlate with the actual physical properties of castings. Federal specification QQ-M-151a indicates the order of magnitude of the difference to be from 25 per cent on the ultimate load and yield load to 75 per cent on the 2-inch gage length elongation, the actual casting coupons giving these lower results. Also, machining frequently exposes defects found deep in the casting which are not approached in the test bars (even when the test bars are machined). It is felt that far more accurate correlation would ultimately result if defects are evaluated on the basis of radiographs of and test coupons cut from actual castings rather than relying on test bars.

Written Discussion: By N. E. Woldman, chief metallurgical engineer, Eclipse-Pioneer Division of Bendix Aviation Corp., Teterboro, N. J.

Leslie Ball has written an excellent paper, but has entered a very controversial subject which to date has not been set down clearly by anyone. This paper outlines a long step in the way to establish a practical method of X-ray standards and interpretation, but could be extended to a national rather than to an individual company code. Mr. Ball apparently intends to correlate the effects various casting imperfections have on the physical properties of castings.

He states on page 546 that the Air Corps Technical Report No. 4796—Static Test Requirements—are very welcome and valuable when used as a general guide, but if applied as an absolute criterion of aircraft serviceability, these static load tests would probably lead to service failures under nonstatic loading. We are inclined to agree with Mr. Ball in this regard although a metallurgist of the Aluminum Company of America and one of the General Electric Company have indicated that static load tests on properly designed castings are a good indication of how the part will stand up under the circumstances normally encountered in service.

Mr. Ball suggests X-ray micrographs of varying degrees of porosity, microshrinkage and other casting defects which had been taken from tensile test bars of known strength as standards to be used for indicating the seriousness of the defects in a production casting. Borderline castings will then be cut and slices taken from time to time and compared with standards of the test bars. We do not see where this will be any better than the ordinary X-ray standards of minimum acceptable quality which should be established by some borderline tests: either static or dynamic laboratory tests or service tests. Perhaps a different approach to the problem would offer a more practical solution.

Castings should be divided into two groups: one which we term in our specification as "average commercial quality castings" and which Mr. Ball terms "a commercially perfect casting". Here X-rays should be used not as a basis for rejection, but as a check on the consistency of quality of successive shipments. The other grade of casting should be the high stress casting which is X-rayed from 10 to 100 per cent. On these castings where the application is so critical as to require expensive X-ray examination, the breakdown tests should be as much a requirement of the specification as the approval of pre-production samples. Then with minimum standards of acceptable quality established by these tests, there should be no dispute as to the disposition of questionable castings.

The short section on defects due to secondary radiation could be enlarged with considerable benefit to most of the people who view X-ray negatives but have had little experience or training. The shadows due to secondary radiation are very deceiving and have caused a number of unwarranted rejections due to the interpreter's failure to recognize the cause of the apparent defect.

A great deal of work must be done in the way of standardizing the reading and interpretation of X-rays before radiography can more than suggest its true value to anyone who uses castings that are stressed to any degree. Mr. Ball has set a course that could well be followed and explored by the engineering societies that would benefit by the resultant standards.

Written Discussion: By H. H. Lester, principal physicist, Watertown Arsenal, Watertown, Mass.

Mr. Ball has selected a very timely subject. There have been different opinions expressed with regard to the specific objectives of radiographic inspection. There cannot be much argument, however, about the overall objective which is to help in the securing of structural units that are dependably consistent in service performance. Radiography permits the examination of one factor that contributes to consistent performance of the part, namely, the factor of metal soundness. The term "essential soundness" is often used. It means that in any structural unit or in any part of it the metal shall be sufficiently free from gross defects so that design strength may be realized. Since all parts of the unit are not stressed to the same extent, essential soundness may vary from region to region in the same unit. Mr. Ball recognizes this fact in his thought that the interpreter of the negative must determine from the blueprint where high stresses may occur. The present commentator desires to point out that if this idea were taken seriously the man who interprets the negative would have to be qualified as a high class design engineer, and

if he were he would probably refuse to classify regions as subject to particularly high stresses in a great many types of castings whatever the indications of the blueprint because such castings (possibly constituting a majority of those ordinarily examined radiographically) are subject to unpredictable stresses. That is, in the case of mobile artillery designed for travel at high speeds over rough terrain, road shocks bring in stresses many of which cannot be easily determined from blueprints. Such units are subject also to shocks due to shells which might explode in the immediate vicinities and to actual impact of enemy ammunition. The above is an extreme case but similar situations hold with regard to airplane structures which may be subject to unusual wind conditions or unusual conditions encountered in landing.

Even if it were possible to determine the stress pattern for the part with certainty there is still the question of what constitutes essential soundness for any particular region. "Radiographic standards" are necessary so that the designer may designate required soundness in specifications. This thought brings up the question as to what should be the basis for the establishment of radiographic standards. Obviously such standards should be based upon definite correlation of defects imaged in radiographic negatives with desired quality characteristics of the material. The evidence for direct correlation is not easily obtainable. The evidence from studies of test specimens is not satisfactory. It could be obtained perhaps from elaborate statistical studies of defective parts. Mr. Ball approaches the solution through comparisons between radiographs of the part as ordinarily viewed and microradiographs taken of cut sections. Such comparisons are valuable in that they serve to make diagnoses of radiographic negatives more accurate but they do not answer the more fundamental question, "To what extent is the actual strength or ductility of the part impaired by the actual presence of the defects imaged in the negative?"

It is suggested that a further approach to a solution of this important question is now possible through radiography itself. That is, there has been developed recently* a 2-million-volt tube with an exceedingly fine focal spot that will yield pictures of the structural details of a mechanism or of a complicated casting with remarkable clarity and accuracy and with sharpness of definition that will permit actual strain measurements to a preciseness of probably better than 0.005 inch. With such a tube it should be practicable to make measurements on actual sound and unsound castings while stressed and unstressed and thus to arrive at actual evaluations of the effects on elastic strength of imaged defects. Such tests would go far toward making radiographic standards mean more to the design engineer. There would still be questions of ductility. The microradiograph comparisons that Mr. Ball describes probably constitute the best approach to an answer to this question that has been thus far suggested in connection with the estimation of the effects of certain types of porosity on ductility.

Author's Reply

One of the purposes of any paper that deals with policies and methods is to provoke constructive discussion. In the present case, the response from so many

*The Machlett tube, introduced to the world in a public showing September 26, 1944.

of the leaders in the radiographic field forms a very important part of the whole paper.

It is evident that there is some misunderstanding as to the personnel involved in the interpretation function. It was not the author's intention to suggest that the radiographer carries out interpretation entirely by himself. It is quite practical and desirable that many metallurgists and engineers should themselves become qualified interpreters. However, their function is supplementary to the "production reader" who inspects about one thousand films per day. Even though metallurgists and engineers guide the production reader, the latter must have professional status in order to apply the guidance he receives.

The difficulties of establishing radiographic standards remain formidable until it is realized that the need is not for "absolute standards" which can be used by the layman, but for "reference standards" which can be applied by the professional interpreter. Only in a very few cases will absolute standards ever be possible.

Mr. Jenks inquires if all the subdivisions of the classifications are necessary. For use as a national standard, they are not all necessary and their number should be reduced. For example, in Group 2, shrinkage cavity and shrinkage sponge are sufficient for national use. However, all the groups are essential and a great advantage of the system is that it allows the addition within the groups of terms which are needed locally or for special types of fabrication. As to whether all the subdivisions can be clearly distinguished, there is no doubt that they can. Our library radiographs fully illustrate this point.

The definition of "the ideal system of interpretation" deserves careful study. The suggested objective can be achieved, but for this purpose the classification and rating of defects have to be supplemented by dimensional statements and sketches. One case in which we do this is the B-17 control wheel, the reports on which include a sketch showing the location and size of any cavities.

The knowledge of the origin and nature of defects which determines "why certain appearances in the radiograph are interpreted as a given defect" is, in many cases, provided by X-ray micrograph studies. The dark areas on radiographs of manganese bronze castings, which might be due to dross, are interpreted as sponge shrinkage because X-ray micrographs have shown that the images are caused by a honeycombed structure containing dendritic crystals.

Table II is intended to provide serviceability ratings, not quantity ratings. We have tried quantity ratings based solely on the size of the defect, but they do not lend themselves to rapid interpretation on production parts. On non-production parts, the serviceability code can be replaced by a more extensive description which does not involve prejudicial terms such as "excessive".

The eight degrees of serviceability are more than enough for production reading. For some types of defect, all the degrees are never used. However, for teaching purposes, and to show trends in foundry control, all eight degrees are valuable. There is no difficulty in illustrating eight distinct degrees of some defects, for example, shrink porosity.

The effect of section thickness is important. One compensating factor is, that the technique can be chosen to give an almost constant contrast in terms

of percentage of total thickness. This compensation is destroyed when a section radiographed thick is machined into a thin one.

In response to H. W. Hiemke, the principle of standards, "based almost entirely on the ability of producers to meet such a standard", is quite practicable particularly if we add the phrase, "at the contract price". However, the foundries themselves seldom welcome adjusting the price per pound to the quality of casting required, so an initial fee may be required to develop high quality in critical castings.

In answer to Mr. Isenburger, the defect classification is intended to apply to all types of castings, forgings and welds.

The variations in the shrinkage conditions in steel are excellently illustrated by the figures to which reference is made. The term, shrinkage crack, appears to be a good one. However, our procedure is to use combined terms to describe intermediate conditions. For example, we may use the combinations "2.1, 2.2," meaning "cavity surrounded by sponge shrinkage," or "2.2, 1.2," meaning "sponge shrinkage including a hot tear."

The effect of X-ray technique factors, such as direction and superimposed sections, does greatly affect the appearance of defects. Fortunately, in the aircraft industry, we are usually able to study critical parts very thoroughly because we receive many thousands of the same part. Under these circumstances interpretation standards become individual to a particular technique.

Replying to Messrs. Lace and Oyster, it is interesting to note that this company has achieved some of the stress marking of prints and standardization of techniques that have sometimes been refused on the grounds that they were impractical. Our own technique files include photographs of each orientation, etc. Under present war conditions this recording has the added advantage that aircraft manufacturers can specify the radiography for subcontractors shall be carried out in the same approved manner as used for the prime contractor. The "higher authority" which disposes of borderline conditions, in our case may be an engineer of the consuming company or the consultant interpreter on our own staff.

The tendency for only one particular type of defect to occur in a particular spot can be easily overestimated. The purchasing departments of many aircraft companies change vendors quite frequently and even the same vendors have periods of quite different difficulties.

Replying to Mr. Austin, the proposed eighth objective is important, particularly for improving the relations between the foundries and the radiographers. We have attempted to accomplish it by making a general reading on the prevailing condition in each shipment of castings and by using sufficient ratings to indicate improvement or deterioration in general quality.

It is true that the designer of castings does have the necessary stress information. Our experience has been that the radiographer has to specify just what information he requires; otherwise, the designer is reticent to prepare stress data because he overestimates what is needed.

In response to A. E. Cartwright, general standards are very much the concern of the A.S.T.M. However, individual laboratories do need to set up standards for particular projects. For example, in our case, we have made a

complete study of several aircraft models and set up standards specific to the manufacturer's requirements on each model.

Very great assistance is provided by "a small diagram indicating the relative location and function of the part." However, a rather simpler and almost as effective method is to have vectors on the print showing all the loads on the part, i.e., showing both applied and reaction loads. Although Mr. Cartwright's comments are justified, there are several cases in which aircraft companies have merited a great deal of credit for the work they have done in guiding X-ray inspection.

To M. A. Miner, I would say that emphasis on foundry control is important and it should be increased beyond the present practice. A radiographic interpreter can learn to associate certain appearances with the practice of individual foundries. For example, a foundry that makes a habit of gating aluminum castings through a thin flange and placing a large riser on the runner, will produce many castings showing a particular type of shrinkage porosity in the flange, and the interpreter can definitely assign this defect to too slow cooling adjacent to the gate.

The point of view that a salvage engineer rather than a radiographer should decide the disposition of doubtful castings, is very much appreciated. However, in those cases where salvage engineers have learned enough of radiography, they have become, in fact, radiographic interpreters and they should receive added recognition for this accomplishment. The term "radiographic reader" is very suitable for describing the man whose duties only go as far as sorting out the definitely bad, the doubtful, and the definitely good parts. If professional engineers trained in radiography are employed by radiographic laboratories it allows rapid and co-ordinated disposition of all parts. On the other hand, there are very good reasons why aircraft manufacturers may choose to have their own salvage engineers decide the usability of borderline parts.

As noted by Mr. Miner, caution is required in applying results obtained by test bars and test coupons. This is emphasized by Table III, where their use is restricted to just one group of defects.

Replying to N. E. Woldman, the reasons that the X-ray micrograph procedure is "better than the ordinary X-ray standards" are, first, because it discloses the exact type of dispersed defect by showing the shape, size and distribution of the individual microcavities, and, second, because it eliminates making allowance for technique factors, such as section thickness.

The principle of "checking on the consistency of quality of successive shipments" of all classes of aircraft castings is well stated. However, it is to the quality of the high stressed 100 per cent X-ray castings to which we apply the term "commercially perfect".

The comment, that there is considerable interest in secondary radiation images, is appreciated. A reference to a fuller description of them has been added to the text.

As Mr. Lester observes, complete stress analysis can be made only by high class engineers, and they are very conscious of the difficulties, uncertainties and expense involved. For this reason, it is important that the radiographer should limit and define his requests for stress information. In judging any defect, his

prime question is, "Is it possible for a fracture to pass through the defect?" If so, the defect is in a critical area and may cause rejection. If no conceivable fracture can pass through the defect, it is not rejectable except for other than stress reasons.

The reference to mobile artillery may emphasize an important difference between judging radiographs of welded and bolted or riveted assemblies. In the latter types of construction, many failures occur through the attachment holes, often through bearing stress failure, and so the critical regions are liable to be adjacent to these holes.

Two-million-volt studies of complete assemblies may well furnish needed service data. The technical session, on this subject, to be held by Committee E-7 at the next A.S.T.M. Convention, should help to assess this possibility.

CHARACTERISTICS AND PROPERTIES OF SOME CAST CHROMIUM-MOLYBDENUM STEELS

BY N. A. ZIEGLER AND W. L. MEINHART

Abstract

The 5.0 to 9.0 per cent chromium, 0.5 to 1.0 per cent molybdenum steels commonly used in castings for corrosion and elevated temperature service are noted for their thermal sluggishness, which makes them susceptible to cracking during welding and heat treatment. More detailed data on alloy steels of this type have been desired; therefore, the individual effects of carbon (0.05 to 0.30 per cent), chromium (2.5 to 9.0 per cent), and molybdenum (0 to 1.5 per cent) on a series of steels have been studied. Results of thermal analyses, metallographic examination, physical property determinations, and welding experiments are presented.

Thermal sluggishness and hardenability vary according to the percentage of carbon, chromium and/or molybdenum in the steel and are not increased appreciably even at 9 per cent chromium and 1 per cent molybdenum, if carbon is held under 0.07 per cent. The air hardening tendency becomes strong when carbon exceeds 0.20 per cent. Increasing carbon in these alloys has a more pronounced effect than chromium and/or molybdenum in raising the strength and hardness and reducing the ductility. More than 1.0 per cent molybdenum or a combination of 7.0 to 9.0 per cent chromium plus 0.25 per cent molybdenum or higher tend to close the gamma loop in the constitutional diagram, which results in decreased thermal sluggishness, strength and hardness.

INTRODUCTION

CHROMIUM-MOLYBDENUM steels have been studied by many investigators and reported in numerous books and technical articles. Perhaps the most complete information on this subject may be obtained from the two Alloys of Iron Research Mono-

A paper presented before the Twenty-sixth Annual Convention of the Society held in Cleveland, October 16 to 20, 1944. Of the authors, N. A. Ziegler is research metallurgist and W. L. Meinhart is assistant research metallurgist, Crane Company, Chicago. Manuscript received June 20, 1944.

graphs by Kinzel and Crafts (1)¹ and by Gregg (2). The appended bibliography is a testimony of considerable work done and information accumulated on chromium-molybdenum steels.

It is quite well known that both chromium and molybdenum, when added to a carbon steel in amounts up to about 10 and 2 per cent respectively, increase the strength and thermal sluggishness, i.e., hardenability. Chromium also improves the corrosion resistance at room temperatures as well as oxidation resistance at elevated temperatures. One of the important functions of molybdenum is the improvement it imparts in high temperature creep resistance. Each of these elements, with iron, form a gamma loop in their respective constitutional diagrams. If the carbon content is not too high, a sufficiently large amount of either element may completely eliminate the austenitic state at any temperature, thus making a steel continuously ferritic up to its melting point, unheat-treatable (in the sense of grain refining) and unhardenable. In this respect molybdenum is more potent than chromium, because in carbon-free iron it closes the gamma loop in the amount of about 3 per cent while it requires over 12 per cent chromium to produce the same effect.

As is well known, increasing carbon extends the nose of the gamma loop in the diagram so that larger amounts of chromium and/or molybdenum are required to eliminate the austenitic state. Moreover, it is known that the effect of chromium and/or molybdenum in increasing thermal sluggishness of the metal (which in turn causes the increase in strength and hardenability) is due not so much to the presence of these two elements per se (in solution in iron), but rather to their effect on the type and distribution of carbides in the microstructure as determined by rate and temperature of transformation. It thus follows that in order to produce the desired beneficial effect, a certain minimum percentage of carbon is necessary.

Most of the work done so far has been with wrought steels, therefore less information is available for "as-cast" and heat treated steels. Many of the general characteristics of the steels discussed above are common to both wrought and cast alloys. However, it is well known that there are certain structural differences between cast and wrought alloys, which heat treatment will not eliminate, and which are reflected in the resultant physical properties. A more detailed study of these cast alloys is desirable, particularly of those in

¹The figures appearing in parentheses pertain to the references appended to this paper.

the range used in high temperature oil refinery or similar severe service.

Two of the common alloys used for making castings for the above service are chromium-molybdenum steels of the following nominal compositions:

C	Si	Mn	S	P	Cr	Mo
0.15-0.30	0.20-1.25	0.45-0.75	0.06 max.	0.05 max.	4.0-6.0	0.40-0.65
0.15-0.30	0.20-1.25	0.45-0.75	0.06 max.	0.05 max.	8.0-10.0	0.75-1.50

The physical properties usually required for both of these steels are as follows:

T.S.	Y.P.	El.	R.A.
90,000 psi. min.	65,000 psi. min.	18 per cent min.	30 per cent min.
Charpy I.R. (70° F.)		B.H.N.	
15 ft-lbs. min.		235 max.	

Even though these and related steels are extensively used in various welded installations, their thermal sluggishness and hardenability necessitate rather specialized welding technique in the sense of careful preheating, weld metal deposition, and stress relieving. Unless the prescribed welding rules and regulations are strictly observed, there is danger of the weld or the affected zone cracking because of the internal strains set up by the thermal sluggishness of the metal. What has been said about welding also applies, perhaps to a lesser degree, to heat treating: heat treating cracks are not uncommon in castings made of these types of steel.

In general, the weldability of a steel is improved in proportion to the decrease of (a) its carbon content, and (b) its alloying elements. In this case, chromium is required to impart the necessary corrosion resistance, and molybdenum—the creep resistance. Both influence the physical properties developed by normalizing and drawing heat treatment. A certain minimum percentage of carbon is necessary to develop the desired properties; but the exact amount of this minimum was not definitely known. In view of many factors involved in developing suitable properties in this type of steel, it was decided to investigate cast alloys made of iron, carbon, chromium and molybdenum within the following compositional limits: 0 (theoretical) to 0.30 per cent carbon, 2.5 to 9 per cent chromium and 0 to 1.5 per cent molybdenum. It was expected that the effect of each one of these elements could be quantitatively detected from data thus accumulated. It also was hoped that the additional knowl-

^aStandard Charpy test bar with a keyhole notch.

tometer. Welding tests were made on all experimental castings ("tees") after they were given the same heat treatment as the test bar blanks. Test data thus accumulated (with the exception of welding tests) are presented in Table I, together with the chemical analysis of each heat. It may be noted that all compositions may be divided into four main groups: those containing 2.5, 5, 7, and 9 per cent chromium. Each group, in turn, may be subdivided into five sub-groups, those containing 0, 0.25, 0.5, 1.0 and 1.5 per cent molybdenum. Each sub-group is composed of three or more steels containing progressively higher carbon, from theoretical zero and up to about 0.3 per cent carbon. Figures representing physical test data were averaged from two or more tests.⁴

The silicon, manganese, sulphur and phosphorus contents (Table I) vary within the specification limits previously referred to, except for a few cases where the manganese content is a little too high. Analyses of chosen variable elements (chromium, molybdenum and carbon) are reasonably uniform, and thus permit drawing certain conclusions.

THERMAL ANALYSIS AND MICROEXAMINATION

Most of the compositions presented in Table I were subjected to thermal analysis by means of a differential dilatometer. This instrument is so constructed that a thermal expansion-contraction curve is automatically recorded on a photographic film. In each case a specimen (50 millimeters long and 4 millimeters in diameter) was heated to about 1000 degrees Cent. (1830 degrees Fahr.) in 2 hours, and then cooled to room temperature at an average rate of (a) 50 degrees Cent. per minute (90 degrees Fahr. per minute) and (b) 3.2 degrees Cent. per minute (5.8 degrees Fahr. per minute). In other words, each composition was subjected to thermal analysis by cooling two specimens from 1000 degrees Cent. (1830 degrees Fahr.), one at a slow and the other at a more rapid rate. Representative dilatometer curves are reproduced in Figs. 2 to 7. The chemical analysis and the Vickers pyramid hardness numbers (V.P.N.) are given adjacent to each curve. Figs. 2 and 3 represent the low carbon (0.02 to 0.08 per cent carbon) steels, Figs. 4 and 5, the intermediate (0.13 to 0.20 per cent carbon), and Figs. 6 and 7—the high (0.20 to 0.35 per cent carbon). Moreover, Figs. 2, 4 and 6 illustrate the

⁴Variations in test results represented by each average figure come within normal limits of experimental error.

Table I

Serial No.	Nominal Composition		Chemical Analysis							Dilatometer Data				Air Cooling
			C		5-Hour Cooling					Run		V.P.N.		
	Cr	Mo	Si	Mn	S	P	C	Cr	Mo	Run No.	V.P.N.	Run No.	V.P.N.	
1	2.5	0	0.74	0.45	0.030	0.017	0.07	2.33	0.02	659	124	658	135	
2	2.5	0	0.92	0.49	0.031	0.015	0.14	2.28	0.02	656	155	657	217	
3	2.5	0	0.82	0.69	0.018	0.018	0.30	2.29	0.04	696	226	697	500	
4	2.5	0.25	0.94	0.43	0.025	0.018	0.07	2.49	0.26	671	123	670	126	
5	2.5	0.25	0.52	0.45	0.029	0.018	0.15	2.08	0.28	661	160	660	271	
6	2.5	0.25	0.80	0.72	0.028	0.020	0.34	2.60	0.30	668	313	669	413	
7	2.5	0.5	0.83	0.72	0.013	0.015	0.02	2.51	0.51	297	135	305	128	
8	2.5	0.5	0.56	0.70	0.020	0.016	0.08	2.63	0.58	554	139	553	173	
9	2.5	0.5	0.65	0.79	0.023	0.014	0.10	2.80	0.61	556	173	555	199	
10	2.5	0.5	0.76	0.70	0.014	0.016	0.14	2.75	0.60	373	350	377	380	
11	2.5	0.5	0.86	0.74	0.023	0.022	0.24	2.71	0.52	387	363	388	417	
12	2.5	1.0	0.77	0.75	0.015	0.010	0.02	2.35	1.16	300	136	307	144	
13	2.5	1.0	0.60	0.61	0.017	0.020	0.17	2.64	0.88	356	262	357	376	
14	2.5	1.0	0.65	0.74	0.015	0.024	0.23	2.53	0.90	343	404	344	420	
15	2.5	1.5	0.70	0.68	0.015	0.017	0.03	2.45	1.75	375	176	382	409	
16	2.5	1.5	0.82	0.42	0.015	0.023	0.19	2.86	1.72	375	176	382	409	
17	2.5	1.5	0.84	0.49	0.017	0.021	0.35	3.06	1.56	317	394	348	514	
18	5.0	0	0.82	0.44	0.025	0.020	0.08	5.22	0.03	673	130	672	177	
19	5.0	0	0.54	0.52	0.024	0.022	0.20	4.82	0.08	674	190	675	419	
20	5.0	0	0.93	0.75	0.021	0.022	0.27	4.85	0	676	222	677	454	
21	5.0	0.25	0.80	0.45	0.020	0.014	0.07	4.87	0.26	678	133	679	236	
22	5.0	0.25	0.63	0.43	0.022	0.016	0.15	4.52	0.21	681	163	680	420	
23	5.0	0.25	0.98	0.70	0.021	0.018	0.24	4.80	0.25	682	272	683	572	
24	5.0	0.5	0.86	0.73	0.005	0.014	0.02	4.88	0.50	354	151	355	159	
25	5.0	0.5	0.75	0.65	0.015	0.014	0.07	4.53	0.55	546	141	545	230	
26	5.0	0.5	0.70	0.75	0.019	0.014	0.09	5.16	0.57	544	172	543	405	
27	5.0	0.5	0.82	0.73	0.026	0.016	0.13	5.06	0.54	548	221	547	405	
28	5.0	0.5	0.72	0.64	0.010	0.016	0.15	5.13	0.52	237	300	342	360	
29	5.0	0.5	0.84	0.69	0.014	0.016	0.28	5.13	0.57	550	462	549	489	
30	5.0	0.5	0.71	0.68	0.012	0.022	0.32	5.44	0.51	229	464	231	600	
31	5.0	0.5	0.77	0.74	0.023	0.016	0.39	5.30	0.54	552	409	551	644	
32	5.0	1.0	0.77	0.80	0.015	0.015	0.03	5.06	1.12	299	149	306	145	
33	5.0	1.0	0.80	0.65	0.009	0.023	0.18	5.87	1.04	298	421	304	459	
34	5.0	1.0	0.87	0.56	0.015	0.023	0.35	5.47	1.12	323	473	346	620	
35	5.0	1.5	0.70	0.74	0.015	0.017	0.03	5.08	1.62	303	153	311	153	
36	5.0	1.5	0.82	0.45	0.015	0.024	0.20	5.33	1.67	376	339	378	478	
37	5.0	1.5	0.89	0.58	0.015	0.015	0.34	5.41	1.62	340	493	345	657	

*Heats from which experimental castings (tees) were made.

Table I—(Continued)

Serial No.	Nominal Composition—			Chemical Analysis—					Dilatometer Data—			
									5-Hour Cooling—		Air Cooling—	
	Cr	Mo	C	Si	Mn	S	P	C	Cr	Mo	Run No.	V.P.N.
38	7.0	0	0	0.87	0.43	0.018	0.016	0.07	6.65	0.02	686	146
39	7.0	0	0.15	0.77	0.68	0.021	0.018	0.14	6.62	0.06	685	217
40	7.0	0	0.30	0.61	0.73	0.021	0.024	0.27	6.27	0.03	689	209
41	7.0	0.25	0	0.94	0.47	0.016	0.016	0.05	7.06	0.25	691	139
42	7.0	0.25	0.15	0.75	0.63	0.014	0.016	0.13	7.20	0.27	699	394
43	7.0	0.25	0.30	0.93	0.76	0.022	0.013	0.23	7.36	0.24	724	413
44	7.0	0.5	0	0.82	0.74	0.015	0.012	0.02	7.53	0.55	301	147
45	7.0	0.5	0.15	0.76	0.69	0.011	0.016	0.13	7.06	0.52	384	397
46	7.0	0.5	0.30	0.92	0.76	0.006	0.025	0.32	7.03	0.54	374	514
47	7.0	1.0	0	0.75	0.80	0.015	0.014	0.03	7.01	1.03	302	147
48	7.0	1.0	0.13	0.75	0.73	0.018	0.016	0.13	7.35	1.04	558	354
49	7.0	1.0	0.15	0.85	0.70	0.011	0.024	0.17	7.03	1.12	294	364
50	7.0	1.0	0.30	0.84	0.45	0.015	0.032	0.34	7.66	1.08	313	563
51	7.0	1.5	0	0.75	0.69	0.015	0.019	0.02	7.09	1.59	316	125
52	7.0	1.5	0.15	0.89	0.56	0.015	0.028	0.20	8.33	1.70	318	170
53	7.0	1.5	0.30	0.84	0.45	0.015	0.022	0.33	7.20	1.70	327	409
54	7.0	1.5	0.30	0.83	0.53	0.015	0.022	0.31	7.50	1.64	322	493
55	9.0	0	0	0.96	0.66	0.020	0.016	0.05	9.02	Tr	693	142
56	9.0	0	0.15	0.90	0.73	0.019	0.012	0.14	8.70	0.06	700	344
57	9.0	0	0.30	0.80	0.74	0.029	0.018	0.28	9.08	0.01	703	308
58	9.0	0.25	0	0.87	0.65	0.018	0.014	0.04	8.97	0.23	695	168
59	9.0	0.25	0.15	0.80	0.73	0.024	0.018	0.18	9.22	0.30	705	421
60	9.0	0.25	0.30	0.75	0.75	0.023	0.018	0.28	9.21	0.31	706	419
61	9.0	0.5	0	0.75	0.75	0.010	0.016	0.03	9.00	0.54	392	145
62	9.0	0.5	0.10	0.68	0.73	0.012	0.014	0.13	8.84	0.58	560	276
63	9.0	0.5	0.15	0.35	0.79	0.010	0.020	0.14	8.88	0.61	402	409
64	9.0	0.5	0.30	0.51	0.80	0.011	0.018	0.25	8.90	0.60	410	468
65	9.0	1.0	0	0.75	0.71	0.010	0.018	0.03	8.90	1.08	394	152
66	9.0	1.0	0.15	0.89	0.71	0.010	0.021	0.13	9.20	1.14	399	222
67	9.0	1.0	0.30	0.87	0.73	0.010	0.020	0.28	9.34	1.10	412	464
68	9.0	1.5	0	0.77	0.71	0.010	0.016	0.02	8.76	1.65	409	165
69	9.0	1.5	0.10	0.87	0.72	0.021	0.016	0.12	8.77	1.80	562	240
70	9.0	1.5	0.15	0.87	0.76	0.010	0.016	0.14	8.78	1.80	400	216
71	9.0	1.5	0.30	0.89	0.68	0.010	0.018	0.26	9.08	1.62	413	376
72	9.0	1.5	0.30	0.45	0.63	0.010	0.020	0.22	9.29	1.69	396	276

*Heats from which experimental castings (tees) were made.

Table 1—(Continued)

Serial No.	Physical Properties					Charpy Impact				
	Tensile Properties					Resistance				
	T. S.	Y. P.	P. L.	B. S.	El.	R. A.	P. S. I.	M. E.	Y. R.	R. T.
		P. S. I.			(Per Cent)	(Per Cent)	× 10 ⁶			(Ft.-Lbs.)
										—25° F.
1	60,300	37,200	38,200	140,200	40.8	77.0	29.9	0.62	0.53	53.3
2	74,800	39,400	40,900	142,000	32.5	60.3	30.3	0.53	0.51	36.0
3	99,300	50,000	52,000	151,700	27.0	57.0	31.0	0.51	0.55	16.8
4	59,800	33,100	34,400	120,000	40.8	75.0	32.5	0.55	0.56	49.0
5	80,300	44,600	43,500	146,100	30.8	59.5	30.3	0.56	0.68	36.5
6	114,800	77,700	56,200	162,700	19.8	43.5	29.5	0.68	0.57	17.0
7	53,400	30,500	25,500	85,000	42.3	70.5	23.0	0.57	0.52	18.8
8	71,200	37,300	32,300	130,500	33.5	68.0	28.8	0.52	0.53	47.0
9	76,300	40,800	35,000	149,500	31.5	67.5	31.4	0.53	0.69	45.3
10	101,000	70,000	56,700	159,000	24.0	51.0	29.0	0.69	0.72	46.4
11	112,000	80,200	64,900	160,000	18.8	48.8	29.3	0.72	0.56	15.3
12	53,100	29,500	24,900	81,500	34.3	57.0	24.6	0.56	0.69	4.8
13	100,900	69,100	44,200	150,000	21.8	48.6	28.4	0.69	0.71	1.5
14	113,100	80,100	68,100	164,300	20.3	43.0	28.5	0.71	0.54	17.8
15	55,000	31,200	24,000	84,500	35.1	54.1	26.3	0.54	0.66	10.3
16	106,000	66,500	41,000	160,500	24.0	50.0	32.5	0.66	0.70	3.0
17	122,600	82,300	73,900	182,300	16.0	37.8	30.7	0.70	0.48	2.3
18	64,500	30,600	26,100	144,000	39.0	74.5	30.3	0.48	0.67	3.8
19	86,200	57,200	36,800	161,000	25.8	67.5	32.0	0.67	0.64	26.5
20	107,300	69,100	49,100	189,000	20.5	52.0	...	0.64	0.51	17.5
21	64,500	32,700	24,700	155,900	36.8	76.0	31.3	0.51	0.80	8.0
22	99,500	81,900	55,700	190,000	23.0	67.0	30.6	0.82	0.80	49.5
23	117,400	94,000	77,900	192,200	20.0	55.0	32.5	0.80	0.73	32.0
24	58,500	34,000	24,500	111,000	35.8	61.5	28.5	0.59	0.51	17.3
25	66,000	33,800	25,500	111,000	36.5	70.5	30.1	0.51	0.77	47.5
26	91,800	67,300	46,500	165,500	27.5	61.5	29.2	0.73	0.75	27.0
27	101,200	80,500	70,000	175,600	23.0	58.0	29.9	0.80	0.77	...
28	106,600	82,300	72,100	184,000	23.0	55.8	28.7	0.77	0.75	...
29	115,500	86,800	75,500	172,000	21.3	48.0	29.0	0.75	0.77	...
30	116,600	83,600	73,100	171,200	20.3	52.8	28.3	0.77	0.74	...
31	117,600	87,500	72,500	170,800	20.5	45.0	29.6	0.74	0.57	...
32	60,500	34,000	24,900	117,500	36.8	60.5	28.0	0.57	0.76	...
33	111,100	83,500	67,000	180,300	19.8	52.0	29.0	0.76	0.59	...
34	125,200	91,500	71,500	166,000	16.3	35.5	31.2	0.73	0.67	...
35	61,400	36,000	27,500	91,000	32.0	64.0	28.8	0.59	0.67	...
36	100,700	67,500	42,000	136,500	24.0	58.5	31.8	0.67	0.71	...
37	125,300	88,500	65,900	155,500	19.3	37.0	31.6	0.71	0.71	...

*Heats from which experimental castings (tees) were made.

Table I—(Continued)

Serial No.	Physical Properties						Charpy Impact Resistance— R. T. —25° F.
	Tensile Properties						
	T. S.	Y. P.	P. L.	B. S.	El.	R. A.	
		P.S.I.			Per Cent		
38	70,300	33,600	34,000	155,000	35.3	74.5	46.5
39	99,600	81,200	52,000	188,200	27.3	61.5	23.3
40	105,300	88,500	68,500	193,200	26.3	61.0	18.8
41	66,800	33,800	29,000	146,900	38.3	71.5	35.3
42	94,700	60,700	39,300	172,000	24.5	59.9	11.0
43	116,000	93,500	81,900	172,800	19.3	44.5	3.3
44	62,600	35,600	27,400	142,000	36.0	62.5	25.0
45	103,100	73,100	60,900	166,300	26.5	52.0	13.3
46	105,800	77,100	66,400	165,800	21.0	47.8	4.0
47	63,000	36,500	26,500	122,000	41.8	65.5	30.0
48	95,300	66,800	52,000	154,000	36.0	53.0	31.8
49	107,000	79,300	62,800	182,000	33.0	52.3	25.3
50	117,400	83,300	64,400	167,000	19.3	35.8	9.5
51	63,400	37,300	24,000	90,800	31.8	57.5	41.3
52	102,500	84,500	59,000	158,300	16.5	45.5	17.5
53	116,700	88,500	65,000	161,500	15.8	29.5	4.0
54	116,800	84,500	66,600	159,500	16.0	27.5	1.5
55	67,700	35,400	29,800	146,200	35.3	69.0	3.0
56	186,700	85,100	71,300	183,100	22.5	57.5	16.0
57	109,800	87,300	79,300	182,500	19.3	44.5	11.5
58	65,600	35,700	29,700	118,300	32.8	58.0	6.0
59	104,100	76,900	75,200	177,300	22.5	57.0	3.3
60	108,400	79,800	76,300	179,200	19.3	38.5	25.8
61	64,500	40,000	32,700	105,000	31.0	52.5	15.5
62	85,400	52,000	38,500	138,000	28.0	49.5	14.5
63	105,400	79,300	66,000	171,000	22.3	30.3	23.5
64	105,600	77,500	62,300	170,000	24.0	47.3	13.8
65	62,800	33,400	23,900	103,000	29.3	50.0	21.0
66	96,200	65,300	51,000	172,500	27.3	55.5	32.0
67	108,500	78,800	65,800	174,000	23.3	45.0	22.0
68	66,800	39,500	27,500	98,000	29.0	64.0	15.8
69	86,500	53,500	43,500	148,000	21.5	50.0	30.5
70	96,300	62,600	47,800	169,500	24.8	48.3	27.0
71	109,100	78,600	65,800	170,000	21.3	37.8	1.5
72	102,800	76,900	54,400	133,000	23.0	43.5	3.5
							...

*Heats from which experimental castings (tees) were made.

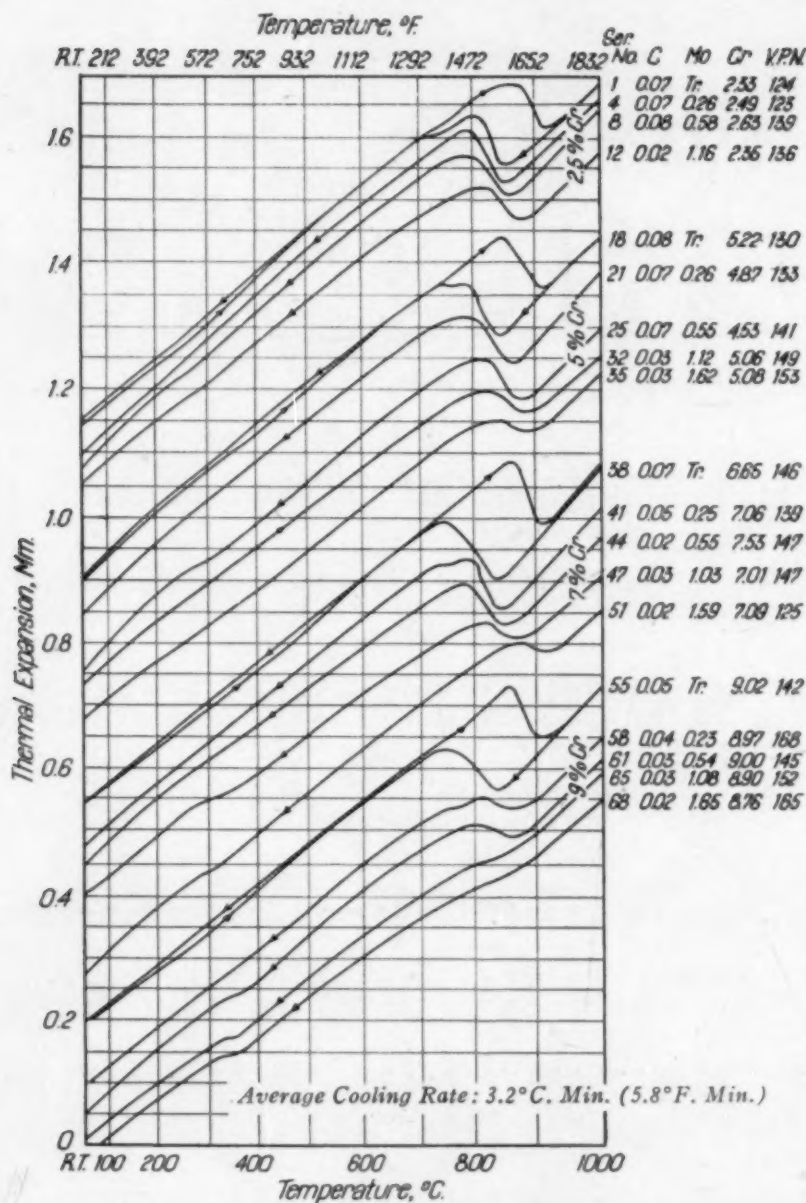


Fig. 2—Thermal Cooling Curves of Chromium Molybdenum Steels Containing 0.02 to 0.08 Per Cent Carbon and Various Amounts of Chromium and Molybdenum. (Slow Cooling Rate).

slow cooling rate (3.2 degrees Cent. per minute or 5.8 degrees Fahr. per minute), and Figs. 3, 5 and 7—more rapid cooling (50 degrees Cent. per minute or 90 degrees Fahr. per minute). In each of these figures, thermal curves are arranged into four groups: steels containing 2.5, 5, 7 and 9 per cent chromium. Within each group they represent steels with molybdenum increasing from 0 to 1.5 per cent. Curves obtained from steels with no molybdenum (the top curves within each group) have been drawn with heating as well as cooling

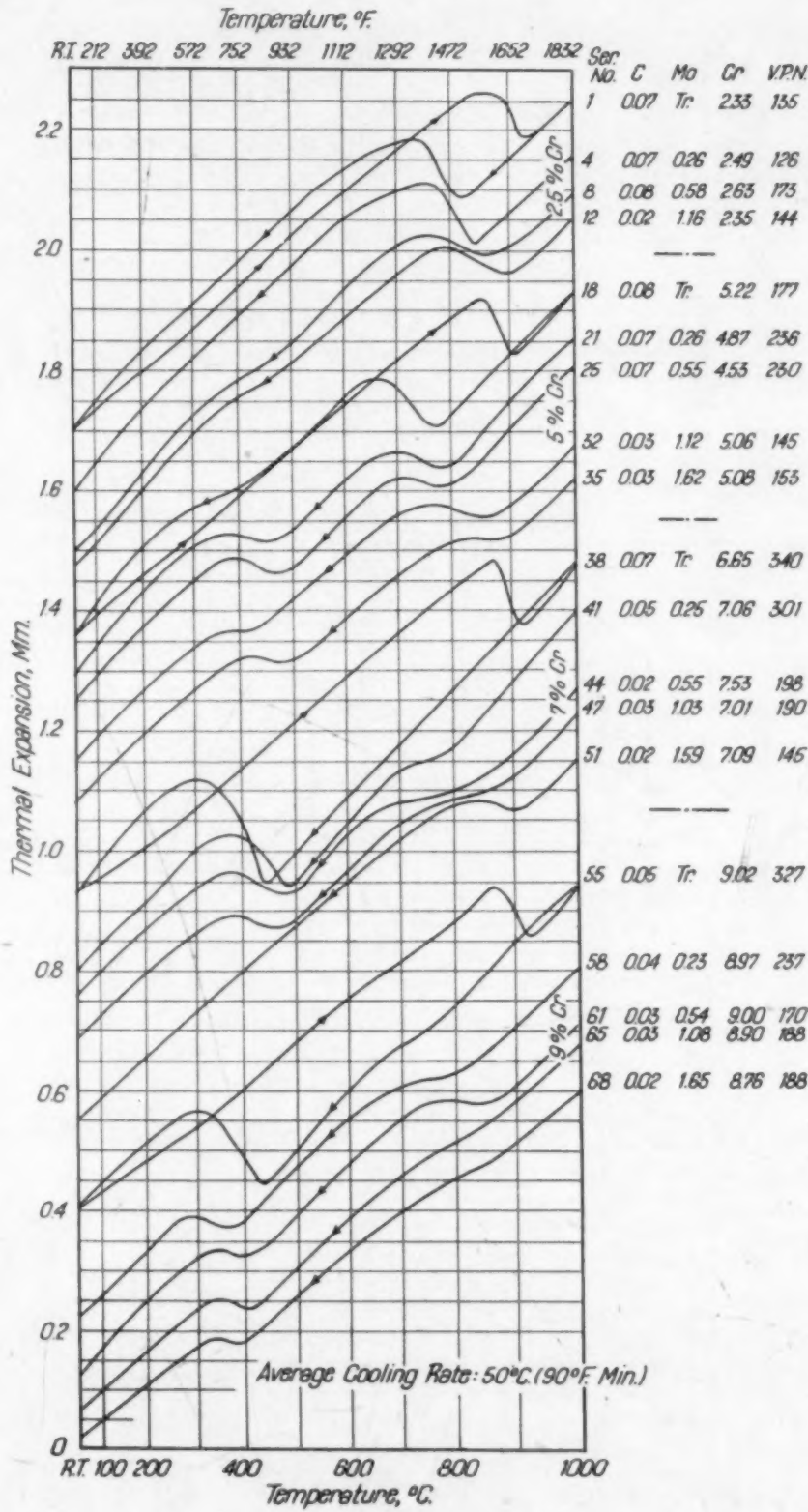


Fig. 3—Thermal Cooling Curves of Chromium-Molybdenum Steels Containing 0.02 to 0.08 Per Cent Carbon and Various Amounts of Chromium and Molybdenum. (Rapid Cooling Rate.)

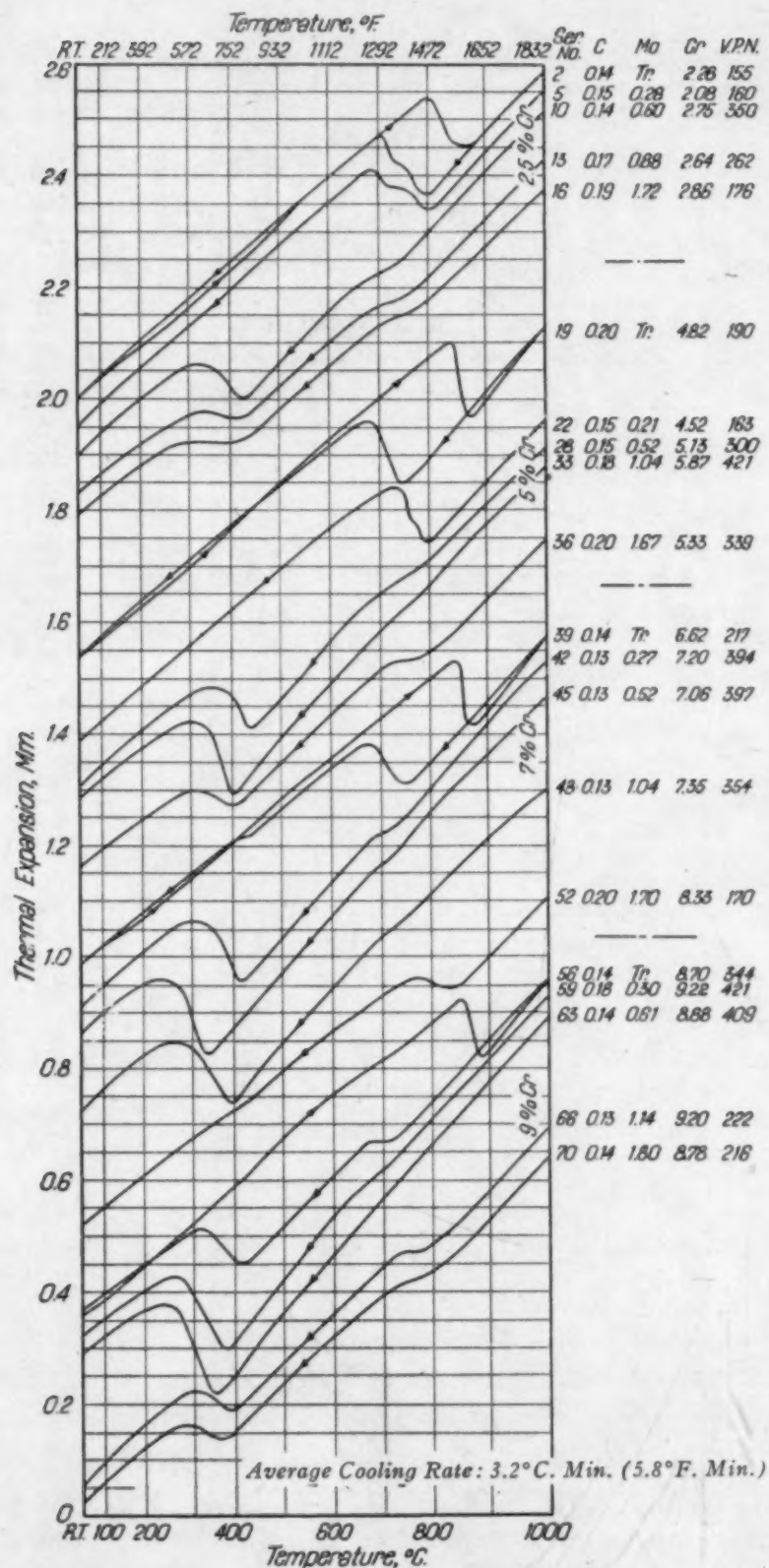


Fig. 4—Thermal Cooling Curves of Chromium-Molybdenum Steels Containing 0.13 to 0.20 Per Cent Carbon and Various Amounts of Chromium and Molybdenum. (Slow Cooling Rate.)

branches. The remainder (for the sake of space economy) have only the cooling branches reproduced, inasmuch as the heating branches for the curves within each group are reasonably similar. All of these curves are tracings of the original photographically recorded dilatometer curves.

In general the uniform cooling of steels of this type from the austenitic state, with the rates employed, results in a majority of transformations occurring at temperatures either over 650 degrees Cent. (1200 degrees Fahr.) such as in No. 1 (Fig. 2) or below 450 degrees Cent. (840 degrees Fahr.) like those in Fig. 7.

The former transformation results in ferrite plus laminated pearlite of various degrees of coarseness and the latter in hard martensite and needlelike bainite structures usually arranged in Widmanstätten pattern. Between these two extreme cases there are steels which with the same cooling rates will partially transform at the upper temperature range and partially at the lower, like curves Nos. 21 and 25 (Fig. 3). In the intermediate range, i.e., between 450 and 650 degrees Cent. (840 and 1200 degrees Fahr.), transformations are extremely slow, as demonstrated by many investigators engaged in studying isothermal transformations and by numerous S-curves published in the literature.

The characteristic of a steel which causes it to transform at either the upper or lower temperature range is determined by three independent factors:

(a) Inherent thermal sluggishness of the metal, which in turn is a function of its chemical composition.

(b) Cooling rate.

(c) Presence in the austenite of a second phase, such as some residual ferrite, a result of the position of the given steel with respect to the gamma loop in the constitutional space diagram.

The third factor may be considered as a special case of the first, but, as will be shown, it may be convenient to differentiate between the two. It should be understood that all these remarks are based on uniform cooling, which does not include some of the phenomena observed in connection with isothermal heat treatments.

Each of the resultant dilatometer specimens was subjected to microexamination.⁵ For the sake of conserving space, however,

⁵Samples were etched in 5 per cent picral, 1 per cent HCl solution. This reagent develops more detail in bainite and martensite than nital without seriously overetching the fine pearlite frequently associated with them in the same samples.

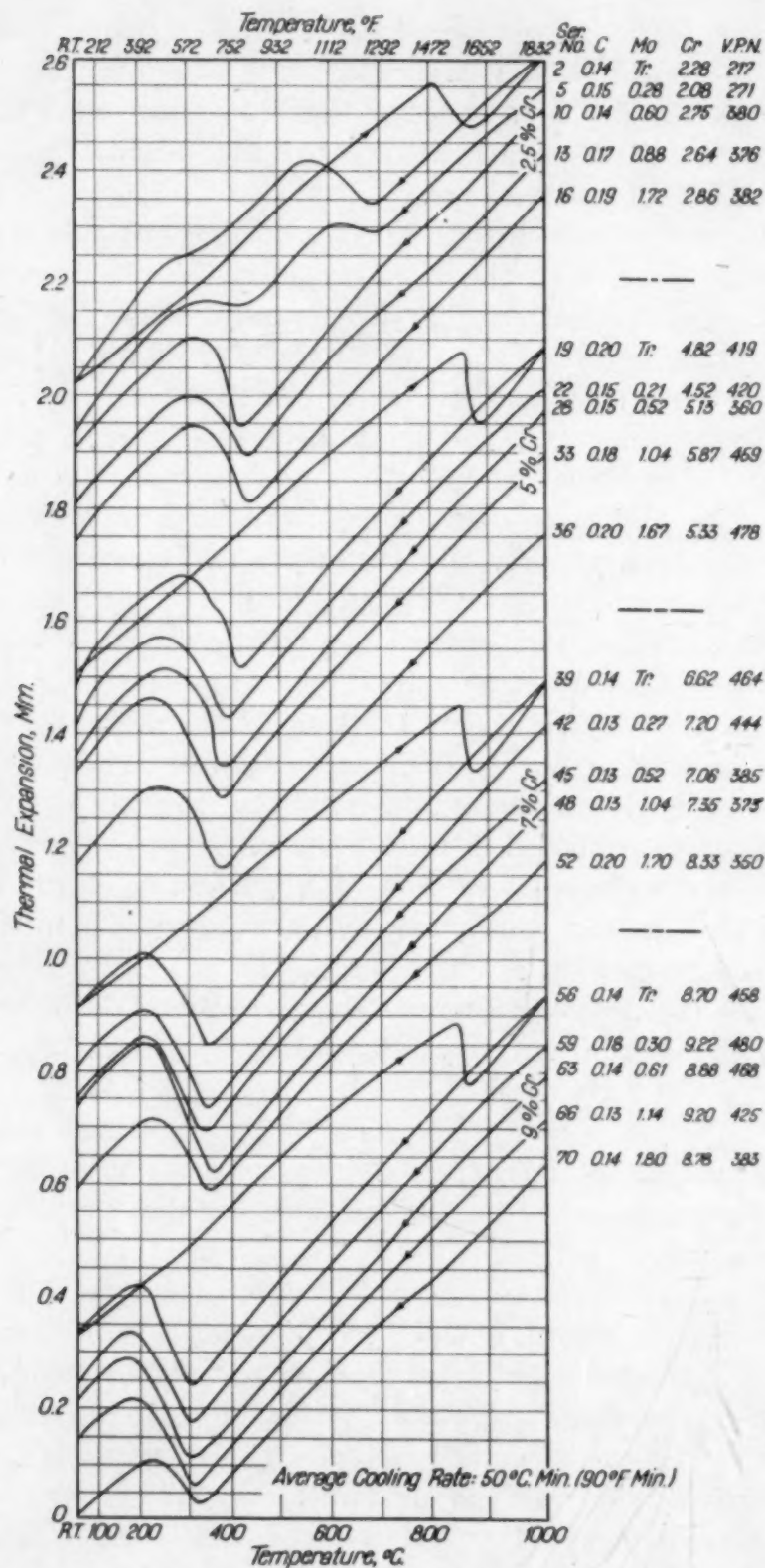


Fig. 5—Thermal Cooling Curves of Chromium-Molybdenum Steel, Containing 0.13 to 0.20 Per Cent Carbon and Various Amounts of Chromium and Molybdenum. (Rapid Cooling Rate.)

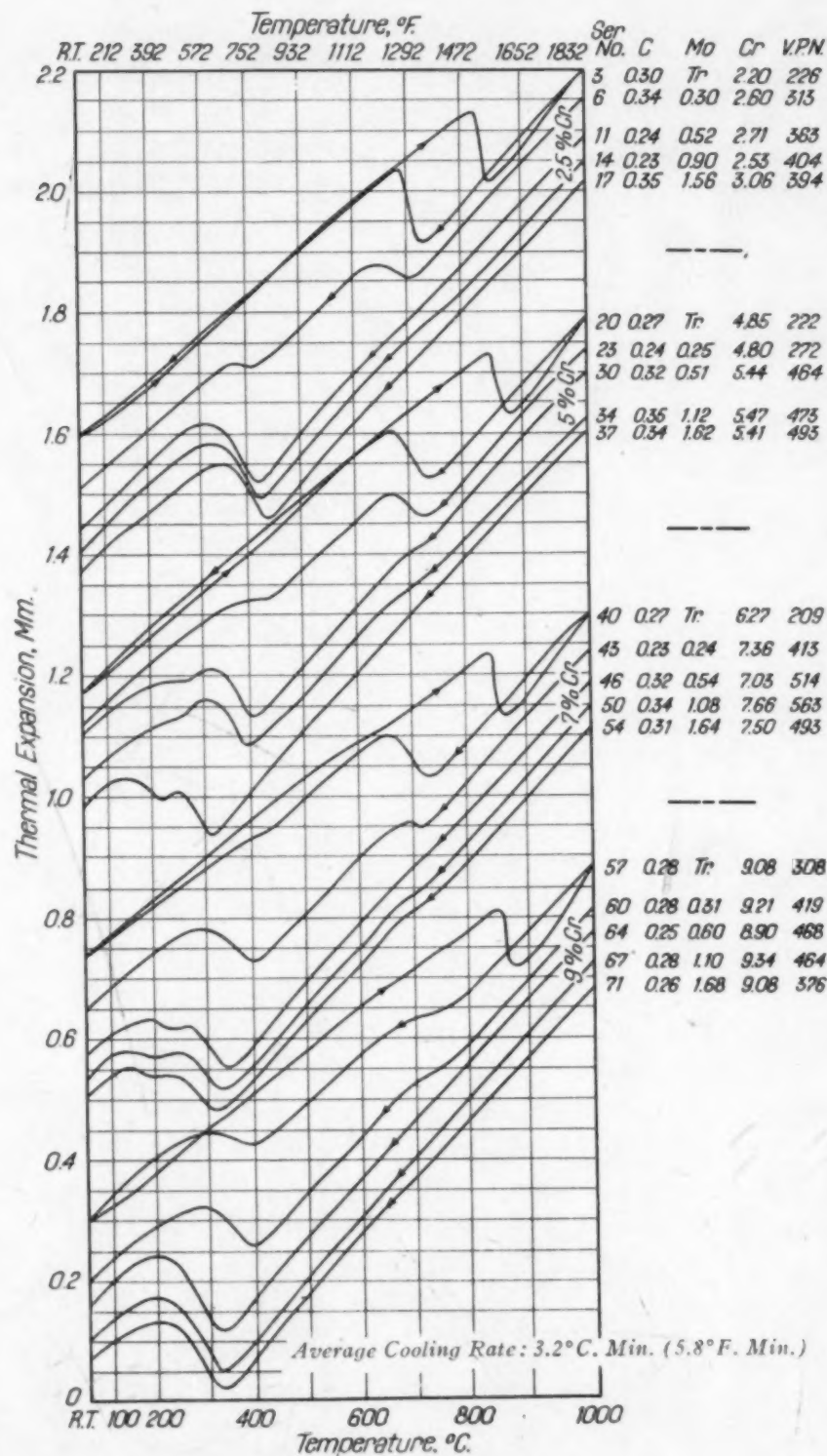


Fig. 6—Thermal Cooling Curves of Chromium-Molybdenum Steels, Containing 0.20 to 0.35 Per Cent Carbon and Various Amounts of Chromium and Molybdenum. (Slow Cooling Rate.)

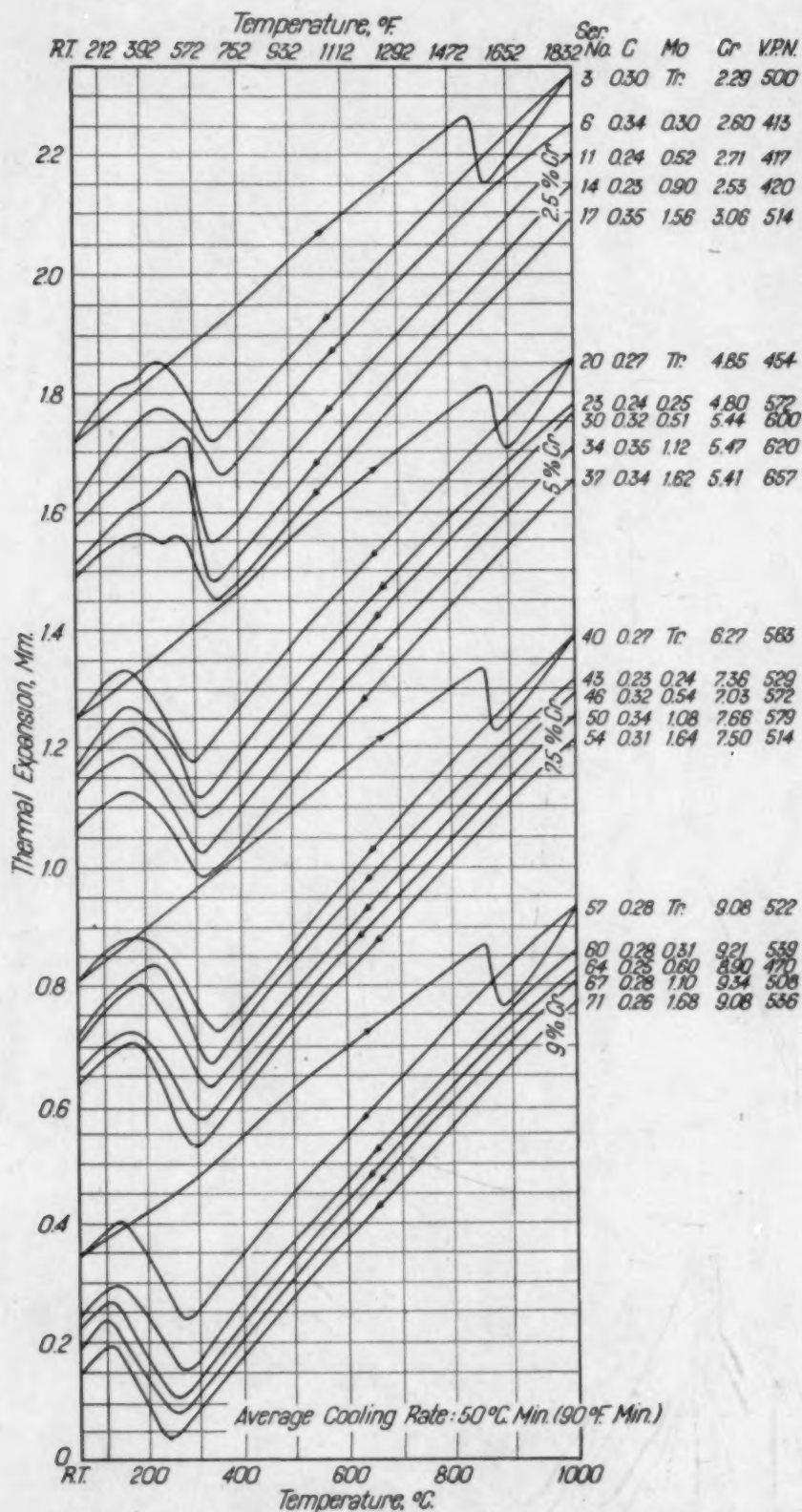


Fig. 7—Thermal Cooling Curves of Chromium-Molybdenum Steels, Containing 0.20 to 0.35 Per Cent Carbon and Various Amounts of Chromium and Molybdenum. (Rapid Cooling Rate.)

only a few typical structures are presented herewith in Figs. 8 to 21.

When the transformation occurs above about 700 degrees Cent. (1290 degrees Fahr.), the resultant structure is composed of well defined pearlite, with variations in lamellae size, and greater or lesser amounts of ferrite, depending on the percentage of carbon. Curves of this type produced by low carbon steels (Fig. 2, thermal curve type, Nos. 1, 18, 38, 55 and Fig. 3, No. 1) are represented by a corresponding structure in Fig. 8. Fig. 9 illustrates the structures of "medium" carbon steels (Fig. 4, thermal curve type, Nos. 2 and 19) and Fig. 10 of "high" carbon steels (Fig. 6, thermal curve type, Nos. 3 and 20).

The pearlite formed at just below 700 degrees Cent. (1290 degrees Fahr.) (sometimes called "nodular troostite") is very fine and merges into a feathery upper bainite type of structure, at or just below 650 degrees Cent. (1200 degrees Fahr.).

As soon as slight traces of a suppressed transformation can be observed on the cooling curve, this immediately is manifested by the appearance in the resultant structure of a new constituent, referred to as "lower bainite". This light etching structure looks like a diluted pearlite and usually has a needlelike or Widmanstätten pattern. This constituent, associated with fine pearlite (dark), is illustrated in Fig. 11 for "low" carbon steels (Fig. 2, thermal curve type, Nos. 8, 25 and 44), Fig. 12—for "medium" carbon steels (Fig. 5, thermal curve type, No. 2) and Fig. 13—for "high" carbon steels (Fig. 6, thermal curve type, No. 6). The amount of this constituent is directly proportional to the degree of suppressed transformation as exhibited by the deflection on the cooling curve.

With further increase in thermal sluggishness, most of the transformation may be suppressed to the low temperature range, which is illustrated by the resultant structure in Fig. 14 for the "medium" carbon steels (Fig. 4, thermal curve type, Nos. 28 and 42, and also Fig. 5, No. 10), and by Fig. 15 for the "high" carbon steels (Fig. 6, thermal curve type, No. 30). In the former case, the structure is composed of fine bainite, martensite and ferrite, and in the latter—of acicular bainite and pearlite ("troostite").

Finally, a condition is reached, when the entire transformation is suppressed to the low temperature range, and the resultant structure is fully bainitic or martensitic. This is represented for the low carbon steels by Fig. 16 (Fig. 3, thermal curve type, No. 38), for the "medium" carbon steels, by Fig. 17 (Fig. 5, thermal curve

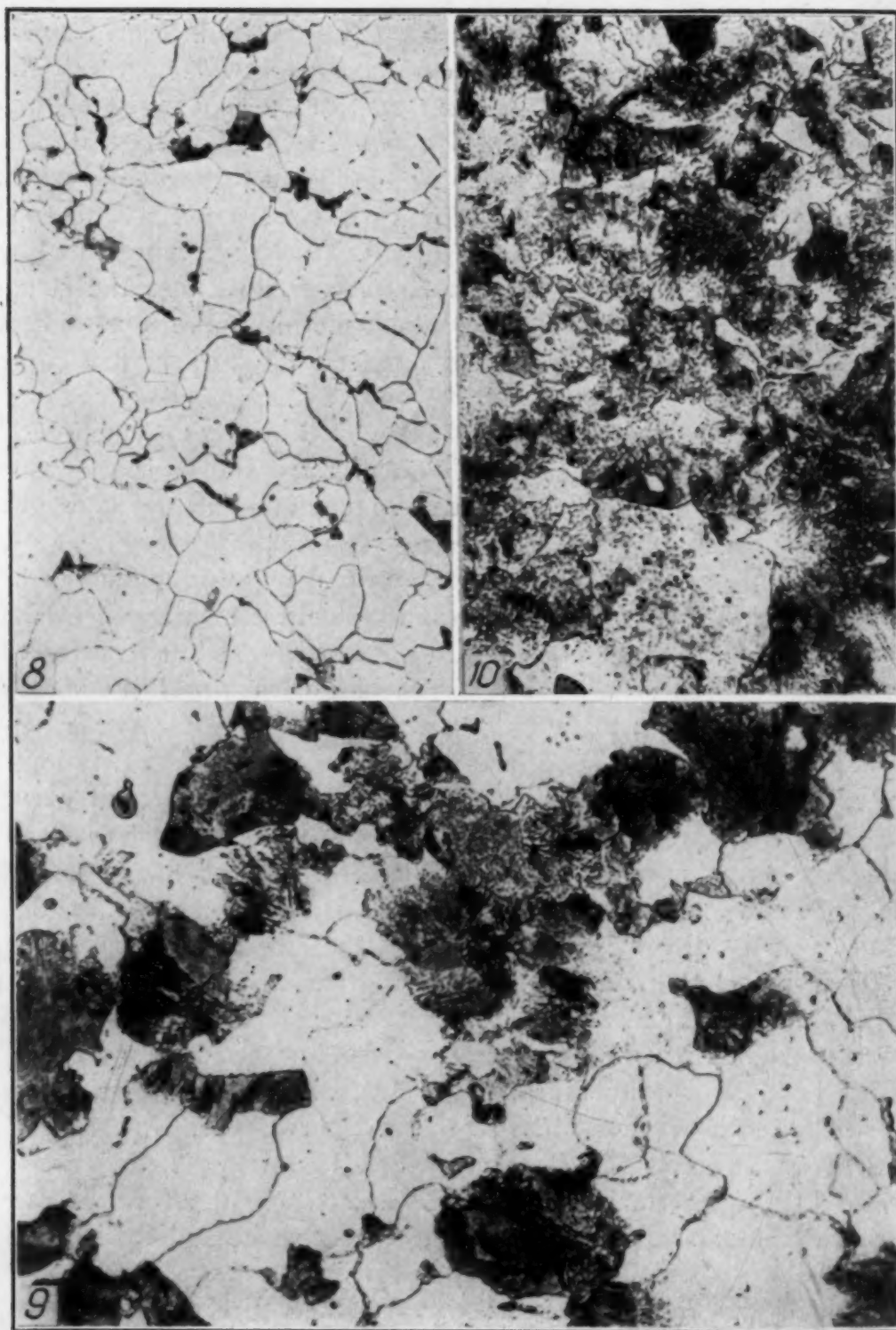


Fig. 8—(Serial No. 1) 0.07 Per Cent Carbon, 0 Per Cent Molybdenum, 2.33 Per Cent Chromium, VPN 124, $\times 150$. Fig. 9—(Serial No. 2) 0.14 Per Cent Carbon, 0 Per Cent Molybdenum, 2.28 Per Cent Chromium, VPN 155, $\times 500$. Fig. 10—(Serial No. 3) 0.30 Per Cent Carbon, 0 Per Cent Molybdenum, 2.29 Per Cent Chromium, VPN 226, $\times 500$. All Specimens Cooled from 1000 Degrees Cent. at 3.2 Degrees Cent. Per Minute. Etched in Picral-HCl Solution. No Suppressed Transformations.

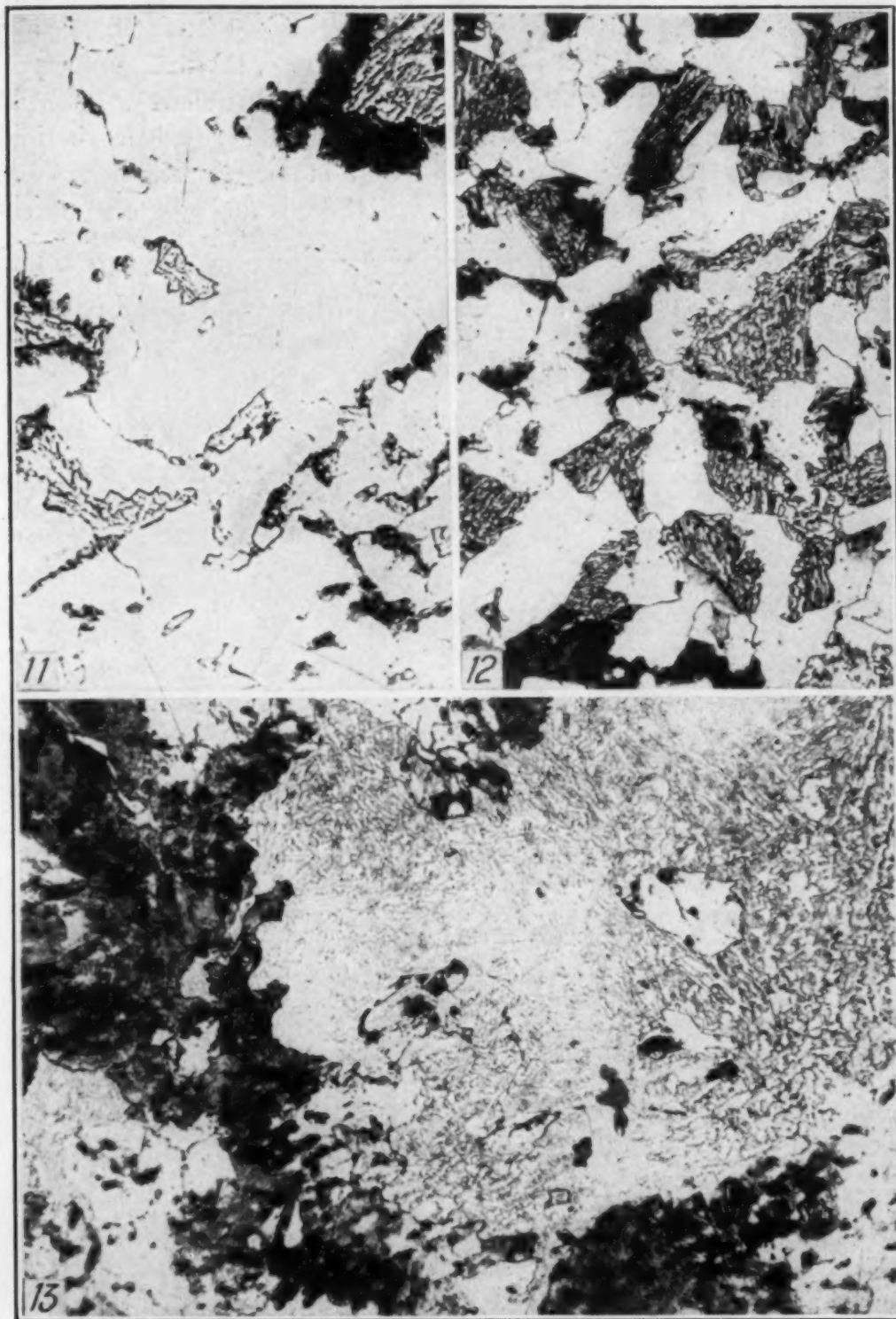


Fig. 11—(Serial No. 8) 0.08 Per Cent Carbon, 0.58 Per Cent Molybdenum, 2.63 Per Cent Chromium, VPN 139, $\times 500$. Fig. 12—(Serial No. 2) 0.14 Per Cent Carbon, 0 Per Cent Molybdenum, 2.28 Per Cent Chromium, VPN 217, $\times 500$. Fig. 13 (Serial No. 13) 0.34 Per Cent Carbon, 0.30 Per Cent Molybdenum, 2.60 Per Cent Chromium, VPN 313, $\times 500$. Figs. 11 and 13 Cooled from 1000 Degrees Cent. at 3.2 Degrees Cent. Per Minute. Fig. 12 Cooled from 1000 Degrees Cent. at 50 Degrees Cent. Per Minute. All Specimens Etched in Picral-HCl Solution. Slight Suppressed Transformations.

type, No. 28, as well as most of the other curves of this chart) and for the "high" carbon steels—by Fig. 18 (Fig. 7, thermal curve type, No. 17, as well as most of the other curves of this chart).

It is believed that structures of Figs. 16, 17, and 18, besides being composed of lower bainite, also contain some martensite. With cooling rates used in this work, however, there is no definite demarca-

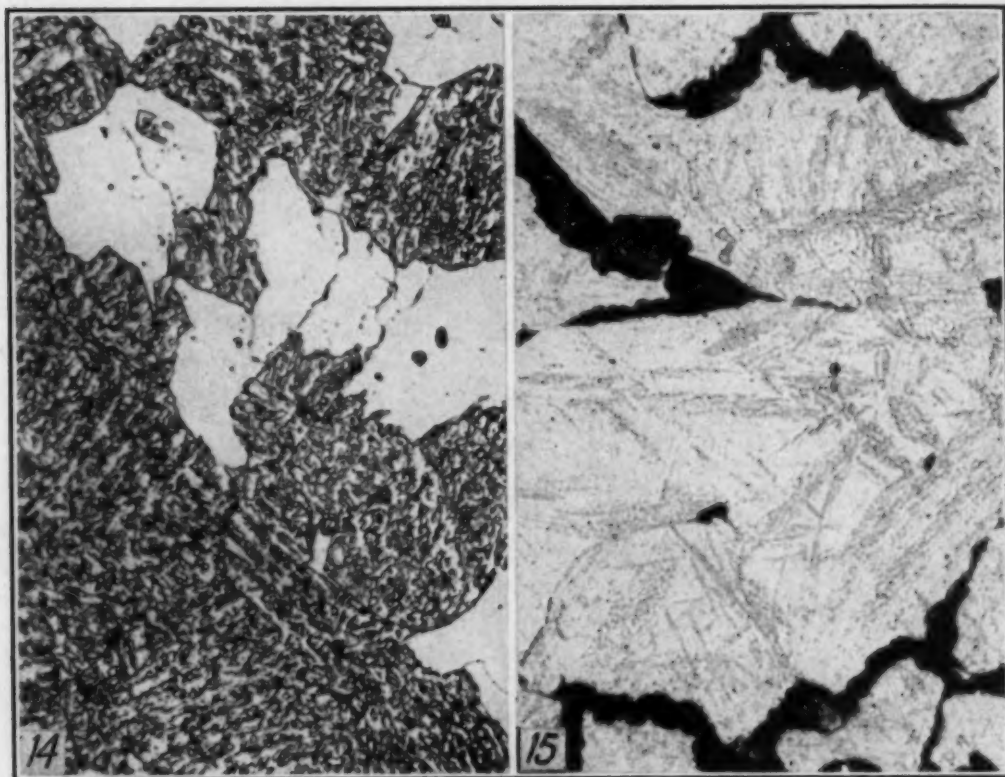


Fig. 14—(Serial No. 10) 0.14 Per Cent Carbon, 0.60 Per Cent Molybdenum, 2.75 Per Cent Chromium, VPN 350, $\times 500$. Fig. 15—(Serial No. 30) 0.32 Per Cent Carbon, 0.51 Per Cent Molybdenum, 5.44 Per Cent Chromium, VPN 464, $\times 500$. Both Specimens Cooled from 1000 Degrees Cent. at 3.2 Per Cent Per Minute. Etched in Picral-HCl Solution. Most of the Transformation Suppressed.

tion between lower bainite and martensite as observed under the microscope as well as manifested by the degree of suppressed transformation. The main visual difference between the two is that lower bainite etches darker and faster than martensite and also has a more "feathery" appearance. Moreover, dilatometer curves show that the austenite-bainite transformation occurs at higher temperatures than austenite-martensite.

As previously stated, the thermal sluggishness of these types of steel increases in proportion to the chromium content and/or molybdenum up to a certain maximum. Above this point, increasing

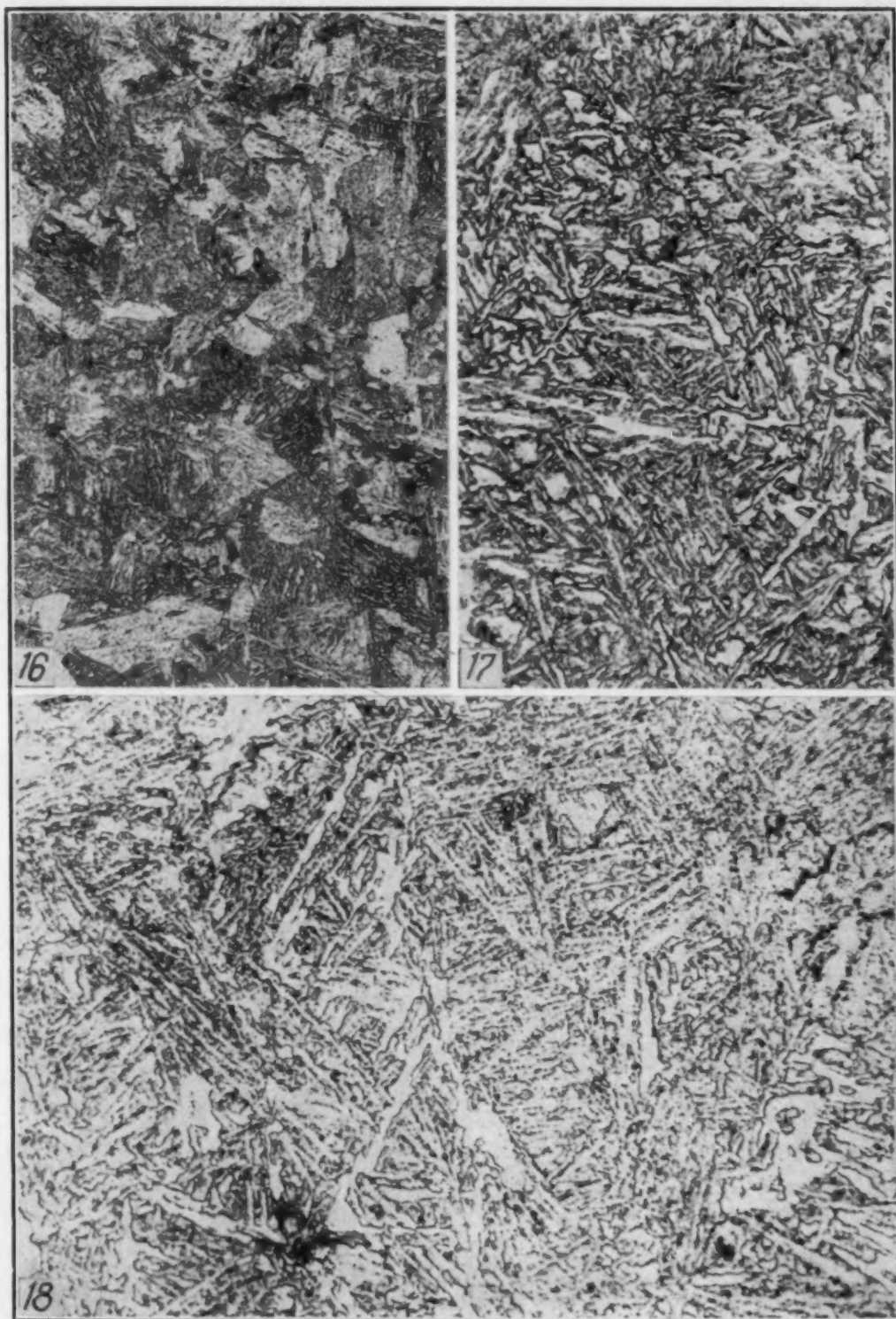


Fig. 16—(Serial No. 38) 0.07 Per Cent Carbon, 0 Per Cent Molybdenum, 6.15 Per Cent Chromium, VPN 340, $\times 150$. Fig. 17—(Serial No. 28) 0.15 Per Cent Carbon, 0.52 Per Cent Molybdenum, 5.31 Per Cent Chromium, VPN 360, $\times 500$. Fig. 18—(Serial No. 17) 0.35 Per Cent Carbon, 1.56 Per Cent Molybdenum, 3.06 Per Cent Chromium, VPN 514, $\times 500$. All Specimens Cooled from 1000 Degrees Cent. at 50 Degrees Cent. Per Minute. Etched in Picral-HCl Solution. Transformation Completely Suppressed.

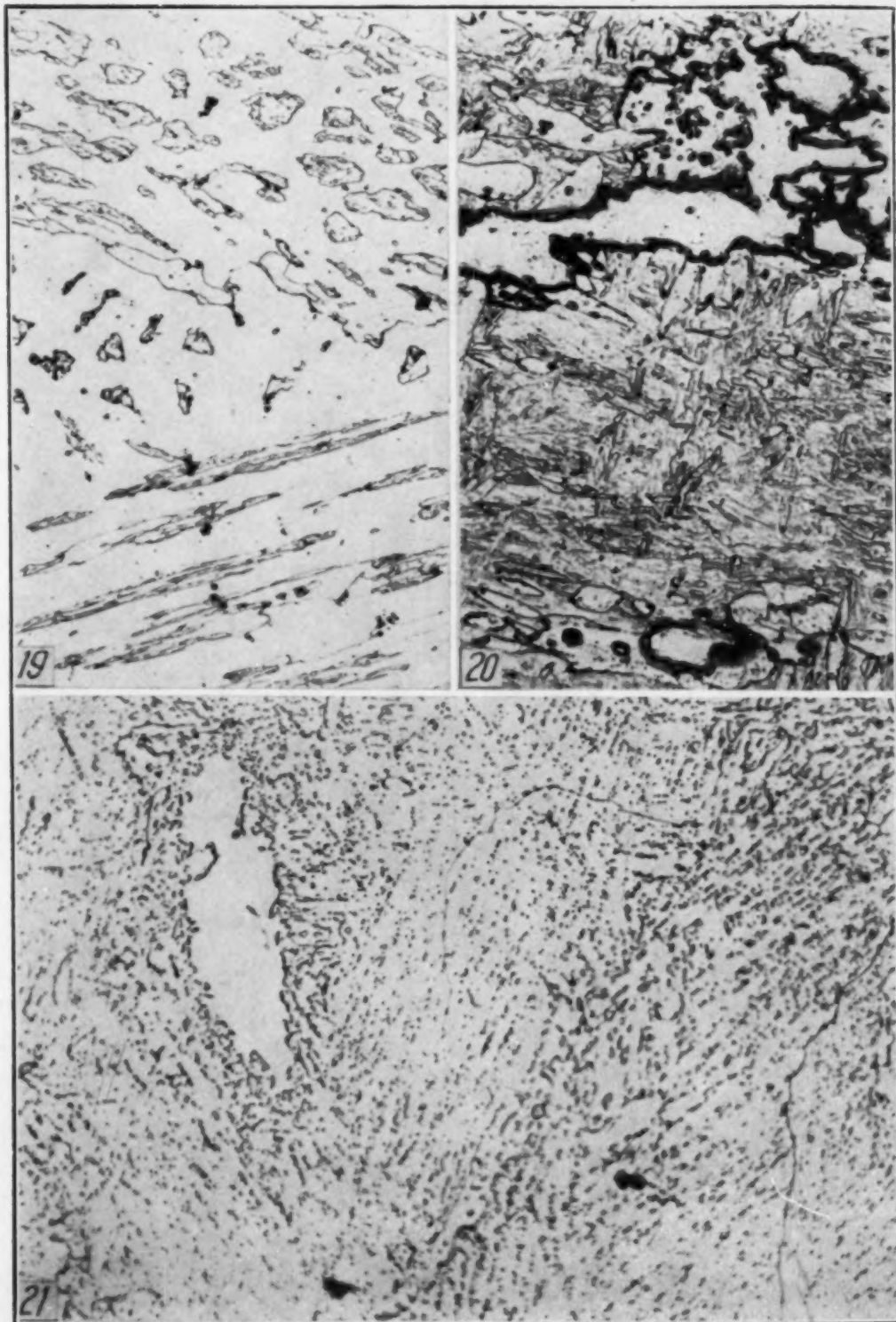


Fig. 19—(Serial No. 65) 0.03 Per Cent Carbon, 1.08 Per Cent Molybdenum, 8.9 Per Cent Chromium, VPN 152, $\times 100$. Fig. 20—(Serial No. 66) 0.13 Per Cent Carbon, 1.14 Per Cent Molybdenum, 9.2 Per Cent Chromium, VPN 222, $\times 500$. Fig. 21—(Serial No. 52) 0.2 Per Cent Carbon, 1.7 Per Cent Molybdenum, 8.33 Per Cent Chromium, VPN 170, $\times 500$. All Specimens Cooled from 1000 Degrees Cent. at 3.2 Degrees Cent. Per Minute. Etched in Picral-HCl Solution. Residual Alpha Ferrite Phase in Austenite at the Heat Treating Temperature.

amounts of these two elements tend to close the gamma loop in the constitutional space diagram. When their combined amount increases beyond this point, such a steel does not become fully austenitic at any temperature, and always contains some residual alpha phase, the amount of which becomes greater with further increase of chromium and/or molybdenum. Moreover, the alpha phase present during cooling from the heat treating temperature begins to act as nuclei for the transformation of austenite, thus causing the metal

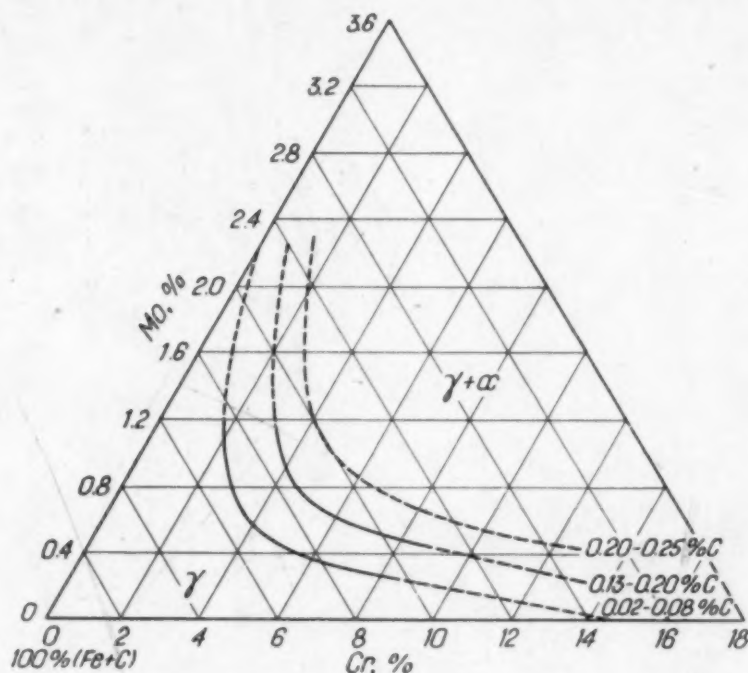


Fig. 22—The Boundary Between Gamma and Gamma Plus Alpha Regions in Iron-Chromium-Molybdenum Diagram at 1000 Degrees Cent. (1830 Degrees Fahr.) for Three Carbon Contents.

to become less thermally sluggish, as can be seen in Fig. 3, thermal curve type, Nos. 44, 47, 58 and 61 for low carbon steels, in Fig. 4, thermal curve type, Nos. 36, 66 and 70 for "medium" carbon steels, and in Fig. 6, thermal curve type, Nos. 50 and 54 for "high" carbon steels. Fig. 19 illustrates the appearance of residual ferrite in low carbon steels, resulting in coarse grain structure and dendritic pattern. Figs. 20 and 21 show the residual alpha ferrite in 0.13 per cent and 0.20 per cent carbon steels respectively. In steels containing over 0.20 per cent carbon, no residual alpha ferrite could be observed, regardless of the contents of chromium and molybdenum used in this work.

Fig. 22 is a graphic representation of dilatometric and metal-

lographic observations, showing the approximate boundary between the gamma and gamma plus alpha regions in the iron-chromium-molybdenum diagram at 1000 degrees Cent. (1830 degrees Fahr.) for each of three different ranges of carbon content. These definite relationships existing between structural characteristics, accompany-

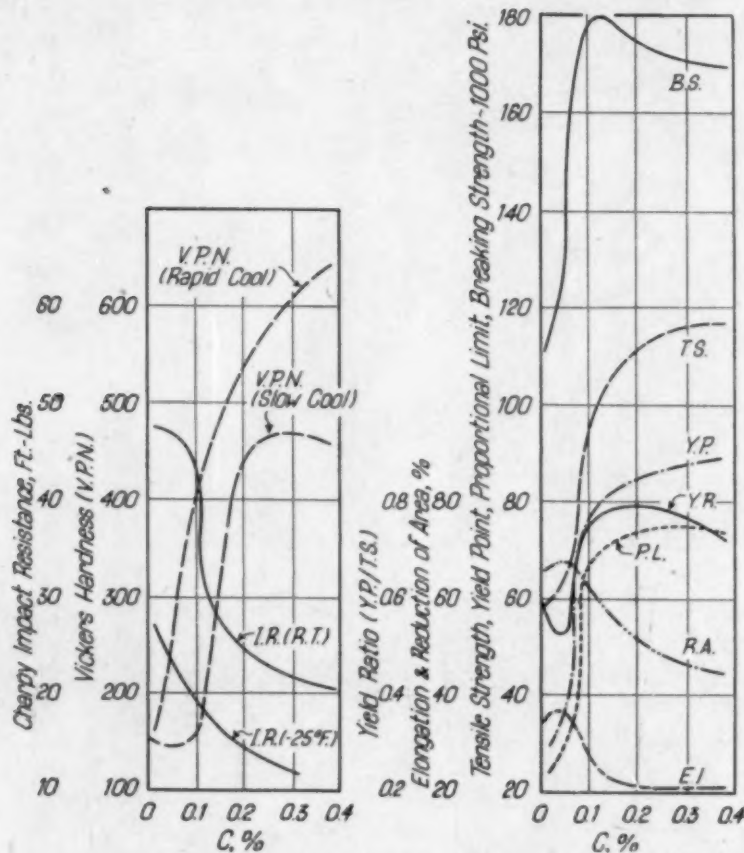


Fig. 23—Effect of Carbon on Physical Properties of Steels Containing 5 Per Cent Chromium and 0.5 Per Cent Molybdenum.

ing hardness values and the shapes of corresponding thermal curves of these alloys, cooled from above their critical temperatures, have been observed in a wide variety of steels (87 and 88).

PHYSICAL PROPERTIES

Variations in physical properties of steels listed in Table I may be considered from three different viewpoints:

1. Effect of carbon (constant chromium and molybdenum).
 2. Effect of molybdenum (constant carbon and chromium).
 3. Effect of chromium (constant carbon and molybdenum).
- A. *Effect of Carbon*—The first step in analyzing physical

properties was to plot them as functions of carbon content. This resulted in twenty individual graphs in each of which chromium and molybdenum were constant. Only one (for steels containing 5 per cent chromium and 0.5 per cent molybdenum) is reproduced here as an example (Fig. 23). Increase in the carbon content raises the

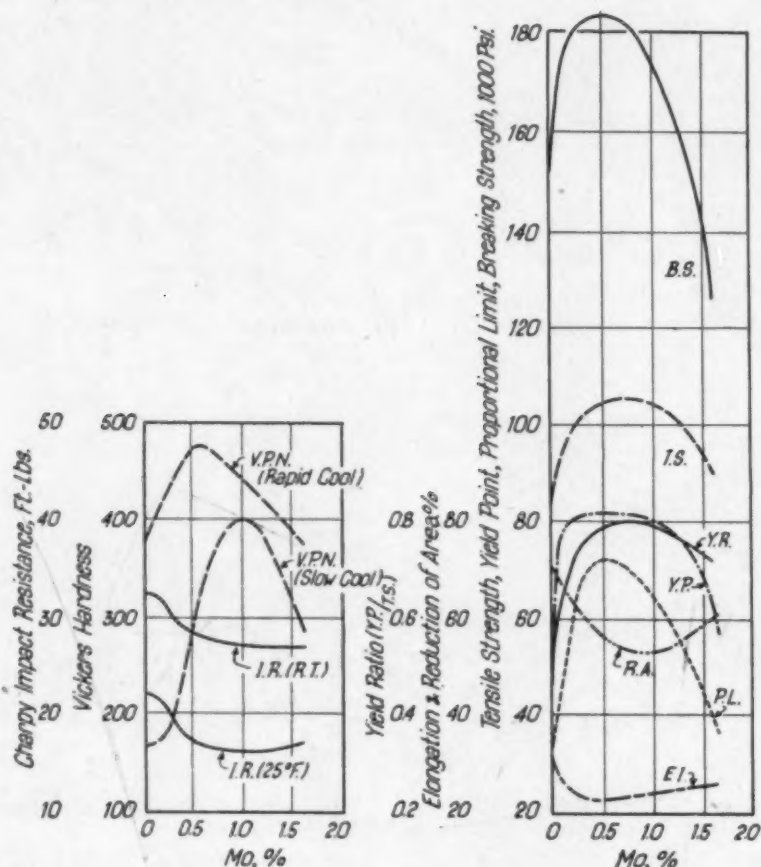


Fig. 24—Effect of Molybdenum on Physical Properties of Steels Containing 5 Per Cent Chromium and 0.15 Per Cent Carbon.

strength and hardness considerably but decreases the ductility and impact resistance.

It may be noted that the effect of carbon is gradual up to about 0.08 per cent, becomes very strong at about 0.12 per cent carbon, and gradually decreases with still higher percentages. Effect of carbon on all other combinations of chromium and molybdenum (not presented here for the sake of conserving space) is of the same nature, although the absolute values of properties are different.

B. Effect of Molybdenum—Since carbon is the most effective element, small variations in its content (particularly in low carbon

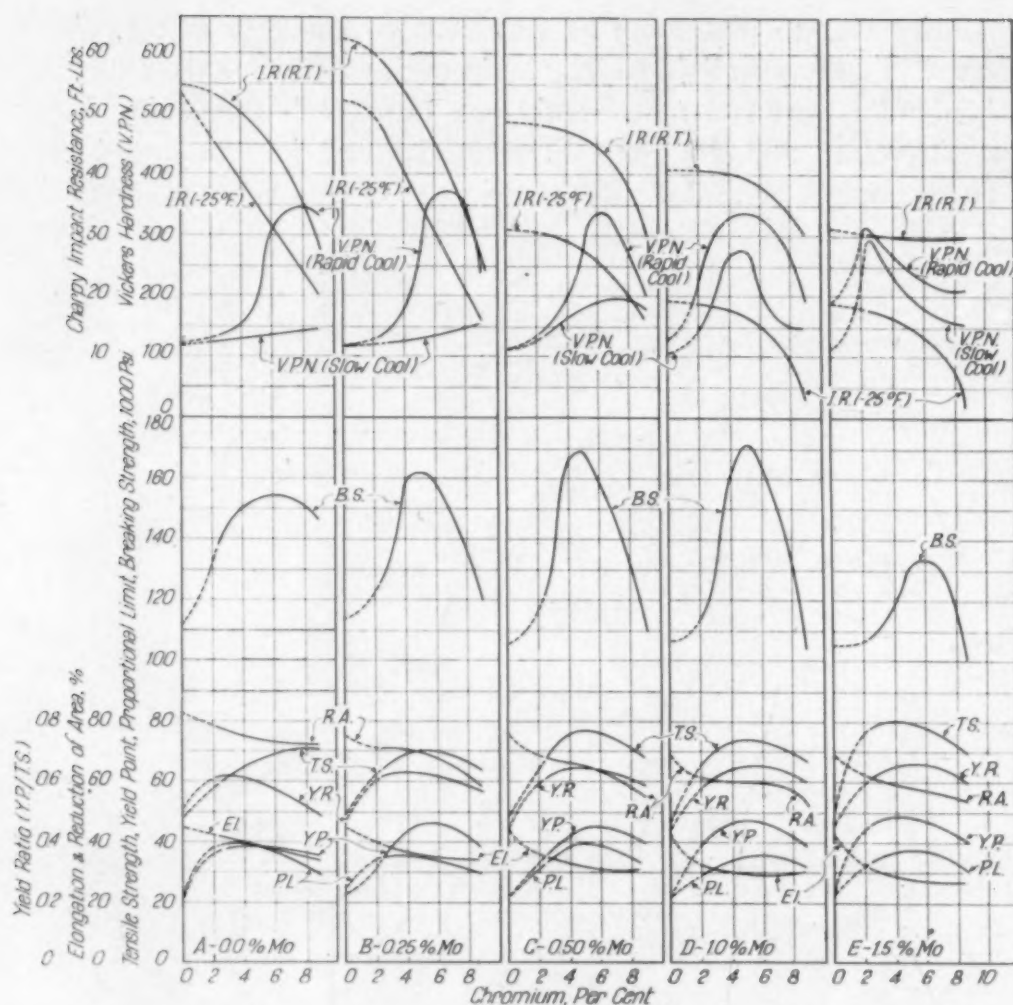


Fig. 25—Effect of Chromium on Physical Properties of Steels Containing 0.05 to 0.07 Per Cent Carbon and Various Amounts of Molybdenum.

steels) have a marked effect on all properties and eclipse the effects of molybdenum and chromium. To correct for these variations, values for carbon of 0.05 to 0.07, 0.15 and 0.24 per cent were taken from the above set of curves and plotted as functions of molybdenum (for constant chromium and carbon), thus resulting in twelve new graphs. Only one (for steels containing 5 per cent chromium and 0.15 per cent carbon) has been reproduced here in Fig. 24. In general, an increase in molybdenum content up to about 1 per cent, in steels containing 2.5 and 5 per cent chromium and various amounts of carbon, raises the strength and hardness, whereas the ductility is somewhat reduced. The addition of further molybdenum up to 1.5 per cent has little additional effect. In 5 per cent chromium steels with molybdenum exceeding 1 per cent, the strength and hardness

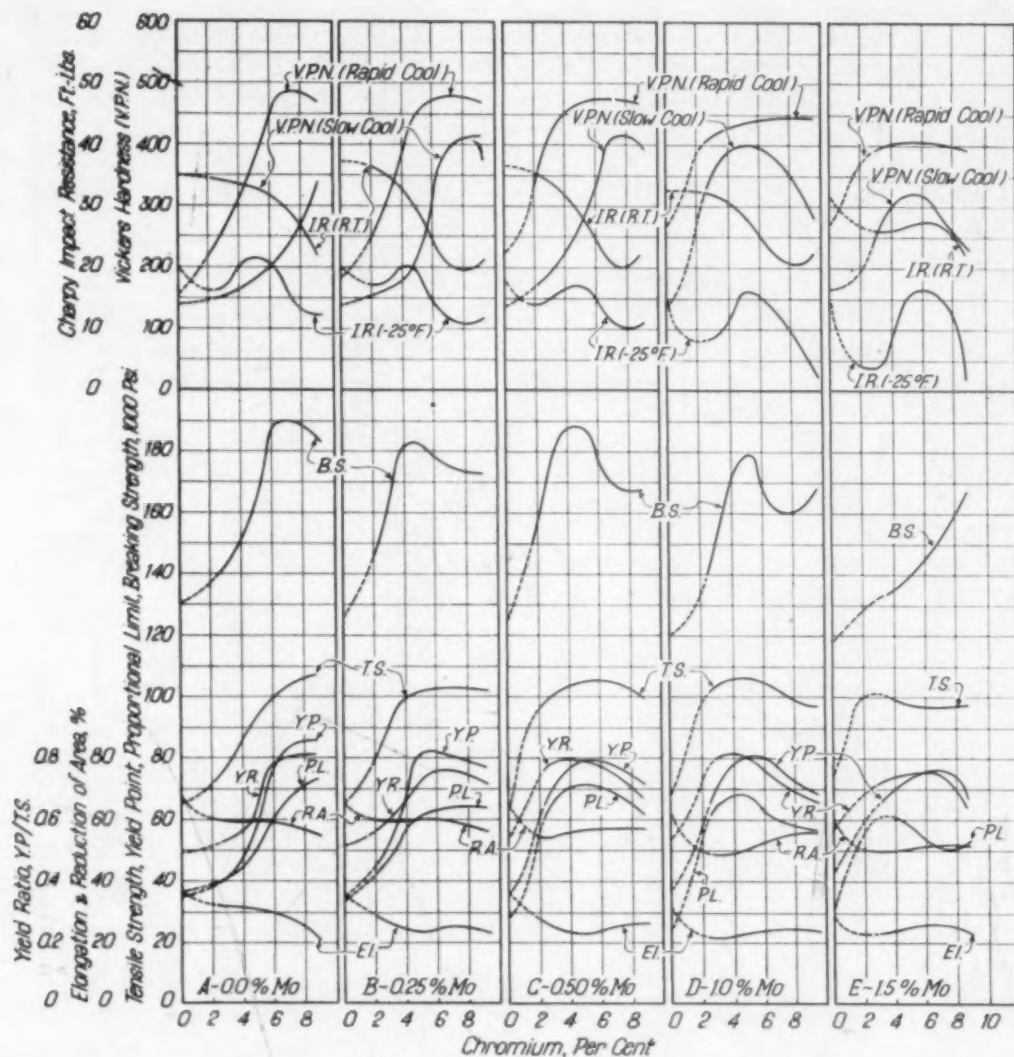


Fig. 26—Effect of Chromium on Physical Properties of Steels Containing 0.15 Per Cent Carbon and Various Amounts of Molybdenum.

even have a tendency to decrease, as shown in Fig. 24. In steels containing 7 and 9 per cent chromium, the effect of molybdenum is quite small, over the entire range.

C. Effect of Chromium—Finally from the set of charts just discussed, values for 0, 0.25, 0.5, 1 and 1.5 per cent molybdenum were taken and plotted as functions of chromium content for 0.05 to 0.07 per cent carbon (Fig. 25), 0.15 per cent carbon (Fig. 26) and 0.24 per cent carbon (Fig. 27), thus resulting in fifteen individual graphs. All of these curves were extrapolated to 0 per cent chromium, using some of our earlier data (87). Generally speaking, chromium up to 6 to 7 per cent increases the strength, yield point, proportional limit and hardness. With further increase in chro-

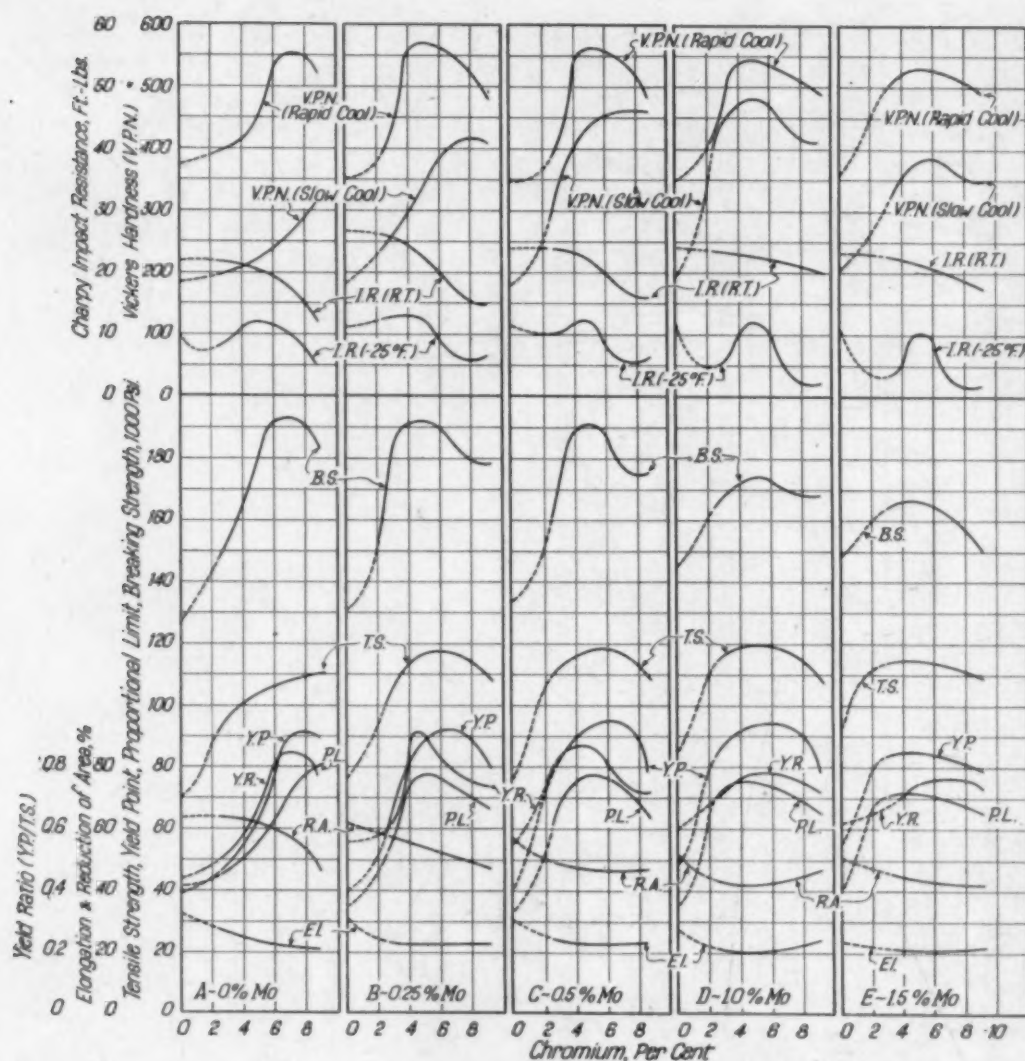


Fig. 27—Effect of Chromium on Physical Properties of Steels, Containing 0.24 Per Cent Carbon and Various Amounts of Molybdenum.

mium, these properties have a tendency to decrease, in all probability because of the appearance of the previously discussed residual alpha ferrite. This effect is most pronounced on the breaking strength. Elongation, reduction of area and impact resistance decrease more or less gradually. The decrease in impact resistance is particularly noticeable in the low carbon, low molybdenum groups (Fig. 25, A and B). The low temperature impact resistance of all higher carbon steels (Figs. 26 and 27) reach a peak at about 6 to 7 per cent chromium. Even though this phenomenon occurs in many cases, its full significance is not quite clear.

WELDING EXPERIMENTS

All experimental castings, "tees", were heat treated by normaliz-

ing from 1750 degrees Fahr. (840 degrees Cent.), air quenching from 1550 degrees Fahr. (840 degrees Cent.) and drawing at 1250 degrees Fahr. (680 degrees Cent.). Then they were cut longitudinally, deep etched and examined. They were found to be quite sound and reasonably free of various defects frequently observed in steel castings. After that, a welding test piece was cut out from each half of the casting, as shown in Fig. 1. The original contact surfaces from the two halves of each casting were machined off, forming a "V" groove, and then were arc welded together in the original shape, using standard chromium-molybdenum electrodes of the following nominal composition:

C	Cr	Mo	Mn	Si	P	S
0.1 max.	4-6	0.4-0.65	0.75 max.	0.75 max.	0.03 max.	0.03 max.

Each resultant "trough" was cut transversely into two halves, and one set of halves was stress relieved at 1300 degrees Fahr. (700 degrees Cent.). From the middle part of each half (as welded, as well as stress relieved), a cross-sectional U-shaped test piece about $\frac{1}{2}$ inch thick was cut out and roughly polished. A hardness survey was made over each of these test pieces, using a Vickers pyramid hardness tester with 30-kilogram load and readings taken at about $\frac{1}{8}$ -inch intervals across the weld and affected zone.

Figs. 28 and 29 are photographs of a set of five deep etched representative welds, all parent metal containing 5 per cent chromium, 0.5 per cent molybdenum and progressively higher carbon contents (0.07 to 0.38 per cent carbon), before and after stress relieving treatment, respectively. It may be noted that after stress relieving (Fig. 29), the acid attack was uniform over the entire surface of each test piece. Before stress relieving, however (Fig. 28), the acid attack of the affected zone increases with increasing carbon. Moreover, there is an abrupt decrease in the corrosion resistance of the affected zone when carbon increases from 0.13 to 0.27 per cent (compare Nos. 27 and 29, Fig. 28). No. 31 containing 0.38 per cent carbon (Fig. 28) has deep grooves etched out in its affected zone which in part is probably due to stresses set up in the affected zone, and in part to the presence of a rapid-etching bainite structure.

Fig. 30 is a graphic representation of hardness distribution across the welds and the affected zones in the same set of specimens, (A) before, and (B) after stress relieving. Before stress relieving (Fig. 30-A), steels with carbon content up to about 0.1 per cent

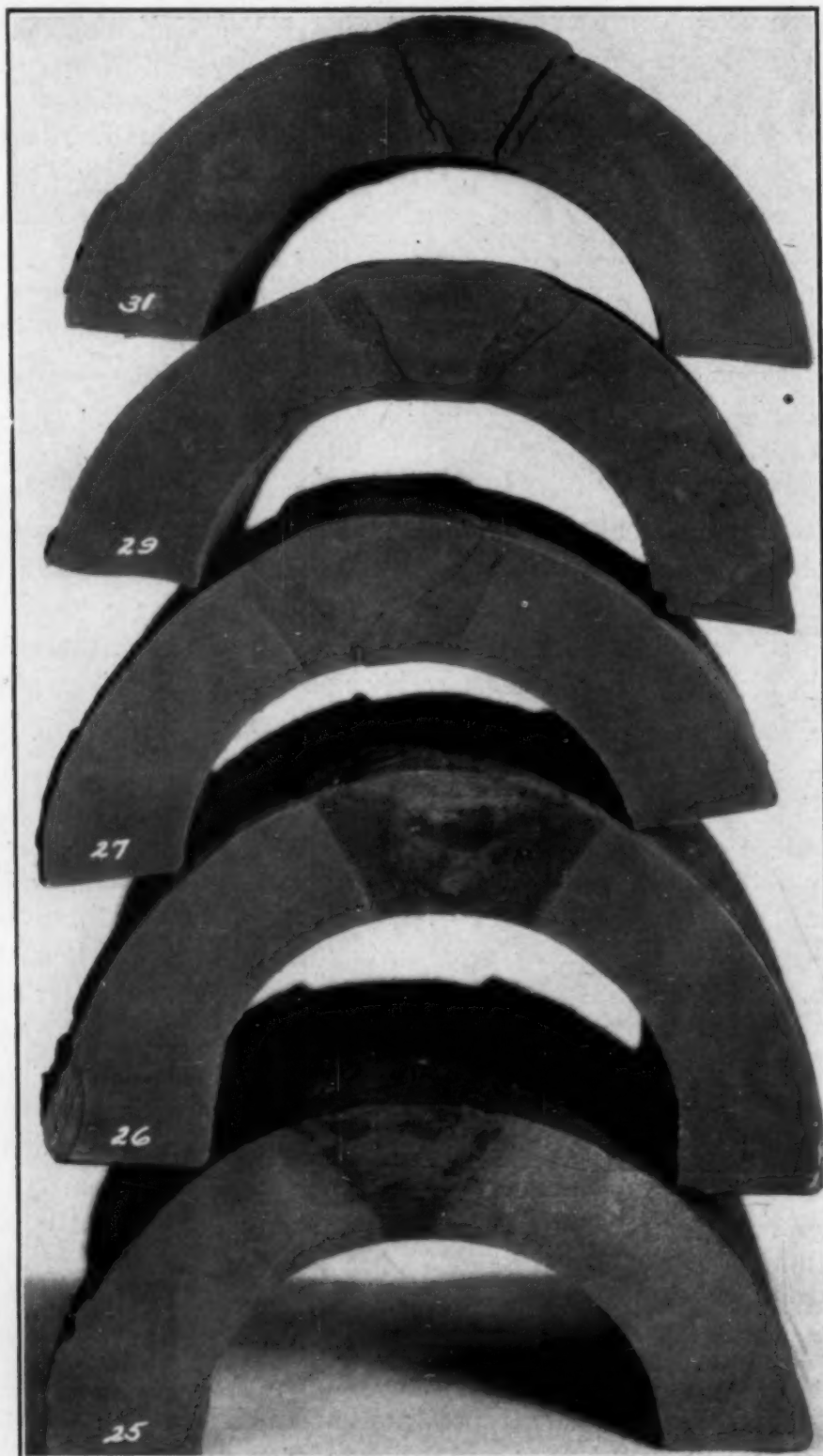


Fig. 28—Deep Etched Cross Sections of Welds in 4 to 6 Per Cent Chromium, 0.5 Per Cent Molybdenum Steels Before Stress Relieving Heat Treatment. Serial No. 31—0.38 Per Cent Carbon. Serial No. 29—0.27 Per Cent Carbon. Serial No. 27—0.13 Per Cent Carbon. Serial No. 26—0.09 Per Cent Carbon. Serial No. 25—0.07 Per Cent Carbon.

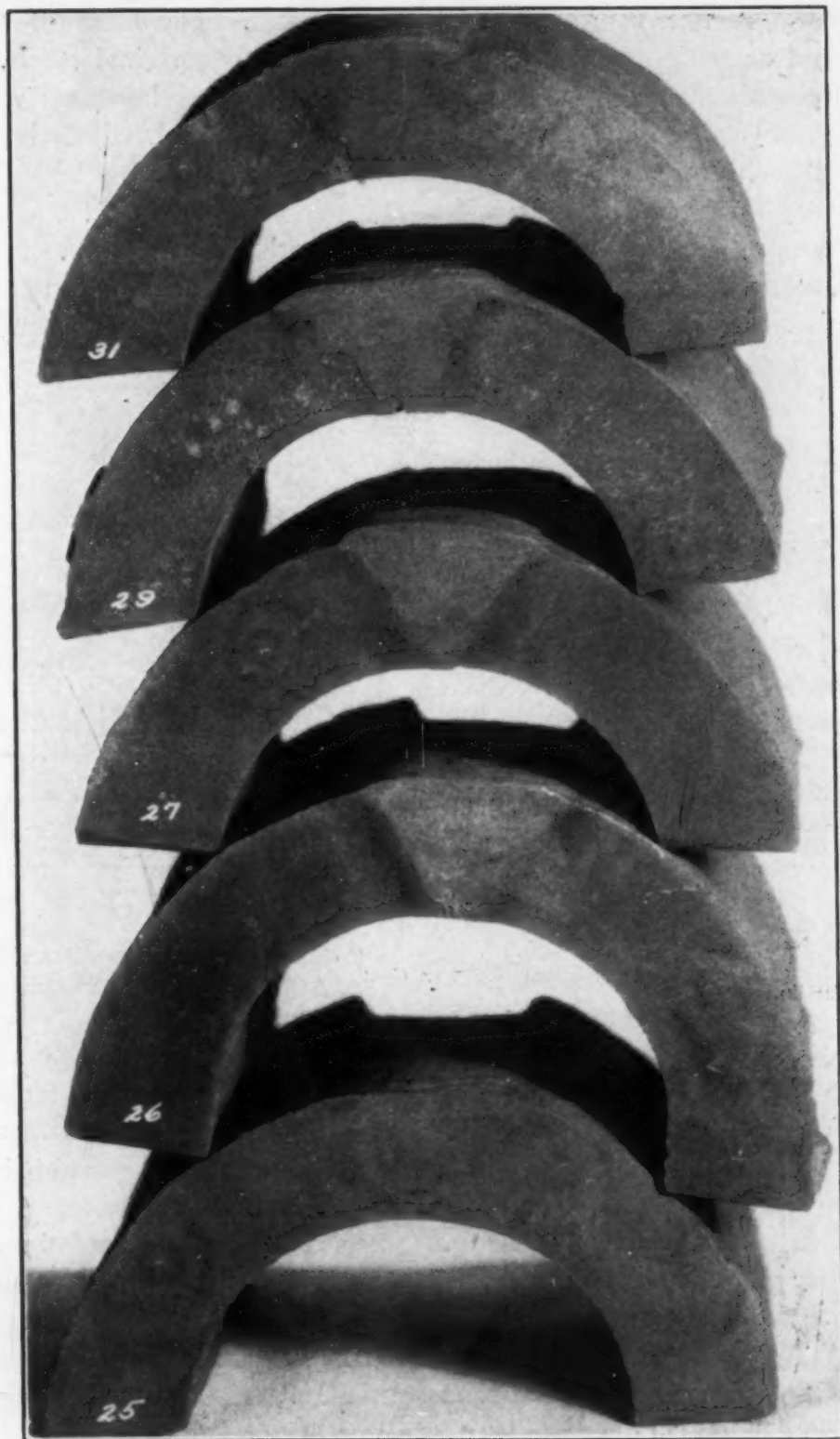


Fig. 29—Deep Etched Cross Sections of Welds in 4 to 6 Per Cent Chromium, 0.5 Per Cent Molybdenum Steels After Stress Relieving Heat Treatment. Serial No. 31—0.38 Per Cent Carbon. Serial No. 29—0.27 Per Cent Carbon. Serial No. 27—0.13 Per Cent Carbon. Serial No. 26—0.09 Per Cent Carbon. Serial No. 25—0.07 Per Cent Carbon.

(No. 25 and 26) are softer than the weld. Hardness of their affected zones is of about the same order as the original steels. A steel containing 0.13 per cent carbon (No. 27) has hardness values in the affected zone about equal to that of the weld, which is considerably higher than the hardness of the steel itself. When the content of carbon increases above 0.2 per cent (Nos. 29 and 31), hardness of the affected zone increases to rather high values. Moreover, all of the hardness values represented by the distribution curves of this series become higher with the increasing carbon content.

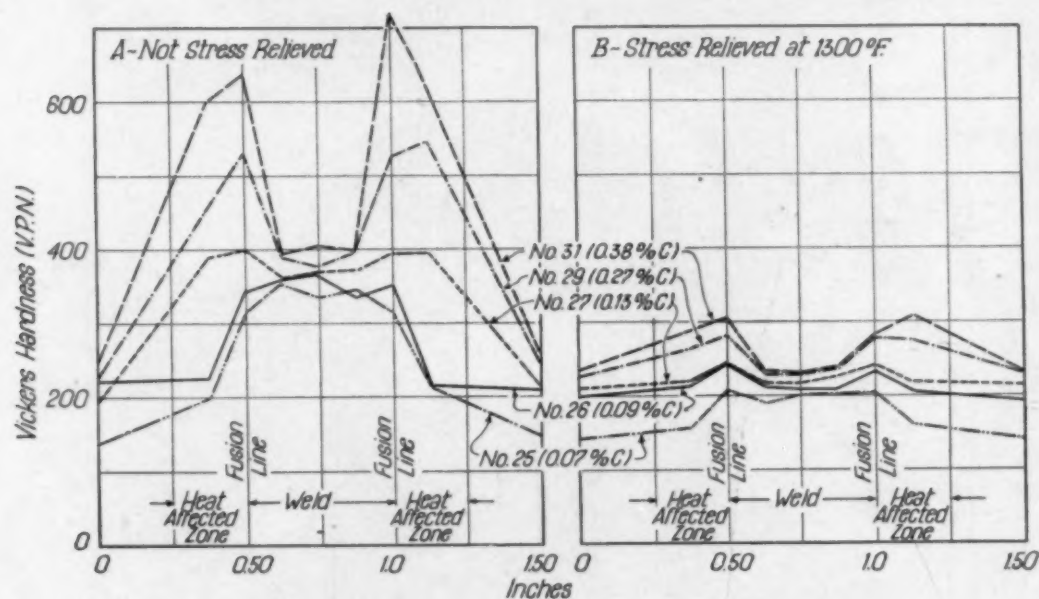


Fig. 30—Hardness Distribution Over the Weld and the Heat Affected Zones Containing 5 Per Cent Chromium, 0.5 Per Cent Molybdenum and Various Amounts of Carbon.

After stress relieving (Fig. 30-B), all of the hardness values represented by the distribution curves decrease quite considerably. Particularly striking is the decrease in hardness of the affected zones. Nonetheless, the absolute hardness values are still proportional to the carbon content.

Other chromium-molybdenum steels (Table I) tested in the same way gave very similar results, regardless of their chromium and molybdenum contents. In other words, hardness values represented by distribution curves are (for constant chromium and molybdenum) functions of carbon content. Variations in chromium and molybdenum influence them only to a lesser degree.

The conclusion which may be reached from these studies is that a stress relieving heat treatment after welding is not nearly so essen-

tial in steels of this type which contain under about 0.15 per cent carbon as in higher carbon compositions. Moreover, many steels can be found among the compositions containing 0.15 per cent carbon (Table I and Fig. 26) which will satisfy the previously referred to specifications.

SUMMARY

1. This paper presents a survey of thermal studies, micro-examination, physical property determinations, and welding experiments performed on a series of steels containing about 0.05 to 0.30 per cent carbon, 2.5 to 9 per cent chromium and 0 to 1.5 per cent molybdenum. A broad selection of steels with widely differing physical and thermal properties is given.

2. The thermal sluggishness and hardenability increase in proportion to the percentage of carbon, chromium and/or molybdenum.

3. These steels remain relatively soft after slow cooling (3.2 degrees Cent. per minute or 5.8 degrees Fahr. per minute) from the austenitic state regardless of the chromium and molybdenum contents, provided that carbon does not exceed about 0.07 per cent. This means that there were no suppressed transformations developed. Even fairly rapid cooling (50 degrees Cent. per minute or 90 degrees Fahr. per minute) did not cause any appreciable hardness increase in steels containing up to and including 2.5 per cent chromium with and without molybdenum and up to 5 per cent chromium in the absence of molybdenum. However, most of the 5 to 9 per cent chromium low carbon steels were somewhat hardened by rapid cooling, which is shown by the appearance of a split transformation in the thermal cooling curves.

4. The 2.5 to 9 per cent chromium steels in the 0.13 to 0.20 per cent carbon range and with less than 0.5 per cent molybdenum do not develop suppressed transformations and remain relatively soft after slow cooling from the austenitic state. Rapid cooling, however, makes them fairly hard. Increasing the molybdenum content to the range of 0.5 to 1.5 per cent results in slightly greater hardness on slow cooling and pronounced hardness and suppressed transformations on rapid cooling.

5. When the carbon content exceeds 0.2 per cent, these steels have marked suppressed transformations and become hard after rapid as well as after slow cooling from the austenitic state.

6. With a given carbon content, increasing percentages of chromium and/or molybdenum increase the thermal sluggishness and hardenability of these steels.

7. Both chromium and molybdenum form gamma loops in their equilibrium diagrams with iron. In view of that fact, their combined effect on a given steel, above certain amounts, is to make it at least partially ferritic at any temperature.

8. With increasing amounts of carbon, higher percentages of chromium and/or molybdenum make steel incompletely austenitic at the heat treating temperature.

9. When a steel is not fully austenitic at the heat treating temperature, it contains a certain amount of residual alpha ferrite, which increases with further increase in chromium and/or molybdenum contents.

10. On cooling from the heat treating temperature this residual ferrite acts as nuclei for the transformation of the austenite, thus making such a steel less thermally sluggish.

11. When the chromium and molybdenum contents are constant, increasing carbon very considerably increases the strength and hardness and reduces ductility and impact resistance. These changes are particularly pronounced, when carbon increases from about 0.07 to 0.15 per cent.

12. When the chromium and carbon contents are constant, the increase of molybdenum from 0 up to about 1 per cent increases the strength and hardness and reduces the ductility and impact resistance. Further increase in molybdenum, due to the appearance of the residual alpha ferrite, reduces the strength and hardness and may increase the ductility and impact resistance.

13. When carbon and molybdenum are constant, the increase in chromium from 0 to about 6 per cent considerably increases the strength and hardness and reduces the ductility and impact resistance. Further increase in chromium up to about 9 per cent reduces strength and hardness and somewhat increases ductility and impact resistance. The latter effect is particularly pronounced in higher molybdenum steels and is due to the presence of the residual alpha ferrite caused by the combined influence of chromium and molybdenum.

14. Some welding experiments illustrate the effect of thermal sluggishness and suppressed transformations on hardness distribution and internal strains in the weld metal and the effected zones.

ACKNOWLEDGMENTS

The authors wish to express their thanks to Crane Co. for permission to publish these results, to Messrs. H. W. Northrup and J. R. Goldsmith for preparation of the steels, heat treating and testing, to Mr. H. A. Peterson for making the dilatometric analyses, and to Mr. R. A. Mueller for performing the welding tests.

References

1. A. B. Kinzel and W. Crafts, "The Alloys of Iron and Chromium," Vol. 1, Low Chromium Alloys. Alloys of Iron Research, Monograph Series, 1937.
2. J. L. Gregg, "Alloys of Iron and Molybdenum," Alloys of Iron Research, Monograph Series, 1932.
3. P. Oberhoffer and H. Esser, "Kinetics of the Iron-Chromium Constitutional Diagram," *Stahl und Eisen*, No. 47, 1927, p. 2021.
4. P. Oberhoffer, "Iron-Chromium Diagram," *Stahl und Eisen*, No. 37, Sept. 15, 1927, p. 1518.
5. A. B. Kinzel, "Critical Points in Chromium-Iron Alloys," *Proceedings, Iron and Steel Division, American Institute of Mining and Metallurgical Engineers*, 1928, p. 301.
6. A. Westgren, G. Phragmen and T. R. Negresco, "The Structure of Iron-Chromium-Carbon System," *Journal, British Iron and Steel Institute*, Vol. 67, 1928, p. 383.
7. Anonymous, "The Alloys of Chromium and Iron," *The Metallurgist*, Feb. 24, 1928, p. 26.
8. J. B. Johnston, "Chromium-Molybdenum Steel in Airplane Construction," *Iron Age*, Vol. 121, No. 16, April 19, 1928, p. 1076.
9. P. Schoenmaker, "Structure of High-Percentage Chromium Steel," *Stahl und Eisen*, Vol. 48, No. 18, May 3, 1928, p. 591.
10. W. H. Hatfield, "Heat Resisting Steels—Mechanical Properties," *Iron and Coal Trades Review*, Vol. 116, No. 3142, May 18, 1928, p. 739.
11. T. Swinden and P. H. Johnson, "Properties of Chromium Steel Rails," *Heat Treating and Forging*, Vol. 14, No. 7, July, 1928, p. 764.
12. E. Maurer and H. Nienhaus, "The Internal Structure of Chromium Steel," *Stahl und Eisen*, Vol. 48, No. 30, July 26, 1928, p. 996.
13. F. T. Sisco and D. M. Wagner, "Effect of Heat Treatment on the Properties of Cr-Mo Sheet Steel," *TRANSACTIONS, American Society for Steel Treating*, Vol. 14, No. 2, Aug. 1928, p. 177.
14. J. Pomey and P. Voulet, "Study of Ternary Chrome Steels," *Rev. de Metallurgie*, Vol. 25, No. 12, Dec. 1928, p. 665.
15. P. Oberhoffer and C. Kreutzer, "Contributions to the Systems Fe-Si, Fe-Cr, Fe-P," *Archiv fuer das Eisenhuettenwesen*, Vol. 2, No. 7, Jan. 1929.
16. M. A. Grossmann, "Chromium as an Alloying Element in Steel," *TRANSACTIONS, American Society for Steel Treating*, Vol. 16, No. 1, July 1929, p. 165.
17. W. M. Mitchell, "Chromium Irons and Steels Exhibit Widely Varying Properties," *Chem. & Met. Eng.*, Vol. 36, No. 9, Sept. 1929, p. 552.
18. J. H. Kindelberger, "Chromium-Molybdenum Steel Tubing," *Journal, Society Automotive Engineers*, Vol. 25, No. 5, Nov. 1929, p. 474.
19. A. R. Page and J. H. Partridge, "The Properties of Some Steels Containing Chromium," *Journal, British Iron and Steel Institute*, Vol. 71, No. 1, 1930, p. 393.

20. V. N. Krivobok and M. A. Grossmann, "A Study of the Iron-Chromium-Carbon Constitutional Diagram," *TRANSACTIONS, American Society for Steel Treating*, Vol. 18, No. 1, July 1930, p. 1.
21. T. Murakami, K. Oka and S. Nishigori, "The Transformation and the Constitution of High Chromium Steels," *Technical Reports of the Tohoku Imp. University*, Nov. 1930, p. 405.
22. F. Wever and A. Heinzl, "Two Examples of Ternary Iron Systems with Closed Gamma Fields," *Mitt. K. W. Inst. Eisenf.*, Vol. 13, 1931, p. 193.
23. F. Wever and W. Jellinghaus, "The Binary System of Iron and Chromium," *Mitt. K. W. Institut Eisenforschung*, Vol. 13, No. 10, 1931, p. 143; *Stahl und Eisen*, Vol. 51, July 16, 1931, p. 918.
24. Anonymous, "The Chromium-Iron Equilibrium Diagram," *The Metallurgist*, Sept. 1931, p. 139.
25. A. Westgren, "High Chromium Steels, Carbides and Inclusions," *METAL PROGRESS*, Vol. 20, No. 5, Nov. 1931, p. 57.
26. F. Wever and W. Jellinghaus, "Influence of Chromium on the Transformations of Carbon Steels," *Mitt. K. W. Institut Eisenforschung*, Vol. 14, No. 8, 1932.
27. A. C. Pruliere, "Study of a C-Cr-Mo Steel at Ordinary Temperature and at High Temperatures," *Rev. de Met. Mem.*, Vol. 29, Jan. 1932, p. 34.
28. H. Franz, "Chromium-Molybdenum Steel in Construction of Automobiles," *Automobiltechnische Z.*, Vol. 35, Sept. 25, 1932, p. 440.
29. E. C. Wright and P. F. Mumma, "Properties of Low-Carbon Medium-Chromium Steels of the Air-Hardening Type," *Proceedings, Iron and Steel Division, American Institute of Mining and Metallurgical Engineers*, 1933, p. 77.
30. K. Bischoff, "Investigations of the Change of Some Properties of Fe-Cr-Ni and Fe-Cr-Mo Alloys by Heat Treatment," *Mitt. Forschungs-Institut, Vereinigte Stahlwerke*, Vol. 3, No. 9, 1933, p. 249.
31. T. Murakami and K. Hatsuta, "On the Structural Constituents of Chromium Steels," *Abs., Metals and Alloys*, Vol. 4, No. 5, May 1933, p. M.A. 140.
32. E. Valenta and F. Poboril, "Influence of Silicon on Critical Points and the Constitution of Chromium Alloys," *Chimie et Industrie*, Vol. 29, June 1933, p. 633.
33. J. H. Critchett, "Chromium in Steel Castings," *Transactions, American Foundrymen's Association*, Vol. 4, No. 3, Oct. 1933, p. 245.
34. L. C. Hicks, "An X-Ray Study of the Diffusion of Chromium into Iron," *Proceedings, Iron and Steel Institute, American Institute of Mining and Metallurgical Engineers*, Vol. 113, 1934, p. 163.
35. F. M. Becket and R. Franks, "Titanium and Columbium in Plain High Chromium Steels," *Proceedings, Iron and Steel Institute, American Institute of Mining and Metallurgical Engineers*, Vol. 113, 1934, p. 143.
36. E. R. Johnson and W. J. Buechling, "A Study of Banding in a Chromium-Molybdenum Steel," *TRANSACTIONS, American Society for Steel Treating*, Vol. 22, No. 3, March 1934, p. 249.
37. E. Scheil, K. Bischoff and E. Schulz, "Precipitation Hardening in Fe-Cr-Mo and Fe-Cr-W Alloys," *Arch. f.d. Eisenhuettenwesen*, Vol. 7, May 1934, p. 637.
38. S. M. Norwood, "Steels With Up to 7 Per Cent Chromium," *METAL PROGRESS*, Vol. 26, No. 3, Sept. 1934, p. 17.
39. R. H. Greaves, "Chromium Steels," London, 1935.
40. J. B. Austin and R. H. H. Pierce, "Linear Thermal Expansion and Transformation Phenomena of Some Low-Carbon Iron-Chromium Alloys," *Proceedings, Iron and Steel Division, American Institute of Mining and Metallurgical Engineers*, Vol. 116, 1935, p. 289.
41. V. N. Krivobok, "Alloys of Iron and Chromium," *TRANSACTIONS, American Society for Metals*, Vol. 23, March 1935, p. 1.

42. H. M. Wilten, "Correlation of Failures from Embrittlement of 4-6 Per Cent Chromium Steel with the Notched Bar Impact Test," *TRANSACTIONS, American Society for Metals*, Vol. 23, No. 4, Dec. 1935, p. 915.
43. A. M. Borzdiko and S. I. Wolfson, "Structure and Properties of 6 Per Cent Chromium Steel and of Molybdenum Steel Containing 6 Per Cent Chromium," *Kachestvennaia Stal*, Vol. 4, No. 4, 1936, p. 43.
44. H. D. Newell, "Properties of the 9 Per Cent Chromium Steel," *METAL PROGRESS*, Vol. 29, No. 2, Feb. 1936, p. 51.
45. A. G. H. Andersen and E. R. Jette, "X-Ray Investigation of the Fe-Cr-Si Phase Diagram," *TRANSACTIONS, American Society for Metals*, Vol. 24, No. 2, June 1936, p. 375.
46. W. Tofaute, A. Sponheur and H. Bennek, "Transformation Hardening and Tempering Phenomena in Steels with up to 1 Per Cent Carbon and up to 12 Per Cent Chromium," *Techn. Mitt. Krupp*, Vol. 4, Nov. 1936, p. 172.
47. T. Murakami and H. Kishimoto, "On the Change of Transformation Points of Chromium Steels Due to Cooling Conditions," *Science Reports of the Tohoku Imperial University*, Dec. 1936, p. 726.
48. H. D. Newell, "Effect of Silicon on Chromium-Molybdenum Steels for High-Temperature Service, with Note on the Effect of Copper," *Proceedings, Iron and Steel Institute, American Institute of Mining and Metallurgical Engineers*, Vol. 131, 1938, p. 419.
49. A. G. H. Andersen and E. R. Jette, "Notes on Microstructure and Hardness of Alloys Consisting Essentially of Iron, Chromium and Silicon," *Proceedings, Iron and Steel Institute, American Institute of Mining and Metallurgical Engineers*, Vol. 131, 1938, p. 318.
50. J. A. Jones and W. C. Hesselwood, "Effect of Chromium and Carbon on the Expansion of Chromium Steels," *Engineering*, May 20, 1938, p. 578; *Journal, British Iron and Steel Institute*, No. 1, 1938, p. 361.
51. A. Pomp and A. Krisch, "Comparative Study of Hardness Penetration of Heat-Treating Chromium-Molybdenum Steels," *Mitt. K. W. Inst. f. Eisenf.*, Vol. 20, 1938, p. 103.
52. R. F. Miller, R. F. Campbell, R. H. Aborn and E. C. Wright, "Influence of Heat Treatment on Creep of Carbon-Molybdenum and Chromium-Molybdenum-Silicon Steels," *TRANSACTIONS, American Society for Metals*, Vol. 26, No. 1, March, 1938, p. 81.
53. V. N. Krivobok, "Plain Chromium Irons—Their Toughness and Weldability," *METAL PROGRESS*, Vol. 34, No. 1, July 1938, p. 47.
54. Anonymous, "Properties of the Principal Cr-Fe Alloys," (Charts) *METAL PROGRESS*, Vol. 24, No. 6, June 1936, p. 56; Vol. 34, No. 4, Oct. 1938, p. 344.
55. W. Crafts and J. L. Lamont, "Hardenability of Low Chromium Steels," *TRANSACTIONS, American Society for Metals, Hardenability of Steels Symposium*, Oct. 1938, p. 197.
56. E. C. Bain and R. H. Aborn, "Constitution of Iron-Chromium Alloys," *ASM METALS HANDBOOK*, 1939, p. 374.
57. W. Crafts, "Chromium in Structural Steel," *Proceedings, Iron and Steel Institute, American Institute of Mining and Metallurgical Engineers*, Vol. 135, 1939, p. 473.
58. A. Rose and W. Fisher, "Influence of Rate of Cooling on Transformation and Properties of Chromium Steels," *Mitt. K. W. Institut f. Eisenforschung*, Vol. 21, 1939, p. 133.
59. Anonymous, "Chromium-Molybdenum Steels," *The Metallurgist*, Feb. 24, 1939, p. 13.
60. H. D. Newell, "Creep of Some Chromium-Molybdenum Steels," *Metals and Alloys*, Vol. 10, No. 11, Nov. 1939, p. 342.
61. W. G. Hildorf, C. L. Clark and A. E. White, "Characteristics of 5.0 and 7.0 Per Cent Chromium Steels with Varying Molybdenum and Vanadium Contents," *TRANSACTIONS, American Society for Metals*, Vol. 27, No. 4, Dec. 1939, p. 1090.

62. K. Roesch, "Chromium Steel Castings," *Die Giesserei*, Vol. 26, 1939, p. 357; *Metallurgist*, Dec. 1939, p. 77.
63. Anonymous, "Chromium-Molybdenum Steels," *The Metallurgist*, Dec. 29, 1939, p. 84.
64. E. K. Smith, "Chromium Steel Castings," *METAL PROGRESS*, Vol. 37, No. 1, Jan. 1940, p. 49.
65. Anonymous, "Creep of Some Chromium-Molybdenum Steels," *Metallurgia*, March 1940, p. 138.
66. H. D. Newell and Z. E. Olzak, "Effect of Phosphorus in 5 Per Cent Chromium, 0.5 Per Cent Molybdenum Steel," *Metals and Alloys*, Vol. 11, No. 4, April 1940, p. 106.
67. H. Hobart, "Tubes for Oil Heaters, Titanium or Columbium in 5 Per Cent Chromium-Molybdenum-Silicon Steel," *METAL PROGRESS*, Vol. 37, No. 4, April 1940, p. 401.
68. Anonymous, "Influence of Rate of Cooling on the Transformations in Chromium Steels," *The Metallurgist*, April 26, 1940, p. 105.
69. K. Roesch, "Cast Chromium Steel," *Iron and Steel*, May 1940, p. 273.
70. Anonymous, "How to Cut Chromium Steel Castings," *Canada's Foundry Journal*, Vol. 13, No. 6, June 1940, p. 5.
71. G. F. Comstock, "Titanium and Some Properties of Chromium-Molybdenum Steel for Airplane Tubing," *Metals and Alloys*, Vol. 12, No. 1, July 1940, p. 21.
72. Anonymous, "3 Per Cent Chromium-Molybdenum Alloy Steels," *Steel*, Vol. 107, No. 6, Aug. 5, 1940, p. 68.
73. Anonymous, "Influence of Titanium on Some Properties of Chromium-Molybdenum Steel," *Metallurgia*, Sept. 1940, p. 165.
74. F. B. Riggan, "Properties and Heat Treatment of 9 Per Cent Chromium, 1½ Per Cent Molybdenum Cast Steels," *Metals and Alloys*, Vol. 12, No. 5, Nov. 1940, p. 615.
75. E. S. Davenport, R. A. Grange and R. J. Hafsten, "Influence of Austenite Grain Size Upon Isothermal Transformation Behavior of S.A.E. 4140 Steel," *Proceedings*, Iron and Steel Institute, American Institute of Mining and Metallurgical Engineers, Vol. 145, 1941, p. 301.
76. H. Eckman, "Welding Chromium-Molybdenum Steel," *Steel*, Feb. 17, 1941, p. 84.
77. C. L. Clark and M. A. Bredig, "Influence of Silicon and Aluminum Additions on the Constitutional Diagram of 4-6 Per Cent Chromium-Molybdenum Steels," *TRANSACTIONS*, American Society for Metals, Vol. 29, No. 1, March 1941, p. 117.
78. Anonymous, "Chromium-Molybdenum Cast Steels," *Foundry Trade Journal*, April 17, 1941, p. 259.
79. R. W. Emerson, "The Weldability of 4-6 Per Cent Chromium, ½ Per Cent Molybdenum Steel and Its Application to Piping Industry," *Welding Journal*, Vol. 20, May 1941, p. 239.
80. H. Scott and T. H. Gray, "Dimensional Changes on Hardening High Chromium Tool Steels," *TRANSACTIONS*, American Society for Metals, Vol. 29, No. 2, June 1941, p. 503.
81. W. Crafts and C. M. Offenbauer, "Carbides in Low-Chromium Steel," *Proceedings*, Iron and Steel Division, American Institute of Mining and Metallurgical Engineers, Vol. 150, 1942, p. 275.
82. R. F. Miller and R. F. Campbell, "Influence of Chromium and Molybdenum on Structure, Hardness and Decarburization of 0.35 Per Cent Carbon Steel," *Proceedings*, Iron and Steel Division, American Institute of Mining and Metallurgical Engineers, Vol. 150, 1942, p. 421.
83. J. G. Ball, "Crack Sensitivity in Welded Chromium-Molybdenum Steels of Thin Sections," *Iron and Steel*, April 1942, p. 233.
84. E. C. Rollason and A. H. Cattrell, "Prevention of Cracks in Welded Light Alloy Steel," *METAL PROGRESS*, Vol. 42, 1942, p. 213.

85. W. Crafts and C. M. Offenbauer, "Carbides in Low-Chromium-Molybdenum Steels," *Transactions, American Institute of Mining and Metallurgical Engineers*, Vol. 154, Iron and Steel Division, 1943, p. 361.
86. Anonymous, "Properties of Important Wrought Chromium-Iron Alloys," (Tables) *METAL PROGRESS*, Vol. 43, No. 4, 1943, p. 560-A; Vol. 44, Nov. 4, 1943, p. 688.
87. N. A. Ziegler and W. L. Meinhart, "The Effect of Copper on Properties of Cast Carbon-Molybdenum Steels," *American Foundrymen's Association*, Preprint 44-28.
88. N. A. Ziegler, "Thermal Characteristics of Some Low Alloyed Steels," *Journal, Western Society of Engineers*, Vol. 45, No. 6, Dec. 1940, p. 277.

DISCUSSION

Written Discussion: By Otto Zmeskal, research metallurgist, Universal-Cyclops Steel Corp., Bridgeville, Pa.

Mr. Ziegler and Mr. Meinhart have concisely presented the results of an exhaustive study on chromium-molybdenum steels. The physical property data are probably applicable to the steels in the cast state only. The transformation data, however, are applicable to either the wrought or the cast states.

Nickel is also a very potent stabilizer of austenite and increases the thermal sluggishness of chromium steels. This is shown by the data plotted in Fig. A, which shows the thermal heating and cooling curves of hot-rolled and annealed 0.10 to 0.13 per cent carbon, 12.30 per cent chromium steel containing various amounts of nickel (0.14 to 1.77 per cent). Each dilatometer specimen ($\frac{1}{4}$ inch diameter by 2 inches long) was cooled at the rate of 400 degrees Fahr. per hour from 1650 degrees Fahr. (900 degrees Cent.).

Increasing the nickel content in chromium steels lowers the critical points both on heating and on cooling. As Gillmor⁶ has shown, the addition of aluminum decreases the thermal sluggishness of chromium steels and raises the critical points on both heating and cooling.

Thus, in evaluating chromium steels for welding applications all of the elements—carbon, molybdenum, nickel, and aluminum—should be considered in writing the analysis specifications.

H. S. BLUMBERG:⁷ I have no discussion, but I have two questions.

The first is, how were these steels made? Do they represent commercial casting material or were they small induction heats?

The second question is this: There are certain very desirable characteristics in the low carbon steels of these groups. What is the lowest carbon content in these steels, or the lowest carbon range, which it is considered practicable to melt in the foundry?

Authors' Reply

Dr. Zmeskal's discussion can be answered only tentatively because our paper deals with chromium-molybdenum steels only. However, it is known that

⁶R. N. Gillmor, "The Influence of Alloying Elements on the Critical Points of Steels as Measured by the Dilatometer," *TRANSACTIONS, American Society for Metals*, Vol. 30, 1942, p. 1377, see p. 1400.

⁷Metallurgist, M. W. Kellogg Co., Jersey City, N. J.

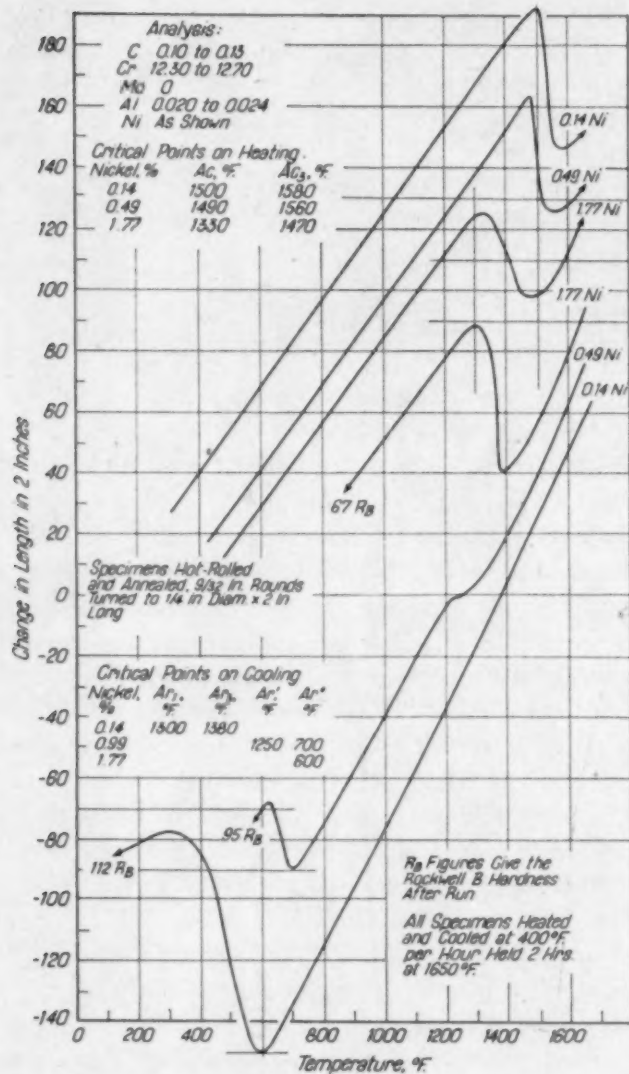


Fig. A—Dilatometer Curves of Chromium Steels Containing Various Amounts of Nickel. Note: The 67 R_b Curve Should be 0.14 Nickel and the 112 R_b Curve Should be 1.77 Nickel. The Curves are in the Reverse Order and are in Error.

nickel has a quite pronounced effect on these types of steels. It increases their thermal sluggishness and hardenability. In plain carbon steels, on the other hand, we find that nickel alone has relatively small effect.

According to Dr. Zmeskal's chart, the thermal sluggishness of 12 per cent chromium steels decreases with increase in nickel. This does not agree with some evidence which we have for steels containing less chromium and from 0.5 to 1.5 per cent molybdenum, but which is not included in this paper. According to our observations, increasing nickel up to about 1 per cent increases thermal sluggishness.

The problem reduces itself to choosing the right combination of chromium, molybdenum, nickel and carbon to produce the desired results. When carbon in a 4 to 6 per cent chromium, 0.5 per cent molybdenum steel is reduced to less

than 0.10 per cent, the resultant steel has low thermal sluggishness and is easily weldable, but its strength is low. By adding nickel, it is possible to improve its physical properties without unduly increasing its hardenability.

The steels were made in an induction furnace of 250 pounds capacity. Whether it is a commercial furnace or not is a matter of definition. We use it at present for research work, but for about a year and a half after the war broke out it was working on production 24 hours a day, when the company was caught short on steel capacity, so we personally would think it is a commercial furnace.

The most desirable carbon content for these steels is indicated in Fig. 30, which graphically portrays the hardness distribution across the welds and the affected zones. It shows that the steel containing 0.13 per cent carbon does not have any abnormal or excessive hardness in the affected zone. The carbon content of the steel in the next curve on that chart is 0.27 per cent. This steel shows a considerable increase in hardness. The desired carbon content thus appears to be somewhere between these two figures. Steels containing 0.15 to 0.20 per cent carbon will give all the desired physical properties, but will not develop any excessive hardness in the affected zone. The latter carbon range is entirely practical for foundry production.

As far as the corrosion resistance is concerned, its increase with increasing chromium is well known, which has been demonstrated by Mr. Franks in his present and previous papers on that subject. But as was pointed out in the discussion to Mr. Frank's paper, we believe that the heat treatment also has a marked influence on the corrosion resistance. From our observations, the best corrosion resistance is obtained in normalized and drawn or quenched and drawn steels.

In conclusion the authors wish to thank those who have contributed to this discussion and especially appreciate Dr. Zmeskal's data and dilatometer curves showing the effect of nickel on 12 per cent chromium steels.

THE EFFECT OF COLD ROLLING ON THE STRUCTURE OF HADFIELD MANGANESE STEEL

BY NORMAN P. GOSS

Abstract

X-ray surface diffraction diagrams of cold-rolled 14 per cent manganese strip steels given a reduction of 87 per cent remained austenitic. X-ray diffraction lines due to alpha iron could not be observed on the diffraction patterns. The X-ray technique was adjusted so that the intense (110) line of the alpha iron could be detected if present.

In view of the X-ray evidence, it is believed that the extreme hardness attainable by cold rolling is due to the smallness of the crystallites as suggested by Nikonoff.

The maximum hardness attainable by cold rolling is of the order of Rockwell C-58.

INTRODUCTION

THE extent to which Hadfield manganese steel can be work hardened by a drop hammer was investigated by D. Nikonoff.^{1, 2} The maximum hardness he was able to attain by his method was Rockwell C-49-52. He observed that the maximum hardness was not developed on the surface but about one millimeter below it. He also found that the maximum hardness was the same whether or not the specimen developed the characteristic slip lines. In the past much significance has been attached to the development of the slip lines, in relationship to the great hardness which could be developed in these steels by work hardening.

These and other experimental observations presented in these excellent papers by Nikonoff led him to conclude that the hardening of austenitic Hadfield manganese steels by cold work is not satisfactorily explained by the decomposition of the unstable austenite. He concluded that "The question remains, to how great a degree do

¹D. Nikonoff, "Quantitative Measurement of Strain Hardness in Austenitic Manganese Steel," *TRANSACTIONS, American Society for Metals*, Vol. 29, 1941, p. 519.

²D. Nikonoff, "Some Aspects of Strain Hardenability of Austenitic Manganese Steel," *TRANSACTIONS, American Society for Metals*, Vol. 31, 1943, p. 716.

A paper presented before the Twenty-sixth Annual Convention of the Society held in Cleveland, October 16 to 20, 1944. The author, Norman P. Goss, is research metallurgist, Cleveland, Ohio. Manuscript received June 20, 1944.

these products contribute to the strain hardening phenomenon? The fact that the strain hardness asserts itself at temperatures as high as 1020 degrees Fahr. (550 degrees Cent.) and that the strain hardened steel does not respond to tempering at 840 degrees Fahr. (450 degrees Cent.) certainly does not indicate that the martensitic reaction is the governing factor."

OBJECT OF THIS INVESTIGATION

The purpose of this investigation was to determine, by means of X-ray diffraction methods, the structure of the strain hardened Hadfield manganese steel resulting from cold rolling, and to compare it with the structure of this alloy in the strain-free state. (To attain the softest condition of this steel it is usually heated to 1800 degrees Fahr. (980 degrees Cent.) or higher and then water-quenched. The hardness after this treatment usually varies from Rockwell B-85 to 95 (Monotron 23-30). By comparing the X-ray diagrams of the drastically cold-rolled and the heat treated and quenched structure, one can determine whether cold working has decomposed the austenite, and the effect it may have upon the sharpness of the diffraction lines. A second purpose of this investigation was to determine the maximum hardness which can be obtained by cold rolling this alloy.

EXPERIMENTAL PROCEDURE

Small specimens of Hadfield manganese steel about 0.5 by 1 by 0.118 inch having the following chemical analysis were used:

C 1.30, Mn 14.00, P 0.010, Si 0.45, S 0.04 per cent

As this material work hardens rapidly and in order to roll the specimens beyond a reduction of 50 per cent in thickness, small specimens were required. These were cold-rolled on a small laboratory two-high mill having rolls 2 inches in diameter. The hardness after each pass was recorded on a Monotron hardness tester. The Rockwell hardness number was obtained by conversion. The reduction in thickness was plotted against the hardness number.

A number of the cold-reduced specimens were examined by the X-ray surface diffraction method, the method most sensitive for the detection of the transformation products. If only 2 per cent of the austenite is transformed into alpha iron (martensite?) the lines will appear on the film, but they will be weak. By a slight alteration in the X-ray technique one can determine the changes in line width,

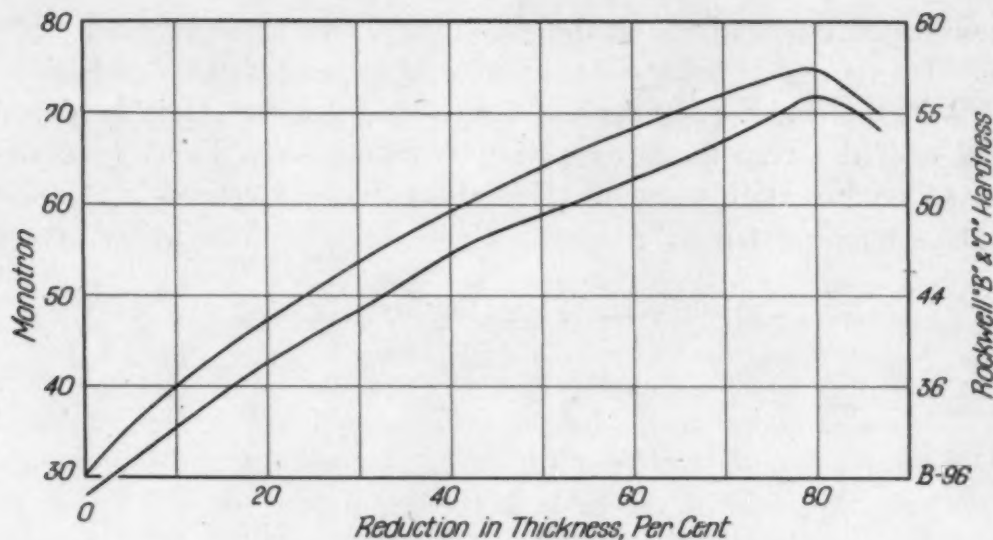


Fig. 1—Relationship Between the Hardness and the Percentage Reduction in Thickness of Hadfield Manganese Steel. Initial Thickness 0.118 Inch.

between the strain-free and after-work-hardening states. By means of the comparator surface diffraction cassette, one can compare the spectra of the work-hardened and the soft as-quenched specimens directly. If any new lines appear they can be easily observed.

If the carbides play an important role in the strain hardenability of the Hadfield manganese steel, the X-ray method may fail to detect the carbides, because of their extreme smallness. It is well known that it is difficult to detect carbides in some hypoeutectoid steels, but they are at times more easily detected in some hypereutectoid steels.

DISCUSSION OF RESULTS

The relationship between the hardness and the percentage reduction in thickness is shown in Fig. 1. It can be seen that the maximum hardness is extremely high. In some specimens Monotron 76 (Rockwell C-58) has been reached. It is therefore possible to strain harden this alloy to a greater extent by cold rolling than by the impact method, as used by Nikonoff. The maximum hardness was also found to extend from the surface to the center of the specimens. This was to be expected since the specimens were rather thin, ranging from 0.015 to 0.118 inch in thickness.

Another interesting point brought out by this investigation was that the specimens given the same percentage reduction in thickness did not harden to the same degree, but varied appreciably. The double curve shown in Fig. 1 indicates this variation and gives ap-

proximately the upper and lower bounds of the hardness for a number of specimens for a given reduction in thickness by cold rolling.

These curves give the further indication that strain hardening is uniform and progressive; however, it was rather surprising to find only a small change in the hardness over a considerable range of reduction in thickness for a given specimen. In other words the hardenability was quite erratic.

The maximum strain hardness was reached near 82 per cent reduction in thickness. When the specimens were given a cold reduction in excess of 85 per cent a definite falling off of the hardness was observed. Specimens given this amount of cold rolling are extremely brittle. It is probable that microscopic fissures begin to form, thereby weakening the structure.

It may be that once the maximum hardness is attained, the grain fragments, called "blocks", crystallites, etc., have reached their limiting size. Further working requires extremely high forces of deformation, to cause further slip, and the number of slip planes now available are very limited in number. In fact, the forces of deformation required to cause further plastic flow may actually exceed the cleavage strength of the crystals, i. e., some crystallites will be favorably oriented so that they have the maximum benefit of the forces of deformation. Also in view of the variation in the strain hardenability of the specimens given the same reductions in thickness, it is reasonable to assume that grains in the same specimen vary considerably in their work hardening characteristics.

No other steel can be work hardened to the extent possible in the Hadfield manganese steel, which strikingly approaches the hardness of martensite.

In Fig. 2, the surface diffraction X-ray diagram of a pure electrolytic iron is compared directly with the structure of the Hadfield manganese steel 1 in its softest condition—Rockwell B-95-96 (Monotron 28-30). These comparator surface diffraction diagrams show clearly that the Hadfield manganese steel is austenitic (gamma iron). This X-ray diagram does not indicate the presence of any alpha iron. If present the amount is extremely small. In other words, if 2 per cent were alpha iron, the X-ray may fail to reveal it.

In Fig. 3, the X-ray diagram of the hot-rolled strip is compared with the same specimen after it has been cold-rolled. The X-ray diagram of each specimen was made on the same film. Direct comparison shows that cold rolling has broadened the lines of the

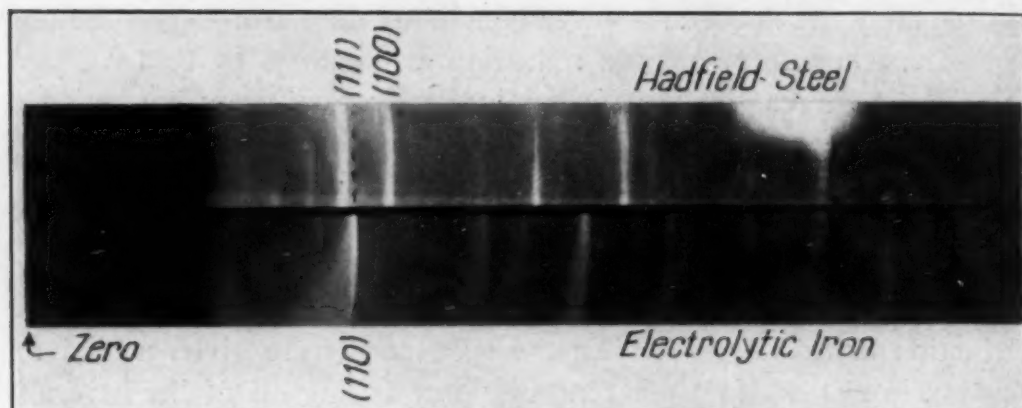


Fig. 2—The X-Ray Spectra of Austenitic Hadfield Manganese Steel and Electrolytic Alpha Iron are Compared Directly Upon the Same Film. The Position of the Strongest Lines in Each Spectrum is Indicated. The (110) Being the Most Intense Line for Alpha Iron, and the (111) Being the Most Intense for the Gamma Iron. Any Alpha Iron Present in the Gamma Iron Would Require the Appearance of the (110) Line in the Position Shown in the X-Ray Diagram of the Alpha Iron, and Indicated by the Dotted Line.

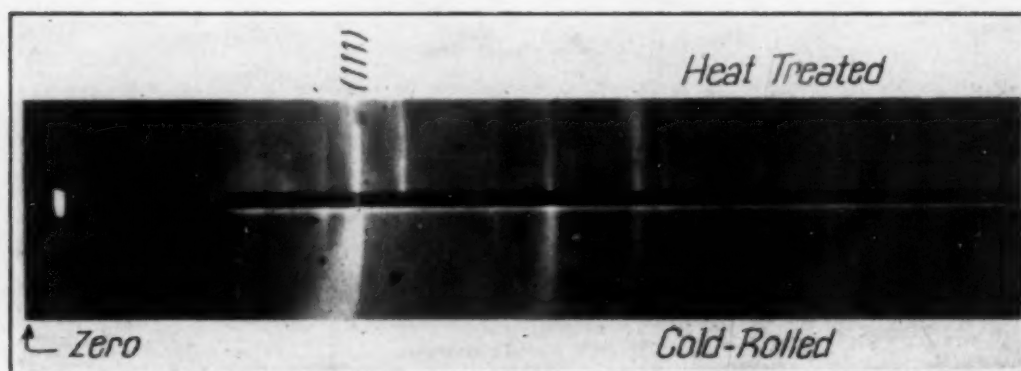


Fig. 3—X-Ray Diffraction Diagrams of Hadfield Manganese Steel in the Soft and Cold-Rolled State, Compared Directly on the Same Film. These Diagrams Were Taken on the Comparator Surface Diffraction Cassette. Molybdenum Filtered Radiation Was Used, and the Angle of Incidence of the X-Ray Beam Striking the Surface of the Specimen Was 10 Degrees. These X-Ray Diagrams Indicate that the Cold Rolling Did Not Transform Any of the Gamma Iron Into Alpha Iron in that the (110) Line Which is the Most Intense Line of the Alpha Iron Spectrum Was Missing.

gamma iron spectrum, but they remain in the same relative position. Drastic cold rolling therefore did not transform the gamma iron into alpha iron. Close examination of this film fails to disclose any lines due to the alpha iron. If the alpha iron has been generated, it is safe to say that less than 2 per cent was produced by the cold working.

It was therefore possible to conclude that Hadfield manganese steel remains austenitic when given a reduction of 75 per cent in thickness. That the structure remained austenitic after severe strain hardening was further substantiated by placing the specimens in a

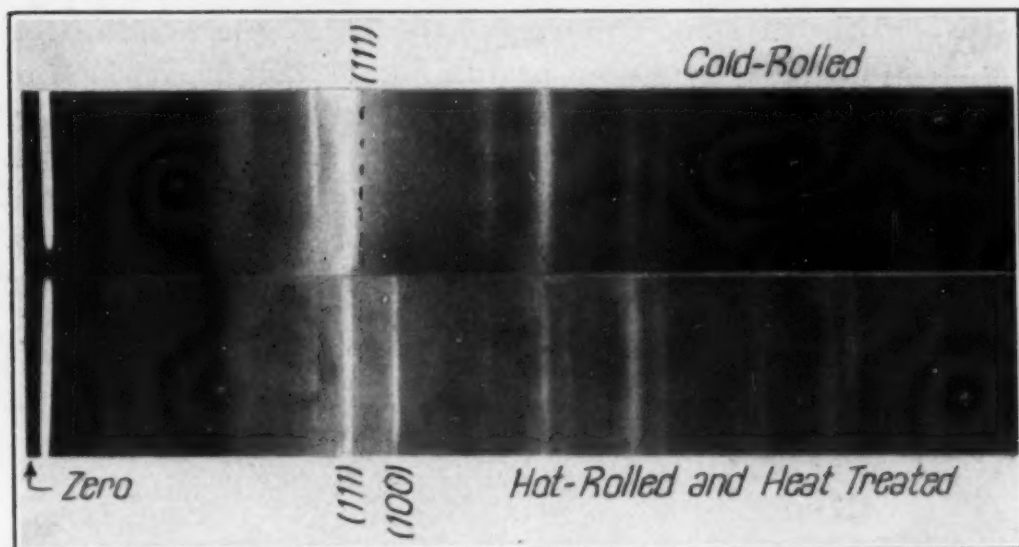


Fig. 4—Another Set of Surface Diffraction Diagrams of Hadfield Manganese Steel in the Cold-Rolled and Softest Condition. Cold Rolling Did Not Transform the Austenite Into Alpha Iron. The Dotted Line Shown in the X-Ray Diagram of the Cold-Rolled Material Gives the Approximate Position of the (110) Line Due to the Alpha Iron If It Were Present. These Diagrams Were Made by Setting the X-Ray Specimen at 10 Degrees to the X-Ray Beam. Molybdenum Radiation Filtered with ZrO Was Used. Specimen Was Cold-Rolled from 0.118 to 0.030 Inch.

powerful magnetic field. This failed to have any effect upon any of the specimens examined.

Fig. 4 compares the surface diffraction diagrams of the soft hot-rolled strip having a Rockwell B-96 (Monotron 30) with a cold-rolled structure having a hardness value of Rockwell C-55 (Monotron 70). It will be observed that the cold rolling has increased the width of the diffraction lines; however, the gamma iron lines persist, and there is no evidence that any alpha iron lines are present. If any alpha iron has been generated by the drastic strain hardening given to this specimen, the amount is exceedingly small. These X-ray diagrams were made by setting the surface of the specimens at 10 degrees to the X-ray beam. The reason for setting the specimens in this manner was to detect the (110) line of the alpha iron, if present. This line is the most intense one for the alpha iron, and would appear before any other line. When present it would occur quite close to the (111) line of austenite. One can readily observe that the (110) line of the alpha iron is definitely missing in both spectrograms.

To show more effectively the extent of the line broadening, the angle of incidence of the X-ray beam impinging upon the surface is increased to 25 degrees. This alteration in the X-ray technique has

been found by experiment to sharpen the lines. The result of this change in the X-ray setup is shown in Fig. 5. The $K\alpha$ doublets of the X-ray diffraction lines of the soft Hadfield steel are clearly resolved. This is believed to indicate that the grains are quite large, i.e., the inherent blocks are aligned so that their common crystal faces tend to lie in the same plane. From the intensity of the lines, one can further conclude that the "blocks" or "crystallites" are

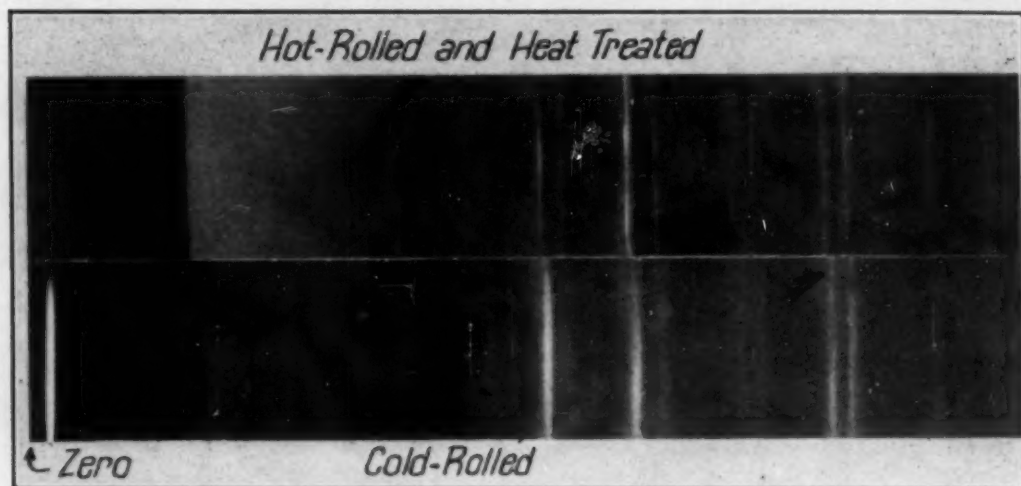


Fig. 5—These X-Ray Surface Diffraction Diagrams Were Taken to Show the Effect of Cold Rolling on the Line Width. On Comparing the Spectra of the Cold-Rolled and the Annealed Hot-Rolled Strip, One Can Observe that the Lines of the X-Ray Diagram Made of the Cold-Reduced Specimen Are Much Broader, and in Many Respects Similar to the X-Ray Diagram of Martensite. In the X-Ray Diagram of Soft Hadfield Austenitic Steel, the $K\alpha$ Doublets Are Definitely Resolved, Though They Are Not as Sharp as One Would Find in a Much Softer Material.

smaller than those found in low carbon steel; however, they are large enough to cause resolution of the $K\alpha$ doublet. According to the writer's viewpoint, a grain is not a true single crystal, but is built up of smaller crystal units called "blocks". The size of these blocks varies depending upon the chemical composition, and the mechanical and thermal treatment given to the material. In the annealed or soft state, the blocks within the grain tend to align themselves so that they have about the same orientation, and therefore have minimum energy content. The alignment of the blocks is more perfect in some grains than in others. For example in silicon ferrite the alignment of the blocks under suitable conditions of heat treatment and mechanical working is nearly perfect. In Hadfield manganese steel, these blocks are not only aligned less perfectly, but they are also much smaller, therefore the initial energy content is greater. These factors in part account for the great difference in hardness

between the soft silicon ferrite and the Hadfield manganese steel in the softest condition.

The diffraction lines of the cold-reduced steel shown in Fig. 5 are very broad and diffuse, and the $K\alpha$ doublets are completely merged, while in the soft Hadfield steel they were clearly resolved. The cold rolling had disorganized the alignment of the "blocks" within the grains and fragmented them into smaller ones, by the process of translatory slip, and rotation on the glide surfaces. (In gamma iron the [111] are the slip planes.) This process of fragmentation and reorientation continues until the limiting "block" size is reached. The limiting block size is associated with the maximum hardness. In other words when the maximum hardness is attained, further plastic deformation does not alter the "limiting" block size, and the hardness is not increased. The limiting block size varies in different metals and alloys. In severely reduced low carbon strip steels, the maximum hardness is about the same as the soft Hadfield manganese steel. Would this mean that the block size of the drastically rolled low carbon steel and the soft Hadfield steel are the same? On comparing the surface diffraction diagrams of these two steels, one finds the $K\alpha$ doublets to be resolved, and the intensity of many lines about the same.

However, in the cold-reduced Hadfield manganese steel the $K\alpha$ doublet lines are no longer resolved, because the lines are definitely broadened. The line width would indicate the crystallite size to lie in the range 10^{-6} to 10^{-7} centimeters. The line widths of the X-ray diffraction patterns of these cold-reduced Hadfield steels appear similar to the surface diffraction patterns of martensite; however, the martensite lines are definitely broader.

CONCLUSION

The results of this X-ray investigation support Niconoff's belief that the strain hardenability is largely due to the fragmentation of the grains into small crystallites or blocks, rather than substantially due to the decomposition products.

The line broadening of the austenite lines of the X-ray diffraction diagrams is believed to be due to the smallness of the "blocks" or the crystallites. It seems that in cold-reduced Hadfield manganese steels, the limiting particle size (blocks) is much smaller than can be produced in carbon steels given the same drastic cold rolling.

The line width observed on the X-ray surface diffraction diagrams would indicate the limiting crystallite size to be of the order of 10^{-6} to 10^{-7} centimeters. In low carbon steels, cold-rolled in excess of 90 per cent, the $K\alpha$ doublets remain resolved. This means that in these steels, the limiting particle size (blocks) is of the order of 10^{-5} centimeters. It is the extent to which the crystallite size (block) can be reduced that determines the hardness of metals.

In Hadfield manganese steels, an extremely small crystallite size (block) can be produced by cold rolling. The experimental results of Nikonoff would indicate that the martensite reaction does not contribute to the strain hardenability.

While the X-ray fails to show the effect the carbides may have upon the strain hardenability, it is evident that the failure of the X-ray diagrams to bring out the carbide lines, indicates that the carbides are in a highly dispersed state. It is quite possible that these highly dispersed carbide particles prevent the recovery of the small crystallites generated by the plastic deformation into larger ones.

This experiment shows that Hadfield austenitic steels can be hardened to values approaching martensite, and that structure remains austenitic.

DISCUSSION

Written Discussion: By C. A. Zapffe, assistant technical director, Rustless Iron and Steel Corporation, Baltimore, Maryland.

There seems to be an unnecessary inhibition on the part of metallurgists in this country to speak freely of the frequently demonstrated fact that the atomic arrangement within a metal grain is not homogeneous, but is of mosaic constitution. Elsewhere, this imperfection-structure of crystals receives much more open discussion.¹

Among the many English scientists who have studied mosaic structure since Darwin's early work with X-rays,^{2,3} Wood has been most concerned with the present problem. Similar to Mr. Goss's work, Wood developed an X-ray method for measuring the "limiting particle size" of the worked metals,^{4,7} and in 1935 showed that the hardness of a worked metal and the diffusion of its diffraction pattern both increase with decreasing size of the mosaic elements.⁴

¹E. N. Dac. Andrade, "The Mechanical Properties of Solids," *Engineer*, Vol. 171, (4457) 1941, p. 380-3.

²C. G. Darwin, "The Theory of X-Ray Reflexion," *Philosophical Magazine*, Vol. 27, 1914, p. 315-33.

³C. G. Darwin, "The Theory of X-Ray Reflexion, Part II," *Philosophical Magazine*, Vol. 27, 1914, p. 675-90.

⁴W. A. Wood, "Differences in the Structure of Electro Deposited Metallic Coatings Shown by X-Ray Diffraction," *Transactions, Faraday Society*, Vol. 31, 1935, p. 1248-53.

⁵W. A. Wood, "The Lower Limiting Crystallite Size and Internal Strains in Some Cold-Worked Metals," *Proceedings, Royal Society*, Vol. 172A, 1939, p. 231-41.

⁶W. A. Wood, "Crystalline Structure and Deformation of Metals," *Proceedings, Physical Society*, Vol. 52, No. 289, 1940, p. 110-6.

⁷W. A. Wood, "X-Ray Diffraction and the Deformation of Metals," *Journal, Scientific Instruments*, Vol. 18, 1941, p. 153-4.

As for the decrease in hardness noted by Mr. Goss beyond a given reduction, Oshiba observed the same phenomenon and states that with still further working the hardness again increases.⁸

Since the nature of hardness is not well understood today, any new theory deserves careful consideration. Once one grants that the grain is subdivided on an ultramicroscopic scale, a rather simple picture of hardness results. Thus, hardness, which is commonly measured as a resistance to indentation by an even harder body, would involve three possible factors: (1) Deformation by shear movements of the mosaic blocks past one another; (2) Deformation by actual submicroscopic cleavage of these blocks; and (3) Deformation by lattice distortion. The hardness of crystals showing little or no slip, such as glass and precious stones, would indicate an unimportance of the last factor, lattice distortion, and a predominating importance of the relative movements of the blocks. Then, decreasing block size would entail increasing hardness because of the increased surface energy opposing the deformation.⁹

If the limiting crystallite size determines hardness, Wood's measurements should be useful in predicting hardness. His values for iron, however, are several times larger than those given for copper, silver, and nickel, which are regarded as softer metals.

Modification of Mr. Goss's simple definition of hardness, on the other hand, may be necessary to include the cohesive strength of the species. Thus, rock-salt and iron might have the same limiting crystallite size, but the fourfold greater cohesive strength of iron atoms would make its hardness much greater.

Certainly the mosaic nature of crystals is no figment of the imagination; but it has been exceedingly difficult to study with existing metallographic tools. The new metallographic technique referred to as "fractography",^{10, 11} however, apparently allows direct observation of this intracrystalline imperfection and could be used, possibly in conjunction with the electron microscope, to check Mr. Goss's theory.

Written Discussion: By Eugene P. Klier, instructor in metallurgy, Pennsylvania State College, State College, Pa.

A study of Hadfield's manganese steel was delivered as the Howe Memorial Lecture in 1929 by J. H. Hall.¹² The work reported was carried out on a 12 per cent manganese steel of unstated carbon content and was primarily concerned with the metallography of this steel. There are reported, however, X-ray data obtained by E. C. Bain, in which it is conclusively shown that some austenite does convert to ferrite after suitable deformation of this steel. In this instance, however, definite ferromagnetism was evinced by the specimen.

It seems reasonable to accept the conclusion, based on the data reported here, that this manganese steel may be reduced to beyond 80 per cent, without

⁸F. Oshiba, "On the Change of Hardness Caused by Repeated Stress and the Effect of Aging on Its Recovery," *Science Reports*, Tohoku Imperial University, Vol. 28, 1940, p. 370-85.

⁹U. Dehlinger, "On the Fundamentals of a Recrystallization Theory," *Zeitschrift Metallkunde*, Vol. 33, (1), 1941, p. 16-20.

¹⁰C. A. Zapffe and Mason Clogg, Jr., "Fractography—A New Tool for Metallurgical Research," *TRANSACTIONS, American Society for Metals*, Vol. 34, 1945, p. 71.

¹¹C. A. Zapffe and Mason Clogg, Jr., "Cleavage Structures of Iron-Silicon Alloys," *TRANSACTIONS, American Society for Metals*, Vol. 34, 1945, p. 108.

¹²J. H. Hall, *Transactions, American Institute of Mining and Metallurgical Engineers*, Vol. 84, 1929, p. 382.

the formation of ferrite in even slight quantities. It is desirable to point out, however, that these data may not be conclusive.

A cold-rolled surface does not possess optimum properties, for the detection of small amounts of a precipitate-structure. On this basis, the estimated 2 per cent ferrite necessary for detection may be somewhat low. Of greater importance is the possibility that the cold rolling has developed a texture in at least the surface layers of the specimen; this might be such as to greatly lessen the chances of observing the (110) α at all. Certain seeming variations in the intensities of the austenite lines for the cold-rolled structure, as compared to the hot-rolled and heat treated structure, might be accounted for in this way.

The failure to observe ferromagnetic properties may not always be conclusive proof that no ferrite exists in the sample. Thus Smith¹³ has shown that for a 6.4 per cent manganese, 0.92 per cent carbon austenite, decomposing under isothermal conditions, the rate of reaction may be very much slower determined from measurement of magnetic flux, than may be observed for several other methods of measurement. (In this instance it appears that the particle size of the ferrite is a factor.) Data of the same character have been reported by Zavarine.¹⁴

Written Discussion: By H. A. Smith, metallurgical engineer, Beech Aircraft Corp., Wichita, Kansas.

It is good to have another paper from the author involving his special field of activity. This time he is investigating a phenomenon, the work hardening of Hadfield steel, which, the writer feels sure, transcends the purely physical effects of cold deformation.

Much good work has been done on the iron-manganese system. From this work we can predict what will occur on cold working such an alloy containing 14 per cent manganese quenched from a high temperature. We would find a structure, originally austenite (face-centered cubic and nonmagnetic), made up almost entirely of ferrite (body-centered cubic, magnetic) supersaturated with respect to manganese, together with traces of epsilon (hexagonal and non-magnetic) and austenite.

In the particular case of the Hadfield steel under consideration, we have a steel made in accordance with commercial melting practice and containing about one atomic per cent silicon and about five and five-tenths atomic per cent carbon, besides iron and manganese. This is definitely not a binary alloy and its behavior on cold working can be expected to be different, especially when one of the components is present in so large an amount forming an interstitial primary solid solution. From the standpoint of thermal equilibrium, alloys of this approximate composition at room temperature would contain an austenitic, a ferritic, and a carbide phase. The formation of this structure is possible only when time is allowed for the necessary diffusion of manganese and of carbon, which are extremely sluggish reactions at ordinary temperatures. On cold working, diffusion of manganese will not occur and if there is any diffusion of carbon it will be restricted to limited regions of atomic dimensions. The formation of martensite in Hadfield steel on cold working has not been adequately demonstrated to the satisfaction of the critical enquirer; however,

¹³H. A. Smith, *ibid.*, Vol. 116, 1935, p. 342.

¹⁴I. N. Zavarine, *ibid.*, Vol. 120, 1936, p. 253.

we must consider its formation possible because this does not involve diffusion. The author has not found evidences of either a body-centered cubic, a hexagonal or a magnetic constituent in his cold-worked Hadfield steel.

It is possible that the author is a little too sanguine in his lower limit for the detection of either of these phases by X-ray diffraction methods. If either of these phases were formed by cold deformation they would most certainly give very diffuse diffraction lines due not only to small block size, but possibly also to solvent lattice distortion caused by solid solution effects. The author further substantiates the absence of a body-centered cubic phase by magnetic methods. In this connection, some remarks from him relative to the sensitivity of his magnetic test would be helpful in judging what quantity of a magnetic constituent might have been present but not detected. It is hoped further work will be attempted correlating conventional and colloidal magnetic photomicrography with X-ray work.

Assuming the use of the proper X-ray technique, which the author has previously so well developed, the broadening of X-ray diffraction lines on cold working may be due to three factors:

- (a) Decrease in crystal fragment block size from normal toward colloidal dimensions.
- (b) Spacial nonregistry of crystal fragment blocks
- (c) Lattice distortion within crystal fragment blocks due to several effects accompanying solid solution.

In any cold-worked metal or alloy, (a) and (b) are certainly operative. The operation of factor (c) in any given case will depend upon the particular conditions of supersaturation, upon stability of the solid solution toward temperatures generated in cold working, and upon the formation of twin bands. Factor (c) will certainly be effective for the steel under consideration, since it is supersaturated to the extent of about four atomic per cent carbon. The steel as a whole will be heated to an appreciable extent by cold working and localized temperatures in the vicinity of slip bands will be much higher. The structure is face-centered cubic and subject to the formation of twin bands. Such bands may be quite large and are composed of highly disturbed lattice conditions following the formation of the twin. The mechanically disturbed lattice conditions in the regions mentioned, as well as the accompanying thermal effects, may easily lead to localized carbide pre-precipitation lattice configurations that would easily lead to the extraordinary hardness found on cold working Hadfield steel. Such an assumption is susceptible to indirect experimental verification. The writer believes that the interpretation given to diffraction line broadening on cold working an alloy will depend upon the condition of the metal relative to thermal equilibrium before cold working begins.

The author is to be congratulated for extending his X-ray investigation of cold-rolled structures from thermally stable to thermally unstable alloys and it is hoped that he will continue this work.

Written Discussion: By Raymond G. Spencer, chairman, Metals Research, Armour Research Foundation, Chicago.

The author of this paper has shown rather conclusively that the high strain hardenability of Hadfield manganese steel is due to a purely physical change

rather than to any decomposition transformation or precipitation products. One can agree readily with his statement that the strain hardness is due to the fragmentation of the grains into their inherent smaller "blocks". This explanation is consistent with the concept of a mosaic structure of crystals.

The author further states that the "blocks" which constitute the mosaic structure in the crystals of Hadfield steel are much smaller than in low carbon steels. This is a possible, but not a necessary, conclusion from the data presented. The broadening of the X-ray diffraction lines is largely due to two causes, (a) the breaking up of the crystals into "blocks" and (b) lattice distortion within these "blocks". It is difficult to determine the amount that each of these contributes to line width. A very significant part of the line width could be due to lattice distortion.

It seems that the results could be explained very satisfactorily by assuming that the crystals break into "blocks" of the order of magnitude of 10^{-5} centimeters and that these blocks have severe lattice distortion.

It is not surprising to learn that Hadfield steel can be worked to a greater hardness by cold rolling than by impact forging. After a certain amount of reduction it is probable that some of the "blocks" are actually fractured on further reduction, thus weakening the steel and reducing its hardness. The phenomenon might readily occur more quickly when metal is worked with a hammer than when rolled. This breakdown caused by extreme working also accounts for the reduction in hardness found by the author when reduction exceeded 80 per cent.

Oral Discussion

V. N. KRIVOBOK:¹⁵ The metallurgical aspects of Hadfield manganese steels have been for a number of years the subject of research in the Metallurgical Research Laboratories of Carnegie Institute of Technology. A number of investigations dealt with the structural stability of austenitic manganese steels and it was invariably found that cold working of the Hadfield manganese steel of common composition resulted in rather pronounced decomposition of austenite. Hence, I find it difficult to accept the statement appearing on page 634 of Mr. Goss's paper which I quote: "Drastic cold rolling did not transform the gamma iron into alpha iron". I searched through the paper for the data on magnetic properties because these can be used as a rather sensitive method of ascertaining the presence of alpha iron, but did not find them included in the text of the paper. Since one should be reluctant to discard results of previous carefully conducted work, it is imperative that an explanation should be found. I note that the specimens of Hadfield steel used by Mr. Goss contained 1.30 per cent carbon and 14 per cent manganese while those which I have investigated contained on the average 1.18 per cent carbon and 12.5 per cent manganese. Although there is a difference in the composition I would not expect that this difference would account for the presence or the absence of magnetic alpha phase in cold-worked steel. I do not wish to state that the interpretation which Mr. Goss gives to this phenomenon is incorrect. I merely wish to point out that perhaps the technique of measuring the magnetic characteristics of the

¹⁵Member, Development and Research Division, International Nickel Co., Inc., New York.

metal was not sufficiently sensitive so as to permit the magnetic change which I believe should be found.

I may further point out the difference in experimental procedure between the work of Mr. Goss and myself. Mr. Goss achieved deformation by cold drawing. In our work we used rapid cold rolling and deformation under the hammer to achieve drastic reduction. Whether the method of cold deformation may have some influence on the final results I do not know but such a subject would appear to be highly speculative.

Author's Reply

Further work on these Hadfield manganese steels shows that some alpha iron can be retained in the specimens when quenched from 1800 degrees Fahr. (980 degrees Cent.) in water. In other specimens no alpha iron could be detected with the X-ray diffraction method. On cold working these specimens, I could not find any evidence of alpha iron in the specimens which did not show any alpha iron lines in the heat treated condition. This and other observations will be presented in another paper. However, I thought that this added information may in part answer the question raised by Drs. Krivobok and Klier. While the magnetic method I used may appear crude, nevertheless it is sensitive enough to detect alpha iron if present. (The specimen is suspended on a fine wire and placed in a magnetic field.)

The fact remains that the presence or the absence of the alpha iron does not have any effect upon the extremely high hardness of this steel.

Therefore, in view of the evidence found in this investigation so far, I must conclude that the extreme hardness of this alloy after cold working is essentially due to the smallness of the crystallites developed by the deformation process.

The line broadening as shown in these X-ray diagrams is believed due to the smallness of the crystals. While I am aware of the fact that others may not agree with this point of view, the evidence as brought out by this work strongly suggests that such a conclusion is reasonable and can be supported by experiment.

The question as to whether line broadening is due to lattice distortion, particle size or both can be tested experimentally.

If line broadening is due to lattice distortion, then the line broadening should remain the same, regardless of the wave length employed. On the other hand if the line broadening is due to smallness of the grain fragments of the crystallites the line width should vary (i.e., the sharpness) depending on the wave length of the $K\alpha$ X-ray radiation used.

Therefore by proper choice of crystallite size and X-ray $K\alpha$ radiations this theory can be tested directly. It is assumed here that the hardness of a metal is largely a function of the particle or crystallite size.

To test this theory, a 17 per cent chromium steel strip was work-hardened by cold rolling it to about Rockwell C-35-40. The specimen was examined with molybdenum $K\alpha$ radiation $\left[\begin{smallmatrix} 0.708 \\ 0.712 \end{smallmatrix} \times 10^{-8} \text{ cm} \right]$. The $K\alpha$ radiation was reflected from the surface of this specimen, and the $K\alpha$ doublet lines were found to be fairly well resolved.

This same specimen was then examined with $K\alpha$ cobalt radiation $\left[\begin{smallmatrix} 1.785 \\ 1.789 \end{smallmatrix} \times 10^{-8} \text{ cm} \right]$ and the $K\alpha$ doublet was completely merged and broadened. In other words the shorter molybdenum $K\alpha$ radiation, being about 2.5 times shorter than the cobalt $K\alpha$ radiation, could diffract the X-ray radiation without appreciable increase in line width.

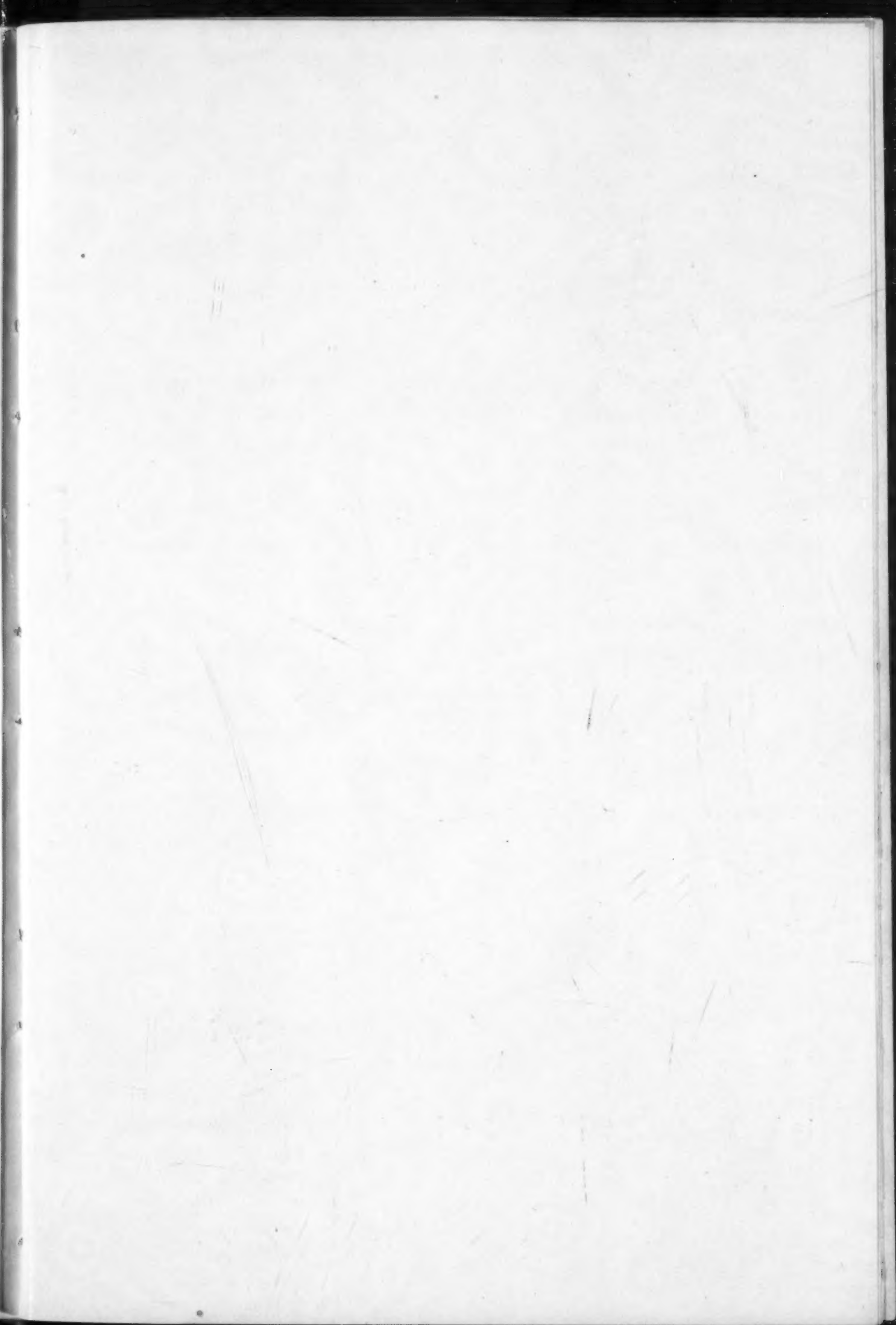
On the basis of this experiment line broadening is due to the smallness of the crystallites.

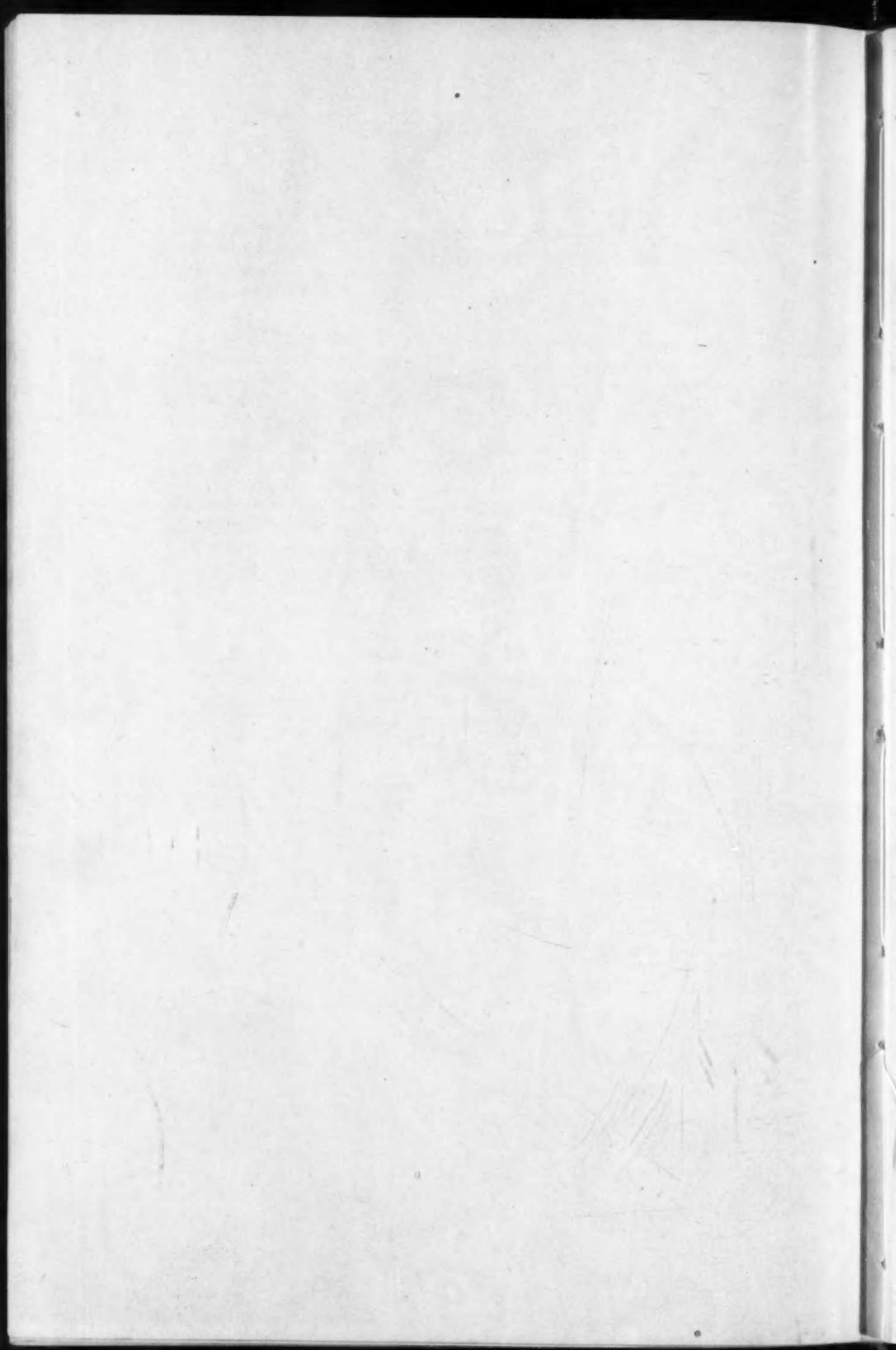
Dr. Wood of England has arrived at the same conclusion independently. He has further attempted to show that while line broadening is due to smallness of particle size, lattice distortion would give the $K\alpha$ lines a definite and measurable shift. So far I have not been able to find this shift on the metals I have studied in this way.

Dr. Klier calls my attention to the X-ray work conducted on Hadfield steels a number of years ago by Dr. Bain, and in which some austenite was reported to have been converted to alpha iron by cold working. While Dr. Bain's samples contained less manganese than those used here, it may well be that some retained alpha iron may have been present in the as-quenched specimen. Or else when the manganese content is 12 per cent, some alpha iron may be transformed from the austenite when cold-worked. I will check this point, and wish to thank Dr. Klier for calling my attention to it. I trust he may also be interested in checking it.

The author appreciates the discussion of Dr. Spencer, and I trust that he will find it possible to test the theory of particle size vs. lattice distortion as suggested above. Dr. Spencer has long advocated the mosaic structure of crystals in explaining certain phases of his own researches.

The discussions of Drs. Smith and Zapffe have added greatly to the mosaic structure theory, and their able discussion is hereby acknowledged. The point brought out by Dr. Smith that one can have lattice parameter variations due to the variation in solid solution will be kept in mind as the work now being done proceeds.





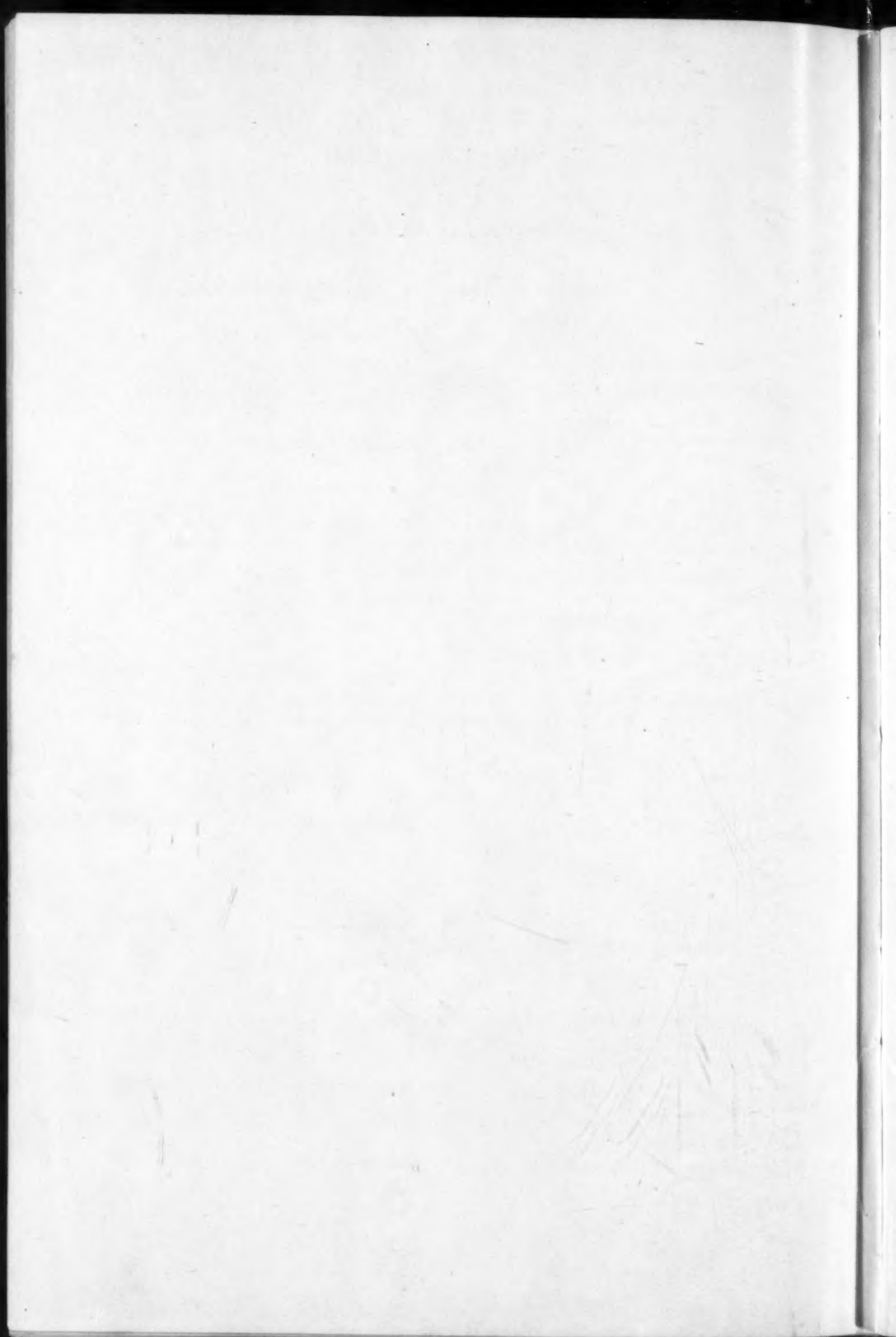
INDEX OF AUTHORS

VOLUME XXXIV

TRANSACTIONS OF AMERICAN SOCIETY FOR METALS

1945

A		K	
Aul, E. L.....	505	Kennedy, Jr., Ralph G.....	250
B		L	
Ball, Leslie W.....	545	Lewis, J. R.....	425
Benninghoff, W. E.....	310	Long, J. R.....	443, 465, 481
Berman, F.	143	Loria, Edward A.....	407
		Lubahn, J. D.....	505, 517
C		M	
Clogg, Jr., Mason.....	71, 108	Martin, D. L.	351
Cohen, Morris	216	Matthews, C. W.....	481
Comstock, G. F.....	425	McIntyre, John	202
		Meinhart, W. L.....	589
D		O	
Dean, R. S.....	443, 465, 481	Osborn, Jr., H. B.....	310
E		P	
Ebert, L. J.....	505, 517	Parker, Earl R.....	156
		Potter, E. V.....	443, 465
F		S	
Fitterer, G. R.....	41	Sachs, G.	505, 517
Fletcher, S. G.....	216	Sykes, W. P.....	415
G		W	
Goss, Norman P.....	630	Wiley, F. E.....	351
Graham, T. R.....	443, 481		
H		Z	
Harker, David	156	Zapffe, Carl A.....	71, 108
Harrington, R. H.....	143	Ziegler, N. A.....	589
Hayes, E. T.....	443		
Huber, R. W.....	465		



INDEX OF SUBJECTS AND AUTHORS OF PAPERS

VOLUME XXXIV

TRANSACTIONS OF AMERICAN SOCIETY FOR METALS

1945

A

Acid Open-Hearth Process; Some Fundamental Problems in the Manufacture of Steel by the—By <i>G. R. Fitterer</i>	41
Age Hardening Copper-Manganese-Nickel Alloys—By <i>R. S. Dean, J. R. Long, T. R. Graham and C. W. Matthews</i>	481
Aircraft Parts; Interpretation of Radiographs—By <i>Leslie W. Ball</i>	545
Aluminum and Titanium Deoxidation for Preventing Strain Aging Embrittlement in Low Carbon Steel; A Comparison of—By <i>G. F. Comstock and J. R. Lewis</i>	425
Amendment of the Constitution of the A.S.M.....	16
Annual Address of President.....	24
Annual Dinner of A.S.M.....	19
Annual Report of Secretary.....	34
Annual Report of Treasurer.....	29
Annual Meeting of A.S.M.....	14
Ar' Reaction in Some Iron-Cobalt-Tungsten Alloys and the Same Modified with Chromium—By <i>W. P. Sykes</i>	415

C

Campbell Memorial Lecture—19th; Some Fundamental Problems in the Manufacture of Steel by the Acid Open-Hearth Process—By <i>G. R. Fitterer</i>	41
Carbon Steels (Plain); Induction Hardening of—By <i>D. L. Martin and F. E. Wiley</i>	351
Cast Chromium-Molybdenum Steels; Characteristics and Properties of Some—By <i>N. A. Ziegler and W. L. Meinhart</i>	589
Characteristics and Properties of Some Cast Chromium-Molybdenum Steels—By <i>N. A. Ziegler and W. L. Meinhart</i>	589
Chromium; Ar' Reaction in Some Iron-Cobalt-Tungsten Alloys and the Same Modified with—By <i>W. P. Sykes</i>	415
Chromium-Molybdenum Steels; Characteristics and Properties of Some Cast—By <i>N. A. Ziegler and W. L. Meinhart</i>	589
Cleavage Structures of Iron-Silicon Alloys—By <i>Carl A. Zappfe and Mason Clogg, Jr.</i>	108
Cobalt-Iron-Tungsten Alloys and the Same Modified with Chromium; Ar' Reaction in Some—By <i>W. P. Sykes</i>	415
Cobalt Steels; Rates of Tempering in—By <i>Edward A. Loria</i>	407
Cold Rolling on the Structure of Hadfield Manganese Steel; Effect of—By <i>Norman P. Goss</i>	630
Comparison of Aluminum and Titanium Deoxidation for Preventing Strain Aging Embrittlement in Low Carbon Steel—By <i>G. F. Comstock and J. R. Lewis</i>	425
Copper-Manganese Alloys; Properties of Transitional Structures in—By <i>R. S. Dean, E. V. Potter, J. R. Long and R. W. Huber</i>	465
Copper-Manganese Equilibrium System—By <i>R. S. Dean, J. R. Long, T. R. Graham, E. V. Potter and E. T. Hayes</i>	443

Copper-Manganese-Nickel Alloys; Age Hardening—By <i>R. S. Dean, J. R. Long, T. R. Graham and C. W. Matthews</i>	481
Cyaniding of High Speed Steel Prior to Hardening; Experiments of Sodium—By <i>John McIntyre</i>	202

D

Dimensional Stability of Steel—Part I—Subatmospheric Transformation of Retained Austenite—By <i>S. G. Fletcher and Morris Cohen</i>	216
---	-----

E

Effect of Cold Rolling on the Structure of Hadfield Manganese Steel—By <i>Norman P. Goss</i>	630
Effect of Fiber on Notched Bar Tensile Strength Properties of a Heat Treated Low Alloy Steel—By <i>G. Sachs, J. D. Lubahn, L. J. Ebert and E. L. Aul</i>	505
Effects of Notches of Varying Depth on the Strength of Heat Treated Low Alloy Steels—By <i>G. Sachs, J. D. Lubahn and L. J. Ebert</i>	517
Election of Officers of A.S.M.....	15
Experiments of Sodium Cyaniding of High Speed Steel Prior to Hardening—By <i>John McIntyre</i>	202

F

Fiber on Notched Bar Tensile Strength Properties of a Heat Treated Low Alloy Steel; Effect of—By <i>G. Sachs, J. D. Lubahn, L. J. Ebert and E. L. Aul</i>	505
Fractography—A New Tool for Metallurgical Research—By <i>Carl A. Zappfe and Mason Clogg, Jr.</i>	71
Fracture Studies of Soldered Joints—By <i>F. Berman and R. H. Harrington</i>	143
Frequency and Time Cycles for the Processing of Metallic Parts with Induction Heating; Practical Aspects of the Selection of—By <i>W. E. Benninghoff and H. B. Osborn, Jr.</i>	310

G

Grain Growth and Grain Shape—By <i>David Harker and Earl R. Parker</i>	156
Grain Shape and Grain Growth—By <i>David Harker and Earl R. Parker</i> ..	156

H

Hadfield Manganese Steel; Effect of Cold Rolling on the Structure of—By <i>Norman P. Goss</i>	630
Hardening; Experiments of Sodium Cyaniding of High Speed Steel Prior to—By <i>John McIntyre</i>	202
Heat Treated Low Alloy Steels; Effects of Notches of Varying Depth on the Strength of—By <i>G. Sachs, J. D. Lubahn and L. J. Ebert</i>	517
High Speed Steel (Molybdenum-Tungsten); A Study of Subzero Treatments Applied to—By <i>Ralph G. Kennedy, Jr.</i>	250
High Speed Steel Prior to Hardening; Experiments of Sodium Cyaniding of—By <i>John McIntyre</i>	202

I

Induction Hardening of Plain Carbon Steels—By <i>D. L. Martin and F. E. Wiley</i>	351
Induction Heating; Practical Aspects of the Selection of Frequency and Time Cycles for the Processing of Metallic Parts with—By <i>W. E. Benninghoff and H. B. Osborn, Jr.</i>	310

Interpretation of Radiographs: Particularly of Aircraft Parts—By <i>Leslie W. Ball</i>	545
Iron-Cobalt-Tungsten Alloys and the Same Modified with Chromium; Ar' Reaction in Some—By <i>W. P. Sykes</i>	415
Iron-Silicon Alloys; Cleavage Structures of—By <i>Carl A. Zapffe and Mason Clogg, Jr.</i>	108

J

Joints; Fracture Studies of Soldered—By <i>F. Berman and R. H. Harrington</i>	143
---	-----

L

Low Alloy Steel; Effect of Fiber on Notched Bar Tensile Strength Properties of a Heat Treated—By <i>G. Sachs, J. D. Lubahn, L. J. Ebert and E. L. Aul</i>	505
Low Alloy Steels; Effects of Notches of Varying Depth on the Strength of Heat Treated—By <i>G. Sachs, J. D. Lubahn and L. J. Ebert</i>	517
Low Carbon Steel; A Comparison of Aluminum and Titanium Deoxidation for Preventing Strain Aging Embrittlement in—By <i>G. F. Comstock and J. R. Lewis</i>	425

M

Manganese-Copper Alloys; Properties of Transitional Structures in—By <i>R. S. Dean, E. V. Potter, J. R. Long and R. W. Huber</i>	465
Manganese-Copper Equilibrium System—By <i>R. S. Dean, J. R. Long, T. R. Graham, E. V. Potter and E. T. Hayes</i>	443
Manganese-Copper-Nickel Alloys; Age Hardening—By <i>R. S. Dean, J. R. Long, T. R. Graham and C. W. Matthews</i>	481
Manganese (Hadfield) Steel; Effect of Cold Rolling on the Structure of—By <i>Norman P. Goss</i>	630
Manufacture of Steel by the Acid Open-Hearth Process; Some Fundamental Problems in the—By <i>G. R. Fitterer</i>	41
Metallic Parts Processing with Induction Heating; Practical Aspects of the Selection of Frequency and Time Cycles for the—By <i>W. E. Benninghoff and H. B. Osborn, Jr.</i>	310
Molybdenum-Chromium Steels; Characteristics and Properties of Some Cast—By <i>N. A. Ziegler and W. L. Meinhart</i>	589
Molybdenum-Tungsten High Speed Steel; Study of Subzero Treatments Applied to—By <i>Ralph G. Kennedy, Jr.</i>	250

N

Nickel-Copper-Manganese Alloys; Age Hardening—By <i>R. S. Dean, J. R. Long, T. R. Graham and C. W. Matthews</i>	481
Notched Bar Tensile Strength Properties of a Heat Treated Low Alloy Steel; Effect of Fiber on—By <i>G. Sachs, J. D. Lubahn, L. J. Ebert and E. L. Aul</i>	505
Notches of Varying Depth on the Strength of Heat Treated Low Alloy Steels; Effects of—By <i>G. Sachs, J. D. Lubahn and L. J. Ebert</i>	517

O

Open-Hearth Process (Acid); Some Fundamental Problems in the Manufacture of Steel by the—By <i>G. R. Fitterer</i>	41
---	----

P

Plain Carbon Steels; Induction Hardening—By <i>D. L. Martin and F. E. Wiley</i>	351
Practical Aspects of the Selection of Frequency and Time Cycles for the Processing of Metallic Parts with Induction Heating—By <i>W. E. Benninghoff and H. B. Osborn, Jr.</i>	310
Presentation of Awards	20, 21, 22
Properties and Characteristics of Some Cast Chromium-Molybdenum Steels—By <i>N. A. Ziegler and W. L. Meinhardt</i>	589
Properties of Transitional Structures in Copper-Manganese Alloys—By <i>R. S. Dean, E. V. Potter, J. R. Long and R. W. Huber</i>	465

R

Radiograph Interpretation: Particularly of Aircraft Parts—By <i>Leslie W. Ball</i>	545
Rates of Tempering in Cobalt Steels—By <i>Edward A. Loria</i>	407
Retained Austenite; Subatmospheric Transformation of (Part I); Dimensional Stability of Steel—By <i>S. G. Fletcher and Morris Cohen</i> ...	216

S

Secretary's Report	34
Selection of Frequency and Time Cycles for the Processing of Metallic Parts with Induction Heating; Practical Aspects of the—By <i>W. E. Benninghoff and H. B. Osborn, Jr.</i>	310
Sodium Cyaniding of High Speed Steel Prior to Hardening; Experiments of—By <i>John McIntyre</i>	202
Soldered Joints; Fracture Studies of—By <i>F. Berman and R. H. Harrington</i>	143
Some Fundamental Problems in the Manufacture of Steel by the Acid Open-Hearth Process—By <i>G. R. Fitterer</i>	41
Stability (Dimensional) of Steel—Part I—Subatmospheric Transformation of Retained Austenite—By <i>S. G. Fletcher and Morris Cohen</i>	216
Strain Aging Embrittlement Prevention in Low Carbon Steel; A Comparison of Aluminum and Titanium Deoxidation for—By <i>G. F. Comstock and J. R. Lewis</i>	425
Study of Subzero Treatments Applied to Molybdenum-Tungsten High Speed Steel—By <i>Ralph G. Kennedy, Jr.</i>	250
Subatmospheric Transformation of Retained Austenite—Part I; Dimensional Stability of Steel—By <i>S. G. Fletcher and Morris Cohen</i>	216
Subzero Treatments Applied to Molybdenum-Tungsten High Speed Steel—By <i>Ralph G. Kennedy, Jr.</i>	250

T

Technical Program and Reports of Officers, A.S.M.—26th Annual Convention, Cleveland, October 16 to 20, 1944	1
Tempering Rates in Cobalt Steels—By <i>Edward A. Loria</i>	407
Titanium and Aluminum Deoxidation for Preventing Strain Aging Embrittlement in Low Carbon Steel; Comparison of—By <i>G. F. Comstock and J. R. Lewis</i>	425
Transitional Structures in Copper-Manganese Alloys; Properties of—By <i>R. S. Dean, E. V. Potter, J. R. Long and R. W. Huber</i>	465
Treasurer's Report	29
Tungsten-Iron-Cobalt Alloys and the Same Modified with Chromium; Ar' Reaction in Some—By <i>W. P. Sykes</i>	415

